

**Ongoing Face Recognition
Vendor Test (FRVT)**
Part 1: Verification

Patrick Grother
Mei Ngan
Kayee Hanaoka
Joyce C. Yang
Austin Hom

*Information Access Division
Information Technology Laboratory*

This publication is available free of charge from:
<https://www.nist.gov/programs-projects/face-recognition-vendor-test-frvt-ongoing>

2023/02/02



ACKNOWLEDGMENTS

The authors are grateful for the long-standing support and collaboration of the the Department of Homeland Security's Science & Technology Directorate (S&T) and the Office of Biometric Identity Management (OBIM).

Additionally, the authors are grateful to staff in the NIST Biometrics Research Laboratory for infrastructure supporting rapid evaluation of algorithms.

DISCLAIMER

Specific hardware and software products identified in this report were used in order to perform the evaluations described in this document. In no case does identification of any commercial product, trade name, or vendor, imply recommendation or endorsement by the National Institute of Standards and Technology, nor does it imply that the products and equipment identified are necessarily the best available for the purpose.

INSTITUTIONAL REVIEW BOARD

The National Institute of Standards and Technology's Research Protections Office reviewed the protocol for this project and determined it is not human subjects research as defined in Department of Commerce Regulations, 15 CFR 27, also known as the Common Rule for the Protection of Human Subjects (45 CFR 46, Subpart A).

FRVT STATUS

This report is a draft NIST Interagency Report, and is open for comment. It is the thirty sixth edition of the report since the first was published in June 2017. Prior editions of this report are maintained on the FRVT [website](#), and may contain useful information about older algorithms and datasets no longer used in FRVT.

FRVT remains open: All [four tracks](#) of the FRVT are open to new algorithm submissions. **2023-02-01** changes

since 2022-12-15:

- ▷ We have added results for first algorithms from four developers: CU-Face, Korea ID, Onfido, and TrueID-VNG.
- ▷ We have added results for new algorithms from 21 returning developers: Alchera, Armatura, Cogent-Thales, Dermalog, Didi ChuXing Global Face, Gorilla, Hyperverge, Innovatrics, Intel Research, IntelliVIX, Intema-LGL, Kasikorn Labs, Paravision, Rank One Computing, Sensetime Group, Suprema AI, Tech5, Unissey, U. Coimbra Visteam, Vixvizion (Imagus), and Yuan High-Tech Development.
- ▷ We have retired results for 20 algorithms per our policy to only list results for two algorithms per developer. Results for retired algorithms appear in prior versions of this report in the [archive](#).
- ▷ We have introduced new set of non-frontal portrait to border comparisons. The new images are described in section [2.3](#) and their use in section [3.2](#).

2022-12-15 changes since 2022-11-06:

- ▷ We have added results for first algorithms from four developers: Maxis Biometrics, PT Autentika Digital Indonesia, PT Qlue Performa Indonesia, and STCON.
- ▷ We have added results for new algorithms from 14 returning developers: Adera Global, Aiseemu Technology, Chunghwa Telecom, chtface, FRP, Griaule, Line Corporation, Maxvision Technology, Mukh Technologies, Papilon Savunma, Qnap Security, Realnetworks, Securif AI, SQISoft, and Veridium.
- ▷ We have retired results for 10 algorithms per our policy to only list results for two algorithms per developer. Results for retired algorithms appear in prior versions of this report in the [archive](#).

2022-11-06 changes since 2022-09-26:

- ▷ We have added results for first algorithms from six developers: AFR Engine, CMC Institute of Science and Technology, Saga Densan Center, Turkcell Technology, UXLabs, and Wise AI SDN BHD.
- ▷ We have added results for new algorithms from 14 returning developers: Coretech Knowledge, Cloudwalk - Moontime, Cloudmatrix, Deepglint, Guangzhou Pixel Solutions, Hangzhuo Allu Network Information Technology, NEO Systems, One More Security, Palit Microsystems, Panasonic R+D Center Singapore, Samsung S1, Seventh Sense Artificial Intelligence, Touchless ID, and Veridas Digital Authentication Solutions S.L.
- ▷ We have retired results for 10 algorithms per our policy to only list results for two algorithms per developer. Results for retired algorithms appear in prior versions of this report in the [archive](#).

2022-09-26 changes since 2022-08-30:

- ▷ We have added results for first algorithms from three developers: Codeline, First Credit Bureau Kazakhstan, and InfoCert.
- ▷ We have added results for new algorithms from 14 returning developers: Advancegroup, Armatura LLC, Beijing Hisign Technology, Cybercore, Cyberlink Corp, Herta Security, ICM Airport Technics, InsightFace AI, Metsakuur, NSENSE Corp, Samsung-SDS, Videmo Intelligent Videoanalyse, Vietnam Posts and Telecommunications Group, and Vision Intelligence Center of Meituan.
- ▷ We have retired results for 11 algorithms per our policy to only list results for two algorithms per developer. Results for retired algorithms appear in prior versions of this report in the [archive](#).

2022-08-30 changes since 2022-07-29:

- ▷ We have added results for first algorithms from two developers: Aximetria, Intellibrain Technological Projects
- ▷ We have added results for new algorithms from twelve returning developers: Alchera Inc, Dermalog, Idemia, Incode Technologies Inc, Intellivision, Kasikorn Labs, Megvii/Face++, Techsign, TuringTech.vip, Universidade de Coimbra, Verijelais, Vixvizon
- ▷ We have retired results for six algorithms per our policy to only list results for two algorithms per developer. Results for retired algorithms appear in prior versions of this report in the [archive](#).

2022-07-29 changes since 2022-06-27:

- ▷ We have added results for first algorithms from seven developers: FRP LLC (Hawaii), IMDS Software, Inspur (Beijing) Electronic Information Industry, Intema - LGL Group, PAPAGO, Qaz Biometric Systems, and VIDA-Digital Identity
- ▷ We have added results for new algorithms from nine returning developers: Cyberextruder, Glory, Maxvision Technology, Rank One Computing, Securif AI, Suprema AI, Suprema ID, Toshiba, and Yuan High-Tech Development.
- ▷ We have retired results for nine algorithms per our policy to only list results for two algorithms per developer. Results for retired algorithms appear in prior versions of this report in the [archive](#).

2022-07-29 changes since 2022-06-27:

- ▷ We have added results for first algorithms from seven developers: FRP LLC (Hawaii), IMDS Software, Inspur (Beijing) Electronic Information Industry, Intema - LGL Group, PAPAGO, Qaz Biometric Systems, and VIDA-Digital Identity
- ▷ We have added results for new algorithms from nine returning developers: Cyberextruder, Glory, Maxvision Technology, Rank One Computing, Securif AI, Suprema AI, Suprema ID, Toshiba, and Yuan High-Tech Development.
- ▷ We have retired results for nine algorithms per our policy to only list results for two algorithms per developer. Results for retired algorithms appear in prior versions of this report in the [archive](#).

2022-06-27 changes since 2022-06-03:

- ▷ We have added results for first algorithms from two developers: Krungthai Bank, and Smartbiometrik.

- ▷ We have added results for new algorithms from thirteen returning developers: Aiseemu, Corsight, Digidata, Griaule, Guangzhou Pixel Solutions, Hangzhuo AI Network Information Technology, Neurotechnology, Real Networks, Samsung S1, Sensetime Group, Smart Engines, Verihubs Inteligensia, and VinBigData.
- ▷ We have retired results for eight algorithms per our policy to only list results for two algorithms per developer. Results for retired algorithms appear in prior versions of this report in the [archive](#).

2022-06-03 changes since 2022-05-05:

- ▷ We have added results for first algorithms from seven developers: Jaak IT, Metsakuur, Palit Microsystems, Smarvist Teknoloji, and Touchless ID.
- ▷ We have added results for new algorithms from sixteen returning developers: Cyberlink, FaceOnLive, Kakao Enterprise, Line Corporation (Line Clova), Multi-Modality Intelligence, NEO Systems, and Unissey
- ▷ We have retired results for four algorithms per our policy to only list results for two algorithms per developer. Results for retired algorithms appear in prior versions of this report in the [archive](#).
- ▷ We have moved the results for the twenty human-difficult pairs used in the May 2018 paper *Face recognition accuracy of forensic examiners, superrecognizers, and face recognition algorithms* by Phillips et al. [1]. to the algorithm-specific report cards (example: [PDF](#)).
- ▷ Likewise, we have added figures showing impostor distribution shifts across demographics to the report card.

2022-05-05 changes since 2022-03-18:

- ▷ We have added results for first algorithms from seven developers: Accurascan, DICIO, FacePhi, Pangiam, University of Surrey-CVSSP, and Veridium.
- ▷ We have added results for new algorithms from sixteen returning developers: ACI Software, Canon Inc, Cloudwalk - Moontime Smart Technology, Cybercore,

2022-05-05 changes since 2022-03-18:

- ▷ We have added results for first algorithms from seven developers: Accurascan, DICIO, FacePhi, Pangiam, University of Surrey-CVSSP, and Veridium.
- ▷ We have added results for new algorithms from sixteen returning developers: ACI Software, Canon Inc, Cloudwalk - Moontime Smart Technology, Cybercore, Cyberextruder, Gemalto Cogent, HyperVerge Inc, KuKe3D Technology, Megvii/Face++, Mobbeel Solutions, Panasonic R+D Center Singapore, Qnap Security, Samsung-SDS, Vietnam Posts and Telecommunications Group, Viettel Group, and Vision Intelligence Center of Meituan.
- ▷ We have retired results for 12 algorithms per our policy to only list results for two algorithms per developer. Results for retired algorithms appear in prior versions of this report in the [archive](#).

2022-03-18 changes since 2022-02-23:

- ▷ We have added support for the detection of multiple people in a single image (see Section 1.2). Specifically the API allows an algorithm to extract features from one or more faces it detects in an image. NIST scores such cases as a correct match when any detected face matches the reference photo, and as a false positive when either face matches a non-mated reference photo. The expected effect of doing this will be to improve reported false non-match rates, and to minimally elevate false match rates. This technique was only applied to images of type “border” and “kiosk”.
- ▷ We have added results for first algorithms from four developers: IntelliVIX, Kasikorn Labs, Lebentech Biometrics, and Wicket.
- ▷ We have added results for new algorithms from 10 returning developers: Chunghwa Telecom, Cloudmatrix, Beijing DeepSense Technologies, FarBar Inc, Imagus Technology Pty, Intellivision, Maxvision Technology, NHN Corp, Seventh Sense Artificial Intelligence, and Verigram.
- ▷ We have retired results for 4 algorithms per our policy to only list results for two algorithms per developer. Results for retired algorithms appear in prior versions of this report in the [archive](#).

2022-02-23 changes since 2022-01-24:

- ▷ We have added results for first algorithms from four developers: AFIS and Biometrics Consulting, Digi-data, Graymatics, Hangzhuo Allu Network Information Technology, KnowUTech LLC, Sukshi Technology Innovation, T4iSB, and TuringTech.vip
- ▷ We have added results for new algorithms from 18 returning developers: Cognitec Systems GmbH, GeoVision Inc, Glory, Herta Security, Intel Research Group, InsightFace AI, Kakao Enterprise, N-Tech Lab, Omnidarde Ltd, Papilon Savunma, Paravision, Realnetworks Inc, Reveal Media Ltd, Shenzhen Inst Adv Integrated Tech CAS, Suprema AI Inc, Toshiba, Universidade de Coimbra, and Yuan High-Tech Development
- ▷ We have retired results for 14 algorithms per our policy to only list results for two algorithms per developer. Results for retired algorithms appear in prior versions of this report in the [archive](#).

2022-01-24 changes since 2022-01-20:

- ▷ We have added results for new algorithms from one returning developer: Vocord.

2022-01-20 changes since 2021-12-18:

- ▷ We have added results for first algorithms from four developers: Armatura, Beyne.AI, One More Security, and VinBigData
- ▷ We have added results for new algorithms from 19 returning developers: AuthenMetric, BOE Technology Group, Cybercore, Cyberlink, Dahua Technology, FaceTag Co, Innovatrics, Megvii, Mobbeel Solutions, Neurotechnology, Oz Forensics, Rank One Computing, Regula Forensics, Samsung S1, Securif AI, Sensetime Group, TigerIT Americas, Videmo Intelligente Videoanalyse, and YooniK.
- ▷ We have retired results for 14 algorithms per our policy to only list results for two algorithms per developer. Results for retired algorithms appear in prior versions of this report in the [archive](#).

: 2021-12-16 changes since 2021-11-22:

- ▷ We have added results for first algorithms from five developers: Alfabeta, Cloudmatrix, Euronovate SA, FaceOnLive Inc, and Mobicin Technology.

- ▷ We have added results for new algorithms from ten returning developers: ACI Software, ITMO University, NEO Systems, Guangzhou Pixel Solutions, Panasonic R+D Center Singapore, Qnap Security, Scanovate, Tevian, Unissey, and Vietnam Posts and Telecommunications Group.
- ▷ We have retired results for eight algorithms per our policy to only list results for two algorithms per developer. Results for retired algorithms appear in prior versions of this report in the [archive](#).
- ▷ We have revamped the figure showing performance on 20 pairs of open-source images. It now color-codes false negatives and positives against a default threshold value.

2021-11-22 changes since 2021-10-28:

- ▷ We have added results to the [website](#) for kiosk-collected images where the design and geometry configuration mean that many images have considerable downward pitch angle. In some images, the face is partially cropped. Some images have other background faces.
- ▷ We have stopped using child exploitation images in FRVT, as we lost access to the imagery. All results for that set have been removed from the [website](#), and will be removed from future PDF reports.
- ▷ We have added results for first algorithms from seven new developers: CUDO Communication, Daon, KuKe3D Technology, Mantra Softtech India, Maxvision Technology, Multi-Modality Intelligence, and Samsung-SDS.
- ▷ We have added results for new algorithms from seven returning developers: Acer Incorporated, Cloudwalk-Moontime Smart Technology, Gorilla Technology, ID3 Technology, Incode Technologies, NSENSE Corp., and SQIssoft.
- ▷ We have retired results for six algorithms per our policy to only list results for two algorithms per developer. Results for retired algorithms appear in prior versions of this report in the [archive](#).

2021-10-28 changes since 2021-09-08:

- ▷ We have substantially revised the algorithm-specific report cards that are linked from the [FRVT results page](#). (Example: [HTML](#)).
- ▷ We have added results for first algorithms from eight new developers: Beijing Mendaxia Technology, Beijing Hisign Technology, Biocube Matrics, Clearview AI, Reveal Media, Toppan ID Gate, Verigram, and Viettel High Technology.
- ▷ We have added results for new algorithms from thirty returning developers: 20Face, 3divi, Canon Inc Chunghwa Telecom, Corsight, Decatur Industries, Deepglint, Dermalog, FaceTag, Fiberhome Telecommunication Technologies, GeoVision, ICM Airport Technics, Imagus Technology, InsightFace AI, Kakao Enterprise, Kookmin University, Line Corporation, N-Tech Lab, NotionTag Technologies, Realnetworks, Suprema ID, Taiwan-Certificate Authority, Toshiba, Tripleize, Trueface.ai, Veridas Digital Authentication, Visidon, VisionLabs, YooniK, and Yuan High-Tech Development.
- ▷ We have retired results for twenty algorithms per our policy to only list results for two algorithms per developer. Results for retired algorithms appear in prior versions of this report in the [archive](#).

2021-09-08 changes since 2021-08-02:

- ▷ We have added results for first algorithms from seven new developers: Griaule, SQIssoft, Qnap Security, Techsign, Smart Engines, Verihubs, and Wuhan Tianyu Information Industry.

- ▷ We have added results for new algorithms from sixteen returning developers: ADVANCE.AI, AuthenMetric, CloudSmart Consulting, Code Everest Pvt, Cognitec Systems, Thales Gemalto Cogent, Intel Research Group, Omnidarde, Oz Forensics, Rank One Computing, Samsung S1 Corp, Securif AI, Tevian, TigerIT Americas, Universidade de Coimbra, and Vigilant Solutions
- ▷ We have retired results for eleven algorithms per our policy to only list results for two algorithms per developer. Results for retired algorithms appear in prior versions of this report in the [archive](#).

2021-08-02 changes since 2021-06-25:

- ▷ We have added results for first algorithms from eight new developers: Bee the Data, Closeli Inc, Coretech Knowledge Inc, Deepsense (France), ioNetworks Inc, Kakao Pay Corp, Seventh Sense Artificial Intelligence, and SK Telecom.
- ▷ We have added results for new algorithms from fifteen returning developers: Alchera Inc, Adera Global PTE, Aware, Bresee Technology, Cyberlink Corp, Expasoft LLC, Fujitsu Research and Development Center, Gorilla Technology, Idemia, Neurotechnology, NEO Systems, NHN Corp, Paravision, Panasonic R+D Center Singapore, and Shenzhen University-Macau University of Science and Technology.
- ▷ We have retired results for twelve algorithms per our policy to only list results for two algorithms per developer. Results for retired algorithms appear in prior versions of this report in the [archive](#).

2021-06-25 changes since 2021-05-21:

- ▷ We have added results for first algorithms from six new developers: Alice Biometrics, BOE Technology Group, Fincore, Neosecu, Sodec App, and Yuntu Data and Technology.
- ▷ We have added results for new algorithms from seven returning developers: Incode Technologies, HyperVerge, Mobbeel Solutions, Guangzhou Pixel Solutions, Remark Holdings, Sensetime, and Vietnam Posts and Telecommunications Group.
- ▷ We have retired results for four algorithms per our policy to only list results for two algorithms per developer. Results for retired algorithms appear in prior versions of this report in the [archive](#).

2021-05-21 changes since 2021-04-26:

- ▷ We have added results for first algorithms from five new developers: Ekin Smart City Technologies, Suprema ID, Tripleize, Taiwan-Certificate Authority, and Vision Intelligence Center of Meituan.
- ▷ We have added results for new algorithms from eight returning developers: ID3 Technology, Imagus Technology, Momentum Digital, N-Tech Lab, NSENSE, Shanghai Jiao Tong University, Vision-Box, and Yuan High-Tech Development
- ▷ We have retired results for seven algorithms per our policy to only list results for two algorithms per developer. Results for retired algorithms appear in prior versions of this report in the [archive](#).

2021-04-26 changes since 2021-04-16:

- ▷ We have added results for first algorithms from three new developers: Quantasoft, Rendip, and NEO Systems.
- ▷ We have added results for new algorithms from four returning developers: 3Divi, Realnetworks, Veridas Digital Authentication Solutions, and Universidade de Coimbra.

- ▷ We have retired results for three algorithms per our policy to only list results for two algorithms per developer. Results for retired algorithms appear in prior versions of this report in the [archive](#).

2021-04-16 changes since 2021-03-19:

- ▷ We have added results for first algorithms from six new developers: 20Face, Beijing DeepSense Technologies, BitCenter UK, Enface, FaceTag, InsightFace AI, Line Corporation, Lema Labs, Nanjing Kiwi Network Technology, Omnidarde, Regula Forensics, and Suprema.
- ▷ We have added results for new algorithms from ten returning developers: CloudSmart Consulting, Dermalog, GeoVision, Neurotechnology, Panasonic R+D Center Singapore, Samsung S1, Securif AI, Trueface.ai, Vigilant Solutions, and Visidon.
- ▷ We have retired results for ten algorithms per our policy to only list results for two algorithms per developer. Results for retired algorithms appear in prior versions of this report in the [archive](#).

2021-03-19 changes since 2021-03-05:

- ▷ We have added results for first algorithms from six new developers: Ajou University, AuthenMetric, Code Everest, Corsight, Papilon Savunma, and NHN Corp
- ▷ We have added results for new algorithms from seven returning developers: Alchera, Deepglint, Fiber-home Telecommunication Technologies, Kakao Enterprise, Kookmin University, Megvii/Face++, and NotionTag Technologies.
- ▷ We have updated many of the hyperlinked HTML report-cards to include seven figures on demographic dependence. Figures of this kind first appeared, and are documented in, the December 2019 document, [NIST Interagency Report 8280](#) on demographic differentials in face recognition. The figures quantify false negative dependence on demographics using “visa-border” comparisons, and false positive dependence using comparisons of “application” photos that uniformly of quality and similar to visa photos.

2021-03-05 changes since 2021-01-19:

- ▷ We have added results for first algorithms from three new developers: IVA Cognitive, Mobbeel, and MoreDian Technology.
- ▷ We have added results for new algorithms from returning developers: Ability Enterprise - Andro Video, ACI Software, Adera Global, AnyVision, BioID Technologies, China Electronics Import-Export, Cognitec Systems, Fujitsu Research and Development Center, Glory, Guangzhou Pixel Solutions, Hengrui AI Technology, Incode Technologies, Intel Research, iQIYI, Mobai, Oz Forensics, Paravision, VisionLabs, and Xforward AI Technology.
- ▷ We have added a new “resources” tab to the main [webpage](#). It includes sortable columns for data related to speed, model size, storage, and memory consumption.
- ▷ We have retired results for 13 algorithms per our policy to only list results for two algorithms per developer. Results for retired algorithms appear in prior versions of this report in the [archive](#).

2021-01-19 changes since 2020-12-18:

- ▷ This report adds results for first algorithms from four developers: Herta Security, Irex AI, Shenzhen University-Macau University of Science and Technology, and Vietnam Posts and Telecommunications Group. See Table 7 for more information.
- ▷ The report also includes results for thirteen developers who have previously submitted algorithms: Bresee Technology, Canon (previously Canon Information Technology (Beijing)), Cyberlink, CSA IntelliCloud Technology, Dahua Technology, ID3 Technology, Imagus Technology (Vixvizon), Moontime Smart Technology, N-Tech Lab, Thales Cogent, Veridas Digital Authentication Solutions, Vocord, and Yuan High-Tech Development.
- ▷ We have retired results for ten algorithms per our policy to only list results for two algorithms per developer. Results for retired algorithms appear in prior versions of this report in the [archive](#).

2020-12-18 changes since 2020-10-09:

- ▷ This report adds results for first algorithms from ten developers: BitCenter UK, CloudSmart Consulting, Cubox, Institute of Computing Technology, Naver Corp, Minivision, NSENSE Corp, Viettel Group, Visage Technologies, and Xiamen University. See Table 7 for more information.
- ▷ The report also includes results for eighteen developers who have previously submitted algorithms: ADVANCE.AI, Awudit Systems, Chosun University, Dermalog, GeoVision, ICM Airport Technics, Idemia, Institute of Information Technologies, Kakao Enterprise, Neurotechnology, Panasonic R+D Center Singapore, Rank One Computing, Sensetime Group, Shanghai Jiao Tong University, TigerIT Americas LLC, Vigilant Solutions, Winsense, and YooniK
- ▷ We have retired results for twelve algorithms per our policy to only list results for two algorithms per developer. Results for retired algorithms appear in prior versions of this report in the [archive](#).

Changes since September 18, 2020:

- ▷ This report adds results for first algorithms from five developers: Aigen, Cortica, Kookmin University, Securif AI and Vinai.
- ▷ The report also includes results for three developers who have previously submitted algorithms: Fujitsu Laboratories, Hengrui AI, and X-Forward AI.
- ▷ In the per-algorithm report-cards linked from tables and the main webpage, we have added a chart to showing reduction in error rates over the course of FRVT i.e. from 2017 onwards for all algorithms supplied by that developer. Similarly we have added a chart showing error rate reductions for our test of protective face mask verification.
- ▷ We plan to continue evaluating algorithms on various mask datasets. We hold that algorithms should be capable of detecting masks and verifying identity of all combinations of masked and unmasked faces. We have accordingly increased the amount of time allowed to extract those features from 1.0 to 1.5 seconds.

Changes since August 25, 2020:

- ▷ This report adds results for first algorithms from eight new developers. Akurat Satu Indonesia, Cybercore, Decatur Industries, Innef Labs, Satellite Innovation/Eocortex, Expasoft, and Mobai.
- ▷ The report includes results for seven developers who have previously submitted algorithms: 3Divi, BioID Technologies, Incode Technologies, Innovatrics, iSAP Solution, Synology, and Tevian.

- ▷ We have retired results for five algorithms per our policy to only list results for two algorithms per developer. Results for retired algorithms appear in prior versions of this report in the [archive](#).

Changes since July 27, 2020:

- ▷ We have introduced per-algorithm report sheets. These are HTML documents linked from the accuracy tables in this report (i.e. Table 29) and on the FRVT 1:1 [homepage](#). The sheets contain interactive graphics allowing, for example, mouseover exploration of FNMR(T) and FMR(T). Some of their content had previously appeared in this document.
- ▷ This report adds results for algorithms from six new developers. ACI Software, Bresee Technology, Fiberhome Telecommunication Technologies, Imageware Systems, Oz Forensics, and Pensees.
- ▷ The report includes results for thirteen developers who have previously submitted algorithms: Canon Information Technology (Beijing), Cyberlink, Dahua Technology, Gorilla Technology, ID3 Technology, Intel Research Group, iQIYI Inc, Momentum Digital, Netbridge Technology, Tech5 SA, Shenzhen AiMall Tech, Vigilant Solutions, and VisionLabs.
- ▷ We have retired results for nine algorithms per our policy to only list results for two algorithms per developer. Results for retired algorithms appear in prior versions of this report in the [archive](#).

Changes since May 18, 2020:

- ▷ The report is the first FRVT update since the pandemic closed it from March to June 2020.
- ▷ This report includes results for algorithms from nine new developers: GeoVision Inc, Su Zhou NaZhi-TianDi Intelligent Technology, YooniK, AYF Technology, PXL Vision AG, Yuan High-Tech Development, Beihang University-ERCACAT, ICM Airport Technics, and Staqu Technologies
- ▷ This report includes results for algorithms from 15 returning developers Acer Incorporated, Antheus Technologia, Chosun University, Chunghwa Telecom, Idemia, Moontime Smart Technology, Neurotechnology, Guangzhou Pixel Solutions, Panasonic R+D Center Singapore, Rank One Computing, Scanovate, Shanghai Universiy - Shanghai Film Academy, Synesis, Trueface.ai, and Veridas Digital Authentication Solutions
- ▷ We have retired results for ten algorithms per our policy to only list results for two algorithms per developer. Results for retired algorithms appear in prior versions of this report in the [archive](#).
- ▷ We separated timing and other resource consumption from the main participation table. The new Table 18 includes template generation durations for four kinds of images, not just mugshots.
- ▷ We have published a separate report, [NIST Interagency Report 8311](#) on accuracy of pre-pandemic algorithms on subjects wearing face masks. We plan to track improvements in accuracy on masked images going forward. In particular, we invite submission of algorithms that can detect whether a person is wearing a mask, extract features from the full face or the exposed periocular region, and do appropriate comparison. We do not intend to evaluate algorithms that assume 100% of images will be of masked individuals.

Changes since March 25, 2020:

- ▷ The report is a maintenance release - it does not add any new algorithms, and FRVT has been closed to new algorithms since mid March 2020.
- ▷ We modified the primary accuracy summary, Table 29, as follows:

- ▷▷ For visa images, the column for FNMR at FMR = 0.0001 has been removed. The visa images are so highly controlled that the error rates for the most accurate algorithms are dominated by false rejection of very young children and by the presence of a few noisy greyscale images. For now, two visa columns remain: FNMR at $FMR = 10^{-6}$ and, for matched covariates, FNMR at $FMR = 10^{-4}$.
- ▷▷ We have inserted a new column labelled “BORDER” giving accuracy for comparison of moderately poor webcam border-crossing photos that exhibit pose variations, poor compression, and low contrast due to strong background illumination. The accuracies are the worst from all cooperative image datasets used in FRVT.
- ▷ Accordingly, we updated the failure-to-template rates in Table 38.
- ▷ We withdrew a figure showing how false matches are concentrated in certain visa images used in cross-comparison, because it didn’t attempt to include demographic information.

Changes since February 27, 2020:

- ▷ The report adds results algorithms from two new developers: Beijing Alleyes Technology, and the Chinese University of Hong Kong. Results for newly submitted algorithms from two other developers will appear in the next report.
- ▷ The report adds results for algorithms from thirteen returning developers: ASUSTek Computer, Aware, Cyberlink Corp, Gorilla Technology, Innovative Technology, Kakao Enterprise, Lomonosov Moscow State University, Panasonic R+D Center Singapore, Shenzhen AiMall Technology, Shenzhen Intellifusion Technologies, Synology, Tech5 SA, and Via Technologies.
- ▷ Per policy to only list results for two algorithms per developer, we have dropped results for algorithms from Aware, Cyberlink, Gorilla Technology, Kakao Enterprise, Lomonosov Moscow State University, Panasonic R+D Center Singapore, and Tech5 SA.

Changes since January 20, 2020:

- ▷ The report adds results for five new developers: Ability Enterprise (Andro Video), Chosun University, Fujitsu Research and Development Center, University of Coimbra, and Xforward AI Technology.
- ▷ The report adds results for algorithms from six returning developers: AlphaSSTG, Incode Technologies, Kneron, Shanghai Jiao Tong University, Vocord, and X-Laboratory.
- ▷ We have corrected template comparison timing numbers for algorithms submitted September 2019 to January 2020. The values reported previously were slower due to a software bug.
- ▷ We have dropped results for algorithms from Vocord and Incode per policy to only list results for two algorithms per developer.
- ▷ The [FRVT 1:1 homepage](#) has been updated with latest accuracy results.
- ▷ The [FRVT 1:N homepage](#) now includes an update to the September 2019 NIST Interagency Report 8271. The new report adds results for one-to-many search algorithms submitted to NIST from June 2019 to January 2020.

Changes since January 6, 2020:

- ▷ Section 2 has been updated to better describe the Visa and Border images. The caption for Table 29 has been updated to better relate the accuracy values to particular image comparisons.

- ▷ The report adds results for five new developers: Acer, Advance.AI, Expasoft, Netbridge Technology, and Videmo Intelligent Videoanalyse.
- ▷ The report adds results for algorithms from 7 returning developers: China Electronics Import-Export Corp, Intel Research Group, ITMO University, Neurotechnology, N-Tech Lab, Rokid, and VisionLabs.
- ▷ We have dropped results from this edition of the report per policy to only list results for two algorithms per developer: N-Tech Lab, Neurotechnology, ITMO, Visionlabs, and CEIEC.
- ▷ The [FRVT homepage](#) has been updated with latest accuracy results.

Changes since November 11, 2019:

- ▷ Table 18 has been updated to include runtime memory usage. This is the first time such a quantity has been reported. The value is the peak size of the resident set size logged during enrollment of single images.
- ▷ We have migrated summary results table to a new platform that supports sortable tables:
<https://pages.nist.gov/frvt/html/frvt11.html>
- ▷ The report adds results for four new developers: Antheus Technologia, BioID Technologies SA, Canon Information Tech. (Beijing), Samsung S1 (listed in the tables as S1), and Taiwan AI Labs.
- ▷ The report adds results for algorithms from 13 returning developers: Anke Investments, Chunghwa Telecom, Deepglint, Institute of Information Technologies, iQIYI, Kneron, Ping An Technology, Paravision, KanKan Ai, Rokid Corporation, Shanghai Universiy - Shanghai Film Academy, Veridas Digital Authentication Solutions, and Videonetics Technology.
- ▷ We have dropped results from this edition of the report per policy to only list results for two algorithms per developer: remarkai-000, veridas-001, sensetime-001, iit-000, anke-003, and everai-002. Results for these are available in prior editions of this report linked from the FRVT page.
- ▷ We issued [NIST Interagency Report 8280: FRVT Part 3: Demographics](#) on 2019-12-19. It includes results for many of the algorithms covered by this report.

Changes since October 16, 2019:

- ▷ The report adds results for ten new developers: Ai-Union Technology, ASUSTek Computer, DiDi ChuXing Technology, Innovative Technology, Luxand, MVision, Pyramid Cyber Security + Forensic, Scanovate, Shenzhen AiMall Tech, and TUPU Technology.
- ▷ The report adds results for 12 returning developers: CTBC Bank Glory Gorilla Technology Guangzhou Pixel Solutions Imagus Technology Incode Technologies Lomonosov Moscow State University Rank One Computing Samtech InfoNet Shanghai Ulucu Electronics Technology Synesis, and Winsense.
- ▷ We have dropped results from this edition of the report per policy to only list results for two algorithms per developer: glory-000, gorilla-002, incode-003, rankone-006, and synesis-004.
- ▷ Results for five recently submitted algorithms will appear in the next report.

Changes since September 11, 2019:

- ▷ The report adds results for five new participants: Awidit Systems (Awiros), Momentum Digital (Sertis), Trueface AI, Shanghai Jiao Tong University, and X-Laboratory.

- ▷ The report adds results for five new algorithms from returning developers: Cyberlink, Hengrui AI Technology, Idemia, Panasonic R+D Singapore, and Tevian. This causes three algorithm, to be de-listed from the report per policy to list results for two algorithms per developer.

Changes since July 31 2019:

- ▷ The HTML table on the [FRVT 1:1 homepage](#) has been updated to include a column for cross-domain Visa-Border verification. Results for this new dataset appeared in the July 29 report under the name "CrossEV" - these are now renamed "Visa-Border".
- ▷ The [FRVT 1:1 homepage](#) lists algorithms according to lowest mean rank accuracy:

$$\begin{aligned} &\text{Rank(FNMR}_{\text{VISA}} \text{ at FMR = 0.000001}) + \\ &\text{Rank(FNMR}_{\text{VISA-BORDER}} \text{ at FMR = 0.000001}) + \\ &\text{Rank(FNMR}_{\text{MUGSHOT}} \text{ at FMR = 0.00001 after 14 years}) + \\ &\text{Rank(FNMR}_{\text{WILD}} \text{ at FMR = 0.00001}) \end{aligned}$$

This ordering rewards high accuracy across all datasets.
- ▷ The main results in Table 29 is now in landscape format to accomodate extra columns for the Visa-Border set, and mugshot comparisons after at least 12 years.
- ▷ The report adds results for nine new participants: Alpha SSTG, Intel Research, ULSee, Chungwa Telecon, iSAP Solution, Rokid, Shenzhen EI Networks, CSA Intellicloud, Shenzhen Intellifusion Technologies.
- ▷ The reports adds results for six new algorithms from returning developers: Innovatrics, Dahua Technology, Tech5 SA, Intellivision, Nodeflux and Imperial College, London. One algorithm, from Imperial has been retired, per policy to list results for two algorithms per developer.
- ▷ The cross-country false match rate heatmaps have been replotted to reveal more structure by listing countries by region instead of alphabetically.
- ▷ The next version of this report will be posted around October 18, 2019.

Changes since July 3 2019:

- ▷ The HTML table on the [FRVT 1:1 homepage](#) has been updated to list the 20 most accurate developers rather than algorithms, choosing the most accurate algorithm from each developer based on visa and mugshot results. Also, the algorithms are ordered in terms of lowest mean rank across mugshot, visa and wild datasets, rewarding broad accuracy over a good result on one particular dataset.
- ▷ This report includes results for a new dataset - see the column labelled "visa-border" in Table 5. It compares a new set of high quality visa-like portraits with a set webcam border-crossing photos that exhibit moderately poor pose variations and background illumination. The two new sets are described in sections 2.2 and 2.4. The comparisons are "cross-domain" in that the algorithm must compare "visa" and "wild" images. Results for other algorithms will be added in future reports as they become available.
- ▷ This report adds results for algorithms from 9 developers submitted in early July 2019. These are from 3DiVi, Camvi, EverAI-Paravision, Facesoft, Farbar (F8), Institute of Information Technologies, Shanghai U. Film Academy, Via Technologies, and Ulucu Electronics Tech. Six of these are new participants.
- ▷ Several other algorithms have been submitted and are being evaluated. Results will be released in the next report, scheduled for September 5. That report will include results for new datasets.
- ▷ Older algorithms from Everai, Camvi and 3DiVi, have been retired, per the policy to list only two algorithms per developer.

Changes since June 20 2019:

- ▷ This report adds results for algorithms from 18 developers submitted in early June 2019. These are from CTBC Bank, Deep Glint, Thales Cogent, Ever AI Paravision, Gorilla Technology, Imagus, Incode, Kneron, N-Tech Lab, Neurotechnology, Notiontag Technologies, Star Hybrid, Videonetics, Vigilant Solutions, Winsense, Anke Investments, CEIEC, and DSK. Nine of these are new participants.

- ▷ Several other algorithms have been submitted and are being evaluated. Results will be released in the next report, scheduled for August 1.
- ▷ Older algorithms from Everai, Thales Cogent, Gorilla Technology, Incode, Neurotechnology, N-Tech Lab and Vigilant Solutions have been retired, per the policy to list only two algorithms per developer.

Changes since April 2019:

- ▷ This report adds results for nine algorithms from nine developers submitted in early June 2019. These are from Tencent Deepsea, Hengrui, Kedacom, Moontime, Guangzhou Pixel, Rank One Computing, Synesis, Sensetime and Vocord.
- ▷ Another 23 algorithms have been submitted and are being evaluated. Results will be released in the next report, scheduled for July 3.
- ▷ Older algorithms for Rank One, Synesis, and Vocord have been retired, per the policy to list only two algorithms per developer.

Changes since February 2019:

- ▷ This report adds results for 49 algorithms from 42 developers submitted in early March 2019.
- ▷ This report omits results for algorithms that we retired. We retired for three reasons: 1. The developer submitted a new algorithm, and we only list two. 2. The algorithm needs a GPU, and we no longer allow GPU-based algorithms. 3. Inoperable algorithms.
- ▷ Previous results for retired algorithms are available in older editions of this report linked [here](#).
- ▷ The mugshot database used from February 2017 to January 2019 has been replaced with an extract of the mugshot database documented in NIST Interagency Report 8238, November 2018. The new mugshot set is described in section [2.5](#) and is adopted because:
 - ▷▷ It has much better identity label integrity, so that false non-match rates are substantially lower than those reported in FRVT 1:1 reports to date - see Figure [114](#).
 - ▷▷ It includes images collected over a 17 year period such that ageing can be much better characterized - - see Figure [359](#).
- ▷ Using the new mugshot database, Figure [359](#) shows accuracy for four demographic groups identified in the biographic metadata that accompanies the data: black females, black males, white females and white males.
- ▷ The report added a figure (now moved to web) with results for the twenty human-difficult pairs used in the May 2018 paper [Face recognition accuracy of forensic examiners, superrecognizers, and face recognition algorithms](#) by Phillips et al. [1].
- ▷ The report uses an update to the wild image database that corrects some ground truth labels.
- ▷ Some results for the child exploitation database are not complete. They are typically updated less frequently than for other image sets.

Contents

ACKNOWLEDGMENTS	1
DISCLAIMER	1
INSTITUTIONAL REVIEW BOARD	1
1 METRICS	55
1.1 CORE ACCURACY	55
1.2 MULTI-TEMPLATE SCORING METHODOLOGY	55
2 DATASETS	56
2.1 VISA IMAGES	56
2.2 APPLICATION IMAGES	56
2.3 APPLICATION IMAGES WITH HEAD YAW	56
2.4 BORDER CROSSING IMAGES	57
2.5 MUGSHOT IMAGES	57
2.6 KIOSK IMAGES	57
2.7 WILD IMAGES	58
3 RESULTS	58
3.1 TEST GOALS	58
3.2 TEST DESIGN	59
3.3 FAILURE TO ENROLL	62
3.4 RECOGNITION ACCURACY	72
3.5 GENUINE DISTRIBUTION STABILITY	361
3.5.1 EFFECT OF BIRTH PLACE ON THE GENUINE DISTRIBUTION	361
3.5.2 EFFECT OF AGEING	401
3.5.3 EFFECT OF AGE ON GENUINE SUBJECTS	431
3.6 IMPOSTOR DISTRIBUTION STABILITY	472
3.6.1 EFFECT OF BIRTH PLACE ON THE IMPOSTOR DISTRIBUTION	472
3.6.2 EFFECT OF AGE ON IMPOSTORS	475

List of Tables

1 PARTICIPANT INFORMATION	24
2 PARTICIPANT INFORMATION	25
3 PARTICIPANT INFORMATION	26
4 PARTICIPANT INFORMATION	27
5 PARTICIPANT INFORMATION	28
6 PARTICIPANT INFORMATION	29
7 PARTICIPANT INFORMATION	30
8 ALGORITHM SUMMARY	31
9 ALGORITHM SUMMARY	32
10 ALGORITHM SUMMARY	33
11 ALGORITHM SUMMARY	34
12 ALGORITHM SUMMARY	35
13 ALGORITHM SUMMARY	36
14 ALGORITHM SUMMARY	37
15 ALGORITHM SUMMARY	38
16 ALGORITHM SUMMARY	39
17 ALGORITHM SUMMARY	40
18 ALGORITHM SUMMARY	41

19	FALSE NON-MATCH RATE	42
20	FALSE NON-MATCH RATE	43
21	FALSE NON-MATCH RATE	44
22	FALSE NON-MATCH RATE	45
23	FALSE NON-MATCH RATE	46
24	FALSE NON-MATCH RATE	47
25	FALSE NON-MATCH RATE	48
26	FALSE NON-MATCH RATE	49
27	FALSE NON-MATCH RATE	50
28	FALSE NON-MATCH RATE	51
29	FALSE NON-MATCH RATE	52
30	FAILURE TO ENROL RATES	63
31	FAILURE TO ENROL RATES	64
32	FAILURE TO ENROL RATES	65
33	FAILURE TO ENROL RATES	66
34	FAILURE TO ENROL RATES	67
35	FAILURE TO ENROL RATES	68
36	FAILURE TO ENROL RATES	69
37	FAILURE TO ENROL RATES	70
38	FAILURE TO ENROL RATES	71

List of Figures

1	PERFORMANCE SUMMARY: FNMR VS. TEMPLATE SIZE TRADEOFF	53
2	PERFORMANCE SUMMARY: FNMR VS. TEMPLATE TIME TRADEOFF	54
3	EXAMPLE IMAGES	58
	(A) VISA	58
	(B) MUGSHOT	58
	(C) WILD	58
	(D) BORDER	58
4	PERFORMANCE ON 20 HUMAN-DIFFICULT PAIRS	73
5	PERFORMANCE ON 20 HUMAN-DIFFICULT PAIRS	74
6	PERFORMANCE ON 20 HUMAN-DIFFICULT PAIRS	75
7	PERFORMANCE ON 20 HUMAN-DIFFICULT PAIRS	76
8	PERFORMANCE ON 20 HUMAN-DIFFICULT PAIRS	77
9	PERFORMANCE ON 20 HUMAN-DIFFICULT PAIRS	78
10	PERFORMANCE ON 20 HUMAN-DIFFICULT PAIRS	79
11	PERFORMANCE ON 20 HUMAN-DIFFICULT PAIRS	80
12	PERFORMANCE ON 20 HUMAN-DIFFICULT PAIRS	81
13	PERFORMANCE ON 20 HUMAN-DIFFICULT PAIRS	82
14	PERFORMANCE ON 20 HUMAN-DIFFICULT PAIRS	83
15	PERFORMANCE ON 20 HUMAN-DIFFICULT PAIRS	84
16	PERFORMANCE ON 20 HUMAN-DIFFICULT PAIRS	85
17	PERFORMANCE ON 20 HUMAN-DIFFICULT PAIRS	86
18	PERFORMANCE ON 20 HUMAN-DIFFICULT PAIRS	87
19	PERFORMANCE ON 20 HUMAN-DIFFICULT PAIRS	88
20	PERFORMANCE ON 20 HUMAN-DIFFICULT PAIRS	89
21	PERFORMANCE ON 20 HUMAN-DIFFICULT PAIRS	90
22	PERFORMANCE ON 20 HUMAN-DIFFICULT PAIRS	91
23	PERFORMANCE ON 20 HUMAN-DIFFICULT PAIRS	92
24	PERFORMANCE ON 20 HUMAN-DIFFICULT PAIRS	93
25	PERFORMANCE ON 20 HUMAN-DIFFICULT PAIRS	94
26	PERFORMANCE ON 20 HUMAN-DIFFICULT PAIRS	95
27	PERFORMANCE ON 20 HUMAN-DIFFICULT PAIRS	96
28	PERFORMANCE ON 20 HUMAN-DIFFICULT PAIRS	97

29	PERFORMANCE ON 20 HUMAN-DIFFICULT PAIRS	98
30	PERFORMANCE ON 20 HUMAN-DIFFICULT PAIRS	99
31	PERFORMANCE ON 20 HUMAN-DIFFICULT PAIRS	100
32	PERFORMANCE ON 20 HUMAN-DIFFICULT PAIRS	101
33	PERFORMANCE ON 20 HUMAN-DIFFICULT PAIRS	102
34	PERFORMANCE ON 20 HUMAN-DIFFICULT PAIRS	103
35	PERFORMANCE ON 20 HUMAN-DIFFICULT PAIRS	104
36	PERFORMANCE ON 20 HUMAN-DIFFICULT PAIRS	105
37	PERFORMANCE ON 20 HUMAN-DIFFICULT PAIRS	106
38	PERFORMANCE ON 20 HUMAN-DIFFICULT PAIRS	107
39	PERFORMANCE ON 20 HUMAN-DIFFICULT PAIRS	108
40	PERFORMANCE ON 20 HUMAN-DIFFICULT PAIRS	109
41	PERFORMANCE ON 20 HUMAN-DIFFICULT PAIRS	110
42	PERFORMANCE ON 20 HUMAN-DIFFICULT PAIRS	111
43	PERFORMANCE ON 20 HUMAN-DIFFICULT PAIRS	112
44	ERROR TRADEOFF CHARACTERISTIC: VISA IMAGES	113
45	ERROR TRADEOFF CHARACTERISTIC: VISA IMAGES	114
46	ERROR TRADEOFF CHARACTERISTIC: VISA IMAGES	115
47	ERROR TRADEOFF CHARACTERISTIC: VISA IMAGES	116
48	ERROR TRADEOFF CHARACTERISTIC: VISA IMAGES	117
49	ERROR TRADEOFF CHARACTERISTIC: VISA IMAGES	118
50	ERROR TRADEOFF CHARACTERISTIC: VISA IMAGES	119
51	ERROR TRADEOFF CHARACTERISTIC: VISA IMAGES	120
52	ERROR TRADEOFF CHARACTERISTIC: VISA IMAGES	121
53	ERROR TRADEOFF CHARACTERISTIC: VISA IMAGES	122
54	ERROR TRADEOFF CHARACTERISTIC: VISA IMAGES	123
55	ERROR TRADEOFF CHARACTERISTIC: VISA IMAGES	124
56	ERROR TRADEOFF CHARACTERISTIC: VISA IMAGES	125
57	ERROR TRADEOFF CHARACTERISTIC: VISA IMAGES	126
58	ERROR TRADEOFF CHARACTERISTIC: VISA IMAGES	127
59	ERROR TRADEOFF CHARACTERISTIC: VISA IMAGES	128
60	ERROR TRADEOFF CHARACTERISTIC: VISA IMAGES	129
61	ERROR TRADEOFF CHARACTERISTIC: VISA IMAGES	130
62	ERROR TRADEOFF CHARACTERISTIC: VISA IMAGES	131
63	ERROR TRADEOFF CHARACTERISTIC: VISA IMAGES	132
64	ERROR TRADEOFF CHARACTERISTIC: VISA IMAGES	133
65	ERROR TRADEOFF CHARACTERISTIC: VISA IMAGES	134
66	ERROR TRADEOFF CHARACTERISTIC: VISA IMAGES	135
67	ERROR TRADEOFF CHARACTERISTIC: VISA IMAGES	136
68	ERROR TRADEOFF CHARACTERISTIC: VISA IMAGES	137
69	ERROR TRADEOFF CHARACTERISTIC: VISA IMAGES	138
70	ERROR TRADEOFF CHARACTERISTIC: VISA IMAGES	139
71	ERROR TRADEOFF CHARACTERISTIC: VISA IMAGES	140
72	ERROR TRADEOFF CHARACTERISTIC: VISA IMAGES	141
73	ERROR TRADEOFF CHARACTERISTIC: VISA IMAGES	142
74	ERROR TRADEOFF CHARACTERISTIC: VISA IMAGES	143
75	ERROR TRADEOFF CHARACTERISTIC: VISA IMAGES	144
76	ERROR TRADEOFF CHARACTERISTIC: VISA IMAGES	145
77	ERROR TRADEOFF CHARACTERISTIC: VISA IMAGES	146
78	ERROR TRADEOFF CHARACTERISTIC: VISA IMAGES	147
79	ERROR TRADEOFF CHARACTERISTIC: VISA IMAGES	148
80	ERROR TRADEOFF CHARACTERISTIC: VISA IMAGES	149
81	ERROR TRADEOFF CHARACTERISTIC: VISA IMAGES	150
82	ERROR TRADEOFF CHARACTERISTIC: VISA IMAGES	151
83	ERROR TRADEOFF CHARACTERISTIC: VISA IMAGES	152
84	ERROR TRADEOFF CHARACTERISTIC: VISA IMAGES	153

85	ERROR TRADEOFF CHARACTERISTIC: VISA IMAGES	154
86	ERROR TRADEOFF CHARACTERISTIC: VISA IMAGES	155
87	ERROR TRADEOFF CHARACTERISTIC: VISA IMAGES	156
88	ERROR TRADEOFF CHARACTERISTIC: VISA IMAGES	157
89	ERROR TRADEOFF CHARACTERISTIC: VISA IMAGES	158
90	ERROR TRADEOFF CHARACTERISTIC: VISA IMAGES	159
91	ERROR TRADEOFF CHARACTERISTIC: MUGSHOT IMAGES	160
92	ERROR TRADEOFF CHARACTERISTIC: MUGSHOT IMAGES	161
93	ERROR TRADEOFF CHARACTERISTIC: MUGSHOT IMAGES	162
94	ERROR TRADEOFF CHARACTERISTIC: MUGSHOT IMAGES	163
95	ERROR TRADEOFF CHARACTERISTIC: MUGSHOT IMAGES	164
96	ERROR TRADEOFF CHARACTERISTIC: MUGSHOT IMAGES	165
97	ERROR TRADEOFF CHARACTERISTIC: MUGSHOT IMAGES	166
98	ERROR TRADEOFF CHARACTERISTIC: MUGSHOT IMAGES	167
99	ERROR TRADEOFF CHARACTERISTIC: MUGSHOT IMAGES	168
100	ERROR TRADEOFF CHARACTERISTIC: MUGSHOT IMAGES	169
101	ERROR TRADEOFF CHARACTERISTIC: MUGSHOT IMAGES	170
102	ERROR TRADEOFF CHARACTERISTIC: MUGSHOT IMAGES	171
103	ERROR TRADEOFF CHARACTERISTIC: MUGSHOT IMAGES	172
104	ERROR TRADEOFF CHARACTERISTIC: MUGSHOT IMAGES	173
105	ERROR TRADEOFF CHARACTERISTIC: MUGSHOT IMAGES	174
106	ERROR TRADEOFF CHARACTERISTIC: MUGSHOT IMAGES	175
107	ERROR TRADEOFF CHARACTERISTIC: MUGSHOT IMAGES	176
108	ERROR TRADEOFF CHARACTERISTIC: MUGSHOT IMAGES	177
109	ERROR TRADEOFF CHARACTERISTIC: MUGSHOT IMAGES	178
110	ERROR TRADEOFF CHARACTERISTIC: MUGSHOT IMAGES	179
111	ERROR TRADEOFF CHARACTERISTIC: MUGSHOT IMAGES	180
112	ERROR TRADEOFF CHARACTERISTIC: MUGSHOT IMAGES	181
113	ERROR TRADEOFF CHARACTERISTIC: MUGSHOT IMAGES	182
114	ERROR TRADEOFF CHARACTERISTIC: MUGSHOT IMAGES	183
115	ERROR TRADEOFF CHARACTERISTIC: WILD IMAGES	184
116	ERROR TRADEOFF CHARACTERISTIC: WILD IMAGES	185
117	ERROR TRADEOFF CHARACTERISTIC: WILD IMAGES	186
118	ERROR TRADEOFF CHARACTERISTIC: WILD IMAGES	187
119	ERROR TRADEOFF CHARACTERISTIC: WILD IMAGES	188
120	ERROR TRADEOFF CHARACTERISTIC: WILD IMAGES	189
121	ERROR TRADEOFF CHARACTERISTIC: WILD IMAGES	190
122	ERROR TRADEOFF CHARACTERISTIC: WILD IMAGES	191
123	ERROR TRADEOFF CHARACTERISTIC: WILD IMAGES	192
124	ERROR TRADEOFF CHARACTERISTIC: WILD IMAGES	193
125	ERROR TRADEOFF CHARACTERISTIC: WILD IMAGES	194
126	ERROR TRADEOFF CHARACTERISTIC: WILD IMAGES	195
127	ERROR TRADEOFF CHARACTERISTIC: WILD IMAGES	196
128	ERROR TRADEOFF CHARACTERISTIC: WILD IMAGES	197
129	ERROR TRADEOFF CHARACTERISTIC: WILD IMAGES	198
130	ERROR TRADEOFF CHARACTERISTIC: WILD IMAGES	199
131	ERROR TRADEOFF CHARACTERISTIC: WILD IMAGES	200
132	ERROR TRADEOFF CHARACTERISTIC: WILD IMAGES	201
133	ERROR TRADEOFF CHARACTERISTIC: WILD IMAGES	202
134	ERROR TRADEOFF CHARACTERISTIC: WILD IMAGES	203
135	FALSE MATCH RATES WITHIN AND ACROSS DEMOGRAPHIC GROUPS	204
136	FALSE MATCH RATES WITHIN AND ACROSS DEMOGRAPHIC GROUPS	205
137	FALSE MATCH RATES WITHIN AND ACROSS DEMOGRAPHIC GROUPS	206
138	FALSE MATCH RATES WITHIN AND ACROSS DEMOGRAPHIC GROUPS	207
139	FALSE MATCH RATES WITHIN AND ACROSS DEMOGRAPHIC GROUPS	208
140	FALSE MATCH RATES WITHIN AND ACROSS DEMOGRAPHIC GROUPS	209
141	FALSE MATCH RATES WITHIN AND ACROSS DEMOGRAPHIC GROUPS	210

142	FALSE MATCH RATES WITHIN AND ACROSS DEMOGRAPHIC GROUPS	211
143	FALSE MATCH RATES WITHIN AND ACROSS DEMOGRAPHIC GROUPS	212
144	FALSE MATCH RATES WITHIN AND ACROSS DEMOGRAPHIC GROUPS	213
145	FALSE MATCH RATES WITHIN AND ACROSS DEMOGRAPHIC GROUPS	214
146	FALSE MATCH RATES WITHIN AND ACROSS DEMOGRAPHIC GROUPS	215
147	FALSE MATCH RATES WITHIN AND ACROSS DEMOGRAPHIC GROUPS	216
148	FALSE MATCH RATES WITHIN AND ACROSS DEMOGRAPHIC GROUPS	217
149	FALSE MATCH RATES WITHIN AND ACROSS DEMOGRAPHIC GROUPS	218
150	FALSE MATCH RATES WITHIN AND ACROSS DEMOGRAPHIC GROUPS	219
151	FALSE MATCH RATES WITHIN AND ACROSS DEMOGRAPHIC GROUPS	220
152	FALSE MATCH RATES WITHIN AND ACROSS DEMOGRAPHIC GROUPS	221
153	FALSE MATCH RATES WITHIN AND ACROSS DEMOGRAPHIC GROUPS	222
154	FALSE MATCH RATES WITHIN AND ACROSS DEMOGRAPHIC GROUPS	223
155	FALSE MATCH RATES WITHIN AND ACROSS DEMOGRAPHIC GROUPS	224
156	FALSE MATCH RATES WITHIN AND ACROSS DEMOGRAPHIC GROUPS	225
157	SEX AND RACE EFFECTS: MUGSHOT IMAGES	226
158	SEX AND RACE EFFECTS: MUGSHOT IMAGES	227
159	SEX AND RACE EFFECTS: MUGSHOT IMAGES	228
160	SEX AND RACE EFFECTS: MUGSHOT IMAGES	229
161	SEX AND RACE EFFECTS: MUGSHOT IMAGES	230
162	SEX AND RACE EFFECTS: MUGSHOT IMAGES	231
163	SEX AND RACE EFFECTS: MUGSHOT IMAGES	232
164	SEX AND RACE EFFECTS: MUGSHOT IMAGES	233
165	SEX AND RACE EFFECTS: MUGSHOT IMAGES	234
166	SEX AND RACE EFFECTS: MUGSHOT IMAGES	235
167	SEX AND RACE EFFECTS: MUGSHOT IMAGES	236
168	SEX AND RACE EFFECTS: MUGSHOT IMAGES	237
169	SEX AND RACE EFFECTS: MUGSHOT IMAGES	238
170	SEX AND RACE EFFECTS: MUGSHOT IMAGES	239
171	SEX AND RACE EFFECTS: MUGSHOT IMAGES	240
172	SEX AND RACE EFFECTS: MUGSHOT IMAGES	241
173	SEX AND RACE EFFECTS: MUGSHOT IMAGES	242
174	SEX AND RACE EFFECTS: MUGSHOT IMAGES	243
175	SEX AND RACE EFFECTS: MUGSHOT IMAGES	244
176	SEX AND RACE EFFECTS: MUGSHOT IMAGES	245
177	SEX AND RACE EFFECTS: MUGSHOT IMAGES	246
178	SEX AND RACE EFFECTS: MUGSHOT IMAGES	247
179	SEX AND RACE EFFECTS: MUGSHOT IMAGES	248
180	SEX AND RACE EFFECTS: MUGSHOT IMAGES	249
181	SEX EFFECTS: VISA IMAGES	250
182	SEX EFFECTS: VISA IMAGES	251
183	SEX EFFECTS: VISA IMAGES	252
184	SEX EFFECTS: VISA IMAGES	253
185	SEX EFFECTS: VISA IMAGES	254
186	SEX EFFECTS: VISA IMAGES	255
187	SEX EFFECTS: VISA IMAGES	256
188	SEX EFFECTS: VISA IMAGES	257
189	SEX EFFECTS: VISA IMAGES	258
190	SEX EFFECTS: VISA IMAGES	259
191	SEX EFFECTS: VISA IMAGES	260
192	SEX EFFECTS: VISA IMAGES	261
193	SEX EFFECTS: VISA IMAGES	262
194	SEX EFFECTS: VISA IMAGES	263
195	SEX EFFECTS: VISA IMAGES	264
196	SEX EFFECTS: VISA IMAGES	265
197	SEX EFFECTS: VISA IMAGES	266
198	SEX EFFECTS: VISA IMAGES	267

199	SEX EFFECTS: VISA IMAGES	268
200	SEX EFFECTS: VISA IMAGES	269
201	SEX EFFECTS: VISA IMAGES	270
202	SEX EFFECTS: VISA IMAGES	271
203	SEX EFFECTS: VISA IMAGES	272
204	SEX EFFECTS: VISA IMAGES	273
205	SEX EFFECTS: VISA IMAGES	274
206	SEX EFFECTS: VISA IMAGES	275
207	SEX EFFECTS: VISA IMAGES	276
208	SEX EFFECTS: VISA IMAGES	277
209	SEX EFFECTS: VISA IMAGES	278
210	SEX EFFECTS: VISA IMAGES	279
211	SEX EFFECTS: VISA IMAGES	280
212	SEX EFFECTS: VISA IMAGES	281
213	SEX EFFECTS: VISA IMAGES	282
214	SEX EFFECTS: VISA IMAGES	283
215	SEX EFFECTS: VISA IMAGES	284
216	SEX EFFECTS: VISA IMAGES	285
217	SEX EFFECTS: VISA IMAGES	286
218	SEX EFFECTS: VISA IMAGES	287
219	SEX EFFECTS: VISA IMAGES	288
220	FALSE MATCH RATE CALIBRATION: MUGSHOT IMAGES	289
221	FALSE MATCH RATE CALIBRATION: MUGSHOT IMAGES	290
222	FALSE MATCH RATE CALIBRATION: MUGSHOT IMAGES	291
223	FALSE MATCH RATE CALIBRATION: MUGSHOT IMAGES	292
224	FALSE MATCH RATE CALIBRATION: MUGSHOT IMAGES	293
225	FALSE MATCH RATE CALIBRATION: MUGSHOT IMAGES	294
226	FALSE MATCH RATE CALIBRATION: MUGSHOT IMAGES	295
227	FALSE MATCH RATE CALIBRATION: MUGSHOT IMAGES	296
228	FALSE MATCH RATE CALIBRATION: MUGSHOT IMAGES	297
229	FALSE MATCH RATE CALIBRATION: MUGSHOT IMAGES	298
230	FALSE MATCH RATE CALIBRATION: MUGSHOT IMAGES	299
231	FALSE MATCH RATE CALIBRATION: MUGSHOT IMAGES	300
232	FALSE MATCH RATE CALIBRATION: MUGSHOT IMAGES	301
233	FALSE MATCH RATE CALIBRATION: MUGSHOT IMAGES	302
234	FALSE MATCH RATE CALIBRATION: MUGSHOT IMAGES	303
235	FALSE MATCH RATE CALIBRATION: MUGSHOT IMAGES	304
236	FALSE MATCH RATE CALIBRATION: MUGSHOT IMAGES	305
237	FALSE MATCH RATE CALIBRATION: MUGSHOT IMAGES	306
238	FALSE MATCH RATE CALIBRATION: MUGSHOT IMAGES	307
239	FALSE MATCH RATE CALIBRATION: MUGSHOT IMAGES	308
240	FALSE MATCH RATE CALIBRATION: MUGSHOT IMAGES	309
241	FALSE MATCH RATE CALIBRATION: MUGSHOT IMAGES	310
242	FALSE MATCH RATE CALIBRATION: MUGSHOT IMAGES	311
243	FALSE MATCH RATE CALIBRATION: MUGSHOT IMAGES	312
244	FALSE MATCH RATE CALIBRATION: VISA IMAGES	313
245	FALSE MATCH RATE CALIBRATION: VISA IMAGES	314
246	FALSE MATCH RATE CALIBRATION: VISA IMAGES	315
247	FALSE MATCH RATE CALIBRATION: VISA IMAGES	316
248	FALSE MATCH RATE CALIBRATION: VISA IMAGES	317
249	FALSE MATCH RATE CALIBRATION: VISA IMAGES	318
250	FALSE MATCH RATE CALIBRATION: VISA IMAGES	319
251	FALSE MATCH RATE CALIBRATION: VISA IMAGES	320
252	FALSE MATCH RATE CALIBRATION: VISA IMAGES	321
253	FALSE MATCH RATE CALIBRATION: VISA IMAGES	322
254	FALSE MATCH RATE CALIBRATION: VISA IMAGES	323
255	FALSE MATCH RATE CALIBRATION: VISA IMAGES	324

256	FALSE MATCH RATE CALIBRATION: VISA IMAGES	325
257	FALSE MATCH RATE CALIBRATION: VISA IMAGES	326
258	FALSE MATCH RATE CALIBRATION: VISA IMAGES	327
259	FALSE MATCH RATE CALIBRATION: VISA IMAGES	328
260	FALSE MATCH RATE CALIBRATION: VISA IMAGES	329
261	FALSE MATCH RATE CALIBRATION: VISA IMAGES	330
262	FALSE MATCH RATE CALIBRATION: VISA IMAGES	331
263	FALSE MATCH RATE CALIBRATION: VISA IMAGES	332
264	FALSE MATCH RATE CALIBRATION: VISA IMAGES	333
265	FALSE MATCH RATE CALIBRATION: VISA IMAGES	334
266	FALSE MATCH RATE CALIBRATION: VISA IMAGES	335
267	FALSE MATCH RATE CALIBRATION: VISA IMAGES	336
268	FALSE MATCH RATE CALIBRATION: VISA IMAGES	337
269	FALSE MATCH RATE CALIBRATION: VISA IMAGES	338
270	FALSE MATCH RATE CALIBRATION: VISA IMAGES	339
271	FALSE MATCH RATE CALIBRATION: VISA IMAGES	340
272	FALSE MATCH RATE CALIBRATION: VISA IMAGES	341
273	FALSE MATCH RATE CALIBRATION: VISA IMAGES	342
274	FALSE MATCH RATE CALIBRATION: VISA IMAGES	343
275	FALSE MATCH RATE CALIBRATION: VISA IMAGES	344
276	FALSE MATCH RATE CALIBRATION: VISA IMAGES	345
277	FALSE MATCH RATE CALIBRATION: VISA IMAGES	346
278	FALSE MATCH RATE CALIBRATION: VISA IMAGES	347
279	FALSE MATCH RATE CALIBRATION: VISA IMAGES	348
280	FALSE MATCH RATE CALIBRATION: VISA IMAGES	349
281	FALSE MATCH RATE CALIBRATION: VISA IMAGES	350
282	FALSE MATCH RATE CALIBRATION: VISA IMAGES	351
283	FALSE MATCH RATE CALIBRATION: VISA IMAGES	352
284	FALSE MATCH RATE CALIBRATION: VISA IMAGES	353
285	FALSE MATCH RATE CALIBRATION: VISA IMAGES	354
286	FALSE MATCH RATE CALIBRATION: VISA IMAGES	355
287	FALSE MATCH RATE CALIBRATION: VISA IMAGES	356
288	FALSE MATCH RATE CALIBRATION: VISA IMAGES	357
289	FALSE MATCH RATE CALIBRATION: VISA IMAGES	358
290	FALSE MATCH RATE CALIBRATION: VISA IMAGES	359
291	FALSE MATCH RATE CALIBRATION: VISA IMAGES	360
292	EFFECT OF COUNTRY OF BIRTH ON FNMR	362
293	EFFECT OF COUNTRY OF BIRTH ON FNMR	363
294	EFFECT OF COUNTRY OF BIRTH ON FNMR	364
295	EFFECT OF COUNTRY OF BIRTH ON FNMR	365
296	EFFECT OF COUNTRY OF BIRTH ON FNMR	366
297	EFFECT OF COUNTRY OF BIRTH ON FNMR	367
298	EFFECT OF COUNTRY OF BIRTH ON FNMR	368
299	EFFECT OF COUNTRY OF BIRTH ON FNMR	369
300	EFFECT OF COUNTRY OF BIRTH ON FNMR	370
301	EFFECT OF COUNTRY OF BIRTH ON FNMR	371
302	EFFECT OF COUNTRY OF BIRTH ON FNMR	372
303	EFFECT OF COUNTRY OF BIRTH ON FNMR	373
304	EFFECT OF COUNTRY OF BIRTH ON FNMR	374
305	EFFECT OF COUNTRY OF BIRTH ON FNMR	375
306	EFFECT OF COUNTRY OF BIRTH ON FNMR	376
307	EFFECT OF COUNTRY OF BIRTH ON FNMR	377
308	EFFECT OF COUNTRY OF BIRTH ON FNMR	378
309	EFFECT OF COUNTRY OF BIRTH ON FNMR	379
310	EFFECT OF COUNTRY OF BIRTH ON FNMR	380
311	EFFECT OF COUNTRY OF BIRTH ON FNMR	381
312	EFFECT OF COUNTRY OF BIRTH ON FNMR	382

313	EFFECT OF COUNTRY OF BIRTH ON FNMR	383
314	EFFECT OF COUNTRY OF BIRTH ON FNMR	384
315	EFFECT OF COUNTRY OF BIRTH ON FNMR	385
316	EFFECT OF COUNTRY OF BIRTH ON FNMR	386
317	EFFECT OF COUNTRY OF BIRTH ON FNMR	387
318	EFFECT OF COUNTRY OF BIRTH ON FNMR	388
319	EFFECT OF COUNTRY OF BIRTH ON FNMR	389
320	EFFECT OF COUNTRY OF BIRTH ON FNMR	390
321	EFFECT OF COUNTRY OF BIRTH ON FNMR	391
322	EFFECT OF COUNTRY OF BIRTH ON FNMR	392
323	EFFECT OF COUNTRY OF BIRTH ON FNMR	393
324	EFFECT OF COUNTRY OF BIRTH ON FNMR	394
325	EFFECT OF COUNTRY OF BIRTH ON FNMR	395
326	EFFECT OF COUNTRY OF BIRTH ON FNMR	396
327	EFFECT OF COUNTRY OF BIRTH ON FNMR	397
328	EFFECT OF COUNTRY OF BIRTH ON FNMR	398
329	EFFECT OF COUNTRY OF BIRTH ON FNMR	399
330	EFFECT OF COUNTRY OF BIRTH ON FNMR	400
331	ERROR TRADEOFF CHARACTERISTIC: MUGSHOT IMAGES	402
332	ERROR TRADEOFF CHARACTERISTIC: MUGSHOT IMAGES	403
333	ERROR TRADEOFF CHARACTERISTIC: MUGSHOT IMAGES	404
334	ERROR TRADEOFF CHARACTERISTIC: MUGSHOT IMAGES	405
335	ERROR TRADEOFF CHARACTERISTIC: MUGSHOT IMAGES	406
336	ERROR TRADEOFF CHARACTERISTIC: MUGSHOT IMAGES	407
337	ERROR TRADEOFF CHARACTERISTIC: MUGSHOT IMAGES	408
338	ERROR TRADEOFF CHARACTERISTIC: MUGSHOT IMAGES	409
339	ERROR TRADEOFF CHARACTERISTIC: MUGSHOT IMAGES	410
340	ERROR TRADEOFF CHARACTERISTIC: MUGSHOT IMAGES	411
341	ERROR TRADEOFF CHARACTERISTIC: MUGSHOT IMAGES	412
342	ERROR TRADEOFF CHARACTERISTIC: MUGSHOT IMAGES	413
343	ERROR TRADEOFF CHARACTERISTIC: MUGSHOT IMAGES	414
344	ERROR TRADEOFF CHARACTERISTIC: MUGSHOT IMAGES	415
345	ERROR TRADEOFF CHARACTERISTIC: MUGSHOT IMAGES	416
346	ERROR TRADEOFF CHARACTERISTIC: MUGSHOT IMAGES	417
347	ERROR TRADEOFF CHARACTERISTIC: MUGSHOT IMAGES	418
348	ERROR TRADEOFF CHARACTERISTIC: MUGSHOT IMAGES	419
349	ERROR TRADEOFF CHARACTERISTIC: MUGSHOT IMAGES	420
350	ERROR TRADEOFF CHARACTERISTIC: MUGSHOT IMAGES	421
351	ERROR TRADEOFF CHARACTERISTIC: MUGSHOT IMAGES	422
352	ERROR TRADEOFF CHARACTERISTIC: MUGSHOT IMAGES	423
353	ERROR TRADEOFF CHARACTERISTIC: MUGSHOT IMAGES	424
354	ERROR TRADEOFF CHARACTERISTIC: MUGSHOT IMAGES	425
355	ERROR TRADEOFF CHARACTERISTIC: MUGSHOT IMAGES	426
356	ERROR TRADEOFF CHARACTERISTIC: MUGSHOT IMAGES	427
357	ERROR TRADEOFF CHARACTERISTIC: MUGSHOT IMAGES	428
358	ERROR TRADEOFF CHARACTERISTIC: MUGSHOT IMAGES	429
359	ERROR TRADEOFF CHARACTERISTIC: MUGSHOT IMAGES	430
360	EFFECT OF SUBJECT AGE ON FNMR	432
361	EFFECT OF SUBJECT AGE ON FNMR	433
362	EFFECT OF SUBJECT AGE ON FNMR	434
363	EFFECT OF SUBJECT AGE ON FNMR	435
364	EFFECT OF SUBJECT AGE ON FNMR	436
365	EFFECT OF SUBJECT AGE ON FNMR	437
366	EFFECT OF SUBJECT AGE ON FNMR	438
367	EFFECT OF SUBJECT AGE ON FNMR	439
368	EFFECT OF SUBJECT AGE ON FNMR	440

369	EFFECT OF SUBJECT AGE ON FNMR	441
370	EFFECT OF SUBJECT AGE ON FNMR	442
371	EFFECT OF SUBJECT AGE ON FNMR	443
372	EFFECT OF SUBJECT AGE ON FNMR	444
373	EFFECT OF SUBJECT AGE ON FNMR	445
374	EFFECT OF SUBJECT AGE ON FNMR	446
375	EFFECT OF SUBJECT AGE ON FNMR	447
376	EFFECT OF SUBJECT AGE ON FNMR	448
377	EFFECT OF SUBJECT AGE ON FNMR	449
378	EFFECT OF SUBJECT AGE ON FNMR	450
379	EFFECT OF SUBJECT AGE ON FNMR	451
380	EFFECT OF SUBJECT AGE ON FNMR	452
381	EFFECT OF SUBJECT AGE ON FNMR	453
382	EFFECT OF SUBJECT AGE ON FNMR	454
383	EFFECT OF SUBJECT AGE ON FNMR	455
384	EFFECT OF SUBJECT AGE ON FNMR	456
385	EFFECT OF SUBJECT AGE ON FNMR	457
386	EFFECT OF SUBJECT AGE ON FNMR	458
387	EFFECT OF SUBJECT AGE ON FNMR	459
388	EFFECT OF SUBJECT AGE ON FNMR	460
389	EFFECT OF SUBJECT AGE ON FNMR	461
390	EFFECT OF SUBJECT AGE ON FNMR	462
391	EFFECT OF SUBJECT AGE ON FNMR	463
392	EFFECT OF SUBJECT AGE ON FNMR	464
393	EFFECT OF SUBJECT AGE ON FNMR	465
394	EFFECT OF SUBJECT AGE ON FNMR	466
395	EFFECT OF SUBJECT AGE ON FNMR	467
396	EFFECT OF SUBJECT AGE ON FNMR	468
397	EFFECT OF SUBJECT AGE ON FNMR	469
398	EFFECT OF SUBJECT AGE ON FNMR	470
399	IMPOSTOR COUNTS FOR CROSS COUNTRY FMR CALCULATIONS	474

	Location	Developer Name	Short Name	Seq. Num.	Validation Date
1	NL	20Face	20face-000	000	2021-04-12
2	NL	20Face	20face-001	001	2021-09-29
3	US	3Divi	3divi-006	006	2021-04-14
4	US	3Divi	3divi-007	007	2021-09-27
5	TH	ACI Software	acisw-007	007	2021-11-15
6	TH	ACI Software	acisw-008	008	2022-03-22
7	US	AFIS and Biometrics Consulting	afisbiometrics-000	000	2022-01-27
8	US	AFR Engine	afrengine-000	000	2022-09-29
9	TW	ASUSTek Computer Inc	asusaics-000	000	2019-10-24
10	TW	ASUSTek Computer Inc	asusaics-001	001	2020-02-25
11	CN	AYF Technology	ayftech-001	001	2020-07-06
12	TW	Ability Enterprise - Andro Video	androvideo-000	000	2021-01-25
13	TW	Acer Incorporated	acer-001	001	2020-06-30
14	TW	Acer Incorporated	acer-002	002	2021-11-10
15	SG	Adera Global PTE	ader-a-003	003	2021-07-12
16	SG	Adera Global PTE	ader-a-004	004	2022-11-14
17	SG	Advancegroup	advance-003	003	2021-08-05
18	SG	Advancegroup	advance-004	004	2022-09-06
19	TH	Ai First	aifirst-001	001	2019-11-21
20	TW	AiUnion Technology	aiunionface-000	000	2019-10-22
21	TH	Aigen	aigen-001	001	2020-10-06
22	TH	Aigen	aigen-002	002	2021-03-15
23	CN	Aiseemu Technology	aiseemu-001	001	2022-06-16
24	CN	Aiseemu Technology	aiseemu-002	002	2022-11-18
25	KR	Ajou University	ajou-001	001	2021-03-08
26	ID	Akurat Satu Indonesia	ptakuratsatu-000	000	2020-09-11
27	KR	Alchera Inc	alchera-004	004	2022-08-12
28	KR	Alchera Inc	alchera-005	005	2023-01-04
29	ID	Alfabeta	alfabeta-001	001	2021-12-02
30	ES	Alice Biometrics	alice-000	000	2021-06-15
31	RU	Alivia / Innovation Sys	isystems-001	001	2018-06-12
32	RU	Alivia / Innovation Sys	isystems-002	002	2018-10-18
33	IN	AllGoVision	allgovision-000	000	2019-03-01
34	CN	AlphaSSTG	alphaface-001	001	2019-09-03
35	CN	AlphaSSTG	alphaface-002	002	2020-02-20
36	GB	Amplified Group	amplifiedgroup-001	001	2019-03-01
37	CN	Anke Investments	anke-004	004	2019-06-27
38	CN	Anke Investments	anke-005	005	2019-11-21
39	BR	Antheus Technologia	antheus-000	000	2019-12-05
40	BR	Antheus Technologia	antheus-001	001	2020-06-25
41	GB	AnyVision	anyvision-004	004	2018-06-15
42	GB	AnyVision	anyvision-005	005	2021-02-03
43	US	Armatura LLC	armatura-001	001	2022-01-04
44	US	Armatura LLC	armatura-003	003	2023-01-13
45	CN	AuthenMetric	authenmetric-003	003	2021-08-09
46	CN	AuthenMetric	authenmetric-004	004	2022-01-03
47	US	Aware	aware-005	005	2020-02-27
48	US	Aware	aware-006	006	2021-07-03
49	IN	Awidit Systems	awiroos-001	001	2019-09-23
50	IN	Awidit Systems	awiroos-002	002	2020-10-28
51	CH	Aximetria	aximetria-001	001	2022-08-10
52	JP	Ayonix	ayonix-000	000	2017-06-22
53	CN	BÖE Technology Group	boetech-001	001	2021-06-22
54	CN	BOE Technology Group	boetech-002	002	2021-12-21
55	ES	Bee the Data	beethedata-000	000	2021-07-26
56	CN	Beihang University-ERCACAT	ercacat-001	001	2020-07-06
57	CN	Beijing Alleyes Technology	alleyes-000	000	2020-03-09
58	CN	Beijing DeepSense Technologies	deepsense-000	000	2021-03-19
59	CN	Beijing DeepSense Technologies	deepsense-001	001	2022-03-11
60	CN	Beijing Hisign Technology	hisign-001	001	2021-09-24
61	CN	Beijing Hisign Technology	hisign-002	002	2022-09-09
62	CN	Beijing Mendaxia Technology	mendaxiatech-000	000	2021-09-15
63	CN	Beijing Vion Technology Inc	vion-000	000	2018-10-19
64	KZ	Beyne.AI	beyneai-000	000	2022-01-03
65	CH	BioID Technologies SA	bioidtechswiss-001	001	2020-08-28
66	CH	BioID Technologies SA	bioidtechswiss-002	002	2021-02-17
67	IN	Biocube Matrics	biocube-001	001	2021-09-08
68	UK	BitCenter UK	farfaces-001	001	2021-04-09
69	CN	Bitmain	bm-001	001	2018-10-17
70	CN	Bresee Technology	bresee-001	001	2020-12-30

Table 1: Summary of participant information included in this report.

	Location	Developer Name	Short Name	Seq. Num.	Validation Date
71	CN	Bresee Technology	bresee-002	002	2021-06-30
72	VN	CMC Institute of Science and Technology	cist-001	001	2022-10-20
73	CN	CSA IntelliCloud Technology	intellicloudai-001	001	2019-08-13
74	CN	CSA IntelliCloud Technology	intellicloudai-002	002	2020-12-17
75	TW	CTBC Bank	ctbcbank-000	000	2019-06-28
76	TW	CTBC Bank	ctbcbank-001	001	2019-10-28
77	KR	CUDO Communication	cudocommunication-001	001	2021-10-20
78	US	Camvi Technologies	camvi-002	002	2018-10-19
79	US	Camvi Technologies	camvi-004	004	2019-07-12
80	JP	Canon Inc	canon-003	003	2021-09-15
81	JP	Canon Inc	canon-004	004	2022-04-25
82	CN	China Electronics Import-Export Corp	ceiec-003	003	2020-01-06
83	CN	China Electronics Import-Export Corp	ceiec-004	004	2021-01-18
84	CN	China University of Petroleum	upc-001	001	2019-06-05
85	CN	Chinese University of Hong Kong	cuhkee-001	001	2020-03-18
86	KR	Chosun University	chosun-001	001	2020-07-01
87	KR	Chosun University	chosun-002	002	2020-11-25
88	TW	Chunghwa Telecom	chtface-005	005	2022-03-09
89	TW	Chunghwa Telecom	chtface-006	006	2022-11-03
90	US	Clearview AI Inc	clearviewai-000	000	2021-09-22
91	CN	Closeli Inc	closeli-001	001	2021-07-15
92	US	CloudSmart Consulting LLC	csc-002	002	2021-03-24
93	US	CloudSmart Consulting LLC	csc-003	003	2021-08-26
94	TW	Cloudmatrix	cloudmatrix-001	001	2022-02-16
95	TW	Cloudmatrix	cloudmatrix-002	002	2022-10-17
96	CN	Cloudwalk - Hengrui AI Technology	cloudwalk-hr-003	003	2020-09-25
97	CN	Cloudwalk - Hengrui AI Technology	cloudwalk-hr-004	004	2021-02-10
98	CN	Cloudwalk - Moontime Smart Technology	cloudwalk-mt-005	005	2022-03-29
99	CN	Cloudwalk - Moontime Smart Technology	cloudwalk-mt-006	006	2022-10-20
100	IN	Code Everest Pvt	facex-001	001	2021-03-08
101	IN	Code Everest Pvt	facex-002	002	2021-08-24
102	KR	Codeline	codeline-000	000	2022-09-13
103	DE	Cognitec Systems GmbH	cognitec-003	003	2021-07-30
104	DE	Cognitec Systems GmbH	cognitec-004	004	2022-02-10
105	TW	Coretech Knowledge Inc	coretech-000	000	2021-07-12
106	TW	Coretech Knowledge Inc	coretech-001	001	2022-09-29
107	IL	Corsight	corsight-002	002	2021-09-01
108	IL	Corsight	corsight-003	003	2022-06-09
109	IL	Cortica	cor-001	001	2020-09-24
110	TW	Cu-Face	cu-face-002	002	2023-01-05
111	KR	Cubox	cubox-001	001	2020-12-07
112	KR	Cubox	cubox-002	002	2021-08-24
113	JP	Cybercore	cybercore-002	002	2022-04-25
114	JP	Cybercore	cybercore-003	003	2022-08-31
115	US	Cyberextruder	cyberextruder-003	003	2022-03-16
116	US	Cyberextruder	cyberextruder-004	004	2022-07-20
117	TW	Cyberlink Corp	cyberlink-009	009	2022-05-12
118	TW	Cyberlink Corp	cyberlink-010	010	2022-09-16
119	MX	DICIO	dicio-001	001	2022-03-22
120	CN	DSK	dsk-000	000	2019-06-28
121	CN	Dahua Technology	dahua-006	006	2020-12-30
122	CN	Dahua Technology	dahua-007	007	2021-12-20
123	IE	Daon	daon-000	000	2021-11-03
124	US	Decatur Industries Inc	decatur-000	000	2020-08-18
125	US	Decatur Industries Inc	decatur-001	001	2021-09-27
126	CN	Deepglint	deepglint-004	004	2021-09-17
127	CN	Deepglint	deepglint-005	005	2022-10-17
128	FR	Deepsense	dps-000	000	2021-07-16
129	DE	Dermalog	dermalog-010	010	2022-07-25
130	DE	Dermalog	dermalog-011	011	2022-12-12
131	CN	DiDi ChuXing Technology	didiglobalface-001	001	2019-10-23
132	CN	DiDi ChuXing Technology	didiglobalface-002	002	2023-01-09
133	IN	Digidata	didata-000	000	2022-01-27
134	IN	Digidata	didata-001	001	2022-06-10
135	GB	Digital Barriers	digitalbarriers-002	002	2019-03-01
136	TR	Ekin Smart City Technologies	ekin-002	002	2021-05-04
137	RU	Enface	enface-000	000	2021-04-09
138	RU	Enface	enface-001	001	2021-12-17
139	CH	Euronovate SA	euronovate-001	001	2021-11-15
140	RU	Expasoft LLC	expasoft-001	001	2020-09-03

Table 2: Summary of participant information included in this report.

	Location	Developer Name	Short Name	Seq. Num.	Validation Date
141	RU	Expasoft LLC	expasoft-002	002	2021-07-26
142	US	FRP LLC	frpkauai-001	001	2022-07-18
143	US	FRP LLC	frpkauai-002	002	2022-11-21
144	DE	FaceOnLive Inc	faceonlive-001	001	2021-11-23
145	DE	FaceOnLive Inc	faceonlive-002	002	2022-04-11
146	ES	FacePhi	facephi-000	000	2022-04-06
147	GB	FaceSoft	facesoft-000	000	2019-07-10
148	KR	FaceTag Co	facetag-000	000	2021-03-22
149	KR	FaceTag Co	facetag-002	002	2022-01-06
150	TW	FarBar Inc	f8-001	001	2019-07-11
151	TW	FarBar Inc	f8-002	002	2022-03-02
152	CN	Fiberhome Telecommunication Technologies	fiberhome-nanjing-003	003	2021-03-12
153	CN	Fiberhome Telecommunication Technologies	fiberhome-nanjing-004	004	2021-09-14
154	UK	Fincore Ltd	fincore-000	000	2021-06-07
155	KZ	First Credit Bureau Kazakhstan	firstcreditKZ-001	001	2022-08-22
156	CN	Fujitsu Research and Development Center	fujitsulab-002	002	2021-02-24
157	CN	Fujitsu Research and Development Center	fujitsulab-003	003	2021-07-12
158	US	Gemalto Cogent	cogent-007	007	2022-04-11
159	US	Gemalto Cogent	cogent-008	008	2023-01-03
160	TW	GeoVision Inc	geo-002	002	2021-04-01
161	TW	GeoVision Inc	geo-004	004	2022-02-10
162	JP	Glory	glory-004	004	2022-02-08
163	JP	Glory	glory-005	005	2022-07-08
164	TW	Gorilla Technology	gorilla-008	008	2021-11-08
165	TW	Gorilla Technology	gorilla-009	009	2022-12-14
166	US	Graymatics	graymatics-001	001	2022-01-13
167	US	Griaule	griaule-001	001	2022-05-31
168	US	Griaule	griaule-002	002	2022-12-02
169	CN	Guangzhou Pixel Solutions	pixelall-008	008	2022-06-16
170	CN	Guangzhou Pixel Solutions	pixelall-009	009	2022-10-26
171	CN	Hangzhuo Allu Network Information Technology	hzailu-002	002	2022-06-02
172	CN	Hangzhuo Allu Network Information Technology	hzailu-003	003	2022-10-11
173	ES	Herta Security	hertasecurity-001	001	2022-01-18
174	ES	Herta Security	hertasecurity-002	002	2022-09-02
175	CN	Hikvision Research Institute	hik-001	001	2019-03-01
176	IN	HyperVerge Inc	hyperverge-003	003	2022-04-11
177	IN	HyperVerge Inc	hyperverge-004	004	2022-12-14
178	AU	ICM Airport Technics	icm-003	003	2021-09-06
179	AU	ICM Airport Technics	icm-004	004	2022-09-07
180	FR	ID3 Technology	id3-006	006	2020-12-17
181	FR	ID3 Technology	id3-008	008	2021-11-10
182	CA	IMDS Software	imds-software-001	001	2022-07-06
183	RU	ITMO University	itmo-007	007	2020-01-06
184	RU	ITMO University	itmo-008	008	2021-11-19
185	RU	IVA Cognitive	ivacognitive-001	001	2021-01-29
186	FR	Idemia	idemia-008	008	2021-07-07
187	FR	Idemia	idemia-009	009	2022-07-27
188	US	Imageware Systems	iws-000	000	2020-08-12
189	GB	Imperial College London	imperial-000	000	2019-03-01
190	GB	Imperial College London	imperial-002	002	2019-08-28
191	US	Incode Technologies Inc	incode-010	010	2021-10-22
192	US	Incode Technologies Inc	incode-011	011	2022-08-10
193	IT	InfoCert	infocert-001	001	2022-09-08
194	IN	Innef Labs	innefulabs-000	000	2020-09-04
195	GB	Innovative Technology	innovativetechnologyltd-001	001	2019-10-22
196	GB	Innovative Technology	innovativetechnologyltd-002	002	2020-02-26
197	SK	Innovatrics	innovatrics-008	008	2021-12-15
198	SK	Innovatrics	innovatrics-009	009	2022-01-19
199	CN	InsightFace AI	insightface-001	001	2021-09-27
200	CN	InsightFace AI	insightface-003	003	2022-08-23
201	CN	Inspur (Beijing) Electronic Information Industry Co	inspur-000	000	2022-07-19
202	CN	Institute of Computing Technology	ichthtc-000	000	2020-11-29
203	RU	Institute of Information Technologies	iit-002	002	2019-12-04
204	RU	Institute of Information Technologies	iit-003	003	2020-12-01
205	IS	Intel Research Group	intelresearch-005	005	2022-02-13
206	IS	Intel Research Group	intelresearch-006	006	2022-12-19
207	KR	IntelliVIX	intellivix-002	002	2022-07-14
208	KR	IntelliVIX	intellivix-003	003	2022-12-12
209	AE	Intellibrain Technological Projects	g42-intellibrain-001	001	2022-07-27
210	US	Intellivision	intellivision-003	003	2022-03-07

Table 3: Summary of participant information included in this report.

	Location	Developer Name	Short Name	Seq. Num.	Validation Date
211	US	Intellivision	intellivision-004	004	2022-07-28
212	LU	Intema-LGL Group	intema-000	000	2022-07-15
213	LU	Intema-LGL Group	intema-001	001	2023-01-11
214	US	IrexAI	irex-000	000	2020-12-17
215	IL	Is It You	isityou-000	000	2017-06-26
216	MX	Jaak IT	jaakit-001	001	2022-05-20
217	KR	Kakao Enterprise	kakao-007	007	2022-01-12
218	KR	Kakao Enterprise	kakao-008	008	2022-05-12
219	KR	Kakao Pay Corp	kakaopay-001	001	2021-07-06
220	TH	Kasikorn Labs	kasikornlabs-000	000	2022-03-02
221	TH	Kasikorn Labs	kasikornlabs-002	002	2022-12-13
222	SG	Kedacom International Pte	kedacom-000	000	2019-06-03
223	US	Kneron Inc	kneron-003	003	2019-07-01
224	US	Kneron Inc	kneron-005	005	2020-02-21
225	US	KnowUTech LLC	knowutech-000	000	2022-02-13
226	KR	Kookmin University	kookmin-002	002	2021-03-05
227	KR	Korea Identification Inc	koreaid-001	001	2022-12-12
228	TH	Krungthai	krungthai-002	002	2022-06-21
229	CN	KuKe3D Technology	kuke3d-001	001	2021-10-28
230	CN	KuKe3D Technology	kuke3d-002	002	2022-04-14
231	MX	Lebentech Biometrics	lebentech-000	000	2022-02-16
232	IN	Lema Labs	lemalabs-001	001	2021-04-13
233	JP	Line Corporation	lineclova-002	002	2022-05-18
234	JP	Line Corporation	lineclova-003	003	2022-11-28
235	RU	Lomonosov Moscow State University	intsysmsu-001	001	2019-10-22
236	RU	Lomonosov Moscow State University	intsysmsu-002	002	2020-03-12
237	IN	Lookman Electroplast Industries	lookman-002	002	2018-06-13
238	IN	Lookman Electroplast Industries	lookman-004	004	2019-06-03
239	US	Luxand Inc	luxand-000	000	2019-11-07
240	RU	MVision	mvision-001	001	2019-11-12
241	IN	Mantra Softech India	mantra-000	000	2021-10-28
242	CN	Maxvision Technology	maxvision-002	002	2022-07-12
243	CN	Maxvision Technology	maxvision-003	003	2022-11-14
244	CN	Megvii/Face++	megvii-005	005	2022-03-28
245	CN	Megvii/Face++	megvii-006	006	2022-08-08
246	KR	Metsakuur	metsakuurcompany-001	001	2022-05-12
247	KR	Metsakuur	metsakuurcompany-002	002	2022-09-14
248	CN	Miaxis Biometrics	miaxis-001	001	2022-11-15
249	GB	MicroFocus	microfocus-001	001	2018-06-13
250	GB	MicroFocus	microfocus-002	002	2018-10-17
251	CN	Minivision	minivision-000	000	2020-10-28
252	NO	Mobai	mobai-000	000	2020-08-26
253	NO	Mobai	mobai-001	001	2021-02-17
254	ES	Mobbeel Solutions	mobbl-001	001	2021-06-16
255	ES	Mobbeel Solutions	mobbl-003	003	2022-04-19
256	KR	Mobipin Technology	mobipintech-000	000	2021-11-23
257	TH	Momentum Digital	sertis-000	000	2019-10-07
258	TH	Momentum Digital	sertis-002	002	2021-05-13
259	CN	MoreDian Technology	moreedian-000	000	2021-02-24
260	US	Mukh Technologies	mukh-001	001	2022-03-22
261	US	Mukh Technologies	mukh-002	002	2022-11-01
262	CN	Multi-Modality Intelligence	multimodality-000	000	2021-10-19
263	CN	Multi-Modality Intelligence	multimodality-001	001	2022-05-16
264	RU	N-Tech Lab	ntechlab-011	011	2021-09-13
265	RU	N-Tech Lab	ntechlab-012	012	2022-01-20
266	CA	NEO Systems	neosystems-004	004	2022-05-02
267	KR	NHN Corp	nhn-002	002	2021-07-15
268	KR	NHN Corp	nhn-003	003	2022-02-22
269	KR	NSENSE Corp	nsensecorp-003	003	2021-10-29
270	KR	NSENSE Corp	nsensecorp-004	004	2022-09-08
271	CN	Nanjing Kiwi Network Technology	kiwitech-000	000	2021-03-19
272	KR	Neosecu Co	openface-001	001	2021-06-15
273	TW	Netbridge Technology Incoporation	netbridgegetech-001	001	2020-01-08
274	TW	Netbridge Technology Incoporation	netbridgegetech-002	002	2020-08-11
275	LT	Neurotechnology	neurotechnology-013	013	2022-01-07
276	LT	Neurotechnology	neurotechnology-015	015	2022-06-07
277	ID	Nodeflux	nodeflux-002	002	2019-08-13
278	IN	NotionTag Technologies Private Limited	notionntag-001	001	2021-03-04
279	IN	NotionTag Technologies Private Limited	notionntag-002	002	2021-09-17
280	US	Omnigarde Ltd	omnigarde-001	001	2021-08-23

Table 4: Summary of participant information included in this report.

	Location	Developer Name	Short Name	Seq. Num.	Validation Date
281	US	Omnigarde Ltd	omnigarde-002	002	2022-01-19
282	KR	One More Security	omface-000	000	2021-12-15
283	KR	One More Security	omface-001	001	2022-10-21
284	UK	Onfido	onfido-000	000	2022-12-13
285	RU	Oz Forensics LLC	oz-003	003	2021-08-09
286	RU	Oz Forensics LLC	oz-004	004	2021-12-13
287	TW	PAPAGO Inc	papago-001	001	2022-07-19
288	ID	PT Autentika Digital Indonesia	autentika-000	000	2022-12-05
289	ID	PT Qlue Performa Indonesia	qluevision-001	001	2022-11-15
290	CH	PXL Vision AG	pxl-001	001	2020-06-30
291	TW	Palit Microsystems	palit-000	000	2022-05-16
292	TW	Palit Microsystems	palit-001	001	2022-09-26
293	SG	Panasonic R+D Center Singapore	psl-010	010	2022-04-19
294	SG	Panasonic R+D Center Singapore	psl-011	011	2022-10-06
295	US	Pangiam	pangiam-000	000	2022-04-04
296	TR	Papilon Savunma	papsav1923-002	002	2022-01-20
297	TR	Papilon Savunma	papsav1923-003	003	2022-11-25
298	US	Paravision (EverAI)	paravision-010	010	2022-02-02
299	US	Paravision (EverAI)	paravision-011	011	2022-12-12
300	SG	Pensees Pte	pensees-001	001	2020-08-17
301	IN	Pyramid Cyber Security + Forensic (P)	pyramid-000	000	2019-11-04
302	KZ	Qaz Biometric Systems	qazbs-000	000	2022-06-22
303	TW	Qnap Security	qnap-002	002	2022-04-15
304	TW	Qnap Security	qnap-003	003	2022-12-09
305	CZ	Quantasoft	quantasoft-003	003	2021-04-19
306	US	Rank One Computing	rankone-012	012	2021-12-27
307	US	Rank One Computing	rankone-013	013	2022-07-09
308	US	Rank One Computing	rankone-014	014	2022-12-21
309	US	Realnetworks Inc	realnetworks-007	007	2022-06-14
310	US	Realnetworks Inc	realnetworks-008	008	2022-11-10
311	US	Regula Forensics	regula-000	000	2021-04-13
312	US	Regula Forensics	regula-001	001	2021-12-14
313	CN	Remark Holdings	remarkai-001	001	2019-03-01
314	CN	Remark Holdings	remarkai-003	003	2021-06-22
315	SG	Rendip	rendip-000	000	2021-04-19
316	UK	Reveal Media Ltd	revealmedia-005	005	2021-09-24
317	UK	Reveal Media Ltd	revealmedia-006	006	2022-01-26
318	CN	Rokid Corporation	rokid-000	000	2019-08-01
319	CN	Rokid Corporation	rokid-001	001	2019-12-13
320	KR	SK Telecom	sktelecom-000	000	2021-07-09
321	KR	SQIsoft	sqisoft-002	002	2021-11-03
322	KR	SQIsoft	sqisoft-003	003	2022-10-26
323	SA	STCON LLC	stcon-000	000	2022-11-02
324	DE	Saffe	saffe-001	001	2018-10-19
325	DE	Saffe	saffe-002	002	2019-03-01
326	JP	Saga Densan Center Co Ltd	sdc-000	000	2022-10-18
327	KR	Samsung S1 Corp	s1-005	005	2022-06-17
328	KR	Samsung S1 Corp	s1-006	006	2022-10-17
329	KR	Samsung-SDS	samsungsds-001	001	2022-04-18
330	KR	Samsung-SDS	samsungsds-002	002	2022-09-16
331	IN	Samtech InfoNet Limited	samtech-001	001	2019-10-15
332	RU	Satellite Innovation/Eocortex	eocortex-000	000	2020-08-26
333	IL	Scanovate	scanovate-002	002	2020-06-26
334	IL	Scanovate	scanovate-003	003	2021-11-15
335	RO	Securif AI	securifai-005	005	2022-05-16
336	RO	Securif AI	securifai-006	006	2022-11-14
337	CN	Sensetime Group	sensetime-007	007	2022-06-17
338	CN	Sensetime Group	sensetime-008	008	2023-01-04
339	SG	Seventh Sense Artificial Intelligence	seventhsense-001	001	2022-03-04
340	SG	Seventh Sense Artificial Intelligence	seventhsense-002	002	2022-10-17
341	US	Shaman Software	shaman-000	000	2017-12-05
342	US	Shaman Software	shaman-001	001	2018-01-13
343	CN	Shanghai Jiao Tong University	sjtu-003	003	2020-11-02
344	CN	Shanghai Jiao Tong University	sjtu-004	004	2021-05-13
345	CN	Shanghai Ulucu Electronics Technology	uluface-002	002	2019-07-10
346	CN	Shanghai Ulucu Electronics Technology	uluface-003	003	2019-11-12
347	CN	Shanghai University - Shanghai Film Academy	shu-002	002	2019-12-10
348	CN	Shanghai University - Shanghai Film Academy	shu-003	003	2020-06-24
349	CN	Shanghai Yitu Technology	yitu-003	003	2019-03-01
350	CN	Shenzhen AiMall Tech	aimall-002	002	2020-03-12

Table 5: Summary of participant information included in this report.

	Location	Developer Name	Short Name	Seq. Num.	Validation Date
351	CN	Shenzhen AiMall Tech	aimall-003	003	2020-08-12
352	CN	Shenzhen EI Networks	einetworks-000	000	2019-08-13
353	CN	Shenzhen Inst Adv Integrated Tech CAS	siat-002	002	2018-06-13
354	CN	Shenzhen Inst Adv Integrated Tech CAS	siat-005	005	2022-02-08
355	CN	Shenzhen Intellifusion Technologies	intellifusion-001	001	2019-08-22
356	CN	Shenzhen Intellifusion Technologies	intellifusion-002	002	2020-03-18
357	CN	Shenzhen University-Macau University of Science and Technology	sztu-000	000	2020-12-17
358	CN	Shenzhen University-Macau University of Science and Technology	sztu-001	001	2021-07-13
359	RU	Smart Engines	smartengines-000	000	2021-08-25
360	RU	Smart Engines	smartengines-001	001	2022-05-31
361	ES	Smartbiometrik	smartbiometrik-001	001	2022-05-16
362	TR	Smarvist Teknoloji	smarvist-000	000	2022-05-10
363	DE	Smilart	smilart-002	002	2018-02-06
364	DE	Smilart	smilart-003	003	2019-03-01
365	TR	Sodec App Inc	sodec-000	000	2021-06-02
366	IN	Staqu Technologies	st aqu-000	000	2020-07-15
367	CN	Star Hybrid Limited	starhybrid-001	001	2019-06-19
368	CN	Su Zhou NaZhiTianDi intelligent technology	nazhai-000	000	2020-06-25
369	IN	Sukshi Technology Innovation	sukshi-000	000	2022-02-13
370	KR	Suprema AI Inc	suprema-003	003	2022-07-20
371	KR	Suprema AI Inc	suprema-004	004	2023-01-09
372	KR	Suprema ID Inc	supremaid-001	001	2021-05-04
373	KR	Suprema ID Inc	supremaid-002	002	2022-06-24
374	RU	Synesis	synesis-006	006	2019-10-10
375	RU	Synesis	synesis-007	007	2020-06-24
376	TW	Synology Inc	synology-000	000	2019-10-23
377	TW	Synology Inc	synology-002	002	2020-08-20
378	BR	T4iSB	t4isb-000	000	2022-01-28
379	CN	TUPU Technology	tuputech-000	000	2019-10-11
380	TW	Taiwan AI Labs	ailabs-001	001	2019-12-18
381	TW	Taiwan-Certificate Authority Incorporation	twface-000	000	2021-05-14
382	TW	Taiwan-Certificate Authority Incorporation	twface-001	001	2021-09-14
383	CH	Tech5 SA	tech5-005	005	2020-07-24
384	CH	Tech5 SA	tech5-007	007	2022-12-30
385	TR	Techsign	techsign-000	000	2021-08-25
386	TR	Techsign	techsign-001	001	2022-07-01
387	CN	Tencent Deepsea Lab	deepsea-001	001	2019-06-03
388	RU	Tevian	tevian-007	007	2021-08-06
389	RU	Tevian	tevian-008	008	2021-12-06
390	US	TigerIT Americas LLC	tiger-005	005	2021-07-29
391	US	TigerIT Americas LLC	tiger-006	006	2021-12-13
392	RU	Tinkoff Bank	tinkoff-001	001	2021-05-13
393	CN	TongYi Transportation Technology	tongyi-005	005	2019-06-12
394	TW	Toppan ID Gate	toppanidgate-000	000	2021-09-28
395	JP	Toshiba	toshiba-004	004	2021-09-27
396	JP	Toshiba	toshiba-006	006	2022-06-29
397	ES	Touchless ID	touchlessid-000	000	2022-05-02
398	ES	Touchless ID	touchlessid-001	001	2022-09-21
399	JP	Tripleize	aize-001	001	2021-04-23
400	JP	Tripleize	aize-002	002	2021-10-08
401	VN	TrueID-VNG	trueidvng-001	001	2023-01-05
402	US	Trueface.ai	trueface-002	002	2021-03-29
403	US	Trueface.ai	trueface-003	003	2021-09-30
404	CN	TuringTech.vip	turingtechvip-001	001	2022-02-03
405	CN	TuringTech.vip	turingtechvip-002	002	2022-07-27
406	TR	Turkcell Technology	turkcell-000	000	2022-10-11
407	CN	ULSee Inc	ulsee-001	001	2019-07-31
408	TW	UXLabs	uxlabs-001	001	2022-09-19
409	FR	Unissey	unissey-002	002	2022-04-29
410	FR	Unissey	unissey-003	003	2022-12-19
411	PT	Universidade de Coimbra	visteam-003	003	2022-01-31
412	PT	Universidade de Coimbra	visteam-004	004	2022-08-01
413	PT	Universidade de Coimbra	visteam-005	005	2023-01-04
414	UK	University of Surrey-CVSSP	surrey-cvssp-000	000	2022-03-25
415	UK	University of Surrey-CVSSP	surrey-cvssp-001	001	2022-09-22
416	US	VCognition	vcog-002	002	2017-06-12
417	ES	Veridas Digital Authentication Solutions S.L.	veridas-007	007	2021-09-02
418	ES	Veridas Digital Authentication Solutions S.L.	veridas-008	008	2022-10-17
419	UK	Veridium	veridium-000	000	2022-03-28
420	UK	Veridium	veridium-001	001	2022-11-03

Table 6: Summary of participant information included in this report.

	Location	Developer Name	Short Name	Seq. Num.	Validation Date
421	KZ	Verigram	verigram-000	000	2021-09-06
422	KZ	Verigram	verigram-001	001	2022-03-09
423	ID	Verihubs	verihubs-inteligensia-000	000	2021-07-27
424	ID	Verihubs	verihubs-inteligensia-001	001	2022-06-16
425	ID	Verijelas	verijelas-000	000	2022-08-01
426	TW	Via Technologies Inc	via-000	000	2019-07-08
427	TW	Via Technologies Inc	via-001	001	2020-01-08
428	DE	Videmo Intelligent Videoanalyse	videmo-001	001	2021-12-22
429	DE	Videmo Intelligent Videoanalyse	videmo-002	002	2022-08-31
430	IN	Videogenetics Technology Pvt	videogenetics-001	001	2019-06-19
431	IN	Videogenetics Technology Pvt	videogenetics-002	002	2019-11-21
432	VN	Vietnam Posts and Telecommunications Group	vnpt-004	004	2022-04-15
433	VN	Vietnam Posts and Telecommunications Group	vnpt-005	005	2022-08-24
434	VN	Viettel Group	vts-000	000	2020-11-04
435	VN	Viettel Group	vts-001	001	2022-04-20
436	VN	Viettel High Technology	viettelhightech-000	000	2021-08-04
437	US	Vigilant Solutions	vigilantsolutions-010	010	2021-04-07
438	US	Vigilant Solutions	vigilantsolutions-011	011	2021-08-07
439	VN	VinAI Research VietNam	vinai-000	000	2020-09-24
440	VN	VinBigData	vinbigdata-001	001	2022-01-06
441	VN	VinBigData	vinbigdata-002	002	2022-06-07
442	SE	Visage Technologies	visage-000	000	2020-12-09
443	FI	Visidon	vd-002	002	2021-04-12
444	FI	Visidon	vd-003	003	2021-10-12
445	CN	Vision Intelligence Center of Meituan	meituan-001	001	2022-03-25
446	CN	Vision Intelligence Center of Meituan	meituan-002	002	2022-09-14
447	PT	Vision-Box	visionbox-001	001	2019-03-01
448	PT	Vision-Box	visionbox-002	002	2021-04-29
449	RU	VisionLabs	visionlabs-010	010	2021-01-25
450	RU	VisionLabs	visionlabs-011	011	2021-10-13
451	AU	Vixvizon	vixvization-006	006	2022-08-11
452	AU	Vixvizon	vixvization-007	007	2023-01-17
453	RU	Vocord	vocord-009	009	2020-12-28
454	RU	Vocord	vocord-010	010	2021-12-20
455	US	Wicket	wicket-000	000	2022-02-14
456	CN	Winsense	winsense-001	001	2019-10-16
457	CN	Winsense	winsense-002	002	2020-11-20
458	MY	Wise AI SDN BHD	wiseai-001	001	2022-10-25
459	CN	Wuhan Tianyu Information Industry	wuhantianyu-001	001	2021-08-05
460	CN	X-Laboratory	x-laboratory-000	000	2019-09-03
461	CN	X-Laboratory	x-laboratory-001	001	2020-01-21
462	CN	Xforward AI Technology	xforwardai-001	001	2020-09-25
463	CN	Xforward AI Technology	xforwardai-002	002	2021-02-10
464	CN	Xiamen Meiya Pico Information	meiya-001	001	2019-03-01
465	CN	Xiamen University	xm-000	000	2020-10-19
466	PT	YooniK	yoonik-002	002	2021-09-06
467	PT	YooniK	yoonik-003	003	2022-01-06
468	TW	Yuan High-Tech Development	yuan-005	005	2022-06-22
469	TW	Yuan High-Tech Development	yuan-006	006	2022-12-14
470	CN	Yuntu Data and Technology	ytu-000	000	2021-06-16
471	CN	Zhuhai Yisheng Electronics Technology	yisheng-004	004	2018-06-12
472	CN	iQIYI Inc	iqface-000	000	2019-06-04
473	CN	iQIYI Inc	iqface-003	003	2021-02-23
474	TW	iSAP Solution Corporation	isap-001	001	2019-08-07
475	TW	iSAP Solution Corporation	isap-002	002	2020-09-01
476	TW	ioNetworks Inc	ionetworks-000	000	2021-07-20

Table 7: Summary of participant information included in this report.

	ALGORITHM	CONFIG	LIBRARY	TEMPLATE								COMPARISON ⁴		
				NAME	DATA		MEMORY	SIZE	GENERATION TIME (ms) ⁴				TIME (ns) ⁵	
					(KB) ¹	(KB) ²			(B)	MUGSHOT	480x720	960x1440	1600x2400	3000x4500
1	20face-000	117155	324083	²¹⁴ 905	²⁷⁰ 2048 ± 0	⁴² 232 ± 1	³⁰ 223 ± 1	²⁶ 226 ± 4	²² 222 ± 1	¹⁶ 224 ± 1	⁴⁴⁷ 44880 ± 134	⁴⁴⁵ 44462 ± 163		
2	20face-001	226824	324119	³⁷³ 1940	⁴⁰⁸ 4096 ± 0	⁵³ 279 ± 2	³⁷ 266 ± 1	²⁹ 266 ± 1	²⁸ 267 ± 1	²³ 267 ± 0	³⁵¹ 5553 ± 54	³⁴⁹ 5541 ± 65		
3	3divi-006	273866	52656	⁹⁰ 472	²⁰³ 2048 ± 0	²¹⁰ 654 ± 1	¹⁷⁵ 651 ± 0	¹⁵⁸ 660 ± 1	¹⁴² 678 ± 2	¹⁴⁰ 759 ± 13	¹¹⁴ 775 ± 19	¹¹³ 770 ± 22		
4	3divi-007	483115	24723	²⁹⁶ 1285	¹⁹¹ 2048 ± 0	¹⁹⁰ 615 ± 1	¹⁶² 616 ± 1	¹⁴⁸ 623 ± 1	¹²⁸ 644 ± 1	¹³¹ 727 ± 5	¹⁰² 707 ± 31	¹⁰² 712 ± 25		
5	acer-001	36650	66086	⁷⁵ 417	²⁸ 512 ± 0	³⁶ 199 ± 0	³³ 237 ± 28	²⁷ 229 ± 26	²⁷ 242 ± 37	²¹ 259 ± 21	²⁶³ 2453 ± 44	²⁶⁴ 2461 ± 62		
6	acer-002	43922	624858	³⁹ 187	²⁶⁷ 2048 ± 0	³¹ 184 ± 0	²³ 184 ± 0	¹⁷ 185 ± 0	¹⁴ 185 ± 0	¹³ 186 ± 0	³⁰⁴ 3370 ± 47	³⁰⁴ 3350 ± 54		
7	acisw-007	267619	36111	⁵³ 286	¹²⁵ 2048 ± 0	⁵⁸ 283 ± 0	⁴⁷ 293 ± 3	⁶² 414 ± 0	⁵⁴ 404 ± 0	⁵⁵ 484 ± 1	¹⁷⁴ 1316 ± 22	¹⁷⁴ 1297 ± 23		
8	acisw-008	171703	39359	²⁵⁷ 1101	²⁹¹ 2048 ± 0	⁹⁶ 400 ± 1	⁶⁶ 362 ± 28	⁵⁰ 369 ± 9	³³ 300 ± 2	²⁸ 336 ± 5	¹⁷⁵ 1327 ± 19	¹⁷⁷ 1337 ± 32		
9	ader-a-003	0	749778	²¹⁹ 917	⁴⁵⁹ 5120 ± 0	⁴⁴³ 1381 ± 12	⁴¹² 1385 ± 1	⁴¹¹ 1394 ± 1	³⁸⁷ 1401 ± 1	³³⁸ 1469 ± 1	²⁴ 2148 ± 34	²⁴⁷ 2130 ± 32		
10	ader-a-004	0	959123	³⁵⁷ 1748	⁴⁶¹ 6144 ± 0	⁴¹⁰ 1246 ± 1	³⁶⁵ 1204 ± 1	³⁵⁷ 1230 ± 2	³²² 1207 ± 2	²⁷² 1254 ± 1	²²¹ 1840 ± 34	²²⁰ 1828 ± 31		
11	advance-003	258867	78699	¹⁰⁴ 518	¹⁹⁷ 2048 ± 0	¹⁷⁶ 586 ± 0	¹⁴⁹ 584 ± 0	¹²⁹ 583 ± 0	¹⁰⁸ 588 ± 0	⁸⁷ 591 ± 1	²²⁰ 1813 ± 17	²¹⁶ 1788 ± 26		
12	advance-004	803133	954494	¹⁴⁶ 679	²⁶¹ 2048 ± 0	³⁶⁸ 1099 ± 20	³³⁸ 1107 ± 15	³²⁰ 1093 ± 21	²⁸³ 1103 ± 21	²⁴¹ 1138 ± 21	²³³ 1935 ± 35	²³⁵ 1936 ± 32		
13	afisbiometrics-000	545886	32882	²⁵⁴ 1088	¹⁶ 512 ± 0	⁴⁰¹ 1219 ± 1	³⁴⁵ 1135 ± 1	³³¹ 1137 ± 2	²⁹⁴ 1137 ± 1	²⁴³ 1147 ± 1	¹⁸¹ 1400 ± 29	¹⁷⁸ 1357 ± 32		
14	affengine-000	151875	382842	³⁸ 177	⁴³⁵ 4096 ± 0	¹⁶ 107 ± 0	¹³ 112 ± 0	³³ 284 ± 2	¹⁵⁰ 697 ± 2	⁴¹³ 3299 ± 17	⁴⁵⁴ 54329 ± 140	⁴⁵³ 56195 ± 256		
15	aifirst-001	224157	808777	⁹¹ 485	¹⁰⁵ 2048 ± 0	¹⁷⁸ 587 ± 2	¹⁴² 568 ± 2	¹³⁰ 584 ± 3	¹¹⁴ 601 ± 6	¹³⁸ 755 ± 5	¹⁵⁶ 1099 ± 14	¹⁵⁸ 1087 ± 45		
16	aigen-001	256958	595227	²⁶⁹ 1136	²⁸⁶ 2048 ± 0	⁴⁶⁴ 1448 ± 9	⁴³⁵ 1451 ± 8	⁴⁴² 1759 ± 6	⁴³⁸ 2594 ± 4	⁴²⁵ 5691 ± 44	³²⁰ 3772 ± 57	³¹⁹ 3736 ± 56		
17	aigen-002	205300	1316138	²⁰⁸ 874	²⁵⁰ 2048 ± 0	¹⁷⁵ 586 ± 24	¹⁴⁸ 582 ± 4	²⁴² 920 ± 4	⁴²³ 1758 ± 5	⁴²⁴ 5427 ± 17	³¹⁷ 3678 ± 44	³¹⁶ 3646 ± 48		
18	ailabs-001	1054663	338989	²⁸⁶ 1252	³⁰⁸ 2048 ± 0	²¹⁵ 664 ± 4	²¹⁶ 774 ± 50	³³⁵ 1145 ± 12	⁴²⁹ 1972 ± 74	⁴²¹ 5205 ± 272	⁴⁶⁹ 104034 ± 661	⁴⁶⁹ 103415 ± 7722		
19	aimall-002	370156	25210	³³⁴ 1576	²⁰⁸ 2048 ± 0	²⁵⁴ 776 ± 4	²⁷⁶ 927 ± 27	²⁵⁰ 940 ± 21	²³² 955 ± 34	¹⁹⁶ 1003 ± 75	⁴⁶⁵ 72811 ± 7399	⁴⁶³ 71216 ± 6286		
20	aimall-003	504324	171935	³⁶⁹ 1913	⁷⁹ 1024 ± 0	²¹³ 662 ± 1	²⁰⁵ 740 ± 51	¹⁸⁹ 752 ± 62	¹⁶⁵ 741 ± 46	¹⁴⁹ 807 ± 47	⁴³⁹ 34565 ± 93	⁴⁴⁰ 34598 ± 118		
21	aiseemu-001	0	1005354	⁴¹⁰ 2697	⁴¹⁴ 4096 ± 0	³⁴⁶ 1001 ± 1	³¹⁰ 1017 ± 0	²⁹⁰ 1014 ± 5	²⁶⁰ 1022 ± 2	²¹⁵ 1059 ± 4	³³⁷ 4864 ± 25	³³⁸ 4855 ± 32		
22	aiseemu-002	0	1216980	⁴³¹ 3446	⁴¹⁸ 4096 ± 0	⁴²⁵ 1298 ± 5	³⁹³ 1303 ± 4	³⁸³ 1313 ± 2	³⁶² 1329 ± 0	³⁰⁰ 1348 ± 2	³⁴⁰ 4917 ± 37	³³⁹ 4916 ± 37		
23	aiunionface-000	241642	840295	⁷² 402	²⁸⁵ 2048 ± 0	²⁰² 637 ± 13	²¹¹ 754 ± 41	²⁹² 1025 ± 28	³¹⁰ 1179 ± 29	³⁶⁶ 1639 ± 47	¹⁵⁰ 1072 ± 19	¹⁵⁶ 1080 ± 47		
24	aize-001	268456	168970	³²⁰ 1436	³²⁹ 2048 ± 0	¹¹² 437 ± 10	⁹ 440 ± 8	¹¹⁶ 542 ± 17	¹⁶⁸ 756 ± 27	³⁶¹ 1583 ± 53	²³⁵ 1937 ± 22	²²⁹ 1919 ± 23		
25	aize-002	257106	182517	¹²⁴ 586	¹⁵¹ 2048 ± 0	¹²⁵ 467 ± 1	¹⁰⁵ 479 ± 1	¹⁹⁰ 756 ± 1	⁴¹⁰ 1477 ± 1	⁶⁵ 597 ± 16	⁶⁹ 598 ± 14			
26	ajou-001	363257	31734	⁸³ 442	¹⁷⁵ 2048 ± 0	¹⁴⁸ 530 ± 0	¹²⁸ 536 ± 0	¹¹¹ 535 ± 0	⁹⁶ 549 ± 0	⁸³ 577 ± 0	⁶⁴ 597 ± 19	⁶⁸ 596 ± 13		
27	alchera-004	1001019	388616	²⁹¹ 1270	¹⁵⁰ 2048 ± 0	³³⁶ 975 ± 0	²⁸³ 955 ± 0	²⁶² 960 ± 0	²⁴⁵ 989 ± 0	²⁴⁴ 1152 ± 1	³¹² 3529 ± 54	³¹² 3530 ± 63		
28	alchera-005	1001019	388616	²⁸⁹ 1268	²⁷⁵ 2048 ± 0	³³³ 969 ± 1	²⁹⁰ 987 ± 3	²⁷³ 985 ± 3	²⁴⁹ 998 ± 0	²⁵⁰ 1162 ± 2	³¹¹ 3481 ± 59	³⁰⁸ 3422 ± 57		
29	alfabeta-001	128232	21780	⁸ 73	³² 512 ± 0	⁴⁹ 271 ± 0	⁴¹ 276 ± 0	⁸⁰ 459 ± 2	²⁰⁸ 886 ± 2	³⁹⁷ 2547 ± 9	⁴⁴ 470 ± 25	⁴⁶ 458 ± 20		
30	alice-000	1741293	19355	³⁵³ 1732	⁴¹⁰ 4096 ± 0	³²⁴ 950 ± 2	²⁷⁸ 933 ± 1	²⁵⁴ 949 ± 1	²⁵⁸ 1011 ± 3	²⁷⁶ 1264 ± 8	⁴⁰⁶ 14975 ± 201	⁴⁰⁶ 14890 ± 229		
31	alleyes-000	507636	997090	²⁰⁵ 857	²⁴³ 2048 ± 0	²⁵⁸ 784 ± 1	²⁸⁹ 970 ± 61	²⁶⁷ 974 ± 62	²²⁸ 943 ± 69	²¹³ 1057 ± 23	¹⁷³ 1298 ± 34	¹⁷⁵ 1303 ± 51		
32	allgovision-000	172509	155862	¹¹⁶ 561	²³⁵ 2048 ± 0	⁹¹ 384 ± 8	⁷⁴ 395 ± 17	⁶¹ 413 ± 14	⁷² 471 ± 14	¹²⁵ 710 ± 21	⁴²⁹ 29903 ± 406	⁴³⁰ 29735 ± 194		
33	alphaface-001	259849	81636	¹⁰⁷ 527	²⁶⁵ 2048 ± 0	¹⁸⁵ 612 ± 1	¹⁵⁹ 613 ± 3	¹⁴¹ 612 ± 1	¹²⁰ 619 ± 1	¹⁰⁵ 640 ± 2	¹⁴¹ 1008 ± 10	¹⁴¹ 1002 ± 19		
34	alphaface-002	768995	70692	³¹⁹ 1434	¹²⁶ 2048 ± 0	¹⁹⁷ 628 ± 2	²⁰⁸ 746 ± 19	¹⁸⁸ 751 ± 18	¹⁷² 779 ± 22	¹⁵⁴ 828 ± 40	¹³¹ 945 ± 25	¹³² 935 ± 17		
35	amplifiedgroup-001	0	47053	¹² 81	⁶⁷ 866 ± 2	¹³ 93 ± 0	-	-	-	-	⁴⁵⁷ 57803 ± 4210	⁴⁵⁴ 56365 ± 1196		
36	androvideo-000	174847	585063	⁷³ 403	¹⁶⁴ 2048 ± 0	⁵¹ 277 ± 0	⁴⁵ 285 ± 0	³⁸ 314 ± 0	⁴⁴ 372 ± 1	⁹⁶ 620 ± 0	²⁸² 2860 ± 28	²⁸¹ 2847 ± 22		
37	anke-004	349388	410776	¹⁵⁶ 706	³⁶⁴ 2056 ± 0	¹⁹⁵ 625 ± 1	¹⁶⁵ 627 ± 2	¹⁵⁰ 635 ± 3	¹³³ 653 ± 2	¹⁹² 982 ± 8	⁸⁵ 633 ± 22	⁸⁵ 632 ± 34		
38	anke-005	328553	429160	²⁶⁷ 1134	³⁷⁴ 2056 ± 0	¹⁷⁹ 590 ± 2	¹⁵³ 594 ± 5	¹³⁸ 601 ± 3	¹²⁷ 638 ± 4	¹⁵³ 821 ± 24	⁹⁶ 685 ± 19	⁹⁸ 687 ± 26		
39	antheus-000	119453	41994	²⁰ 116	⁵² 520 ± 0	¹⁷ 109 ± 1	²⁸ 187 ± 1	¹⁹ 189 ± 1	¹⁶ 195 ± 1	¹⁸ 236 ± 2	³⁶⁷ 6901 ± 268	³⁶⁷ 6936 ± 103		
40	antheus-001	119453	41962	²¹ 118	⁵³ 520 ± 0	²⁰ 120 ± 1	³⁶ 265 ± 13	⁸⁶ 468 ± 22	³²⁵ 1223 ± 27	³⁹⁹ 2660 ± 87	³⁶² 6218 ± 47	³⁶¹ 6216 ± 45		
41	anyvision-004	401001	630797	²⁵⁸ 1102	⁷¹ 1024 ± 0	⁸⁰ 355 ± 1	-	-	-	-	²³⁰ 1891 ± 51	²²¹ 1829 ± 85		
42	anyvision-005	190979	116595	²²⁷ 963	⁷³ 1024 ± 0	³⁴¹ 985 ± 1	³⁰⁰ 997 ± 1	²⁸⁶ 1004 ± 1	²⁴⁷ 995 ± 1	¹⁹⁵ 995 ± 1	¹⁰⁷ 733 ± 14	¹⁰⁷ 733 ± 16		
43	armatura-001	0	374608	²⁷³ 1151	²⁹⁷ 2048 ± 0	²²⁶ 688 ± 1	¹⁹⁰ 689 ± 1	¹⁷² 693 ± 1	¹⁵³ 708 ± 3	¹³⁹ 756 ± 13	¹⁹ 270 ± 17	²³ 268 ± 11		
44	armatura-003	0	836082	³³⁵ 1577	⁴⁶³ 6144 ± 0	³⁵⁶ 1028 ± 1	³¹⁵ 1032 ± 1	²⁹⁵ 1027 ± 0	²⁶³ 1036 ± 1	²⁰⁷ 1041 ± 3	⁴⁵³ 51850 ± 56	⁴⁵² 51835 ± 48		

Notes

- 1 The configuration size does not capture static data included in libraries.
- 2 The library size is the combined total of all files provided in the submission lib folder. These libraries e.g. OpenCV may or may not be installed on any end user's platform natively and would not need to be installed with the algorithm. Some developers put neural network models in their libraries.
- 3 The memory usage is the peak resident set size reported by the ps system call during template generation.
- 4 The median template creation times are measured on Intel®Xeon®CPU E5-2630 v4 @ 2.20GHz processors.
- 5 The comparison durations, in nanoseconds, are estimated using std::chrono::high_resolution_clock which on the machine in (2) counts 1ns clock ticks. Precision is somewhat worse than that however. The \pm value is the median absolute deviation times 1.48 for Normal consistency.

Table 8: Summary of algorithms and properties included in this report. The red superscripts give ranking for the quantity in that column.

	ALGORITHM	CONFIG	LIBRARY	TEMPLATE								COMPARISON ⁴	
	NAME	DATA	DATA	MEMORY	SIZE	MUGSHOT	480x720	960x1440	1600x2400	3000x4500	GENUINE	IMPOSTOR	TIME (ns) ⁵
		(KB) ¹	(KB) ²	(MB) ³	(B)	MUGSHOT	480x720	960x1440	1600x2400	3000x4500	GENUINE	IMPOSTOR	
45	asusaics-000	257418	245320	¹³¹ 605	¹³⁵ 2048 ± 0	¹³⁵ 484 ± 13	¹²¹ 506 ± 21	²¹⁴ 850 ± 26	⁴²⁵ 1789 ± 61	⁴²⁷ 6305 ± 188	³⁴⁹ 5455 ± 78	³⁴⁸ 5422 ± 112	
46	asusaics-001	257418	245330	¹²⁸ 595	⁴¹¹ 4096 ± 0	²⁸³ 842 ± 17	³⁰⁷ 1008 ± 20	⁴⁰³ 1377 ± 28	⁴³⁷ 2423 ± 90	⁴³¹ 7284 ± 277	³⁷⁷ 8618 ± 42	³⁷⁷ 8638 ± 136	
47	autentika-000	266093	3200425	³⁷⁴ 1942	¹⁰⁶ 2048 ± 0	¹⁵⁹ 553 ± 1	¹⁵⁶ 605 ± 1	¹⁴⁰ 609 ± 2	¹¹⁶ 608 ± 1	⁹⁵ 618 ± 2	⁴⁶⁶ 72833 ± 577	⁴⁶⁴ 71829 ± 541	
48	authenmetric-003	293599	39492	²³¹ 982	²⁰⁴ 2048 ± 0	³⁴⁴ 992 ± 1	³⁰⁵ 1006 ± 1	²⁸⁵ 1003 ± 2	²⁵³ 1002 ± 1	²⁰⁵ 1036 ± 1	²¹¹ 1757 ± 19	²¹¹ 1755 ± 19	
49	authenmetric-004	381165	39492	²⁸¹ 1214	¹⁶⁸ 2048 ± 0	³⁰⁸ 910 ± 1	²⁶⁷ 909 ± 1	²³⁸ 915 ± 1	²²⁰ 921 ± 2	¹⁸⁶ 950 ± 1	²⁰⁷ 1724 ± 14	²⁰⁶ 1691 ± 29	
50	aware-005	300017	26320	²⁸⁸ 1265	¹⁰⁰ 1572 ± 0	³⁰² 886 ± 23	³¹⁹ 1038 ± 21	³²⁵ 1121 ± 22	³⁶⁴ 1337 ± 58	³⁸⁶ 2195 ± 144	¹⁹⁰ 1475 ± 63	¹⁸⁷ 1427 ± 115	
51	aware-006	298543	14124	²²⁴ 943	¹⁵ 352 ± 0	³⁸⁶ 1148 ± 3	³⁵⁰ 1146 ± 2	³⁴⁹ 1190 ± 2	³⁴⁸ 1306 ± 20	³⁷⁶ 1754 ± 84	²⁷² 2598 ± 42	²⁷² 2559 ± 60	
52	awiros-001	15499	87480	¹⁴ 88	³¹ 512 ± 0	¹⁴ 97 ± 6	¹¹ 98 ± 4	¹² 138 ± 6	²³ 225 ± 7	⁷⁹ 556 ± 8	¹⁵² 1079 ± 44	¹⁵⁰ 1050 ± 45	
53	awiros-002	289016	203723	¹¹⁷ 562	¹⁸⁷ 2048 ± 0	¹²⁹ 479 ± 0	¹¹⁷ 500 ± 0	¹¹⁰ 534 ± 0	¹¹⁹ 618 ± 0	¹⁸⁴ 946 ± 1	²³⁶ 1966 ± 31	²³⁷ 1957 ± 25	
54	aximetria-001	408902	487912	¹⁴⁵ 674	¹⁴⁶ 2048 ± 0	³⁵¹ 1013 ± 1	³¹¹ 1023 ± 21	²⁹⁶ 1029 ± 5	²⁵⁰ 999 ± 2	²²⁷ 1091 ± 5	³³¹ 4401 ± 94	³³⁰ 4490 ± 80	
55	ayftech-001	195423	43580	¹⁶⁵ 731	³⁴ 512 ± 0	¹⁰³ 408 ± 23	¹⁰³ 476 ± 52	²⁰² 814 ± 108	⁴²⁷ 1827 ± 384	⁴²³ 5412 ± 1029	⁷⁶ 615 ± 16	¹²⁶ 885 ± 44	
56	ayonix-000	58505	5252	⁶ 69	⁸⁷ 1036 ± 0	² 18 ± 2	-	-	-	-	⁷⁸ 621 ± 23	⁸² 620 ± 26	
57	beethedata-000	227849	1087592	¹¹⁵ 555	¹²⁸ 2048 ± 0	¹²³ 465 ± 0	¹⁰¹ 467 ± 0	⁸⁴ 468 ± 0	⁷⁰ 467 ± 0	⁵² 467 ± 0	²⁴⁴ 2121 ± 34	²⁴⁵ 2110 ± 38	
58	beyneai-000	256958	591433	²⁶⁴ 1124	³⁰⁴ 2048 ± 0	¹¹⁵ 451 ± 8	⁹³ 449 ± 1	¹⁹² 767 ± 7	⁴²⁰ 1603 ± 25	⁴¹⁹ 4669 ± 124	³¹⁸ 3730 ± 57	³¹⁷ 3668 ± 54	
59	biocube-001	25030	6192987	⁸⁷ 458	⁴³⁴ 4096 ± 0	⁵⁶ 282 ± 22	⁴⁶ 292 ± 24	¹⁰⁸ 521 ± 57	¹⁴⁷ 684 ± 59	²⁸¹ 1282 ± 68	⁴²⁰ 21787 ± 96	⁴²⁰ 21812 ± 109	
60	bioidtechswiss-001	1178769	120811	³²¹ 1455	¹⁹ 512 ± 0	³³¹ 966 ± 4	³⁸⁴ 1270 ± 270	³⁷⁶ 1294 ± 96	³⁹⁰ 1409 ± 157	³⁸⁰ 1793 ± 79	²⁷³ 2610 ± 25	²⁷³ 2624 ± 32	
61	bioidtechswiss-002	744786	114842	²³⁶ 993	²⁷ 512 ± 0	³¹³ 917 ± 2	²⁷⁷ 930 ± 2	²⁵⁵ 952 ± 2	²²⁹ 947 ± 3	²¹⁴ 1058 ± 11	²⁵⁰ 2177 ± 29	²⁵¹ 2170 ± 31	
62	bm-001	287734	38076	²⁸ 148	¹ 64 ± 0	¹¹³ 444 ± 88	-	-	-	-	²²⁹ 1887 ± 31	²²⁷ 1877 ± 26	
63	boetech-001	261376	88710	³¹¹ 1384	²⁸⁴ 2048 ± 0	⁴⁸ 271 ± 1	³⁸ 268 ± 1	³⁰ 273 ± 0	³¹ 286 ± 1	²⁶ 318 ± 1	⁴⁶² 68519 ± 1921	⁴⁶¹ 67648 ± 822	
64	boetech-002	294347	88710	³²⁶ 1489	²⁵⁷ 2048 ± 0	⁶⁶ 305 ± 4	⁵⁰ 296 ± 1	³⁴ 302 ± 1	³⁴ 313 ± 1	³⁰ 348 ± 2	⁴⁶³ 68921 ± 2137	⁴⁶² 69473 ± 2104	
65	bresee-001	287880	23227	²⁸² 1214	¹³⁹ 2048 ± 0	⁴⁰³ 1223 ± 3	³⁶⁸ 1216 ± 1	³⁸⁷ 1331 ± 1	³²⁸ 1227 ± 1	³⁰⁶ 1360 ± 1	⁴⁴² 37240 ± 655	⁴⁴² 37167 ± 584	
66	bresee-002	313627	30902	³⁷⁶ 1956	²³¹ 2048 ± 0	²⁴⁵ 743 ± 4	³⁴⁸ 1143 ± 2	³³⁶ 1146 ± 2	²⁹⁷ 1148 ± 2	²⁵⁷ 1176 ± 2	²¹⁴ 1778 ± 22	²¹⁴ 1775 ± 23	
67	camvi-002	236278	225285	¹⁶⁷ 737	⁸⁰ 1024 ± 0	²²¹ 677 ± 7	²⁰³ 726 ± 36	²¹⁸ 869 ± 28	²⁹⁰ 1129 ± 43	⁴⁰⁴ 2785 ± 113	⁷⁴ 612 ± 26	⁷⁴ 603 ± 20	
68	camvi-004	280733	615819	²²⁰ 919	³¹¹ 2048 ± 0	²⁴⁸ 759 ± 10	²⁴² 861 ± 17	²⁷⁶ 986 ± 34	³⁴⁵ 1279 ± 51	⁴⁰⁶ 2891 ± 158	¹³² 948 ± 40	¹³³ 963 ± 31	
69	canon-003	2550850	101378	⁴⁵⁹ 5472	⁴⁶⁴ 6180 ± 0	⁴¹⁴ 1263 ± 3	³⁸¹ 1263 ± 1	³⁷³ 1283 ± 1	³⁵⁶ 1320 ± 1	³⁴³ 1482 ± 2	³³⁵ 4783 ± 17	³³³ 4780 ± 19	
70	canon-004	2399160	114188	⁴⁶¹ 5956	⁴⁶⁵ 6200 ± 0	³²² 948 ± 4	²⁸⁴ 955 ± 3	²⁶¹ 959 ± 3	²³⁸ 977 ± 3	²²⁰ 1064 ± 2	³⁷³ 7172 ± 63	³⁷² 7169 ± 51	
71	ceiec-003	260371	88707	⁷⁹ 430	¹¹⁸ 2048 ± 0	²⁷¹ 817 ± 4	²⁵⁶ 883 ± 57	²²⁹ 897 ± 60	²¹³ 899 ± 72	¹⁸² 944 ± 72	²⁵⁷ 2256 ± 38	²⁵⁷ 2241 ± 54	
72	ceiec-004	263476	67011	⁷⁴ 408	¹⁶⁷ 2048 ± 0	³⁵⁴ 1024 ± 1	³¹³ 1027 ± 1	²⁹⁴ 1027 ± 1	²⁶² 1030 ± 1	²¹¹ 1055 ± 1	²²³ 1844 ± 26	²²² 1836 ± 20	
73	chosun-001	765615	707	⁹⁵ 491	¹⁰³ 2048 ± 0	²⁵⁷ 783 ± 2	²³¹ 826 ± 4	⁴⁴¹ 1662 ± 13	⁴⁴² 3679 ± 67	⁴³⁸ 11694 ± 243	¹³⁸ 998 ± 25	¹⁴⁸ 1035 ± 11	
74	chosun-002	234001	31875	⁸⁴ 450	¹⁴³ 2048 ± 0	⁴⁴ 248 ± 3	⁴⁰ 273 ± 3	⁴³⁶ 1495 ± 14	⁴⁴³ 7920 ± 90	⁴³⁹ 80302 ± 1349	⁸⁰ 623 ± 17	⁸⁷ 634 ± 13	
75	chtface-005	408364	311100	³¹⁵ 1412	²⁷³ 2048 ± 0	⁷⁰ 322 ± 0	⁵⁴ 316 ± 1	⁴⁰ 325 ± 2	³⁶ 324 ± 1	⁴² 411 ± 2	²³¹ 1907 ± 19	²²⁸ 1898 ± 23	
76	chtface-006	733645	610439	³⁹⁵ 2417	¹³⁷ 2048 ± 0	¹⁴⁶ 522 ± 1	¹²² 514 ± 1	¹¹² 536 ± 2	⁹⁹ 561 ± 1	¹¹⁹ 693 ± 2	²⁴¹ 2034 ± 41	²⁴² 2049 ± 29	
77	cist-001	0	300551	¹²¹ 583	²²² 2048 ± 0	³³⁴ 972 ± 0	²⁹¹ 977 ± 1	²⁷² 981 ± 0	²⁴¹ 983 ± 0	²¹⁸ 1061 ± 0	²⁸⁸ 2947 ± 20	²⁸⁷ 2940 ± 22	
78	clearviewai-000	342491	211852	⁴¹⁶ 2750	¹⁶⁹ 2048 ± 0	⁴⁵³ 1402 ± 1	⁴²² 1403 ± 1	⁴¹⁹ 1412 ± 1	³⁹³ 1420 ± 1	³²² 1418 ± 1	¹⁹⁶ 1592 ± 37	¹⁹⁴ 1561 ± 37	
79	cloesli-001	420342	9851	¹⁷⁸ 773	⁴³⁰ 4096 ± 0	²⁸² 839 ± 1	²³⁶ 843 ± 1	²¹² 841 ± 1	¹⁹⁴ 845 ± 1	¹⁶⁴ 865 ± 1	³⁴⁸ 5404 ± 17	³⁴⁷ 5400 ± 25	
80	cloudmatrix-001	10390	542121	⁴⁶ 249	²⁰² 2048 ± 0	¹⁹ 114 ± 1	¹⁴ 117 ± 0	¹¹ 118 ± 0	¹⁰ 123 ± 1	¹¹ 169 ± 1	⁴⁵⁰ 50263 ± 212	⁴⁴⁹ 50243 ± 237	
81	cloudmatrix-002	256635	693318	²⁴¹ 1030	¹⁷³ 2048 ± 0	⁹⁵ 395 ± 1	⁷⁶ 398 ± 1	⁵⁷ 399 ± 1	⁵² 402 ± 1	⁴⁷ 437 ± 20	⁴⁴⁹ 49578 ± 120	⁴⁴⁸ 49602 ± 180	
82	cloudwalk-hr-003	383739	144263	²³⁴ 984	³⁷⁸ 2057 ± 0	¹⁸⁴ 606 ± 0	¹⁵¹ 588 ± 0	¹³⁴ 594 ± 0	¹¹⁸ 612 ± 1	-	³⁶⁹ 6982 ± 80	³⁶⁸ 6972 ± 84	
83	cloudwalk-hr-004	502916	520169	³¹⁴ 1394	³³¹ 2049 ± 0	²⁹⁵ 873 ± 1	²⁵¹ 877 ± 1	²²³ 876 ± 1	²⁰⁴ 879 ± 1	¹⁷⁵ 902 ± 3	³⁹¹ 11652 ± 127	³⁹¹ 11608 ± 123	
84	cloudwalk-mt-005	846026	573253	⁴²³ 2928	³⁰⁵ 2048 ± 0	³⁹⁰ 1179 ± 3	³⁶⁴ 1200 ± 3	³⁵⁴ 1209 ± 3	³²⁷ 1226 ± 5	²⁶⁹ 1229 ± 3	³⁹⁸ 12525 ± 225	³⁹⁷ 12394 ± 152	
85	cloudwalk-mt-006	563322	480071	⁴¹⁹ 2836	²⁹⁹ 2048 ± 0	⁴⁴⁶ 1385 ± 0	⁴¹⁶ 1392 ± 1	⁴¹³ 1398 ± 1	³⁸⁵ 1397 ± 4	³³² 1444 ± 2	³⁰³ 3364 ± 96	³⁰² 3324 ± 83	
86	codeline-000	361659	138388	²⁷⁹ 1188	³²⁶ 2048 ± 0	⁴⁶⁵ 1453 ± 0	⁴³⁷ 1456 ± 2	⁴³⁰ 1456 ± 0	⁴⁰³ 1457 ± 0	³⁴⁴ 1483 ± 1	²⁴⁸ 2171 ± 69	²⁵³ 2194 ± 84	
87	cogent-007	621565	72316	³⁶⁸ 1884	⁶² 550 ± 0	⁴³⁴ 1329 ± 2	⁴⁰⁴ 1333 ± 5	³⁹¹ 1337 ± 4	³⁶⁶ 1353 ± 5	³¹⁶ 1390 ± 4	³² 355 ± 8	³⁵ 367 ± 14	
88	cogent-008	856817	73587	³⁸⁷ 2173	⁶³ 550 ± 0	⁴⁵⁷ 1412 ± 1	⁴²⁷ 1419 ± 2	⁴²² 1426 ± 3	³⁹⁸ 1437 ± 3	³⁴¹ 1476 ± 1	⁴⁰ 436 ± 14	⁴³ 441 ± 23	

Notes

- 1 The configuration size does not capture static data included in libraries.
- 2 The library size is the combined total of all files provided in the submission lib folder. These libraries e.g. OpenCV may or may not be installed on any end user's platform natively and would not need to be installed with the algorithm. Some developers put neural network models in their libraries.
- 3 The memory usage is the peak resident set size reported by the ps system call during template generation.
- 4 The median template creation times are measured on Intel®Xeon®CPU E5-2630 v4 @ 2.20GHz processors.
- 5 The comparison durations, in nanoseconds, are estimated using std::chrono::high_resolution_clock which on the machine in (2) counts 1ns clock ticks. Precision is somewhat worse than that however. The ± value is the median absolute deviation times 1.48 for Normal consistency.

Table 9: Summary of algorithms and properties included in this report. The red superscripts give ranking for the quantity in that column.

	ALGORITHM	CONFIG	LIBRARY	TEMPLATE								COMPARISON ⁴									
				NAME	DATA	DATA	MEMORY	SIZE	GENERATION TIME (ms) ⁴				TIME (ns) ⁵								
									(KB) ¹	(KB) ²	(MB) ³	(B)	MUGSHOT	480x720	960x1440	1600x2400	3000x4500	GENUINE	IMPOSTOR		
89	cognitec-003	471458	62502	194	817	351	2052 ± 0	85	366 ± 9	79	403 ± 9	59	408 ± 9	58	424 ± 9	60	509 ± 13	308	3417 ± 51	310	3433 ± 53
90	cognitec-004	705645	62678	123	585	353	2052 ± 0	120	463 ± 9	113	497 ± 9	99	504 ± 10	87	521 ± 10	97	631 ± 12	294	3028 ± 197	295	3059 ± 238
91	cor-001	1194948	11240	285	1249	380	2060 ± 0	235	699 ± 3	244	863 ± 76	217	865 ± 80	201	872 ± 89	187	952 ± 39	472	270145 ± 2259	472	282686 ± 11788
92	coretech-000	186423	43964	71	393	22	512 ± 0	183	602 ± 15	176	659 ± 12	332	1139 ± 24	298	1149 ± 25	251	1165 ± 23	28	333 ± 14	29	321 ± 13
93	coretech-001	235361	305490	330	1524	290	2048 ± 0	227	688 ± 7	193	695 ± 7	219	870 ± 17	205	879 ± 15	168	877 ± 15	81	625 ± 25	90	641 ± 25
94	corsight-002	1474921	32093	380	2061	383	2080 ± 0	423	1290 ± 1	389	1287 ± 1	374	1290 ± 1	349	1307 ± 2	315	1388 ± 4	424	24953 ± 637	423	24263 ± 578
95	corsight-003	1413063	32198	341	1637	380	2080 ± 0	398	1202 ± 2	363	1190 ± 5	352	1199 ± 3	329	1236 ± 3	301	1349 ± 7	428	28754 ± 434	429	28279 ± 446
96	csc-002	0	519768	309	1376	58	544 ± 0	127	473 ± 0	111	494 ± 0	91	481 ± 1	78	490 ± 1	64	514 ± 5	35	367 ± 11	36	371 ± 10
97	csc-003	0	400435	339	1609	59	544 ± 0	139	499 ± 0	116	500 ± 1	98	502 ± 0	84	508 ± 1	72	535 ± 4	38	393 ± 8	38	397 ± 7
98	ctcbcbank-000	257208	599238	119	570	300	2048 ± 0	166	568 ± 43	157	606 ± 38	171	690 ± 53	155	711 ± 50	155	831 ± 51	313	3551 ± 87	335	4805 ± 209
99	ctcbcbank-001	275511	599238	129	603	241	2048 ± 0	207	652 ± 35	218	781 ± 30	222	875 ± 43	212	898 ± 51	203	1030 ± 47	321	3926 ± 45	320	3924 ± 56
100	cu-face-002	812008	38655	166	735	413	4096 ± 0	363	1054 ± 1	324	1059 ± 0	309	1060 ± 0	273	1063 ± 1	222	1070 ± 0	456	57287 ± 1750	456	57027 ± 945
101	cubox-001	369627	75427	139	649	327	2048 ± 0	305	907 ± 1	263	902 ± 1	233	903 ± 0	218	917 ± 0	179	931 ± 0	177	1379 ± 37	184	1417 ± 38
102	cubox-002	542254	90975	377	1964	206	2048 ± 0	315	921 ± 1	271	921 ± 1	243	922 ± 1	224	933 ± 1	197	1003 ± 1	239	2008 ± 72	239	1969 ± 57
103	cudocommunication-001	385258	341277	251	1077	271	2048 ± 0	317	925 ± 1	273	923 ± 1	248	928 ± 1	223	932 ± 0	189	964 ± 1	268	2534 ± 20	270	2537 ± 20
104	cuhkee-001	787853	74917	402	2515	338	2052 ± 0	338	977 ± 31	-	-	-	-	-	-	-	-	274	2719 ± 60	278	2783 ± 56
105	cybercore-002	166096	7374	405	2564	323	2048 ± 0	137	489 ± 1	115	500 ± 4	97	500 ± 1	82	499 ± 2	70	528 ± 1	396	12389 ± 123	396	12352 ± 112
106	cybercore-003	289176	7969	449	4310	402	4096 ± 0	284	844 ± 2	241	855 ± 4	216	864 ± 4	200	862 ± 4	169	878 ± 2	355	5744 ± 41	350	5737 ± 31
107	cyberextruder-003	253300	12354	81	437	37	512 ± 0	93	390 ± 1	71	388 ± 1	55	393 ± 1	50	399 ± 1	46	435 ± 1	10	198 ± 4	11	189 ± 8
108	cyberextruder-004	169301	12354	64	349	2	128 ± 0	38	206 ± 0	28	208 ± 0	23	209 ± 0	24	229 ± 0	20	249 ± 1	5	145 ± 14	6	155 ± 14
109	cyberlink-009	588443	102201	346	1704	451	4164 ± 0	445	1384 ± 2	420	1395 ± 2	412	1398 ± 2	386	1401 ± 2	336	1456 ± 2	24	299 ± 17	26	304 ± 16
110	cyberlink-010	1590818	102180	435	3672	471	8260 ± 0	415	1265 ± 2	390	1314 ± 5	377	1294 ± 2	341	1273 ± 2	289	1305 ± 2	45	476 ± 23	48	472 ± 14
111	dahua-006	831641	119261	455	5068	185	2048 ± 0	451	1398 ± 2	421	1397 ± 1	416	1404 ± 1	388	1402 ± 1	319	1402 ± 1	18	249 ± 13	20	250 ± 11
112	dahua-007	1578737	119418	466	7237	405	4096 ± 0	450	1393 ± 2	411	1373 ± 1	405	1378 ± 1	376	1378 ± 1	311	1379 ± 2	36	367 ± 102	39	434 ± 108
113	daon-000	280726	2307	379	2013	382	2065 ± 0	162	562 ± 3	146	581 ± 5	194	791 ± 9	191	838 ± 15	210	1055 ± 32	409	16052 ± 88	409	16041 ± 85
114	decatur-000	350495	171271	215	907	443	4100 ± 0	353	1024 ± 2	-	-	-	-	-	-	-	-	390	11439 ± 80	390	11418 ± 112
115	decatur-001	342866	253734	327	1507	343	2052 ± 0	370	1103 ± 2	325	1064 ± 2	312	1063 ± 2	275	1067 ± 2	223	1084 ± 2	73	610 ± 19	73	602 ± 8
116	deepglint-004	1073382	261571	426	3084	309	2048 ± 0	467	1470 ± 1	441	1474 ± 1	435	1485 ± 1	408	1474 ± 1	347	1492 ± 2	359	5961 ± 34	359	5955 ± 29
117	deepglint-005	960326	213877	425	2947	133	2048 ± 0	456	1408 ± 1	429	1431 ± 2	421	1424 ± 3	395	1424 ± 3	334	1446 ± 2	365	6765 ± 38	364	6765 ± 40
118	deepsea-001	147497	336250	66	358	81	1024 ± 0	198	630 ± 7	209	752 ± 37	187	746 ± 30	160	727 ± 32	152	820 ± 32	182	1401 ± 37	189	1467 ± 50
119	deepsense-000	357113	936618	467	7618	288	2048 ± 0	216	664 ± 3	174	645 ± 1	159	660 ± 2	145	687 ± 2	150	808 ± 3	46	480 ± 22	47	459 ± 34
120	deepsense-001	73173	1288355	456	5314	43	512 ± 0	383	1142 ± 2	353	1164 ± 3	347	1183 ± 3	319	1201 ± 3	295	1323 ± 2	261	2356 ± 35	261	2354 ± 42
121	dermalog-010	0	525908	239	1023	23	512 ± 0	201	635 ± 0	172	640 ± 1	152	639 ± 4	130	647 ± 3	118	691 ± 5	42	444 ± 13	32	341 ± 26
122	dermalog-011	0	278395	159	715	3	128 ± 0	76	343 ± 0	60	345 ± 0	43	347 ± 0	39	351 ± 0	34	363 ± 0	23	299 ± 19	22	253 ± 14
123	dicio-001	61751	119517	11	77	54	520 ± 0	152	538 ± 0	141	563 ± 10	239	915 ± 3	426	1800 ± 7	422	5286 ± 30	278	2818 ± 20	279	2807 ± 31
124	didiglobalface-001	259849	70680	106	527	186	2048 ± 0	186	612 ± 1	169	633 ± 3	148	634 ± 3	131	650 ± 15	111	666 ± 4	134	973 ± 20	135	988 ± 20
125	didiglobalface-002	260054	161508	196	826	314	2048 ± 0	193	622 ± 1	168	633 ± 1	155	642 ± 2	135	659 ± 4	130	726 ± 15	57	560 ± 10	60	567 ± 13
126	digidata-000	133370	30249	49	257	115	2048 ± 0	84	361 ± 0	64	360 ± 0	48	361 ± 0	42	363 ± 0	36	380 ± 0	243	2084 ± 37	241	2039 ± 42
127	digidata-001	254564	33036	67	367	296	2048 ± 0	161	559 ± 1	139	561 ± 1	122	562 ± 1	100	564 ± 1	91	602 ± 1	387	10308 ± 102	387	10301 ± 121
128	digitalbarriers-002	83002	598577	372	1930	370	2056 ± 0	39	209 ± 11	34	250 ± 19	60	411 ± 37	180	808 ± 72	387	2236 ± 123	399	13409 ± 228	399	13267 ± 206
129	dps-000	0	2211812	245	1058	439	4096 ± 0	289	868 ± 2	260	893 ± 6	427	1445 ± 9	440	2910 ± 38	433	9345 ± 17	189	1473 ± 37	190	1479 ± 37
130	dsk-000	11967	782905	48	252	18	512 ± 0	64	304 ± 47	55	317 ± 33	284	1001 ± 96	439	2660 ± 170	436	10451 ± 832	372	7152 ± 115	370	7134 ± 111
131	einetworks-000	372608	219883	211	880	361	2056 ± 0	205	645 ± 3	-	-	-	-	-	-	-	-	338	4876 ± 66	342	5156 ± 77
132	ekin-002	51434	278	24	139	392	3072 ± 0	395	1186 ± 13	361	1180 ± 12	345	1181 ± 11	317	1191 ± 11	264	1207 ± 8	329	4294 ± 80	351	5569 ± 112

Notes

- 1 The configuration size does not capture static data included in libraries.
- 2 The library size is the combined total of all files provided in the submission lib folder. These libraries e.g. OpenCV may or may not be installed on any end user's platform natively and would not need to be installed with the algorithm. Some developers put neural network models in their libraries.
- 3 The memory usage is the peak resident set size reported by the ps system call during template generation.
- 4 The median template creation times are measured on Intel®Xeon®CPU E5-2630 v4 @ 2.20GHz processors.
- 5 The comparison durations, in nanoseconds, are estimated using std::chrono::high_resolution_clock which on the machine in (2) counts 1ns clock ticks. Precision is somewhat worse than that however. The ± value is the median absolute deviation times 1.48 for Normal consistency.

Table 10: Summary of algorithms and properties included in this report. The red superscripts give ranking for the quantity in that column.

	ALGORITHM	CONFIG	LIBRARY	TEMPLATE								COMPARISON ⁴									
				NAME	DATA	DATA	MEMORY	SIZE	GENERATION TIME (ms) ⁴				TIME (ns) ⁵								
									(KB) ¹	(KB) ²	(MB) ³	(B)	MUGSHOT	480x720	960x1440	1600x2400	3000x4500	GENUINE	IMPOSTOR		
133	enface-000	369598	153781	141	662	75	1024 ± 0	160	555 ± 4	138	558 ± 4	163	669 ± 6	244	987 ± 15	390	2349 ± 54	370	7059 ± 62	369	6980 ± 65
134	enface-001	370710	173609	144	670	68	1024 ± 0	157	550 ± 4	137	555 ± 3	162	668 ± 7	239	981 ± 15	394	2416 ± 59	364	6734 ± 68	365	6766 ± 69
135	eocortex-000	255937	59432	44	224	277	2048 ± 0	63	305 ± 22	59	341 ± 25	74	440 ± 47	69	464 ± 45	62	513 ± 44	130	923 ± 11	131	918 ± 11
136	ercacat-001	811623	58012	418	2816	341	2052 ± 0	362	1052 ± 3	-	-	-	-	-	-	-	270	2551 ± 62	267	2501 ± 81	
137	euronovate-001	0	1774966	302	1308	91	1177 ± 0	357	1034 ± 2	354	1165 ± 3	340	1160 ± 3	308	1177 ± 3	255	1172 ± 2	468	81294 ± 591	468	81631 ± 931
138	expasoft-001	39057	983064	26	142	119	2048 ± 0	9	70 ± 0	74	± 0	77	± 0	673	± 0	574	± 0	202	1660 ± 35	203	1676 ± 48
139	expasoft-002	38760	59825	34	168	205	2048 ± 0	5	34 ± 0	34	± 0	34	± 0	234	± 0	234	± 0	379	8870 ± 78	379	8838 ± 77
140	f8-001	272977	19668	292	1276	268	2048 ± 0	276	822 ± 39	-	-	-	-	-	-	-	408	15262 ± 139	408	15277 ± 212	
141	f8-002	28278	215616	13	83	278	2048 ± 0	63	39 ± 0	441	± 0	675	± 0	18	197 ± 1	122	702 ± 1	405	14765 ± 131	405	14790 ± 133
142	faceonline-001	0	71529	56	302	367	2056 ± 0	28	179 ± 0	20	179 ± 0	21	190 ± 0	21	217 ± 0	29	343 ± 1	148	1064 ± 37	147	1033 ± 35
143	faceonline-002	155220	141019	237	995	142	2048 ± 0	256	783 ± 1	223	797 ± 2	195	794 ± 2	181	809 ± 3	174	901 ± 2	400	13798 ± 197	400	13743 ± 127
144	facephi-000	148904	5219	470	11481	178	2048 ± 0	290	871 ± 2	253	881 ± 3	225	880 ± 4	209	888 ± 4	185	949 ± 12	327	4067 ± 53	326	4047 ± 53
145	facesoft-000	370120	10612	183	796	220	2048 ± 0	219	675 ± 18	180	669 ± 3	168	686 ± 3	140	675 ± 5	115	687 ± 2	256	2239 ± 28	259	2277 ± 96
146	facetag-000	1232331	4022	229	965	66	684 ± 0	79	355 ± 17	67	369 ± 8	278	989 ± 33	436	2408 ± 91	432	7930 ± 316	464	72003 ± 625	465	71912 ± 612
147	facetag-002	819806	4021	162	726	289	2048 ± 0	154	544 ± 1	132	544 ± 0	115	542 ± 0	95	545 ± 0	77	554 ± 0	208	1730 ± 25	208	1733 ± 25
148	facex-001	305074	930372	424	2931	318	2048 ± 0	107	422 ± 4	89	434 ± 4	107	520 ± 7	164	737 ± 13	369	1670 ± 27	226	1871 ± 23	224	1846 ± 29
149	facex-002	305074	928334	427	3095	224	2048 ± 0	108	426 ± 5	87	429 ± 4	105	516 ± 8	162	730 ± 12	375	1738 ± 36	84	631 ± 25	80	614 ± 19
150	farfaces-001	346494	44581	50	261	30	512 ± 0	391	1179 ± 1	360	1180 ± 1	344	1180 ± 0	314	1185 ± 1	265	1209 ± 2	123	855 ± 25	122	860 ± 31
151	fiberhome-nanjing-003	352895	1482309	201	845	236	2048 ± 0	379	1136 ± 7	344	1134 ± 4	330	1132 ± 3	296	1139 ± 3	245	1154 ± 5	155	1097 ± 38	157	1083 ± 42
152	fiberhome-nanjing-004	443779	1482313	244	1048	421	4096 ± 0	431	1321 ± 5	394	1304 ± 3	382	1307 ± 2	351	1308 ± 3	297	1326 ± 5	171	1276 ± 40	172	1265 ± 38
153	fincore-000	256615	19409	111	535	302	2048 ± 0	143	508 ± 3	120	505 ± 0	101	508 ± 1	86	513 ± 2	71	535 ± 1	212	1765 ± 31	212	1763 ± 22
154	firstcreditKZ-001	553811	24803	261	1112	123	2048 ± 0	266	808 ± 0	301	997 ± 0	311	1061 ± 1	307	1174 ± 1	379	1774 ± 54	127	904 ± 20	128	903 ± 23
155	frpkauai-001	507771	24807	250	1076	117	2048 ± 0	229	689 ± 1	192	691 ± 0	174	697 ± 2	157	714 ± 6	143	775 ± 31	110	752 ± 29	112	764 ± 23
156	frpkauai-002	519141	24803	262	1112	141	2048 ± 0	263	799 ± 0	298	987 ± 0	304	1046 ± 1	303	1163 ± 2	378	1769 ± 4	128	907 ± 20	127	886 ± 28
157	fujitsulab-002	0	1088887	340	1613	447	4104 ± 0	406	1237 ± 2	371	1222 ± 2	358	1236 ± 1	332	1251 ± 2	295	1327 ± 2	279	2836 ± 25	280	2809 ± 44
158	fujitsulab-003	662263	318209	465	6907	448	4104 ± 0	326	951 ± 20	279	941 ± 19	256	952 ± 19	237	971 ± 20	208	1045 ± 21	281	2855 ± 16	282	2849 ± 19
159	g42-intelibrain-001	1031335	235521	475	25628	10	269 ± 0	337	976 ± 6	290	975 ± 1	283	997 ± 2	276	1068 ± 3	307	1362 ± 8	357	5878 ± 96	358	5865 ± 71
160	geo-002	369903	98667	238	1018	262	2048 ± 0	259	791 ± 1	221	793 ± 0	196	794 ± 0	175	795 ± 1	147	803 ± 1	307	3407 ± 45	309	3422 ± 65
161	geo-004	168980	107714	294	1280	274	2048 ± 0	416	1268 ± 1	387	1279 ± 1	370	1274 ± 0	336	1259 ± 1	286	1296 ± 1	144	1023 ± 20	146	1028 ± 22
162	glory-004	0	999639	388	2181	454	4182 ± 0	228	688 ± 0	213	759 ± 1	251	941 ± 1	431	2134 ± 4	434	9360 ± 47	341	4982 ± 66	340	4990 ± 63
163	glory-005	0	999999	397	2428	453	4182 ± 0	237	703 ± 1	220	789 ± 0	265	972 ± 1	433	2200 ± 25	435	9679 ± 22	345	5224 ± 93	344	5176 ± 81
164	gorilla-008	450175	707000	360	1789	472	8338 ± 0	182	595 ± 1	152	590 ± 0	137	600 ± 1	123	621 ± 2	127	720 ± 9	333	4530 ± 44	331	4524 ± 38
165	gorilla-009	329584	297395	304	1312	455	4242 ± 0	304	899 ± 2	272	922 ± 1	232	901 ± 3	221	924 ± 4	204	1032 ± 12	260	2294 ± 74	260	2301 ± 66
166	graymatics-001	13095	70406	22	127	406	4096 ± 0	33	191 ± 1	26	203 ± 1	133	592 ± 5	422	1698 ± 9	430	7150 ± 34	444	39874 ± 309	443	39762 ± 295
167	griaule-001	0	412061	290	1269	336	2052 ± 0	388	1164 ± 1	336	1096 ± 5	321	1099 ± 4	293	1136 ± 2	350	1509 ± 2	324	3948 ± 23	323	3957 ± 32
168	griaule-002	0	1320474	363	1815	349	2052 ± 0	277	822 ± 1	274	924 ± 4	237	907 ± 1	266	1038 ± 21	328	1430 ± 9	325	4005 ± 32	325	4012 ± 31
169	hertasecurity-001	0	944427	278	1183	29	512 ± 0	78	346 ± 0	61	345 ± 0	45	349 ± 0	40	354 ± 0	37	388 ± 0	213	1770 ± 45	207	1726 ± 48
170	hertasecurity-002	0	944582	277	1177	24	512 ± 0	134	484 ± 7	104	478 ± 3	89	480 ± 3	81	495 ± 3	68	520 ± 3	259	2289 ± 40	258	2267 ± 48
171	hik-001	667866	9290	463	6597	95	1408 ± 0	206	651 ± 0	179	667 ± 8	165	677 ± 16	144	686 ± 13	134	737 ± 12	48	488 ± 19	49	477 ± 22
172	hisign-001	732412	167488	332	1553	385	2080 ± 0	427	1306 ± 1	398	1320 ± 1	384	1315 ± 1	354	1312 ± 1	296	1325 ± 1	11	201 ± 10	9	185 ± 13
173	hisign-002	1014906	102652	384	2123	384	2080 ± 0	261	797 ± 0	224	800 ± 5	198	800 ± 0	177	801 ± 0	146	803 ± 1	17	232 ± 11	13	207 ± 11
174	hyperverge-003	1167779	282156	415	2748	74	1024 ± 0	471	1477 ± 2	442	1503 ± 3	438	1520 ± 3	414	1525 ± 4	359	1565 ± 3	58	566 ± 11	58	561 ± 8
175	hyperverge-004	4924393	282156	442	3907	131	2048 ± 0	469	1471 ± 2	430	1434 ± 1	428	1446 ± 6	400	1445 ± 3	346	1491 ± 3	137	996 ± 10	139	1000 ± 19
176	hzailu-002	1515880	74047	452	4715	371	2056 ± 0	387	1150 ± 5	343	1127 ± 6	328	1129 ± 7	295	1137 ± 7	254	1172 ± 3	153	1079 ± 53	153	1070 ± 31

Notes

- 1 The configuration size does not capture static data included in libraries.
- 2 The library size is the combined total of all files provided in the submission lib folder. These libraries e.g. OpenCV may or may not be installed on any end user's platform natively and would not need to be installed with the algorithm. Some developers put neural network models in their libraries.
- 3 The memory usage is the peak resident set size reported by the ps system call during template generation.
- 4 The median template creation times are measured on Intel®Xeon®CPU E5-2630 v4 @ 2.20GHz processors.
- 5 The comparison durations, in nanoseconds, are estimated using std::chrono::high_resolution_clock which on the machine in (2) counts 1ns clock ticks. Precision is somewhat worse than that however. The ± value is the median absolute deviation times 1.48 for Normal consistency.

Table 11: Summary of algorithms and properties included in this report. The red superscripts give ranking for the quantity in that column.

ALGORITHM			CONFIG	LIBRARY	TEMPLATE						COMPARISON ⁴										
NAME		DATA	DATA	MEMORY	SIZE	GENERATION TIME (ms) ⁴				TIME (ns) ⁵											
		(KB) ¹	(KB) ²	(MB) ³	(B)	MUGSHOT	480x720	960x1440	1600x2400	3000x4500	GENUINE	IMPOSTOR									
177	hzailu-003	1923030	222185	453	4817	396	3080 ± 0	448	1389 ± 5	403	1331 ± 7	388	1334 ± 2	365	1349 ± 6	325	1424 ± 8	191	1483 ± 35	188	1464 ± 31
178	icm-003	1513988	940	97	500	263	2048 ± 0	222	681 ± 6	182	672 ± 4	180	714 ± 11	190	837 ± 41	312	1381 ± 131	423	24351 ± 161	422	24227 ± 146
179	icm-004	2012129	1089	243	1040	165	2048 ± 0	106	419 ± 6	80	407 ± 6	79	454 ± 15	115	603 ± 51	354	1527 ± 235	404	14730 ± 154	404	14521 ± 152
180	ichttc-000	172459	1471004	361	1805	153	2048 ± 0	75	338 ± 11	58	338 ± 9	71	437 ± 16	152	705 ± 24	373	1719 ± 44	347	5284 ± 63	346	5290 ± 54
181	id3-006	210116	7706	232	2882	52	520 ± 0	223	683 ± 0	329	1088 ± 1	350	1192 ± 1	323	1209 ± 1	277	1270 ± 1	350	5547 ± 34	350	5563 ± 34
182	id3-008	242416	8151	248	1068	9	264 ± 0	272	819 ± 0	367	1209 ± 2	380	1297 ± 2	361	1329 ± 1	329	1433 ± 1	353	5658 ± 44	354	5624 ± 40
183	idemia-008	374017	69922	280	1194	14	348 ± 0	117	457 ± 1	98	461 ± 0	82	466 ± 1	74	476 ± 2	61	513 ± 10	297	3080 ± 41	293	3046 ± 56
184	idemia-009	1066728	70572	411	2702	65	636 ± 0	399	1207 ± 1	369	1218 ± 1	356	1222 ± 2	324	1222 ± 3	279	1280 ± 10	354	5664 ± 84	353	5597 ± 90
185	iit-002	259579	52070	164	731	144	2048 ± 0	144	514 ± 1	124	531 ± 2	119	547 ± 1	104	583 ± 1	132	733 ± 2	149	1023 ± 7	142	1011 ± 66
186	iit-003	261288	53791	19	817	130	2048 ± 0	132	482 ± 0	110	493 ± 0	102	509 ± 0	93	541 ± 0	109	661 ± 0	27	324 ± 17	30	326 ± 8
187	imds-software-001	373399	352623	176	772	229	2048 ± 0	122	465 ± 1	286	958 ± 6	329	1131 ± 5	292	1134 ± 2	234	1119 ± 10	393	11885 ± 120	392	11779 ± 174
188	imperial-000	370120	10623	184	796	214	2048 ± 0	218	669 ± 1	185	675 ± 3	166	683 ± 17	141	676 ± 2	116	689 ± 2	245	2130 ± 32	243	2052 ± 100
189	imperial-002	472327	16134	364	1826	225	2048 ± 0	168	569 ± 1	147	581 ± 15	126	575 ± 5	103	576 ± 2	85	588 ± 3	258	2278 ± 90	248	2131 ± 44
190	incode-010	627808	21014	407	2628	209	2048 ± 0	392	1180 ± 2	358	1178 ± 1	346	1182 ± 1	311	1184 ± 1	267	1221 ± 1	165	1164 ± 32	164	1144 ± 32
191	incode-011	477280	21781	349	1708	259	2048 ± 0	293	872 ± 0	250	875 ± 0	226	881 ± 1	211	892 ± 1	180	939 ± 0	158	1117 ± 31	160	1109 ± 37
192	infocert-001	1204340	38972	325	1483	218	2048 ± 0	296	874 ± 1	258	891 ± 1	305	1050 ± 5	407	1473 ± 2	411	3174 ± 8	343	5055 ± 108	341	5008 ± 100
193	inefulabs-000	370588	162172	82	439	110	2048 ± 0	349	1006 ± 3	312	1025 ± 3	297	1030 ± 4	267	1041 ± 2	239	1135 ± 3	356	5782 ± 41	357	5741 ± 45
194	innovativetechnologyltd-001	177232	335757	61	341	134	2048 ± 0	111	433 ± 7	92	446 ± 8	72	439 ± 4	63	452 ± 4	57	485 ± 7	228	1877 ± 42	232	1924 ± 97
195	innovativetechnologyltd-002	173939	372324	21	912	116	2048 ± 0	212	661 ± 2	204	726 ± 4	271	981 ± 27	248	997 ± 40	142	766 ± 3	222	1841 ± 50	226	1857 ± 59
196	innovatrics-008	307323	59842	317	1424	56	538 ± 0	255	778 ± 6	214	767 ± 3	193	770 ± 3	179	803 ± 3	160	853 ± 10	293	3021 ± 66	275	2673 ± 88
197	innovatrics-009	624485	105187	370	1917	450	4136 ± 0	375	1116 ± 1	339	1107 ± 5	323	1104 ± 5	285	1110 ± 5	242	1146 ± 6	342	5051 ± 54	332	4733 ± 102
198	insightface-001	776777	16606	437	3852	211	2048 ± 0	438	1366 ± 2	409	1368 ± 3	400	1372 ± 3	375	1375 ± 5	314	1386 ± 4	159	1119 ± 29	159	1108 ± 34
199	insightface-003	1016917	26668	328	1515	319	2048 ± 0	365	1073 ± 0	330	1092 ± 2	315	1070 ± 1	280	1082 ± 1	228	1101 ± 1	63	597 ± 16	67	595 ± 17
200	inspur-000	364844	91926	183	808	423	4096 ± 0	439	1367 ± 1	402	1331 ± 2	398	1368 ± 2	406	1465 ± 1	383	1861 ± 3	385	9831 ± 37	384	9860 ± 40
201	intelllicloudai-001	220831	868246	141	655	280	2048 ± 0	126	468 ± 2	96	456 ± 1	82	466 ± 3	79	492 ± 1	98	632 ± 2	147	1056 ± 4	151	1051 ± 72
202	intelllicloudai-002	259047	58559	433	3584	442	4100 ± 0	285	847 ± 1	237	847 ± 2	213	849 ± 1	190	853 ± 1	170	878 ± 4	119	822 ± 28	118	818 ± 23
203	intellifusion-001	271872	289387	172	762	147	2048 ± 0	249	764 ± 38	217	774 ± 39	197	797 ± 42	178	803 ± 34	148	805 ± 33	157	1112 ± 28	161	1112 ± 41
204	intellifusion-002	762731	385841	223	941	418	4096 ± 0	323	950 ± 2	335	1096 ± 42	317	1088 ± 33	305	1168 ± 31	252	1171 ± 10	206	1713 ± 57	202	1665 ± 87
205	intellivision-003	64023	133748	185	799	372	2056 ± 0	98	407 ± 3	78	398 ± 2	65	418 ± 2	62	450 ± 1	86	591 ± 4	388	11069 ± 56	388	11066 ± 75
206	intellivision-004	117727	131310	103	515	369	2056 ± 0	72	330 ± 0	57	330 ± 0	44	347 ± 0	45	382 ± 0	63	514 ± 0	389	11197 ± 63	389	11165 ± 72
207	intellivix-002	361566	116162	276	1172	182	2048 ± 0	328	956 ± 0	282	947 ± 6	268	976 ± 0	242	984 ± 4	225	1089 ± 1	431	30096 ± 128	433	31287 ± 140
208	intellivix-003	234409	116167	300	1299	324	2048 ± 0	306	908 ± 0	268	916 ± 1	249	930 ± 0	234	961 ± 1	238	1129 ± 3	430	30025 ± 137	432	31190 ± 131
209	intelresearch-005	398137	85290	274	1158	251	2048 ± 0	433	1328 ± 1	405	1334 ± 2	393	1344 ± 2	367	1356 ± 2	323	1423 ± 4	332	4524 ± 87	329	4461 ± 74
210	intelresearch-006	445223	101126	240	1028	200	2048 ± 0	314	918 ± 1	254	881 ± 0	228	892 ± 0	217	913 ± 1	198	1008 ± 3	361	6137 ± 410	360	6024 ± 109
211	intema-000	1532392	19488	256	1097	47	513 ± 0	350	1010 ± 0	302	1001 ± 4	281	994 ± 0	246	993 ± 5	212	1056 ± 1	129	910 ± 29	130	906 ± 32
212	intema-001	1122562	19536	322	1460	48	513 ± 0	436	1354 ± 1	397	1318 ± 5	390	1336 ± 4	360	1328 ± 2	309	1375 ± 0	135	977 ± 31	134	980 ± 31
213	intsysmsu-001	384409	172480	182	789	244	2048 ± 0	188	614 ± 2	161	615 ± 2	156	642 ± 2	166	750 ± 3	248	1159 ± 4	79	621 ± 8	77	611 ± 31
214	intsysmsu-002	765921	172298	181	786	77	1024 ± 0	181	593 ± 1	222	793 ± 2	207	827 ± 1	202	875 ± 104	285	1293 ± 3	53	549 ± 25	56	548 ± 29
215	ionetworks-000	287609	51236	65	351	109	2048 ± 0	110	430 ± 0	90	435 ± 0	70	433 ± 0	60	432 ± 0	49	444 ± 0	368	6913 ± 102	371	7150 ± 160
216	iqface-000	268819	596337	155	704	457	4750 ± 32	153	538 ± 26	112	494 ± 2	117	543 ± 3	163	734 ± 4	317	1393 ± 4	475	636433 ± 38446	475	632654 ± 85615
217	iqface-003	370803	963398	193	817	458	4763 ± 37	147	529 ± 1	120	532 ± 2	136	599 ± 8	195	850 ± 2	370	1694 ± 2	474	575924 ± 2601	474	576653 ± 2051
218	irex-000	741899	47419	382	2086	395	3080 ± 0	287	852 ± 2	239	850 ± 1	221	874 ± 2	226	939 ± 1	271	1249 ± 5	13	201 ± 11	14	208 ± 8
219	isap-001	99049	204201	1	18	404	4096 ± 0	1	0 ± 0	-	-	-	-	-	-	-	-	43	459 ± 17	44	456 ± 11
220	isap-002	256765	49931	54	288	198	2048 ± 0	252	769 ± 3	314	1027 ± 2	224	877 ± 2	171	761 ± 1	176	912 ± 2	295	3045 ± 94	289	2973 ± 66

Notes

1 The configuration size does not capture static data included in libraries.

2 The library size is the combined total of all files provided in the submission lib folder. These libraries e.g. OpenCV may or may not be installed on any end user's platform natively and would not need to be installed with the algorithm. Some developers put neural network models in their libraries.

3 The memory usage is the peak resident set size reported by the ps system call during template generation.

4 The median template creation times are measured on Intel®Xeon®CPU E5-2630 v4 @ 2.20GHz processors.

5 The comparison durations, in nanoseconds, are estimated using std::chrono::high_resolution_clock which on the machine in (2) counts 1ns clock ticks. Precision is somewhat worse than that however. The ± value is the median absolute deviation times 1.48 for Normal consistency.

	ALGORITHM	CONFIG	LIBRARY	TEMPLATE								COMPARISON ⁴							
				NAME		DATA		MEMORY		SIZE		GENERATION TIME (ms) ⁴				TIME (ns) ⁵			
				(KB) ¹	(KB) ²	(MB) ³	(B)	MUGSHOT	480x720	960x1440	1600x2400	3000x4500	GENUINE	IMPOSTOR					
221	isityou-000	48010	36621	17	110	473	19200 ± 0	18	113 ± 5	-	-	-	-	471	237517 ± 1318	471 237374 ± 1279			
222	isystems-001	274621	639268	255	1091	253	2048 ± 0	59	291 ± 9	-	-	-	-	55	557 ± 16	59 564 ± 22			
223	isystems-002	358984	803389	337	1595	260	2048 ± 0	278	822 ± 8	-	-	-	-	109	749 ± 31	86 632 ± 28			
224	itmo-007	415979	245376	391	2199	238	2048 ± 0	244	741 ± 2	-	-	-	-	269	2551 ± 50	269 2529 ± 80			
225	itmo-008	726866	318238	310	1377	438	4096 ± 0	364	1060 ± 1	323	1058 ± 1	308	1059 ± 1	278	1072 ± 4	230 1104 ± 1	315 3578 ± 25	315 3580 ± 28	
226	ivacognitive-001	256958	62791	226	947	172	2048 ± 0	424	1292 ± 3	390	1288 ± 4	375	1292 ± 4	347	1292 ± 3	293 1321 ± 4	328 4228 ± 41	327 4226 ± 41	
227	iws-000	30875	3063	10	77	26	512 ± 0	50	277 ± 5	44	283 ± 1	95	494 ± 3	243	984 ± 3	407 2987 ± 39	139 999 ± 40	137 992 ± 22	
228	jaakit-001	99024	24754	47	251	42	512 ± 0	10	76 ± 0	8	77 ± 0	89	70 ± 0	78	81 ± 0	79	93 ± 0	264 2466 ± 57	265 2465 ± 66
229	kakao-007	526993	129545	445	3953	279	2048 ± 0	327	952 ± 1	287	961 ± 1	260	958 ± 1	236	962 ± 1	191	968 ± 1	146 1056 ± 16	149 1047 ± 28
230	kakao-008	734583	104820	439	3876	207	2048 ± 0	378	1135 ± 3	351	1148 ± 3	337	1150 ± 3	300	1156 ± 1	256	1175 ± 1	108 736 ± 23	105 727 ± 22
231	kakaopay-001	397864	179869	148	684	401	4096 ± 0	114	448 ± 0	130	542 ± 0	114	542 ± 0	94	542 ± 0	76	553 ± 0	86 633 ± 22	84 630 ± 22
232	kasikornlabs-000	256471	61000	151	693	152	2048 ± 0	307	908 ± 36	252	878 ± 22	264	969 ± 39	312	1184 ± 54	392	2382 ± 145	433 31669 ± 188	434 31714 ± 182
233	kasikornlabs-002	256431	61063	171	757	283	2048 ± 0	312	917 ± 35	266	907 ± 13	263	963 ± 13	357	1320 ± 45	398	2629 ± 178	432 31025 ± 180	431 31054 ± 186
234	kedacom-000	245292	37401	474	23574	13	292 ± 0	141	506 ± 3	135	547 ± 10	143	614 ± 9	109	588 ± 10	110	665 ± 24	94 684 ± 14	96 682 ± 16
235	kiwitech-000	369711	21375	190	808	166	2048 ± 0	180	591 ± 0	154	594 ± 0	135	595 ± 1	113	596 ± 0	92	609 ± 0	210 1755 ± 20	209 1734 ± 16
236	kneron-003	58366	1747	40	188	192	2048 ± 0	54	281 ± 3	43	280 ± 1	39	315 ± 13	43	365 ± 7	268	1224 ± 30	346 5237 ± 63	346 5274 ± 99
237	kneron-005	375374	13633	86	457	104	2048 ± 0	145	518 ± 2	123	522 ± 4	121	556 ± 5	169	757 ± 19	377	1922 ± 25	232 1922 ± 11	233 1926 ± 20
238	knowutech-000	808045	32886	301	1303	97	1536 ± 0	458	1419 ± 2	410	1372 ± 1	404	1377 ± 1	377	1382 ± 2	313	1386 ± 2	319 3743 ± 31	318 3693 ± 38
239	kookmin-002	371771	30734	19	827	156	2048 ± 0	359	1038 ± 2	321	1047 ± 1	302	1045 ± 1	272	1061 ± 1	232	1116 ± 1	89 638 ± 19	88 636 ± 20
240	koreaid-001	256261	20152	362	1811	249	2048 ± 0	90	384 ± 2	72	390 ± 1	76	444 ± 2	97	556 ± 6	145	795 ± 5	88 636 ± 11	89 636 ± 10
241	krungthai-002	2360957	15033	275	1171	158	2048 ± 0	67	308 ± 0	53	314 ± 5	35	309 ± 0	35	319 ± 0	33	362 ± 0	291 3014 ± 20	290 2980 ± 22
242	kuke3d-001	403462	68786	109	530	426	4096 ± 0	269	814 ± 2	226	811 ± 2	203	814 ± 2	182	814 ± 1	158	834 ± 1	363 6412 ± 57	363 6413 ± 51
243	kuke3d-002	270544	1227855	191	809	217	2048 ± 0	140	504 ± 3	119	504 ± 1	103	511 ± 1	89	523 ± 2	84	585 ± 1	287 2943 ± 22	288 2966 ± 38
244	lebentech-000	0	10360	18	110	33	512 ± 0	3	322 ± 0	12	22 ± 0	122	± 0	123	± 0	123	± 0	117 801 ± 42	119 825 ± 51
245	lemalabs-001	748400	198794	414	2738	171	2048 ± 0	267	810 ± 0	227	812 ± 0	201	813 ± 0	184	819 ± 0	159	844 ± 1	394 11930 ± 35	394 11913 ± 37
246	lineclova-002	475779	406756	306	1353	312	2048 ± 0	420	1284 ± 1	386	1275 ± 2	371	1275 ± 1	342	1273 ± 2	280	1281 ± 2	277 2765 ± 10	277 2767 ± 31
247	lineclova-003	585149	410482	351	1726	210	2048 ± 0	461	1444 ± 1	432	1438 ± 1	424	1439 ± 2	399	1440 ± 1	333	1446 ± 2	284 2890 ± 23	285 2899 ± 29
248	lookman-002	138200	25410	472	16518	61	548 ± 0	20	173 ± 1	-	-	-	-	-	-	-	72 610 ± 19	79 612 ± 22	
249	lookman-004	244775	37401	473	23548	60	548 ± 0	142	507 ± 5	133	545 ± 12	142	613 ± 12	110	590 ± 11	106	656 ± 16	124 871 ± 29	124 878 ± 29
250	luxand-000	0	57908	308	1366	88	1040 ± 0	102	407 ± 23	88	433 ± 11	75	444 ± 14	68	464 ± 14	80	562 ± 25	120 828 ± 28	120 828 ± 32
251	mantra-000	471458	62566	169	749	344	2052 ± 0	104	413 ± 18	109	487 ± 19	96	494 ± 18	85	511 ± 18	89	598 ± 19	300 3151 ± 51	298 3127 ± 63
252	maxvision-002	171894	60623	367	1863	226	2048 ± 0	25	172 ± 0	19	171 ± 0	16	172 ± 0	13	174 ± 0	15	221 ± 0	106 725 ± 5	104 725 ± 5
253	maxvision-003	234062	61252	393	2292	176	2048 ± 0	128	474 ± 0	102	468 ± 0	87	471 ± 0	73	475 ± 0	67	519 ± 0	266 2467 ± 28	266 2488 ± 23
254	megvii-005	1378009	44038	447	4036	333	2049 ± 0	430	1319 ± 5	377	1247 ± 6	360	1240 ± 2	331	1245 ± 2	287	1298 ± 3	437 32025 ± 121	438 32008 ± 114
255	megvii-006	1554938	44038	450	4354	330	2049 ± 0	422	1287 ± 3	388	1286 ± 0	409	1393 ± 5	355	1319 ± 1	304	1360 ± 1	435 31845 ± 100	436 31872 ± 118
256	meituan-001	615387	333249	259	1106	148	2048 ± 0	352	1017 ± 4	308	1008 ± 3	289	1010 ± 2	257	1010 ± 3	199	1011 ± 4	90 654 ± 10	93 658 ± 14
257	meituan-002	686111	244091	389	2191	419	4096 ± 0	361	1052 ± 0	328	1086 ± 1	313	1064 ± 2	271	1060 ± 5	219	1063 ± 1	149 1064 ± 10	152 1070 ± 16
258	meiya-001	280055	264913	99	507	332	2049 ± 0	194	622 ± 12	-	-	-	-	-	-	-	373 8356 ± 615	375 8134 ± 97	
259	mendaxiatech-000	1941475	45484	430	3195	440	4097 ± 0	408	1243 ± 2	379	1255 ± 1	401	1373 ± 2	419	1598 ± 3	400	2689 ± 8	448 46906 ± 275	447 46872 ± 217
260	metsakurcompany-001	445177	1091558	333	1572	368	2056 ± 0	170	578 ± 1	150	587 ± 3	131	590 ± 1	136	659 ± 1	161	854 ± 1	370 8600 ± 192	376 8155 ± 298
261	metsakurcompany-002	0	957558	233	983	359	2056 ± 0	339	980 ± 1	293	978 ± 1	269	976 ± 2	254	1005 ± 1	229	1103 ± 2	378 8766 ± 326	378 8786 ± 324
262	miaxis-001	0	215019	58	322	35	512 ± 0	52	279 ± 0	42	278 ± 0	31	278 ± 1	30	285 ± 0	25	297 ± 0	125 872 ± 14	125 881 ± 22
263	microfocus-001	104524	27242	41	190	5	256 ± 0	47	264 ± 18	-	-	-	-	-	-	-	16 215 ± 8	17 217 ± 10	
264	microfocus-002	96288	27362	37	176	4	256 ± 0	45	259 ± 18	-	-	-	-	-	-	-	29 337 ± 34	18 230 ± 25	

Notes

- 1 The configuration size does not capture static data included in libraries.
- 2 The library size is the combined total of all files provided in the submission lib folder. These libraries e.g. OpenCV may or may not be installed on any end user's platform natively and would not need to be installed with the algorithm. Some developers put neural network models in their libraries.
- 3 The memory usage is the peak resident set size reported by the ps system call during template generation.
- 4 The median template creation times are measured on Intel®Xeon®CPU E5-2630 v4 @ 2.20GHz processors.
- 5 The comparison durations, in nanoseconds, are estimated using std::chrono::high_resolution_clock which on the machine in (2) counts 1ns clock ticks. Precision is somewhat worse than that however. The ± value is the median absolute deviation times 1.48 for Normal consistency.

Table 13: Summary of algorithms and properties included in this report. The red superscripts give ranking for the quantity in that column.

ALGORITHM	CONFIG	LIBRARY	TEMPLATE								COMPARISON ⁴										
			NAME		DATA		MEMORY		SIZE		GENERATION TIME (ms) ⁴										
			(KB) ¹	(KB) ²	(MB) ³	(B)	MUGSHOT	480x720	960x1440	1600x2400	3000x4500	GENUINE	IMPOSTOR								
265	minivision-000	836697	16597	446	4013	4096 ± 0	358	1035 ± 1	318	1033 ± 2	298	1035 ± 1	264	1037 ± 1	216	1059 ± 2	265	2466 ± 26	263	2460 ± 25	
266	mobai-000	365451	80573	180	786	460	6144 ± 0	251	766 ± 8	245	869 ± 6	353	1205 ± 31	428	1867 ± 45	416	3549 ± 190	410	16458 ± 333	410	16423 ± 1473
267	mobai-001	265297	60164	110	534	188	2048 ± 0	187	612 ± 3	166	614 ± 3	169	687 ± 9	206	886 ± 31	371	1707 ± 103	178	1386 ± 25	179	1377 ± 26
268	mobbl-001	231160	58706	43	223	252	2048 ± 0	30	183 ± 32	241	184 ± 25	47	354 ± 76	186	823 ± 396	403	2781 ± 1166	392	11832 ± 109	393	11851 ± 88
269	mobbl-003	172248	60960	52	270	179	2048 ± 0	217	664 ± 6	177	661 ± 5	161	663 ± 5	137	665 ± 6	117	691 ± 5	397	12506 ± 111	398	12509 ± 100
270	mobiptimech-000	370514	303291	265	1130	132	2048 ± 0	409	1245 ± 1	372	1234 ± 1	366	1264 ± 1	371	1360 ± 1	372	1707 ± 1	403	14506 ± 214	403	14433 ± 197
271	moreedian-000	525259	21374	222	932	292	2048 ± 0	233	694 ± 0	194	698 ± 0	176	699 ± 0	151	700 ± 0	126	713 ± 1	217	1803 ± 11	215	1779 ± 23
272	mukh-001	866223	451194	342	1637	72	1024 ± 0	441	1375 ± 17	414	1390 ± 12	417	1406 ± 8	382	1394 ± 10	305	1360 ± 11	39	433 ± 14	41	435 ± 14
273	mukh-002	693809	454936	260	1109	228	2048 ± 0	332	968 ± 1	270	921 ± 12	259	957 ± 2	231	954 ± 6	188	953 ± 5	75	612 ± 13	76	611 ± 17
274	multimodality-000	0	503924	316	1417	127	2048 ± 0	105	416 ± 0	85	420 ± 0	67	423 ± 0	59	427 ± 0	51	463 ± 0	122	848 ± 25	116	800 ± 28
275	multimodality-001	185719	545045	312	1388	415	4096 ± 0	397	1190 ± 2	355	1169 ± 2	341	1165 ± 2	304	1167 ± 2	258	1177 ± 2	185	1424 ± 35	181	1384 ± 42
276	mvision-001	227502	149531	161	723	38	512 ± 0	231	691 ± 21	195	702 ± 19	175	697 ± 24	154	708 ± 29	124	710 ± 27	160	1123 ± 40	166	1154 ± 38
277	nazhiai-000	547484	16141	412	2716	281	2048 ± 0	223	683 ± 3	189	687 ± 2	210	835 ± 27	193	840 ± 31	157	834 ± 34	255	2230 ± 34	249	2133 ± 81
278	neosystems-004	243546	352623	108	529	227	2048 ± 0	71	324 ± 0	199	711 ± 3	208	827 ± 7	197	854 ± 2	177	916 ± 2	402	14437 ± 176	402	14355 ± 173
279	netbridgetech-001	133108	205875	100	508	422	4096 ± 0	12	85 ± 1	10	83 ± 0	9	84 ± 0	9	92 ± 0	9	113 ± 4	380	9280 ± 74	380	9446 ± 512
280	netbridgetech-002	257687	49931	55	299	223	2048 ± 0	28	838 ± 6	239	838 ± 2	211	839 ± 1	192	839 ± 3	162	859 ± 3	285	2893 ± 65	294	3050 ± 123
281	neurotechnology-013	474749	85552	422	2894	49	514 ± 0	345	1000 ± 1	306	1006 ± 2	291	1022 ± 2	269	1053 ± 2	259	1195 ± 8	2	109 ± 4	110	110 ± 4
282	neurotechnology-015	474782	86045	404	2564	50	515 ± 0	355	1028 ± 3	317	1033 ± 3	307	1055 ± 4	281	1097 ± 4	288	1304 ± 18	4	130 ± 2	4	130 ± 4
283	nhn-002	363471	817674	143	667	433	4096 ± 0	381	1141 ± 3	346	1138 ± 2	333	1141 ± 2	299	1151 ± 6	261	1203 ± 2	455	56608 ± 579	455	56549 ± 606
284	nhn-003	933665	432730	323	1464	409	4096 ± 0	404	1229 ± 2	380	1261 ± 1	365	1263 ± 3	344	1279 ± 2	310	1375 ± 3	451	50560 ± 105	450	50592 ± 142
285	nodeflux-002	774668	690213	89	466	310	2048 ± 0	239	708 ± 4	198	709 ± 4	181	716 ± 7	159	716 ± 7	133	736 ± 3	310	3475 ± 62	307	3408 ± 143
286	notiontag-001	92753	427967	118	566	64	584 ± 0	318	929 ± 35	331	1092 ± 39	444	3709 ± 81	444	10233 ± 180	-	445	43636 ± 286	444	43724 ± 330	
287	notiontag-002	271987	967207	420	2840	389	2120 ± 0	110	453 ± 2	97	453 ± 3	78	453 ± 3	64	458 ± 2	53	471 ± 3	418	20278 ± 194	418	20195 ± 186
288	nsensecorp-003	199895	117041	158	710	201	2048 ± 0	211	661 ± 0	178	664 ± 0	160	662 ± 1	134	659 ± 1	107	659 ± 0	446	44658 ± 51	446	44654 ± 72
289	nsensecorp-004	513276	139178	343	1663	321	2048 ± 0	460	1433 ± 0	433	1445 ± 7	429	1450 ± 3	412	1487 ± 5	-	262	2388 ± 42	262	2385 ± 63	
290	ntechlab-011	786933	209458	464	6867	94	1280 ± 0	385	1148 ± 2	347	1142 ± 1	339	1159 ± 1	313	1185 ± 1	283	1290 ± 3	7	179 ± 11	8	173 ± 11
291	ntechlab-012	570796	212350	458	5451	391	2560 ± 0	429	1309 ± 1	400	1323 ± 1	386	1331 ± 1	370	1360 ± 1	337	1460 ± 3	18	211 ± 8	16	211 ± 7
292	omface-000	45945	844976	30	150	69	1024 ± 0	37	185 ± 1	27	206 ± 2	22	203 ± 1	15	195 ± 1	14	193 ± 1	47	481 ± 42	45	456 ± 20
293	omface-001	146370	1799745	27	145	82	1024 ± 0	34	194 ± 2	29	222 ± 2	24	209 ± 0	19	216 ± 1	17	233 ± 1	412	18369 ± 19	412	18366 ± 32
294	omnigarde-001	200523	32882	88	464	17	512 ± 0	319	941 ± 0	257	883 ± 1	227	886 ± 1	210	891 ± 1	172	898 ± 0	183	1405 ± 31	180	1379 ± 26
295	omnigarde-002	368860	32882	170	757	70	1024 ± 0	426	1303 ± 1	376	1246 ± 1	363	1249 ± 1	334	1253 ± 1	275	1261 ± 1	276	2727 ± 34	276	2686 ± 32
296	onfido-000	273478	959781	216	908	245	2048 ± 0	118	459 ± 17	94	451 ± 15	77	451 ± 14	67	462 ± 15	59	505 ± 18	199	1617 ± 50	200	1637 ± 53
297	openface-001	0	40111	16	100	189	2048 ± 0	22	148 ± 1	10	154 ± 0	49	365 ± 3	56	409 ± 9	94	616 ± 31	70	608 ± 14	70	604 ± 13
298	oz-003	484147	519652	471	11949	354	2053 ± 0	440	1375 ± 12	413	1388 ± 3	443	1773 ± 16	430	2039 ± 6	412	3209 ± 5	467	73905 ± 456	467	73892 ± 444
299	oz-004	373982	1075452	468	8071	355	2053 ± 0	280	832 ± 7	246	871 ± 6	231	899 ± 10	279	1078 ± 12	363	1608 ± 10	459	61654 ± 418	458	61749 ± 450
300	palit-000	428754	144958	307	1355	428	4096 ± 0	169	570 ± 1	144	578 ± 1	127	576 ± 3	105	583 ± 1	93	614 ± 1	254	2227 ± 16	256	2226 ± 16
301	palit-001	173886	145564	122	583	247	2048 ± 0	40	227 ± 0	31	224 ± 1	25	224 ± 1	22	229 ± 3	22	262 ± 2	161	1150 ± 16	162	1135 ± 23
302	pangiam-000	464252	24512	444	3919	136	2048 ± 0	196	627 ± 5	162	618 ± 4	144	615 ± 3	122	620 ± 3	104	639 ± 3	3	118 ± 7	3	113 ± 7
303	papago-001	669274	52817	394	2341	140	2048 ± 0	418	1272 ± 6	392	1296 ± 7	379	1295 ± 6	346	1281 ± 3	299	1345 ± 3	407	15236 ± 169	407	15184 ± 142
304	papsav1923-002	491185	24727	268	1136	340	2052 ± 0	260	792 ± 1	292	978 ± 1	300	1042 ± 1	301	1158 ± 1	166	1641 ± 19	166	1209 ± 29	168	1206 ± 38
305	papsav1923-003	515576	24803	263	1112	193	2048 ± 0	262	797 ± 0	297	987 ± 1	301	1043 ± 1	309	1178 ± 1	381	1809 ± 7	126	903 ± 26	129	905 ± 34
306	paravision-010	688291	205854	385	2150	441	4100 ± 0	200	634 ± 0	171	635 ± 0	151	635 ± 0	125	635 ± 0	101	635 ± 1	195	1577 ± 35	196	1571 ± 32
307	paravision-011	781138	95589	396	2420	446	4100 ± 0	286	852 ± 0	24	871 ± 1	218	858 ± 1	198	854 ± 0	167	873 ± 1	198	1608 ± 35	198	1625 ± 32
308	pensees-001	1619431	408932	371	1922	469	8200 ± 0	372	1108 ± 3	434	1448 ± 17	423	1439 ± 10	405	1464 ± 5	357	1546 ± 9	299	3151 ± 34	299	3143 ± 25

Notes

- 1 The configuration size does not capture static data included in libraries.
 - 2 The library size is the combined total of all files provided in the submission lib folder. These libraries e.g. OpenCV may or may not be installed on any end user's platform natively and would not need to be installed with the algorithm. Some developers put neural network models in their libraries.
 - 3 The memory usage is the peak resident set size reported by the ps system call during template generation.
 - 4 The median template creation times are measured on Intel®Xeon®CPU E5-2630 v4 @ 2.20GHz processors.
 - 5 The comparison durations, in nanoseconds, are estimated using std::chrono::high_resolution_clock which on the machine in (2) counts 1ns clock ticks. Precision is somewhat worse than that however. The \pm value is the median absolute deviation times 1.48 for Normal consistency.

Table 14: Summary of algorithms and properties included in this report. The red superscripts give ranking for the quantity in that column.

	ALGORITHM	CONFIG	LIBRARY	TEMPLATE								COMPARISON ⁴									
				NAME	DATA	DATA	MEMORY	SIZE	GENERATION TIME (ms) ⁴				TIME (ns) ⁵								
									(KB) ¹	(KB) ²	(MB) ³	(B)	MUGSHOT	480x720	960x1440	1600x2400	3000x4500	GENUINE	IMPOSTOR		
309	pixelall-008	0	992249	356	1741	468	8192 ± 0	468	1471 ± 3	424	1405 ± 4	418	1409 ± 4	392	1413 ± 3	326	1426 ± 4	216	1799 ± 50	219	1807 ± 48
310	pixelall-009	0	1009114	352	1731	467	8192 ± 0	475	1484 ± 3	419	1395 ± 3	414	1400 ± 4	380	1391 ± 3	330	1433 ± 3	224	1848 ± 13	223	1842 ± 19
311	psl-010	411027	591157	457	5361	452	4168 ± 0	455	1403 ± 9	417	1393 ± 3	408	1392 ± 3	383	1395 ± 3	318	1396 ± 3	31	354 ± 53	31	329 ± 29
312	psl-011	814579	606050	454	4984	470	8248 ± 0	432	1324 ± 2	399	1323 ± 8	385	1326 ± 8	358	1324 ± 8	294	1322 ± 4	204	1680 ± 37	205	1688 ± 40
313	ptakuratsatu-000	0	585434	305	1347	57	538 ± 0	297	875 ± 3	243	863 ± 48	247	928 ± 9	233	958 ± 17	221	1066 ± 26	358	5900 ± 103	359	5687 ± 167
314	pxl-001	110116	78231	33	168	41	512 ± 0	15	101 ± 5	12	104 ± 5	20	189 ± 12	55	408 ± 27	339	1470 ± 144	352	5598 ± 45	352	5590 ± 68
315	pyramid-000	372608	219883	186	804	366	2056 ± 0	172	583 ± 2	-	-	-	-	-	-	371	7147 ± 59	373	7586 ± 425		
316	qazbs-000	362015	805258	204	856	160	2048 ± 0	428	1307 ± 1	375	1243 ± 0	362	1248 ± 9	333	1253 ± 1	278	1270 ± 0	344	5181 ± 62	343	5167 ± 93
317	qluevision-001	173605	205230	70	376	466	8192 ± 0	41	229 ± 1	32	230 ± 1	28	231 ± 1	26	233 ± 1	19	239 ± 1	305	3374 ± 38	305	3365 ± 41
318	qnap-002	346963	33284	153	700	269	2048 ± 0	274	821 ± 1	230	824 ± 1	206	824 ± 1	189	826 ± 1	156	832 ± 1	21	293 ± 13	24	287 ± 17
319	qnap-003	245476	61427	175	770	322	2048 ± 0	92	387 ± 0	73	393 ± 0	56	393 ± 0	49	393 ± 1	41	400 ± 2	92	683 ± 20	91	651 ± 17
320	quantasoft-003	370518	211354	246	1058	317	2048 ± 0	199	632 ± 2	170	634 ± 0	147	632 ± 0	124	631 ± 1	100	634 ± 0	12	201 ± 7	12	203 ± 8
321	rankone-012	0	264182	23	134	6	261 ± 0	163	564 ± 3	136	554 ± 1	123	564 ± 1	106	586 ± 1	120	695 ± 1	20	273 ± 17	19	231 ± 14
322	rankone-013	0	228729	29	149	8	261 ± 0	230	690 ± 5	181	672 ± 1	179	712 ± 1	174	780 ± 1	233	1118 ± 3	33	356 ± 23	27	304 ± 23
323	rankone-014	0	243130	31	163	7	261 ± 0	236	701 ± 1	197	705 ± 0	185	732 ± 1	176	800 ± 1	231	1113 ± 1	26	306 ± 16	21	251 ± 13
324	realnetworks-007	570797	101527	428	3137	365	2056 ± 0	435	1348 ± 2	407	1358 ± 11	397	1363 ± 10	378	1386 ± 9	352	1517 ± 6	56	559 ± 31	54	539 ± 35
325	realnetworks-008	73346	75421	68	369	362	2056 ± 0	62	296 ± 3	48	294 ± 3	46	353 ± 4	41	361 ± 5	56	485 ± 5	52	539 ± 31	55	543 ± 29
326	regula-000	262444	29384	133	610	212	2048 ± 0	396	1187 ± 1	342	1126 ± 1	327	1129 ± 0	291	1132 ± 1	249	1159 ± 1	50	491 ± 16	51	500 ± 22
327	regula-001	256075	25980	230	976	180	2048 ± 0	421	1284 ± 1	370	1220 ± 1	355	1222 ± 1	326	1226 ± 1	273	1255 ± 1	34	361 ± 10	33	342 ± 25
328	remarkai-001	241857	868314	163	730	335	2052 ± 0	279	831 ± 6	238	849 ± 18	306	1055 ± 25	318	1198 ± 34	353	1519 ± 38	169	1229 ± 20	117	805 ± 56
329	remarkai-003	280516	58559	441	3896	445	4100 ± 0	342	986 ± 1	299	993 ± 1	280	992 ± 1	251	999 ± 3	200	1019 ± 2	116	787 ± 20	114	793 ± 22
330	rendip-000	0	437653	147	682	242	2048 ± 0	121	464 ± 2	97	458 ± 0	88	473 ± 0	75	483 ± 1	78	556 ± 4	59	576 ± 13	61	573 ± 11
331	revealmedia-005	293933	202465	174	763	444	4100 ± 0	109	428 ± 0	86	428 ± 0	69	430 ± 0	61	433 ± 0	48	442 ± 0	240	2023 ± 38	240	2009 ± 26
332	revealmedia-006	293933	200912	168	741	346	2052 ± 0	88	381 ± 0	68	381 ± 0	52	382 ± 0	46	384 ± 0	39	394 ± 0	82	626 ± 35	71	600 ± 2
333	rokid-000	258612	396624	283	1218	360	2056 ± 0	155	546 ± 3	131	542 ± 2	118	545 ± 1	88	522 ± 3	81	563 ± 4	309	3457 ± 62	311	3463 ± 77
334	rokid-001	641223	413733	249	1071	381	2060 ± 0	309	911 ± 2	262	901 ± 5	230	899 ± 2	214	900 ± 3	173	901 ± 3	302	3345 ± 50	303	3346 ± 149
335	s1-005	482369	95685	271	1137	129	2048 ± 0	347	1001 ± 0	304	1002 ± 0	287	1004 ± 0	255	1008 ± 0	202	1029 ± 2	83	626 ± 74	63	589 ± 14
336	s1-006	482372	95681	270	1137	325	2048 ± 0	325	951 ± 0	285	956 ± 0	258	957 ± 0	235	962 ± 0	193	983 ± 0	98	696 ± 23	100	696 ± 29
337	saffe-001	85973	62488	35	168	92	1280 ± 0	55	281 ± 1	-	-	-	-	-	-	-	170	1274 ± 19	173	1277 ± 26	
338	saffe-002	260622	28285	203	855	138	2048 ± 0	270	817 ± 11	225	805 ± 15	200	809 ± 19	183	815 ± 29	151	813 ± 23	103	717 ± 7	103	714 ± 29
339	samsungsd-001	1189592	147444	440	3893	407	4096 ± 0	380	1140 ± 3	349	1145 ± 4	392	1344 ± 5	373	1366 ± 5	351	1514 ± 7	452	51559 ± 773	451	51721 ± 1003
340	samsungsd-002	1040732	147475	398	2431	376	2056 ± 0	377	1118 ± 1	356	1175 ± 12	399	1372 ± 6	359	1324 ± 2	345	1489 ± 4	440	35803 ± 266	441	36181 ± 674
341	samtech-001	288082	219883	130	605	373	2056 ± 0	60	294 ± 3	-	-	-	-	-	-	374	7694 ± 59	374	7678 ± 91		
342	scanovate-002	256986	457227	202	850	293	2048 ± 0	234	696 ± 32	200	713 ± 33	186	738 ± 28	173	779 ± 32	253	1172 ± 53	292	3021 ± 38	297	3120 ± 163
343	scanovate-003	135585	89469	188	808	303	2048 ± 0	174	585 ± 1	158	613 ± 12	132	591 ± 1	117	610 ± 2	114	684 ± 1	286	2926 ± 22	286	2925 ± 20
344	sdc-000	256814	481583	179	786	298	2048 ± 0	310	913 ± 14	265	906 ± 9	334	1142 ± 19	424	1774 ± 45	420	4719 ± 222	438	32645 ± 93	439	32653 ± 112
345	securifai-005	252532	81777	105	525	199	2048 ± 0	442	1377 ± 2	406	1355 ± 1	395	1353 ± 0	303	1356 ± 0	227	1873 ± 25	225	1847 ± 35		
346	securifai-006	452474	81856	177	773	432	4096 ± 0	366	1090 ± 2	327	1086 ± 3	319	1093 ± 1	284	1104 ± 10	226	1090 ± 2	306	3376 ± 42	306	3399 ± 40
347	sensetime-007	765353	37533	460	5699	83	1028 ± 0	447	1386 ± 41	401	1323 ± 2	394	1347 ± 2	372	1366 ± 2	187	1460 ± 29	186	1425 ± 26		
348	sensetime-008	1176483	60067	462	5976	84	1028 ± 0	473	1479 ± 31	431	1436 ± 4	434	1482 ± 4	415	1525 ± 5	368	1669 ± 2	172	1283 ± 51	170	1240 ± 47
349	sertis-000	265572	68770	77	427	184	2048 ± 0	247	754 ± 0	212	759 ± 0	191	764 ± 0	170	760 ± 0	141	763 ± 0	192	1497 ± 29	197	1582 ± 38
350	sertis-002	460790	68929	313	1391	258	2048 ± 0	394	1181 ± 1	357	1178 ± 0	348	1183 ± 0	316	1187 ± 0	266	1221 ± 0	154	1086 ± 32	154	1076 ± 31
351	seventhsense-001	369850	3183365	192	811	342	2052 ± 0	413	1255 ± 2	391	1294 ± 15	372	1277 ± 3	343	1275 ± 2	282	1288 ± 3	234	1936 ± 26	236	1943 ± 34
352	seventhsense-002	452197	1567903	225	944	352	2052 ± 0	412	1252 ± 1	385	1271 ± 1	368	1269 ± 1	340	1272 ± 1	284	1290 ± 1	246	2131 ± 45	246	2123 ± 45

Notes

- 1 The configuration size does not capture static data included in libraries.
- 2 The library size is the combined total of all files provided in the submission lib folder. These libraries e.g. OpenCV may or may not be installed on any end user's platform natively and would not need to be installed with the algorithm. Some developers put neural network models in their libraries.
- 3 The memory usage is the peak resident set size reported by the ps system call during template generation.
- 4 The median template creation times are measured on Intel®Xeon®CPU E5-2630 v4 @ 2.20GHz processors.
- 5 The comparison durations, in nanoseconds, are estimated using std::chrono::high_resolution_clock which on the machine in (2) counts 1ns clock ticks. Precision is somewhat worse than that however. The ± value is the median absolute deviation times 1.48 for Normal consistency.

	ALGORITHM	CONFIG	LIBRARY	TEMPLATE								COMPARISON ⁴			
				NAME		DATA		MEMORY		SIZE		GENERATION TIME (ms) ⁴			
				(KB) ¹	(KB) ²	(MB) ³	(B)	MUGSHOT	480x720	960x1440	1600x2400	3000x4500	GENUINE	IMPOSTOR	
353	shaman-000	0	120033	98 ⁵⁰⁷	436 ^{4096 ± 0}	208 ^{653 ± 16}	-	-	-	-	-	37 ^{380 ± 25}	37 ^{379 ± 31}		
354	shaman-001	0	174446	102 ⁵¹¹	412 ^{4096 ± 0}	61 ^{294 ± 2}	-	-	-	-	-	87 ^{635 ± 19}	42 ^{441 ± 25}		
355	shu-002	731250	148309	212 ⁸⁹⁰	399 ^{4096 ± 0}	246 ^{751 ± 2}	215 ^{769 ± 4}	244 ^{922 ± 4}	397 ^{1431 ± 9}	415 ^{3489 ± 47}	476 ^{2930763 ± 47355}	476 ^{2929759 ± 39149}			
356	shu-003	428774	146940	101 ⁵¹¹	276 ^{2048 ± 0}	273 ^{820 ± 6}	233 ^{828 ± 3}	252 ^{941 ± 9}	352 ^{1308 ± 15}	408 ^{3045 ± 44}	267 ^{2506 ± 26}	268 ^{2512 ± 38}			
357	siat-002	486842	7738	399 ²⁴³⁴	348 ^{2052 ± 0}	171 ^{579 ± 0}	-	-	-	-	-	113 ^{769 ± 13}	110 ^{750 ± 13}		
358	siat-005	380936	16935	299 ¹²⁹⁸	232 ^{2048 ± 0}	98 ^{403 ± 0}	78 ^{400 ± 0}	58 ^{401 ± 0}	53 ^{403 ± 1}	42 ^{422 ± 7}	60 ^{577 ± 13}	62 ^{580 ± 17}			
359	sjtu-003	480795	148243	113 ⁵³⁸	237 ^{2048 ± 0}	275 ^{821 ± 2}	228 ^{820 ± 2}	245 ^{923 ± 3}	320 ^{1201 ± 3}	391 ^{2373 ± 9}	194 ^{1560 ± 20}	193 ^{1560 ± 14}			
360	sjtu-004	1953267	241108	413 ²⁷²⁷	456 ^{4608 ± 0}	405 ^{1236 ± 2}	366 ^{1209 ± 2}	378 ^{1294 ± 4}	417 ^{1554 ± 5}	402 ^{2738 ± 8}	296 ^{3057 ± 14}	296 ^{3070 ± 20}			
361	sktelecom-000	527132	298496	303 ¹³¹¹	96 ^{1536 ± 0}	373 ^{1110 ± 1}	340 ^{1113 ± 1}	324 ^{1114 ± 1}	286 ^{1120 ± 1}	246 ^{1155 ± 1}	427 ^{26583 ± 128}	426 ^{26508 ± 126}			
362	smartbiometrik-001	30875	92620	71	40 ^{512 ± 0}	192 ^{620 ± 7}	164 ^{625 ± 7}	161 ^{640 ± 4}	161 ^{728 ± 6}	209 ^{1047 ± 8}	100 ^{703 ± 31}	101 ^{710 ± 40}			
363	smartengines-000	17111	3025	450	12 ^{288 ± 0}	24 ^{168 ± 7}	21 ^{180 ± 1}	18 ^{188 ± 3}	20 ^{217 ± 3}	24 ^{275 ± 1}	9 ^{197 ± 5}	7 ^{167 ± 11}			
364	smartengines-001	7095	4601	346	11 ^{288 ± 0}	74 ^{333 ± 89}	81 ^{408 ± 1}	66 ^{423 ± 1}	65 ^{460 ± 2}	75 ^{553 ± 5}	6 ^{153 ± 11}	5 ^{143 ± 13}			
365	smartvist-000	5959	134084	32165	36 ^{512 ± 0}	859 ± 0	656 ± 0	556 ± 0	558 ± 0	690 ± 1	186 ^{1435 ± 31}	185 ^{1422 ± 48}			
366	smilart-002	111826	87805	51 ²⁶³	76 ^{1024 ± 0}	27 ^{176 ± 16}	-	-	-	-	413 ^{18784 ± 136}	414 ^{18795 ± 151}			
367	smilart-003	67339	91670	42 ¹⁹²	20 ^{512 ± 0}	29 ^{180 ± 12}	22 ^{181 ± 10}	37 ^{313 ± 22}	139 ^{665 ± 49}	388 ^{2299 ± 196}	179 ^{1395 ± 74}	145 ^{1027 ± 66}			
368	sodec-000	836592	13142	429 ³¹⁸⁶	424 ^{4096 ± 0}	360 ^{1041 ± 2}	316 ^{1032 ± 1}	299 ^{1035 ± 1}	265 ^{1037 ± 2}	217 ^{1061 ± 2}	215 ^{1794 ± 37}	213 ^{1775 ± 23}			
369	sqisoft-002	278039	386291	142 ⁶⁶⁶	377 ^{2056 ± 0}	124 ^{466 ± 8}	100 ^{466 ± 2}	85 ^{468 ± 11}	66 ^{461 ± 6}	54 ^{472 ± 4}	111 ^{758 ± 11}	111 ^{760 ± 23}			
370	sqisoft-003	362737	607964	187 ⁸⁰⁵	356 ^{2056 ± 0}	203 ^{638 ± 2}	183 ^{674 ± 7}	182 ^{718 ± 17}	138 ^{665 ± 6}	128 ^{720 ± 6}	121 ^{844 ± 11}	121 ^{844 ± 23}			
371	stachu-000	879661	624676	247 ¹⁰⁶⁴	417 ^{4096 ± 0}	268 ^{813 ± 25}	-	-	-	-	289 ^{2979 ± 31}	292 ^{3007 ± 75}			
372	starhybrid-001	100509	289356	200 ⁸⁴⁵	114 ^{2048 ± 0}	82 ^{358 ± 82}	63 ^{355 ± 49}	51 ^{379 ± 58}	51 ^{401 ± 79}	38 ^{393 ± 67}	151 ^{1075 ± 51}	155 ^{1078 ± 53}			
373	stcon-000	408095	49619	266 ¹¹³¹	78 ^{1024 ± 0}	191 ^{617 ± 1}	167 ^{632 ± 4}	149 ^{634 ± 1}	129 ^{645 ± 2}	113 ^{676 ± 6}	41 ^{437 ± 10}	40 ^{434 ± 11}			
374	sukshi-000	94035	688738	69 ³⁷²	475 ^{32768 ± 0}	101 ^{407 ± 11}	82 ^{413 ± 8}	100 ^{504 ± 8}	146 ^{689 ± 11}	360 ^{1574 ± 28}	384 ^{9817 ± 50}	383 ^{9787 ± 62}			
375	suprema-003	498231	116054	284 ¹²³⁹	328 ^{2048 ± 0}	463 ^{1448 ± 1}	426 ^{1417 ± 4}	420 ^{1418 ± 3}	394 ^{1421 ± 4}	335 ^{1451 ± 5}	251 ^{2201 ± 10}	254 ^{2198 ± 13}			
376	suprema-004	1430475	116085	392 ²²⁷²	429 ^{4096 ± 0}	472 ^{1478 ± 2}	439 ^{1472 ± 2}	433 ^{1469 ± 1}	409 ^{1476 ± 1}	348 ^{1496 ± 1}	301 ^{3201 ± 14}	301 ^{3202 ± 22}			
377	supremaid-001	258193	23479	114 ⁵⁴¹	113 ^{2048 ± 0}	130 ^{479 ± 1}	107 ^{481 ± 0}	90 ^{481 ± 0}	77 ^{490 ± 0}	65 ^{522 ± 0}	101 ^{704 ± 19}	92 ^{652 ± 19}			
378	supremaid-002	256273	23899	60 ³³⁵	174 ^{2048 ± 0}	133 ^{483 ± 0}	118 ^{501 ± 0}	94 ^{488 ± 0}	83 ^{503 ± 0}	82 ^{565 ± 0}	238 ^{1990 ± 19}	231 ^{1923 ± 29}			
379	surrey-cvssp-000	158030	70795	210 ⁸⁷⁹	162 ^{2048 ± 0}	382 ^{1141 ± 3}	352 ^{1157 ± 3}	338 ^{1158 ± 4}	302 ^{1163 ± 3}	270 ^{1245 ± 3}	382 ^{9557 ± 143}	381 ^{9602 ± 186}			
380	surrey-cvssp-001	900280	76392	348 ¹⁷⁰⁷	161 ^{2048 ± 0}	402 ^{1221 ± 1}	373 ^{1238 ± 2}	339 ^{1240 ± 0}	330 ^{1243 ± 0}	274 ^{1257 ± 0}	415 ^{18970 ± 161}	412 ^{18999 ± 176}			
381	synesis-006	731941	21817	324 ¹⁴⁷²	449 ^{4104 ± 0}	156 ^{549 ± 1}	134 ^{546 ± 1}	120 ^{552 ± 1}	98 ^{558 ± 2}	103 ^{639 ± 28}	99 ^{697 ± 32}	99 ^{688 ± 31}			
382	synesis-007	1442961	24145	400 ²⁴⁴³	394 ^{3080 ± 0}	400 ^{1215 ± 5}	383 ^{1268 ± 30}	381 ^{1306 ± 67}	353 ^{1311 ± 58}	324 ^{1423 ± 52}	95 ^{684 ± 32}	97 ^{686 ± 25}			
383	synology-000	221021	25809	85 ⁴⁵³	307 ^{2048 ± 0}	100 ^{407 ± 14}	83 ^{415 ± 14}	173 ^{694 ± 31}	384 ^{1396 ± 58}	417 ^{4568 ± 211}	417 ^{19720 ± 203}	416 ^{19767 ± 379}			
384	synology-002	256713	25943	93 ⁴⁸⁸	107 ^{2048 ± 0}	303 ^{886 ± 4}	259 ^{892 ± 3}	241 ^{920 ± 2}	252 ^{1000 ± 5}	291 ^{1317 ± 12}	188 ^{1466 ± 32}	191 ^{1496 ± 45}			
385	sztu-000	338637	15871	297 ¹²⁹⁸	316 ^{2048 ± 0}	150 ^{531 ± 0}	125 ^{532 ± 0}	109 ^{533 ± 0}	91 ^{537 ± 0}	73 ^{548 ± 0}	61 ^{585 ± 11}	66 ^{592 ± 13}			
386	sztu-001	338650	15871	298 ¹²⁹⁸	266 ^{2048 ± 0}	151 ^{535 ± 0}	129 ^{537 ± 0}	113 ^{538 ± 0}	92 ^{540 ± 0}	74 ^{553 ± 0}	67 ^{599 ± 10}	70 ^{598 ± 10}			
387	t4isb-000	234227	115237	62 ³⁴³	256 ^{2048 ± 0}	348 ^{1006 ± 5}	303 ^{1001 ± 1}	288 ^{1006 ± 1}	256 ^{1009 ± 1}	201 ^{1022 ± 2}	316 ^{3586 ± 34}	313 ^{3534 ± 34}			
388	tech5-005	1178769	120517	318 ¹⁴²⁶	25 ^{512 ± 0}	417 ^{1272 ± 109}	320 ^{1038 ± 63}	303 ^{1046 ± 39}	287 ^{1124 ± 38}	302 ^{1351 ± 44}	271 ^{2573 ± 37}	271 ^{2545 ± 32}			
389	tech5-007	0	340324	409 ²⁶⁴³	21 ^{512 ± 0}	437 ^{1360 ± 0}	408 ^{1366 ± 0}	402 ^{1376 ± 0}	374 ^{1373 ± 0}	331 ^{1438 ± 6}	51 ^{538 ± 19}	52 ^{516 ± 22}			
390	techsign-000	0	1101622	375 ¹⁹⁵⁵	194 ^{2048 ± 0}	86 ^{366 ± 1}	77 ^{398 ± 1}	342 ^{1172 ± 3}	441 ^{3065 ± 18}	437 ^{10460 ± 65}	334 ^{4758 ± 112}	334 ^{4789 ± 93}			
391	techsign-001	0	586983	355 ¹⁷⁴¹	108 ^{2048 ± 0}	253 ^{772 ± 35}	219 ^{788 ± 23}	199 ^{802 ± 42}	230 ^{949 ± 10}	321 ^{1409 ± 26}	62 ^{592 ± 11}	65 ^{592 ± 13}			
392	tevian-007	779934	19523	350 ¹⁷¹⁴	88 ^{1032 ± 0}	173 ^{583 ± 1}	145 ^{579 ± 0}	128 ^{580 ± 0}	107 ^{588 ± 1}	102 ^{636 ± 0}	339 ^{4894 ± 65}	337 ^{4841 ± 83}			
393	tevian-008	847177	19519	432 ³⁴⁹⁰	86 ^{1032 ± 0}	300 ^{884 ± 2}	264 ^{903 ± 1}	234 ^{903 ± 1}	216 ^{911 ± 1}	183 ^{946 ± 1}	336 ^{4828 ± 40}	336 ^{4811 ± 41}			
394	tiger-005	342866	253734	331 ¹⁵³¹	337 ^{2052 ± 0}	367 ^{1097 ± 2}	326 ^{1065 ± 2}	314 ^{1066 ± 2}	274 ^{1067 ± 3}	224 ^{1088 ± 3}	77 ^{620 ± 19}	81 ^{615 ± 16}			
395	tiger-006	421186	394688	157 ⁷⁰⁷	339 ^{2052 ± 0}	449 ^{1392 ± 16}	425 ^{1411 ± 10}	425 ^{1444 ± 10}	416 ^{1531 ± 11}	382 ^{1848 ± 10}	219 ^{1810 ± 20}	218 ^{1801 ± 13}			
396	tinkoff-001	274660	389272	127 ⁵⁹²	254 ^{2048 ± 0}	389 ^{1176 ± 3}	359 ^{1179 ± 3}	343 ^{1178 ± 3}	306 ^{1169 ± 2}	262 ^{1203 ± 3}	330 ^{4361 ± 74}	328 ^{4364 ± 75}			

Notes

- 1 The configuration size does not capture static data included in libraries.
- 2 The library size is the combined total of all files provided in the submission lib folder. These libraries e.g. OpenCV may or may not be installed on any end user's platform natively and would not need to be installed with the algorithm. Some developers put neural network models in their libraries.
- 3 The memory usage is the peak resident set size reported by the ps system call during template generation.
- 4 The median template creation times are measured on Intel®Xeon®CPU E5-2630 v4 @ 2.20GHz processors.
- 5 The comparison durations, in nanoseconds, are estimated using std::chrono::high_resolution_clock which on the machine in (2) counts 1ns clock ticks. Precision is somewhat worse than that however. The ± value is the median absolute deviation times 1.48 for Normal consistency.

	ALGORITHM	CONFIG	LIBRARY	TEMPLATE								COMPARISON ⁴		
				NAME	DATA	DATA	MEMORY	SIZE	GENERATION TIME (ms) ⁴				TIME (ns) ⁵	
									(KB) ¹	(KB) ²	(MB) ³	(B)	MUGSHOT	480x720
397	tongyi-005	1140701	138919	³⁸³ 2121	³⁸⁸ 2089 ± 0	²³ 165 ± 1	-	-	-	-	-	-	⁴¹⁴ 18924 ± 65	⁴¹⁷ 20158 ± 103
398	toppanidgate-000	671181	711850	³⁵⁹ 1786	⁴²⁷ 4096 ± 0	³¹¹ 915 ± 1	²⁶⁹ 916 ± 1	²⁴⁰ 916 ± 1	²¹⁹ 917 ± 1	¹⁷⁸ 917 ± 1	⁴²⁵ 25262 ± 84	⁴²⁴ 25264 ± 97		
399	toshiba-004	599297	27880	³³⁸ 1595	³⁶³ 2056 ± 0	⁴⁶² 1447 ± 3	⁴³⁶ 1453 ± 2	⁴³¹ 1457 ± 9	⁴⁰² 1457 ± 3	³⁴² 1479 ± 4	¹⁴² 1020 ± 25	¹³⁸ 998 ± 32		
400	toshiba-006	599566	44078	³³⁶ 1588	³⁵⁸ 2056 ± 0	⁴⁷⁴ 1481 ± 16	⁴⁴³ 1515 ± 7	⁴³⁷ 1506 ± 6	⁴¹³ 1521 ± 2	³⁵⁸ 1546 ± 30	¹⁴³ 1022 ± 17	¹⁴⁴ 1022 ± 23		
401	touchlessid-000	92561	64467	¹⁶⁰ 716	¹⁵⁷ 2048 ± 0	⁶⁸ 309 ± 5	⁵¹ 305 ± 2	³⁶ 312 ± 5	²⁹ 277 ± 4	³¹ 349 ± 17	⁴³⁶ 31935 ± 292	⁴³⁷ 31958 ± 243		
402	touchlessid-001	255274	14355	¹¹² 537	²⁹⁵ 2048 ± 0	⁷⁷ 344 ± 1	⁶² 347 ± 1	⁶³ 414 ± 3	¹¹² 595 ± 10	³⁷⁴ 1732 ± 61	²¹⁸ 1806 ± 35	²¹⁷ 1800 ± 35		
403	trueface-002	253947	123116	⁹² 486	¹⁰² 2000 ± 0	⁸³ 360 ± 0	⁶⁵ 361 ± 0	⁶⁸ 423 ± 0	¹¹¹ 590 ± 1	-	⁸ 192 ± 14	¹⁰ 186 ± 19		
404	trueface-003	346530	24308	⁴⁴³ 3915	¹⁵⁴ 2048 ± 0	³⁷¹ 1107 ± 22	¹⁸⁶ 677 ± 3	¹⁸⁴ 732 ± 7	²¹⁵ 905 ± 5	-	¹ 103 ± 11	² 112 ± 29		
405	trueidvng-001	766071	37721	³⁴⁴ 1692	⁴⁶² 6144 ± 0	³³⁵ 975 ± 1	²⁹⁵ 985 ± 1	²⁷⁹ 989 ± 1	²⁵⁹ 1016 ± 1	²³⁷ 1128 ± 2	⁴⁴¹ 37129 ± 216	⁴⁶⁶ 72067 ± 305		
406	tuputech-000	11476	17185	²³³	²⁵⁵ 2048 ± 0	²¹ 122 ± 4	¹⁵ 120 ± 1	¹³ 142 ± 2	¹⁷ 196 ± 5	⁴³ 411 ± 14	⁴²² 23893 ± 406	⁴²⁵ 25279 ± 406		
407	turingtechvip-001	399874	54535	¹³⁵ 617	²¹⁵ 2048 ± 0	⁴⁴⁴ 1384 ± 4	⁴¹⁵ 1391 ± 1	⁴¹⁰ 1393 ± 1	³⁹¹ 1411 ± 1	³⁴⁰ 1476 ± 2	²⁰⁹ 1733 ± 19	²¹⁰ 1734 ± 20		
408	turingtechvip-002	167556	140995	²⁰⁹ 876	¹⁸³ 2048 ± 0	⁴⁷⁶ 1493 ± 2	³⁹⁵ 1306 ± 1	⁴⁰⁶ 1382 ± 1	³⁶³ 1337 ± 1	³²⁷ 1426 ± 3	⁴⁰¹ 13819 ± 103	⁴⁰¹ 13807 ± 137		
409	turkcell-000	271083	133553	¹³⁸ 637	¹⁸¹ 2048 ± 0	³⁷⁴ 1110 ± 1	³³³ 1094 ± 0	³²² 1103 ± 0	²⁸⁹ 1126 ± 1	²⁶⁰ 1201 ± 1	²⁸³ 2866 ± 23	²⁸⁴ 2873 ± 40		
410	twface-000	661735	11782	⁴⁰⁶ 2610	¹²⁴ 2048 ± 0	²⁹¹ 871 ± 1	²⁴⁸ 873 ± 1	²²⁰ 873 ± 2	²⁰³ 876 ± 2	¹⁷⁷ 898 ± 1	¹⁹³ 1504 ± 29	¹⁹² 1510 ± 34		
411	twface-001	671511	11782	⁴²¹ 2855	²⁴⁸ 2048 ± 0	³¹⁶ 923 ± 1	²⁷⁵ 925 ± 2	²⁴⁶ 926 ± 1	²²² 929 ± 2	¹⁸¹ 940 ± 2	¹⁸⁰ 1400 ± 32	¹⁸² 1402 ± 37		
412	ulsee-001	370519	57261	-	²³³ 2048 ± 0	²⁰⁹ 654 ± 2	-	-	-	-	³⁶⁰ 6065 ± 94	³⁶² 6228 ± 77		
413	uluface-002	0	480761	²⁵³ 1088	²⁴⁰ 2048 ± 0	²⁹⁴ 873 ± 42	²⁴⁰ 855 ± 9	²⁷⁰ 978 ± 24	³³⁷ 1271 ± 40	³⁸⁹ 2333 ± 68	⁴¹⁶ 19207 ± 1114	⁴¹³ 18501 ± 274		
414	uluface-003	97357	529422	²⁸⁷ 1264	³⁹³ 3072 ± 0	³³⁰ 965 ± 11	²⁸⁸ 968 ± 10	³¹⁶ 1087 ± 20	³⁷⁹ 1387 ± 36	³⁹⁶ 2469 ± 86	⁴²⁶ 26057 ± 195	⁴²⁸ 26865 ± 566		
415	unissey-002	0	1443765	¹⁷³ 763	⁴³⁷ 4096 ± 0	²⁴³ 736 ± 1	²¹⁰ 752 ± 1	²⁸² 994 ± 1	³⁹⁶ 1426 ± 1	⁴¹⁴ 3331 ± 2	³⁹⁵ 12308 ± 91	³⁹⁵ 12302 ± 137		
416	unissey-003	0	814526	¹³⁷ 618	⁴²⁰ 4096 ± 0	²⁴⁰ 718 ± 1	²⁰⁷ 744 ± 0	²⁵⁷ 956 ± 1	³⁸⁹ 1403 ± 1	⁴⁰⁹ 3055 ± 2	¹⁹⁷ 1594 ± 20	¹⁹⁵ 1570 ± 44		
417	upc-001	0	89914	²⁵² 1077	⁸⁹ 1052 ± 0	¹⁵⁸ 551 ± 15	¹⁹⁶ 703 ± 56	¹⁸³ 724 ± 51	¹⁶⁷ 751 ± 49	¹⁶³ 863 ± 33	²⁹⁸ 3114 ± 44	³⁰⁰ 3165 ± 97		
418	uxlabs-001	291127	39378	¹⁵⁴ 700	⁴²⁵ 4096 ± 0	⁹⁴ 395 ± 0	⁷⁰ 387 ± 0	⁵⁴ 388 ± 0	⁴⁸ 390 ± 0	⁴⁰ 396 ± 0	²²⁵ 1863 ± 31	²³⁰ 1921 ± 45		
419	vcog-002	3229434	118946	⁴³⁴ 3666	⁴⁷⁶ 61504 ± 5	⁸¹ 357 ± 25	-	-	-	-	⁴⁷³ 296154 ± 3077	⁴⁷³ 296436 ± 4183		
420	vd-002	254498	34389	¹⁵⁰ 688	⁵¹ 516 ± 0	²²⁵ 684 ± 5	¹⁸⁷ 679 ± 4	¹⁶⁴ 676 ± 5	¹⁴⁸ 693 ± 5	¹³⁷ 754 ± 5	²⁹ 300 ± 14	²⁸ 319 ± 32		
421	vd-003	254505	44051	¹⁵² 696	³⁴⁷ 2052 ± 0	²³² 691 ± 5	¹⁹¹ 690 ± 5	¹⁶⁷ 683 ± 4	¹⁴⁷ 691 ± 5	¹²⁹ 722 ± 5	¹⁴⁰ 1003 ± 11	¹⁴⁰ 1001 ± 7		
422	veridas-007	355105	891492	⁴⁰³ 2527	²⁷² 2048 ± 0	²⁹² 872 ± 9	²⁴⁹ 875 ± 8	³⁶⁴ 1261 ± 18	⁴³⁴ 2238 ± 38	⁴²⁸ 6374 ± 147	⁹¹ 655 ± 16	⁹⁴ 660 ± 19		
423	veridas-008	1100495	1190915	⁴⁶⁹ 8932	¹¹¹ 2048 ± 0	³²¹ 944 ± 12	²⁸¹ 945 ± 11	³⁸⁹ 1334 ± 27	⁴³⁵ 2382 ± 48	⁴²⁹ 6959 ± 172	¹⁰⁴ 723 ± 14	¹⁰⁶ 731 ± 16		
424	veridium-000	0	47198	¹⁵⁸ 98	⁴⁷⁴ 29399 ± 2045	¹⁷ 79 ± 0	⁹ 80 ± 0	¹⁰ 89 ± 0	⁸ 90 ± 0	⁸ 111 ± 0	⁴⁶¹ 64880 ± 171	⁴⁶⁰ 64697 ± 247		
425	veridium-001	0	40561	²⁵ 142	³⁹⁰ 2489 ± 0	⁷ 44 ± 0	⁵ 45 ± 0	⁴ 48 ± 0	⁴ 50 ± 0	⁴ 72 ± 0	⁴⁶⁰ 63417 ± 1061	⁴⁵⁹ 63225 ± 2133		
426	verigram-000	256209	7798	³⁶⁵ 1842	²⁴⁶ 2048 ± 0	²⁶⁴ 807 ± 1	²²⁹ 821 ± 1	²⁶⁶ 972 ± 2	³⁶⁹ 1358 ± 3	⁴⁰⁵ 2848 ± 13	¹⁶⁸ 1222 ± 17	¹⁶⁹ 1219 ± 17		
427	verigram-001	282155	11773	⁴⁰⁸ 2638	³⁰¹ 2048 ± 0	²¹⁴ 664 ± 2	¹⁸⁴ 675 ± 2	²⁰⁹ 833 ± 4	³²¹ 1202 ± 7	⁴⁰¹ 2733 ± 32	²⁰³ 1664 ± 60	²⁰¹ 1648 ± 56		
428	verihubs-inteligensia-000	209562	51877	⁷⁸ 427	²⁸⁷ 2048 ± 0	¹⁶⁵ 567 ± 0	⁴⁴⁴ 1558 ± 8	⁴⁴⁰ 1560 ± 8	⁴¹⁸ 1568 ± 8	³⁶⁴ 1621 ± 8	⁴²¹ 22351 ± 91	⁴²¹ 22371 ± 81		
429	verihubs-inteligensia-001	216524	51916	⁸⁰ 437	¹⁶³ 2048 ± 0	¹⁶⁴ 564 ± 0	¹⁴⁰ 562 ± 0	¹²⁴ 566 ± 1	¹⁰¹ 566 ± 0	⁹⁰ 600 ± 0	⁴¹⁹ 21770 ± 84	⁴¹⁹ 21735 ± 102		
430	verijelas-000	254540	10322	³⁵⁴ 1736	¹¹² 2048 ± 0	⁶⁹ 321 ± 0	⁵⁶ 325 ± 1	⁴² 329 ± 0	³⁸ 335 ± 5	³² 360 ± 0	³⁸⁶ 10267 ± 143	³⁸⁶ 10218 ± 109		
431	via-000	124422	11151	²²⁸ 964	¹²¹ 2048 ± 0	²³⁸ 707 ± 8	²⁰⁶ 740 ± 5	²³⁵ 906 ± 41	²²⁷ 941 ± 40	²⁰⁶ 1040 ± 5	¹³³ 966 ± 28	¹⁴³ 1021 ± 44		
432	via-001	370255	11151	³⁴⁵ 1697	¹⁷⁷ 2048 ± 0	³²⁹ 964 ± 3	³⁰⁹ 1011 ± 3	²⁹³ 1026 ± 4	²⁶⁸ 1045 ± 3	²⁴⁰ 1137 ± 28	¹³⁶ 983 ± 31	¹³⁶ 989 ± 40		
433	videmo-001	212051	95063	⁵⁷ 304	³⁰⁶ 2048 ± 0	³⁵ 199 ± 0	¹⁷ 164 ± 0	¹⁴ 164 ± 0	¹¹ 164 ± 0	¹⁰ 165 ± 0	²² 296 ± 17	²⁵ 288 ± 16		
434	videmo-002	212053	32963	⁵⁹ 332	¹⁷⁰ 2048 ± 0	³⁷ 199 ± 0	¹⁸ 169 ± 0	¹⁵ 169 ± 0	¹² 170 ± 0	¹² 170 ± 0	¹⁴ 209 ± 7	¹⁵ 208 ± 8		
435	videonetics-001	30875	5963	⁵ 61	³⁹ 512 ± 0	⁴⁶ 262 ± 3	³⁹ 273 ± 1	⁷³ 439 ± 3	¹⁸⁵ 820 ± 3	³⁹³ 2393 ± 43	¹⁶² 1153 ± 38	¹⁶³ 1142 ± 65		
436	videonetics-002	121981	6289	¹⁹ 115	³³⁴ 2052 ± 0	⁵⁷ 282 ± 5	⁴⁹ 295 ± 1	¹⁰⁴ 513 ± 4	²⁶¹ 1029 ± 3	⁴¹⁰ 3151 ± 46	¹⁶⁷ 1219 ± 57	¹⁷¹ 1262 ± 56		
437	viettelhightech-000	259471	215557	⁷⁶ 419	³²⁰ 2048 ± 0	¹¹⁹ 461 ± 1	⁹⁹ 461 ± 2	⁸¹ 461 ± 1	⁷¹ 467 ± 2	⁵⁸ 494 ± 0	⁶⁶ 599 ± 11	⁶⁴ 591 ± 13		
438	vigilantsolutions-010	348798	49973	¹⁹⁹ 840	⁹⁹ 1548 ± 0	¹⁸⁹ 615 ± 0	¹⁶⁶ 631 ± 0	¹⁴⁶ 632 ± 0	¹²⁶ 636 ± 0	¹⁰⁸ 659 ± 0	⁴⁹ 490 ± 13	⁵⁰ 488 ± 11		
439	vigilantsolutions-011	255661	49973	¹²⁶ 591	⁹⁸ 1548 ± 0	⁹⁷ 402 ± 0	⁸⁴ 418 ± 0	⁶⁴ 418 ± 0	⁵⁷ 422 ± 0	⁵⁰ 445 ± 0	³⁰ 339 ± 20	³⁴ 366 ± 37		
440	vinai-000	402391	866522	²⁴² 1032	¹⁴⁵ 2048 ± 0	³⁶⁹ 1099 ± 1	³³⁴ 1095 ± 1	³¹⁸ 1093 ± 1	²⁸² 1099 ± 1	²³⁶ 1126 ± 1	²⁹⁰ 2996 ± 20	²⁹¹ 2993 ± 26		

Notes

- 1 The configuration size does not capture static data included in libraries.
- 2 The library size is the combined total of all files provided in the submission lib folder. These libraries e.g. OpenCV may or may not be installed on any end user's platform natively and would not need to be installed with the algorithm. Some developers put neural network models in their libraries.
- 3 The memory usage is the peak resident set size reported by the ps system call during template generation.
- 4 The median template creation times are measured on Intel®Xeon®CPU E5-2630 v4 @ 2.20GHz processors.
- 5 The comparison durations, in nanoseconds, are estimated using std::chrono::high_resolution_clock which on the machine in (2) counts 1ns clock ticks. Precision is somewhat worse than that however. The ± value is the median absolute deviation times 1.48 for Normal consistency.

Table 17: Summary of algorithms and properties included in this report. The red superscripts give ranking for the quantity in that column.

	ALGORITHM	CONFIG	LIBRARY	TEMPLATE								COMPARISON ⁴									
				NAME	DATA	DATA	MEMORY	SIZE	GENERATION TIME (ms) ⁴				TIME (ns) ⁵								
									(KB) ¹	(KB) ²	(MB) ³	(B)	MUGSHOT	480x720	960x1440	1600x2400	3000x4500	GENUINE	IMPOSTOR		
441	vinbigdata-001	271405	44746	125	589	195	2048 ± 0	452	1400 ± 5	418	1393 ± 2	407	1391 ± 2	381	1393 ± 1	320	1404 ± 1	176	1351 ± 50	176	1310 ± 38
442	vinbigdata-002	256322	138864	132	606	313	2048 ± 0	167	569 ± 2	143	572 ± 1	125	571 ± 1	102	572 ± 1	88	596 ± 1	249	2175 ± 44	250	2160 ± 53
443	vion-000	228219	7533	96	498	345	2052 ± 0	73	333 ± 1	-	-	-	-	-	-	443	39839 ± 3561	427	26830 ± 2241		
444	visageo-000	49218	70150	9	73	44	512 ± 0	427	27 ± 0	227	27 ± 0	231	27 ± 0	338	38 ± 0	3	63 ± 0	253	2220 ± 14	255	2218 ± 14
445	visionbox-001	256869	190645	120	579	264	2048 ± 0	340	983 ± 7	332	1093 ± 46	396	1360 ± 68	432	2181 ± 105	426	5955 ± 281	164	1161 ± 22	165	1154 ± 20
446	visionbox-002	259063	135281	134	612	379	2059 ± 0	131	482 ± 1	108	482 ± 0	93	484 ± 1	80	492 ± 1	65	517 ± 3	237	1969 ± 44	234	1931 ± 42
447	visionlabs-010	1067280	19357	213	902	45	513 ± 0	241	730 ± 0	201	717 ± 1	177	709 ± 0	156	713 ± 1	135	739 ± 0	69	600 ± 41	83	626 ± 35
448	visionlabs-011	1067280	19353	206	862	40	513 ± 0	242	731 ± 1	202	717 ± 1	178	710 ± 1	158	714 ± 1	136	741 ± 1	54	556 ± 26	57	559 ± 25
449	visteam-003	215359	33730	94	489	398	4096 ± 0	411	1249 ± 4	378	1251 ± 4	367	1266 ± 5	338	1272 ± 5	308	1370 ± 9	366	6816 ± 111	366	6816 ± 105
450	visteam-004	61594	35369	36	168	315	2048 ± 0	63	303 ± 5	52	313 ± 6	32	278 ± 4	32	288 ± 4	35	377 ± 7	323	3936 ± 72	322	3938 ± 79
451	visteam-005	288140	35427	63	348	239	2048 ± 0	376	1117 ± 6	337	1106 ± 6	310	1060 ± 4	277	1071 ± 4	247	1156 ± 8	322	3932 ± 97	321	3932 ± 71
452	vixvizion-006	594053	396294	218	914	230	2048 ± 0	298	876 ± 9	232	828 ± 3	205	817 ± 1	188	825 ± 2	166	871 ± 1	68	600 ± 23	78	611 ± 25
453	vixvizion-007	594053	470119	295	1282	155	2048 ± 0	301	885 ± 35	234	828 ± 1	204	816 ± 1	187	825 ± 1	165	870 ± 1	70	600 ± 28	72	602 ± 34
454	vnpt-004	370110	240841	235	988	216	2048 ± 0	407	1238 ± 1	374	1241 ± 1	361	1242 ± 2	350	1307 ± 2	349	1505 ± 2	326	4047 ± 48	324	4008 ± 108
455	vnpt-005	560630	240888	272	1141	282	2048 ± 0	454	1403 ± 0	423	1404 ± 6	415	1403 ± 6	401	1456 ± 0	365	1630 ± 10	314	3562 ± 23	314	3554 ± 29
456	vocord-009	1380132	201560	448	4162	101	1920 ± 0	470	1472 ± 2	440	1472 ± 1	439	1549 ± 1	421	1667 ± 2	385	2064 ± 2	242	2052 ± 50	244	2056 ± 39
457	vocord-010	902552	206873	438	3858	90	1088 ± 0	466	1459 ± 2	438	1459 ± 1	432	1463 ± 2	411	1484 ± 1	355	1535 ± 3	275	2724 ± 31	274	2653 ± 45
458	vts-000	256589	169760	347	1704	122	2048 ± 0	136	486 ± 1	106	481 ± 0	92	484 ± 0	76	485 ± 1	66	517 ± 0	470	124209 ± 352	470	123652 ± 358
459	vts-001	293000	475743	136	618	219	2048 ± 0	220	676 ± 1	188	683 ± 6	170	687 ± 3	149	695 ± 2	123	709 ± 2	383	9620 ± 44	382	9618 ± 54
460	wicket-000	826392	641802	381	2071	213	2048 ± 0	459	1419 ± 2	428	1429 ± 3	426	1444 ± 4	404	1460 ± 3	356	1537 ± 6	458	60976 ± 232	457	61096 ± 323
461	winsense-001	264428	32035	221	922	93	1280 ± 0	250	766 ± 7	322	1058 ± 47	273	983 ± 97	270	1053 ± 119	292	1320 ± 84	200	1631 ± 28	238	1964 ± 171
462	winsense-002	281379	25780	358	1781	294	2048 ± 0	138	494 ± 2	114	498 ± 1	106	519 ± 1	90	537 ± 1	99	634 ± 1	205	1683 ± 8	204	1685 ± 7
463	wiseai-001	189467	60781	45	245	120	2048 ± 0	43	240 ± 0	35	251 ± 0	41	328 ± 1	37	327 ± 0	27	332 ± 0	280	2850 ± 29	283	2852 ± 31
464	wuhantianyu-001	465118	66457	207	866	221	2048 ± 0	204	642 ± 1	173	642 ± 1	157	644 ± 0	132	652 ± 0	121	697 ± 0	381	9502 ± 151	385	9920 ± 253
465	x-laboratory-000	520020	197310	329	1524	375	2056 ± 0	265	808 ± 7	261	897 ± 113	236	907 ± 103	207	886 ± 103	112	673 ± 39	105	725 ± 19	109	749 ± 34
466	x-laboratory-001	625140	398792	366	1844	357	2056 ± 0	177	586 ± 2	155	596 ± 5	139	603 ± 6	121	620 ± 7	144	793 ± 14	118	813 ± 28	123	872 ± 32
467	xforwardai-001	340100	51163	386	2173	149	2048 ± 0	393	1180 ± 2	362	1182 ± 1	351	1194 ± 1	315	1186 ± 2	263	1203 ± 1	115	779 ± 17	115	797 ± 13
468	xforwardai-002	707715	51163	378	1989	400	4096 ± 0	320	944 ± 1	280	942 ± 1	253	943 ± 4	228	935 ± 1	190	967 ± 1	184	1406 ± 8	183	1405 ± 13
469	xm-000	578041	148920	149	688	350	2052 ± 0	299	878 ± 2	255	882 ± 1	277	988 ± 2	335	1258 ± 3	395	2434 ± 7	201	1634 ± 17	199	1632 ± 20
470	yisheng-004	486351	38653	293	1279	397	3704 ± 0	87	378 ± 12	-	-	-	-	-	-	97	693 ± 137	53	526 ± 34		
471	yitu-003	1525719	138919	436	3737	387	2082 ± 0	288	860 ± 0	-	-	-	-	-	-	411	18305 ± 71	411	18286 ± 62		
472	yoonik-002	453720	265415	417	2755	190	2048 ± 0	384	1145 ± 4	341	1123 ± 2	326	1124 ± 2	288	1125 ± 2	235	1126 ± 3	112	761 ± 32	108	736 ± 32
473	yoonik-003	346691	265415	390	2196	196	2048 ± 0	343	991 ± 3	294	980 ± 1	274	984 ± 4	240	982 ± 1	194	983 ± 1	93	684 ± 45	95	678 ± 41
474	ytu-000	1477360	44032	401	2484	159	2048 ± 0	149	530 ± 0	127	533 ± 0	153	640 ± 0	199	861 ± 2	384	1949 ± 8	434	31797 ± 131	435	31794 ± 133
475	yuan-005	258312	145564	198	839	234	2048 ± 0	89	381 ± 0	69	386 ± 0	53	387 ± 2	47	390 ± 4	44	421 ± 3	163	1156 ± 8	167	1196 ± 26
476	yuan-006	1622733	145572	451	4365	431	4096 ± 0	419	1280 ± 2	382	1268 ± 1	369	1273 ± 0	339	1272 ± 2	290	1306 ± 3	252	2202 ± 19	252	2190 ± 20

Notes

- 1 The configuration size does not capture static data included in libraries.
- 2 The library size is the combined total of all files provided in the submission lib folder. These libraries e.g. OpenCV may or may not be installed on any end user's platform natively and would not need to be installed with the algorithm. Some developers put neural network models in their libraries.
- 3 The memory usage is the peak resident set size reported by the ps system call during template generation.
- 4 The median template creation times are measured on Intel®Xeon®CPU E5-2630 v4 @ 2.20GHz processors.
- 5 The comparison durations, in nanoseconds, are estimated using std::chrono::high_resolution_clock which on the machine in (2) counts 1ns clock ticks. Precision is somewhat worse than that however. The ± value is the median absolute deviation times 1.48 for Normal consistency.

Table 18: Summary of algorithms and properties included in this report. The red superscripts give ranking for the quantity in that column.

	Algorithm	FALSE NON-MATCH RATE (FNMR)										LESS CONSTRAINED, NON-COOP.					
		CONSTRAINED, COOPERATIVE								WILD							
		Name	VISAMC	VISA	MUGSHOT	MUGSHOT12+YRS	VISABORDER	BORDER	BORDER	1E-05							
	FMR	0.0001	1E-06	1E-05	1E-05	1E-06	1E-06	1E-06	1E-05	0.0001							
1	20face-000	0.1268	417	0.1828	412	0.1748	421	0.2768	421	0.1765	405	0.1864	308	0.0927	342	0.0405	299
2	20face-001	0.0521	393	0.0732	394	0.1414	419	0.2549	420	0.0769	381	0.1354	299	0.0419	298	0.0295	186
3	3divi-006	0.0064	204	0.0094	203	0.0047	187	0.0066	190	0.0091	196	0.0191	164	0.0113	163	0.0289	156
4	3divi-007	0.0024	69	0.0038	75	0.0028	78	0.0034	74	0.0046	109	0.0101	93	0.0082	112	0.0300	201
5	acer-001	0.0294	374	0.0504	376	0.0240	367	0.0463	369	0.0436	360	0.0622	264	0.0360	291	0.0307	217
6	acer-002	0.0169	339	0.0262	339	0.0103	302	0.0167	311	0.0182	294	0.0281	204	0.0159	216	0.0297	193
7	acisw-007	0.4276	446	0.5493	448	0.8425	462	0.9185	462	0.8424	445	0.9976	430	0.9930	448	0.4963	445
8	acisw-008	0.0100	271	0.0147	266	0.0094	298	0.0126	269	0.1740	404	0.6651	366	0.4545	395	0.0925	381
9	ader-a-003	0.0043	140	0.0059	138	0.0036	137	0.0043	117	0.0076	168	0.0151	130	0.0128	183	0.0989	382
10	ader-a-004	0.0014	25	0.0022	25	0.0035	133	0.0050	142	0.0023	12	0.0212	176	0.0058	56	0.0278	43
11	advance-003	0.0060	196	0.0087	193	0.0052	202	0.0067	191	0.0389	353	0.4914	348	0.1291	348	0.0508	330
12	advance-004	0.0083	248	0.0101	218	0.0037	144	0.0054	153	0.0051	122	0.3555	337	0.1088	346	0.1635	401
13	afisbiometrics-000	0.0051	158	0.0073	162	0.0030	98	0.0050	143	0.0044	104	0.0077	55	0.0057	53	0.0282	102
14	afrengine-000	0.6244	466	0.7336	465	0.8318	461	0.9083	460	0.8122	442	0.9980	432	0.9895	446	0.6480	452
15	aifirst-001	0.0119	297	0.0170	287	0.0084	279	0.0127	274	0.0131	253	0.0212	175	0.0138	192	0.0432	313
16	aigen-001	0.0124	303	0.0219	317	0.0143	337	0.0217	334	0.0236	319	0.8960	397	0.3255	380	0.0681	356
17	aigen-002	0.0192	351	0.0343	356	0.0256	368	0.0402	363	0.0389	352	0.9196	401	0.3876	389	0.1096	387
18	ailabs-001	0.0158	332	0.0276	344	0.0192	353	0.0317	354	0.0352	347	0.0608	261	0.0434	301	0.0338	262
19	aimall-002	0.0119	298	0.0167	285	0.0224	362	0.0411	365	0.0233	317	0.0373	235	0.0235	263	0.0327	249
20	aimall-003	0.0033	107	0.0041	83	0.0033	125	0.0035	86	0.0056	135	0.0109	100	0.0087	123	0.0312	227
21	aiseemu-001	0.0021	54	0.0029	47	0.0027	64	0.0033	69	0.0038	80	0.0339	224	0.0057	54	0.0282	93
22	aiseemu-002	0.0023	66	0.0032	53	0.0026	50	0.0027	32	0.0036	73	0.0439	242	0.0057	50	0.0280	78
23	aiunionface-000	0.0104	275	0.0154	276	0.0082	276	0.0122	264	0.0141	260	0.0243	189	0.0169	221	0.0306	214
24	aize-001	0.0223	359	0.0344	357	0.0199	354	0.0313	353	0.0367	349	0.0522	254	0.0359	290	0.0446	318
25	aize-002	0.0210	356	0.0327	352	0.0280	372	0.0489	373	0.0504	367	0.0692	269	0.0434	300	0.0854	376
26	ajou-001	0.0093	261	0.0147	267	0.0071	252	0.0126	270	0.0173	291	0.0274	199	0.0186	237	0.0348	267
27	alchera-004	0.0035	116	0.0052	126	0.0028	85	0.0039	103	0.0029	32	0.0075	51	0.0044	18	0.0304	209
28	alchera-005	0.0027	79	0.0040	78	0.0026	46	0.0030	50	0.0025	18	0.0055	21	0.0040	13	0.0306	216
29	alfabeta-001	0.4867	453	0.5831	451	0.6855	447	0.8156	449	0.8253	444	0.7765	382	0.6416	411	0.3427	433
30	alice-000	0.0119	299	0.0192	305	0.0106	308	0.0170	312	0.0167	282	0.0265	196	0.0150	210	0.0288	144
31	alleyes-000	0.0058	186	0.0090	198	0.0055	213	0.0087	232	0.0068	156	0.0105	99	0.0076	100	0.0282	101
32	allgovision-000	0.0346	383	0.0527	380	0.0232	364	0.0339	355	0.0372	351	0.0620	263	0.0443	305	0.0607	344
33	alphaface-001	0.0065	206	0.0097	211	0.0039	153	0.0063	185	0.0083	182	-	-	-	-	0.0280	80
34	alphaface-002	0.0052	163	0.0075	167	0.0030	92	0.0044	122	1.0000	467	0.0115	106	0.0084	117	0.0279	66
35	amplifiedgroup-001	0.5034	455	0.5848	452	0.6973	450	0.8316	450	0.7807	439	0.7724	380	0.6354	408	0.4250	440
36	androvideo-000	0.0243	363	0.0438	371	0.0239	366	0.0365	360	0.0483	365	0.1870	309	0.0635	325	0.1163	390
37	anke-004	0.0080	240	0.0154	275	0.0073	254	0.0112	256	0.0102	223	0.0178	157	0.0118	171	0.0288	148
38	anke-005	0.0070	215	0.0109	231	0.0059	224	0.0094	239	0.0105	225	0.0142	121	0.0102	143	0.0289	155
39	antheus-000	0.2564	431	0.3776	434	0.7240	451	0.8699	455	0.8899	452	0.9872	419	0.9483	436	0.7668	456
40	antheus-001	0.1311	418	0.2306	420	0.5113	439	0.6797	441	0.8748	451	0.9908	424	0.9649	441	0.7586	455
41	anyvision-004	0.0267	368	0.0385	367	0.0258	369	0.0487	372	0.0234	318	0.0301	210	0.0191	240	0.0470	323
42	anyvision-005	0.0023	67	0.0037	72	0.0027	74	0.0035	82	0.0049	118	0.0084	70	0.0069	85	0.0285	119
43	armatura-001	0.0033	104	0.0042	90	0.0031	102	0.0037	94	0.0056	134	0.0110	101	0.0092	129	0.0815	373
44	armatura-003	0.0020	49	0.0029	44	0.0026	55	0.0028	37	0.0025	19	0.0049	11	0.0043	17	0.0292	176

Table 19: FNMR is the proportion of mated comparisons below a threshold set to achieve the FMR given in the header on the fourth row. FMR is the proportion of impostor comparisons at or above that threshold. The light grey values give rank over all algorithms in that column. The pink columns use only same-sex impostors; others are selected regardless of demographics. The exception, in the green column, uses “matched-covariates” i.e. impostors of the same sex, age group, and country of birth. The second pink column includes effects of extended ageing. Missing entries for border, visa, mugshot and wild images generally mean the algorithm did not run to completion. The VISA columns compare images described in section 2.1. The MUGSHOT columns compare images described in section 2.5. The VISA-BORDER column compare images described in section 2.2 with those of section 2.4. The BORDER column compares images described in section 2.4. The WILD columns compare images described in section 2.7.

	Algorithm	FALSE NON-MATCH RATE (FNMR)										LESS CONSTRAINED, NON-COOP.					
		CONSTRAINED, COOPERATIVE								WILD							
		Name	VISAMC	VISA	MUGSHOT	MUGSHOT12+YRS	VISABORDER	BORDER	BORDER								
	FMR	0.0001	1E-06	1E-05	1E-05	1E-05	1E-06	1E-06	1E-05	0.0001							
45	asusaics-000	0.0125	307	0.0209	313	0.0085	281	0.0134	282	0.0143	264	0.7189	370	0.0285	275	0.0295	184
46	asusaics-001	0.0125	306	0.0210	314	0.0085	283	0.0134	283	0.0143	265	0.7437	374	0.0289	277	0.0295	183
47	autentika-000	0.1415	420	0.1916	414	0.4130	433	0.5521	433	0.4217	426	0.9998	445	0.9954	450	0.3183	431
48	authenmetric-003	0.0036	123	0.0053	128	0.0039	158	0.0051	144	0.0095	209	0.9930	426	0.5932	405	0.0290	160
49	authenmetric-004	0.0027	80	0.0042	89	0.0033	120	0.0036	91	0.0083	185	0.9879	420	0.4058	391	0.0290	165
50	aware-005	0.0457	390	0.0643	388	0.0603	401	0.1094	404	0.0613	374	0.1075	290	0.0491	309	0.0314	232
51	aware-006	0.0487	391	0.0819	397	0.0529	395	0.1090	402	0.1011	393	0.1058	287	0.0502	312	0.0317	238
52	awiros-001	0.4044	444	0.4622	440	0.5530	441	0.6518	438	0.2008	409	0.1994	312	0.1386	353	0.5584	448
53	awiros-002	0.1990	425	0.2561	422	0.3319	427	0.4411	427	0.3821	424	0.9938	427	0.2634	370	0.0997	383
54	aximetria-001	0.0111	286	0.0186	299	0.0110	314	0.0148	298	0.0170	286	0.3928	340	0.2090	363	0.0409	303
55	ayftech-001	0.0946	411	0.1941	415	0.2438	423	0.3625	423	0.1558	401	0.1589	303	0.0936	343	0.0785	365
56	ayonix-000	0.4351	448	0.4872	442	0.6150	446	0.7510	446	0.6557	434	0.6361	362	0.4981	397	0.3635	435
57	beethedata-000	0.0127	311	0.0195	306	0.0092	292	0.0157	304	0.0171	288	0.0306	211	0.0204	250	0.0285	122
58	beyneai-000	0.0071	223	0.0107	228	0.0104	305	0.0131	280	0.0170	287	0.9837	416	0.6171	407	0.0597	343
59	biocube-001	0.5596	461	0.6834	460	0.7700	458	0.8712	456	0.8446	446	0.9661	412	0.7922	422	0.2377	416
60	bioidtechswiss-001	0.0054	169	0.0072	158	0.0069	245	0.0124	267	0.0060	142	0.0094	84	0.0065	76	0.0313	231
61	bioidtechswiss-002	0.0049	150	0.0067	151	0.0064	233	0.0116	259	0.0067	155	0.0117	108	0.0086	120	0.0279	55
62	bm-001	0.7431	470	0.9494	471	0.9586	466	0.9843	466	0.9049	454	0.9021	400	0.8395	428	0.9935	466
63	boetech-001	0.0662	403	0.0802	396	0.0493	393	0.0791	392	0.0682	378	0.1074	289	0.0758	333	0.1719	403
64	boetech-002	0.0535	396	0.0565	384	0.0114	322	0.0136	285	0.0403	354	0.0650	265	0.0606	323	0.1697	402
65	bresee-001	0.0085	250	0.0143	263	0.0086	285	0.0153	301	0.0108	229	0.0168	147	0.0115	168	0.0355	280
66	bresee-002	0.0079	239	0.0101	217	0.0065	236	0.0079	216	0.0129	248	0.0263	195	0.0224	260	0.0327	250
67	camvi-002	0.0125	308	0.0221	319	0.0089	289	0.0145	296	0.0142	261	0.2650	326	0.0166	220	0.0288	142
68	camvi-004	0.0171	344	0.0316	351	0.0042	169	0.0049	140	0.0097	216	0.6636	365	0.0141	197	0.0284	109
69	canon-003	0.0041	137	0.0059	136	0.0030	90	0.0040	105	0.0040	87	0.0073	48	0.0059	61	0.0274	20
70	canon-004	0.0052	164	0.0091	201	0.0033	124	0.0058	168	0.0037	75	0.0770	273	0.0494	310	0.0267	2
71	ceiec-003	0.0071	221	0.0107	225	0.0061	230	0.0079	219	0.0160	274	0.0316	213	0.0260	271	0.0308	223
72	ceiec-004	0.0038	130	0.0051	121	0.0045	181	0.0053	148	0.0062	148	0.3939	341	0.0104	149	0.0325	246
73	chosun-001	0.0525	394	0.0936	399	0.0742	407	0.1263	410	0.0978	392	1.0000	458	0.9354	434	0.4446	442
74	chosun-002	0.0390	385	0.0646	389	0.0339	384	0.0576	383	0.0455	364	0.6904	368	0.1746	360	0.0696	358
75	chtface-005	0.0033	106	0.0049	114	0.0029	87	0.0041	109	0.0044	103	0.0317	214	0.0066	79	0.0306	215
76	chtface-006	0.0029	87	0.0043	92	0.0026	59	0.0034	79	0.0040	88	0.2701	327	0.0065	75	0.0305	213
77	cist-001	0.0046	145	0.0065	150	0.0042	170	0.0063	184	0.9675	461	0.9997	443	0.9994	457	0.0407	300
78	clearviewai-000	0.0010	8	0.0019	18	0.0024	20	0.0028	38	0.0030	35	0.0058	25	0.0050	29	0.0271	5
79	closeli-001	0.0136	314	0.0163	279	0.0039	156	0.0054	152	0.0072	161	1.0000	452	0.0094	133	0.0318	239
80	cloudmatrix-001	0.0668	404	0.1141	403	0.0539	396	0.0905	397	0.3509	421	0.9819	415	0.9010	431	0.0636	348
81	cloudmatrix-002	0.0075	233	0.0113	236	0.0084	280	0.0120	261	0.9248	457	0.9997	442	0.9985	456	0.0358	282
82	cloudwalk-hr-003	0.0026	76	0.0041	80	0.0040	163	0.0058	167	0.0060	146	0.9992	435	0.0094	131	0.7206	454
83	cloudwalk-hr-004	0.0009	6	0.0018	13	0.0034	128	0.0028	44	0.0052	124	0.9992	436	0.0093	130	0.1625	400
84	cloudwalk-mt-005	0.0006	1	0.0009	2	0.0025	36	0.0022	9	0.0017	2	0.9286	404	0.5956	406	0.0287	136
85	cloudwalk-mt-006	0.0006	2	0.0006	1	0.0023	12	0.0019	1	0.0016	1	0.0032	1	0.0030	2	0.0290	162
86	codeline-000	0.0057	180	0.0079	179	0.0037	141	0.0053	151	0.2721	415	1.0000	453	0.9763	443	0.0273	13
87	cogent-007	0.0022	62	0.0038	74	0.0028	82	0.0031	56	0.0040	90	0.0082	64	0.0067	80	0.0438	316
88	cogent-008	0.0015	30	0.0027	41	0.0023	14	0.0025	21	0.0033	54	0.0063	32	0.0055	47	0.0281	84

Table 20: FNMR is the proportion of mated comparisons below a threshold set to achieve the FMR given in the header on the fourth row. FMR is the proportion of impostor comparisons at or above that threshold. The light grey values give rank over all algorithms in that column. The pink columns use only same-sex impostors; others are selected regardless of demographics. The exception, in the green column, uses “matched-covariates” i.e. impostors of the same sex, age group, and country of birth. The second pink column includes effects of extended ageing. Missing entries for border, visa, mugshot and wild images generally mean the algorithm did not run to completion. The VISA columns compare images described in section 2.1. The MUGSHOT columns compare images described in section 2.5. The VISA-BORDER column compare images described in section 2.2 with those of section 2.4. The BORDER column compares images described in section 2.4. The WILD columns compare images described in section 2.7.

Algorithm	FALSE NON-MATCH RATE (FNMR)										WILD					
	CONSTRAINED, COOPERATIVE								LESS CONSTRAINED, NON-COOP.							
	Name	VISAMC	VISA	MUGSHOT	MUGSHOT12+YRS	VISABORDER	BORDER	BORDER	1E-05	0.0001						
FMR	0.0001	1E-06	1E-05	1E-05	1E-06	1E-06	1E-06	1E-05								
89 cognitec-003	0.0038	128	0.0052	123	0.0054	211	0.0057	164	0.0225	312	0.0416	241	0.0388	294	0.0348	268
90 cognitec-004	0.0036	118	0.0053	127	0.0053	204	0.0056	160	0.0098	217	0.0202	173	0.0154	212	0.0352	278
91 cor-001	0.0075	232	0.0113	235	0.0055	215	0.0084	224	0.0091	198	0.0148	127	0.0092	128	0.0277	41
92 coretech-000	0.7699	472	1.0000	478	1.0000	475	-		1.0000	478	1.0000	475	1.0000	467	1.0000	471
93 coretech-001	0.0052	159	0.0067	153	0.0083	278	0.0092	236	0.0346	346	0.1363	300	0.0252	267	0.0793	368
94 corsight-002	0.0053	165	0.0068	155	0.0030	95	0.0041	110	0.0039	84	0.0079	58	0.0054	45	0.0276	35
95 corsight-003	0.0026	77	0.0040	79	0.0028	79	0.0045	125	0.0035	71	0.0059	27	0.0046	22	0.0279	59
96 csc-002	0.0099	268	0.0132	253	0.0077	261	0.0142	293	0.0126	247	0.0195	166	0.0146	204	0.1779	405
97 csc-003	0.0053	166	0.0065	148	0.0037	142	0.0047	131	0.0074	163	0.0124	113	0.0112	162	0.1773	404
98 ctbcbank-000	0.0168	337	0.0250	332	0.0146	339	0.0224	336	0.0211	309	0.8964	398	0.3779	388	1.0000	475
99 ctbcbank-001	0.0155	330	0.0235	327	0.0148	344	0.0243	341	0.0207	306	0.9279	403	0.3469	382	1.0000	472
100 cu-face-002	0.0105	279	0.0116	238	0.0650	404	0.0568	380	0.0271	332	0.0139	120	0.0076	99	0.3984	438
101 cubox-001	0.0064	205	0.0080	180	0.0037	139	0.0055	156	0.0060	143	0.0111	103	0.0077	101	0.0300	199
102 cubox-002	0.0034	115	0.0041	81	0.0025	33	0.0025	24	0.0033	53	0.0064	34	0.0058	57	0.0480	326
103 cudocommunication-001	0.4777	451	1.0000	477	0.4373	434	0.5360	430	1.0000	472	1.0000	474	1.0000	474		
104 cuhkee-001	0.0036	121	0.0045	103	0.0031	108	0.0046	128	0.0051	123	0.0095	87	0.0079	104	0.1492	395
105 cybercore-002	0.0092	260	0.0119	241	0.0049	193	0.0072	197	0.9105	456	1.0000	457	1.0000	462	0.5484	447
106 cybercore-003	0.0155	329	0.0164	281	0.0032	116	0.0033	73	0.0024	13	0.9719	413	0.8213	426	0.0705	360
107 cyberextruder-003	0.0109	283	0.0169	286	0.0071	250	0.0112	257	0.0165	280	0.0410	240	0.0272	274	0.0302	207
108 cyberextruder-004	0.0118	295	0.0181	296	0.0081	273	0.0133	281	0.0191	301	0.0329	217	0.0268	272	0.0679	355
109 cyberlink-009	0.0018	41	0.0027	40	0.0047	183	0.0046	126	0.0040	93	0.0086	77	0.0062	71	0.0280	79
110 cyberlink-010	0.0011	13	0.0019	17	0.0041	165	0.0041	106	0.0039	82	0.1829	307	0.0054	46	0.0280	72
111 dahua-006	0.0027	78	0.0039	76	0.0031	105	0.0039	104	0.0039	83	0.0067	41	0.0058	55	0.0280	69
112 dahua-007	0.0017	36	0.0023	27	0.0026	53	0.0032	62	0.0033	49	0.0060	28	0.0054	44	0.0278	46
113 daon-000	0.0095	264	0.0117	240	0.0068	241	0.0077	211	0.0092	202	0.0174	153	0.0137	191	0.0331	254
114 decatur-000	0.0714	405	0.1115	402	0.0608	402	0.1106	405	0.0866	385	1.0000	455	0.0714	331	0.0658	351
115 decatur-001	0.0424	387	0.0711	392	0.0237	365	0.0458	368	0.0447	362	1.0000	449	0.9969	453	0.0280	76
116 deepglint-004	0.0025	74	0.0034	61	0.0039	157	0.0061	180	0.0050	119	0.0091	81	0.0082	111	0.0285	126
117 deepglint-005	0.0052	160	0.0059	140	0.0030	91	0.0031	57	0.0033	57	0.7620	379	0.1535	356	0.0320	243
118 deepsea-001	0.0136	315	0.0215	316	0.0142	336	0.0214	333	0.0163	278	0.0250	192	0.0192	241	0.0347	266
119 deepsense-000	0.0145	323	0.0265	340	0.0113	320	0.0196	326	0.0151	268	0.0215	180	0.0129	185	0.0290	161
120 deepsense-001	0.0013	23	0.0019	16	0.0024	25	0.0025	22	0.0027	27	0.0115	107	0.0053	38	0.0285	120
121 dermalog-010	0.0030	92	0.0041	85	0.0034	129	0.0037	96	0.0075	164	0.5181	353	0.2530	366	0.0275	22
122 dermalog-011	0.0045	143	0.0062	143	0.0035	132	0.0059	172	0.0057	137	0.2242	318	0.0407	296	0.0276	30
123 dicio-001	0.5486	460	0.6442	454	0.7516	454	0.8607	452	0.8678	450	0.8268	390	0.7034	415	0.3605	434
124 didiglobalface-001	0.0055	173	0.0092	202	0.0030	94	0.0045	124	0.0088	191	0.0119	111	0.0085	118	0.0282	100
125 didiglobalface-002	0.0033	110	0.0051	122	0.0026	54	0.0034	81	0.0033	52	0.0085	71	0.0047	25	0.0277	39
126 digidata-000	0.0967	412	0.1410	408	0.2596	424	0.3462	422	0.0293	336	0.0363	231	0.0212	254	0.0310	224
127 digidata-001	0.0224	360	0.0352	359	0.0330	381	0.0570	382	0.0109	231	0.0481	249	0.0123	181	0.0288	140
128 digitalbarriers-002	0.3360	440	0.3690	432	0.0877	411	0.1557	411	0.0971	391	0.0951	282	0.0497	311	0.0436	315
129 dps-000	0.0115	291	0.0176	293	0.0149	346	0.0185	321	0.0173	290	0.0275	201	0.0180	230	0.1067	385
130 dsk-000	0.1526	422	0.2169	419	0.3787	429	0.5426	432	0.3115	417	0.3089	330	0.1994	362	0.2201	412
131 einetworks-000	0.0099	269	0.0180	295	0.0088	288	0.0140	290	0.0130	249	0.0225	184	0.0147	206	0.0293	178
132 ekin-002	0.1168	415	0.2042	417	0.1530	420	0.2524	419	0.1777	406	0.2773	329	0.1347	351	0.4801	444

Table 21: FNMR is the proportion of mated comparisons below a threshold set to achieve the FMR given in the header on the fourth row. FMR is the proportion of impostor comparisons at or above that threshold. The light grey values give rank over all algorithms in that column. The pink columns use only same-sex impostors; others are selected regardless of demographics. The exception, in the green column, uses “matched-covariates” i.e. impostors of the same sex, age group, and country of birth. The second pink column includes effects of extended ageing. Missing entries for border, visa, mugshot and wild images generally mean the algorithm did not run to completion. The VISA columns compare images described in section 2.1. The MUGSHOT columns compare images described in section 2.5. The VISA-BORDER column compare images described in section 2.2 with those of section 2.4. The BORDER column compares images described in section 2.4. The WILD columns compare images described in section 2.7.

Algorithm	FALSE NON-MATCH RATE (FNMR)									
	CONSTRAINED, COOPERATIVE								LESS CONSTRAINED, NON-COOP.	
	Name	VISAMC	VISA	MUGSHOT	MUGSHOT12+YRS	VISABORDER	BORDER	BORDER	WILD	
FMR	0.0001	1E-06	1E-05	1E-05	1E-06	1E-06	1E-06	1E-05	0.0001	
133	enface-000	0.0028	85	0.0049	116	0.0043	172	0.0072	195	0.0058
134	enface-001	0.0072	226	0.0107	226	0.0071	247	0.0138	287	0.0068
135	eocortex-000	0.3485	441	0.6943	461	0.1122	412	0.1574	412	0.2155
136	ercacat-001	0.0036	124	0.0044	97	0.0033	119	0.0047	132	0.0106
137	euronovate-001	0.2786	434	0.3608	431	0.4489	436	0.6105	437	0.5010
138	expasoft-001	0.0328	380	0.0488	373	0.0211	359	0.0342	357	0.0629
139	expasoft-002	0.0170	341	0.0274	342	0.0787	410	0.0768	391	0.1629
140	f8-001	0.0249	365	0.0336	354	0.0178	351	0.0232	337	0.0303
141	f8-002	0.0340	382	0.0591	387	0.0213	361	0.0374	361	0.0452
142	faceonlive-001	0.0269	370	0.0359	362	0.0387	387	0.0721	389	0.0246
143	faceonlive-002	0.0121	300	0.0135	256	0.0033	121	0.0041	108	0.0037
144	facephi-000	0.0044	141	0.0059	137	0.0047	184	0.0057	165	0.0088
145	facesoft-000	0.0085	249	0.0112	233	0.0064	234	0.0107	252	0.0091
146	facetag-000	0.2836	435	0.4081	437	0.2933	426	0.4303	426	0.3448
147	facetag-002	0.0098	267	0.0147	268	0.0064	235	0.0110	254	0.0116
148	facex-001	1.0000	476	1.0000	475	1.0000	471	-	1.0000	474
149	facex-002	0.0803	407	0.1404	407	0.1283	415	0.1979	416	0.1440
150	farfaces-001	0.4890	454	0.5860	453	0.5650	442	0.7268	444	0.8015
151	fiberhome-nanjing-003	0.0090	253	0.0139	260	0.0082	275	0.0144	294	0.0110
152	fiberhome-nanjing-004	0.0037	127	0.0056	134	0.0031	103	0.0043	116	0.0043
153	fincore-000	0.0309	378	0.0502	375	0.0281	373	0.0510	376	0.0521
154	firstcreditKZ-001	0.0024	72	0.0034	58	0.0024	30	0.0024	17	0.0034
155	frpkauai-001	0.0023	64	0.0035	68	0.0026	43	0.0030	53	0.0040
156	frpkauai-002	0.0024	73	0.0035	66	0.0024	28	0.0024	15	0.0033
157	fujitsulab-002	0.0091	256	0.0124	248	0.0105	306	0.0156	302	0.0169
158	fujitsulab-003	0.0045	144	0.0065	149	0.0057	219	0.0083	222	0.0080
159	g42-intelibrain-001	0.0006	3	0.0009	3	0.0037	140	0.0044	119	0.0030
160	geo-002	0.0171	343	0.0187	301	0.0035	131	0.0051	146	0.0064
161	geo-004	0.0030	91	0.0041	84	0.0025	39	0.0030	49	0.0035
162	glory-004	0.0077	236	0.0123	245	0.0074	258	0.0098	247	0.0122
163	glory-005	0.0056	176	0.0076	168	0.0054	212	0.0072	198	0.0075
164	gorilla-008	0.0058	189	0.0091	200	0.0049	192	0.0079	218	0.0079
165	gorilla-009	0.0049	151	0.0072	160	0.0038	146	0.0056	161	0.0065
166	graymatrics-001	0.1039	413	0.1620	411	0.1344	417	0.1917	415	0.1648
167	griaule-001	0.0057	178	0.0078	175	0.0045	180	0.0065	188	0.0070
168	griaule-002	0.0021	56	0.0032	54	0.0025	42	0.0027	33	0.0034
169	hertasecurity-001	0.0249	364	0.0309	349	0.0105	307	0.0161	306	0.0245
170	hertasecurity-002	0.0206	355	0.0315	350	0.0060	227	0.0078	214	0.0253
171	hik-001	0.0096	266	0.0125	251	0.0093	297	0.0164	309	0.0108
172	hisign-001	0.0036	122	0.0050	117	0.0034	126	0.0046	127	0.0079
173	hisign-002	0.0029	88	0.0044	100	0.0027	71	0.0032	67	0.0028
174	hyperverge-003	0.0019	46	0.0030	49	0.0025	34	0.0029	47	0.0027
175	hyperverge-004	0.0072	227	0.0116	239	0.0040	161	0.0071	194	0.0058
176	hzailu-002	0.0051	156	0.0072	157	0.0038	151	0.0055	157	0.0040

Table 22: FNMR is the proportion of mated comparisons below a threshold set to achieve the FMR given in the header on the fourth row. FMR is the proportion of impostor comparisons at or above that threshold. The light grey values give rank over all algorithms in that column. The pink columns use only same-sex impostors; others are selected regardless of demographics. The exception, in the green column, uses “matched-covariates” i.e. impostors of the same sex, age group, and country of birth. The second pink column includes effects of extended ageing. Missing entries for border, visa, mugshot and wild images generally mean the algorithm did not run to completion. The VISA columns compare images described in section 2.1. The MUGSHOT columns compare images described in section 2.5. The VISA-BORDER column compare images described in section 2.2 with those of section 2.4. The BORDER column compares images described in section 2.4. The WILD columns compare images described in section 2.7.

	Algorithm	FALSE NON-MATCH RATE (FNMR)								LESS CONSTRAINED, NON-COOP.							
		CONSTRAINED, COOPERATIVE															
		Name	VISAMC	VISA	MUGSHOT	MUGSHOT12+YRS	VISABORDER	BORDER	BORDER								
	FMR		0.0001	1E-06	1E-05	1E-05	1E-06	1E-06	1E-05	0.0001							
177	hzailu-003	0.0178	346	0.0291	347	0.0031	109	0.0042	114	0.0035	65	0.0061	31	0.0052	34	0.0524	334
178	icm-003	0.0138	317	0.0222	321	0.0149	345	0.0282	348	0.0227	313	0.0384	236	0.0257	268	0.0333	256
179	icm-004	0.0079	238	0.0120	242	0.0074	256	0.0107	251	0.0091	199	0.0281	205	0.0128	184	0.0315	234
180	icthtc-000	0.0260	367	0.0396	368	0.0207	358	0.0339	356	0.0291	335	0.0474	248	0.0346	286	0.0459	321
181	id3-006	0.0072	225	0.0103	220	0.0049	194	0.0074	203	0.0095	207	0.0165	145	0.0119	175	0.9938	467
182	id3-008	0.0039	131	0.0055	132	0.0032	114	0.0042	112	0.0081	178	0.0155	136	0.0134	188	0.8856	460
183	idemria-008	0.0023	65	0.0032	55	0.0023	15	0.0028	35	0.0034	64	0.0067	40	0.0056	49	0.0290	164
184	idemria-009	0.0022	60	0.0030	50	0.0022	7	0.0023	14	0.0023	11	0.0046	7	0.0039	10	0.0285	118
185	iit-002	0.0111	288	0.0177	294	0.0085	282	0.0140	289	0.0193	302	0.0332	220	0.0260	270	0.1373	393
186	iit-003	0.0082	246	0.0151	273	0.0053	206	0.0084	225	0.0122	243	0.0199	170	0.0137	190	0.0407	301
187	imds-software-001	0.0126	310	0.0228	322	0.0130	333	0.0221	335	0.0231	315	0.0469	247	0.0199	248	0.0365	285
188	imperial-000	0.0067	209	0.0108	230	0.0080	270	0.0134	284	0.0087	189	0.0581	257	0.0102	144	0.0281	86
189	imperial-002	0.0058	188	0.0081	183	0.0055	214	0.0085	228	0.0083	183	0.0157	137	0.0103	145	0.0273	15
190	incode-010	0.0041	136	0.0063	145	0.0028	83	0.0043	115	0.0047	113	0.0077	56	0.0061	67	0.0296	192
191	incode-011	0.0032	98	0.0044	96	0.0026	57	0.0034	78	0.0032	45	0.0359	229	0.0140	195	0.0295	187
192	infocert-001	0.0105	280	0.0172	288	0.0078	264	0.0125	268	0.0159	272	0.1573	302	0.0565	319	0.0307	219
193	innefulabs-000	0.0122	302	0.0199	309	0.0112	319	0.0197	327	0.0222	311	0.0372	234	0.0271	273	0.0348	269
194	innovativetechnologyltd-001	0.0578	399	0.0938	400	0.0501	394	0.0981	398	0.0592	373	0.0779	274	0.0422	299	0.0449	320
195	innovativetechnologyltd-002	0.0451	389	0.0716	393	0.0541	397	0.1009	400	0.0506	368	0.0682	267	0.0371	292	0.0804	371
196	innovatrics-008	0.0047	146	0.0064	147	0.0038	149	0.0052	147	0.0053	126	0.0088	78	0.0069	87	0.0287	134
197	innovatrics-009	0.0022	57	0.0031	52	0.0028	76	0.0032	65	0.0034	60	0.1165	294	0.0326	281	0.0279	57
198	insightface-001	0.0009	7	0.0014	5	0.0027	63	0.0024	16	0.0035	69	0.0070	44	0.0065	73	0.0279	62
199	insightface-003	0.0015	29	0.0021	22	0.0045	179	0.0034	80	0.1298	395	1.0000	466	0.9407	435	0.0277	38
200	inspur-000	0.0060	197	0.0078	173	0.7415	453	0.9093	461	0.2838	416	0.9996	439	0.9976	454	0.0283	106
201	intellicloudai-001	0.0142	320	0.0234	326	0.0092	294	0.0145	295	0.0162	276	0.0371	233	0.0171	223	0.0409	304
202	intellicloudai-002	0.0059	192	0.0085	189	0.0060	228	0.0069	193	0.0108	228	0.2477	324	0.0171	222	0.0303	208
203	intellifusion-001	0.0072	224	0.0094	205	0.0056	218	0.0085	229	0.0111	235	0.0212	177	0.0143	200	0.0289	153
204	intellifusion-002	0.0059	190	0.0077	169	0.0040	162	0.0074	202	0.0085	187	0.5352	354	0.0104	150	0.0305	212
205	intellivision-003	0.1177	416	0.2006	416	0.0760	408	0.1244	409	0.1069	394	0.1431	301	0.0839	336	0.0829	375
206	intellivision-004	0.0271	371	0.0559	383	0.0294	379	0.0503	375	0.0327	343	0.0461	245	0.0293	280	0.0645	350
207	intellivix-002	0.0062	199	0.0085	190	0.0039	155	0.0056	159	0.0060	145	0.3464	334	0.0857	339	0.0289	154
208	intellivix-003	0.0075	231	0.0125	249	0.0052	203	0.0091	235	0.0066	153	0.0297	208	0.0096	136	0.0286	132
209	intelresearch-005	0.0016	32	0.0023	28	0.0028	75	0.0034	76	0.0042	100	0.0084	68	0.0066	78	0.0290	163
210	intelresearch-006	0.0010	11	0.0015	8	0.0026	62	0.0028	41	0.0032	47	0.8123	386	0.4742	396	0.0291	170
211	intema-000	0.0012	18	0.0017	11	0.0023	8	0.0022	10	0.0022	9	0.0172	150	0.0061	66	0.0279	61
212	intema-001	0.0010	10	0.0014	6	0.0021	3	0.0020	5	0.0019	6	0.0037	4	0.0030	3	0.0282	96
213	intsyssmu-001	0.9543	475	0.9888	473	0.9923	467	-	0.9977	462	0.9955	428	0.9892	445	0.7871	458	
214	intsyssmu-002	0.0130	312	0.0254	334	0.0137	334	0.0267	346	0.0160	273	0.0267	198	0.0145	203	0.0289	157
215	ionetworks-000	0.0060	195	0.0087	192	0.0044	174	0.0058	170	0.0080	177	0.0144	125	0.0112	160	0.0319	241
216	iqface-000	0.0091	257	0.0143	262	0.0075	259	0.0110	255	0.0171	289	0.2234	317	0.0359	288	0.0381	291
217	iqface-003	0.0058	187	0.0079	177	0.0051	200	0.0058	171	0.0104	224	0.0200	171	0.0193	242	0.0402	296
218	irex-000	0.0052	161	0.0099	215	0.0056	217	0.0083	223	0.0137	258	0.0163	143	0.0078	102	0.0285	121
219	isap-001	0.5092	456	0.6588	457	0.6899	449	0.7978	447	0.7200	435	0.7253	371	0.5373	401	0.1931	407
220	isap-002	0.0114	290	0.0186	300	0.0087	286	0.0151	300	0.0156	271	0.5134	350	0.0333	282	0.0354	279

Table 23: FNMR is the proportion of mated comparisons below a threshold set to achieve the FMR given in the header on the fourth row. FMR is the proportion of impostor comparisons at or above that threshold. The light grey values give rank over all algorithms in that column. The pink columns use only same-sex impostors; others are selected regardless of demographics. The exception, in the green column, uses “matched-covariates” i.e. impostors of the same sex, age group, and country of birth. The second pink column includes effects of extended ageing. Missing entries for border, visa, mugshot and wild images generally mean the algorithm did not run to completion. The VISA columns compare images described in section 2.1. The MUGSHOT columns compare images described in section 2.5. The VISA-BORDER column compare images described in section 2.2 with those of section 2.4. The BORDER column compares images described in section 2.4. The WILD columns compare images described in section 2.7.

	Algorithm	FALSE NON-MATCH RATE (FNMR)									
		CONSTRAINED, COOPERATIVE								LESS CONSTRAINED, NON-COOP.	
		Name	VISAMC	VISA	MUGSHOT	MUGSHOT12+YRS	VISABORDER	BORDER	BORDER	WILD	
	FMR	0.0001	1E-06	1E-05	1E-05	1E-05	1E-06	1E-06	1E-05	0.0001	
221	isityou-000	0.5682	462	0.7033	463	1.0000	474	-	1.0000	473	1.0000
222	isystems-001	0.0149	326	0.0245	330	0.0138	335	0.0210	331	0.0209	308
223	isystems-002	0.0118	293	0.0182	297	0.0111	316	0.0162	307	0.0166	281
224	itmo-007	0.0080	241	0.0125	250	0.0107	309	0.0185	319	0.0167	283
225	itmo-008	0.0090	254	0.0150	270	0.0058	221	0.0059	174	0.0187	297
226	ivacognitive-001	0.0189	349	0.0351	358	0.0123	329	0.0235	338	0.0198	304
227	iws-000	0.4824	452	0.5801	450	0.6859	448	0.8155	448	0.8251	443
228	jaakit-001	0.5830	463	0.7146	464	0.8173	460	0.8893	458	0.8950	453
229	kakao-007	0.0019	47	0.0028	42	0.0024	19	0.0026	26	0.0033	51
230	kakao-008	0.0011	14	0.0018	14	0.0023	9	0.0023	12	0.0021	8
231	kakaopay-001	0.0152	328	0.0252	333	0.0145	338	0.0270	347	0.0232	316
232	kasikornlabs-000	0.0112	289	0.0184	298	0.0086	284	0.0137	286	0.0130	251
233	kasikornlabs-002	0.0069	214	0.0091	199	0.0048	188	0.0063	183	0.0076	167
234	kedacom-000	0.0055	172	0.0081	182	0.0111	318	0.0120	262	0.0415	356
235	kiwitech-000	0.0076	234	0.0105	223	0.0081	274	0.0128	276	0.0096	211
236	kneron-003	0.0542	398	0.0902	398	0.0346	385	0.0562	379	0.0919	388
237	kneron-005	0.0157	331	0.0259	336	0.0126	332	0.0212	332	0.0406	355
238	knowutech-000	0.0039	132	0.0055	130	0.0028	86	0.0042	111	0.0042	98
239	kookmin-002	0.0054	170	0.0077	172	0.0043	171	0.0065	187	0.0123	245
240	koreaid-001	0.0031	96	0.0045	102	0.0026	52	0.0032	63	0.0043	101
241	krungthai-002	0.0105	277	0.0161	277	0.0091	291	0.0141	291	0.7350	437
242	kuke3d-001	0.0058	183	0.0104	222	0.0083	277	0.0093	238	0.0270	331
243	kuke3d-002	0.0077	237	0.0135	257	0.0069	244	0.0098	246	0.0111	234
244	lebentech-000	0.5940	464	0.7032	462	0.8854	463	0.9511	463	0.9089	455
245	lemalabs-001	0.0111	287	0.0175	291	0.0088	287	0.0142	292	0.0143	262
246	lineclova-002	0.0021	53	0.0035	65	0.0025	32	0.0027	31	0.0041	94
247	lineclova-003	0.0018	43	0.0030	48	0.0028	84	0.0031	58	0.0041	95
248	lookman-002	0.0297	376	0.0547	382	0.0339	383	0.0562	378	0.0614	375
249	lookman-004	0.0074	230	0.0099	214	0.0124	331	0.0149	299	0.0430	359
250	luxand-000	0.2056	426	0.2814	424	0.4053	431	0.5365	431	0.3497	420
251	mantra-000	0.0037	125	0.0052	125	0.0054	209	0.0056	162	0.0097	215
252	maxvision-002	0.0070	219	0.0107	227	0.0061	229	0.0093	237	0.0080	174
253	maxvision-003	0.0056	175	0.0083	187	0.0038	150	0.0060	175	0.0061	147
254	megvii-005	0.0010	9	0.0015	7	0.0026	51	0.0031	61	0.0019	5
255	megvii-006	0.0011	12	0.0016	9	0.0026	58	0.0033	72	0.0025	17
256	meituan-001	0.0164	336	0.1886	413	0.0025	35	0.0026	25	0.0030	38
257	meituan-002	0.0017	37	0.0025	31	0.0024	22	0.0023	11	0.0024	16
258	meiya-001	0.0171	342	0.0275	343	0.0159	348	0.0261	345	0.0311	340
259	mendaxiatech-000	0.0027	81	0.0036	69	0.0029	88	0.0036	92	0.0031	43
260	metsakuurcompany-001	0.0068	212	0.0087	195	0.0068	242	0.0078	213	0.0095	208
261	metsakuurcompany-002	0.0048	148	0.0071	156	0.0030	97	0.0043	118	0.0032	48
262	maxis-001	0.0068	211	0.0099	213	0.0059	225	0.0097	245	0.0096	213
263	microfocus-001	0.4482	449	0.5524	449	0.7256	452	0.8416	451	0.7301	436
264	microfocus-002	0.3605	442	0.5057	444	0.5783	444	0.7223	443	0.5909	431

Table 24: FNMR is the proportion of mated comparisons below a threshold set to achieve the FMR given in the header on the fourth row. FMR is the proportion of impostor comparisons at or above that threshold. The light grey values give rank over all algorithms in that column. The pink columns use only same-sex impostors; others are selected regardless of demographics. The exception, in the green column, uses “matched-covariates” i.e. impostors of the same sex, age group, and country of birth. The second pink column includes effects of extended ageing. Missing entries for border, visa, mugshot and wild images generally mean the algorithm did not run to completion. The VISA columns compare images described in section 2.1. The MUGSHOT columns compare images described in section 2.5. The VISA-BORDER column compare images described in section 2.2 with those of section 2.4. The BORDER column compares images described in section 2.4. The WILD columns compare images described in section 2.7.

	Algorithm	FALSE NON-MATCH RATE (FNMR)										LESS CONSTRAINED, NON-COOP.					
		CONSTRAINED, COOPERATIVE								WILD							
		Name	VISAMC	VISA	MUGSHOT	MUGSHOT12+YRS	VISABORDER	BORDER	BORDER	WILD							
	FMR	0.0001	1E-06	1E-05	1E-05	1E-05	1E-06	1E-06	1E-05	0.0001							
265	minivision-000	0.0033	103	0.0048	111	0.0038	148	0.0049	136	0.0055	131	0.0094	86	0.0079	106	0.0273	12
266	mobai-000	0.0360	384	0.0439	372	0.0372	386	0.0700	387	0.0367	350	0.0939	280	0.0795	335	0.2640	426
267	mobai-001	0.0199	353	0.0219	318	0.0047	185	0.0061	177	0.0093	205	0.0174	152	0.0138	193	0.1045	384
268	mobbl-001	0.3208	436	0.4375	438	0.5680	443	0.7193	442	0.6282	432	0.5783	358	0.3984	390	0.1866	406
269	mobbl-003	0.0087	251	0.0134	255	0.0062	231	0.0087	231	0.0099	218	0.0197	167	0.0122	180	0.0312	228
270	mobipintech-000	0.0090	255	0.0149	269	0.0039	160	0.0057	163	0.0115	239	0.0465	246	0.0182	232	0.0315	235
271	moreedian-000	0.3874	443	0.4912	443	0.9988	469	-	9990	464	0.9999	446	0.9998	459	0.4788	443	
272	mukh-001	0.0170	340	0.0285	345	0.0225	363	0.0405	364	0.0272	333	0.0950	281	0.0291	279	0.0301	203
273	mukh-002	0.0269	369	0.0357	361	0.0435	391	0.0799	393	0.0143	263	0.0213	178	0.0122	179	0.0345	263
274	multimodality-000	0.0034	112	0.0047	108	0.0036	138	0.0044	121	0.0077	169	0.9976	431	0.4456	394	0.0287	135
275	multimodality-001	0.0029	86	0.0042	88	0.0031	101	0.0035	83	0.0038	78	0.0071	45	0.0059	62	0.0281	85
276	mvision-001	0.0191	350	0.0233	324	0.0204	356	0.0356	359	0.0198	305	0.0337	222	0.0242	264	0.0431	312
277	nazhiai-000	0.0040	133	0.0059	139	0.0036	134	0.0048	134	0.0057	136	0.0125	114	0.0083	114	0.0275	27
278	neosystems-004	0.0279	373	0.0495	374	0.0289	375	0.0585	385	0.0439	361	0.9621	410	0.1296	349	0.0333	258
279	netbridge-tech-001	0.4749	450	0.6599	458	0.4438	435	0.5676	434	0.4491	427	1.0000	451	0.9541	437	0.1098	388
280	netbridge-tech-002	0.0101	272	0.0166	284	0.0077	262	0.0127	273	0.0133	254	0.8215	388	0.0523	315	0.0351	275
281	neurotechnology-013	0.0032	99	0.0045	104	0.0026	61	0.0036	87	0.0037	76	0.0068	43	0.0052	37	0.0278	47
282	neurotechnology-015	0.0022	59	0.0036	70	0.0024	18	0.0028	40	0.0030	36	0.0052	15	0.0041	14	0.0276	33
283	nhn-002	0.0068	213	0.0096	208	0.0057	220	0.0087	233	0.0136	257	0.0253	194	0.0186	238	0.0302	205
284	nhn-003	0.0033	105	0.0048	113	0.0027	68	0.0038	99	0.0036	74	0.0198	168	0.0071	90	0.0285	127
285	nodeflux-002	0.0186	348	0.0340	355	0.0261	370	0.0451	367	0.0548	371	1.0000	456	1.0000	463	0.0299	197
286	notiontag-001	0.6846	468	0.8006	468	0.3955	430	0.5247	429	0.8669	448	0.8313	392	0.6362	409	0.2221	413
287	notiontag-002	0.0066	207	0.0089	196	0.0045	178	0.0061	178	0.0077	170	0.0137	119	0.0104	148	0.0299	196
288	nsensecorp-003	0.0251	366	0.0295	348	0.0212	360	0.0305	351	0.0131	252	0.2139	316	0.0141	198	0.0872	378
289	nsensecorp-004	0.1370	419	0.1397	406	0.0066	238	0.0094	240	1.0000	477	1.0000	478	1.0000	469	0.0805	372
290	ntechlab-011	0.0012	21	0.0019	15	0.0024	23	0.0028	45	0.0029	34	0.0055	19	0.0047	24	0.0288	145
291	ntechlab-012	0.0011	15	0.0016	10	0.0023	16	0.0030	51	0.0026	21	0.0050	14	0.0043	16	0.0280	75
292	omface-000	0.2573	432	0.3835	435	0.3590	428	0.4903	428	0.3956	425	0.5003	349	0.2595	367	0.2400	417
293	omface-001	0.0137	316	0.0212	315	0.0114	324	0.0187	322	0.0174	292	1.0000	472	0.0214	256	0.0789	367
294	omnigarde-001	0.0168	338	0.0260	337	0.0203	355	0.0402	362	0.0243	323	0.0327	216	0.0177	226	0.0288	143
295	omnigarde-002	0.0033	109	0.0046	106	0.0027	72	0.0039	101	0.0041	96	0.0076	52	0.0059	65	0.0278	51
296	onfido-000	0.1472	421	0.2881	425	0.0335	382	0.0731	390	0.0515	369	0.9915	425	0.9579	438	0.0731	362
297	openface-001	0.1804	423	0.2921	426	0.2878	425	0.3906	425	0.2054	411	0.2338	322	0.1549	357	0.2445	418
298	oz-003	0.0095	265	0.0143	261	0.0054	210	0.0077	210	0.0096	212	0.0175	155	0.0118	172	0.0288	149
299	oz-004	0.0033	111	0.0049	115	0.0038	152	0.0055	155	0.0081	179	0.0163	144	0.0142	199	0.0329	252
300	palit-000	0.0062	200	0.0084	188	0.0039	154	0.0055	154	0.0055	132	0.4610	346	0.2468	365	0.0280	74
301	palit-001	0.0050	152	0.0068	154	0.0032	117	0.0047	133	0.0045	106	0.0110	102	0.0058	60	0.0287	138
302	pangiam-000	0.0031	94	0.0043	94	0.0026	45	0.0030	55	0.0038	79	0.0071	46	0.0061	70	0.0424	309
303	papago-001	0.0067	210	0.0096	210	0.0051	201	0.0077	209	0.0071	159	0.0126	115	0.0086	121	0.0816	374
304	papsav1923-002	0.0021	55	0.0034	59	0.0026	47	0.0030	54	0.0048	114	0.0093	83	0.0086	119	0.0312	229
305	papsav1923-003	0.0025	75	0.0035	62	0.0024	31	0.0025	19	0.0034	59	0.0066	38	0.0058	59	0.0281	89
306	paravision-010	0.0012	17	0.0021	20	0.0022	6	0.0021	7	0.0027	26	0.0055	20	0.0050	30	0.0288	150
307	paravision-011	0.0008	5	0.0020	19	0.0021	4	0.0020	4	0.0026	22	0.0053	16	0.0049	28	0.0289	158
308	pensees-001	0.0087	252	0.0133	254	0.0071	249	0.0122	266	0.0145	266	0.0252	193	0.0195	245	0.0283	105

Table 25: FNMR is the proportion of mated comparisons below a threshold set to achieve the FMR given in the header on the fourth row. FMR is the proportion of impostor comparisons at or above that threshold. The light grey values give rank over all algorithms in that column. The pink columns use only same-sex impostors; others are selected regardless of demographics. The exception, in the green column, uses “matched-covariates” i.e. impostors of the same sex, age group, and country of birth. The second pink column includes effects of extended ageing. Missing entries for border, visa, mugshot and wild images generally mean the algorithm did not run to completion. The VISA columns compare images described in section 2.1. The MUGSHOT columns compare images described in section 2.5. The VISA-BORDER column compare images described in section 2.2 with those of section 2.4. The BORDER column compares images described in section 2.4. The WILD columns compare images described in section 2.7.

	Algorithm	FALSE NON-MATCH RATE (FNMR)										LESS CONSTRAINED, NON-COOP.					
		CONSTRAINED, COOPERATIVE															
		Name	VISAMC	VISA	MUGSHOT	MUGSHOT12+YRS	VISABORDER	BORDER	BORDER	WILD							
		FMR	0.0001	1E-06	1E-05	1E-05	1E-06	1E-06	1E-05	0.0001							
309	pixelall-008	0.0015	26	0.0023	29	0.0034	130	0.0049	135	0.0031	42	0.0057	23	0.0052	33	0.0278	44
310	pixelall-009	0.0018	42	0.0025	33	0.0024	27	0.0026	27	0.0031	44	0.3475	335	0.0053	40	0.0276	31
311	psl-010	0.0017	40	0.0035	67	0.0023	10	0.0025	18	0.0035	68	0.0104	95	0.0052	36	0.0282	91
312	psl-011	0.0013	22	0.0026	35	0.0021	1	0.0021	6	0.0024	14	0.0047	8	0.0035	7	0.0285	123
313	ptakuratsatu-000	0.0060	194	0.0089	197	0.0070	246	0.0104	250	0.0096	214	0.0152	132	0.0100	139	0.0284	110
314	pxl-001	0.0488	392	0.0752	395	0.0586	400	0.1087	401	0.0946	389	0.1065	288	0.0625	324	0.1088	386
315	pyramid-000	0.0136	313	0.0233	325	0.0117	326	0.0192	324	0.0185	296	0.0322	215	0.0206	252	0.0304	211
316	qazbs-000	0.0058	182	0.0083	185	0.0046	182	0.0072	196	0.0130	250	0.0244	190	0.0196	246	0.0297	194
317	qluevision-001	0.0223	358	0.0419	370	0.0205	357	0.0343	358	0.0327	344	0.8762	395	0.7413	419	0.0460	322
318	qnap-002	0.0122	301	0.0191	303	0.0075	260	0.0095	243	0.0146	267	0.0281	206	0.0184	234	0.0352	277
319	qnap-003	0.0637	401	0.0657	390	0.0058	222	0.0078	212	0.0082	181	0.9985	434	0.9658	442	0.0287	137
320	quantasoft-003	0.0081	244	0.0113	234	0.0056	216	0.0076	206	0.0091	200	0.0161	141	0.0107	154	0.0414	306
321	rankone-012	0.0043	139	0.0058	135	0.0031	110	0.0038	98	0.0047	111	0.0081	62	0.0065	74	0.0358	281
322	rankone-013	0.0028	82	0.0041	82	0.0026	48	0.0033	70	0.0028	31	0.0055	22	0.0040	11	0.0291	169
323	rankone-014	0.0016	34	0.0021	21	0.0024	17	0.0027	30	0.0022	10	0.0047	9	0.0035	5	0.0293	177
324	realnetworks-007	0.0031	95	0.0051	119	0.0028	81	0.0035	84	0.0048	115	0.0091	80	0.0074	96	0.0279	54
325	realnetworks-008	0.0022	61	0.0039	77	0.0038	145	0.0045	123	0.0055	129	0.0100	92	0.0080	109	0.0292	173
326	regula-000	0.0184	347	0.0376	366	0.0103	303	0.0185	318	0.0120	241	0.9983	433	0.0231	261	0.0273	14
327	regula-001	0.0072	228	0.0107	229	0.0102	301	0.0179	316	0.0123	246	0.0333	221	0.0174	224	0.0295	182
328	remarkai-001	0.0144	321	0.0256	335	0.0102	300	0.0159	305	0.0162	277	0.0582	258	0.0185	236	0.0308	222
329	remarkai-003	0.0047	147	0.0063	146	0.0033	123	0.0049	138	0.0054	127	0.0100	91	0.0072	93	0.0275	28
330	rendip-000	0.0055	174	0.0077	171	0.0048	190	0.0060	176	0.0080	175	0.0142	123	0.0110	159	0.0433	314
331	revealmedia-005	0.0050	154	0.0074	166	0.0050	196	0.0068	192	0.0075	166	0.0124	112	0.0104	151	0.3960	437
332	revealmedia-006	0.0040	134	0.0067	152	0.0041	167	0.0056	158	0.0056	133	0.0085	72	0.0068	82	0.0278	49
333	rokid-000	0.0093	262	0.0145	264	0.0073	255	0.0102	249	0.0164	279	0.0280	203	0.0214	255	0.0857	377
334	rokid-001	0.0105	278	0.0162	278	0.0094	299	0.0163	308	0.0181	293	0.0276	202	0.0165	219	0.0325	247
335	s1-005	0.0024	70	0.0036	71	0.0025	41	0.0029	48	0.0026	23	0.0048	10	0.0038	9	0.0359	283
336	s1-006	0.0029	89	0.0044	98	0.0028	77	0.0033	68	0.0035	66	0.0073	47	0.0044	19	0.0367	286
337	saffe-001	0.4339	447	0.5261	446	0.7539	456	0.8736	457	0.7977	440	0.9810	414	0.7435	420	0.3887	436
338	saffe-002	0.0119	296	0.0206	310	0.0107	312	0.0177	314	0.0244	324	0.9998	444	0.2785	372	0.0308	221
339	samsungsds-001	0.0015	31	0.0026	37	0.0023	13	0.0023	13	0.0024	15	0.1660	304	0.0536	316	0.0282	90
340	samsungsds-002	0.0017	39	0.0027	38	0.0023	11	0.0022	8	0.0021	7	0.0043	6	0.0036	8	0.0283	103
341	samtech-001	0.0197	352	0.0365	363	0.0146	342	0.0241	340	0.0238	322	0.0394	237	0.0251	266	0.0337	259
342	scanovate-002	0.0175	345	0.0355	360	0.0146	340	0.0286	349	0.0269	330	0.0301	209	0.0178	228	0.0301	204
343	scanovate-003	0.0054	168	0.0080	181	0.0054	207	0.0072	200	0.0312	341	0.0599	259	0.0568	320	0.0283	104
344	sdc-000	0.0303	377	0.0526	379	0.0572	399	0.1094	403	0.0867	386	0.6230	360	0.3682	386	0.1201	392
345	securifai-005	0.0125	305	0.0190	302	0.0080	271	0.0126	271	0.0134	255	0.9861	417	0.9205	432	0.0329	251
346	securifai-006	0.0140	319	0.0196	308	0.0067	240	0.0102	248	0.0113	237	0.9888	421	0.9239	433	0.0346	265
347	sensetime-007	0.0012	16	0.0022	23	0.0021	5	0.0020	3	0.0018	3	0.0034	2	0.0029	1	0.0280	70
348	sensetime-008	0.0008	4	0.0014	4	0.0021	2	0.0020	2	0.0018	4	0.0036	3	0.0033	4	0.0284	116
349	sertis-000	0.0118	294	0.0208	312	0.0080	267	0.0127	272	0.0110	233	0.0176	156	0.0114	165	0.0285	125
350	sertis-002	0.0049	149	0.0061	141	0.0039	159	0.0061	181	0.0055	130	0.0099	90	0.0070	89	0.0281	83
351	seventhSense-001	0.0034	114	0.0047	110	0.0025	40	0.0031	60	0.0029	33	0.0338	223	0.0109	156	0.0279	56
352	seventhSense-002	0.0036	120	0.0050	118	0.0028	80	0.0036	88	0.0035	67	0.0811	275	0.0183	233	0.0278	48

Table 26: FNMR is the proportion of mated comparisons below a threshold set to achieve the FMR given in the header on the fourth row. FMR is the proportion of impostor comparisons at or above that threshold. The light grey values give rank over all algorithms in that column. The pink columns use only same-sex impostors; others are selected regardless of demographics. The exception, in the green column, uses “matched-covariates” i.e. impostors of the same sex, age group, and country of birth. The second pink column includes effects of extended ageing. Missing entries for border, visa, mugshot and wild images generally mean the algorithm did not run to completion. The VISA columns compare images described in section 2.1. The MUGSHOT columns compare images described in section 2.5. The VISA-BORDER column compare images described in section 2.2 with those of section 2.4. The BORDER column compares images described in section 2.4. The WILD columns compare images described in section 2.7.

Algorithm	FALSE NON-MATCH RATE (FNMR)										LESS CONSTRAINED, NON-COOP.					
	CONSTRAINED, COOPERATIVE								WILD							
	Name	VISAMC	VISA	MUGSHOT	MUGSHOT12+YRS	VISABORDER	BORDER	BORDER	1E-06	1E-05						
FMR	0.0001	1E-06	1E-05	1E-05	1E-05	1E-06	1E-06	1E-06	1E-05	0.0001						
353 shaman-000	0.9297	474	0.9774	472	0.9990	470	-	0.9999	465	1.0000	454	0.9999	461	0.9575	464	
354 shaman-001	0.3346	439	0.4616	439	0.2368	422	0.3723	424	0.3574	422	0.3527	336	0.2304	364	0.1498	397
355 shu-002	-	0.0079	178	0.0146	341	0.0308	352	1.0000	466	0.0183	159	0.0115	167	0.0284	111	
356 shu-003	0.0028	83	0.0041	86	0.0050	195	0.0088	234	0.0081	180	0.0133	118	0.0094	132	0.0283	108
357 siat-002	0.0091	258	0.0126	252	0.0109	313	0.0190	323	0.0276	334	0.0516	253	0.0464	308	0.0520	332
358 siat-005	0.0021	52	0.0038	73	0.0059	223	0.0049	139	0.0742	379	0.9623	411	0.6801	412	0.0279	60
359 sjiu-003	0.0017	38	0.0033	57	0.0030	96	0.0037	95	0.0058	138	0.0104	96	0.0081	110	0.0284	117
360 sjiu-004	0.0014	24	0.0025	32	0.0027	65	0.0028	46	0.0046	107	0.0086	75	0.0073	94	0.0272	8
361 sktelecom-000	0.0038	129	0.0054	129	0.0031	99	0.0051	145	0.0042	97	0.3418	332	0.0061	69	0.0293	179
362 smartbiometrik-001	0.5485	459	0.6442	455	0.7550	457	0.8611	454	0.8677	449	0.8270	391	0.7030	414	0.3144	430
363 smartengines-000	0.6240	465	0.7562	466	0.9552	465	0.9784	465	0.9515	460	0.9288	406	0.8200	425	0.8037	459
364 smartengines-001	0.6434	467	0.7666	467	0.9446	464	0.9750	464	0.9387	459	0.9556	409	0.8647	430	0.7748	457
365 smartvist-000	0.0912	409	0.1587	410	0.1163	414	0.1841	413	0.1397	398	0.9372	407	0.7107	417	0.0779	364
366 smilart-002	0.2440	428	0.3532	430	-	-	-	0.3785	423	0.4145	343	0.2611	369	-	-	-
367 smilart-003	0.6944	469	0.8836	469	0.0695	406	0.1193	407	0.0894	387	0.1221	295	0.0737	332	0.1190	391
368 sodec-000	0.0033	108	0.0044	101	0.0040	164	0.0053	150	0.0054	128	0.0096	88	0.0080	107	0.0274	18
369 sqisoft-002	0.0082	247	0.0124	246	0.0051	199	0.0086	230	0.0102	222	0.0183	160	0.0122	178	0.0287	139
370 sqisoft-003	0.0041	138	0.0055	131	0.0026	44	0.0032	66	0.0039	85	1.0000	461	1.0000	478	0.0295	185
371 staqu-000	0.0139	318	0.0208	311	0.0104	304	0.0145	297	0.0156	270	0.8063	385	0.1408	354	0.0332	255
372 starhybrid-001	0.0108	281	0.0138	258	0.0081	272	0.0113	258	0.0152	269	0.0265	197	0.0189	239	0.0350	273
373 stcon-000	0.0040	135	0.0056	133	0.0031	106	0.0047	130	0.0048	116	0.9863	418	0.3562	384	0.0300	202
374 sukshi-000	0.5409	457	0.6612	459	0.4556	437	0.6567	439	0.9296	458	0.8898	396	0.7384	418	0.6892	453
375 suprema-003	0.0028	84	0.0041	87	0.0034	127	0.0039	102	0.0030	39	0.3095	331	0.0580	322	0.0284	112
376 suprema-004	0.0024	68	0.0035	64	0.0032	113	0.0036	89	0.0028	28	0.0053	17	0.0045	21	0.0281	82
377 supremaid-001	0.0053	167	0.0073	163	0.0045	177	0.0066	189	0.0099	220	0.0186	161	0.0148	207	0.0352	276
378 supremaid-002	0.0063	202	0.0094	206	0.0044	173	0.0062	182	0.0072	162	0.0229	186	0.0095	135	0.0345	264
379 surrey-cvssp-000	0.9084	473	0.9909	474	0.9923	468	0.9950	467	0.9981	463	0.9994	437	0.9979	455	0.9389	461
380 surrey-cvssp-001	1.0000	477	1.0000	476	0.0077	263	0.0079	217	0.0266	329	0.3822	339	0.0551	318	1.0000	478
381 synesis-006	0.0070	216	0.0096	209	0.0107	310	0.0166	310	-	0.0128	117	0.0089	124	0.0292	172	
382 synesis-007	0.0050	155	0.0073	165	0.0062	232	0.0076	205	-	0.0105	97	0.0080	108	0.0288	141	
383 synology-000	0.0149	324	0.0238	328	0.0148	343	0.0261	343	0.0221	310	0.0331	218	0.0209	253	0.0330	253
384 synology-002	0.0104	276	0.0153	274	0.0107	311	0.0184	317	0.0189	299	0.2032	313	0.0180	229	0.0312	226
385 sztu-000	0.0092	259	0.0139	259	0.0091	290	0.0201	329	0.0136	256	0.0685	268	0.0118	174	0.0270	4
386 sztu-001	0.0031	93	0.0043	95	0.0025	37	0.0028	43	0.0051	120	0.0113	104	0.0089	125	0.0275	21
387 t4isb-000	0.0058	184	0.0087	194	0.0041	168	0.0064	186	0.0083	184	0.0157	138	0.0103	146	0.0282	97
388 tech5-005	0.0054	171	0.0072	159	0.0069	243	0.0122	265	0.0060	144	0.0094	85	0.0066	77	0.0349	271
389 tech5-007	0.0020	48	0.0029	45	0.0024	21	0.0028	36	0.0034	62	0.8622	394	0.5335	400	0.0280	67
390 techsign-000	0.0325	379	0.0511	377	0.0435	390	0.0710	388	0.0746	380	0.1104	291	0.0841	337	0.0639	349
391 techsign-001	0.0110	284	0.0196	307	0.0067	239	0.0120	263	0.0087	190	0.2475	323	0.0883	341	0.0299	198
392 tevian-007	0.0019	45	0.0027	39	0.0032	115	0.0041	107	0.0045	105	0.0086	74	0.0078	103	0.0310	225
393 tevian-008	0.0012	20	0.0017	12	0.0033	118	0.0042	113	0.0042	99	0.0081	61	0.0068	83	0.0290	159
394 tiger-005	0.0624	400	0.2450	421	0.0292	377	0.0556	377	0.0430	358	1.0000	448	0.9964	451	0.0278	45
395 tiger-006	0.0066	208	0.0101	219	0.0050	198	0.0075	204	0.0089	194	0.0158	139	0.0117	170	0.0290	168
396 tinkoff-001	0.0145	322	0.0244	329	0.0318	380	0.0636	386	0.0236	320	1.0000	469	0.0339	284	0.0563	341

Table 27: FNMR is the proportion of mated comparisons below a threshold set to achieve the FMR given in the header on the fourth row. FMR is the proportion of impostor comparisons at or above that threshold. The light grey values give rank over all algorithms in that column. The pink columns use only same-sex impostors; others are selected regardless of demographics. The exception, in the green column, uses “matched-covariates” i.e. impostors of the same sex, age group, and country of birth. The second pink column includes effects of extended ageing. Missing entries for border, visa, mugshot and wild images generally mean the algorithm did not run to completion. The VISA columns compare images described in section 2.1. The MUGSHOT columns compare images described in section 2.5. The VISA-BORDER column compare images described in section 2.2 with those of section 2.4. The BORDER column compares images described in section 2.4. The WILD columns compare images described in section 2.7.

Algorithm	Name	FALSE NON-MATCH RATE (FNMR)										LESS CONSTRAINED, NON-COOP.					
		CONSTRAINED, COOPERATIVE								WILD							
		VISAMC	VISA	MUGSHOT	MUGSHOT12+YRS	VISABORDER	BORDER	BORDER	1E-05	0.0001							
FMR		0.0001	1E-06	1E-05	1E-05	1E-06	1E-06	1E-06	1E-05								
397	tongyi-005	0.0073	229	0.0146	265	0.0187	352	0.0421	366	0.0161	275	0.0215	179	0.0149	209	0.0399	295
398	toppanidgate-000	0.0021	51	0.0033	56	0.0026	49	0.0028	39	0.0039	86	0.0075	50	0.0068	81	0.0376	290
399	toshiba-004	0.0030	90	0.0042	91	0.0025	38	0.0027	34	0.0034	61	0.0063	33	0.0053	43	0.0278	42
400	toshiba-006	0.0022	63	0.0035	63	0.0024	26	0.0025	23	0.0027	25	0.7425	373	0.3070	378	0.0275	24
401	touchlessid-000	0.3296	438	0.4804	441	0.4111	432	0.6026	436	0.5324	430	0.9996	440	0.9964	452	0.2521	422
402	touchlessid-001	0.0076	235	0.0104	221	0.0680	405	0.0842	395	0.1358	396	1.0000	450	0.9995	458	0.0499	328
403	trueface-002	0.0060	193	0.0096	207	0.0048	189	0.0061	179	0.0112	236	0.0198	169	0.0155	214	0.0793	369
404	trueface-003	0.0070	217	0.0094	204	0.0053	205	0.0081	220	0.0122	242	0.0217	181	0.0159	217	0.0785	366
405	trueidvng-001	0.0063	201	0.0077	170	0.0033	122	0.0044	120	0.0046	108	0.0086	76	0.0069	86	0.0628	346
406	tuputech-000	0.3218	437	0.3696	433	-	-	-	0.3237	418	0.4304	344	0.2973	377	0.9415	462	
407	turingtechvip-001	0.0330	381	0.0540	381	0.0458	392	0.1007	399	0.4715	428	0.9286	405	0.8448	429	0.4035	439
408	turingtechvip-002	0.0126	309	0.0163	280	0.0092	295	0.0118	260	0.2264	413	1.0000	476	0.9925	447	0.2144	411
409	turkcell-000	0.1134	414	0.1288	405	0.0770	409	0.1112	406	0.2570	414	1.0000	447	0.9999	460	0.9556	463
410	twface-000	0.0051	157	0.0072	161	0.0041	166	0.0058	166	0.0071	160	0.0153	133	0.0100	138	0.0276	32
411	twface-001	0.0036	117	0.0051	120	0.0031	107	0.0038	97	0.0049	117	0.0091	82	0.0075	97	0.0277	36
412	ulsee-001	0.0151	327	0.0246	331	0.0113	321	0.0185	320	0.0187	298	0.6766	367	0.0181	231	0.0316	237
413	ultinous-000	0.2343	427	0.3484	429	-	-	-	-	-	-	-	-	-	-	-	
414	ultinous-001	0.2485	429	0.4003	436	-	-	-	-	-	-	-	-	-	-	-	
415	uluface-002	0.0081	242	0.0123	244	0.0071	248	0.0095	244	0.0107	227	1.0000	464	0.0140	196	0.0444	317
416	uluface-003	0.0100	270	0.0150	271	0.0079	265	0.0128	275	-	-	-	-	-	-	0.0635	347
417	unissey-002	0.0094	263	0.0151	272	0.0079	266	0.0110	253	0.0114	238	0.4424	345	0.1914	361	0.0420	308
418	unissey-003	0.0057	177	0.0082	184	0.0047	186	0.0082	221	0.0067	154	0.5179	352	0.2863	375	0.0288	146
419	upc-001	0.0234	361	0.0519	378	0.0291	376	0.0490	374	0.0294	337	0.2316	321	0.0389	295	0.0314	233
420	uxlabs-001	0.0534	395	0.0570	385	0.0118	327	0.0131	279	0.0237	321	0.0399	238	0.0288	276	0.0876	379
421	vcog-002	0.7522	471	0.9033	470	-	-	-	-	-	-	-	-	-	-	-	
422	vd-002	0.0429	388	0.0704	391	0.0569	398	0.0844	396	0.0801	382	0.0937	278	0.0577	321	0.0556	340
423	vd-003	0.0199	354	0.0222	320	0.0115	325	0.0130	278	0.0138	259	0.0239	188	0.0177	227	0.0389	292
424	veridas-007	0.0063	203	0.0083	186	0.0044	175	0.0058	169	0.0080	176	0.0152	131	0.0120	177	0.0284	113
425	veridas-008	0.0032	100	0.0045	105	0.0030	93	0.0033	71	0.0085	188	0.0206	174	0.0143	201	0.0288	147
426	veridium-000	0.0726	406	0.1248	404	0.5226	440	0.6652	440	0.6425	433	0.8150	387	0.7989	424	0.4988	446
427	veridium-001	0.0274	372	0.0368	365	0.0292	378	0.0475	370	0.0488	366	0.0673	266	0.0463	307	0.0800	370
428	verigram-000	0.0032	97	0.0043	93	0.0031	100	0.0034	75	0.0093	204	0.0175	154	0.0164	218	0.0276	29
429	verigram-001	0.0032	101	0.0044	99	0.0027	66	0.0032	64	0.0030	37	0.9995	438	0.9953	449	0.0276	34
430	verihubs-inteligensia-000	0.0070	218	0.0098	212	0.0048	191	0.0076	208	0.0092	201	0.0160	140	0.0117	169	0.0283	107
431	verihubs-inteligensia-001	0.0071	220	0.0114	237	0.0050	197	0.0076	207	0.0096	210	0.0165	146	0.0114	166	0.0282	94
432	verijelas-000	0.2488	430	0.3431	428	0.4861	438	0.6004	435	0.0811	383	0.1148	292	0.0440	302	0.0524	335
433	via-000	0.0216	357	0.0365	364	0.0177	350	0.0287	350	0.0296	338	0.0572	256	0.0290	278	0.0349	270
434	via-001	0.0149	325	0.0229	323	0.0114	323	0.0177	315	0.0183	295	0.4056	342	0.0176	225	0.0373	288
435	videmo-001	0.0295	375	0.0417	369	0.0164	349	0.0261	344	0.0355	348	0.0603	260	0.0442	304	0.1473	394
436	videmo-002	0.0158	333	0.0288	346	0.0149	347	0.0249	342	0.0230	314	0.3429	333	0.1468	355	0.0294	181
437	videonetics-001	0.5483	458	0.6446	456	0.7517	455	0.8607	453	0.8664	447	0.8255	389	0.6956	413	0.2986	427
438	videonetics-002	0.4274	445	0.5329	447	0.6081	445	0.7438	445	0.7775	438	0.7297	372	0.5756	403	0.1976	409
439	viettelhightech-000	0.0117	292	0.0166	283	0.0110	315	0.0198	328	0.0167	284	0.0249	191	0.0158	215	0.0409	305
440	vigilantsolutions-010	0.0109	282	0.0164	282	0.0074	257	0.0095	242	0.0209	307	0.0365	232	0.0233	262	0.0277	37

Table 28: FNMR is the proportion of mated comparisons below a threshold set to achieve the FMR given in the header on the fourth row. FMR is the proportion of impostor comparisons at or above that threshold. The light grey values give rank over all algorithms in that column. The pink columns use only same-sex impostors; others are selected regardless of demographics. The exception, in the green column, uses “matched-covariates” i.e. impostors of the same sex, age group, and country of birth. The second pink column includes effects of extended ageing. Missing entries for border, visa, mugshot and wild images generally mean the algorithm did not run to completion. The VISA columns compare images described in section 2.1. The MUGSHOT columns compare images described in section 2.5. The VISA-BORDER column compare images described in section 2.2 with those of section 2.4. The BORDER column compares images described in section 2.4. The WILD columns compare images described in section 2.7.

Algorithm	FALSE NON-MATCH RATE (FNMR)																
	CONSTRAINED, COOPERATIVE											LESS CONSTRAINED, NON-COOP.					
	Name	VISAMC	VISA	MUGSHOT	MUGSHOT12+YRS	VISABORDER	BORDER	BORDER	WILD								
FMR	0.0001	1E-06	1E-05	1E-05	1E-06	1E-06	1E-06	1E-05	0.0001								
441	vigilantsolutions-011	0.0124	304	0.0176	292	0.0073	253	0.0095	241	0.0196	303	0.0360	230	0.0221	258	0.0274	17
442	vinai-000	0.0081	243	0.0124	247	0.0045	176	0.0072	199	0.0089	193	0.1814	306	0.0112	161	0.0274	19
443	vinbigdata-001	0.2576	433	0.2763	423	0.1404	418	0.1988	417	0.1407	399	0.1150	293	0.0703	330	0.9767	465
444	vinbigdata-002	0.0102	273	0.0175	290	0.0071	251	0.0084	226	0.0090	195	0.8017	384	0.3134	379	0.0304	210
445	vion-000	0.0419	386	0.0590	386	0.0422	389	0.0478	371	0.0581	372	0.0968	285	0.0847	338	0.2479	419
446	visage-000	0.0933	410	0.1441	409	0.1316	416	0.2416	418	0.1395	397	0.1920	310	0.1001	345	0.0500	329
447	visionbox-001	0.0159	334	0.0270	341	0.0111	317	0.0173	313	0.0190	300	0.0315	212	0.0205	251	0.0389	293
448	visionbox-002	0.0058	181	0.0079	176	0.0060	226	0.0074	201	0.0084	186	0.0149	128	0.0113	164	0.0447	319
449	visionlabs-010	0.0017	35	0.0024	30	0.0026	56	0.0030	52	0.0033	55	0.0061	30	0.0052	35	0.0282	99
450	visionlabs-011	0.0012	19	0.0022	24	0.0024	29	0.0026	28	0.0028	29	0.0053	18	0.0046	23	0.0280	73
451	visteam-003	0.0804	408	0.2166	418	0.0613	403	0.1204	408	0.0963	390	0.1269	297	0.0441	303	0.0296	191
452	visteam-004	0.0541	397	0.5202	445	0.0406	388	0.0827	394	0.1879	407	0.1795	305	0.0347	287	0.0289	152
453	visteam-005	0.0235	362	0.0333	353	0.0265	371	0.0583	384	0.0341	345	0.0524	255	0.0259	269	0.0292	171
454	vixvizion-006	0.0082	245	0.0122	243	0.0093	296	0.0194	325	0.0099	219	0.0169	148	0.0108	155	0.0268	3
455	vixvizion-007	0.0110	285	0.0191	304	0.0080	269	0.0157	303	0.0101	221	0.0190	162	0.0118	173	0.0273	16
456	vnpt-004	0.0058	185	0.0078	174	0.0037	143	0.0053	149	0.0051	121	0.4640	347	0.1384	352	0.0275	25
457	vnpt-005	0.0036	119	0.0052	124	0.0027	67	0.0031	59	0.0036	72	0.0066	39	0.0056	48	0.0286	130
458	vocard-009	0.0022	58	0.0029	46	0.0036	135	0.0046	129	0.0052	125	0.0098	89	0.0086	122	0.0284	115
459	vocard-010	0.0024	71	0.0031	51	0.0036	136	0.0049	141	0.0025	20	0.0065	35	0.0040	12	0.0280	71
460	vts-000	0.0103	274	0.0174	289	0.0080	268	0.0129	277	0.0250	327	0.0450	244	0.0372	293	0.0596	342
461	vts-001	0.0033	102	0.0048	112	0.0027	69	0.0036	90	0.0032	46	0.6519	364	0.3563	385	0.0338	261
462	wicket-000	0.0018	44	0.0028	43	0.0024	24	0.0027	29	0.0031	41	0.7968	383	0.4340	393	0.0323	244
463	winsense-001	0.0062	198	0.0099	216	0.0092	293	0.0210	330	0.0093	203	0.0144	126	0.0098	137	0.0320	242
464	winsense-002	0.0050	153	0.0073	164	0.0038	147	0.0059	173	0.0064	150	0.0118	110	0.0084	116	0.0307	218
465	wiseai-001	0.0658	402	0.0964	401	0.7743	459	0.8956	459	0.1967	408	0.7526	377	0.3419	381	0.5780	449
466	wuhantianyu-001	0.0163	335	0.0262	338	0.0281	374	0.0569	381	0.0316	342	0.0486	250	0.0344	285	0.0324	245
467	x-laboratory-000	0.0071	222	0.0106	224	0.0123	330	0.0138	288	0.0419	357	0.5629	356	0.2852	374	0.0295	188
468	x-laboratory-001	0.0059	191	0.0110	232	0.0054	208	0.0078	215	0.0094	206	0.0142	122	0.0100	140	0.0294	180
469	xforwardai-001	0.0021	50	0.0034	60	0.0027	70	0.0028	42	0.0046	110	0.0088	79	0.0079	105	0.0281	88
470	xforwardai-002	0.0016	33	0.0023	26	0.0026	60	0.0025	20	0.0040	91	0.0081	63	0.0074	95	0.0282	92
471	xm-000	0.0015	27	0.0026	36	0.0031	104	0.0038	100	0.0058	139	0.0105	98	0.0082	113	0.0282	98
472	yisheng-004	0.1988	424	0.3329	427	0.1147	413	0.1849	414	0.2044	410	-	-	-	0.0908	380	
473	yitu-003	0.0015	28	0.0026	34	0.0066	237	0.0085	227	0.0064	151	0.0114	105	0.0103	147	0.0325	248
474	yoonik-002	0.0052	162	0.0062	144	0.0029	89	0.0034	77	0.0615	376	0.1279	298	0.1166	347	0.0549	338
475	yoonik-003	0.0034	113	0.0047	109	0.0032	112	0.0037	93	0.0816	384	0.2033	314	0.1601	358	0.0699	359
476	ytu-000	0.0057	179	0.0087	191	0.0121	328	0.0238	339	0.0047	112	0.0078	57	0.0059	64	0.0286	131
477	yuan-005	0.0037	126	0.0046	107	0.0027	73	0.0035	85	0.0033	50	0.2706	328	0.0876	340	0.0288	151
478	yuan-006	0.0045	142	0.0062	142	0.0032	111	0.0049	137	0.0038	81	0.0084	69	0.0049	27	0.0273	11

Table 29: FNMR is the proportion of mated comparisons below a threshold set to achieve the FMR given in the header on the fourth row. FMR is the proportion of impostor comparisons at or above that threshold. The light grey values give rank over all algorithms in that column. The pink columns use only same-sex impostors; others are selected regardless of demographics. The exception, in the green column, uses “matched-covariates” i.e. impostors of the same sex, age group, and country of birth. The second pink column includes effects of extended ageing. Missing entries for border, visa, mugshot and wild images generally mean the algorithm did not run to completion. The VISA columns compare images described in section 2.1. The MUGSHOT columns compare images described in section 2.5. The VISA-BORDER column compare images described in section 2.2 with those of section 2.4. The BORDER column compares images described in section 2.4. The WILD columns compare images described in section 2.7.

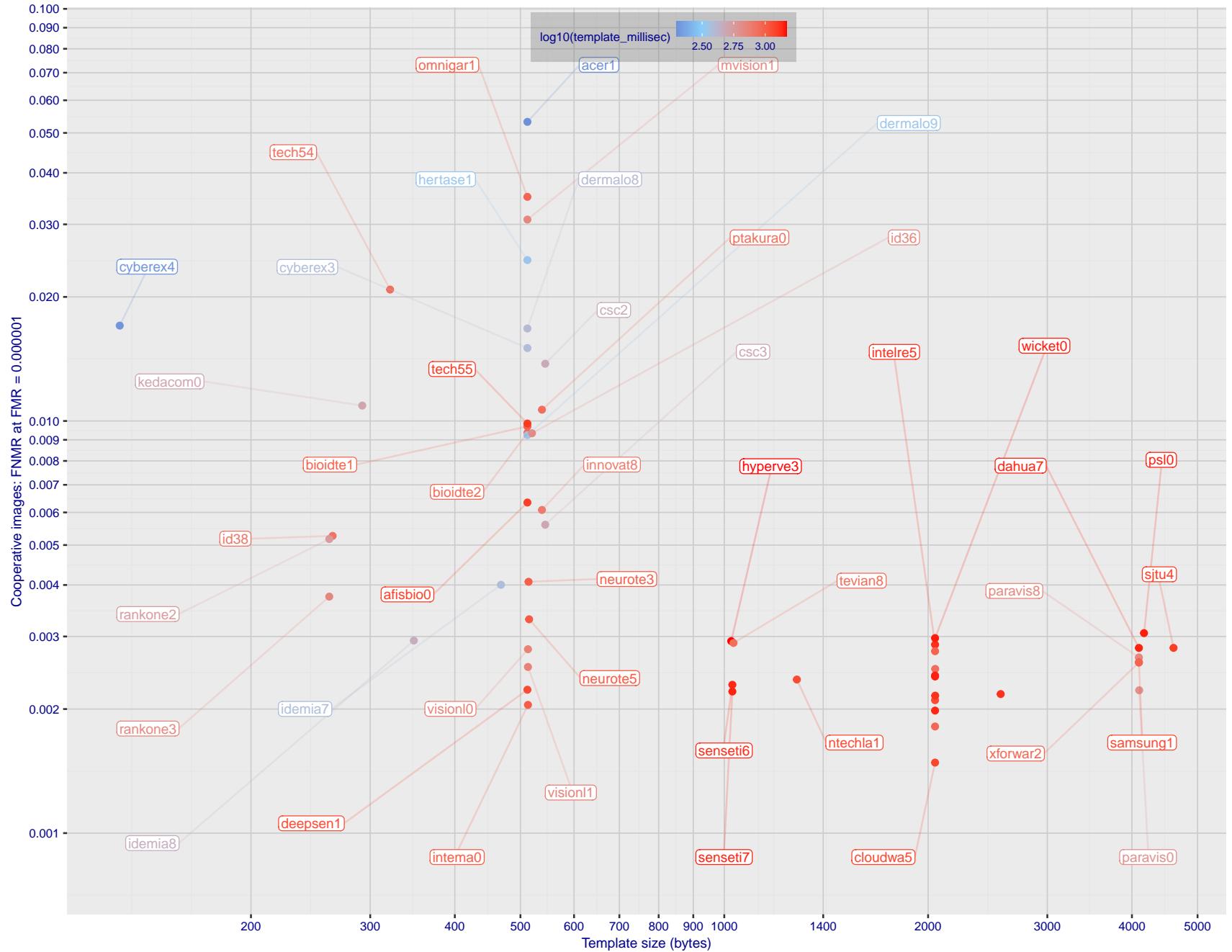


Figure 1: The points show false non-match rates (FNMR) versus the size of the encoded template. FNMR is the geometric mean of FNMR values for visa and mugshot images (from Figs. 90 and 114) at the false match rate (FMR) given in the y-axis label. The color of the points encodes template generation time - which spans at least one order of magnitude. Durations are measured on a single core of a c. 2016 Intel Xeon CPU E5-2630 v4 running at 2.20GHz. Algorithms with poor FNMR are omitted.

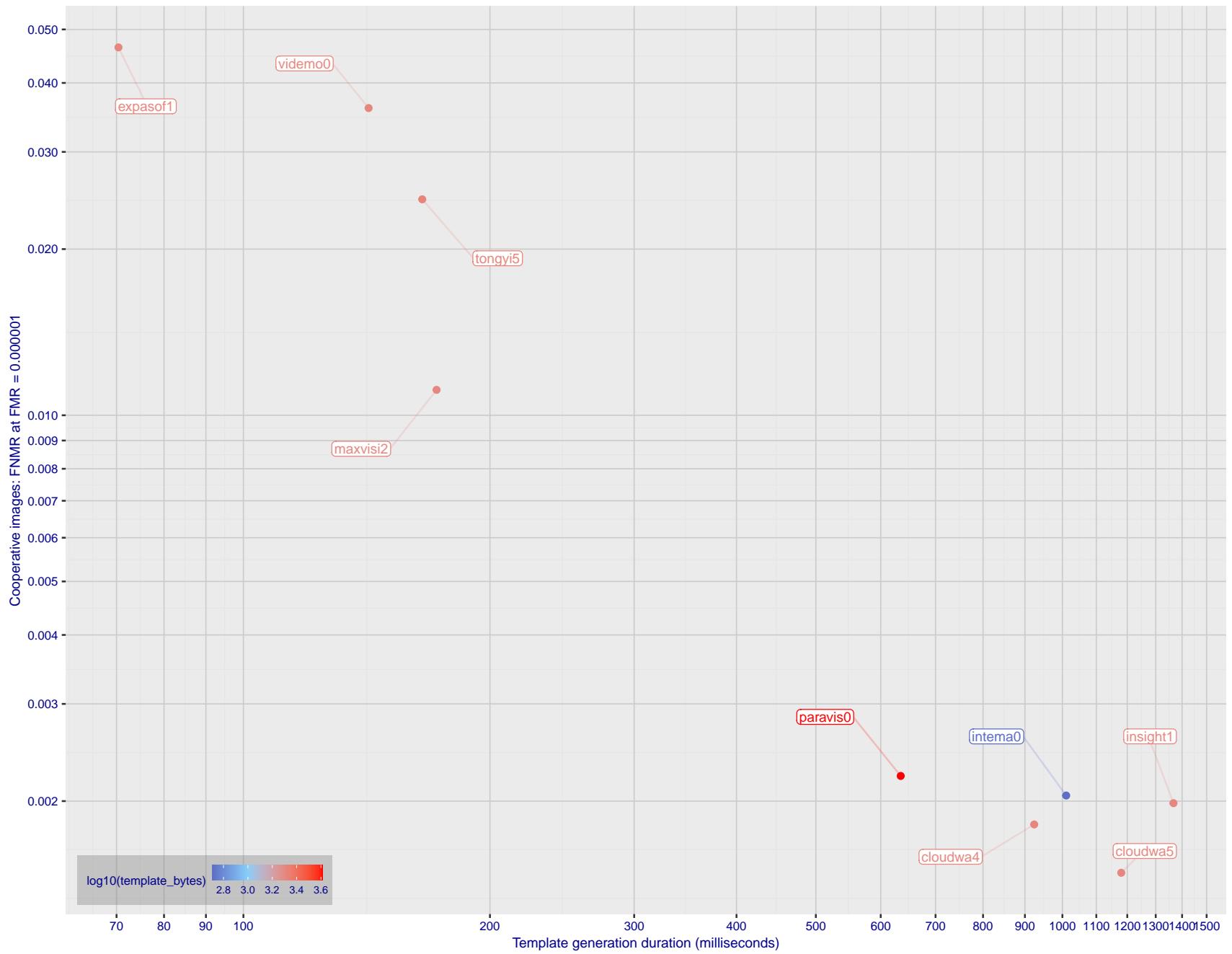


Figure 2: The points show false non-match rates (FNMR) versus the duration of the template generation operation. FNMR is the geometric mean of FNMR values for visa and mugshot images (from Figs. 90 and 114) at a false match rate (FMR) given in the y-axis label. Template generation time is a median estimated over 640 x 480 pixel portraits. It is measured on a single core of a c. 2016 Intel Xeon CPU E5-2630 v4 running at 2.20GHz. The color of the points encodes template size - which span two orders of magnitude. Algorithms with poor FNMR are omitted.

1 Metrics

1.1 Core accuracy

Given a vector of N genuine scores, u , the false non-match rate (FNMR) is computed as the proportion below some threshold, T:

$$\text{FNMR}(T) = 1 - \frac{1}{N} \sum_{i=1}^N H(u_i - T) \quad (1)$$

where $H(x)$ is the unit step function, and $H(0)$ taken to be 1.

Similarly, given a vector of N impostor scores, v , the false match rate (FMR) is computed as the proportion above T:

$$\text{FMR}(T) = \frac{1}{N} \sum_{i=1}^N H(v_i - T) \quad (2)$$

The threshold, T, can take on any value. We typically generate a set of thresholds from quantiles of the observed impostor scores, v , as follows. Given some interesting false match rate range, $[\text{FMR}_L, \text{FMR}_U]$, we form a vector of K thresholds corresponding to FMR measurements evenly spaced on a logarithmic scale

$$T_k = Q_v(1 - \text{FMR}_k) \quad (3)$$

where Q is the quantile function, and FMR_k comes from

$$\log_{10} \text{FMR}_k = \log_{10} \text{FMR}_L + \frac{k}{K} [\log_{10} \text{FMR}_U - \log_{10} \text{FMR}_L] \quad (4)$$

Error tradeoff characteristics are plots of FNMR(T) vs. FMR(T). These are plotted with $\text{FMR}_U \rightarrow 1$ and FMR_L as low as is sustained by the number of impostor comparisons, N. This is somewhat higher than the “rule of three” limit $3/N$ because samples are not independent, due to re-use of images.

1.2 Multi-template scoring methodology

There are some scenarios when one or more people exist and are detected in an image, and some of the proposed test images include $K > 1$ persons for some images and situations where the subject of interest may or may not be the foreground face (largest face in the image). The NIST FRVT 1:1 API supports this by allowing generation of multiple templates representing each person detected in an image. When this occurs, NIST will match all templates generated from the enrollment image with all templates generated from the verification image and use the **maximum** similarity score across all template comparisons. This scoring approach will be used in our calculation of FMR and FNMR (this applies to both genuine and imposter comparisons).

2 Datasets

2.1 Visa images

- ▷ The number of images is on the order of 10^5 .
- ▷ The number of subjects is on the order of 10^5 .
- ▷ The number of subjects with two images is on the order of 10^4 .
- ▷ The images have geometry in reasonable conformance with the ISO/IEC 19794-5 Full Frontal image type. Pose is generally excellent.
- ▷ The images are of size 252x300 pixels. The mean interocular distance (IOD) is 69 pixels.
- ▷ The images are of subjects from greater than 100 countries, with significant imbalance due to visa issuance patterns.
- ▷ The images are of subjects of all ages, including children, again with imbalance due to visa issuance demand.
- ▷ Many of the images are live capture. A substantial number of the images are photographs of paper photographs.
- ▷ When these images are input to the algorithm, they are labelled as being of type "ISO" - see Table 4 of the FRVT API.

2.2 Application images

- ▷ The number of images is on the order of 10^6 .
- ▷ The number of subjects is on the order of 10^6 .
- ▷ The number of subjects with two images is on the order of 10^6 .
- ▷ The images have geometry in good conformance with the ISO/IEC 19794-5 Full Frontal image type. Pose is generally excellent.
- ▷ The images are of size 300x300 pixels. The mean interocular distance (IOD) is 61 pixels.
- ▷ The images are of subjects from greater than 100 countries, with significant imbalance due to population and immigration patterns.
- ▷ The images are of subjects of adults.
- ▷ All of the images are live capture.
- ▷ When these images are input to the algorithm, they are labelled as being of type "ISO" - see Table 4 of the FRVT API.

2.3 Application images with head yaw

- ▷ The number of images is on the order of 10^5 .
- ▷ The number of subjects is on the order of 10^5 .
- ▷ The number of subjects with two images is on the order of 10^5 .
- ▷ The images have geometry in good conformance with the ISO/IEC 19794-5 Full Frontal image type *except* the yaw angle is between 25 and 85 degrees. Our pose estimates are approximate, with an angular error that increases with yaw. The angular estimates will be improved over time.
- ▷ The images are of size 300x300 pixels. The mean interocular distance (IOD), if frontal, would be about pixels, but reduces with cosine of yaw.
- ▷ The images are of subjects from greater than 100 countries, with significant imbalance due to population and immigration patterns.

- ▷ The images are of subjects of adults.
- ▷ All of the images are live capture.
- ▷ When these images are input to the algorithm, they are labelled as being of type "WILD" - see Table 4 of the FRVT API.

2.4 Border crossing images

- ▷ The number of images is on the order of 10^6 .
- ▷ The number of subjects is on the order of 10^6 .
- ▷ The number of subjects with two images is on the order of 10^6 .
- ▷ The images are taken with a camera oriented by an attendant toward a cooperating subject. This is done under time constraints so there are roll, pitch and yaw angle variations. Also background illumination is sometimes strong, so the face is under-exposed. There is some perspective distortion due to close range images. Some faces are partially cropped.
- ▷ The images have mean IOD of 38 pixels.
- ▷ The images are of subjects of adults and children aged 12 or above.
- ▷ The images are of subjects from greater than 100 countries, with significant imbalance due to population and immigration patterns.
- ▷ The images are all live capture.
- ▷ When these images are input to the algorithm, they are labelled as being of type "WILD" - see Table 4 of the FRVT API.

2.5 Mugshot images

- ▷ The number of images is on the order of 10^6 .
- ▷ The number of subjects is on the order of 10^6 .
- ▷ The number of subjects with two images is on the order of 10^6 .
- ▷ The images have geometry in reasonable conformance with the ISO/IEC 19794-5 Full Frontal image type.
- ▷ The images are of variable sizes. The median IOD is 105 pixels. The mean IOD is 113 pixels. The 1-st, 5-th, 10-th, 25-th, 75-th, 90-th and 99-th percentiles are 34, 58, 70, 87, 121, 161 and 297 pixels.
- ▷ The images are of subjects from the United States.
- ▷ The images are of adults.
- ▷ The images are all live capture.
- ▷ When these images are input to the algorithm, they are labelled as being of type "mugshot" - see Table 4 of the FRVT API.

2.6 Kiosk images

- ▷ The number of images is on the order of 10^6 .
- ▷ The number of subjects is on the order of 10^5 .
- ▷ The number of subjects with multiple images is the order of 10^5 .



Figure 3: The figure gives simulated samples of image types used in this report.

- ▷ The images are taken at kiosk equipped with a camera intended to capture a centered face. However the images have specific quality defects arising from the camera triggering before the subject looks at it. These are downward pitch of the face relative to the optical axis; cropping of the forehead; and cropping of left or right part of the face. Partial cropping affects perhaps 10% of the images. Resolution does not vary widely.
 - ▷ The images are of adults.
 - ▷ The images have mean IOD of 44 pixels, with maximum below 75, and minimum when both eyes are present above 25 pixels.
 - ▷ All of the images are live capture, none are scanned.
 - ▷ When these images are input to the algorithm, they are labelled as being of type "WILD" - see Table 4 of the FRVT API.

2.7 Wild images

- ▷ The number of images is on the order of 10^5 .
 - ▷ The number of subjects is on the order of 10^4 .
 - ▷ The number of subjects with two images on the order of 10^4 .
 - ▷ The images include many photojournalism-style images. Images are given to the algorithm using a variable but generally tight crop of the head. Resolution varies very widely. The images are very unconstrained, with wide yaw and pitch pose variation. Faces can be occluded, including hair and hands.
 - ▷ The images are of adults.
 - ▷ All of the images are live capture, none are scanned.
 - ▷ When these images are input to the algorithm, they are labelled as being of type "WILD" - see Table 4 of the FRVT API.

3 Results

3.1 Test goals

- To state absolute accuracy for different kinds of images, including those with and without subject cooperation.

- ▷ To state comparative accuracy, across algorithms.

3.2 Test design

Method: For visa images:

- ▷ The comparisons are of visa photos against visa photos.
- ▷ The number of genuine comparisons is on the order of 10^4 .
- ▷ The number of impostor comparisons is on the order of 10^{10} .
- ▷ The comparisons are fully zero-effort, meaning impostors are paired without attention to sex, age or other covariates. However, later analysis is conducted on subsets.
- ▷ The number of persons is on the order of 10^5 .
- ▷ The number of images used to make a template is one.
- ▷ The number of templates used to make each comparison score is two corresponding to simple one-to-one verification.

Method: For mugshot images:

- ▷ The comparisons are of mugshot photos against mugshot photos.
- ▷ The number of genuine comparisons is on the order of 10^6 .
- ▷ The number of impostor comparisons is on the order of 10^8 .
- ▷ The impostors are paired by sex, but not by age or other covariates.
- ▷ The number of persons is on the order of 10^6 .
- ▷ The number of images used to make a template is one.
- ▷ The number of templates used to make each comparison score is two, corresponding to simple one-to-one verification.

Method: For visa-border comparisons:

- ▷ The comparisons are of visa-like frontals against border crossing webcam photos.
- ▷ The number of genuine comparisons is on the order of 10^6 .
- ▷ The number of impostor comparisons is on the order of 10^8 .
- ▷ The impostors are paired by sex, but not by age or other covariates.
- ▷ The number of persons is on the order of 10^6 .
- ▷ The number of images used to make a template is one.
- ▷ The number of templates used to make each comparison score is two, corresponding to simple one-to-one verification.

Method: For visa-border non-frontal yaw comparisons:

- ▷ The comparisons are of visa-like images with yaw 25 to 85 degrees against border crossing webcam photos.
- ▷ The number of genuine comparisons is on the order of 10^5 .
- ▷ The number of impostor comparisons is on the order of 10^8 .
- ▷ The impostors are paired by sex, but not by age or other covariates.

- ▷ The number of persons is on the order of 10^5 .
- ▷ The number of images used to make a template is one.
- ▷ The number of templates used to make each comparison score is two, corresponding to simple one-to-one verification.

Method: For kiosk-border comparisons:

- ▷ The comparisons are of visa-like frontals against kiosk-style photos.
- ▷ The number of genuine comparisons is on the order of 10^6 .
- ▷ The number of impostor comparisons is on the order of 10^8 .
- ▷ The impostors are paired by sex, but not by age or other covariates.
- ▷ The number of persons is on the order of 10^5 .
- ▷ The number of images used to make a template is one.
- ▷ The number of templates used to make each comparison score is two, corresponding to simple one-to-one verification.

Method: For border-border comparisons:

- ▷ The comparisons are of border crossing webcam photos.
- ▷ The number of genuine comparisons is on the order of 10^6 .
- ▷ The number of impostor comparisons is on the order of 10^8 .
- ▷ The impostors are paired by sex, but not by age or other covariates.
- ▷ The number of persons is on the order of 10^6 .
- ▷ The number of images used to make a template is one.
- ▷ The number of templates used to make each comparison score is two corresponding to simple one-to-one verification.

Method: For wild images:

- ▷ The comparisons are of wild photos against wild photos.
- ▷ The number of genuine comparisons is on the order of 10^6 .
- ▷ The number of impostor comparisons is on the order of 10^8 .
- ▷ The comparisons are fully zero-effort, meaning impostors are paired without attention to sex, age or other covariates.
- ▷ The number of persons is on the order of 10^4 .
- ▷ The number of images used to make a template is one.
- ▷ The number of templates used to make each comparison score is two corresponding to simple one-to-one verification.

Method: For child exploitation images:

- ▷ The comparisons are of unconstrained child exploitation photos against others of the same type.
- ▷ The number of genuine comparisons is on the order of 10^4 .
- ▷ The number of impostor comparisons is on the order of 10^7 .

- ▷ The comparisons are fully zero-effort, meaning impostors are paired without attention to sex, age or other covariates.
- ▷ The number of persons is on the order of 10^3 .
- ▷ The number of images used to make 1 template is 1.
- ▷ The number of templates used to make each comparison score is two corresponding to simple one-to-one verification.
- ▷ We produce two performance statements. First, is a DET as used for visa and mugshot images. The second is a cumulative match characteristic (CMC) summarizing a simulated one-to-many search process. This is done as follows.
 - We regard M enrollment templates as items in a gallery.
 - These M templates come from $M > N$ individuals, because multiple images of a subject are present in the gallery under separate identifiers.
 - We regard the verification templates as search templates.
 - For each search we compute the rank of the highest scoring mate.
 - This process should properly be conducted with a 1:N algorithm, such as those tested in NIST IR 8009. We use the 1:1 algorithms in a simulated 1:N mode here to a) better reflect what a child exploitation analyst does, and b) to show algorithm efficacy is better than that revealed in the verification DETs.

3.3 Failure to enroll

	Algorithm	Failure to Enrol Rate ¹											
		APPLICATION	BORDER	KIOSK	MUGSHOT	VISA	WILD	SEC. 2.2	SEC. 2.4	SEC. 2.6	SEC. 2.5	SEC. 2.1	SEC. 2.7
1	20face-000	0.0000	265	0.0008	237	0.0217	172	0.0000	136	0.0004	274	0.0004	200
2	20face-001	0.0000	279	0.0008	236	0.0000	2	0.0000	137	0.0004	276	0.0004	203
3	3divi-006	0.0000	283	0.0007	204	0.0214	169	0.0001	256	0.0002	139	0.0005	261
4	3divi-007	0.0000	264	0.0007	205	0.0214	170	0.0001	255	0.0002	138	0.0005	260
5	acer-001	0.0000	218	0.0011	297	-	410	0.0001	224	0.0004	291	0.0004	218
6	acer-002	0.0000	392	0.0008	229	0.0191	149	0.0003	347	0.0004	288	0.0011	318
7	acisw-007	0.0000	7	0.0000	7	0.0000	31	0.0000	55	0.0000	40	0.0000	74
8	acisw-008	0.0000	288	0.0009	261	0.0173	133	0.0004	372	0.0004	200	0.0007	292
9	adera-003	0.0000	375	0.0034	395	0.0403	254	0.0003	352	0.0005	390	0.0505	439
10	adera-004	0.0000	318	0.0008	226	0.0202	155	0.0003	360	0.0004	251	0.0003	161
11	advance-003	0.0000	365	0.0012	308	0.0247	191	0.0001	280	0.0004	339	0.0011	316
12	advance-004	0.0001	427	0.0010	288	0.0157	124	0.0008	419	0.0006	404	0.0222	419
13	afisbiometrics-000	0.0000	285	0.0008	221	0.0213	167	0.0000	138	0.0004	296	0.0003	191
14	afrengine-000	0.0000	275	0.0015	329	0.0254	200	0.0008	418	0.0004	228	0.0265	427
15	aifirst-001	0.0000	30	0.0000	26	-	401	0.0000	36	0.0000	54	0.0000	107
16	aigen-001	0.0000	77	0.0000	34	-	456	0.0000	26	0.0000	15	0.0000	53
17	aigen-002	0.0000	135	0.0000	69	0.0000	9	0.0000	116	0.0000	105	0.0000	28
18	ailabs-001	0.0000	240	0.0090	436	-	460	0.0007	411	0.0005	363	0.0016	331
19	aimall-002	0.0000	381	0.0043	413	-	343	0.0012	430	0.0005	383	0.0005	270
20	aimall-003	0.0000	356	0.0012	314	-	318	0.0004	366	0.0005	358	0.0004	232
21	aiseemu-001	0.0000	60	0.0000	24	0.0000	24	0.0000	54	0.0000	62	0.0000	103
22	aiseemu-002	0.0000	71	0.0000	47	0.0000	55	0.0000	20	0.0000	4	0.0000	46
23	aiunionface-000	0.0000	34	0.0000	29	-	404	0.0000	39	0.0000	56	0.0000	111
24	aize-001	0.0001	428	0.0040	408	0.0652	271	0.0026	452	0.0022	456	0.0058	374
25	aize-002	0.0000	163	0.0014	324	0.0230	185	0.0005	396	0.0004	271	0.0071	380
26	ajou-001	0.0000	210	0.0020	354	-	432	0.0001	259	0.0004	341	0.0045	363
27	alchera-004	0.0000	277	0.0009	258	0.0228	181	0.0001	289	0.0004	229	0.0003	178
28	alchera-005	0.0000	291	0.0009	259	0.0228	182	0.0001	288	0.0004	221	0.0003	174
29	alfabeta-001	0.0005	450	0.0650	471	0.2142	303	0.0024	448	0.0018	451	0.1071	459
30	alice-000	0.0000	168	0.0006	177	0.0133	107	0.0000	157	0.0004	215	0.0004	230
31	alleyes-000	0.0000	269	0.0010	277	-	319	0.0002	299	0.0004	320	0.0004	243
32	allgvision-000	0.0007	454	0.0062	429	-	334	0.0026	451	0.0052	467	0.0131	400
33	alphaface-001	0.0000	282	0.0012	303	-	313	0.0000	210	0.0004	321	0.0004	207
34	alphaface-002	0.0000	241	0.0012	301	-	445	0.0000	206	0.0004	314	0.0004	210
35	amplifiedgroup-001	0.0114	470	0.1023	473	-	409	0.0189	472	0.0279	475	0.1390	467
36	androvideo-000	0.0000	197	0.0000	99	-	345	0.0000	77	0.0000	90	0.0002	124
37	anke-004	0.0000	238	0.0011	293	-	464	0.0001	269	0.0004	324	0.0006	285
38	anke-005	0.0000	301	0.0012	305	-	372	0.0001	283	0.0004	337	0.0007	291
39	antheus-000	0.0000	2	0.0000	9	-	421	0.0000	56	0.0000	37	0.0242	422
40	antheus-001	0.0000	51	0.0000	20	-	390	0.0000	50	0.0000	65	0.0242	423
41	anyvision-004	0.0000	360	0.0017	342	-	427	0.0001	282	0.0004	279	0.0080	384
42	anyvision-005	0.0000	250	0.0013	315	-	442	0.0000	172	0.0004	213	0.0004	235
43	armatura-001	0.0000	384	0.0021	361	0.0257	203	0.0005	389	0.0005	369	0.0357	436
44	armatura-003	0.0000	256	0.0012	309	0.0333	233	0.0004	370	0.0004	266	0.0008	301
45	asusaics-000	0.0000	151	0.0000	82	-	310	0.0000	106	0.0000	118	0.0000	39
46	asusaics-001	0.0000	56	0.0000	22	-	395	0.0000	52	0.0000	60	0.0000	102
47	autentika-000	0.0000	54	0.0000	18	0.0000	22	0.0000	46	0.0000	68	0.0000	97
48	authenmetric-003	0.0000	95	0.0000	63	0.0000	43	0.0000	7	0.0000	26	0.0000	65
49	authenmetric-004	0.0000	180	0.0000	92	0.0000	18	0.0000	96	0.0000	78	0.0000	11
50	aware-005	0.0000	326	0.0020	352	-	467	0.0001	297	0.0004	323	0.0011	312
51	aware-006	0.0000	259	0.0009	255	0.0249	194	0.0000	177	0.0004	286	0.0006	281
52	awiros-001	0.0039	458	0.0369	463	-	396	0.0386	473	0.0872	478	0.3415	472
53	awiros-002	0.0000	395	0.0038	405	-	444	0.0007	410	0.0012	441	0.0208	415
54	aximetria-001	0.0000	346	0.0010	289	0.0217	173	0.0001	298	0.0004	273	0.0024	342
55	ayftech-001	0.0002	441	0.0046	417	-	402	0.0043	461	0.0011	425	0.0091	389
56	ayonix-000	0.0053	462	0.0341	460	-	371	0.0113	470	0.0137	472	0.1194	463
57	beethedata-000	0.0005	448	0.0042	412	0.0366	241	0.0002	311	0.0010	420	0.0006	275
58	beyneai-000	0.0000	103	0.0000	64	0.0000	44	0.0000	8	0.0000	20	0.0000	67

Table 30: FTE is the proportion of failed template generation attempts. Failures can occur because the software throws an exception, or because the software electively refuses to process the input image. This would typically occur if a face is not detected. FTE is measured as the number of function calls that give EITHER a non-zero error code OR that give a “small” template. This is defined as one whose size is less than 0.3 times the median template size for that algorithm. This second rule is needed because some algorithms incorrectly fail to return a non-zero error code when template generation fails.

A hyphen “-” indicates the dataset was not produced.¹ The effects of FTE are included in the accuracy results of this report by regarding any template comparison involving a failed template to produce a low similarity score. Thus higher FTE results in higher FNMR and lower FMR.

	Algorithm	Failure to Enrol Rate ¹											
		APPLICATION	BORDER	KIOSK	MUGSHOT	VISA	WILD	SEC. 2.2	SEC. 2.4	SEC. 2.6	SEC. 2.5	SEC. 2.1	SEC. 2.7
59	biocube-001	0.0006	452	0.0391	464	0.1207	294	0.0015	436	0.0020	454	0.0253	426
60	biodtechswiss-001	0.0000	286	0.0007	200	-	315	0.0000	165	0.0004	311	0.0025	344
61	biodtechswiss-002	0.0000	315	0.0007	203	-	348	0.0000	167	0.0004	301	0.0005	271
62	bm-001	0.0000	29	0.0000	5	-	415	0.0000	124	0.0000	45	0.0000	84
63	boetech-001	0.0087	466	0.0272	454	0.2117	301	0.0032	457	0.0160	473	0.0946	455
64	boetech-002	0.0087	467	0.0272	455	0.2117	300	0.0032	458	0.0160	474	0.0946	454
65	breecee-001	0.0000	226	0.0010	283	-	398	0.0002	310	0.0003	170	0.0003	138
66	breecee-002	0.0000	372	0.0020	358	0.0219	175	0.0008	412	0.0004	254	0.0031	353
67	camvi-002	0.0000	120	0.0000	73	-	335	0.0000	110	0.0000	97	0.0000	24
68	camvi-004	0.0000	3	0.0000	116	-	420	0.0000	58	0.0000	39	0.0000	78
69	canon-003	0.0000	280	0.0008	220	0.0234	188	0.0000	199	0.0004	298	0.0003	183
70	canon-004	0.0000	222	0.0008	219	0.0234	189	0.0000	198	0.0004	292	0.0003	186
71	ceiec-003	0.0000	131	0.0013	322	-	328	0.0001	236	0.0004	307	0.0004	199
72	ceiec-004	0.0000	175	0.0008	234	-	365	0.0000	171	0.0004	224	0.0004	241
73	chosun-001	0.0000	199	0.0000	103	-	352	0.0000	81	0.0000	91	0.0000	19
74	chosun-002	0.0000	205	0.0000	105	-	358	0.0000	84	0.0000	88	0.0000	22
75	chtface-005	0.0000	32	0.0017	338	0.0320	223	0.0000	184	0.0004	317	0.0020	340
76	chtface-006	0.0000	70	0.0017	339	0.0320	224	0.0000	183	0.0004	312	0.0020	339
77	cist-001	0.0000	156	0.0005	171	0.0087	88	0.0000	107	0.0000	111	0.0000	40
78	clearviewai-000	0.0000	289	0.0003	136	0.0081	85	0.0000	187	0.0003	154	0.0003	137
79	closeli-001	0.0000	91	0.0000	59	0.0000	41	0.0000	3	0.0000	22	0.0001	121
80	cloudmatrix-001	0.0000	332	0.0028	374	0.0225	179	0.0001	225	0.0004	204	0.0004	227
81	cloudmatrix-002	0.0000	345	0.0028	375	0.0225	178	0.0001	229	0.0004	209	0.0004	226
82	cloudwalk-hr-003	0.0000	261	0.0008	239	-	329	0.0001	240	0.0004	217	0.0113	395
83	cloudwalk-hr-004	0.0000	219	0.0011	300	-	411	0.0004	368	0.0003	187	0.0129	399
84	cloudwalk-mt-005	0.0000	247	0.0005	163	0.0130	106	0.0003	343	0.0004	327	0.0004	216
85	cloudwalk-mt-006	0.0000	253	0.0006	179	0.0158	125	0.0002	322	0.0004	326	0.0004	212
86	codeline-000	0.0000	82	0.0000	39	0.0000	48	0.0000	32	0.0000	16	0.0000	57
87	cogent-007	0.0000	373	0.0000	115	0.0000	57	0.0000	173	0.0000	125	0.0001	118
88	cogent-008	0.0000	134	0.0010	290	0.0304	218	0.0000	196	0.0004	201	0.0003	153
89	cognitec-003	0.0001	418	0.0194	449	0.0820	289	0.0003	358	0.0005	368	0.0039	359
90	cognitec-004	0.0001	419	0.0037	404	0.0580	265	0.0003	357	0.0005	366	0.0035	354
91	cor-001	0.0000	249	0.0006	182	-	436	0.0002	337	0.0004	278	0.0004	256
92	coretech-000	0.0000	150	0.0000	78	0.0000	1	0.0000	102	0.0000	117	0.0000	35
93	coretech-001	0.0000	414	0.0033	391	0.0677	276	0.0005	393	0.0011	432	0.0027	347
94	corsight-002	0.0000	245	0.0005	174	0.0152	119	0.0001	270	0.0004	259	0.0003	184
95	corsight-003	0.0000	317	0.0006	189	0.0175	134	0.0001	263	0.0004	272	0.0003	189
96	csc-002	0.0015	457	0.0033	388	-	462	0.0006	405	0.0006	408	0.0968	457
97	csc-003	0.0015	456	0.0033	389	0.0445	260	0.0006	404	0.0006	407	0.0968	456
98	ctcbcbank-000	0.0001	422	0.0051	422	-	359	0.0011	428	0.0019	452	0.0868	450
99	ctcbcbank-001	0.0000	394	0.0036	403	-	440	0.0005	390	0.0010	419	0.0844	447
100	cu-face-002	0.0000	178	0.0000	91	0.0000	17	0.0000	95	0.0000	77	0.0000	10
101	cubox-001	0.0000	55	0.0000	17	-	389	0.0000	47	0.0000	69	0.0000	98
102	cubox-002	0.0000	323	0.0006	185	0.0159	127	0.0002	338	0.0005	384	0.0016	330
103	cudocommunication-001	0.0000	92	0.0000	57	0.0000	38	0.0000	1	0.0000	24	0.0000	108
104	cuhkee-001	0.0000	305	0.0011	299	-	374	0.0000	135	0.0004	265	0.1278	465
105	cybercore-002	0.0000	378	0.0001	123	0.0014	64	0.0002	304	0.0002	132	0.0018	335
106	cybercore-003	0.0000	213	0.0003	137	0.0060	73	0.0005	395	0.0003	157	0.0192	414
107	cyberextruder-003	0.0000	376	0.0077	434	0.0887	291	0.0001	293	0.0006	402	0.0009	307
108	cyberextruder-004	0.0000	374	0.0097	437	0.1025	293	0.0001	286	0.0007	409	0.0213	416
109	cyberlink-009	0.0000	20	0.0004	153	0.0106	94	0.0000	128	0.0003	169	0.0002	133
110	cyberlink-010	0.0000	111	0.0004	154	0.0106	95	0.0000	126	0.0003	168	0.0002	132
111	dahua-006	0.0000	193	0.0000	112	-	364	0.0000	192	0.0003	190	0.0000	16
112	dahua-007	0.0000	97	0.0000	111	0.0000	59	0.0000	188	0.0003	186	0.0000	66
113	daon-000	0.0000	399	0.0028	378	0.0577	264	0.0014	434	0.0015	445	0.0030	352
114	decatur-000	0.0000	333	0.0020	351	-	437	0.0004	378	0.0005	356	0.0236	420
115	decatur-001	0.0000	217	0.0009	264	0.0194	151	0.0001	241	0.0004	247	0.0004	247
116	deepglint-004	0.0000	304	0.0005	158	0.0130	105	0.0002	336	0.0004	223	0.0003	162

Table 31: FTE is the proportion of failed template generation attempts. Failures can occur because the software throws an exception, or because the software electively refuses to process the input image. This would typically occur if a face is not detected. FTE is measured as the number of function calls that give EITHER a non-zero error code OR that give a “small” template. This is defined as one whose size is less than 0.3 times the median template size for that algorithm. This second rule is needed because some algorithms incorrectly fail to return a non-zero error code when template generation fails.

A hyphen “-” indicates the dataset was not produced.¹ The effects of FTE are included in the accuracy results of this report by regarding any template comparison involving a failed template to produce a low similarity score. Thus higher FTE results in higher FNMR and lower FMR.

	Algorithm	Failure to Enrol Rate ¹											
		Name	APPLICATION	BORDER	KIOSK	MUGSHOT	VISA	WILD					
			SEC. 2.2	SEC. 2.4	SEC. 2.6	SEC. 2.5	SEC. 2.1	SEC. 2.7					
117	deepglint-005	0.0000	350	0.0019	346	0.0438	259	0.0006	401	0.0006	405	0.0028	351
118	deepsea-001	0.0000	26	0.0000	4	-	416	0.0000	70	0.0000	46	0.0000	86
119	deepsense-000	0.0000	196	0.0006	190	-	347	0.0000	152	0.0004	195	0.0003	165
120	deepsense-001	0.0000	153	0.0006	192	0.0191	148	0.0000	159	0.0004	203	0.0003	179
121	dermalog-010	0.0000	386	0.0031	385	0.0148	116	0.0006	398	0.0003	147	0.0002	122
122	dermalog-011	0.0000	409	0.0005	159	0.0116	99	0.0001	222	0.0003	152	0.0002	123
123	dicio-001	0.0005	451	0.0649	468	0.2136	302	0.0024	446	0.0012	436	0.0935	452
124	didiglobalface-001	0.0000	244	0.0012	302	-	447	0.0000	207	0.0004	316	0.0004	211
125	didiglobalface-002	0.0000	296	0.0012	304	0.0247	193	0.0000	209	0.0004	318	0.0004	205
126	digidata-000	0.0000	234	0.0023	365	0.0375	248	0.0004	381	0.0006	398	0.0006	278
127	digidata-001	0.0000	308	0.0023	367	0.0375	247	0.0004	383	0.0006	399	0.0006	277
128	digitalbarriers-002	0.0001	431	0.0045	415	-	428	0.0028	454	0.0027	460	0.0071	379
129	dps-000	0.0000	93	0.0000	56	0.0000	39	0.0000	2	0.0000	25	0.0000	61
130	dsk-000	0.0000	176	0.0000	89	-	369	0.0000	93	0.0000	81	0.0000	9
131	einetworks-000	0.0000	393	0.0017	340	-	412	0.0002	325	0.0005	380	0.0008	304
132	ekin-002	0.0000	130	0.0000	117	0.0004	62	0.0000	130	0.0000	124	0.0019	337
133	enface-000	0.0000	107	0.0012	312	0.0305	220	0.0000	180	0.0004	270	0.0004	229
134	enface-001	0.0000	157	0.0012	311	0.0304	219	0.0000	164	0.0004	269	0.0004	215
135	eocortex-000	0.0095	468	0.0602	467	-	468	0.0094	468	0.0059	468	0.1405	468
136	ercacat-001	0.0000	73	0.0005	166	-	477	0.0000	181	0.0003	171	0.0002	126
137	euronovate-001	0.0255	474	0.0102	439	0.0517	263	0.0021	443	0.0004	348	0.2451	470
138	expasoft-001	0.0000	100	0.0000	65	-	453	0.0000	9	0.0000	19	0.0000	68
139	expasoft-002	0.0000	4	0.0000	10	0.0000	34	0.0000	57	0.0000	38	0.0000	76
140	f8-001	0.0003	444	0.0059	427	-	406	0.0035	459	0.0030	465	0.0087	387
141	f8-002	0.0000	416	0.0150	447	0.0685	280	0.0005	385	0.0013	443	0.0883	451
142	faceonlive-001	0.0000	406	0.0029	382	0.0481	261	0.0013	432	0.0011	426	0.0160	405
143	faceonlive-002	0.0002	439	0.0009	267	0.0075	79	0.0008	415	0.0008	416	0.0083	385
144	facephi-000	0.0000	183	0.0004	141	0.0090	89	0.0001	271	0.0004	208	0.0003	164
145	facesoft-000	0.0000	45	0.0000	32	-	407	0.0000	43	0.0000	53	0.0000	92
146	facetag-000	0.0000	149	0.0000	77	0.0000	3	0.0000	101	0.0000	116	0.0000	34
147	facetag-002	0.0000	170	0.0000	96	0.0000	20	0.0000	88	0.0000	71	0.0000	4
148	facex-001	0.0001	437	0.0360	461	-	419	0.0047	463	0.0027	461	0.1109	461
149	facex-002	0.0001	438	0.0360	462	0.2663	305	0.0047	464	0.0027	462	0.1109	460
150	farfaces-001	0.0000	391	0.0007	202	0.0061	74	0.0003	354	0.0003	163	0.0006	286
151	fiberhome-nanjing-003	0.0000	61	0.0004	147	-	466	0.0000	18	0.0003	148	0.0001	113
152	fiberhome-nanjing-004	0.0000	12	0.0004	146	-	433	0.0000	64	0.0003	149	0.0001	114
153	fincore-000	0.0000	276	0.0008	240	0.0185	142	0.0001	216	0.0004	310	0.0006	279
154	firstcreditKZ-001	0.0000	347	0.0019	348	0.0321	226	0.0000	204	0.0004	263	0.0007	289
155	frpkauai-001	0.0000	358	0.0024	370	0.0360	239	0.0001	232	0.0004	334	0.0007	297
156	frpkauai-002	0.0000	353	0.0019	349	0.0321	227	0.0000	203	0.0004	257	0.0007	288
157	fujitsulab-002	0.0000	127	0.0009	251	-	341	0.0001	281	0.0003	150	0.0003	144
158	fujitsulab-003	0.0000	184	0.0008	225	0.0166	131	0.0001	268	0.0001	129	0.0003	139
159	g42-intellibrain-001	0.0000	182	0.0000	107	0.0000	15	0.0000	72	0.0000	85	0.0000	12
160	geo-002	0.0000	235	0.0015	328	0.0332	231	0.0001	213	0.0004	336	0.0017	334
161	geo-004	0.0000	267	0.0005	173	0.0138	110	0.0001	254	0.0004	242	0.0009	308
162	glory-004	0.0000	330	0.0020	356	0.0345	235	0.0001	274	0.0004	330	0.0167	407
163	glory-005	0.0000	335	0.0020	357	0.0345	234	0.0001	276	0.0004	333	0.0167	406
164	gorilla-008	0.0000	306	0.0009	270	0.0259	204	0.0001	242	0.0004	306	0.0004	219
165	gorilla-009	0.0000	220	0.0010	278	0.0276	212	0.0001	227	0.0004	290	0.0004	213
166	graymatics-001	0.0000	102	0.0010	271	0.0210	163	0.0001	291	0.0004	246	0.0006	283
167	griaule-001	0.0000	119	0.0012	313	0.0366	242	0.0000	154	0.0004	302	0.0005	264
168	griaule-002	0.0000	145	0.0007	207	0.0209	161	0.0000	201	0.0004	256	0.0004	202
169	hertasecurity-001	0.0000	190	0.0000	119	0.0000	60	0.0000	142	0.0001	126	0.0002	131
170	hertasecurity-002	0.0000	204	0.0000	106	0.0000	13	0.0000	143	0.0000	121	0.0000	23
171	hik-001	0.0000	189	0.0000	120	-	362	0.0000	76	0.0000	82	0.0000	15
172	hisign-001	0.0000	185	0.0000	109	0.0000	16	0.0000	74	0.0000	86	0.0000	14
173	hisign-002	0.0000	321	0.0006	186	0.0150	117	0.0001	277	0.0003	181	0.0005	268
174	hyperverge-003	0.0000	194	0.0008	223	0.0210	164	0.0002	339	0.0004	250	0.0004	244

Table 32: FTE is the proportion of failed template generation attempts. Failures can occur because the software throws an exception, or because the software electively refuses to process the input image. This would typically occur if a face is not detected. FTE is measured as the number of function calls that give EITHER a non-zero error code OR that give a “small” template. This is defined as one whose size is less than 0.3 times the median template size for that algorithm. This second rule is needed because some algorithms incorrectly fail to return a non-zero error code when template generation fails.

A hyphen “-” indicates the dataset was not produced.¹ The effects of FTE are included in the accuracy results of this report by regarding any template comparison involving a failed template to produce a low similarity score. Thus higher FTE results in higher FNMR and lower FMR.

	Algorithm	Failure to Enrol Rate ¹											
		APPLICATION	BORDER	KIOSK	MUGSHOT	VISA	WILD	SEC. 2.2	SEC. 2.4	SEC. 2.6	SEC. 2.5	SEC. 2.1	SEC. 2.7
175	hyperverge-004	0.0000	215	0.0008	238	0.0218	174	0.0002	327	0.0004	262	0.0004	233
176	hzailiu-002	0.0000	383	0.0015	331	0.0424	255	0.0003	359	0.0005	382	0.0075	381
177	hzailiu-003	0.0000	257	0.0004	142	0.0081	86	0.0002	305	0.0003	178	0.0003	158
178	icm-003	0.0000	188	0.0001	122	0.0023	65	0.0000	75	0.0000	120	0.0000	109
179	icm-004	0.0000	401	0.0033	394	0.0698	281	0.0006	403	0.0010	424	0.0026	346
180	icthtc-000	0.0001	436	0.0047	420	-	333	0.0028	455	0.0029	463	0.0086	386
181	id3-006	0.0000	359	0.0009	269	-	375	0.0004	373	0.0005	377	0.0008	302
182	id3-008	0.0000	42	0.0006	188	0.0184	139	0.0001	290	0.0004	199	0.0003	141
183	idemia-008	0.0000	23	0.0004	155	0.0078	83	0.0000	140	0.0003	175	0.0003	155
184	idemia-009	0.0000	192	0.0004	151	0.0077	81	0.0000	141	0.0003	177	0.0003	157
185	iit-002	0.0000	398	0.0021	360	-	472	0.0009	424	0.0005	388	0.0443	437
186	iit-003	0.0000	294	0.0008	241	-	382	0.0000	170	0.0004	206	0.0069	378
187	imds-software-001	0.0000	75	0.0000	37	0.0000	46	0.0000	29	0.0000	12	0.0000	55
188	imperial-000	0.0000	89	0.0000	60	-	446	0.0000	5	0.0000	21	0.0000	63
189	imperial-002	0.0000	165	0.0000	93	-	377	0.0000	85	0.0000	75	0.0000	3
190	incode-010	0.0000	325	0.0009	256	0.0255	202	0.0002	313	0.0004	237	0.0007	298
191	incode-011	0.0000	336	0.0009	257	0.0255	201	0.0002	314	0.0004	240	0.0007	296
192	infocert-001	0.0000	366	0.0059	428	0.0424	256	0.0001	248	0.0006	394	0.0018	336
193	innefulabs-000	0.0000	312	0.0024	369	-	346	0.0003	355	0.0005	373	0.0004	225
194	innovativetechnologyltd-001	0.0001	435	0.0050	421	-	357	0.0024	449	0.0025	459	0.0055	371
195	innovativetechnologyltd-002	0.0000	355	0.0046	416	-	331	0.0057	467	0.0005	375	0.0247	425
196	innovatrics-008	0.0000	300	0.0009	263	0.0204	156	0.0000	179	0.0004	194	0.0003	188
197	innovatrics-009	0.0000	22	0.0005	157	0.0142	113	0.0000	68	0.0000	123	0.0000	110
198	insightface-001	0.0000	64	0.0000	44	0.0000	52	0.0000	16	0.0000	9	0.0000	43
199	insightface-003	0.0000	1	0.0000	8	0.0000	33	0.0000	59	0.0000	36	0.0000	77
200	inspur-000	0.0000	171	0.0000	98	0.0000	21	0.0000	90	0.0000	72	0.0000	6
201	intellicloudai-001	0.0000	133	0.0000	70	-	327	0.0000	117	0.0000	103	0.0001	120
202	intellicloudai-002	0.0000	28	0.0008	230	-	418	0.0000	169	0.0004	198	0.0012	321
203	intellifusion-001	0.0000	228	0.0005	169	-	473	0.0001	239	0.0003	179	0.0005	266
204	intellifusion-002	0.0000	186	0.0000	118	-	360	0.0000	125	0.0000	87	0.0001	119
205	intellivision-003	0.0000	224	0.0012	307	0.0308	222	0.0003	349	0.0004	354	0.0185	412
206	intellivision-004	0.0000	273	0.0011	294	0.0266	209	0.0002	341	0.0004	349	0.0179	410
207	intellivix-002	0.0000	44	0.0009	268	0.0184	140	0.0000	42	0.0000	52	0.0000	93
208	intellivix-003	0.0000	90	0.0000	58	0.0000	40	0.0000	4	0.0000	23	0.0000	62
209	intelresearch-005	0.0000	271	0.0006	181	0.0144	114	0.0000	158	0.0004	227	0.0003	166
210	intelresearch-006	0.0000	136	0.0000	113	0.0004	63	0.0000	132	0.0004	226	0.0003	182
211	intemta-000	0.0000	19	0.0005	161	0.0126	102	0.0000	191	0.0004	205	0.0003	154
212	intemta-001	0.0000	295	0.0004	150	0.0106	96	0.0000	129	0.0003	189	0.0003	175
213	intsysmsu-001	0.0000	47	0.0010	280	-	386	0.0001	258	0.0004	283	0.0004	240
214	intsysmsu-002	0.0000	13	0.0010	279	-	429	0.0001	260	0.0004	281	0.0004	238
215	ionetworks-000	0.0000	109	0.0016	336	0.0387	250	0.0004	363	0.0005	364	0.0004	246
216	iqface-000	0.0000	69	0.0000	48	-	476	0.0000	21	0.0000	3	0.0000	47
217	iqface-003	0.0000	396	0.0076	433	-	430	0.0006	399	0.0005	391	0.0069	377
218	irex-000	0.0000	363	0.0009	266	-	435	0.0000	186	0.0005	357	0.0003	185
219	isap-001	0.0000	27	0.0000	3	-	417	0.0000	69	0.0000	47	0.0000	85
220	isap-002	0.0000	66	0.0000	49	-	471	0.0000	22	0.0000	1	0.0000	48
221	isityou-000	0.0068	465	0.0316	458	-	338	0.0023	445	0.0010	422	0.0663	444
222	isystems-001	0.0000	404	0.0035	399	-	326	0.0010	426	0.0007	411	0.0128	398
223	isystems-002	0.0000	405	0.0035	400	-	353	0.0010	425	0.0007	410	0.0128	397
224	itm0-007	0.0000	137	0.0009	250	-	332	0.0003	361	0.0000	100	0.0004	214
225	itm0-008	0.0000	144	0.0135	444	0.1239	295	0.0024	450	0.0000	109	0.0836	446
226	ivacognitive-001	0.0000	327	0.0011	296	-	475	0.0001	226	0.0004	335	0.0011	313
227	iws-000	0.0005	449	0.0650	470	-	373	0.0024	447	0.0012	437	0.0936	453
228	jaakit-001	0.0008	455	0.0858	472	0.2713	306	0.0042	460	0.0021	455	0.1062	458
229	kakao-007	0.0000	88	0.0007	193	0.0165	130	0.0001	250	0.0004	218	0.0097	393
230	kakao-008	0.0000	203	0.0009	253	0.0209	162	0.0001	252	0.0004	225	0.0097	392
231	kakaopay-001	0.0000	339	0.0013	320	0.0322	228	0.0001	234	0.0004	338	0.0078	383
232	kasikornlabs-000	0.0000	412	0.0035	398	0.0713	284	0.0004	379	0.0012	440	0.0270	429

Table 33: FTE is the proportion of failed template generation attempts. Failures can occur because the software throws an exception, or because the software electively refuses to process the input image. This would typically occur if a face is not detected. FTE is measured as the number of function calls that give EITHER a non-zero error code OR that give a “small” template. This is defined as one whose size is less than 0.3 times the median template size for that algorithm. This second rule is needed because some algorithms incorrectly fail to return a non-zero error code when template generation fails.

A hyphen “-” indicates the dataset was not produced.¹ The effects of FTE are included in the accuracy results of this report by regarding any template comparison involving a failed template to produce a low similarity score. Thus higher FTE results in higher FNMR and lower FMR.

	Algorithm	Failure to Enrol Rate ¹											
		APPLICATION	BORDER	KIOSK	MUGSHOT	VISA	WILD	SEC. 2.2	SEC. 2.4	SEC. 2.6	SEC. 2.5	SEC. 2.1	SEC. 2.7
233	kasikornlabs-002	0.0000	410	0.0033	390	0.0698	282	0.0004	375	0.0012	434	0.0269	428
234	kedacom-000	0.0000	41	0.0000	33	-	408	0.0000	44	0.0000	51	0.0000	94
235	kiwitech-000	0.0000	239	0.0009	247	-	463	0.0004	374	0.0005	361	0.0004	250
236	kneron-003	0.0239	472	0.0306	456	-	336	0.0044	462	0.0016	449	0.1823	469
237	kneron-005	0.0000	407	0.0226	450	-	317	0.0006	397	0.0005	372	0.0097	391
238	knowutech-000	0.0000	292	0.0008	222	0.0215	171	0.0000	175	0.0004	293	0.0003	187
239	kokmin-002	0.0000	115	0.0000	55	-	443	0.0000	15	0.0000	29	0.0000	73
240	koreaid-001	0.0000	116	0.0023	368	0.0371	245	0.0000	197	0.0005	355	0.0027	348
241	krungthai-002	0.0000	223	0.0005	164	0.0111	98	0.0002	324	0.0003	188	0.0005	257
242	kuke3d-001	0.0000	10	0.0000	12	0.0000	35	0.0000	61	0.0000	42	0.0000	79
243	kuke3d-002	0.0000	206	0.0000	104	0.0000	12	0.0000	83	0.0000	89	0.0000	21
244	lebentech-000	0.0042	459	0.0029	384	0.0252	198	0.0051	466	0.0066	469	0.0154	404
245	lemalabs-001	0.0000	158	0.0005	172	0.0141	111	0.0002	323	0.0004	210	0.0004	208
246	lineclova-002	0.0000	11	0.0007	194	0.0181	137	0.0000	63	0.0000	33	0.0000	106
247	lineclova-003	0.0000	389	0.0023	364	0.0700	283	0.0002	340	0.0005	359	0.0038	356
248	lookman-002	0.0000	141	0.0000	86	-	321	0.0000	99	0.0000	107	0.0000	32
249	lookman-004	0.0000	155	0.0000	81	-	311	0.0000	105	0.0000	119	0.0000	38
250	luxand-000	0.0000	126	0.0000	75	-	339	0.0000	112	0.0000	96	0.0000	26
251	mantra-000	0.0001	420	0.0041	411	0.0680	279	0.0003	353	0.0004	346	0.0037	355
252	maxvision-002	0.0000	293	0.0009	246	0.0229	183	0.0002	302	0.0004	264	0.0004	252
253	maxvision-003	0.0000	207	0.0009	245	0.0229	184	0.0002	301	0.0004	261	0.0004	254
254	megvii-005	0.0000	237	0.0010	272	0.0206	159	0.0002	332	0.0004	313	0.0011	315
255	megvii-006	0.0000	298	0.0010	274	0.0206	158	0.0002	333	0.0004	319	0.0011	314
256	meituan-001	0.0000	307	0.0014	325	0.0295	215	0.0001	262	0.0004	300	0.0013	326
257	meituan-002	0.0000	284	0.0013	319	0.0251	197	0.0001	264	0.0004	297	0.0020	338
258	meiya-001	0.0000	402	0.0028	379	-	381	0.0004	380	0.0010	423	0.0025	343
259	mendaxiatech-000	0.0000	242	0.0010	273	0.0206	157	0.0002	334	0.0004	315	0.0011	317
260	metsakuurcompany-001	0.0000	159	0.0011	292	0.0208	160	0.0002	331	0.0004	230	0.0003	181
261	metsakuurcompany-002	0.0000	122	0.0000	74	0.0000	11	0.0000	111	0.0000	98	0.0000	25
262	maxis-001	0.0000	232	0.0013	316	0.0262	207	0.0001	292	0.0003	156	0.0003	193
263	microfocus-001	0.0001	432	0.0053	424	-	394	0.0008	417	0.0016	448	0.0220	418
264	microfocus-002	0.0001	433	0.0053	425	-	470	0.0008	416	0.0016	447	0.0220	417
265	minivision-000	0.0000	201	0.0000	101	-	349	0.0000	79	0.0000	93	0.0000	17
266	mobai-000	0.0000	369	0.0114	441	-	368	0.0003	356	0.0012	439	0.1242	464
267	mobai-001	0.0000	340	0.0040	407	-	361	0.0001	272	0.0012	438	0.0523	441
268	mobbl-001	0.0000	397	0.0052	423	0.0678	277	0.0002	308	0.0005	381	0.0181	411
269	mobbl-003	0.0000	408	0.0029	383	0.0633	270	0.0002	328	0.0009	418	0.0026	345
270	mobipintech-000	0.0000	21	0.0000	2	0.0000	29	0.0000	67	0.0000	43	0.0000	83
271	moreedian-000	0.0000	297	0.0009	248	-	384	0.0004	377	0.0005	362	0.0004	248
272	mukh-001	0.0000	99	0.0010	281	0.0154	122	0.0001	267	0.0003	142	0.0010	309
273	mukh-002	0.0000	195	0.0022	363	0.0513	262	0.0002	306	0.0004	255	0.0016	332
274	multimodality-000	0.0000	18	0.0000	1	0.0000	28	0.0000	66	0.0000	48	0.0000	82
275	multimodality-001	0.0000	74	0.0009	244	0.0259	205	0.0000	24	0.0000	6	0.0000	50
276	mvision-001	0.0000	14	0.0000	14	-	431	0.0000	65	0.0000	34	0.0000	81
277	nazhiai-000	0.0000	113	0.0000	53	-	438	0.0000	13	0.0000	28	0.0000	71
278	neosystems-004	0.0000	6	0.0000	11	0.0000	32	0.0000	60	0.0000	35	0.0000	75
279	netbridgeotech-001	0.0000	49	0.0000	15	-	385	0.0000	45	0.0000	64	0.0000	95
280	netbridgeotech-002	0.0000	81	0.0000	40	-	458	0.0000	31	0.0000	17	0.0000	58
281	neurotechnology-013	0.0000	43	0.0008	242	0.0185	141	0.0000	134	0.0001	127	0.0004	224
282	neurotechnology-015	0.0000	200	0.0004	143	0.0082	87	0.0000	82	0.0000	122	0.0003	140
283	nhn-002	0.0000	5	0.0004	156	0.0091	90	0.0000	166	0.0003	153	0.0003	143
284	nhn-003	0.0000	352	0.0000	42	0.0000	51	0.0001	296	0.0004	299	0.0010	310
285	nodeflux-002	0.0000	252	0.0261	453	-	441	0.0008	414	0.0005	374	0.0008	305
286	notiontag-001	0.0000	187	0.0000	110	-	363	0.0027	453	0.0000	83	0.0132	401
287	notiontag-002	0.0000	181	0.0000	108	0.0000	14	0.0000	73	0.0000	84	0.0000	13
288	nsensecorp-003	0.0000	110	0.0000	121	0.0002	61	0.0000	155	0.0007	413	0.0150	402
289	nsensecorp-004	0.0406	475	0.0035	397	0.0181	136	0.0016	438	0.0760	477	0.0509	440
290	ntechlab-011	0.0000	164	0.0003	128	0.0057	71	0.0000	193	0.0004	193	0.0003	167

Table 34: FTE is the proportion of failed template generation attempts. Failures can occur because the software throws an exception, or because the software electively refuses to process the input image. This would typically occur if a face is not detected. FTE is measured as the number of function calls that give EITHER a non-zero error code OR that give a “small” template. This is defined as one whose size is less than 0.3 times the median template size for that algorithm. This second rule is needed because some algorithms incorrectly fail to return a non-zero error code when template generation fails.

A hyphen “-” indicates the dataset was not produced.¹ The effects of FTE are included in the accuracy results of this report by regarding any template comparison involving a failed template to produce a low similarity score. Thus higher FTE results in higher FNMR and lower FMR.

	Algorithm	Failure to Enrol Rate ¹										
		Name	APPLICATION		BORDER		KIOSK		MUGSHOT		VISA	WILD
			SEC. 2.2	SEC. 2.4	SEC. 2.6	SEC. 2.5	SEC. 2.1	SEC. 2.7				
291	ntechlab-012	0.0000	121	0.0003	127	0.0057	70	0.0000	195	0.0004	196	0.0003 170
292	omface-000	0.0000	96	0.0000	62	0.0000	42	0.0000	6	0.0000	27	0.1160 462
293	omface-001	0.0000	143	0.0000	114	0.0000	58	0.0000	98	0.0000	108	0.0000 105
294	omnigarde-001	0.0000	274	0.0008	217	0.0213	165	0.0000	163	0.0004	287	0.0003 190
295	omnigarde-002	0.0000	233	0.0008	216	0.0213	166	0.0000	160	0.0004	277	0.0003 194
296	onfido-000	0.0000	403	0.0040	406	0.0804	288	0.0004	365	0.0012	435	0.0052 370
297	openface-001	0.0000	379	0.0104	440	0.0668	272	0.0004	371	0.0006	406	0.0856 449
298	oz-003	0.0000	84	0.0002	125	0.0042	67	0.0000	127	0.0003	141	0.0002 125
299	oz-004	0.0000	385	0.0003	132	0.0041	66	0.0000	133	0.0002	131	0.0006 274
300	palit-000	0.0000	214	0.0005	165	0.0134	109	0.0002	315	0.0004	219	0.0004 239
301	palit-001	0.0000	302	0.0007	215	0.0201	154	0.0002	316	0.0004	222	0.0004 236
302	pangiam-000	0.0000	15	0.0021	362	0.0364	240	0.0001	215	0.0005	360	0.0095 390
303	papago-001	0.0000	329	0.0008	224	0.0159	128	0.0002	342	0.0004	253	0.0190 413
304	papsav1923-002	0.0000	263	0.0018	345	0.0268	210	0.0000	182	0.0004	295	0.0004 223
305	papsav1923-003	0.0000	357	0.0019	350	0.0321	225	0.0000	205	0.0004	268	0.0007 287
306	paravision-010	0.0000	112	0.0010	275	0.0201	153	0.0001	244	0.0004	197	0.0003 195
307	paravision-011	0.0000	161	0.0010	276	0.0201	152	0.0001	249	0.0004	202	0.0003 192
308	pensees-001	0.0000	314	0.0000	100	-	351	0.0000	78	0.0000	94	0.0000 18
309	pixelall-008	0.0000	53	0.0008	233	0.0247	192	0.0000	49	0.0000	66	0.0000 99
310	pixelall-009	0.0000	38	0.0000	31	0.0000	26	0.0000	41	0.0000	49	0.0000 91
311	psl-010	0.0000	225	0.0004	145	0.0095	91	0.0000	123	0.0004	192	0.0003 160
312	psl-011	0.0000	216	0.0003	129	0.0063	76	0.0000	122	0.0003	176	0.0003 151
313	ptakuratsatu-000	0.0000	209	0.0007	213	-	423	0.0001	214	0.0003	162	0.0003 159
314	pxl-001	0.0000	417	0.0044	414	-	356	0.0005	388	0.0022	457	0.0323 432
315	pyramid-000	0.0001	430	0.0041	410	-	367	0.0005	387	0.0007	412	0.0015 329
316	qazbs-000	0.0000	33	0.0009	254	0.0265	208	0.0000	150	0.0004	248	0.0003 197
317	qluevision-001	0.0000	364	0.0008	228	0.0153	120	0.0008	413	0.0004	350	0.0041 360
318	qnap-002	0.0000	400	0.0033	387	0.0761	286	0.0004	367	0.0002	130	0.0017 333
319	qnap-003	0.0000	118	0.0016	334	0.0402	253	0.0000	200	0.0001	128	0.0003 142
320	quantasoft-003	0.0000	370	0.0015	332	0.0355	237	0.0005	386	0.0006	401	0.0088 388
321	rankone-012	0.0000	138	0.0000	72	0.0000	10	0.0000	119	0.0000	99	0.0000 30
322	rankone-013	0.0000	58	0.0005	162	0.0126	103	0.0000	147	0.0003	146	0.0003 147
323	rankone-014	0.0000	172	0.0005	160	0.0129	104	0.0000	149	0.0002	134	0.0002 134
324	realnetworks-007	0.0000	258	0.0013	321	0.0425	257	0.0000	131	0.0004	267	0.0004 242
325	realnetworks-008	0.0000	229	0.0002	126	0.0045	68	0.0000	121	0.0002	140	0.0003 150
326	regula-000	0.0000	105	0.0000	52	0.0000	36	0.0000	12	0.0000	31	0.0000 70
327	regula-001	0.0000	160	0.0000	84	0.0000	6	0.0000	109	0.0000	112	0.0000 42
328	remarkai-001	0.0000	125	0.0000	76	-	340	0.0000	113	0.0000	95	0.0000 112
329	remarkai-003	0.0000	319	0.0007	201	0.0187	143	0.0000	185	0.0004	216	0.0004 228
330	rendip-000	0.0000	351	0.0016	335	0.0293	214	0.0002	312	0.0004	345	0.0013 327
331	revealmedia-005	0.0000	362	0.0007	208	0.0189	145	0.0009	423	0.0004	352	0.0076 382
332	revealmedia-006	0.0000	146	0.0009	262	0.0238	190	0.0001	265	0.0004	309	0.0004 253
333	rokid-000	0.0000	78	0.0072	431	-	457	0.0001	251	0.0005	371	0.0354 435
334	rokid-001	0.0000	106	0.0013	318	-	434	0.0000	11	0.0000	32	0.0007 294
335	s1-005	0.0000	8	0.0004	148	0.0120	101	0.0001	228	0.0002	133	0.0050 368
336	s1-006	0.0000	36	0.0003	130	0.0074	78	0.0001	223	0.0002	135	0.0050 369
337	saffe-001	0.0000	86	0.0000	43	-	461	0.0000	34	0.0000	11	0.0000 60
338	saffe-002	0.0000	140	0.0000	87	-	320	0.0000	100	0.0000	106	0.0000 33
339	samsungsds-001	0.0000	16	0.0005	168	0.0146	115	0.0001	246	0.0003	180	0.0003 196
340	samsungsds-002	0.0000	202	0.0004	149	0.0119	100	0.0001	247	0.0003	172	0.0003 169
341	samtech-001	0.0001	429	0.0032	386	-	378	0.0004	376	0.0008	414	0.0013 324
342	scanovate-002	0.0000	344	0.0018	344	-	350	0.0000	208	0.0004	344	0.0008 303
343	scanovate-003	0.0000	334	0.0233	451	0.3371	308	0.0006	400	0.0004	351	0.0007 295
344	sdc-000	0.0000	413	0.0035	396	0.0678	278	0.0005	394	0.0011	429	0.0028 350
345	securifai-005	0.0000	166	0.0000	95	0.0000	19	0.0000	87	0.0000	73	0.0000 2
346	securifai-006	0.0000	62	0.0000	45	0.0000	54	0.0000	17	0.0000	8	0.0000 45
347	sensetime-007	0.0000	154	0.0004	144	0.0106	93	0.0000	168	0.0003	164	0.0002 130
348	sensetime-008	0.0000	65	0.0007	212	0.0250	195	0.0000	120	0.0003	185	0.0003 136

Table 35: FTE is the proportion of failed template generation attempts. Failures can occur because the software throws an exception, or because the software electively refuses to process the input image. This would typically occur if a face is not detected. FTE is measured as the number of function calls that give EITHER a non-zero error code OR that give a "small" template. This is defined as one whose size is less than 0.3 times the median template size for that algorithm. This second rule is needed because some algorithms incorrectly fail to return a non-zero error code when template generation fails.

A hyphen "-" indicates the dataset was not produced.¹ The effects of FTE are included in the accuracy results of this report by regarding any template comparison involving a failed template to produce a low similarity score. Thus higher FTE results in higher FNMR and lower FMR.

	Algorithm Name	Failure to Enrol Rate ¹							
		APPLICATION		BORDER		KIOSK	MUGSHOT	VISA	WILD
		SEC. 2.2	SEC. 2.4	SEC. 2.6	SEC. 2.5	SEC. 2.1	SEC. 2.7		
349	sertis-000	0.0000	39	0.0007	206	-	405	0.0000	211
350	sertis-002	0.0000	87	0.0007	197	0.0152	118	0.0000	202
351	seventhsense-001	0.0000	316	0.0006	191	0.0184	138	0.0001	218
352	seventhsense-002	0.0000	46	0.0003	140	0.0076	80	0.0000	212
353	shaman-000	0.0000	174	0.0000	88	-	366	0.0000	91
354	shaman-001	0.0000	129	0.0000	67	-	325	0.0000	114
355	shu-002	0.0000	343	0.0010	284	-	342	0.0005	384
356	shu-003	0.0000	24	0.0007	195	-	414	0.0001	219
357	siat-002	0.0000	243	0.0012	310	-	448	0.0000	178
358	siat-005	0.0000	147	0.0000	80	0.0000	56	0.0000	104
359	sjtu-003	0.0000	152	0.0005	175	-	309	0.0000	194
360	sjtu-004	0.0000	83	0.0000	38	0.0000	49	0.0000	30
361	sktelecom-000	0.0000	211	0.0008	232	0.0190	146	0.0000	190
362	smartbiometrik-001	0.0005	447	0.0649	469	0.2147	304	0.0017	439
363	smartengines-000	0.0066	464	0.0150	446	0.1656	297	0.0022	444
364	smartengines-001	0.0003	443	0.0073	432	0.0714	285	0.0007	407
365	smartvist-000	0.0000	179	0.0026	373	0.0357	238	0.0002	300
366	smilart-002	0.0000	411	0.0036	401	-	455	-	474
367	smilart-003	0.0003	442	0.0100	438	-	413	0.0014	433
368	sodec-000	0.0000	101	0.0000	66	0.0000	45	0.0000	10
369	sqisoft-002	0.0000	68	0.0003	135	0.0078	82	0.0000	146
370	sqisoft-003	0.0000	191	0.0003	138	0.0078	84	0.0000	148
371	staqu-000	0.0000	72	0.0000	51	-	478	0.0000	25
372	starhybrid-001	0.0001	434	0.0033	393	-	314	0.0009	422
373	stcon-000	0.0000	266	0.0017	343	0.0301	217	0.0000	161
374	sukshi-000	0.0000	57	0.0000	23	0.0000	23	0.0000	53
375	suprema-003	0.0000	287	0.0008	235	0.0231	186	0.0000	144
376	suprema-004	0.0000	260	0.0014	323	0.0299	216	0.0000	145
377	supremaid-001	0.0000	254	0.0020	355	0.0330	230	0.0001	257
378	supremaid-002	0.0000	212	0.0020	353	0.0330	229	0.0001	261
379	surrey-cvssp-000	0.0000	132	0.0000	71	0.0000	8	0.0000	118
380	surrey-cvssp-001	0.0173	471	0.0007	198	0.0179	135	0.0011	429
381	synesis-006	0.0000	114	0.0003	139	-	439	0.0000	189
382	synesis-007	0.0000	246	0.0013	317	-	452	0.0002	330
383	synology-000	0.0000	67	0.0000	50	-	474	0.0000	23
384	synology-002	0.0000	198	0.0000	102	-	354	0.0000	80
385	sztu-000	0.0000	35	0.0000	28	-	403	0.0000	38
386	sztu-001	0.0000	37	0.0000	27	0.0000	25	0.0000	37
387	t4isb-000	0.0000	76	0.0000	36	0.0000	47	0.0000	28
388	tech5-005	0.0000	272	0.0007	214	-	323	0.0000	162
389	tech5-007	0.0000	281	0.0014	326	0.0305	221	0.0000	153
390	techsign-000	0.0007	453	0.0334	459	0.2093	299	0.0020	442
391	techsign-001	0.0000	270	0.0008	243	0.0253	199	0.0002	318
392	tevian-007	0.0000	262	0.0015	333	0.0429	258	0.0002	326
393	tevian-008	0.0000	248	0.0006	178	0.0109	97	0.0000	156
394	tiger-005	0.0000	313	0.0009	265	0.0194	150	0.0001	243
395	tiger-006	0.0000	320	0.0011	298	0.0396	251	0.0001	287
396	tinkoff-001	0.0000	331	0.0008	231	0.0171	132	0.0001	279
397	tongyi-005	0.0000	9	0.0000	13	-	422	0.0000	62
398	toppanidgate-000	0.0000	221	0.0008	227	0.0232	187	0.0004	364
399	toshiba-004	0.0000	63	0.0000	46	0.0000	53	0.0000	19
400	toshiba-006	0.0000	230	0.0004	152	0.0050	69	0.0001	284
401	touchlessid-000	0.0042	460	0.0133	443	0.2009	298	0.0018	441
402	touchlessid-001	0.0000	173	0.0036	402	0.0923	292	0.0000	92
403	trueface-002	0.0000	324	0.0046	418	-	391	0.0003	344
404	trueface-003	0.0000	338	0.0046	419	0.0397	252	0.0003	346
405	trueidvng-001	0.0000	328	0.0020	359	0.0385	249	0.0002	320
406	tuputech-000	0.0003	445	0.0116	442	-	344	-	476

Table 36: FTE is the proportion of failed template generation attempts. Failures can occur because the software throws an exception, or because the software electively refuses to process the input image. This would typically occur if a face is not detected. FTE is measured as the number of function calls that give EITHER a non-zero error code OR that give a “small” template. This is defined as one whose size is less than 0.3 times the median template size for that algorithm. This second rule is needed because some algorithms incorrectly fail to return a non-zero error code when template generation fails.

A hyphen “-” indicates the dataset was not produced.¹ The effects of FTE are included in the accuracy results of this report by regarding any template comparison involving a failed template to produce a low similarity score. Thus higher FTE results in higher FNMR and lower FMR.

	Algorithm	Failure to Enrol Rate ¹						
	Name	APPLICATION	BORDER	KIOSK	MUGSHOT	VISA	WILD	
	Name	SEC. 2.2	SEC. 2.4	SEC. 2.6	SEC. 2.5	SEC. 2.1	SEC. 2.7	
407	turingtechvip-001	0.0001	424	0.0007	209	0.0061	75	0.0007
408	turingtechvip-002	0.0001	425	0.0017	341	0.0097	92	0.0007
409	turkcell-000	0.0110	469	0.0234	452	0.0350	236	0.0103
410	twface-000	0.0000	85	0.0000	41	0.0000	50	0.0000
411	twface-001	0.0000	162	0.0000	83	0.0000	5	0.0000
412	ulsee-001	0.0000	50	0.0000	19	-	392	0.0000
413	ultinous-000	-	477	-	477	-	383	-
414	ultinous-001	-	476	-	475	-	399	-
415	uluface-002	0.0000	79	0.0000	35	-	454	0.0000
416	uluface-003	0.0000	80	0.0001	124	-	459	0.0002
417	unissey-002	0.0000	117	0.0000	54	0.0000	37	0.0000
418	unissey-003	0.0000	52	0.0008	218	0.0191	147	0.0001
419	upc-001	0.0000	382	0.0003	133	-	424	0.0003
420	uxlabs-001	0.0000	25	0.0000	6	0.0000	30	0.0000
421	vcog-002	-	478	-	478	-	355	-
422	vd-002	0.0000	59	0.0000	21	1.0000	393	0.0000
423	vd-003	0.0001	426	0.0041	409	0.0676	275	0.0030
424	veridas-007	0.0000	377	0.0026	371	0.0595	267	0.0001
425	veridas-008	0.0000	380	0.0026	372	0.0595	266	0.0001
426	veridium-000	0.0061	463	0.5956	474	0.2889	307	0.0050
427	veridium-001	0.0001	423	0.0087	435	0.1615	296	0.0014
428	verigram-000	0.0000	354	0.0068	430	0.0822	290	0.0003
429	verigram-001	0.0000	322	0.0003	134	0.0060	72	0.0002
430	verihubs-inteligensia-000	0.0000	299	0.0029	381	0.0669	274	0.0001
431	verihubs-inteligensia-001	0.0000	303	0.0029	380	0.0669	273	0.0001
432	verijelas-000	0.0000	309	0.0023	366	0.0375	246	0.0004
433	via-000	0.0000	31	0.0000	25	-	400	0.0000
434	via-001	0.0000	177	0.0000	90	-	370	0.0000
435	videomo-001	0.0000	367	0.0170	448	0.0332	232	0.0010
436	videomo-002	0.0000	108	0.0006	187	0.0189	144	0.0001
437	videonetics-001	0.0004	446	0.0309	457	-	450	0.0015
438	videonetics-002	0.0000	349	0.0459	466	-	397	0.0006
439	viettelhightech-000	0.0000	390	0.0019	347	0.0368	243	0.0007
440	vigilantsolutions-010	0.0000	371	0.0028	377	0.0609	269	0.0001
441	vigilantsolutions-011	0.0000	368	0.0028	376	0.0609	268	0.0001
442	vinaí-000	0.0000	169	0.0000	97	-	380	0.0000
443	vinbigdata-001	0.0000	148	0.0000	79	0.0000	4	0.0000
444	vinbigdata-002	0.0000	94	0.0015	330	0.0250	196	0.0000
445	vion-000	0.0050	461	0.0392	465	-	451	0.0130
446	visage-000	0.0000	388	0.0054	426	-	330	0.0009
447	visionbox-001	0.0000	415	0.0033	392	-	312	0.0005
448	visionbox-002	0.0000	17	0.0017	337	0.0270	211	0.0000
449	visionlabs-010	0.0000	361	0.0009	252	-	426	0.0001
450	visionlabs-011	0.0000	98	0.0006	184	0.0156	123	0.0001
451	visteam-003	0.0000	310	0.0010	287	0.0225	180	0.0001
452	visteam-004	0.0000	255	0.0010	286	0.0225	177	0.0001
453	visteam-005	0.0000	251	0.0010	285	0.0224	176	0.0001
454	vixvizioni-006	0.0000	142	0.0000	85	0.0000	7	0.0000
455	vixvizioni-007	0.0000	40	0.0000	30	0.0000	27	0.0000
456	vnpt-004	0.0000	236	0.0006	180	0.0160	129	0.0002
457	vnpt-005	0.0000	139	0.0006	176	0.0154	121	0.0002
458	vocord-009	0.0000	231	0.0006	183	-	469	0.0001
459	vocord-010	0.0000	342	0.0005	170	0.0141	112	0.0002
460	vts-000	0.0000	348	0.0011	295	-	387	0.0001
461	vts-001	0.0000	104	0.0003	131	0.0073	77	0.0000
462	wicket-000	0.0000	311	0.0009	249	0.0260	206	0.0000
463	winsense-001	0.0000	128	0.0000	68	-	324	0.0000
464	winsense-002	0.0000	167	0.0000	94	-	376	0.0000

Table 37: FTE is the proportion of failed template generation attempts. Failures can occur because the software throws an exception, or because the software electively refuses to process the input image. This would typically occur if a face is not detected. FTE is measured as the number of function calls that give EITHER a non-zero error code OR that give a "small" template. This is defined as one whose size is less than 0.3 times the median template size for that algorithm. This second rule is needed because some algorithms incorrectly fail to return a non-zero error code when template generation fails.

A hyphen "-" indicates the dataset was not produced.¹ The effects of FTE are included in the accuracy results of this report by regarding any template comparison involving a failed template to produce a low similarity score. Thus higher FTE results in higher FNMR and lower FMR.

	Algorithm Name	Failure to Enrol Rate ¹											
		APPLICATION	BORDER	KIOSK	MUGSHOT	VISA	WILD	SEC. 2.1	SEC. 2.2	SEC. 2.4	SEC. 2.5		
465	wiseai-001	0.0001	421	0.0137	445	0.0768	287	0.0018	440	0.0018	450	0.0624	443
466	wuhantianyu-001	0.0000	124	0.0007	199	0.0159	126	0.0001	217	0.0004	285	0.0002	128
467	x-laboratory-000	0.0247	473	0.0000	61	-	449	0.0005	391	0.0002	137	0.0000	64
468	x-laboratory-001	0.0000	208	0.0012	306	-	425	0.0001	278	0.0004	331	0.0007	290
469	xforwardai-001	0.0000	290	0.0007	211	-	379	0.0003	350	0.0004	328	0.0004	198
470	xforwardai-002	0.0000	268	0.0007	210	-	322	0.0003	351	0.0004	329	0.0004	201
471	xm-000	0.0000	123	0.0007	196	-	337	0.0001	221	0.0003	161	0.0004	249
472	yisheng-004	0.0002	440	-	476	-	316	0.0013	431	0.0006	403	0.0321	431
473	yitu-003	0.0000	48	0.0000	16	-	388	0.0009	420	0.0000	63	0.0000	96
474	yoonik-002	0.0000	341	0.0010	282	0.0284	213	0.0003	345	0.0006	392	0.0005	265
475	yoonik-003	0.0000	337	0.0009	260	0.0214	168	0.0002	307	0.0004	303	0.0008	299
476	ytu-000	0.0000	227	0.0010	291	-	465	0.0002	335	0.0004	322	0.0011	319
477	yuan-005	0.0000	278	0.0005	167	0.0134	108	0.0002	317	0.0004	231	0.0004	237
478	yuan-006	0.0000	387	0.0014	327	0.0369	244	0.0004	369	0.0005	378	0.0038	357

Table 38: FTE is the proportion of failed template generation attempts. Failures can occur because the software throws an exception, or because the software electively refuses to process the input image. This would typically occur if a face is not detected. FTE is measured as the number of function calls that give EITHER a non-zero error code OR that give a “small” template. This is defined as one whose size is less than 0.3 times the median template size for that algorithm. This second rule is needed because some algorithms incorrectly fail to return a non-zero error code when template generation fails.

A hyphen “-” indicates the dataset was not produced.¹ The effects of FTE are included in the accuracy results of this report by regarding any template comparison involving a failed template to produce a low similarity score. Thus higher FTE results in higher FNMR and lower FMR.

3.4 Recognition accuracy

Core algorithm accuracy is stated via:

▷ **Cooperative subjects**

- The summary table of Figure 29;
- The visa image DETs of Figure 90;
- The mugshot DETs of Figure 114;
- The mugshot ageing profiles of Figure 359;
- The human-difficult pairs of Figure 43

▷ **Non-cooperative subjects**

- The photojournalism DET of Figure 134

Figure 291 shows dependence of false match rate on algorithm score threshold. This allows a deployer to set a threshold to target a particular false match rate appropriate to the security objectives of the application.

Figure 243 likewise shows FMR(T) but for mugshots, and specially four subsets of the population.

Note that in both the mugshot and visa sets false match rates vary with the ethnicity, age, and sex, of the enrollee and impostor. For example figure 156 summarizes FMR for impostors paired from four groups black females, black males, white females, white males.

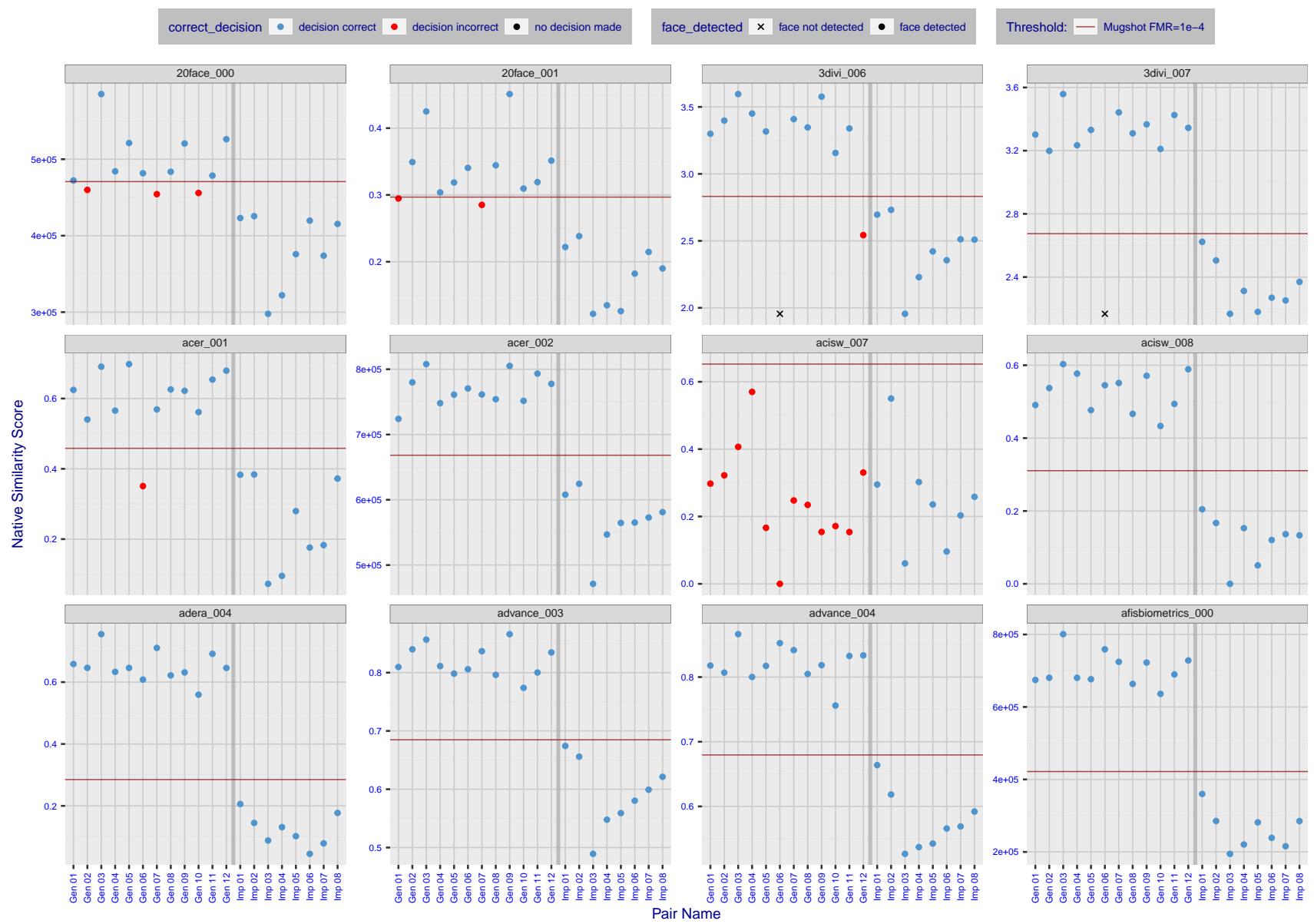


Figure 4: The figure shows algorithms' similarity scores for 12 genuine and 8 impostor image pairs used in a May 2018 paper by Phillips et al. ([1]). The threshold (red horizontal line) is a value calibrated to give $FMR = 0.0001$ on mugshot images. Points above the threshold correspond to pairs determined to be genuine, and points below the threshold correspond to pairs determined to be impostors. If the determined class (genuine or impostor) matches the real class, points will be blue; if not, red. An X represents face detection failure in either of the images in the pair. Note that the sample size ($n=20$) is small, and the figure may change substantially if larger or different sets are used. The images can be viewed on p. 13 of the Appendix, where Gen 01 corresponds to Same-Identity Pair 1, Gen 02 corresponds to Same-Identity Pair 2, and so on.

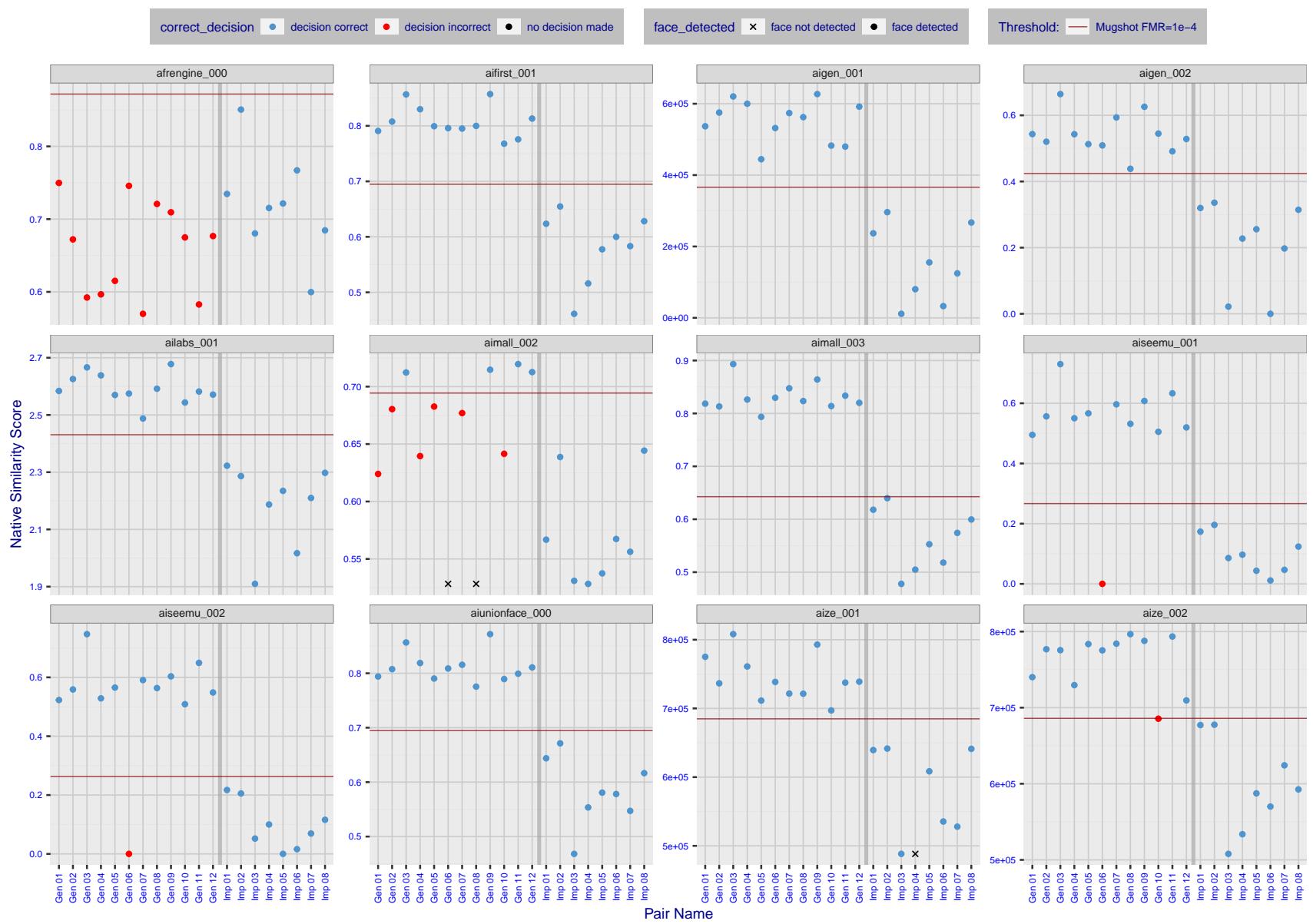


Figure 5: The figure shows algorithms' similarity scores for 12 genuine and 8 impostor image pairs used in a May 2018 paper by Phillips et al. ([1]). The threshold (red horizontal line) is a value calibrated to give $FMR = 0.0001$ on mugshot images. Points above the threshold correspond to pairs determined to be genuine, and points below the threshold correspond to pairs determined to be impostors. If the determined class (genuine or impostor) matches the real class, points will be blue; if not, red. An X represents face detection failure in either of the images in the pair. Note that the sample size ($n=20$) is small, and the figure may change substantially if larger or different sets are used. The images can be viewed on p. 13 of the Appendix, where Gen 01 corresponds to Same-Identity Pair 1, Gen 02 corresponds to Same-Identity Pair 2, and so on.

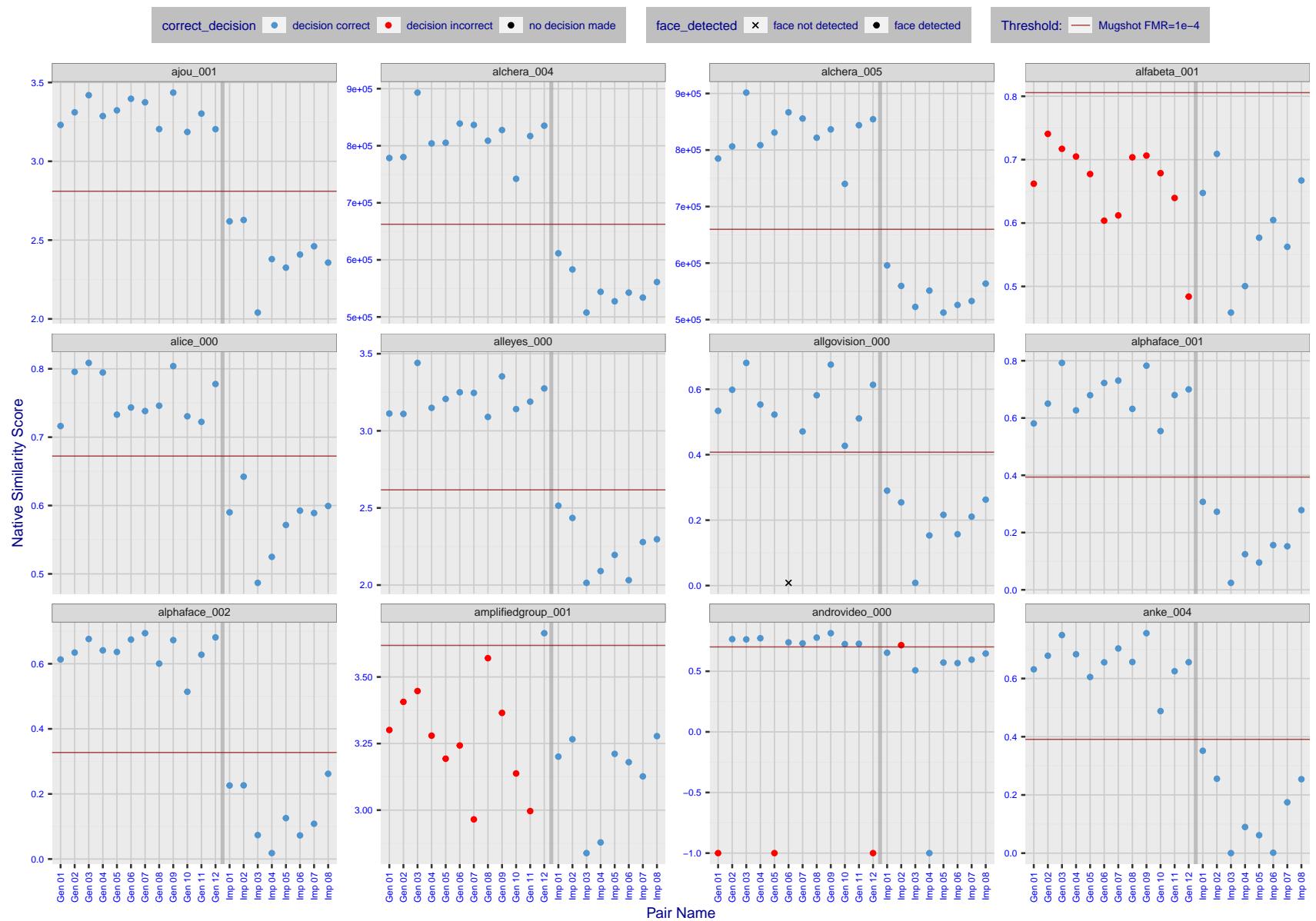


Figure 6: The figure shows algorithms' similarity scores for 12 genuine and 8 impostor image pairs used in a May 2018 paper by Phillips et al. ([1]). The threshold (red horizontal line) is a value calibrated to give $FMR = 0.0001$ on mugshot images. Points above the threshold correspond to pairs determined to be genuine, and points below the threshold correspond to pairs determined to be impostors. If the determined class (genuine or impostor) matches the real class, points will be blue; if not, red. An X represents face detection failure in either of the images in the pair. Note that the sample size ($n=20$) is small, and the figure may change substantially if larger or different sets are used. The images can be viewed on p. 13 of the Appendix, where Gen 01 corresponds to Same-Identity Pair 1, Gen 02 corresponds to Same-Identity Pair 2, and so on.

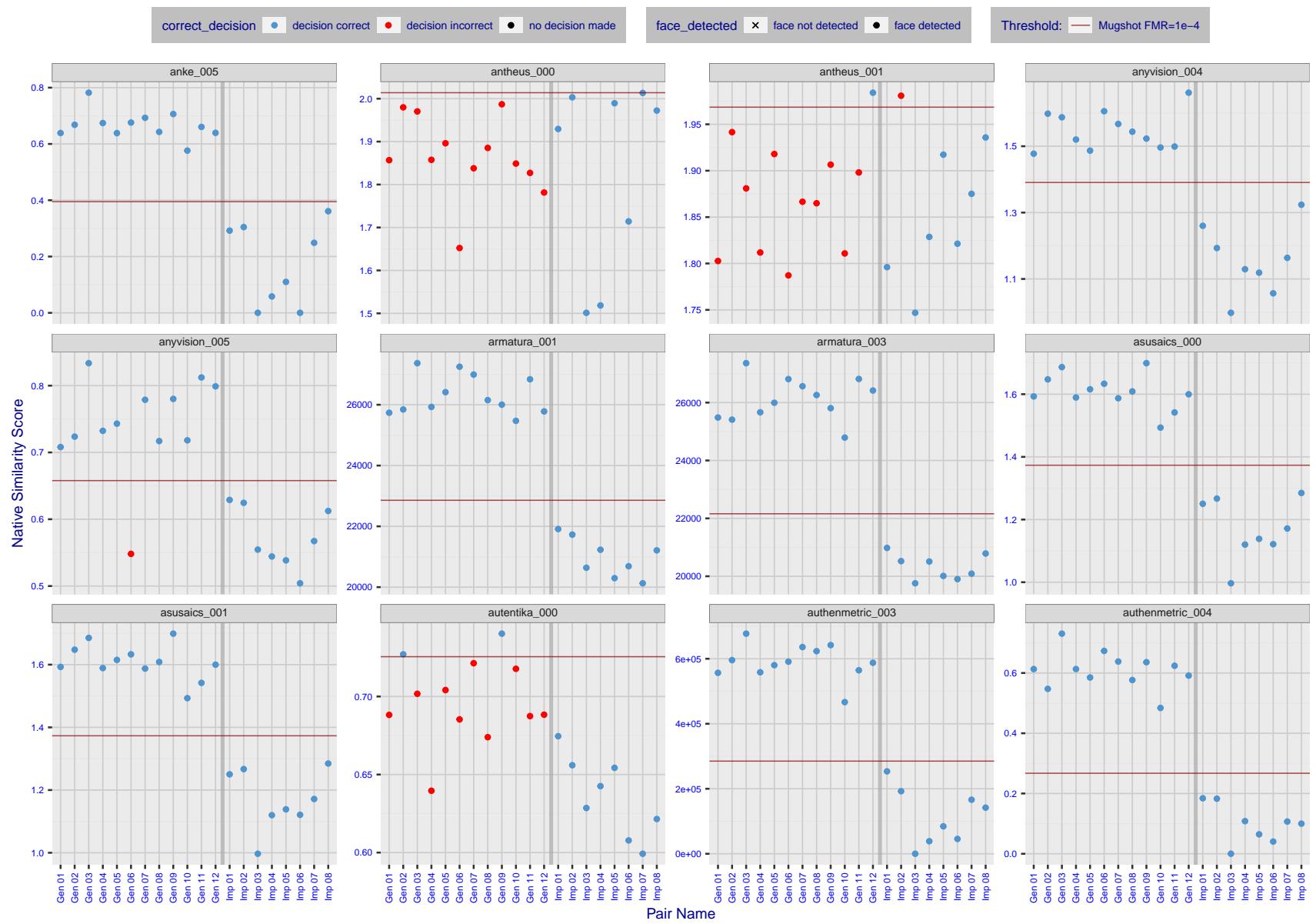


Figure 7: The figure shows algorithms' similarity scores for 12 genuine and 8 impostor image pairs used in a May 2018 paper by Phillips et al. ([1]). The threshold (red horizontal line) is a value calibrated to give $FMR = 0.0001$ on mugshot images. Points above the threshold correspond to pairs determined to be genuine, and points below the threshold correspond to pairs determined to be impostors. If the determined class (genuine or impostor) matches the real class, points will be blue; if not, red. An X represents face detection failure in either of the images in the pair. Note that the sample size ($n=20$) is small, and the figure may change substantially if larger or different sets are used. The images can be viewed on p. 13 of the Appendix, where Gen 01 corresponds to Same-Identity Pair 1, Gen 02 corresponds to Same-Identity Pair 2, and so on.

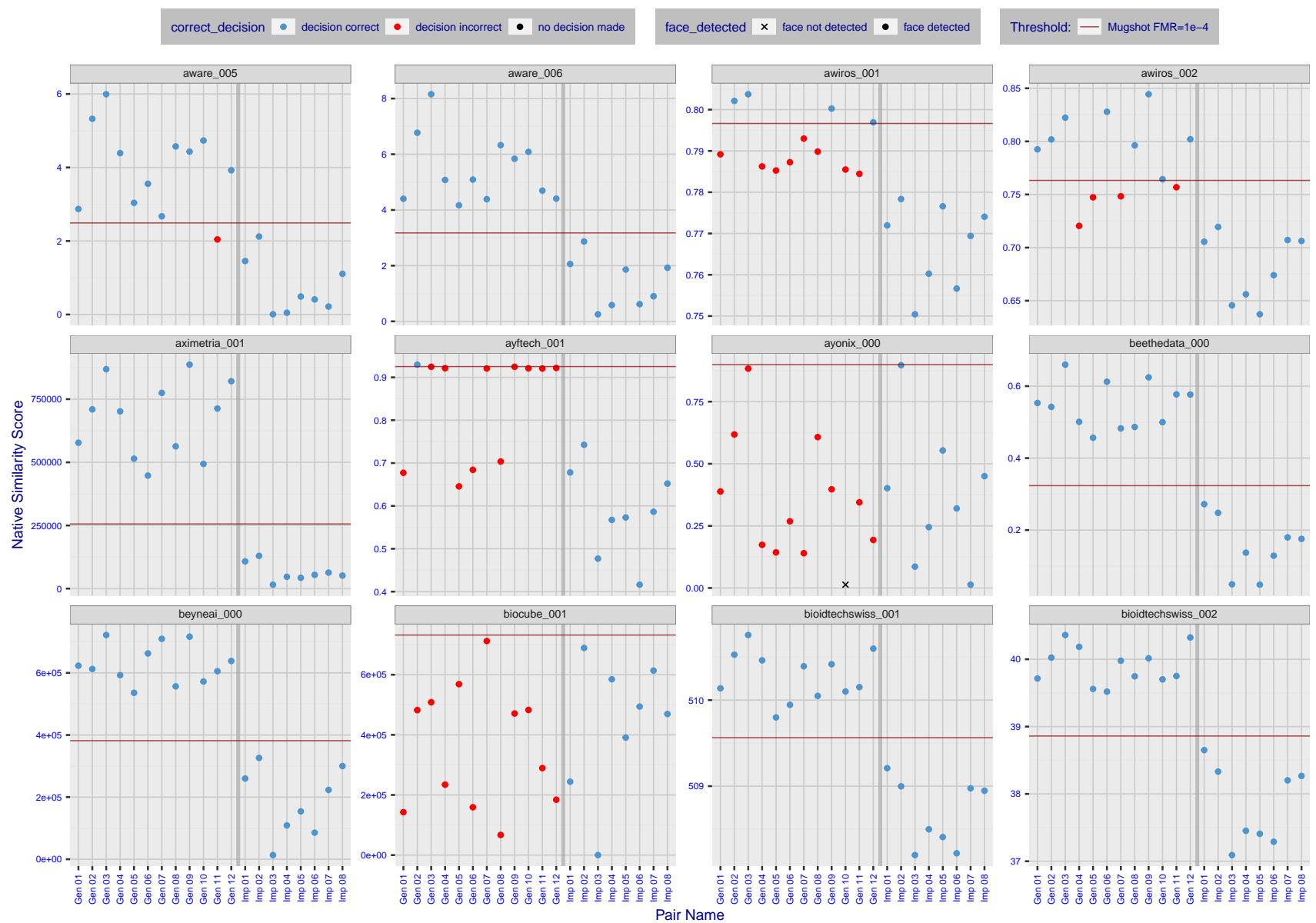


Figure 8: The figure shows algorithms' similarity scores for 12 genuine and 8 impostor image pairs used in a May 2018 paper by Phillips et al. ([1]). The threshold (red horizontal line) is a value calibrated to give $FMR = 0.0001$ on mugshot images. Points above the threshold correspond to pairs determined to be genuine, and points below the threshold correspond to pairs determined to be impostors. If the determined class (genuine or impostor) matches the real class, points will be blue; if not, red. An X represents face detection failure in either of the images in the pair. Note that the sample size ($n=20$) is small, and the figure may change substantially if larger or different sets are used. The images can be viewed on p. 13 of the Appendix, where Gen 01 corresponds to Same-Identity Pair 1, Gen 02 corresponds to Same-Identity Pair 2, and so on.

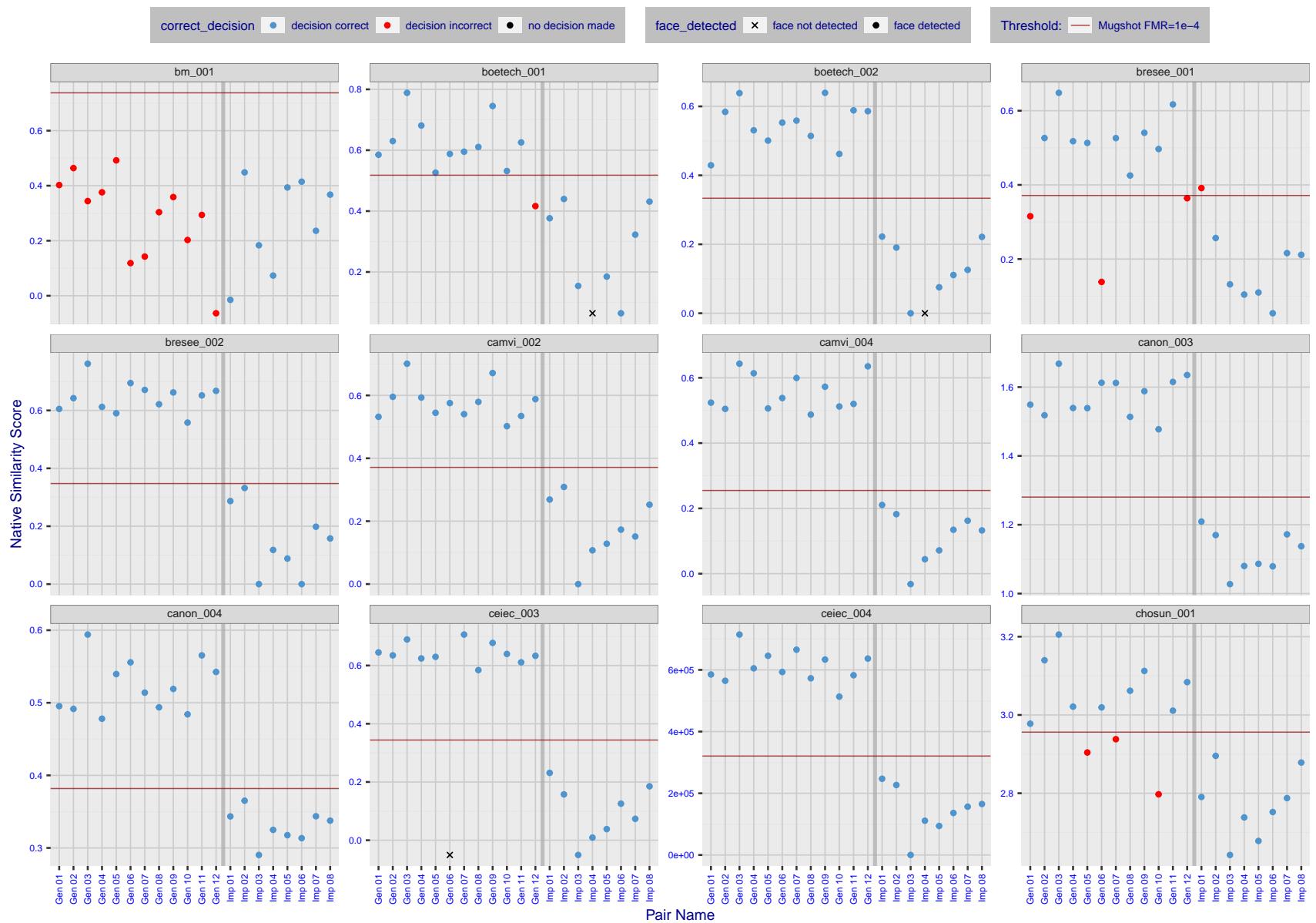


Figure 9: The figure shows algorithms' similarity scores for 12 genuine and 8 impostor image pairs used in a May 2018 paper by Phillips et al. ([1]). The threshold (red horizontal line) is a value calibrated to give $FMR = 0.0001$ on mugshot images. Points above the threshold correspond to pairs determined to be genuine, and points below the threshold correspond to pairs determined to be impostors. If the determined class (genuine or impostor) matches the real class, points will be blue; if not, red. An X represents face detection failure in either of the images in the pair. Note that the sample size ($n=20$) is small, and the figure may change substantially if larger or different sets are used. The images can be viewed on p. 13 of the Appendix, where Gen 01 corresponds to Same-Identity Pair 1, Gen 02 corresponds to Same-Identity Pair 2, and so on.

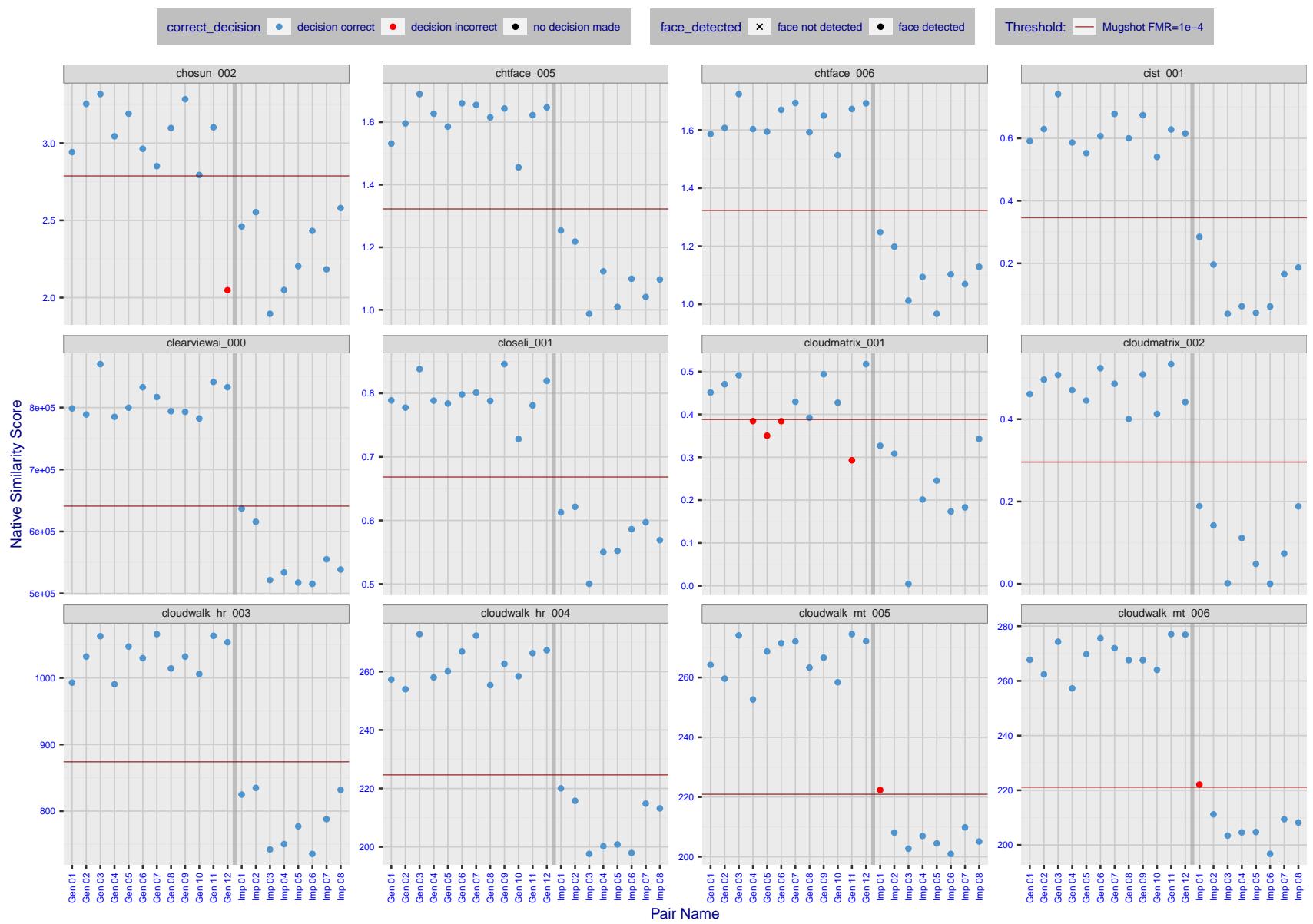


Figure 10: The figure shows algorithms' similarity scores for 12 genuine and 8 impostor image pairs used in a May 2018 paper by Phillips et al. ([1]). The threshold (red horizontal line) is a value calibrated to give $FMR = 0.0001$ on mugshot images. Points above the threshold correspond to pairs determined to be genuine, and points below the threshold correspond to pairs determined to be impostors. If the determined class (genuine or impostor) matches the real class, points will be blue; if not, red. An X represents face detection failure in either of the images in the pair. Note that the sample size ($n=20$) is small, and the figure may change substantially if larger or different sets are used. The images can be viewed on p. 13 of the Appendix, where Gen 01 corresponds to Same-Identity Pair 1, Gen 02 corresponds to Same-Identity Pair 2, and so on.

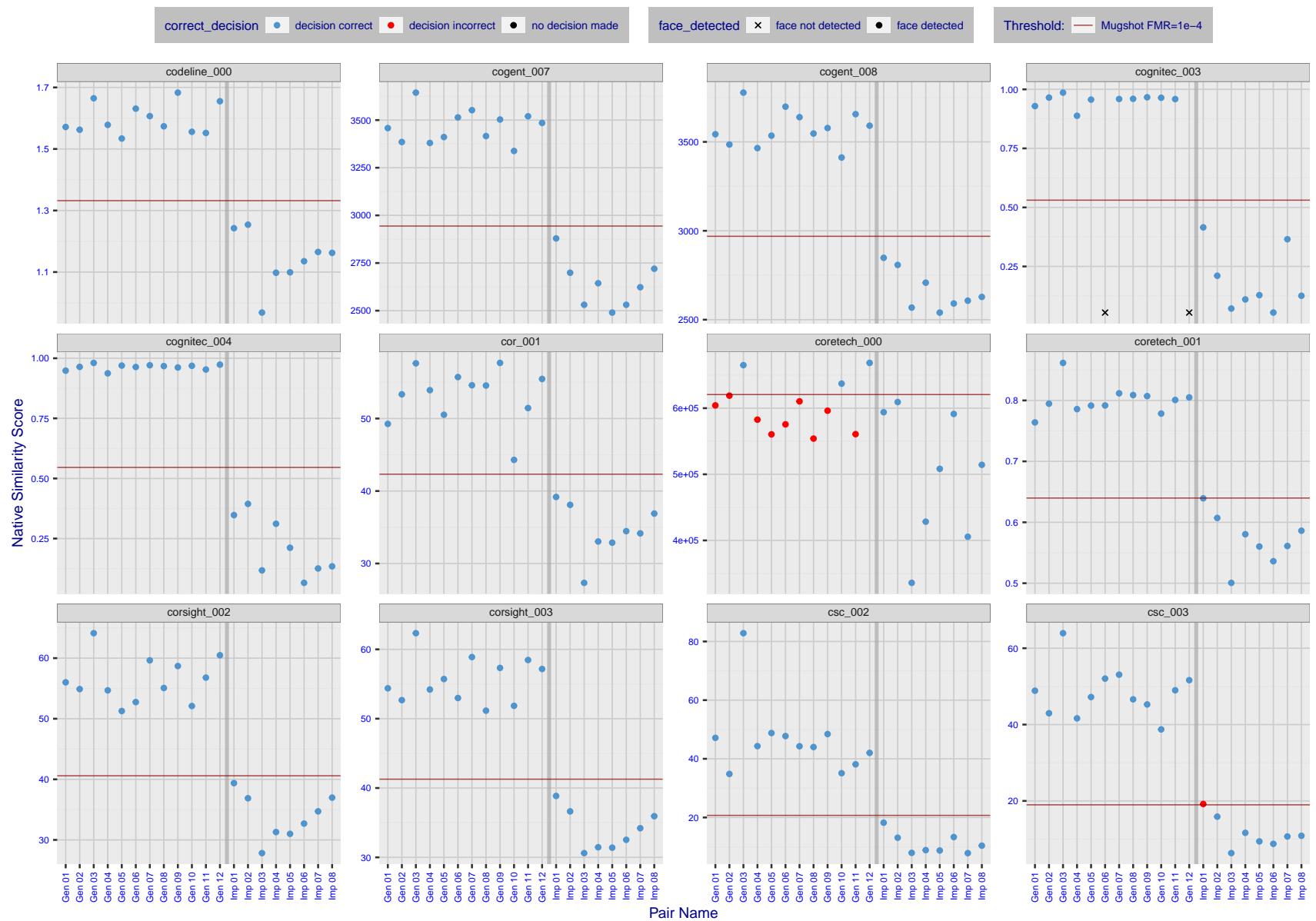


Figure 11: The figure shows algorithms' similarity scores for 12 genuine and 8 impostor image pairs used in a May 2018 paper by Phillips et al. ([1]). The threshold (red horizontal line) is a value calibrated to give $FMR = 0.0001$ on mugshot images. Points above the threshold correspond to pairs determined to be genuine, and points below the threshold correspond to pairs determined to be impostors. If the determined class (genuine or impostor) matches the real class, points will be blue; if not, red. An X represents face detection failure in either of the images in the pair. Note that the sample size ($n=20$) is small, and the figure may change substantially if larger or different sets are used. The images can be viewed on p. 13 of the Appendix, where Gen 01 corresponds to Same-Identity Pair 1, Gen 02 corresponds to Same-Identity Pair 2, and so on.

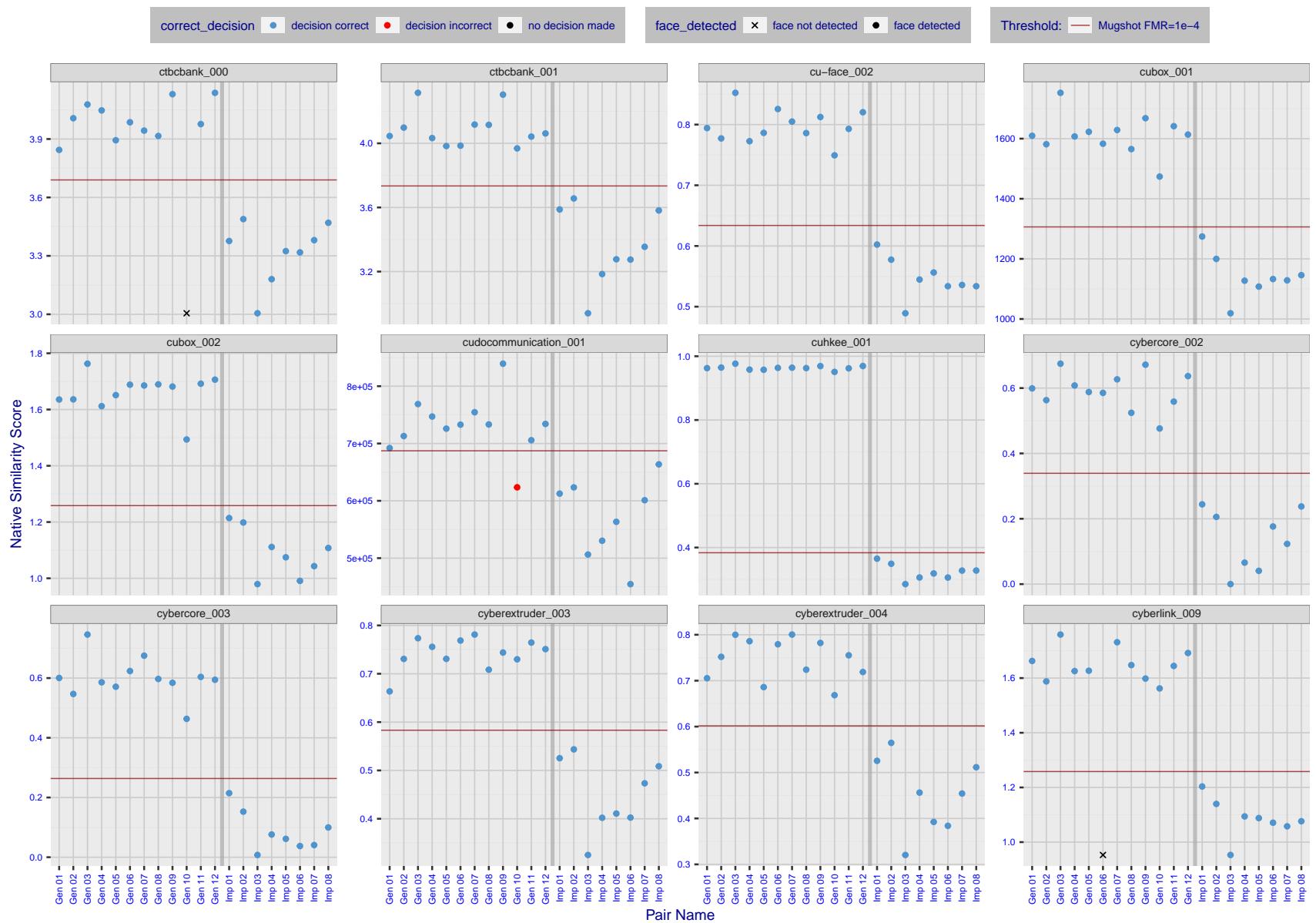


Figure 12: The figure shows algorithms' similarity scores for 12 genuine and 8 impostor image pairs used in a May 2018 paper by Phillips et al. ([1]). The threshold (red horizontal line) is a value calibrated to give $FMR = 0.0001$ on mugshot images. Points above the threshold correspond to pairs determined to be genuine, and points below the threshold correspond to pairs determined to be impostors. If the determined class (genuine or impostor) matches the real class, points will be blue; if not, red. An X represents face detection failure in either of the images in the pair. Note that the sample size ($n=20$) is small, and the figure may change substantially if larger or different sets are used. The images can be viewed on p. 13 of the Appendix, where Gen 01 corresponds to Same-Identity Pair 1, Gen 02 corresponds to Same-Identity Pair 2, and so on.

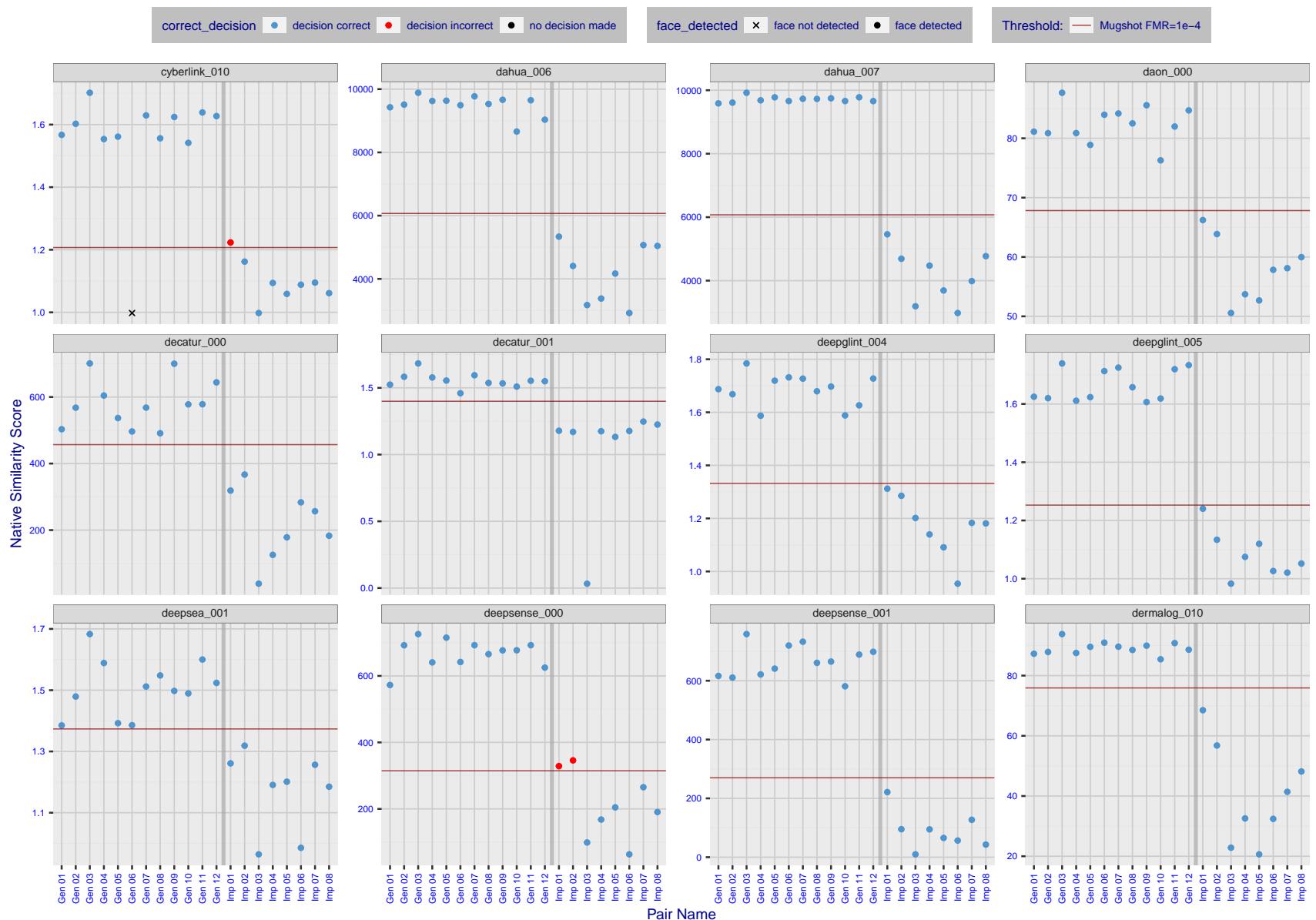


Figure 13: The figure shows algorithms' similarity scores for 12 genuine and 8 impostor image pairs used in a May 2018 paper by Phillips et al. ([1]). The threshold (red horizontal line) is a value calibrated to give $FMR = 0.0001$ on mugshot images. Points above the threshold correspond to pairs determined to be genuine, and points below the threshold correspond to pairs determined to be impostors. If the determined class (genuine or impostor) matches the real class, points will be blue; if not, red. An X represents face detection failure in either of the images in the pair. Note that the sample size ($n=20$) is small, and the figure may change substantially if larger or different sets are used. The images can be viewed on p. 13 of the Appendix, where Gen 01 corresponds to Same-Identity Pair 1, Gen 02 corresponds to Same-Identity Pair 2, and so on.

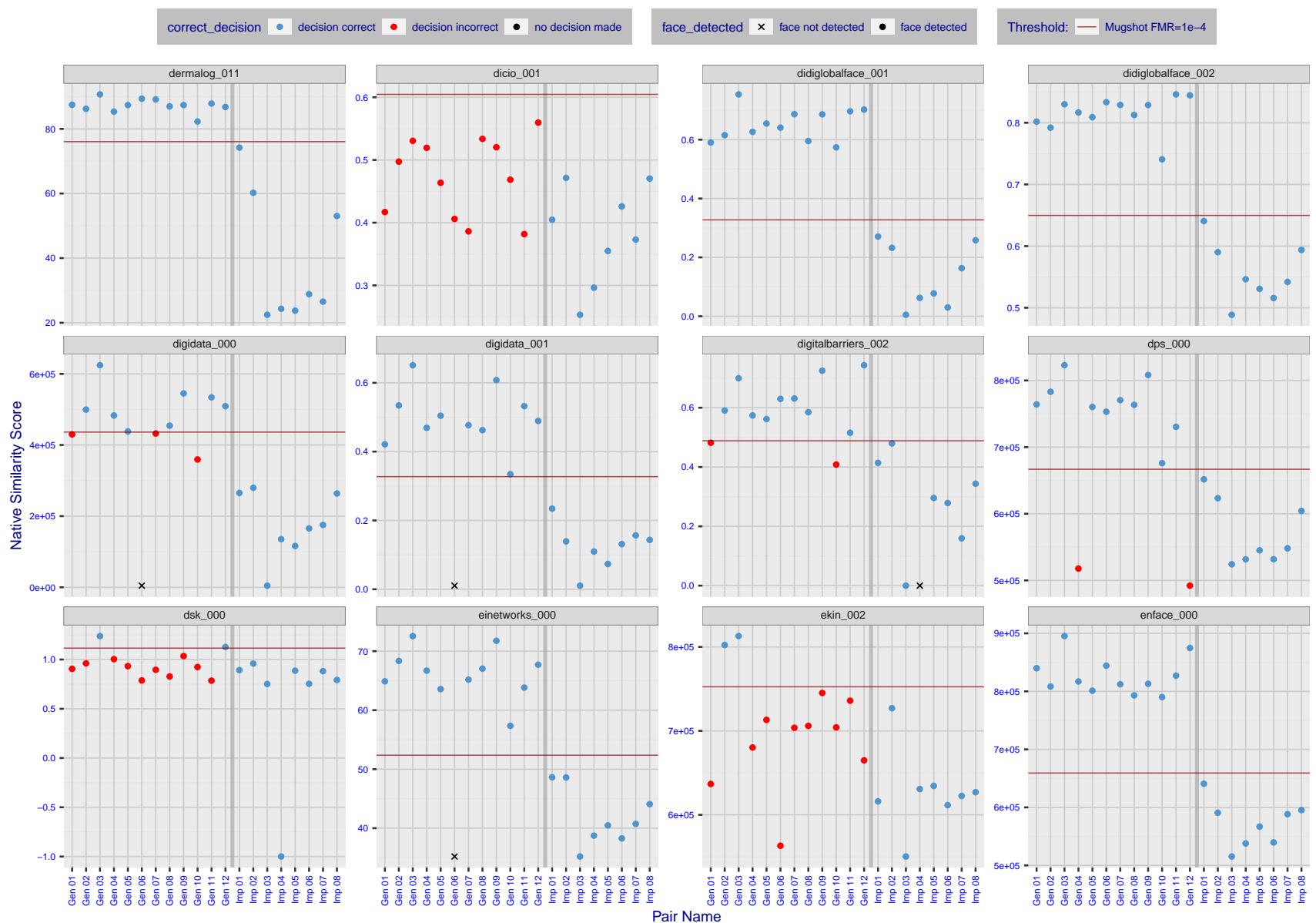


Figure 14: The figure shows algorithms' similarity scores for 12 genuine and 8 impostor image pairs used in a May 2018 paper by Phillips et al. ([1]). The threshold (red horizontal line) is a value calibrated to give $FMR = 0.0001$ on mugshot images. Points above the threshold correspond to pairs determined to be genuine, and points below the threshold correspond to pairs determined to be impostors. If the determined class (genuine or impostor) matches the real class, points will be blue; if not, red. An X represents face detection failure in either of the images in the pair. Note that the sample size ($n=20$) is small, and the figure may change substantially if larger or different sets are used. The images can be viewed on p. 13 of the Appendix, where Gen 01 corresponds to Same-Identity Pair 1, Gen 02 corresponds to Same-Identity Pair 2, and so on.

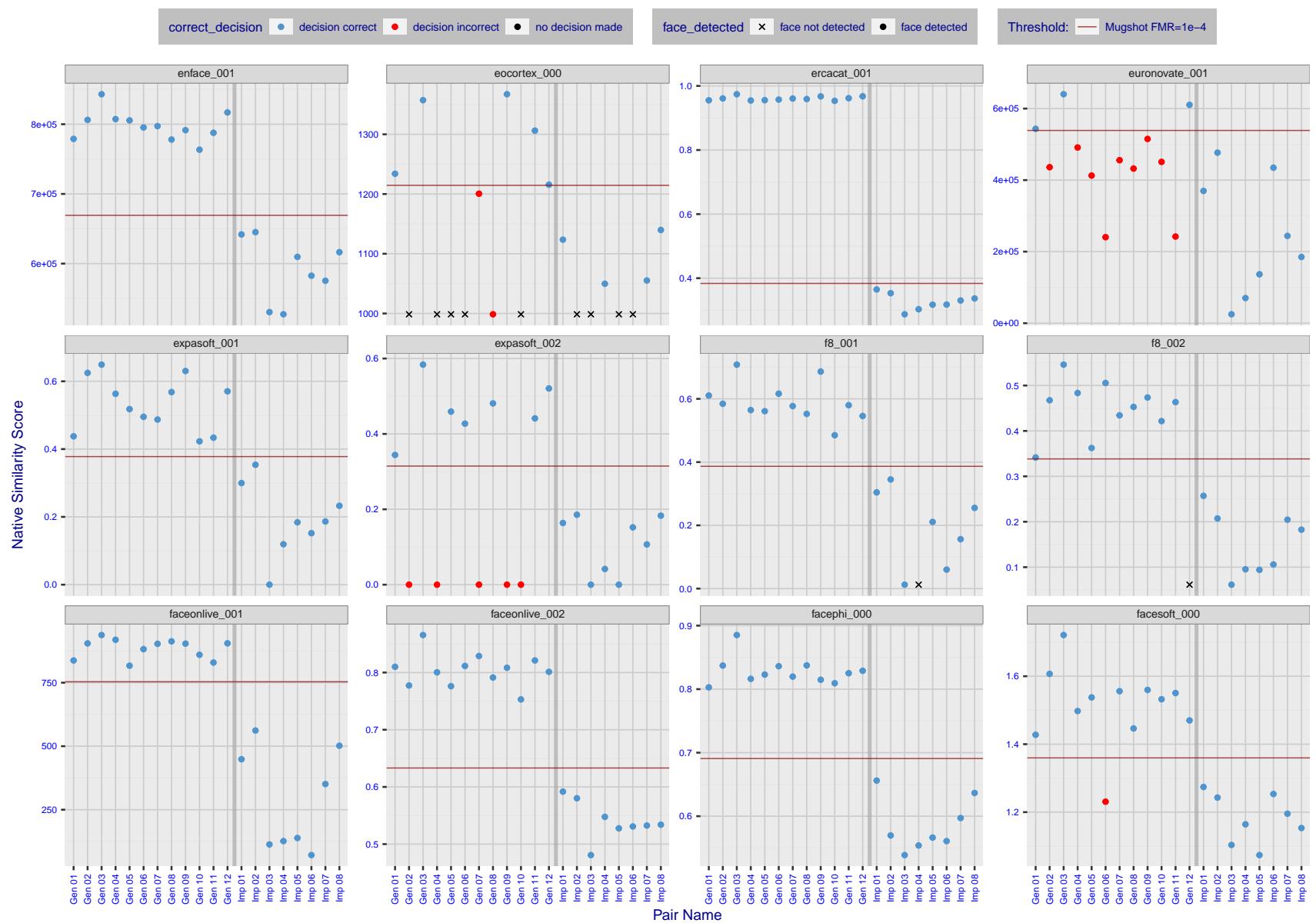


Figure 15: The figure shows algorithms' similarity scores for 12 genuine and 8 impostor image pairs used in a May 2018 paper by Phillips et al. ([1]). The threshold (red horizontal line) is a value calibrated to give $FMR = 0.0001$ on mugshot images. Points above the threshold correspond to pairs determined to be genuine, and points below the threshold correspond to pairs determined to be impostors. If the determined class (genuine or impostor) matches the real class, points will be blue; if not, red. An X represents face detection failure in either of the images in the pair. Note that the sample size ($n=20$) is small, and the figure may change substantially if larger or different sets are used. The images can be viewed on p. 13 of the Appendix, where Gen 01 corresponds to Same-Identity Pair 1, Gen 02 corresponds to Same-Identity Pair 2, and so on.

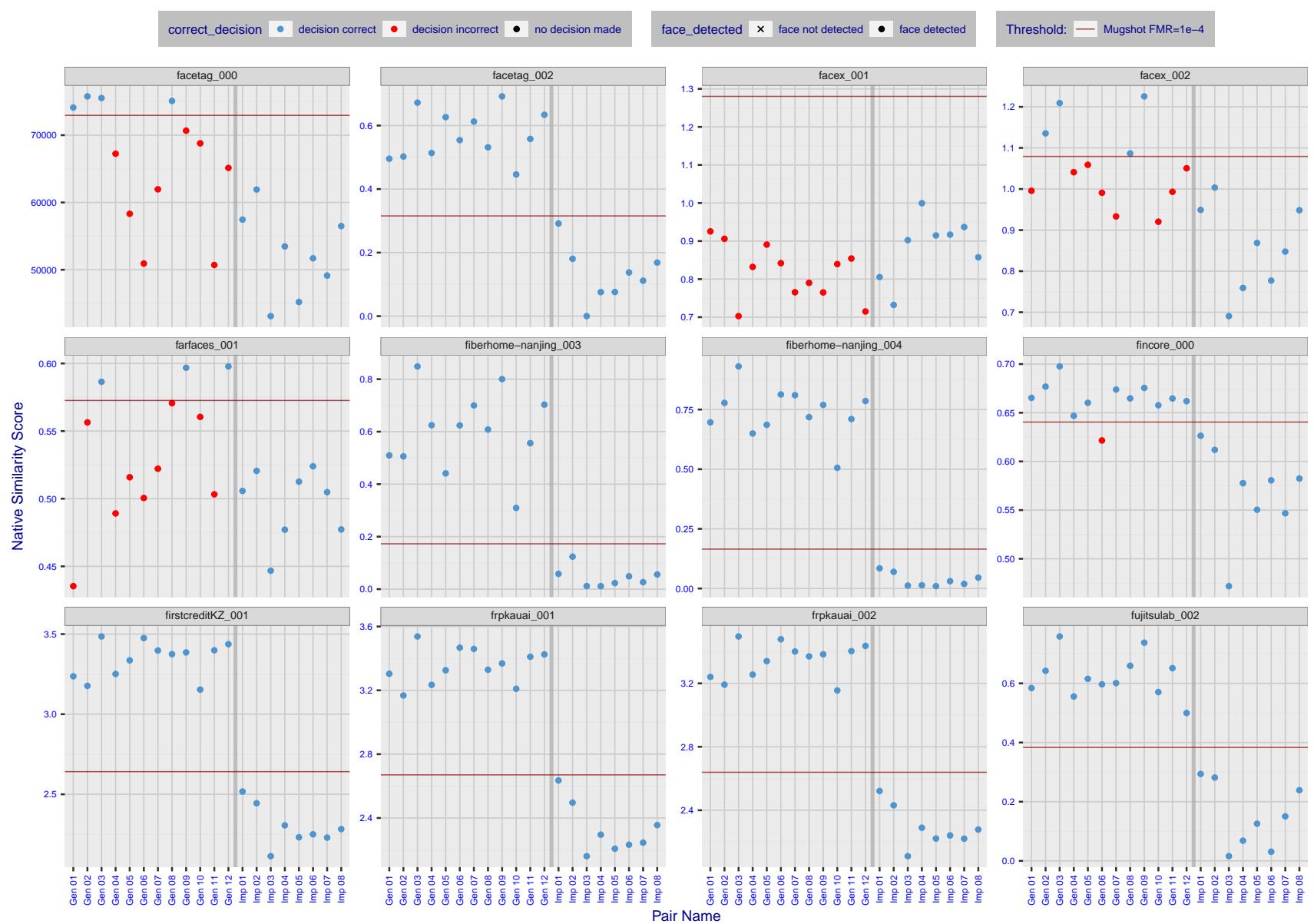


Figure 16: The figure shows algorithms' similarity scores for 12 genuine and 8 impostor image pairs used in a May 2018 paper by Phillips et al. ([1]). The threshold (red horizontal line) is a value calibrated to give $FMR = 0.0001$ on mugshot images. Points above the threshold correspond to pairs determined to be genuine, and points below the threshold correspond to pairs determined to be impostors. If the determined class (genuine or impostor) matches the real class, points will be blue; if not, red. An X represents face detection failure in either of the images in the pair. Note that the sample size ($n=20$) is small, and the figure may change substantially if larger or different sets are used. The images can be viewed on p. 13 of the Appendix, where Gen 01 corresponds to Same-Identity Pair 1, Gen 02 corresponds to Same-Identity Pair 2, and so on.

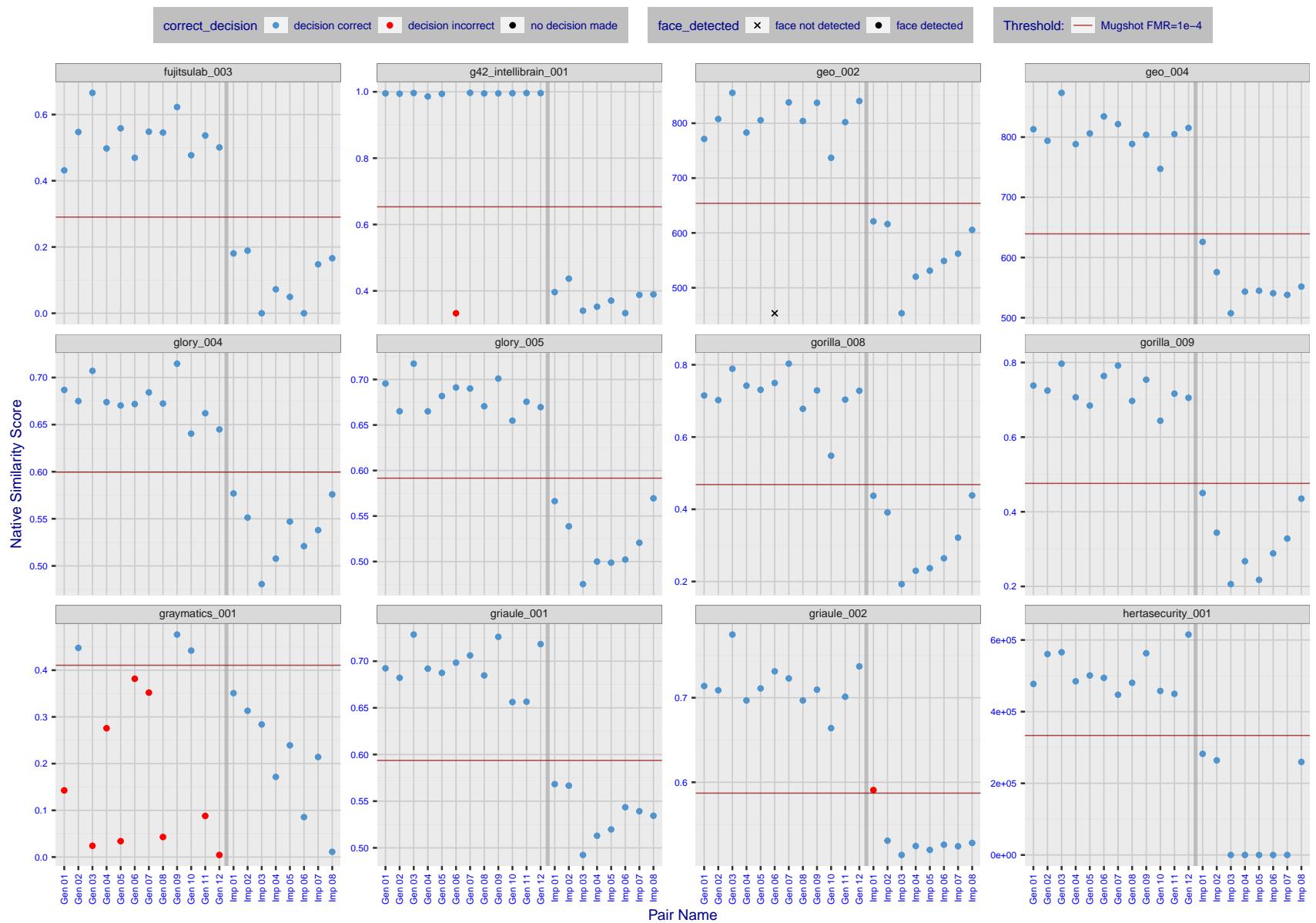


Figure 17: The figure shows algorithms' similarity scores for 12 genuine and 8 impostor image pairs used in a May 2018 paper by Phillips et al. ([1]). The threshold (red horizontal line) is a value calibrated to give $FMR = 0.0001$ on mugshot images. Points above the threshold correspond to pairs determined to be genuine, and points below the threshold correspond to pairs determined to be impostors. If the determined class (genuine or impostor) matches the real class, points will be blue; if not, red. An X represents face detection failure in either of the images in the pair. Note that the sample size ($n=20$) is small, and the figure may change substantially if larger or different sets are used. The images can be viewed on p. 13 of the Appendix, where Gen 01 corresponds to Same-Identity Pair 1, Gen 02 corresponds to Same-Identity Pair 2, and so on.

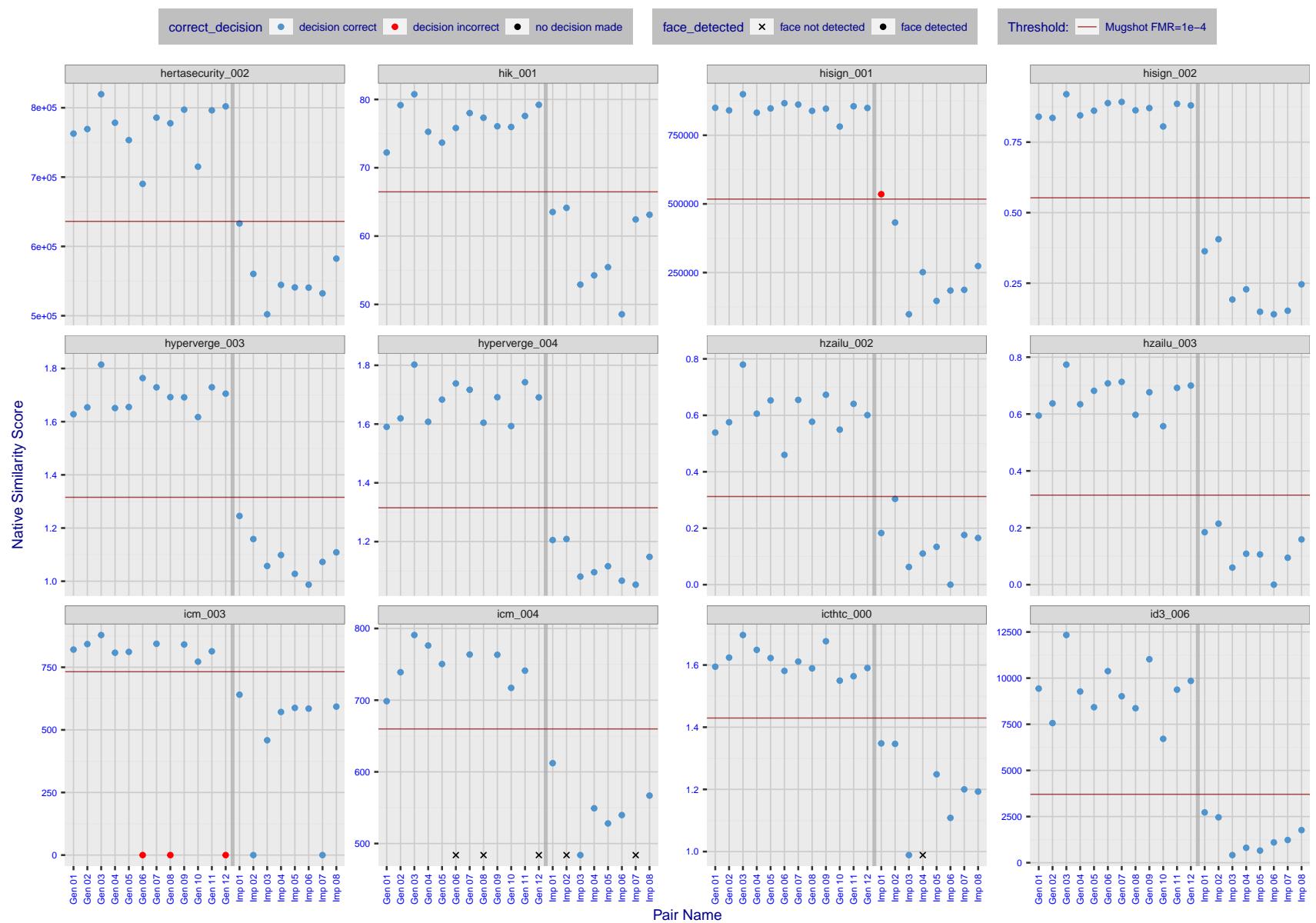


Figure 18: The figure shows algorithms' similarity scores for 12 genuine and 8 impostor image pairs used in a May 2018 paper by Phillips et al. ([1]). The threshold (red horizontal line) is a value calibrated to give $\text{FMR} = 0.0001$ on mugshot images. Points above the threshold correspond to pairs determined to be genuine, and points below the threshold correspond to pairs determined to be impostors. If the determined class (genuine or impostor) matches the real class, points will be blue; if not, red. An X represents face detection failure in either of the images in the pair. Note that the sample size ($n=20$) is small, and the figure may change substantially if larger or different sets are used. The images can be viewed on p. 13 of the Appendix, where Gen 01 corresponds to Same-Identity Pair 1, Gen 02 corresponds to Same-Identity Pair 2, and so on.

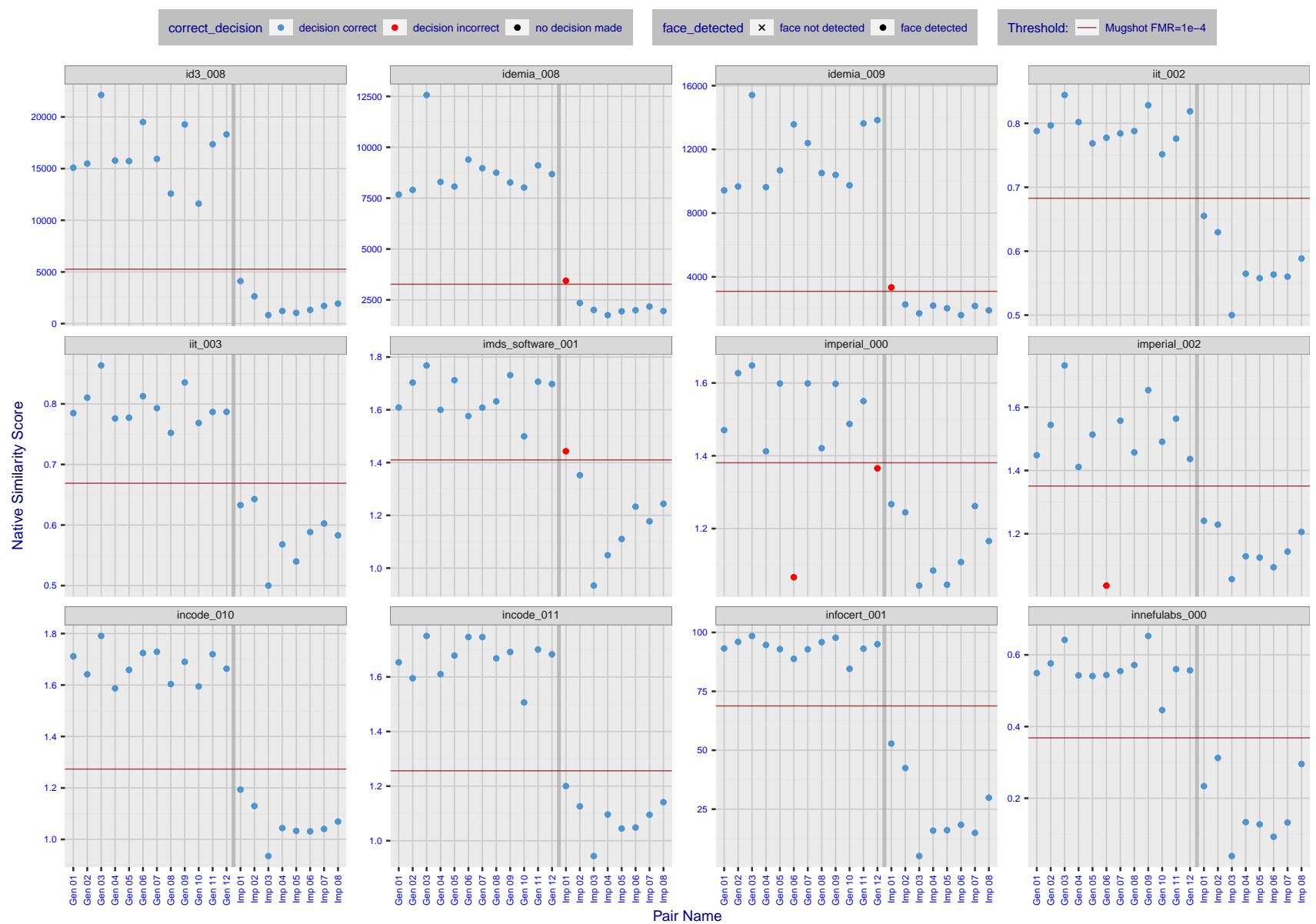


Figure 19: The figure shows algorithms' similarity scores for 12 genuine and 8 impostor image pairs used in a May 2018 paper by Phillips et al. ([1]). The threshold (red horizontal line) is a value calibrated to give $FMR = 0.0001$ on mugshot images. Points above the threshold correspond to pairs determined to be genuine, and points below the threshold correspond to pairs determined to be impostors. If the determined class (genuine or impostor) matches the real class, points will be blue; if not, red. An X represents face detection failure in either of the images in the pair. Note that the sample size ($n=20$) is small, and the figure may change substantially if larger or different sets are used. The images can be viewed on p. 13 of the Appendix, where Gen 01 corresponds to Same-Identity Pair 1, Gen 02 corresponds to Same-Identity Pair 2, and so on.

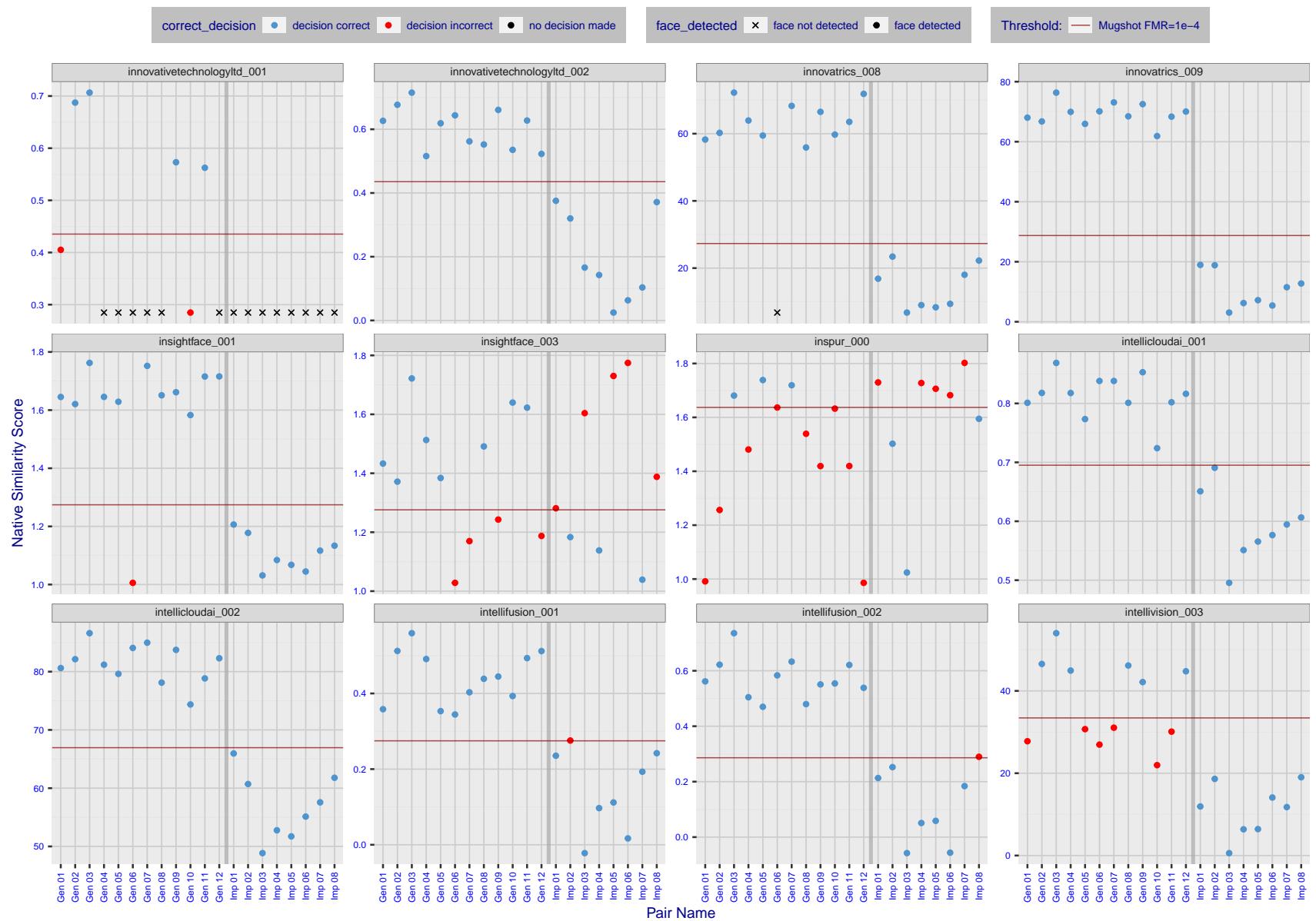


Figure 20: The figure shows algorithms' similarity scores for 12 genuine and 8 impostor image pairs used in a May 2018 paper by Phillips et al. ([1]). The threshold (red horizontal line) is a value calibrated to give $FMR = 0.0001$ on mugshot images. Points above the threshold correspond to pairs determined to be genuine, and points below the threshold correspond to pairs determined to be impostors. If the determined class (genuine or impostor) matches the real class, points will be blue; if not, red. An X represents face detection failure in either of the images in the pair. Note that the sample size ($n=20$) is small, and the figure may change substantially if larger or different sets are used. The images can be viewed on p. 13 of the Appendix, where Gen 01 corresponds to Same-Identity Pair 1, Gen 02 corresponds to Same-Identity Pair 2, and so on.

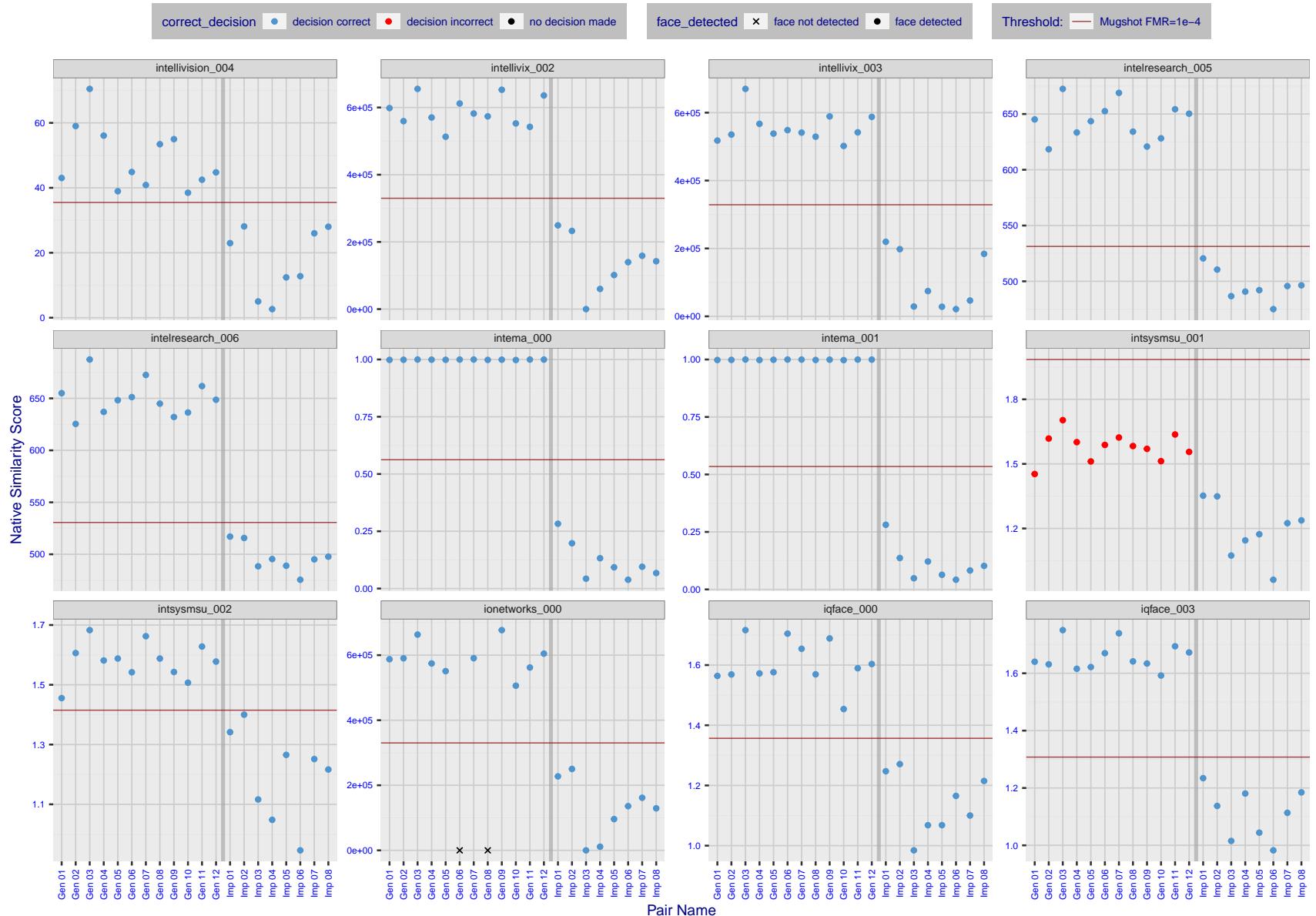


Figure 21: The figure shows algorithms' similarity scores for 12 genuine and 8 impostor image pairs used in a May 2018 paper by Phillips et al. ([1]). The threshold (red horizontal line) is a value calibrated to give $FMR = 0.0001$ on mugshot images. Points above the threshold correspond to pairs determined to be genuine, and points below the threshold correspond to pairs determined to be impostors. If the determined class (genuine or impostor) matches the real class, points will be blue; if not, red. An X represents face detection failure in either of the images in the pair. Note that the sample size ($n=20$) is small, and the figure may change substantially if larger or different sets are used. The images can be viewed on p. 13 of the Appendix, where Gen 01 corresponds to Same-Identity Pair 1, Gen 02 corresponds to Same-Identity Pair 2, and so on.

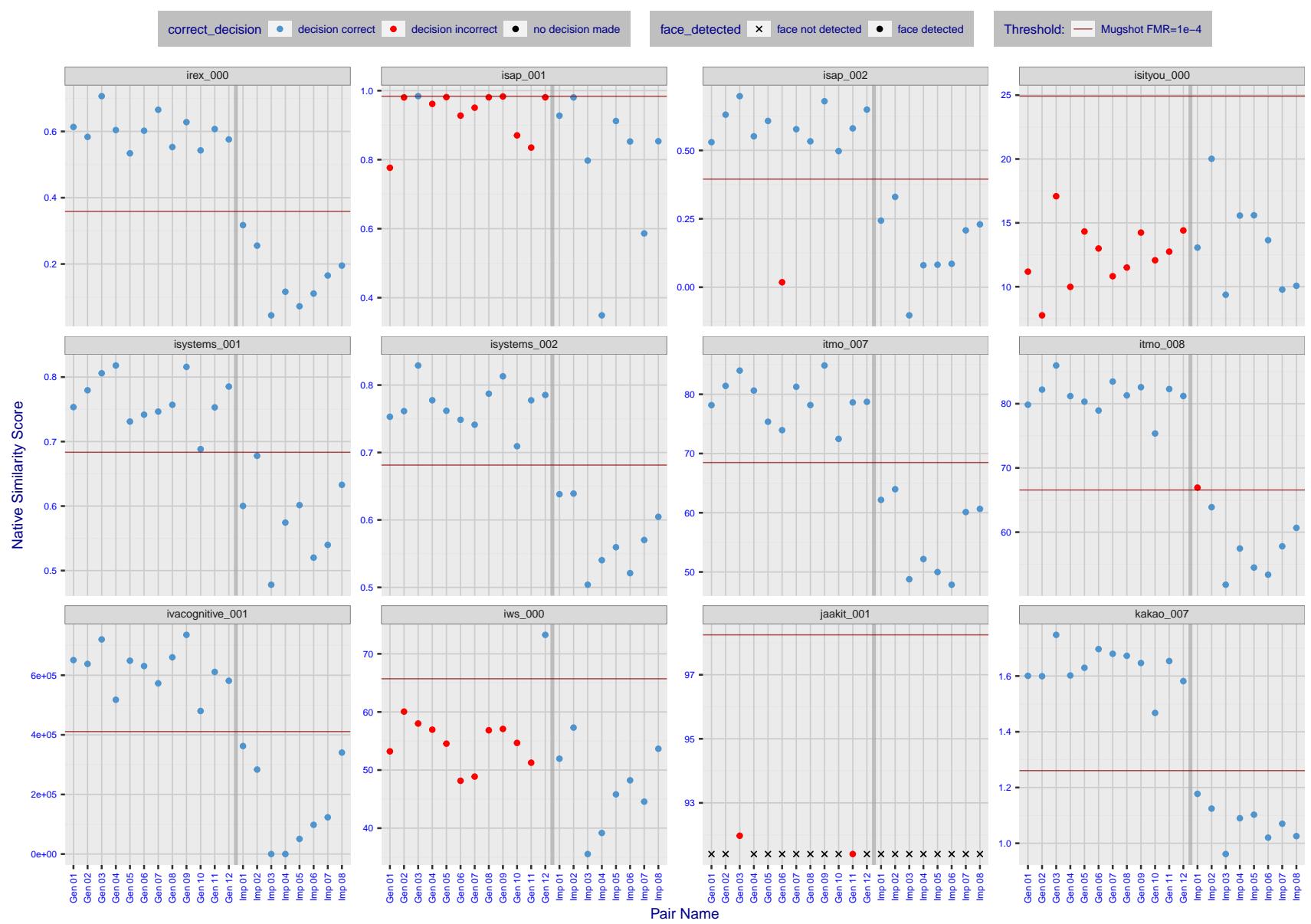


Figure 22: The figure shows algorithms' similarity scores for 12 genuine and 8 impostor image pairs used in a May 2018 paper by Phillips et al. ([1]). The threshold (red horizontal line) is a value calibrated to give $FMR = 0.0001$ on mugshot images. Points above the threshold correspond to pairs determined to be genuine, and points below the threshold correspond to pairs determined to be impostors. If the determined class (genuine or impostor) matches the real class, points will be blue; if not, red. An X represents face detection failure in either of the images in the pair. Note that the sample size ($n=20$) is small, and the figure may change substantially if larger or different sets are used. The images can be viewed on p. 13 of the Appendix, where Gen 01 corresponds to Same-Identity Pair 1, Gen 02 corresponds to Same-Identity Pair 2, and so on.

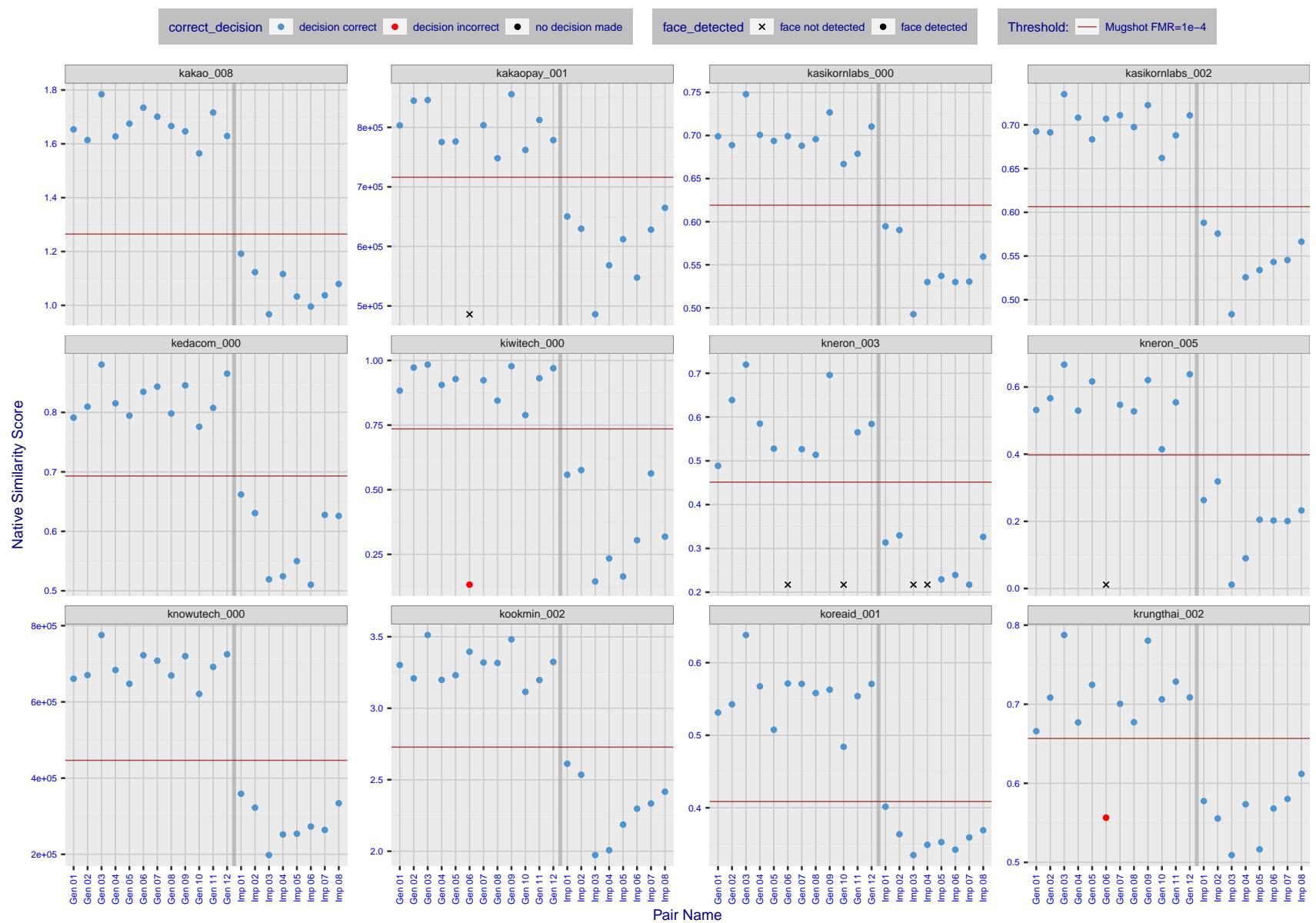


Figure 23: The figure shows algorithms' similarity scores for 12 genuine and 8 impostor image pairs used in a May 2018 paper by Phillips et al. ([1]). The threshold (red horizontal line) is a value calibrated to give $FMR = 0.0001$ on mugshot images. Points above the threshold correspond to pairs determined to be genuine, and points below the threshold correspond to pairs determined to be impostors. If the determined class (genuine or impostor) matches the real class, points will be blue; if not, red. An X represents face detection failure in either of the images in the pair. Note that the sample size ($n=20$) is small, and the figure may change substantially if larger or different sets are used. The images can be viewed on p. 13 of the Appendix, where Gen 01 corresponds to Same-Identity Pair 1, Gen 02 corresponds to Same-Identity Pair 2, and so on.

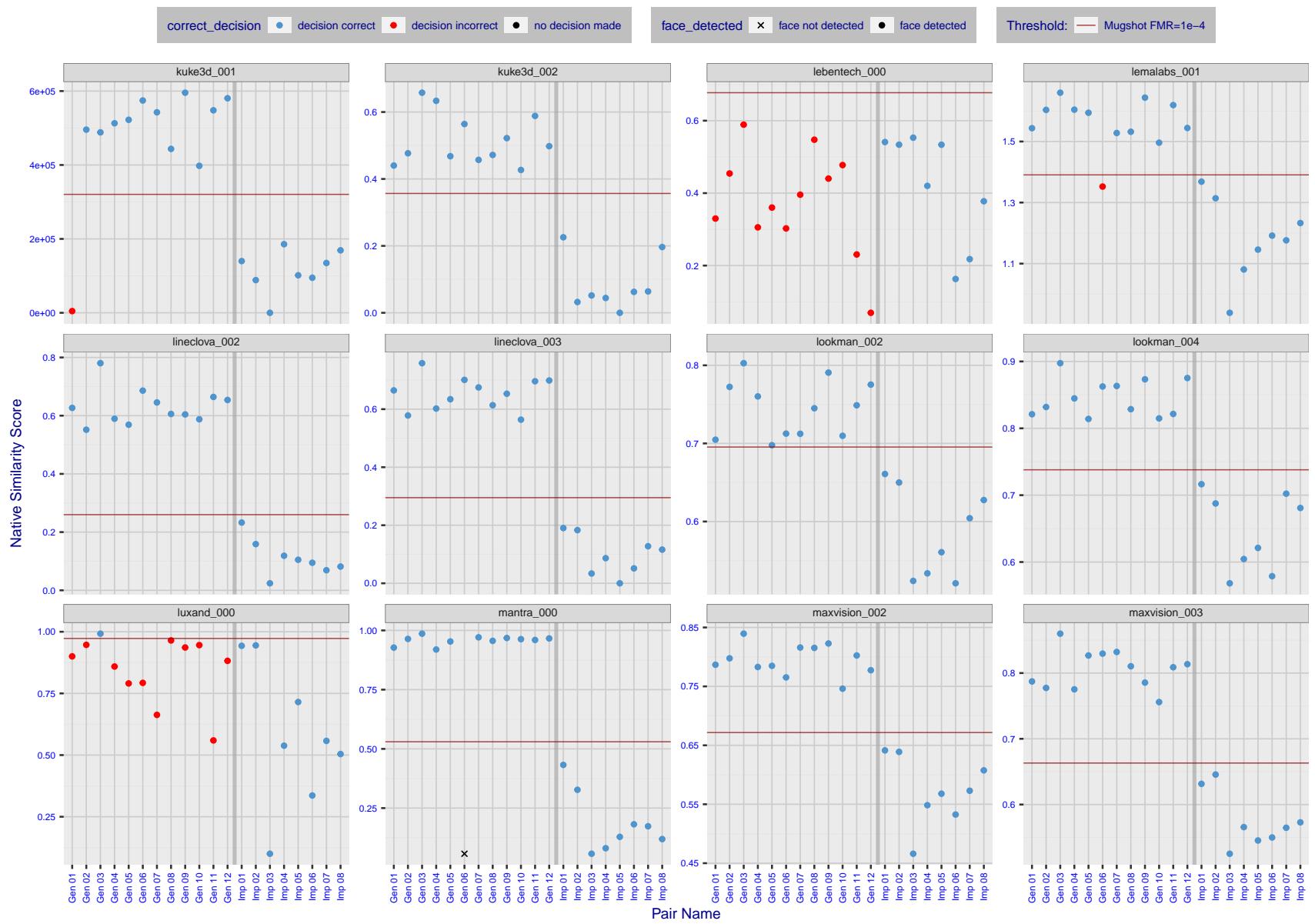


Figure 24: The figure shows algorithms' similarity scores for 12 genuine and 8 impostor image pairs used in a May 2018 paper by Phillips et al. ([1]). The threshold (red horizontal line) is a value calibrated to give $FMR = 0.0001$ on mugshot images. Points above the threshold correspond to pairs determined to be genuine, and points below the threshold correspond to pairs determined to be impostors. If the determined class (genuine or impostor) matches the real class, points will be blue; if not, red. An X represents face detection failure in either of the images in the pair. Note that the sample size ($n=20$) is small, and the figure may change substantially if larger or different sets are used. The images can be viewed on p. 13 of the Appendix, where Gen 01 corresponds to Same-Identity Pair 1, Gen 02 corresponds to Same-Identity Pair 2, and so on.

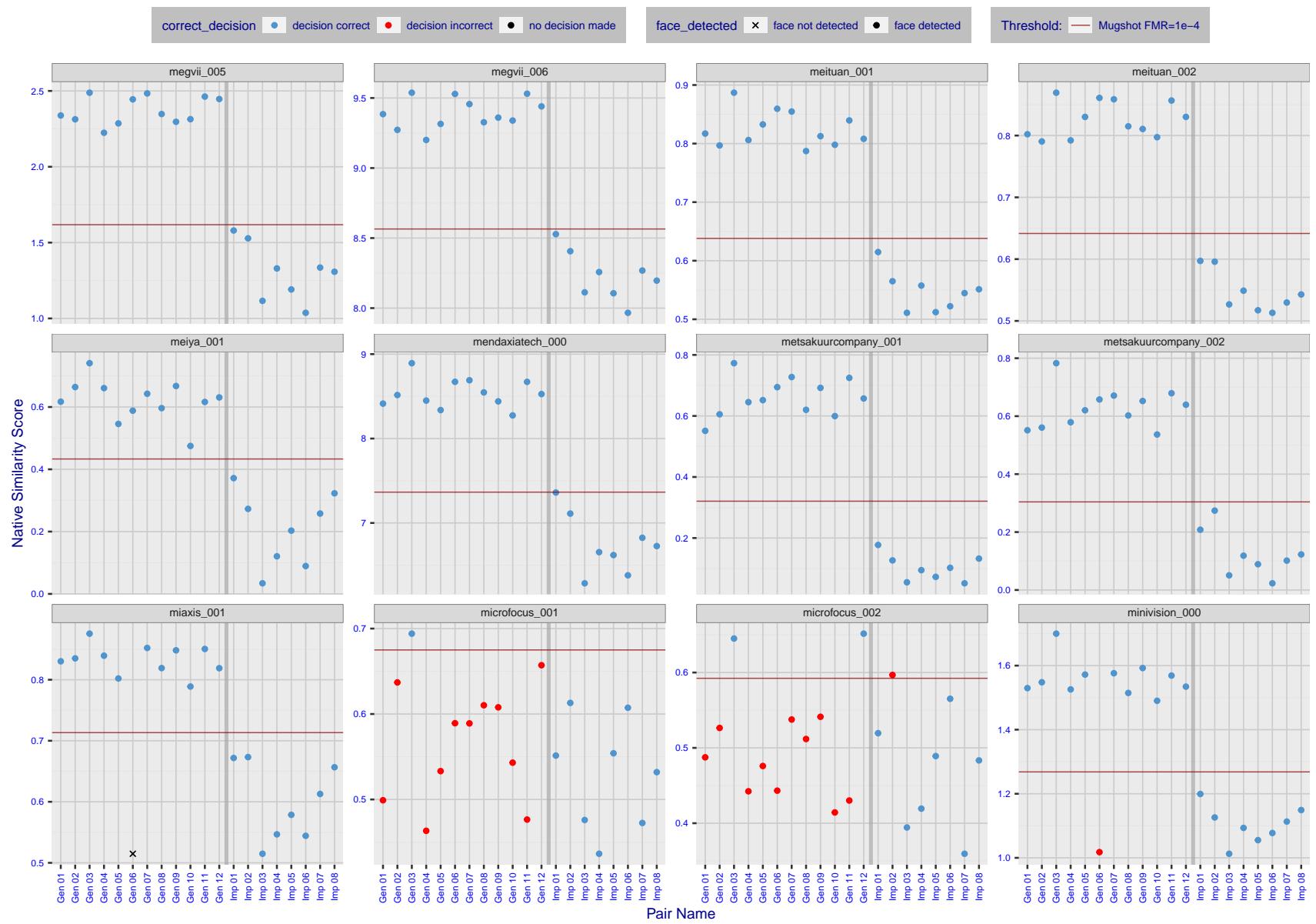


Figure 25: The figure shows algorithms' similarity scores for 12 genuine and 8 impostor image pairs used in a May 2018 paper by Phillips et al. ([1]). The threshold (red horizontal line) is a value calibrated to give $FMR = 0.0001$ on mugshot images. Points above the threshold correspond to pairs determined to be genuine, and points below the threshold correspond to pairs determined to be impostors. If the determined class (genuine or impostor) matches the real class, points will be blue; if not, red. An X represents face detection failure in either of the images in the pair. Note that the sample size ($n=20$) is small, and the figure may change substantially if larger or different sets are used. The images can be viewed on p. 13 of the Appendix, where Gen 01 corresponds to Same-Identity Pair 1, Gen 02 corresponds to Same-Identity Pair 2, and so on.

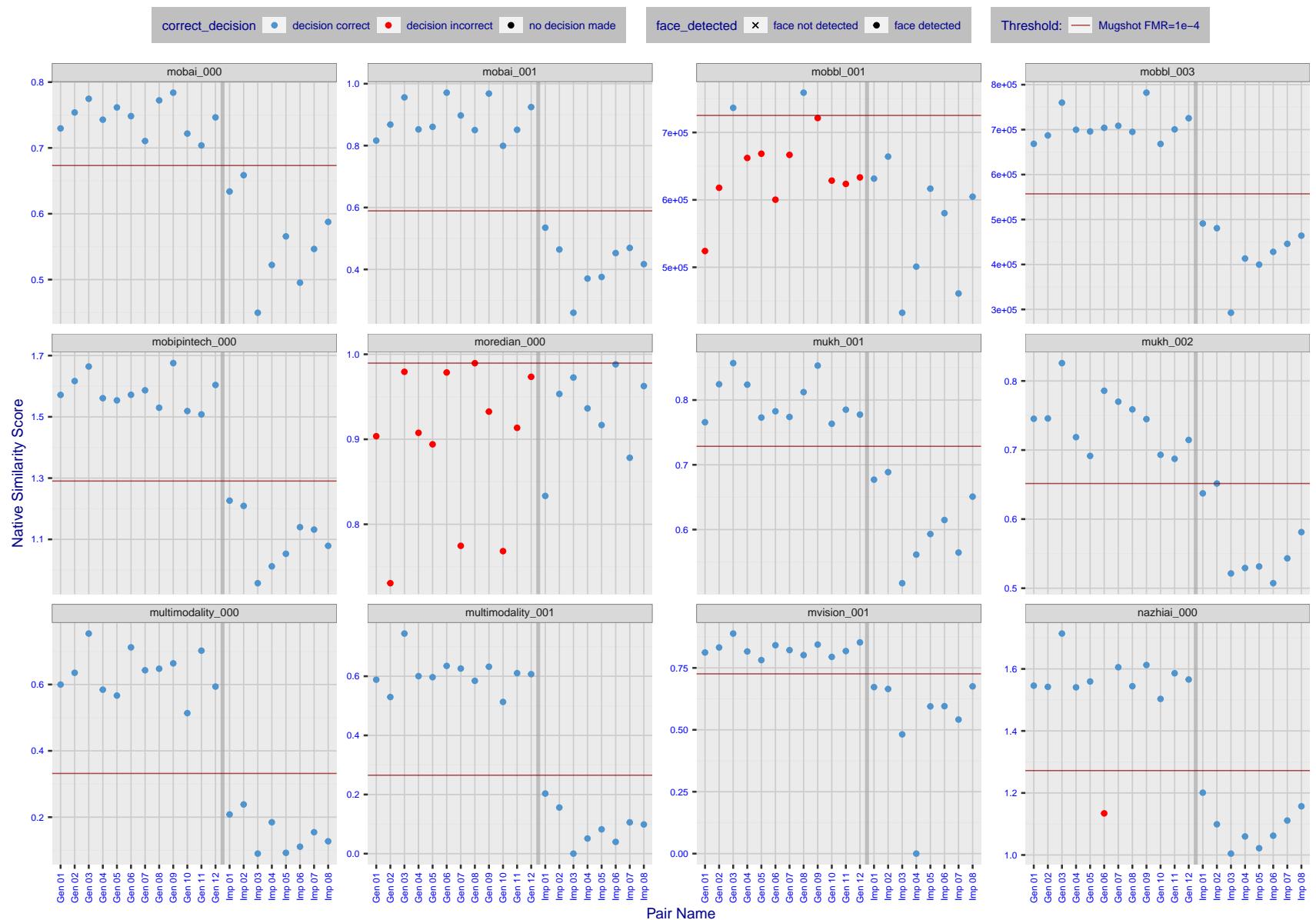


Figure 26: The figure shows algorithms' similarity scores for 12 genuine and 8 impostor image pairs used in a May 2018 paper by Phillips et al. ([1]). The threshold (red horizontal line) is a value calibrated to give $FMR = 0.0001$ on mugshot images. Points above the threshold correspond to pairs determined to be genuine, and points below the threshold correspond to pairs determined to be impostors. If the determined class (genuine or impostor) matches the real class, points will be blue; if not, red. An X represents face detection failure in either of the images in the pair. Note that the sample size ($n=20$) is small, and the figure may change substantially if larger or different sets are used. The images can be viewed on p. 13 of the Appendix, where Gen 01 corresponds to Same-Identity Pair 1, Gen 02 corresponds to Same-Identity Pair 2, and so on.

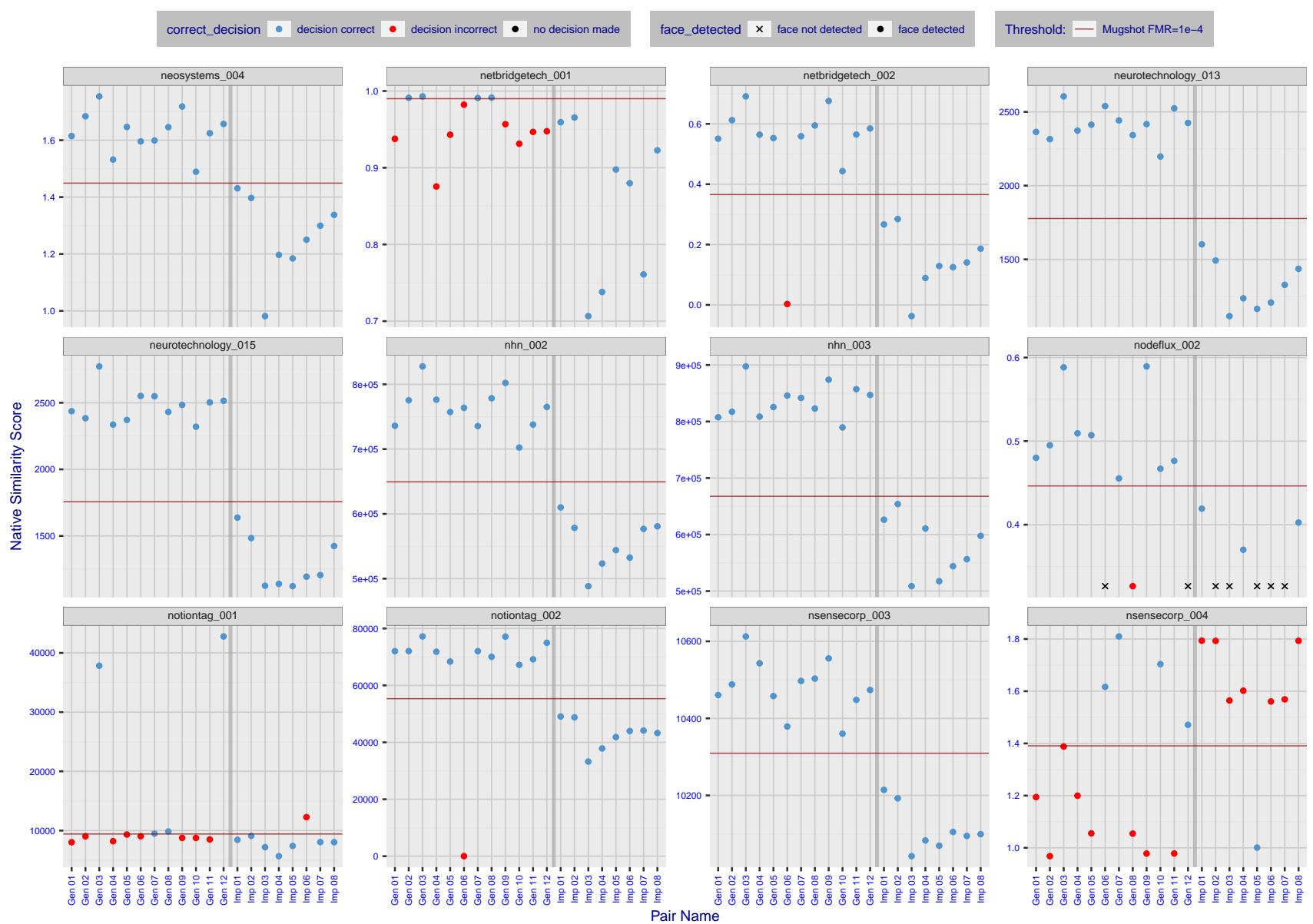


Figure 27: The figure shows algorithms' similarity scores for 12 genuine and 8 impostor image pairs used in a May 2018 paper by Phillips et al. ([1]). The threshold (red horizontal line) is a value calibrated to give $FMR = 0.0001$ on mugshot images. Points above the threshold correspond to pairs determined to be genuine, and points below the threshold correspond to pairs determined to be impostors. If the determined class (genuine or impostor) matches the real class, points will be blue; if not, red. An X represents face detection failure in either of the images in the pair. Note that the sample size ($n=20$) is small, and the figure may change substantially if larger or different sets are used. The images can be viewed on p. 13 of the Appendix, where Gen 01 corresponds to Same-Identity Pair 1, Gen 02 corresponds to Same-Identity Pair 2, and so on.

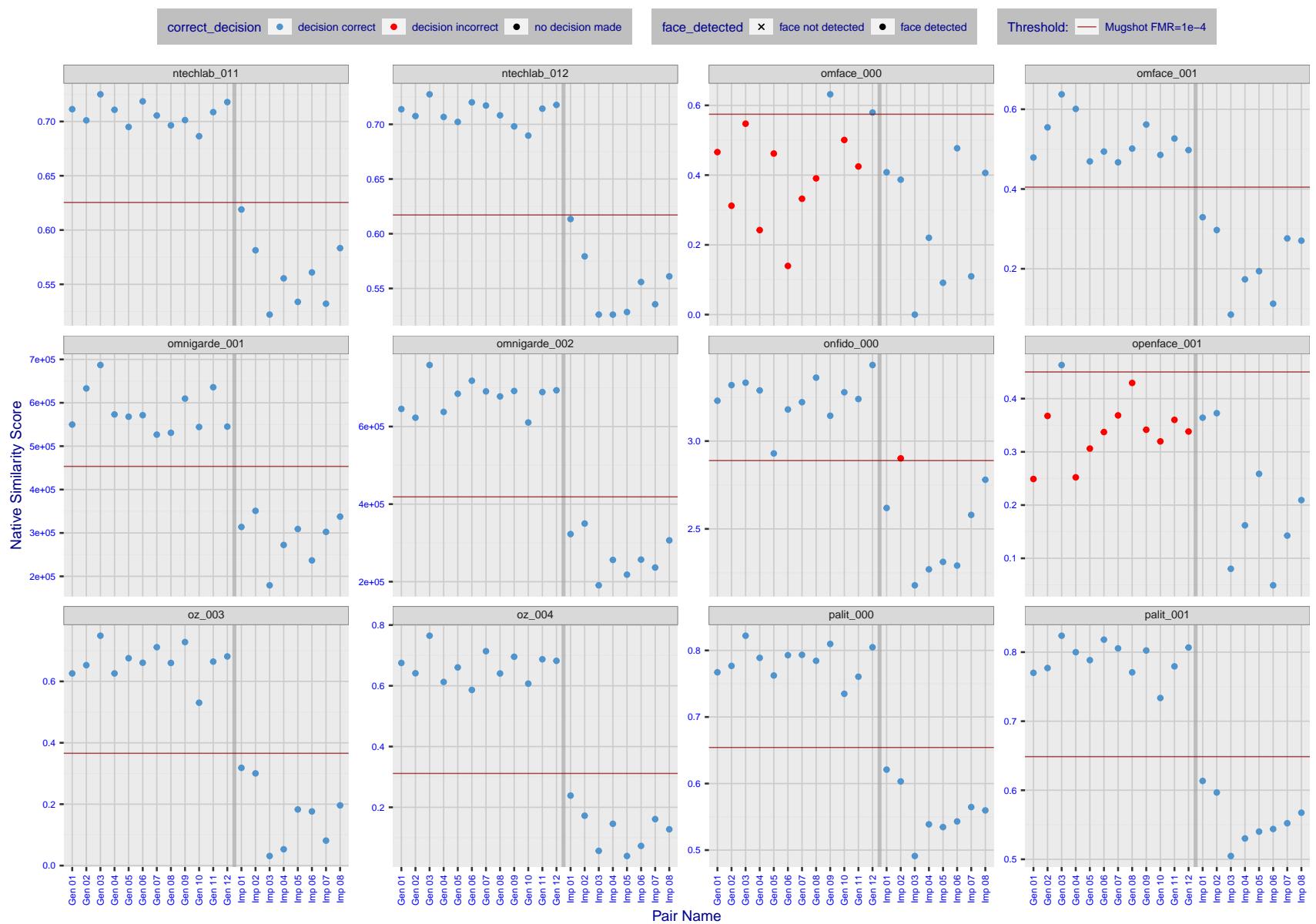


Figure 28: The figure shows algorithms' similarity scores for 12 genuine and 8 impostor image pairs used in a May 2018 paper by Phillips et al. ([1]). The threshold (red horizontal line) is a value calibrated to give $FMR = 0.0001$ on mugshot images. Points above the threshold correspond to pairs determined to be genuine, and points below the threshold correspond to pairs determined to be impostors. If the determined class (genuine or impostor) matches the real class, points will be blue; if not, red. An X represents face detection failure in either of the images in the pair. Note that the sample size ($n=20$) is small, and the figure may change substantially if larger or different sets are used. The images can be viewed on p. 13 of the Appendix, where Gen 01 corresponds to Same-Identity Pair 1, Gen 02 corresponds to Same-Identity Pair 2, and so on.

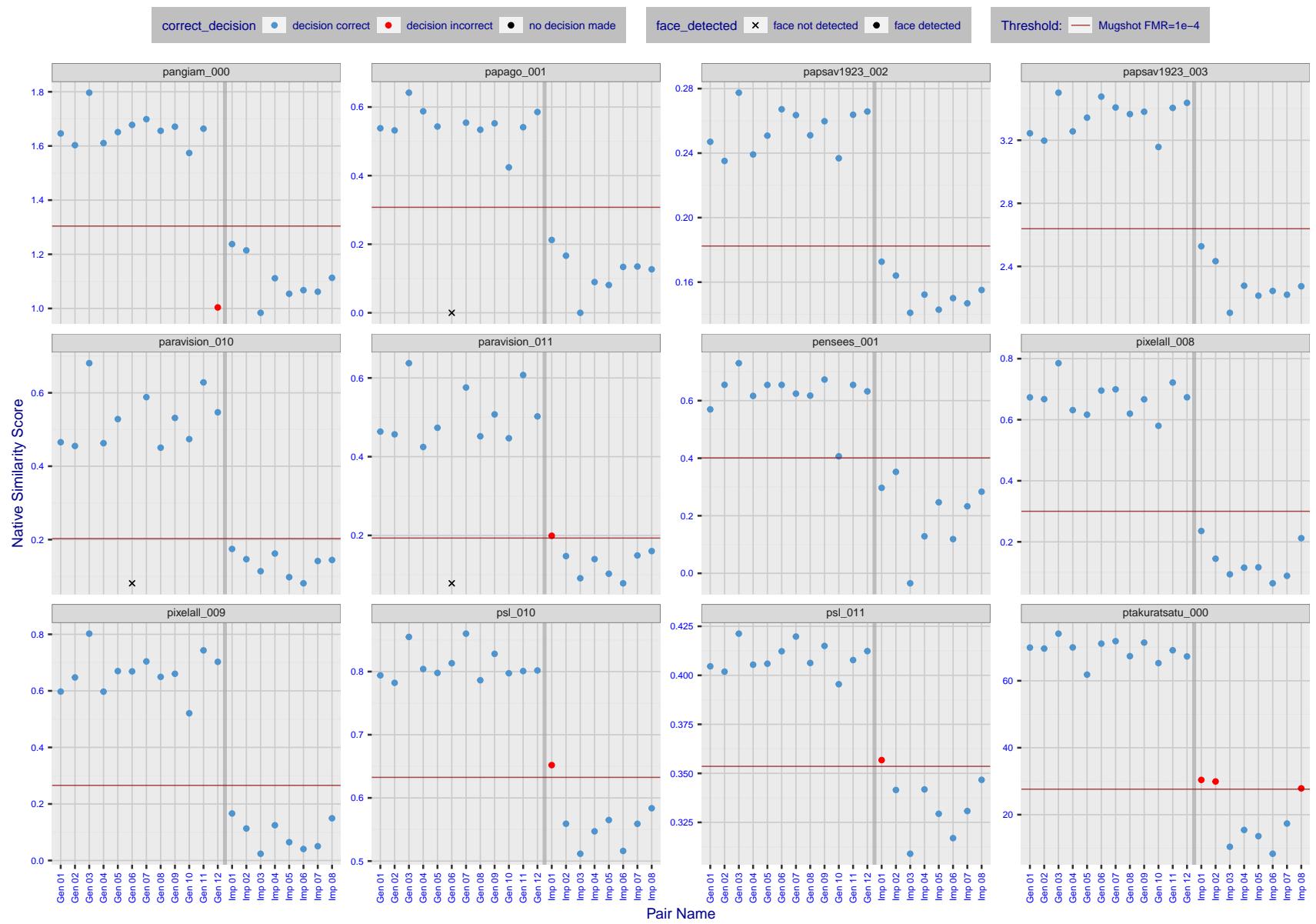


Figure 29: The figure shows algorithms' similarity scores for 12 genuine and 8 impostor image pairs used in a May 2018 paper by Phillips et al. ([1]). The threshold (red horizontal line) is a value calibrated to give $FMR = 0.0001$ on mugshot images. Points above the threshold correspond to pairs determined to be genuine, and points below the threshold correspond to pairs determined to be impostors. If the determined class (genuine or impostor) matches the real class, points will be blue; if not, red. An X represents face detection failure in either of the images in the pair. Note that the sample size ($n=20$) is small, and the figure may change substantially if larger or different sets are used. The images can be viewed on p. 13 of the Appendix, where Gen 01 corresponds to Same-Identity Pair 1, Gen 02 corresponds to Same-Identity Pair 2, and so on.

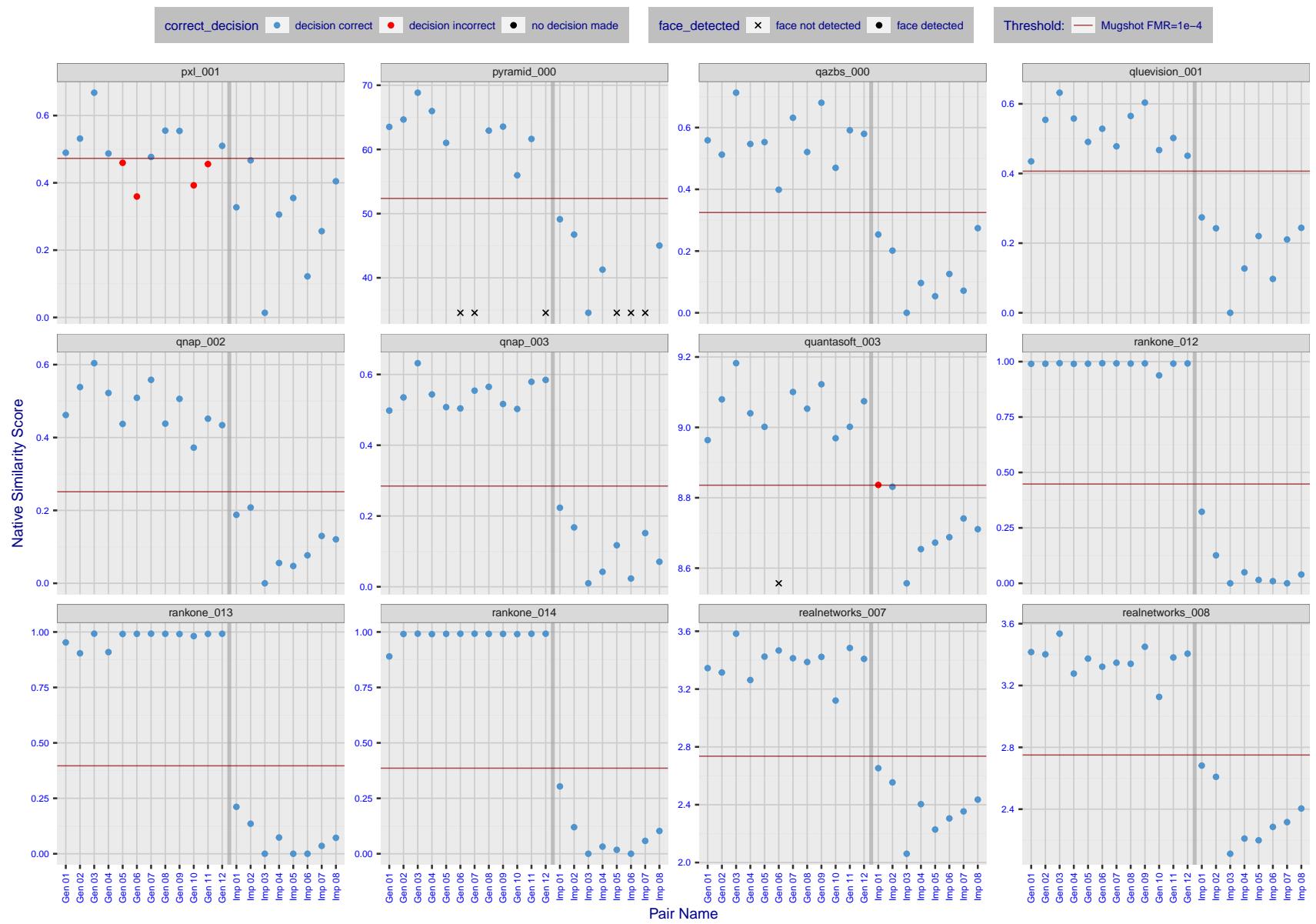


Figure 30: The figure shows algorithms' similarity scores for 12 genuine and 8 impostor image pairs used in a May 2018 paper by Phillips et al. ([1]). The threshold (red horizontal line) is a value calibrated to give $FMR = 0.0001$ on mugshot images. Points above the threshold correspond to pairs determined to be genuine, and points below the threshold correspond to pairs determined to be impostors. If the determined class (genuine or impostor) matches the real class, points will be blue; if not, red. An X represents face detection failure in either of the images in the pair. Note that the sample size ($n=20$) is small, and the figure may change substantially if larger or different sets are used. The images can be viewed on p. 13 of the Appendix, where Gen 01 corresponds to Same-Identity Pair 1, Gen 02 corresponds to Same-Identity Pair 2, and so on.

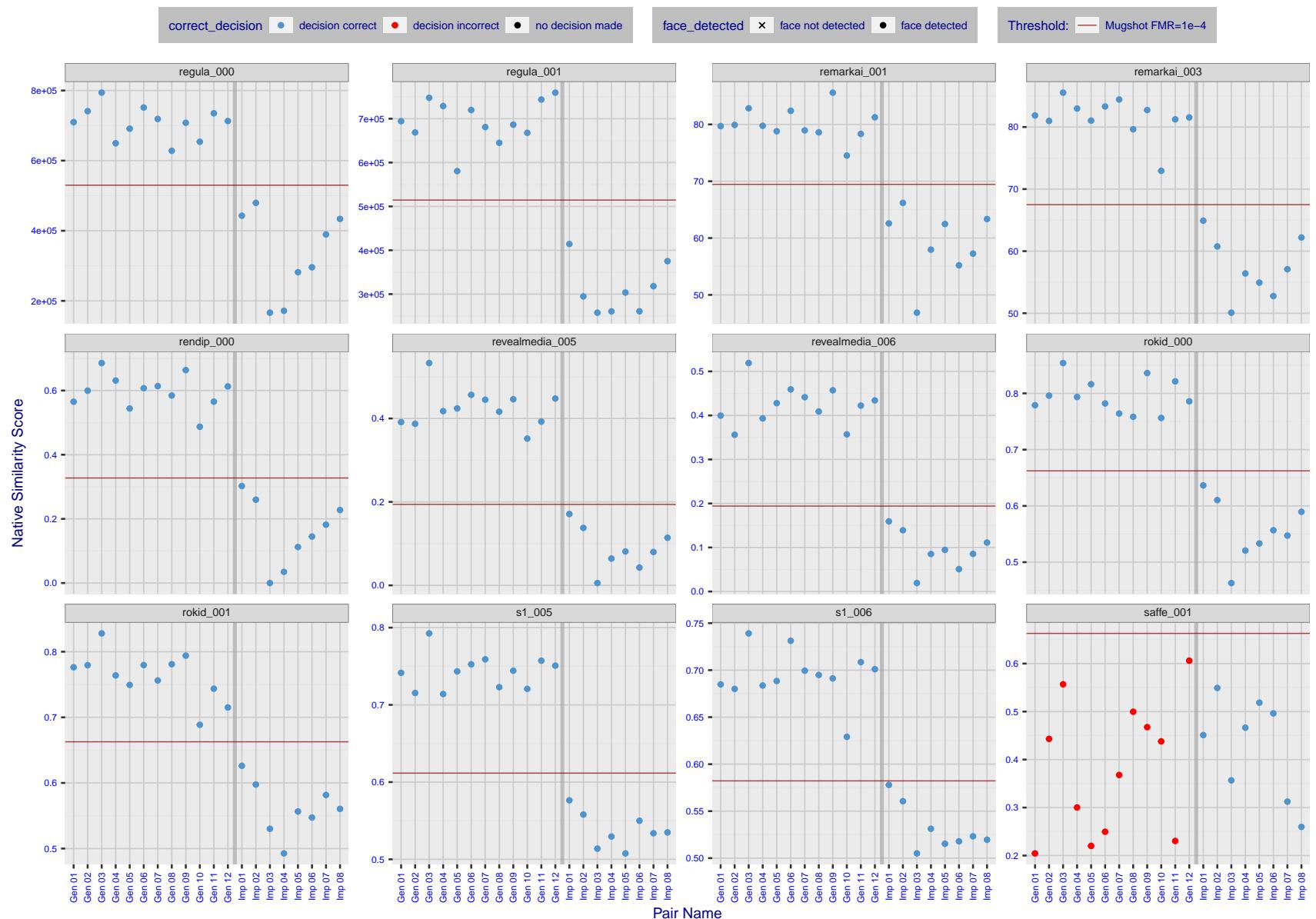


Figure 31: The figure shows algorithms' similarity scores for 12 genuine and 8 impostor image pairs used in a May 2018 paper by Phillips et al. ([1]). The threshold (red horizontal line) is a value calibrated to give $FMR = 0.0001$ on mugshot images. Points above the threshold correspond to pairs determined to be genuine, and points below the threshold correspond to pairs determined to be impostors. If the determined class (genuine or impostor) matches the real class, points will be blue; if not, red. An X represents face detection failure in either of the images in the pair. Note that the sample size ($n=20$) is small, and the figure may change substantially if larger or different sets are used. The images can be viewed on p. 13 of the Appendix, where Gen 01 corresponds to Same-Identity Pair 1, Gen 02 corresponds to Same-Identity Pair 2, and so on.

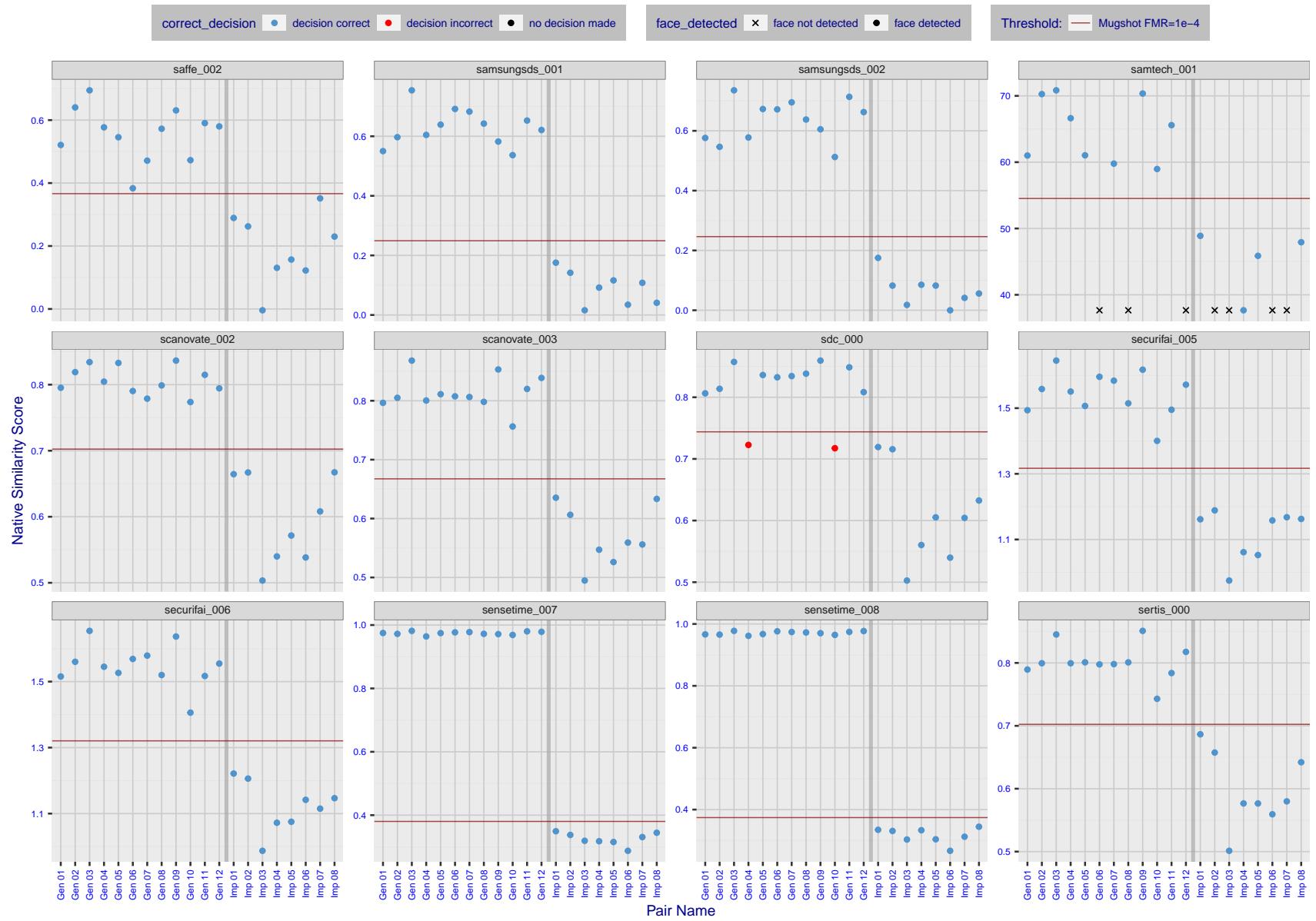


Figure 32: The figure shows algorithms' similarity scores for 12 genuine and 8 impostor image pairs used in a May 2018 paper by Phillips et al. ([1]). The threshold (red horizontal line) is a value calibrated to give $FMR = 0.0001$ on mugshot images. Points above the threshold correspond to pairs determined to be genuine, and points below the threshold correspond to pairs determined to be impostors. If the determined class (genuine or impostor) matches the real class, points will be blue; if not, red. An X represents face detection failure in either of the images in the pair. Note that the sample size ($n=20$) is small, and the figure may change substantially if larger or different sets are used. The images can be viewed on p. 13 of the Appendix, where Gen 01 corresponds to Same-Identity Pair 1, Gen 02 corresponds to Same-Identity Pair 2, and so on.

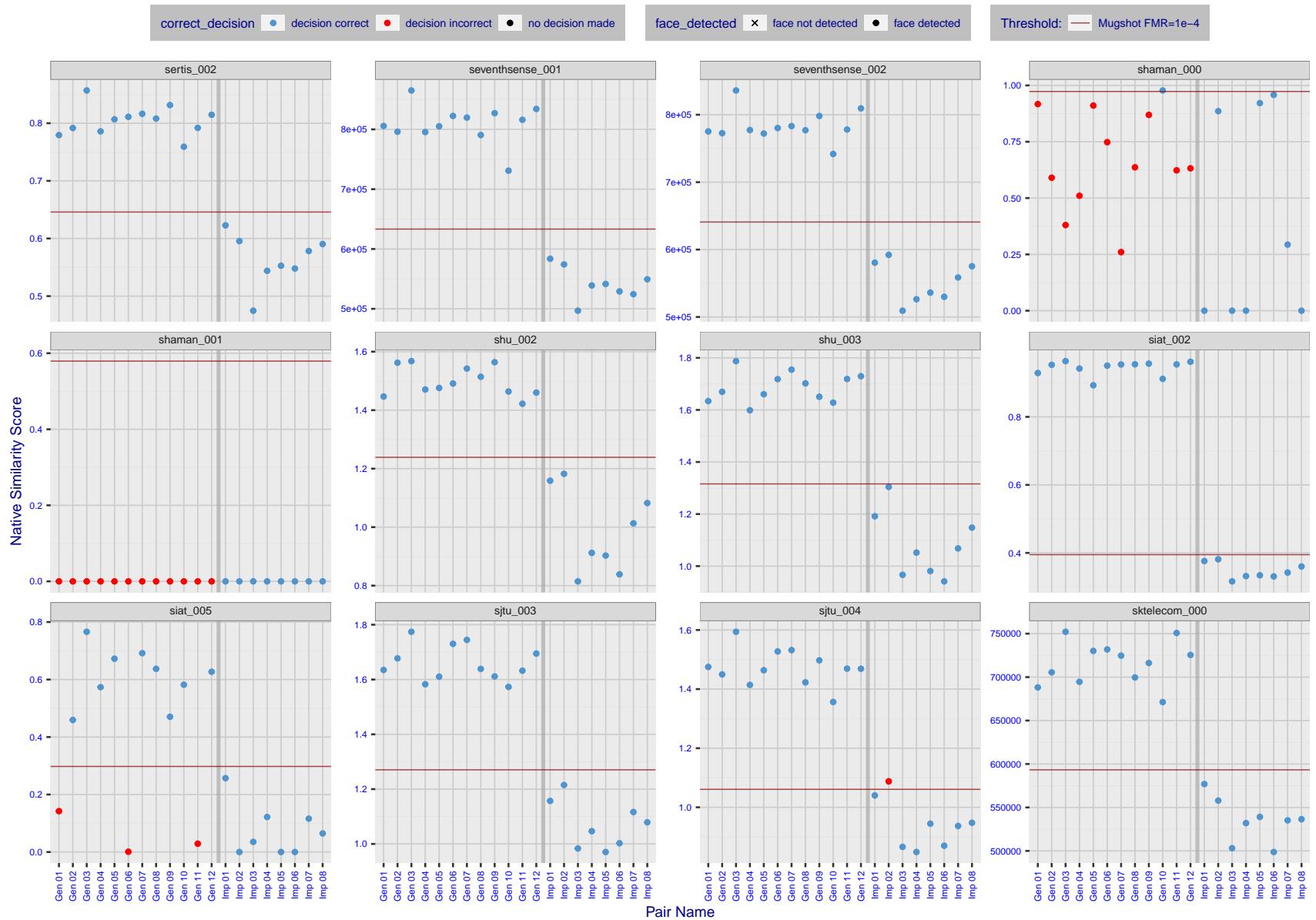


Figure 33: The figure shows algorithms' similarity scores for 12 genuine and 8 impostor image pairs used in a May 2018 paper by Phillips et al. ([1]). The threshold (red horizontal line) is a value calibrated to give $FMR = 0.0001$ on mugshot images. Points above the threshold correspond to pairs determined to be genuine, and points below the threshold correspond to pairs determined to be impostors. If the determined class (genuine or impostor) matches the real class, points will be blue; if not, red. An X represents face detection failure in either of the images in the pair. Note that the sample size ($n=20$) is small, and the figure may change substantially if larger or different sets are used. The images can be viewed on p. 13 of the Appendix, where Gen 01 corresponds to Same-Identity Pair 1, Gen 02 corresponds to Same-Identity Pair 2, and so on.

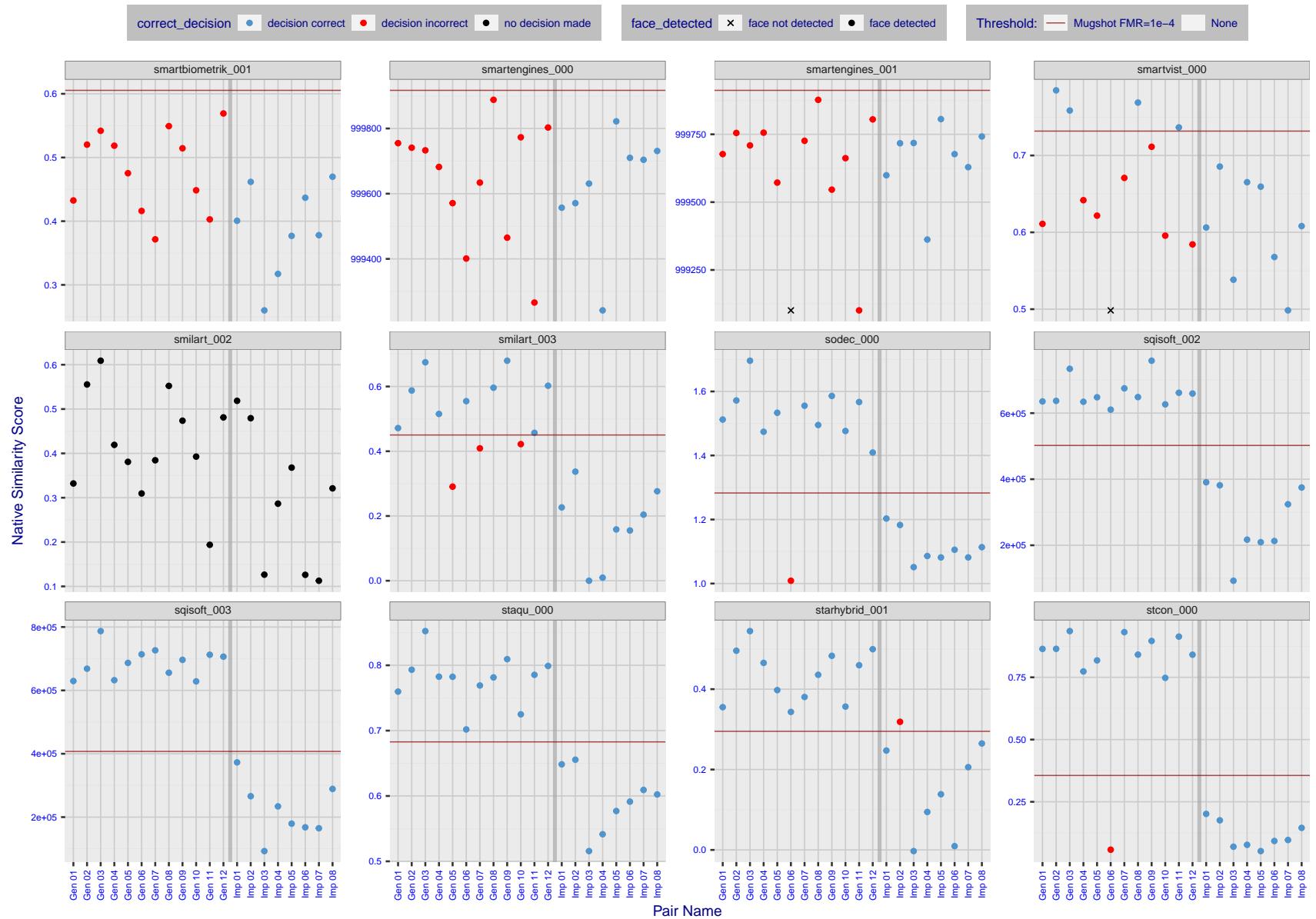


Figure 34: The figure shows algorithms' similarity scores for 12 genuine and 8 impostor image pairs used in a May 2018 paper by Phillips et al. ([1]). The threshold (red horizontal line) is a value calibrated to give $FMR = 0.0001$ on mugshot images. Points above the threshold correspond to pairs determined to be genuine, and points below the threshold correspond to pairs determined to be impostors. If the determined class (genuine or impostor) matches the real class, points will be blue; if not, red. An X represents face detection failure in either of the images in the pair. Note that the sample size ($n=20$) is small, and the figure may change substantially if larger or different sets are used. The images can be viewed on p. 13 of the Appendix, where Gen 01 corresponds to Same-Identity Pair 1, Gen 02 corresponds to Same-Identity Pair 2, and so on.

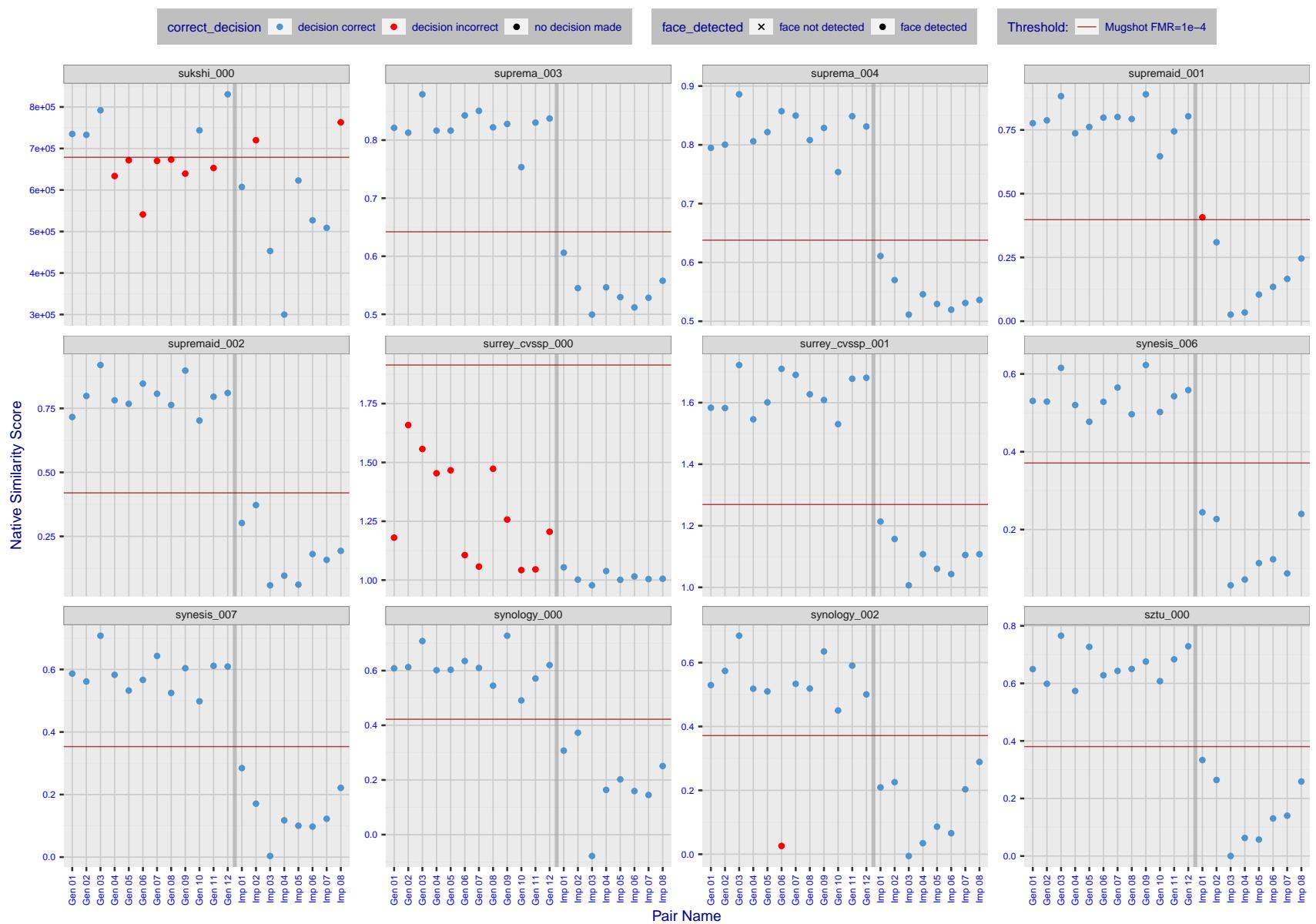


Figure 35: The figure shows algorithms' similarity scores for 12 genuine and 8 impostor image pairs used in a May 2018 paper by Phillips et al. ([1]). The threshold (red horizontal line) is a value calibrated to give $FMR = 0.0001$ on mugshot images. Points above the threshold correspond to pairs determined to be genuine, and points below the threshold correspond to pairs determined to be impostors. If the determined class (genuine or impostor) matches the real class, points will be blue; if not, red. An X represents face detection failure in either of the images in the pair. Note that the sample size ($n=20$) is small, and the figure may change substantially if larger or different sets are used. The images can be viewed on p. 13 of the Appendix, where Gen 01 corresponds to Same-Identity Pair 1, Gen 02 corresponds to Same-Identity Pair 2, and so on.

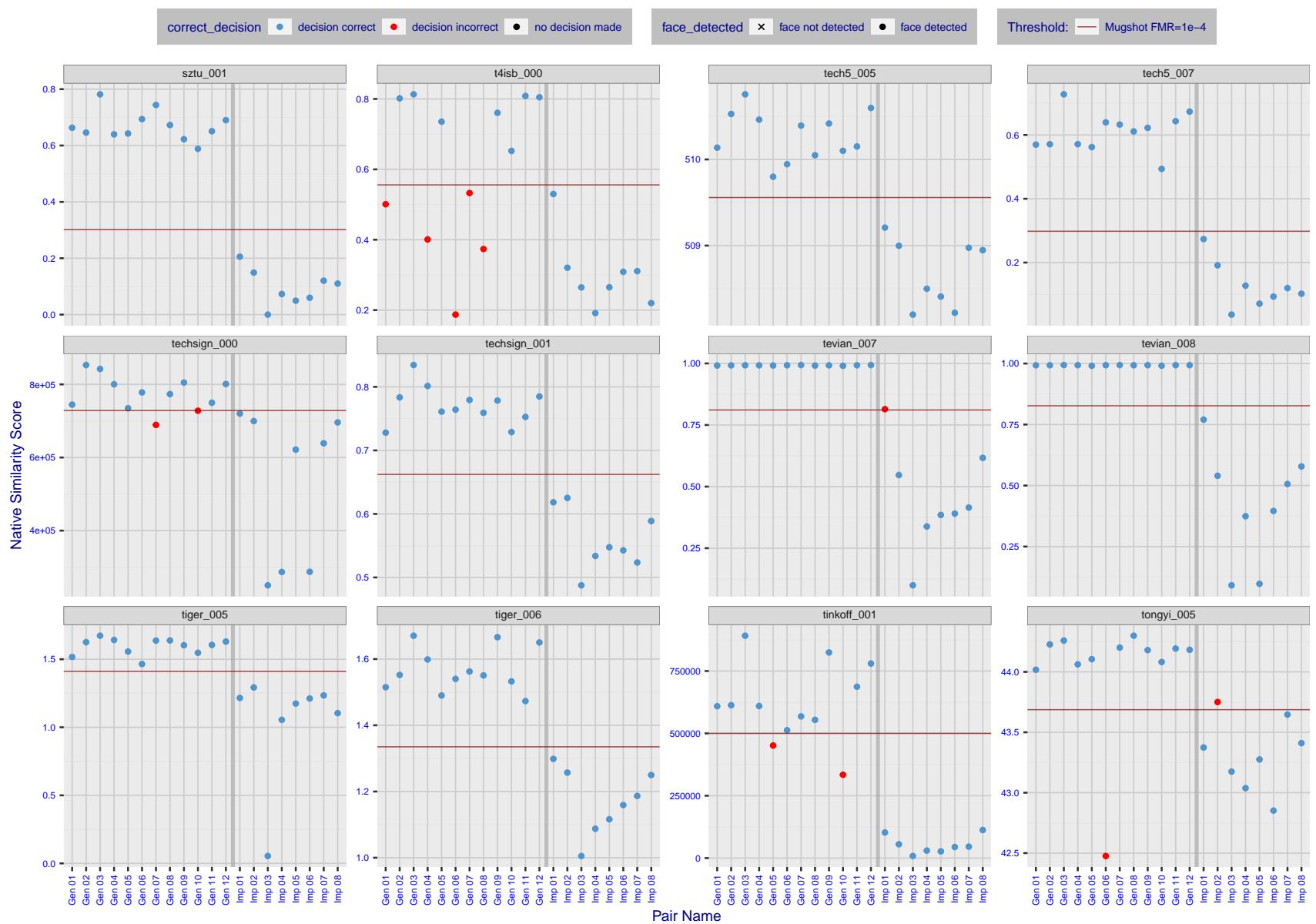


Figure 36: The figure shows algorithms' similarity scores for 12 genuine and 8 impostor image pairs used in a May 2018 paper by Phillips et al. ([1]). The threshold (red horizontal line) is a value calibrated to give $FMR = 0.0001$ on mugshot images. Points above the threshold correspond to pairs determined to be genuine, and points below the threshold correspond to pairs determined to be impostors. If the determined class (genuine or impostor) matches the real class, points will be blue; if not, red. An X represents face detection failure in either of the images in the pair. Note that the sample size ($n=20$) is small, and the figure may change substantially if larger or different sets are used. The images can be viewed on p. 13 of the Appendix, where Gen 01 corresponds to Same-Identity Pair 1, Gen 02 corresponds to Same-Identity Pair 2, and so on.

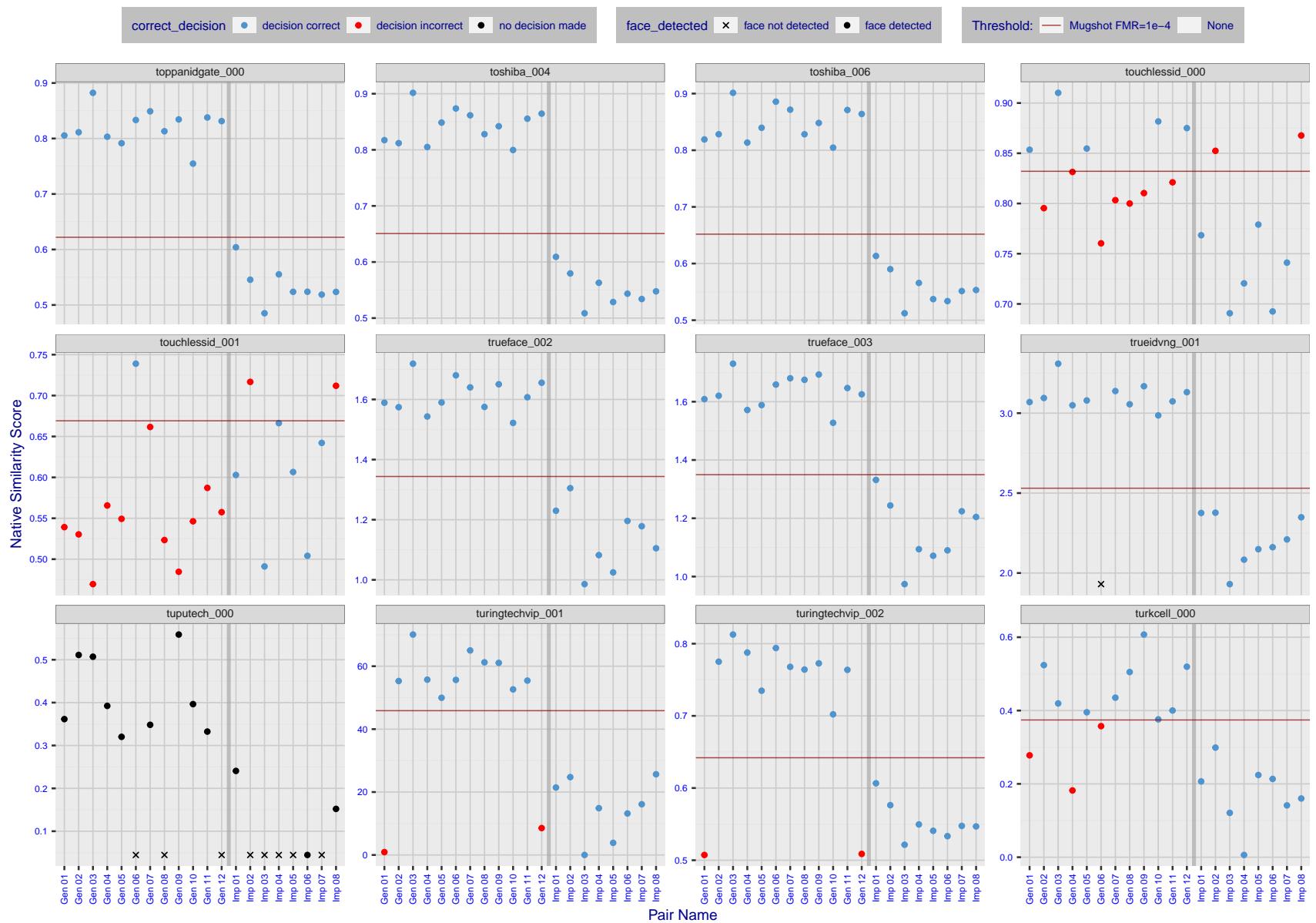


Figure 37: The figure shows algorithms' similarity scores for 12 genuine and 8 impostor image pairs used in a May 2018 paper by Phillips et al. ([1]). The threshold (red horizontal line) is a value calibrated to give $FMR = 0.0001$ on mugshot images. Points above the threshold correspond to pairs determined to be genuine, and points below the threshold correspond to pairs determined to be impostors. If the determined class (genuine or impostor) matches the real class, points will be blue; if not, red. An X represents face detection failure in either of the images in the pair. Note that the sample size ($n=20$) is small, and the figure may change substantially if larger or different sets are used. The images can be viewed on p. 13 of the Appendix, where Gen 01 corresponds to Same-Identity Pair 1, Gen 02 corresponds to Same-Identity Pair 2, and so on.

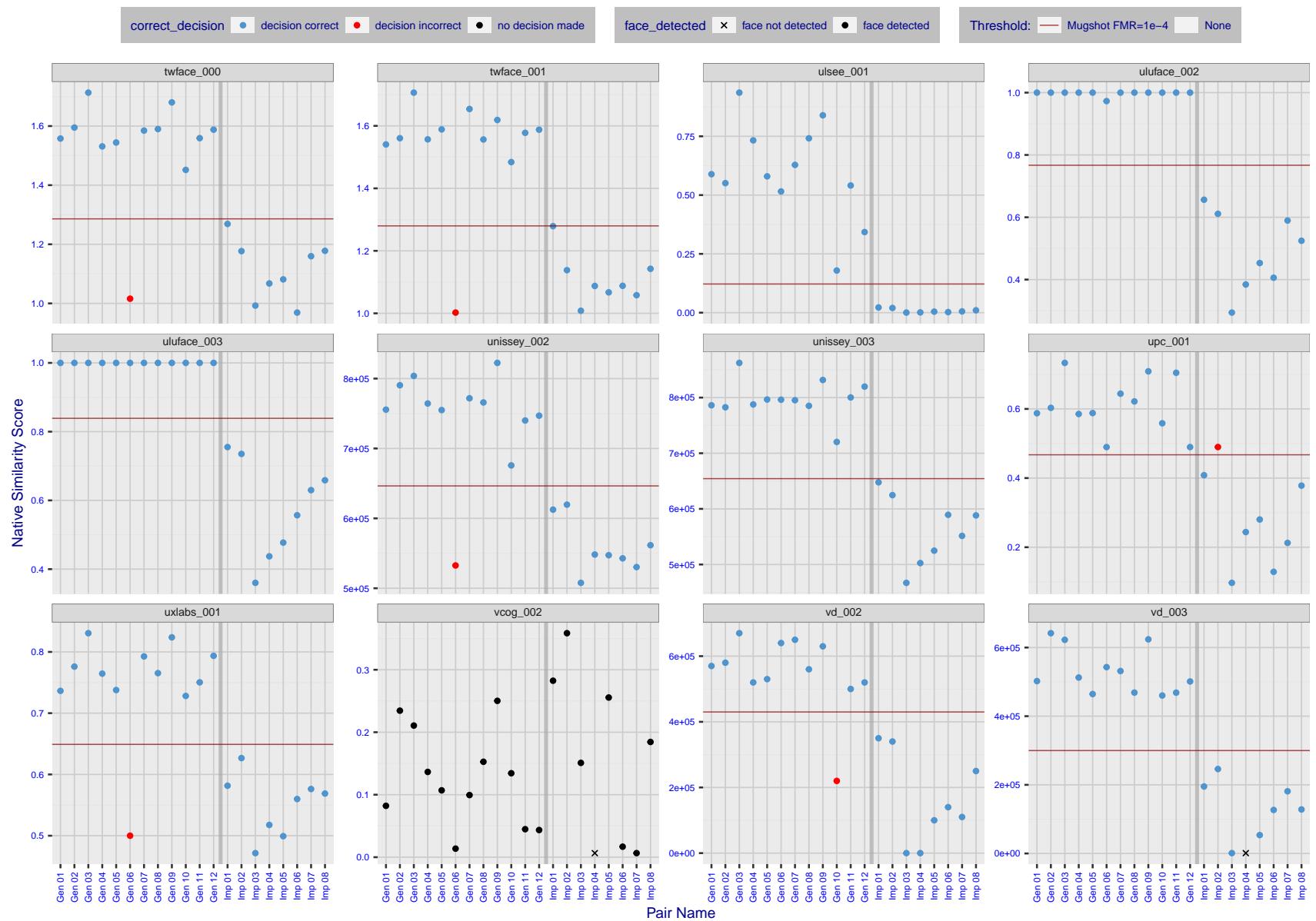


Figure 38: The figure shows algorithms' similarity scores for 12 genuine and 8 impostor image pairs used in a May 2018 paper by Phillips et al. ([1]). The threshold (red horizontal line) is a value calibrated to give $FMR = 0.0001$ on mugshot images. Points above the threshold correspond to pairs determined to be genuine, and points below the threshold correspond to pairs determined to be impostors. If the determined class (genuine or impostor) matches the real class, points will be blue; if not, red. An X represents face detection failure in either of the images in the pair. Note that the sample size ($n=20$) is small, and the figure may change substantially if larger or different sets are used. The images can be viewed on p. 13 of the Appendix, where Gen 01 corresponds to Same-Identity Pair 1, Gen 02 corresponds to Same-Identity Pair 2, and so on.

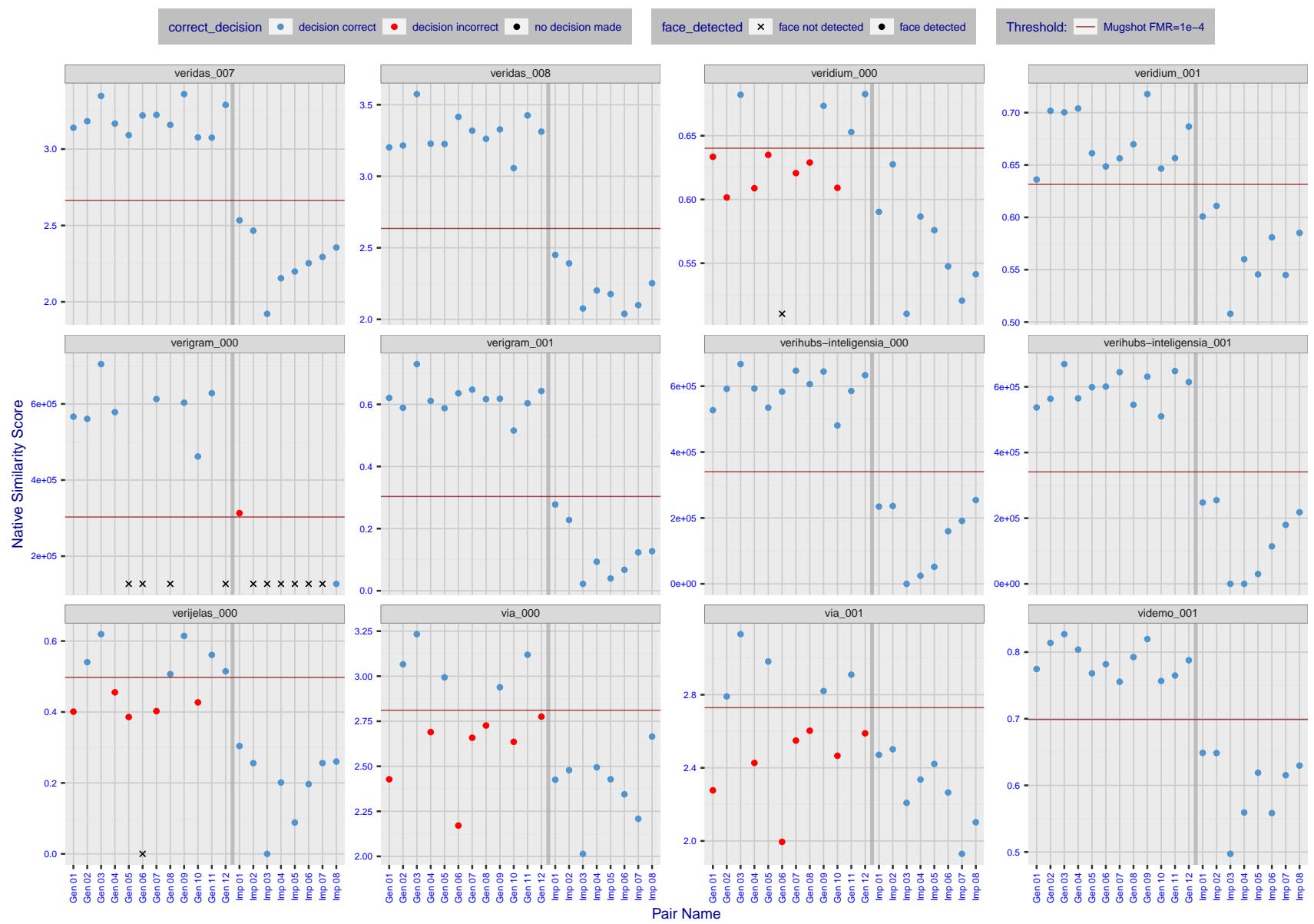


Figure 39: The figure shows algorithms' similarity scores for 12 genuine and 8 impostor image pairs used in a May 2018 paper by Phillips et al. ([1]). The threshold (red horizontal line) is a value calibrated to give $FMR = 0.0001$ on mugshot images. Points above the threshold correspond to pairs determined to be genuine, and points below the threshold correspond to pairs determined to be impostors. If the determined class (genuine or impostor) matches the real class, points will be blue; if not, red. An X represents face detection failure in either of the images in the pair. Note that the sample size ($n=20$) is small, and the figure may change substantially if larger or different sets are used. The images can be viewed on p. 13 of the Appendix, where Gen 01 corresponds to Same-Identity Pair 1, Gen 02 corresponds to Same-Identity Pair 2, and so on.

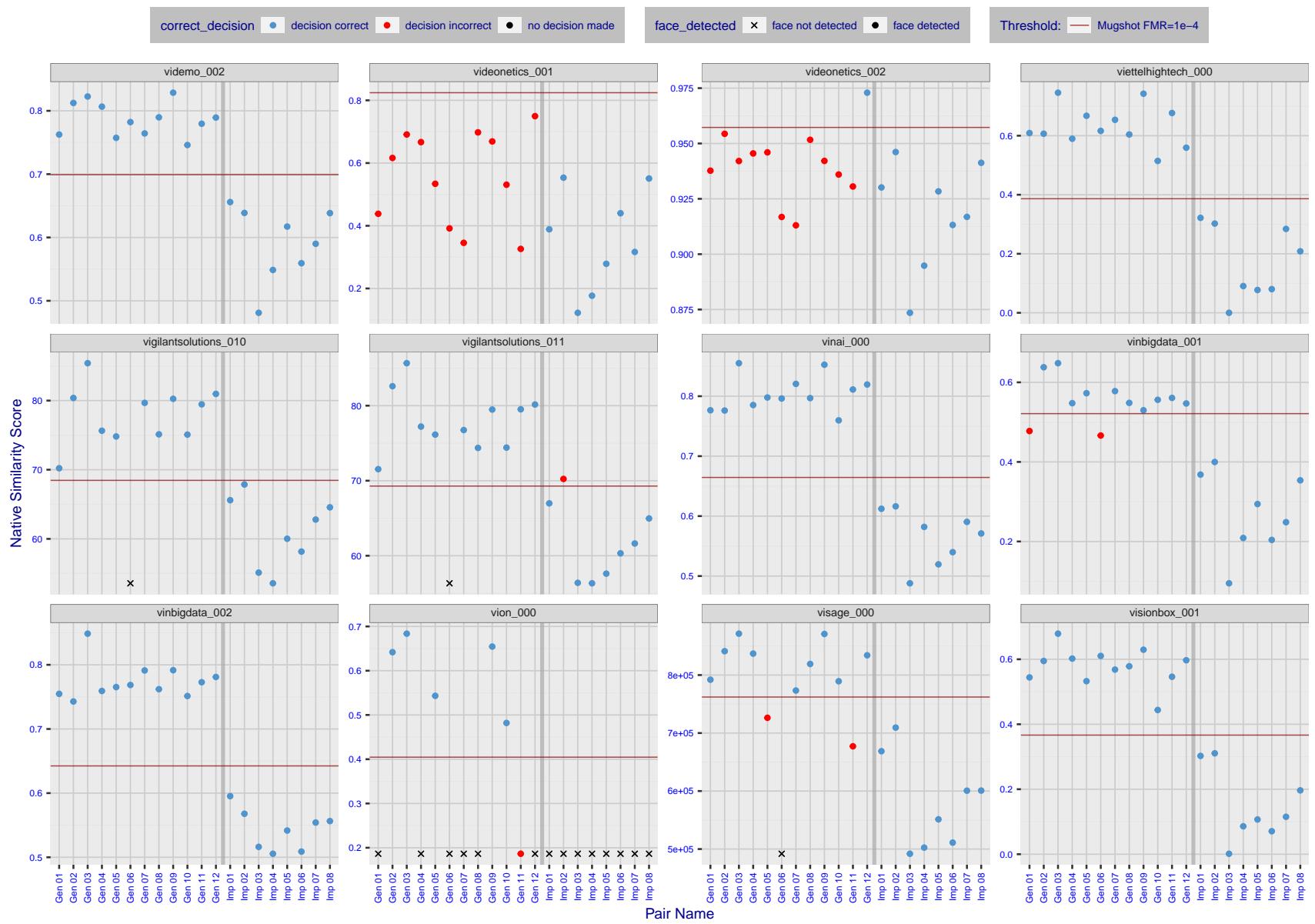


Figure 40: The figure shows algorithms' similarity scores for 12 genuine and 8 impostor image pairs used in a May 2018 paper by Phillips et al. ([1]). The threshold (red horizontal line) is a value calibrated to give $FMR = 0.0001$ on mugshot images. Points above the threshold correspond to pairs determined to be genuine, and points below the threshold correspond to pairs determined to be impostors. If the determined class (genuine or impostor) matches the real class, points will be blue; if not, red. An X represents face detection failure in either of the images in the pair. Note that the sample size ($n=20$) is small, and the figure may change substantially if larger or different sets are used. The images can be viewed on p. 13 of the Appendix, where Gen 01 corresponds to Same-Identity Pair 1, Gen 02 corresponds to Same-Identity Pair 2, and so on.

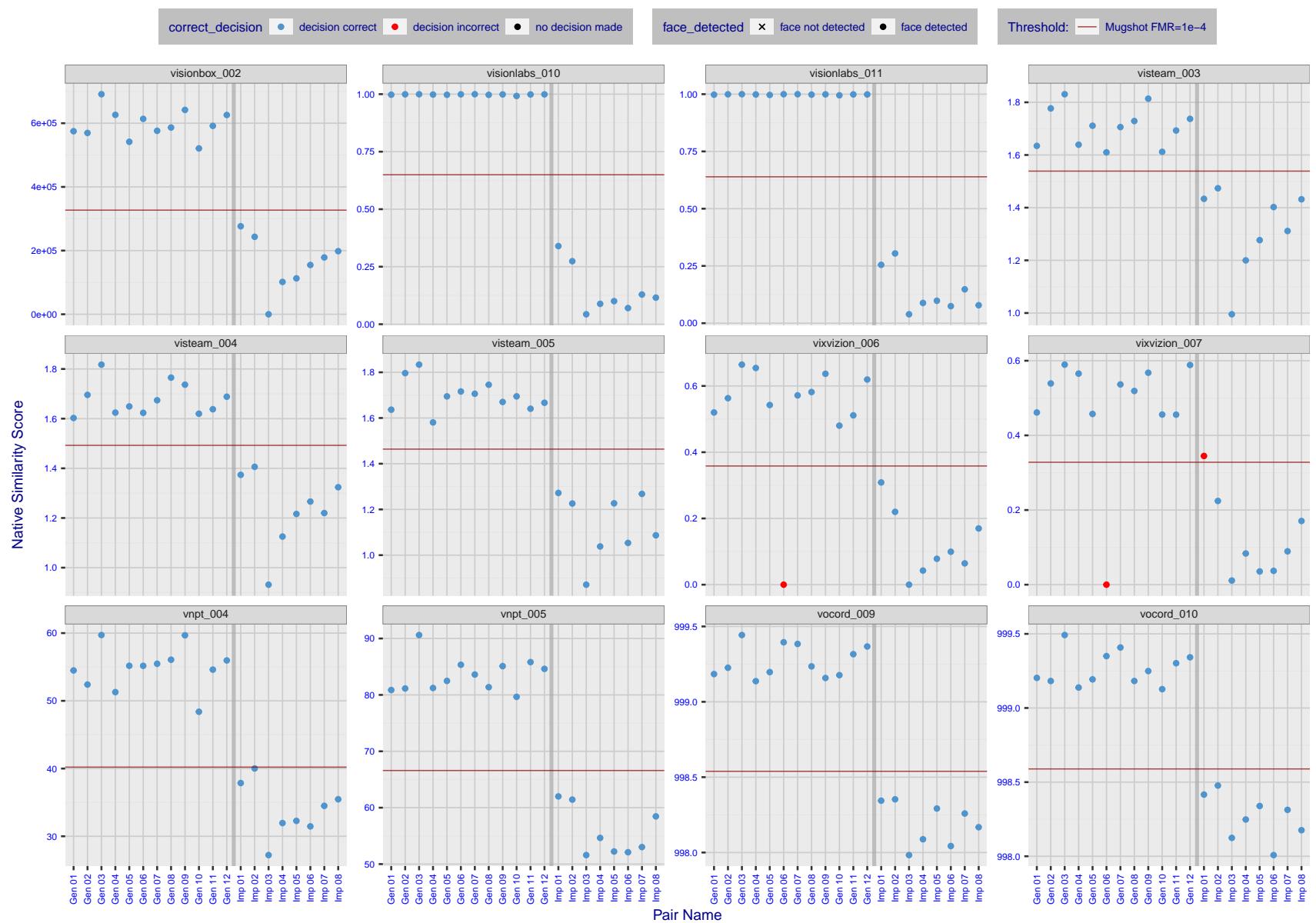


Figure 41: The figure shows algorithms' similarity scores for 12 genuine and 8 impostor image pairs used in a May 2018 paper by Phillips et al. ([1]). The threshold (red horizontal line) is a value calibrated to give $FMR = 0.0001$ on mugshot images. Points above the threshold correspond to pairs determined to be genuine, and points below the threshold correspond to pairs determined to be impostors. If the determined class (genuine or impostor) matches the real class, points will be blue; if not, red. An X represents face detection failure in either of the images in the pair. Note that the sample size ($n=20$) is small, and the figure may change substantially if larger or different sets are used. The images can be viewed on p. 13 of the Appendix, where Gen 01 corresponds to Same-Identity Pair 1, Gen 02 corresponds to Same-Identity Pair 2, and so on.

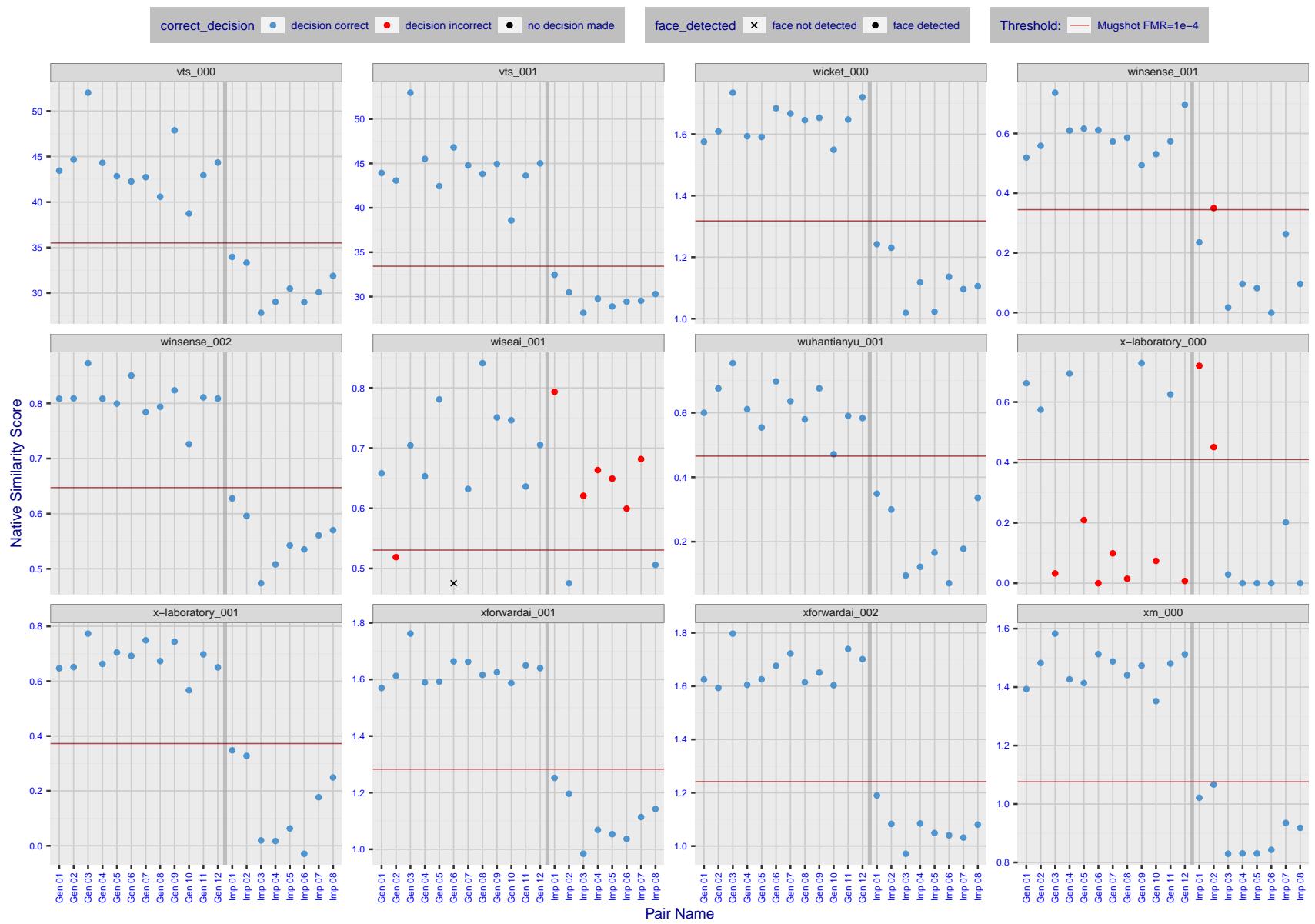


Figure 42: The figure shows algorithms' similarity scores for 12 genuine and 8 impostor image pairs used in a May 2018 paper by Phillips et al. ([1]). The threshold (red horizontal line) is a value calibrated to give $FMR = 0.0001$ on mugshot images. Points above the threshold correspond to pairs determined to be genuine, and points below the threshold correspond to pairs determined to be impostors. If the determined class (genuine or impostor) matches the real class, points will be blue; if not, red. An X represents face detection failure in either of the images in the pair. Note that the sample size ($n=20$) is small, and the figure may change substantially if larger or different sets are used. The images can be viewed on p. 13 of the Appendix, where Gen 01 corresponds to Same-Identity Pair 1, Gen 02 corresponds to Same-Identity Pair 2, and so on.

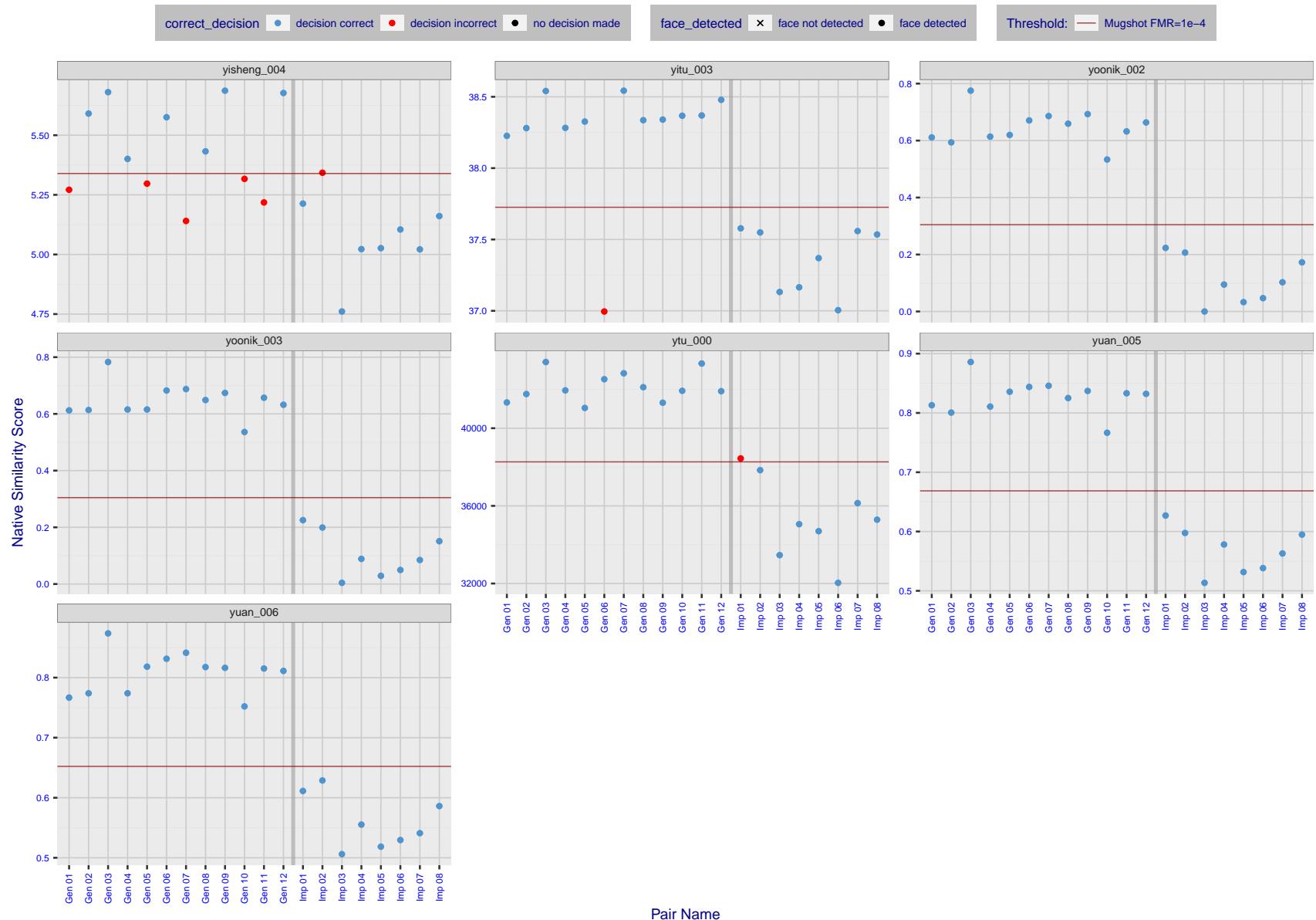


Figure 43: The figure shows algorithms' similarity scores for 12 genuine and 8 impostor image pairs used in a May 2018 paper by Phillips et al. ([1]). The threshold (red horizontal line) is a value calibrated to give $FMR = 0.0001$ on mugshot images. Points above the threshold correspond to pairs determined to be genuine, and points below the threshold correspond to pairs determined to be impostors. If the determined class (genuine or impostor) matches the real class, points will be blue; if not, red. An X represents face detection failure in either of the images in the pair. Note that the sample size ($n=20$) is small, and the figure may change substantially if larger or different sets are used. The images can be viewed on p. 13 of the Appendix, where Gen 01 corresponds to Same-Identity Pair 1, Gen 02 corresponds to Same-Identity Pair 2, and so on.

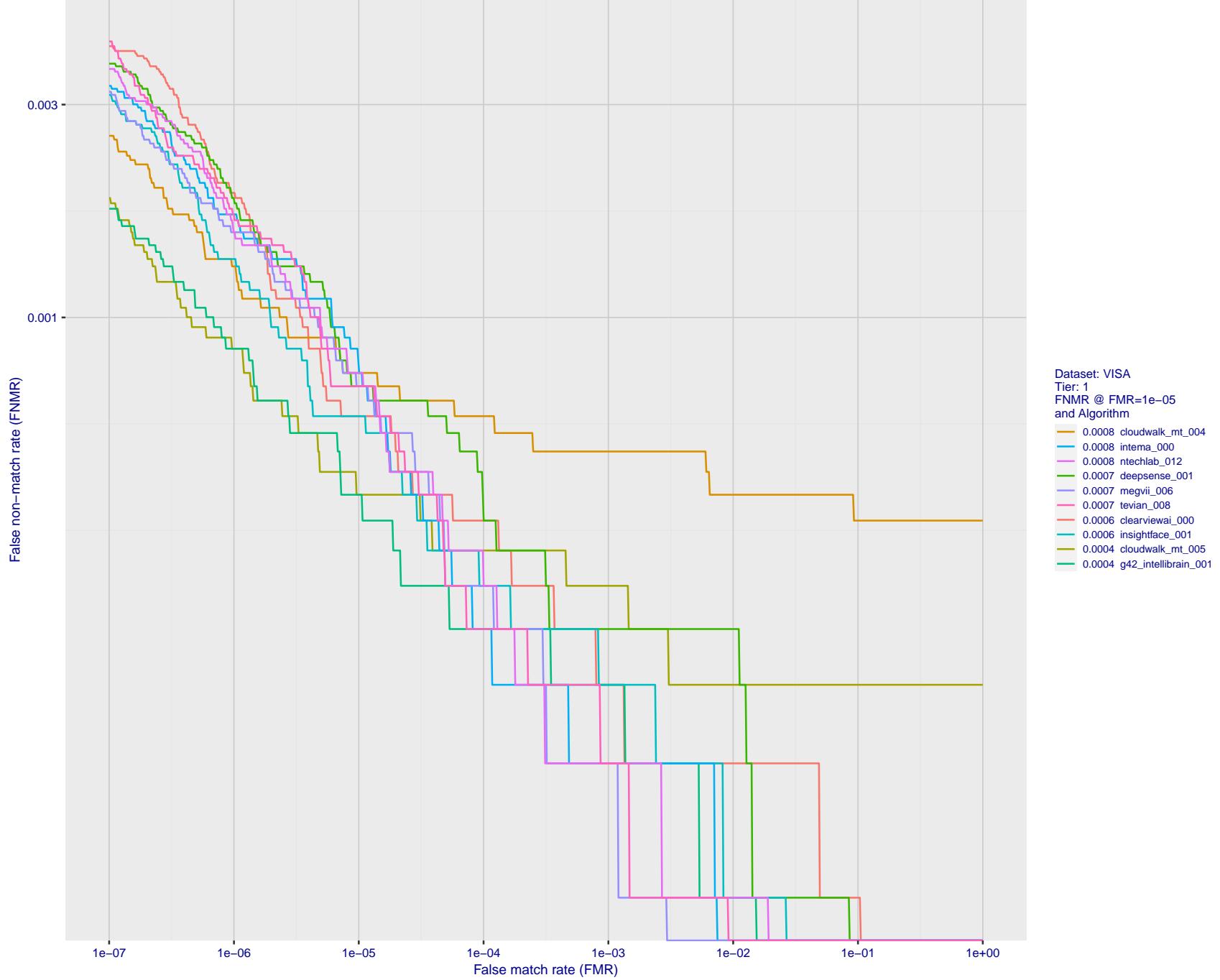


Figure 44: For the visa images, detection error tradeoff (DET) characteristics showing false non-match rate vs. false match rate plotted parametrically on threshold, T . The scales are logarithmic in order to show many decades of FMR.

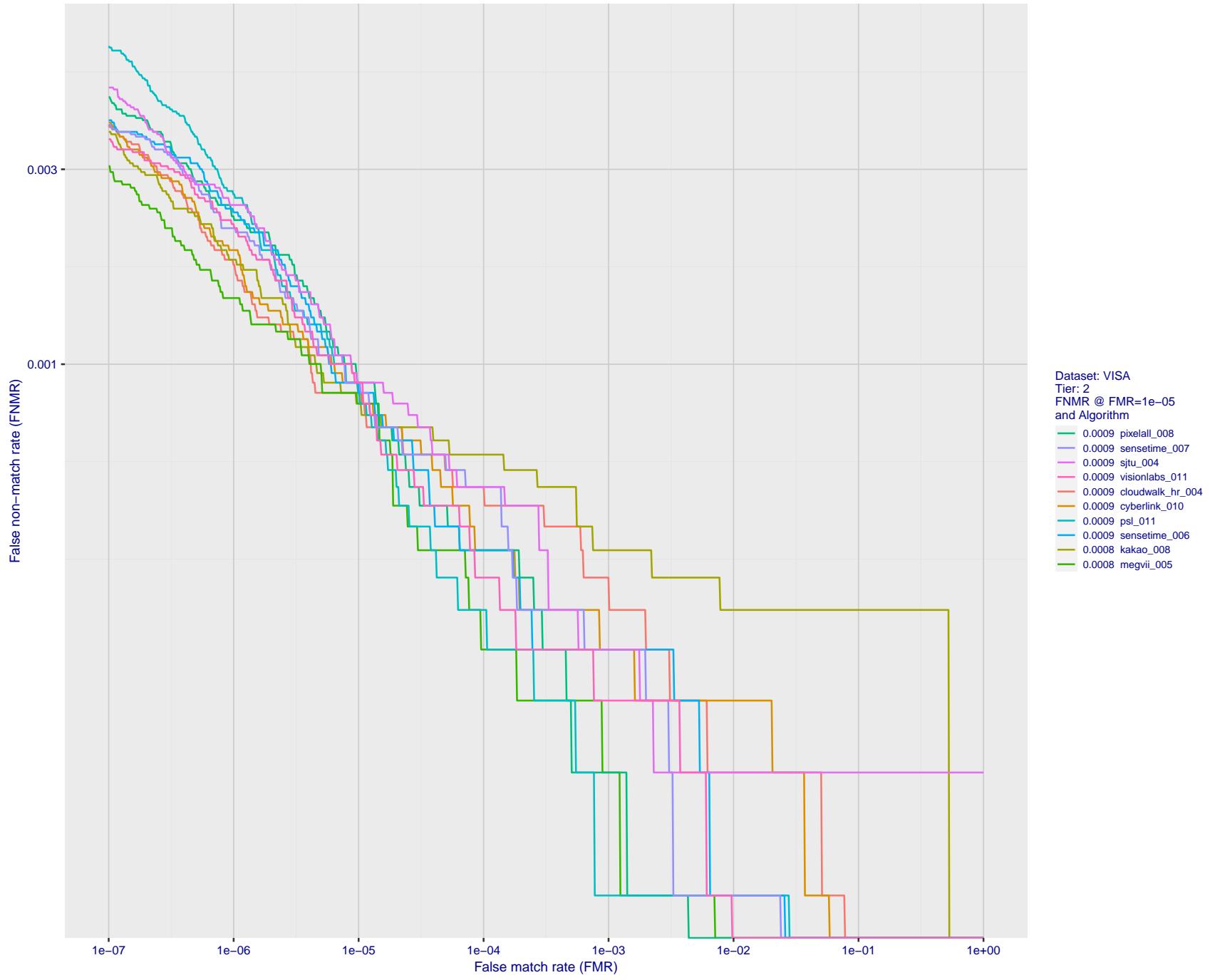


Figure 45: For the visa images, detection error tradeoff (DET) characteristics showing false non-match rate vs. false match rate plotted parametrically on threshold, T . The scales are logarithmic in order to show many decades of FMR.

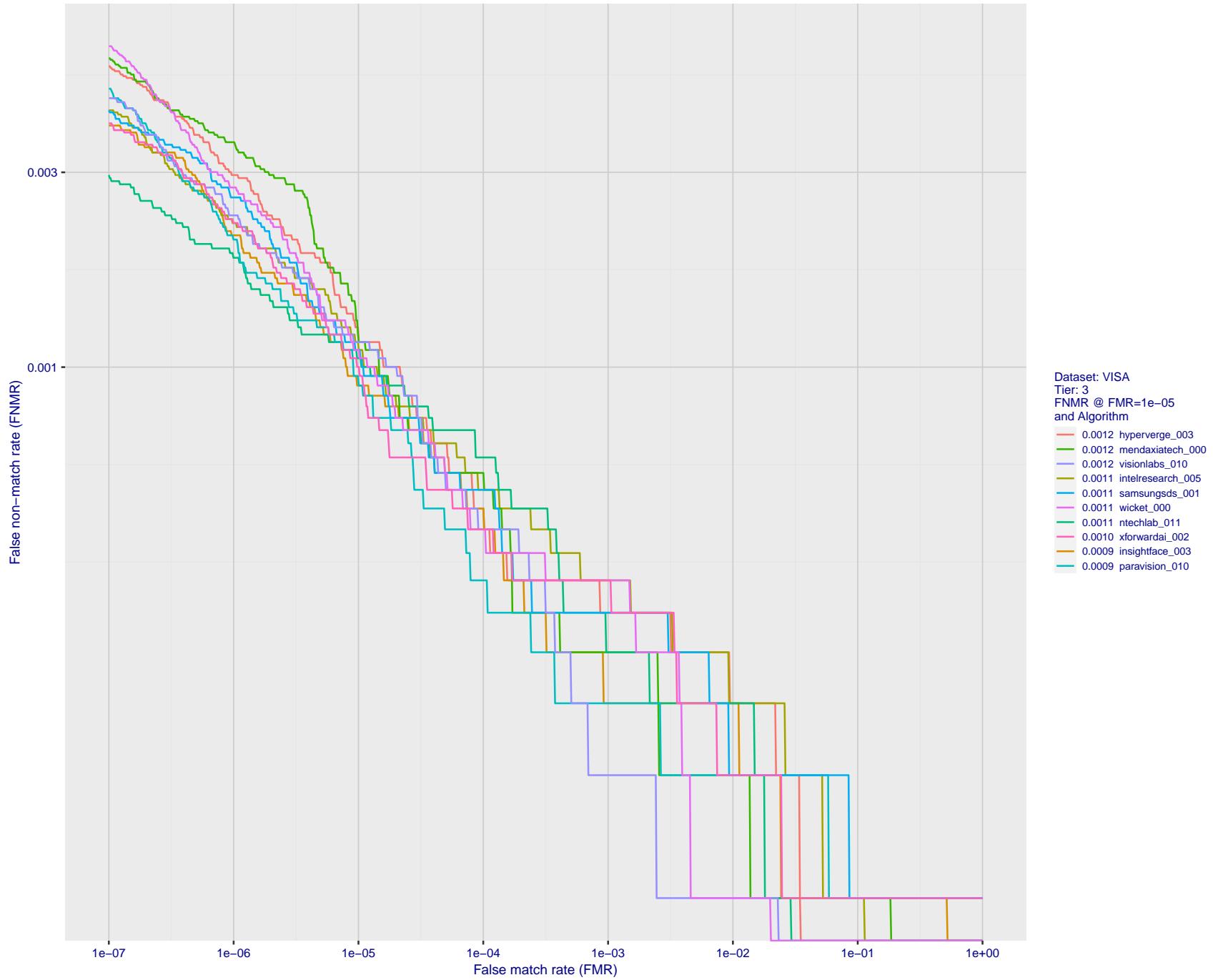


Figure 46: For the visa images, detection error tradeoff (DET) characteristics showing false non-match rate vs. false match rate plotted parametrically on threshold, T . The scales are logarithmic in order to show many decades of FMR.

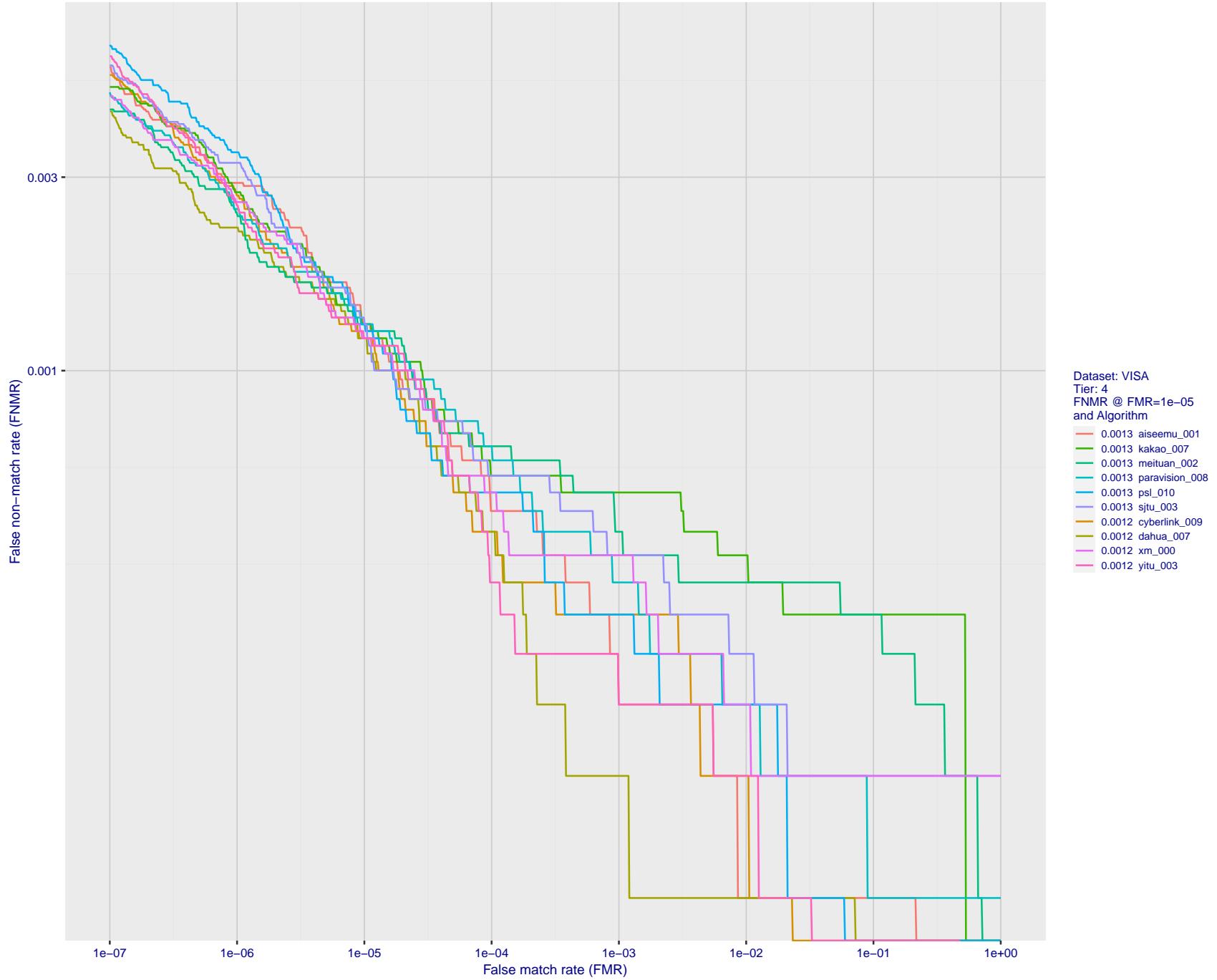


Figure 47: For the visa images, detection error tradeoff (DET) characteristics showing false non-match rate vs. false match rate plotted parametrically on threshold, T . The scales are logarithmic in order to show many decades of FMR.

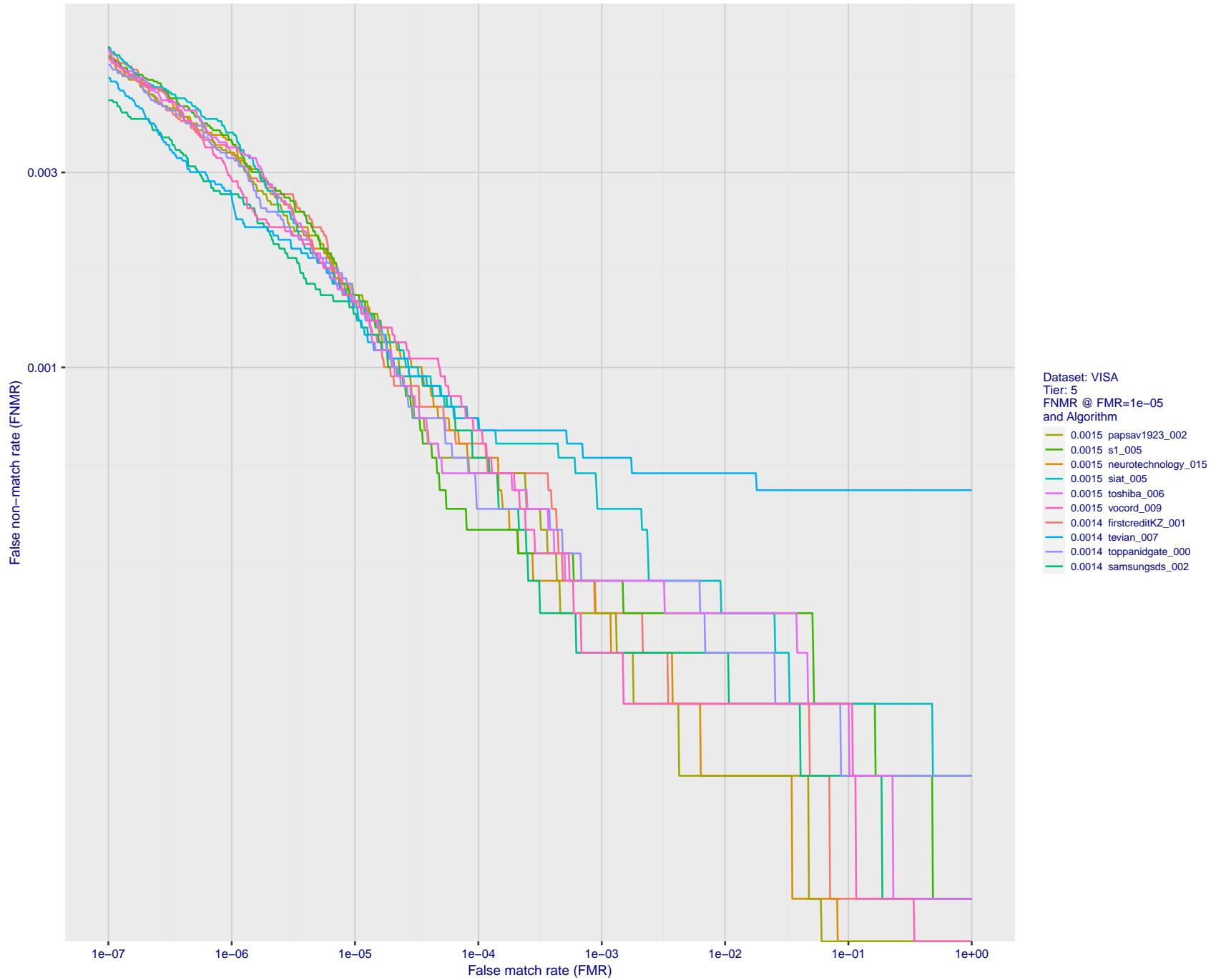


Figure 48: For the visa images, detection error tradeoff (DET) characteristics showing false non-match rate vs. false match rate plotted parametrically on threshold, T . The scales are logarithmic in order to show many decades of FMR.

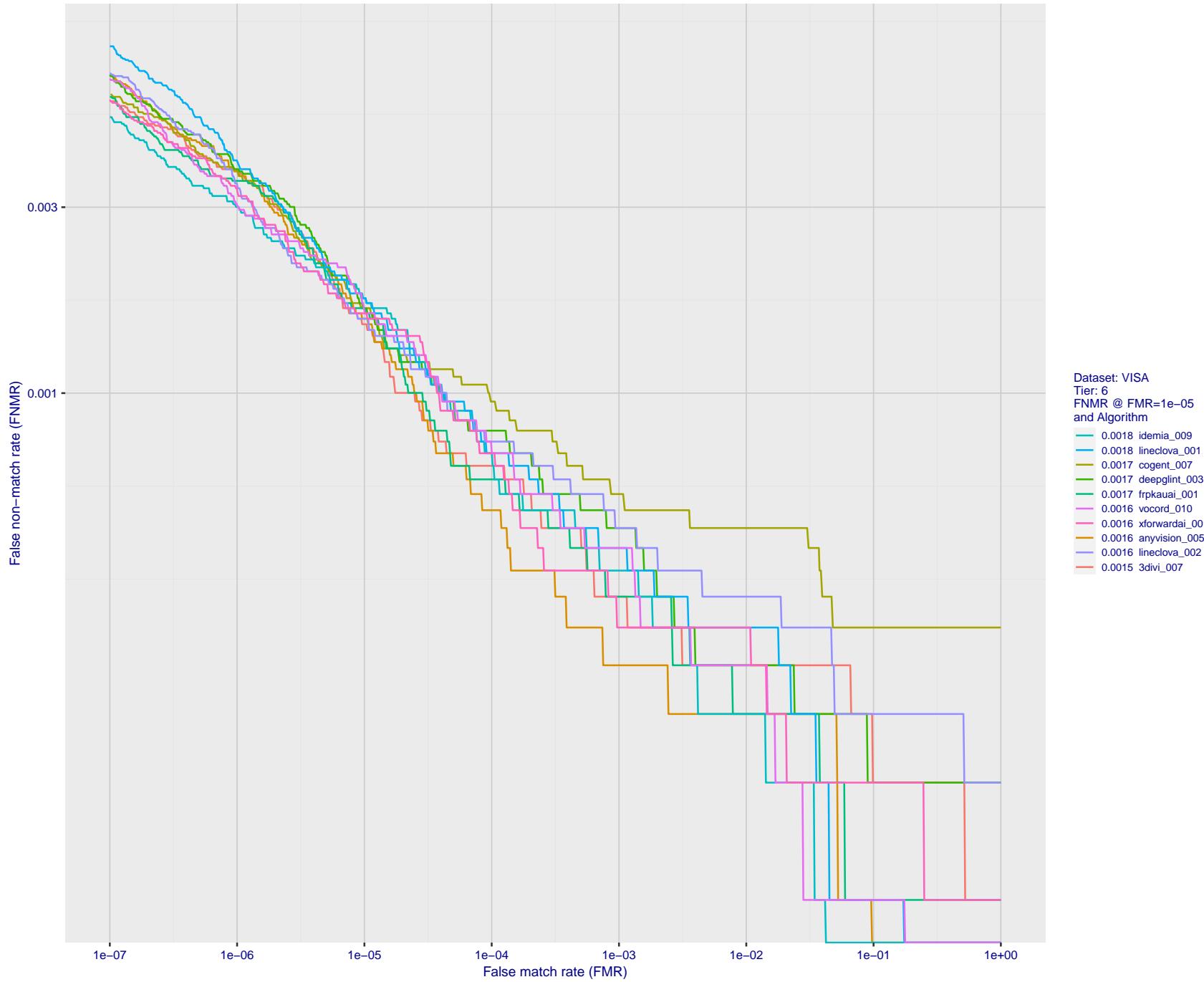


Figure 49: For the visa images, detection error tradeoff (DET) characteristics showing false non-match rate vs. false match rate plotted parametrically on threshold, T . The scales are logarithmic in order to show many decades of FMR.

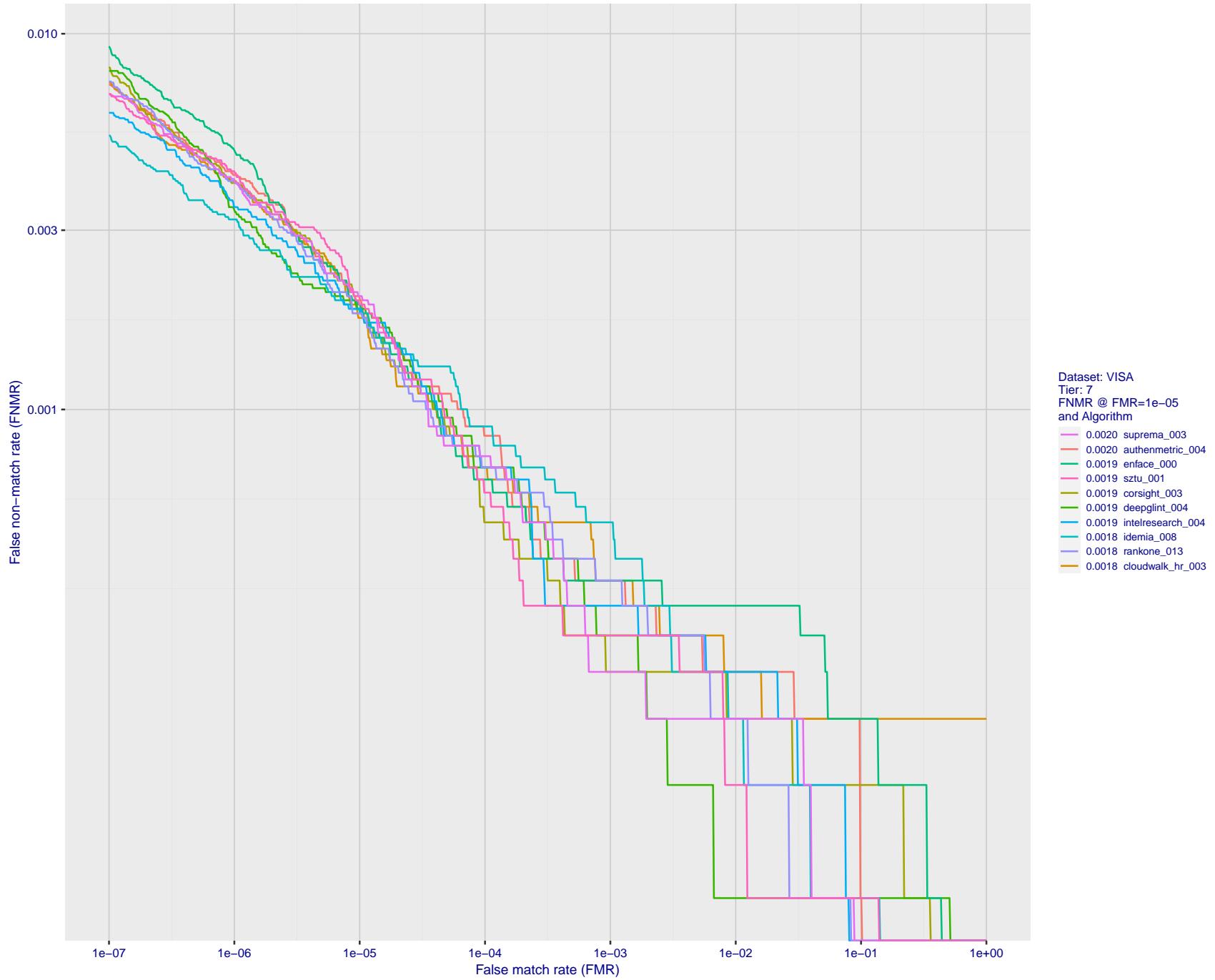


Figure 50: For the visa images, detection error tradeoff (DET) characteristics showing false non-match rate vs. false match rate plotted parametrically on threshold, T . The scales are logarithmic in order to show many decades of FMR.

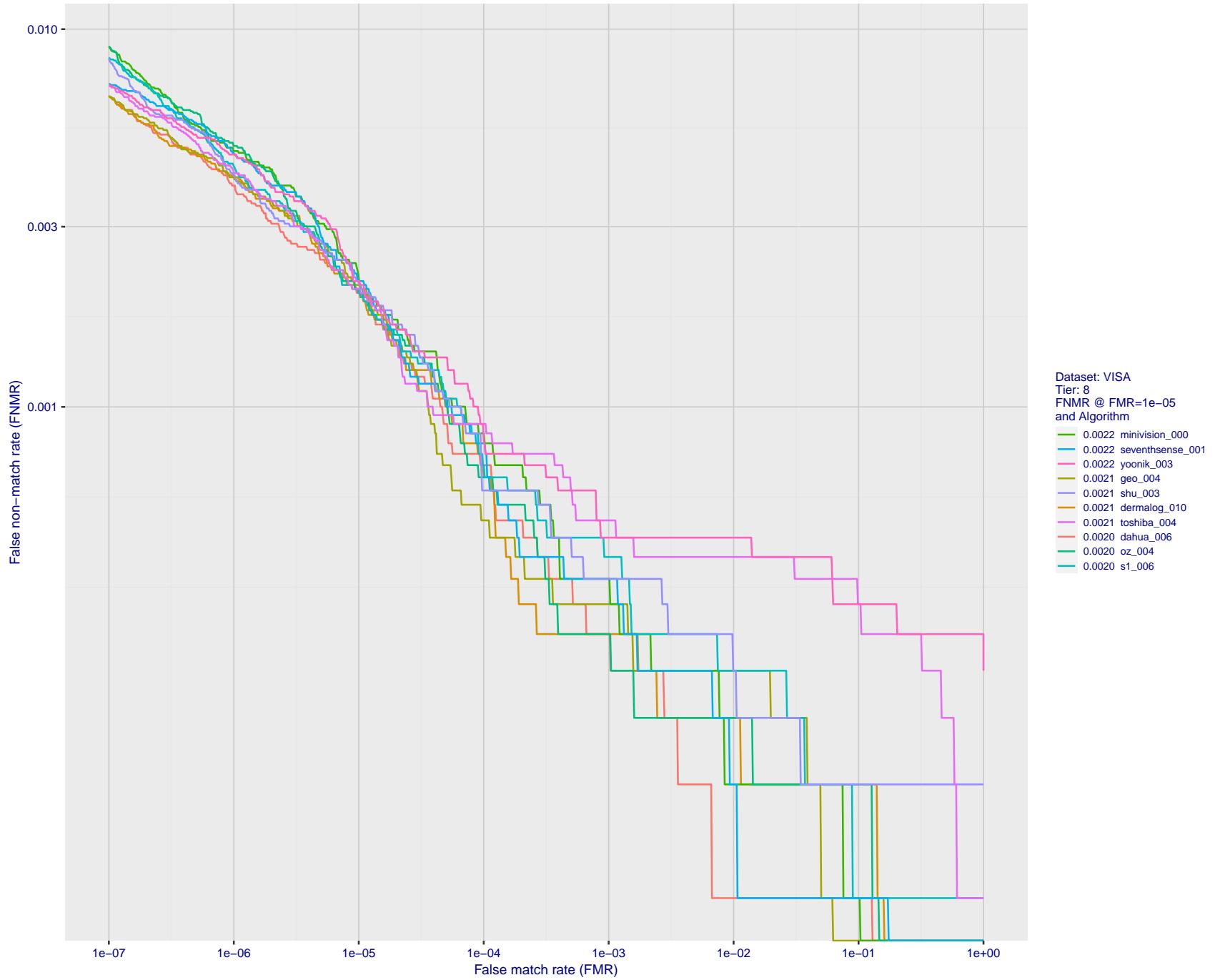


Figure 51: For the visa images, detection error tradeoff (DET) characteristics showing false non-match rate vs. false match rate plotted parametrically on threshold, T . The scales are logarithmic in order to show many decades of FMR.

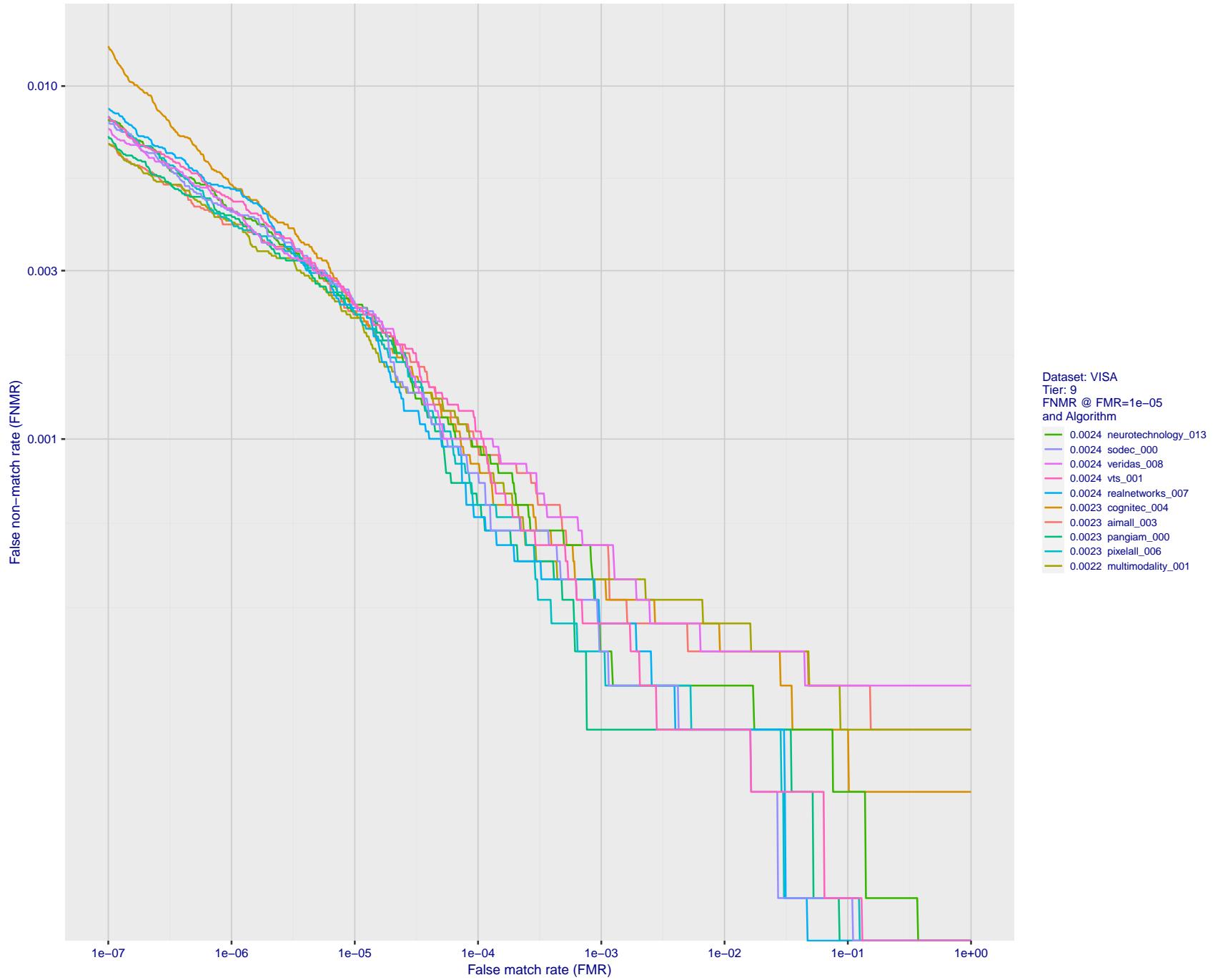


Figure 52: For the visa images, detection error tradeoff (DET) characteristics showing false non-match rate vs. false match rate plotted parametrically on threshold, T . The scales are logarithmic in order to show many decades of FMR.

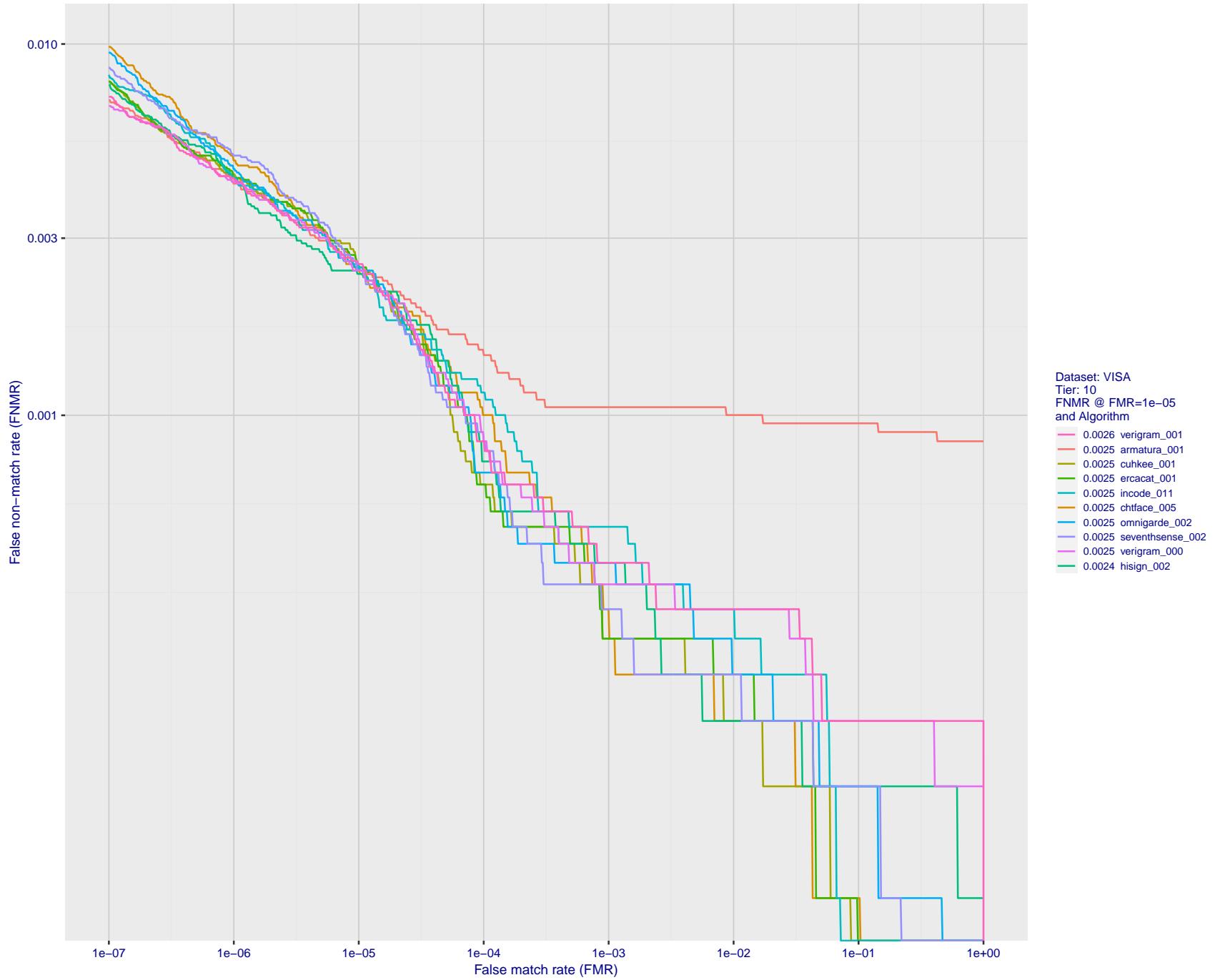


Figure 53: For the visa images, detection error tradeoff (DET) characteristics showing false non-match rate vs. false match rate plotted parametrically on threshold, T . The scales are logarithmic in order to show many decades of FMR.

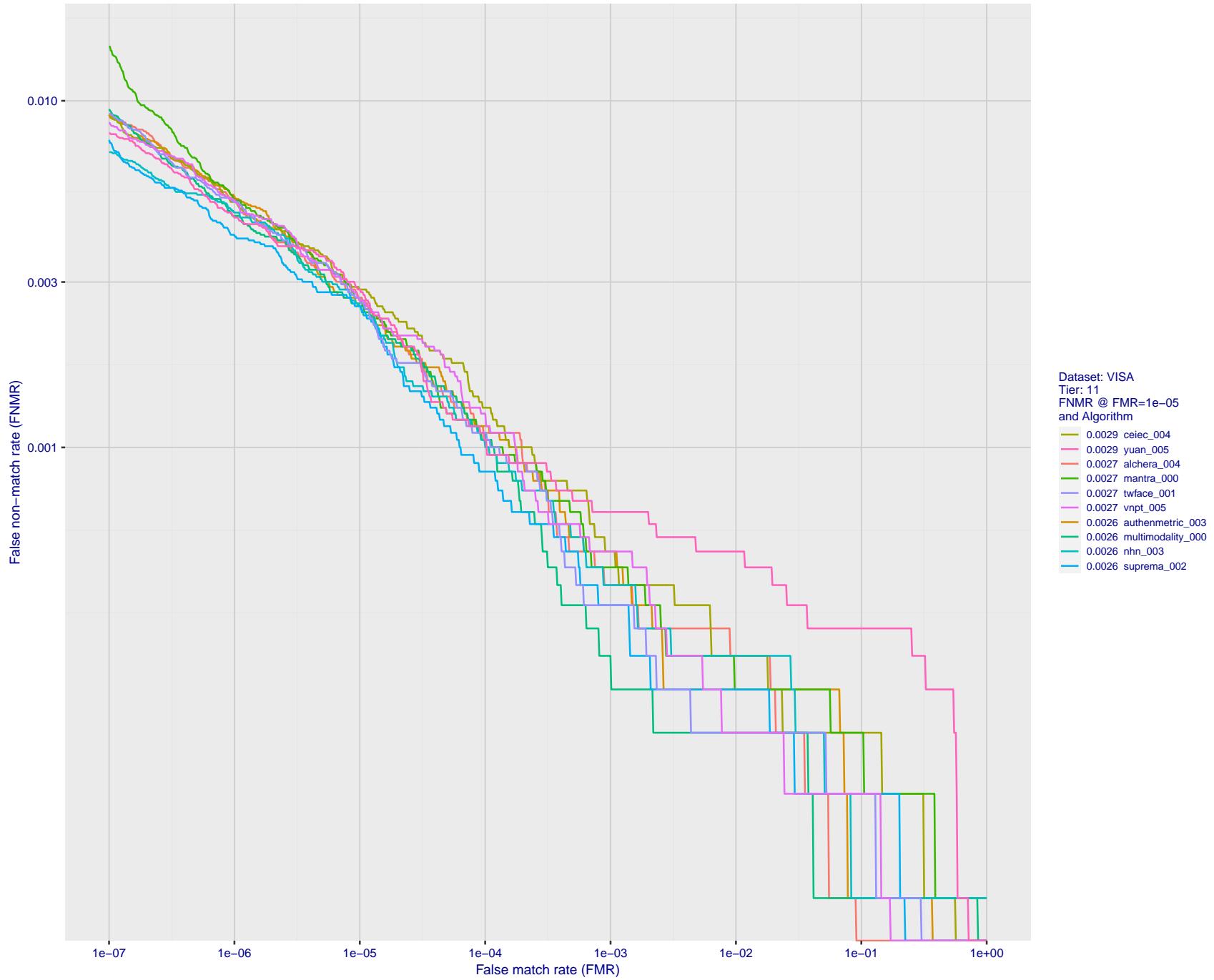


Figure 54: For the visa images, detection error tradeoff (DET) characteristics showing false non-match rate vs. false match rate plotted parametrically on threshold, T . The scales are logarithmic in order to show many decades of FMR.

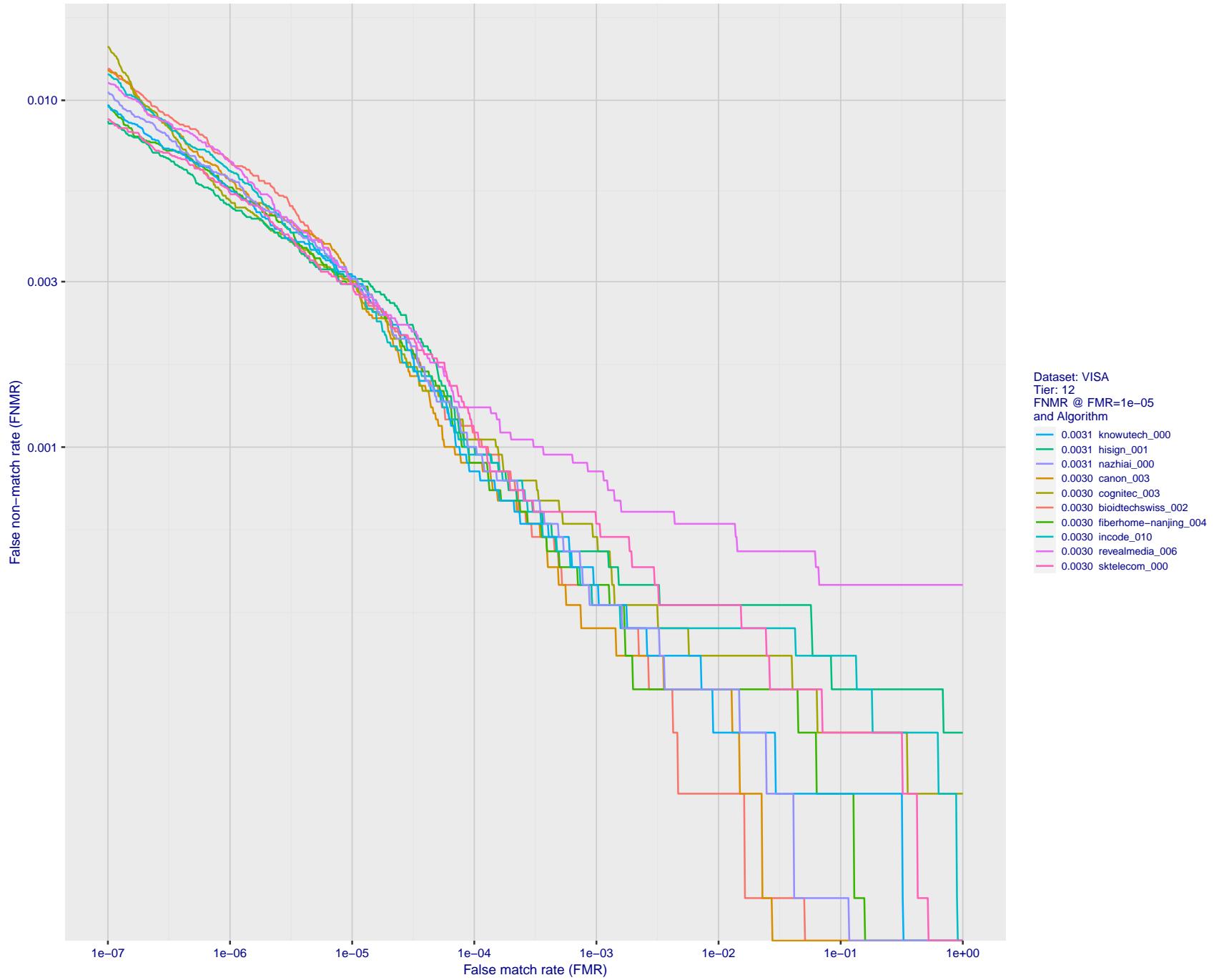


Figure 55: For the visa images, detection error tradeoff (DET) characteristics showing false non-match rate vs. false match rate plotted parametrically on threshold, T . The scales are logarithmic in order to show many decades of FMR.

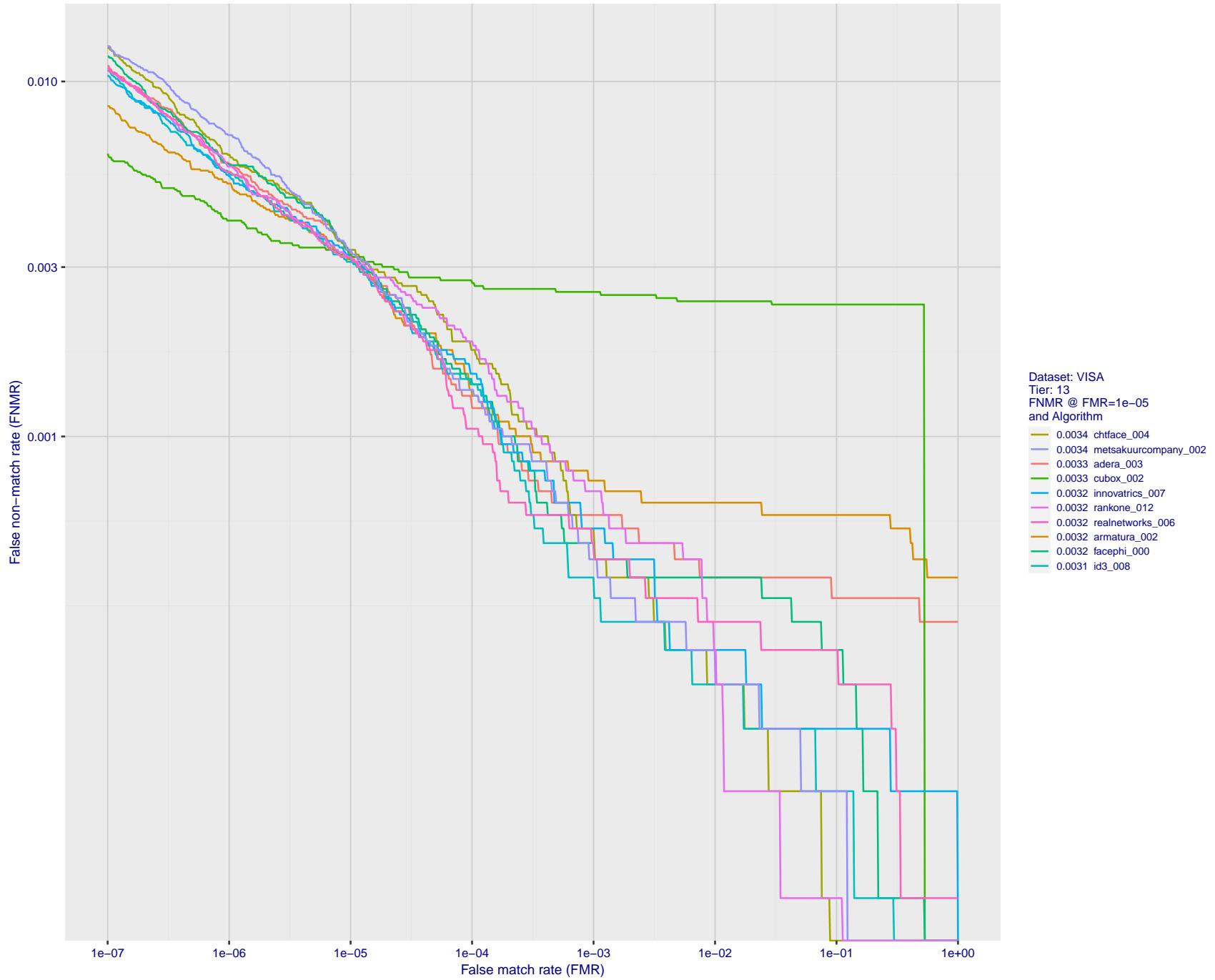


Figure 56: For the visa images, detection error tradeoff (DET) characteristics showing false non-match rate vs. false match rate plotted parametrically on threshold, T . The scales are logarithmic in order to show many decades of FMR.

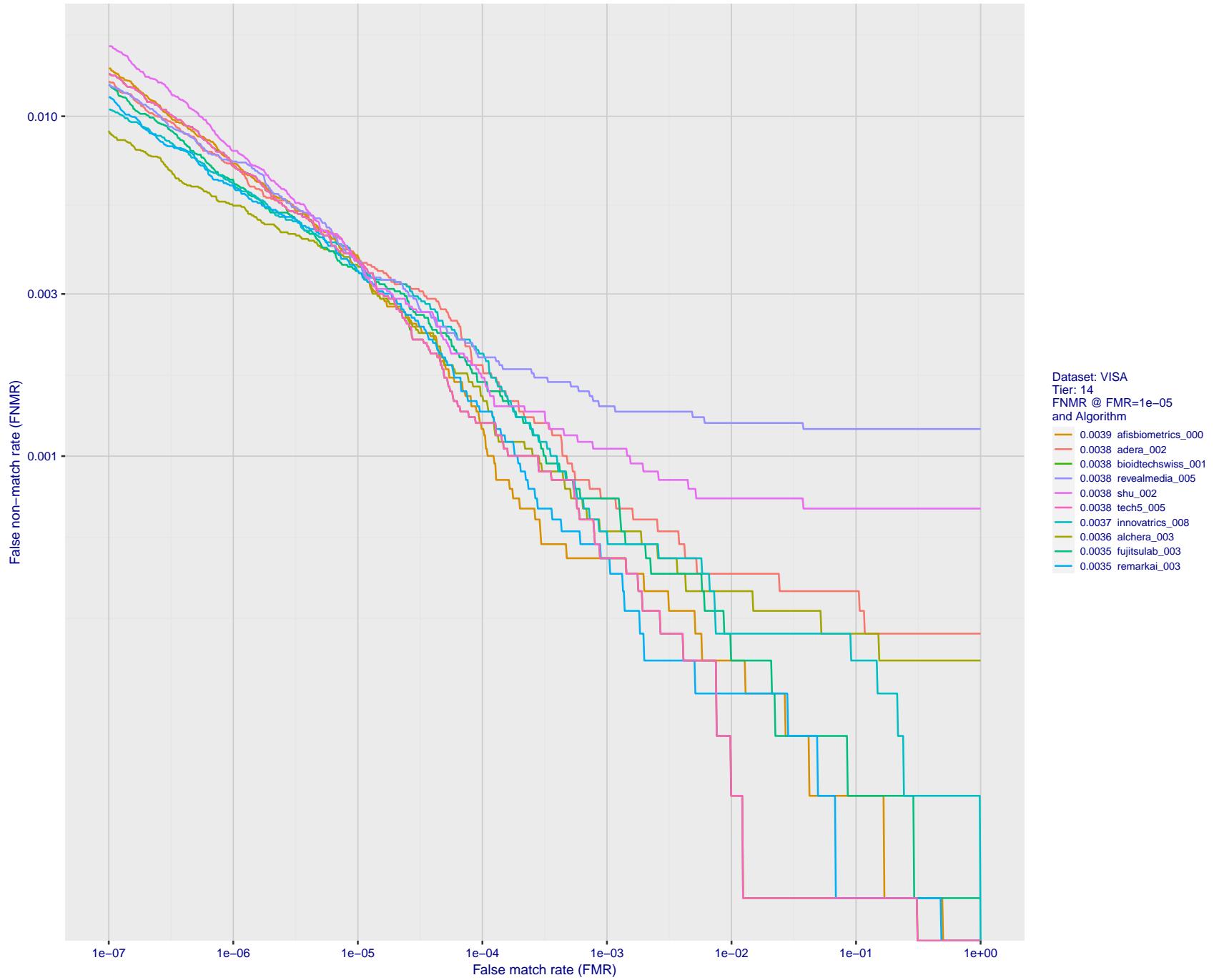


Figure 57: For the visa images, detection error tradeoff (DET) characteristics showing false non-match rate vs. false match rate plotted parametrically on threshold, T . The scales are logarithmic in order to show many decades of FMR.

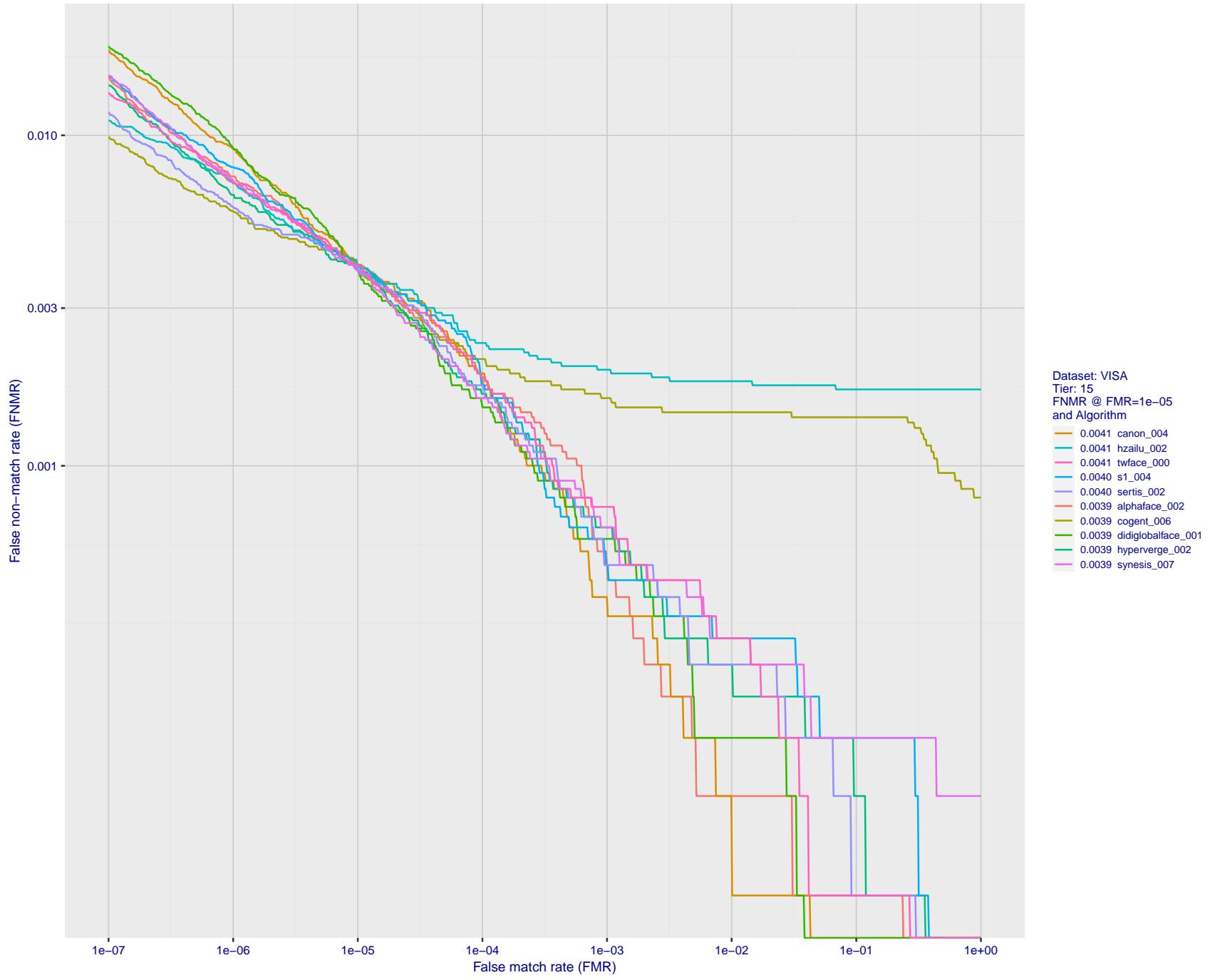


Figure 58: For the visa images, detection error tradeoff (DET) characteristics showing false non-match rate vs. false match rate plotted parametrically on threshold, T . The scales are logarithmic in order to show many decades of FMR.

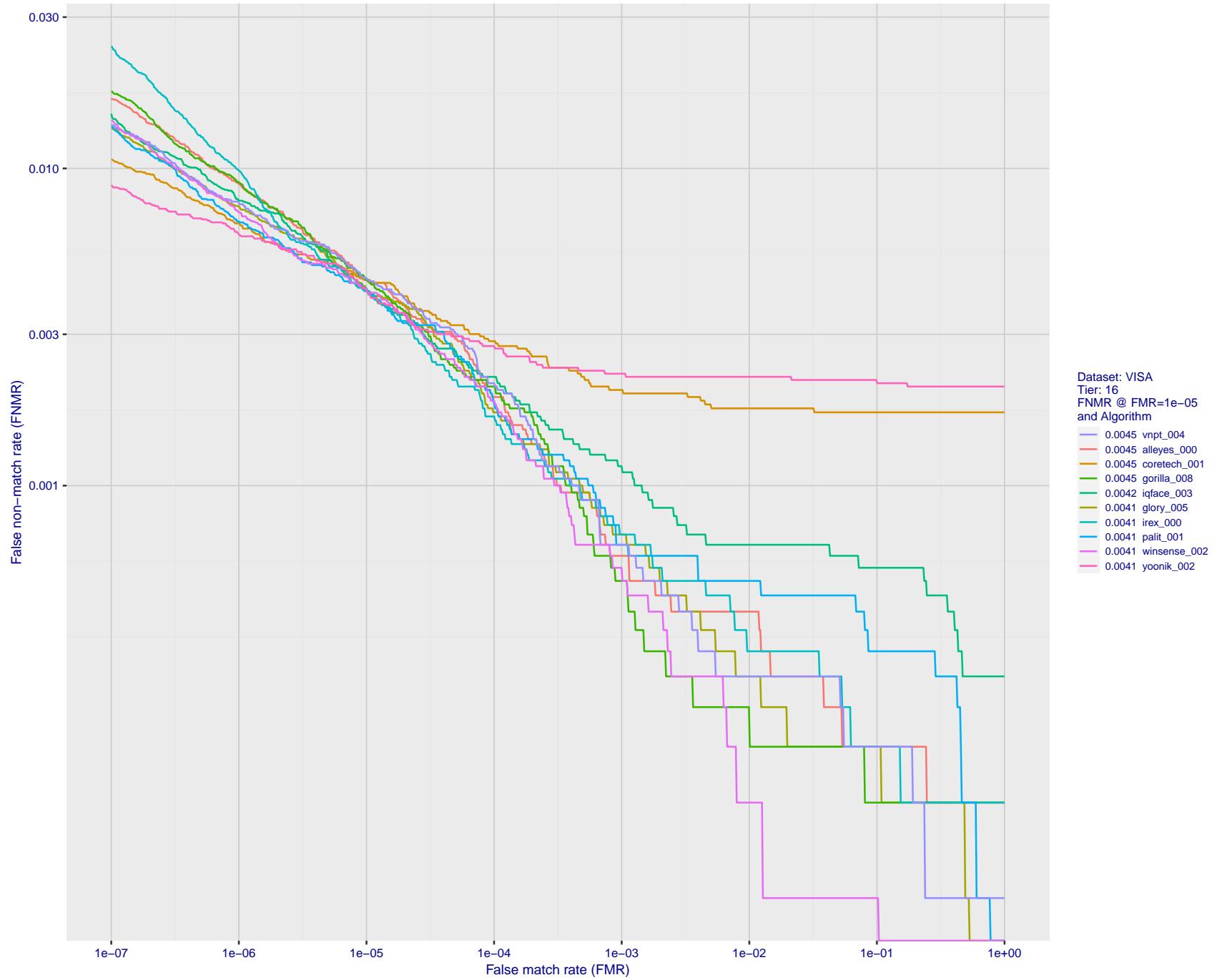


Figure 59: For the visa images, detection error tradeoff (DET) characteristics showing false non-match rate vs. false match rate plotted parametrically on threshold, T . The scales are logarithmic in order to show many decades of FMR.

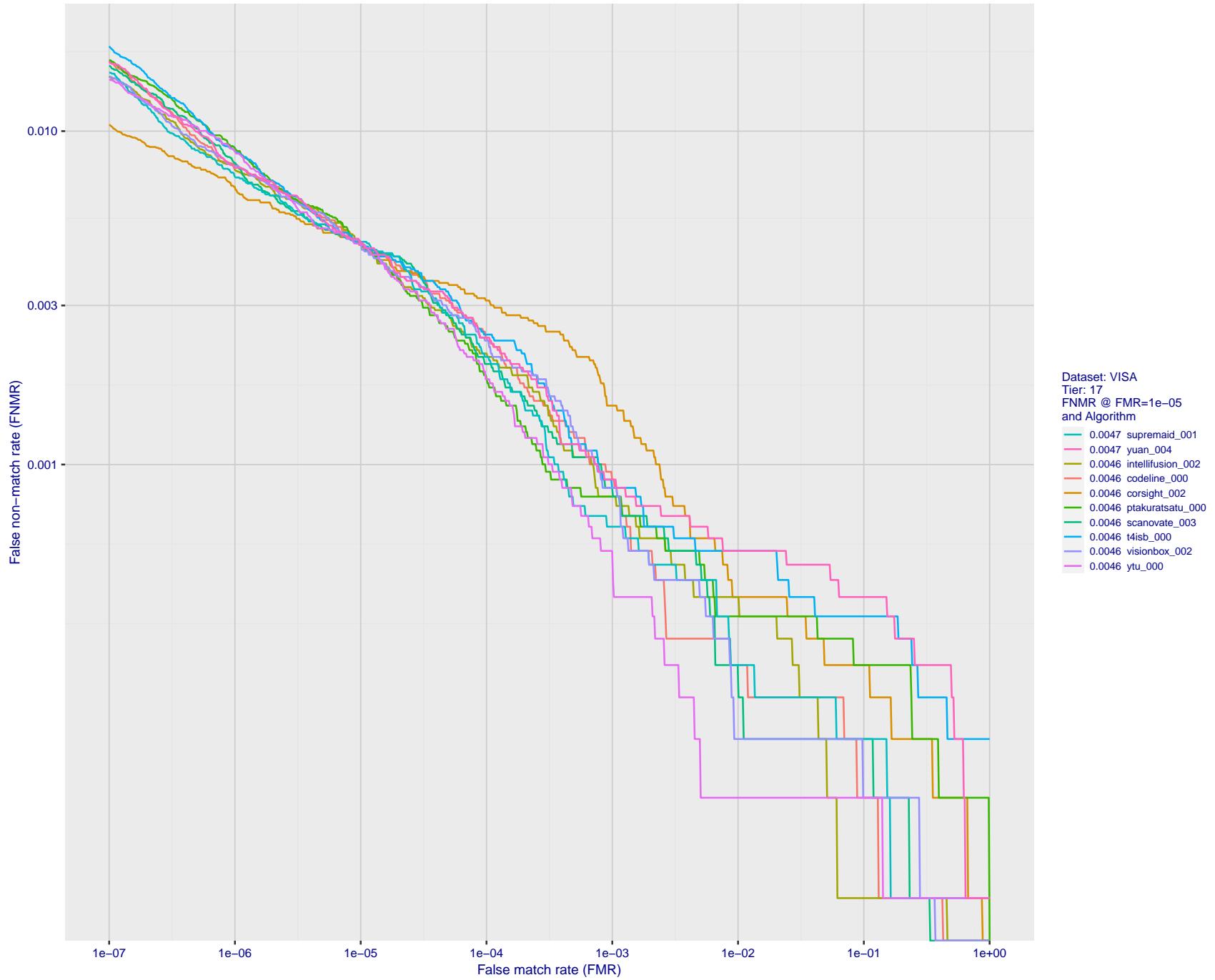


Figure 60: For the visa images, detection error tradeoff (DET) characteristics showing false non-match rate vs. false match rate plotted parametrically on threshold, T . The scales are logarithmic in order to show many decades of FMR.

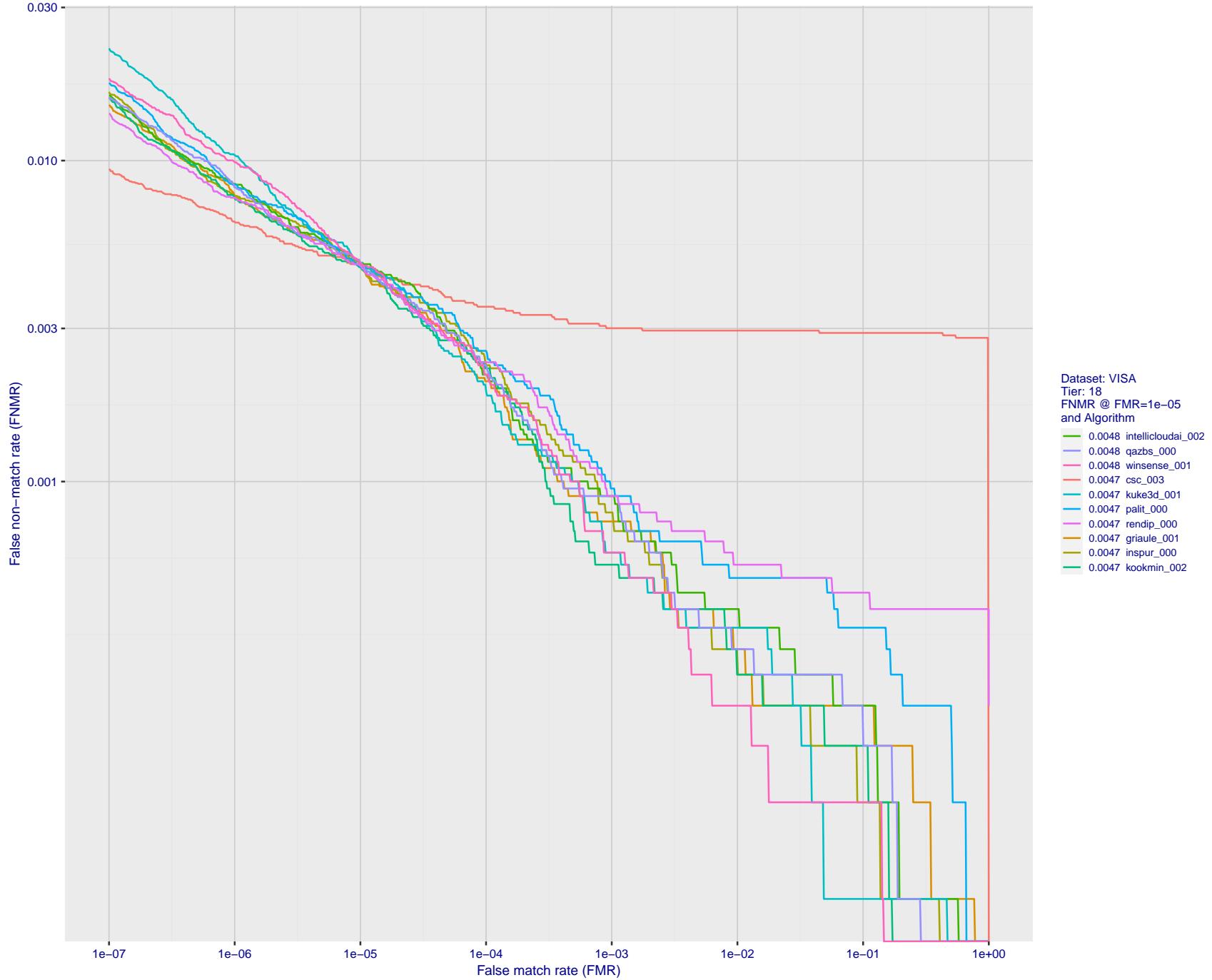


Figure 61: For the visa images, detection error tradeoff (DET) characteristics showing false non-match rate vs. false match rate plotted parametrically on threshold, T . The scales are logarithmic in order to show many decades of FMR.

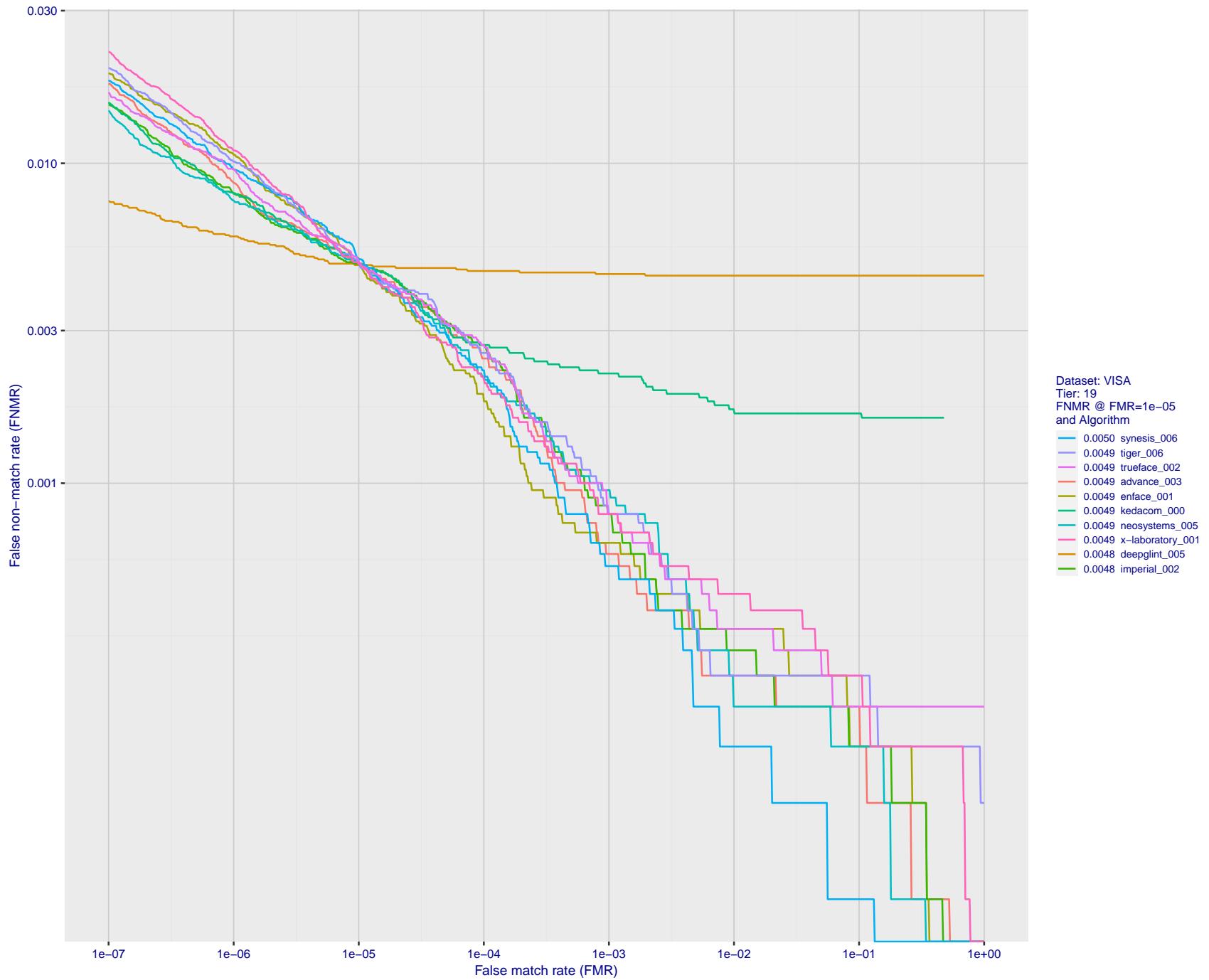


Figure 62: For the visa images, detection error tradeoff (DET) characteristics showing false non-match rate vs. false match rate plotted parametrically on threshold, T . The scales are logarithmic in order to show many decades of FMR.

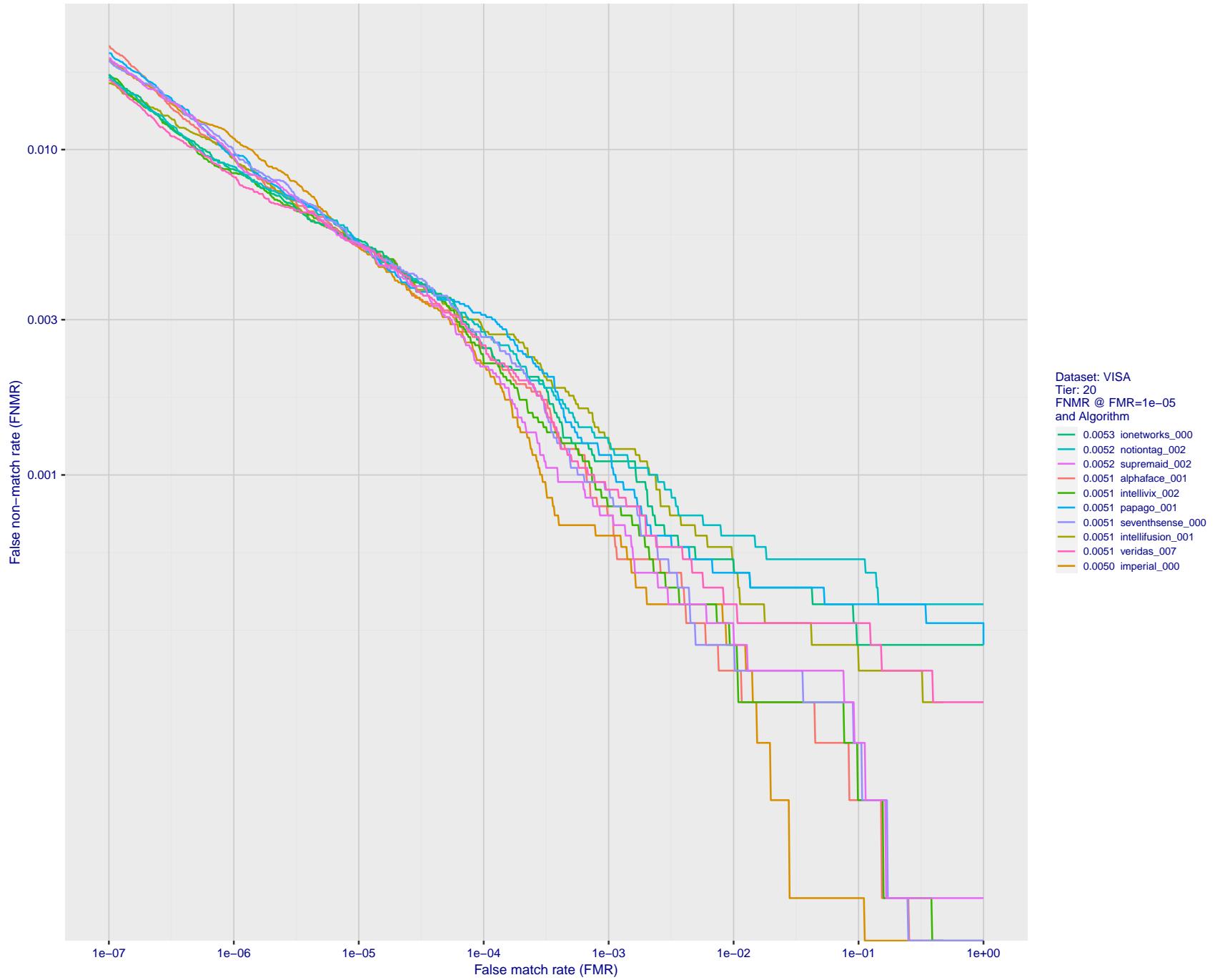


Figure 63: For the visa images, detection error tradeoff (DET) characteristics showing false non-match rate vs. false match rate plotted parametrically on threshold, T . The scales are logarithmic in order to show many decades of FMR.

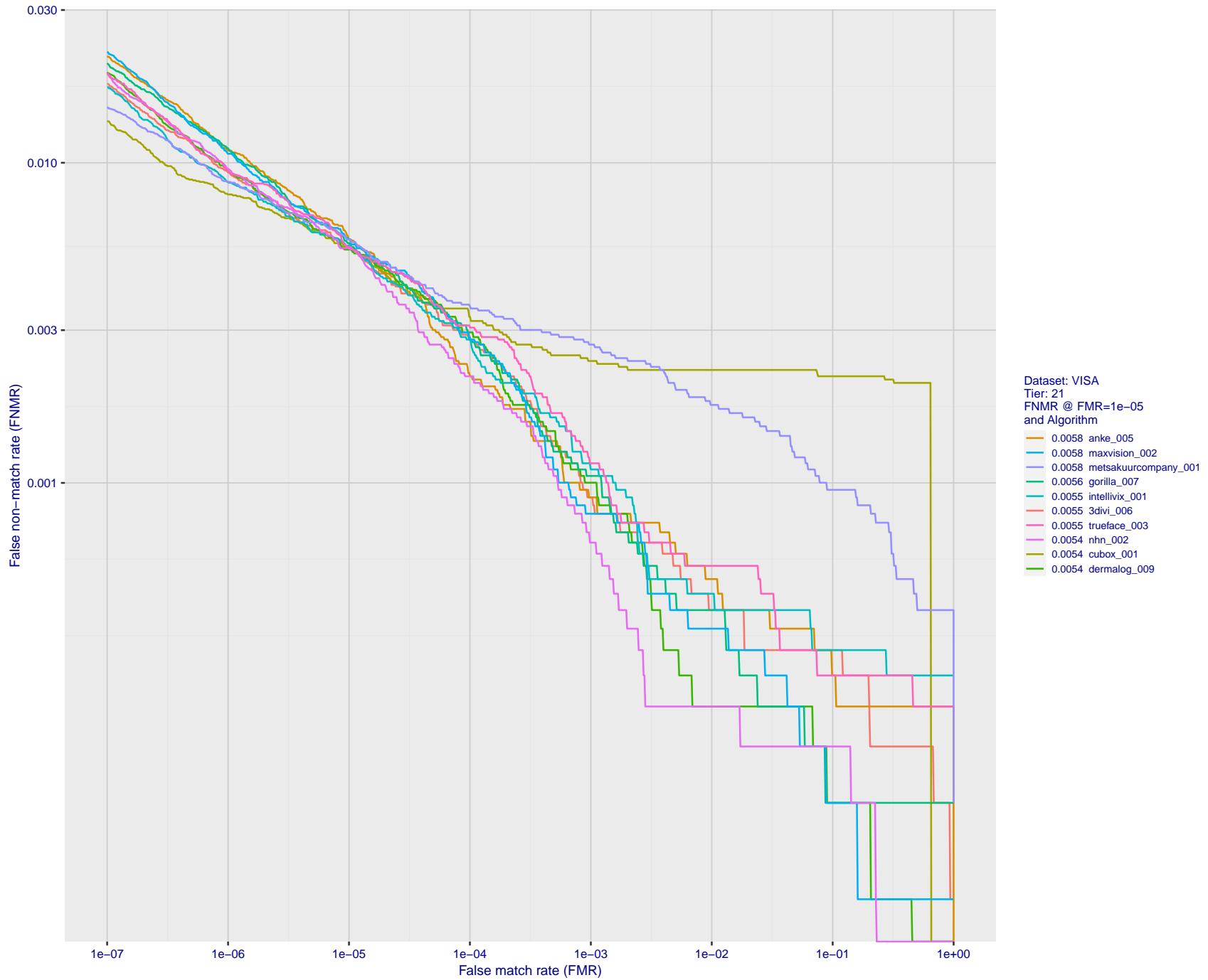


Figure 64: For the visa images, detection error tradeoff (DET) characteristics showing false non-match rate vs. false match rate plotted parametrically on threshold, T . The scales are logarithmic in order to show many decades of FMR.

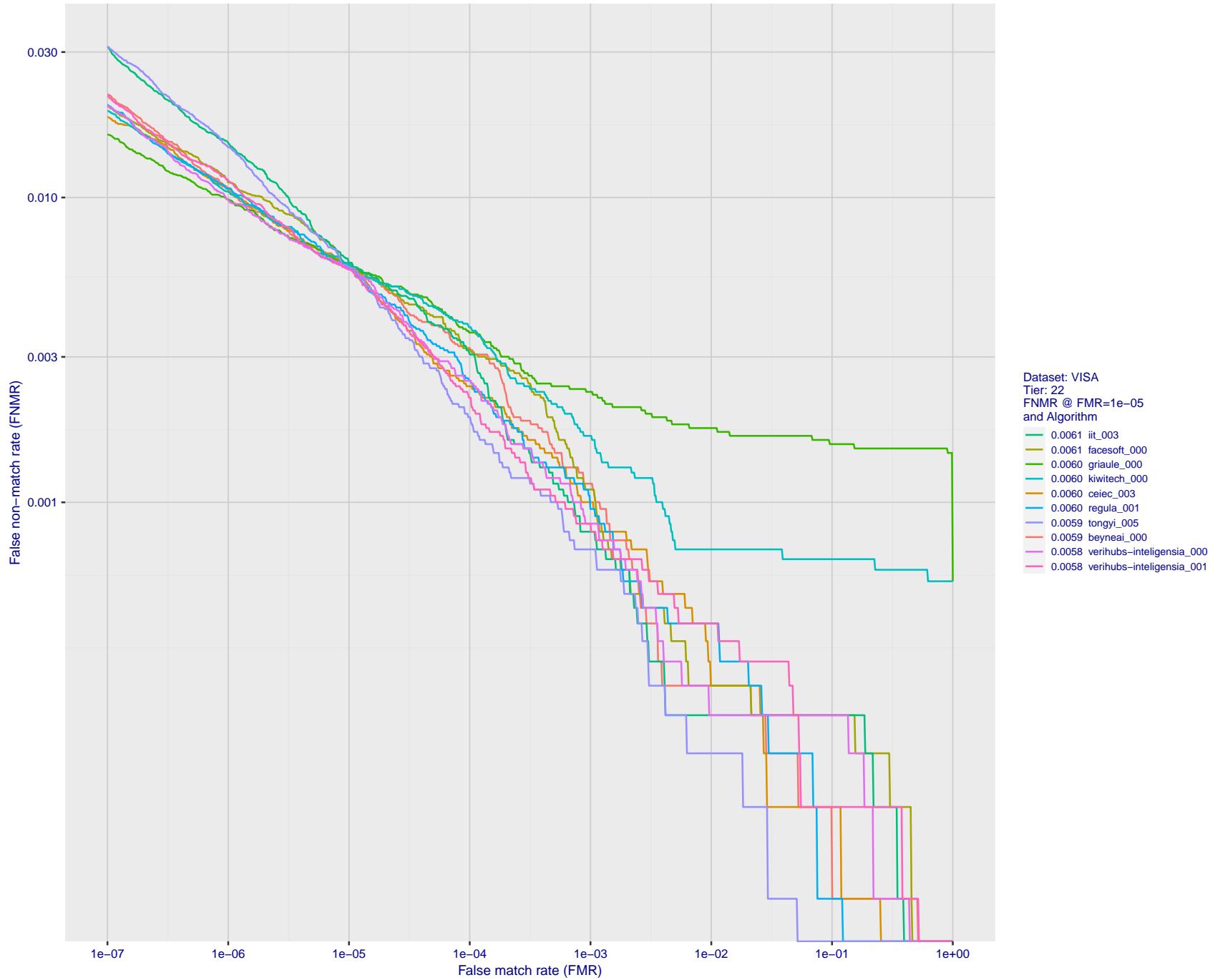


Figure 65: For the visa images, detection error tradeoff (DET) characteristics showing false non-match rate vs. false match rate plotted parametrically on threshold, T . The scales are logarithmic in order to show many decades of FMR.

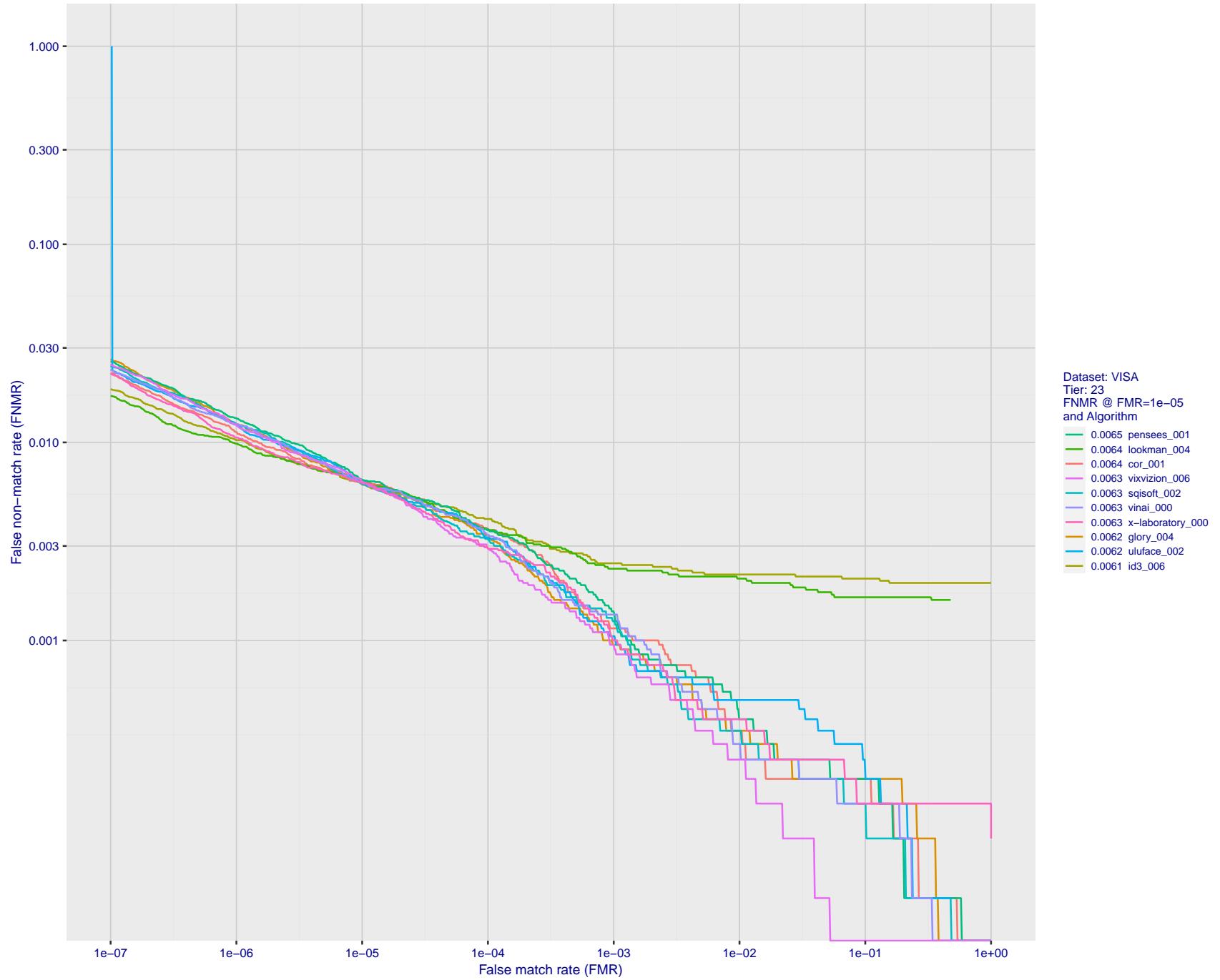


Figure 66: For the visa images, detection error tradeoff (DET) characteristics showing false non-match rate vs. false match rate plotted parametrically on threshold, T . The scales are logarithmic in order to show many decades of FMR.

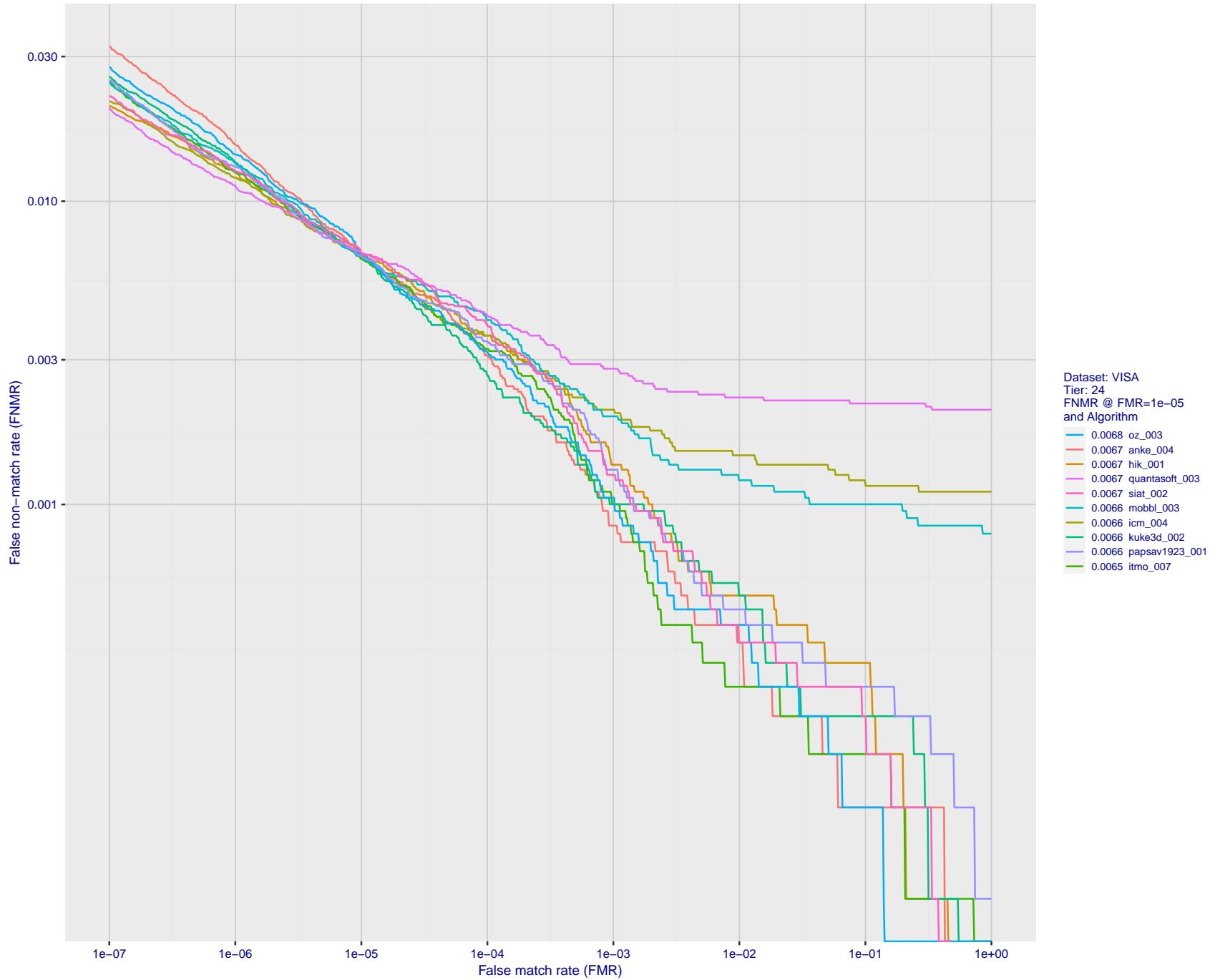


Figure 67: For the visa images, detection error tradeoff (DET) characteristics showing false non-match rate vs. false match rate plotted parametrically on threshold, T . The scales are logarithmic in order to show many decades of FMR.

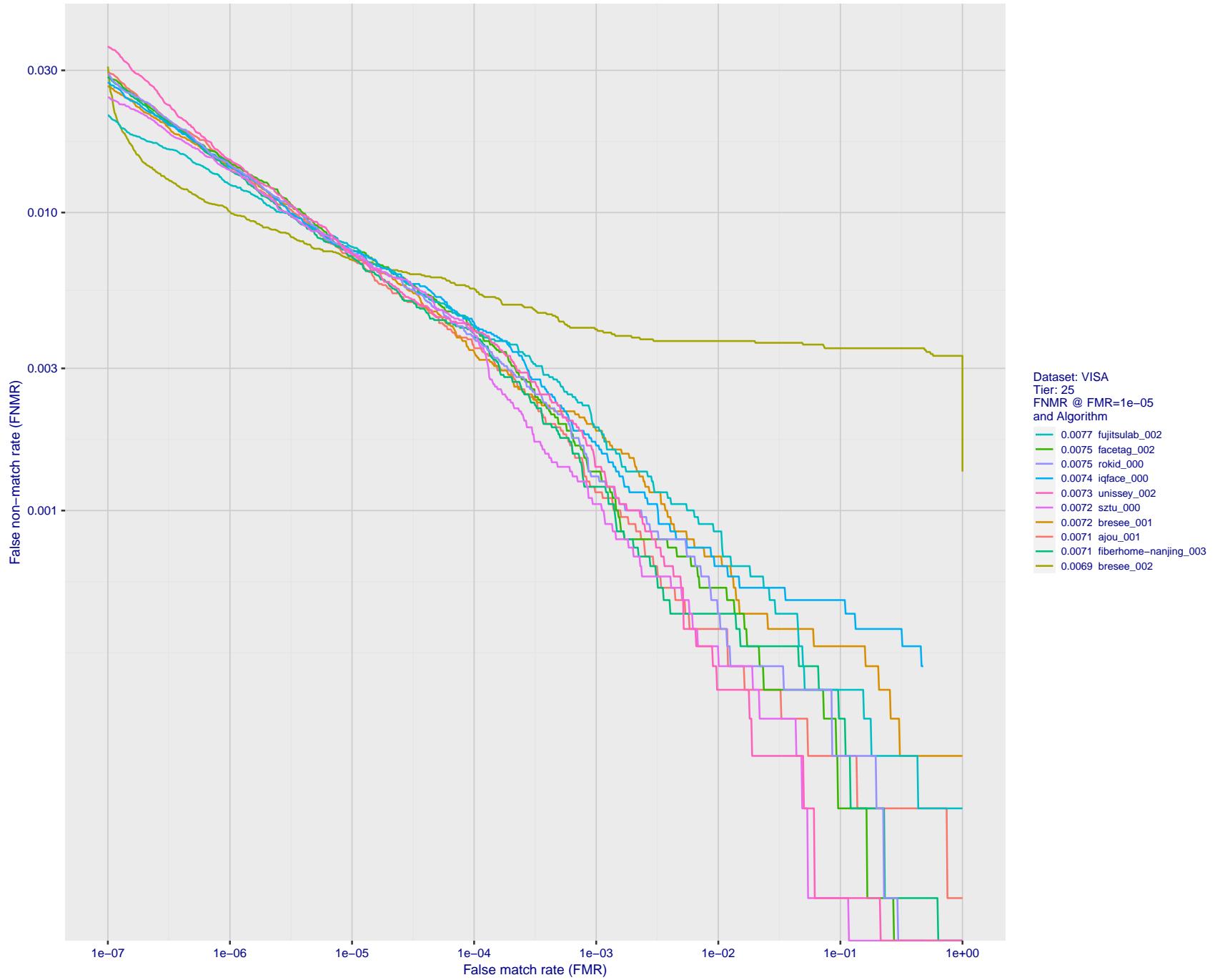


Figure 68: For the visa images, detection error tradeoff (DET) characteristics showing false non-match rate vs. false match rate plotted parametrically on threshold, T . The scales are logarithmic in order to show many decades of FMR.

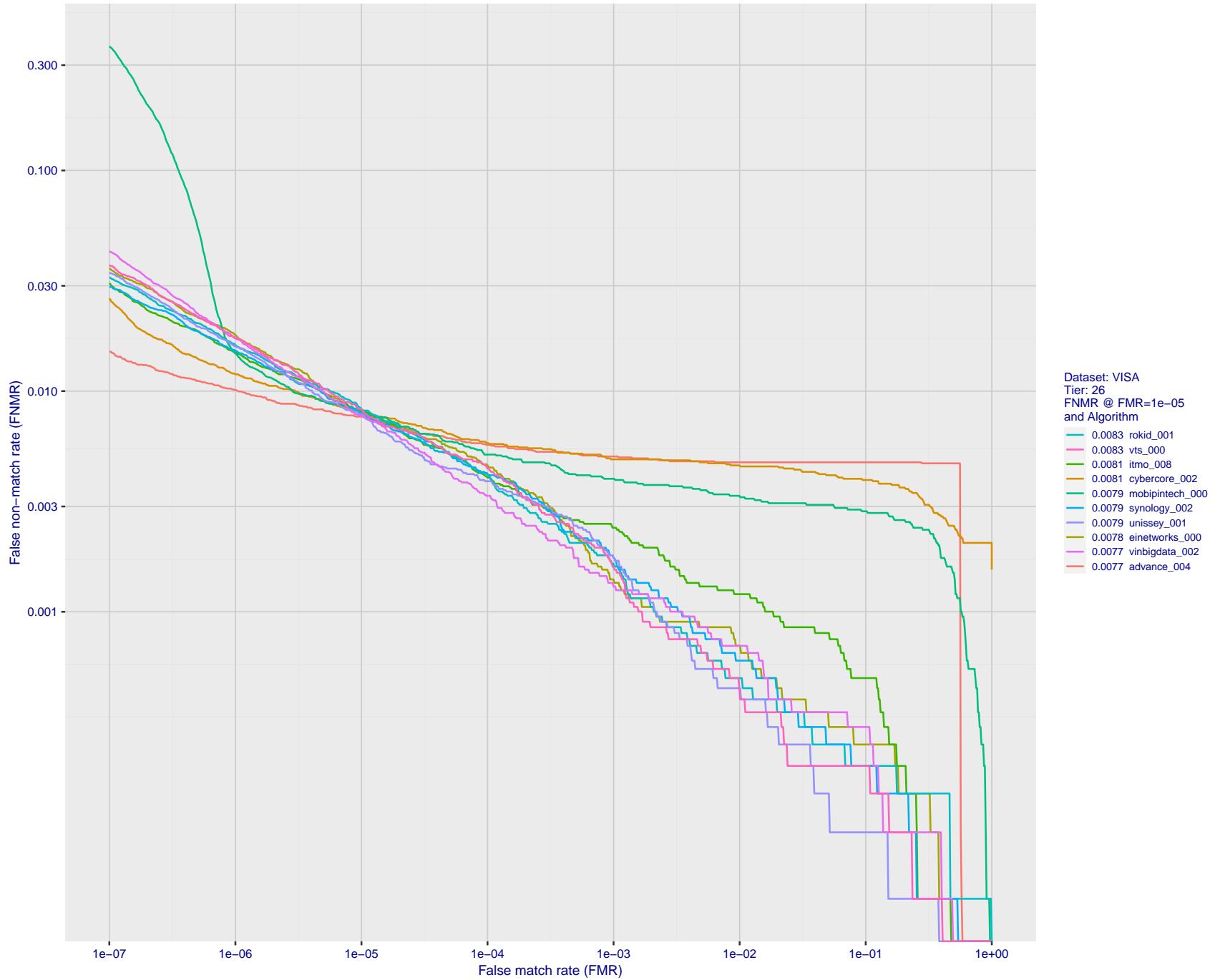


Figure 69: For the visa images, detection error tradeoff (DET) characteristics showing false non-match rate vs. false match rate plotted parametrically on threshold, T . The scales are logarithmic in order to show many decades of FMR.

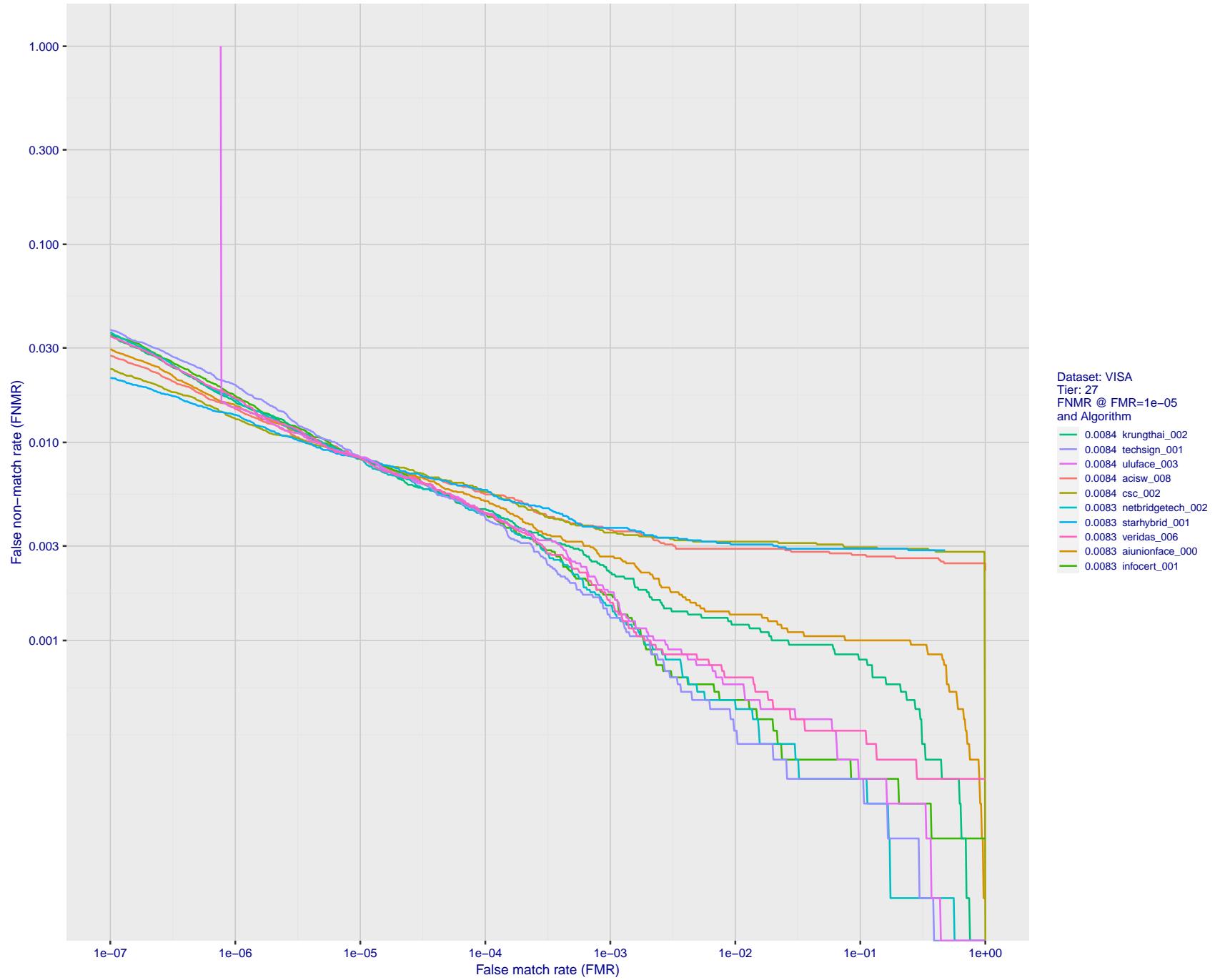


Figure 70: For the visa images, detection error tradeoff (DET) characteristics showing false non-match rate vs. false match rate plotted parametrically on threshold, T . The scales are logarithmic in order to show many decades of FMR.

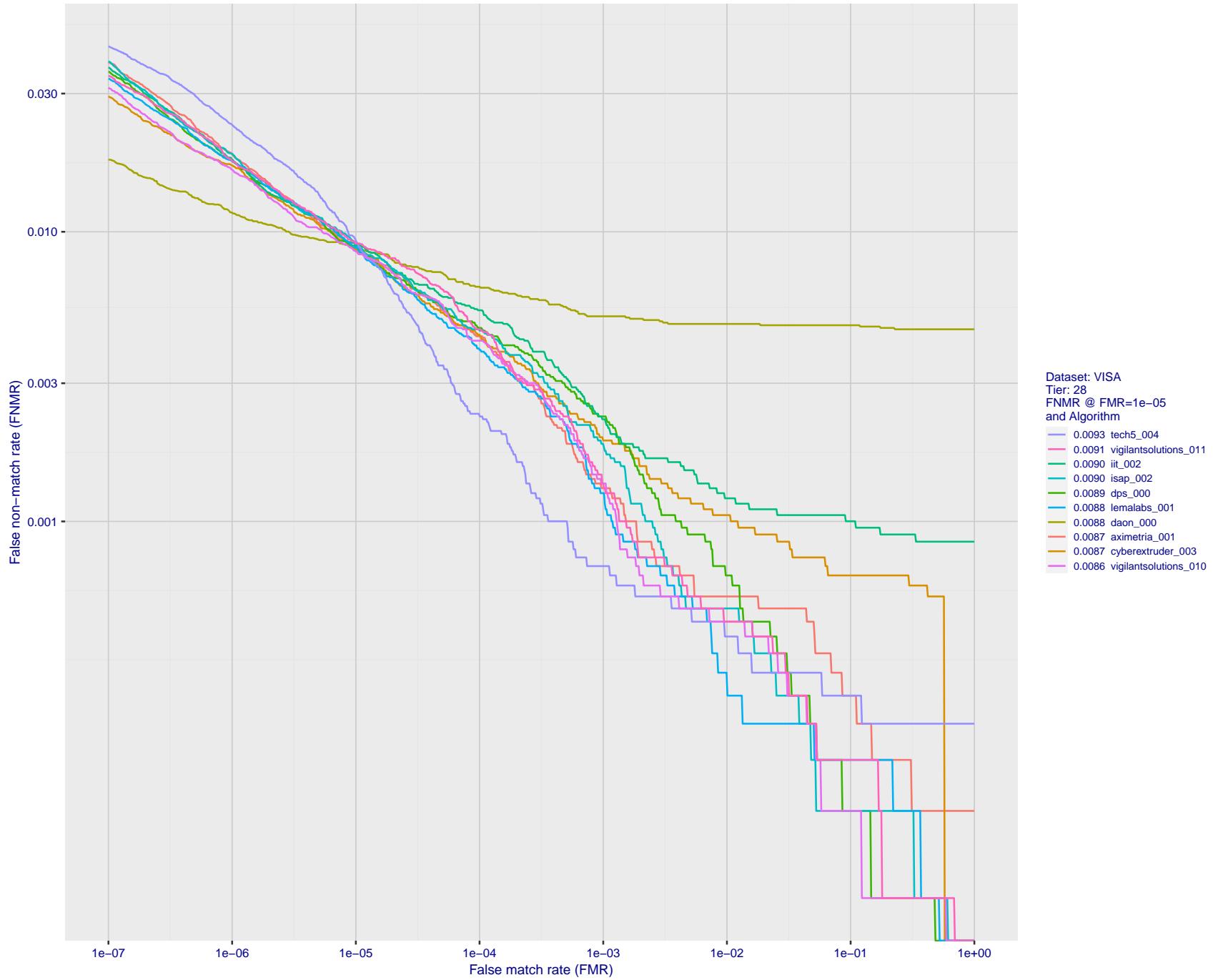


Figure 71: For the visa images, detection error tradeoff (DET) characteristics showing false non-match rate vs. false match rate plotted parametrically on threshold, T . The scales are logarithmic in order to show many decades of FMR.

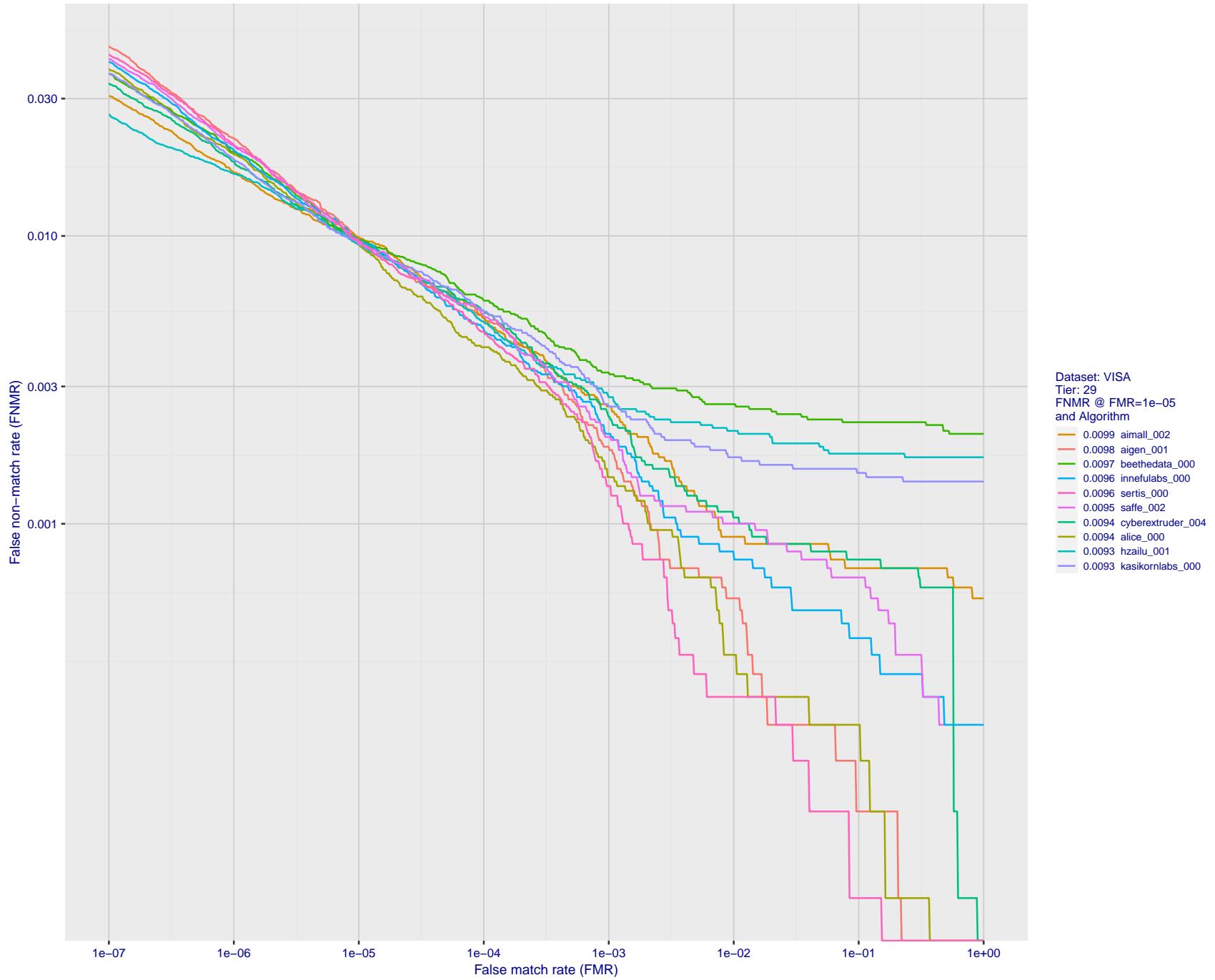


Figure 72: For the visa images, detection error tradeoff (DET) characteristics showing false non-match rate vs. false match rate plotted parametrically on threshold, T . The scales are logarithmic in order to show many decades of FMR.

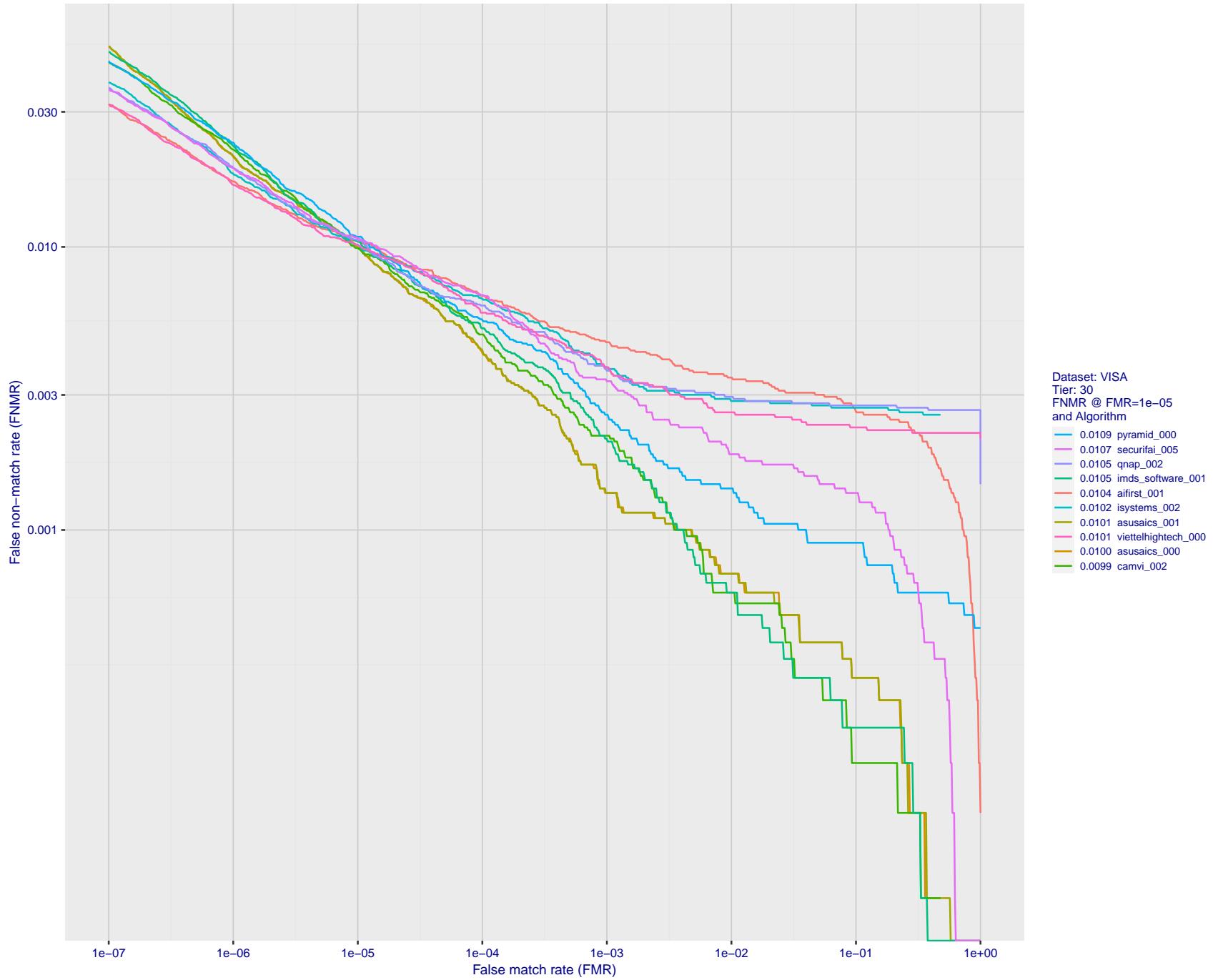


Figure 73: For the visa images, detection error tradeoff (DET) characteristics showing false non-match rate vs. false match rate plotted parametrically on threshold, T . The scales are logarithmic in order to show many decades of FMR.

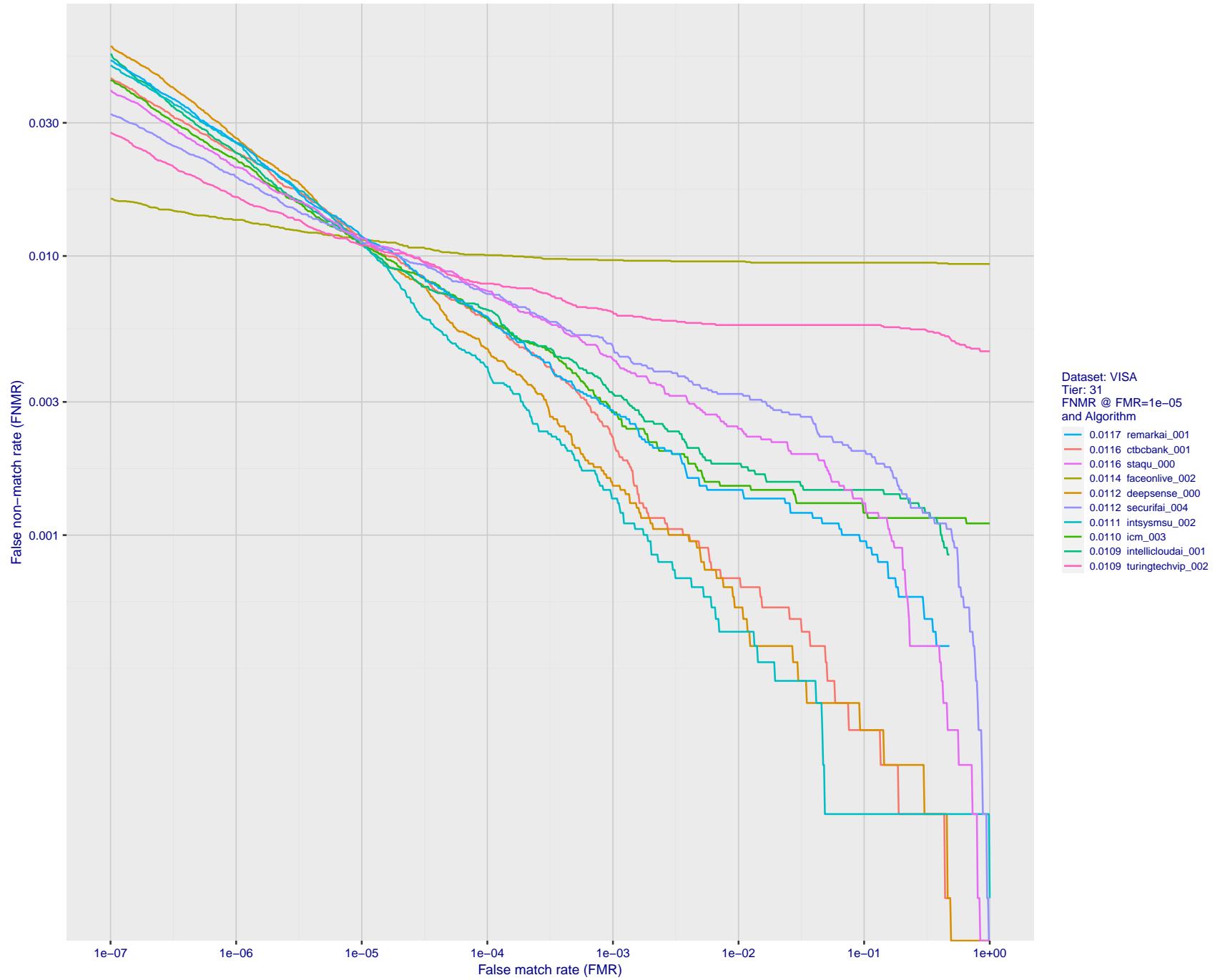


Figure 74: For the visa images, detection error tradeoff (DET) characteristics showing false non-match rate vs. false match rate plotted parametrically on threshold, T . The scales are logarithmic in order to show many decades of FMR.

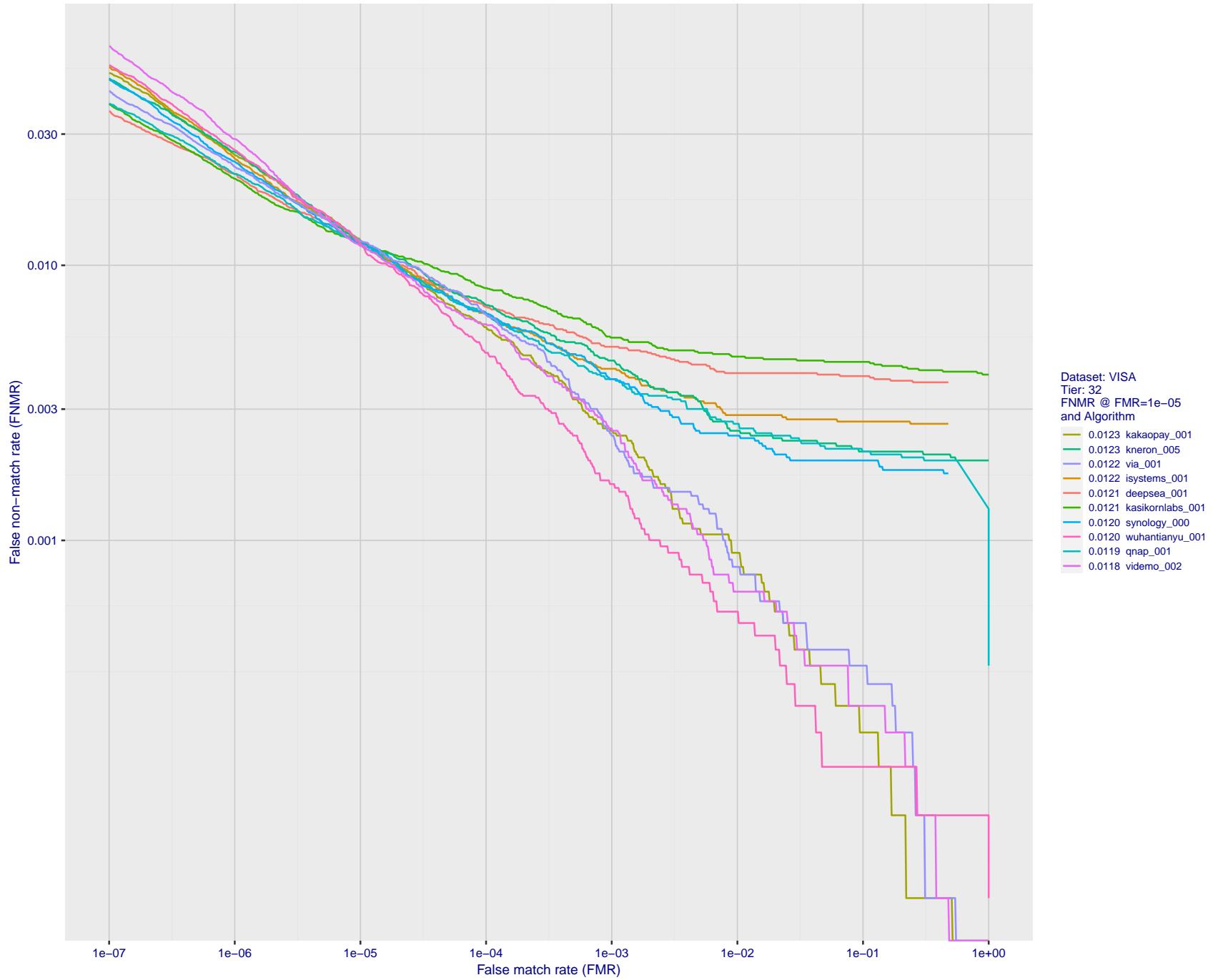


Figure 75: For the visa images, detection error tradeoff (DET) characteristics showing false non-match rate vs. false match rate plotted parametrically on threshold, T . The scales are logarithmic in order to show many decades of FMR.

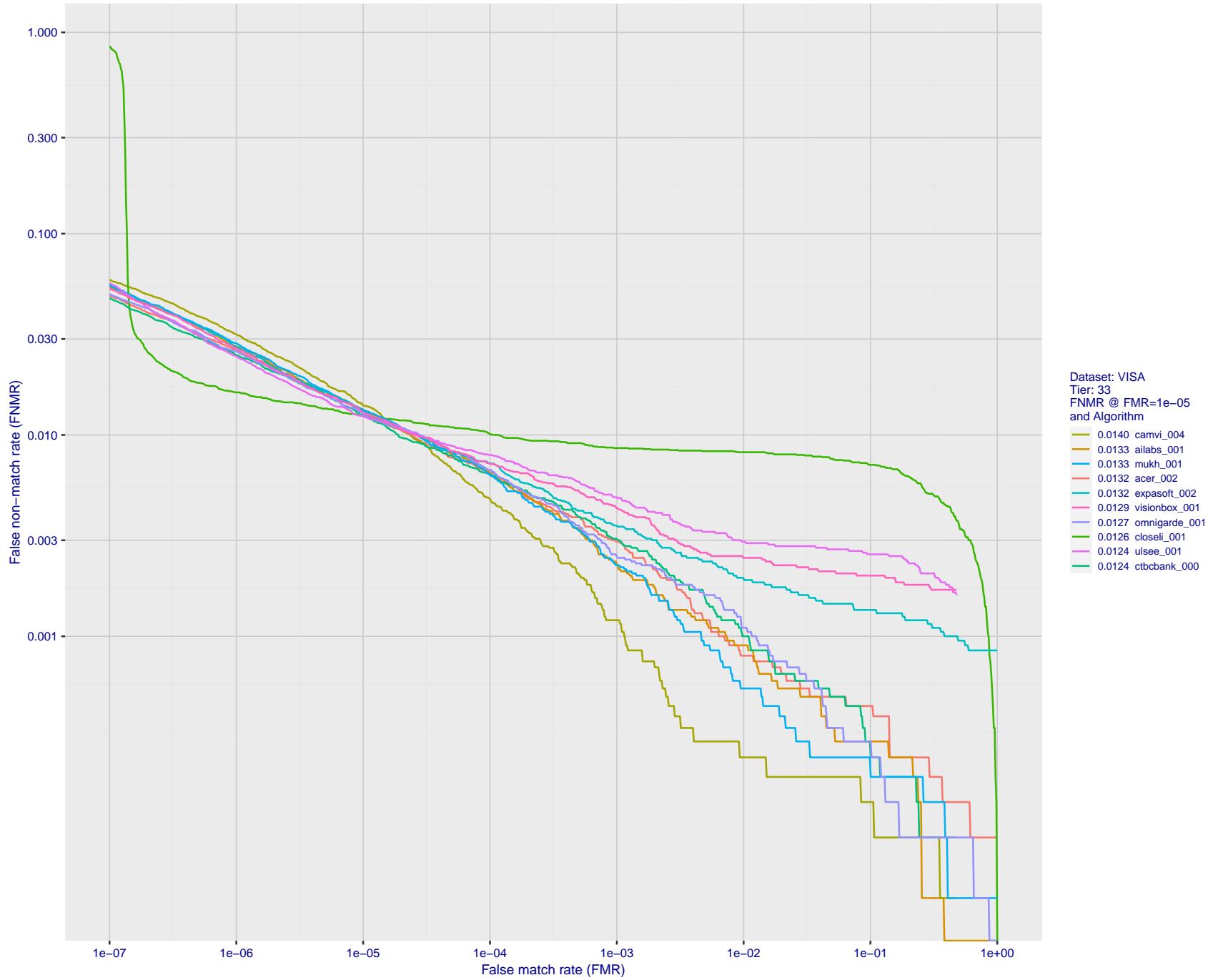


Figure 76: For the visa images, detection error tradeoff (DET) characteristics showing false non-match rate vs. false match rate plotted parametrically on threshold, T . The scales are logarithmic in order to show many decades of FMR.

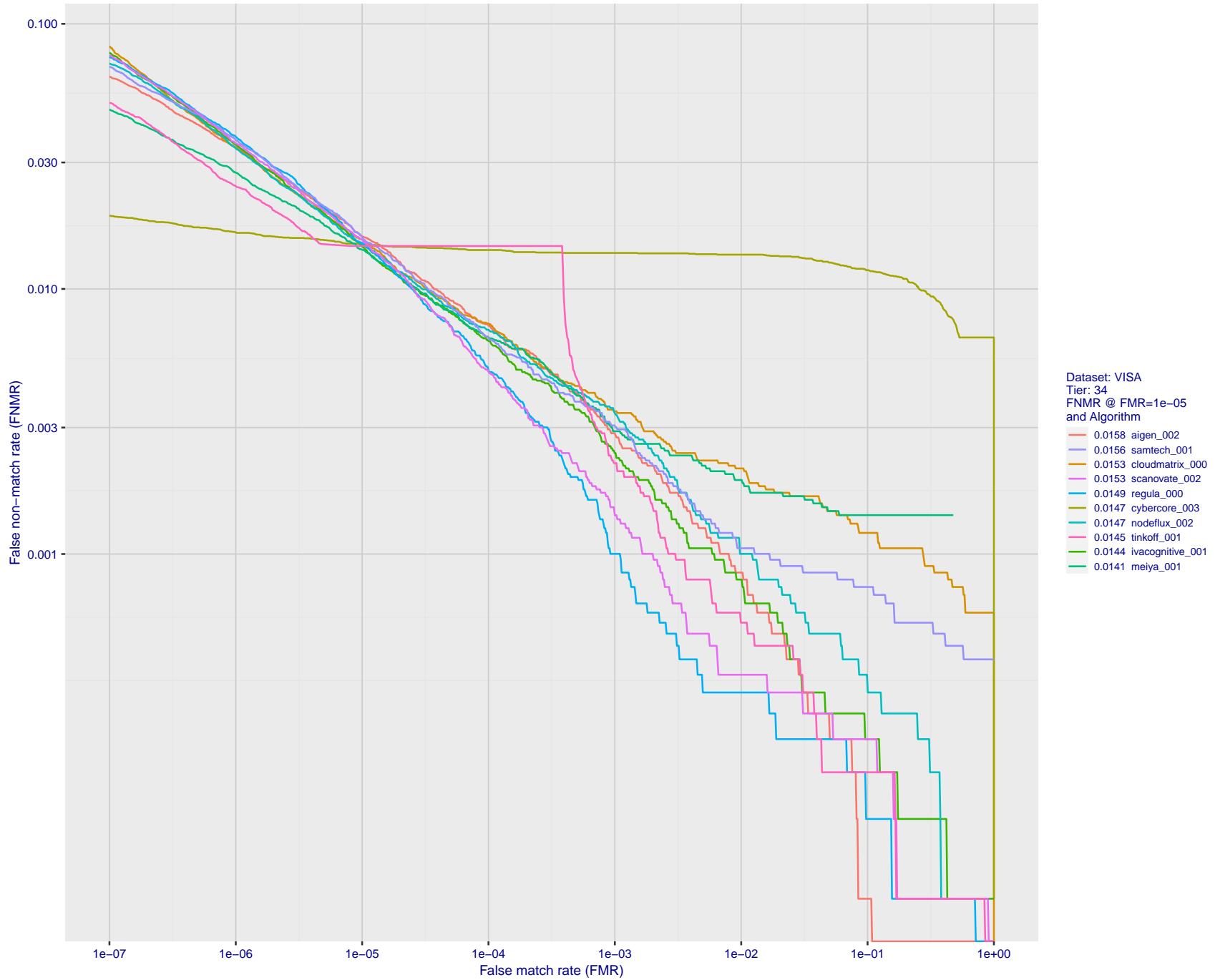


Figure 77: For the visa images, detection error tradeoff (DET) characteristics showing false non-match rate vs. false match rate plotted parametrically on threshold, T . The scales are logarithmic in order to show many decades of FMR.

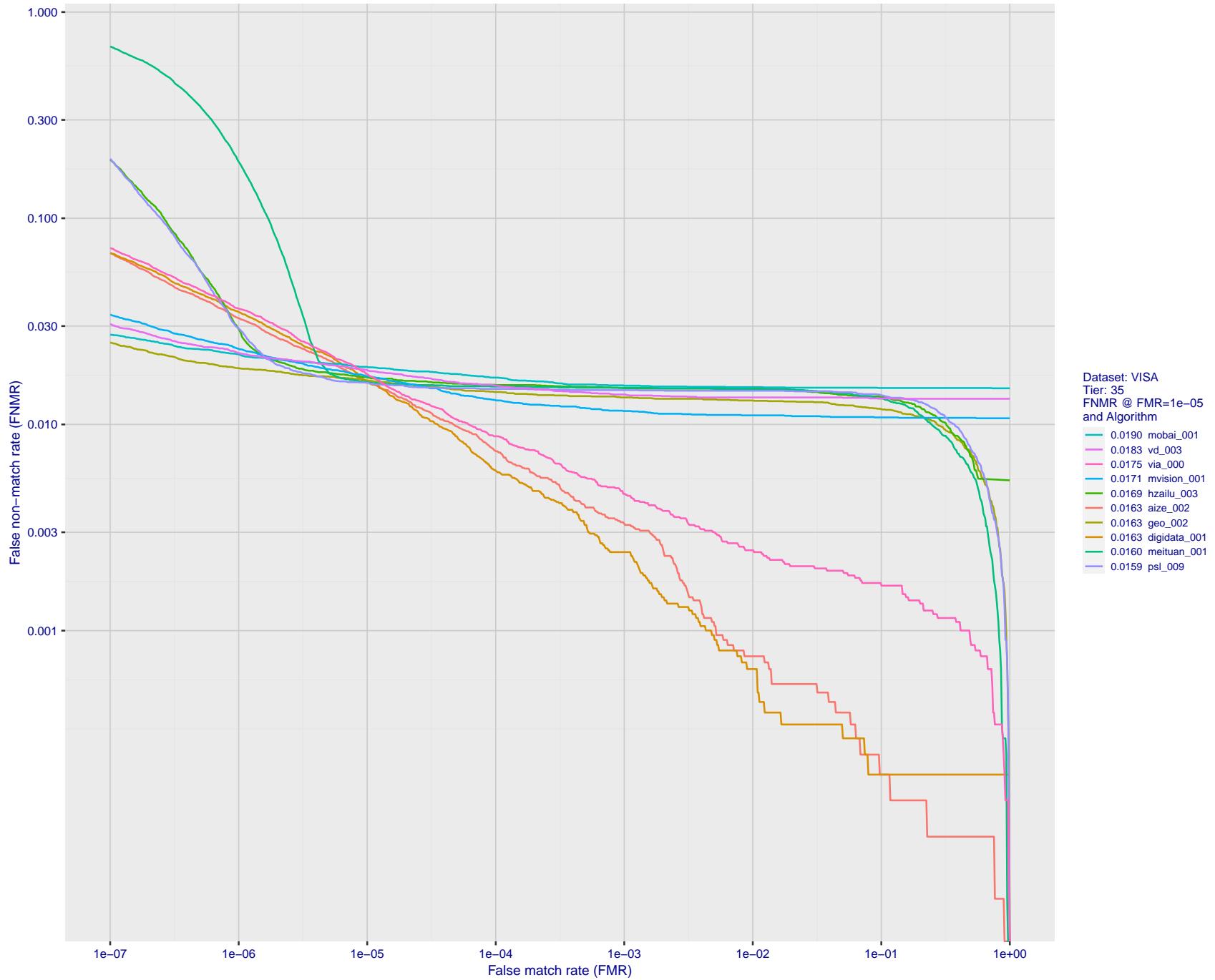


Figure 78: For the visa images, detection error tradeoff (DET) characteristics showing false non-match rate vs. false match rate plotted parametrically on threshold, T . The scales are logarithmic in order to show many decades of FMR.

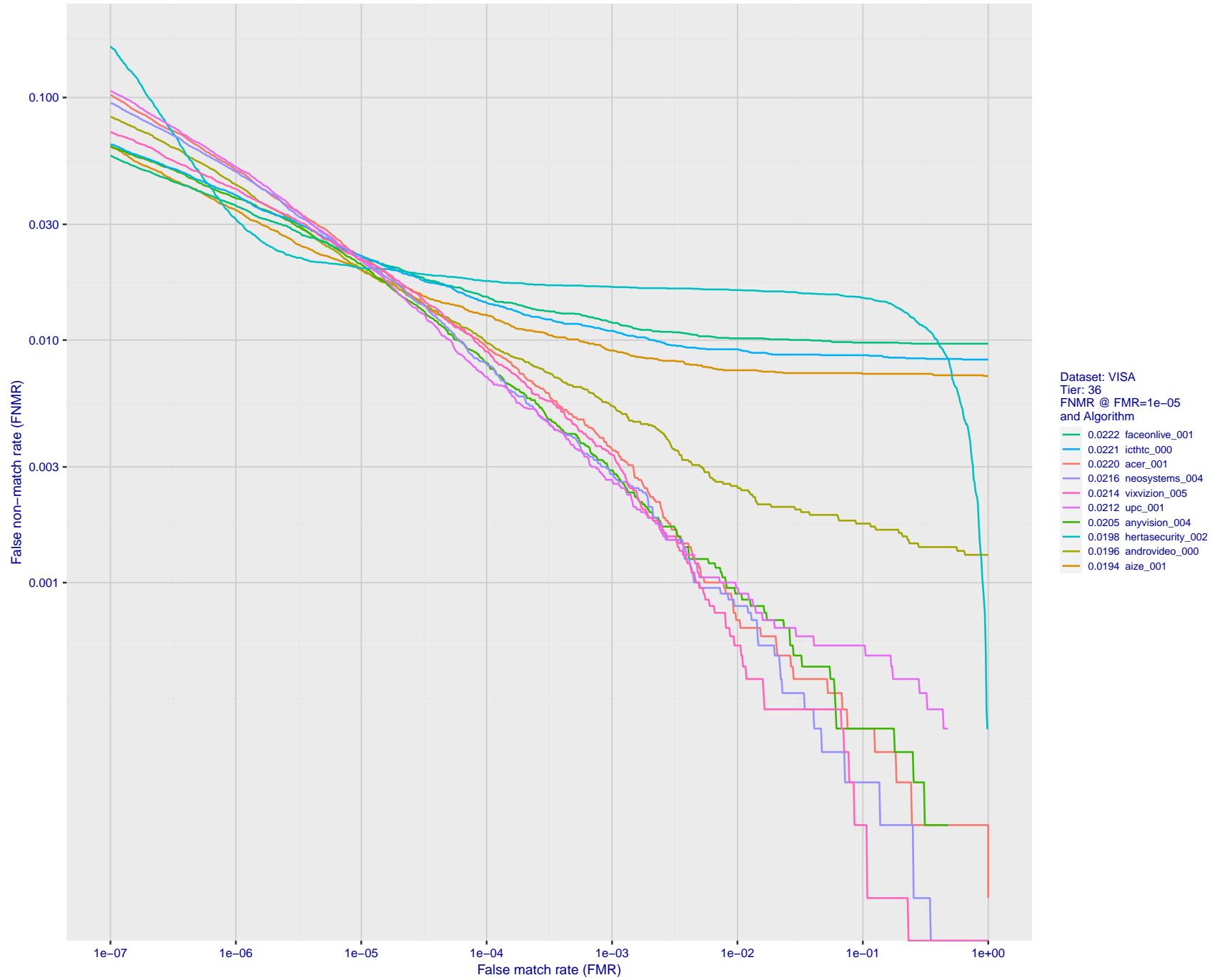


Figure 79: For the visa images, detection error tradeoff (DET) characteristics showing false non-match rate vs. false match rate plotted parametrically on threshold, T . The scales are logarithmic in order to show many decades of FMR.

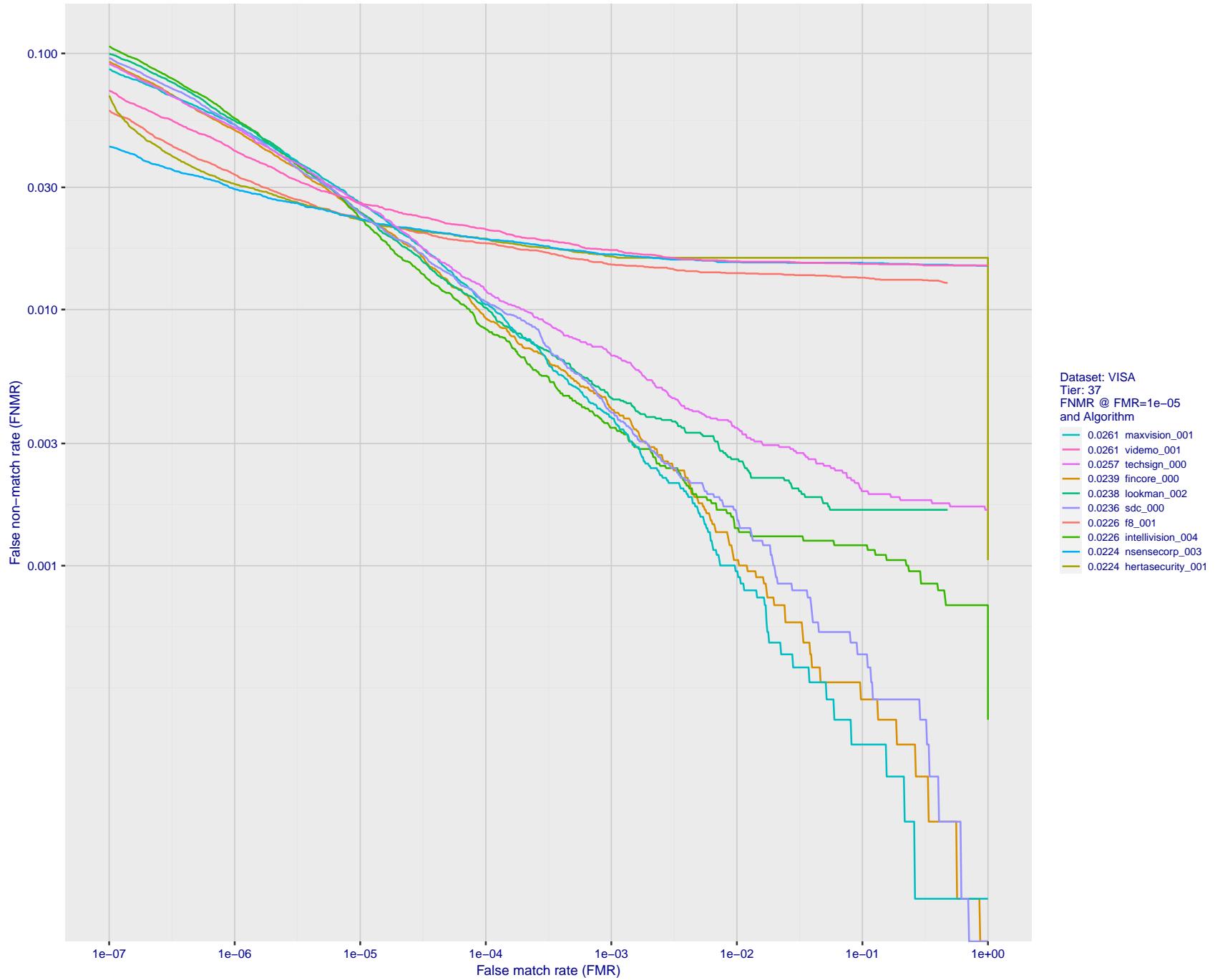


Figure 80: For the visa images, detection error tradeoff (DET) characteristics showing false non-match rate vs. false match rate plotted parametrically on threshold, T . The scales are logarithmic in order to show many decades of FMR.

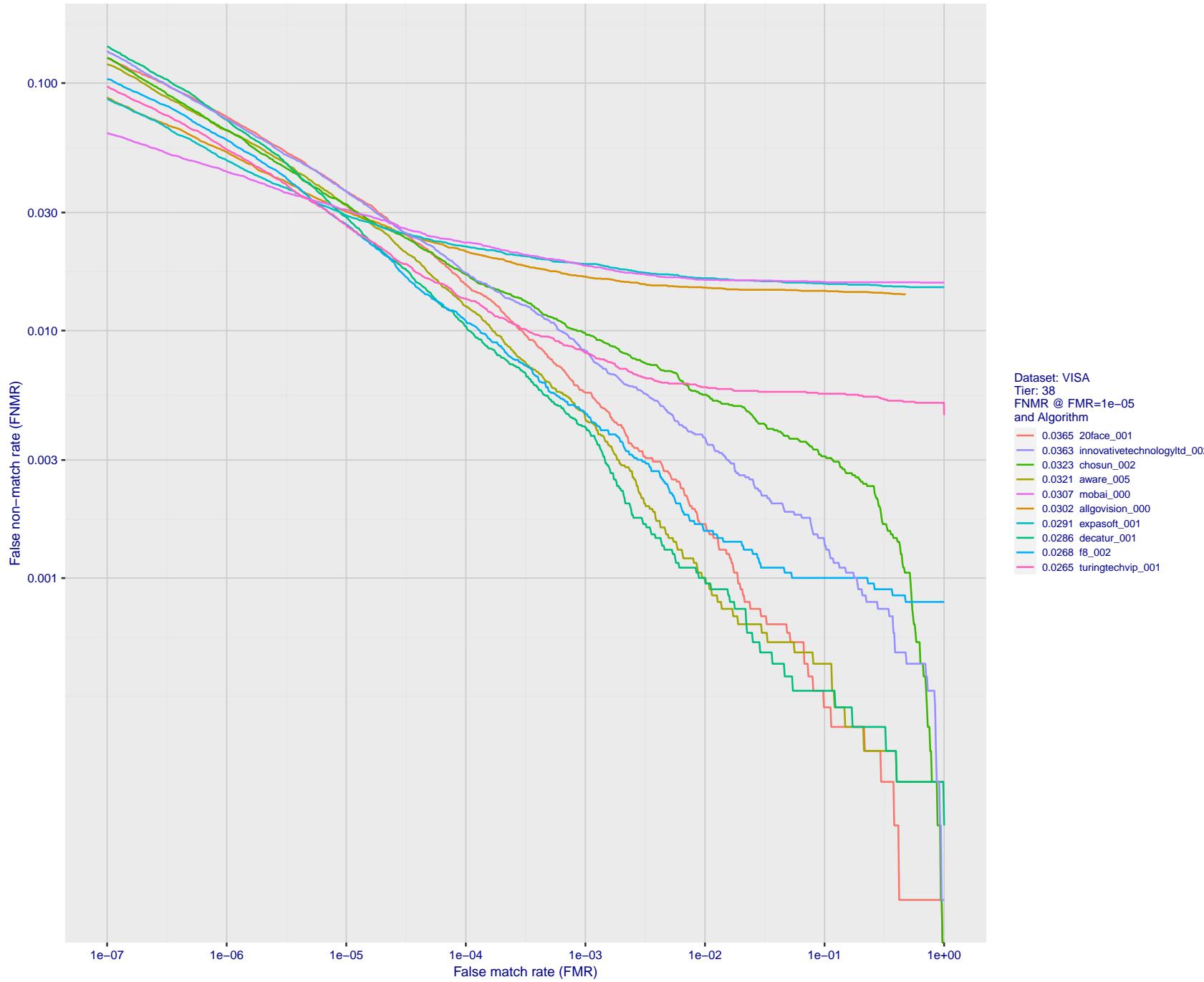


Figure 81: For the visa images, detection error tradeoff (DET) characteristics showing false non-match rate vs. false match rate plotted parametrically on threshold, T . The scales are logarithmic in order to show many decades of FMR.

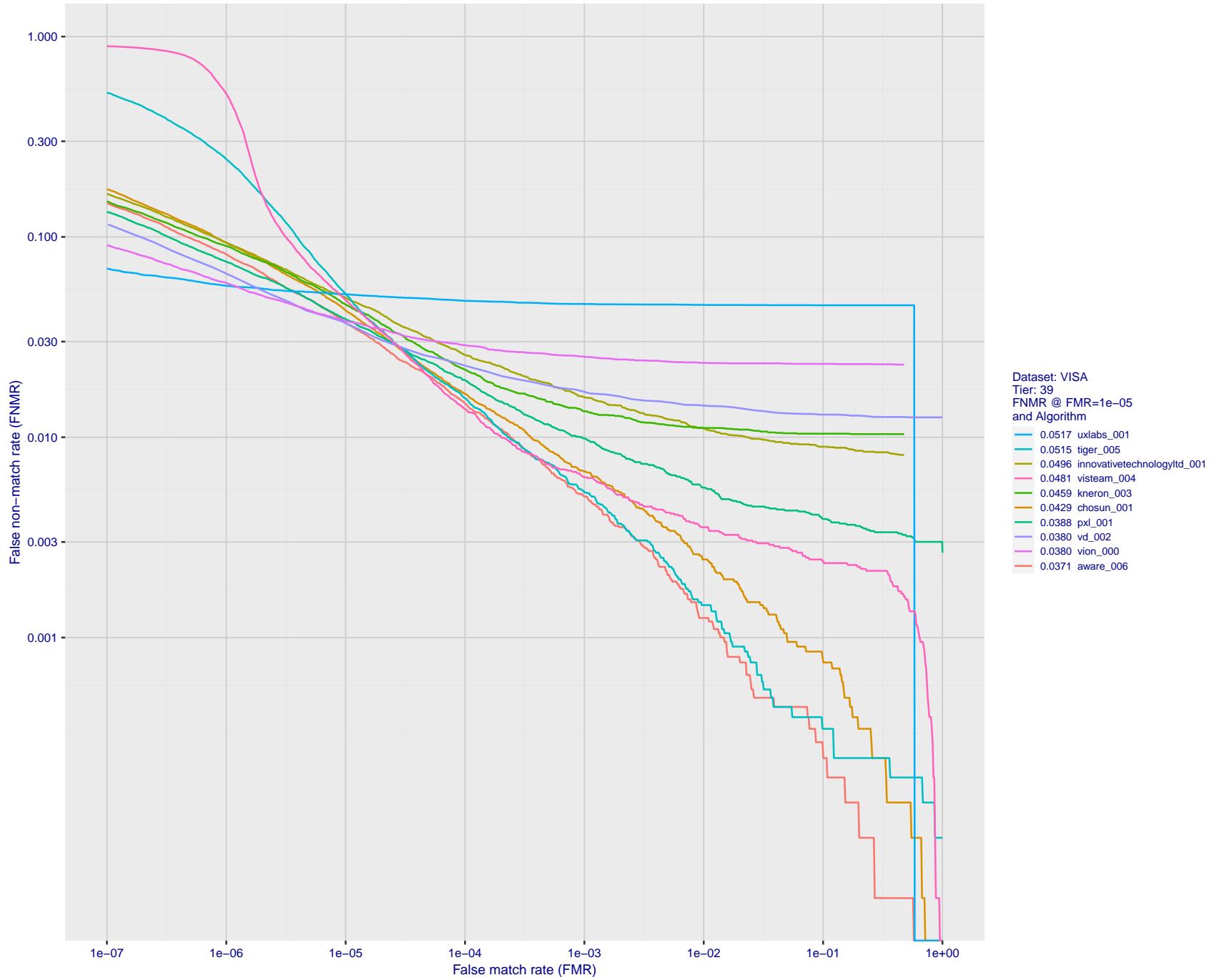


Figure 82: For the visa images, detection error tradeoff (DET) characteristics showing false non-match rate vs. false match rate plotted parametrically on threshold, T . The scales are logarithmic in order to show many decades of FMR.

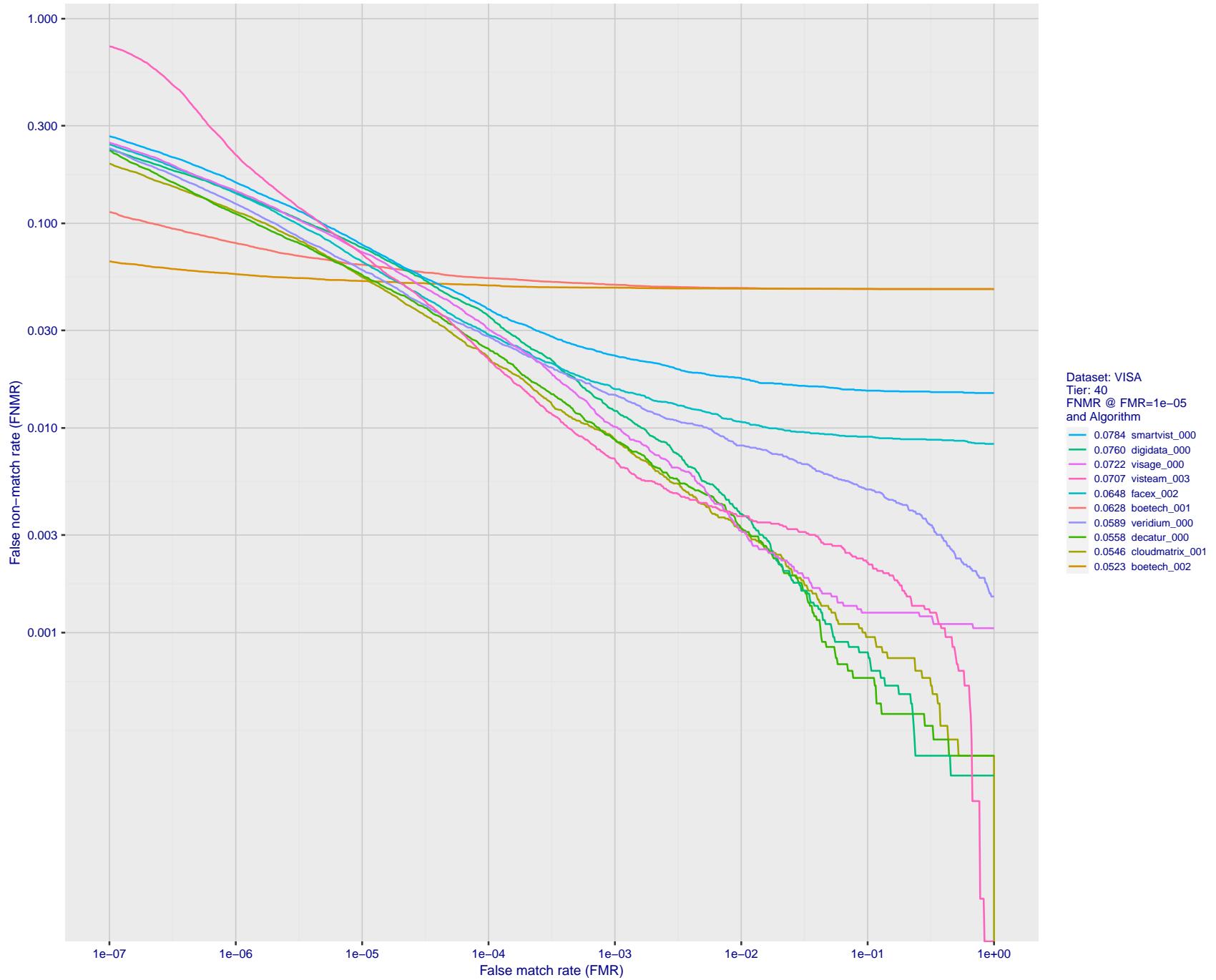


Figure 83: For the visa images, detection error tradeoff (DET) characteristics showing false non-match rate vs. false match rate plotted parametrically on threshold, T . The scales are logarithmic in order to show many decades of FMR.

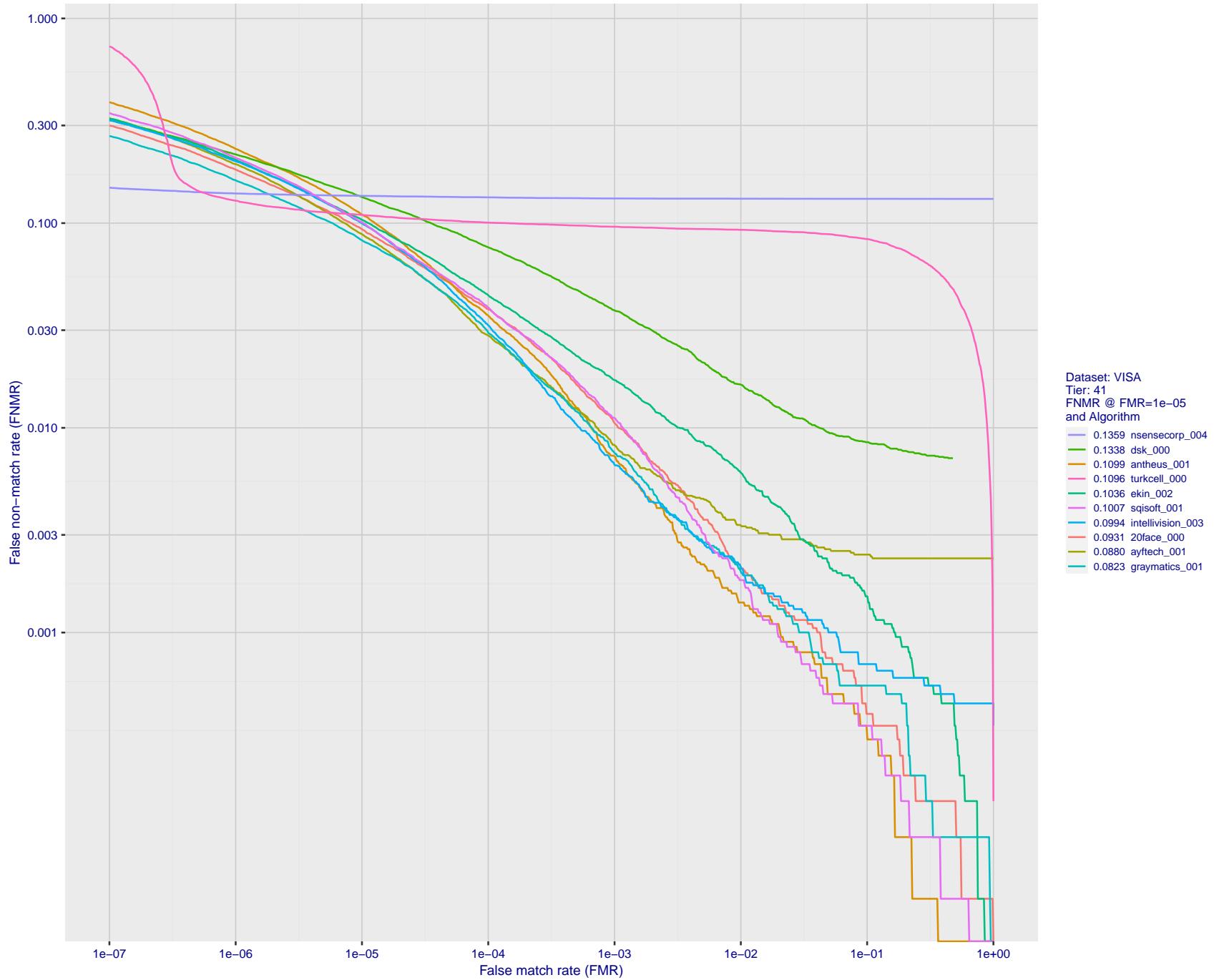


Figure 84: For the visa images, detection error tradeoff (DET) characteristics showing false non-match rate vs. false match rate plotted parametrically on threshold, T . The scales are logarithmic in order to show many decades of FMR.

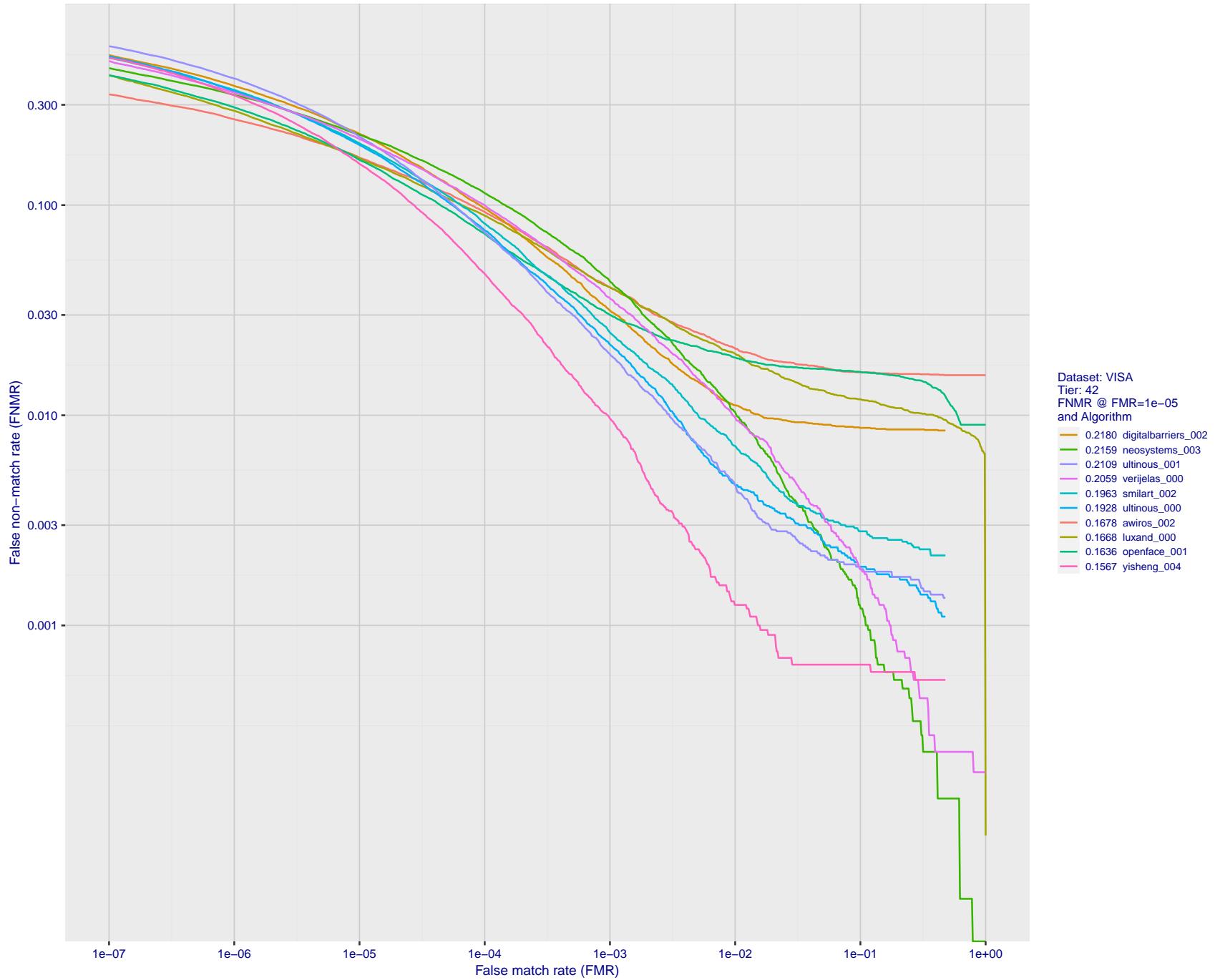


Figure 85: For the visa images, detection error tradeoff (DET) characteristics showing false non-match rate vs. false match rate plotted parametrically on threshold, T . The scales are logarithmic in order to show many decades of FMR.

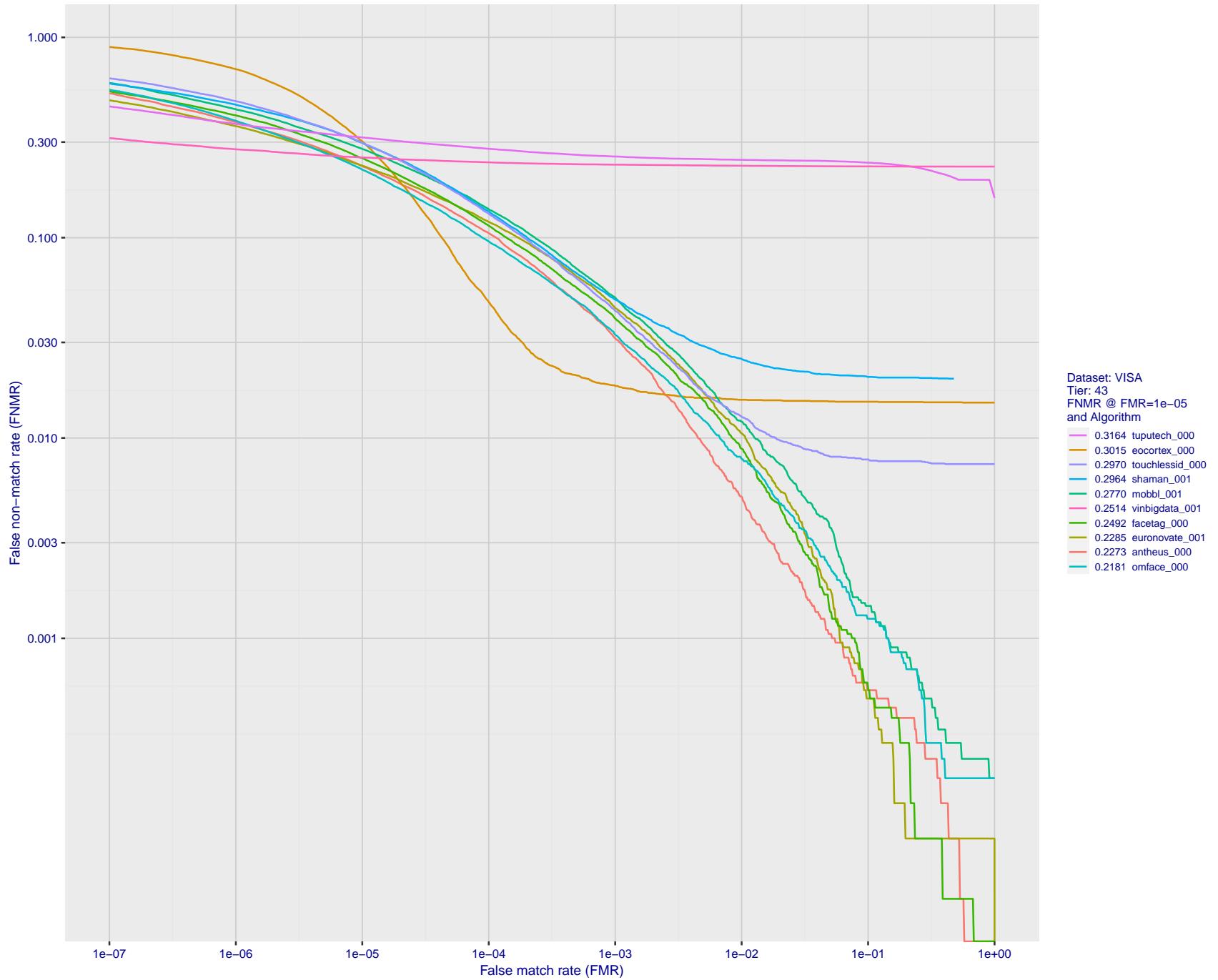


Figure 86: For the visa images, detection error tradeoff (DET) characteristics showing false non-match rate vs. false match rate plotted parametrically on threshold, T . The scales are logarithmic in order to show many decades of FMR.

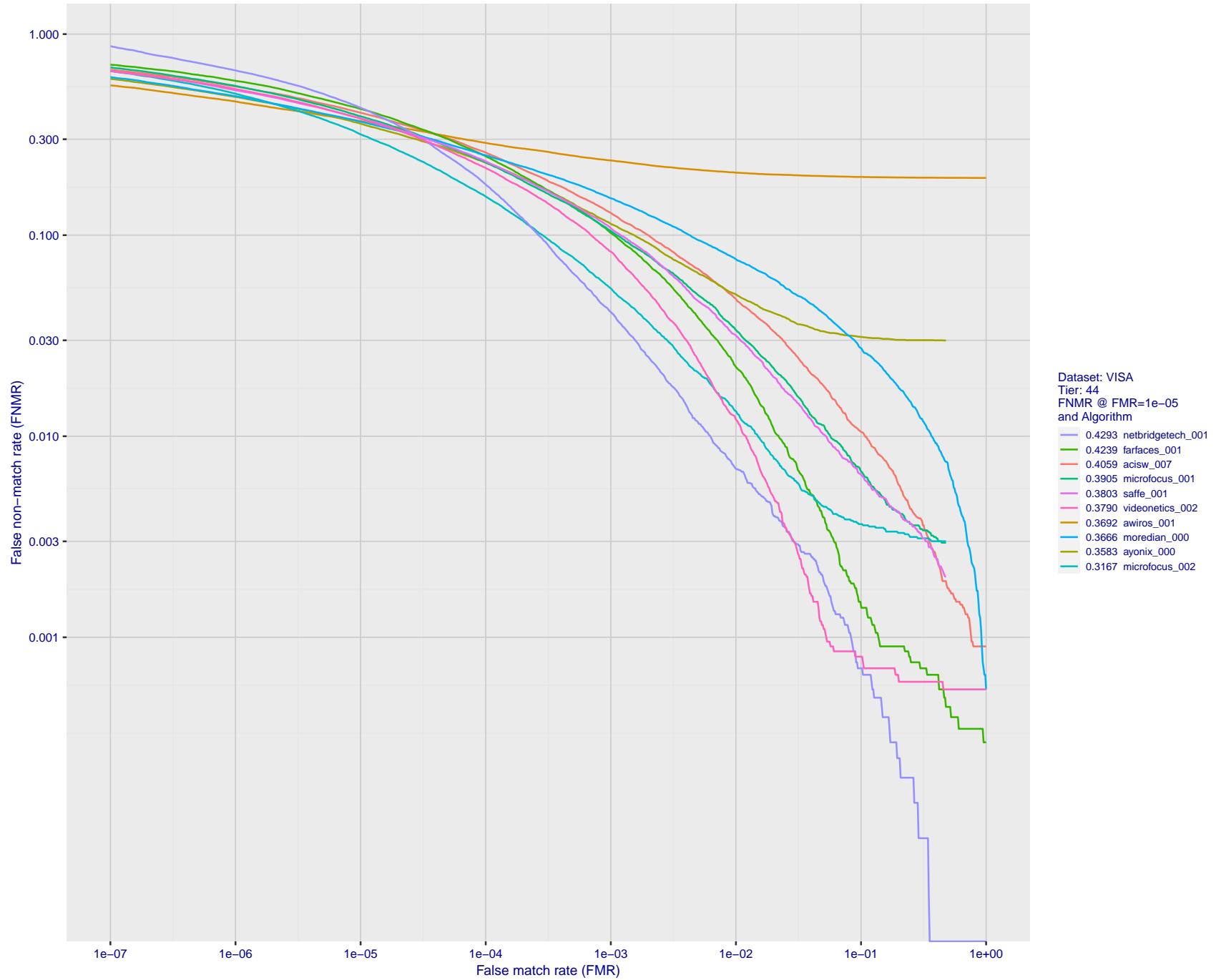


Figure 87: For the visa images, detection error tradeoff (DET) characteristics showing false non-match rate vs. false match rate plotted parametrically on threshold, T . The scales are logarithmic in order to show many decades of FMR.

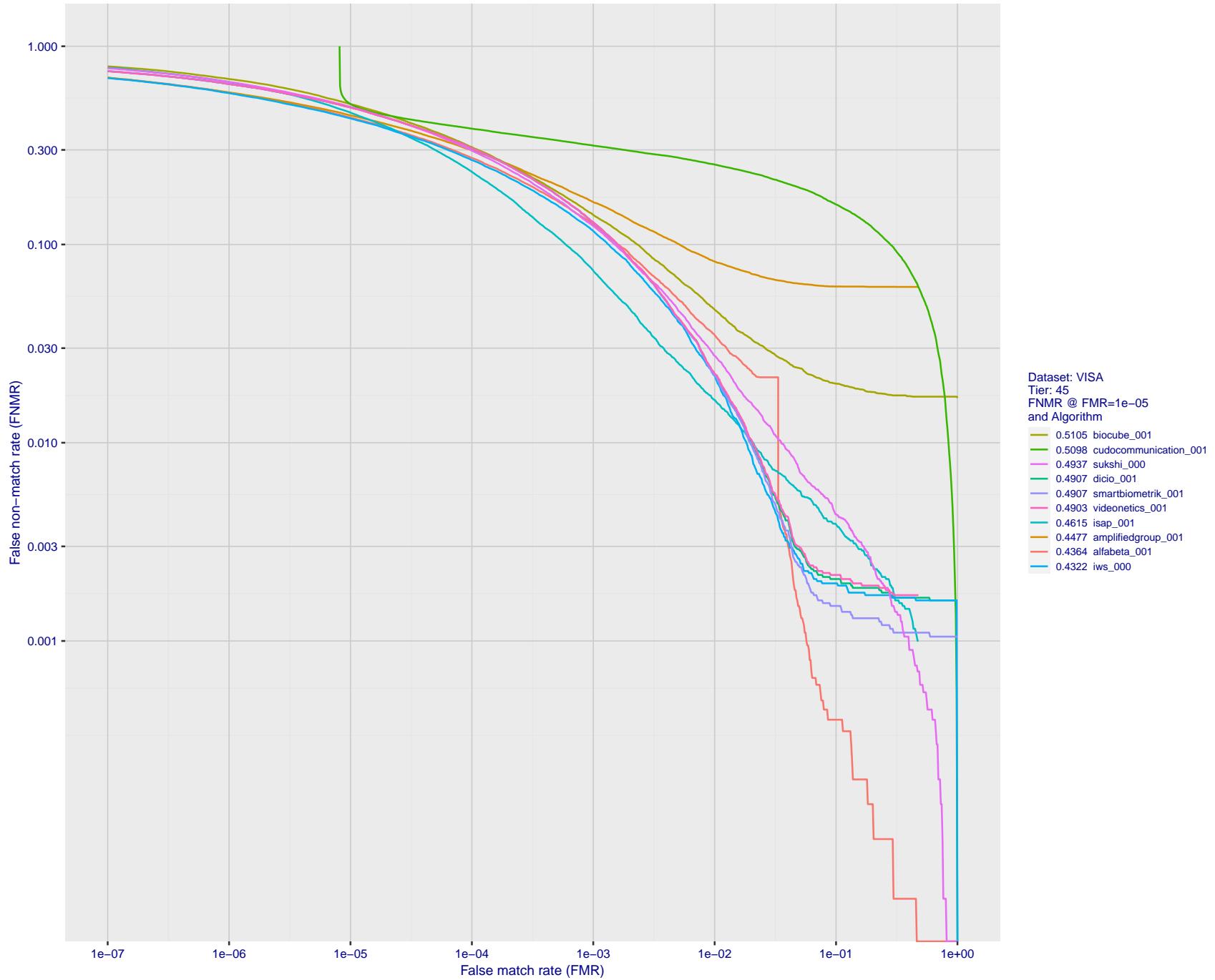


Figure 88: For the visa images, detection error tradeoff (DET) characteristics showing false non-match rate vs. false match rate plotted parametrically on threshold, T . The scales are logarithmic in order to show many decades of FMR.

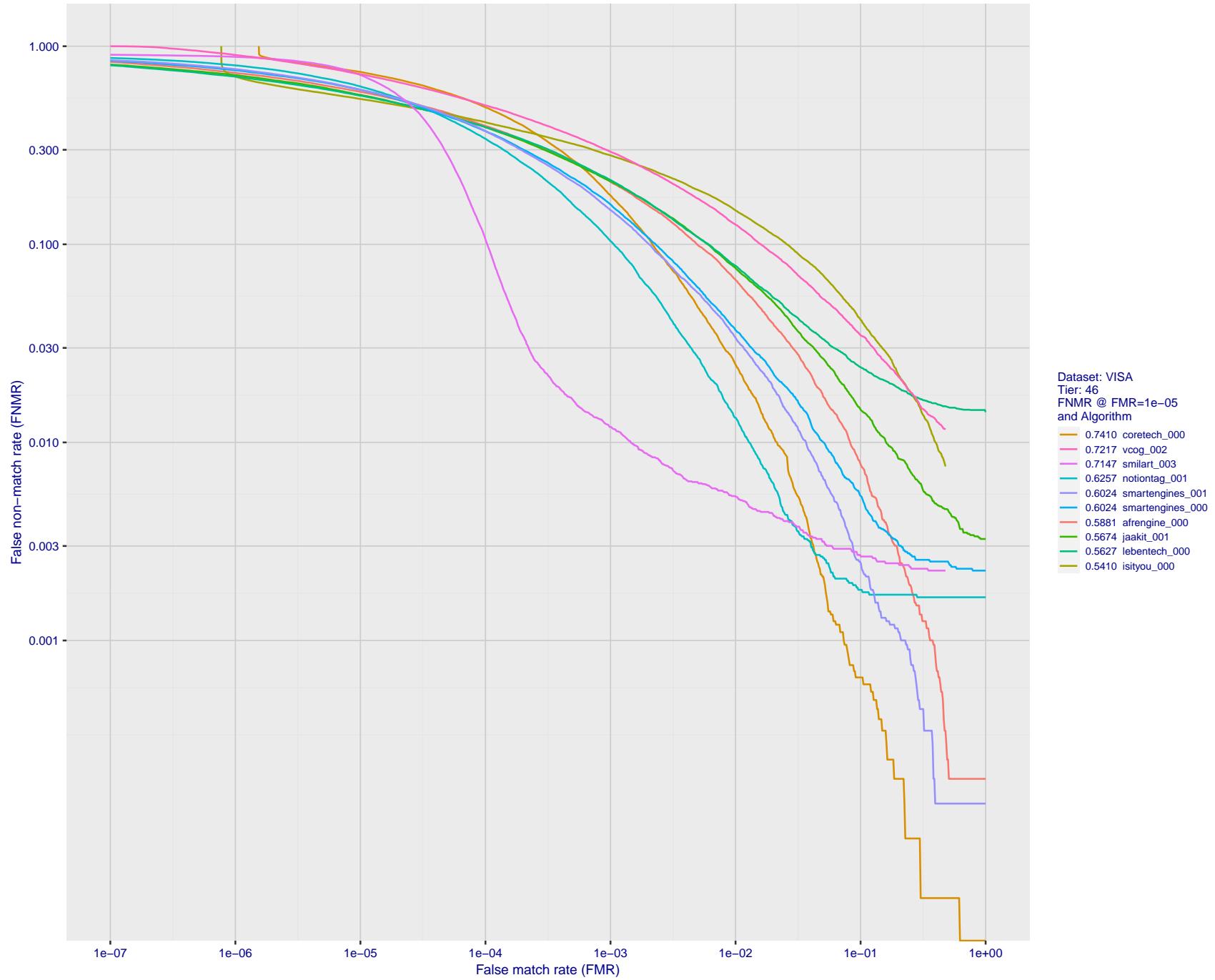


Figure 89: For the visa images, detection error tradeoff (DET) characteristics showing false non-match rate vs. false match rate plotted parametrically on threshold, T . The scales are logarithmic in order to show many decades of FMR.

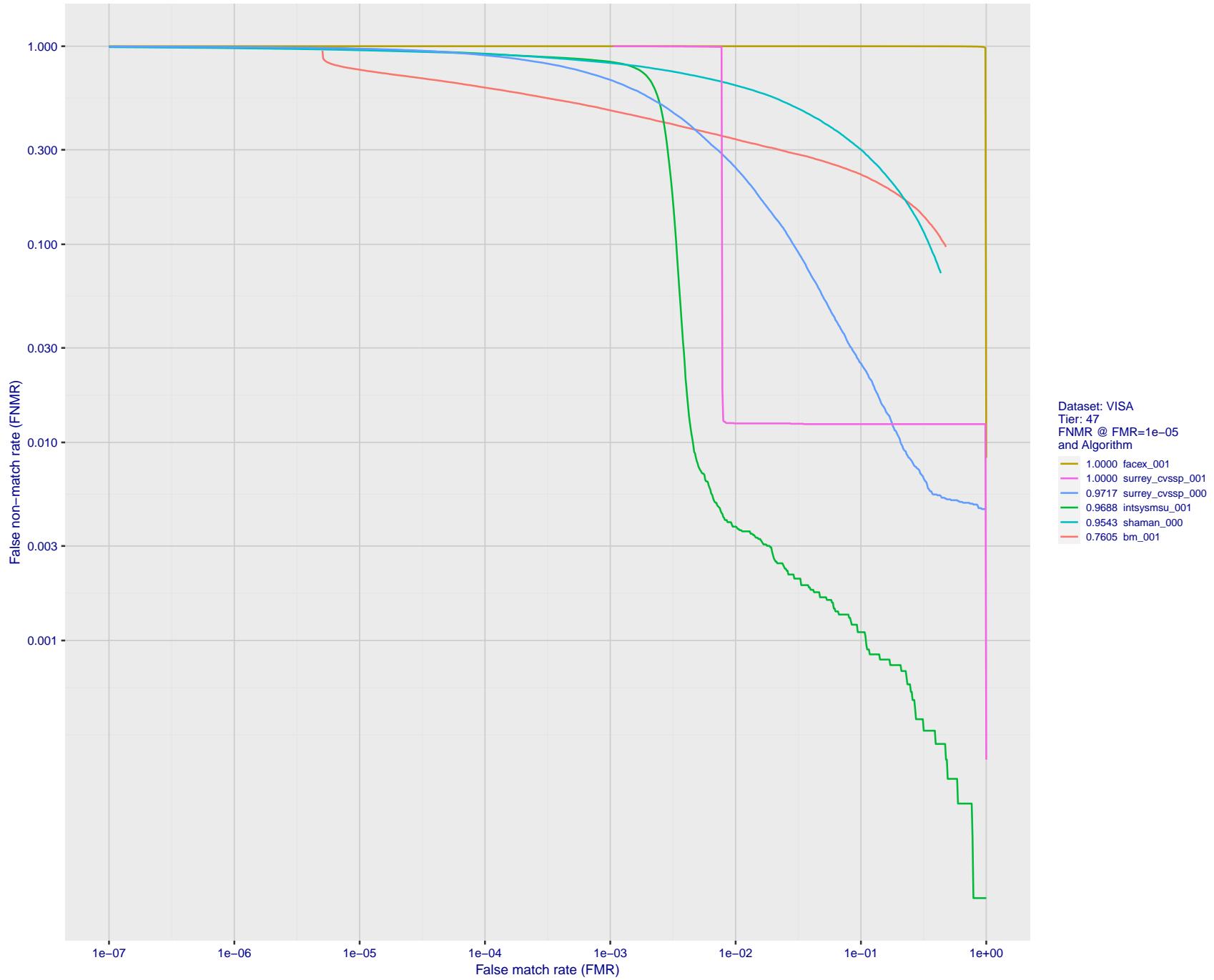


Figure 90: For the visa images, detection error tradeoff (DET) characteristics showing false non-match rate vs. false match rate plotted parametrically on threshold, T . The scales are logarithmic in order to show many decades of FMR.

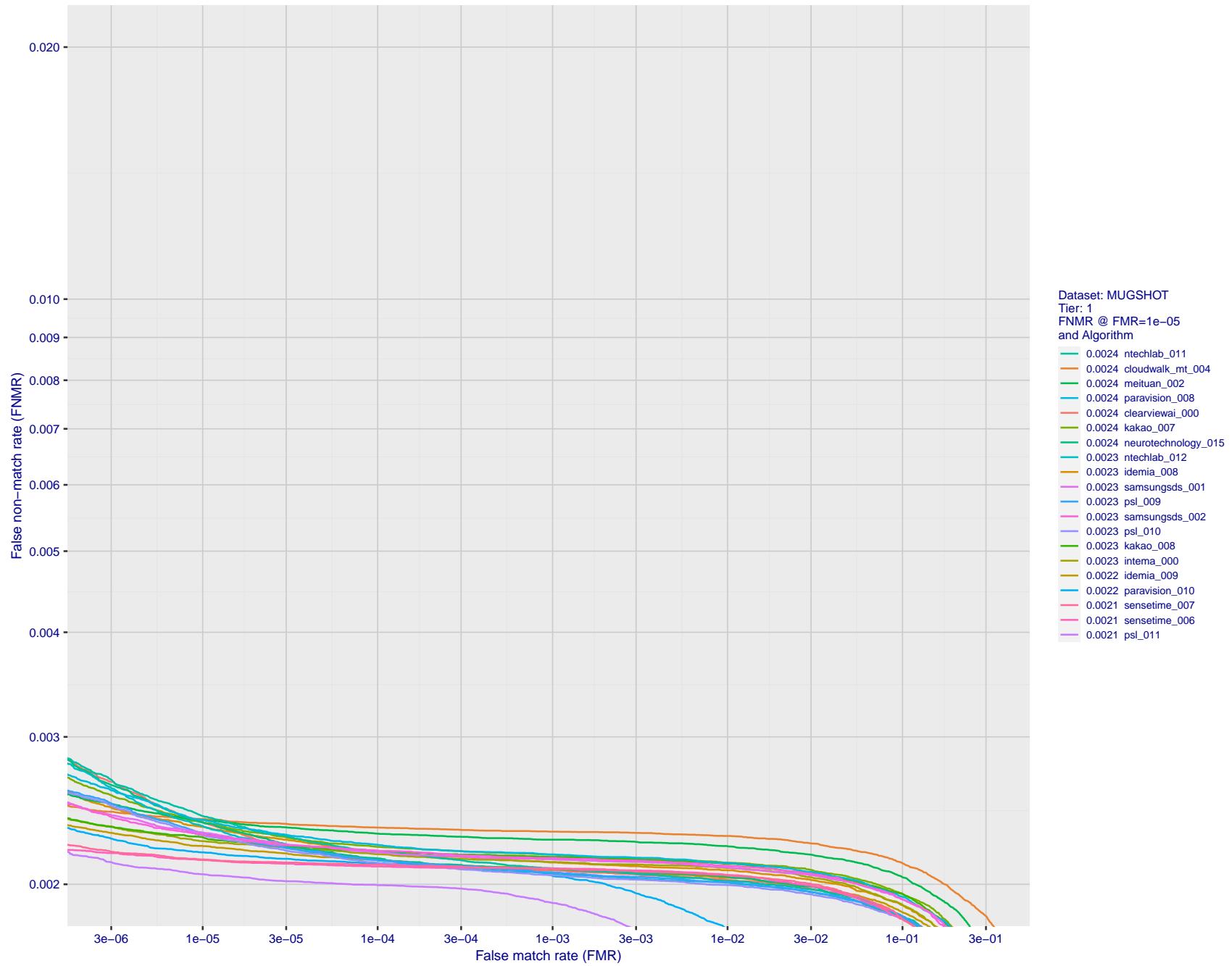


Figure 91: For the mugshot images, detection error tradeoff (DET) characteristics showing false non-match rate vs. false match rate plotted parametrically on threshold, T . The scales are logarithmic in order to show decades of FMR.

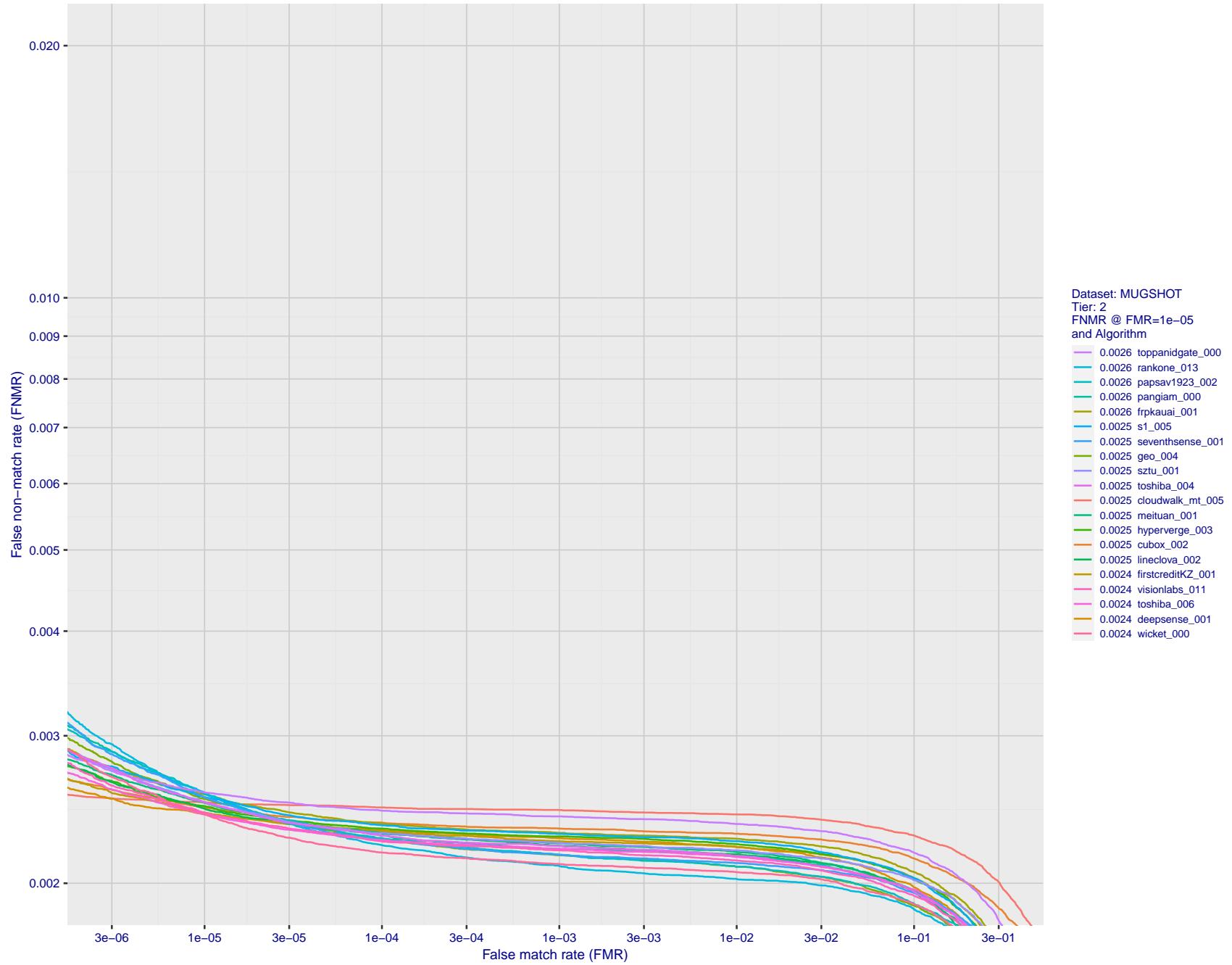


Figure 92: For the mugshot images, detection error tradeoff (DET) characteristics showing false non-match rate vs. false match rate plotted parametrically on threshold, T . The scales are logarithmic in order to show decades of FMR.

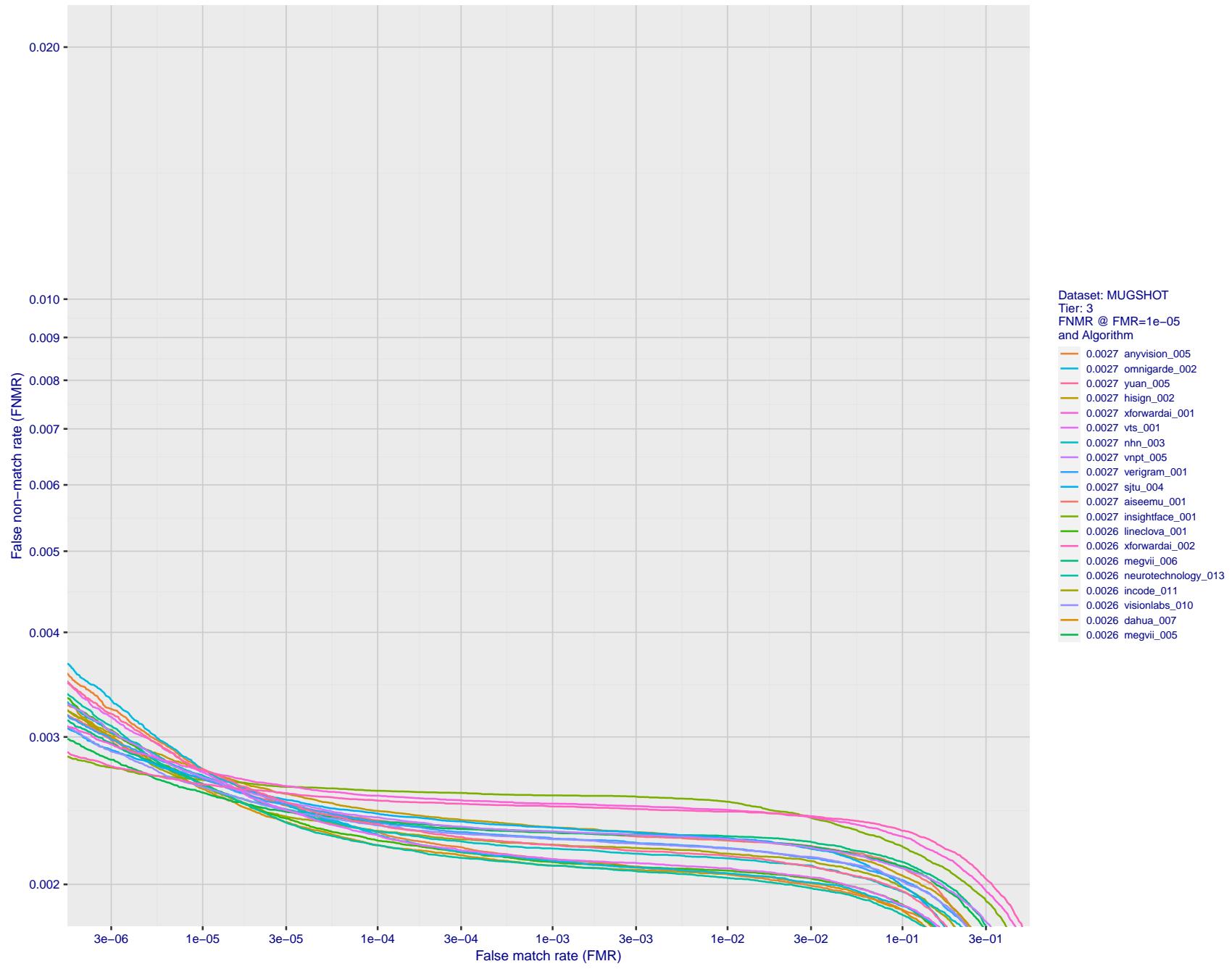


Figure 93: For the mugshot images, detection error tradeoff (DET) characteristics showing false non-match rate vs. false match rate plotted parametrically on threshold, T . The scales are logarithmic in order to show decades of FMR.

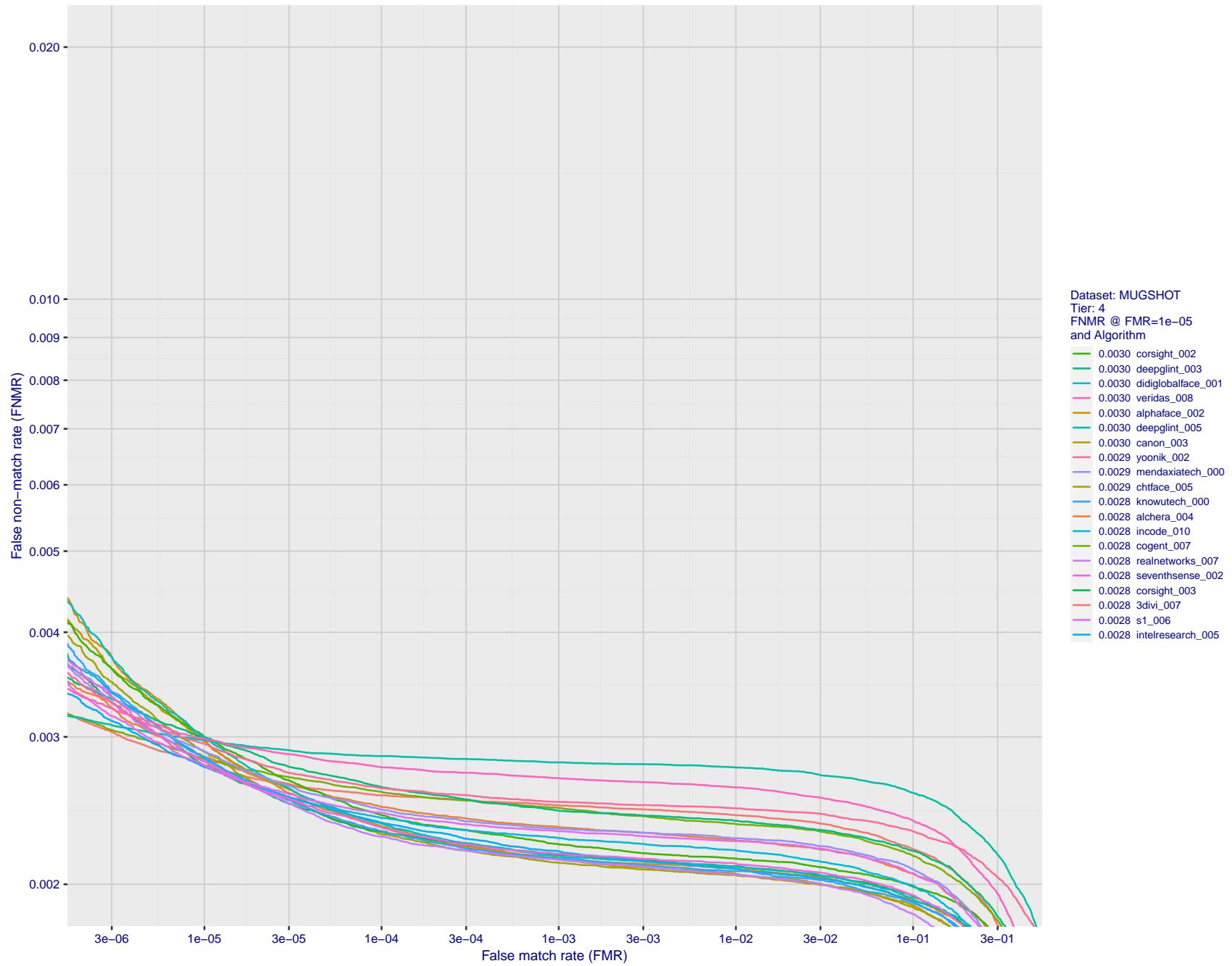


Figure 94: For the mugshot images, detection error tradeoff (DET) characteristics showing false non-match rate vs. false match rate plotted parametrically on threshold, T . The scales are logarithmic in order to show decades of FMR.

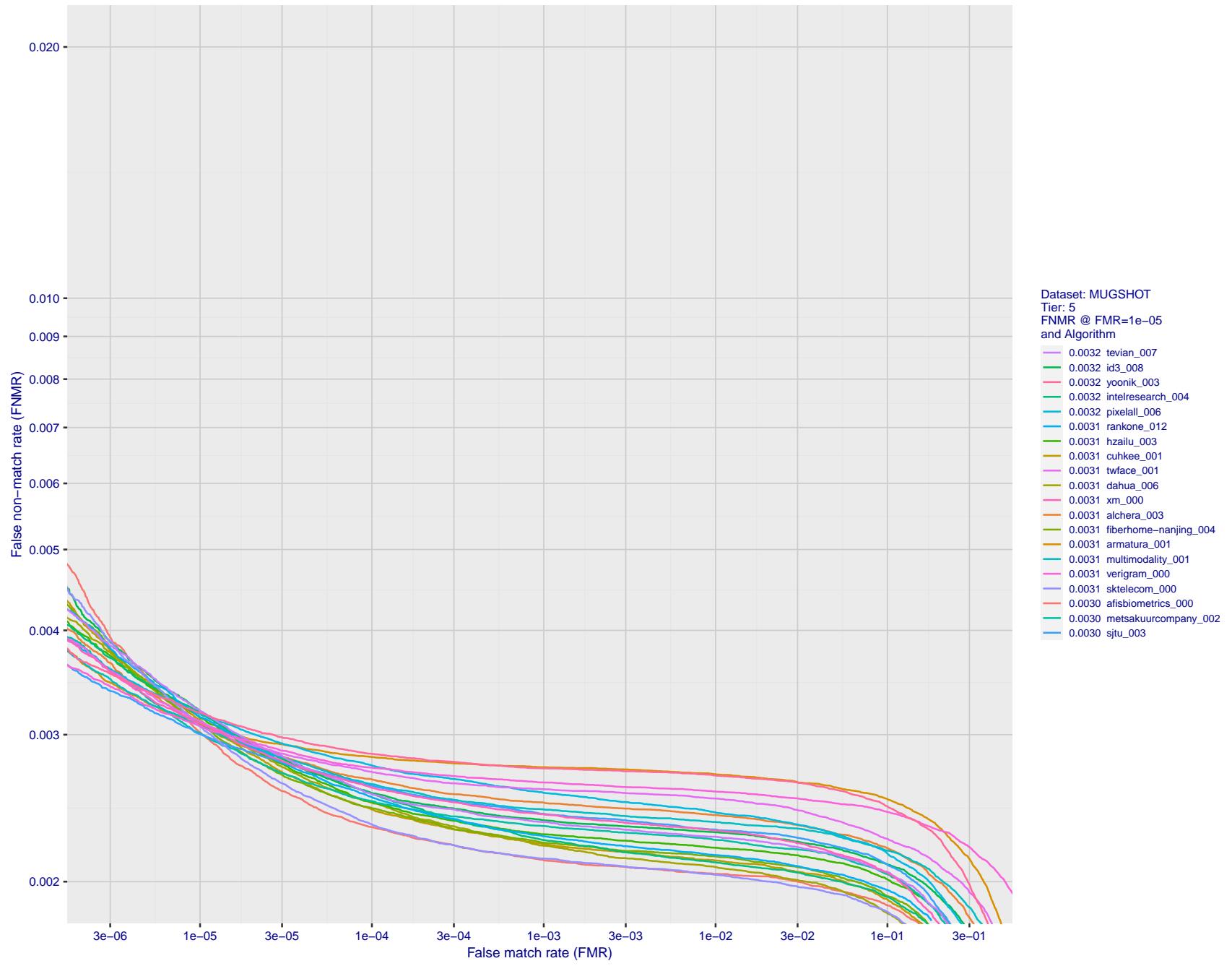


Figure 95: For the mugshot images, detection error tradeoff (DET) characteristics showing false non-match rate vs. false match rate plotted parametrically on threshold, T . The scales are logarithmic in order to show decades of FMR.

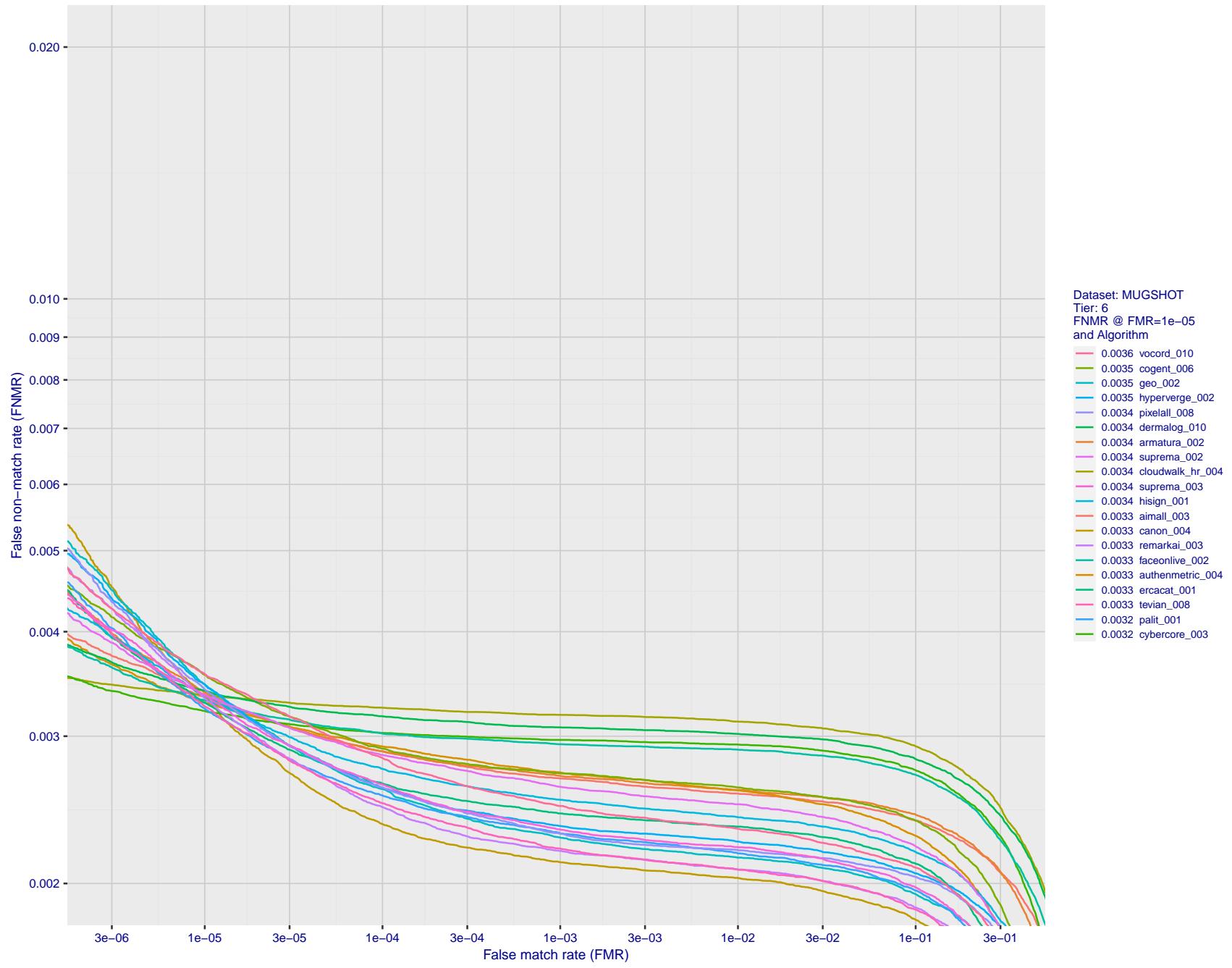


Figure 96: For the mugshot images, detection error tradeoff (DET) characteristics showing false non-match rate vs. false match rate plotted parametrically on threshold, T . The scales are logarithmic in order to show decades of FMR.

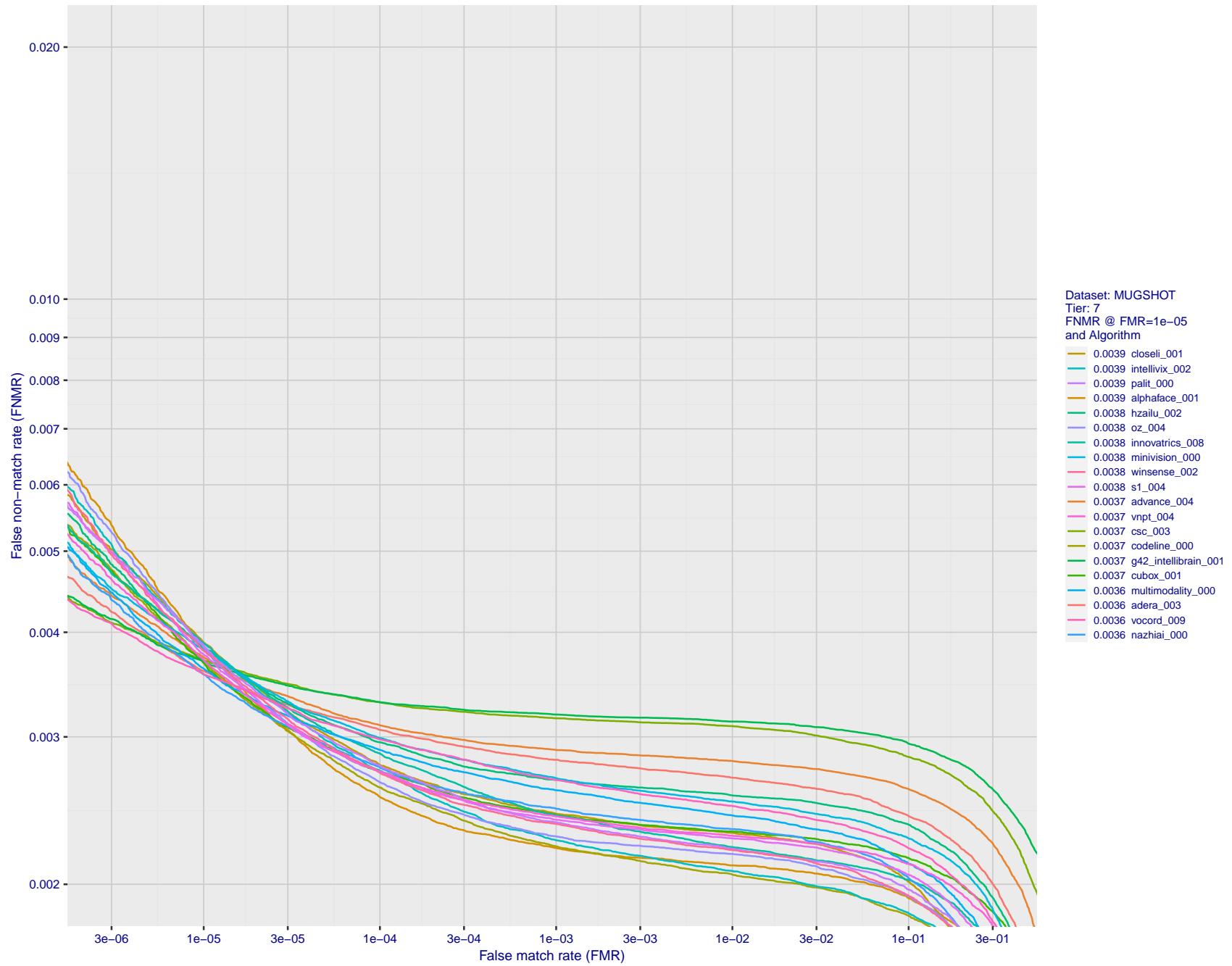


Figure 97: For the mugshot images, detection error tradeoff (DET) characteristics showing false non-match rate vs. false match rate plotted parametrically on threshold, T . The scales are logarithmic in order to show decades of FMR.

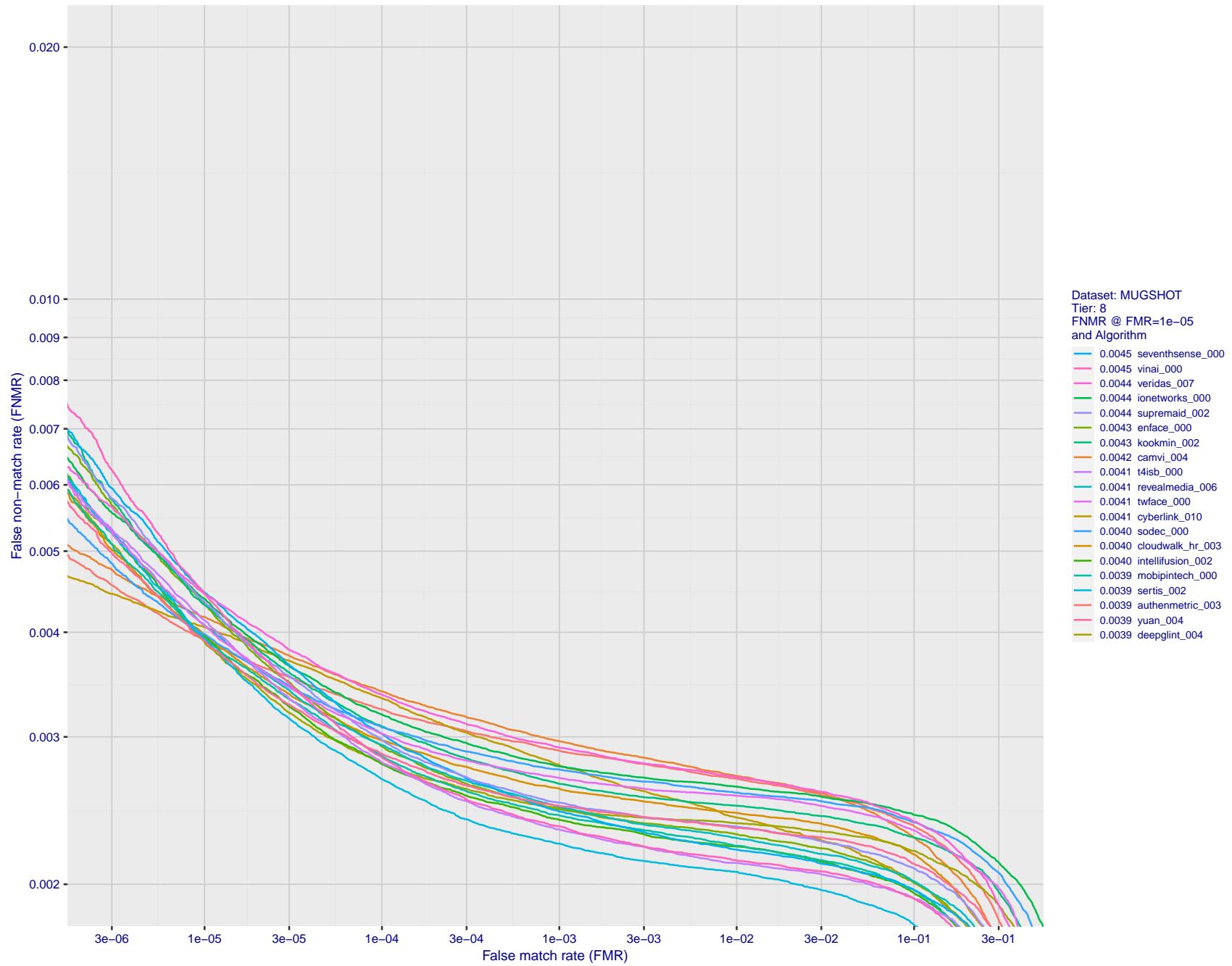


Figure 98: For the mugshot images, detection error tradeoff (DET) characteristics showing false non-match rate vs. false match rate plotted parametrically on threshold, T . The scales are logarithmic in order to show decades of FMR.

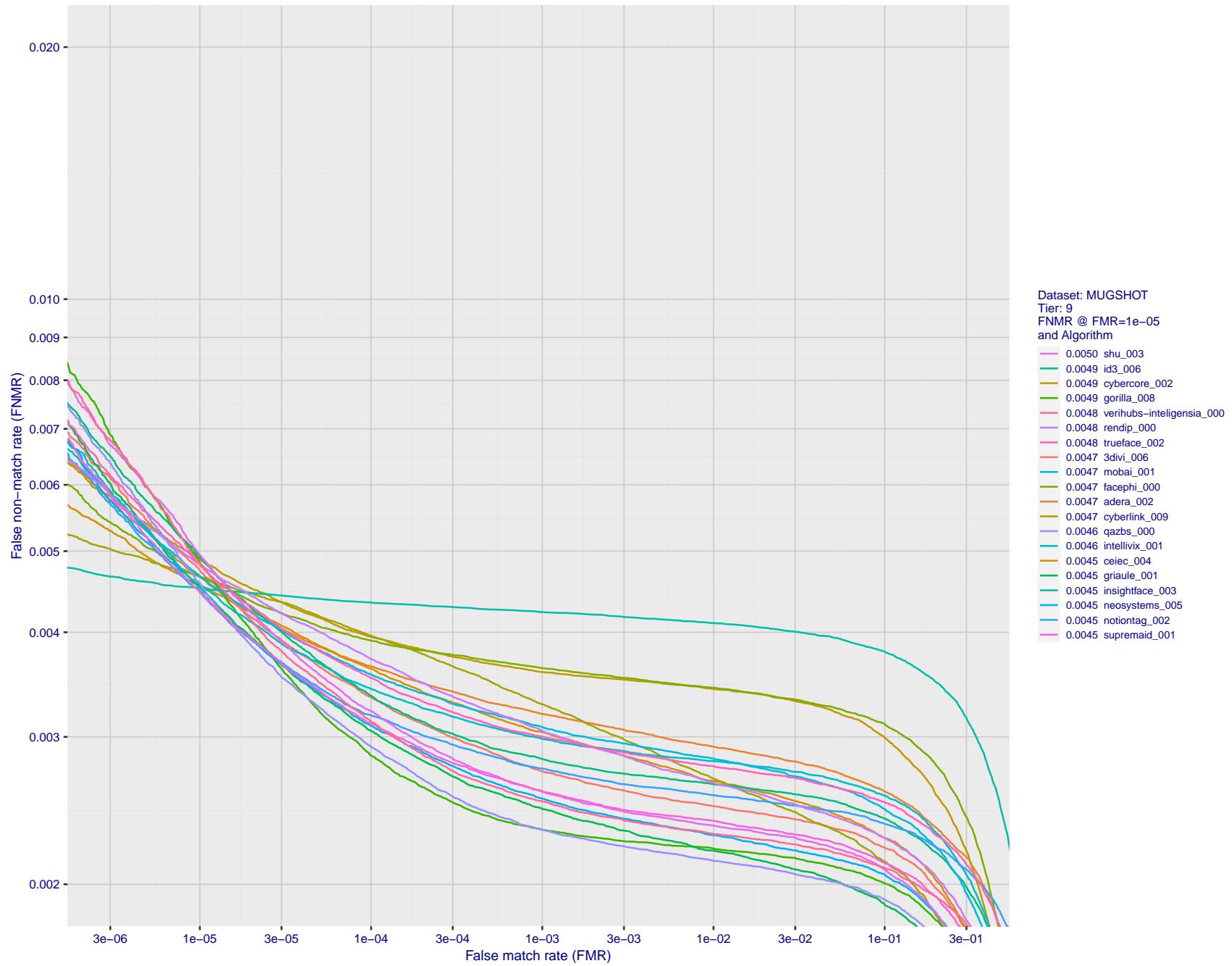


Figure 99: For the mugshot images, detection error tradeoff (DET) characteristics showing false non-match rate vs. false match rate plotted parametrically on threshold, T . The scales are logarithmic in order to show decades of FMR.

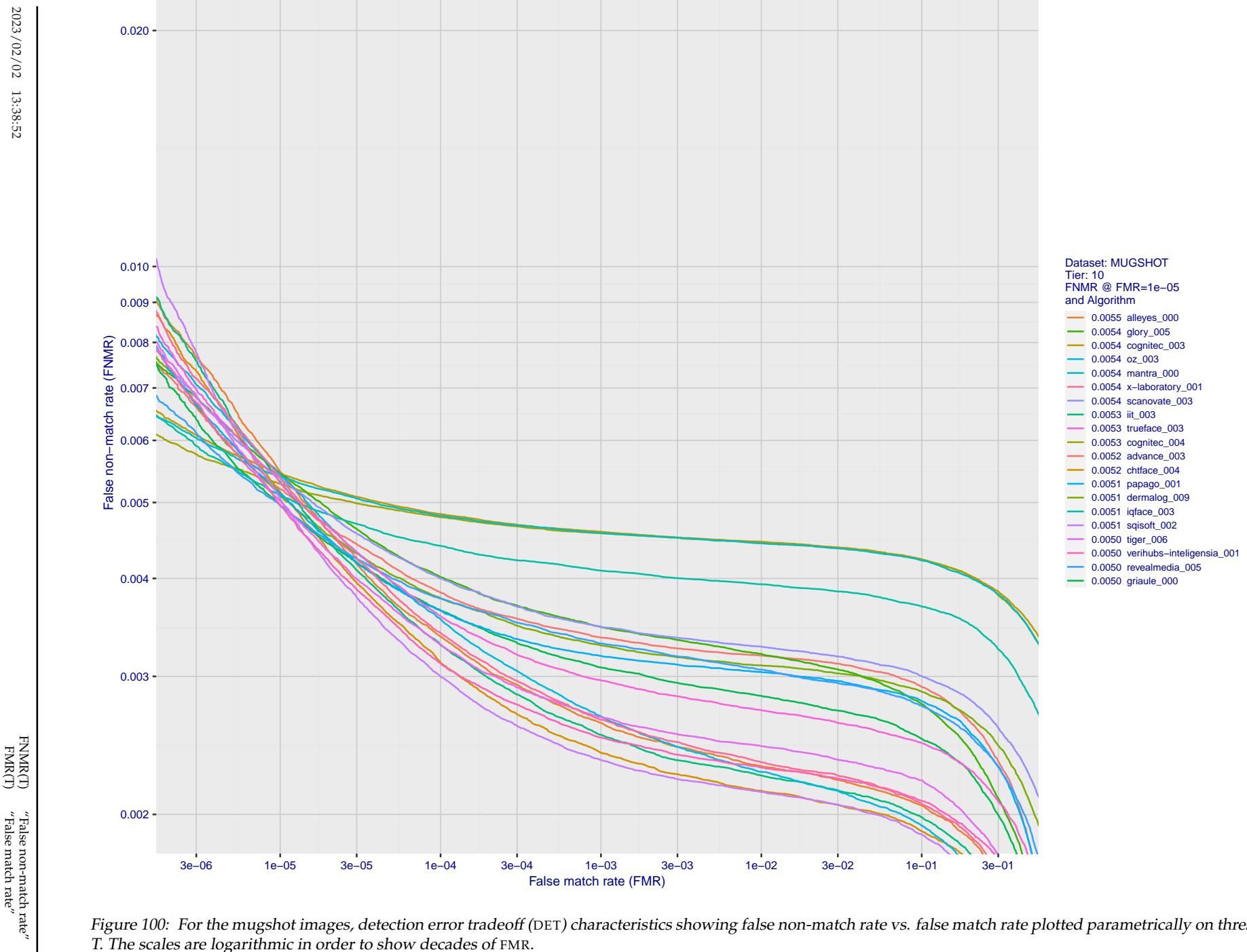


Figure 100: For the mugshot images, detection error tradeoff (DET) characteristics showing false non-match rate vs. false match rate plotted parametrically on threshold, T . The scales are logarithmic in order to show decades of FMR.

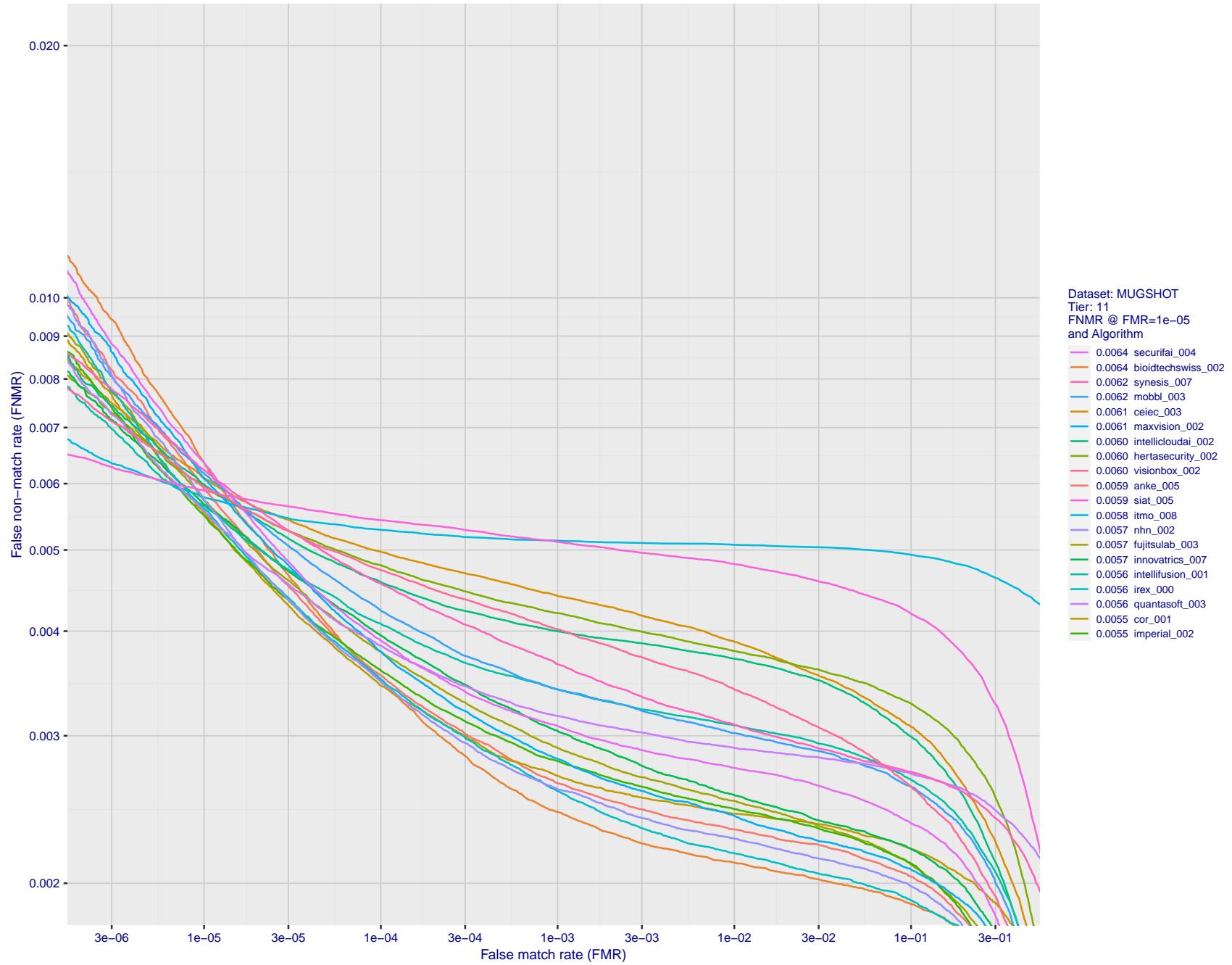


Figure 101: For the mugshot images, detection error tradeoff (DET) characteristics showing false non-match rate vs. false match rate plotted parametrically on threshold, T . The scales are logarithmic in order to show decades of FMR.

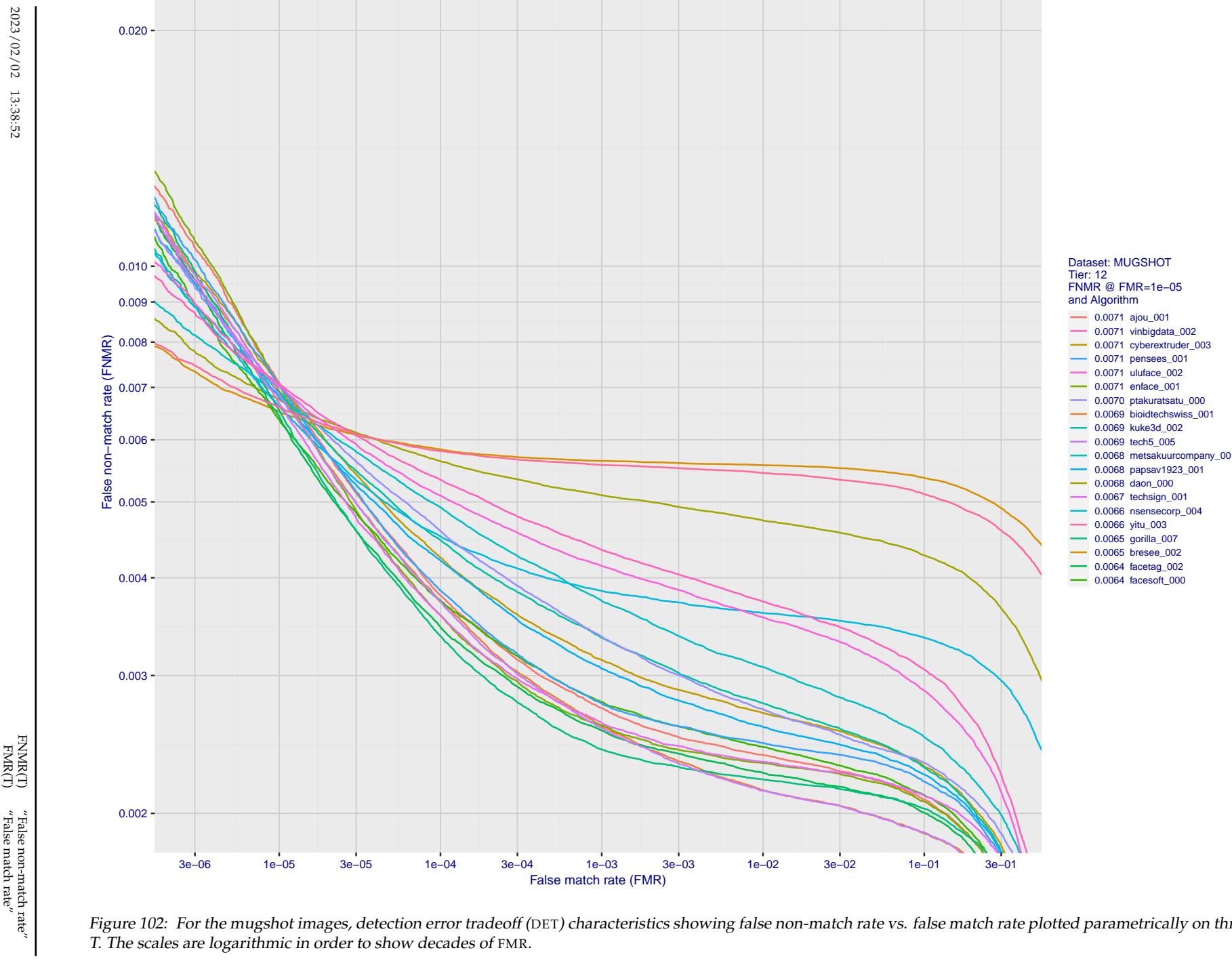


Figure 102: For the mugshot images, detection error tradeoff (DET) characteristics showing false non-match rate vs. false match rate plotted parametrically on threshold, T . The scales are logarithmic in order to show decades of FMR.

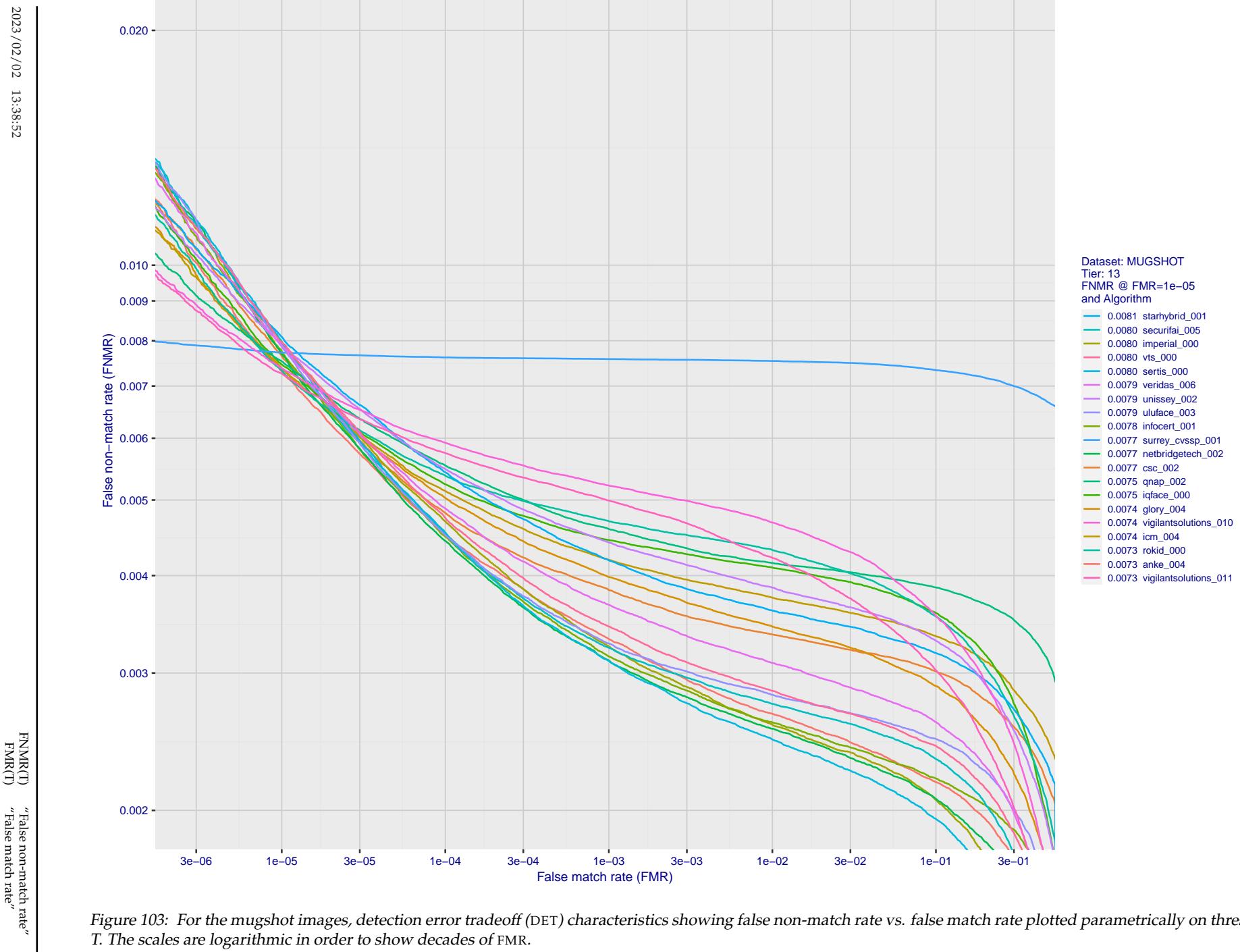


Figure 103: For the mugshot images, detection error tradeoff (DET) characteristics showing false non-match rate vs. false match rate plotted parametrically on threshold, T . The scales are logarithmic in order to show decades of FMR.

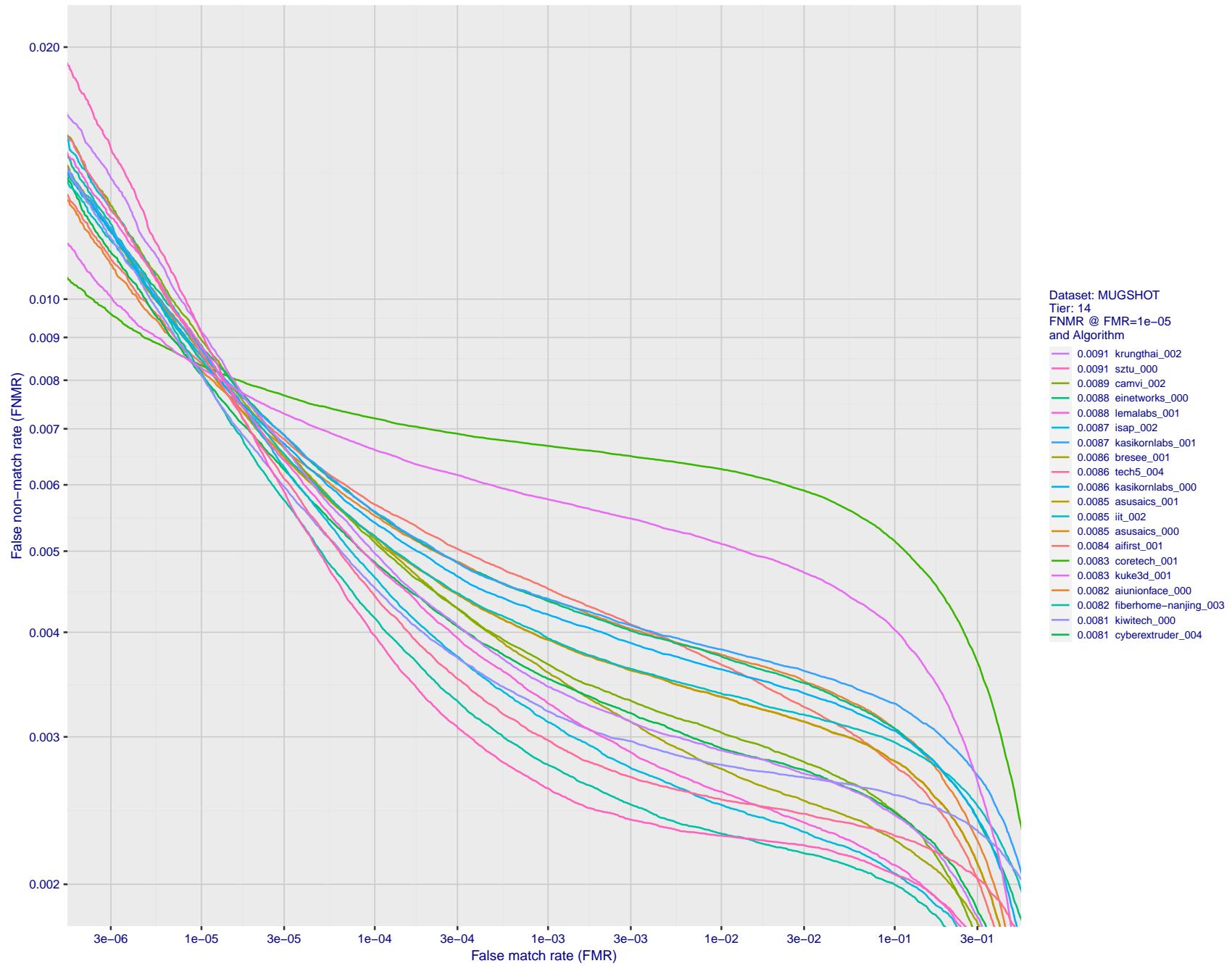


Figure 104: For the mugshot images, detection error tradeoff (DET) characteristics showing false non-match rate vs. false match rate plotted parametrically on threshold, T . The scales are logarithmic in order to show decades of FMR.

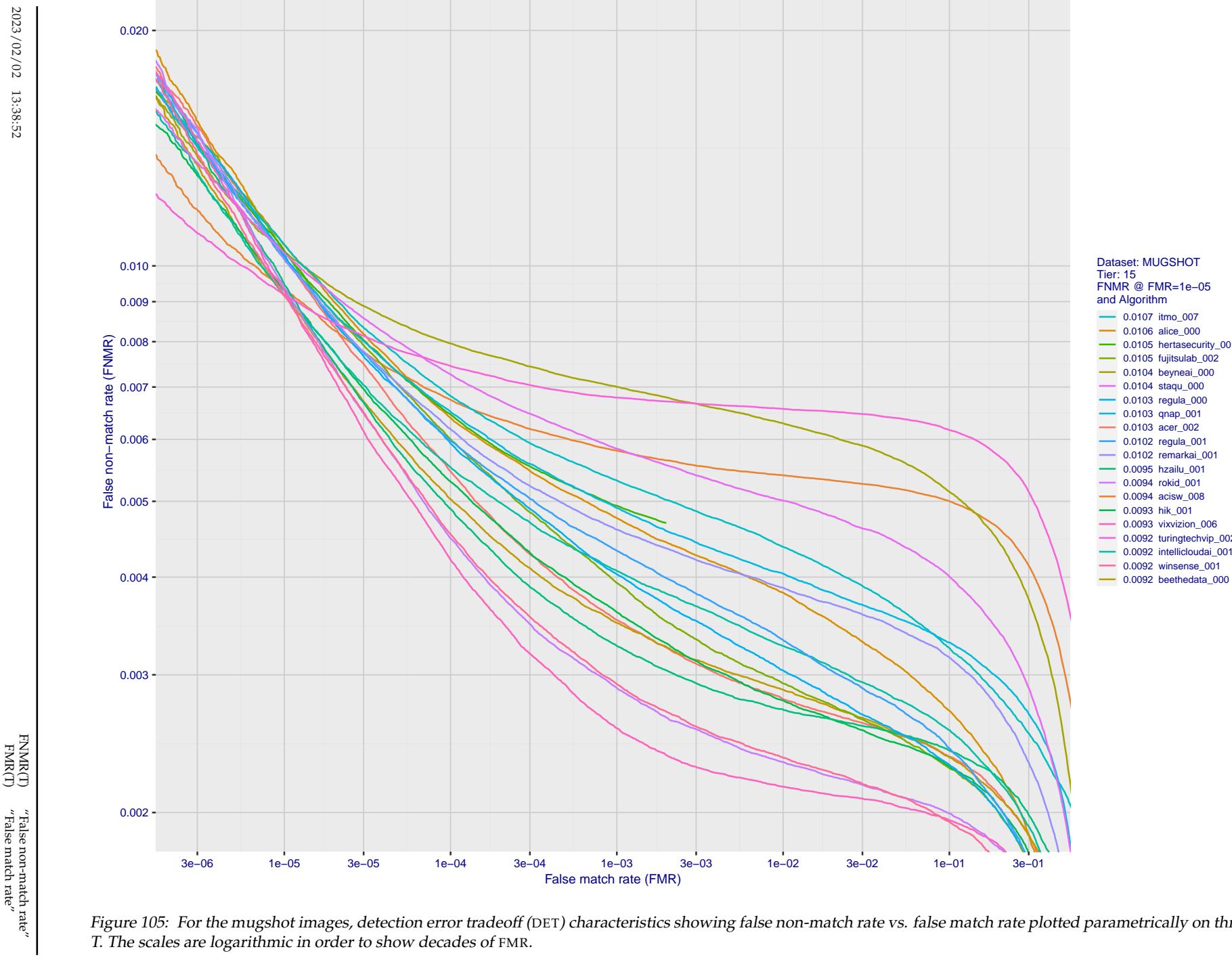


Figure 105: For the mugshot images, detection error tradeoff (DET) characteristics showing false non-match rate vs. false match rate plotted parametrically on threshold, T. The scales are logarithmic in order to show decades of FMR.

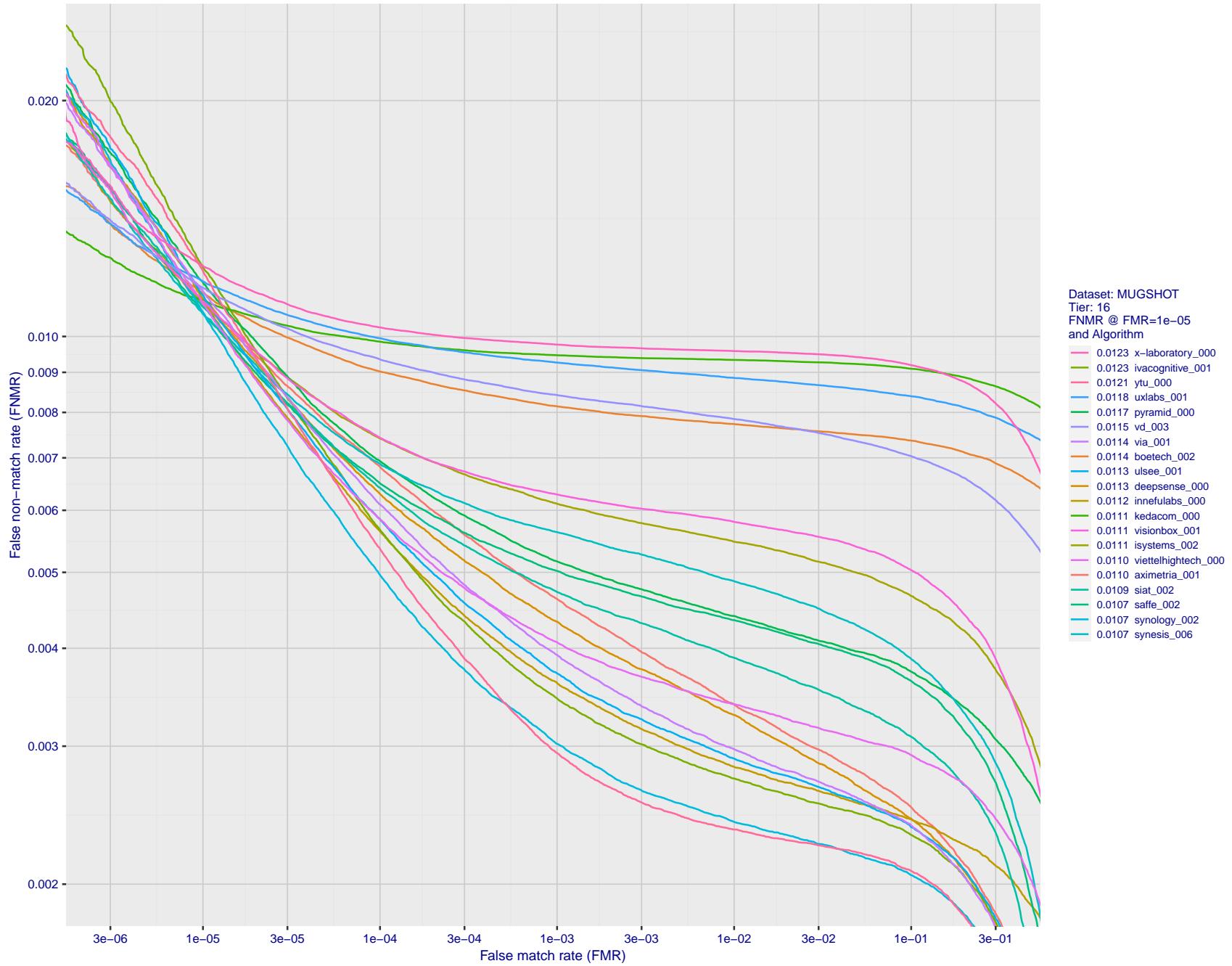


Figure 106: For the mugshot images, detection error tradeoff (DET) characteristics showing false non-match rate vs. false match rate plotted parametrically on threshold, T. The scales are logarithmic in order to show decades of FMR.

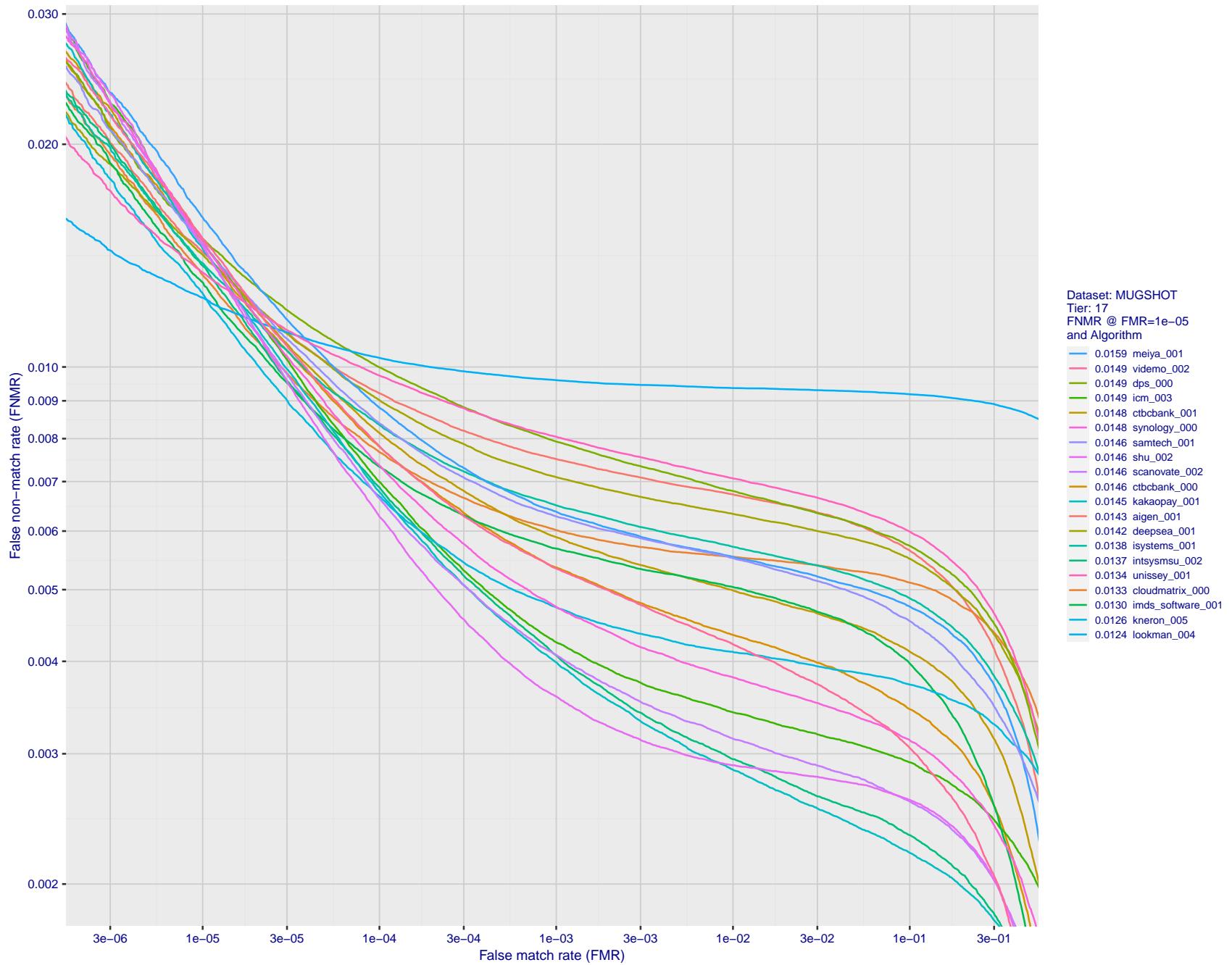


Figure 107: For the mugshot images, detection error tradeoff (DET) characteristics showing false non-match rate vs. false match rate plotted parametrically on threshold, T . The scales are logarithmic in order to show decades of FMR.

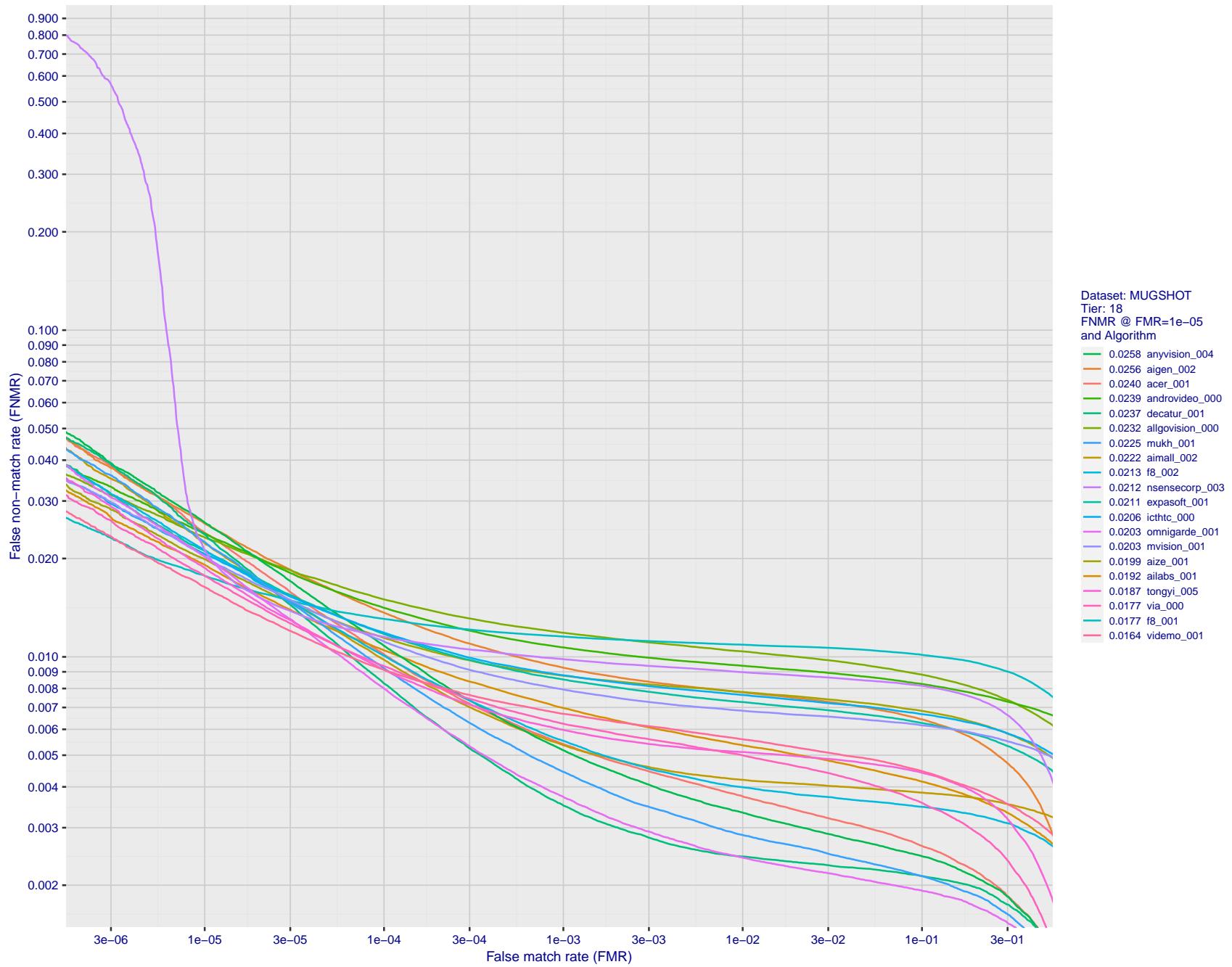


Figure 108: For the mugshot images, detection error tradeoff (DET) characteristics showing false non-match rate vs. false match rate plotted parametrically on threshold, T . The scales are logarithmic in order to show decades of FMR.

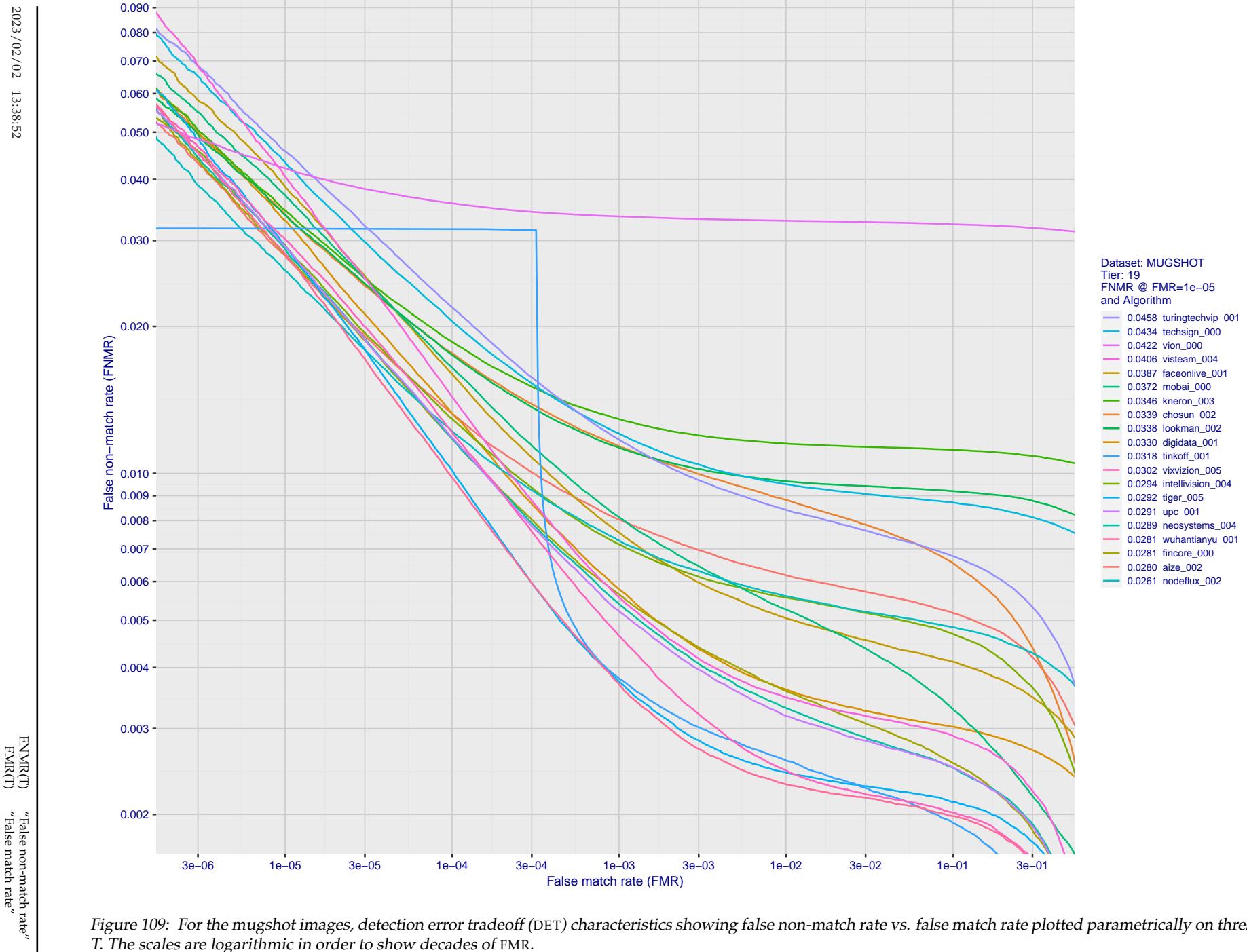


Figure 109: For the mugshot images, detection error tradeoff (DET) characteristics showing false non-match rate vs. false match rate plotted parametrically on threshold, T . The scales are logarithmic in order to show decades of FMR.

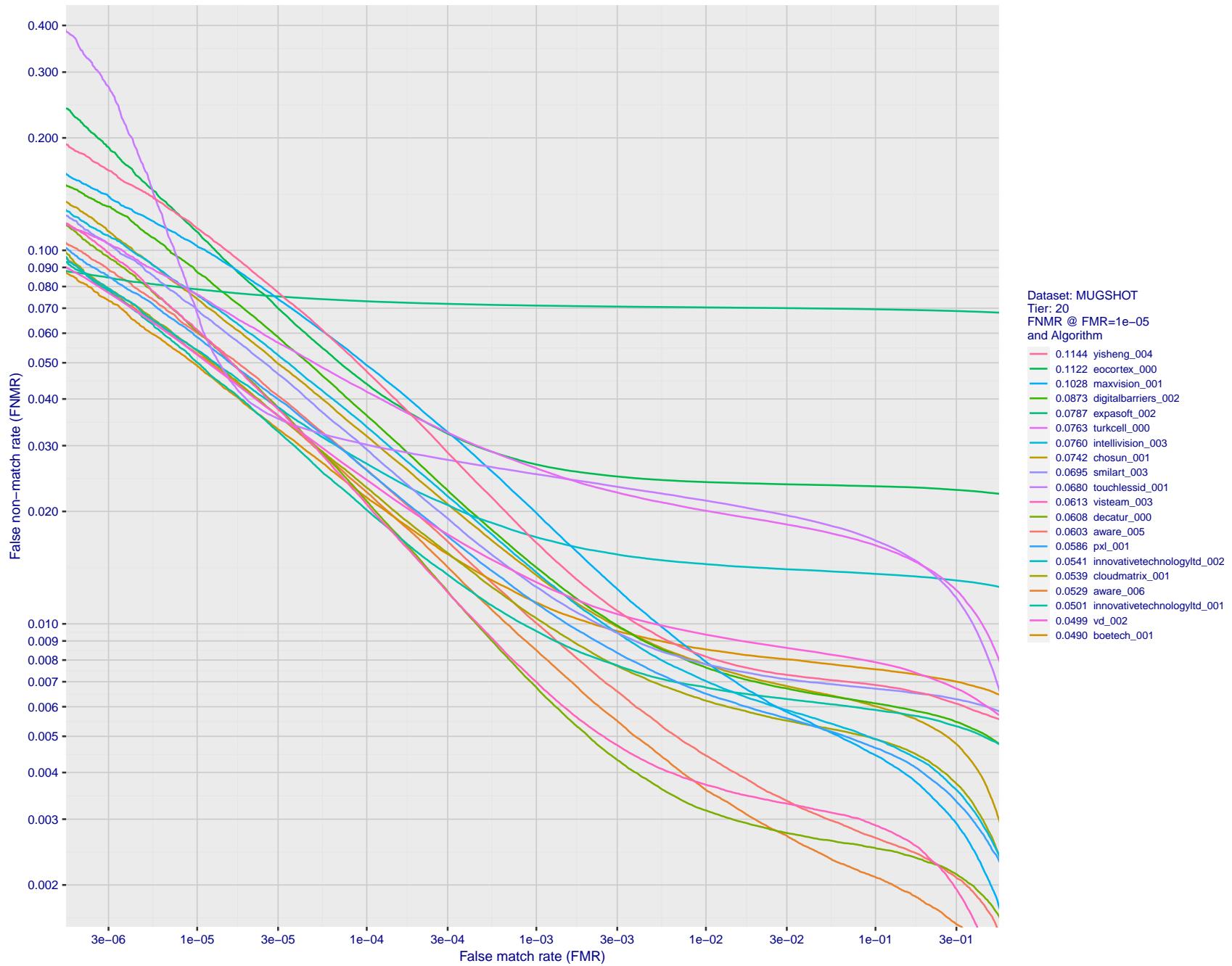


Figure 110: For the mugshot images, detection error tradeoff (DET) characteristics showing false non-match rate vs. false match rate plotted parametrically on threshold, T . The scales are logarithmic in order to show decades of FMR.

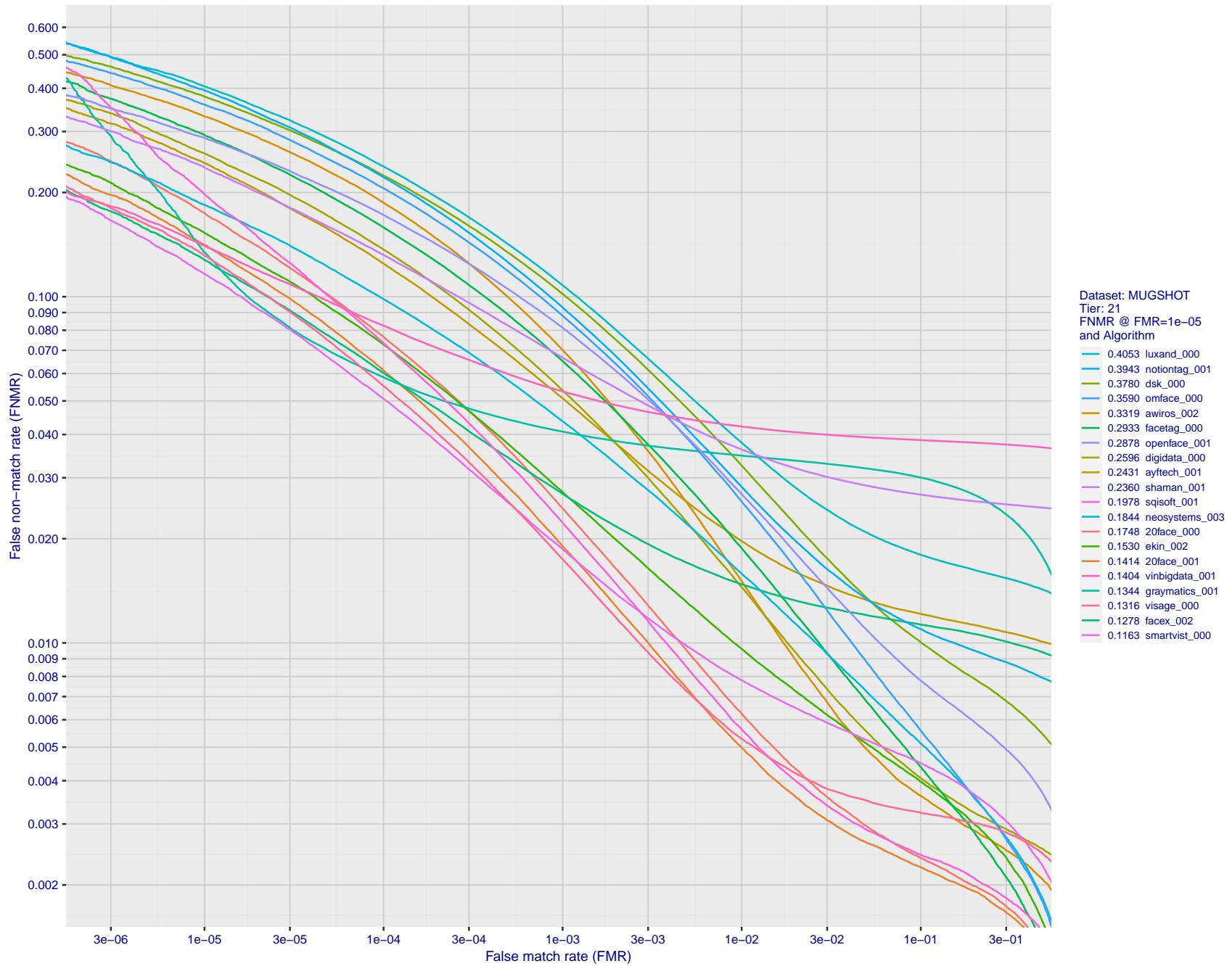


Figure 111: For the mugshot images, detection error tradeoff (DET) characteristics showing false non-match rate vs. false match rate plotted parametrically on threshold, T . The scales are logarithmic in order to show decades of FMR.

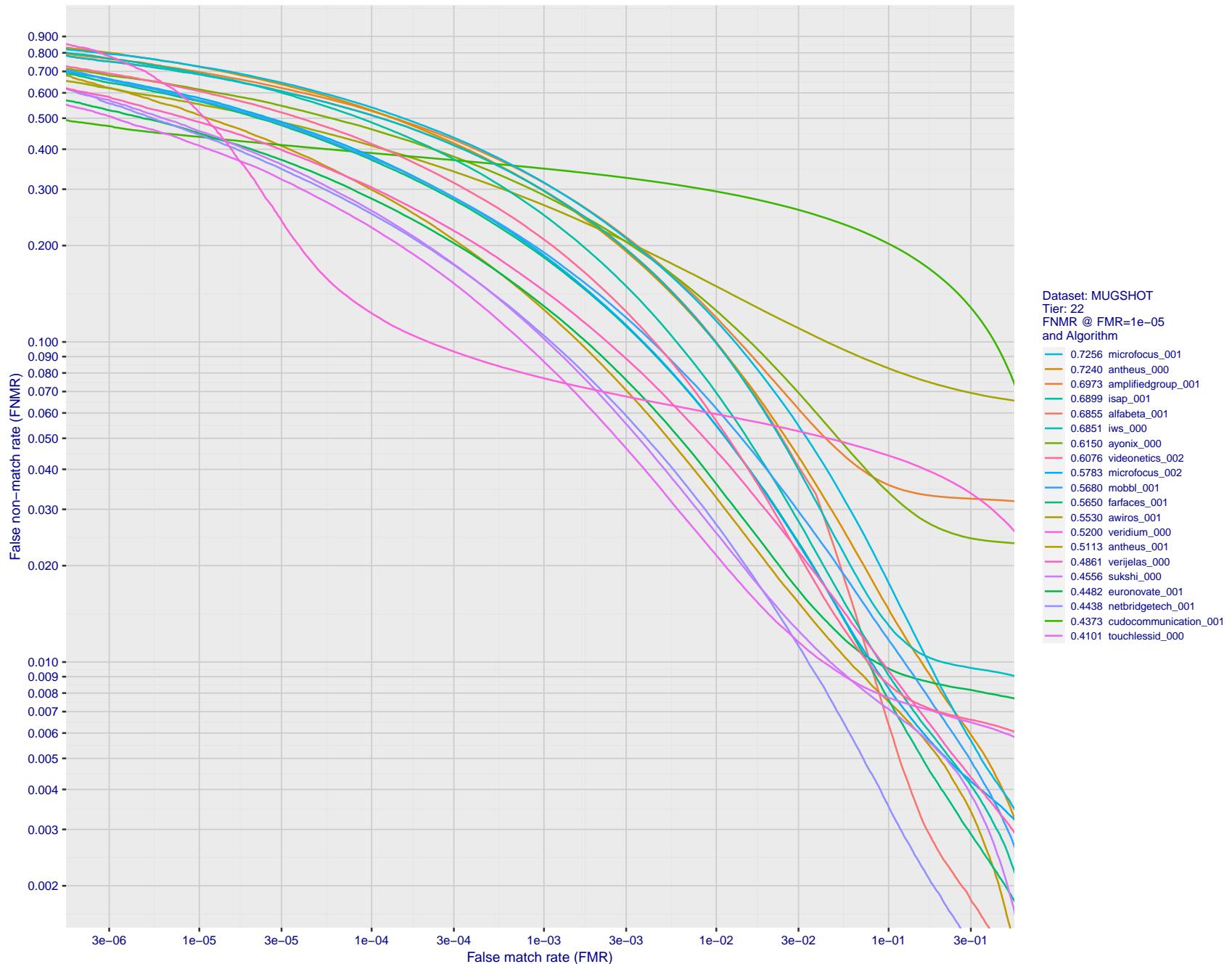


Figure 112: For the mugshot images, detection error tradeoff (DET) characteristics showing false non-match rate vs. false match rate plotted parametrically on threshold, T . The scales are logarithmic in order to show decades of FMR.

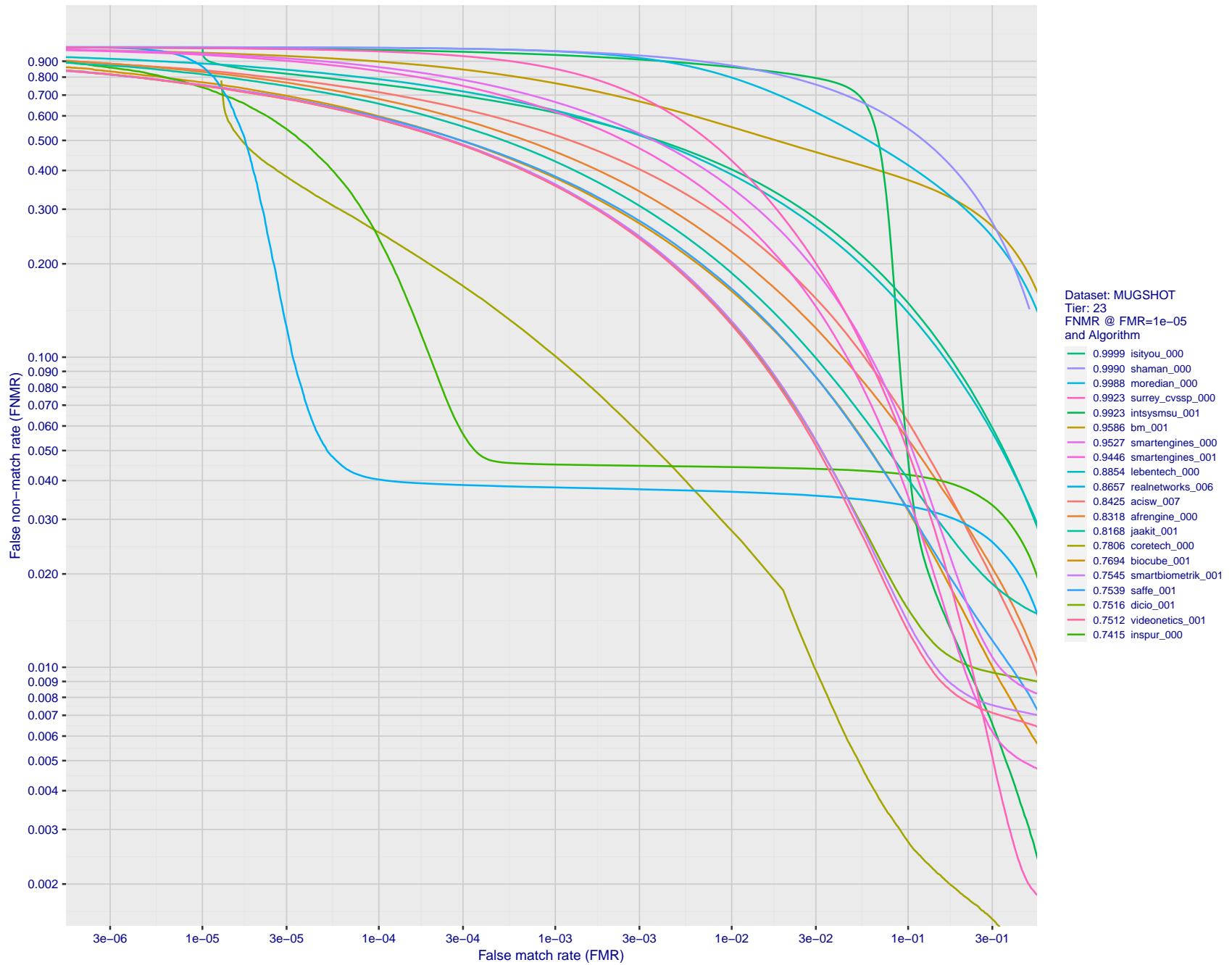


Figure 113: For the mugshot images, detection error tradeoff (DET) characteristics showing false non-match rate vs. false match rate plotted parametrically on threshold, T . The scales are logarithmic in order to show decades of FMR.

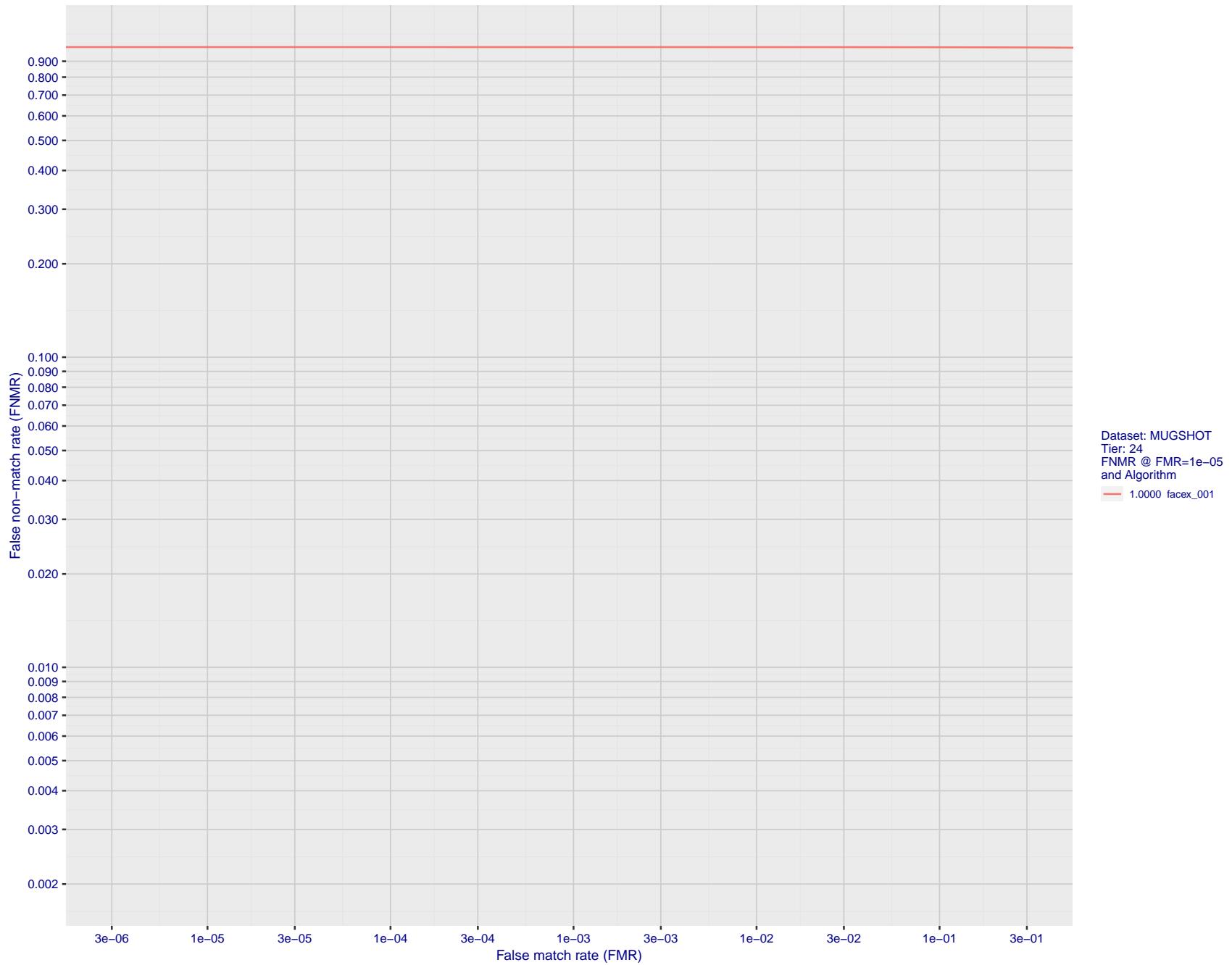


Figure 114: For the mugshot images, detection error tradeoff (DET) characteristics showing false non-match rate vs. false match rate plotted parametrically on threshold, T . The scales are logarithmic in order to show decades of FMR.

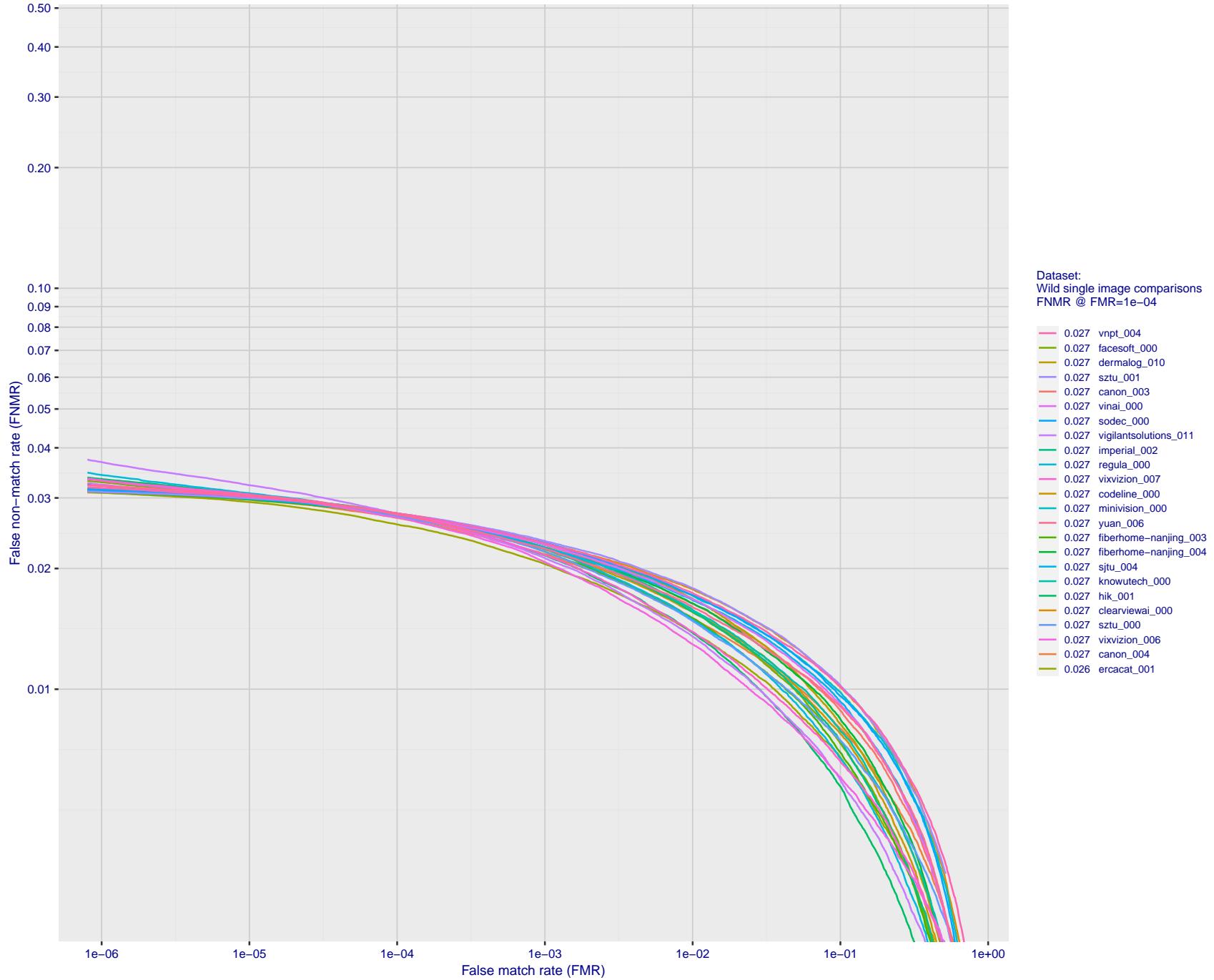


Figure 115: For the 2018 wild image comparisons, detection error tradeoff (DET) characteristics showing false non-match rate vs. false match rate plotted parametrically on threshold, T. The scales are logarithmic in order to show several decades of FMR.

2023/02/02 13:38:52

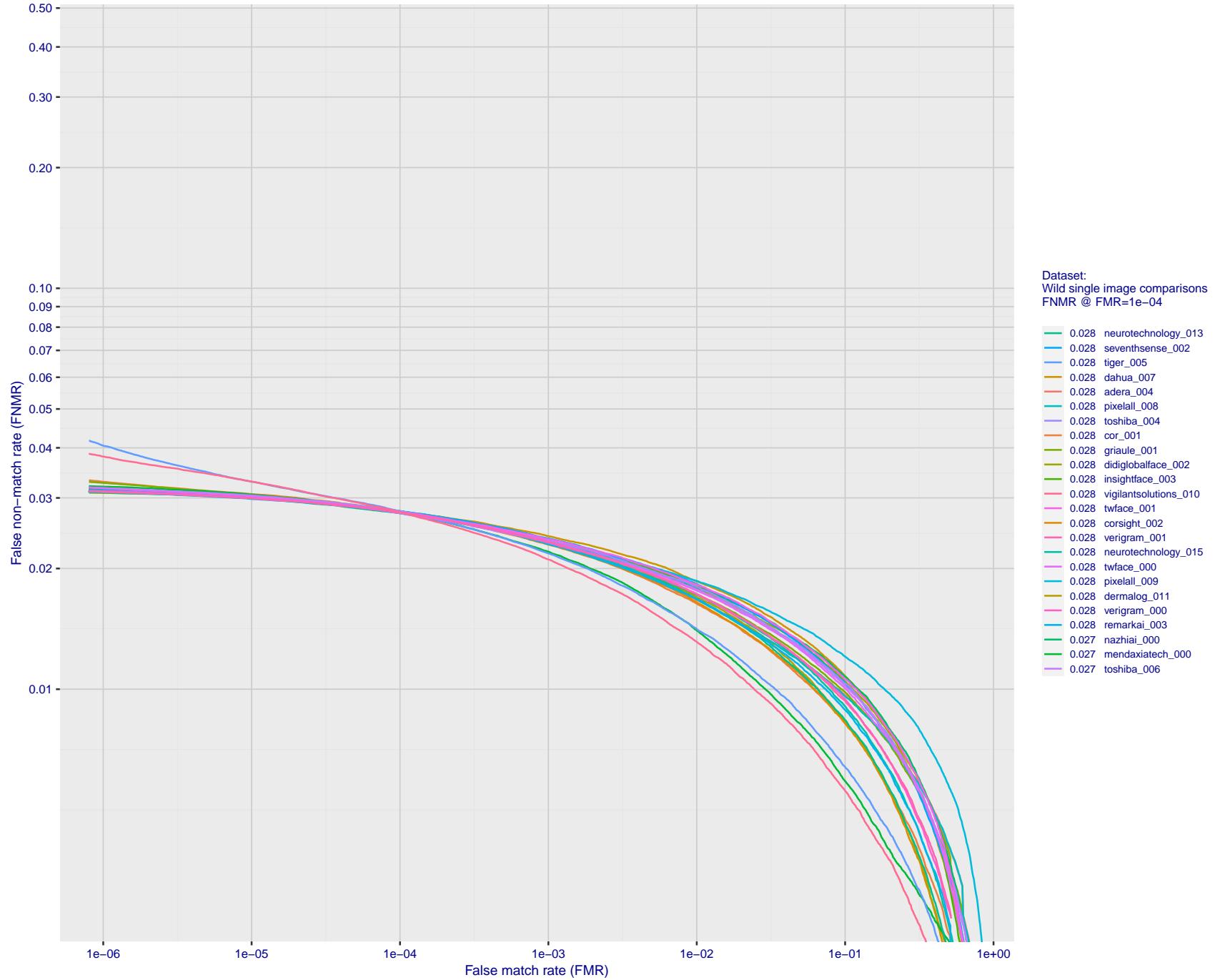


Figure 116: For the 2018 wild image comparisons, detection error tradeoff (DET) characteristics showing false non-match rate vs. false match rate plotted parametrically on threshold, T. The scales are logarithmic in order to show several decades of FMR.

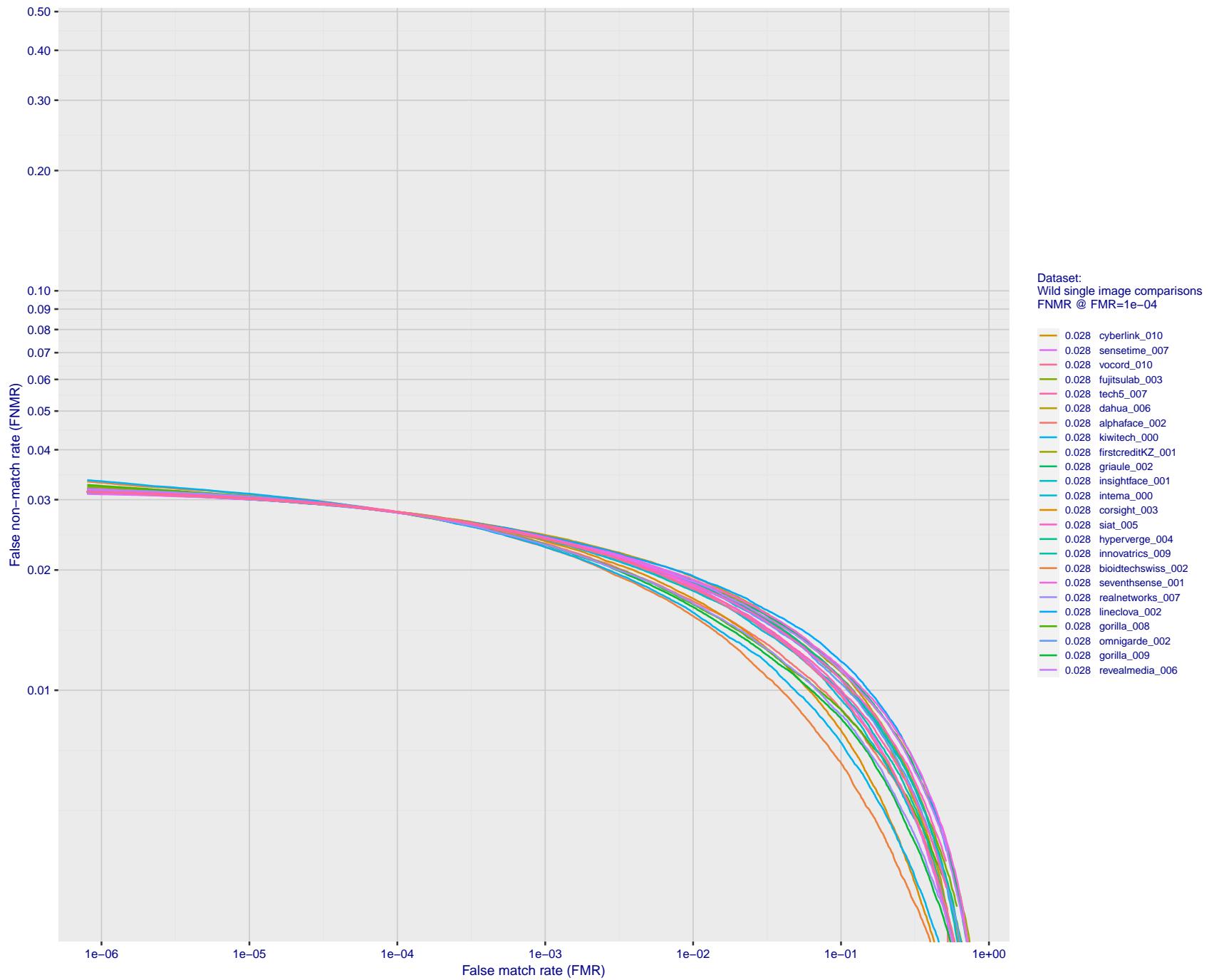


Figure 117: For the 2018 wild image comparisons, detection error tradeoff (DET) characteristics showing false non-match rate vs. false match rate plotted parametrically on threshold, T . The scales are logarithmic in order to show several decades of FMR.

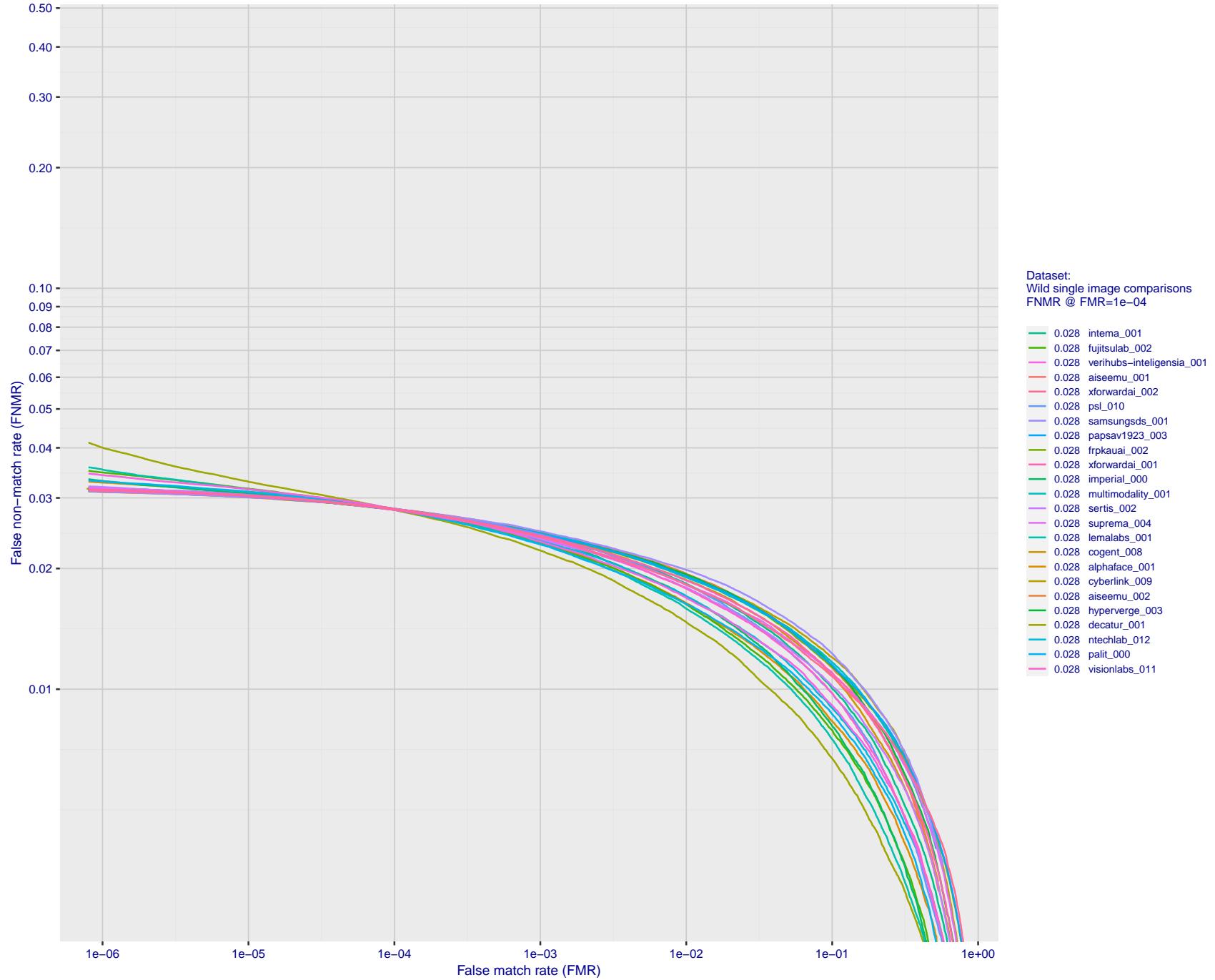


Figure 118: For the 2018 wild image comparisons, detection error tradeoff (DET) characteristics showing false non-match rate vs. false match rate plotted parametrically on threshold, T . The scales are logarithmic in order to show several decades of FMR.

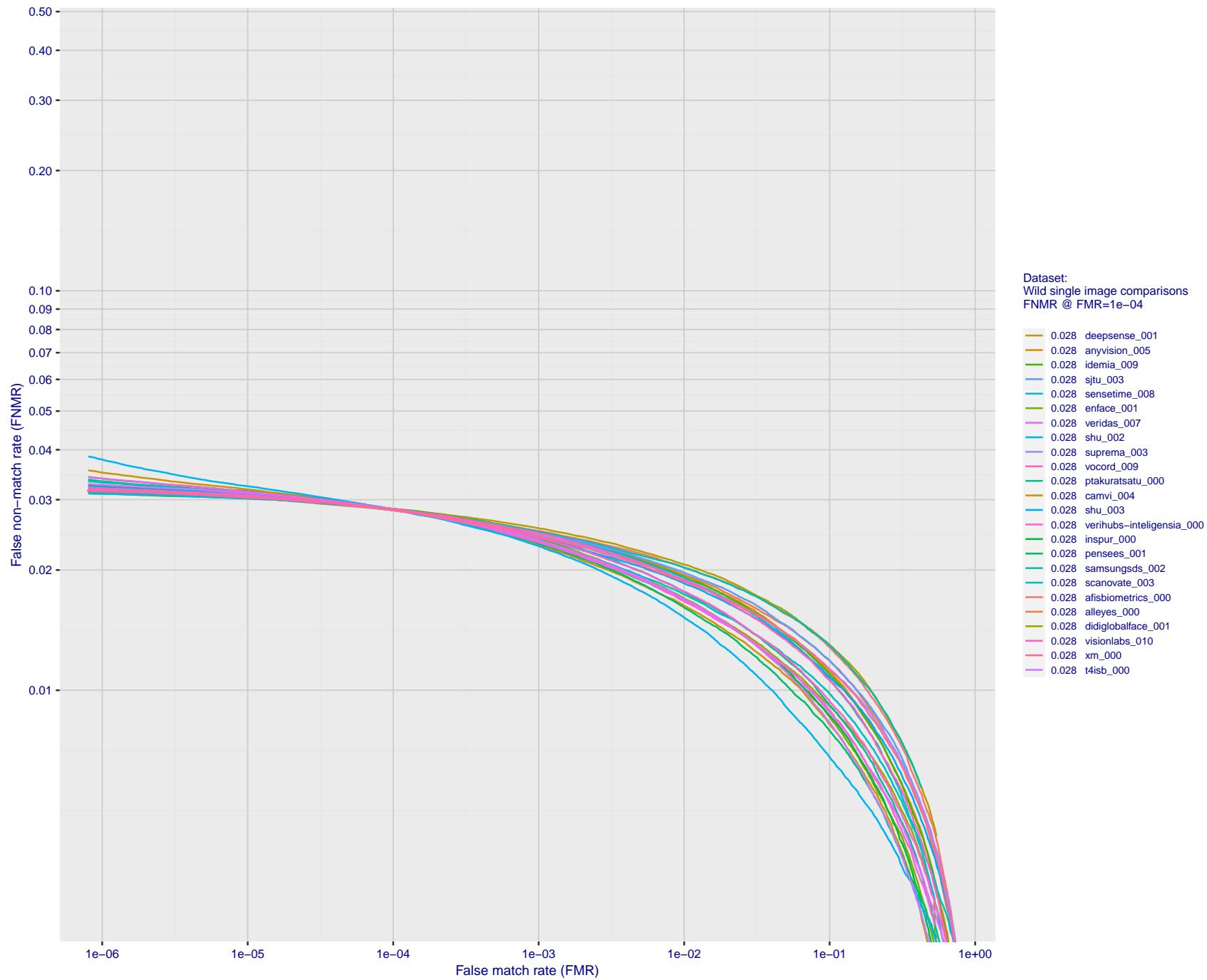


Figure 119: For the 2018 wild image comparisons, detection error tradeoff (DET) characteristics showing false non-match rate vs. false match rate plotted parametrically on threshold, T . The scales are logarithmic in order to show several decades of FMR.

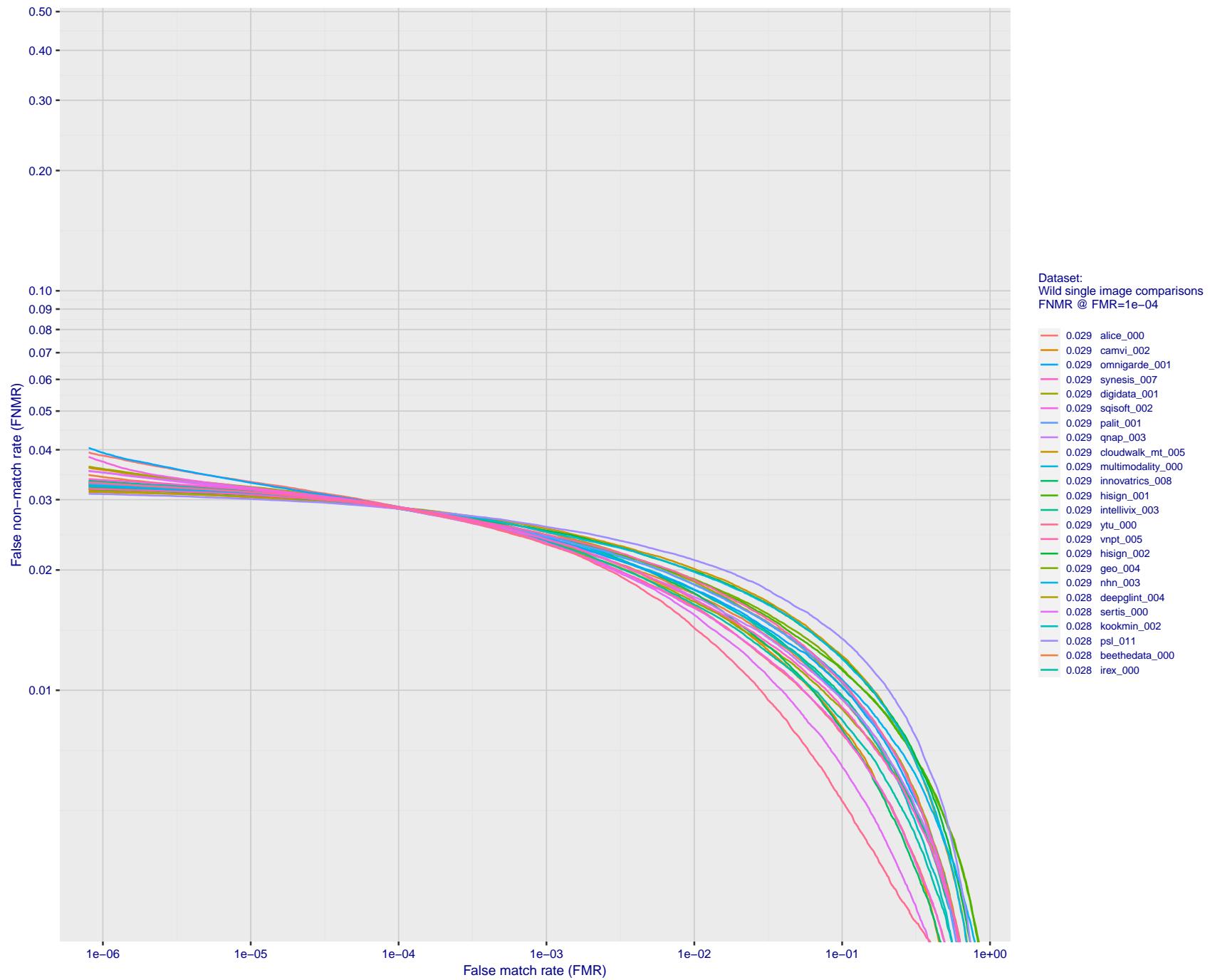


Figure 120: For the 2018 wild image comparisons, detection error tradeoff (DET) characteristics showing false non-match rate vs. false match rate plotted parametrically on threshold, T . The scales are logarithmic in order to show several decades of FMR.

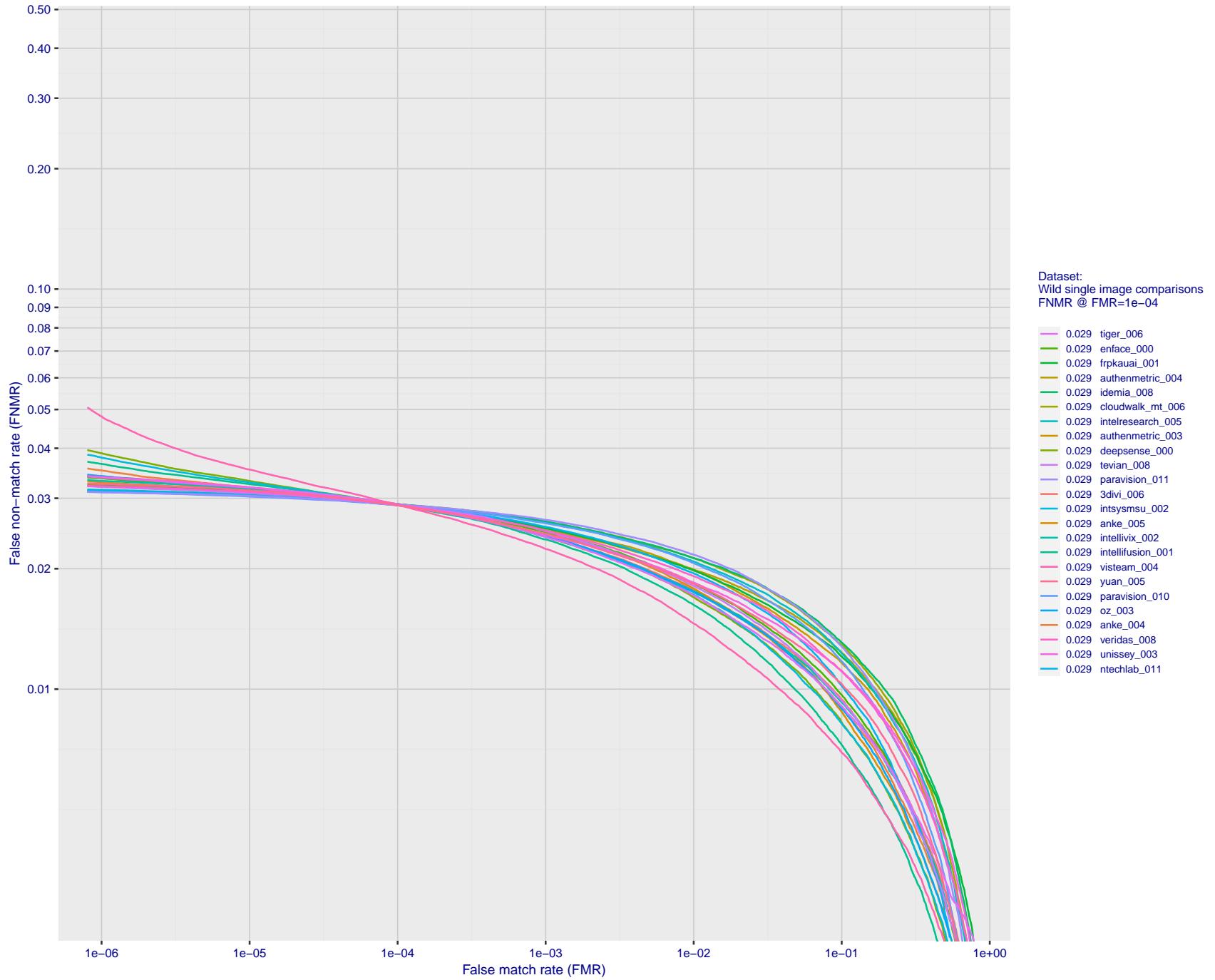


Figure 121: For the 2018 wild image comparisons, detection error tradeoff (DET) characteristics showing false non-match rate vs. false match rate plotted parametrically on threshold, T . The scales are logarithmic in order to show several decades of FMR.

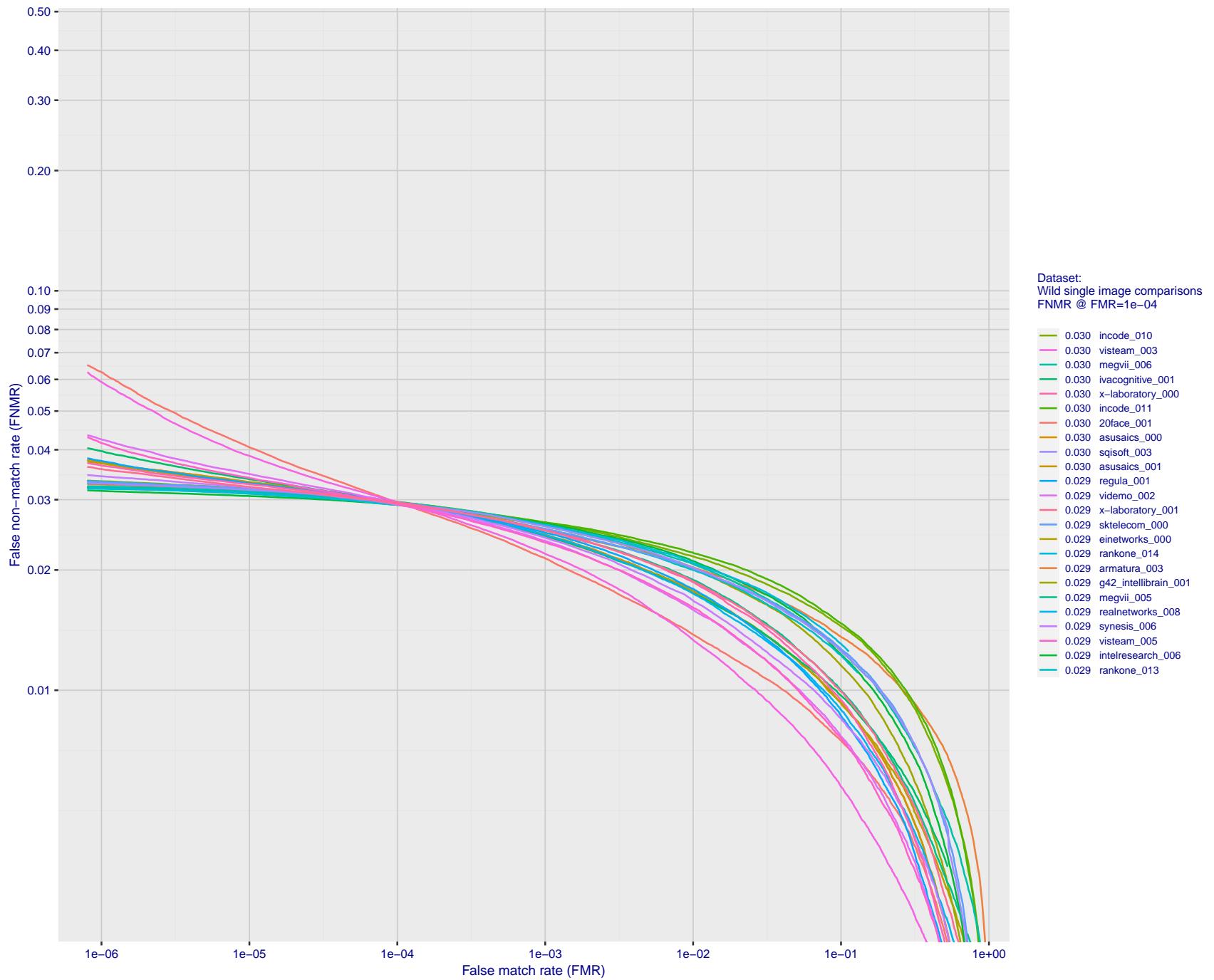


Figure 122: For the 2018 wild image comparisons, detection error tradeoff (DET) characteristics showing false non-match rate vs. false match rate plotted parametrically on threshold, T . The scales are logarithmic in order to show several decades of FMR.

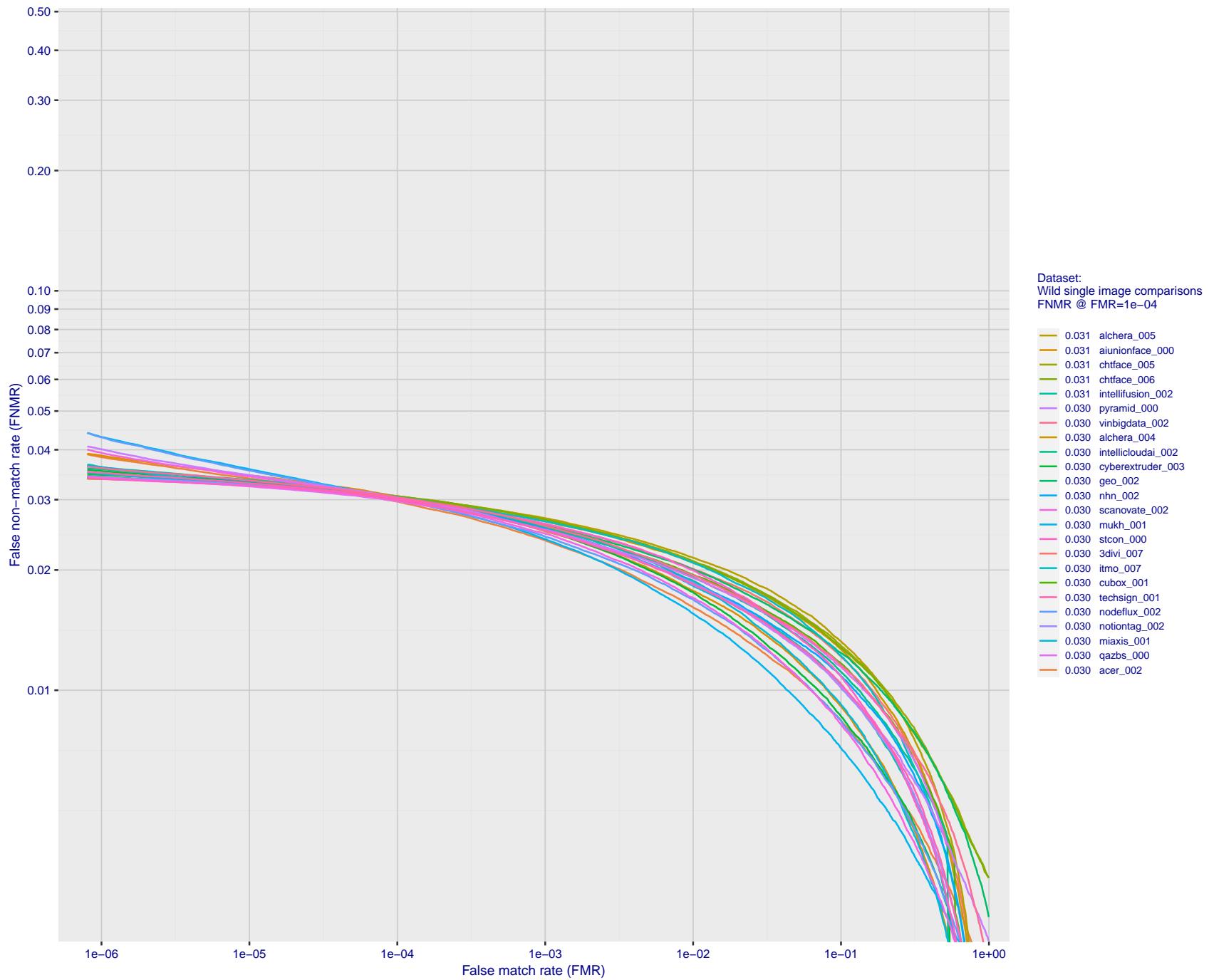


Figure 123: For the 2018 wild image comparisons, detection error tradeoff (DET) characteristics showing false non-match rate vs. false match rate plotted parametrically on threshold, T . The scales are logarithmic in order to show several decades of FMR.

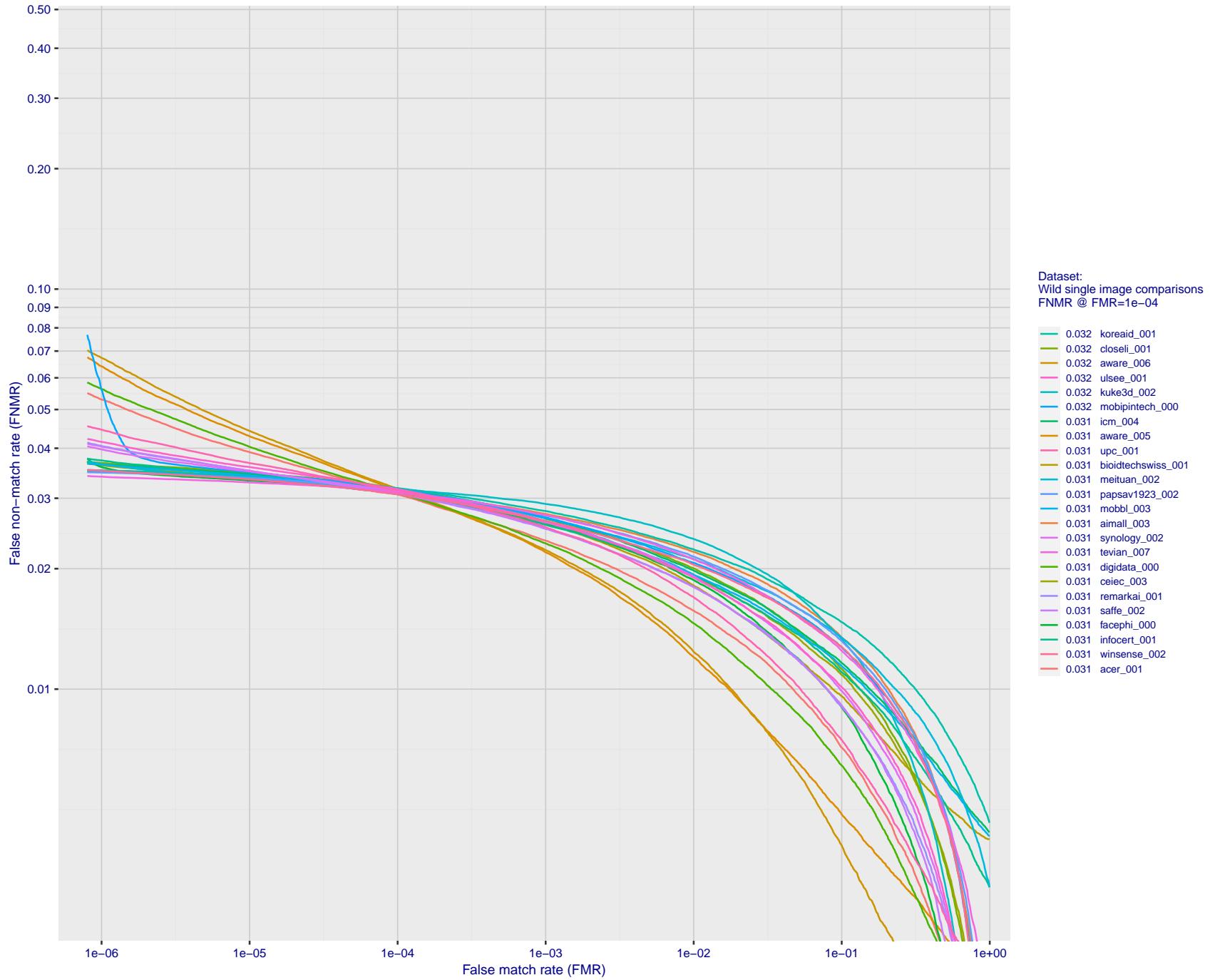


Figure 124: For the 2018 wild image comparisons, detection error tradeoff (DET) characteristics showing false non-match rate vs. false match rate plotted parametrically on threshold, T. The scales are logarithmic in order to show several decades of FMR.

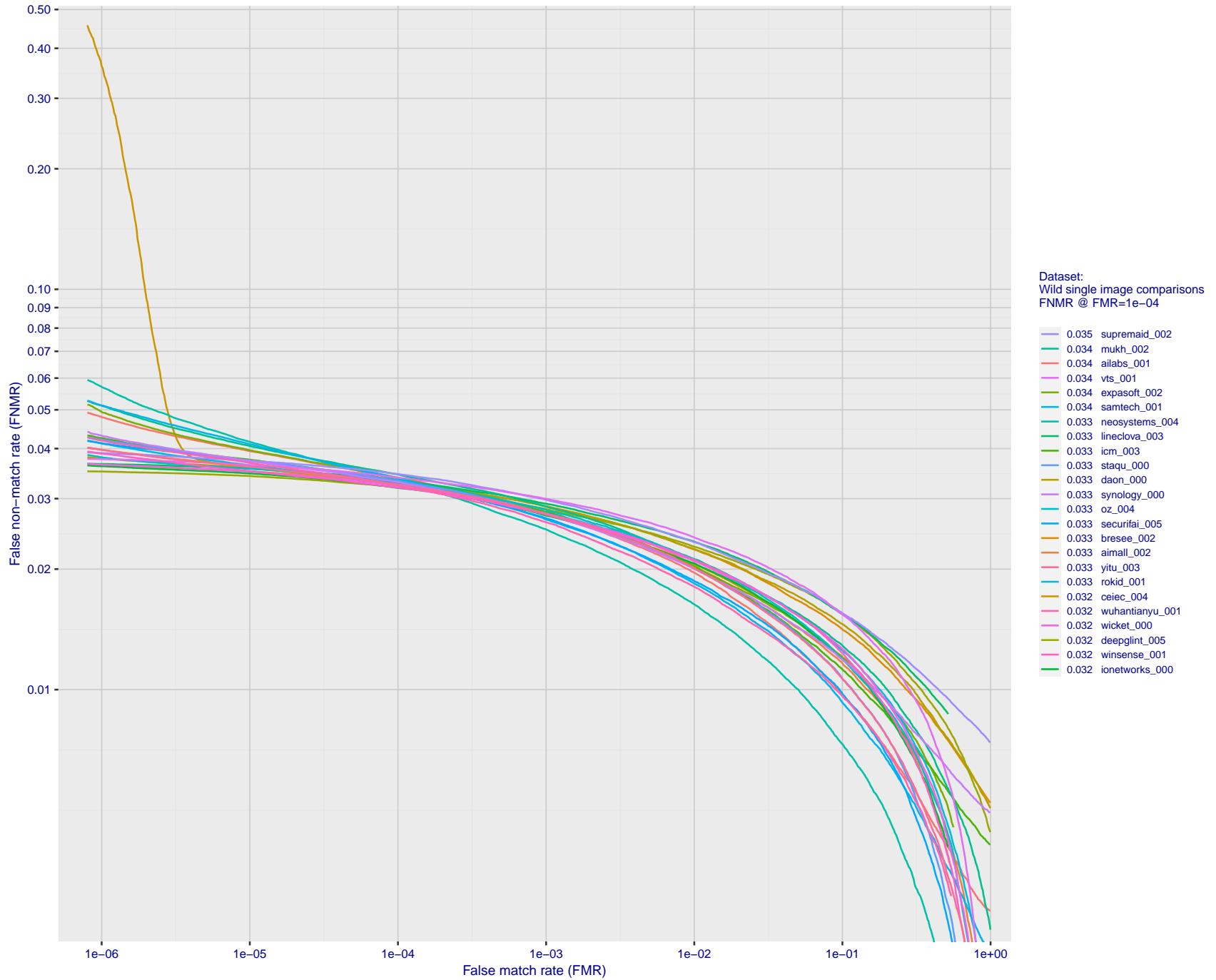


Figure 125: For the 2018 wild image comparisons, detection error tradeoff (DET) characteristics showing false non-match rate vs. false match rate plotted parametrically on threshold, T . The scales are logarithmic in order to show several decades of FMR.

2023/02/02
13:38:52

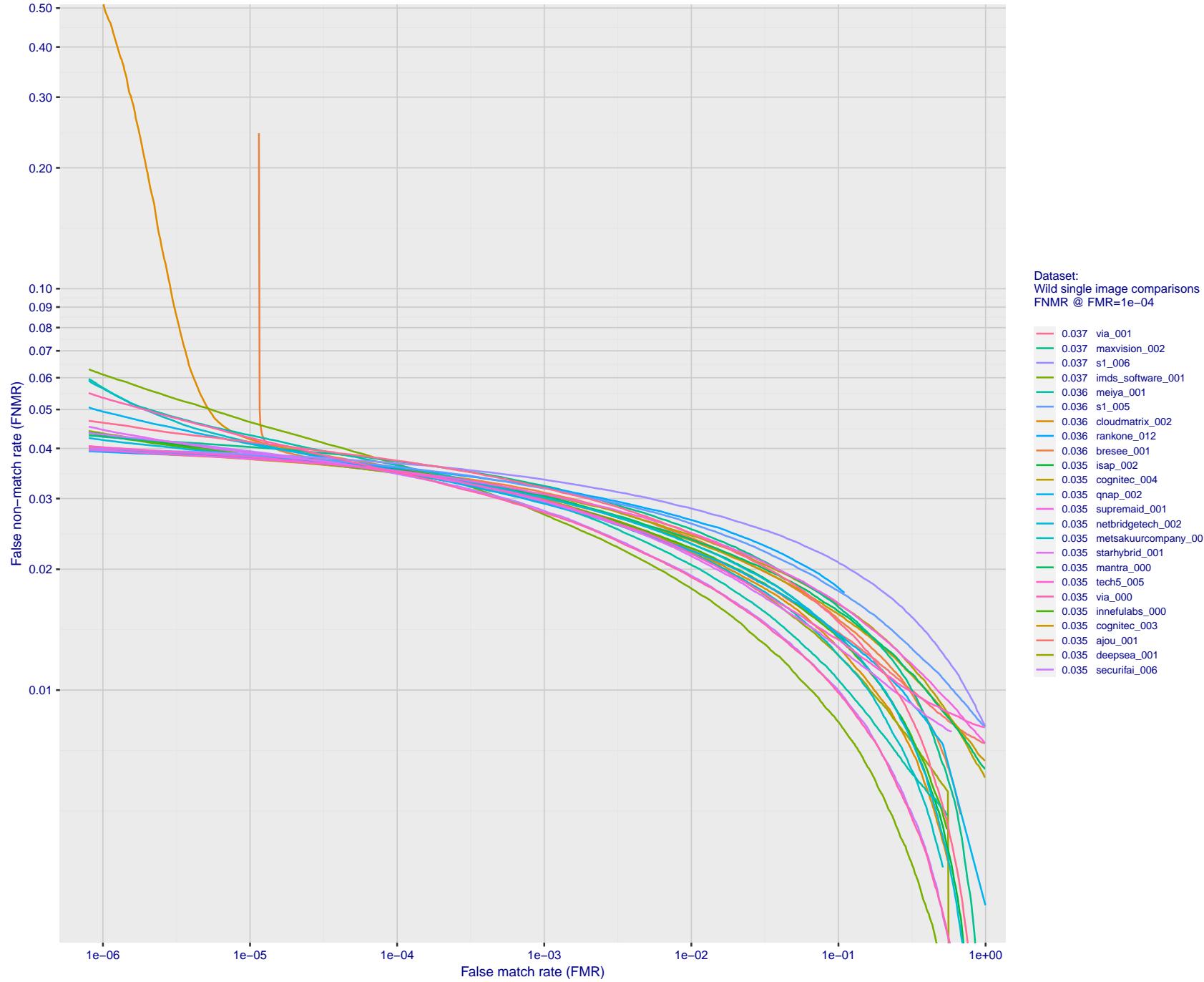


Figure 126: For the 2018 wild image comparisons, detection error tradeoff (DET) characteristics showing false non-match rate vs. false match rate plotted parametrically on threshold, T. The scales are logarithmic in order to show several decades of FMR.

2023/02/02 13:38:52

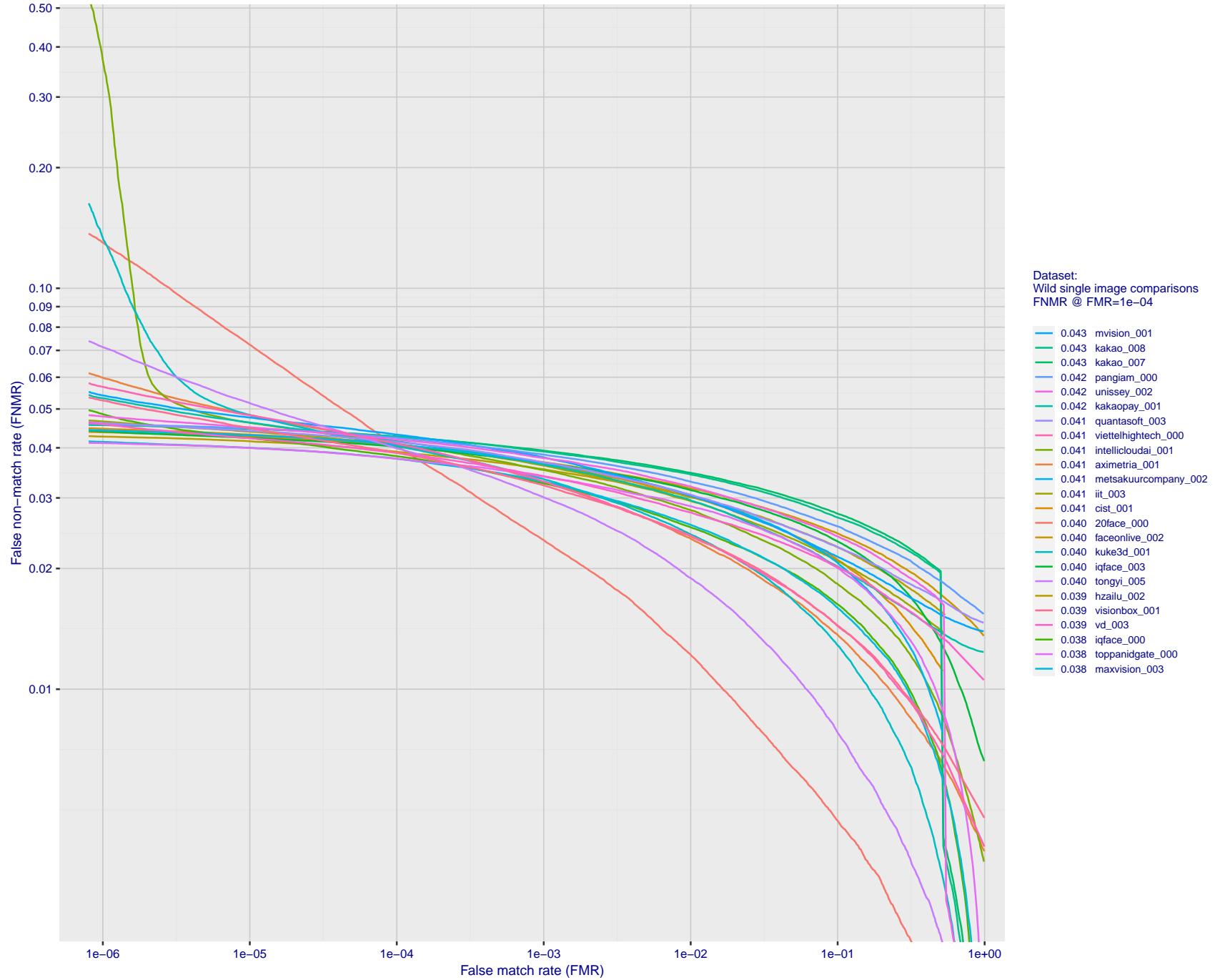


Figure 127: For the 2018 wild image comparisons, detection error tradeoff (DET) characteristics showing false non-match rate vs. false match rate plotted parametrically on threshold, T . The scales are logarithmic in order to show several decades of FMR.

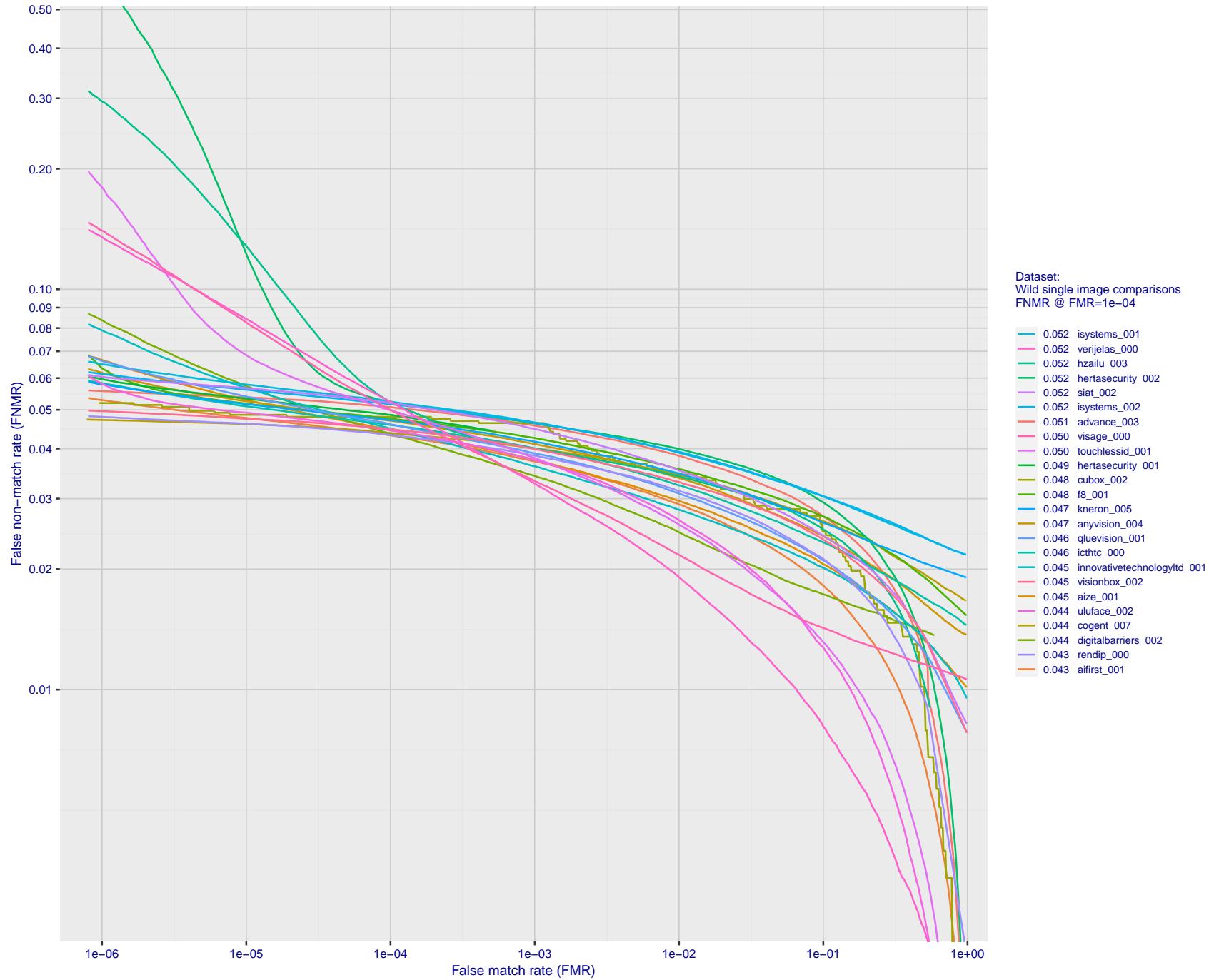


Figure 128: For the 2018 wild image comparisons, detection error tradeoff (DET) characteristics showing false non-match rate vs. false match rate plotted parametrically on threshold, T . The scales are logarithmic in order to show several decades of FMR.

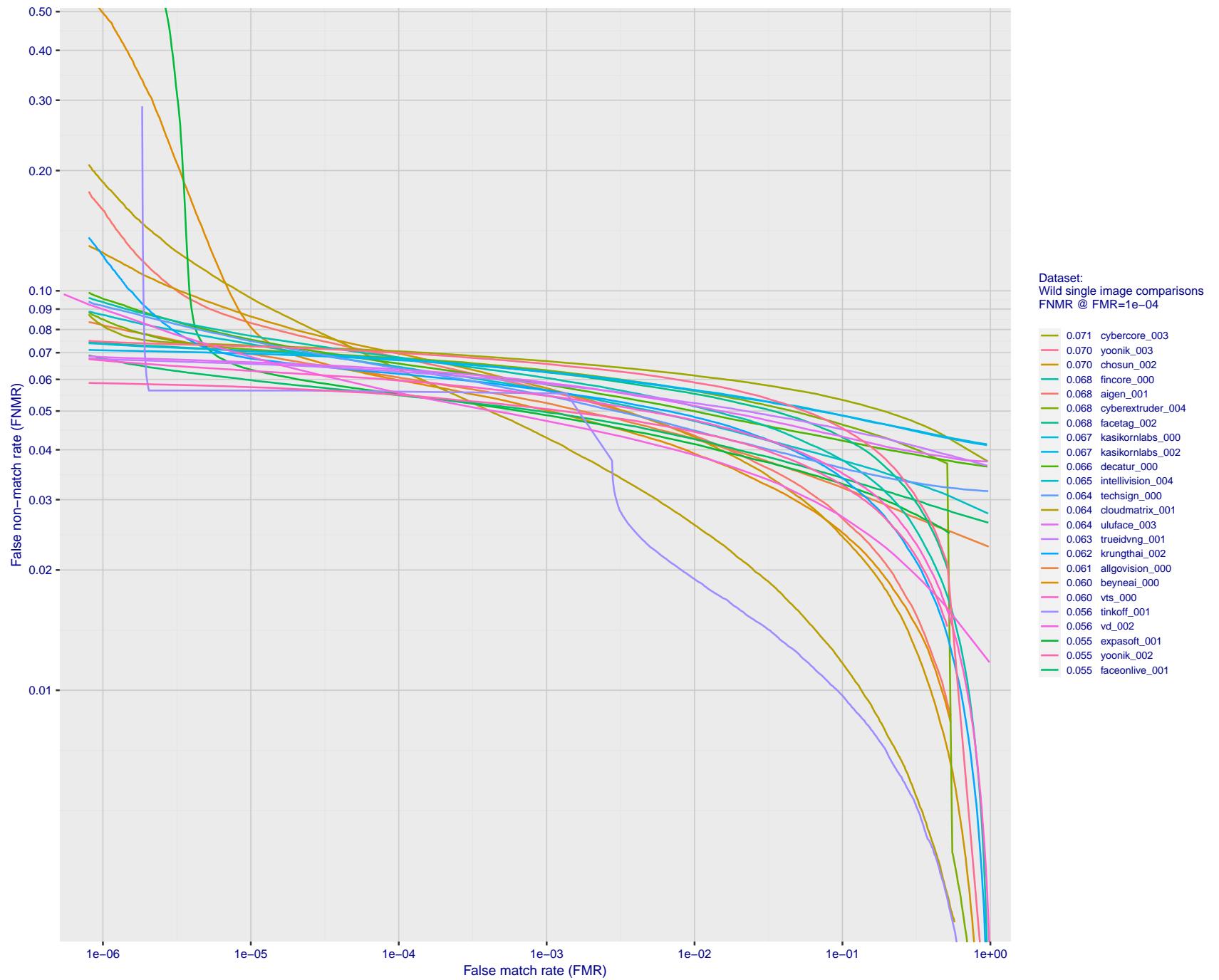


Figure 129: For the 2018 wild image comparisons, detection error tradeoff (DET) characteristics showing false non-match rate vs. false match rate plotted parametrically on threshold, T . The scales are logarithmic in order to show several decades of FMR.

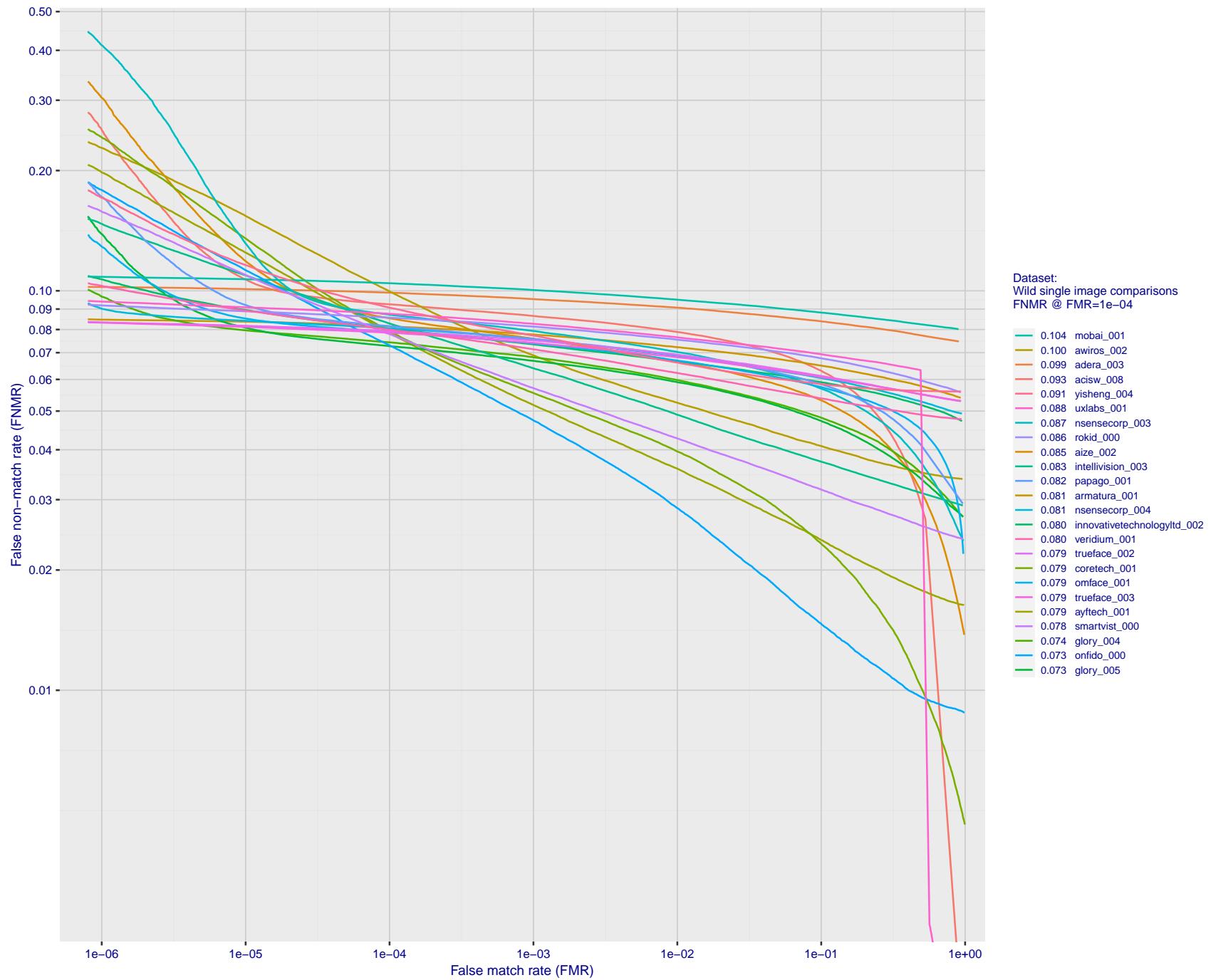


Figure 130: For the 2018 wild image comparisons, detection error tradeoff (DET) characteristics showing false non-match rate vs. false match rate plotted parametrically on threshold, T. The scales are logarithmic in order to show several decades of FMR.

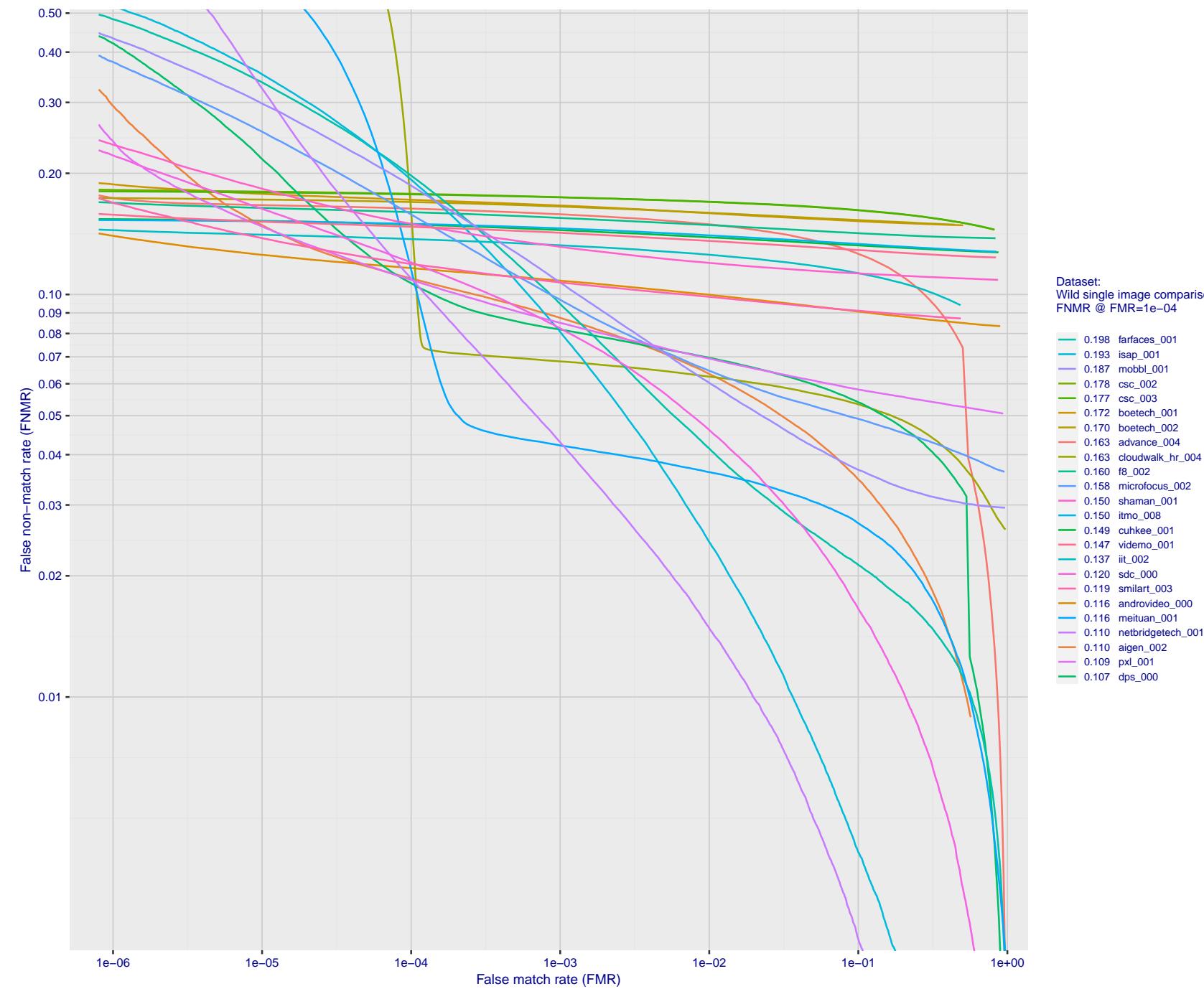


Figure 131: For the 2018 wild image comparisons, detection error tradeoff (DET) characteristics showing false non-match rate vs. false match rate plotted parametrically on threshold, T . The scales are logarithmic in order to show several decades of FMR.

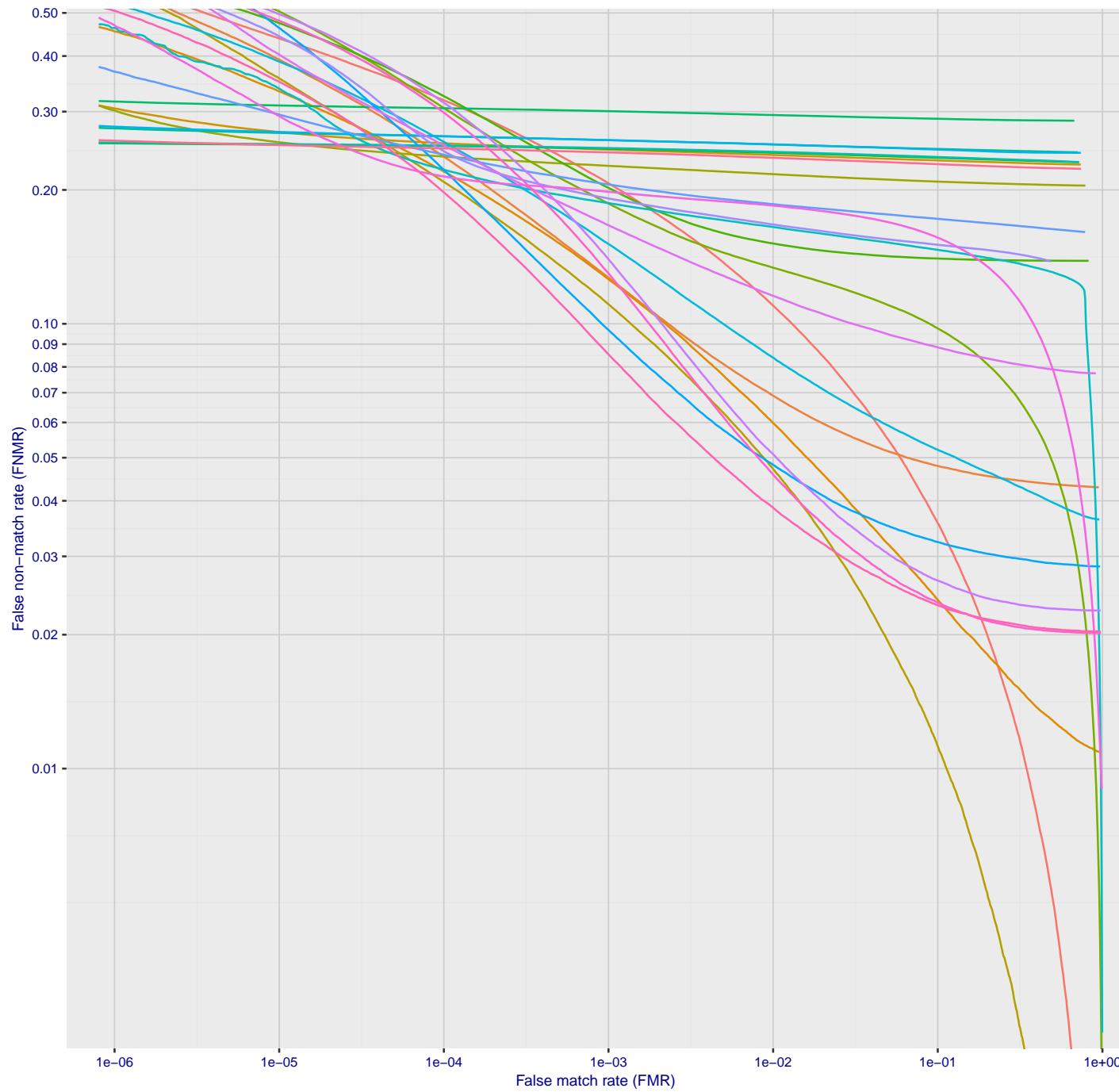


Figure 132: For the 2018 wild image comparisons, detection error tradeoff (DET) characteristics showing false non-match rate vs. false match rate plotted parametrically on threshold, T . The scales are logarithmic in order to show several decades of FMR.

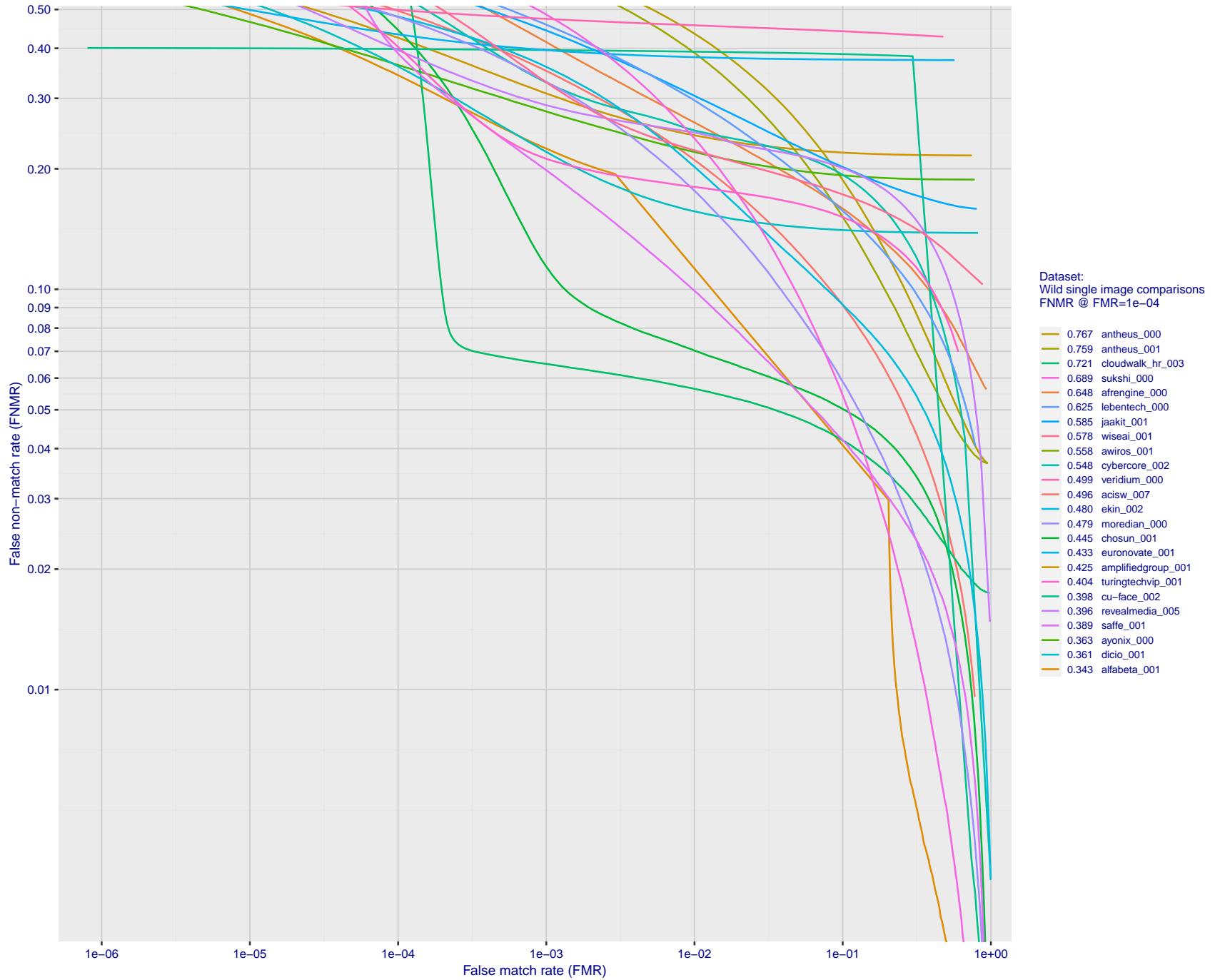


Figure 133: For the 2018 wild image comparisons, detection error tradeoff (DET) characteristics showing false non-match rate vs. false match rate plotted parametrically on threshold, T . The scales are logarithmic in order to show several decades of FMR.

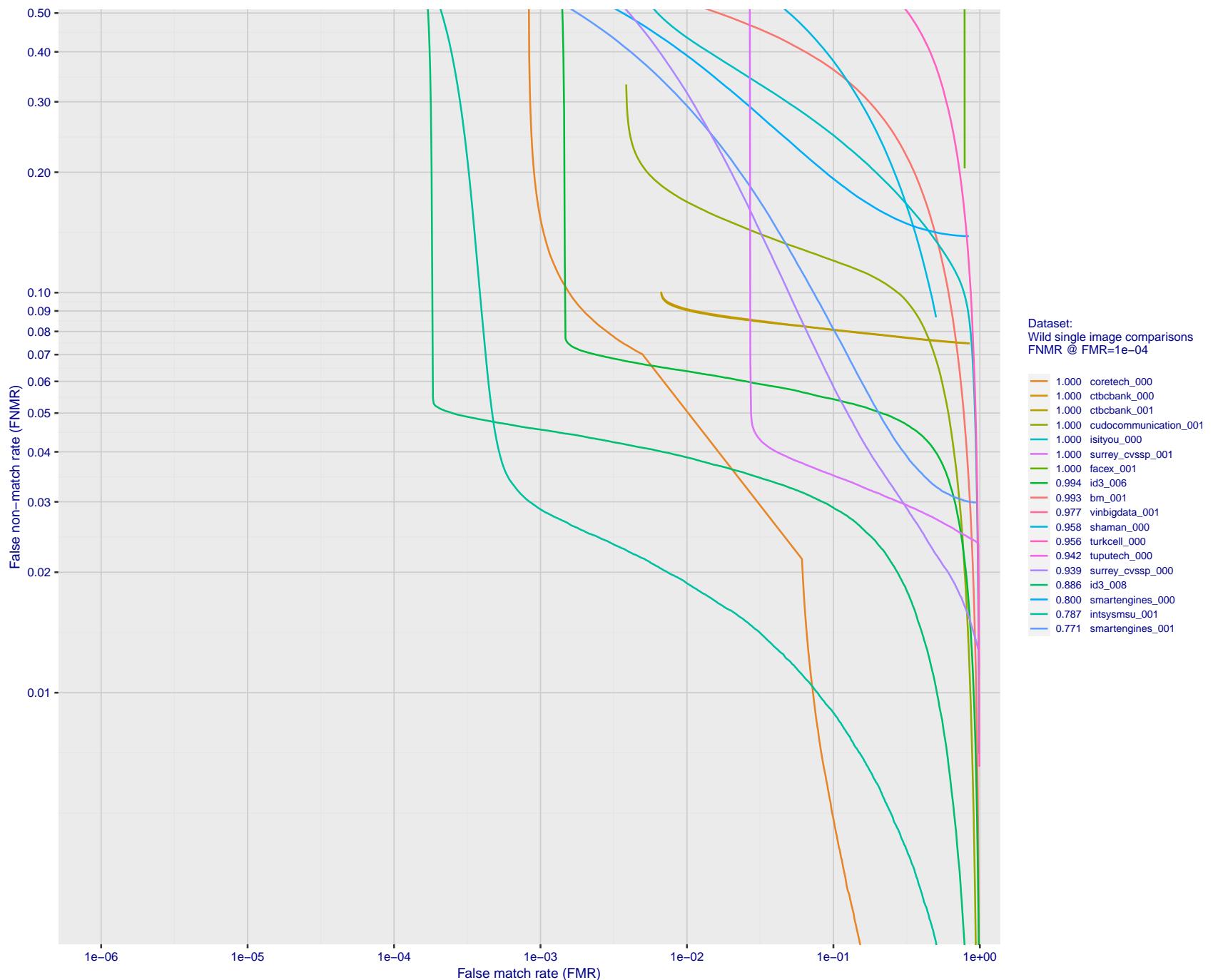


Figure 134: For the 2018 wild image comparisons, detection error tradeoff (DET) characteristics showing false non-match rate vs. false match rate plotted parametrically on threshold, T. The scales are logarithmic in order to show several decades of FMR.

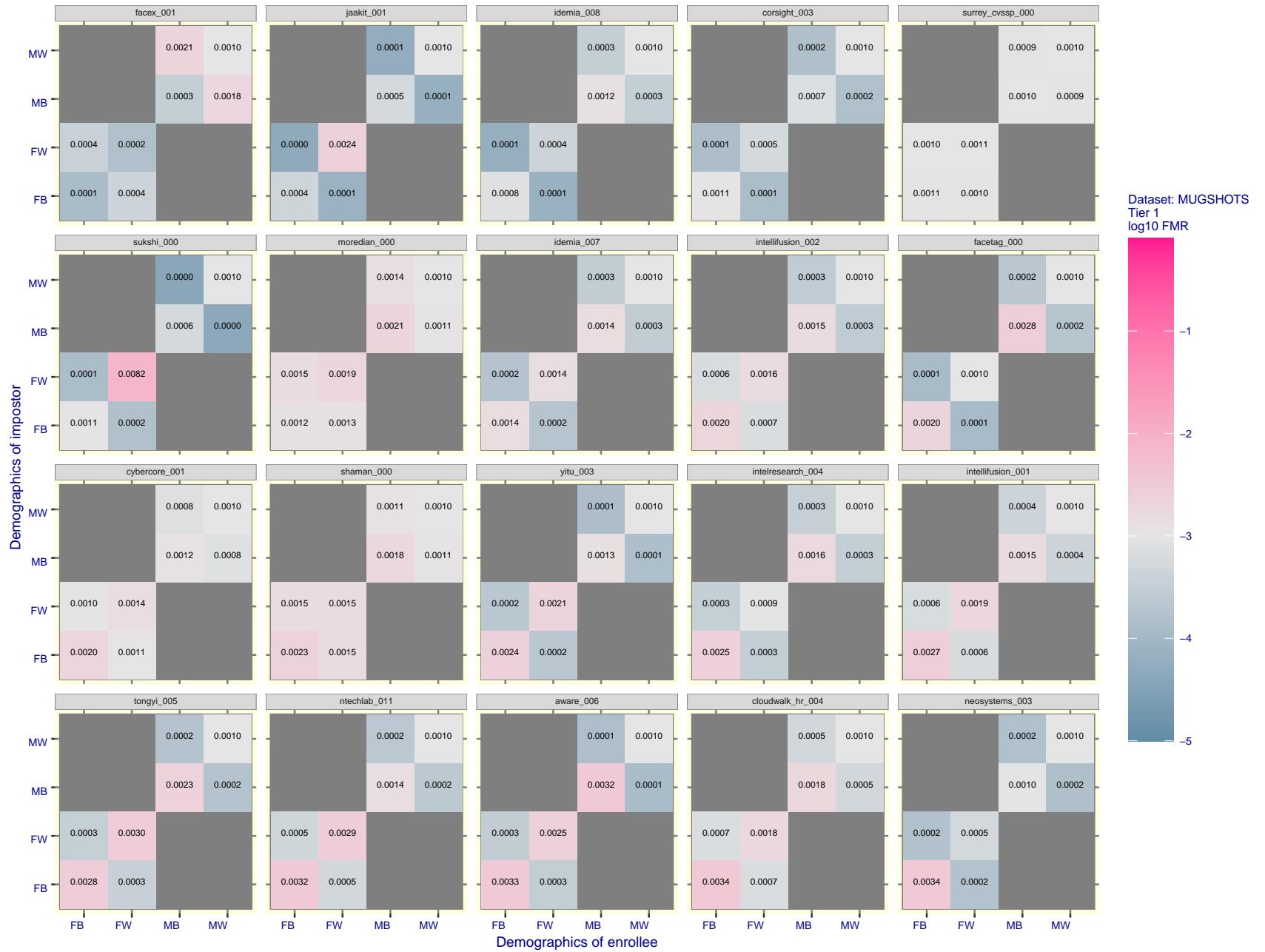


Figure 135: For the mugshot images, FMR for same-sex impostor pairs of images annotated with codes for black female, black male, white female, white male. The threshold is set for each algorithm to give $FMR = 0.001$ for white males which is the demographic that usually gives the lowest FMR. This means the top right box is the same color in all panels. The panels are sorted over multiple pages in order of FMR on black females, which is the demographic that usually gives the highest FMR.

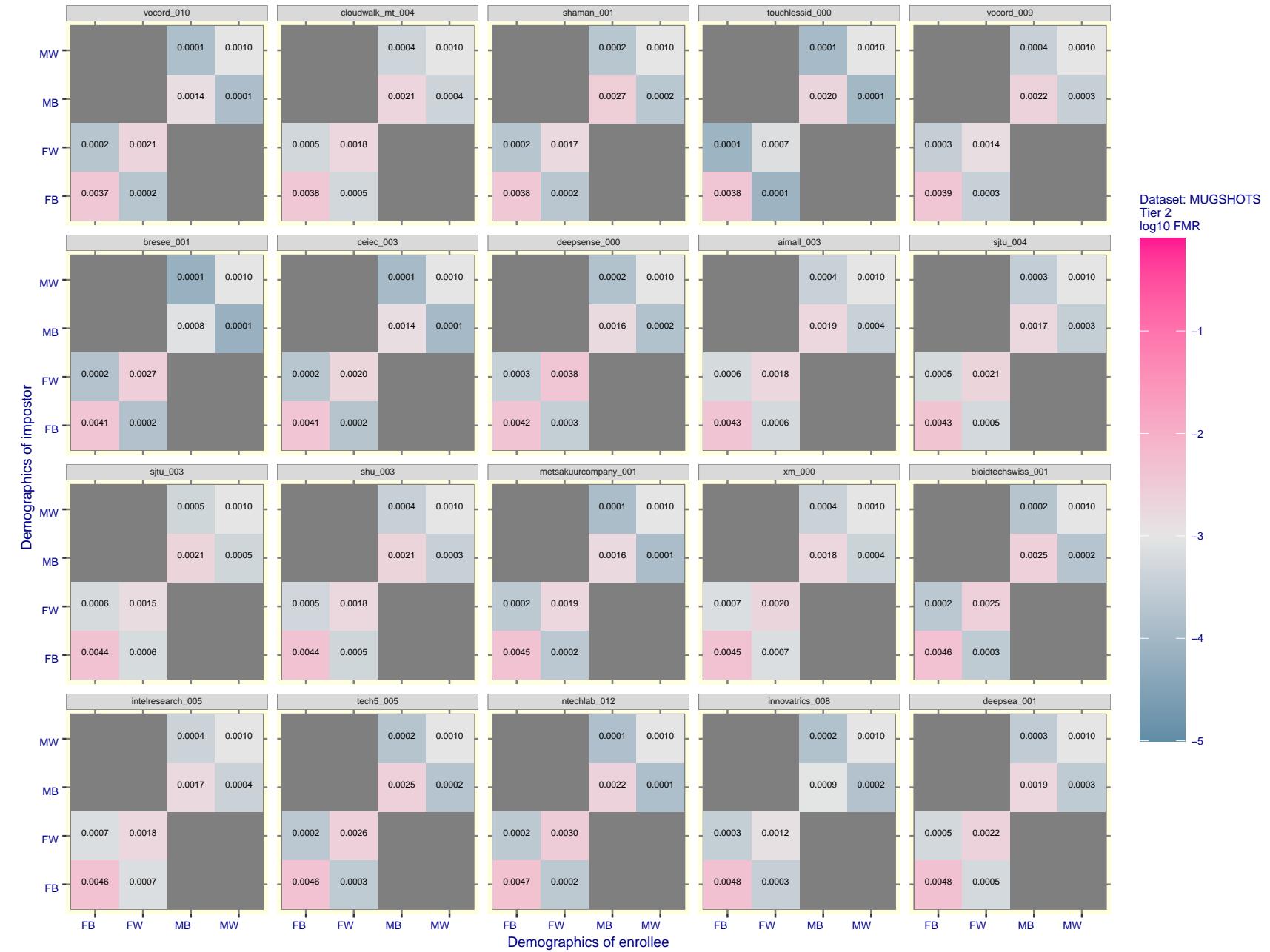


Figure 136: For the mugshot images, FMR for same-sex impostor pairs of images annotated with codes for black female, black male, white female, white male. The threshold is set for each algorithm to give FMR = 0.001 for white males which is the demographic that usually gives the lowest FMR. This means the top right box is the same color in all panels. The panels are sorted over multiple pages in order of FMR on black females, which is the demographic that usually gives the highest FMR.

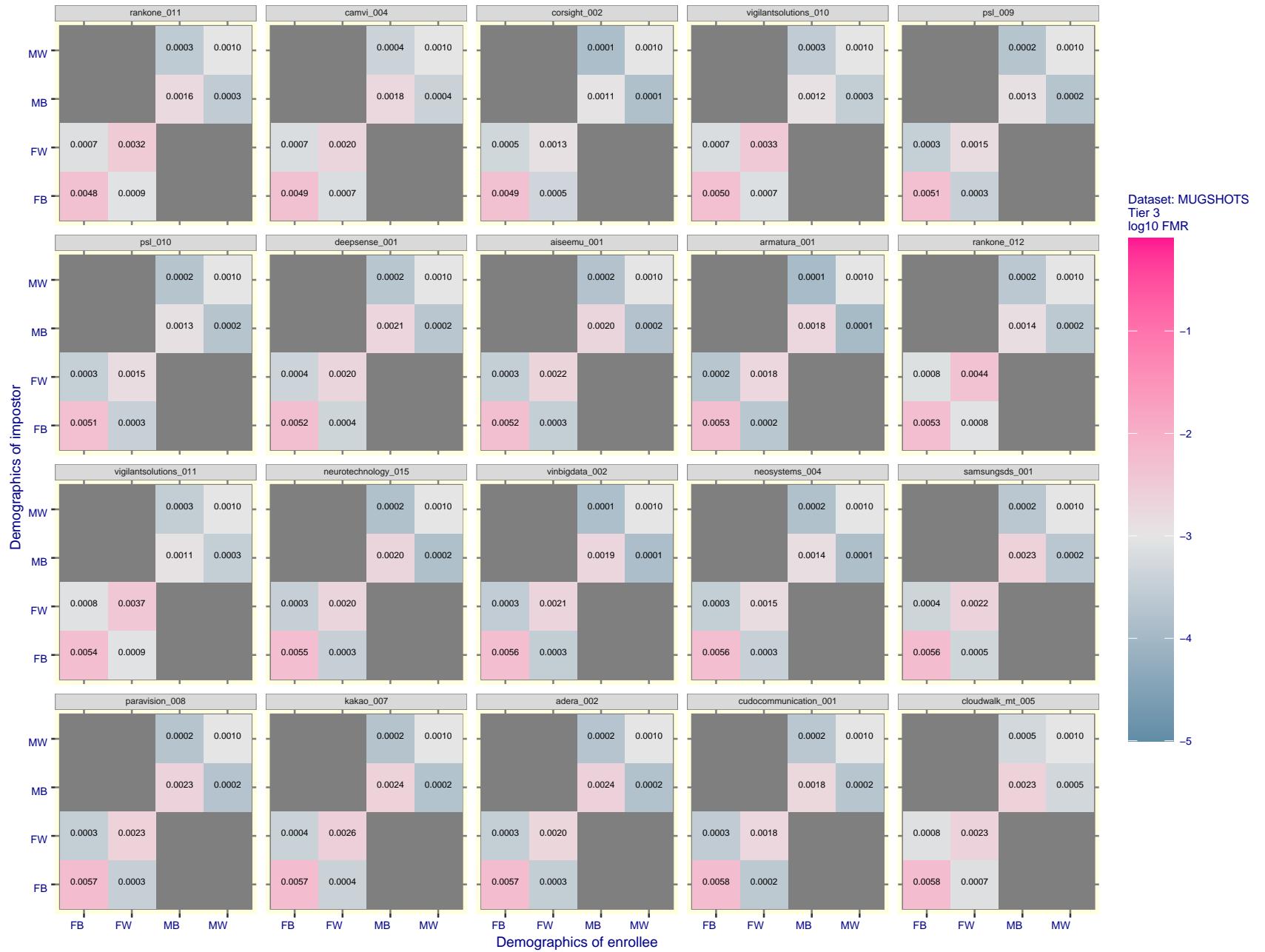


Figure 137: For the mugshot images, FMR for same-sex impostor pairs of images annotated with codes for black female, black male, white female, white male. The threshold is set for each algorithm to give FMR = 0.001 for white males which is the demographic that usually gives the lowest FMR. This means the top right box is the same color in all panels. The panels are sorted over multiple pages in order of FMR on black females, which is the demographic that usually gives the highest FMR.

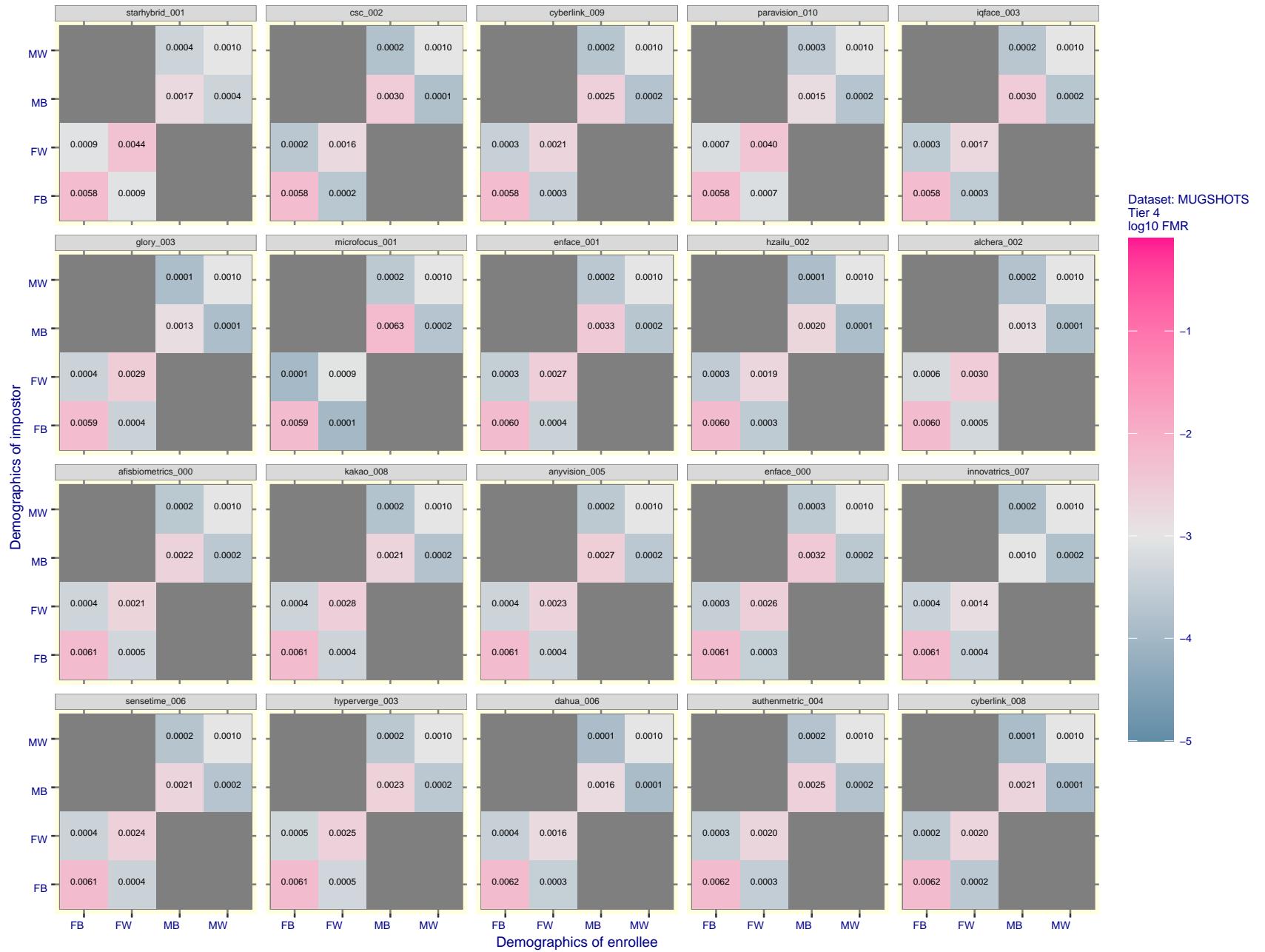


Figure 138: For the mugshot images, FMR for same-sex impostor pairs of images annotated with codes for black female, black male, white female, white male. The threshold is set for each algorithm to give $\text{FMR} = 0.001$ for white males which is the demographic that usually gives the lowest FMR. This means the top right box is the same color in all panels. The panels are sorted over multiple pages in order of FMR on black females, which is the demographic that usually gives the highest FMR.

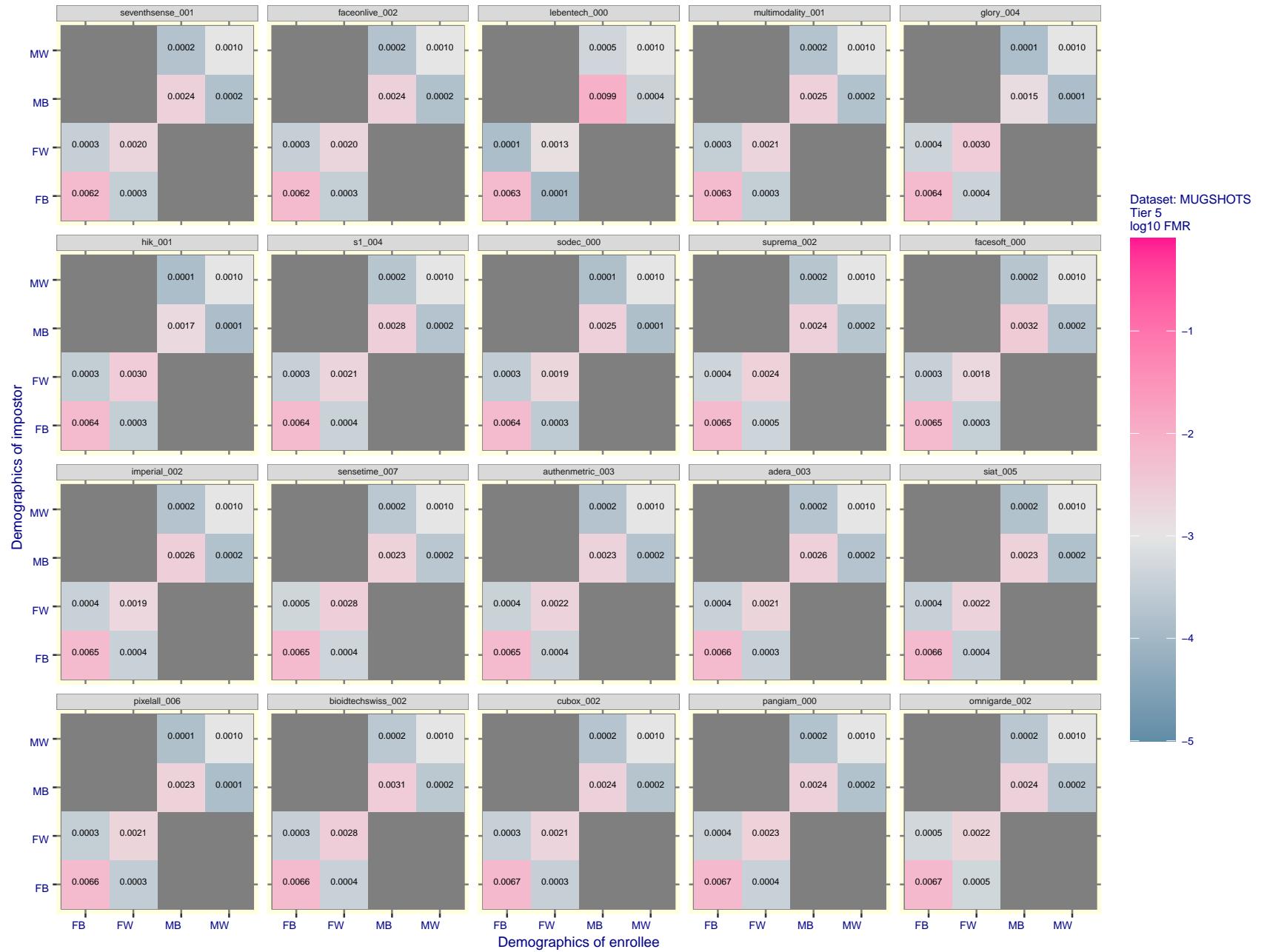


Figure 139: For the mugshot images, FMR for same-sex impostor pairs of images annotated with codes for black female, black male, white female, white male. The threshold is set for each algorithm to give $FMR = 0.001$ for white males which is the demographic that usually gives the lowest FMR. This means the top right box is the same color in all panels. The panels are sorted over multiple pages in order of FMR on black females, which is the demographic that usually gives the highest FMR.

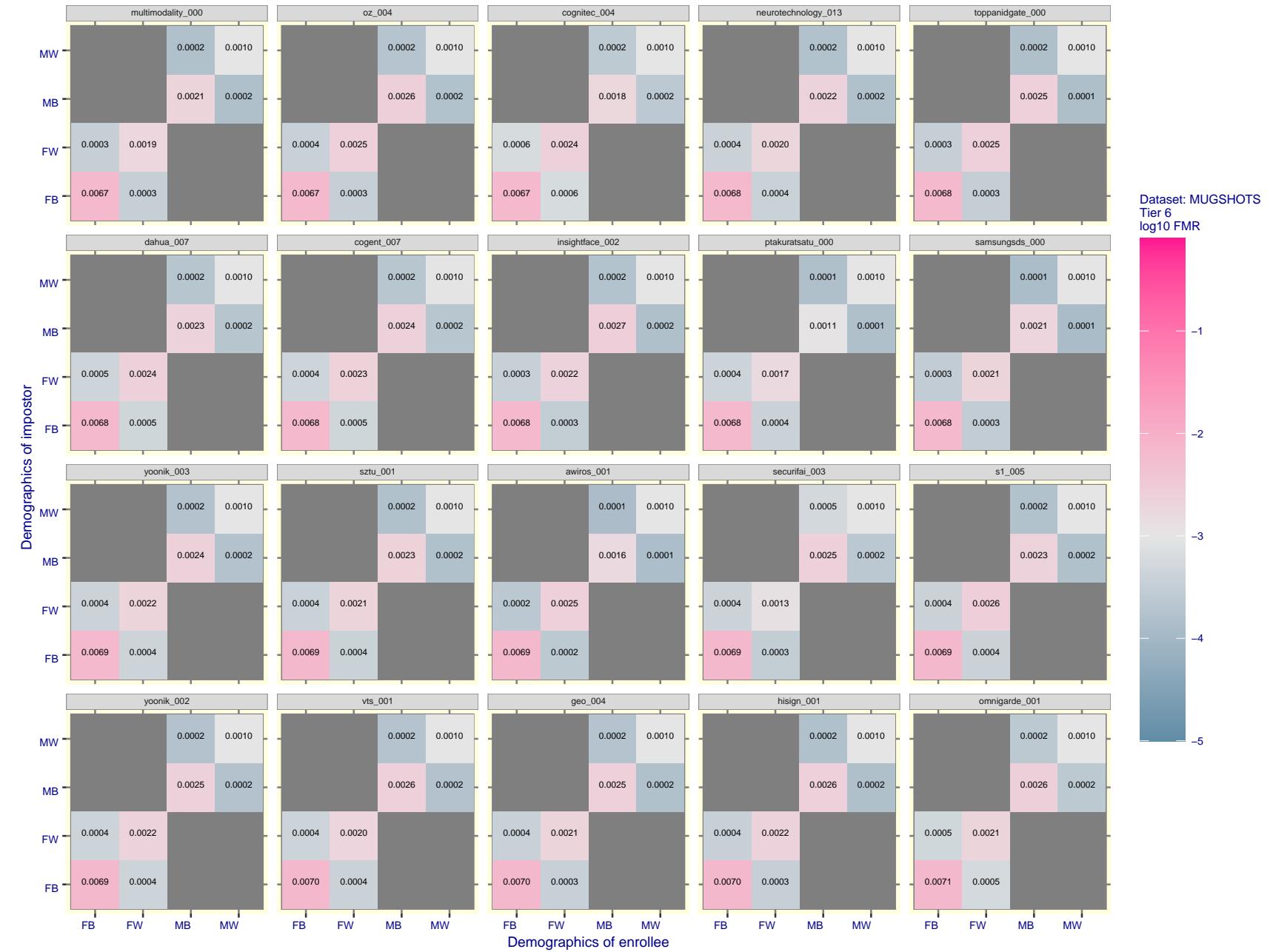


Figure 140: For the mugshot images, FMR for same-sex impostor pairs of images annotated with codes for black female, black male, white female, white male. The threshold is set for each algorithm to give $FMR = 0.001$ for white males which is the demographic that usually gives the lowest FMR. This means the top right box is the same color in all panels. The panels are sorted over multiple pages in order of FMR on black females, which is the demographic that usually gives the highest FMR.

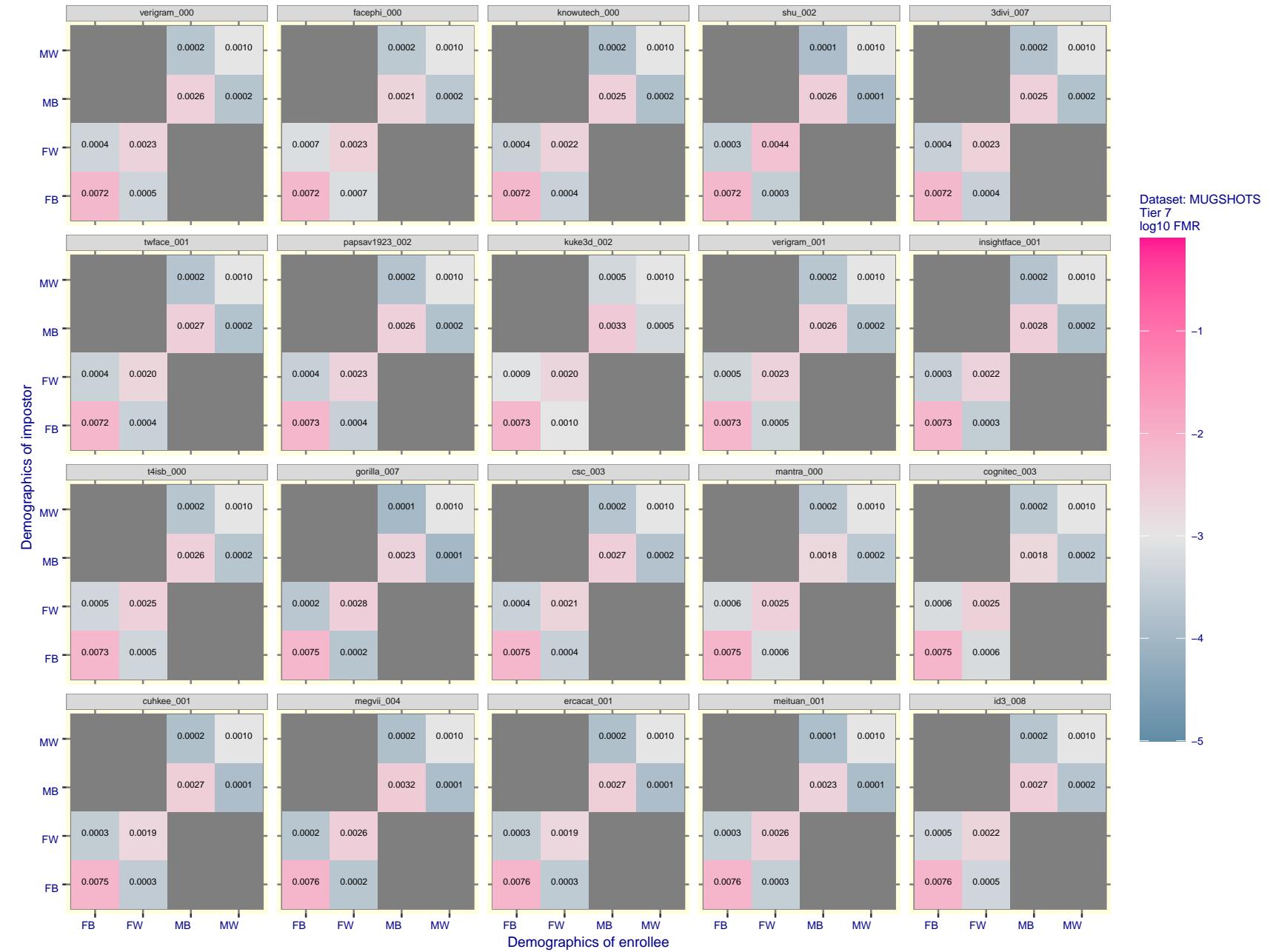


Figure 141: For the mugshot images, FMR for same-sex impostor pairs of images annotated with codes for black female, black male, white female, white male. The threshold is set for each algorithm to give FMR = 0.001 for white males which is the demographic that usually gives the lowest FMR. This means the top right box is the same color in all panels. The panels are sorted over multiple pages in order of FMR on black females, which is the demographic that usually gives the highest FMR.

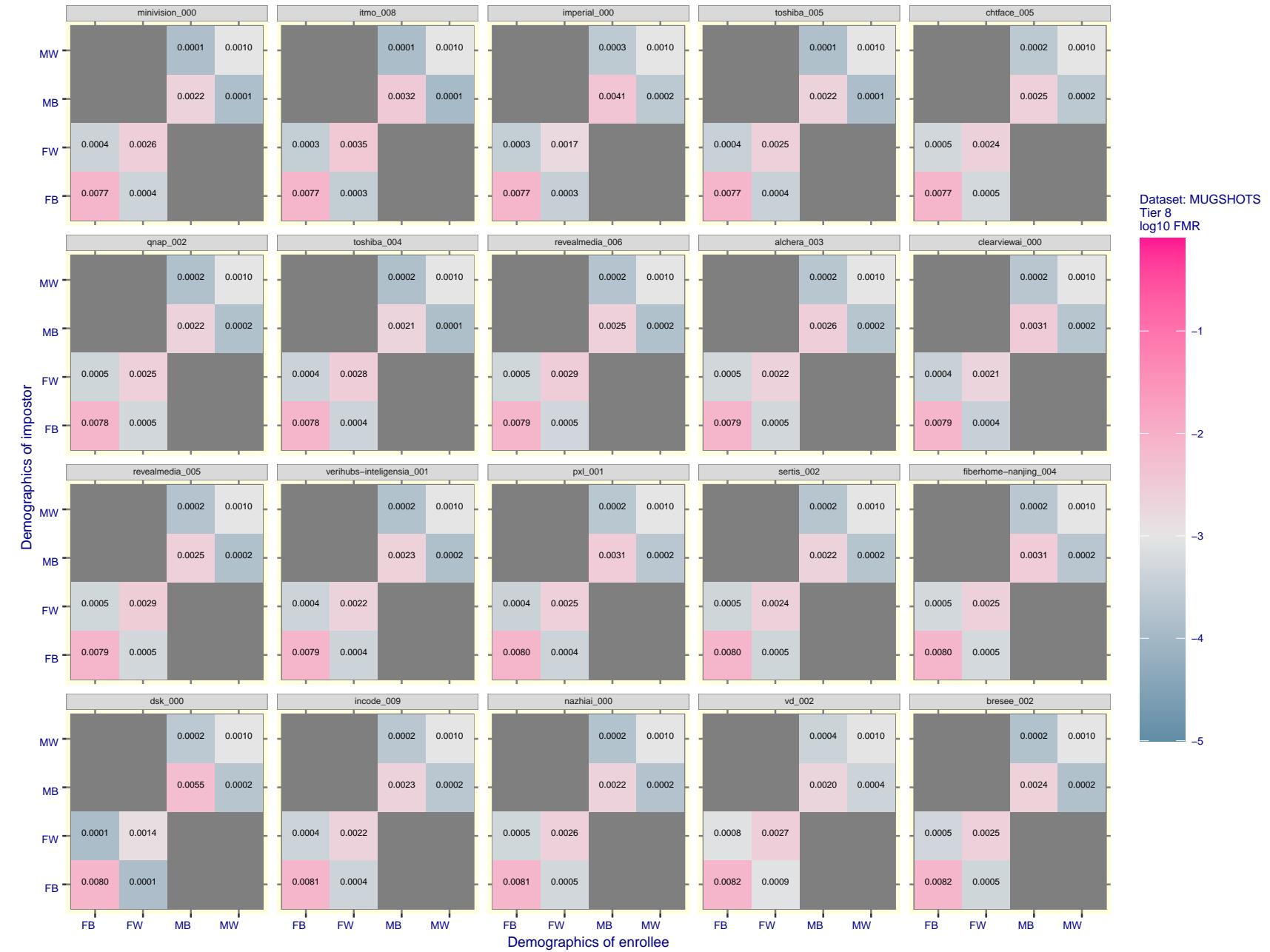


Figure 142: For the mugshot images, FMR for same-sex impostor pairs of images annotated with codes for black female, black male, white female, white male. The threshold is set for each algorithm to give $FMR = 0.001$ for white males which is the demographic that usually gives the lowest FMR. This means the top right box is the same color in all panels. The panels are sorted over multiple pages in order of FMR on black females, which is the demographic that usually gives the highest FMR.

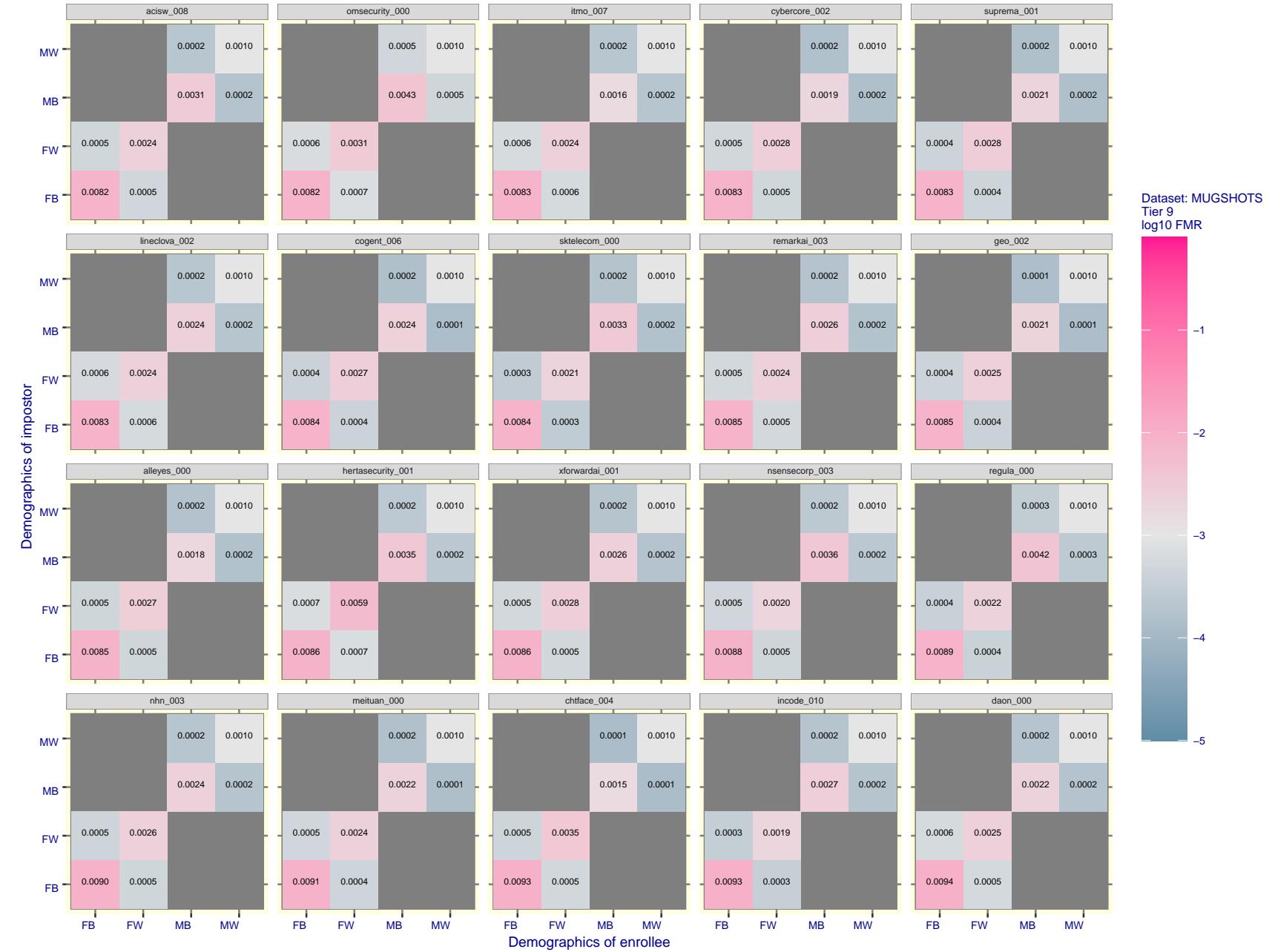


Figure 143: For the mugshot images, FMR for same-sex impostor pairs of images annotated with codes for black female, black male, white female, white male. The threshold is set for each algorithm to give $\text{FMR} = 0.001$ for white males which is the demographic that usually gives the lowest FMR. This means the top right box is the same color in all panels. The panels are sorted over multiple pages in order of FMR on black females, which is the demographic that usually gives the highest FMR.

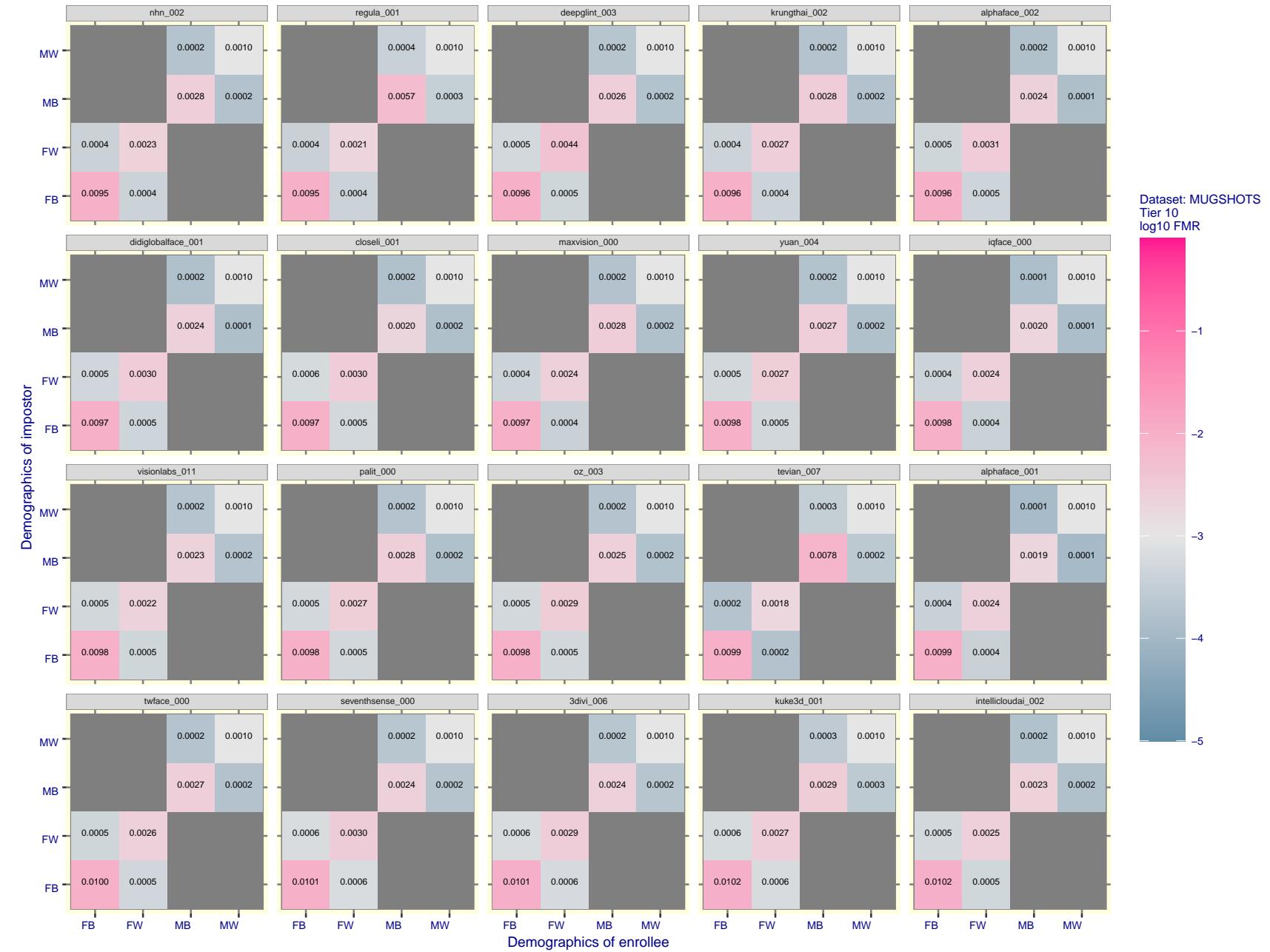


Figure 144: For the mugshot images, FMR for same-sex impostor pairs of images annotated with codes for black female, black male, white female, white male. The threshold is set for each algorithm to give $FMR = 0.001$ for white males which is the demographic that usually gives the lowest FMR. This means the top right box is the same color in all panels. The panels are sorted over multiple pages in order of FMR on black females, which is the demographic that usually gives the highest FMR.

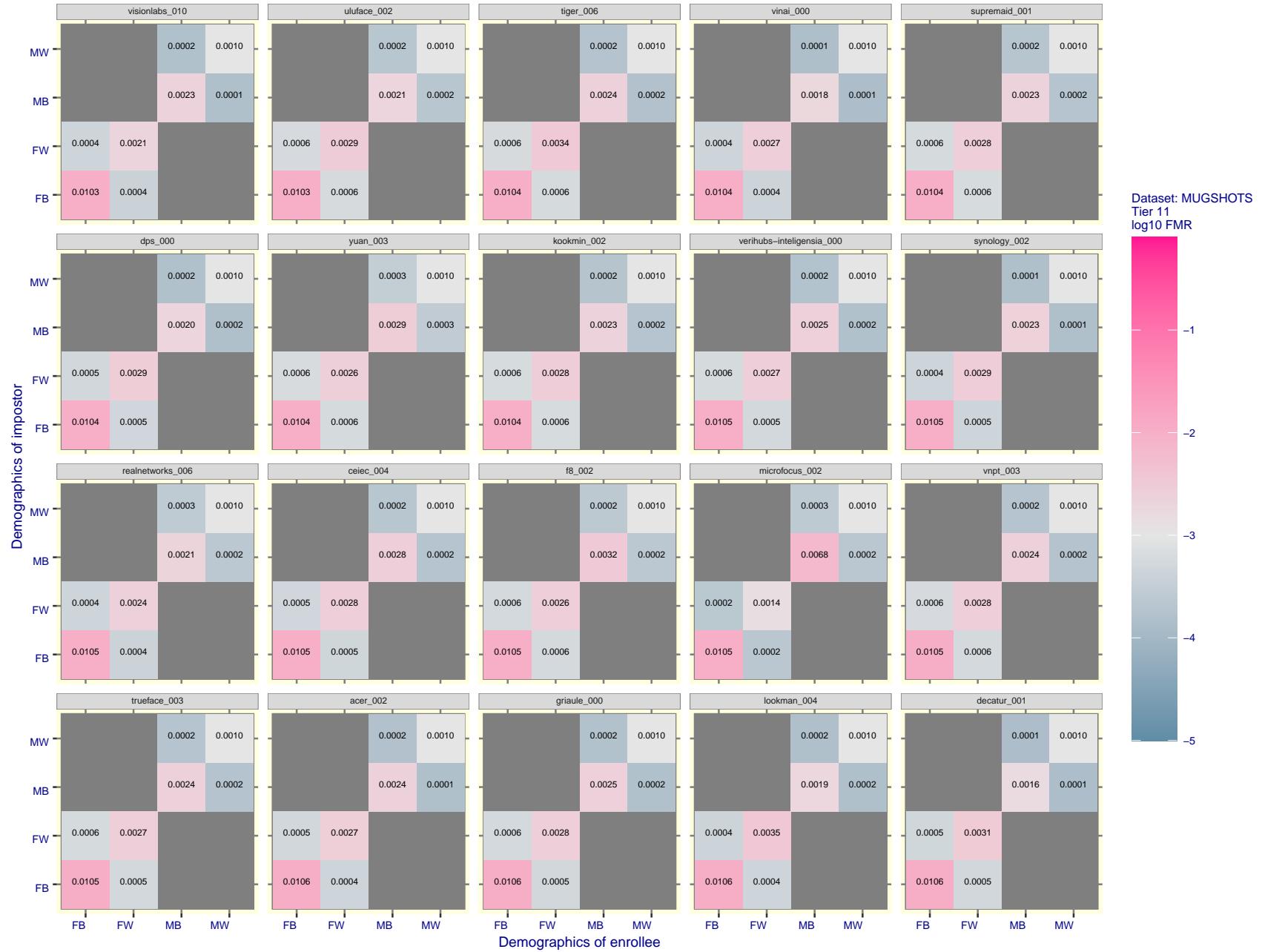


Figure 145: For the mugshot images, FMR for same-sex impostor pairs of images annotated with codes for black female, black male, white female, white male. The threshold is set for each algorithm to give $FMR = 0.001$ for white males which is the demographic that usually gives the lowest FMR. This means the top right box is the same color in all panels. The panels are sorted over multiple pages in order of FMR on black females, which is the demographic that usually gives the highest FMR.

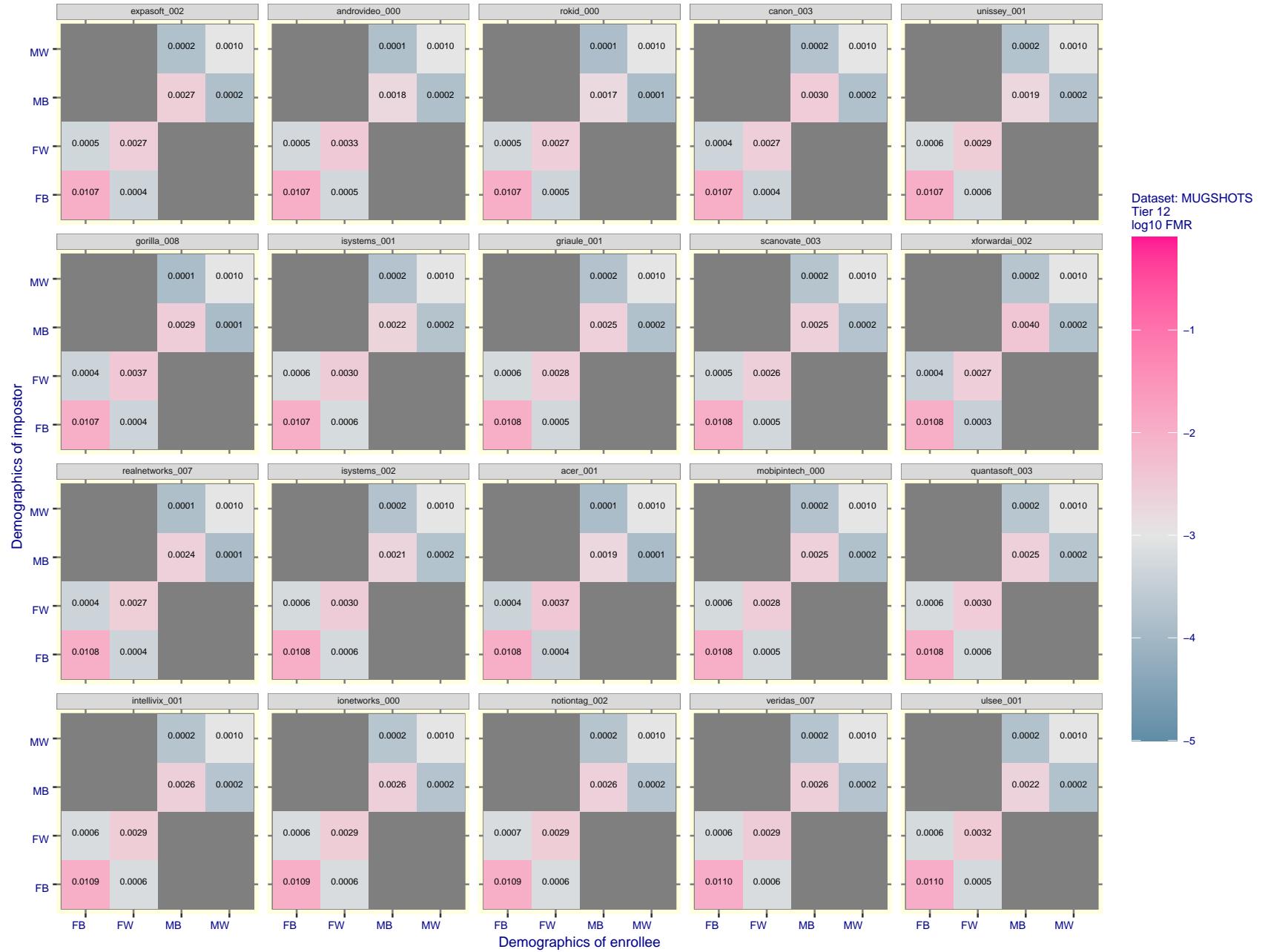


Figure 146: For the mugshot images, FMR for same-sex impostor pairs of images annotated with codes for black female, black male, white female, white male. The threshold is set for each algorithm to give $FMR = 0.001$ for white males which is the demographic that usually gives the lowest FMR. This means the top right box is the same color in all panels. The panels are sorted over multiple pages in order of FMR on black females, which is the demographic that usually gives the highest FMR.

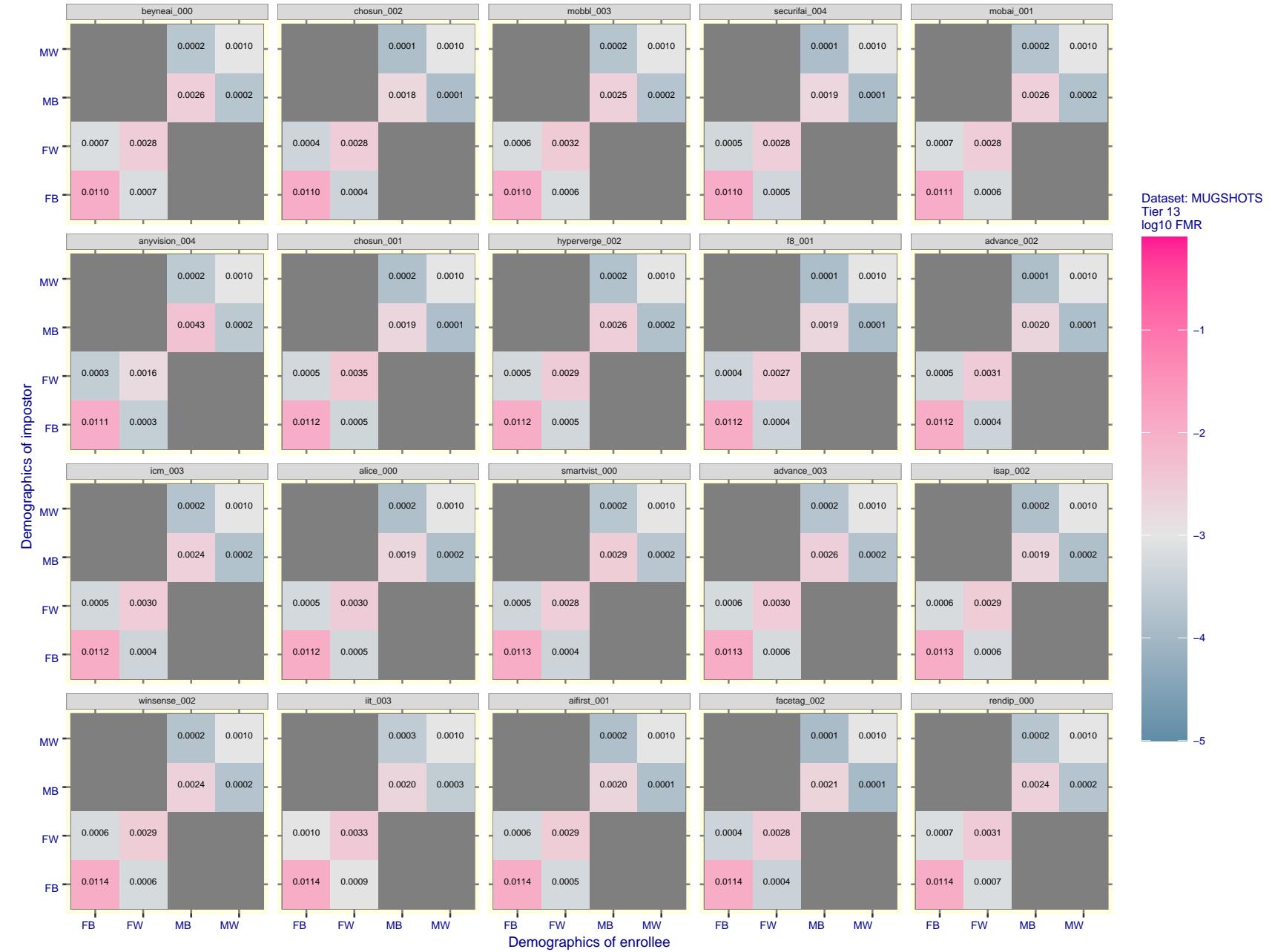


Figure 147: For the mugshot images, FMR for same-sex impostor pairs of images annotated with codes for black female, black male, white female, white male. The threshold is set for each algorithm to give $FMR = 0.001$ for white males which is the demographic that usually gives the lowest FMR. This means the top right box is the same color in all panels. The panels are sorted over multiple pages in order of FMR on black females, which is the demographic that usually gives the highest FMR.

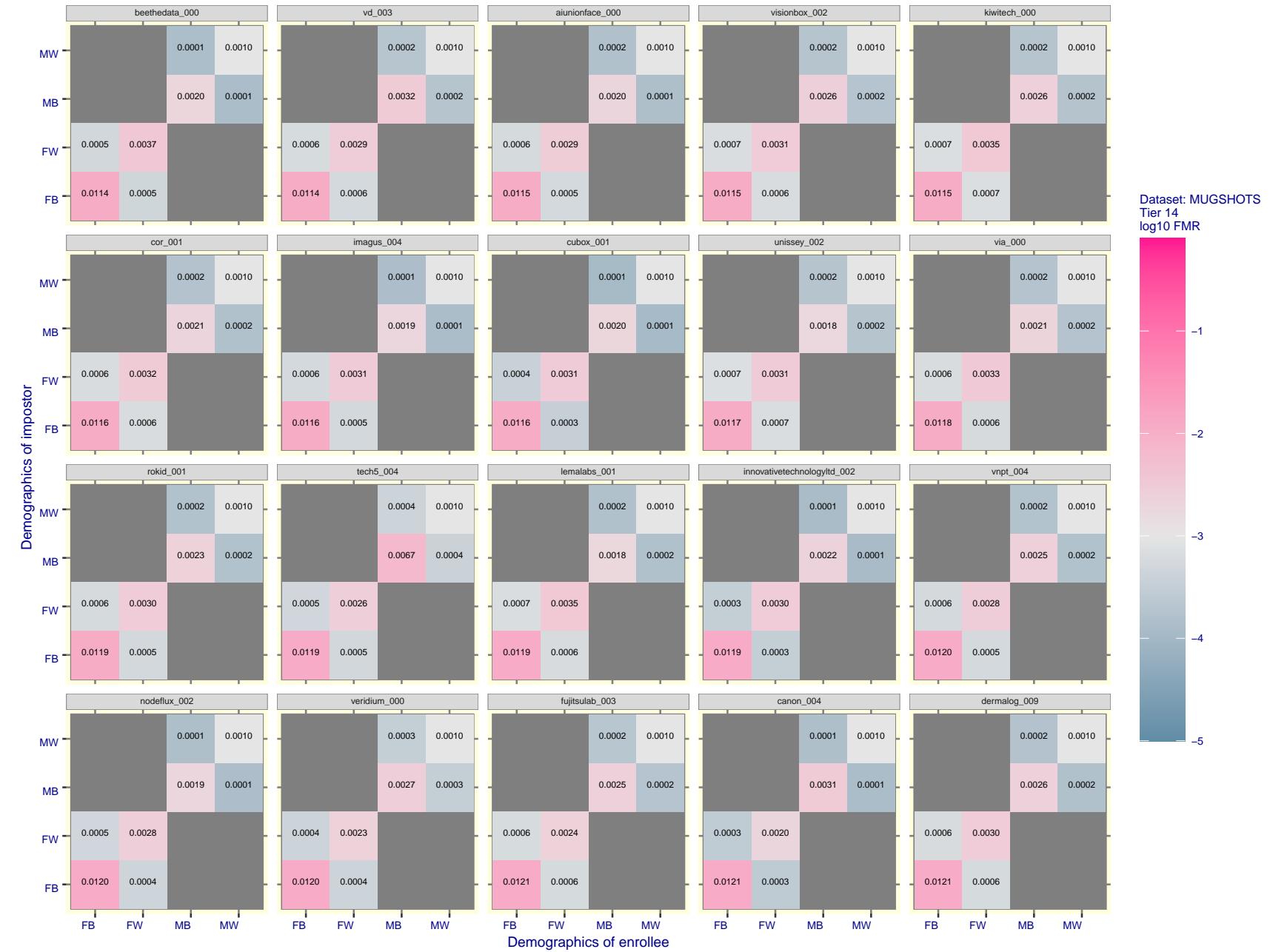


Figure 148: For the mugshot images, FMR for same-sex impostor pairs of images annotated with codes for black female, black male, white female, white male. The threshold is set for each algorithm to give $FMR = 0.001$ for white males which is the demographic that usually gives the lowest FMR. This means the top right box is the same color in all panels. The panels are sorted over multiple pages in order of FMR on black females, which is the demographic that usually gives the highest FMR.

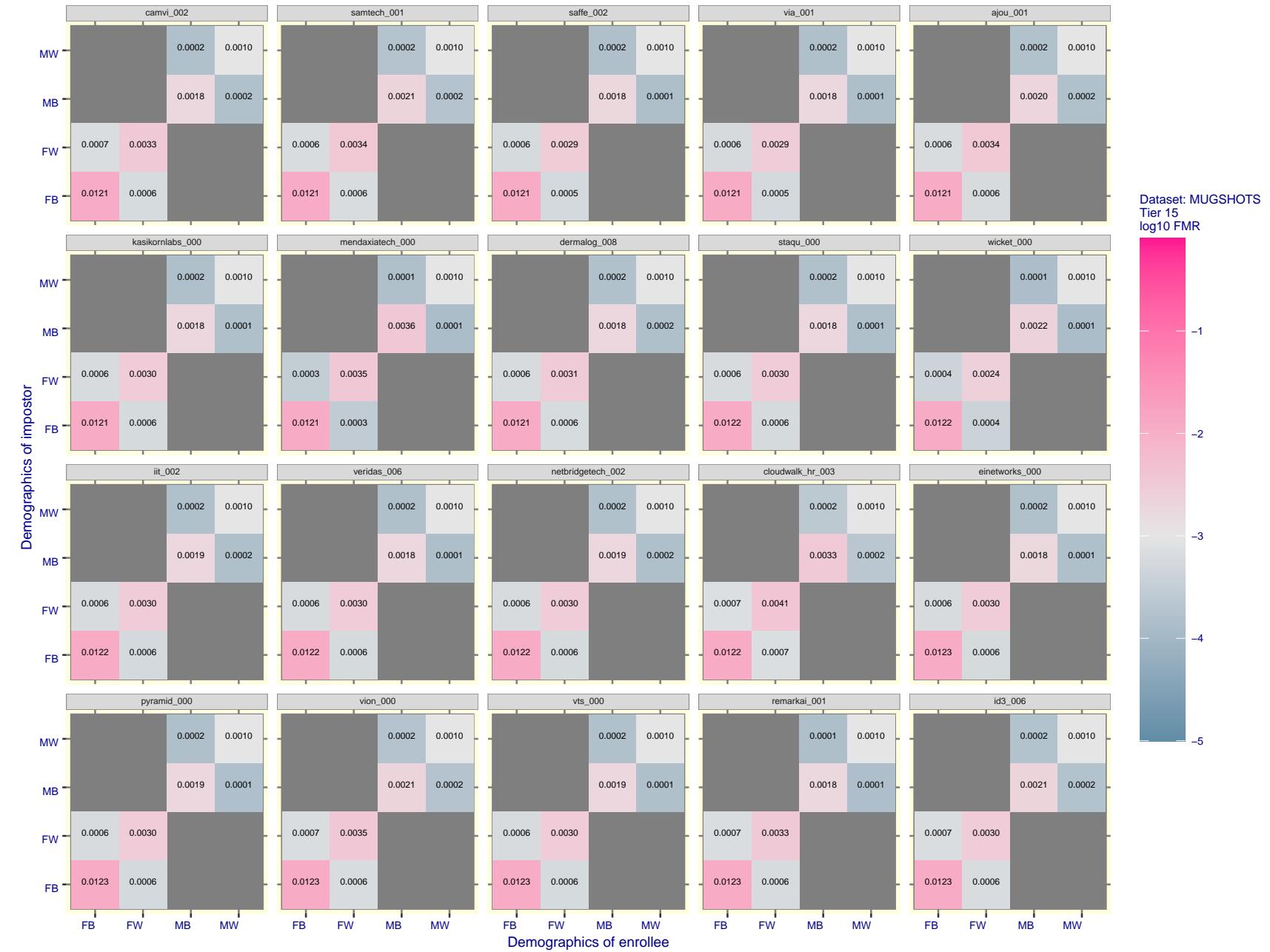


Figure 149: For the mugshot images, FMR for same-sex impostor pairs of images annotated with codes for black female, black male, white female, white male. The threshold is set for each algorithm to give $FMR = 0.001$ for white males which is the demographic that usually gives the lowest FMR. This means the top right box is the same color in all panels. The panels are sorted over multiple pages in order of FMR on black females, which is the demographic that usually gives the highest FMR.

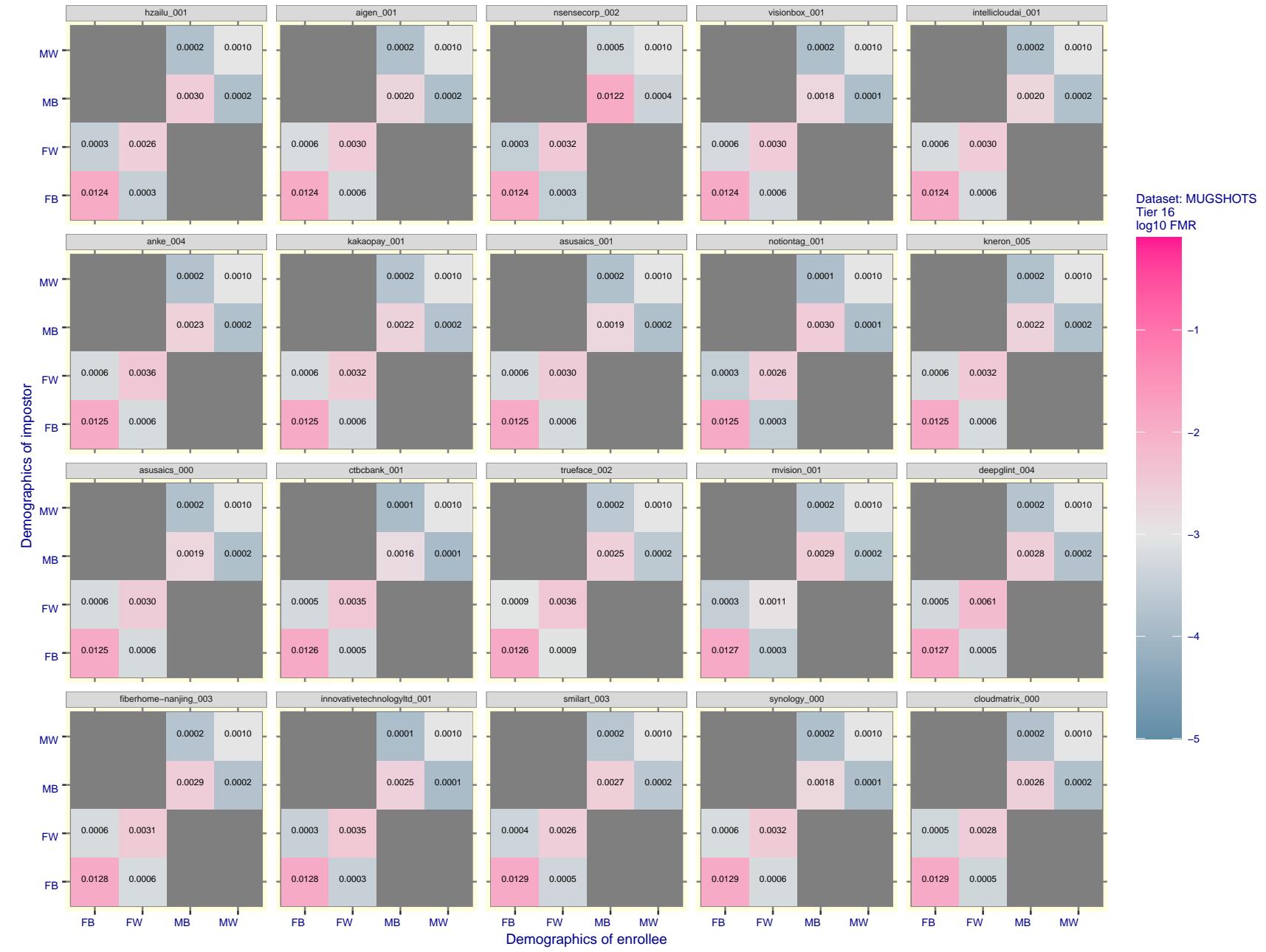


Figure 150: For the mugshot images, FMR for same-sex impostor pairs of images annotated with codes for black female, black male, white female, white male. The threshold is set for each algorithm to give $FMR = 0.001$ for white males which is the demographic that usually gives the lowest FMR. This means the top right box is the same color in all panels. The panels are sorted over multiple pages in order of FMR on black females, which is the demographic that usually gives the highest FMR.

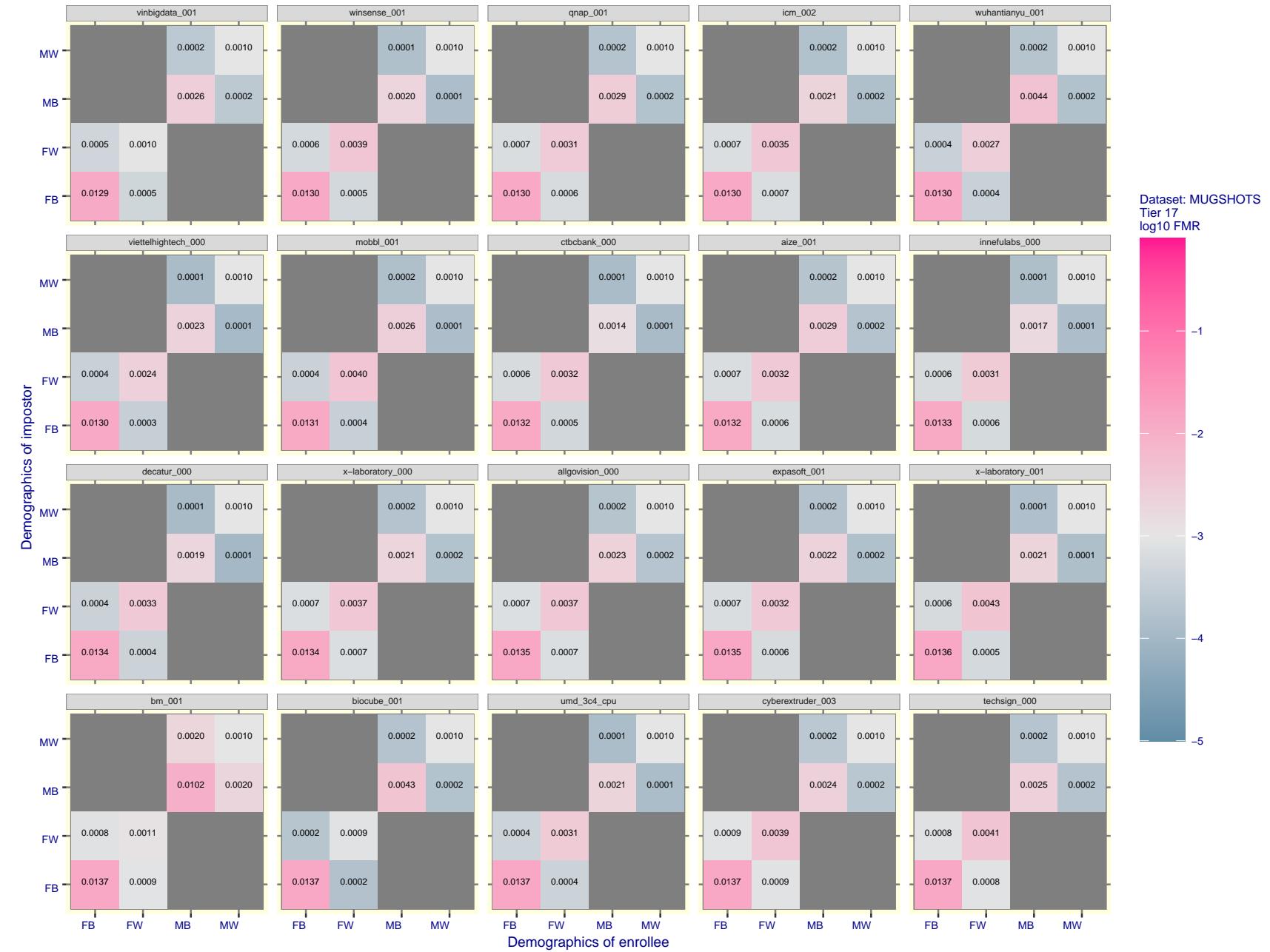


Figure 151: For the mugshot images, FMR for same-sex impostor pairs of images annotated with codes for black female, black male, white female, white male. The threshold is set for each algorithm to give $FMR = 0.001$ for white males which is the demographic that usually gives the lowest FMR. This means the top right box is the same color in all panels. The panels are sorted over multiple pages in order of FMR on black females, which is the demographic that usually gives the highest FMR.

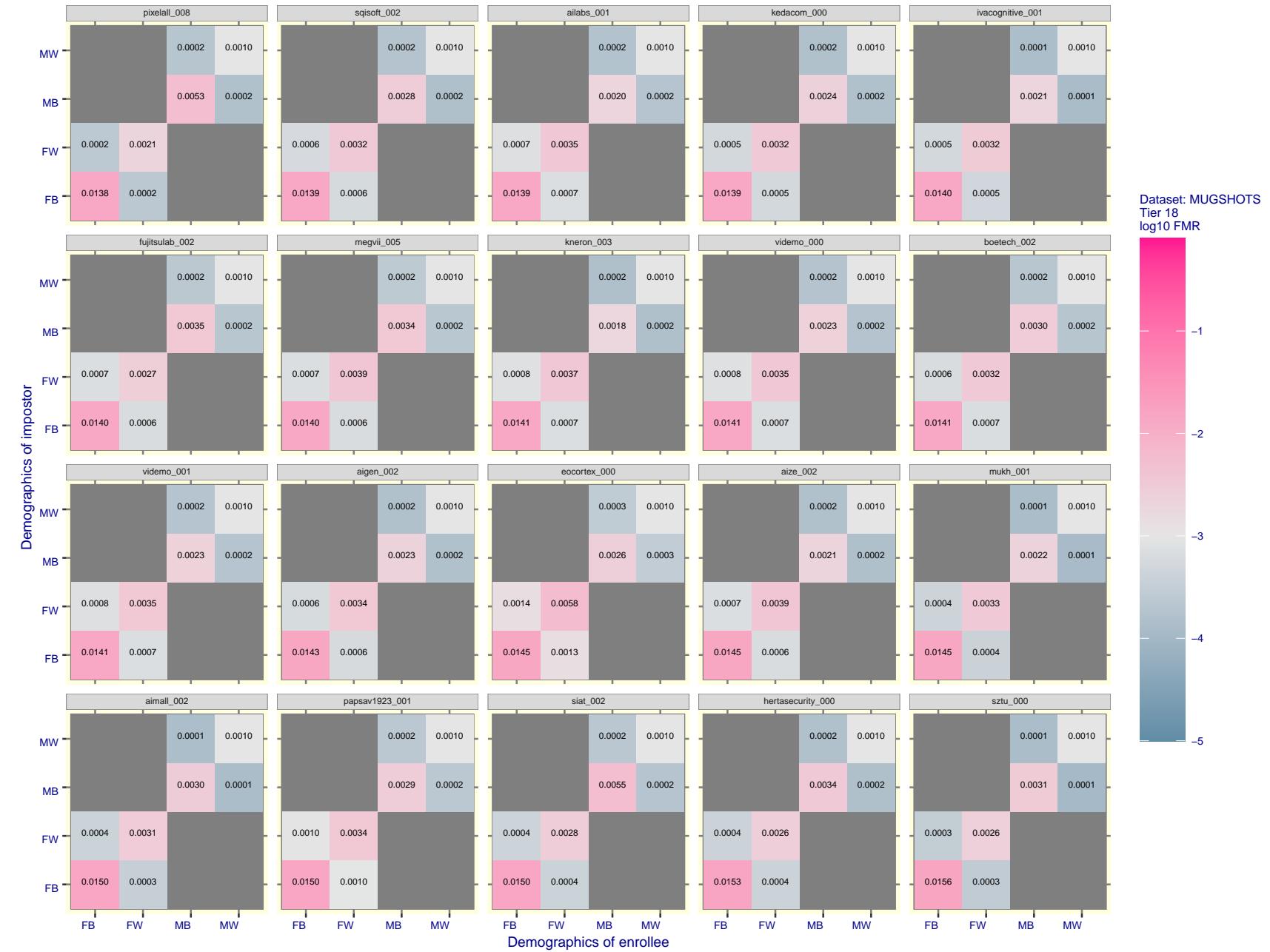


Figure 152: For the mugshot images, FMR for same-sex impostor pairs of images annotated with codes for black female, black male, white female, white male. The threshold is set for each algorithm to give FMR = 0.001 for white males which is the demographic that usually gives the lowest FMR. This means the top right box is the same color in all panels. The panels are sorted over multiple pages in order of FMR on black females, which is the demographic that usually gives the highest FMR.

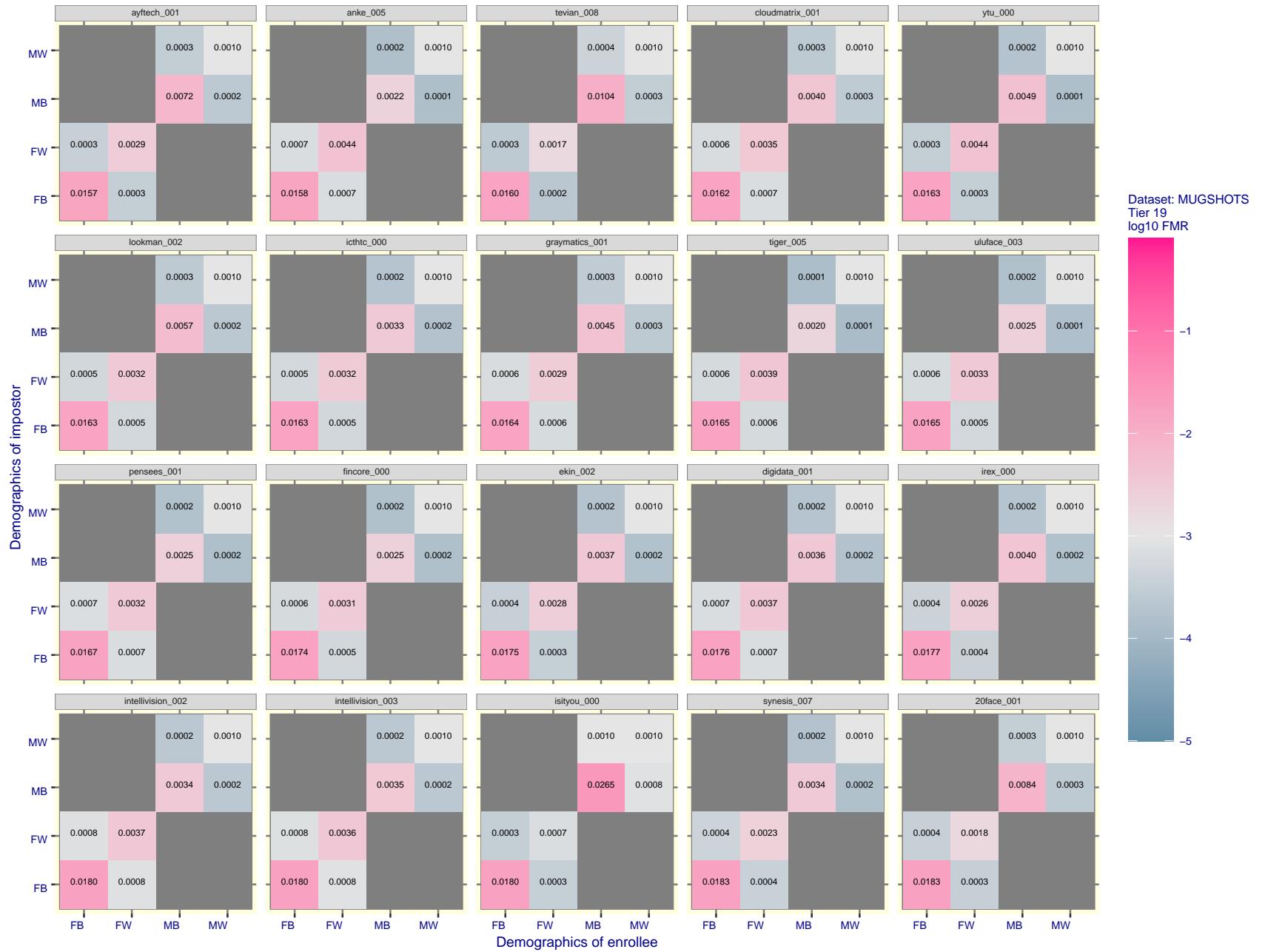


Figure 153: For the mugshot images, FMR for same-sex impostor pairs of images annotated with codes for black female, black male, white female, white male. The threshold is set for each algorithm to give FMR = 0.001 for white males which is the demographic that usually gives the lowest FMR. This means the top right box is the same color in all panels. The panels are sorted over multiple pages in order of FMR on black females, which is the demographic that usually gives the highest FMR.

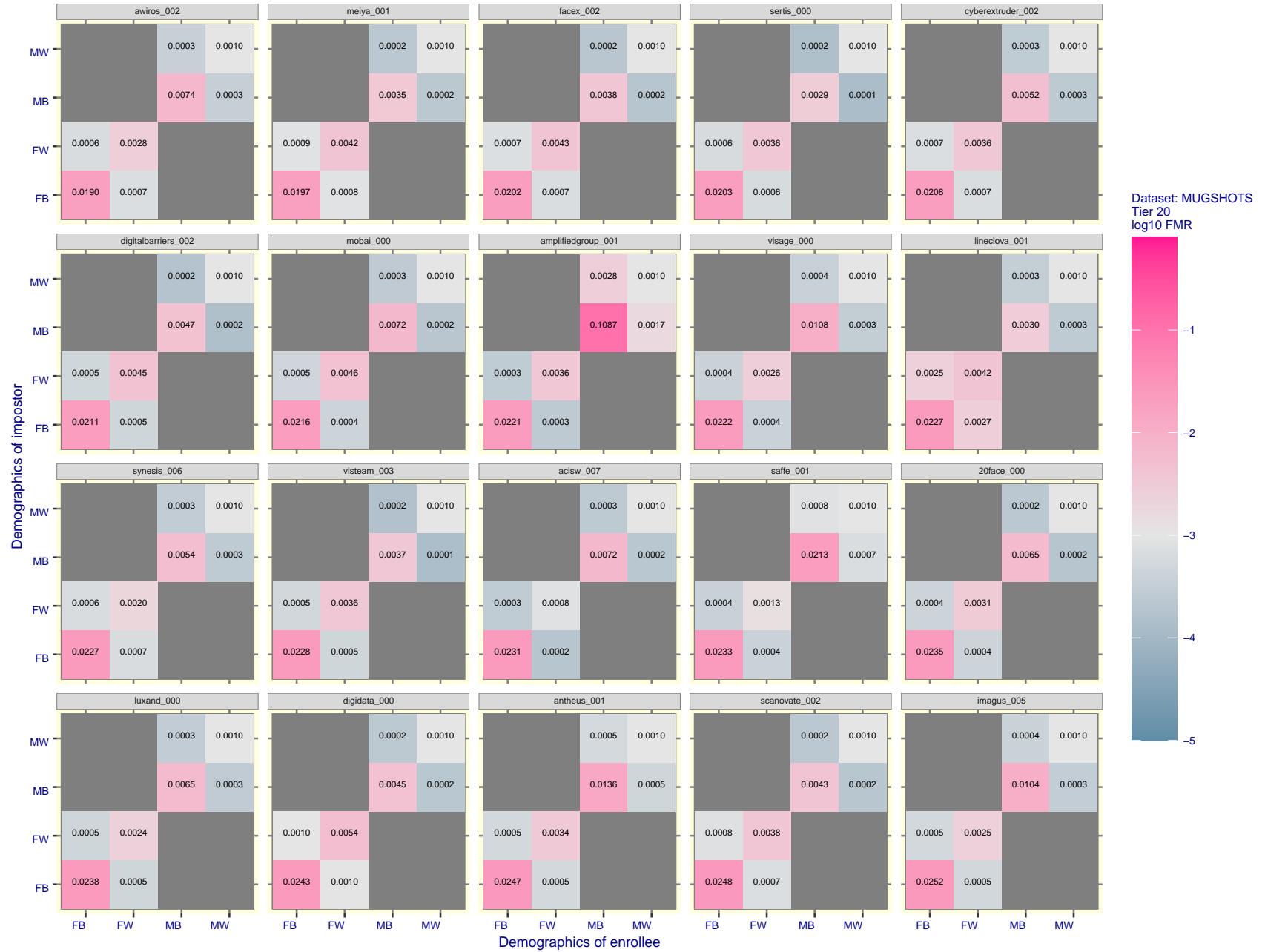


Figure 154: For the mugshot images, FMR for same-sex impostor pairs of images annotated with codes for black female, black male, white female, white male. The threshold is set for each algorithm to give FMR = 0.001 for white males which is the demographic that usually gives the lowest FMR. This means the top right box is the same color in all panels. The panels are sorted over multiple pages in order of FMR on black females, which is the demographic that usually gives the highest FMR.

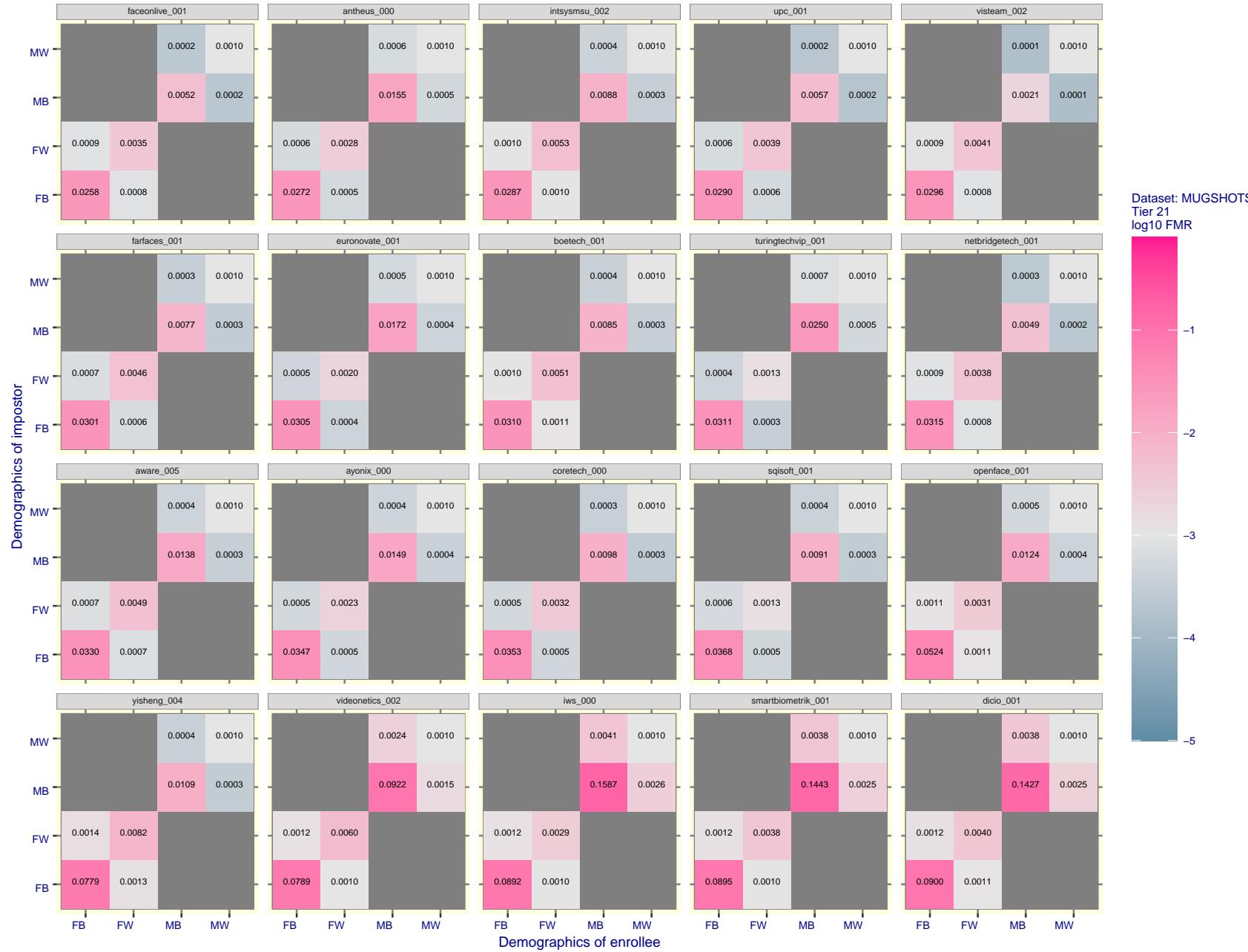


Figure 155: For the mugshot images, FMR for same-sex impostor pairs of images annotated with codes for black female, black male, white female, white male. The threshold is set for each algorithm to give FMR = 0.001 for white males which is the demographic that usually gives the lowest FMR. This means the top right box is the same color in all panels. The panels are sorted over multiple pages in order of FMR on black females, which is the demographic that usually gives the highest FMR.

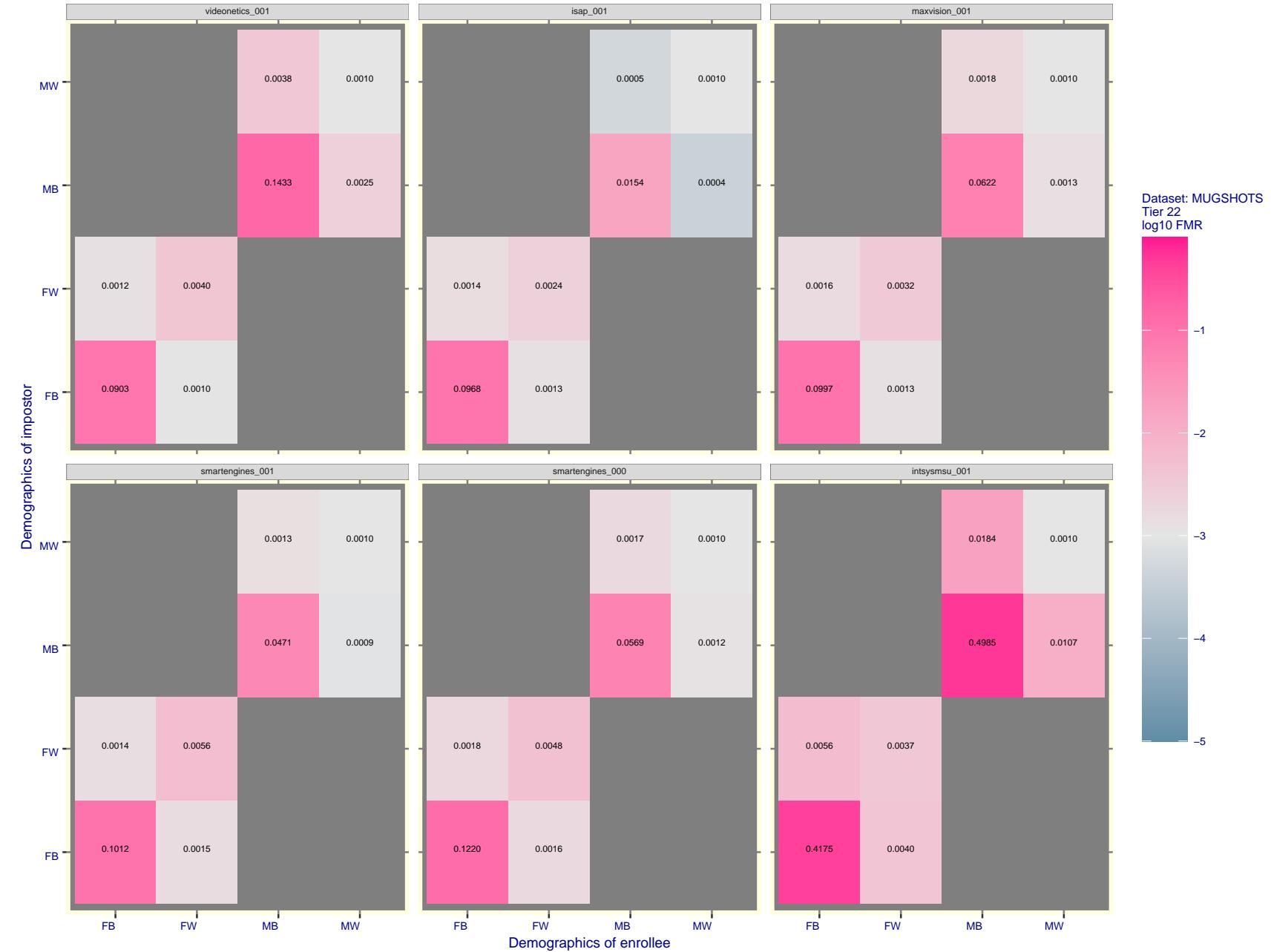


Figure 156: For the mugshot images, FMR for same-sex impostor pairs of images annotated with codes for black female, black male, white female, white male. The threshold is set for each algorithm to give $\text{FMR} = 0.001$ for white males which is the demographic that usually gives the lowest FMR. This means the top right box is the same color in all panels. The panels are sorted over multiple pages in order of FMR on black females, which is the demographic that usually gives the highest FMR.

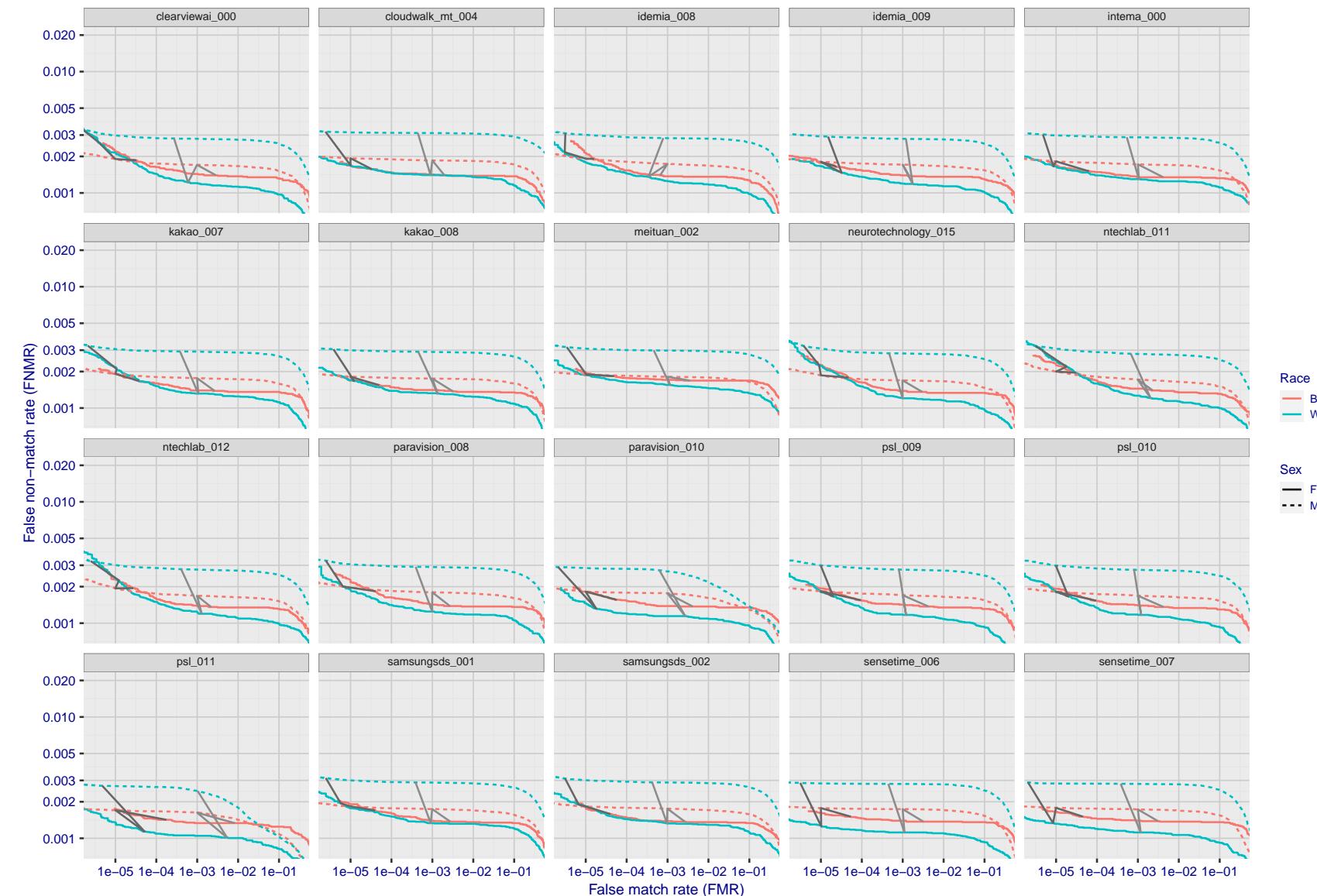


Figure 157: For the mugshot images, error tradeoff characteristics for white females, black females, black males and white males. The Z-shaped grey lines correspond to fixed thresholds, showing both FNMR and FMR vary at one T value. Note: Many of the plots will naively be read as saying women gives worse error rates than men because the solid traces lie above the dotted ones. However, this is misleading and incomplete: The grey lines show the traces reveal horizontal shifts. Thus for the cogent-003 algorithm FNMR for men is higher than for women at a fixed threshold but, at the same time, FMR is higher for women - see Figure 243. As access control systems almost always operate at a fixed threshold, the naive interpretation is incorrect.

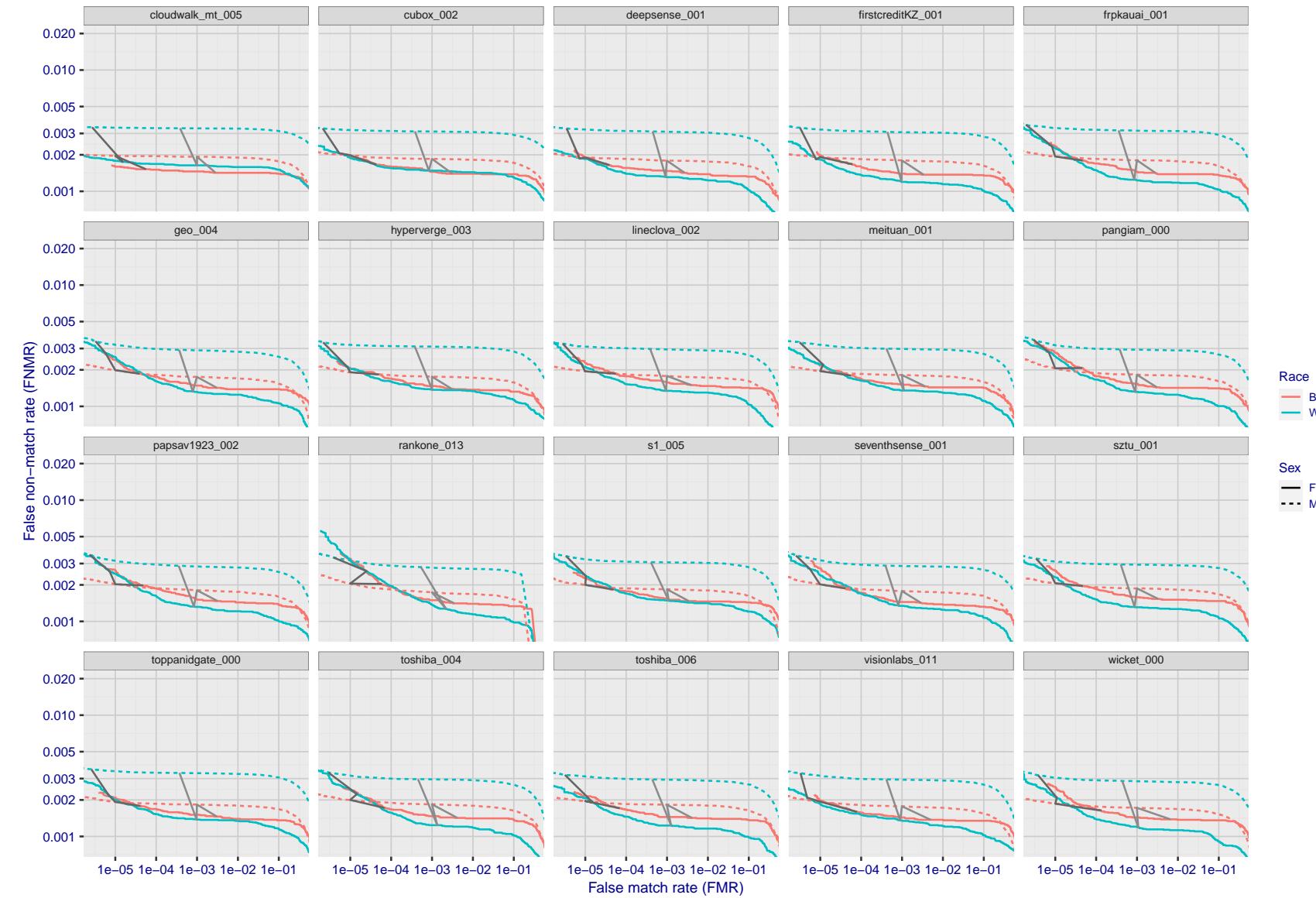


Figure 158: For the mugshot images, error tradeoff characteristics for white females, black females, black males and white males. The Z-shaped grey lines correspond to fixed thresholds, showing both FNMR and FMR vary at one T value. Note: Many of the plots will naively be read as saying women gives worse error rates than men because the solid traces lie above the dotted ones. However, this is misleading and incomplete: The grey lines show the traces reveal horizontal shifts. Thus for the cogent-003 algorithm FNMR for men is higher than for women at a fixed threshold but, at the same time, FMR is higher for women - see Figure 243. As access control systems almost always operate at a fixed threshold, the naive interpretation is incorrect.

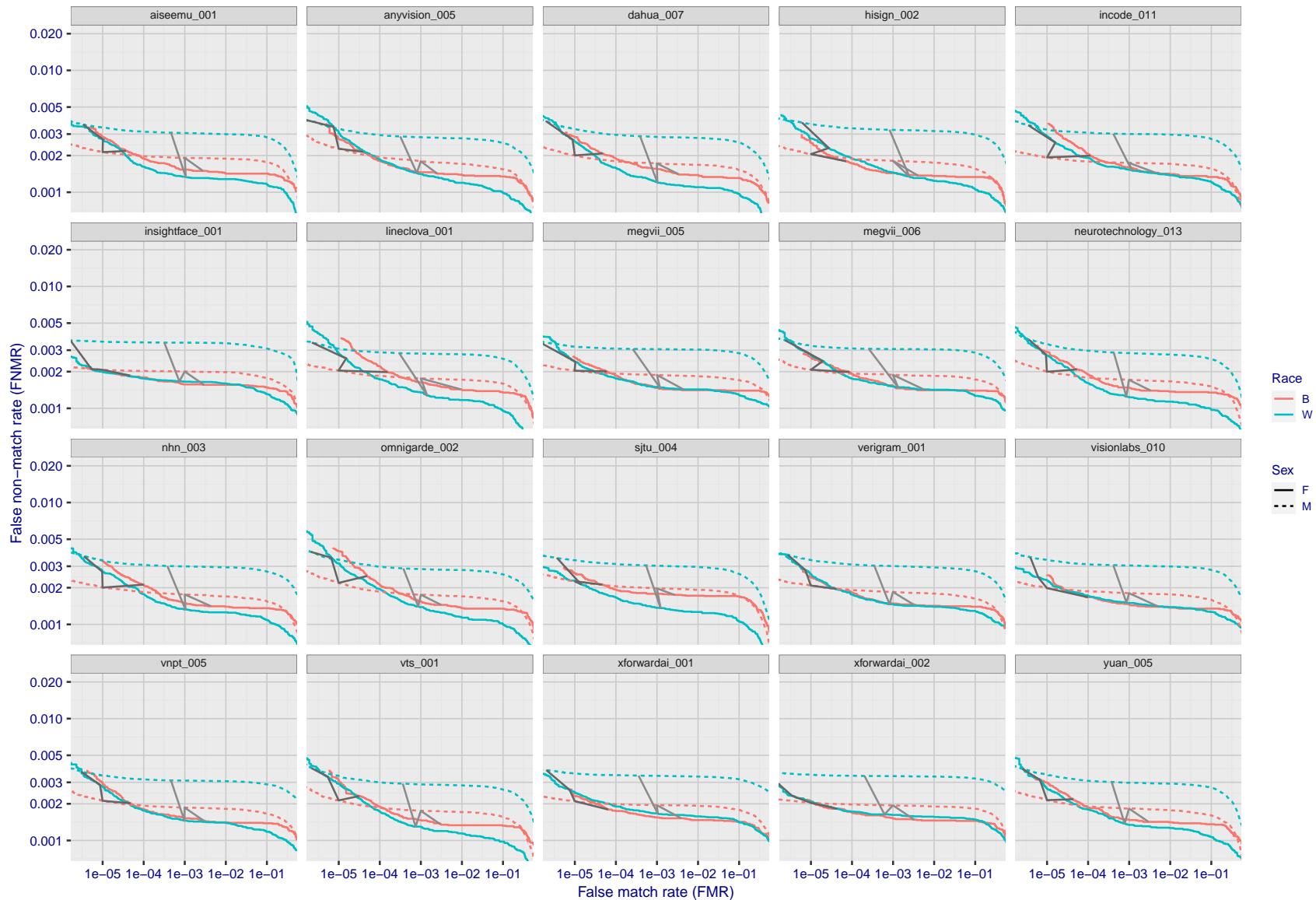


Figure 159: For the mugshot images, error tradeoff characteristics for white females, black females, black males and white males. The Z-shaped grey lines correspond to fixed thresholds, showing both FNMR and FMR vary at one T value. Note: Many of the plots will naively be read as saying women gives worse error rates than men because the solid traces lie above the dotted ones. However, this is misleading and incomplete: The grey lines show the traces reveal horizontal shifts. Thus for the cogent-003 algorithm FNMR for men is higher than for women at a fixed threshold but, at the same time, FMR is higher for women - see Figure 243. As access control systems almost always operate at a fixed threshold, the naive interpretation is incorrect.

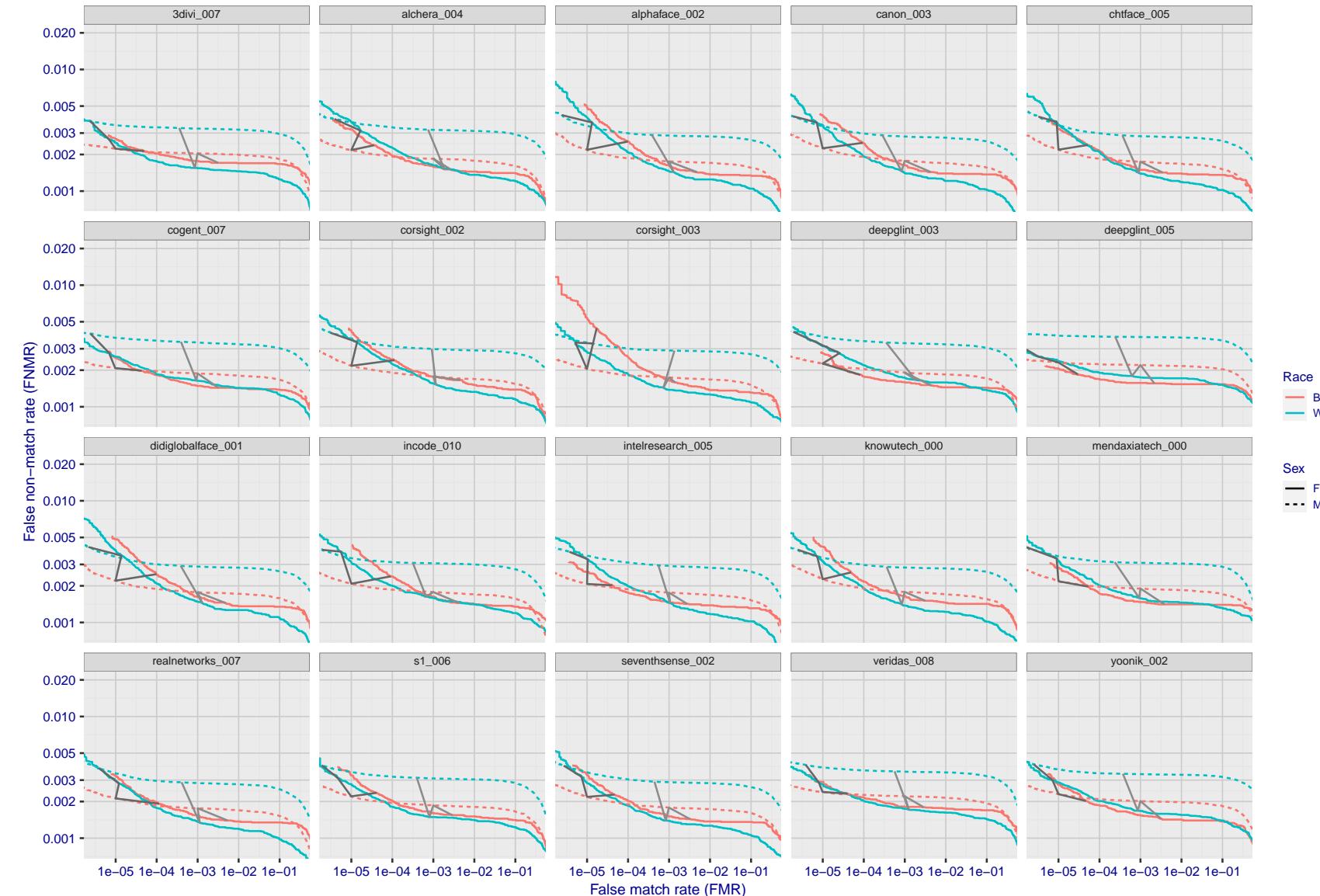


Figure 160: For the mugshot images, error tradeoff characteristics for white females, black females, black males and white males. The Z-shaped grey lines correspond to fixed thresholds, showing both FNMR and FMR vary at one T value. Note: Many of the plots will naively be read as saying women gives worse error rates than men because the solid traces lie above the dotted ones. However, this is misleading and incomplete: The grey lines show the traces reveal horizontal shifts. Thus for the cogent-003 algorithm FNMR for men is higher than for women at a fixed threshold but, at the same time, FMR is higher for women - see Figure 243. As access control systems almost always operate at a fixed threshold, the naive interpretation is incorrect.

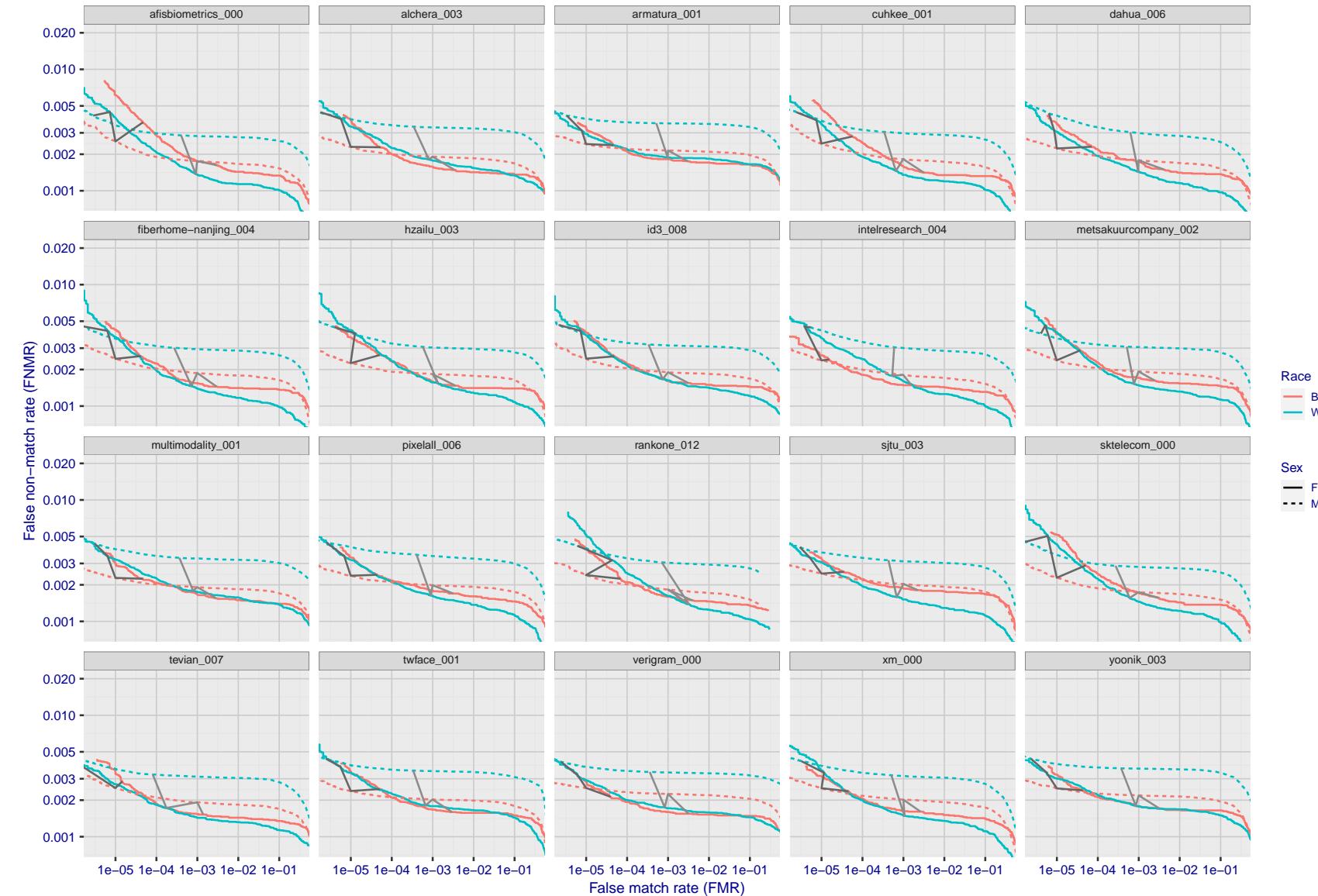


Figure 161: For the mugshot images, error tradeoff characteristics for white females, black females, black males and white males. The Z-shaped grey lines correspond to fixed thresholds, showing both FNMR and FMR vary at one T value. Note: Many of the plots will naively be read as saying women gives worse error rates than men because the solid traces lie above the dotted ones. However, this is misleading and incomplete: The grey lines show the traces reveal horizontal shifts. Thus for the cogent-003 algorithm FNMR for men is higher than for women at a fixed threshold but, at the same time, FMR is higher for women - see Figure 243. As access control systems almost always operate at a fixed threshold, the naive interpretation is incorrect.

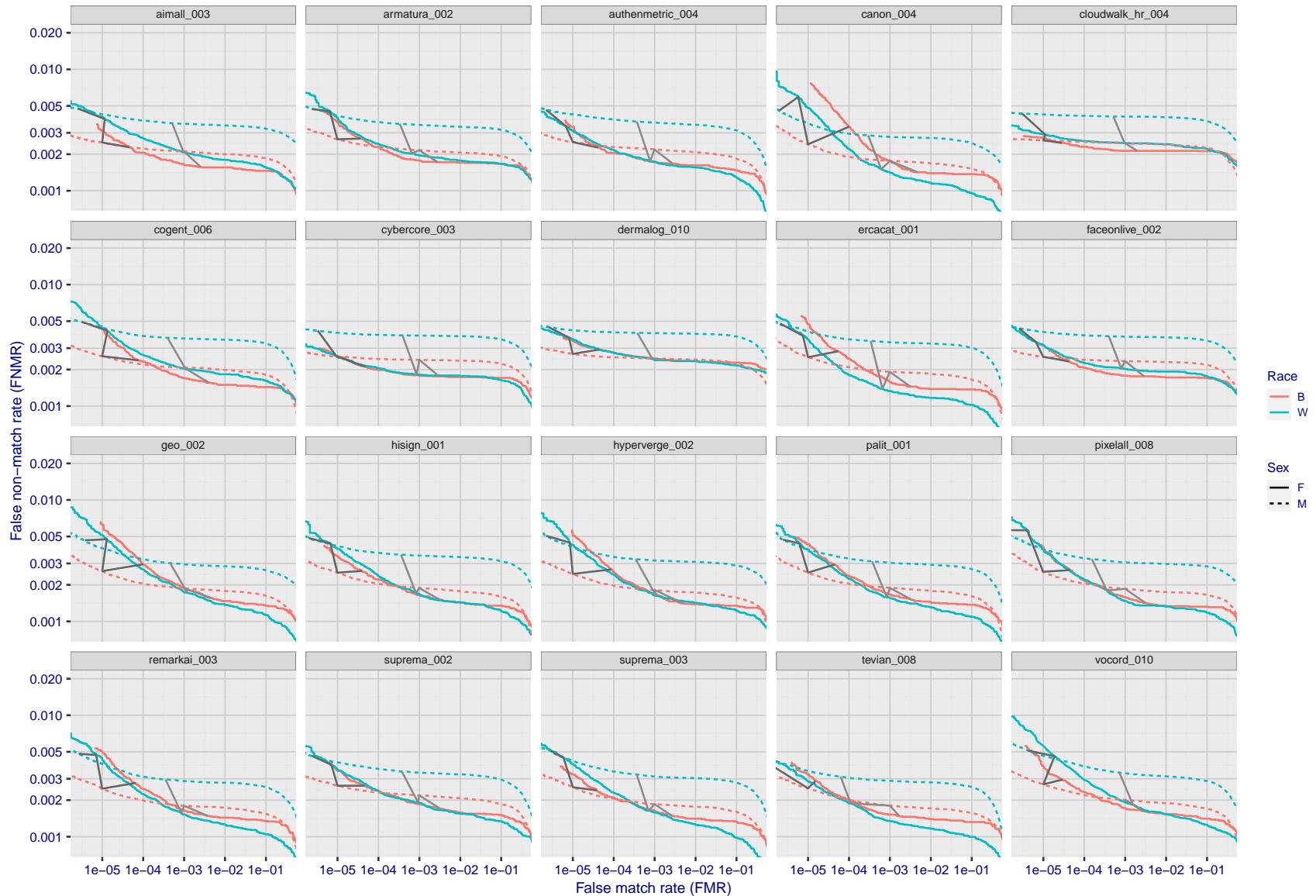


Figure 162: For the mugshot images, error tradeoff characteristics for white females, black females, black males and white males. The Z-shaped grey lines correspond to fixed thresholds, showing both FNMR and FMR vary at one T value. Note: Many of the plots will naively be read as saying women gives worse error rates than men because the solid traces lie above the dotted ones. However, this is misleading and incomplete: The grey lines show the traces reveal horizontal shifts. Thus for the cogent-003 algorithm FNMR for men is higher than for women at a fixed threshold but, at the same time, FMR is higher for women - see Figure 243. As access control systems almost always operate at a fixed threshold, the naive interpretation is incorrect.

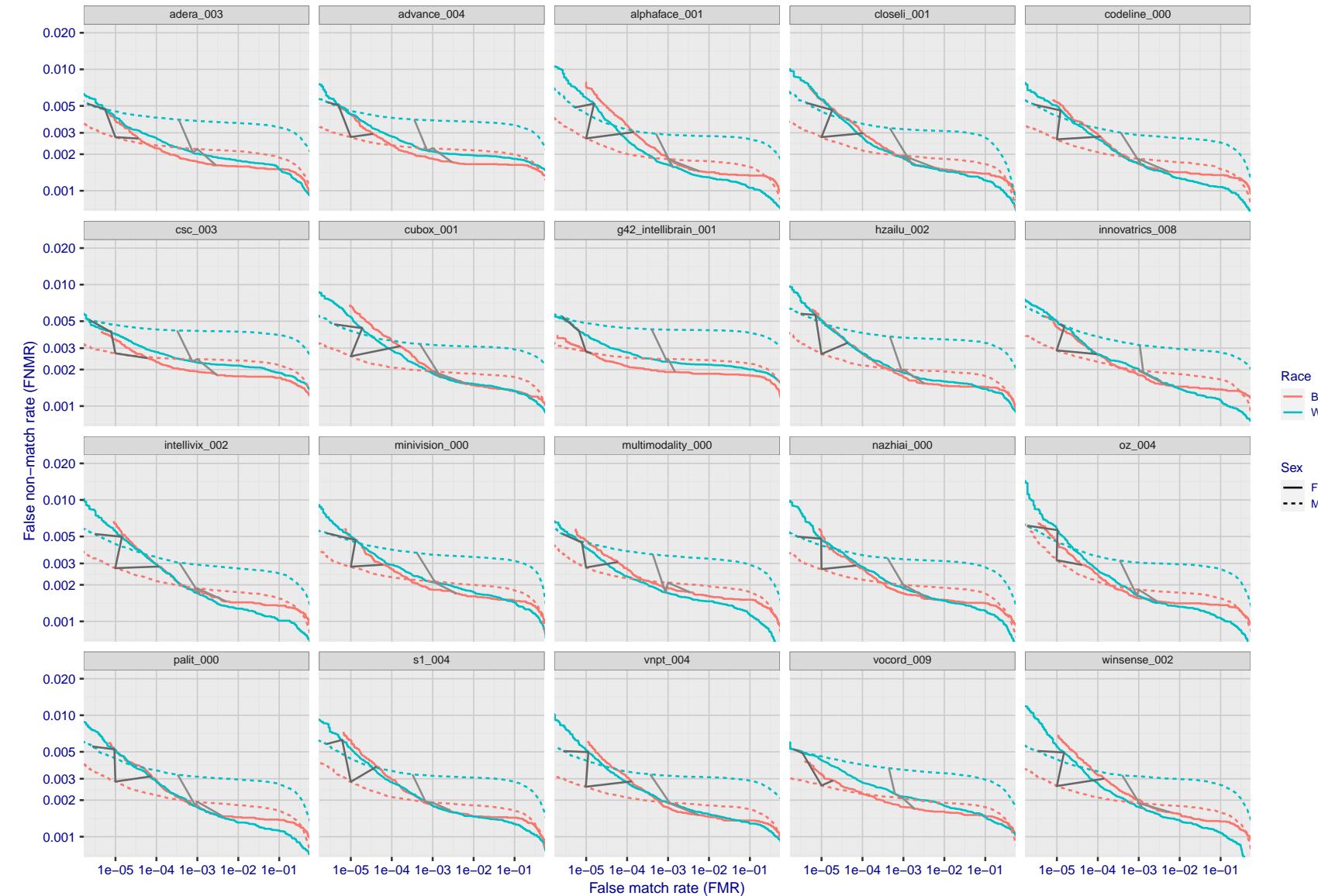


Figure 163: For the mugshot images, error tradeoff characteristics for white females, black females, black males and white males. The Z-shaped grey lines correspond to fixed thresholds, showing both FNMR and FMR vary at one T value. Note: Many of the plots will naively be read as saying women gives worse error rates than men because the solid traces lie above the dotted ones. However, this is misleading and incomplete: The grey lines show the traces reveal horizontal shifts. Thus for the cogent-003 algorithm FNMR for men is higher than for women at a fixed threshold but, at the same time, FMR is higher for women - see Figure 243. As access control systems almost always operate at a fixed threshold, the naive interpretation is incorrect.

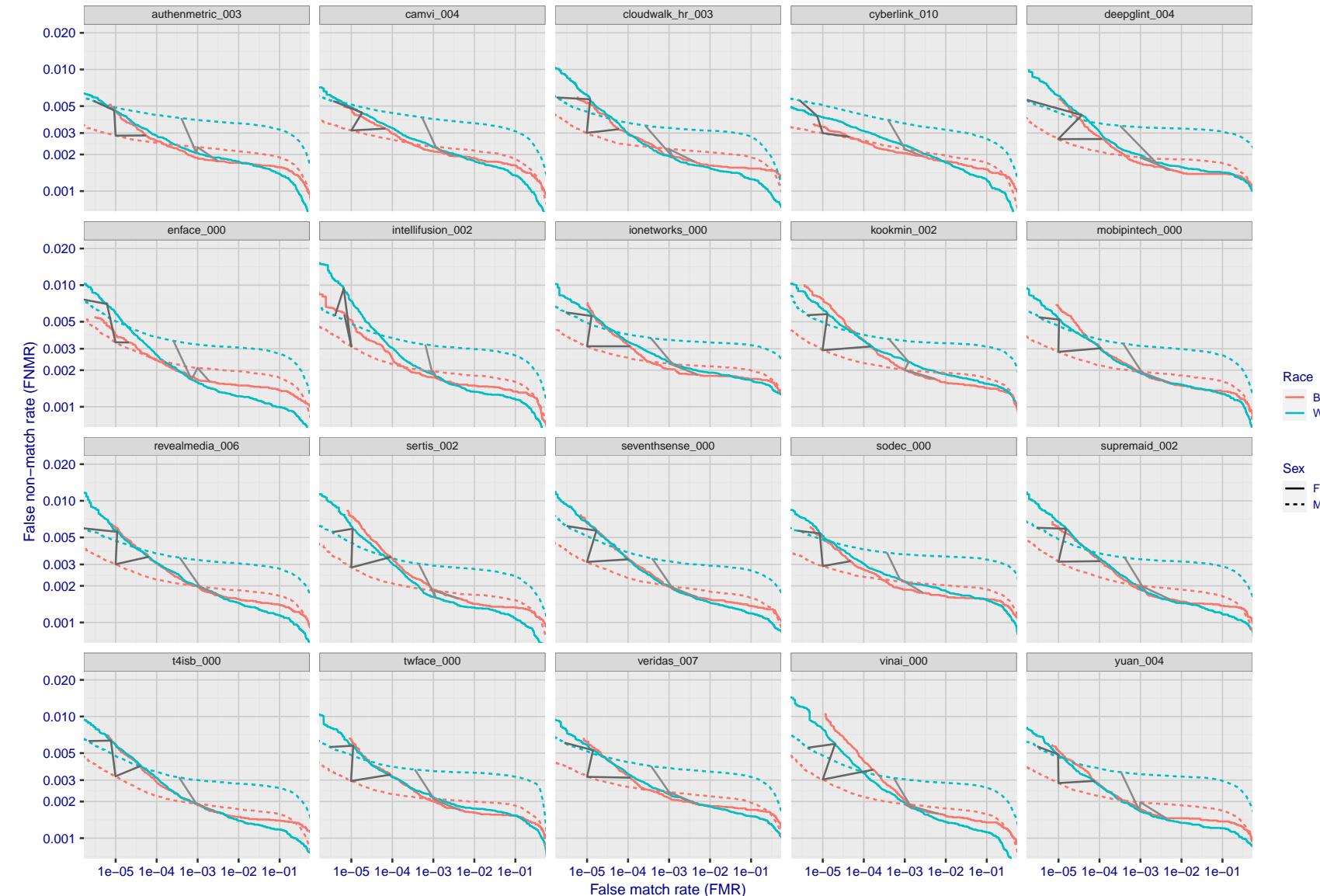


Figure 164: For the mugshot images, error tradeoff characteristics for white females, black females, black males and white males. The Z-shaped grey lines correspond to fixed thresholds, showing both FNMR and FMR vary at one T value. Note: Many of the plots will naively be read as saying women gives worse error rates than men because the solid traces lie above the dotted ones. However, this is misleading and incomplete: The grey lines show the traces reveal horizontal shifts. Thus for the cogent-003 algorithm FNMR for men is higher than for women at a fixed threshold but, at the same time, FMR is higher for women - see Figure 243. As access control systems almost always operate at a fixed threshold, the naive interpretation is incorrect.

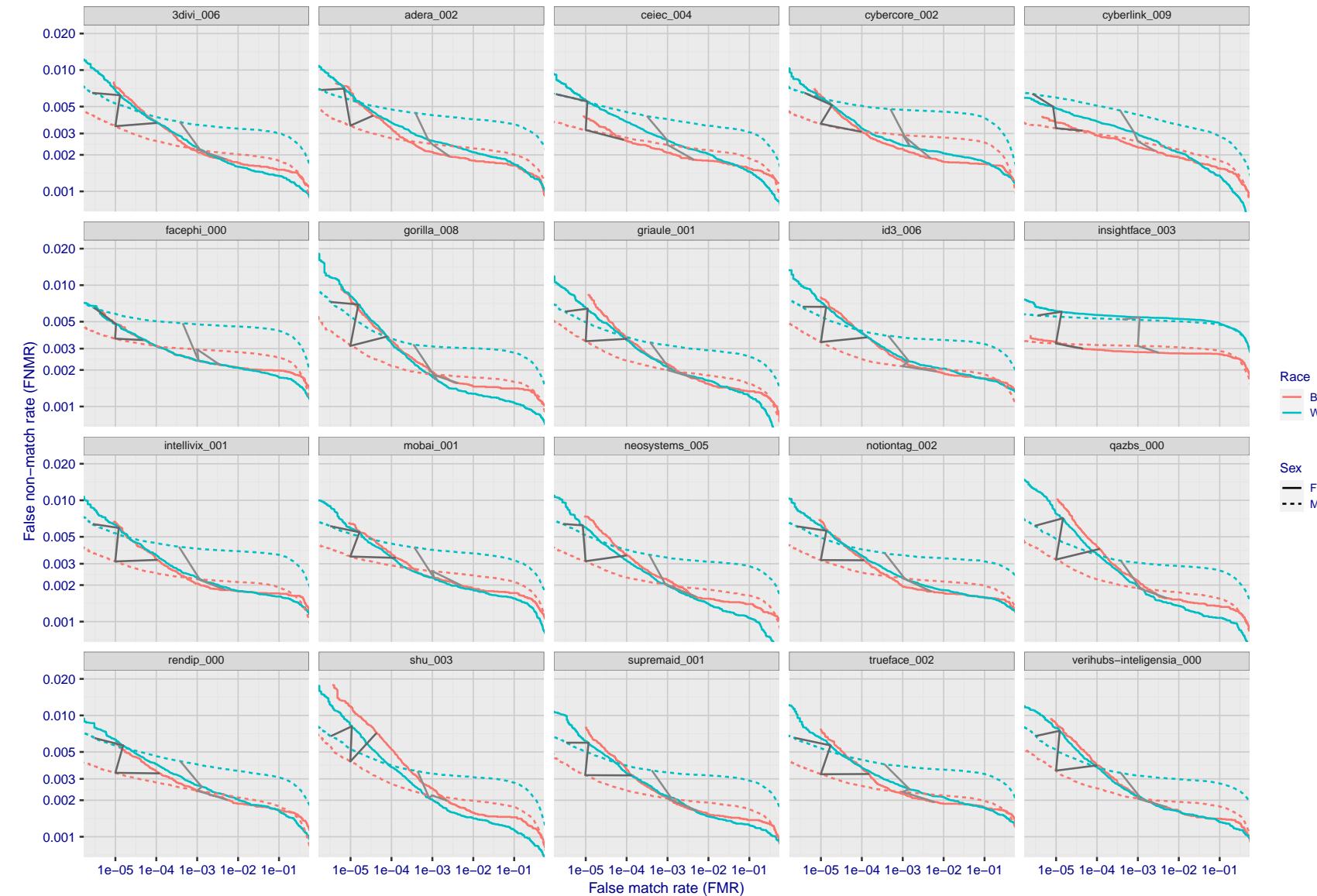


Figure 165: For the mugshot images, error tradeoff characteristics for white females, black females, black males and white males. The Z-shaped grey lines correspond to fixed thresholds, showing both FNMR and FMR vary at one T value. Note: Many of the plots will naively be read as saying women gives worse error rates than men because the solid traces lie above the dotted ones. However, this is misleading and incomplete: The grey lines show the traces reveal horizontal shifts. Thus for the cogent-003 algorithm FNMR for men is higher than for women at a fixed threshold but, at the same time, FMR is higher for women - see Figure 243. As access control systems almost always operate at a fixed threshold, the naive interpretation is incorrect.

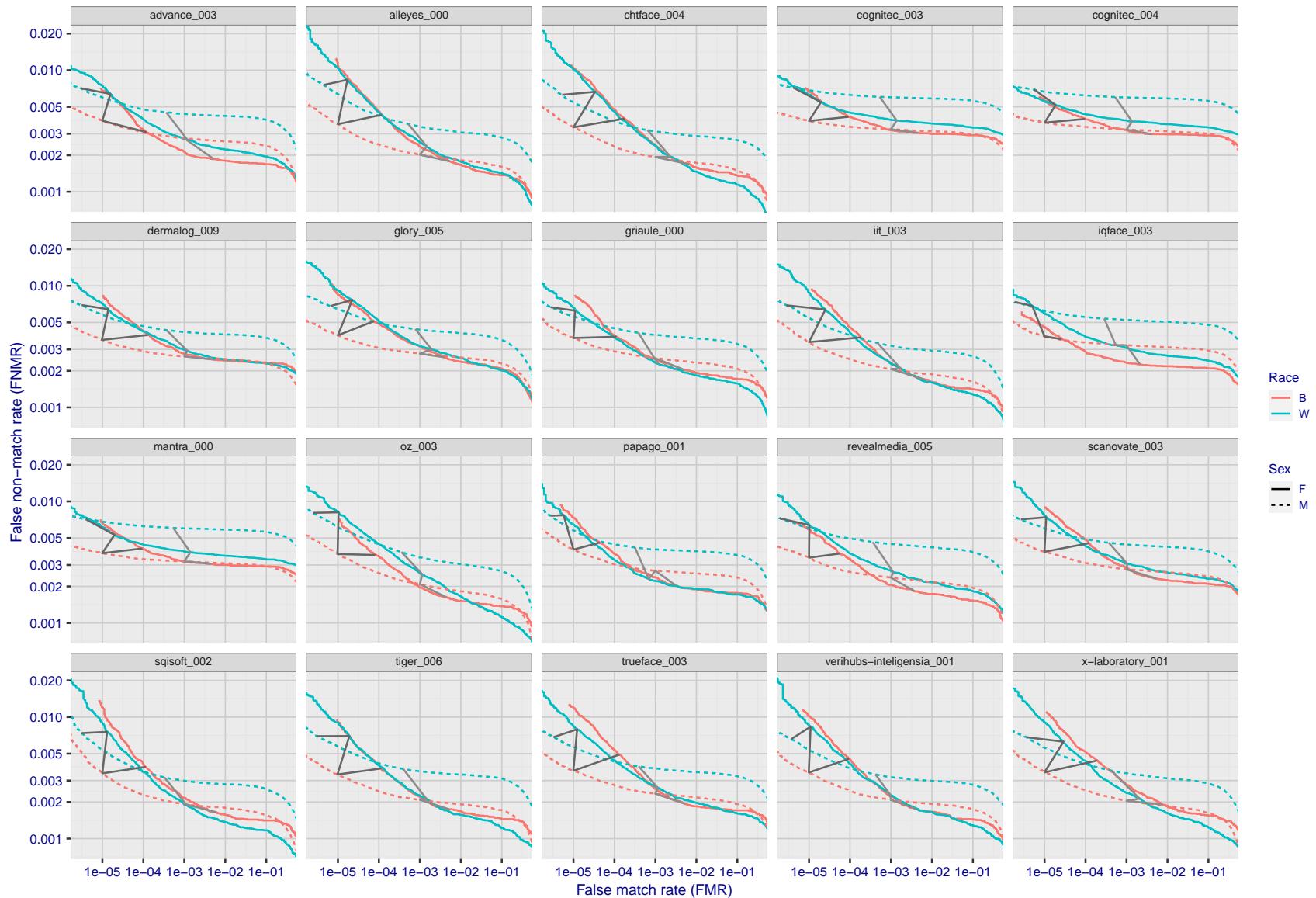


Figure 166: For the mugshot images, error tradeoff characteristics for white females, black females, black males and white males. The Z-shaped grey lines correspond to fixed thresholds, showing both FNMR and FMR vary at one T value. Note: Many of the plots will naively be read as saying women gives worse error rates than men because the solid traces lie above the dotted ones. However, this is misleading and incomplete: The grey lines show the traces reveal horizontal shifts. Thus for the cogent-003 algorithm FNMR for men is higher than for women at a fixed threshold but, at the same time, FMR is higher for women - see Figure 243. As access control systems almost always operate at a fixed threshold, the naive interpretation is incorrect.

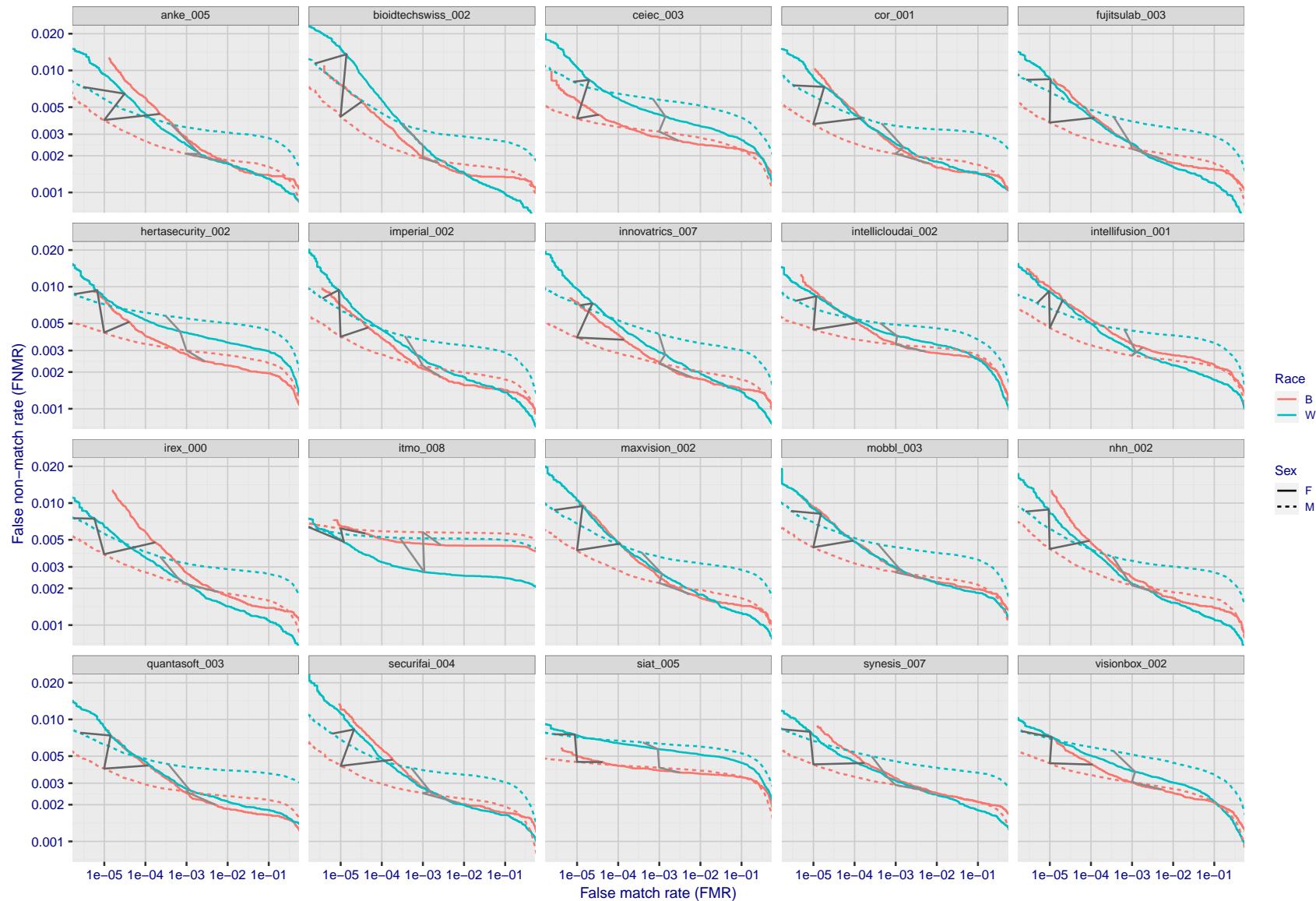


Figure 167: For the mugshot images, error tradeoff characteristics for white females, black females, black males and white males. The Z-shaped grey lines correspond to fixed thresholds, showing both FNMR and FMR vary at one T value. Note: Many of the plots will naively be read as saying women gives worse error rates than men because the solid traces lie above the dotted ones. However, this is misleading and incomplete: The grey lines show the traces reveal horizontal shifts. Thus for the cogent-003 algorithm FNMR for men is higher than for women at a fixed threshold but, at the same time, FMR is higher for women - see Figure 243. As access control systems almost always operate at a fixed threshold, the naive interpretation is incorrect.

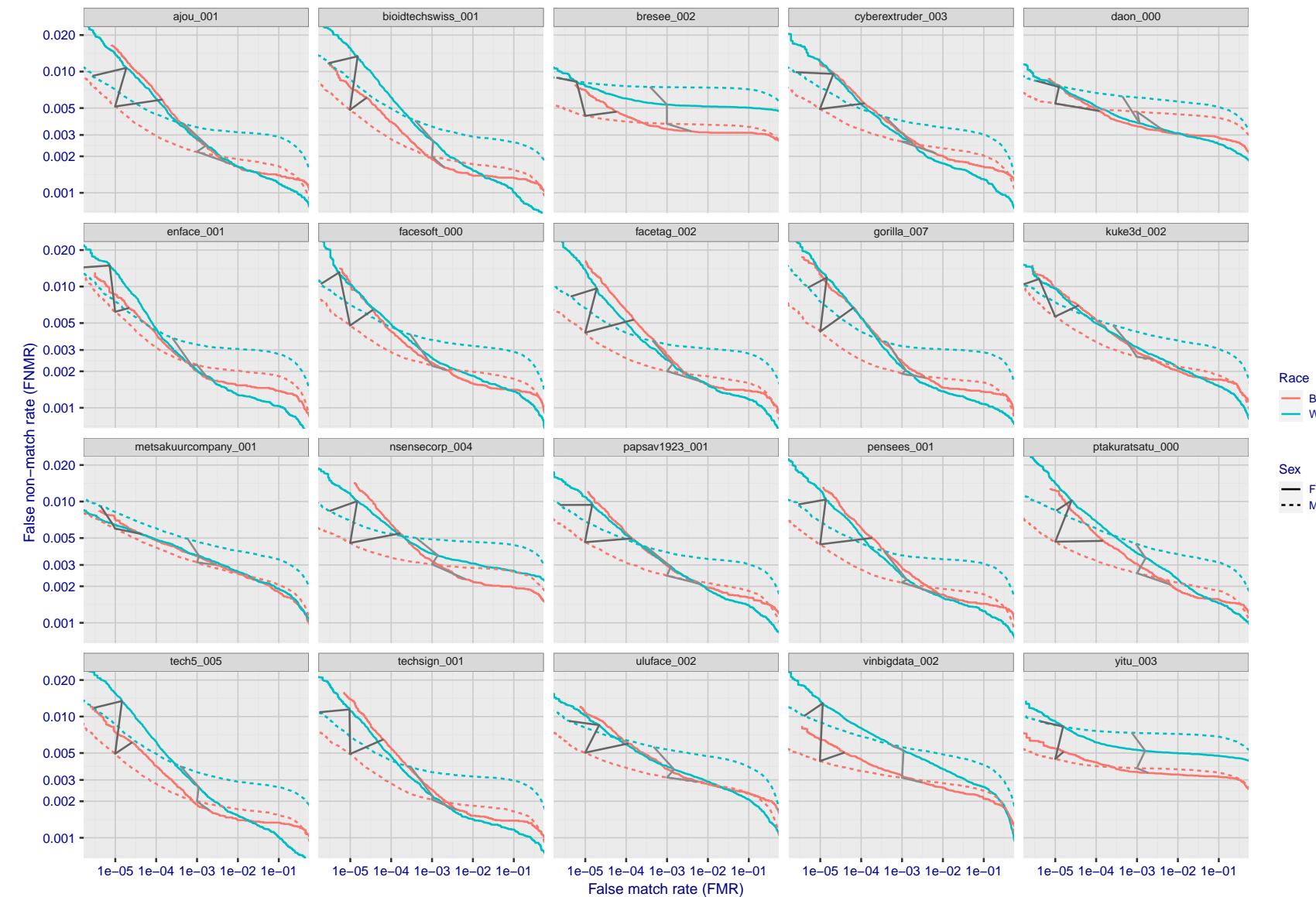


Figure 168: For the mugshot images, error tradeoff characteristics for white females, black females, black males and white males. The Z-shaped grey lines correspond to fixed thresholds, showing both FNMR and FMR vary at one T value. Note: Many of the plots will naively be read as saying women gives worse error rates than men because the solid traces lie above the dotted ones. However, this is misleading and incomplete: The grey lines show the traces reveal horizontal shifts. Thus for the cogent-003 algorithm FNMR for men is higher than for women at a fixed threshold but, at the same time, FMR is higher for women - see Figure 243. As access control systems almost always operate at a fixed threshold, the naive interpretation is incorrect.

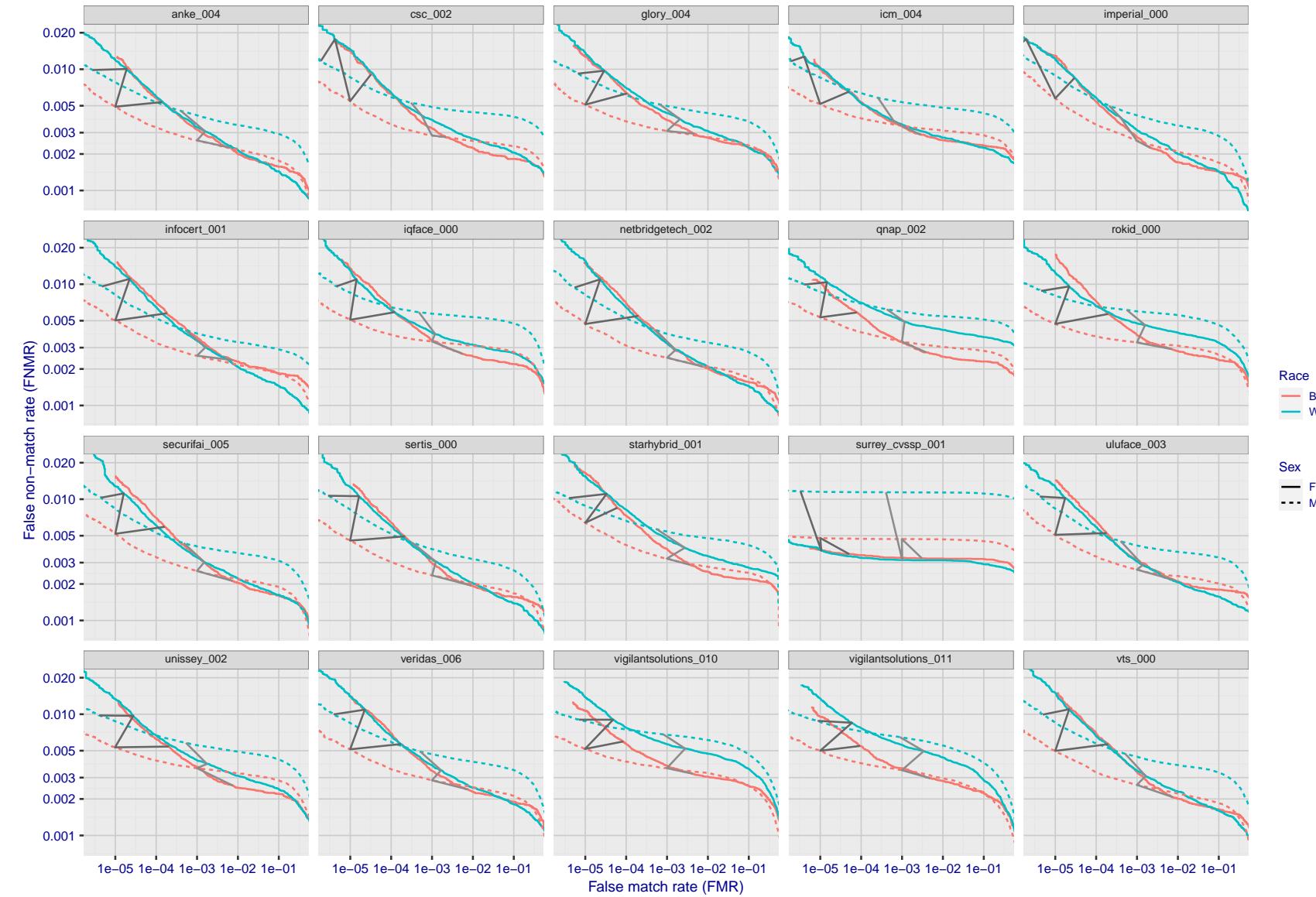


Figure 169: For the mugshot images, error tradeoff characteristics for white females, black females, black males and white males. The Z-shaped grey lines correspond to fixed thresholds, showing both FNMR and FMR vary at one T value. Note: Many of the plots will naively be read as saying women gives worse error rates than men because the solid traces lie above the dotted ones. However, this is misleading and incomplete: The grey lines show the traces reveal horizontal shifts. Thus for the cogent-003 algorithm FNMR for men is higher than for women at a fixed threshold but, at the same time, FMR is higher for women - see Figure 243. As access control systems almost always operate at a fixed threshold, the naive interpretation is incorrect.

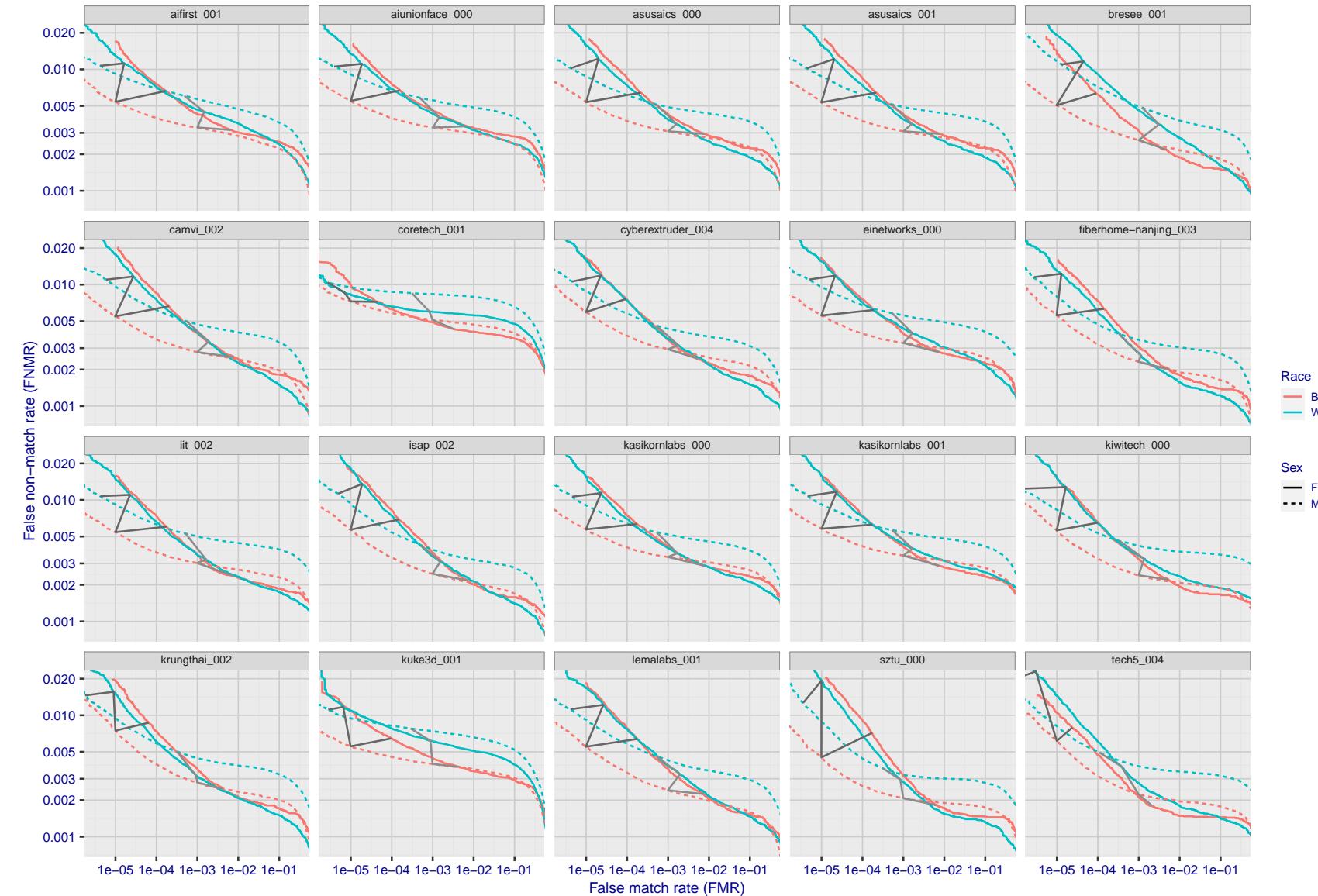


Figure 170: For the mugshot images, error tradeoff characteristics for white females, black females, black males and white males. The Z-shaped grey lines correspond to fixed thresholds, showing both FNMR and FMR vary at one T value. Note: Many of the plots will naively be read as saying women gives worse error rates than men because the solid traces lie above the dotted ones. However, this is misleading and incomplete: The grey lines show the traces reveal horizontal shifts. Thus for the cogent-003 algorithm FNMR for men is higher than for women at a fixed threshold but, at the same time, FMR is higher for women - see Figure 243. As access control systems almost always operate at a fixed threshold, the naive interpretation is incorrect.

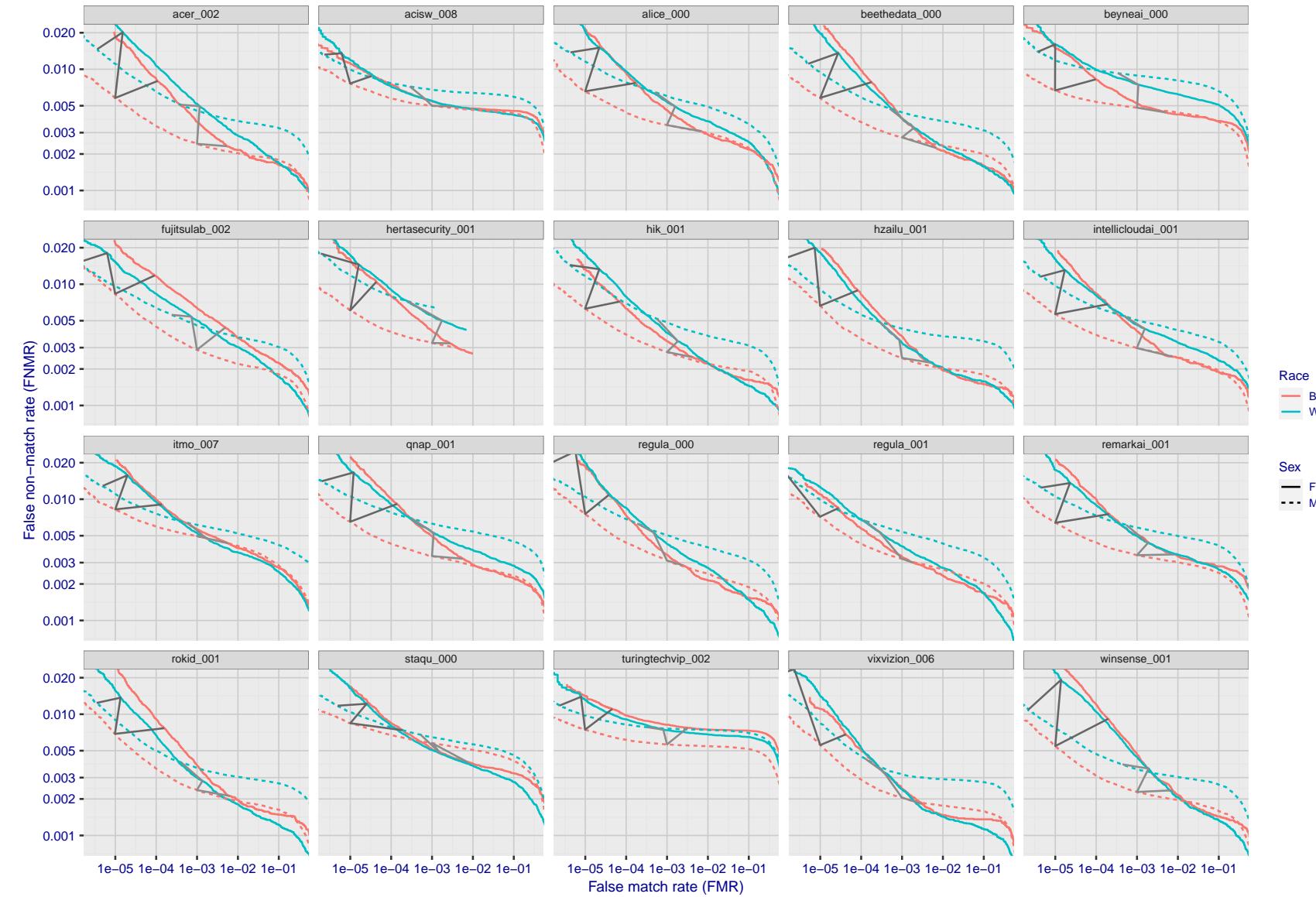


Figure 171: For the mugshot images, error tradeoff characteristics for white females, black females, black males and white males. The Z-shaped grey lines correspond to fixed thresholds, showing both FNMR and FMR vary at one T value. Note: Many of the plots will naively be read as saying women gives worse error rates than men because the solid traces lie above the dotted ones. However, this is misleading and incomplete: The grey lines show the traces reveal horizontal shifts. Thus for the cogent-003 algorithm FNMR for men is higher than for women at a fixed threshold but, at the same time, FMR is higher for women - see Figure 243. As access control systems almost always operate at a fixed threshold, the naive interpretation is incorrect.

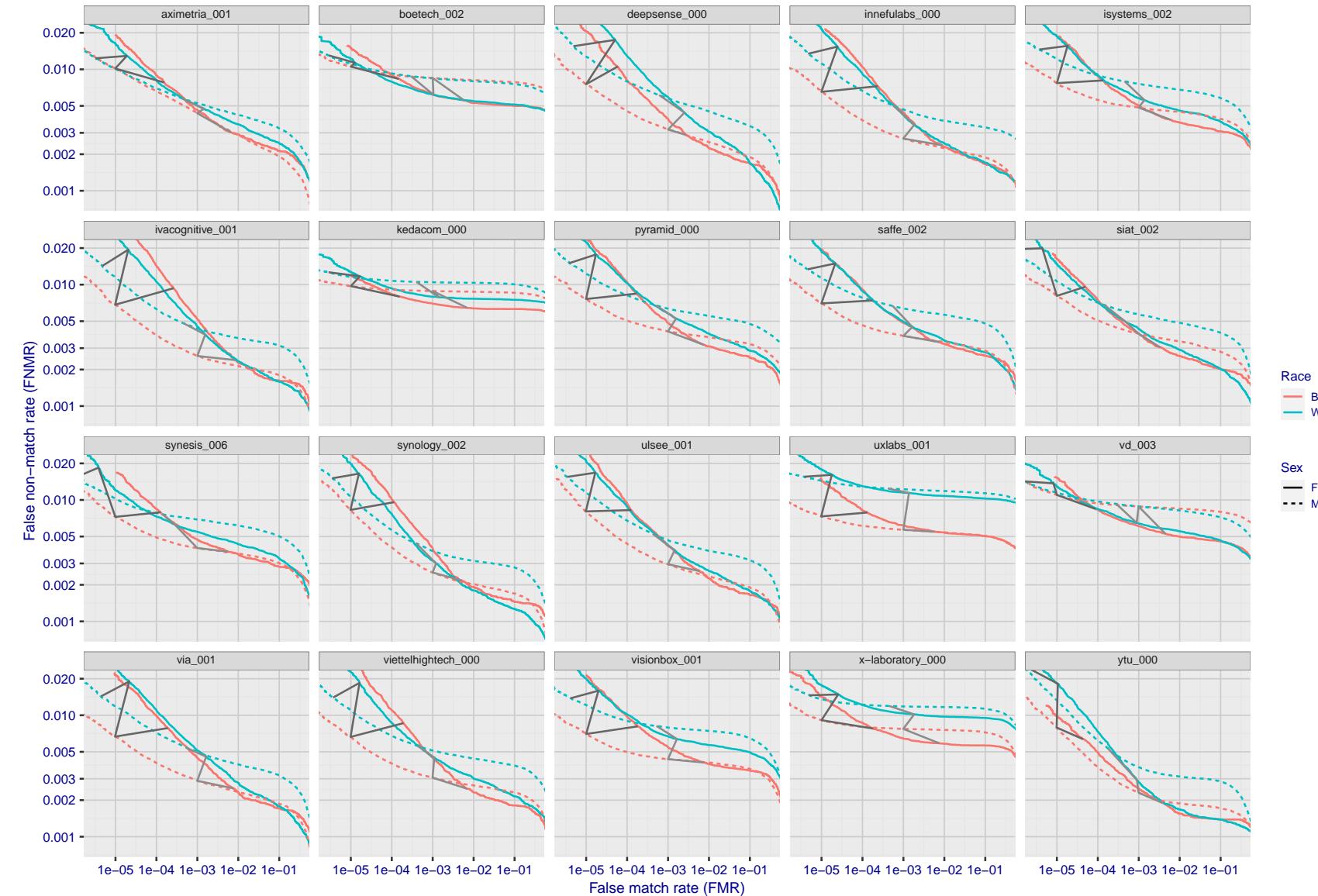


Figure 172: For the mugshot images, error tradeoff characteristics for white females, black females, black males and white males. The Z-shaped grey lines correspond to fixed thresholds, showing both FNMR and FMR vary at one T value. Note: Many of the plots will naively be read as saying women gives worse error rates than men because the solid traces lie above the dotted ones. However, this is misleading and incomplete: The grey lines show the traces reveal horizontal shifts. Thus for the cogent-003 algorithm FNMR for men is higher than for women at a fixed threshold but, at the same time, FMR is higher for women - see Figure 243. As access control systems almost always operate at a fixed threshold, the naive interpretation is incorrect.

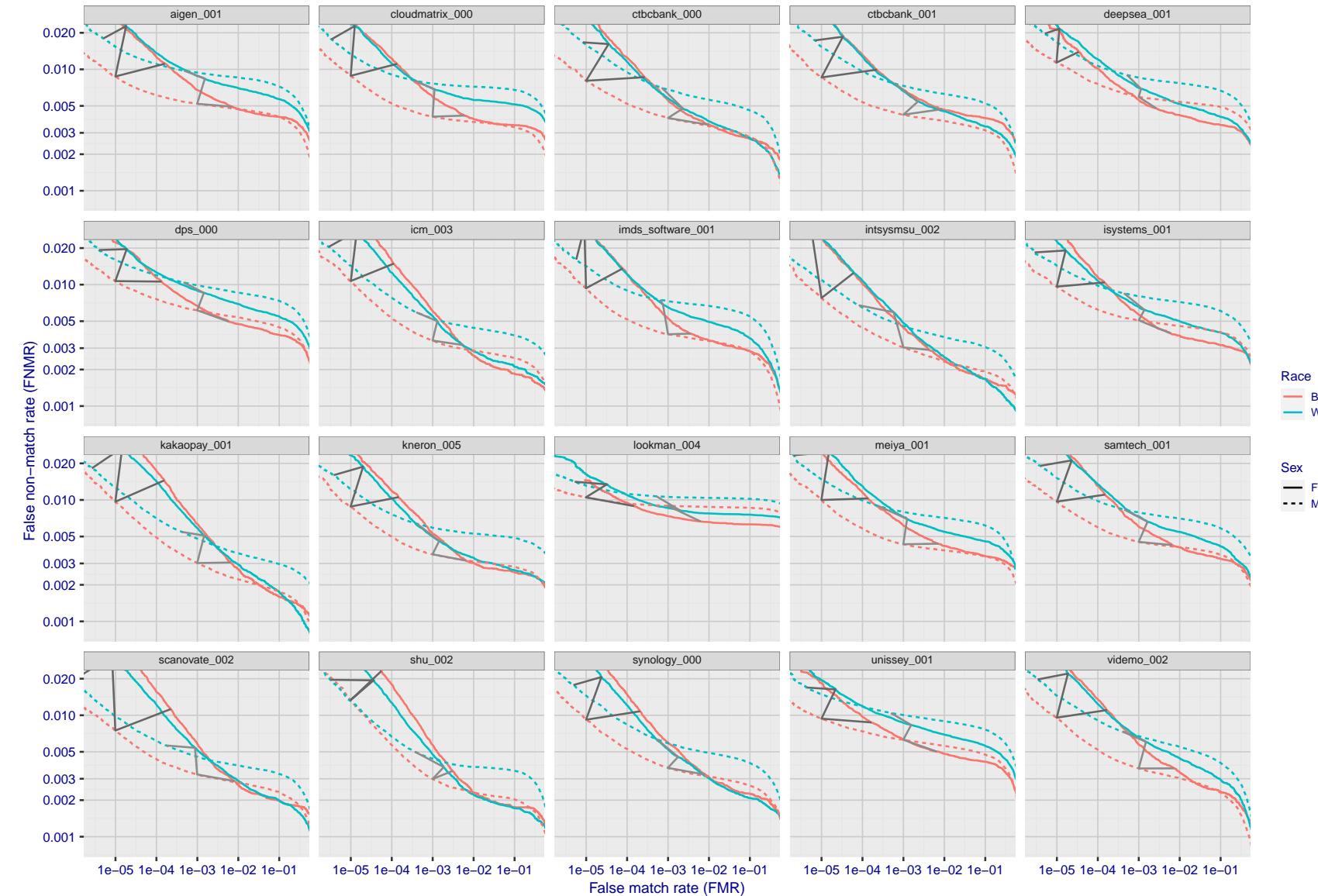


Figure 173: For the mugshot images, error tradeoff characteristics for white females, black females, black males and white males. The Z-shaped grey lines correspond to fixed thresholds, showing both FNMR and FMR vary at one T value. Note: Many of the plots will naively be read as saying women gives worse error rates than men because the solid traces lie above the dotted ones. However, this is misleading and incomplete: The grey lines show the traces reveal horizontal shifts. Thus for the cogent-003 algorithm FNMR for men is higher than for women at a fixed threshold but, at the same time, FMR is higher for women - see Figure 243. As access control systems almost always operate at a fixed threshold, the naive interpretation is incorrect.

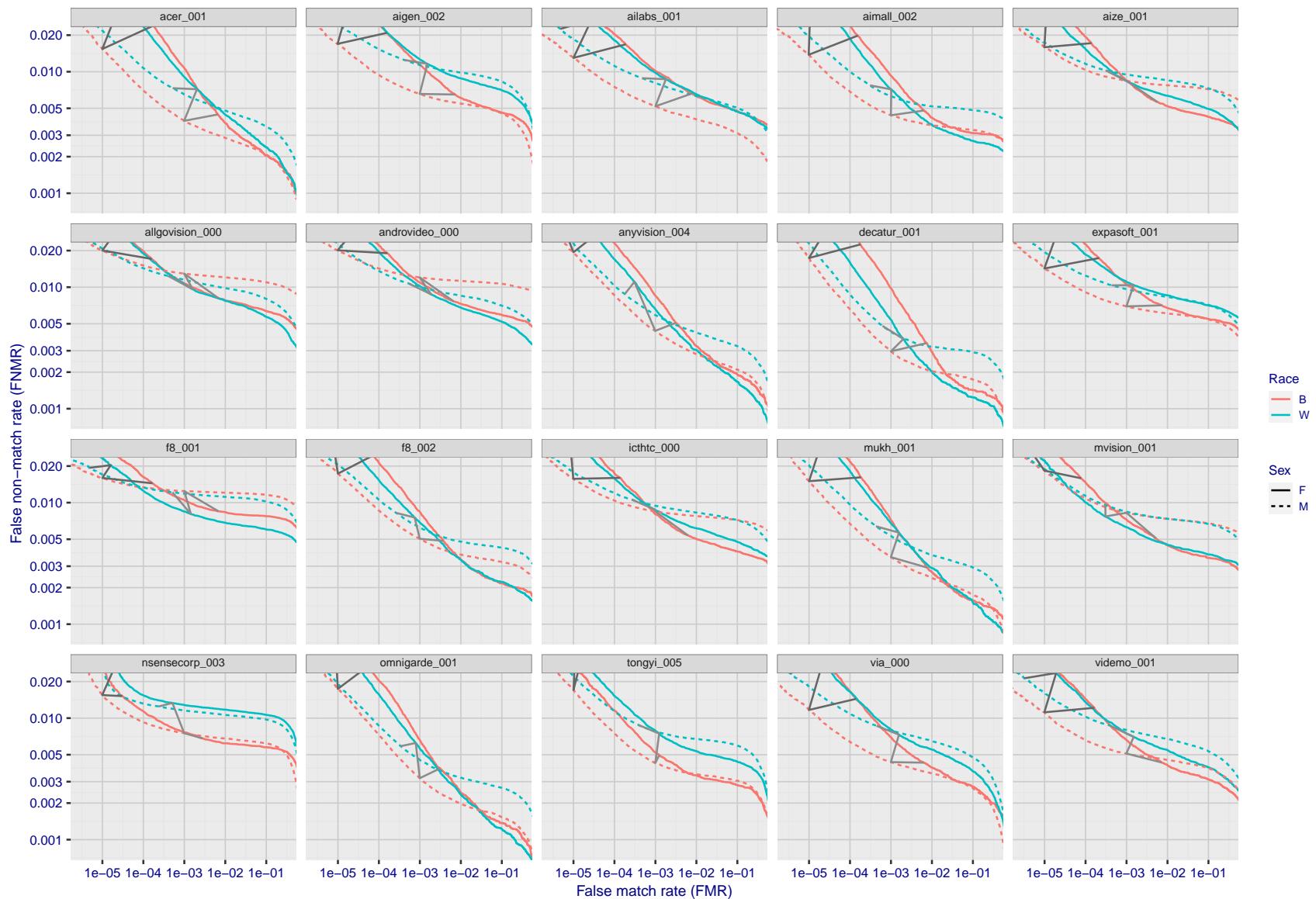


Figure 174: For the mugshot images, error tradeoff characteristics for white females, black females, black males and white males. The Z-shaped grey lines correspond to fixed thresholds, showing both FNMR and FMR vary at one T value. Note: Many of the plots will naively be read as saying women gives worse error rates than men because the solid traces lie above the dotted ones. However, this is misleading and incomplete: The grey lines show the traces reveal horizontal shifts. Thus for the cogent-003 algorithm FNMR for men is higher than for women at a fixed threshold but, at the same time, FMR is higher for women - see Figure 243. As access control systems almost always operate at a fixed threshold, the naive interpretation is incorrect.

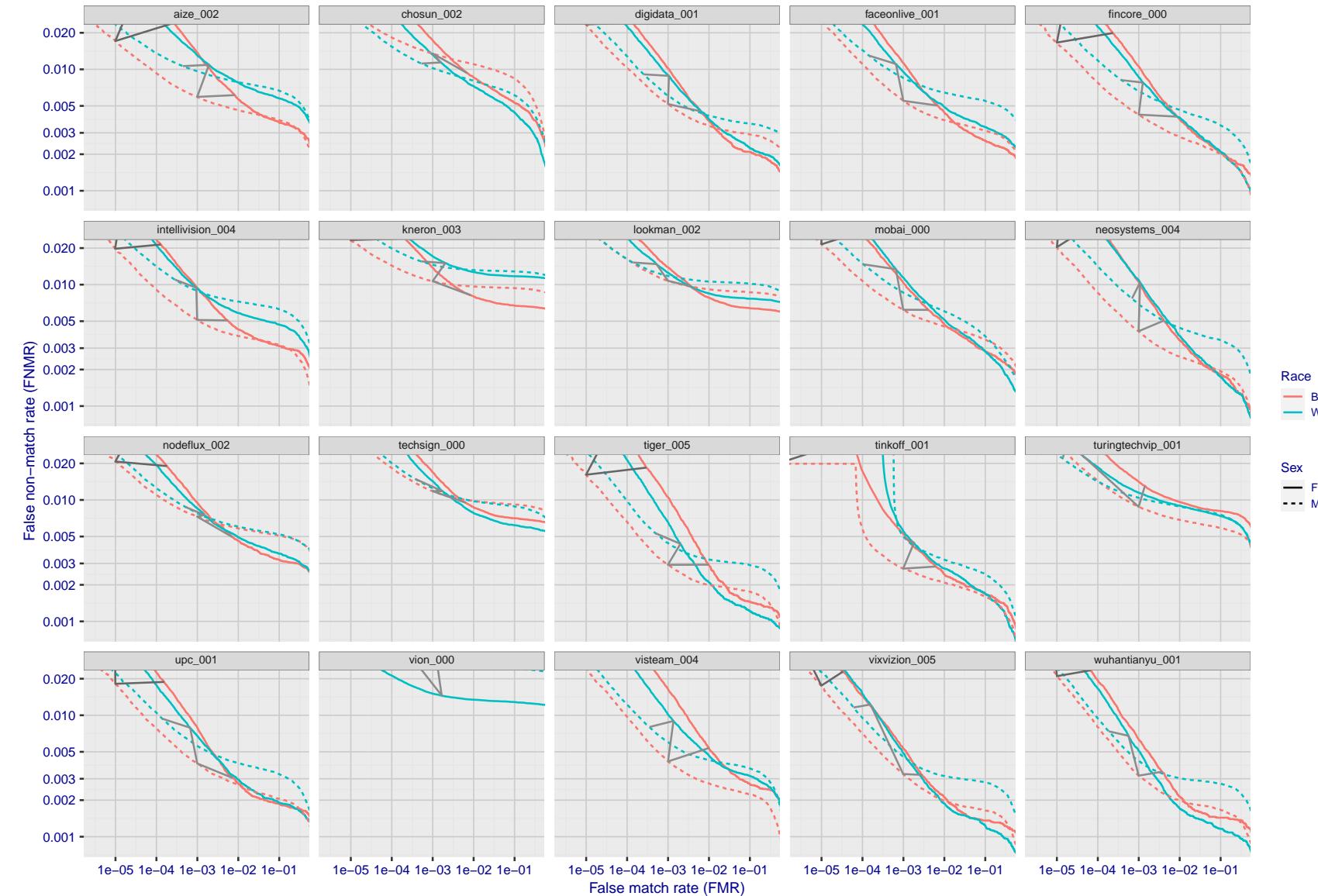


Figure 175: For the mugshot images, error tradeoff characteristics for white females, black females, black males and white males. The Z-shaped grey lines correspond to fixed thresholds, showing both FNMR and FMR vary at one T value. Note: Many of the plots will naively be read as saying women gives worse error rates than men because the solid traces lie above the dotted ones. However, this is misleading and incomplete: The grey lines show the traces reveal horizontal shifts. Thus for the cogent-003 algorithm FNMR for men is higher than for women at a fixed threshold but, at the same time, FMR is higher for women - see Figure 243. As access control systems almost always operate at a fixed threshold, the naive interpretation is incorrect.

2023/02/02 13:38:52

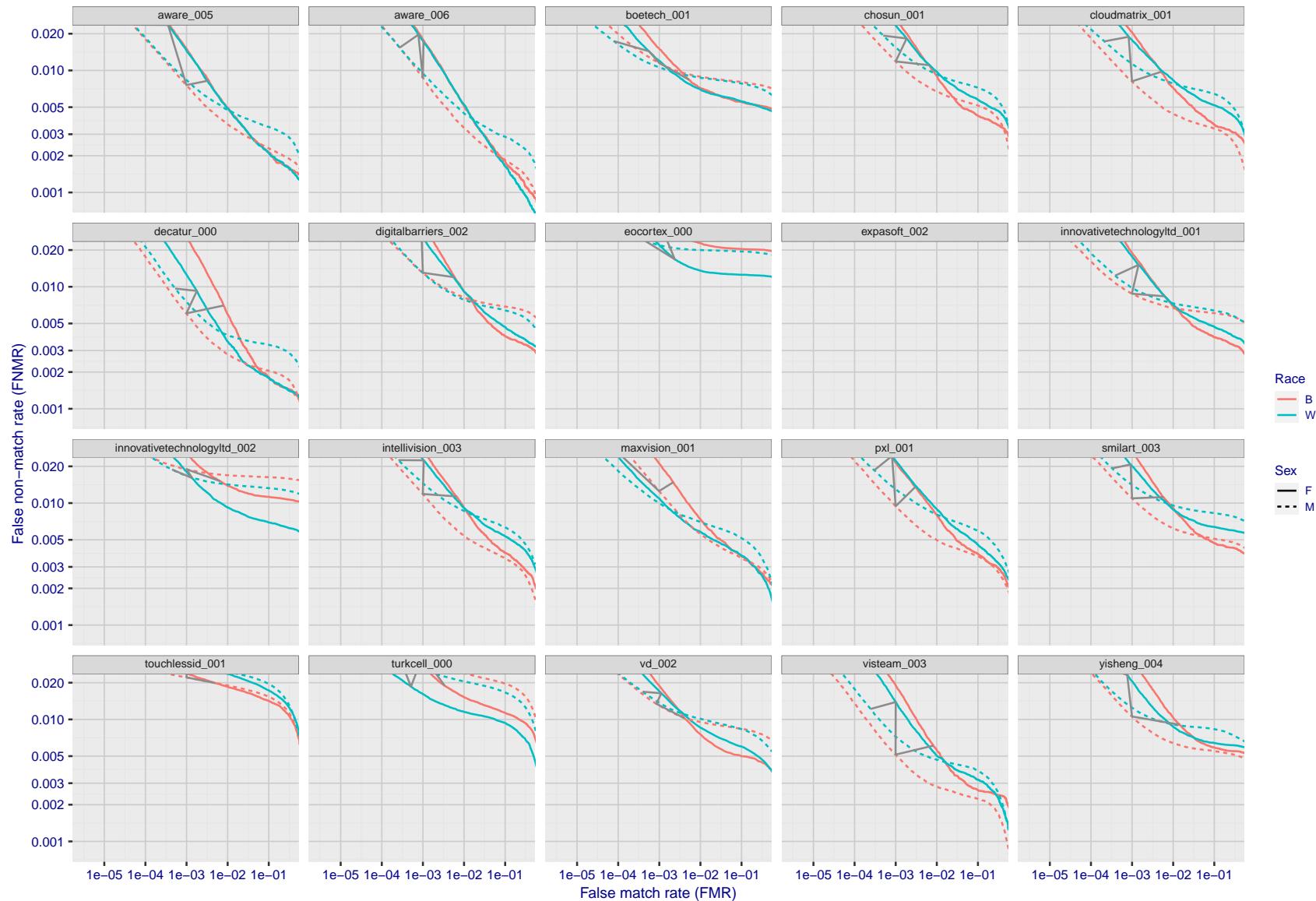


Figure 176: For the mugshot images, error tradeoff characteristics for white females, black females, black males and white males. The Z-shaped grey lines correspond to fixed thresholds, showing both FNMR and FMR vary at one T value. Note: Many of the plots will naively be read as saying women gives worse error rates than men because the solid traces lie above the dotted ones. However, this is misleading and incomplete: The grey lines show the traces reveal horizontal shifts. Thus for the cogent-003 algorithm FNMR for men is higher than for women at a fixed threshold but, at the same time, FMR is higher for women - see Figure 243. As access control systems almost always operate at a fixed threshold, the naive interpretation is incorrect.

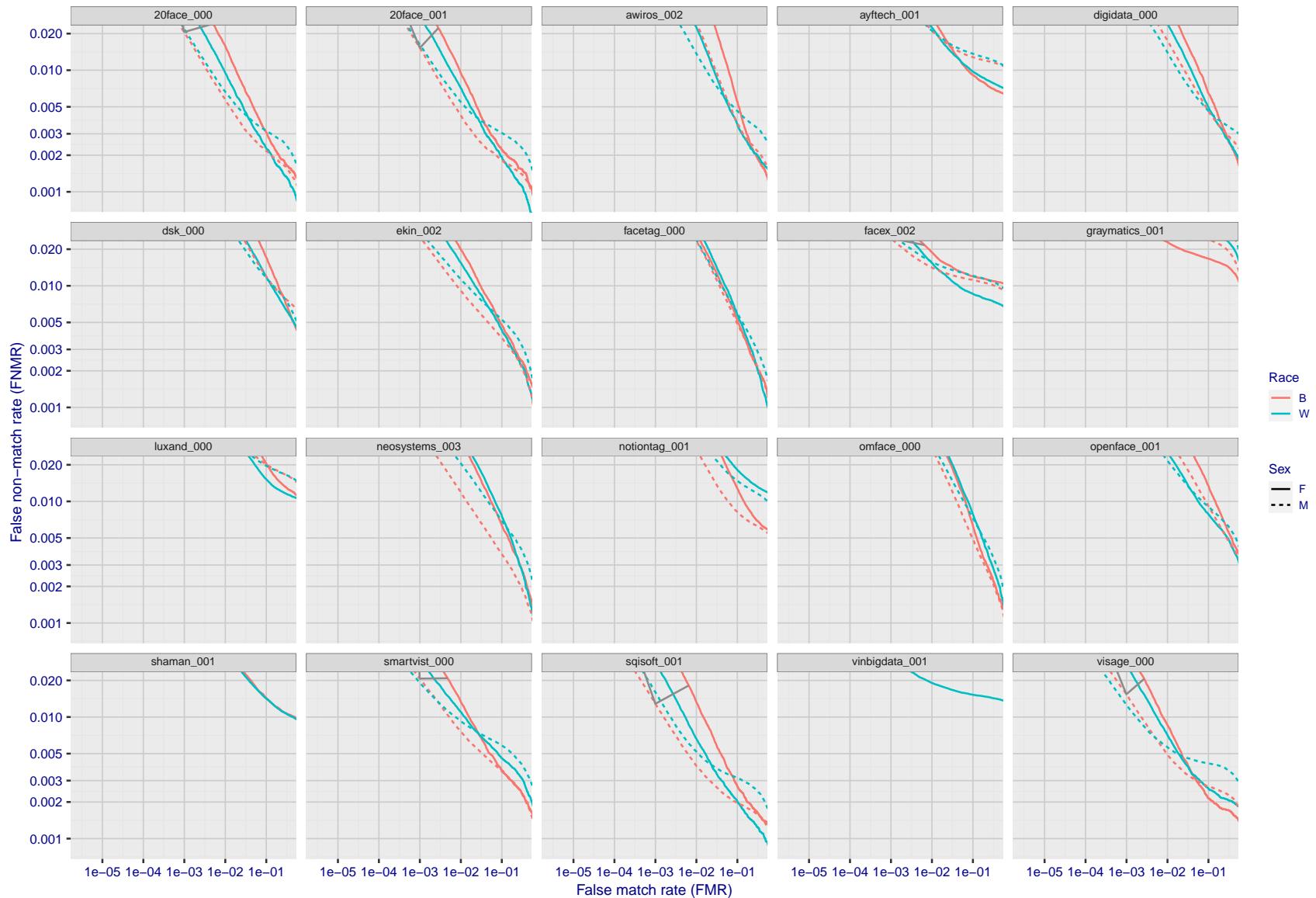


Figure 177: For the mugshot images, error tradeoff characteristics for white females, black females, black males and white males. The Z-shaped grey lines correspond to fixed thresholds, showing both FNMR and FMR vary at one T value. Note: Many of the plots will naively be read as saying women gives worse error rates than men because the solid traces lie above the dotted ones. However, this is misleading and incomplete: The grey lines show the traces reveal horizontal shifts. Thus for the cogent-003 algorithm FNMR for men is higher than for women at a fixed threshold but, at the same time, FMR is higher for women - see Figure 243. As access control systems almost always operate at a fixed threshold, the naive interpretation is incorrect.

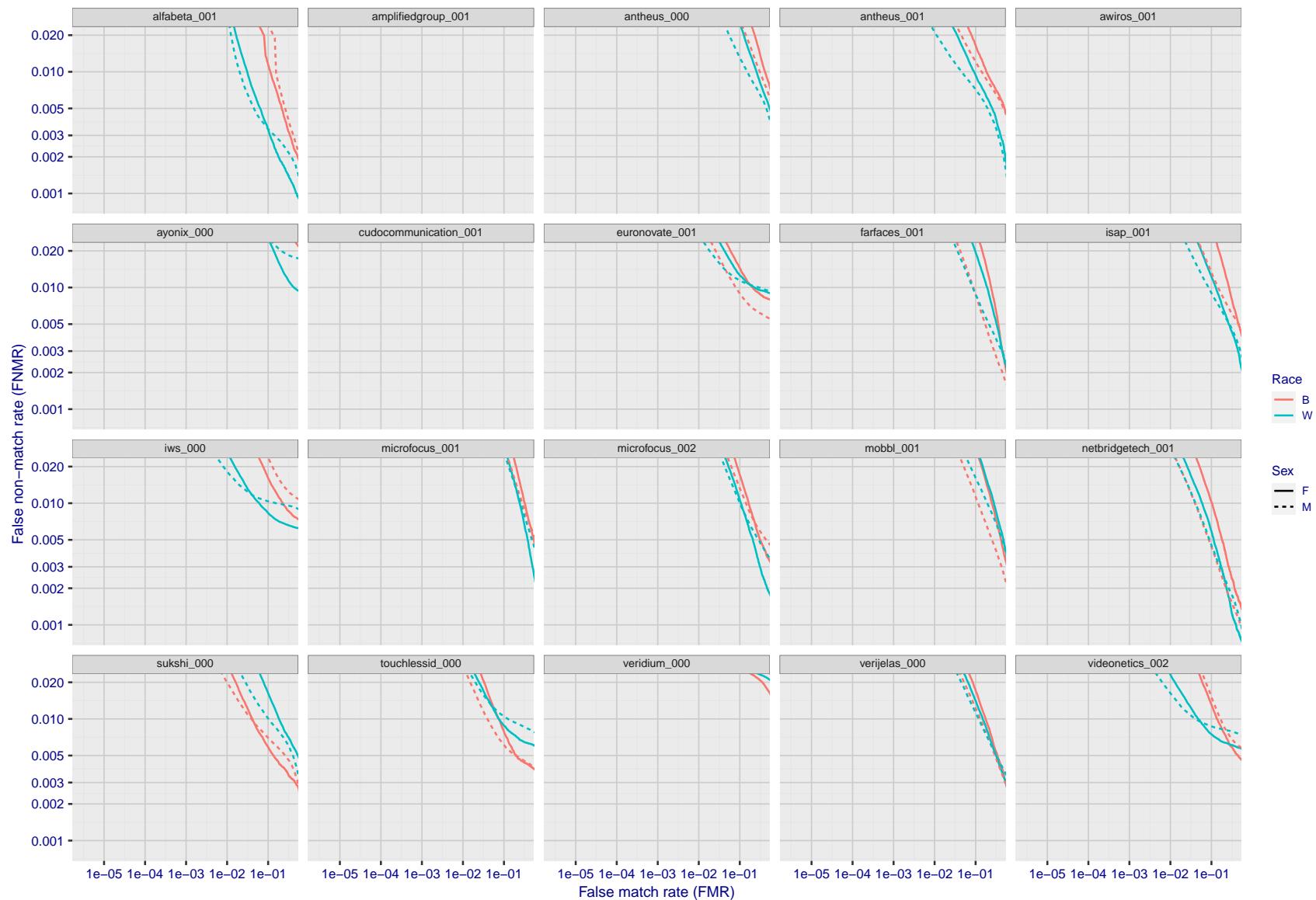


Figure 178: For the mugshot images, error tradeoff characteristics for white females, black females, black males and white males. The Z-shaped grey lines correspond to fixed thresholds, showing both FNMR and FMR vary at one T value. Note: Many of the plots will naively be read as saying women gives worse error rates than men because the solid traces lie above the dotted ones. However, this is misleading and incomplete: The grey lines show the traces reveal horizontal shifts. Thus for the cogent-003 algorithm FNMR for men is higher than for women at a fixed threshold but, at the same time, FMR is higher for women - see Figure 243. As access control systems almost always operate at a fixed threshold, the naive interpretation is incorrect.

2023/02/02 13:38:52

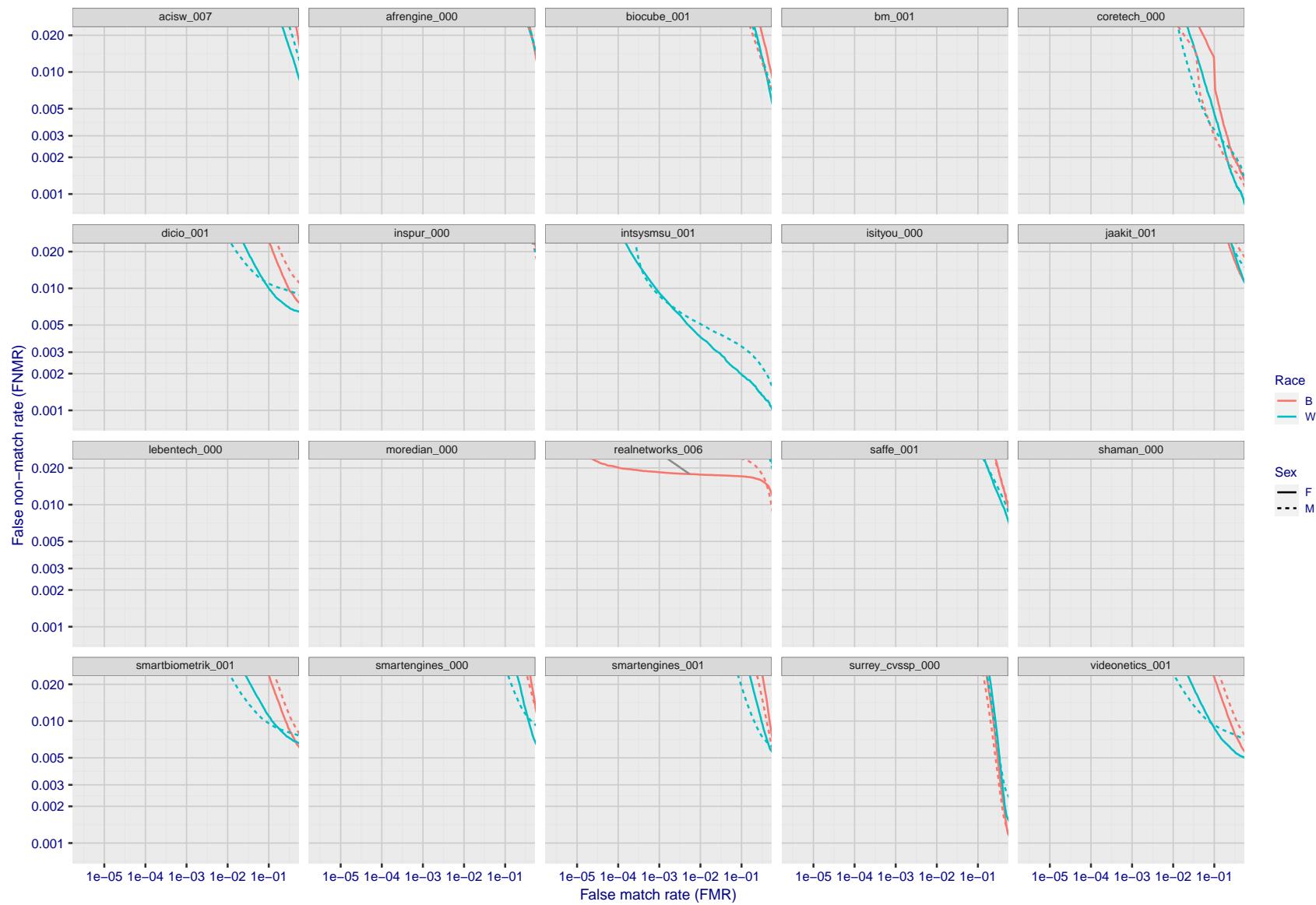


Figure 179: For the mugshot images, error tradeoff characteristics for white females, black females, black males and white males. The Z-shaped grey lines correspond to fixed thresholds, showing both FNMR and FMR vary at one T value. Note: Many of the plots will naively be read as saying women gives worse error rates than men because the solid traces lie above the dotted ones. However, this is misleading and incomplete: The grey lines show the traces reveal horizontal shifts. Thus for the cogent-003 algorithm FNMR for men is higher than for women at a fixed threshold but, at the same time, FMR is higher for women - see Figure 243. As access control systems almost always operate at a fixed threshold, the naive interpretation is incorrect.

FNMR(T)"False non-match rate"
"False match rate"

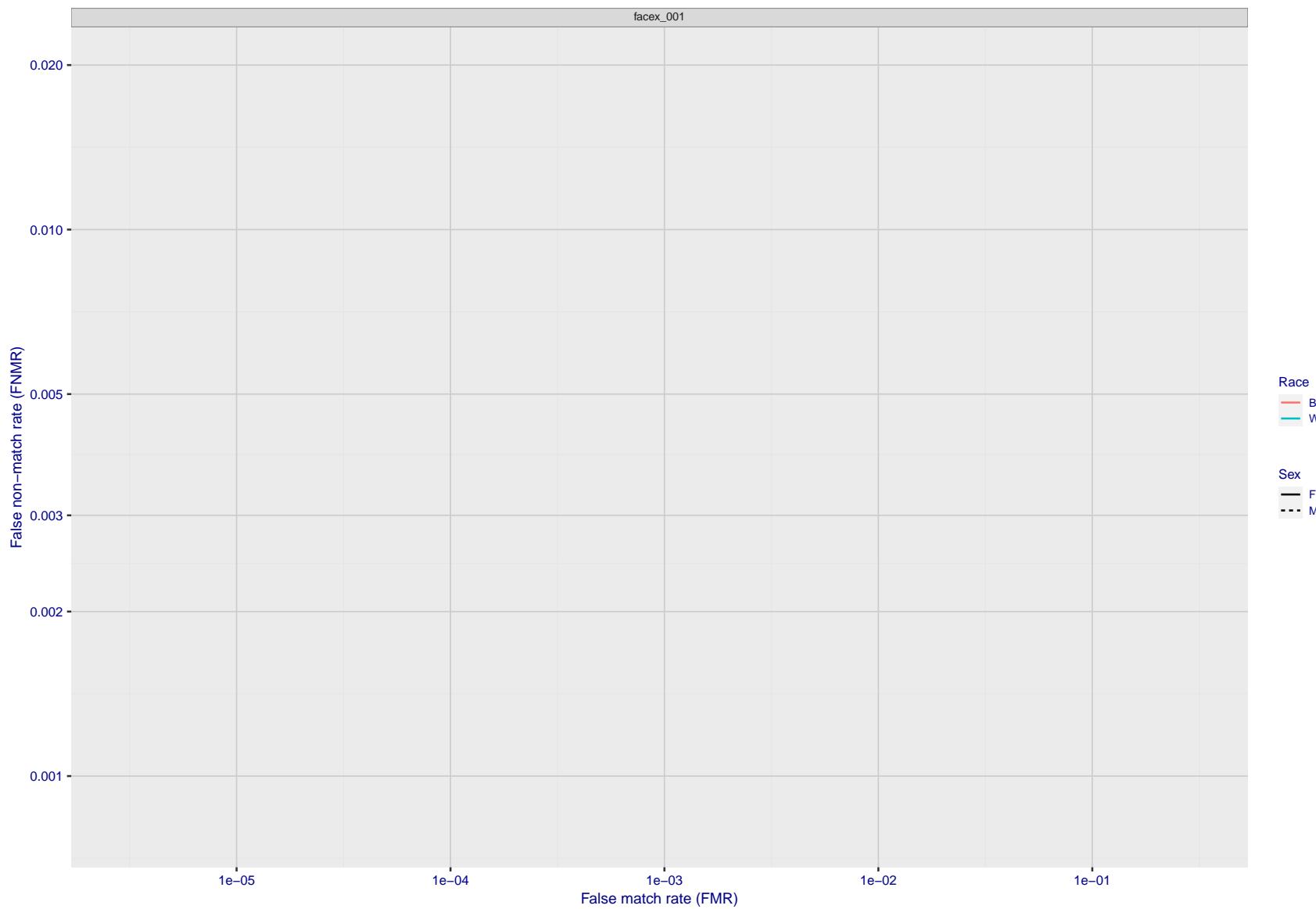


Figure 180: For the mugshot images, error tradeoff characteristics for white females, black females, black males and white males. The Z-shaped grey lines correspond to fixed thresholds, showing both FNMR and FMR vary at one T value. Note: Many of the plots will naively be read as saying women gives worse error rates than men because the solid traces lie above the dotted ones. However, this is misleading and incomplete: The grey lines show the traces reveal horizontal shifts. Thus for the cogent-003 algorithm FNMR for men is higher than for women at a fixed threshold but, at the same time, FMR is higher for women - see Figure 243. As access control systems almost always operate at a fixed threshold, the naive interpretation is incorrect.

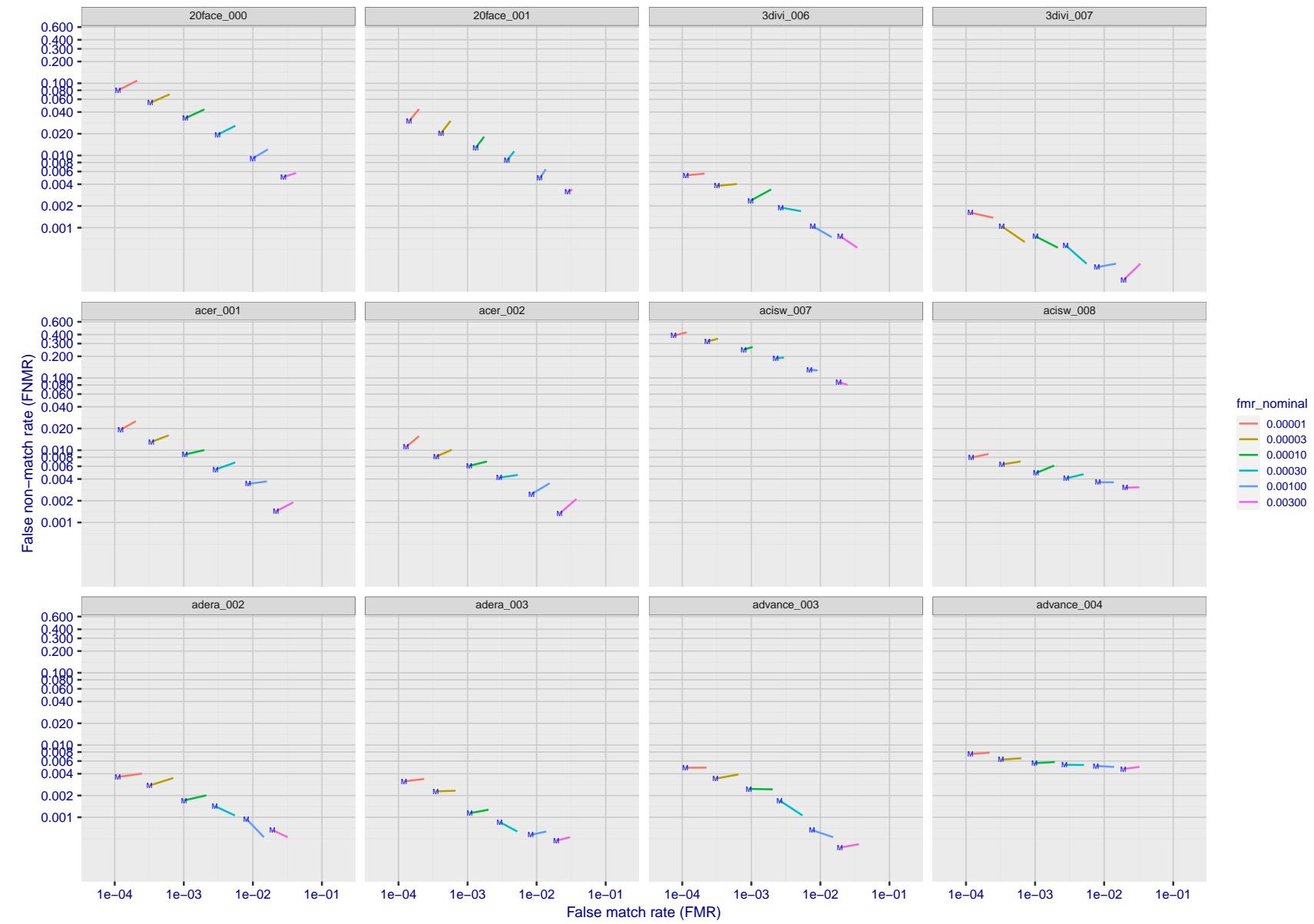


Figure 181: For the visa images, FNMR and FMR at six operating points along the DET characteristic. At each point a line is drawn between $(FMR, FNMR)_{MALE}$ and $(FMR, FNMR)_{FEMALE}$ showing how which sex has lower FMR and/or FNMR. The "M" label denotes male, the other end of the line corresponds to female. The six operating thresholds are selected to give the nominal false match rates given in the legend, and are computed over all impostor pairs regardless of age, sex, and place of birth. The plotted FMR values are broadly an order of magnitude larger than the nominal rates because FMR is computed over demographically-matched impostor pairs i.e individuals of the same sex, from the same geographic region (see section 3.6.1), and the same age group (see section 3.6.2).

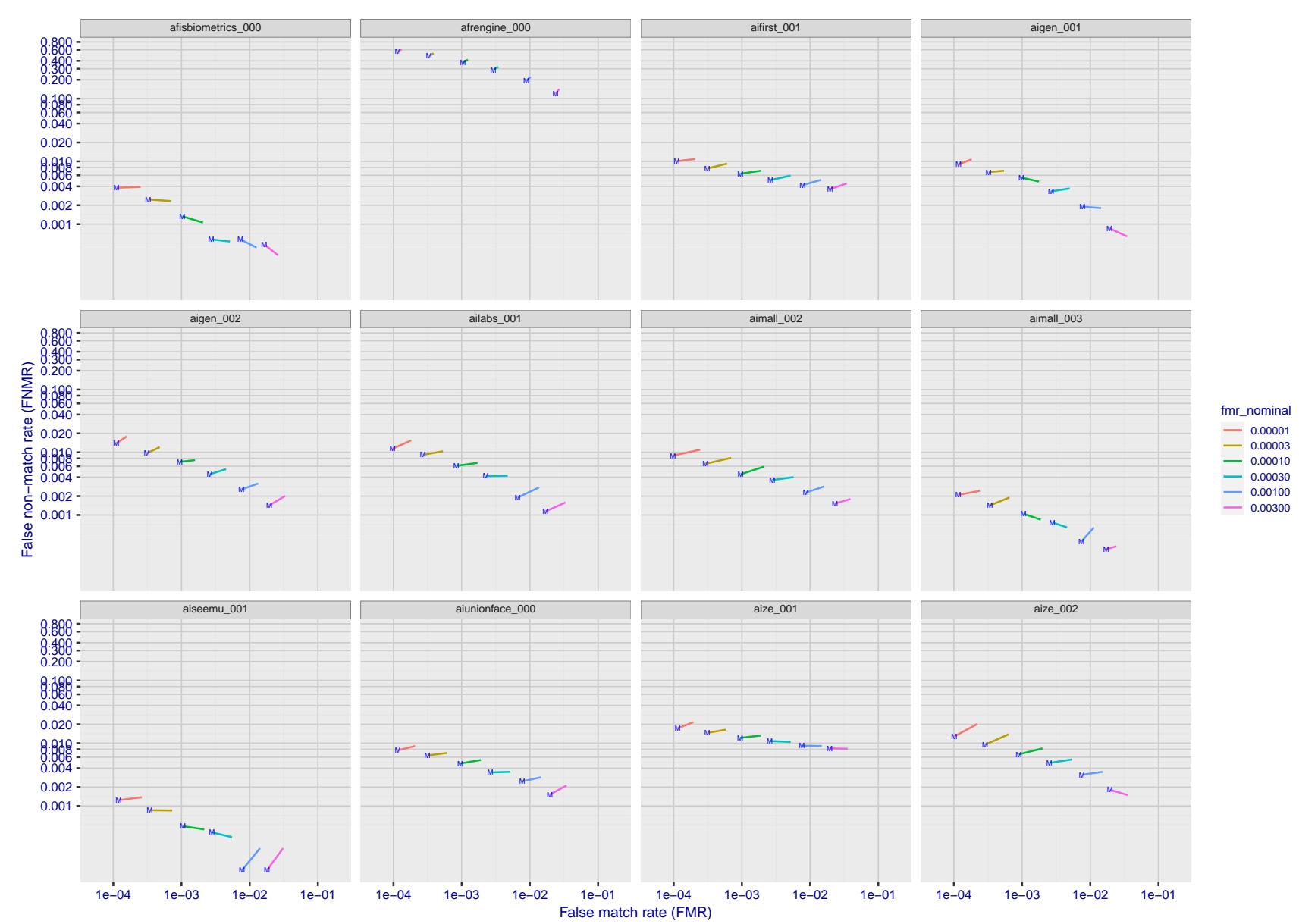


Figure 182: For the visa images, FNMR and FMR at six operating points along the DET characteristic. At each point a line is drawn between $(FMR, FNMR)_{MALE}$ and $(FMR, FNMR)_{FEMALE}$ showing how which sex has lower FMR and/or FNMR. The "M" label denotes male, the other end of the line corresponds to female. The six operating thresholds are selected to give the nominal false match rates given in the legend, and are computed over all impostor pairs regardless of age, sex, and place of birth. The plotted FMR values are broadly an order of magnitude larger than the nominal rates because FMR is computed over demographically-matched impostor pairs i.e individuals of the same sex, from the same geographic region (see section 3.6.1), and the same age group (see section 3.6.2).

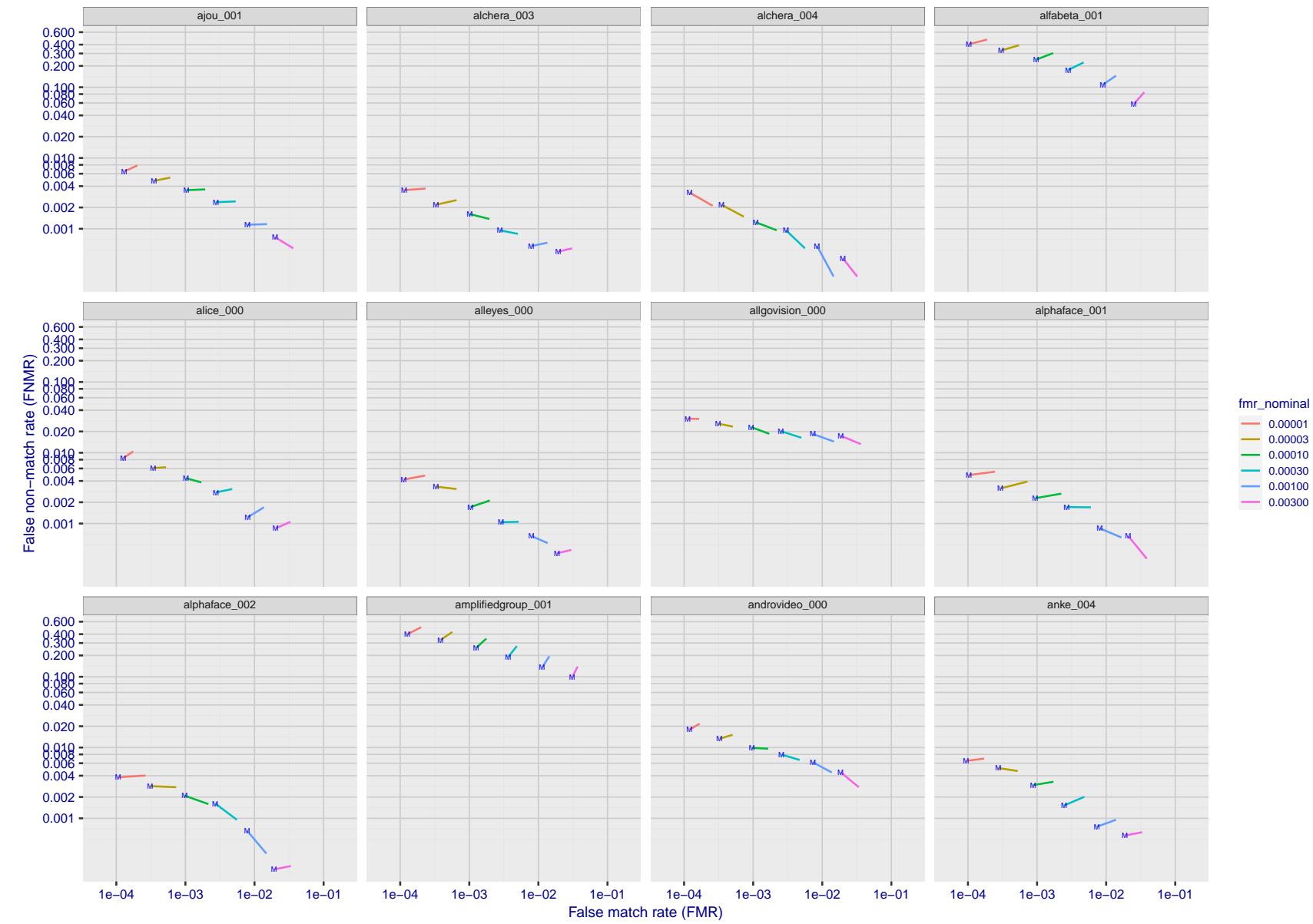


Figure 183: For the visa images, FNMR and FMR at six operating points along the DET characteristic. At each point a line is drawn between $(FMR, FNMR)_{MALE}$ and $(FMR, FNMR)_{FEMALE}$ showing how which sex has lower FMR and/or FNMR. The "M" label denotes male, the other end of the line corresponds to female. The six operating thresholds are selected to give the nominal false match rates given in the legend, and are computed over all impostor pairs regardless of age, sex, and place of birth. The plotted FMR values are broadly an order of magnitude larger than the nominal rates because FMR is computed over demographically-matched impostor pairs i.e individuals of the same sex, from the same geographic region (see section 3.6.1), and the same age group (see section 3.6.2).

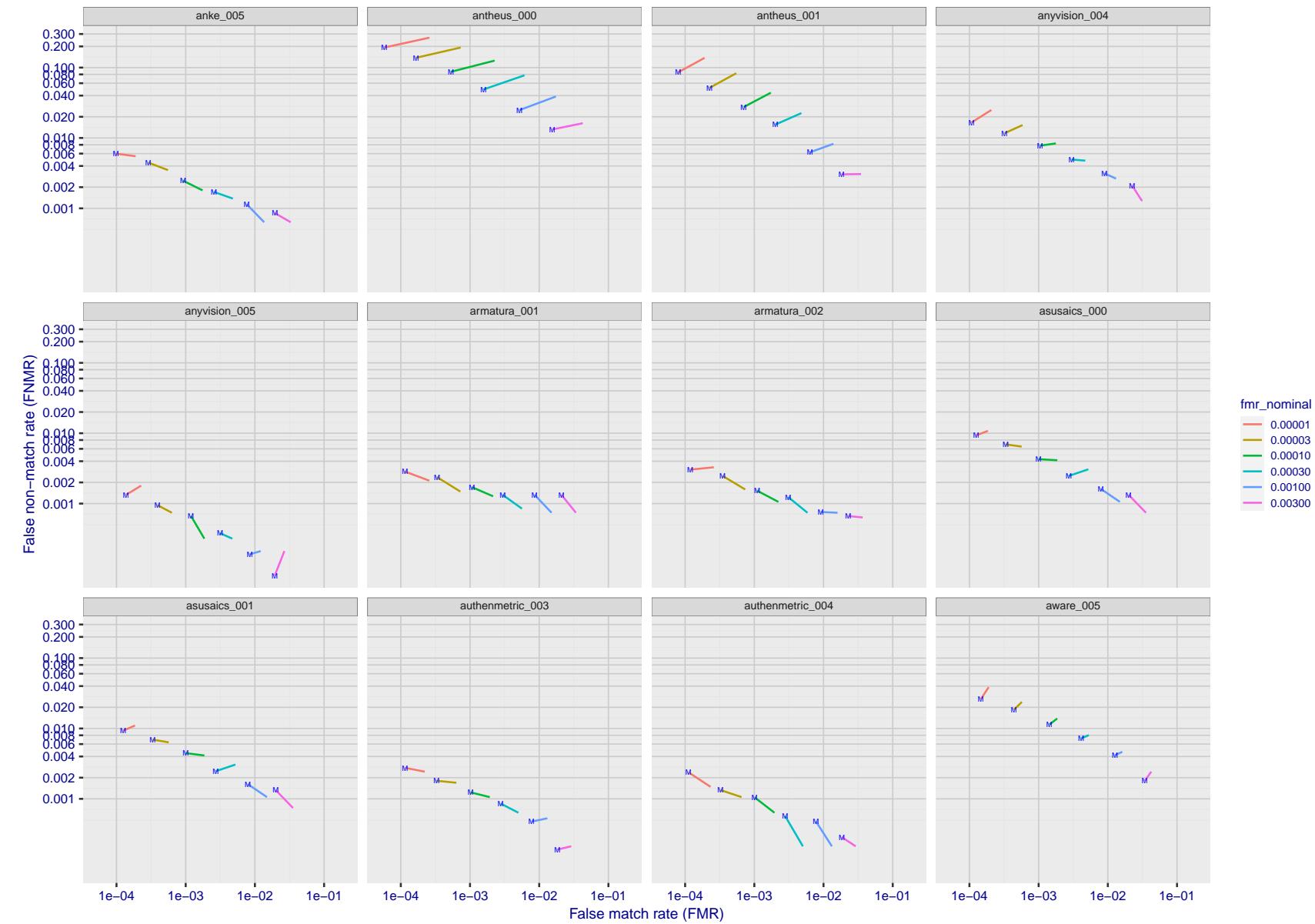


Figure 184: For the visa images, FNMR and FMR at six operating points along the DET characteristic. At each point a line is drawn between $(FMR, FNMR)_{MALE}$ and $(FMR, FNMR)_{FEMALE}$ showing how which sex has lower FMR and/or FNMR. The "M" label denotes male, the other end of the line corresponds to female. The six operating thresholds are selected to give the nominal false match rates given in the legend, and are computed over all impostor pairs regardless of age, sex, and place of birth. The plotted FMR values are broadly an order of magnitude larger than the nominal rates because FMR is computed over demographically-matched impostor pairs i.e individuals of the same sex, from the same geographic region (see section 3.6.1), and the same age group (see section 3.6.2).

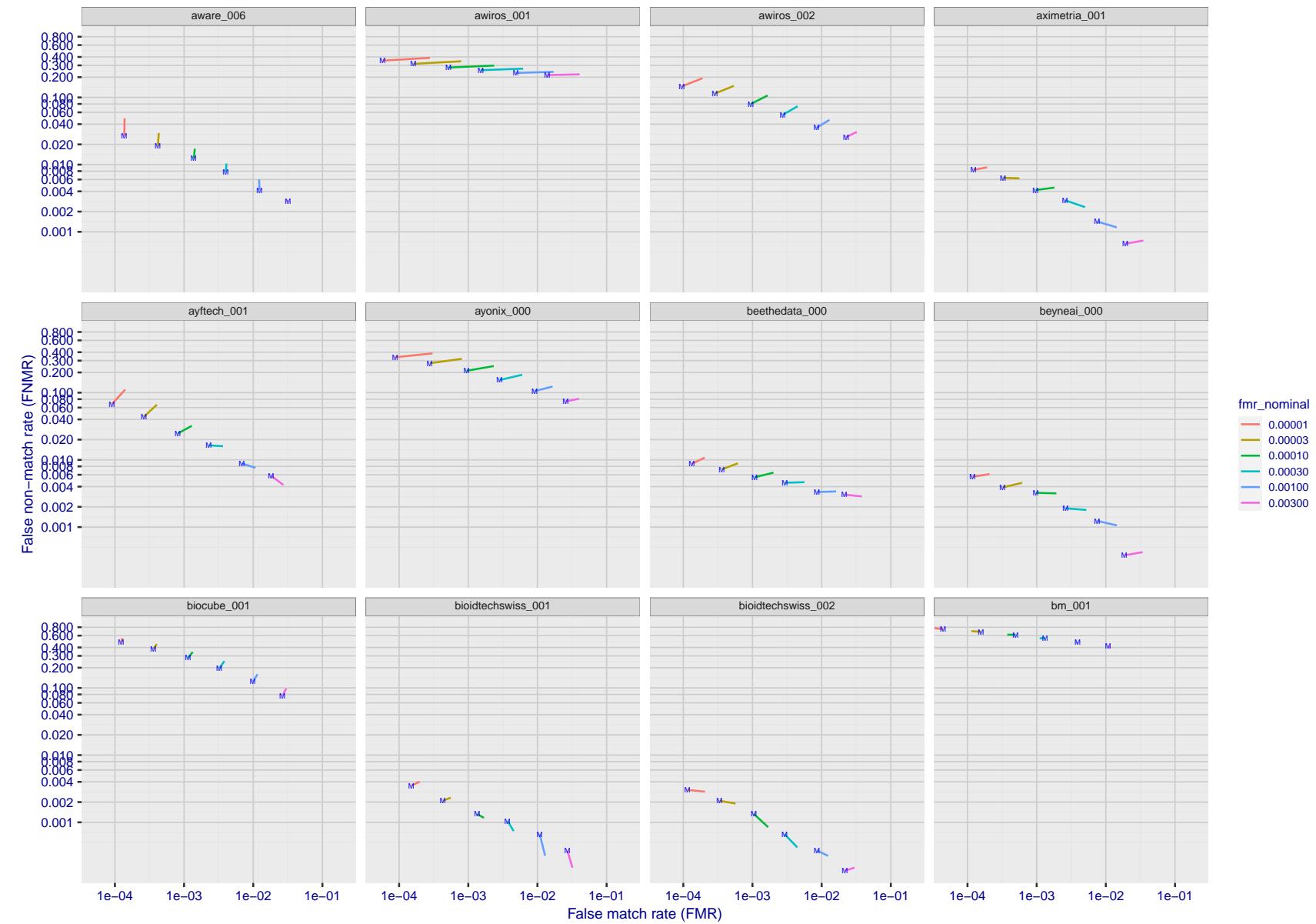


Figure 185: For the visa images, FNMR and FMR at six operating points along the DET characteristic. At each point a line is drawn between $(FMR, FNMR)_{MALE}$ and $(FMR, FNMR)_{FEMALE}$ showing how which sex has lower FMR and/or FNMR. The "M" label denotes male, the other end of the line corresponds to female. The six operating thresholds are selected to give the nominal false match rates given in the legend, and are computed over all impostor pairs regardless of age, sex, and place of birth. The plotted FMR values are broadly an order of magnitude larger than the nominal rates because FMR is computed over demographically-matched impostor pairs i.e individuals of the same sex, from the same geographic region (see section 3.6.1), and the same age group (see section 3.6.2).

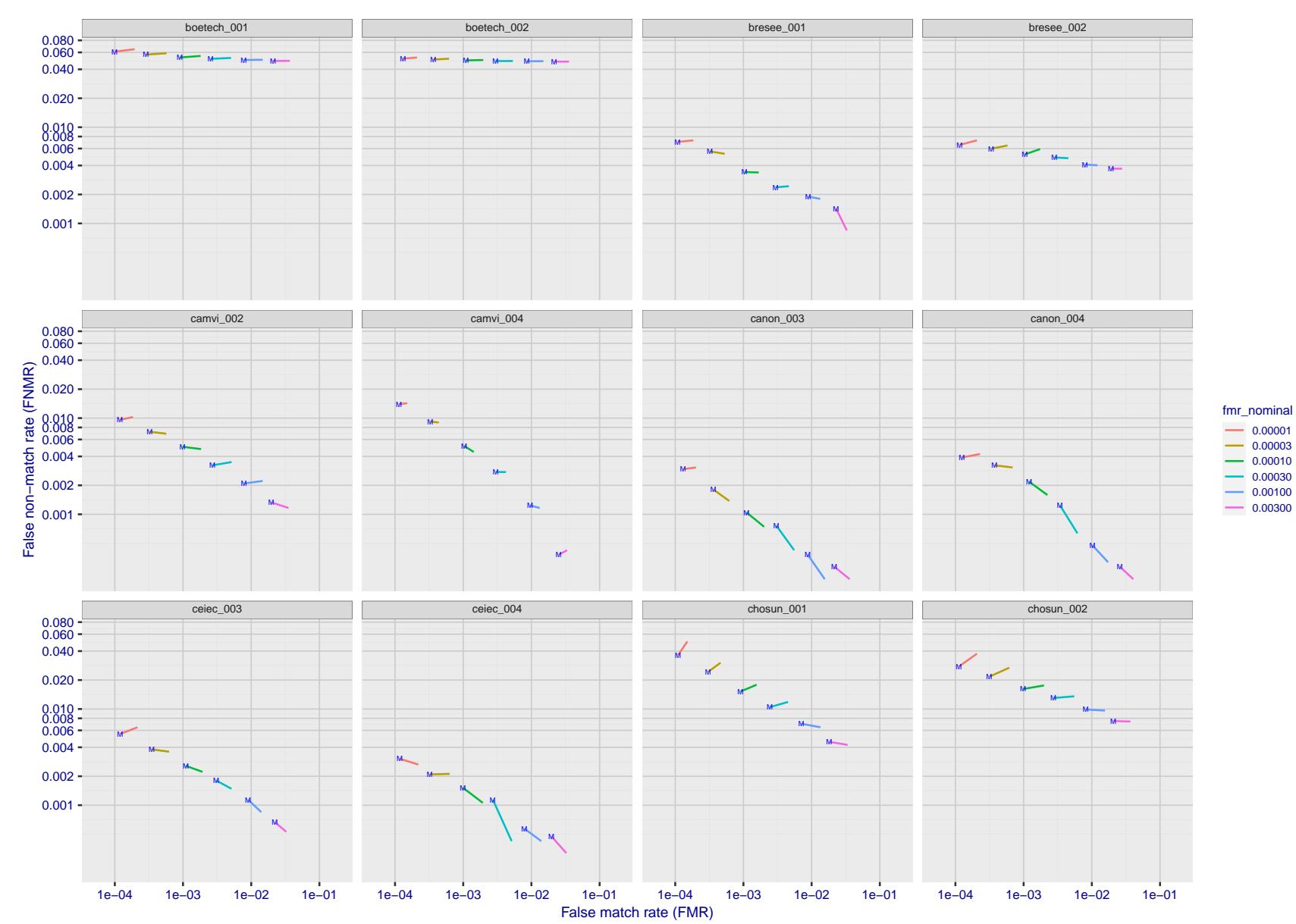


Figure 186: For the visa images, FNMR and FMR at six operating points along the DET characteristic. At each point a line is drawn between $(FMR, FNMR)_{MALE}$ and $(FMR, FNMR)_{FEMALE}$ showing how which sex has lower FMR and/or FNMR. The "M" label denotes male, the other end of the line corresponds to female. The six operating thresholds are selected to give the nominal false match rates given in the legend, and are computed over all impostor pairs regardless of age, sex, and place of birth. The plotted FMR values are broadly an order of magnitude larger than the nominal rates because FMR is computed over demographically-matched impostor pairs i.e individuals of the same sex, from the same geographic region (see section 3.6.1), and the same age group (see section 3.6.2).

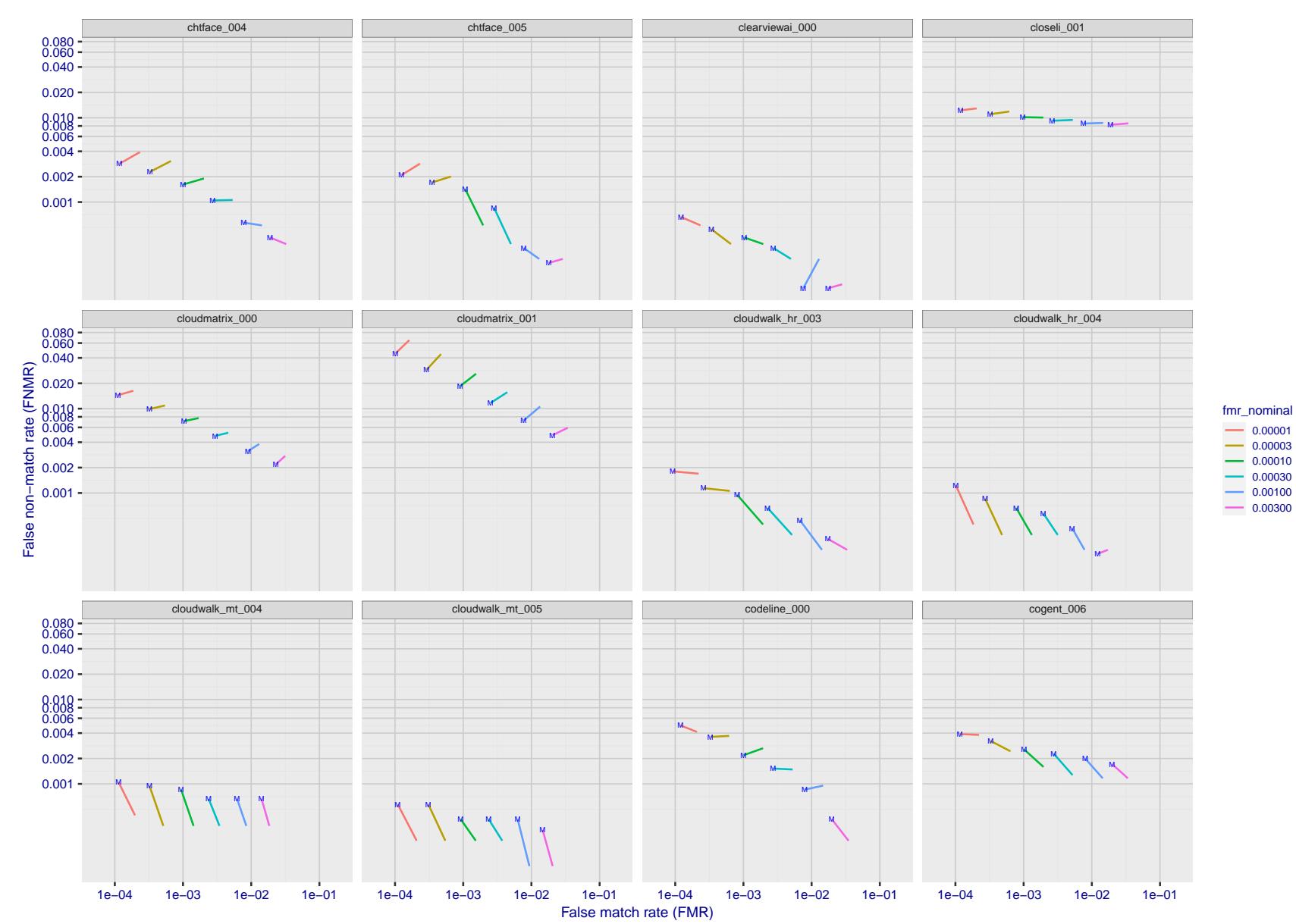


Figure 187: For the visa images, FNMR and FMR at six operating points along the DET characteristic. At each point a line is drawn between $(FMR, FNMR)_{MALE}$ and $(FMR, FNMR)_{FEMALE}$ showing how which sex has lower FMR and/or FNMR. The "M" label denotes male, the other end of the line corresponds to female. The six operating thresholds are selected to give the nominal false match rates given in the legend, and are computed over all impostor pairs regardless of age, sex, and place of birth. The plotted FMR values are broadly an order of magnitude larger than the nominal rates because FMR is computed over demographically-matched impostor pairs i.e individuals of the same sex, from the same geographic region (see section 3.6.1), and the same age group (see section 3.6.2).

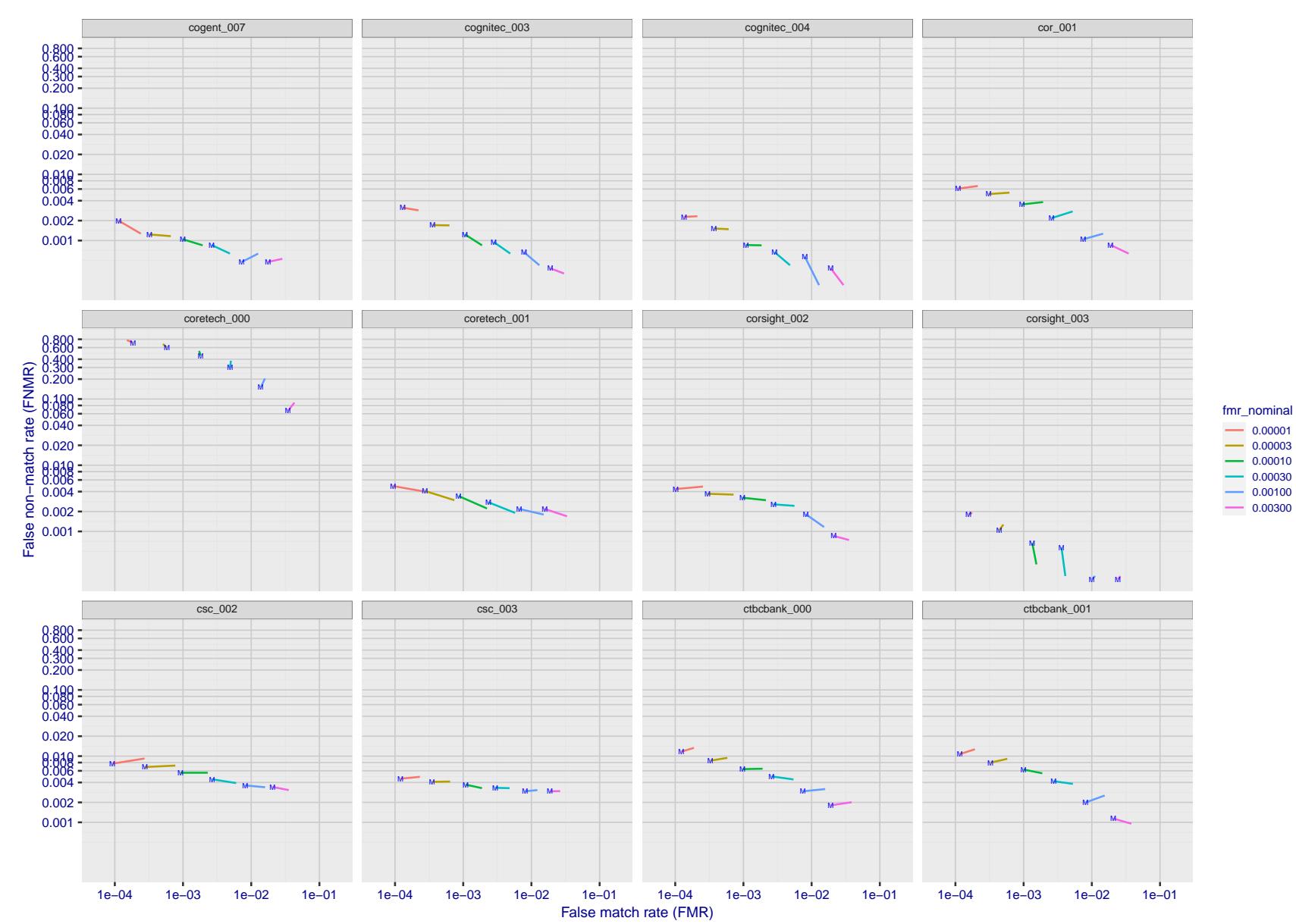


Figure 188: For the visa images, FNMR and FMR at six operating points along the DET characteristic. At each point a line is drawn between $(FMR, FNMR)_{MALE}$ and $(FMR, FNMR)_{FEMALE}$ showing how which sex has lower FMR and/or FNMR. The "M" label denotes male, the other end of the line corresponds to female. The six operating thresholds are selected to give the nominal false match rates given in the legend, and are computed over all impostor pairs regardless of age, sex, and place of birth. The plotted FMR values are broadly an order of magnitude larger than the nominal rates because FMR is computed over demographically-matched impostor pairs i.e individuals of the same sex, from the same geographic region (see section 3.6.1), and the same age group (see section 3.6.2).

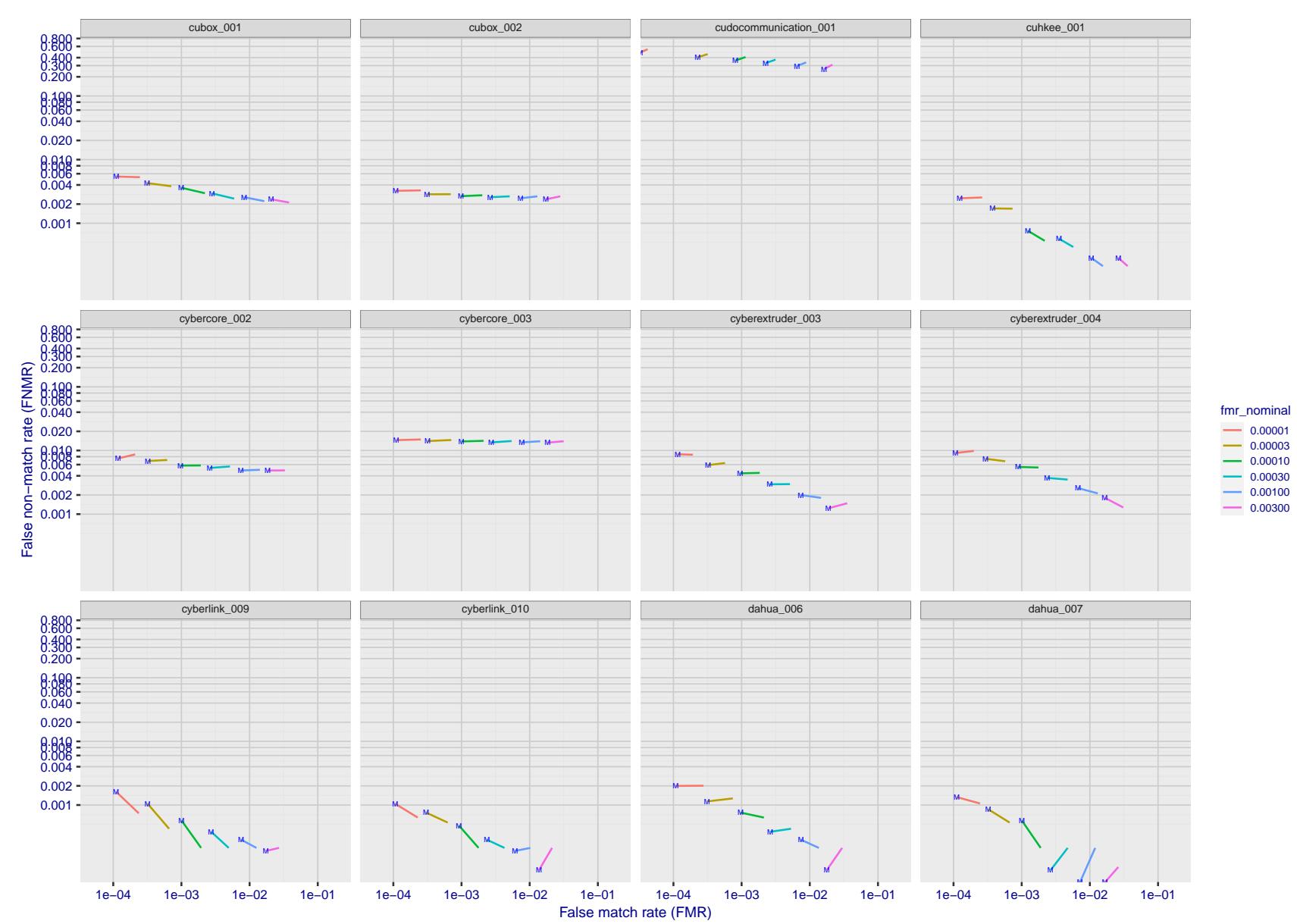


Figure 189: For the visa images, FNMR and FMR at six operating points along the DET characteristic. At each point a line is drawn between $(FMR, FNMR)_{MALE}$ and $(FMR, FNMR)_{FEMALE}$ showing how which sex has lower FMR and/or FNMR. The "M" label denotes male, the other end of the line corresponds to female. The six operating thresholds are selected to give the nominal false match rates given in the legend, and are computed over all impostor pairs regardless of age, sex, and place of birth. The plotted FMR values are broadly an order of magnitude larger than the nominal rates because FMR is computed over demographically-matched impostor pairs i.e individuals of the same sex, from the same geographic region (see section 3.6.1), and the same age group (see section 3.6.2).

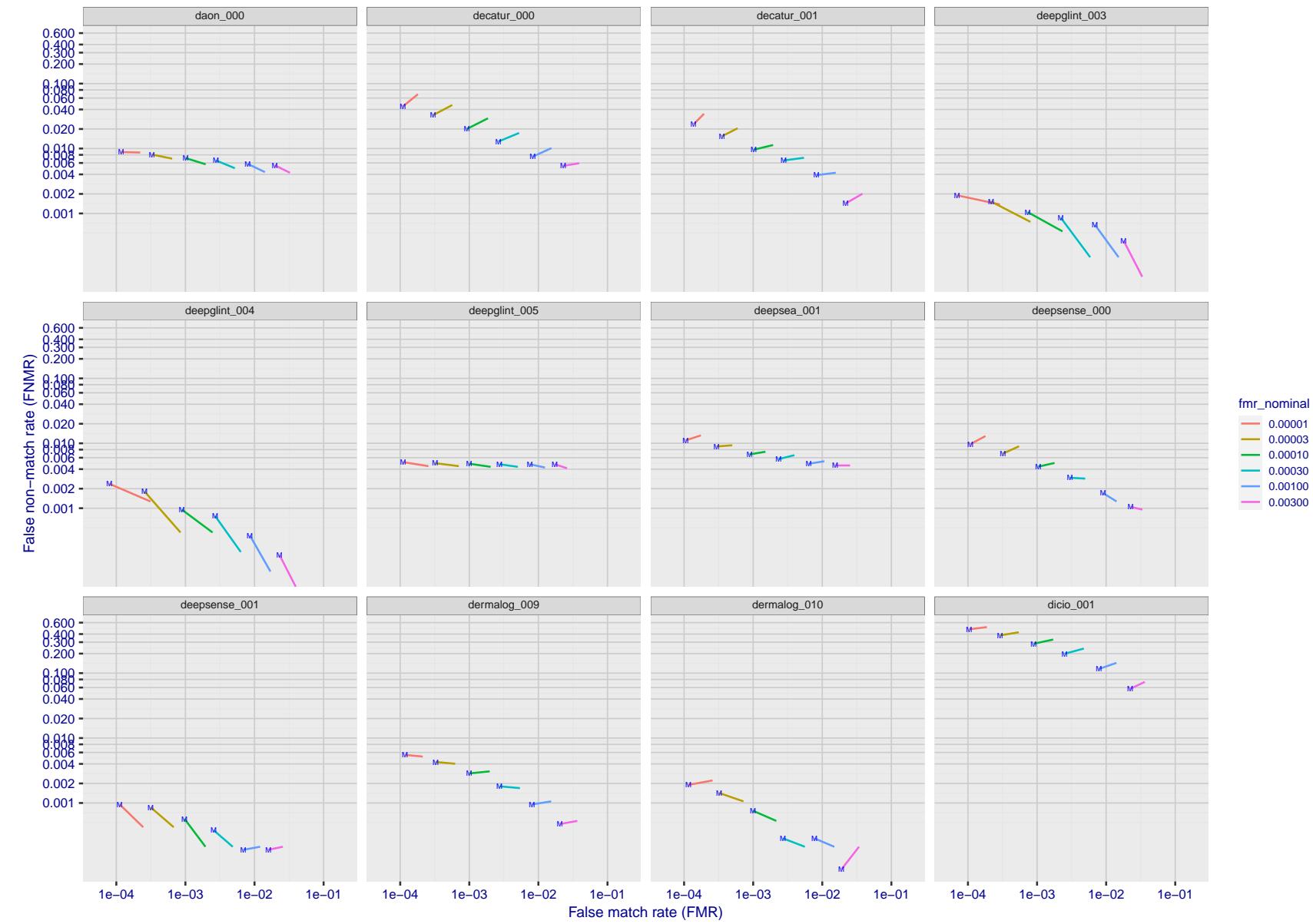


Figure 190: For the visa images, FNMR and FMR at six operating points along the DET characteristic. At each point a line is drawn between $(FMR, FNMR)_{MALE}$ and $(FMR, FNMR)_{FEMALE}$ showing how which sex has lower FMR and/or FNMR. The "M" label denotes male, the other end of the line corresponds to female. The six operating thresholds are selected to give the nominal false match rates given in the legend, and are computed over all impostor pairs regardless of age, sex, and place of birth. The plotted FMR values are broadly an order of magnitude larger than the nominal rates because FMR is computed over demographically-matched impostor pairs i.e individuals of the same sex, from the same geographic region (see section 3.6.1), and the same age group (see section 3.6.2).

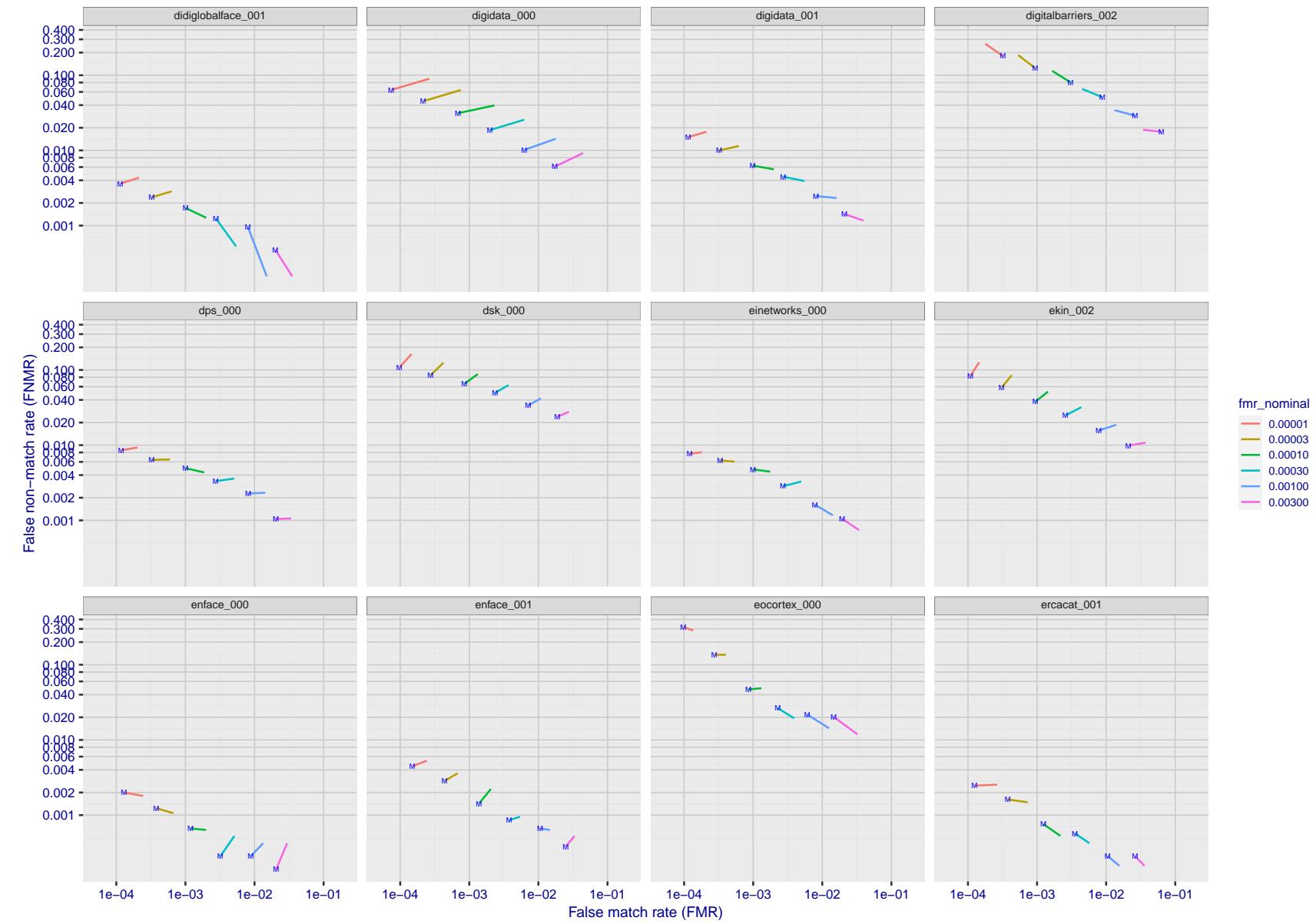


Figure 191: For the visa images, FNMR and FMR at six operating points along the DET characteristic. At each point a line is drawn between $(FMR, FNMR)_{MALE}$ and $(FMR, FNMR)_{FEMALE}$ showing how which sex has lower FMR and/or FNMR. The "M" label denotes male, the other end of the line corresponds to female. The six operating thresholds are selected to give the nominal false match rates given in the legend, and are computed over all impostor pairs regardless of age, sex, and place of birth. The plotted FMR values are broadly an order of magnitude larger than the nominal rates because FMR is computed over demographically-matched impostor pairs i.e individuals of the same sex, from the same geographic region (see section 3.6.1), and the same age group (see section 3.6.2).

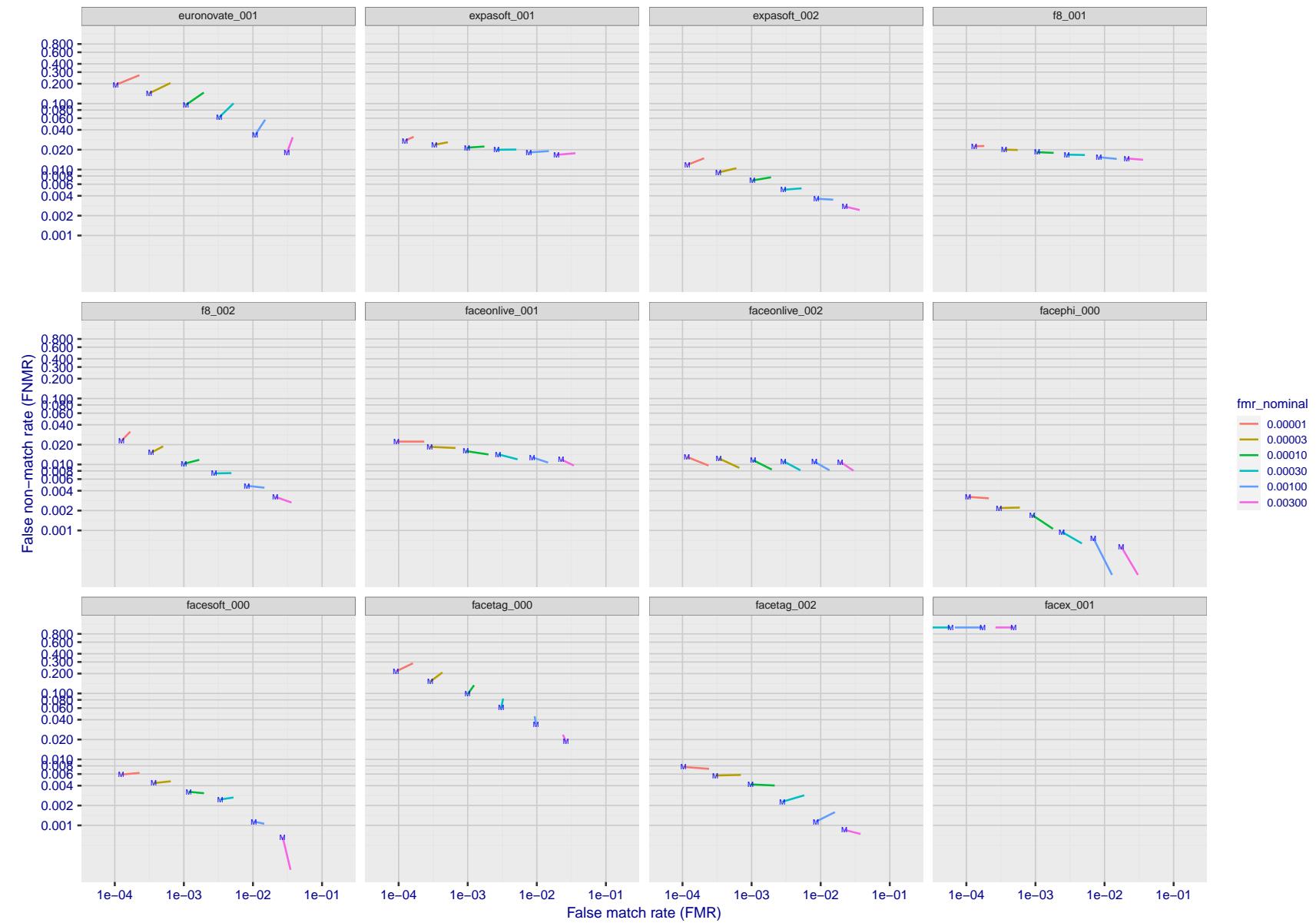


Figure 192: For the visa images, FNMR and FMR at six operating points along the DET characteristic. At each point a line is drawn between $(FMR, FNMR)_{MALE}$ and $(FMR, FNMR)_{FEMALE}$ showing how which sex has lower FMR and/or FNMR. The "M" label denotes male, the other end of the line corresponds to female. The six operating thresholds are selected to give the nominal false match rates given in the legend, and are computed over all impostor pairs regardless of age, sex, and place of birth. The plotted FMR values are broadly an order of magnitude larger than the nominal rates because FMR is computed over demographically-matched impostor pairs i.e individuals of the same sex, from the same geographic region (see section 3.6.1), and the same age group (see section 3.6.2).

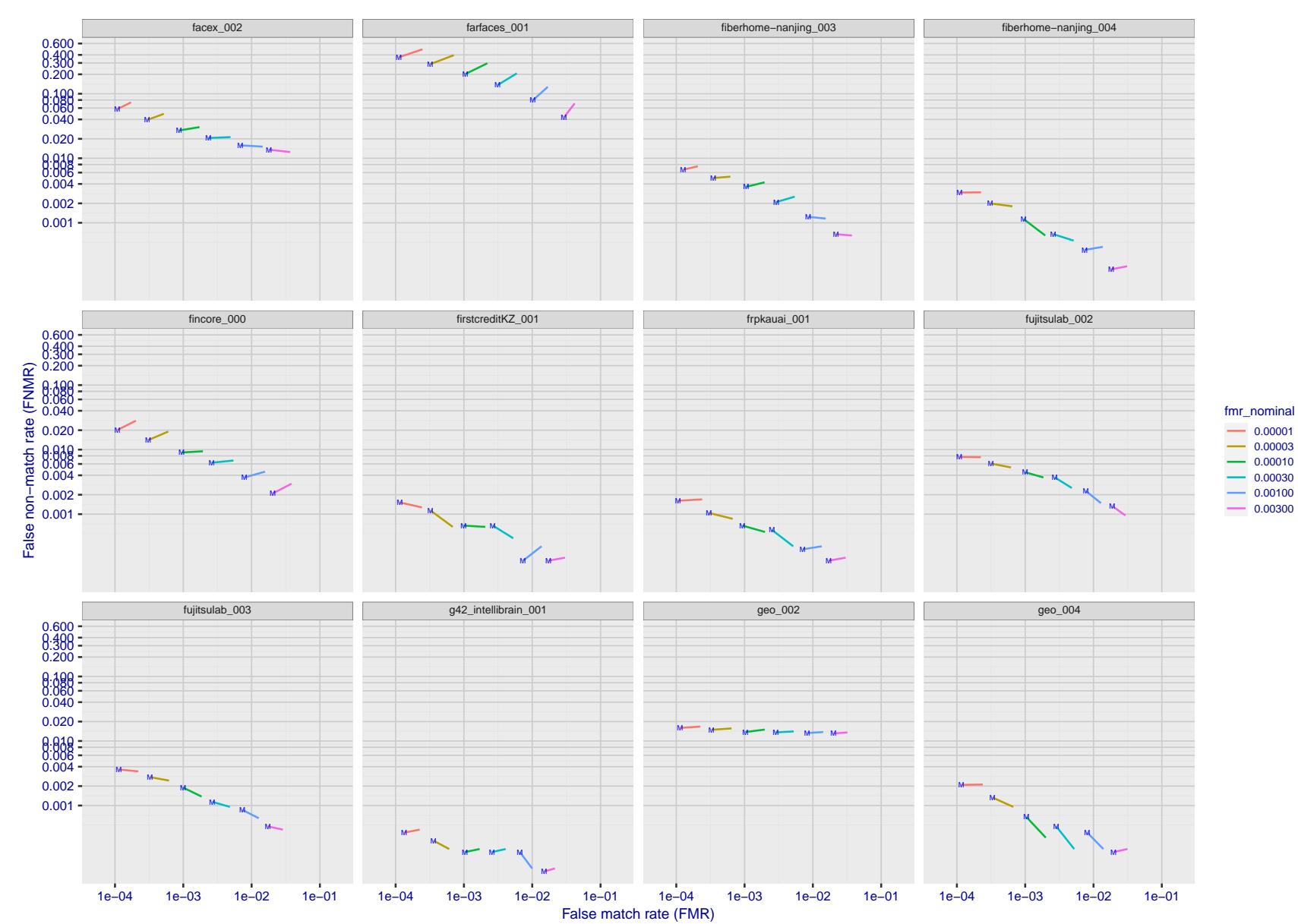


Figure 193: For the visa images, FNMR and FMR at six operating points along the DET characteristic. At each point a line is drawn between $(FMR, FNMR)_{MALE}$ and $(FMR, FNMR)_{FEMALE}$ showing how which sex has lower FMR and/or FNMR. The "M" label denotes male, the other end of the line corresponds to female. The six operating thresholds are selected to give the nominal false match rates given in the legend, and are computed over all impostor pairs regardless of age, sex, and place of birth. The plotted FMR values are broadly an order of magnitude larger than the nominal rates because FMR is computed over demographically-matched impostor pairs i.e individuals of the same sex, from the same geographic region (see section 3.6.1), and the same age group (see section 3.6.2).

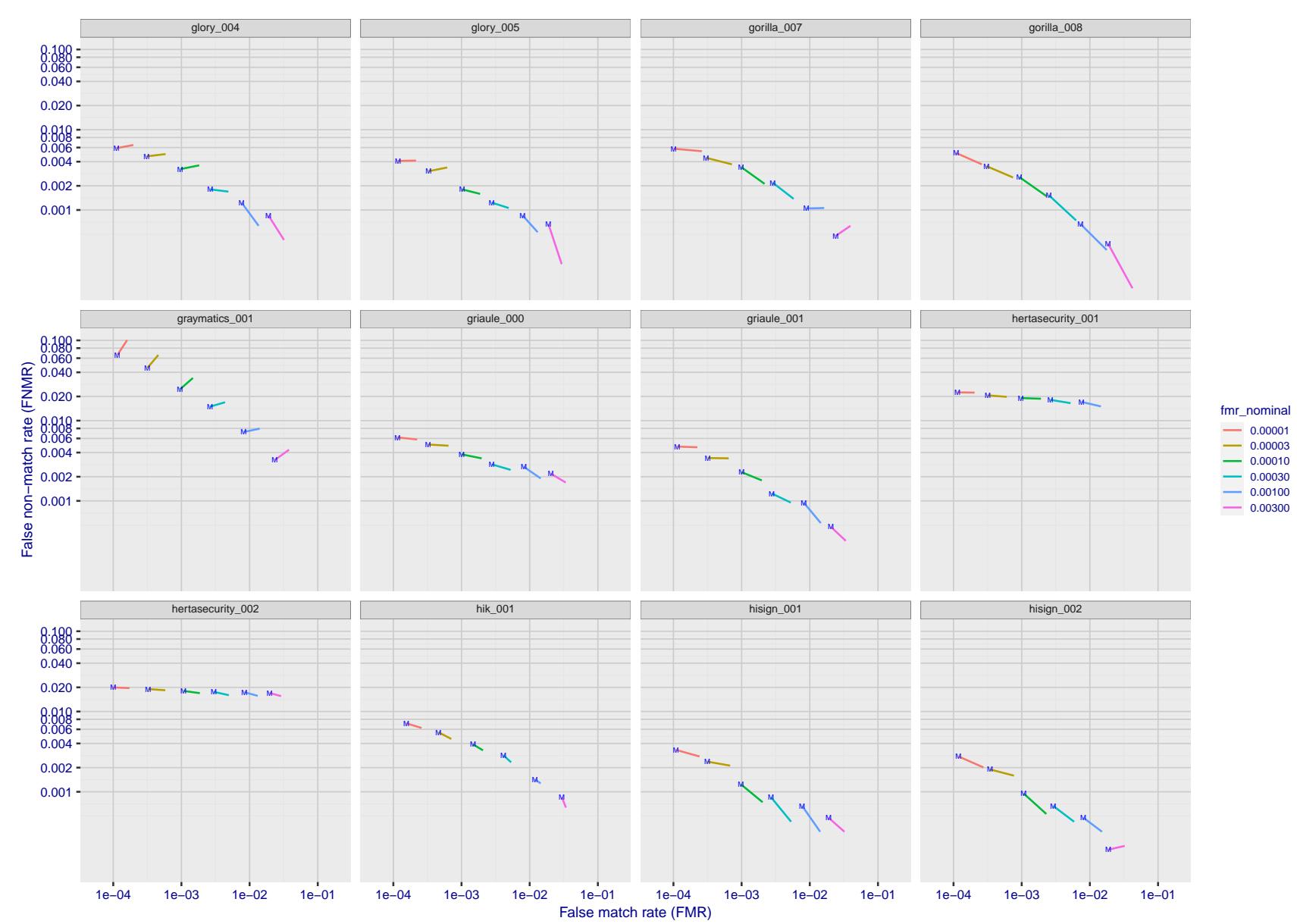


Figure 194: For the visa images, FNMR and FMR at six operating points along the DET characteristic. At each point a line is drawn between $(FMR, FNMR)_{MALE}$ and $(FMR, FNMR)_{FEMALE}$ showing how which sex has lower FMR and/or FNMR. The "M" label denotes male, the other end of the line corresponds to female. The six operating thresholds are selected to give the nominal false match rates given in the legend, and are computed over all impostor pairs regardless of age, sex, and place of birth. The plotted FMR values are broadly an order of magnitude larger than the nominal rates because FMR is computed over demographically-matched impostor pairs i.e individuals of the same sex, from the same geographic region (see section 3.6.1), and the same age group (see section 3.6.2).

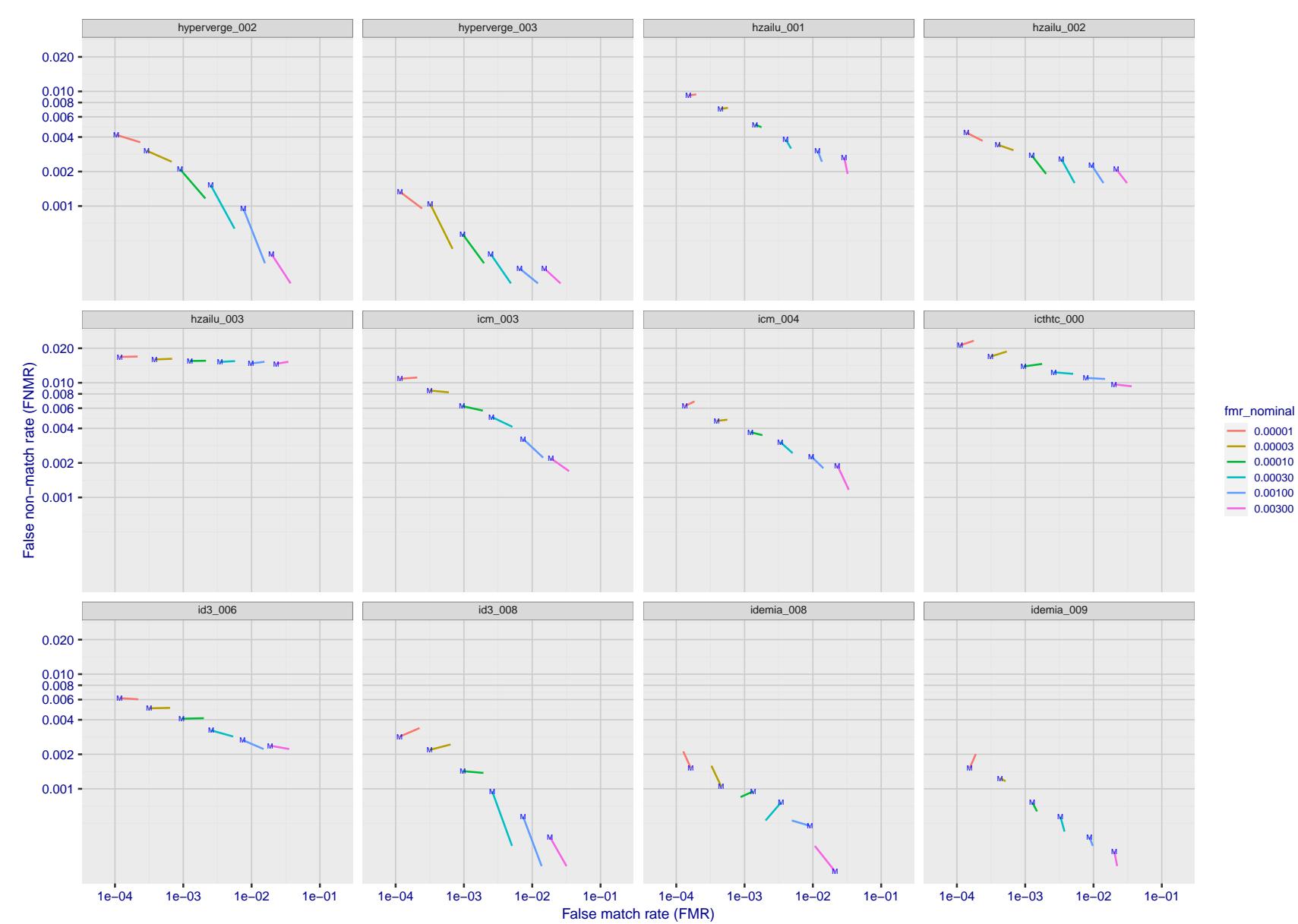


Figure 195: For the visa images, FNMR and FMR at six operating points along the DET characteristic. At each point a line is drawn between $(FMR, FNMR)_{MALE}$ and $(FMR, FNMR)_{FEMALE}$ showing how which sex has lower FMR and/or FNMR. The "M" label denotes male, the other end of the line corresponds to female. The six operating thresholds are selected to give the nominal false match rates given in the legend, and are computed over all impostor pairs regardless of age, sex, and place of birth. The plotted FMR values are broadly an order of magnitude larger than the nominal rates because FMR is computed over demographically-matched impostor pairs i.e individuals of the same sex, from the same geographic region (see section 3.6.1), and the same age group (see section 3.6.2).

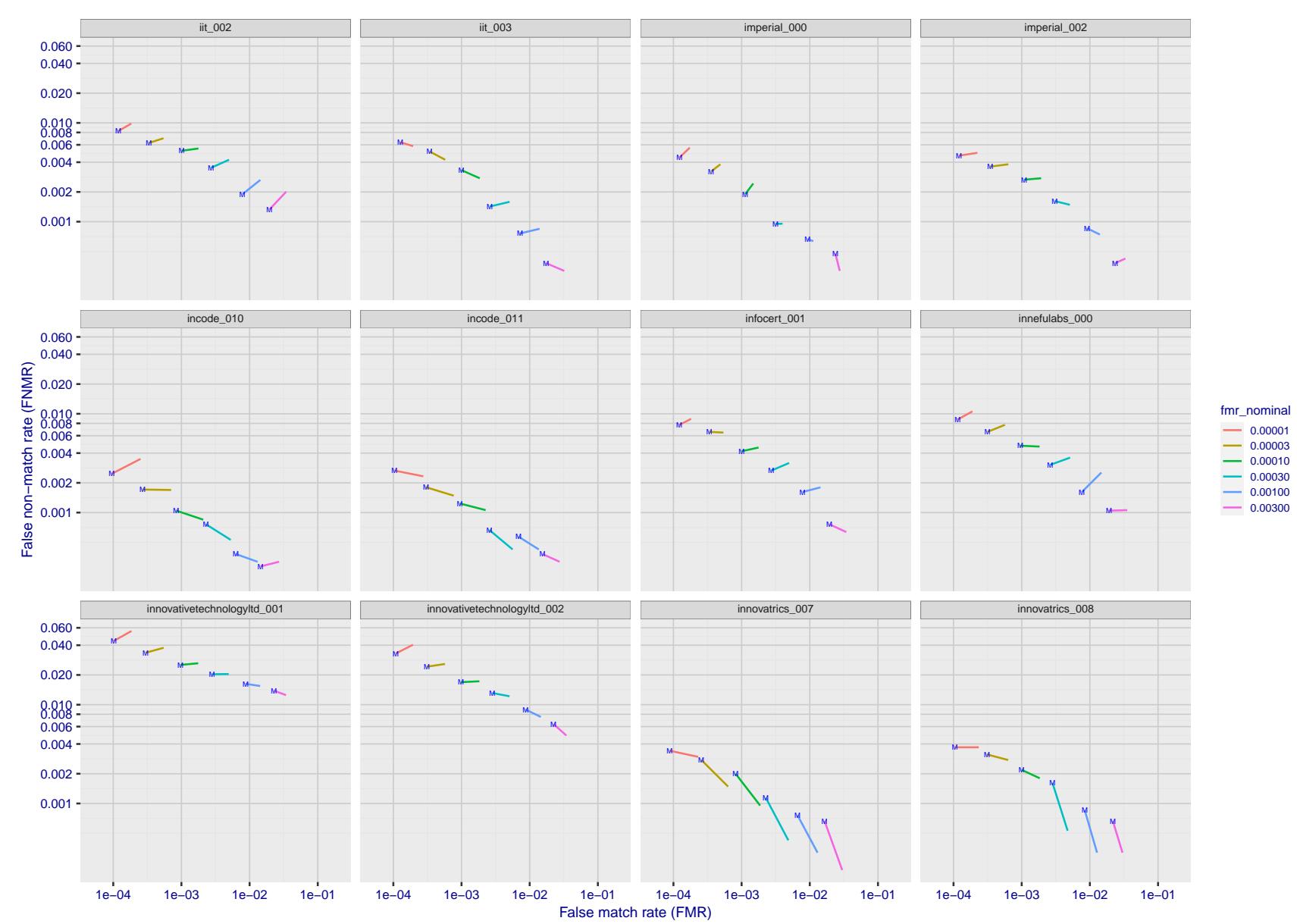


Figure 196: For the visa images, FNMR and FMR at six operating points along the DET characteristic. At each point a line is drawn between $(FMR, FNMR)_{MALE}$ and $(FMR, FNMR)_{FEMALE}$ showing how which sex has lower FMR and/or FNMR. The "M" label denotes male, the other end of the line corresponds to female. The six operating thresholds are selected to give the nominal false match rates given in the legend, and are computed over all impostor pairs regardless of age, sex, and place of birth. The plotted FMR values are broadly an order of magnitude larger than the nominal rates because FMR is computed over demographically-matched impostor pairs i.e individuals of the same sex, from the same geographic region (see section 3.6.1), and the same age group (see section 3.6.2).

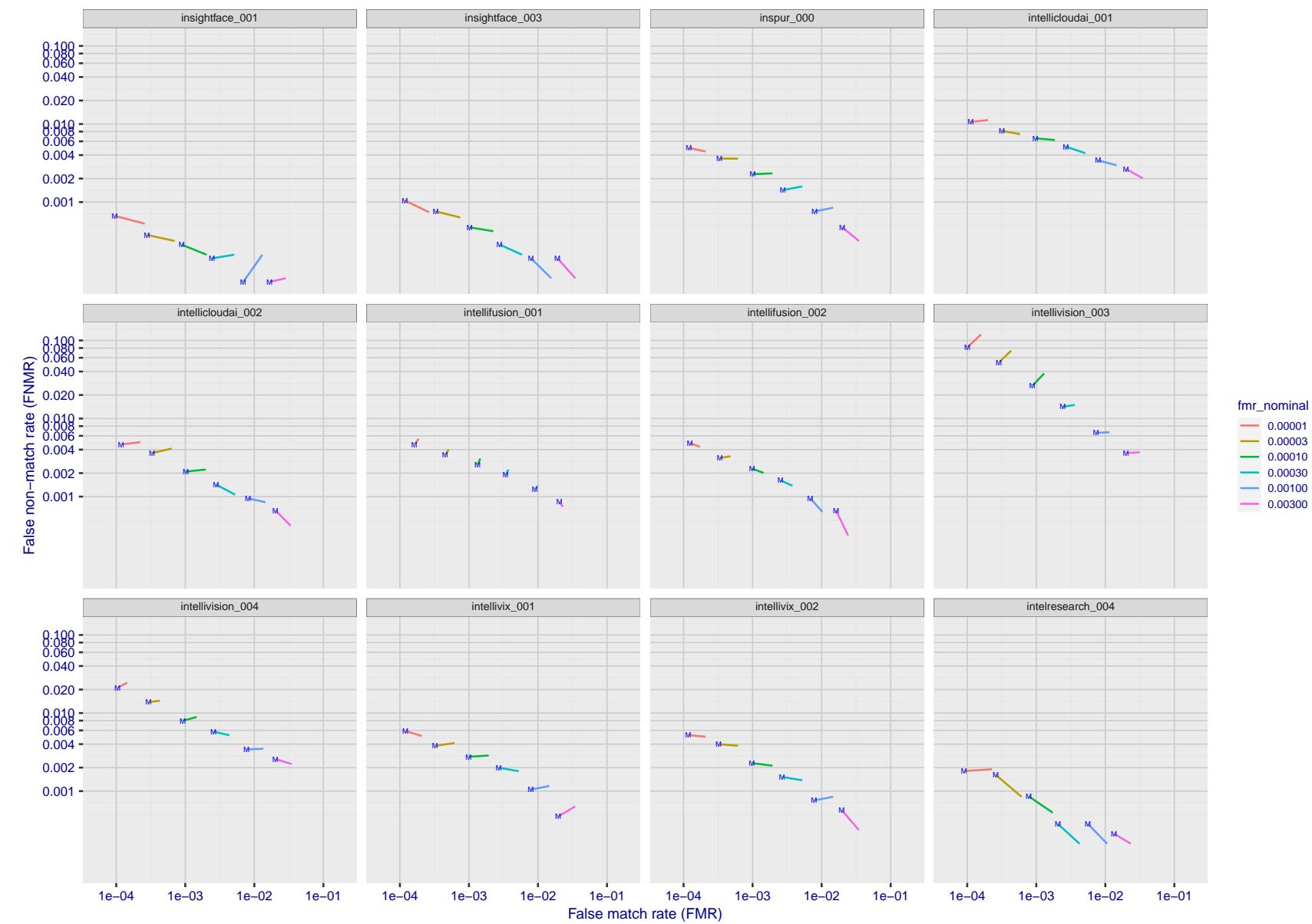


Figure 197: For the visa images, FNMR and FMR at six operating points along the DET characteristic. At each point a line is drawn between $(FMR, FNMR)_{MALE}$ and $(FMR, FNMR)_{FEMALE}$ showing how which sex has lower FMR and/or FNMR. The "M" label denotes male, the other end of the line corresponds to female. The six operating thresholds are selected to give the nominal false match rates given in the legend, and are computed over all impostor pairs regardless of age, sex, and place of birth. The plotted FMR values are broadly an order of magnitude larger than the nominal rates because FMR is computed over demographically-matched impostor pairs i.e individuals of the same sex, from the same geographic region (see section 3.6.1), and the same age group (see section 3.6.2).

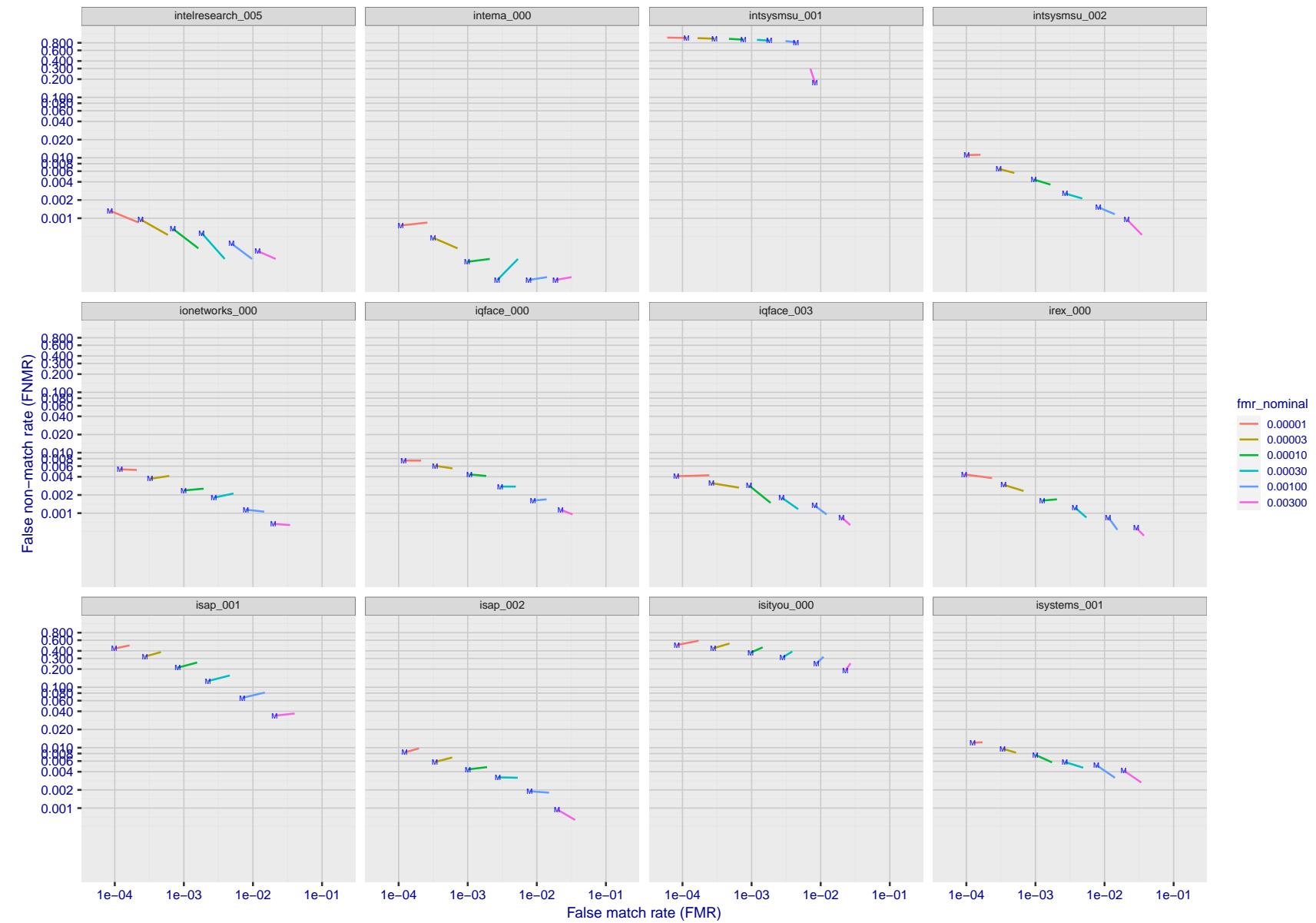


Figure 198: For the visa images, FNMR and FMR at six operating points along the DET characteristic. At each point a line is drawn between $(FMR, FNMR)_{MALE}$ and $(FMR, FNMR)_{FEMALE}$ showing how which sex has lower FMR and/or FNMR. The "M" label denotes male, the other end of the line corresponds to female. The six operating thresholds are selected to give the nominal false match rates given in the legend, and are computed over all impostor pairs regardless of age, sex, and place of birth. The plotted FMR values are broadly an order of magnitude larger than the nominal rates because FMR is computed over demographically-matched impostor pairs i.e individuals of the same sex, from the same geographic region (see section 3.6.1), and the same age group (see section 3.6.2).

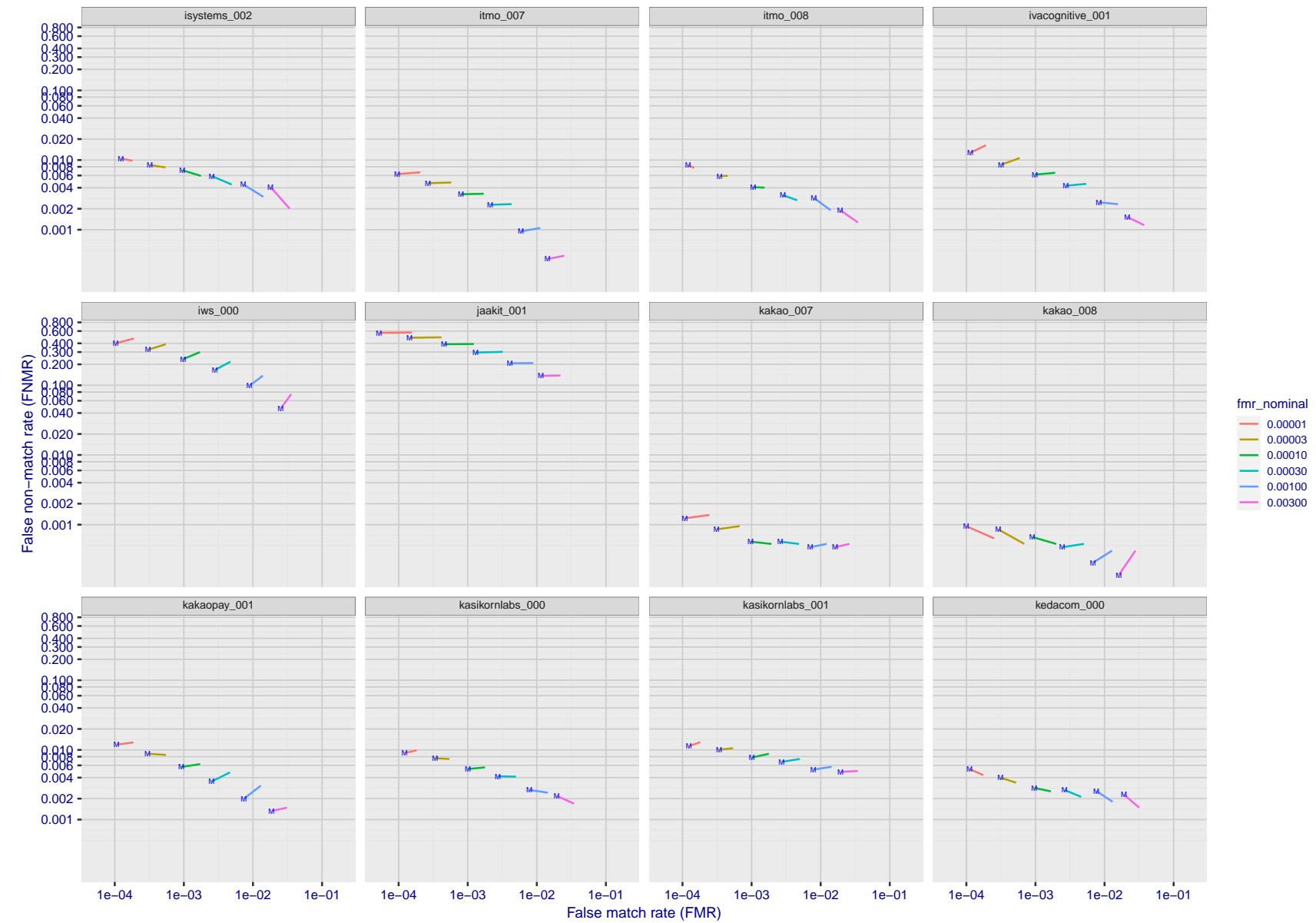


Figure 199: For the visa images, FNMR and FMR at six operating points along the DET characteristic. At each point a line is drawn between $(FMR, FNMR)_{MALE}$ and $(FMR, FNMR)_{FEMALE}$ showing how which sex has lower FMR and/or FNMR. The "M" label denotes male, the other end of the line corresponds to female. The six operating thresholds are selected to give the nominal false match rates given in the legend, and are computed over all impostor pairs regardless of age, sex, and place of birth. The plotted FMR values are broadly an order of magnitude larger than the nominal rates because FMR is computed over demographically-matched impostor pairs i.e individuals of the same sex, from the same geographic region (see section 3.6.1), and the same age group (see section 3.6.2).

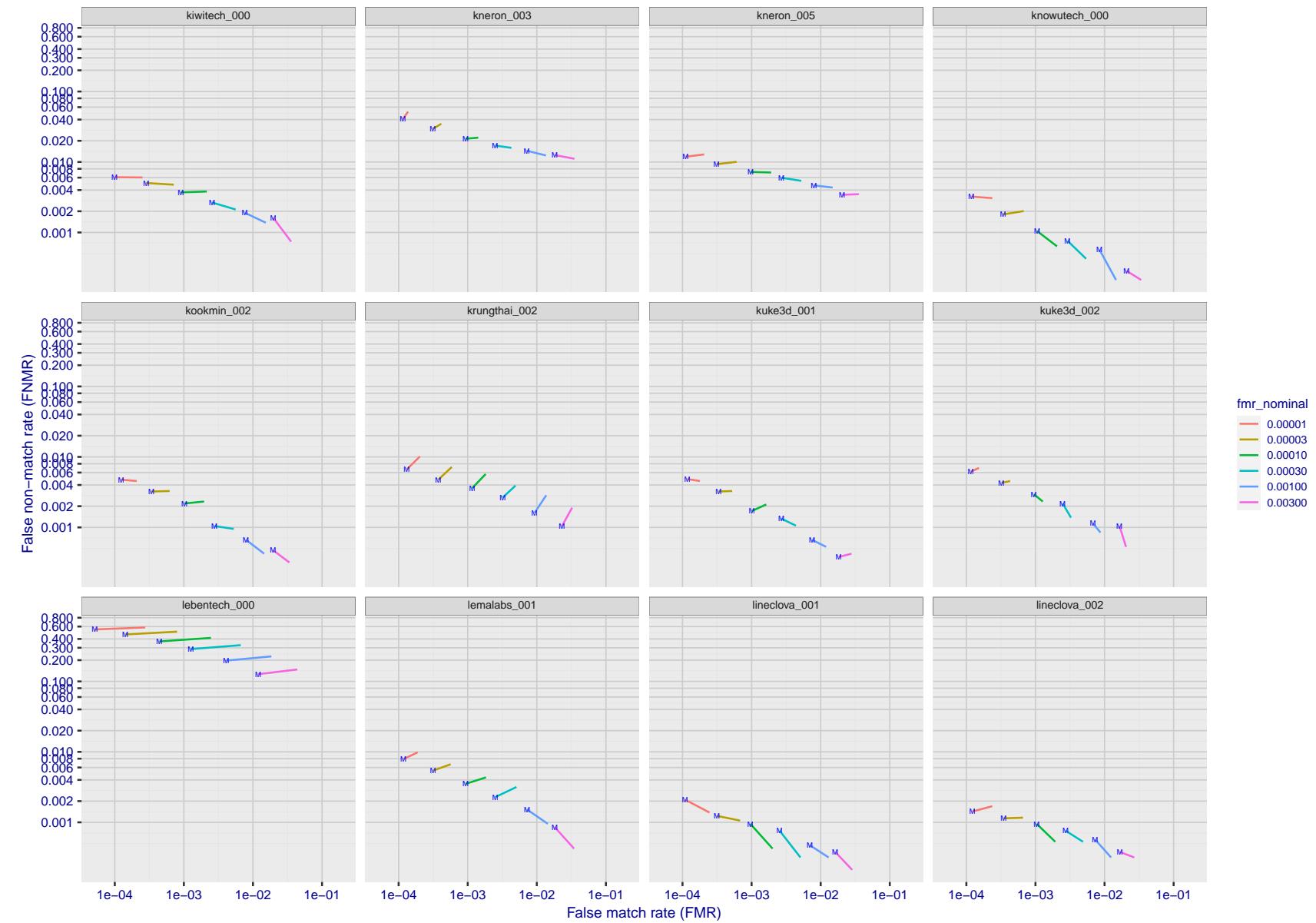


Figure 200: For the visa images, FNMR and FMR at six operating points along the DET characteristic. At each point a line is drawn between $(FMR, FNMR)_{MALE}$ and $(FMR, FNMR)_{FEMALE}$ showing how which sex has lower FMR and/or FNMR. The "M" label denotes male, the other end of the line corresponds to female. The six operating thresholds are selected to give the nominal false match rates given in the legend, and are computed over all impostor pairs regardless of age, sex, and place of birth. The plotted FMR values are broadly an order of magnitude larger than the nominal rates because FMR is computed over demographically-matched impostor pairs i.e individuals of the same sex, from the same geographic region (see section 3.6.1), and the same age group (see section 3.6.2).

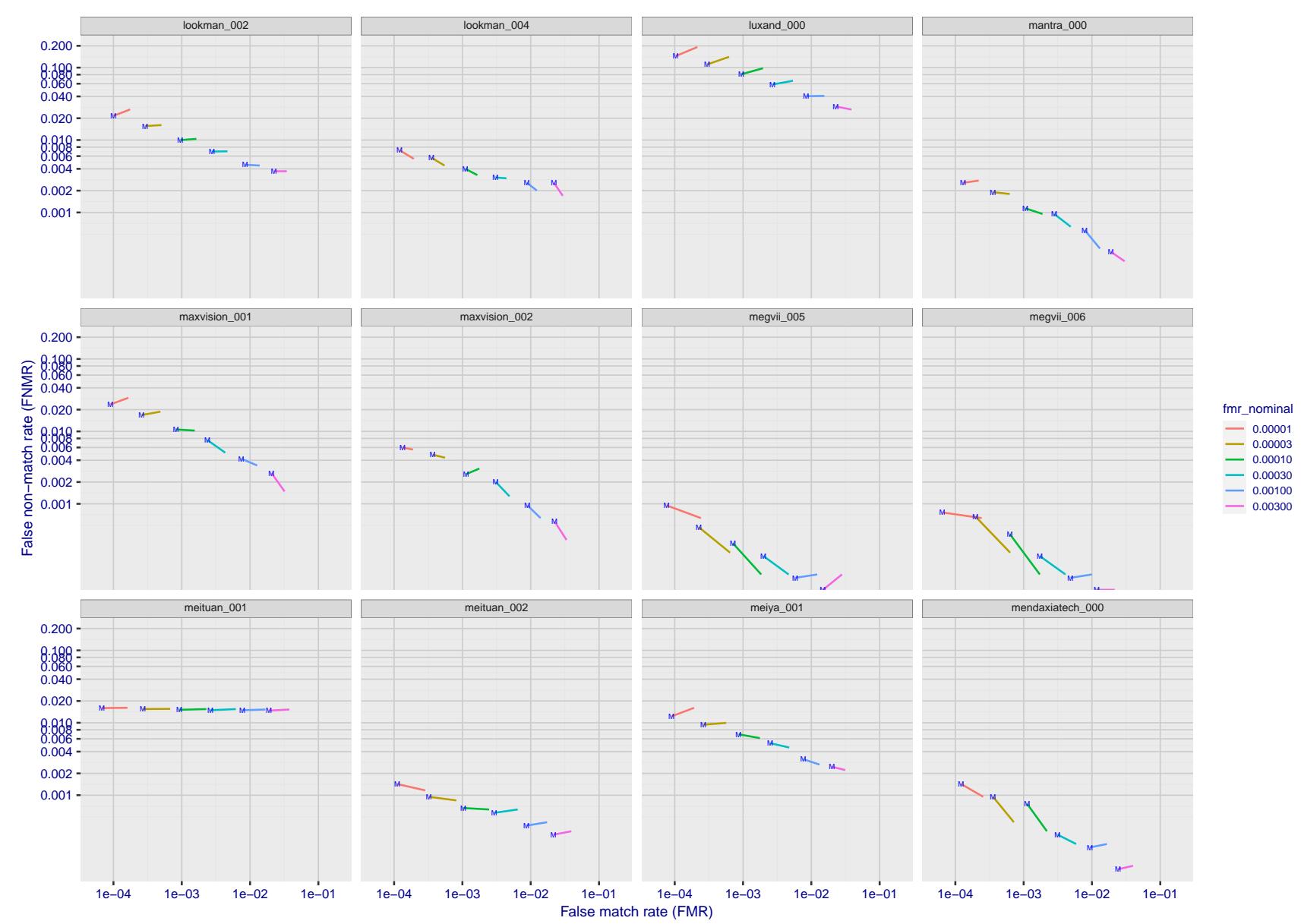


Figure 201: For the visa images, FNMR and FMR at six operating points along the DET characteristic. At each point a line is drawn between $(FMR, FNMR)_{MALE}$ and $(FMR, FNMR)_{FEMALE}$ showing how which sex has lower FMR and/or FNMR. The "M" label denotes male, the other end of the line corresponds to female. The six operating thresholds are selected to give the nominal false match rates given in the legend, and are computed over all impostor pairs regardless of age, sex, and place of birth. The plotted FMR values are broadly an order of magnitude larger than the nominal rates because FMR is computed over demographically-matched impostor pairs i.e individuals of the same sex, from the same geographic region (see section 3.6.1), and the same age group (see section 3.6.2).

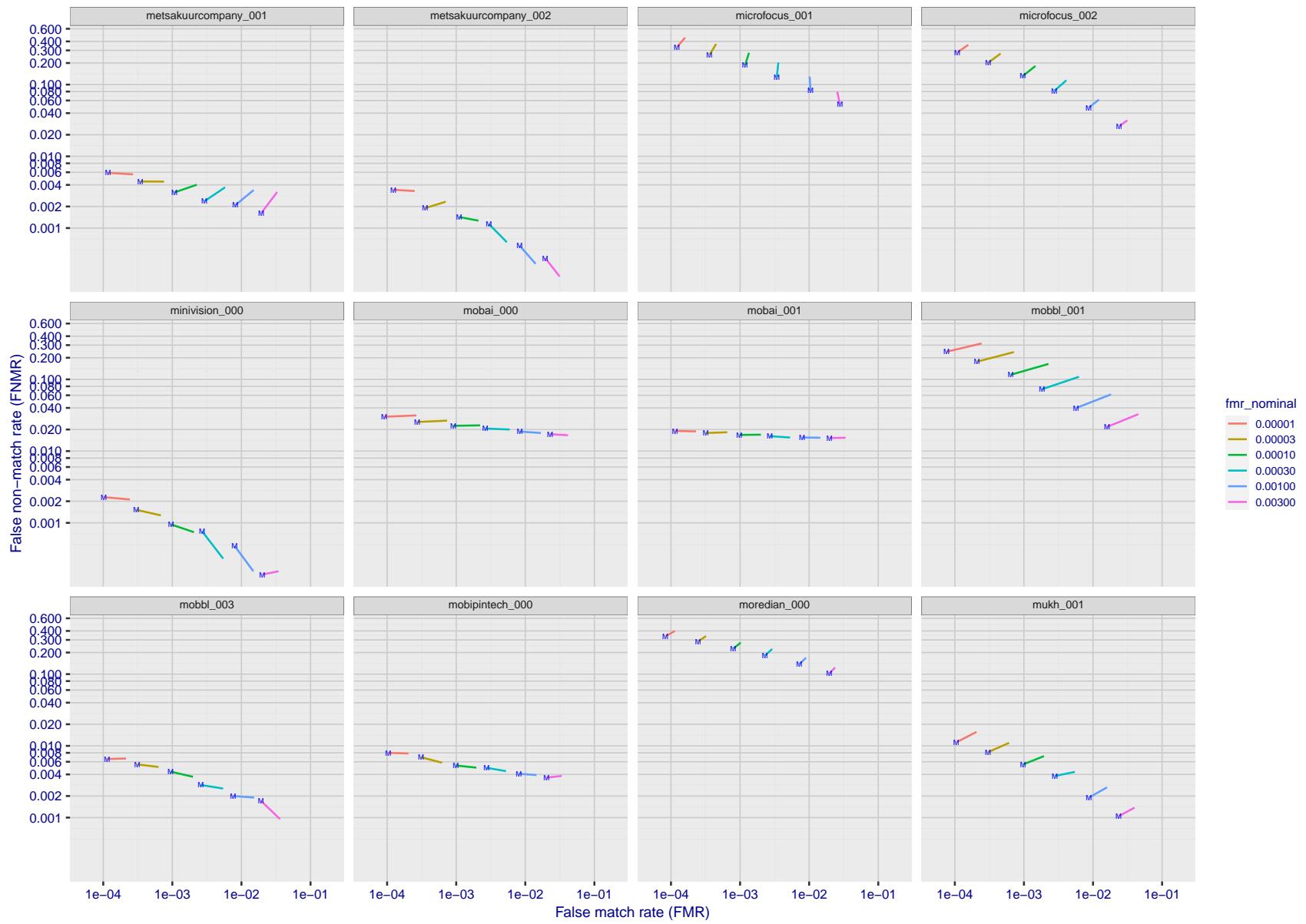


Figure 202: For the visa images, FNMR and FMR at six operating points along the DET characteristic. At each point a line is drawn between $(FMR, FNMR)_{MALE}$ and $(FMR, FNMR)_{FEMALE}$ showing how which sex has lower FMR and/or FNMR. The "M" label denotes male, the other end of the line corresponds to female. The six operating thresholds are selected to give the nominal false match rates given in the legend, and are computed over all impostor pairs regardless of age, sex, and place of birth. The plotted FMR values are broadly an order of magnitude larger than the nominal rates because FMR is computed over demographically-matched impostor pairs i.e individuals of the same sex, from the same geographic region (see section 3.6.1), and the same age group (see section 3.6.2).

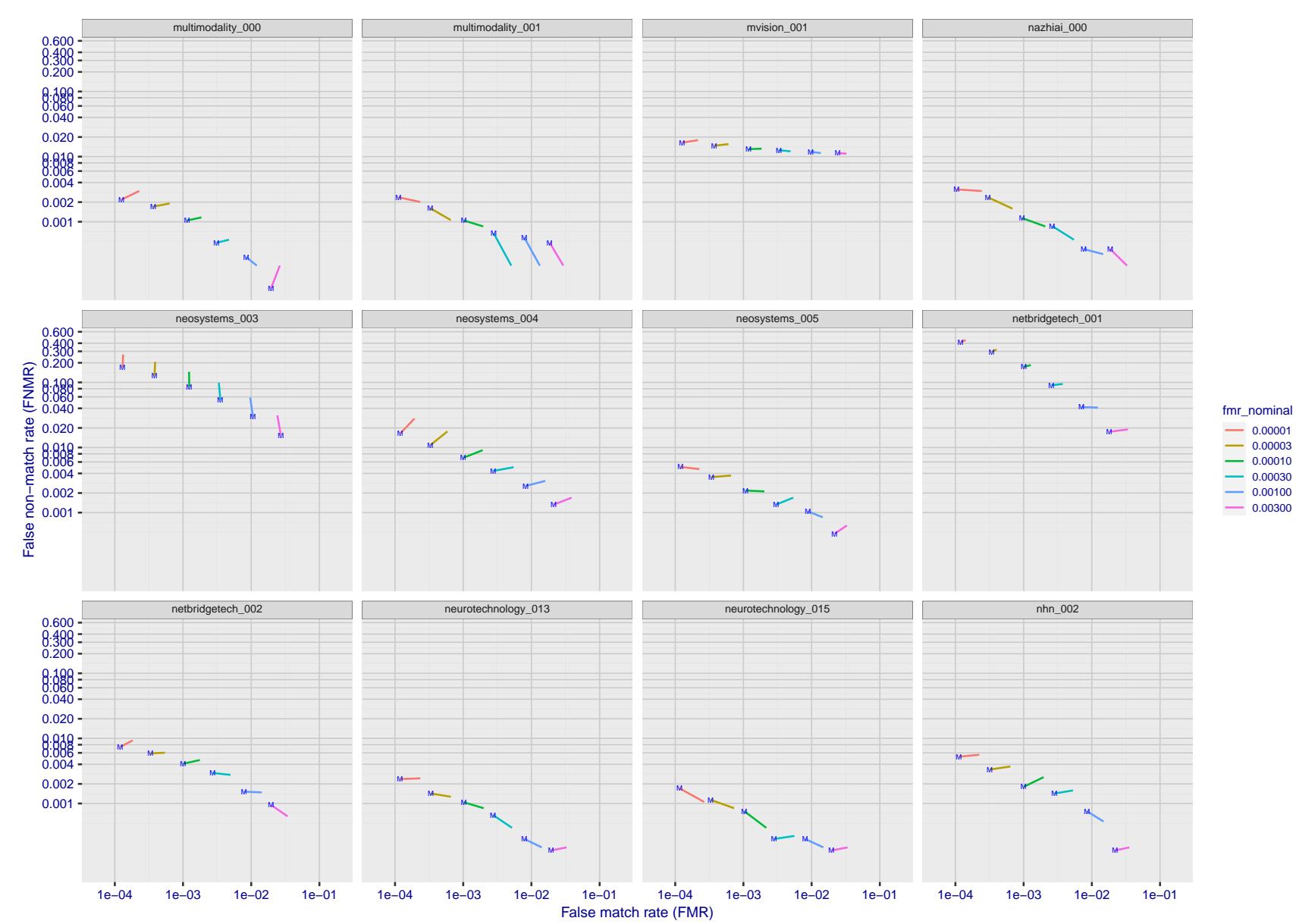


Figure 203: For the visa images, FNMR and FMR at six operating points along the DET characteristic. At each point a line is drawn between $(FMR, FNMR)_{MALE}$ and $(FMR, FNMR)_{FEMALE}$ showing how which sex has lower FMR and/or FNMR. The "M" label denotes male, the other end of the line corresponds to female. The six operating thresholds are selected to give the nominal false match rates given in the legend, and are computed over all impostor pairs regardless of age, sex, and place of birth. The plotted FMR values are broadly an order of magnitude larger than the nominal rates because FMR is computed over demographically-matched impostor pairs i.e individuals of the same sex, from the same geographic region (see section 3.6.1), and the same age group (see section 3.6.2).

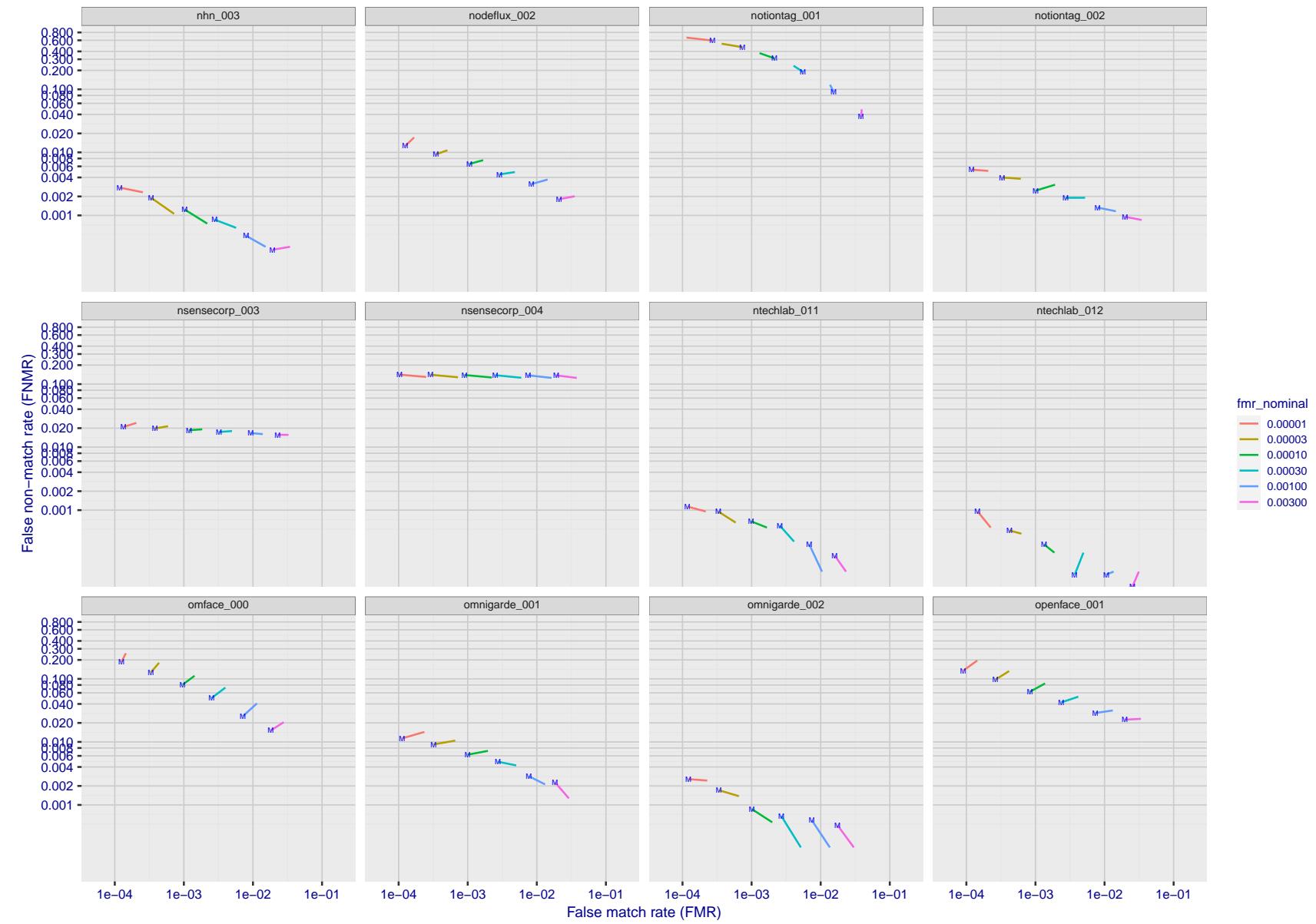


Figure 204: For the visa images, FNMR and FMR at six operating points along the DET characteristic. At each point a line is drawn between $(FMR, FNMR)_{MALE}$ and $(FMR, FNMR)_{FEMALE}$ showing how which sex has lower FMR and/or FNMR. The "M" label denotes male, the other end of the line corresponds to female. The six operating thresholds are selected to give the nominal false match rates given in the legend, and are computed over all impostor pairs regardless of age, sex, and place of birth. The plotted FMR values are broadly an order of magnitude larger than the nominal rates because FMR is computed over demographically-matched impostor pairs i.e individuals of the same sex, from the same geographic region (see section 3.6.1), and the same age group (see section 3.6.2).

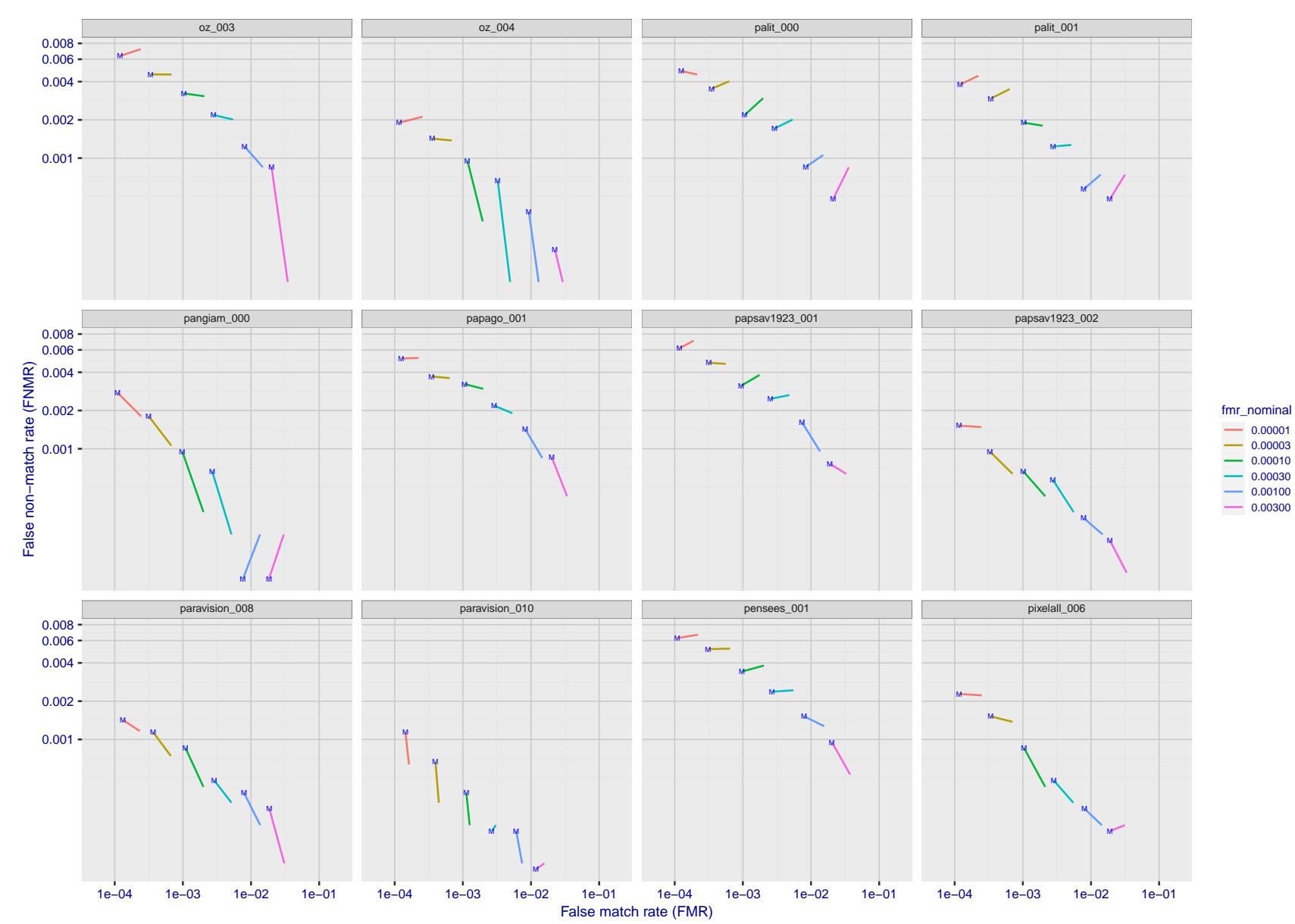


Figure 205: For the visa images, FNMR and FMR at six operating points along the DET characteristic. At each point a line is drawn between $(FMR, FNMR)_{MALE}$ and $(FMR, FNMR)_{FEMALE}$ showing how which sex has lower FMR and/or FNMR. The "M" label denotes male, the other end of the line corresponds to female. The six operating thresholds are selected to give the nominal false match rates given in the legend, and are computed over all impostor pairs regardless of age, sex, and place of birth. The plotted FMR values are broadly an order of magnitude larger than the nominal rates because FMR is computed over demographically-matched impostor pairs i.e individuals of the same sex, from the same geographic region (see section 3.6.1), and the same age group (see section 3.6.2).

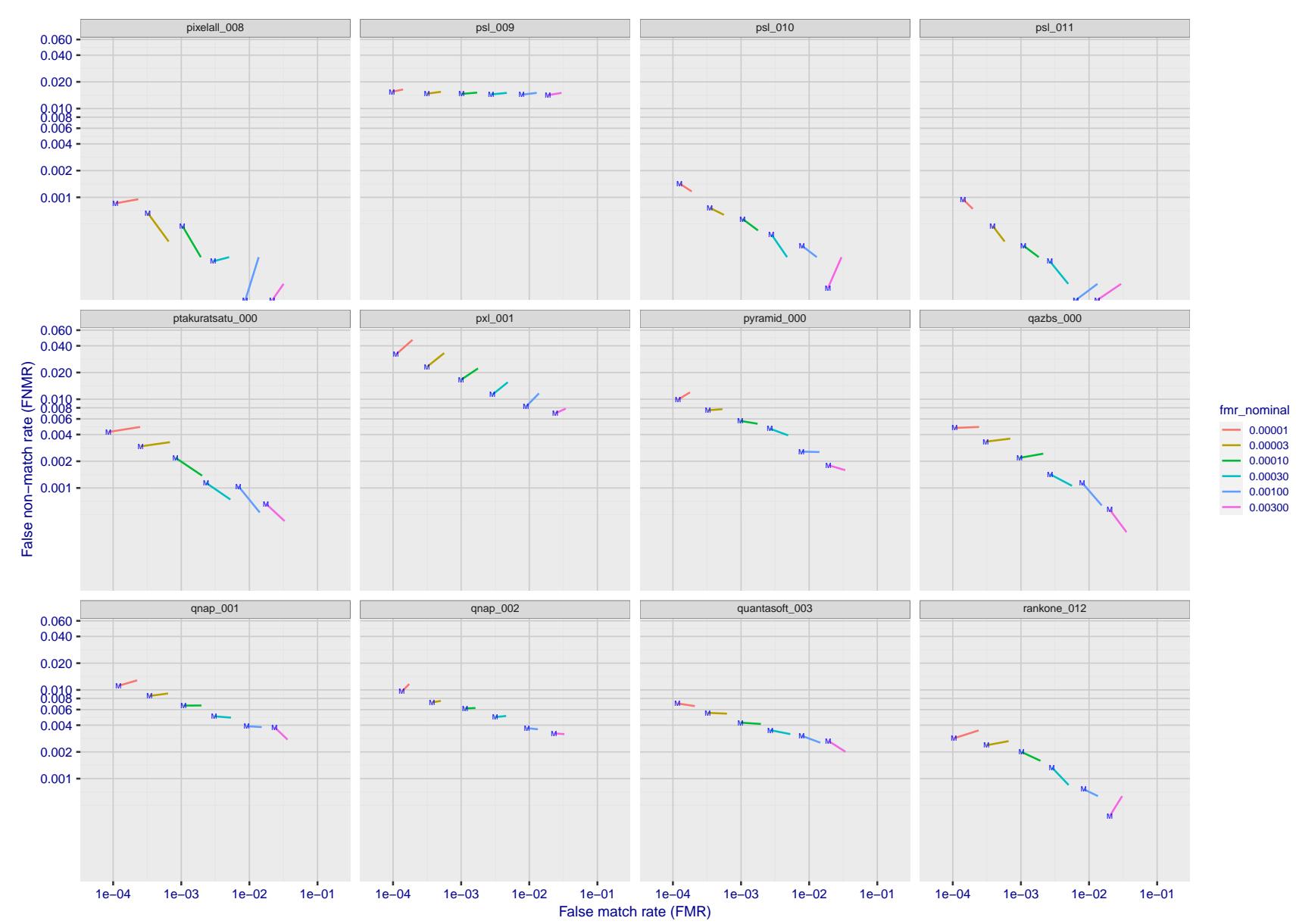


Figure 206: For the visa images, FNMR and FMR at six operating points along the DET characteristic. At each point a line is drawn between $(FMR, FNMR)_{MALE}$ and $(FMR, FNMR)_{FEMALE}$ showing how which sex has lower FMR and/or FNMR. The "M" label denotes male, the other end of the line corresponds to female. The six operating thresholds are selected to give the nominal false match rates given in the legend, and are computed over all impostor pairs regardless of age, sex, and place of birth. The plotted FMR values are broadly an order of magnitude larger than the nominal rates because FMR is computed over demographically-matched impostor pairs i.e individuals of the same sex, from the same geographic region (see section 3.6.1), and the same age group (see section 3.6.2).

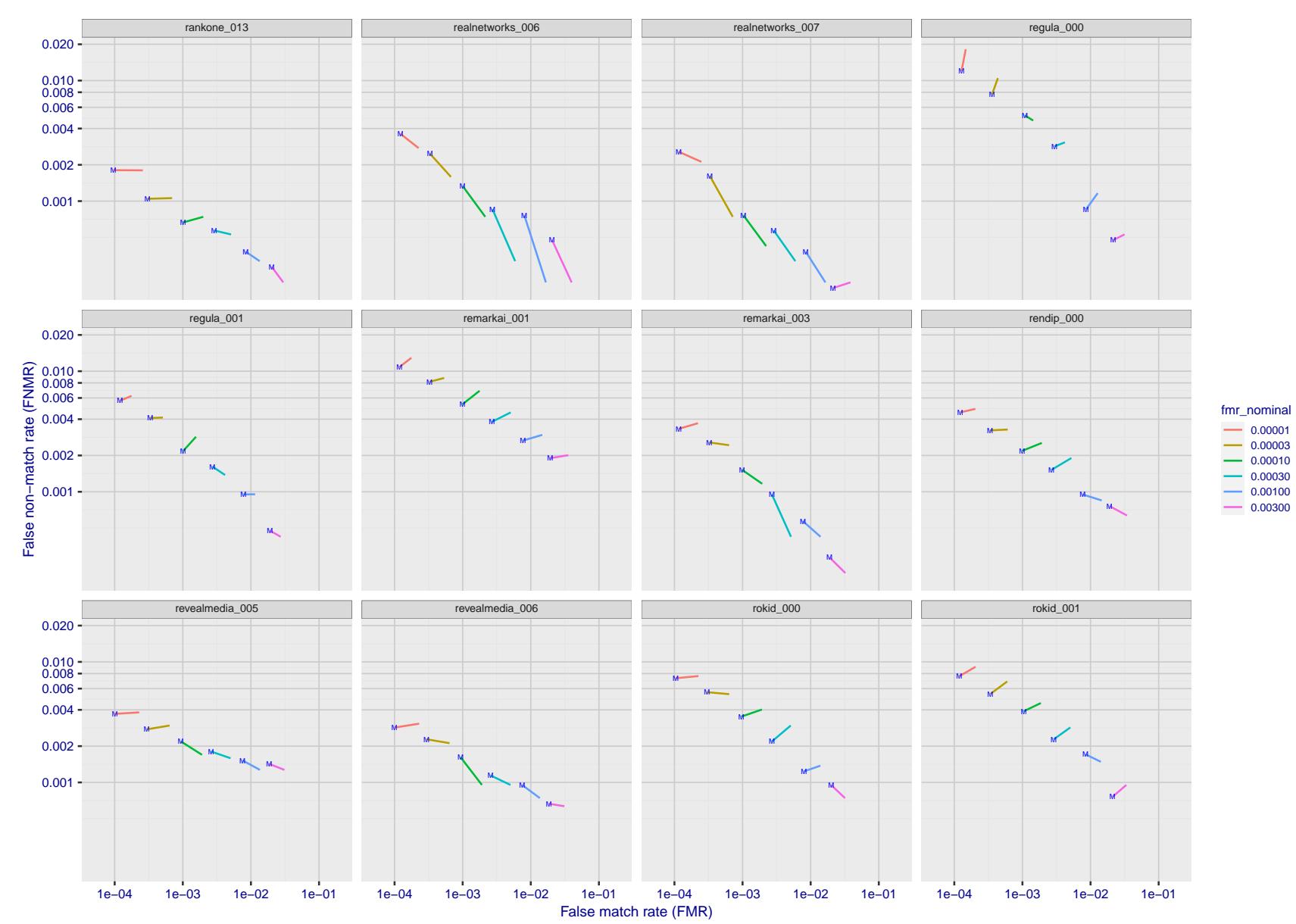


Figure 207: For the visa images, FNMR and FMR at six operating points along the DET characteristic. At each point a line is drawn between $(FMR, FNMR)_{MALE}$ and $(FMR, FNMR)_{FEMALE}$ showing how which sex has lower FMR and/or FNMR. The "M" label denotes male, the other end of the line corresponds to female. The six operating thresholds are selected to give the nominal false match rates given in the legend, and are computed over all impostor pairs regardless of age, sex, and place of birth. The plotted FMR values are broadly an order of magnitude larger than the nominal rates because FMR is computed over demographically-matched impostor pairs i.e individuals of the same sex, from the same geographic region (see section 3.6.1), and the same age group (see section 3.6.2).

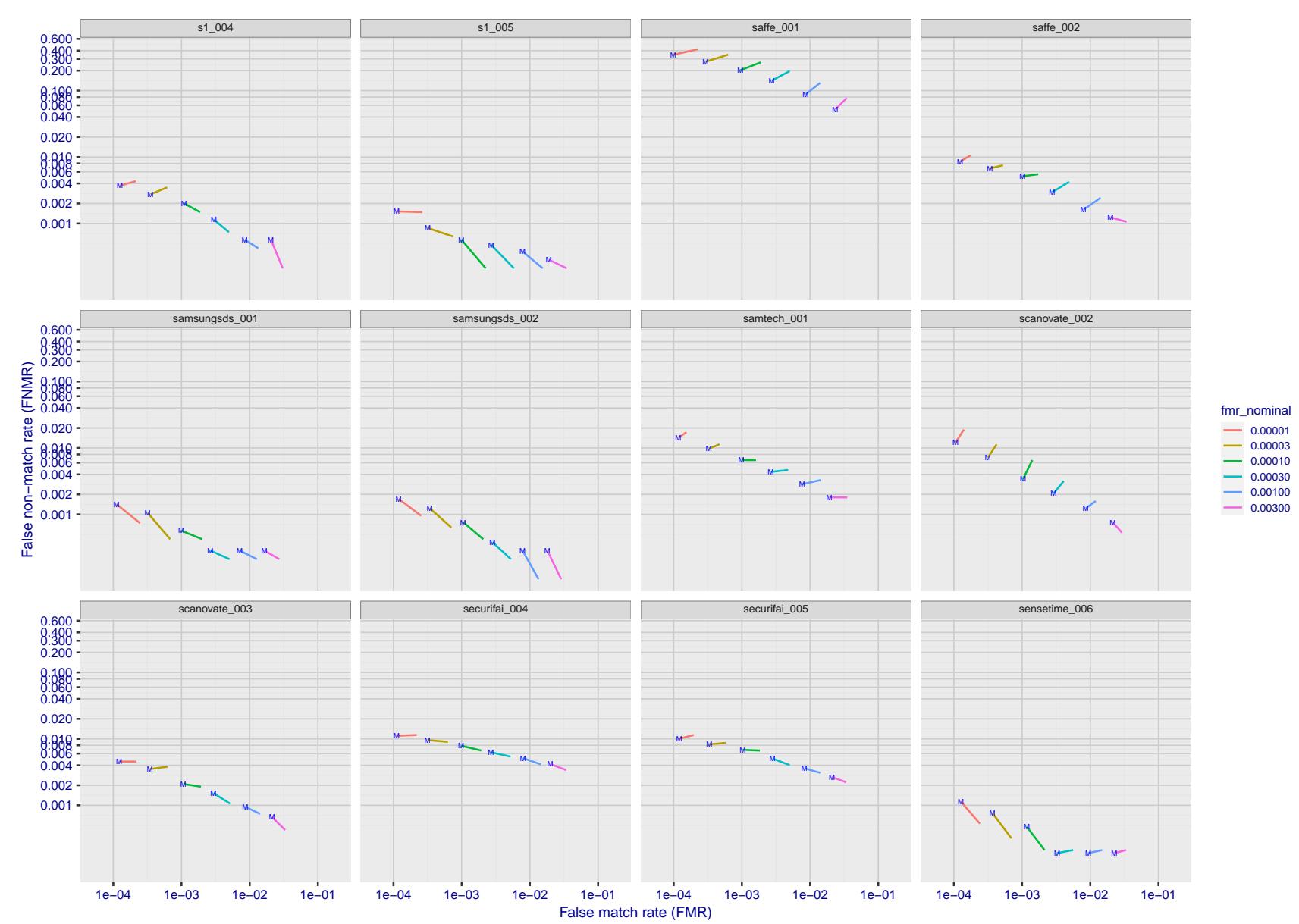


Figure 208: For the visa images, FNMR and FMR at six operating points along the DET characteristic. At each point a line is drawn between $(FMR, FNMR)_{MALE}$ and $(FMR, FNMR)_{FEMALE}$ showing how which sex has lower FMR and/or FNMR. The "M" label denotes male, the other end of the line corresponds to female. The six operating thresholds are selected to give the nominal false match rates given in the legend, and are computed over all impostor pairs regardless of age, sex, and place of birth. The plotted FMR values are broadly an order of magnitude larger than the nominal rates because FMR is computed over demographically-matched impostor pairs i.e individuals of the same sex, from the same geographic region (see section 3.6.1), and the same age group (see section 3.6.2).

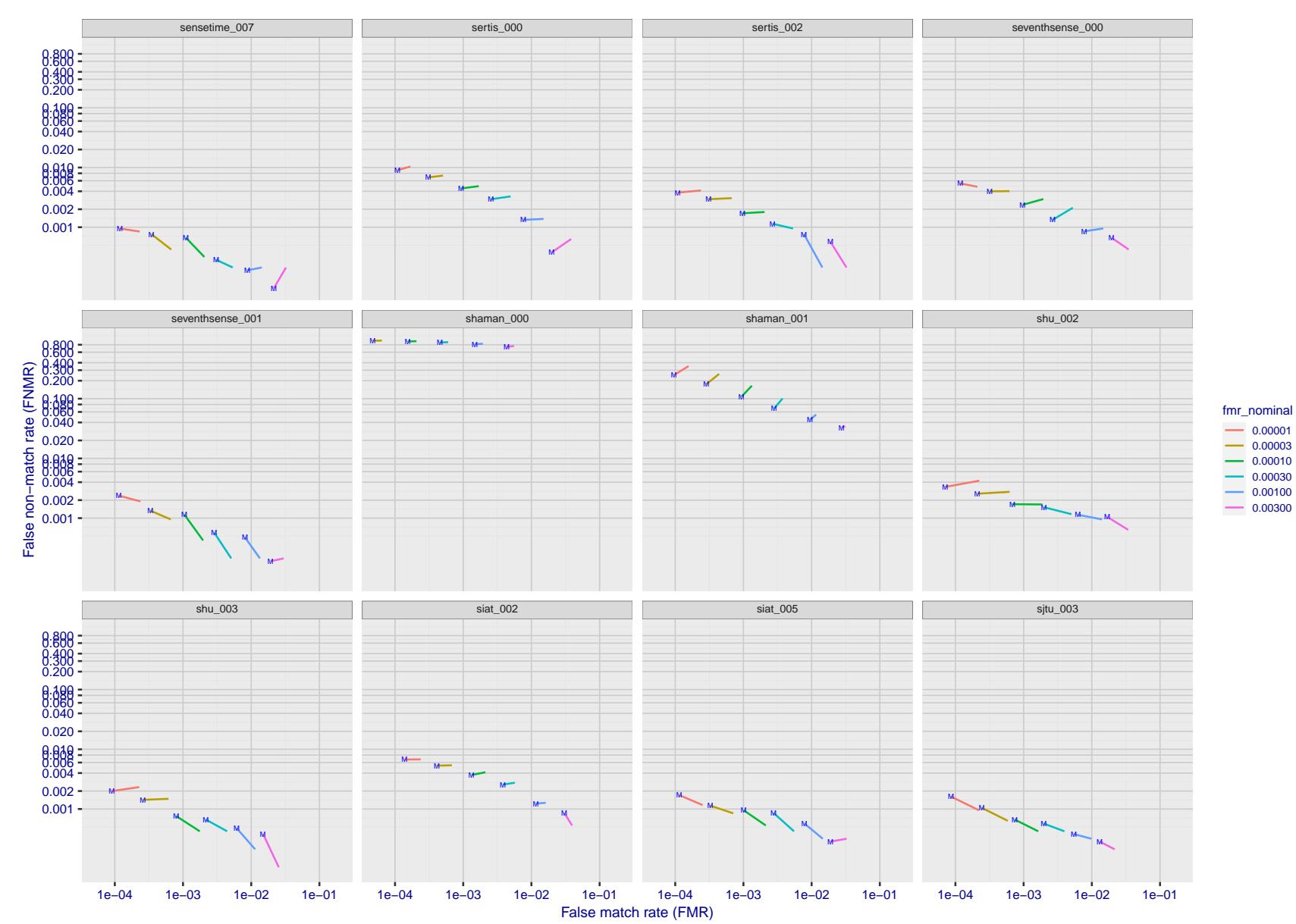


Figure 209: For the visa images, FNMR and FMR at six operating points along the DET characteristic. At each point a line is drawn between $(FMR, FNMR)_{MALE}$ and $(FMR, FNMR)_{FEMALE}$ showing how which sex has lower FMR and/or FNMR. The "M" label denotes male, the other end of the line corresponds to female. The six operating thresholds are selected to give the nominal false match rates given in the legend, and are computed over all impostor pairs regardless of age, sex, and place of birth. The plotted FMR values are broadly an order of magnitude larger than the nominal rates because FMR is computed over demographically-matched impostor pairs i.e individuals of the same sex, from the same geographic region (see section 3.6.1), and the same age group (see section 3.6.2).

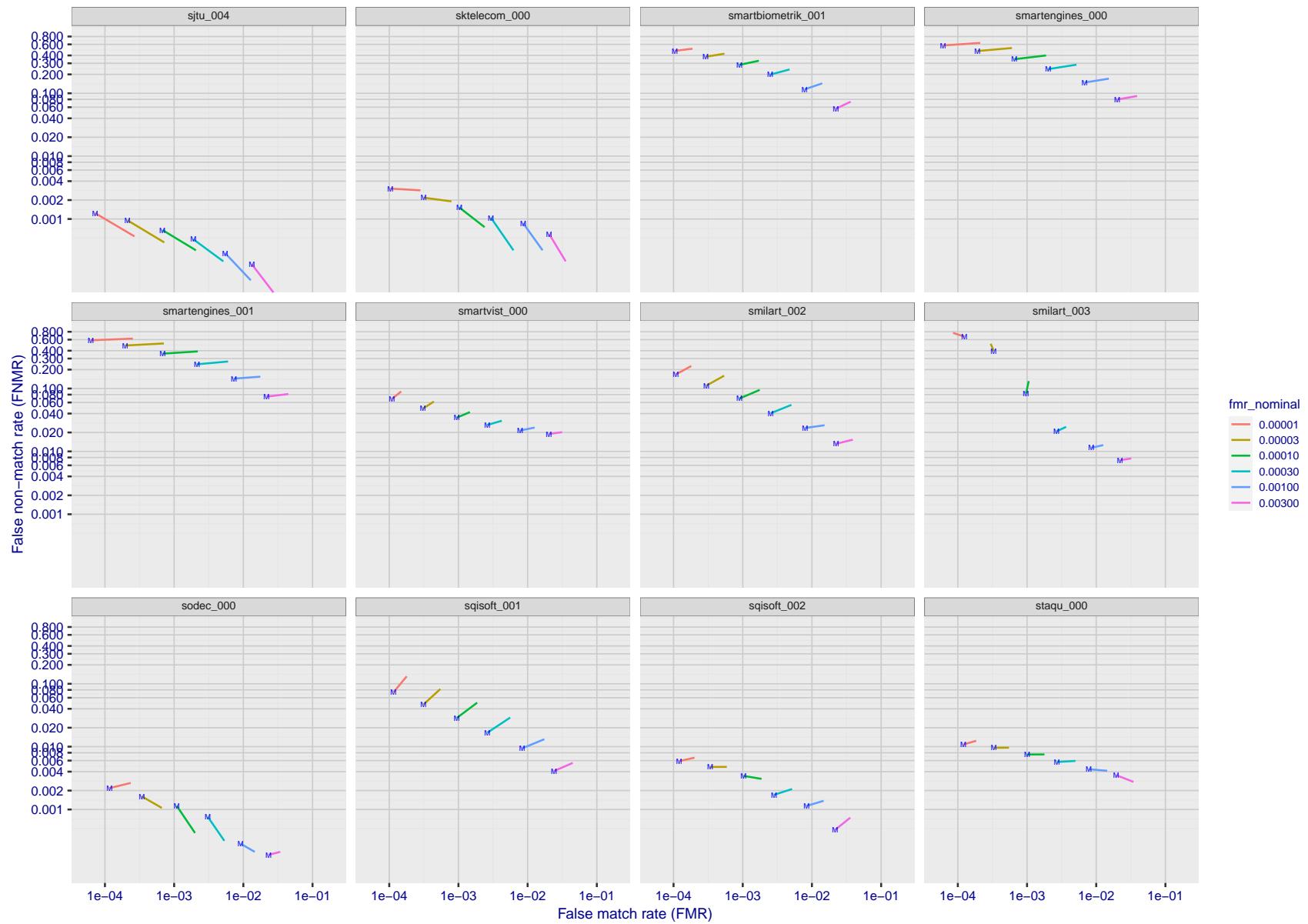


Figure 210: For the visa images, FNMR and FMR at six operating points along the DET characteristic. At each point a line is drawn between $(FMR, FNMR)_{MALE}$ and $(FMR, FNMR)_{FEMALE}$ showing how which sex has lower FMR and/or FNMR. The "M" label denotes male, the other end of the line corresponds to female. The six operating thresholds are selected to give the nominal false match rates given in the legend, and are computed over all impostor pairs regardless of age, sex, and place of birth. The plotted FMR values are broadly an order of magnitude larger than the nominal rates because FMR is computed over demographically-matched impostor pairs i.e individuals of the same sex, from the same geographic region (see section 3.6.1), and the same age group (see section 3.6.2).

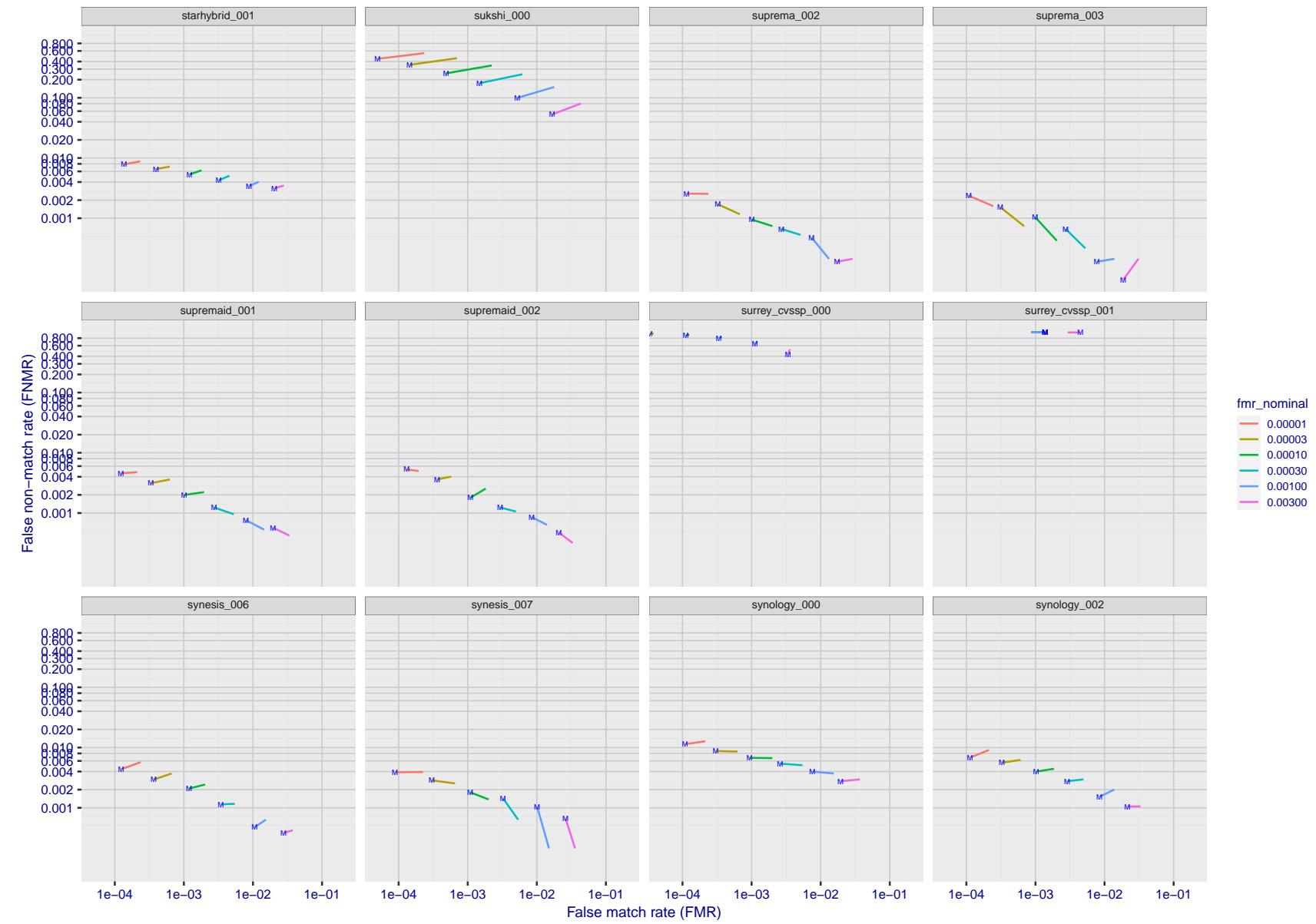


Figure 211: For the visa images, FNMR and FMR at six operating points along the DET characteristic. At each point a line is drawn between $(FMR, FNMR)_{MALE}$ and $(FMR, FNMR)_{FEMALE}$ showing how which sex has lower FMR and/or FNMR. The "M" label denotes male, the other end of the line corresponds to female. The six operating thresholds are selected to give the nominal false match rates given in the legend, and are computed over all impostor pairs regardless of age, sex, and place of birth. The plotted FMR values are broadly an order of magnitude larger than the nominal rates because FMR is computed over demographically-matched impostor pairs i.e individuals of the same sex, from the same geographic region (see section 3.6.1), and the same age group (see section 3.6.2).

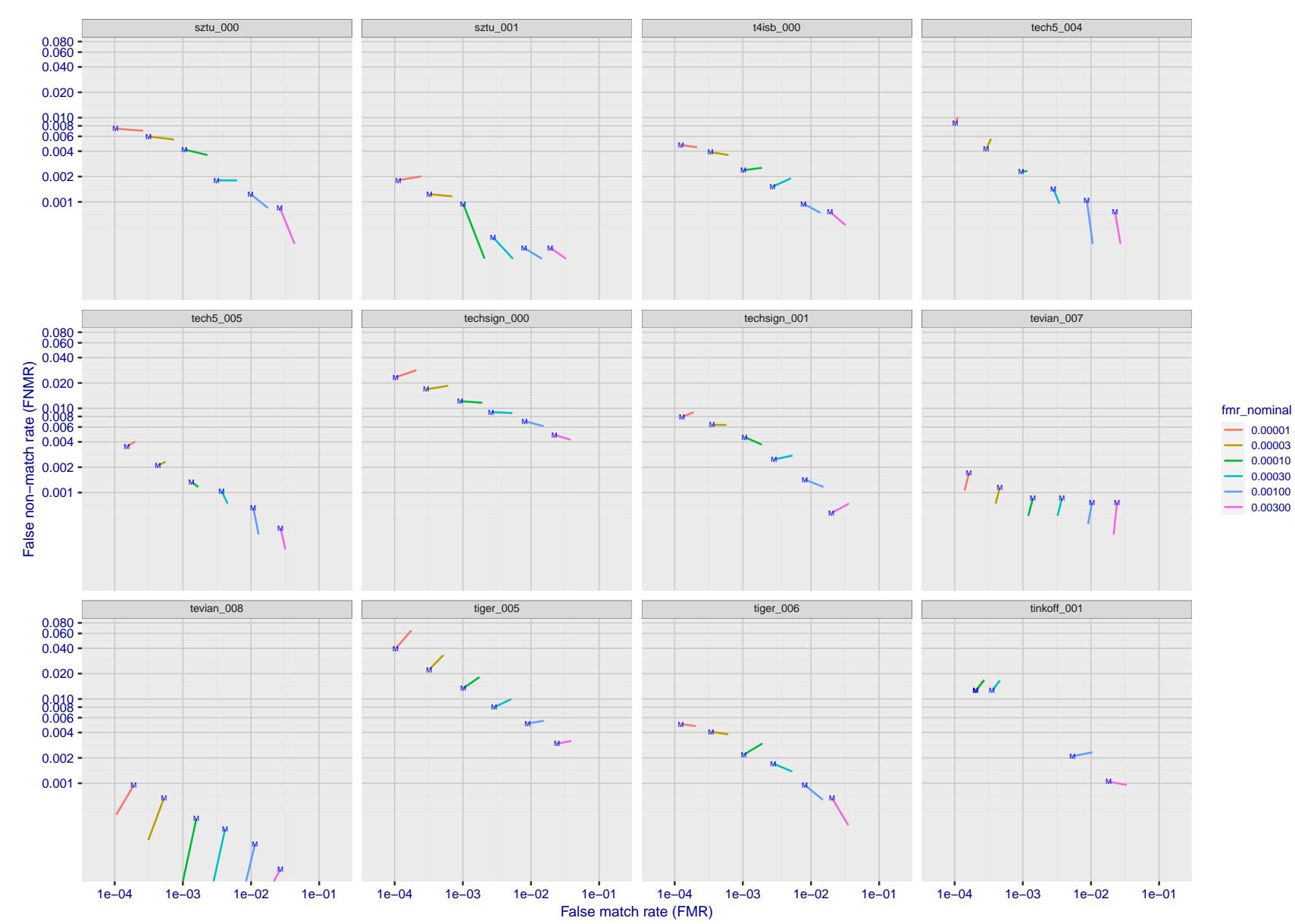


Figure 212: For the visa images, FNMR and FMR at six operating points along the DET characteristic. At each point a line is drawn between $(FMR, FNMR)_{MALE}$ and $(FMR, FNMR)_{FEMALE}$ showing how which sex has lower FMR and/or FNMR. The "M" label denotes male, the other end of the line corresponds to female. The six operating thresholds are selected to give the nominal false match rates given in the legend, and are computed over all impostor pairs regardless of age, sex, and place of birth. The plotted FMR values are broadly an order of magnitude larger than the nominal rates because FMR is computed over demographically-matched impostor pairs i.e individuals of the same sex, from the same geographic region (see section 3.6.1), and the same age group (see section 3.6.2).

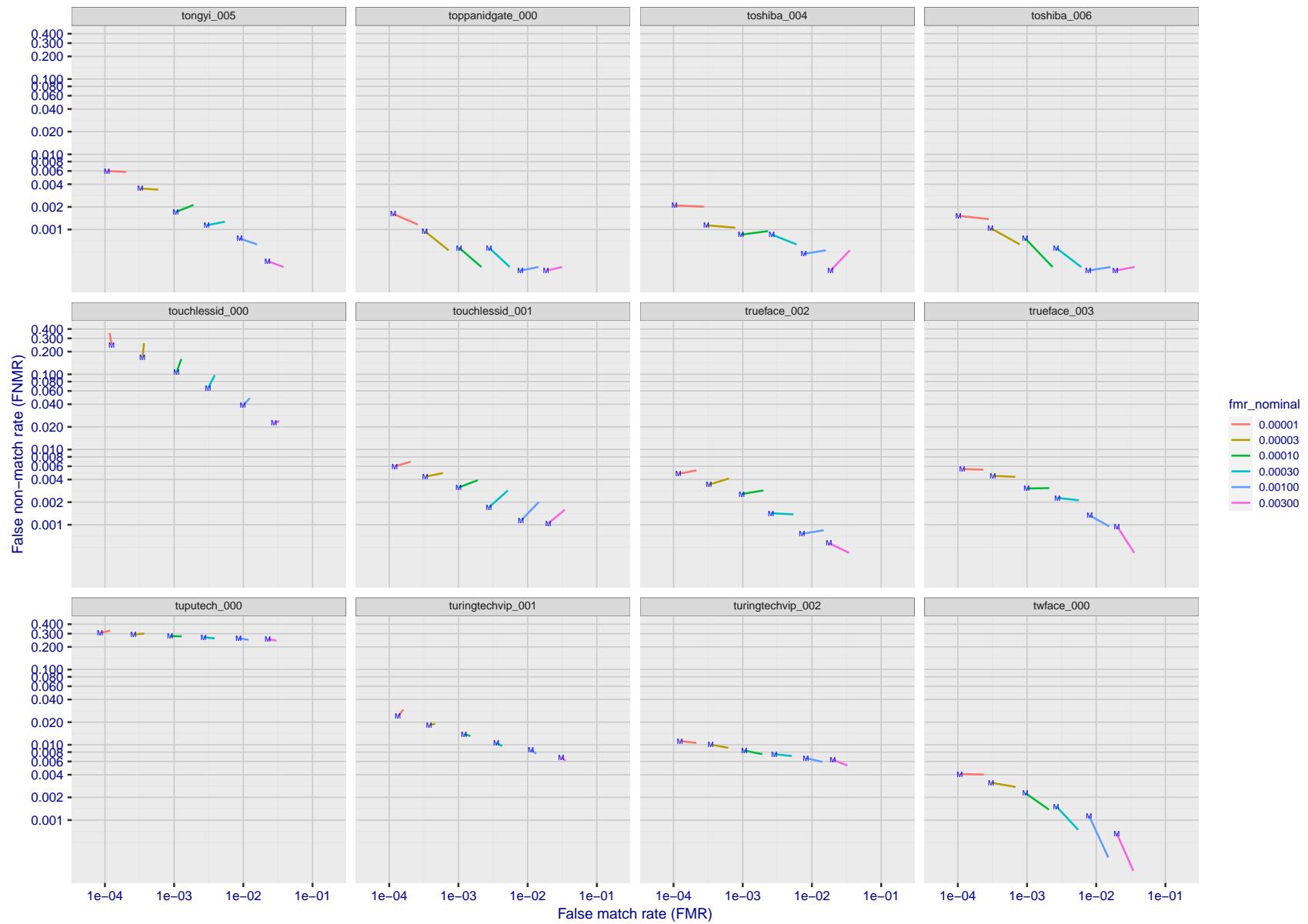


Figure 213: For the visa images, FNMR and FMR at six operating points along the DET characteristic. At each point a line is drawn between $(FMR, FNMR)_{MALE}$ and $(FMR, FNMR)_{FEMALE}$ showing how which sex has lower FMR and/or FNMR. The "M" label denotes male, the other end of the line corresponds to female. The six operating thresholds are selected to give the nominal false match rates given in the legend, and are computed over all impostor pairs regardless of age, sex, and place of birth. The plotted FMR values are broadly an order of magnitude larger than the nominal rates because FMR is computed over demographically-matched impostor pairs i.e individuals of the same sex, from the same geographic region (see section 3.6.1), and the same age group (see section 3.6.2).

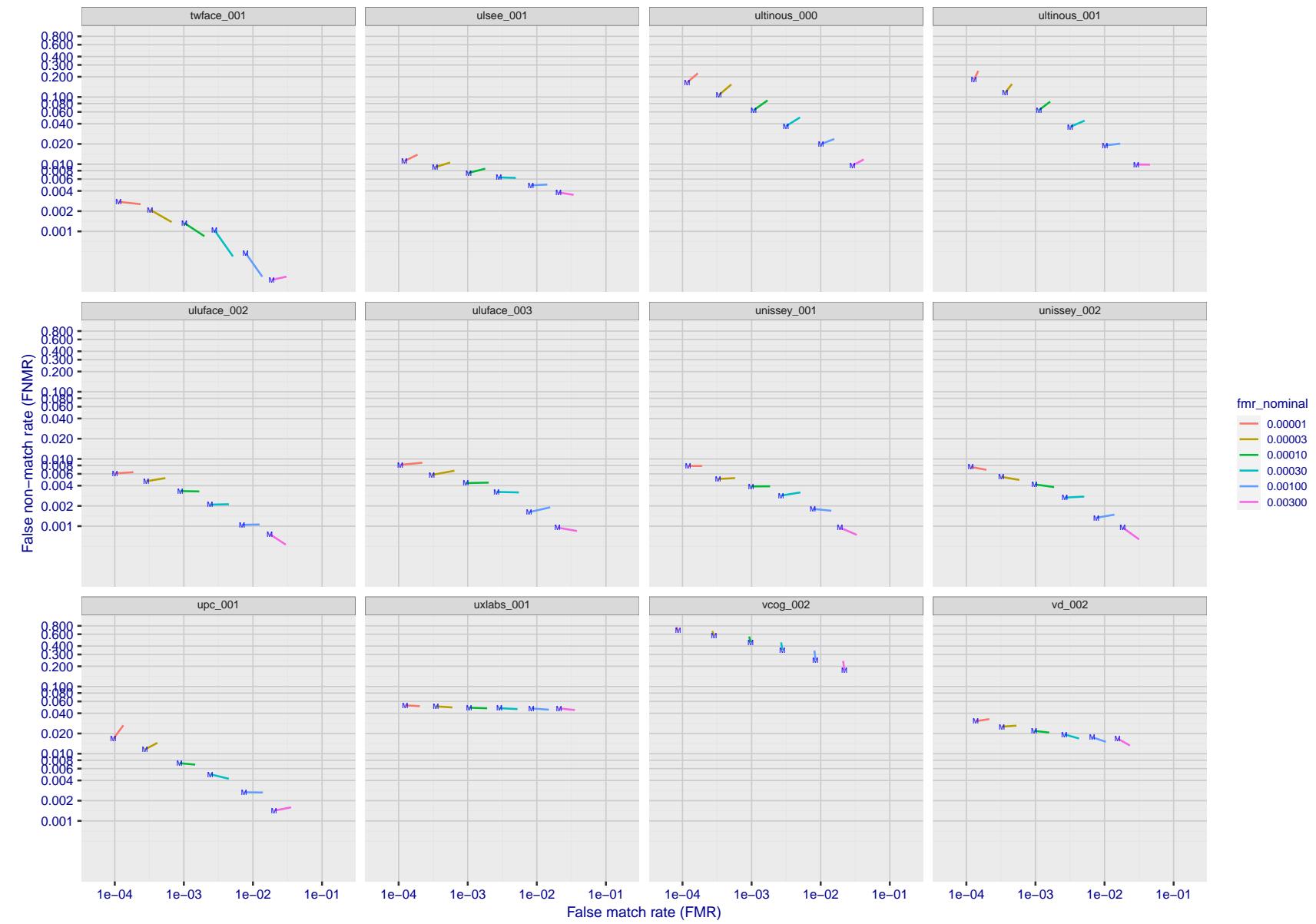


Figure 214: For the visa images, FNMR and FMR at six operating points along the DET characteristic. At each point a line is drawn between $(FMR, FNMR)_{MALE}$ and $(FMR, FNMR)_{FEMALE}$ showing how which sex has lower FMR and/or FNMR. The "M" label denotes male, the other end of the line corresponds to female. The six operating thresholds are selected to give the nominal false match rates given in the legend, and are computed over all impostor pairs regardless of age, sex, and place of birth. The plotted FMR values are broadly an order of magnitude larger than the nominal rates because FMR is computed over demographically-matched impostor pairs i.e individuals of the same sex, from the same geographic region (see section 3.6.1), and the same age group (see section 3.6.2).

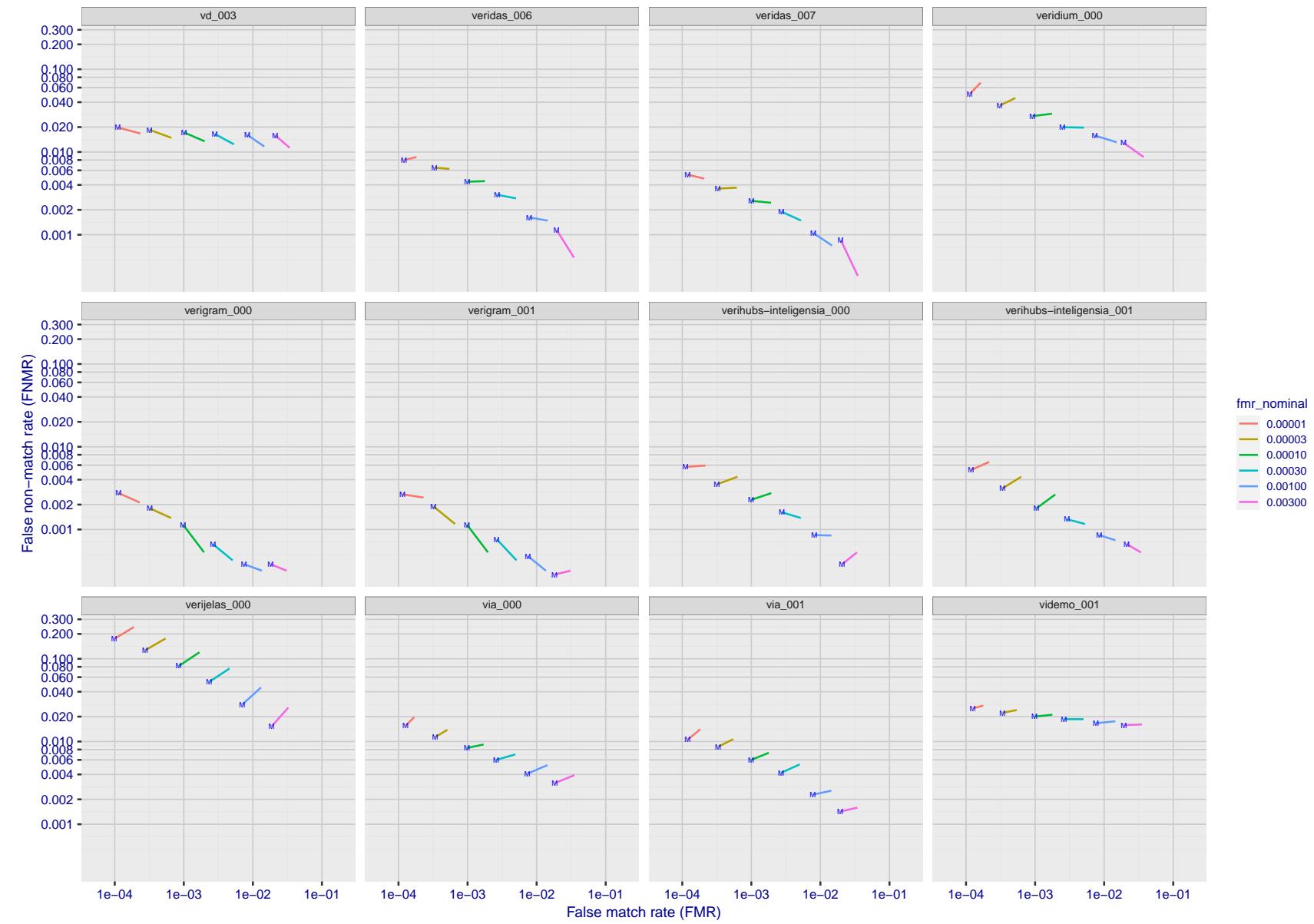


Figure 215: For the visa images, FNMR and FMR at six operating points along the DET characteristic. At each point a line is drawn between $(FMR, FNMR)_{MALE}$ and $(FMR, FNMR)_{FEMALE}$ showing how which sex has lower FMR and/or FNMR. The "M" label denotes male, the other end of the line corresponds to female. The six operating thresholds are selected to give the nominal false match rates given in the legend, and are computed over all impostor pairs regardless of age, sex, and place of birth. The plotted FMR values are broadly an order of magnitude larger than the nominal rates because FMR is computed over demographically-matched impostor pairs i.e individuals of the same sex, from the same geographic region (see section 3.6.1), and the same age group (see section 3.6.2).

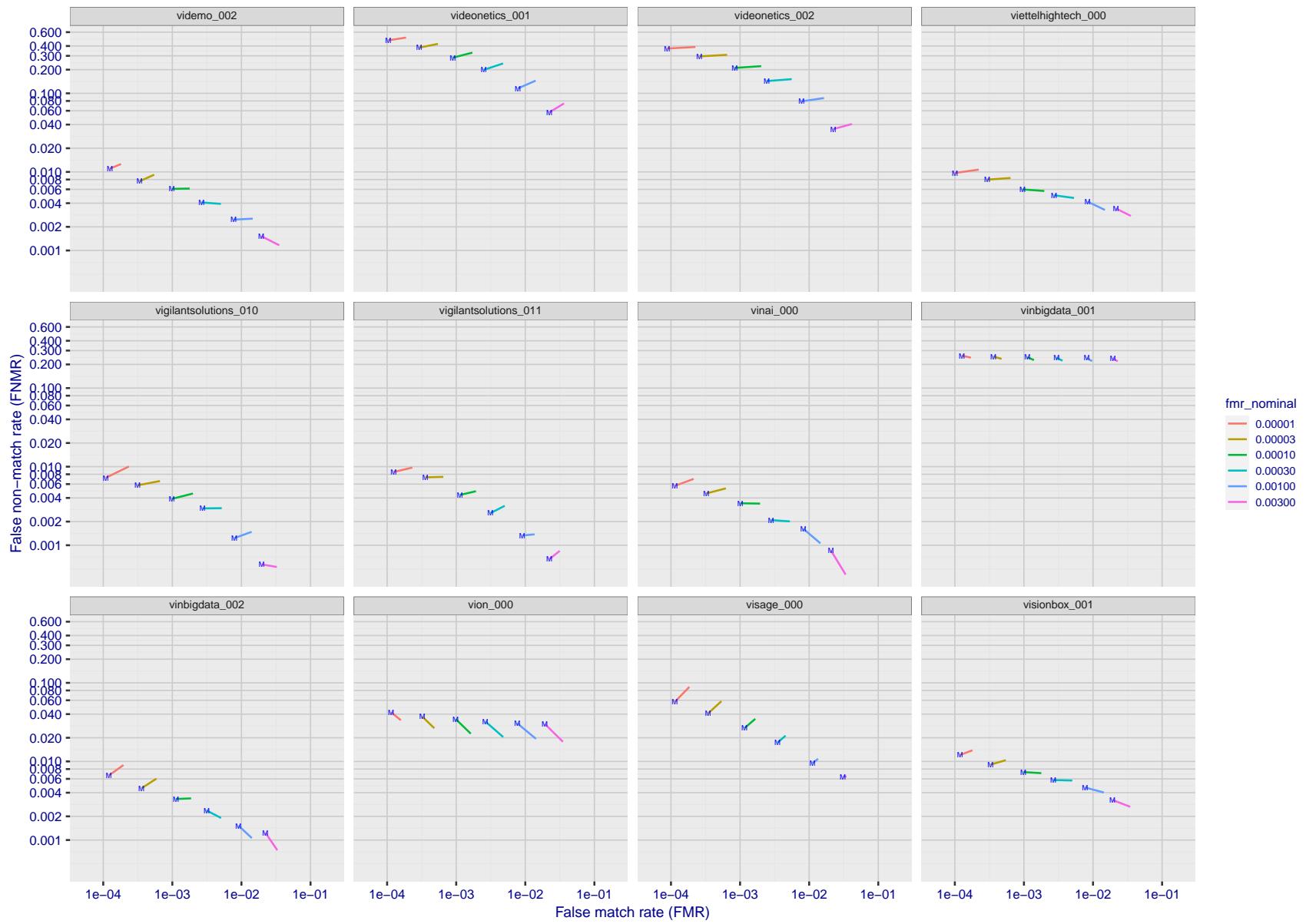


Figure 216: For the visa images, FNMR and FMR at six operating points along the DET characteristic. At each point a line is drawn between $(FMR, FNMR)_{MALE}$ and $(FMR, FNMR)_{FEMALE}$ showing how which sex has lower FMR and/or FNMR. The "M" label denotes male, the other end of the line corresponds to female. The six operating thresholds are selected to give the nominal false match rates given in the legend, and are computed over all impostor pairs regardless of age, sex, and place of birth. The plotted FMR values are broadly an order of magnitude larger than the nominal rates because FMR is computed over demographically-matched impostor pairs i.e individuals of the same sex, from the same geographic region (see section 3.6.1), and the same age group (see section 3.6.2).

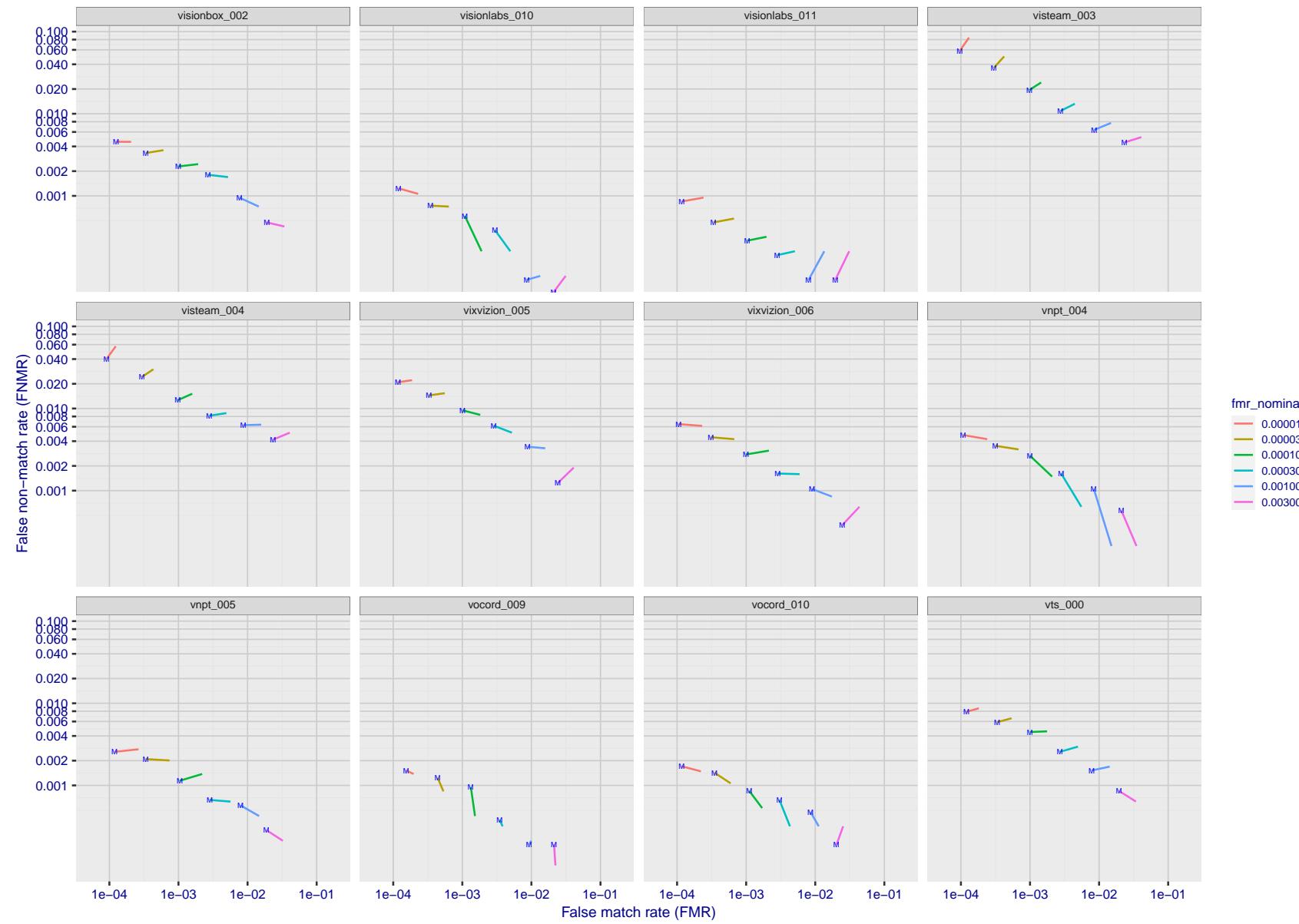


Figure 217: For the visa images, FNMR and FMR at six operating points along the DET characteristic. At each point a line is drawn between $(FMR, FNMR)_{MALE}$ and $(FMR, FNMR)_{FEMALE}$ showing how which sex has lower FMR and/or FNMR. The "M" label denotes male, the other end of the line corresponds to female. The six operating thresholds are selected to give the nominal false match rates given in the legend, and are computed over all impostor pairs regardless of age, sex, and place of birth. The plotted FMR values are broadly an order of magnitude larger than the nominal rates because FMR is computed over demographically-matched impostor pairs i.e individuals of the same sex, from the same geographic region (see section 3.6.1), and the same age group (see section 3.6.2).

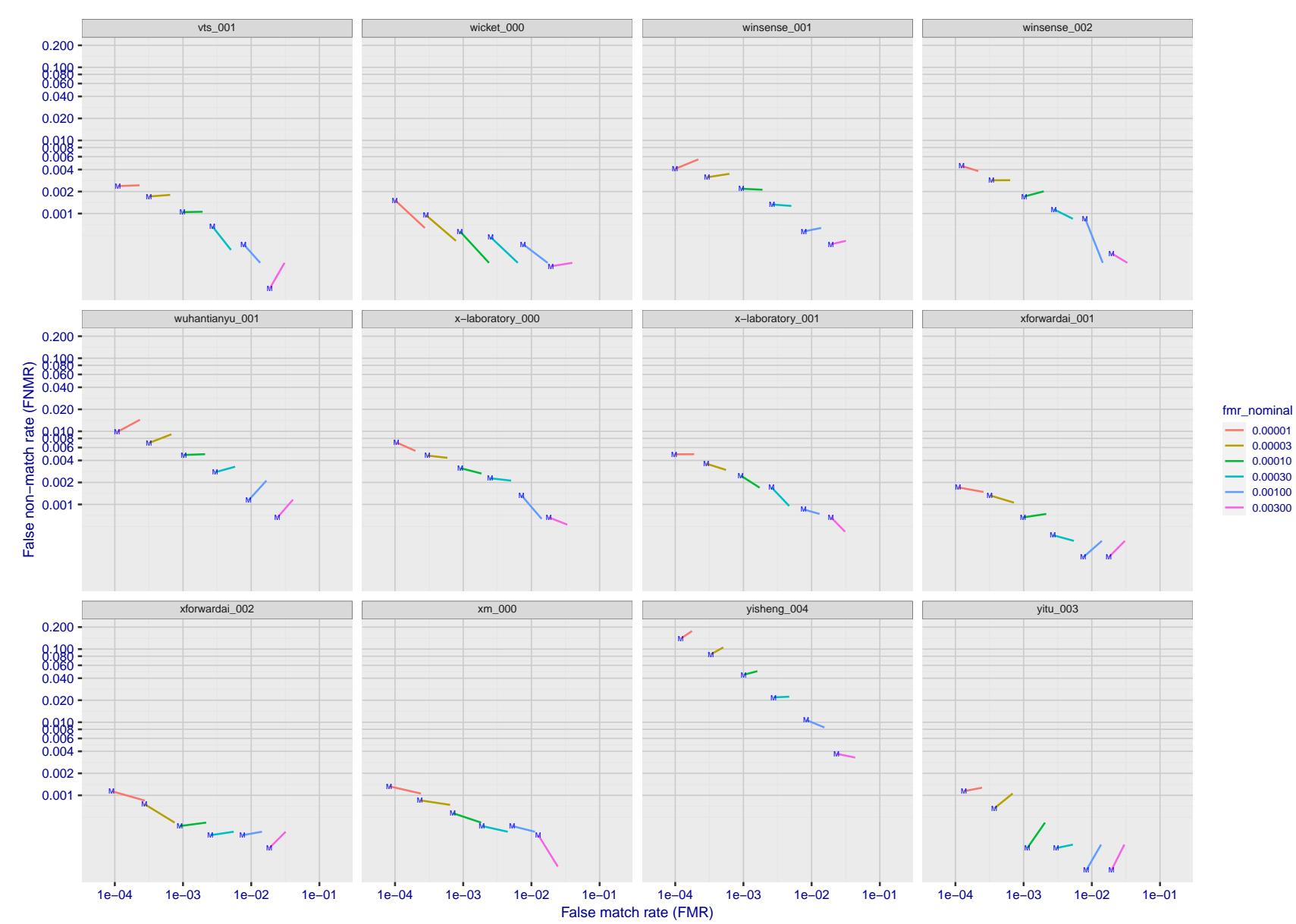


Figure 218: For the visa images, FNMR and FMR at six operating points along the DET characteristic. At each point a line is drawn between $(FMR, FNMR)_{MALE}$ and $(FMR, FNMR)_{FEMALE}$ showing how which sex has lower FMR and/or FNMR. The "M" label denotes male, the other end of the line corresponds to female. The six operating thresholds are selected to give the nominal false match rates given in the legend, and are computed over all impostor pairs regardless of age, sex, and place of birth. The plotted FMR values are broadly an order of magnitude larger than the nominal rates because FMR is computed over demographically-matched impostor pairs i.e individuals of the same sex, from the same geographic region (see section 3.6.1), and the same age group (see section 3.6.2).

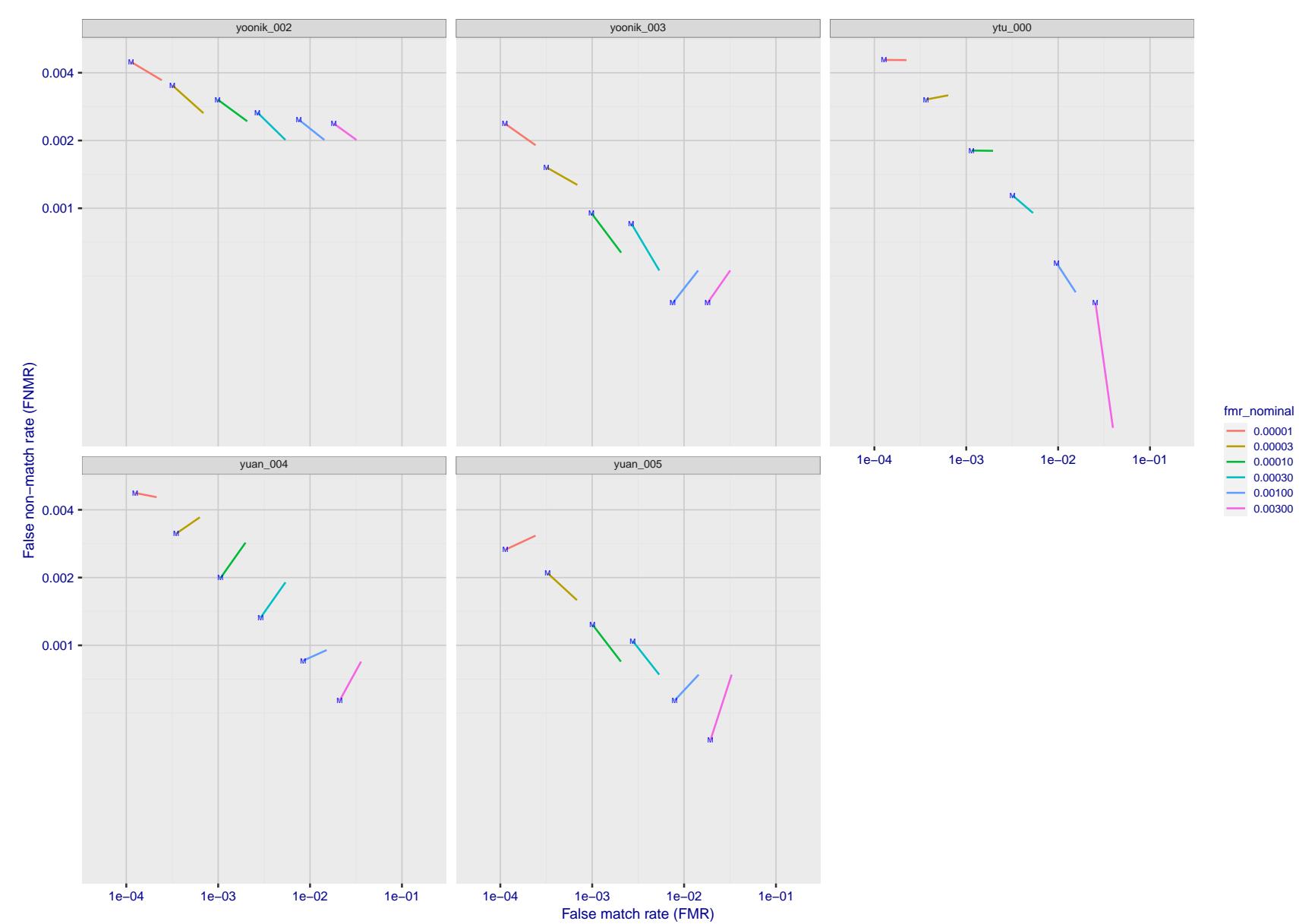


Figure 219: For the visa images, FNMR and FMR at six operating points along the DET characteristic. At each point a line is drawn between $(FMR, FNMR)_{MALE}$ and $(FMR, FNMR)_{FEMALE}$ showing how which sex has lower FMR and/or FNMR. The "M" label denotes male, the other end of the line corresponds to female. The six operating thresholds are selected to give the nominal false match rates given in the legend, and are computed over all impostor pairs regardless of age, sex, and place of birth. The plotted FMR values are broadly an order of magnitude larger than the nominal rates because FMR is computed over demographically-matched impostor pairs i.e individuals of the same sex, from the same geographic region (see section 3.6.1), and the same age group (see section 3.6.2).

2023/02/02 13:38:52

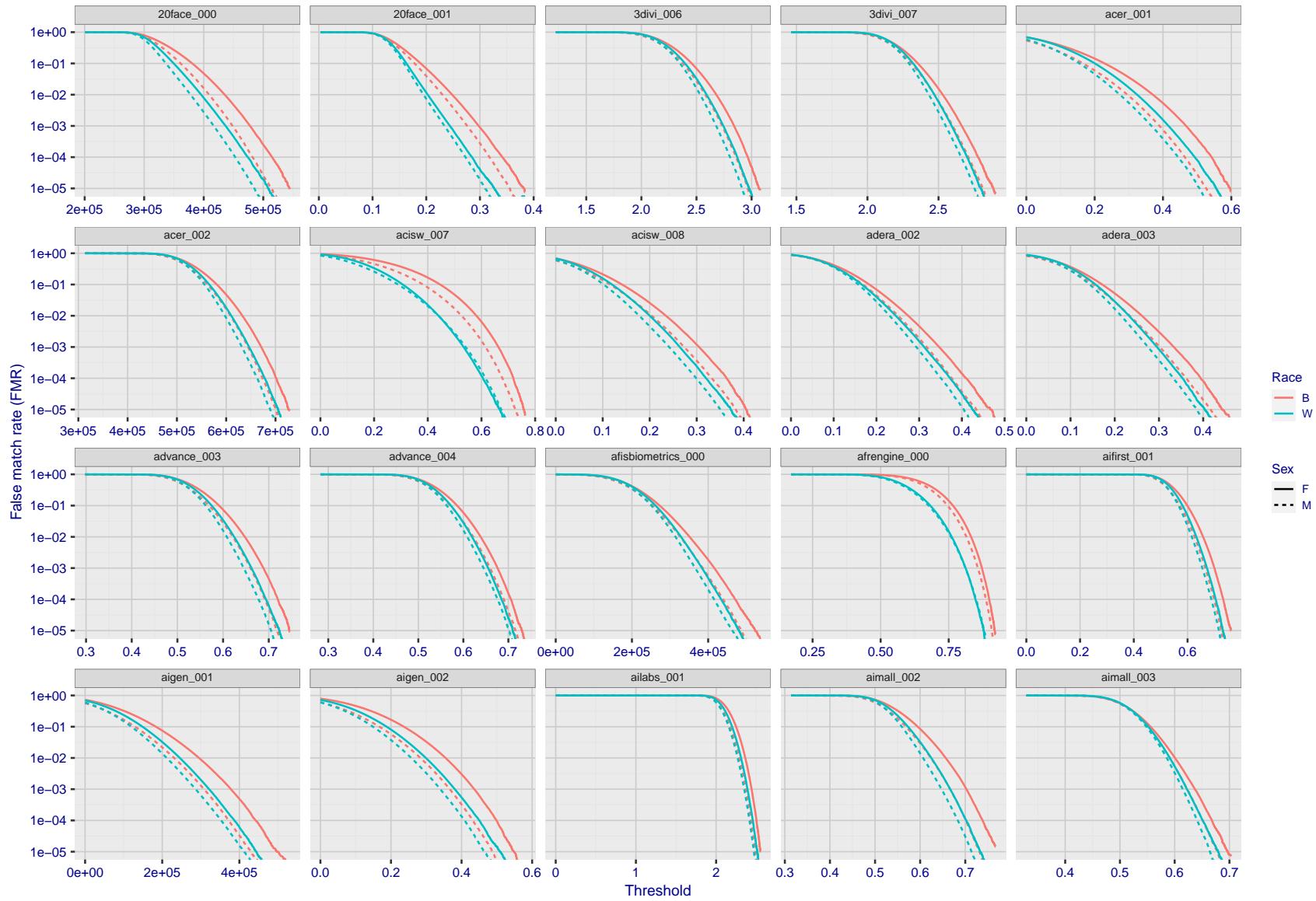


Figure 220: For the mugshot images, the false match calibration curves show false match rate vs. threshold. Separate curves appear for white females, black females, black males and white males.

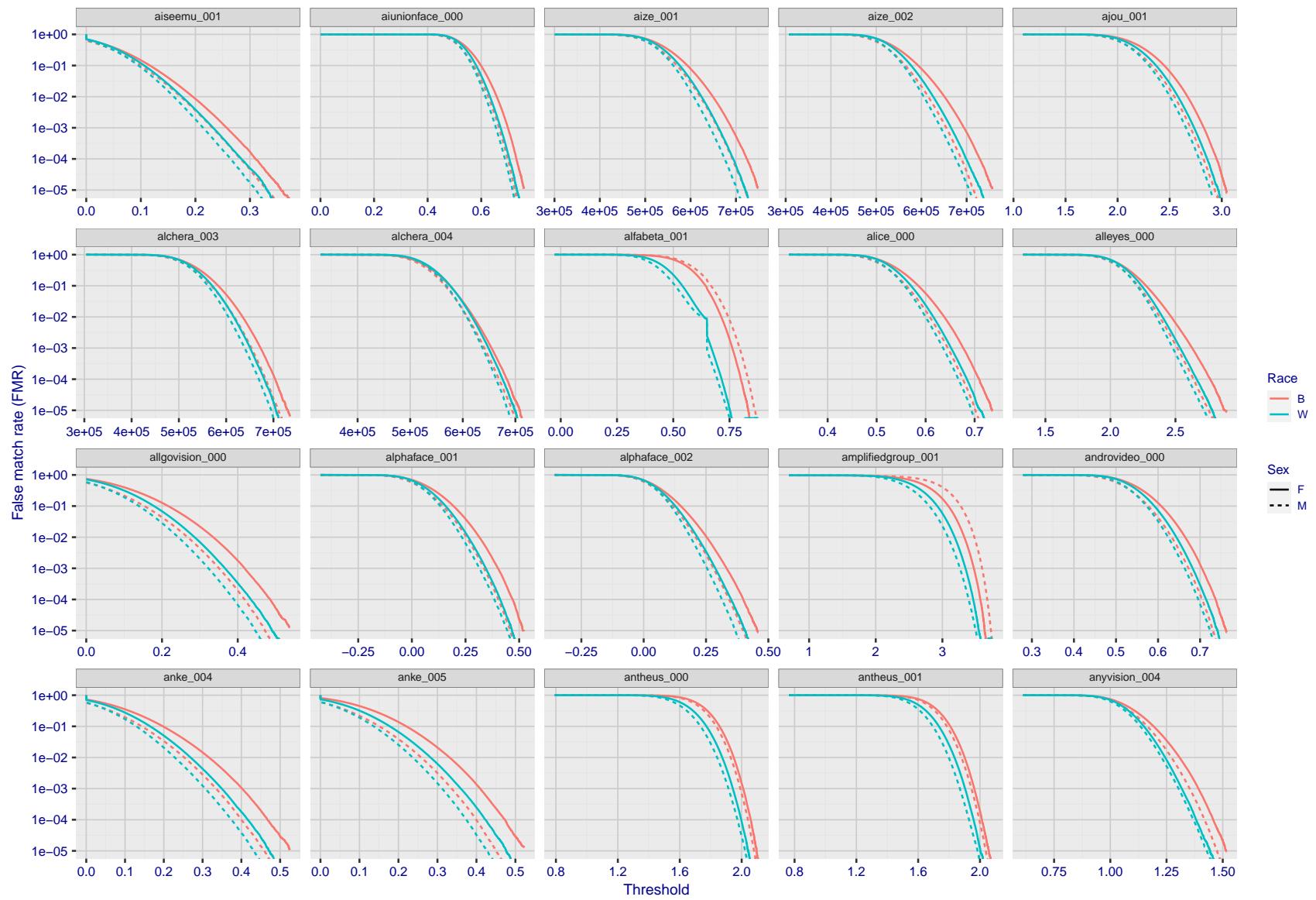


Figure 221: For the mugshot images, the false match calibration curves show false match rate vs. threshold. Separate curves appear for white females, black females, black males and white males.

2023/02/02 13:38:52

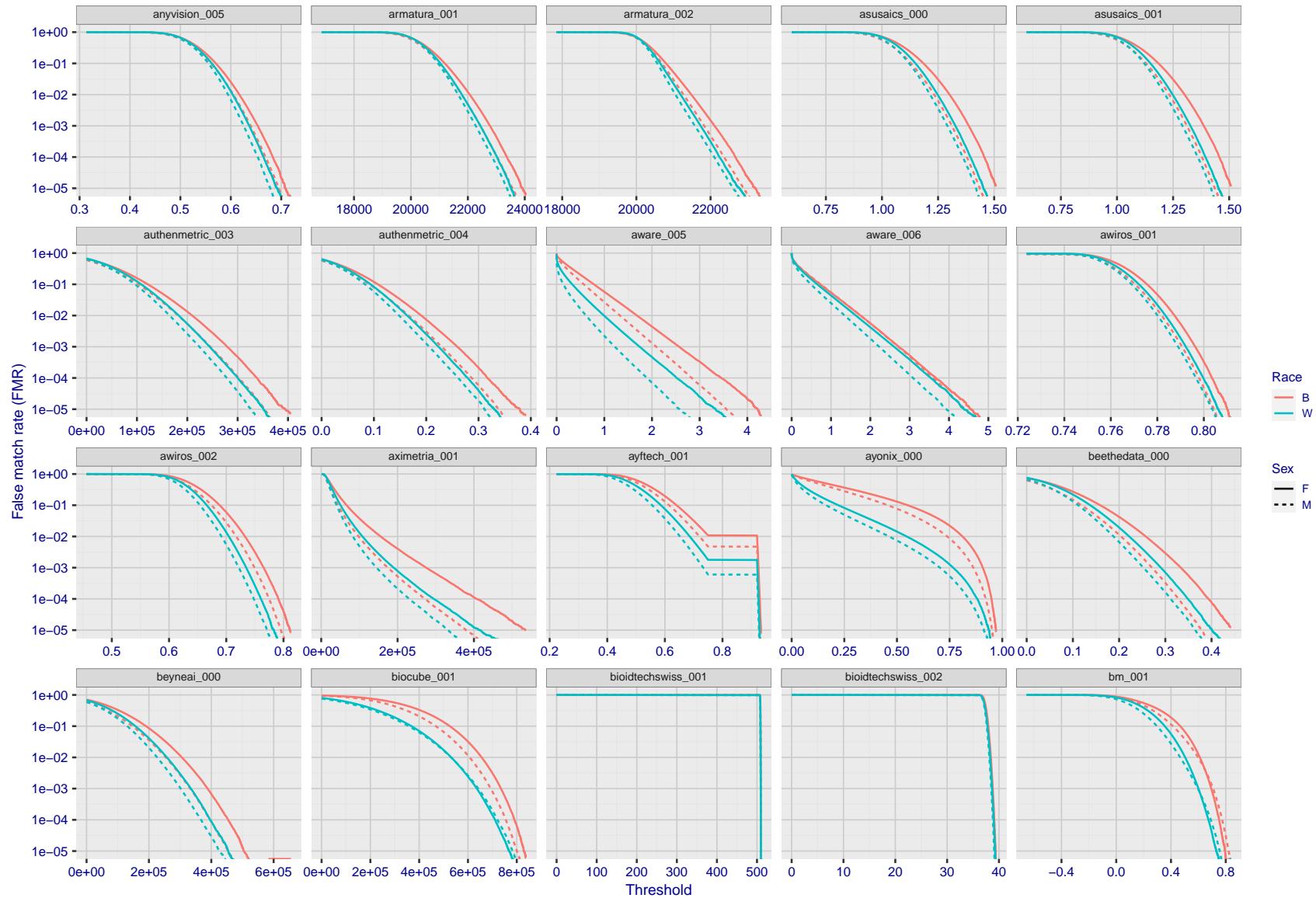


Figure 222: For the mugshot images, the false match calibration curves show false match rate vs. threshold. Separate curves appear for white females, black females, black males and white males.

2023/02/02 13:38:52

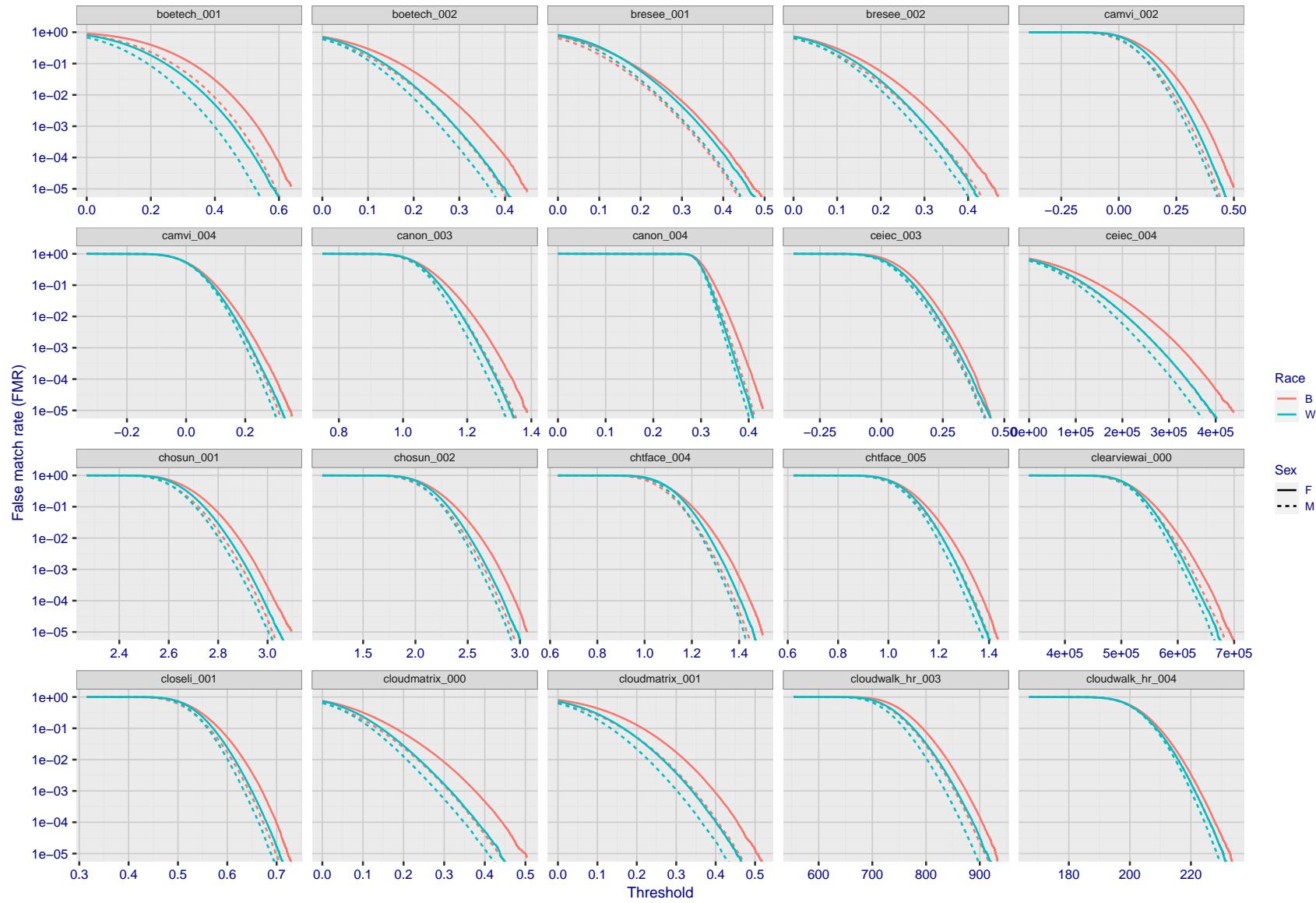


Figure 223: For the mugshot images, the false match calibration curves show false match rate vs. threshold. Separate curves appear for white females, black females, black males and white males.

2023/02/02 13:38:52

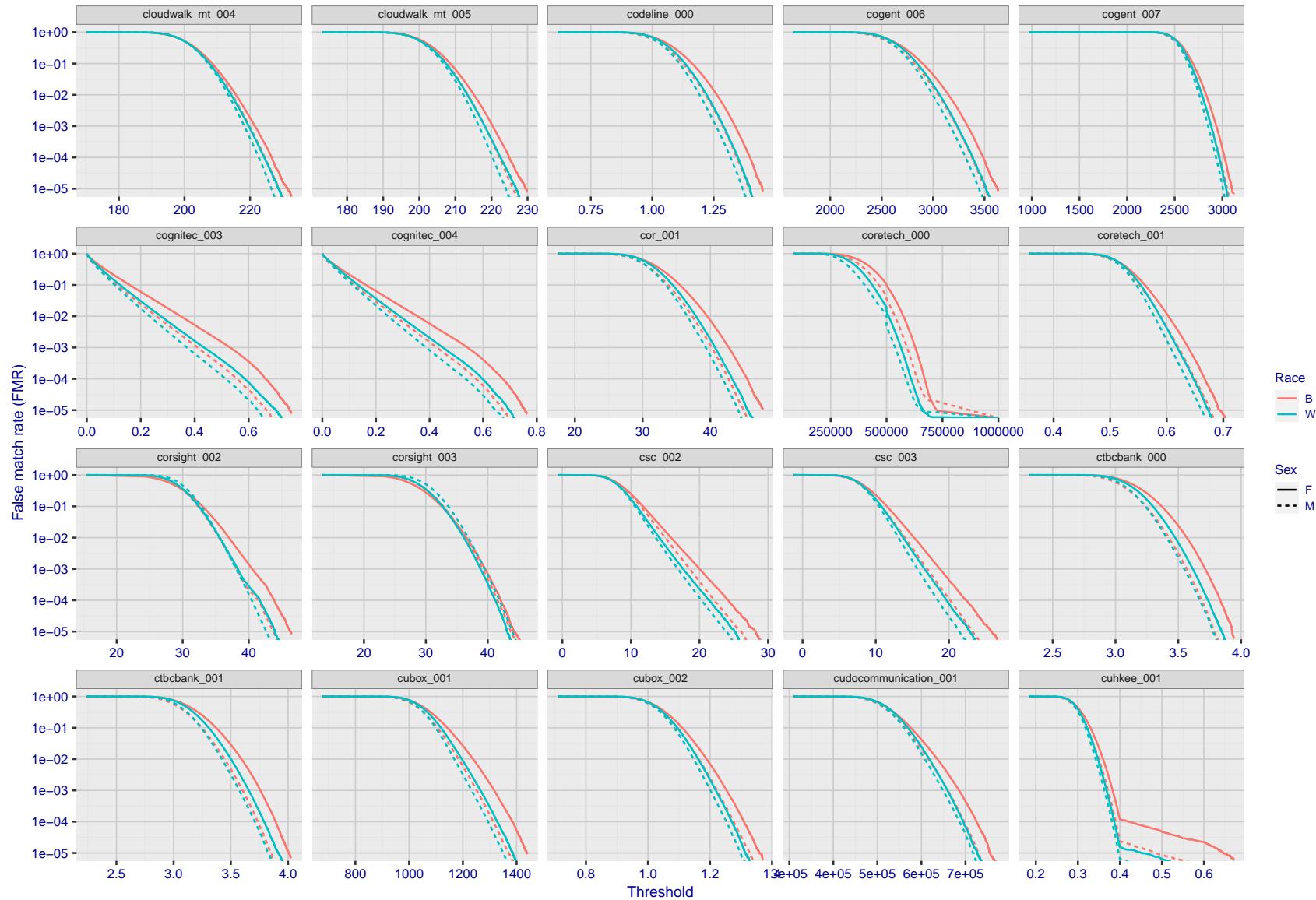


Figure 224: For the mugshot images, the false match calibration curves show false match rate vs. threshold. Separate curves appear for white females, black females, black males and white males.

2023/02/02 13:38:52

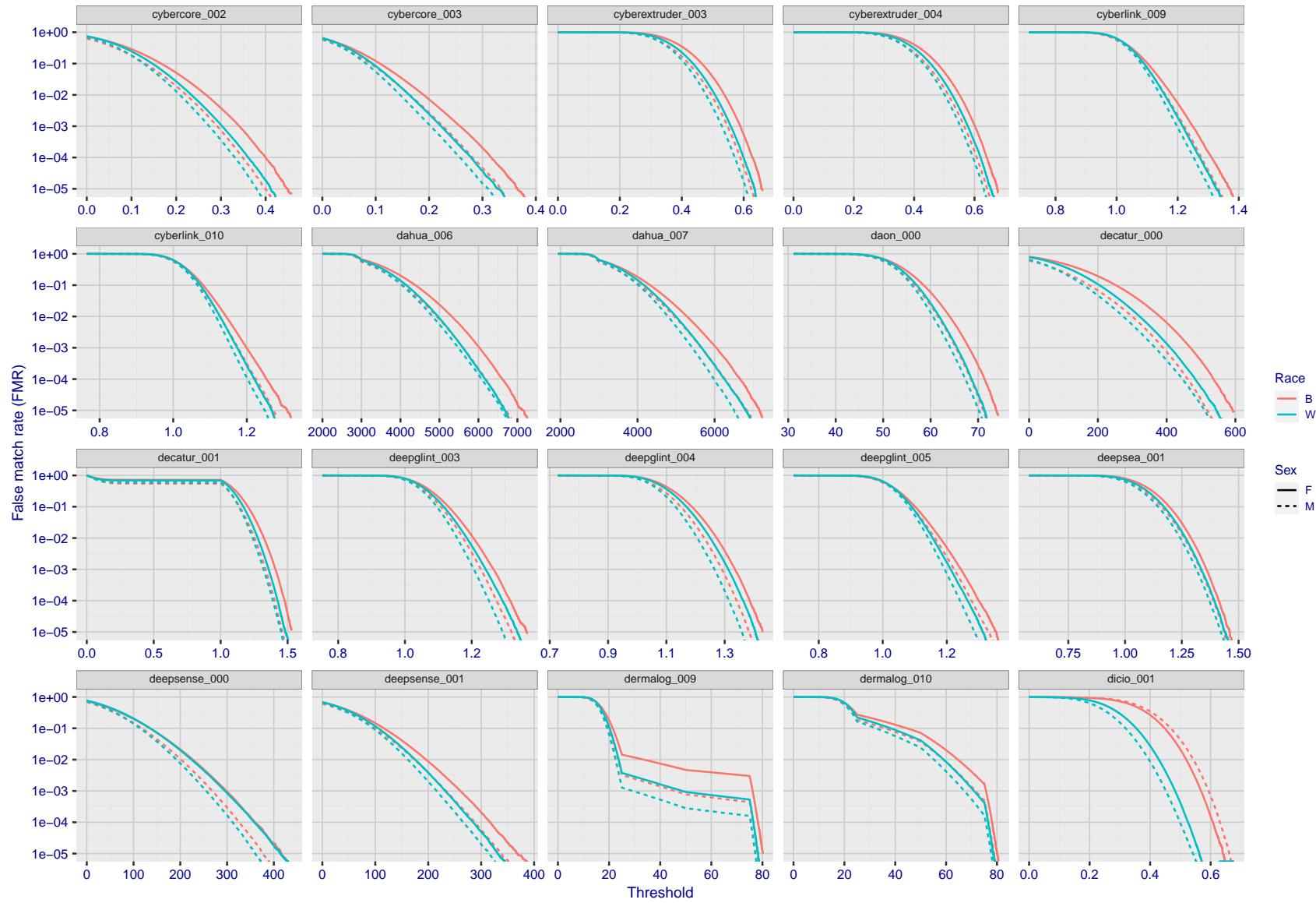


Figure 225: For the mugshot images, the false match calibration curves show false match rate vs. threshold. Separate curves appear for white females, black females, black males and white males.

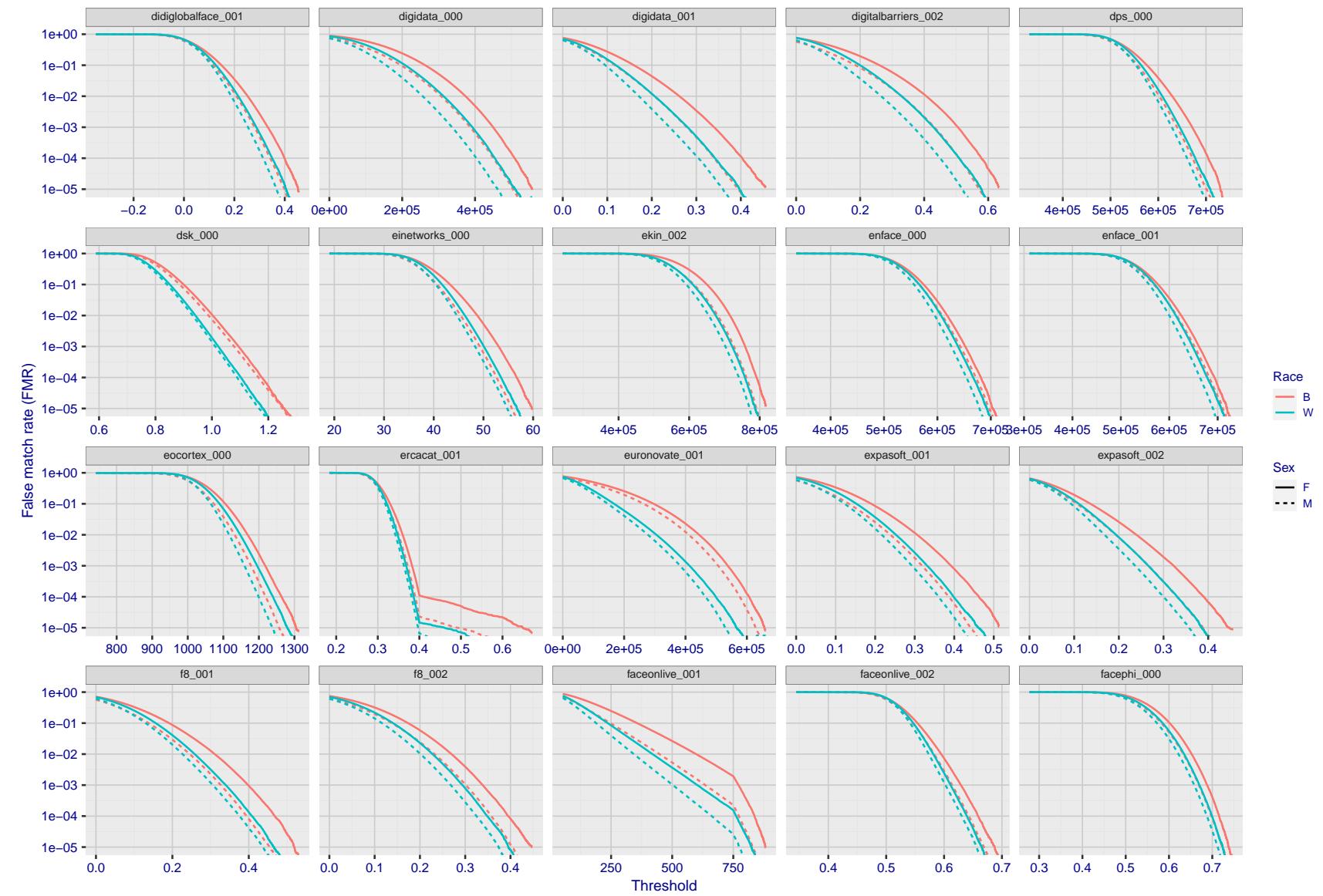


Figure 226: For the mugshot images, the false match calibration curves show false match rate vs. threshold. Separate curves appear for white females, black females, black males and white males.

2023/02/02 13:38:52

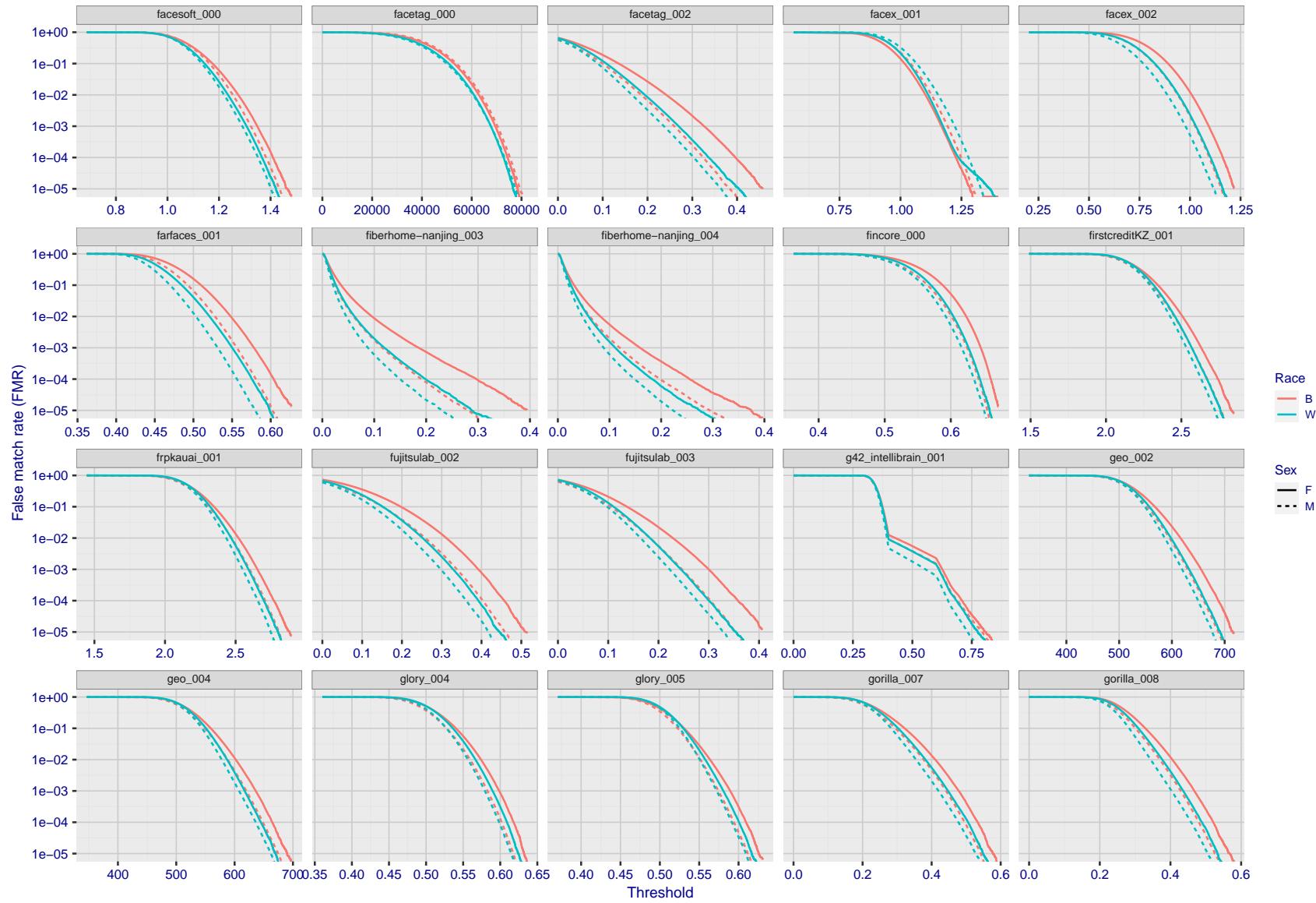


Figure 227: For the mugshot images, the false match calibration curves show false match rate vs. threshold. Separate curves appear for white females, black females, black males and white males.

2023/02/02 13:38:52

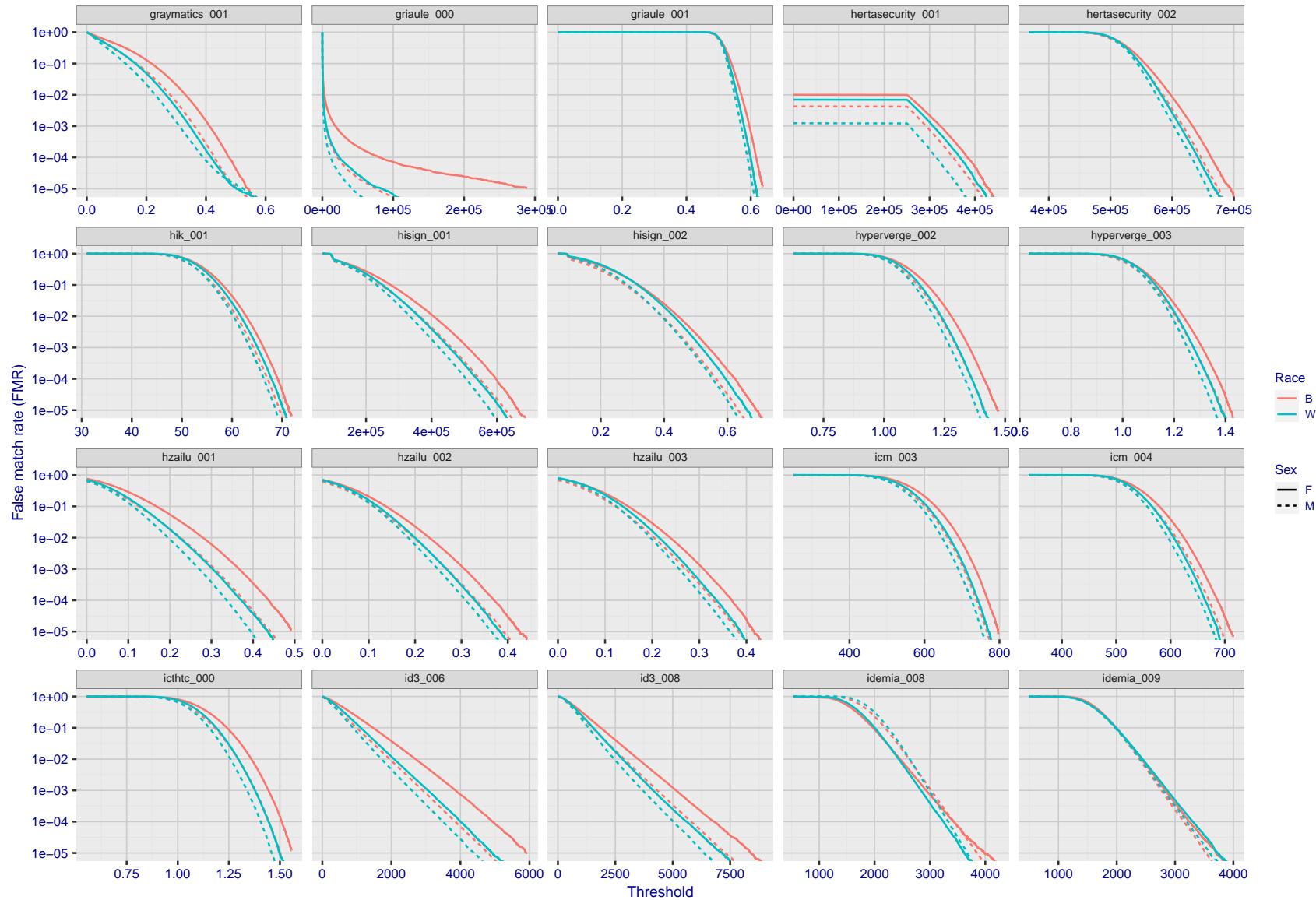


Figure 228: For the mugshot images, the false match calibration curves show false match rate vs. threshold. Separate curves appear for white females, black females, black males and white males.

2023/02/02 13:38:52

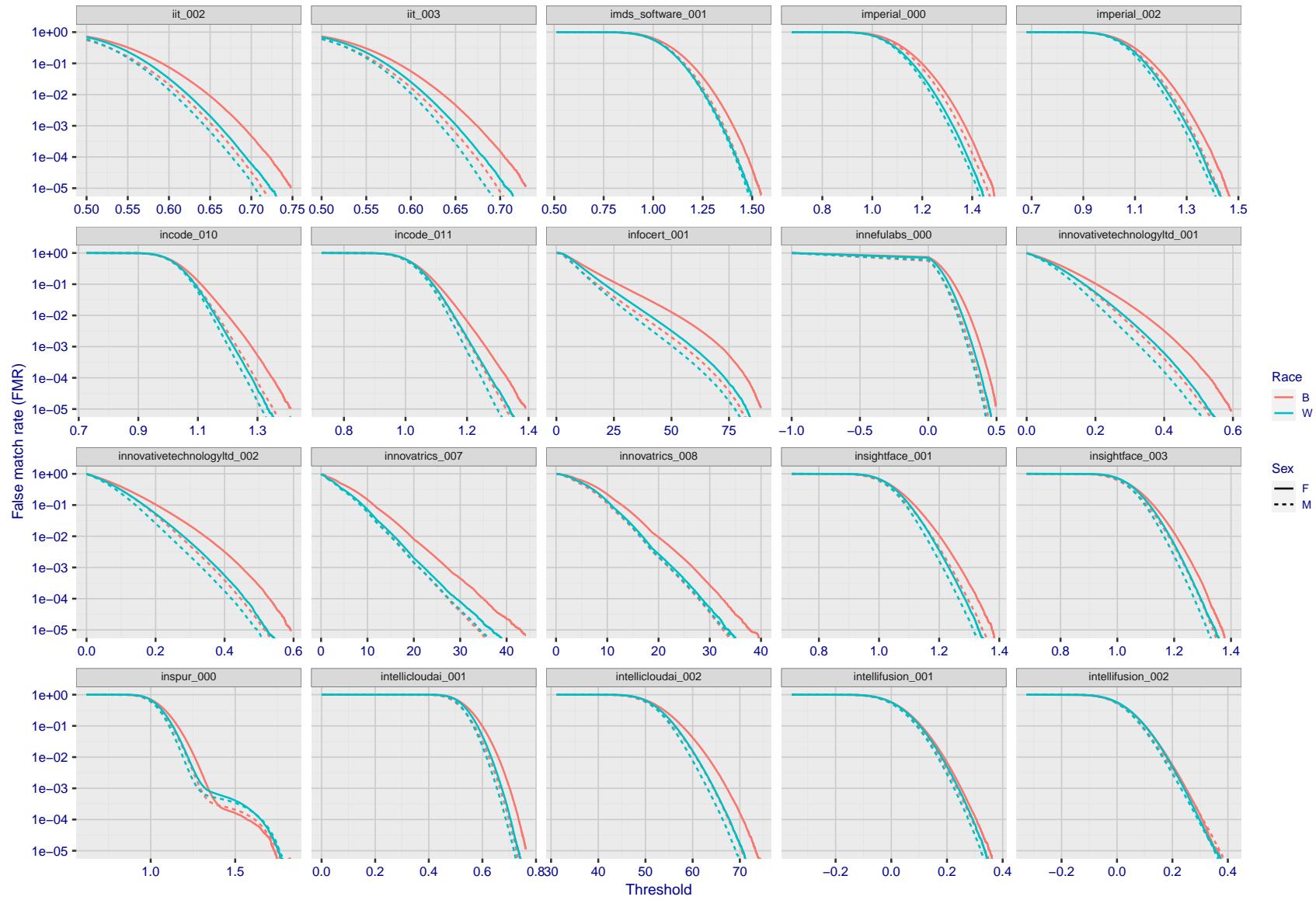


Figure 229: For the mugshot images, the false match calibration curves show false match rate vs. threshold. Separate curves appear for white females, black females, black males and white males.

2023/02/02 13:38:52

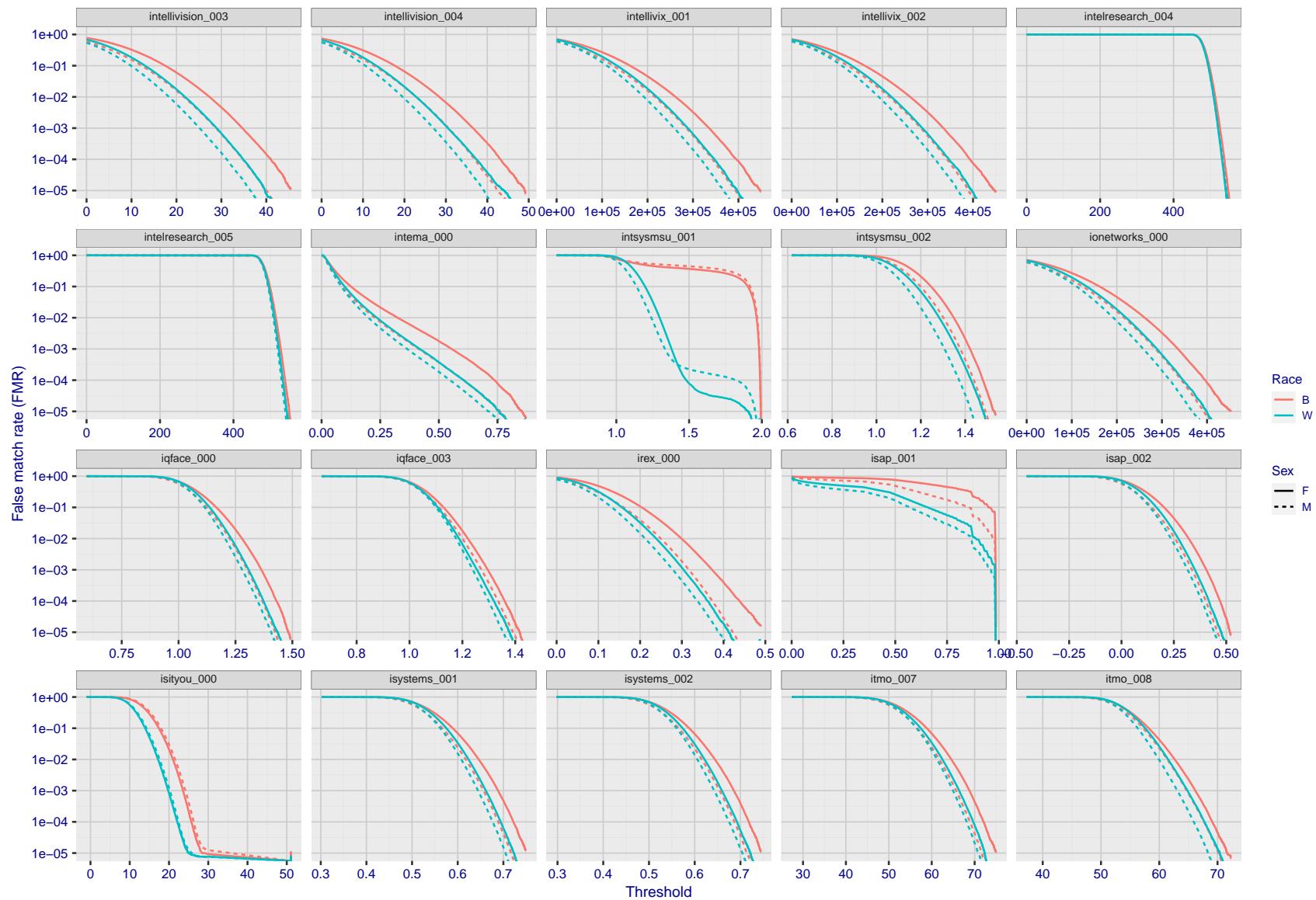


Figure 230: For the mugshot images, the false match calibration curves show false match rate vs. threshold. Separate curves appear for white females, black females, black males and white males.

2023/02/02 13:38:52

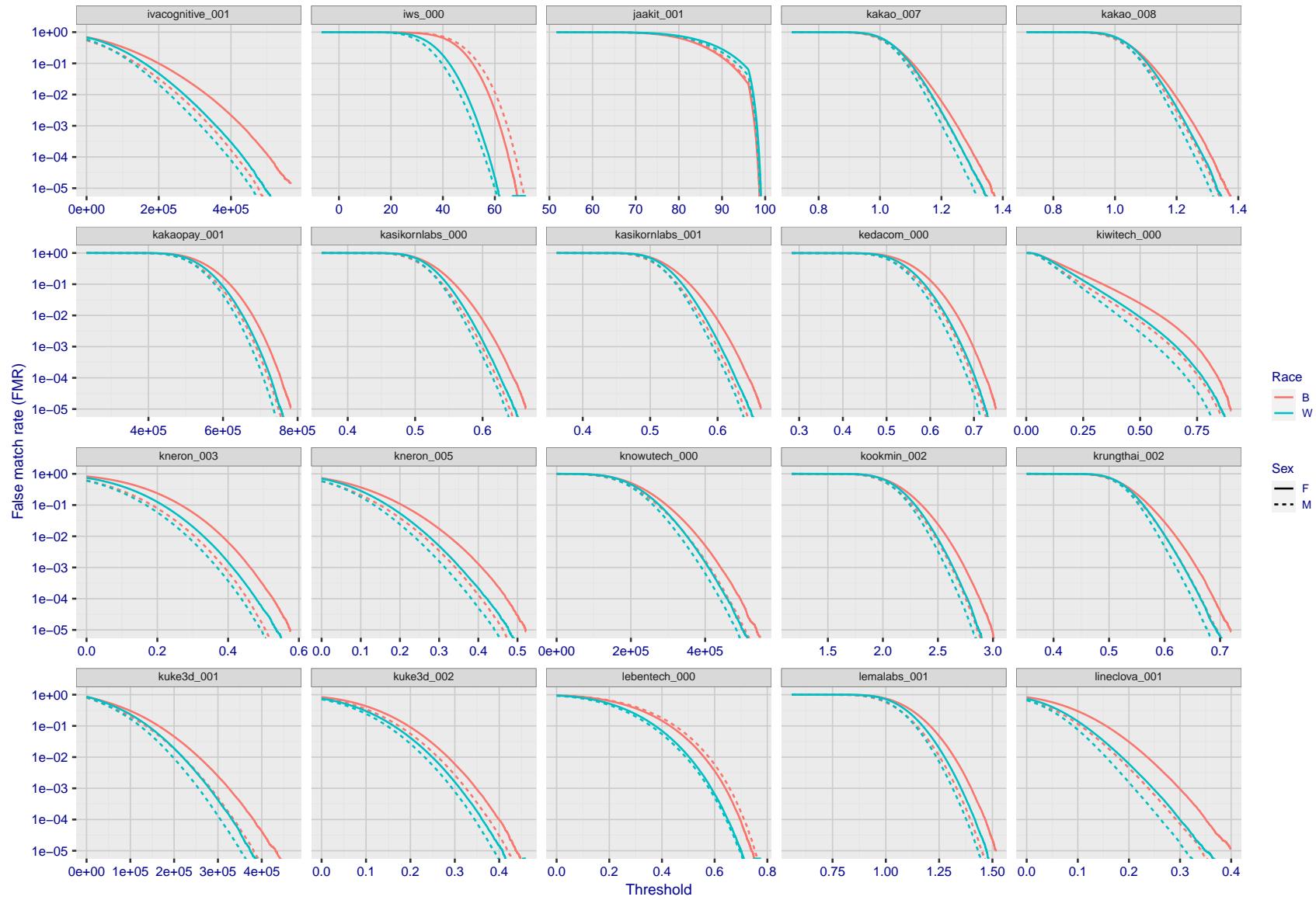


Figure 231: For the mugshot images, the false match calibration curves show false match rate vs. threshold. Separate curves appear for white females, black females, black males and white males.

FNMR(T)
"False non-match rate"FMR(T)
"False match rate"

2023/02/02 13:38:52

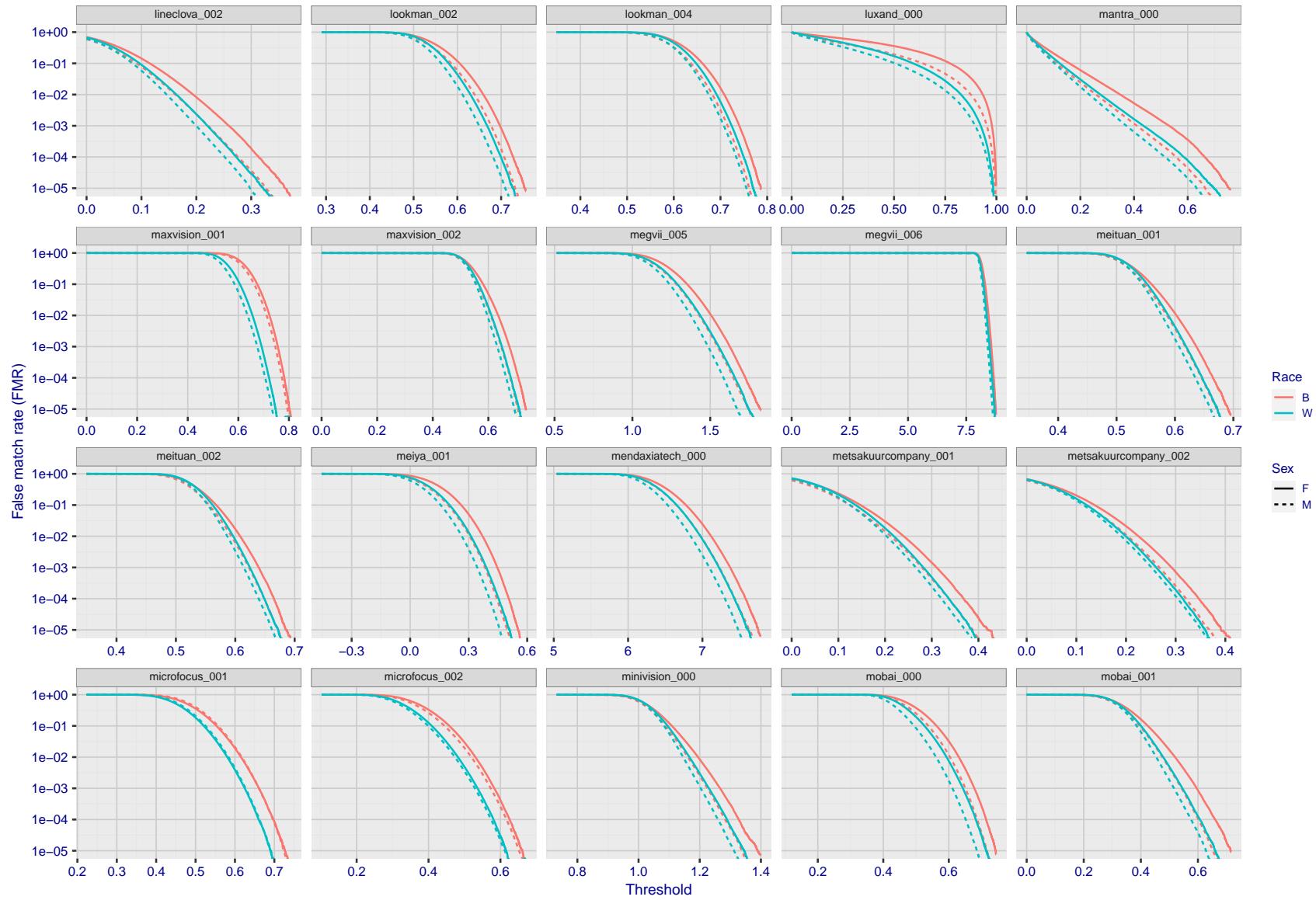


Figure 232: For the mugshot images, the false match calibration curves show false match rate vs. threshold. Separate curves appear for white females, black females, black males and white males.

2023/02/02 13:38:52

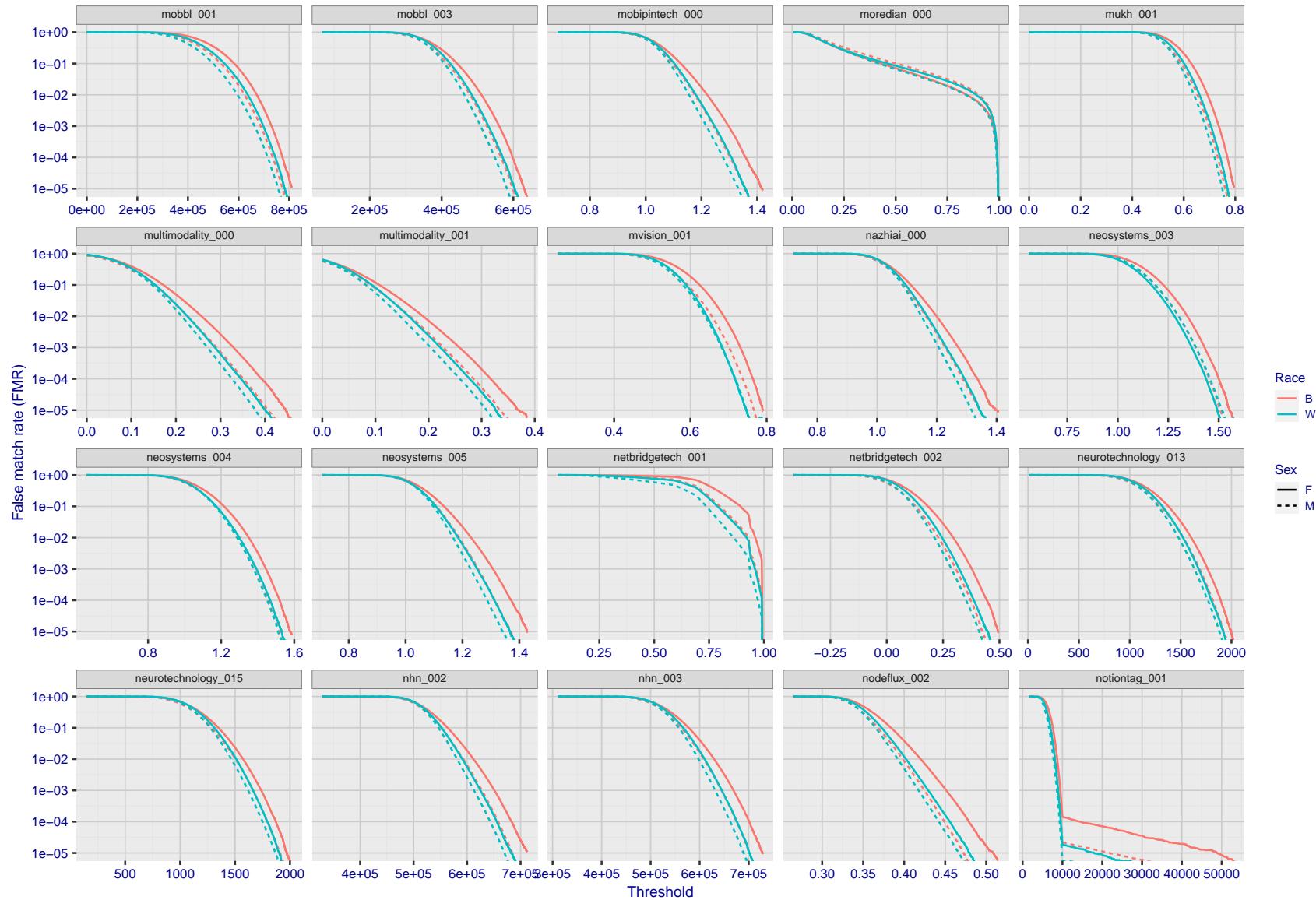


Figure 233: For the mugshot images, the false match calibration curves show false match rate vs. threshold. Separate curves appear for white females, black females, black males and white males.

FNMR(T)
"False non-match rate"
"False match rate"

2023/02/02 13:38:52

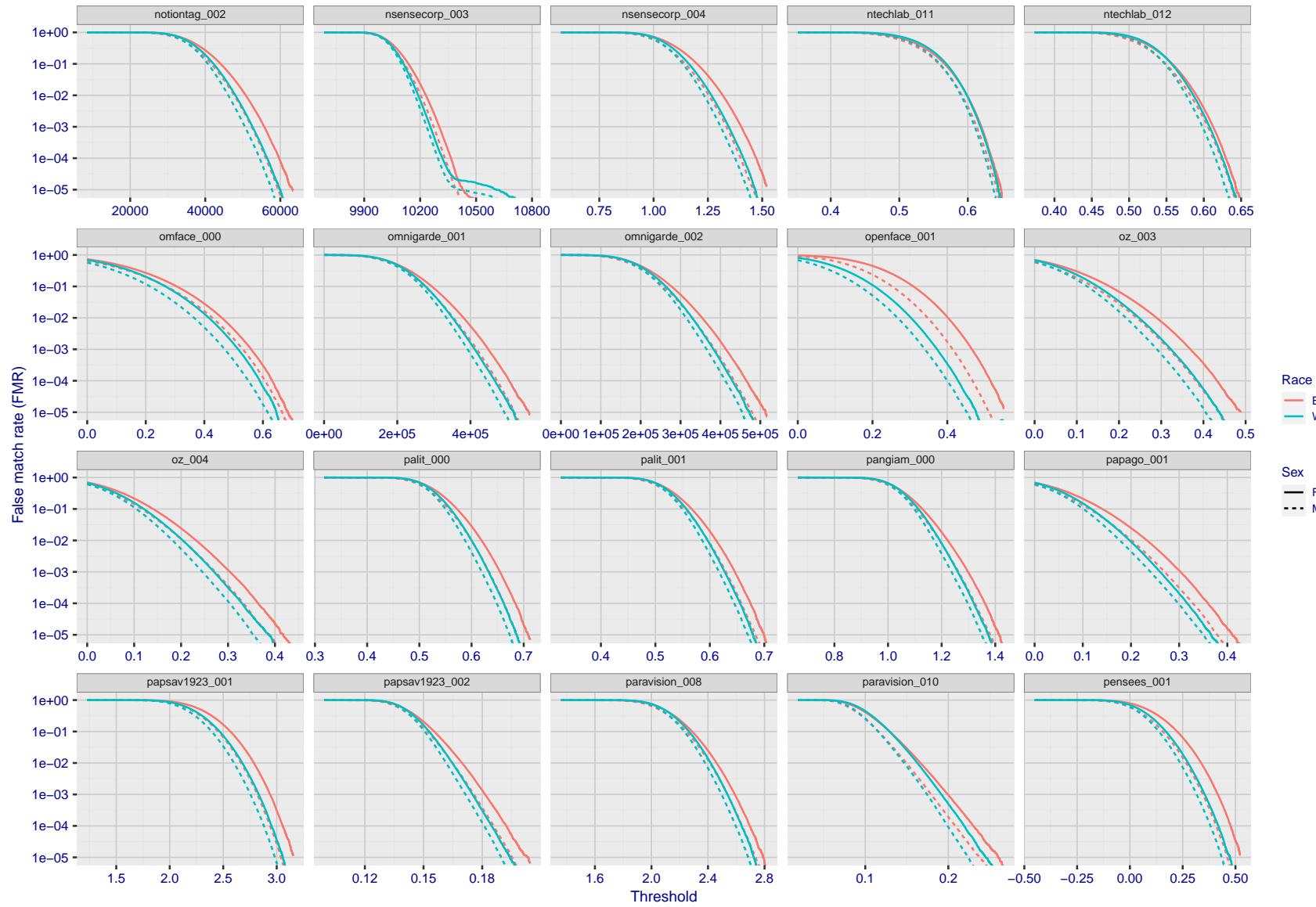


Figure 234: For the mugshot images, the false match calibration curves show false match rate vs. threshold. Separate curves appear for white females, black females, black males and white males.

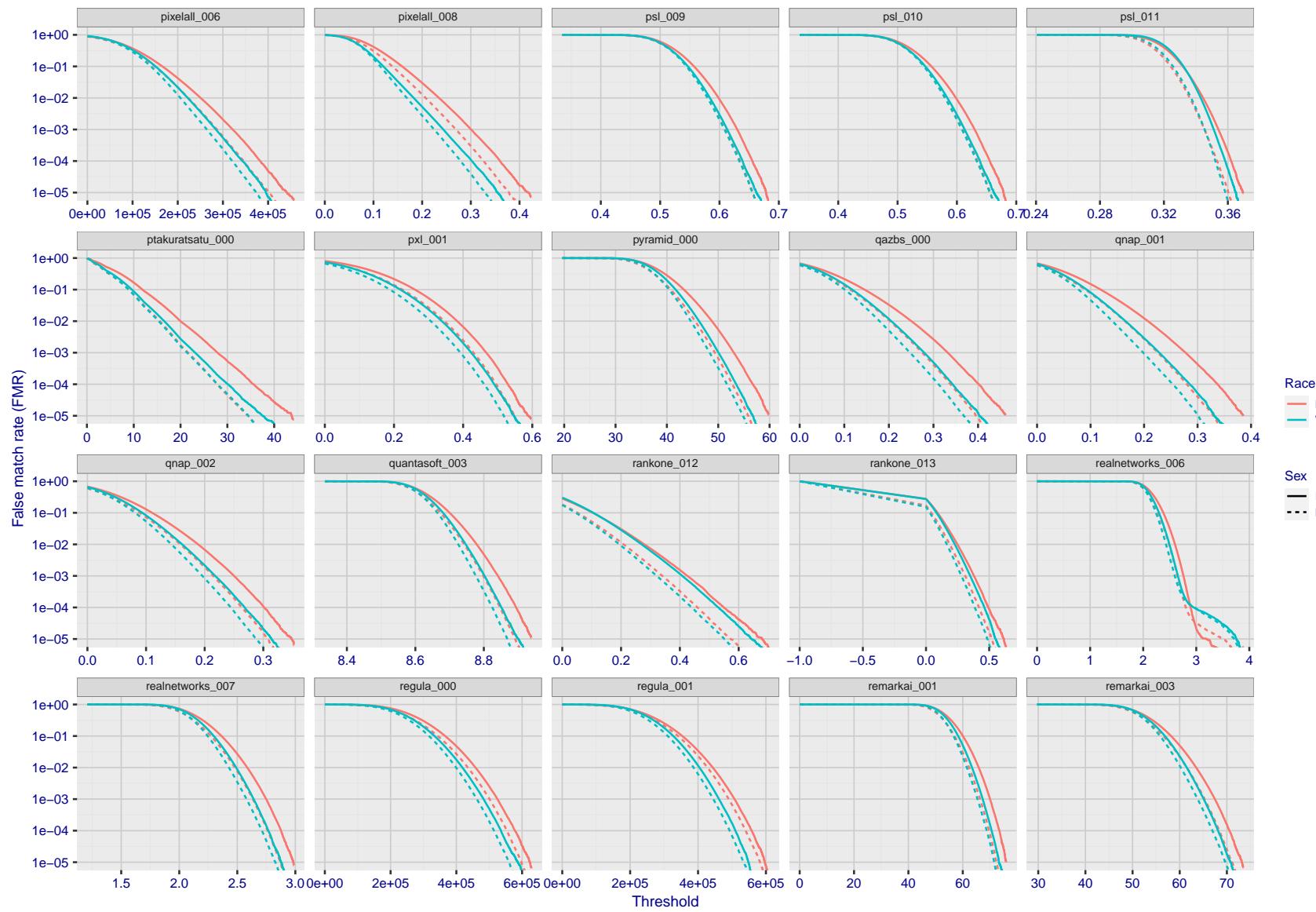


Figure 235: For the mugshot images, the false match calibration curves show false match rate vs. threshold. Separate curves appear for white females, black females, black males and white males.

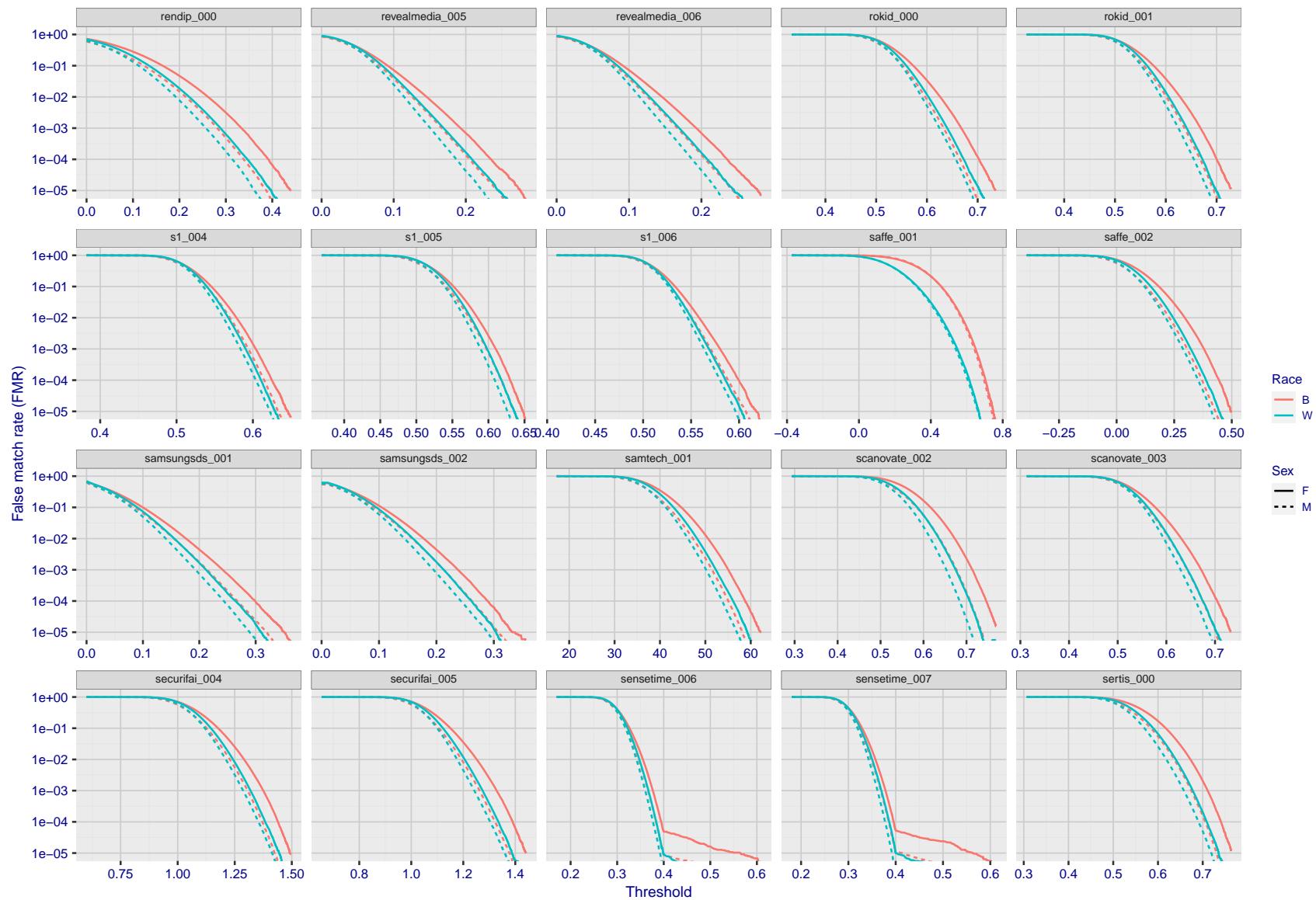


Figure 236: For the mugshot images, the false match calibration curves show false match rate vs. threshold. Separate curves appear for white females, black females, black males and white males.

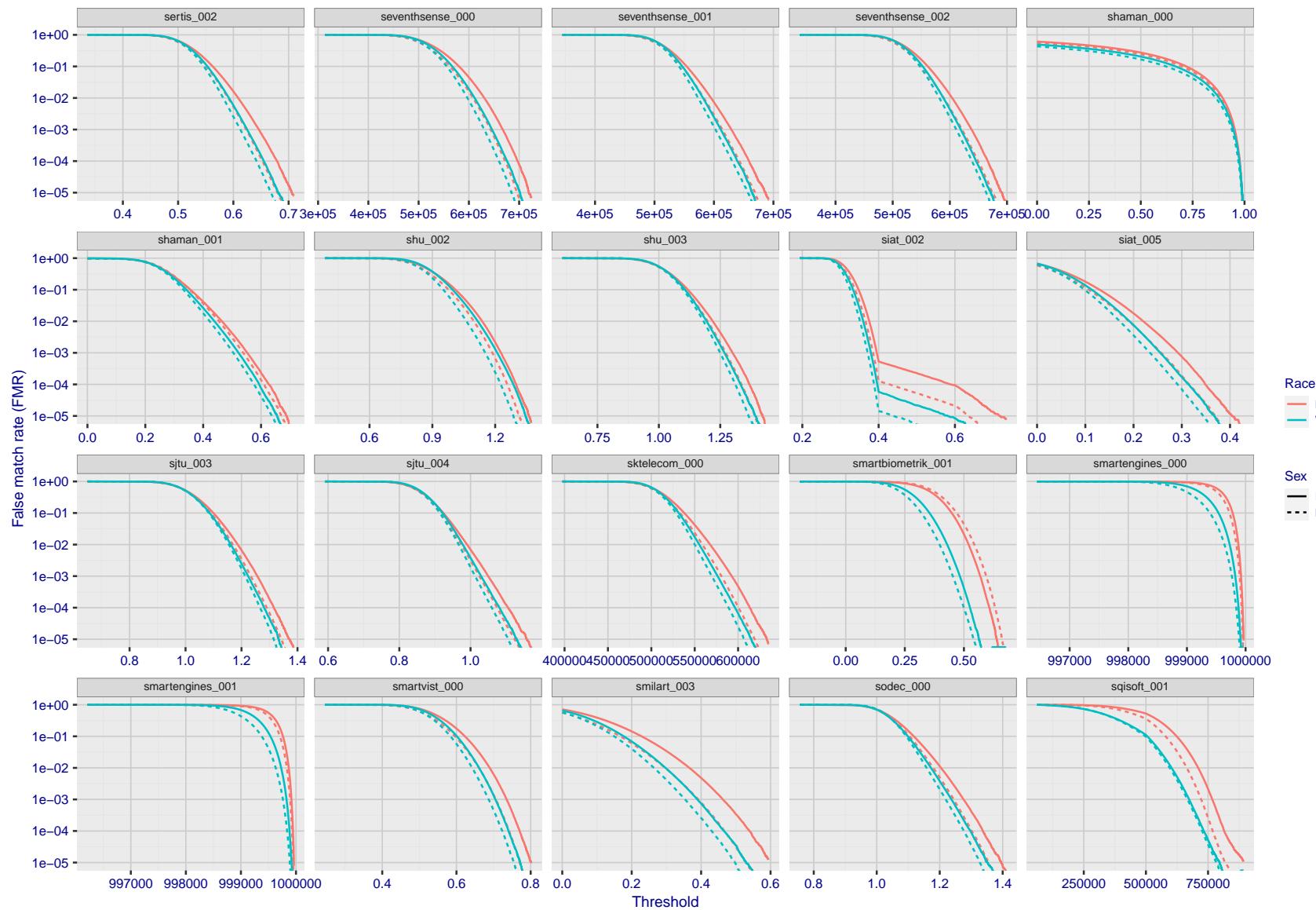


Figure 237: For the mugshot images, the false match calibration curves show false match rate vs. threshold. Separate curves appear for white females, black females, black males and white males.

2023/02/02 13:38:52

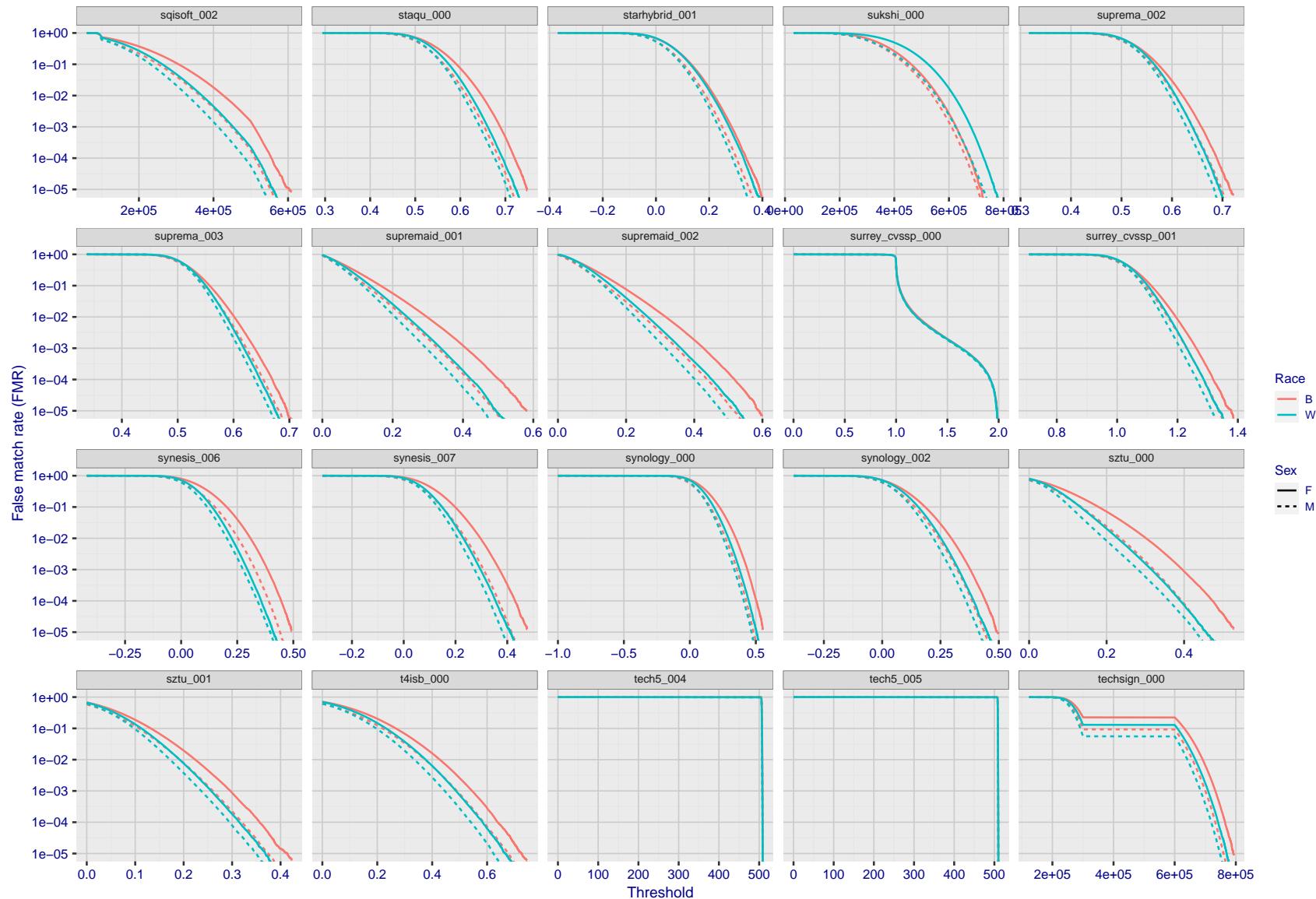


Figure 238: For the mugshot images, the false match calibration curves show false match rate vs. threshold. Separate curves appear for white females, black females, black males and white males.

FNMR(T)
"False non-match rate"
"False match rate"

2023/02/02 13:38:52

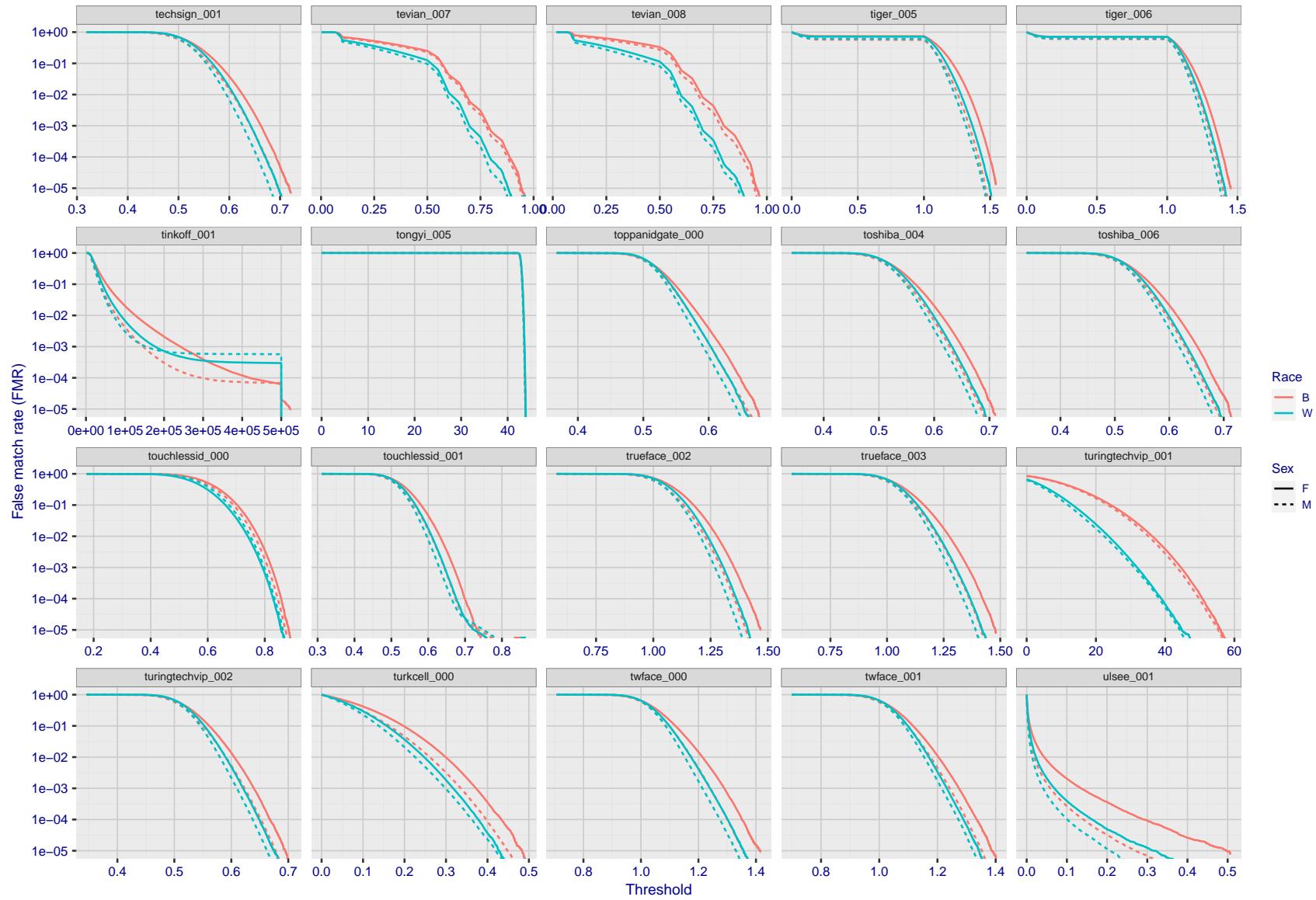


Figure 239: For the mugshot images, the false match calibration curves show false match rate vs. threshold. Separate curves appear for white females, black females, black males and white males.

2023/02/02 13:38:52

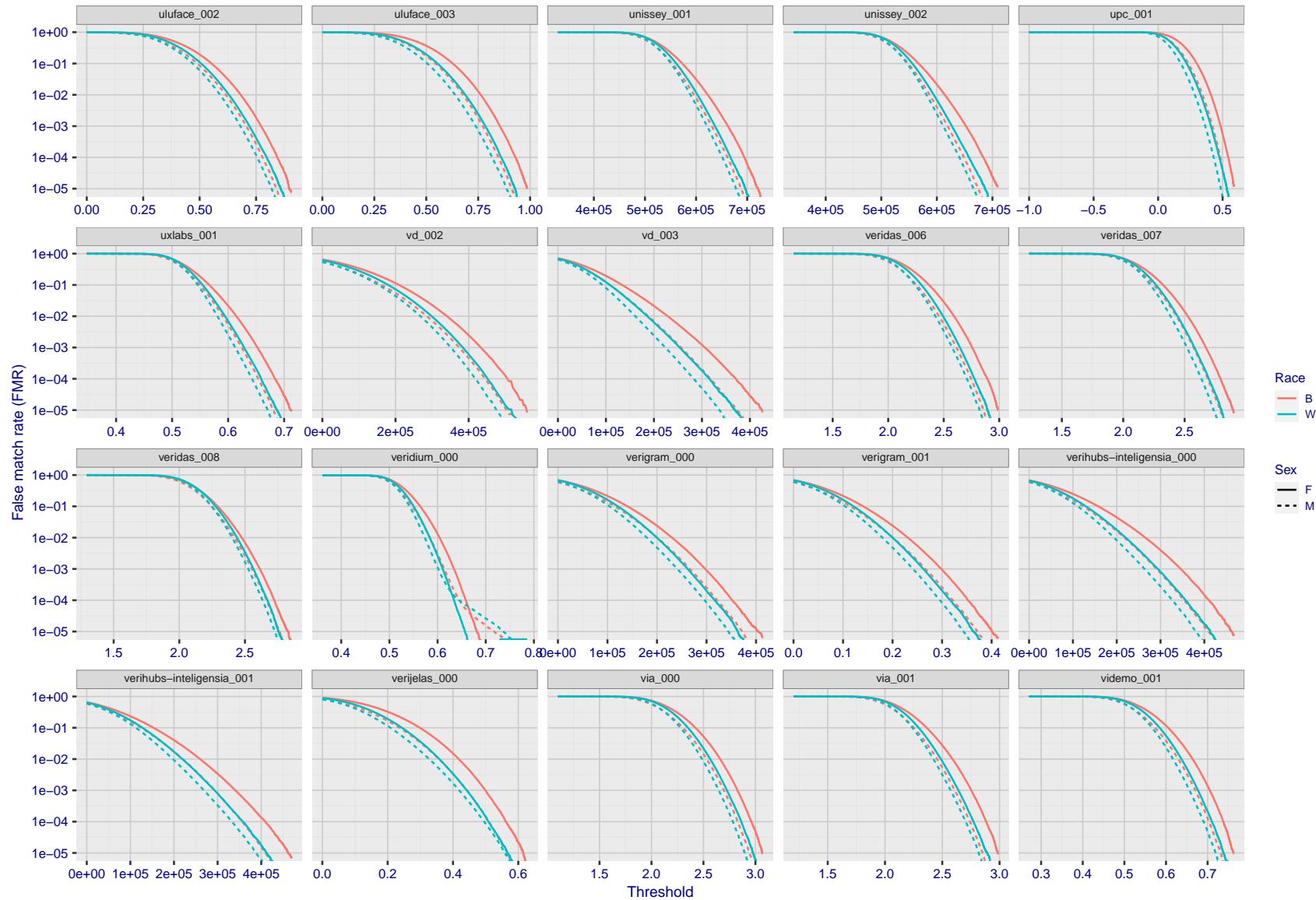


Figure 240: For the mugshot images, the false match calibration curves show false match rate vs. threshold. Separate curves appear for white females, black females, black males and white males.

FNMR(T)
"False non-match rate"
"False match rate"

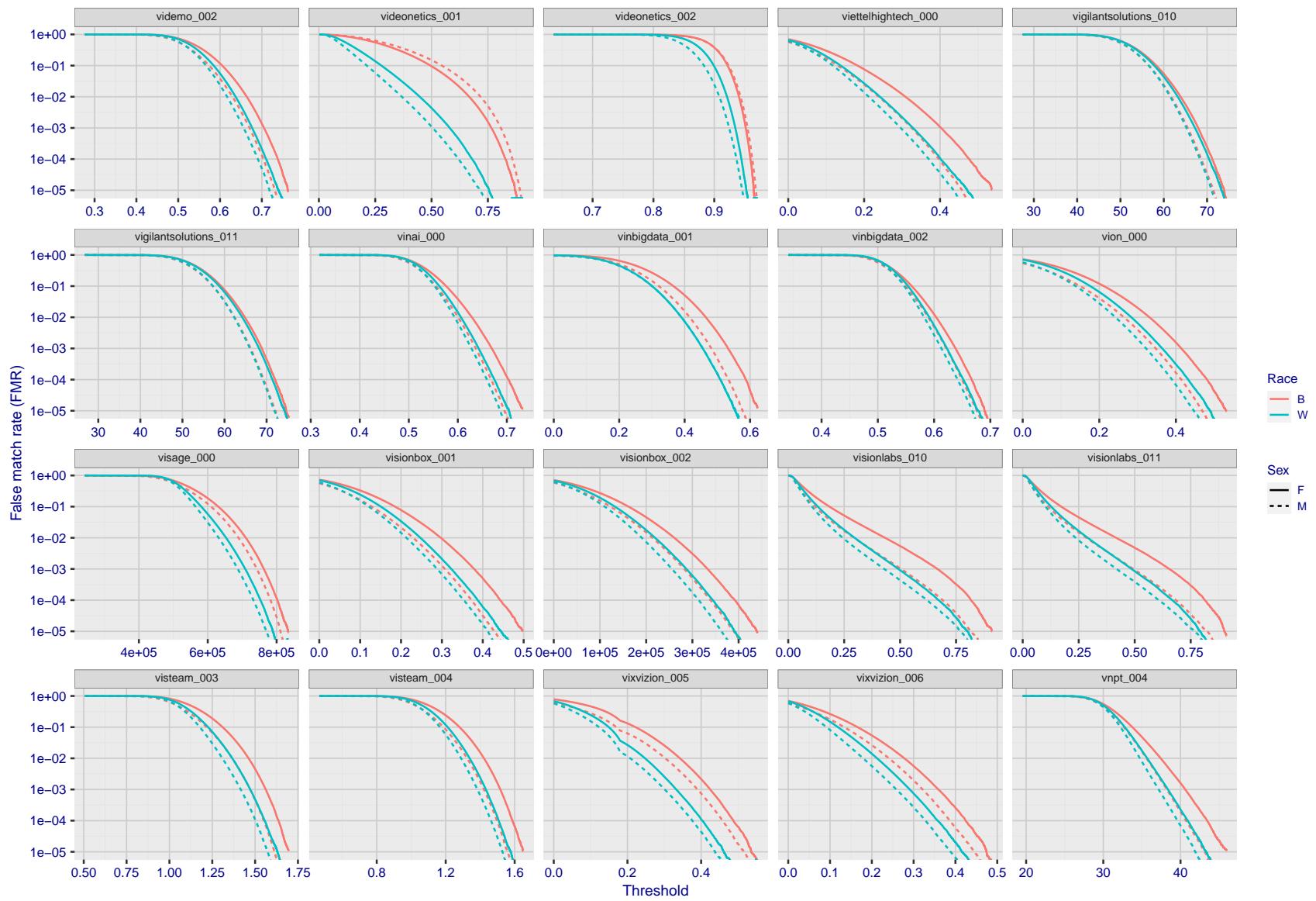


Figure 241: For the mugshot images, the false match calibration curves show false match rate vs. threshold. Separate curves appear for white females, black females, black males and white males.

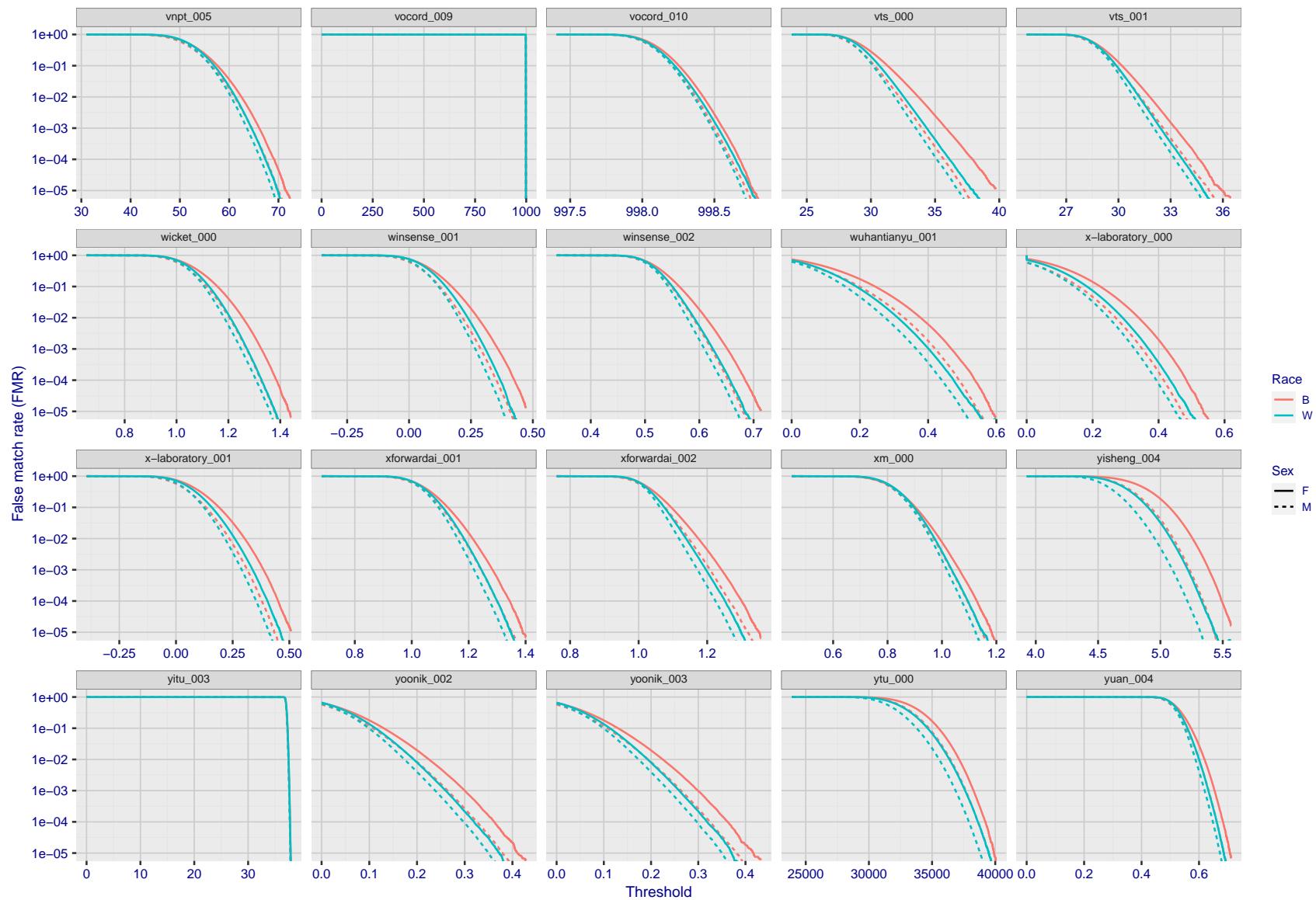


Figure 242: For the mugshot images, the false match calibration curves show false match rate vs. threshold. Separate curves appear for white females, black females, black males and white males.

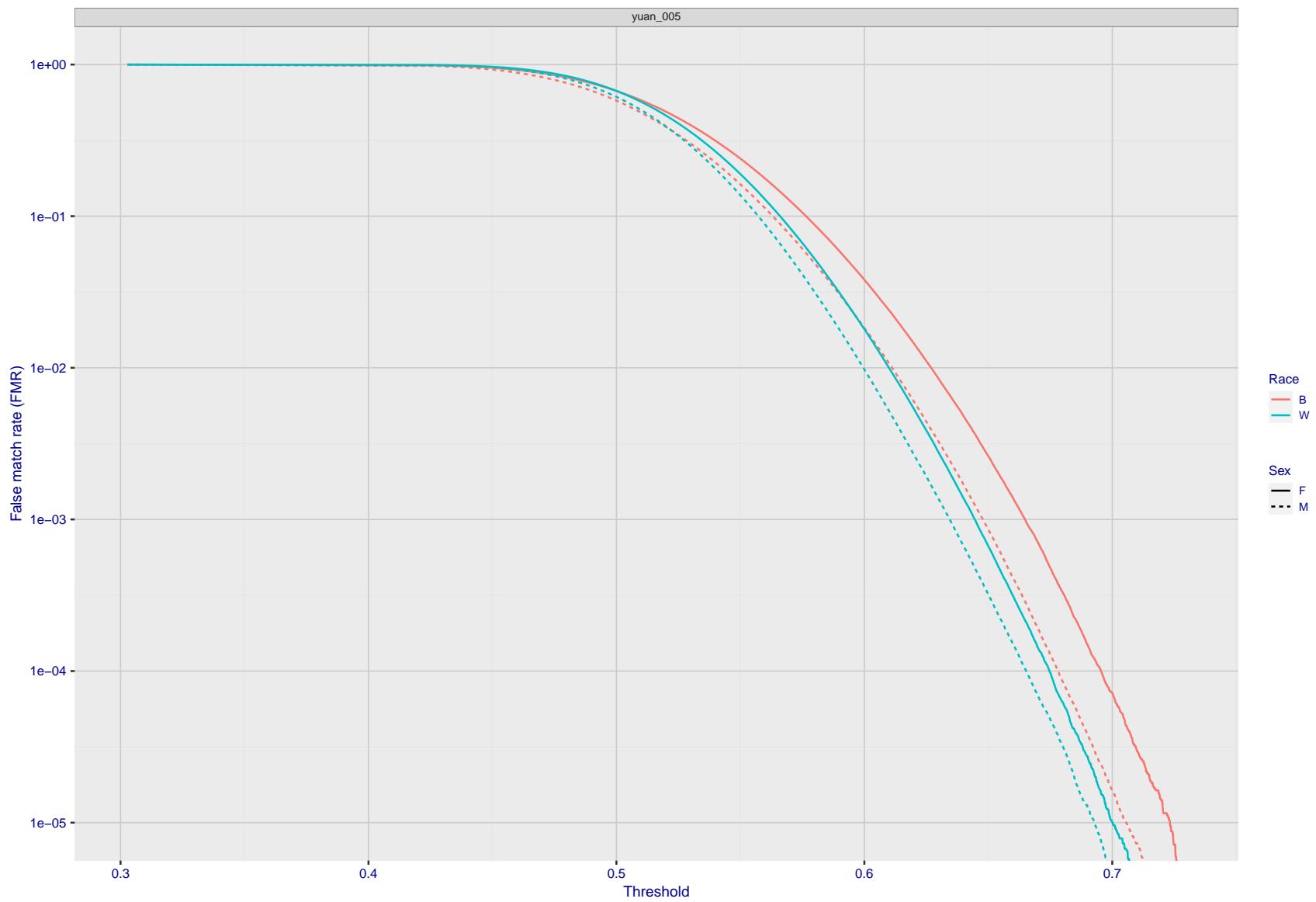


Figure 243: For the mugshot images, the false match calibration curves show false match rate vs. threshold. Separate curves appear for white females, black females, black males and white males.

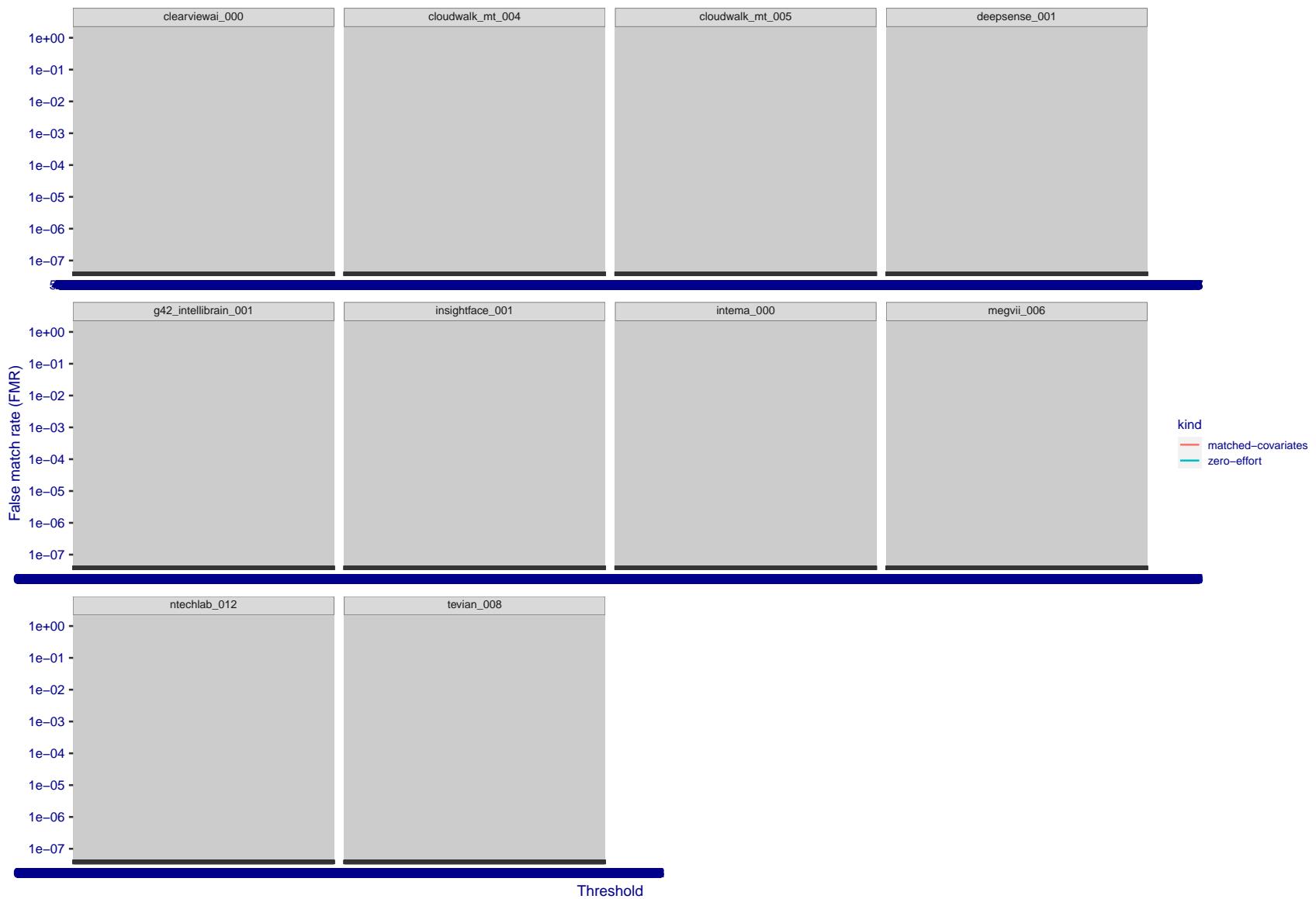


Figure 244: For the visa images, the false match calibration curves show FMR vs. threshold, T . The blue (lower) curves are for zero-effort impostors (i.e. comparing all images against all). The red (upper) curves are for persons of the same-sex, same-age, and same national-origin. This shows that FMR is underestimated (by a factor of 10 or more) by using a zero-effort impostor calculation to calibrate T . As shown later (sec. 3.6), FMR is higher for demographic-matched impostors.

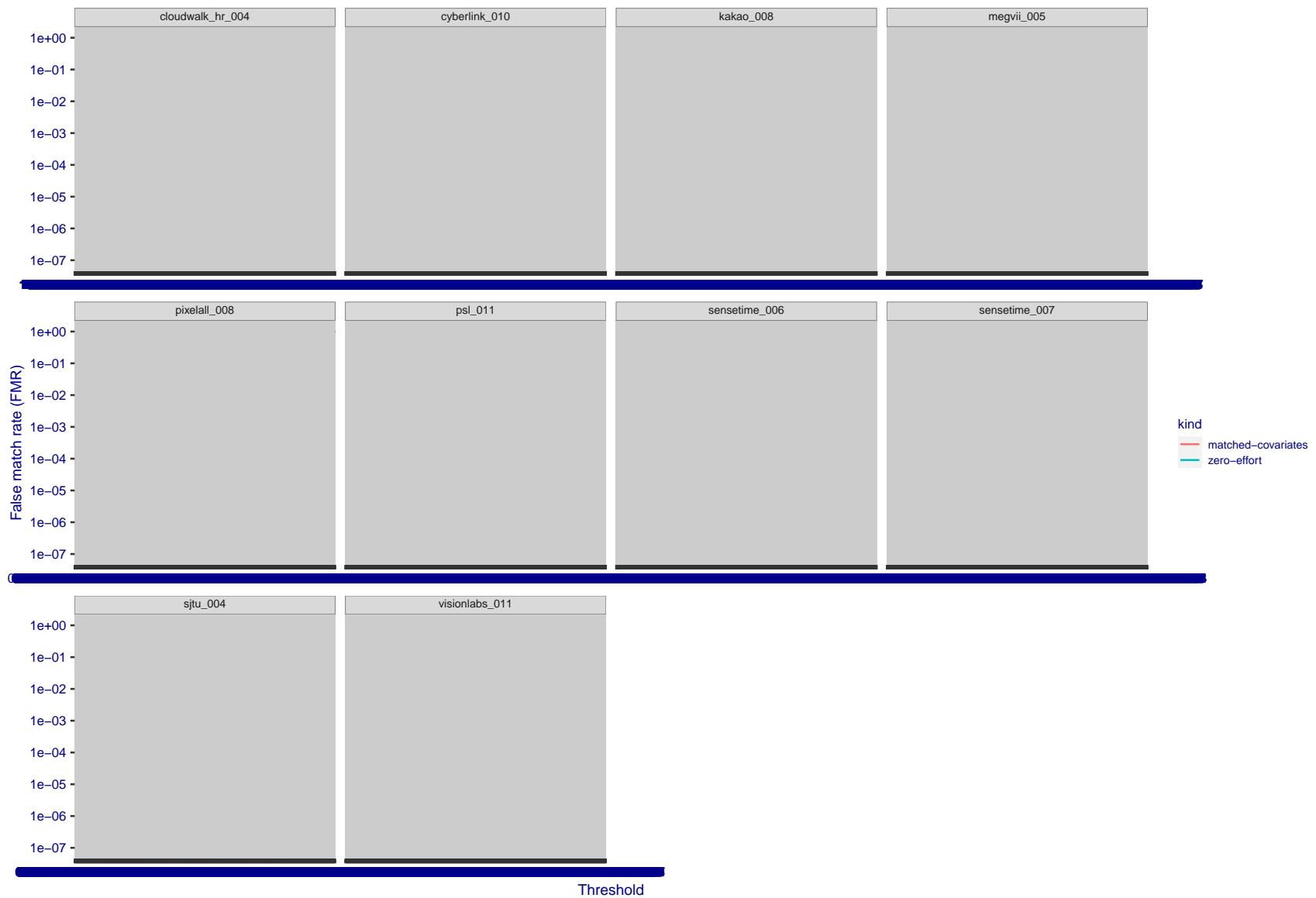


Figure 245: For the visa images, the false match calibration curves show FMR vs. threshold, T . The blue (lower) curves are for zero-effort impostors (i.e. comparing all images against all). The red (upper) curves are for persons of the same-sex, same-age, and same national-origin. This shows that FMR is underestimated (by a factor of 10 or more) by using a zero-effort impostor calculation to calibrate T . As shown later (sec. 3.6), FMR is higher for demographic-matched impostors.

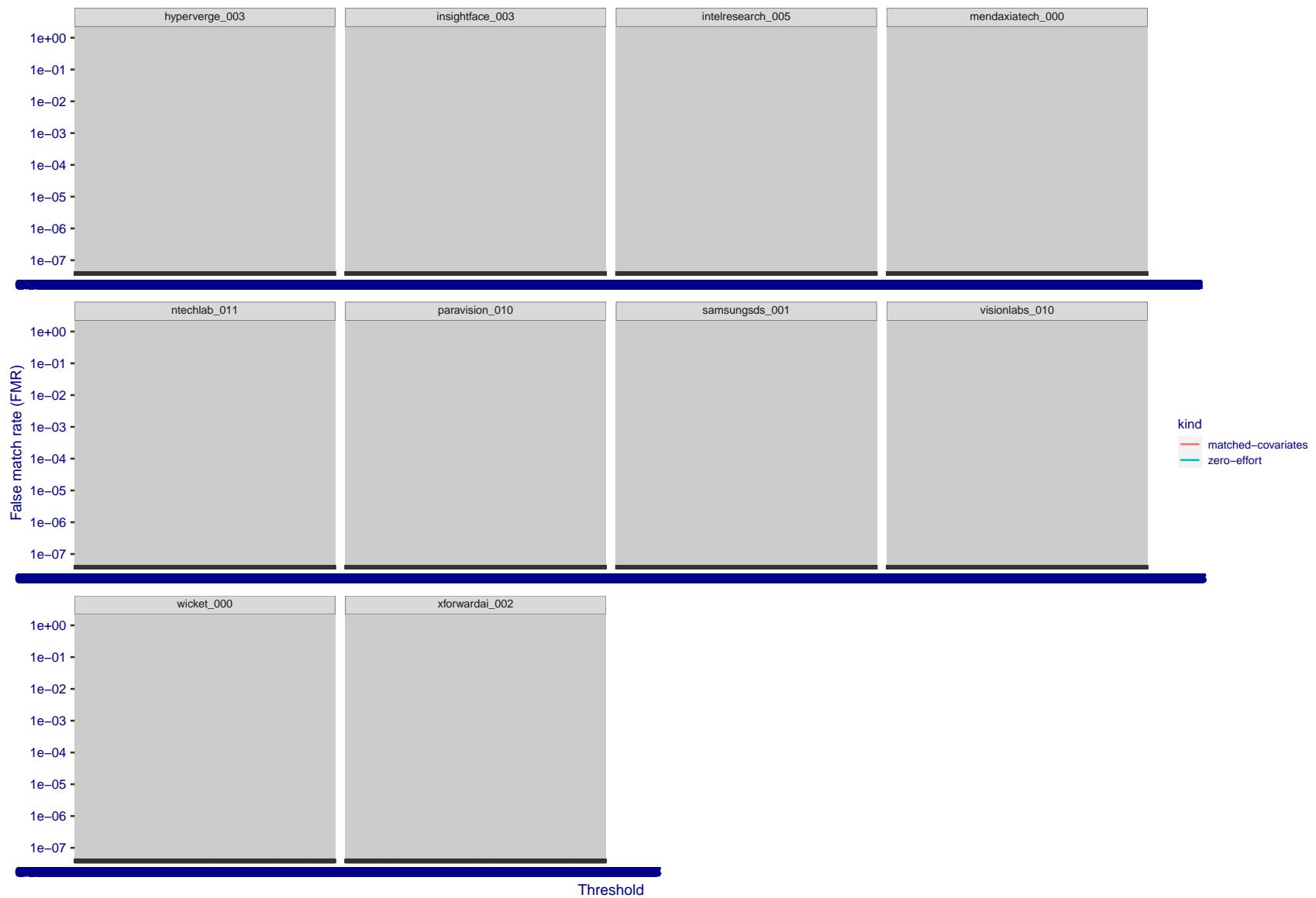


Figure 246: For the visa images, the false match calibration curves show FMR vs. threshold, T . The blue (lower) curves are for zero-effort impostors (i.e. comparing all images against all). The red (upper) curves are for persons of the same-sex, same-age, and same national-origin. This shows that FMR is underestimated (by a factor of 10 or more) by using a zero-effort impostor calculation to calibrate T . As shown later (sec. 3.6), FMR is higher for demographic-matched impostors.

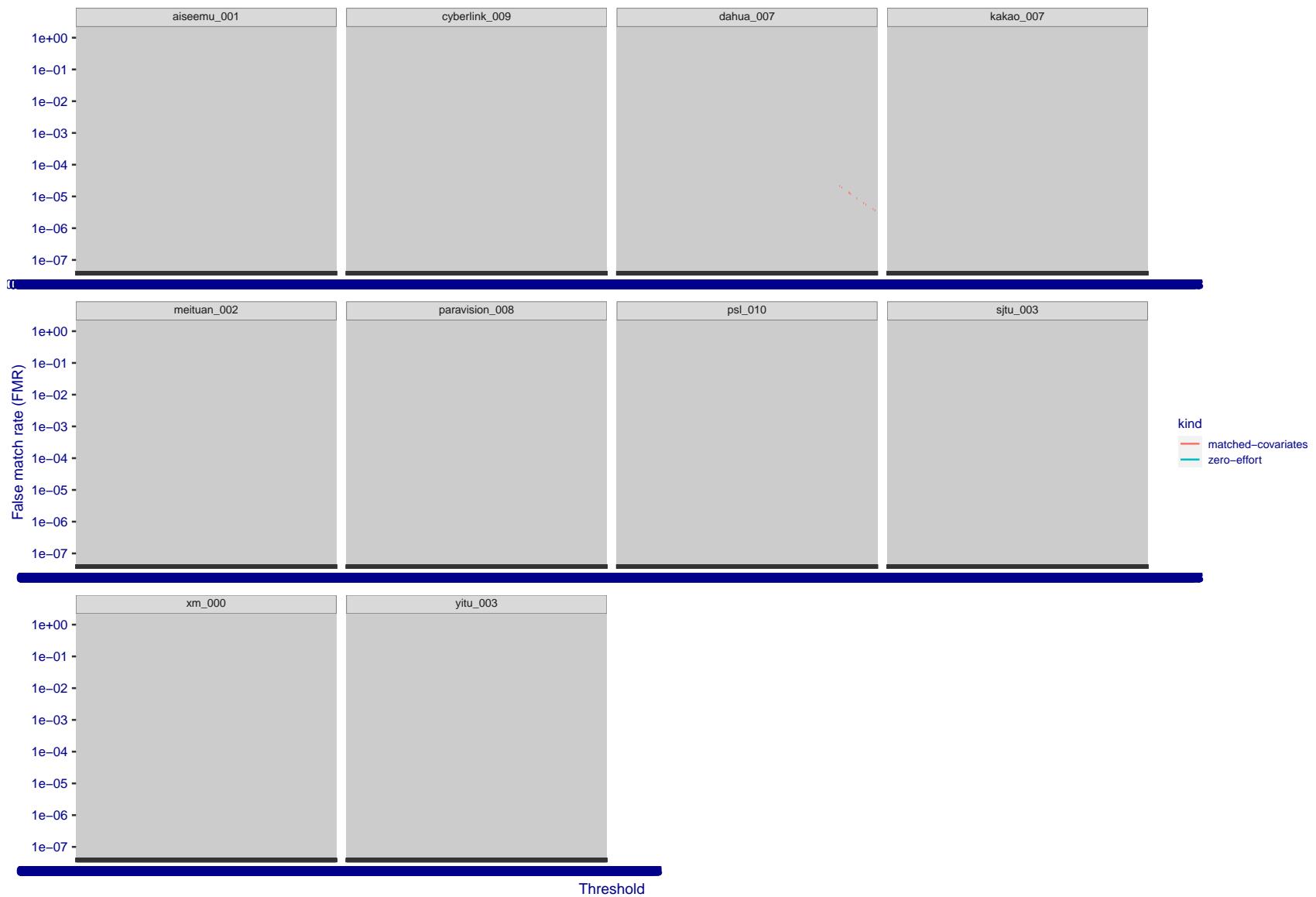


Figure 247: For the visa images, the false match calibration curves show FMR vs. threshold, T . The blue (lower) curves are for zero-effort impostors (i.e. comparing all images against all). The red (upper) curves are for persons of the same-sex, same-age, and same national-origin. This shows that FMR is underestimated (by a factor of 10 or more) by using a zero-effort impostor calculation to calibrate T . As shown later (sec. 3.6), FMR is higher for demographic-matched impostors.

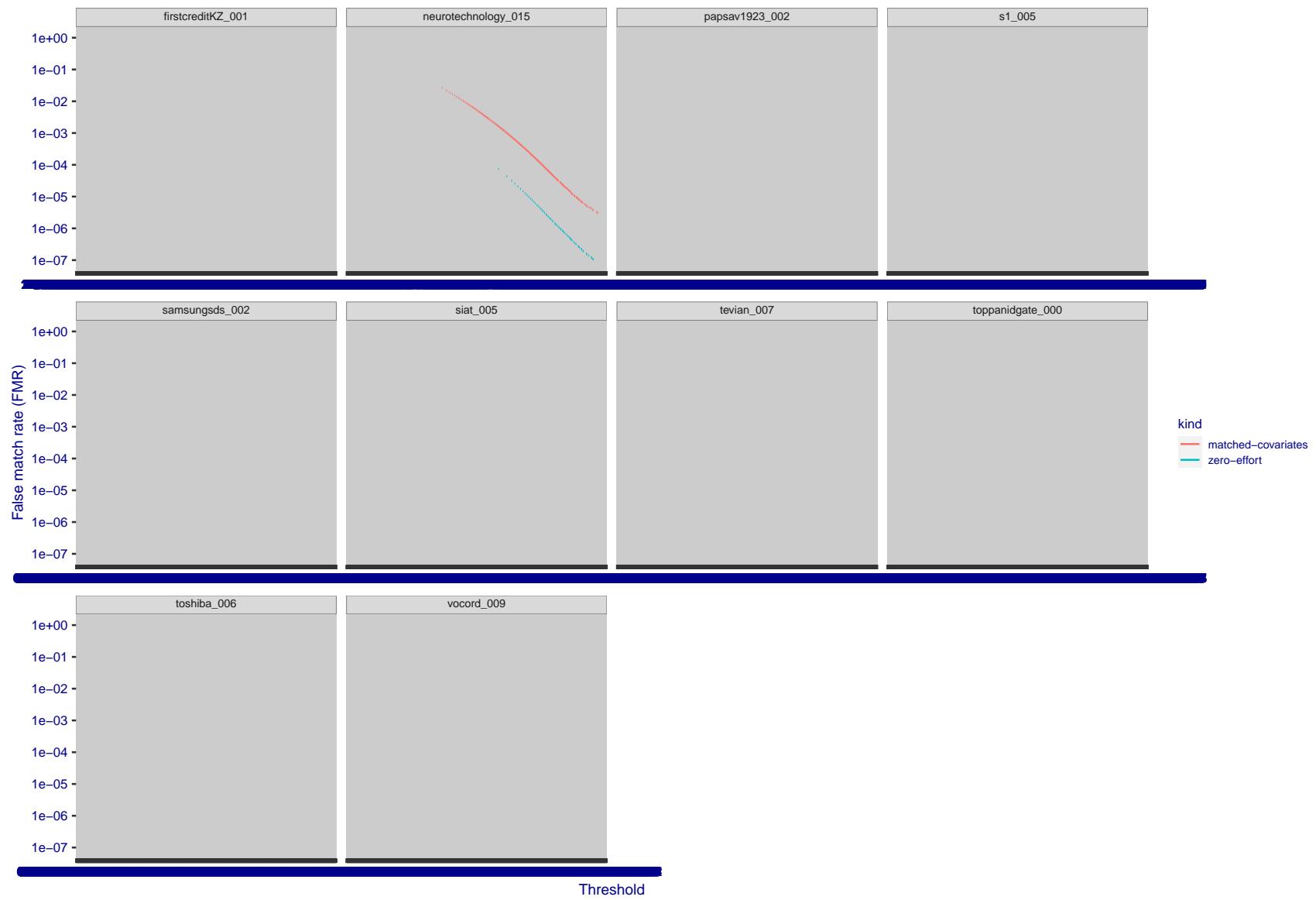


Figure 248: For the visa images, the false match calibration curves show FMR vs. threshold, T . The blue (lower) curves are for zero-effort impostors (i.e. comparing all images against all). The red (upper) curves are for persons of the same-sex, same-age, and same national-origin. This shows that FMR is underestimated (by a factor of 10 or more) by using a zero-effort impostor calculation to calibrate T . As shown later (sec. 3.6), FMR is higher for demographic-matched impostors.

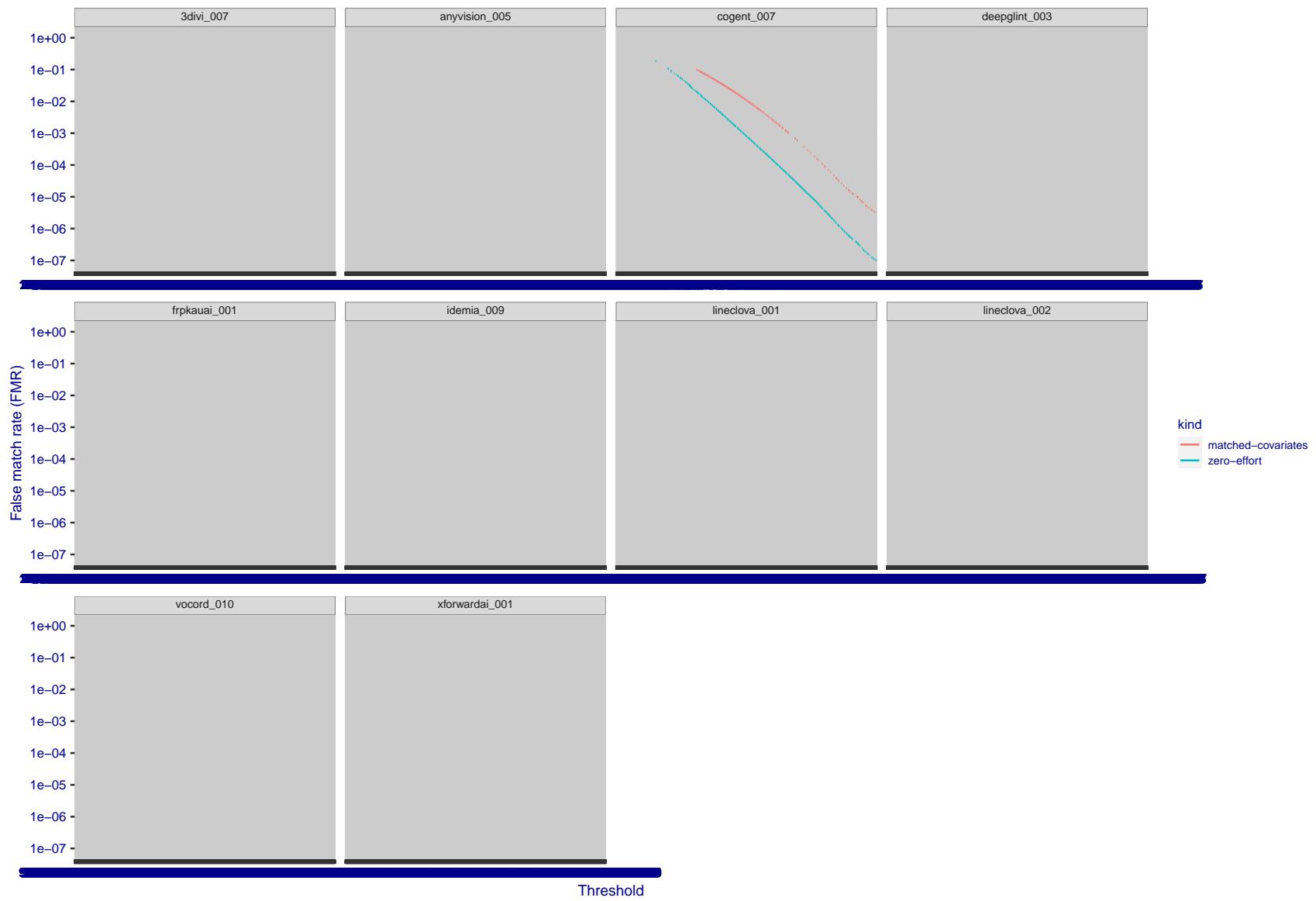


Figure 249: For the visa images, the false match calibration curves show FMR vs. threshold, T . The blue (lower) curves are for zero-effort impostors (i.e. comparing all images against all). The red (upper) curves are for persons of the same-sex, same-age, and same national-origin. This shows that FMR is underestimated (by a factor of 10 or more) by using a zero-effort impostor calculation to calibrate T . As shown later (sec. 3.6), FMR is higher for demographic-matched impostors.

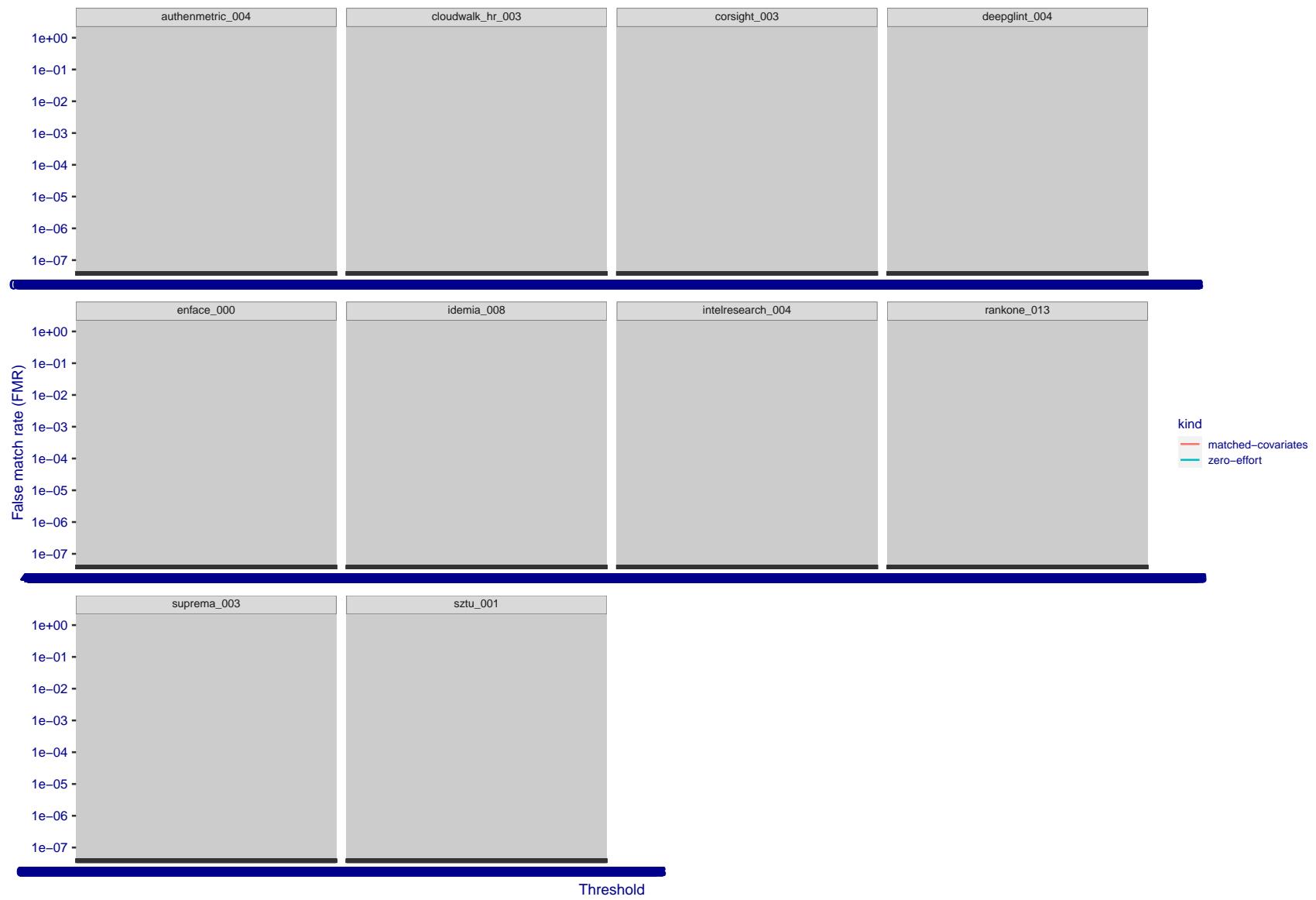


Figure 250: For the visa images, the false match calibration curves show FMR vs. threshold, T . The blue (lower) curves are for zero-effort impostors (i.e. comparing all images against all). The red (upper) curves are for persons of the same-sex, same-age, and same national-origin. This shows that FMR is underestimated (by a factor of 10 or more) by using a zero-effort impostor calculation to calibrate T . As shown later (sec. 3.6), FMR is higher for demographic-matched impostors.

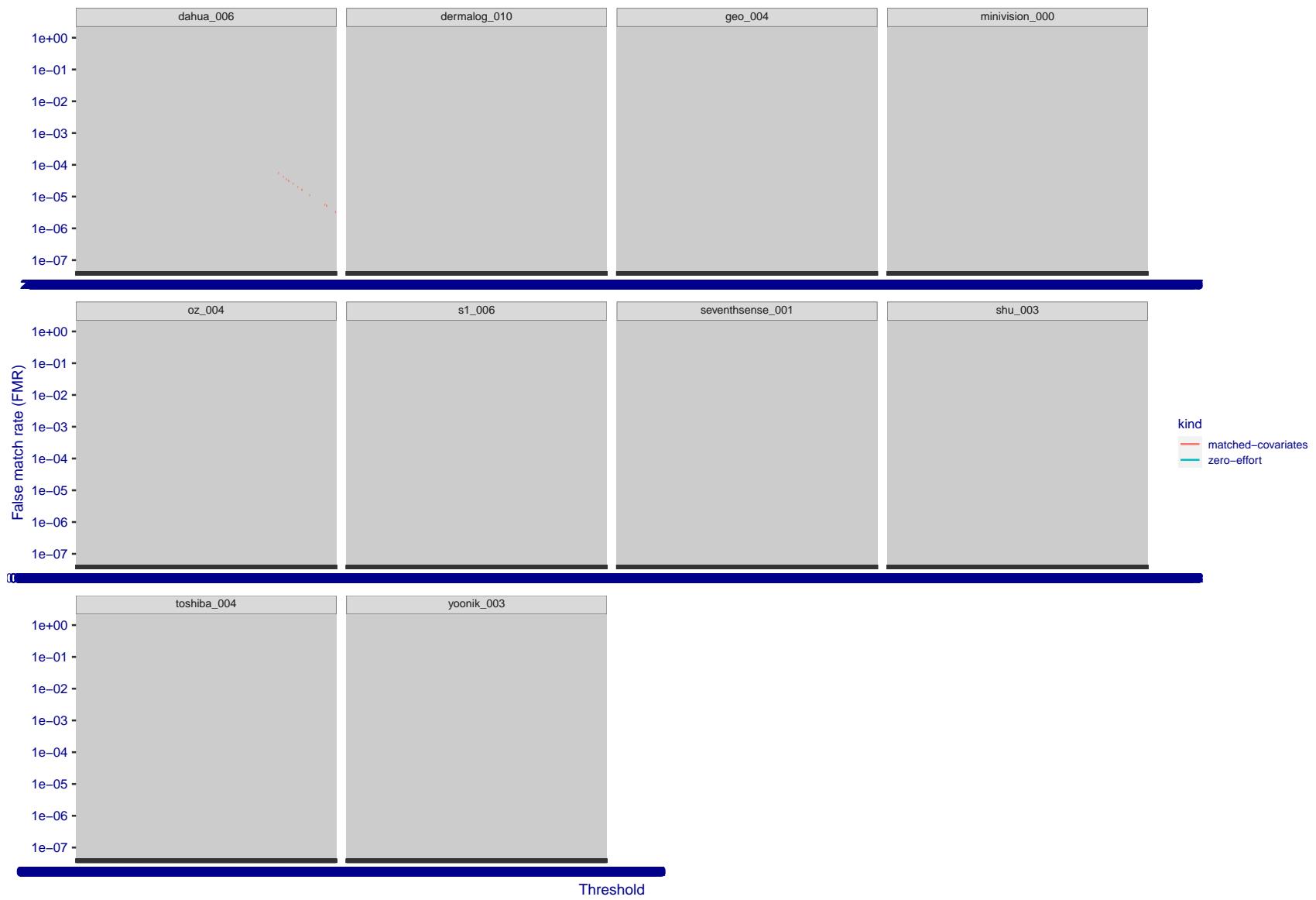


Figure 251: For the visa images, the false match calibration curves show FMR vs. threshold, T . The blue (lower) curves are for zero-effort impostors (i.e. comparing all images against all). The red (upper) curves are for persons of the same-sex, same-age, and same national-origin. This shows that FMR is underestimated (by a factor of 10 or more) by using a zero-effort impostor calculation to calibrate T . As shown later (sec. 3.6), FMR is higher for demographic-matched impostors.

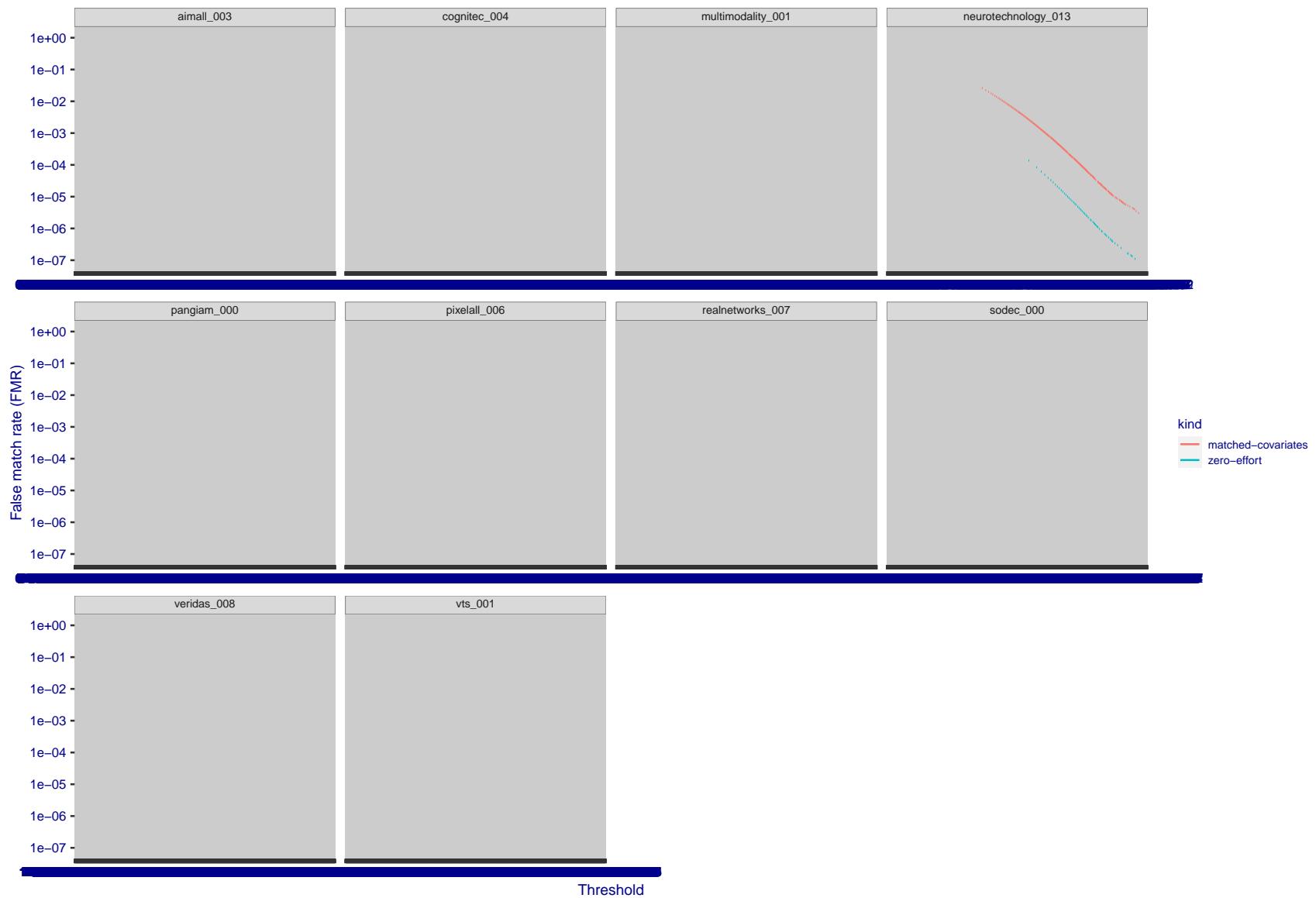


Figure 252: For the visa images, the false match calibration curves show FMR vs. threshold, T . The blue (lower) curves are for zero-effort impostors (i.e. comparing all images against all). The red (upper) curves are for persons of the same-sex, same-age, and same national-origin. This shows that FMR is underestimated (by a factor of 10 or more) by using a zero-effort impostor calculation to calibrate T . As shown later (sec. 3.6), FMR is higher for demographic-matched impostors.

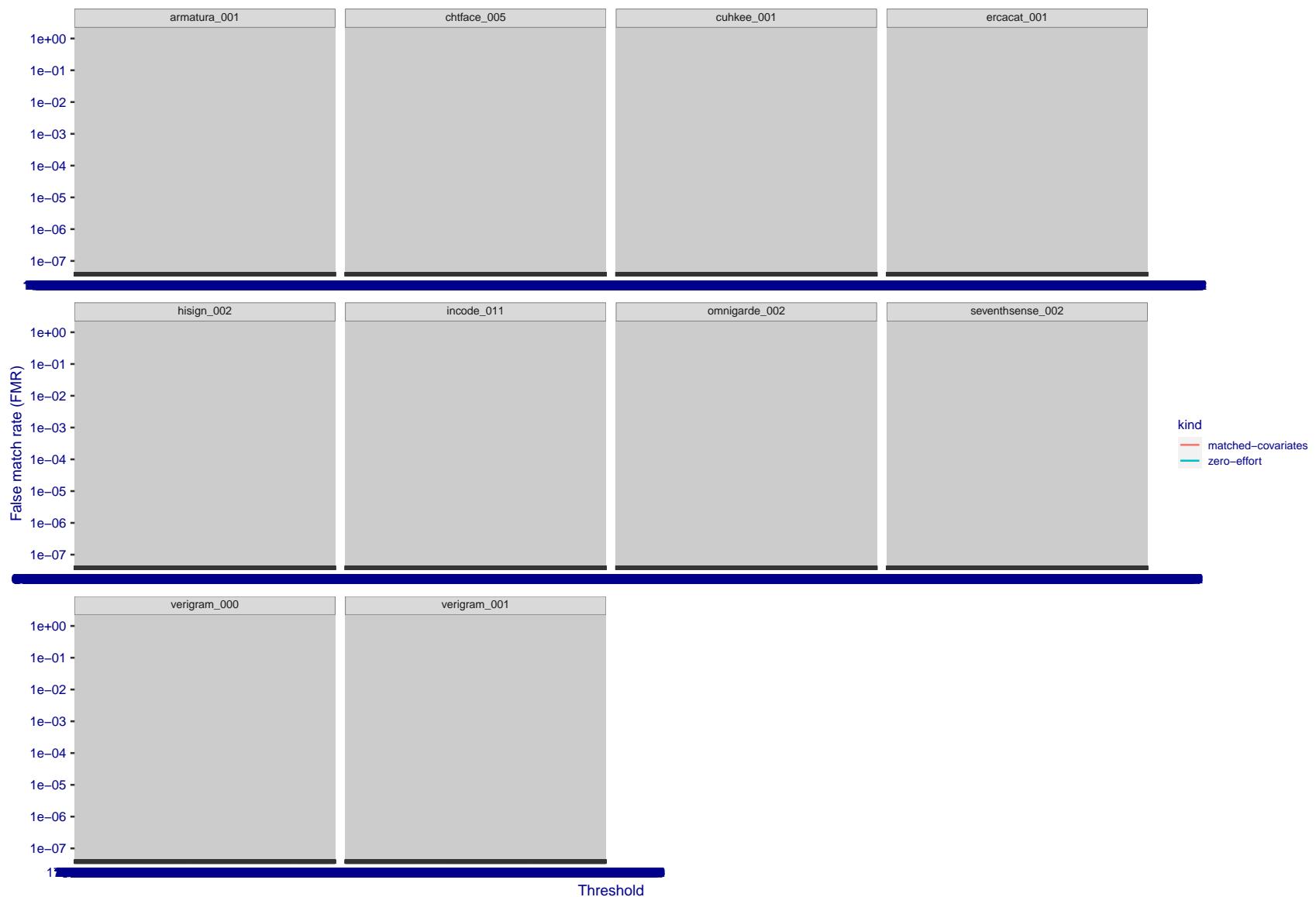


Figure 253: For the visa images, the false match calibration curves show FMR vs. threshold, T . The blue (lower) curves are for zero-effort impostors (i.e. comparing all images against all). The red (upper) curves are for persons of the same-sex, same-age, and same national-origin. This shows that FMR is underestimated (by a factor of 10 or more) by using a zero-effort impostor calculation to calibrate T . As shown later (sec. 3.6), FMR is higher for demographic-matched impostors.

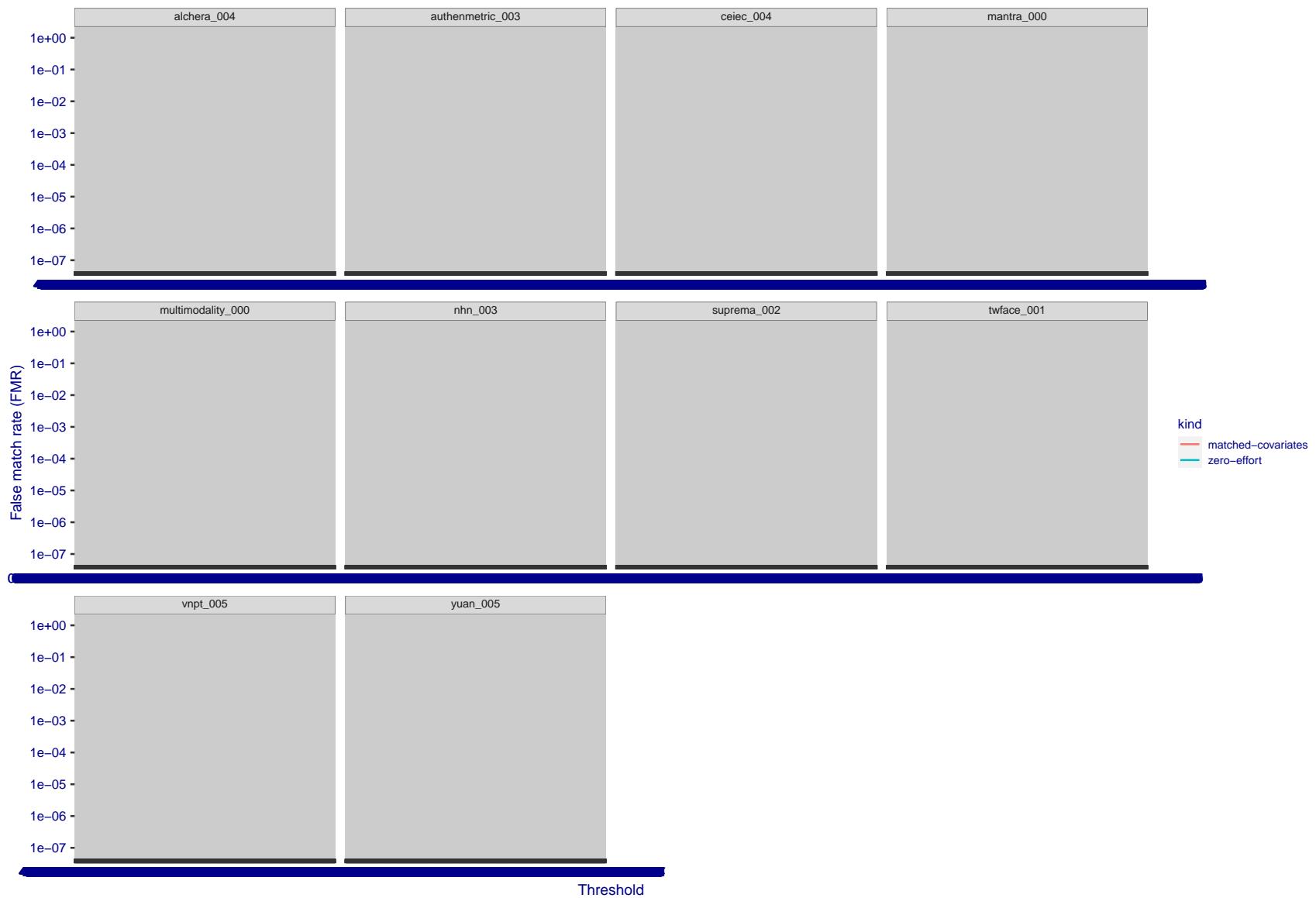


Figure 254: For the visa images, the false match calibration curves show FMR vs. threshold, T . The blue (lower) curves are for zero-effort impostors (i.e. comparing all images against all). The red (upper) curves are for persons of the same-sex, same-age, and same national-origin. This shows that FMR is underestimated (by a factor of 10 or more) by using a zero-effort impostor calculation to calibrate T . As shown later (sec. 3.6), FMR is higher for demographic-matched impostors.



Figure 255: For the visa images, the false match calibration curves show FMR vs. threshold, T . The blue (lower) curves are for zero-effort impostors (i.e. comparing all images against all). The red (upper) curves are for persons of the same-sex, same-age, and same national-origin. This shows that FMR is underestimated (by a factor of 10 or more) by using a zero-effort impostor calculation to calibrate T . As shown later (sec. 3.6), FMR is higher for demographic-matched impostors.

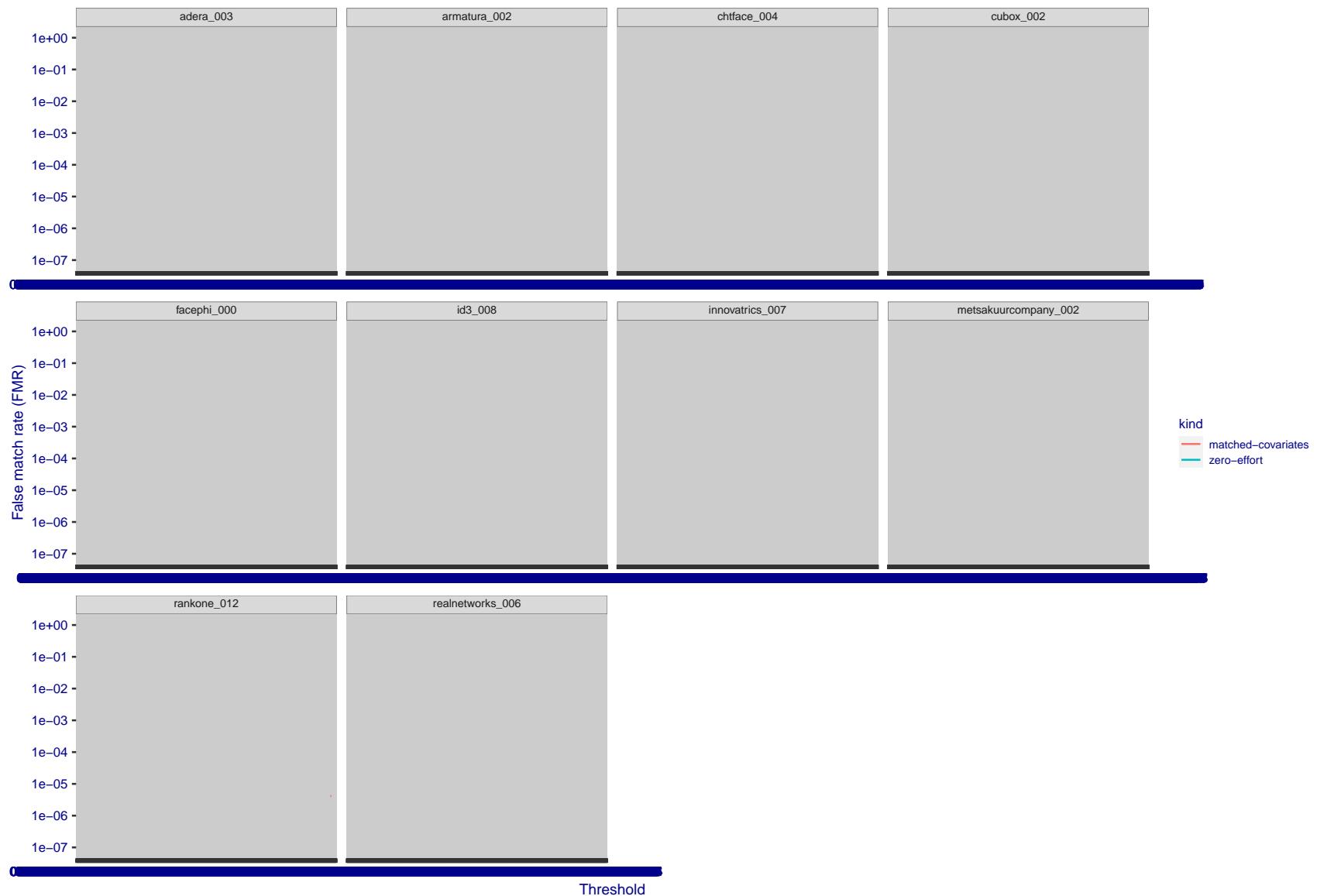


Figure 256: For the visa images, the false match calibration curves show FMR vs. threshold, T . The blue (lower) curves are for zero-effort impostors (i.e. comparing all images against all). The red (upper) curves are for persons of the same-sex, same-age, and same national-origin. This shows that FMR is underestimated (by a factor of 10 or more) by using a zero-effort impostor calculation to calibrate T . As shown later (sec. 3.6), FMR is higher for demographic-matched impostors.

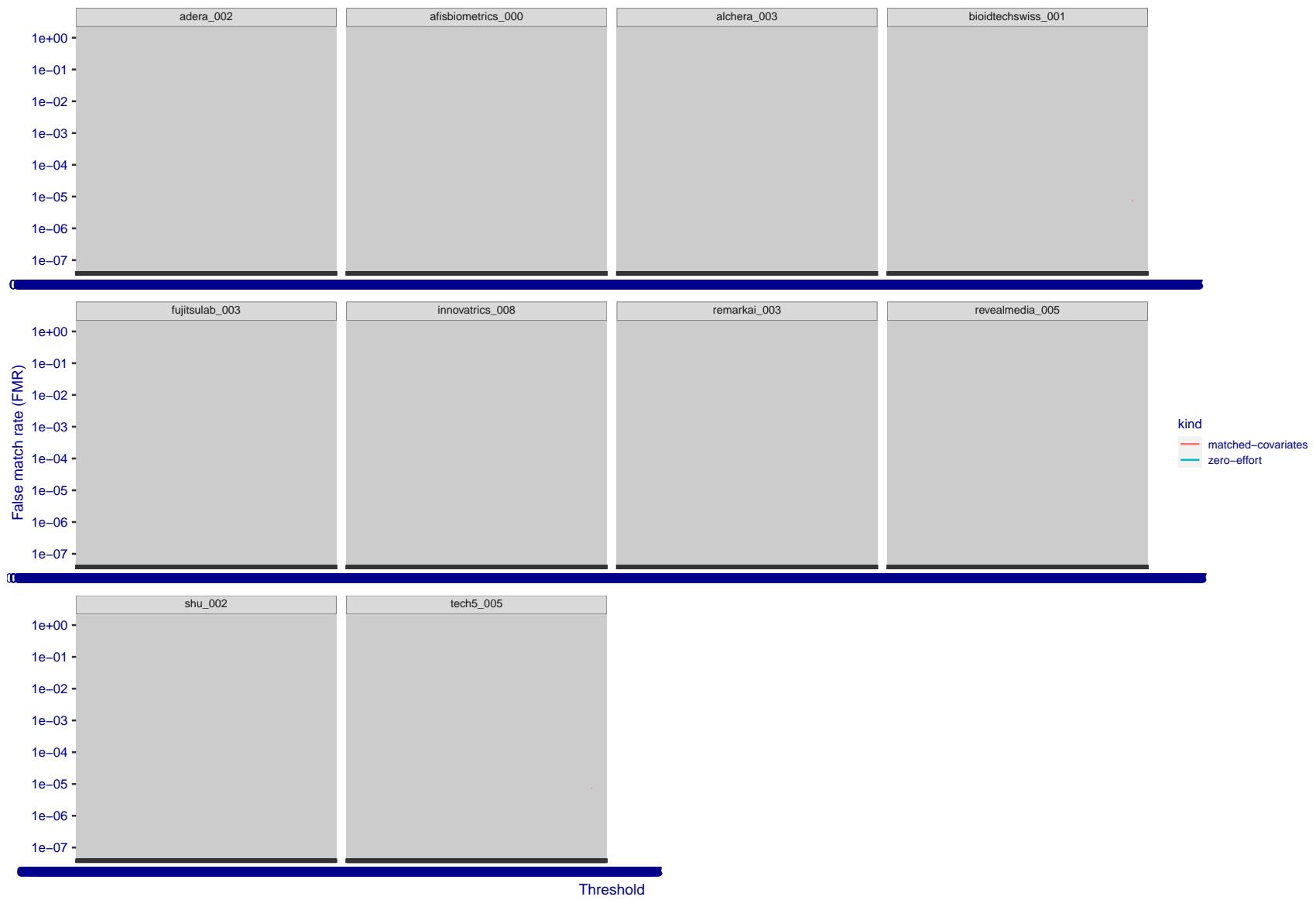


Figure 257: For the visa images, the false match calibration curves show FMR vs. threshold, T . The blue (lower) curves are for zero-effort impostors (i.e. comparing all images against all). The red (upper) curves are for persons of the same-sex, same-age, and same national-origin. This shows that FMR is underestimated (by a factor of 10 or more) by using a zero-effort impostor calculation to calibrate T . As shown later (sec. 3.6), FMR is higher for demographic-matched impostors.

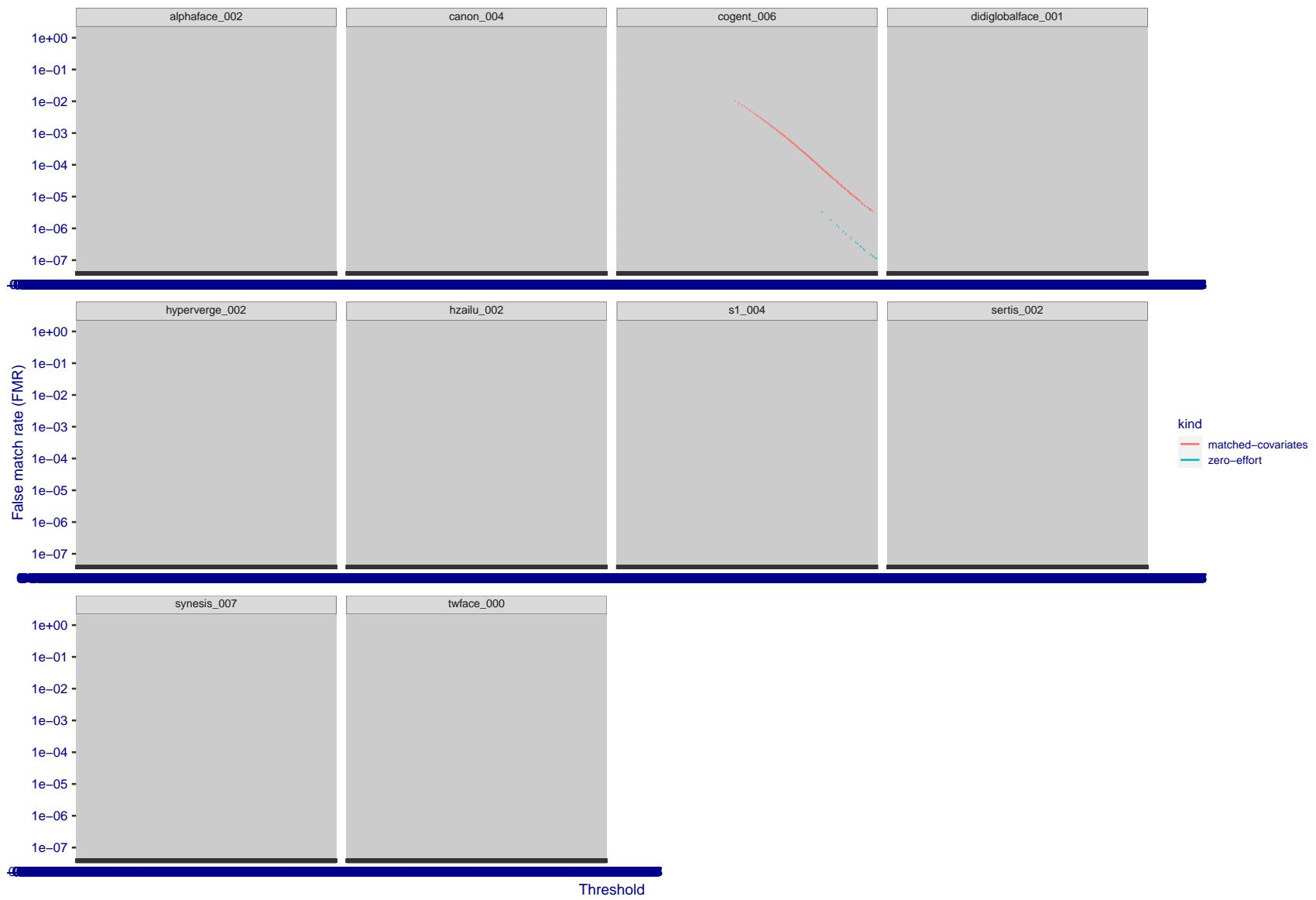


Figure 258: For the visa images, the false match calibration curves show FMR vs. threshold, T . The blue (lower) curves are for zero-effort impostors (i.e. comparing all images against all). The red (upper) curves are for persons of the same-sex, same-age, and same national-origin. This shows that FMR is underestimated (by a factor of 10 or more) by using a zero-effort impostor calculation to calibrate T . As shown later (sec. 3.6), FMR is higher for demographic-matched impostors.

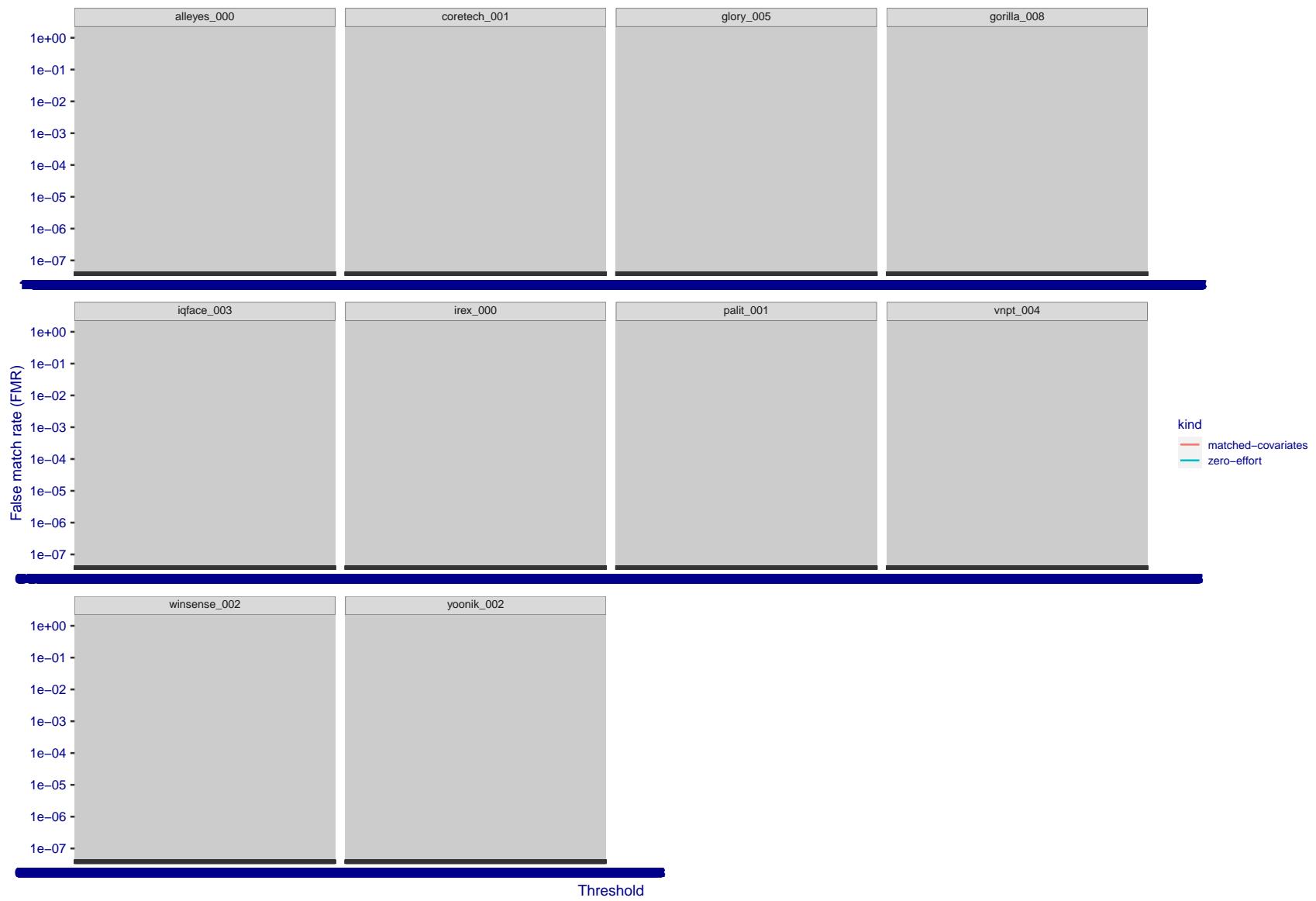


Figure 259: For the visa images, the false match calibration curves show FMR vs. threshold, T . The blue (lower) curves are for zero-effort impostors (i.e. comparing all images against all). The red (upper) curves are for persons of the same-sex, same-age, and same national-origin. This shows that FMR is underestimated (by a factor of 10 or more) by using a zero-effort impostor calculation to calibrate T . As shown later (sec. 3.6), FMR is higher for demographic-matched impostors.

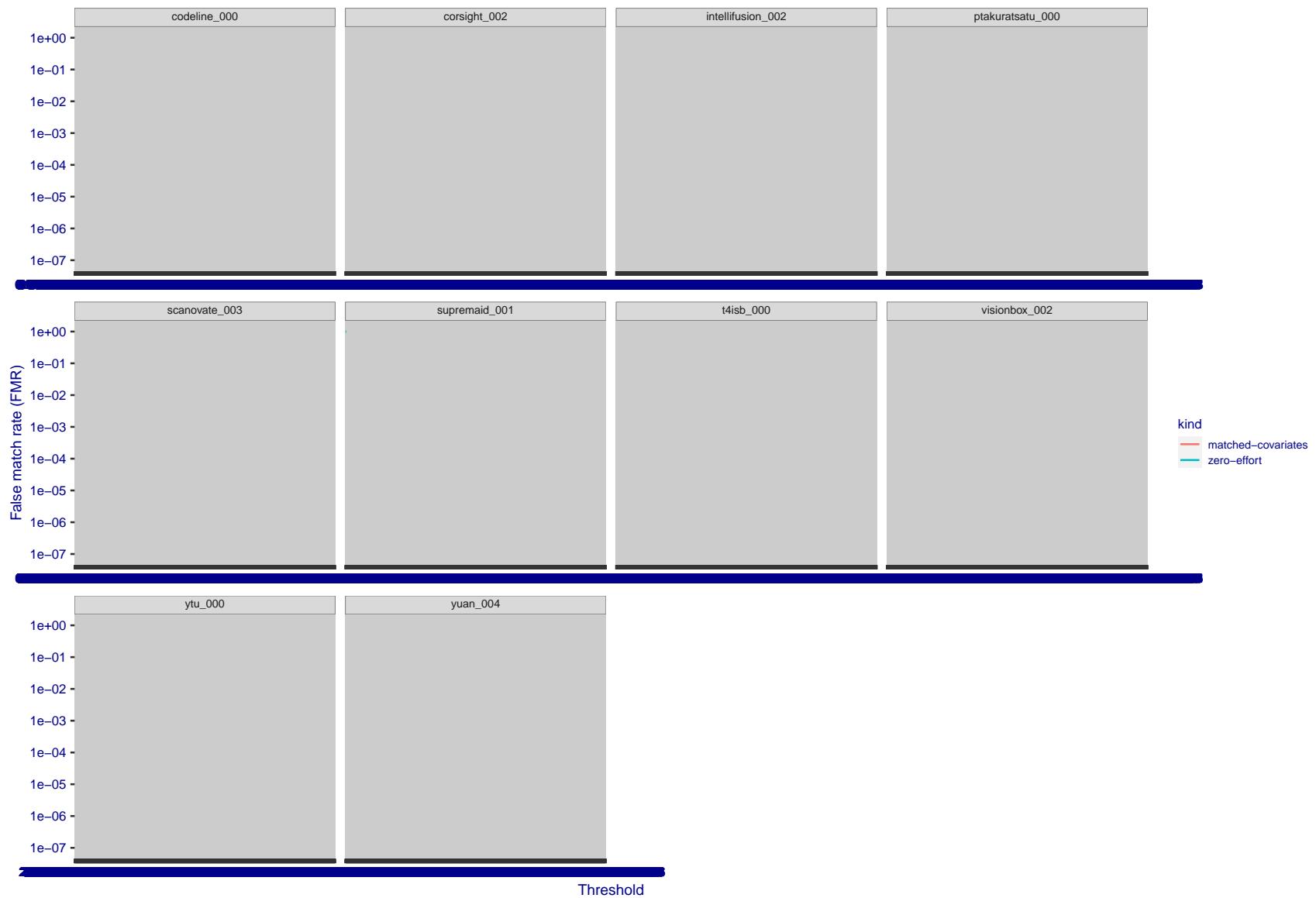


Figure 260: For the visa images, the false match calibration curves show FMR vs. threshold, T . The blue (lower) curves are for zero-effort impostors (i.e. comparing all images against all). The red (upper) curves are for persons of the same-sex, same-age, and same national-origin. This shows that FMR is underestimated (by a factor of 10 or more) by using a zero-effort impostor calculation to calibrate T . As shown later (sec. 3.6), FMR is higher for demographic-matched impostors.

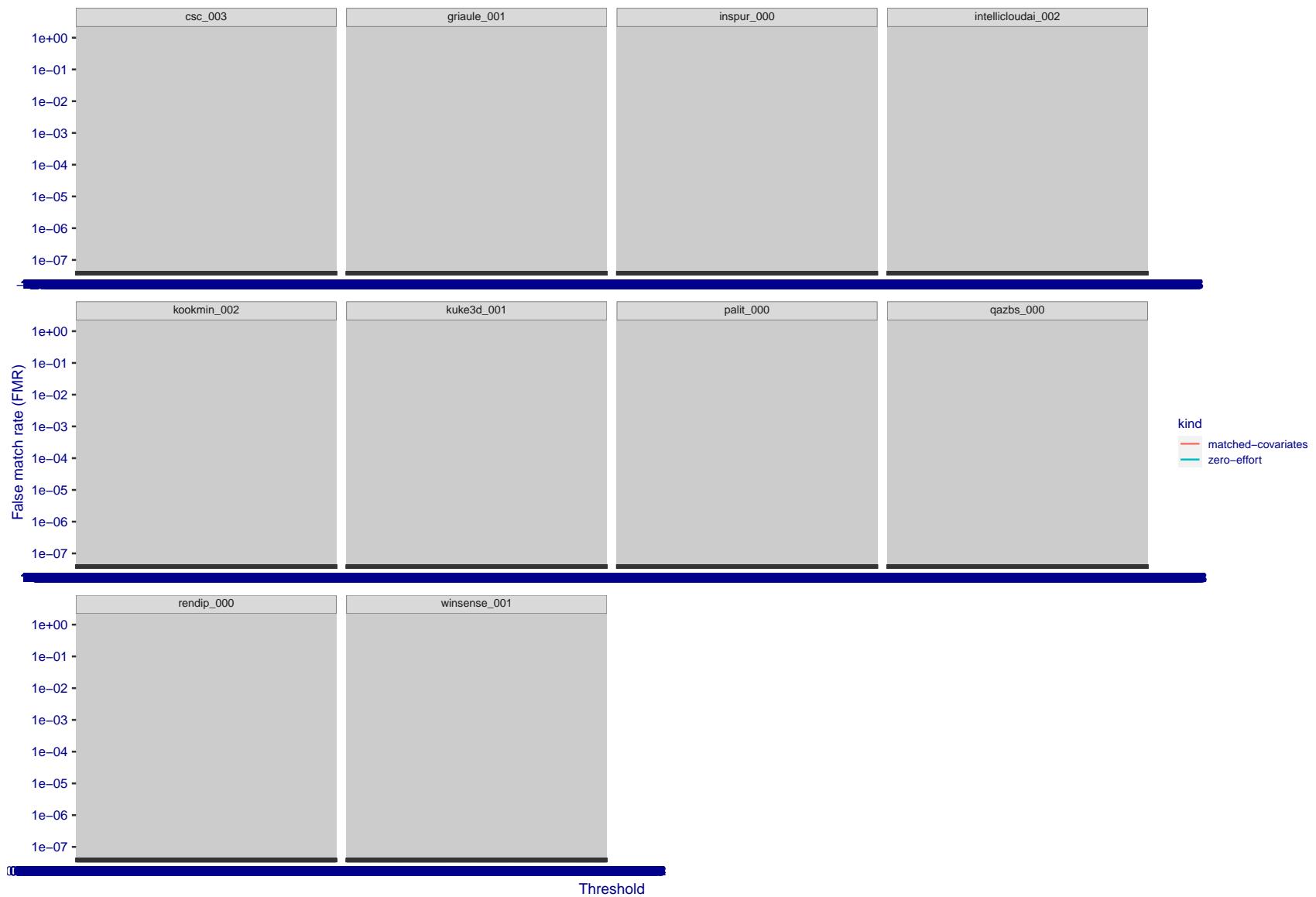


Figure 261: For the visa images, the false match calibration curves show FMR vs. threshold, T . The blue (lower) curves are for zero-effort impostors (i.e. comparing all images against all). The red (upper) curves are for persons of the same-sex, same-age, and same national-origin. This shows that FMR is underestimated (by a factor of 10 or more) by using a zero-effort impostor calculation to calibrate T . As shown later (sec. 3.6), FMR is higher for demographic-matched impostors.

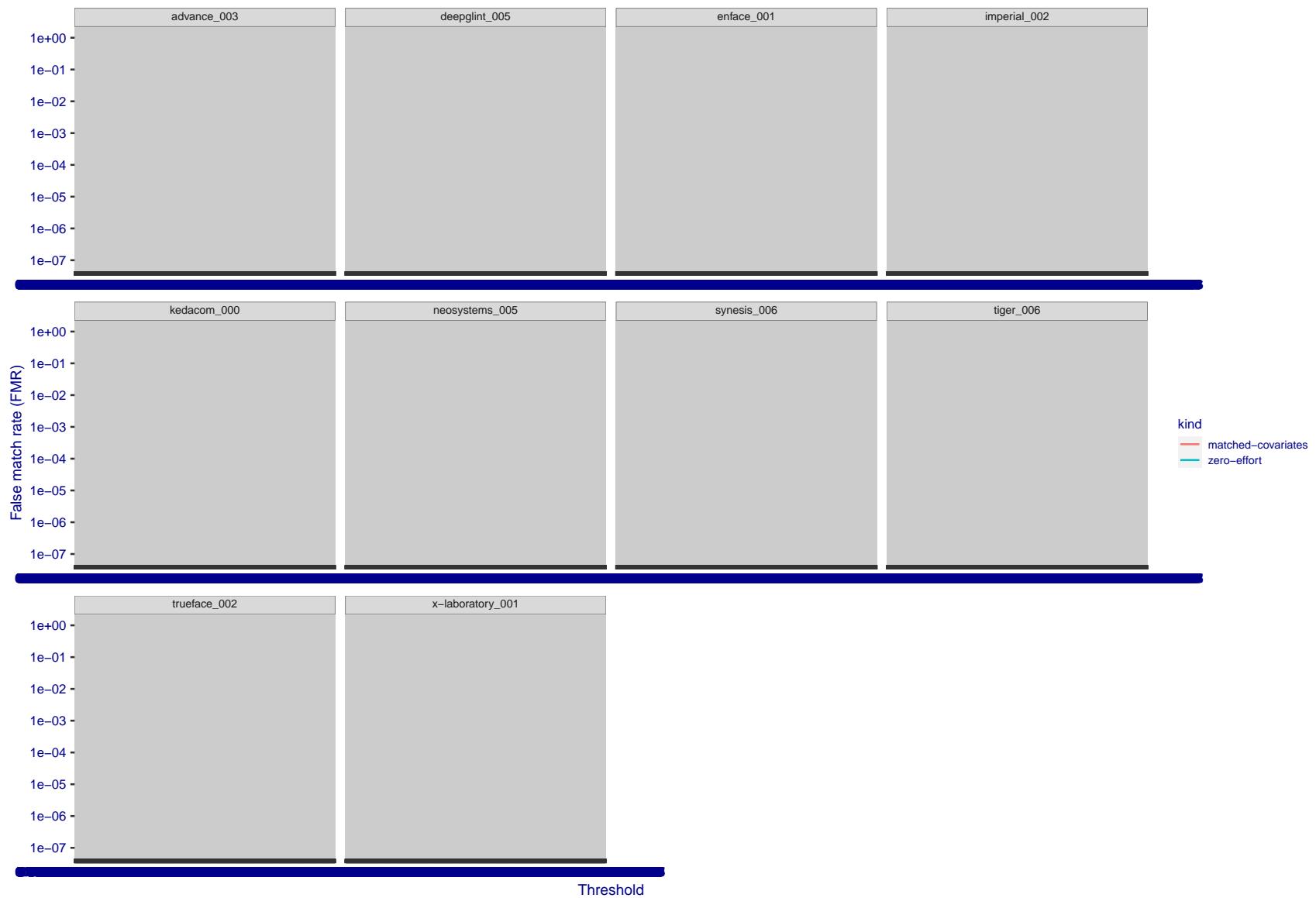


Figure 262: For the visa images, the false match calibration curves show FMR vs. threshold, T . The blue (lower) curves are for zero-effort impostors (i.e. comparing all images against all). The red (upper) curves are for persons of the same-sex, same-age, and same national-origin. This shows that FMR is underestimated (by a factor of 10 or more) by using a zero-effort impostor calculation to calibrate T . As shown later (sec. 3.6), FMR is higher for demographic-matched impostors.

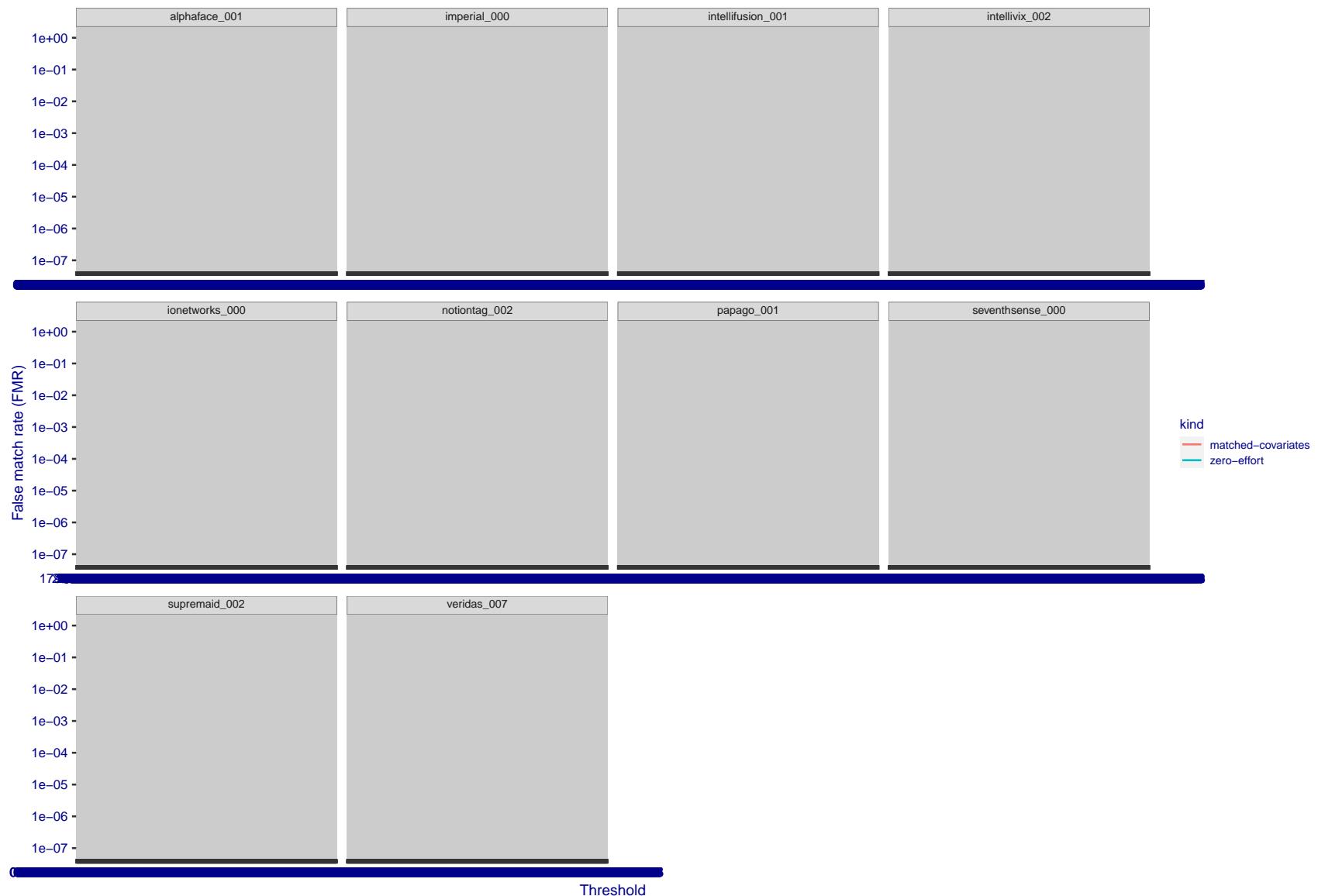


Figure 263: For the visa images, the false match calibration curves show FMR vs. threshold, T . The blue (lower) curves are for zero-effort impostors (i.e. comparing all images against all). The red (upper) curves are for persons of the same-sex, same-age, and same national-origin. This shows that FMR is underestimated (by a factor of 10 or more) by using a zero-effort impostor calculation to calibrate T . As shown later (sec. 3.6), FMR is higher for demographic-matched impostors.

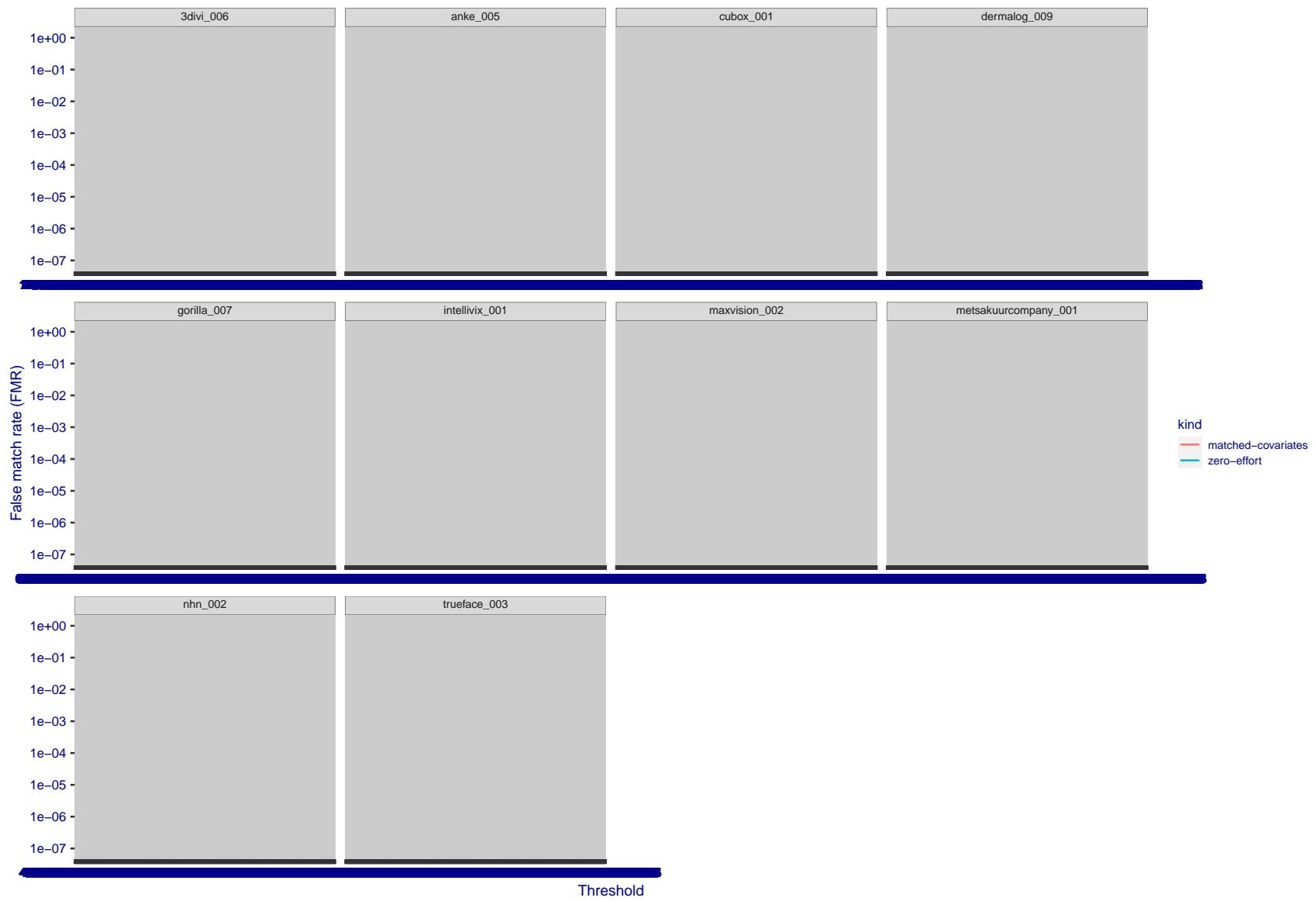


Figure 264: For the visa images, the false match calibration curves show FMR vs. threshold, T . The blue (lower) curves are for zero-effort impostors (i.e. comparing all images against all). The red (upper) curves are for persons of the same-sex, same-age, and same national-origin. This shows that FMR is underestimated (by a factor of 10 or more) by using a zero-effort impostor calculation to calibrate T . As shown later (sec. 3.6), FMR is higher for demographic-matched impostors.

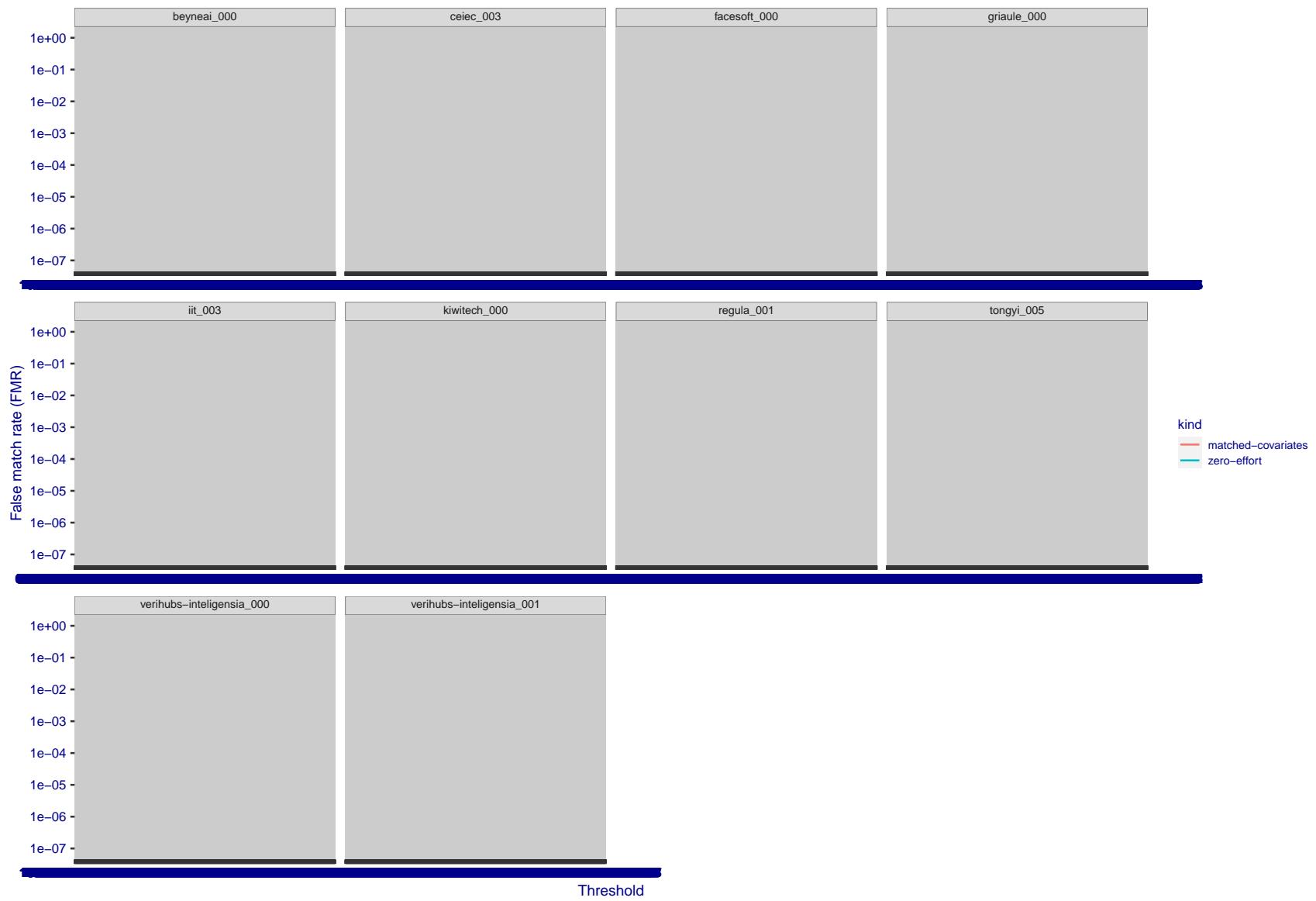


Figure 265: For the visa images, the false match calibration curves show FMR vs. threshold, T . The blue (lower) curves are for zero-effort impostors (i.e. comparing all images against all). The red (upper) curves are for persons of the same-sex, same-age, and same national-origin. This shows that FMR is underestimated (by a factor of 10 or more) by using a zero-effort impostor calculation to calibrate T . As shown later (sec. 3.6), FMR is higher for demographic-matched impostors.

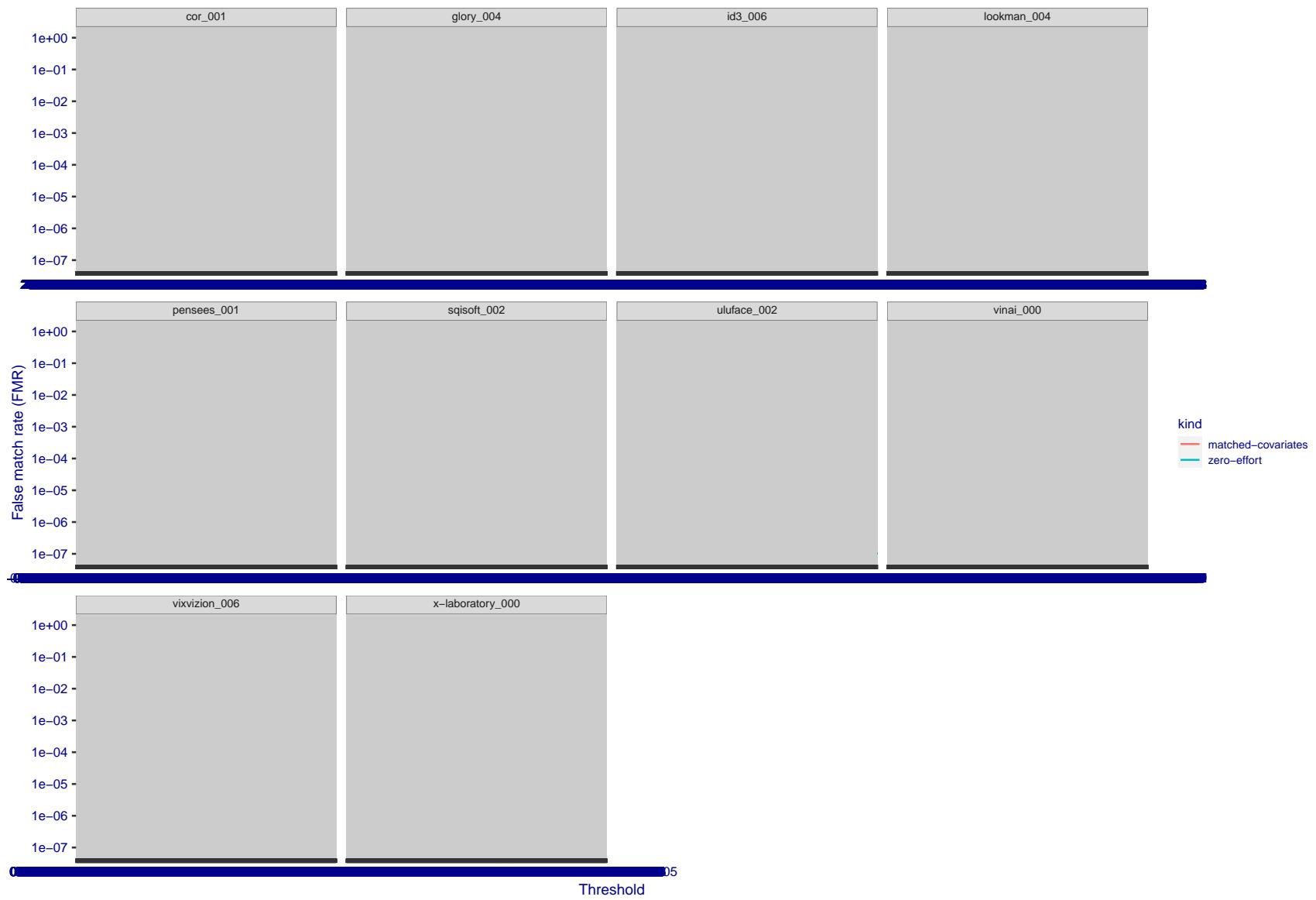


Figure 266: For the visa images, the false match calibration curves show FMR vs. threshold, T . The blue (lower) curves are for zero-effort impostors (i.e. comparing all images against all). The red (upper) curves are for persons of the same-sex, same-age, and same national-origin. This shows that FMR is underestimated (by a factor of 10 or more) by using a zero-effort impostor calculation to calibrate T . As shown later (sec. 3.6), FMR is higher for demographic-matched impostors.

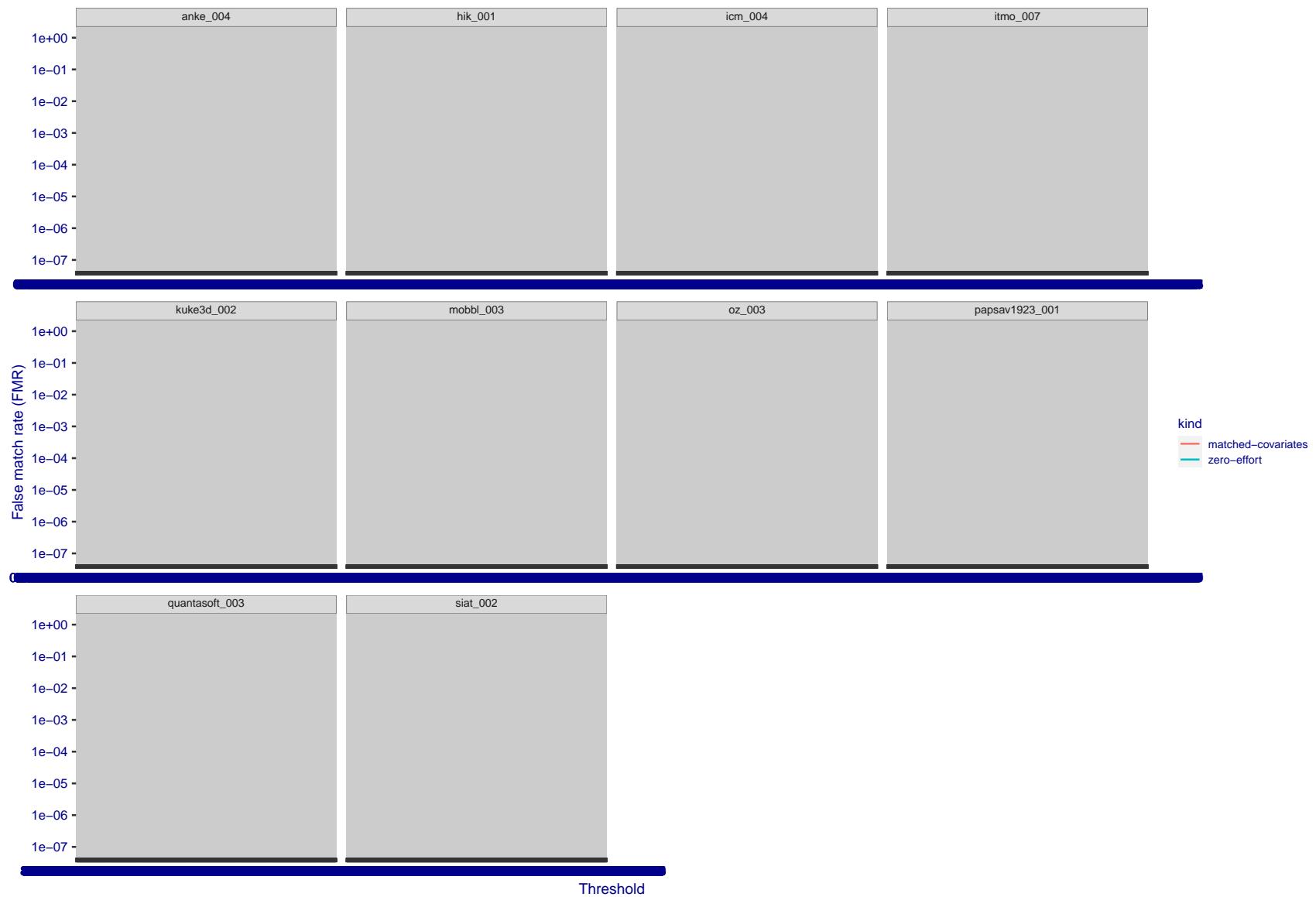


Figure 267: For the visa images, the false match calibration curves show FMR vs. threshold, T . The blue (lower) curves are for zero-effort impostors (i.e. comparing all images against all). The red (upper) curves are for persons of the same-sex, same-age, and same national-origin. This shows that FMR is underestimated (by a factor of 10 or more) by using a zero-effort impostor calculation to calibrate T . As shown later (sec. 3.6), FMR is higher for demographic-matched impostors.

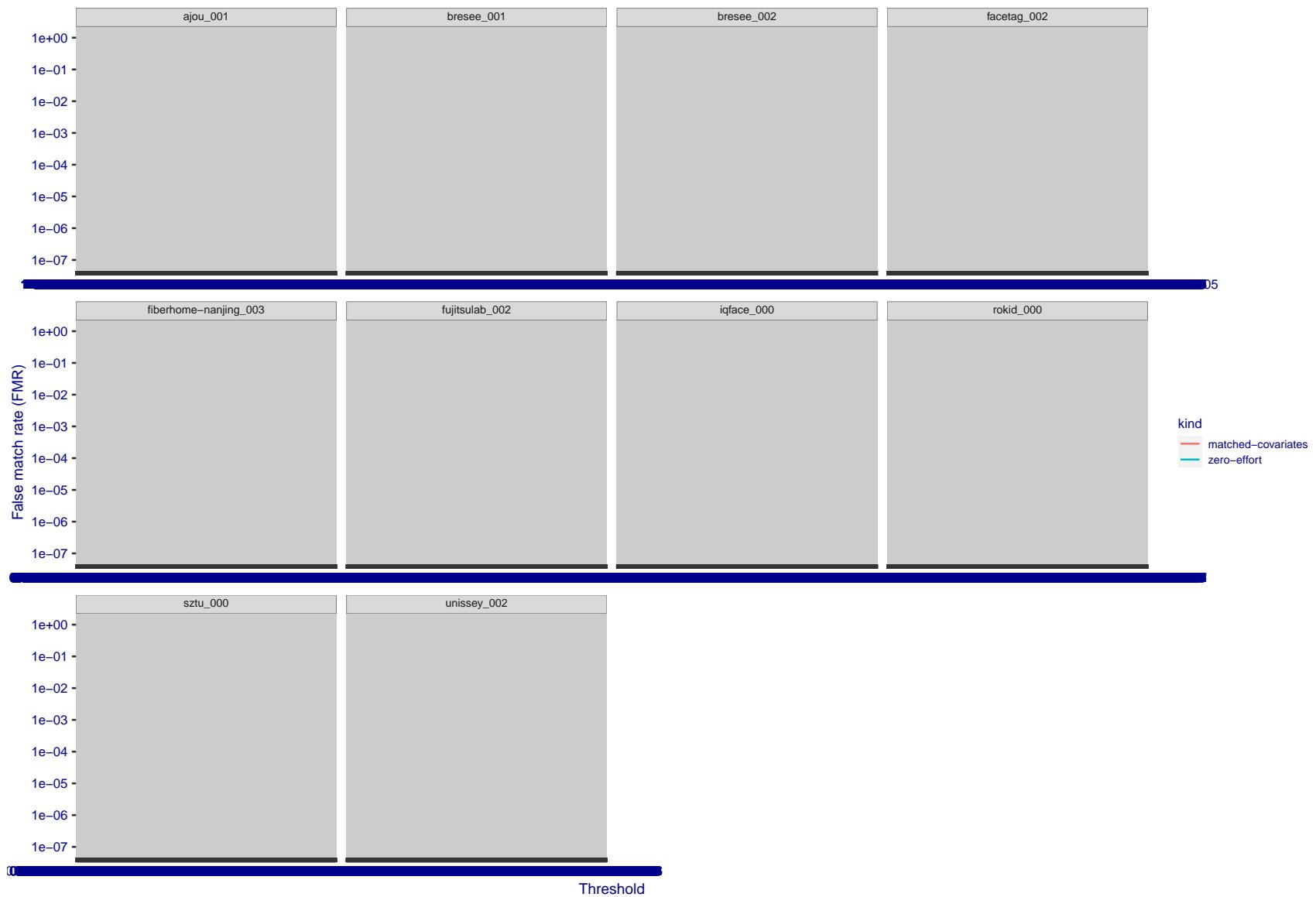


Figure 268: For the visa images, the false match calibration curves show FMR vs. threshold, T . The blue (lower) curves are for zero-effort impostors (i.e. comparing all images against all). The red (upper) curves are for persons of the same-sex, same-age, and same national-origin. This shows that FMR is underestimated (by a factor of 10 or more) by using a zero-effort impostor calculation to calibrate T . As shown later (sec. 3.6), FMR is higher for demographic-matched impostors.

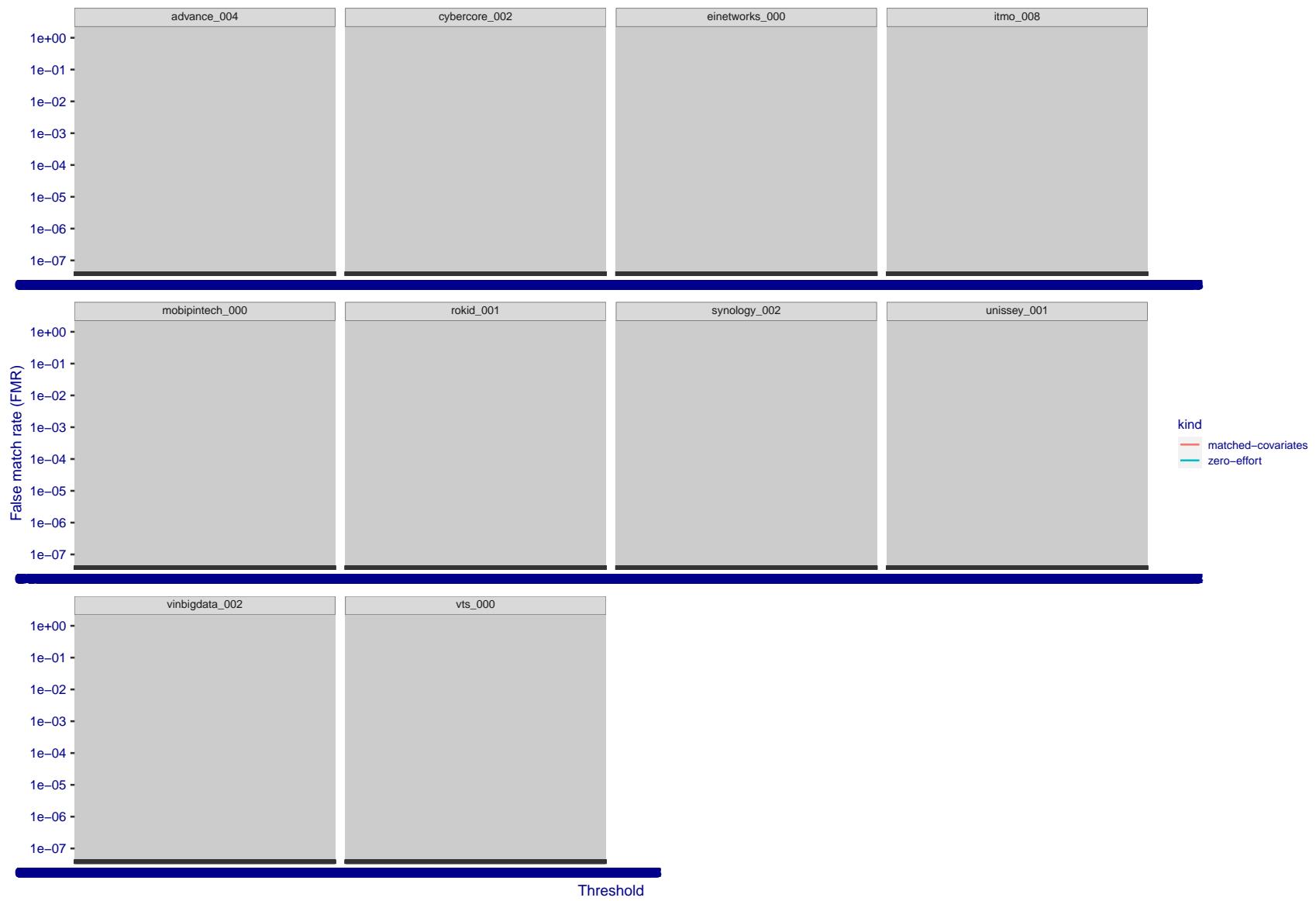


Figure 269: For the visa images, the false match calibration curves show FMR vs. threshold, T . The blue (lower) curves are for zero-effort impostors (i.e. comparing all images against all). The red (upper) curves are for persons of the same-sex, same-age, and same national-origin. This shows that FMR is underestimated (by a factor of 10 or more) by using a zero-effort impostor calculation to calibrate T . As shown later (sec. 3.6), FMR is higher for demographic-matched impostors.

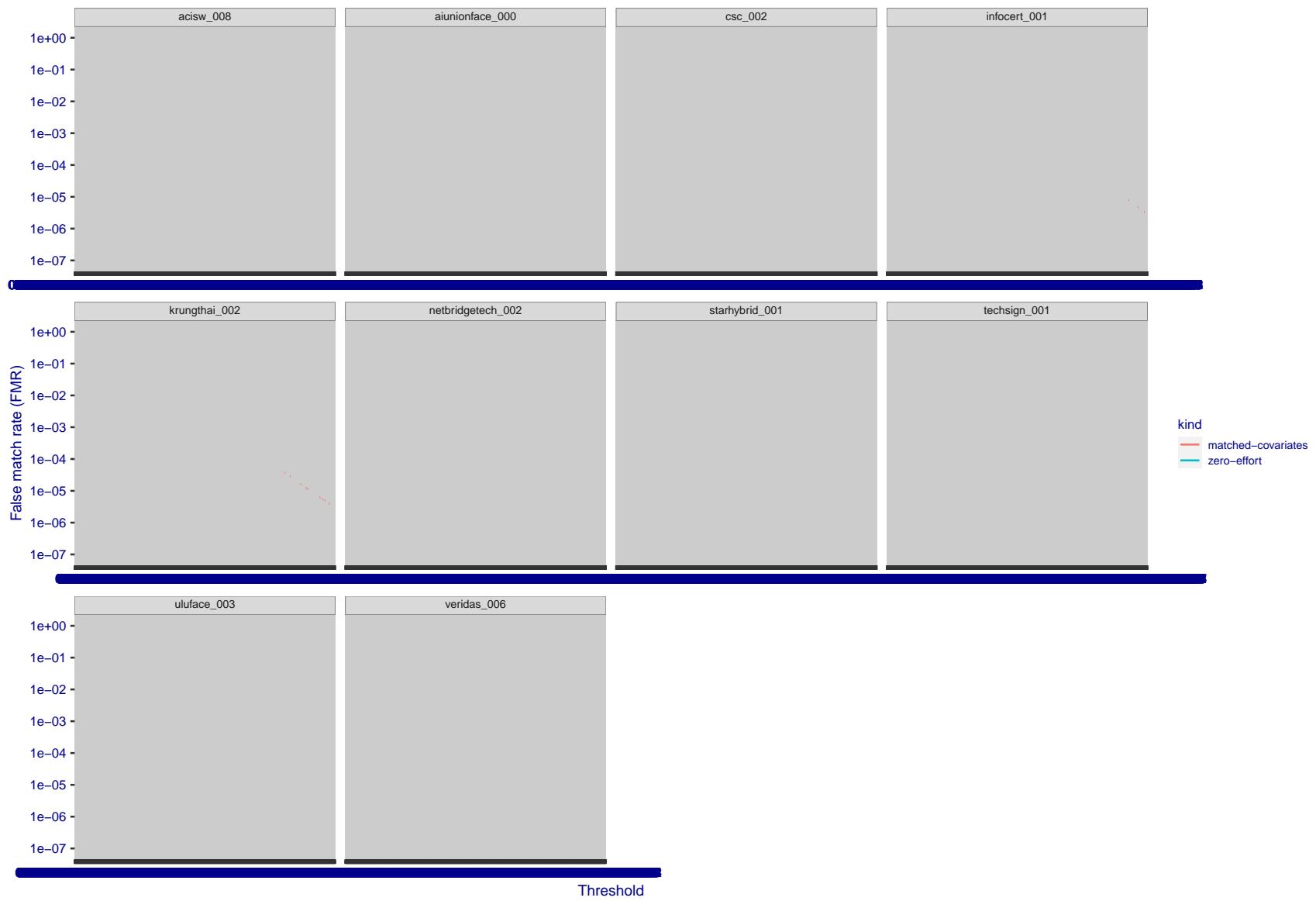


Figure 270: For the visa images, the false match calibration curves show FMR vs. threshold, T . The blue (lower) curves are for zero-effort impostors (i.e. comparing all images against all). The red (upper) curves are for persons of the same-sex, same-age, and same national-origin. This shows that FMR is underestimated (by a factor of 10 or more) by using a zero-effort impostor calculation to calibrate T . As shown later (sec. 3.6), FMR is higher for demographic-matched impostors.

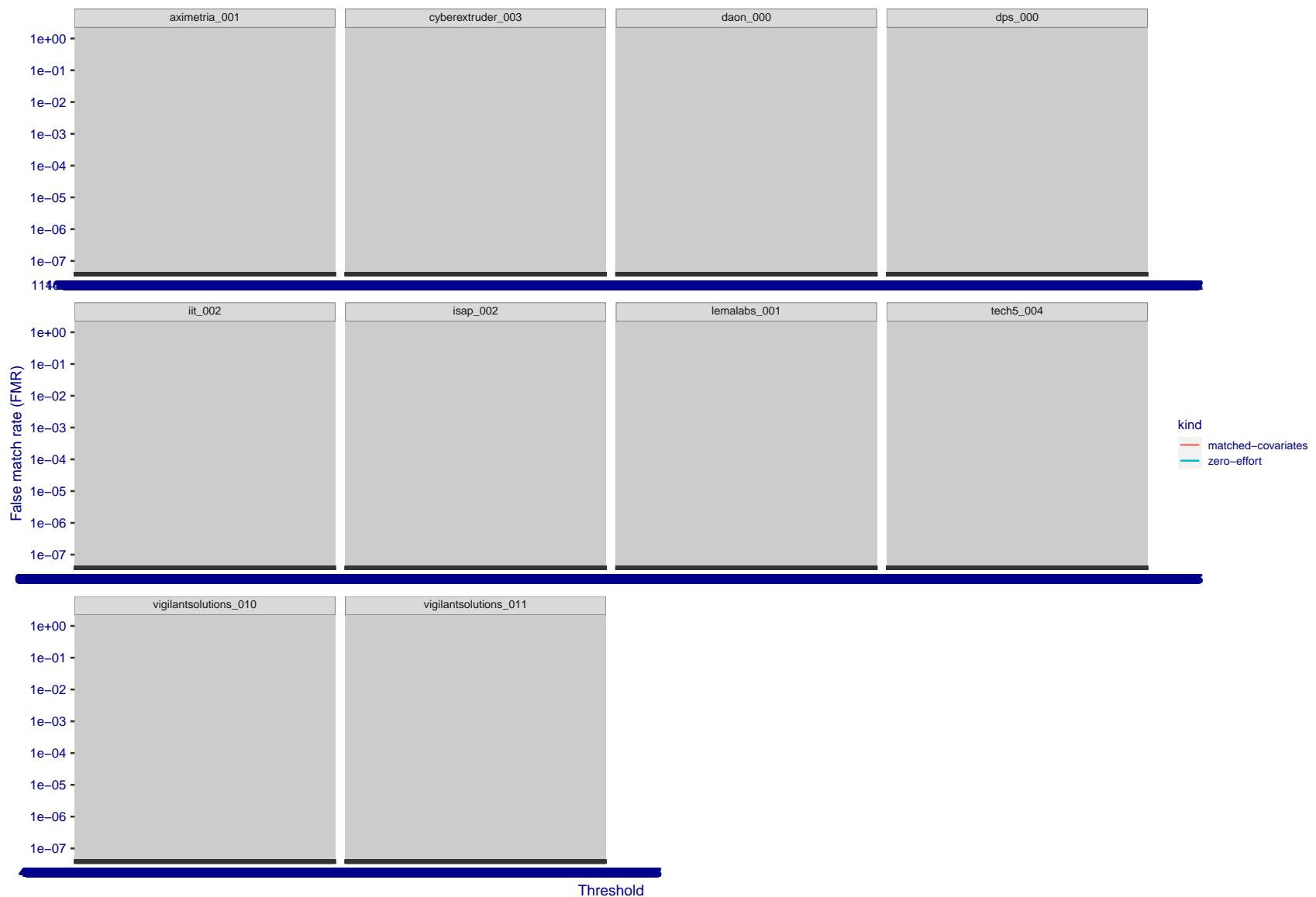


Figure 271: For the visa images, the false match calibration curves show FMR vs. threshold, T . The blue (lower) curves are for zero-effort impostors (i.e. comparing all images against all). The red (upper) curves are for persons of the same-sex, same-age, and same national-origin. This shows that FMR is underestimated (by a factor of 10 or more) by using a zero-effort impostor calculation to calibrate T . As shown later (sec. 3.6), FMR is higher for demographic-matched impostors.

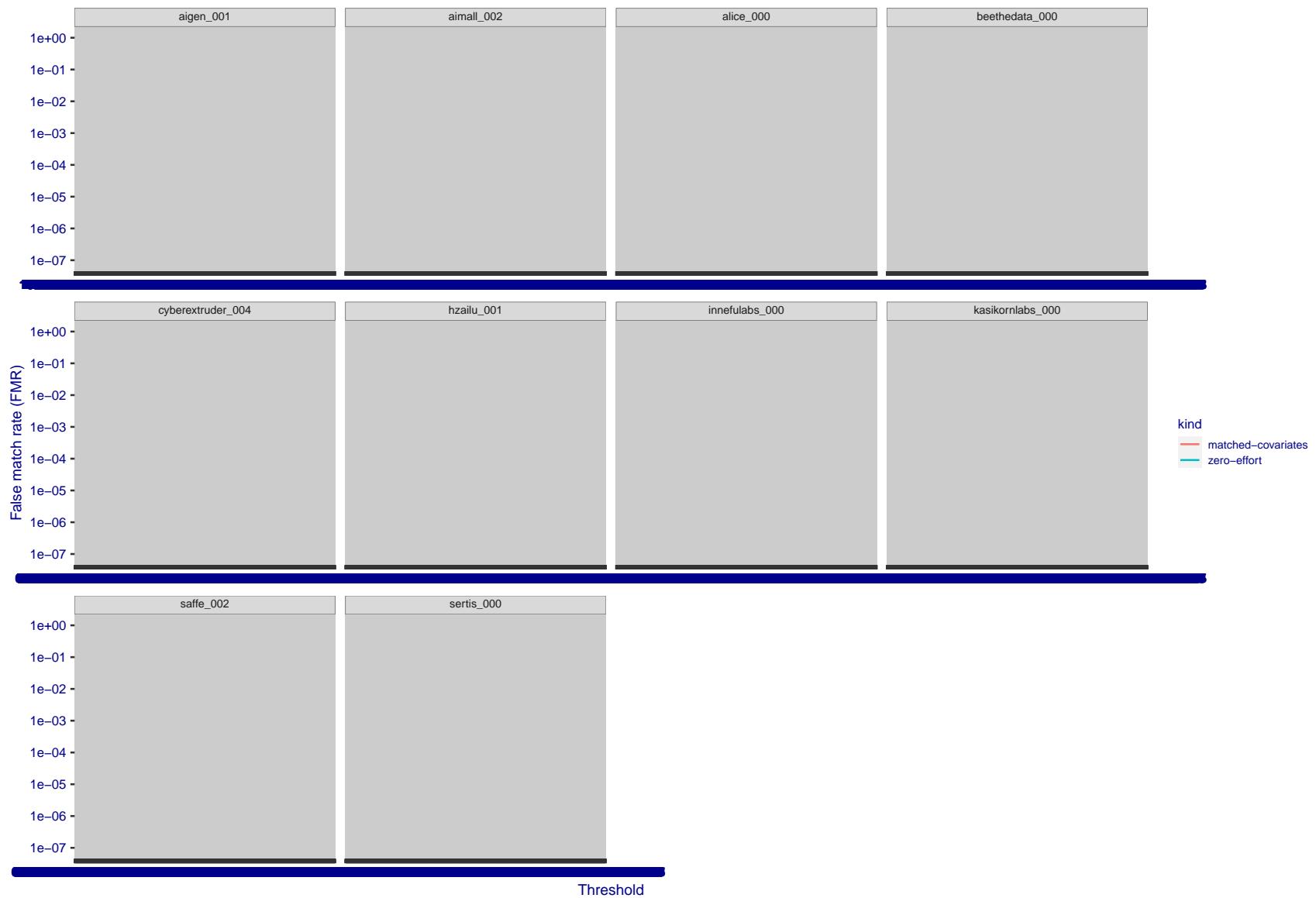


Figure 272: For the visa images, the false match calibration curves show FMR vs. threshold, T . The blue (lower) curves are for zero-effort impostors (i.e. comparing all images against all). The red (upper) curves are for persons of the same-sex, same-age, and same national-origin. This shows that FMR is underestimated (by a factor of 10 or more) by using a zero-effort impostor calculation to calibrate T . As shown later (sec. 3.6), FMR is higher for demographic-matched impostors.

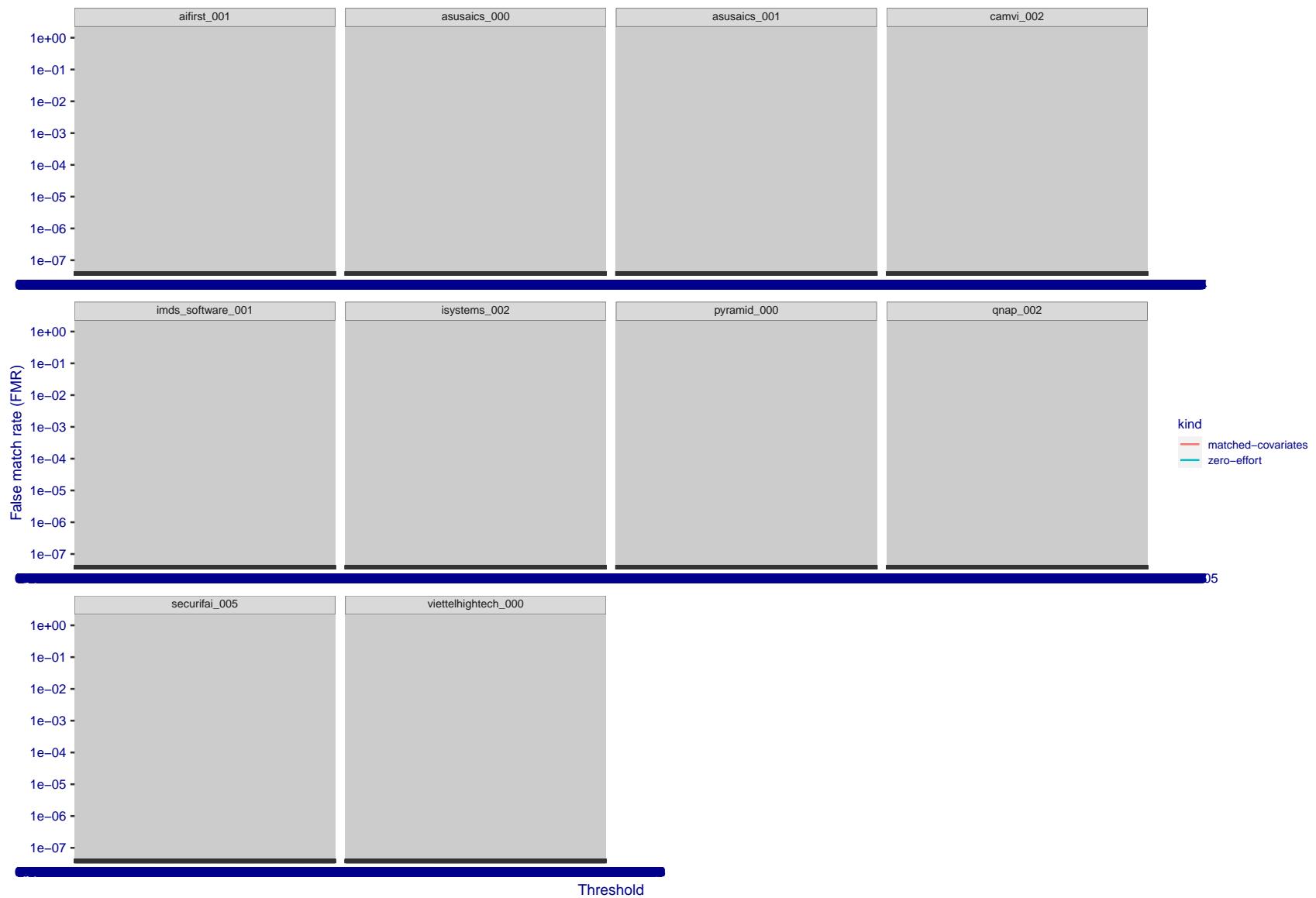


Figure 273: For the visa images, the false match calibration curves show FMR vs. threshold, T . The blue (lower) curves are for zero-effort impostors (i.e. comparing all images against all). The red (upper) curves are for persons of the same-sex, same-age, and same national-origin. This shows that FMR is underestimated (by a factor of 10 or more) by using a zero-effort impostor calculation to calibrate T . As shown later (sec. 3.6), FMR is higher for demographic-matched impostors.

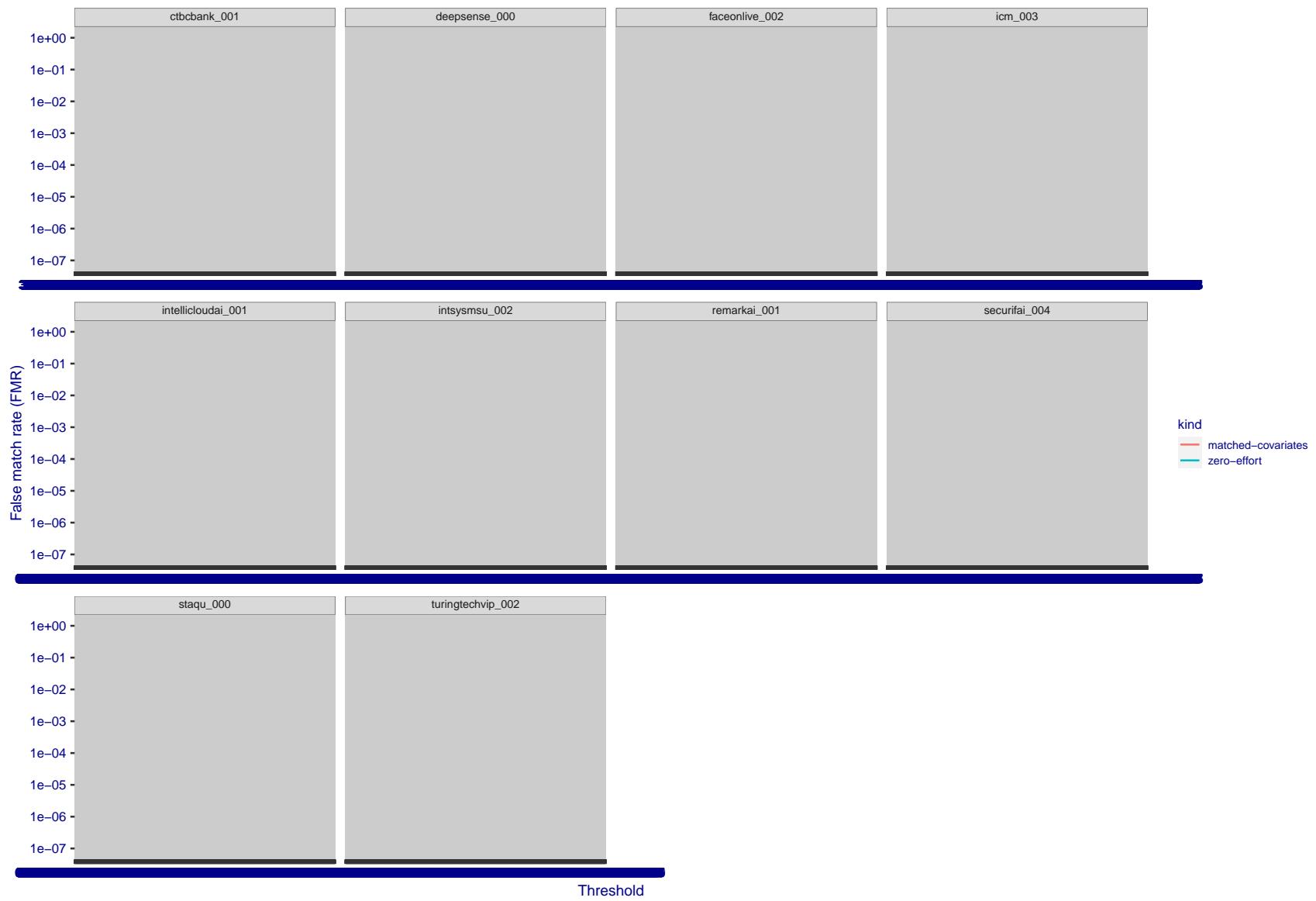


Figure 274: For the visa images, the false match calibration curves show FMR vs. threshold, T . The blue (lower) curves are for zero-effort impostors (i.e. comparing all images against all). The red (upper) curves are for persons of the same-sex, same-age, and same national-origin. This shows that FMR is underestimated (by a factor of 10 or more) by using a zero-effort impostor calculation to calibrate T . As shown later (sec. 3.6), FMR is higher for demographic-matched impostors.

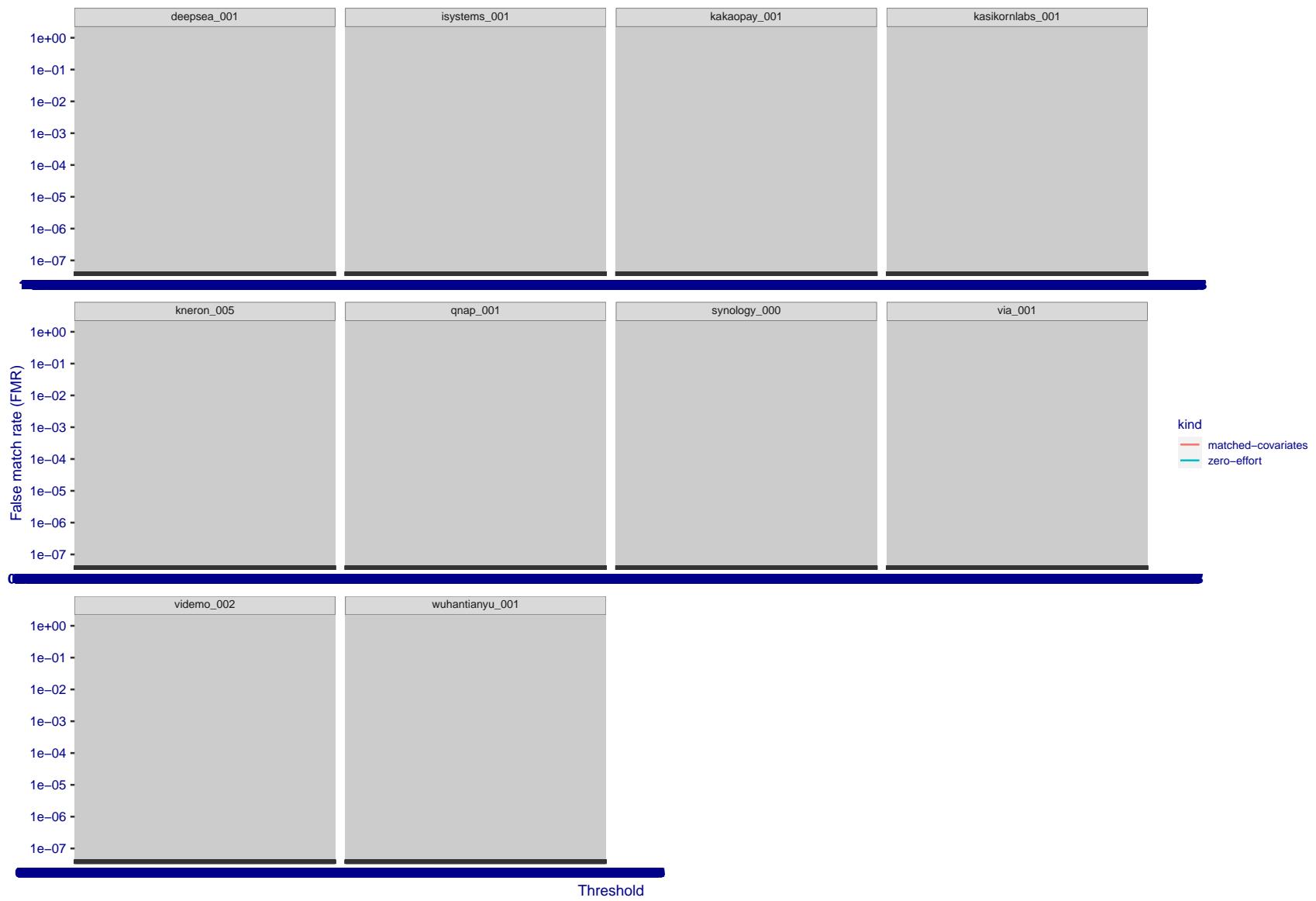


Figure 275: For the visa images, the false match calibration curves show FMR vs. threshold, T . The blue (lower) curves are for zero-effort impostors (i.e. comparing all images against all). The red (upper) curves are for persons of the same-sex, same-age, and same national-origin. This shows that FMR is underestimated (by a factor of 10 or more) by using a zero-effort impostor calculation to calibrate T . As shown later (sec. 3.6), FMR is higher for demographic-matched impostors.

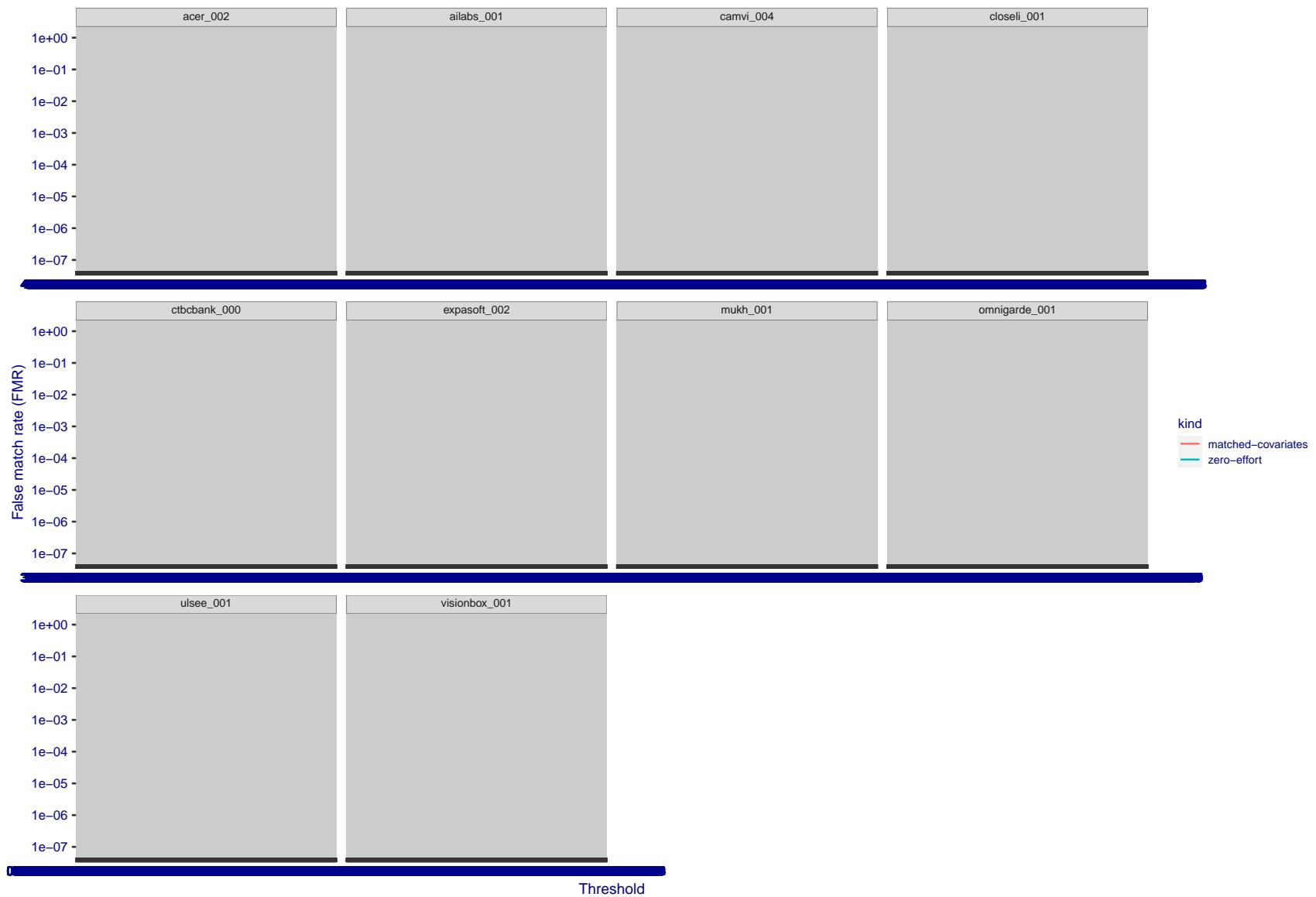


Figure 276: For the visa images, the false match calibration curves show FMR vs. threshold, T . The blue (lower) curves are for zero-effort impostors (i.e. comparing all images against all). The red (upper) curves are for persons of the same-sex, same-age, and same national-origin. This shows that FMR is underestimated (by a factor of 10 or more) by using a zero-effort impostor calculation to calibrate T . As shown later (sec. 3.6), FMR is higher for demographic-matched impostors.

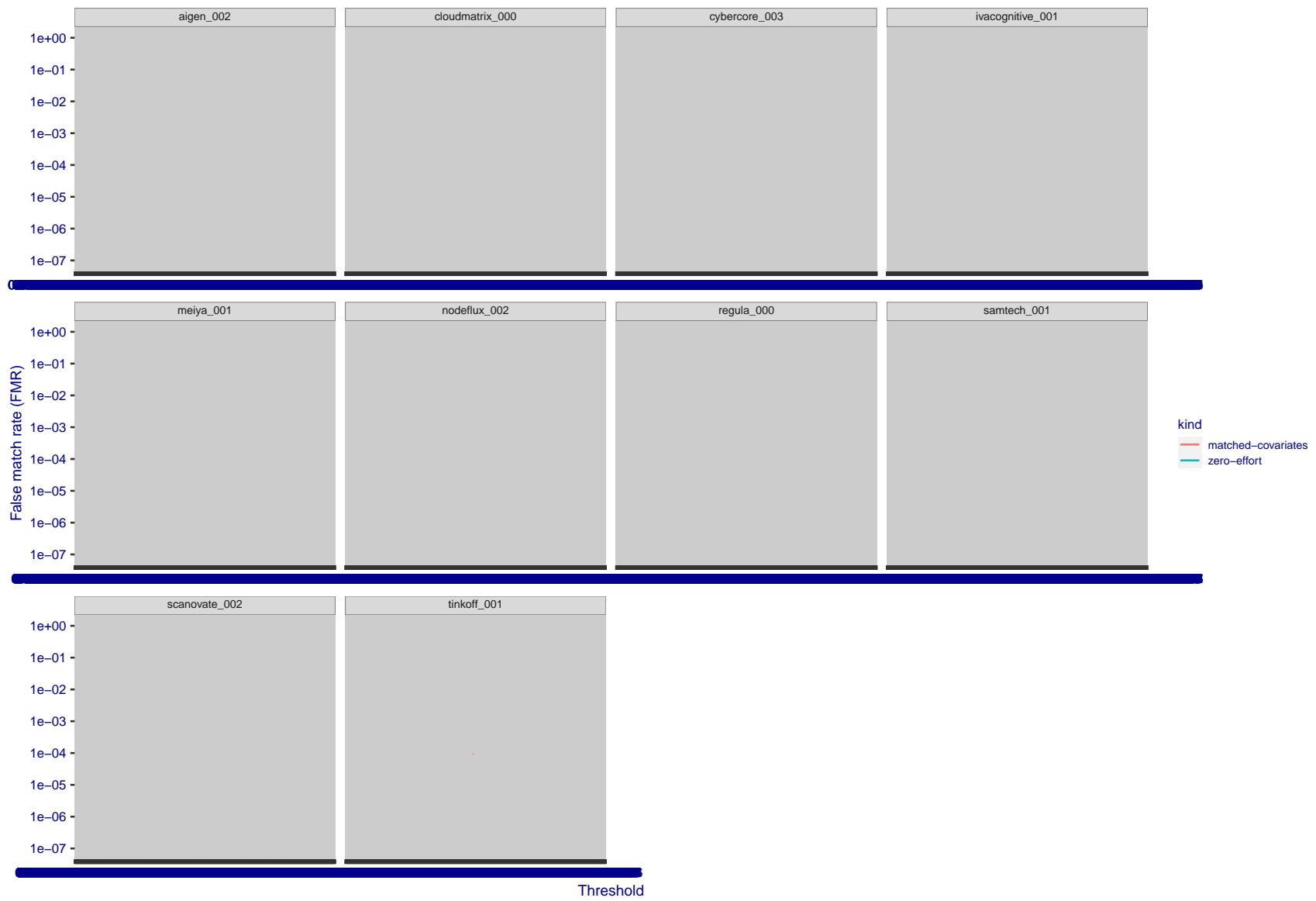


Figure 277: For the visa images, the false match calibration curves show FMR vs. threshold, T . The blue (lower) curves are for zero-effort impostors (i.e. comparing all images against all). The red (upper) curves are for persons of the same-sex, same-age, and same national-origin. This shows that FMR is underestimated (by a factor of 10 or more) by using a zero-effort impostor calculation to calibrate T . As shown later (sec. 3.6), FMR is higher for demographic-matched impostors.

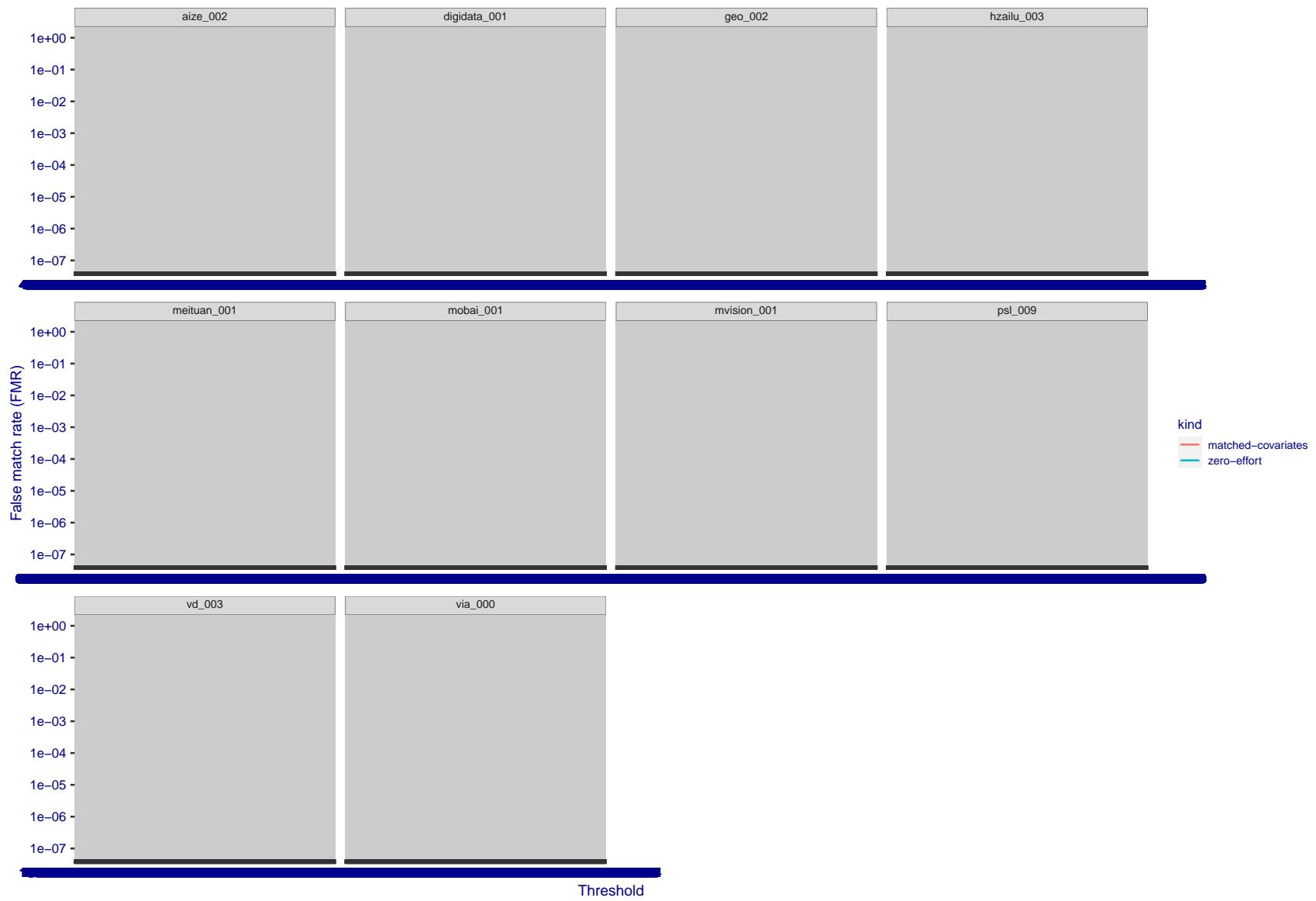


Figure 278: For the visa images, the false match calibration curves show FMR vs. threshold, T . The blue (lower) curves are for zero-effort impostors (i.e. comparing all images against all). The red (upper) curves are for persons of the same-sex, same-age, and same national-origin. This shows that FMR is underestimated (by a factor of 10 or more) by using a zero-effort impostor calculation to calibrate T . As shown later (sec. 3.6), FMR is higher for demographic-matched impostors.

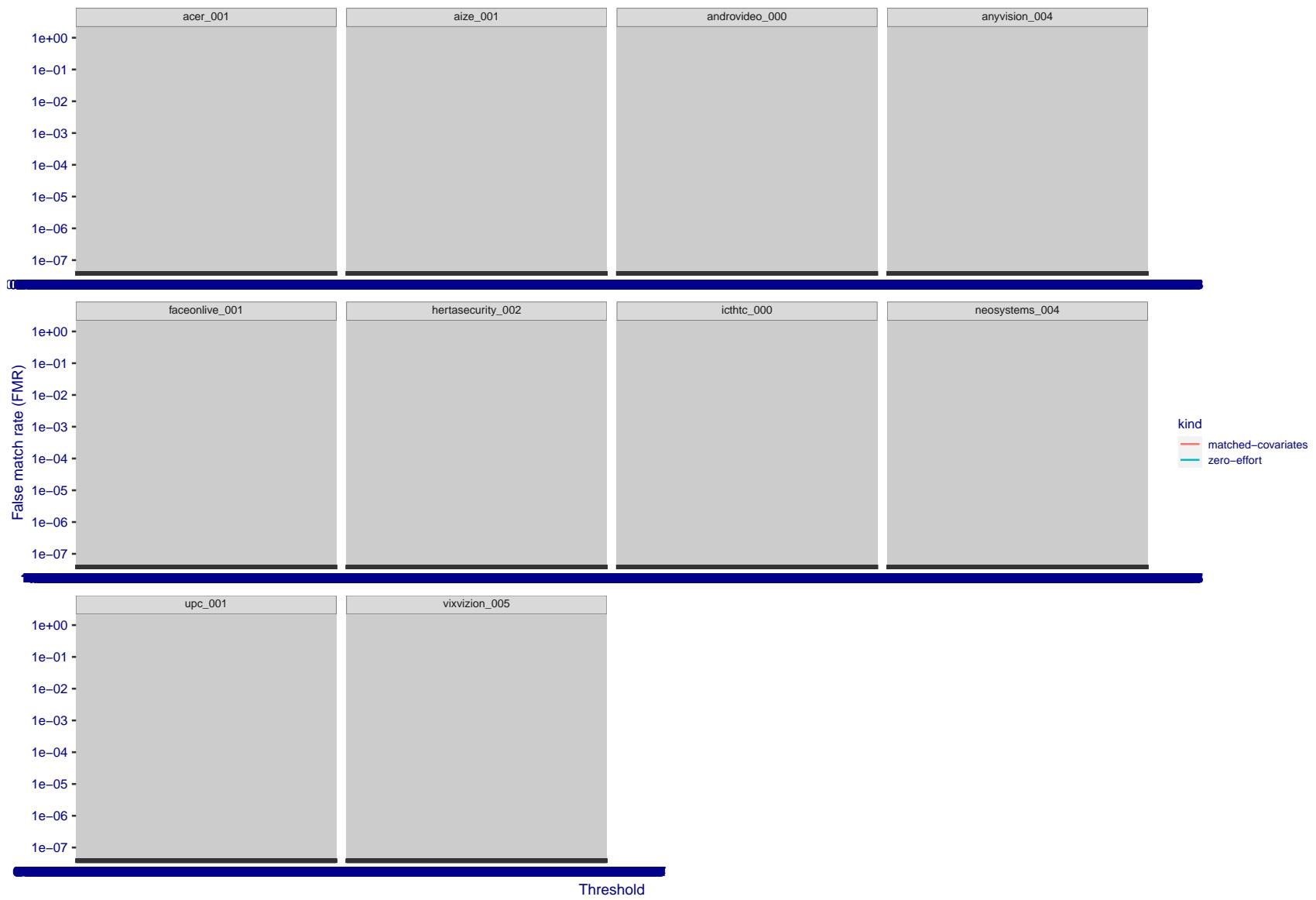


Figure 279: For the visa images, the false match calibration curves show FMR vs. threshold, T . The blue (lower) curves are for zero-effort impostors (i.e. comparing all images against all). The red (upper) curves are for persons of the same-sex, same-age, and same national-origin. This shows that FMR is underestimated (by a factor of 10 or more) by using a zero-effort impostor calculation to calibrate T . As shown later (sec. 3.6), FMR is higher for demographic-matched impostors.

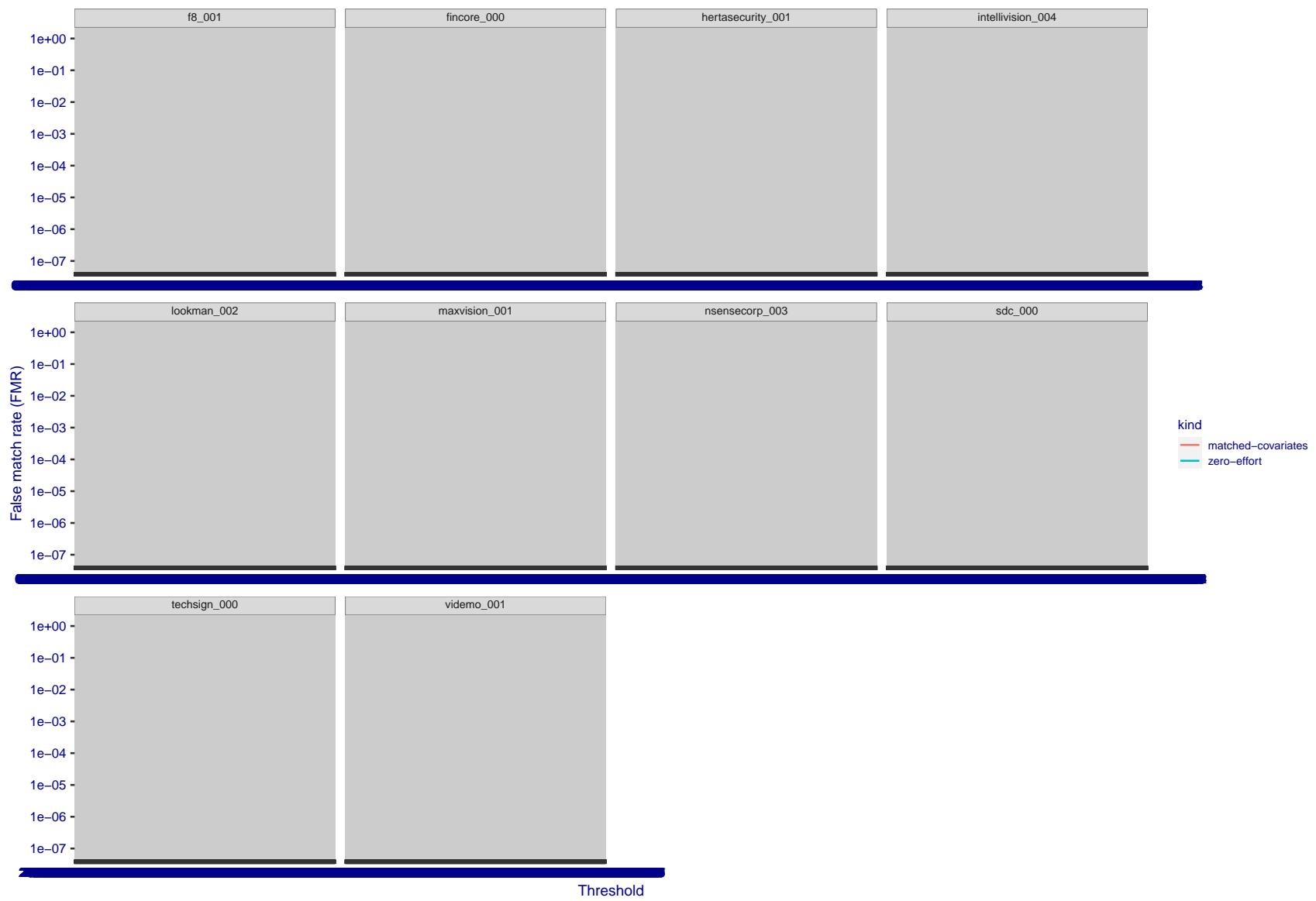


Figure 280: For the visa images, the false match calibration curves show FMR vs. threshold, T . The blue (lower) curves are for zero-effort impostors (i.e. comparing all images against all). The red (upper) curves are for persons of the same-sex, same-age, and same national-origin. This shows that FMR is underestimated (by a factor of 10 or more) by using a zero-effort impostor calculation to calibrate T . As shown later (sec. 3.6), FMR is higher for demographic-matched impostors.

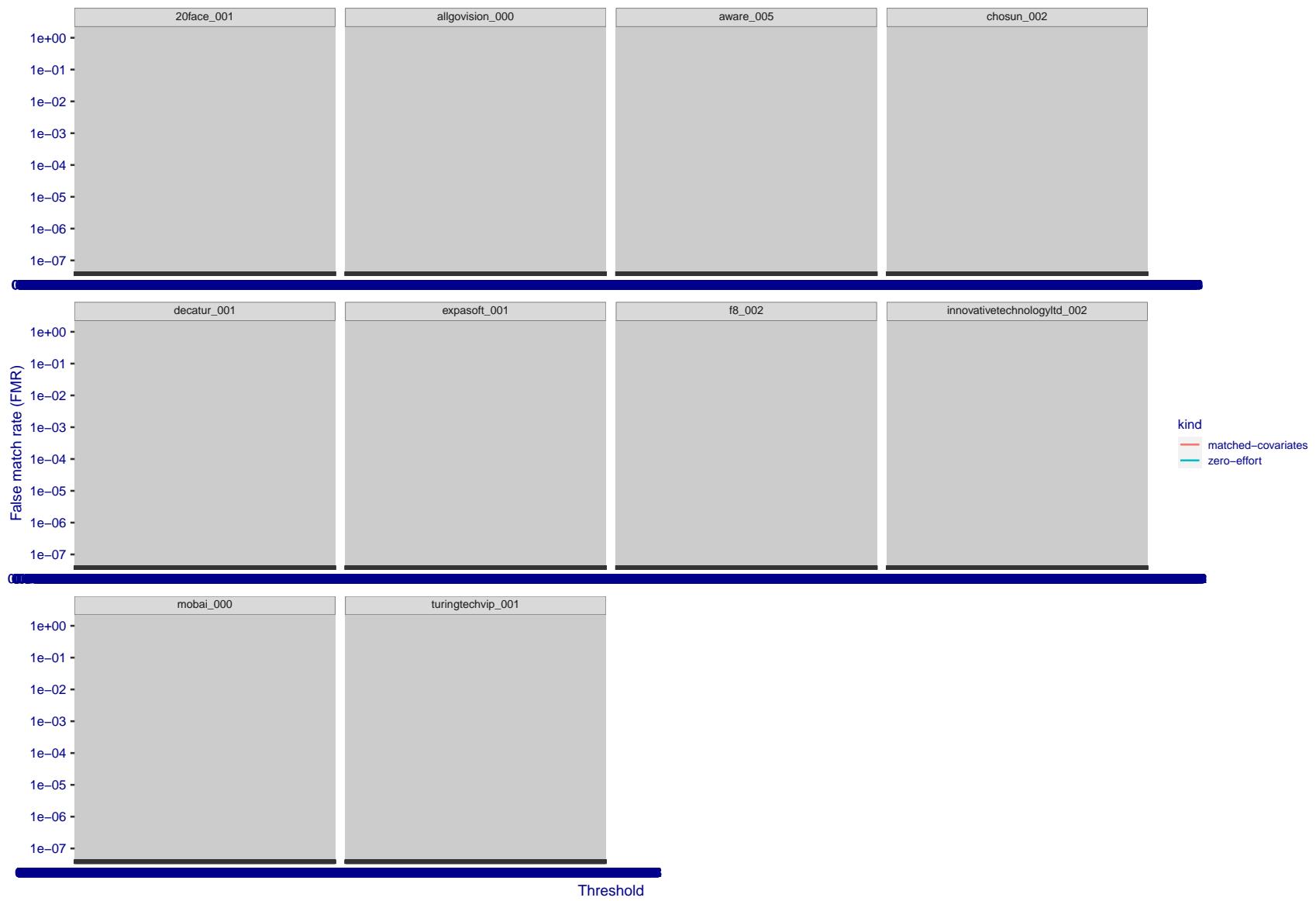


Figure 281: For the visa images, the false match calibration curves show FMR vs. threshold, T . The blue (lower) curves are for zero-effort impostors (i.e. comparing all images against all). The red (upper) curves are for persons of the same-sex, same-age, and same national-origin. This shows that FMR is underestimated (by a factor of 10 or more) by using a zero-effort impostor calculation to calibrate T . As shown later (sec. 3.6), FMR is higher for demographic-matched impostors.

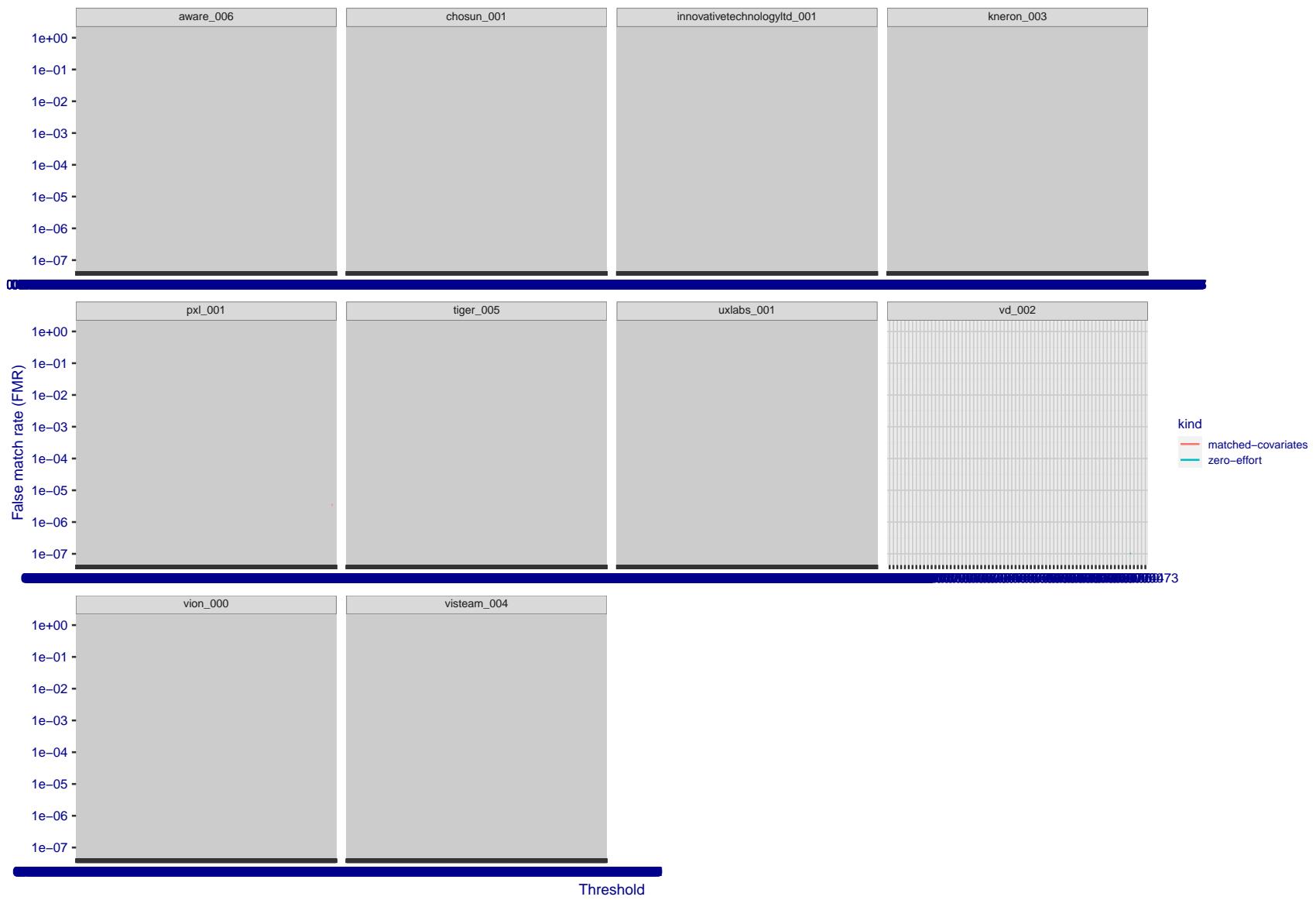


Figure 282: For the visa images, the false match calibration curves show FMR vs. threshold, T . The blue (lower) curves are for zero-effort impostors (i.e. comparing all images against all). The red (upper) curves are for persons of the same-sex, same-age, and same national-origin. This shows that FMR is underestimated (by a factor of 10 or more) by using a zero-effort impostor calculation to calibrate T . As shown later (sec. 3.6), FMR is higher for demographic-matched impostors.

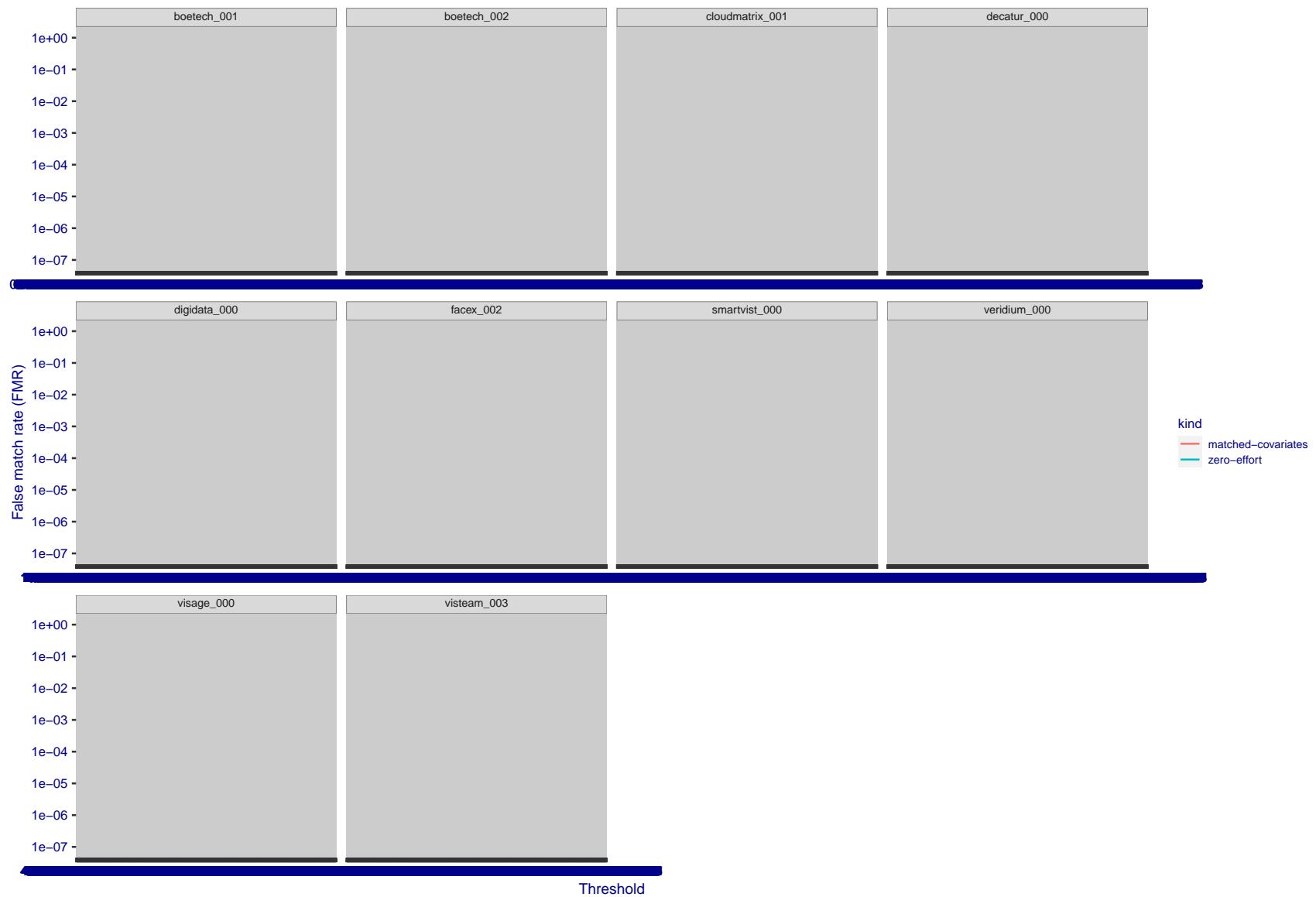


Figure 283: For the visa images, the false match calibration curves show FMR vs. threshold, T . The blue (lower) curves are for zero-effort impostors (i.e. comparing all images against all). The red (upper) curves are for persons of the same-sex, same-age, and same national-origin. This shows that FMR is underestimated (by a factor of 10 or more) by using a zero-effort impostor calculation to calibrate T . As shown later (sec. 3.6), FMR is higher for demographic-matched impostors.

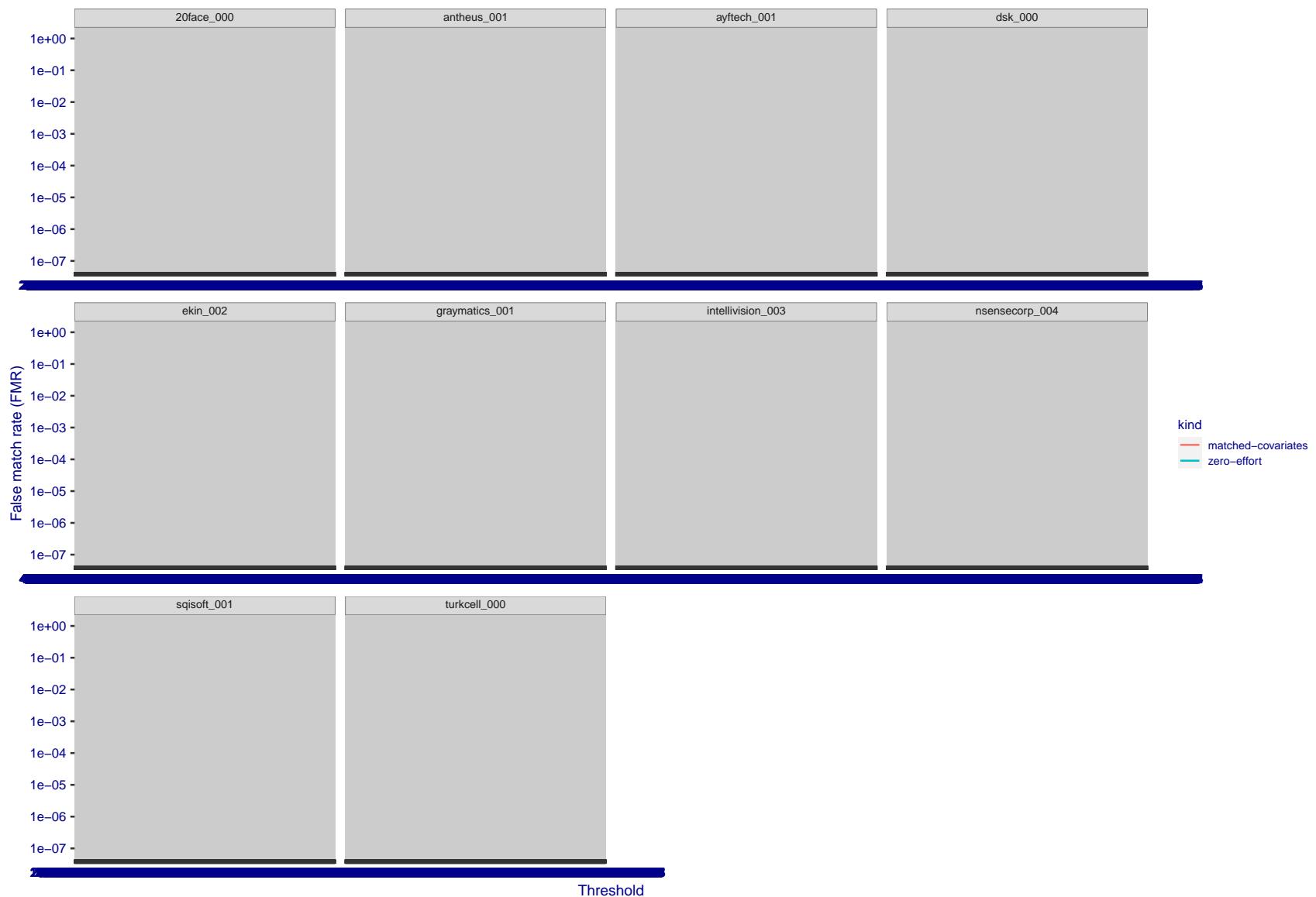


Figure 284: For the visa images, the false match calibration curves show FMR vs. threshold, T . The blue (lower) curves are for zero-effort impostors (i.e. comparing all images against all). The red (upper) curves are for persons of the same-sex, same-age, and same national-origin. This shows that FMR is underestimated (by a factor of 10 or more) by using a zero-effort impostor calculation to calibrate T . As shown later (sec. 3.6), FMR is higher for demographic-matched impostors.

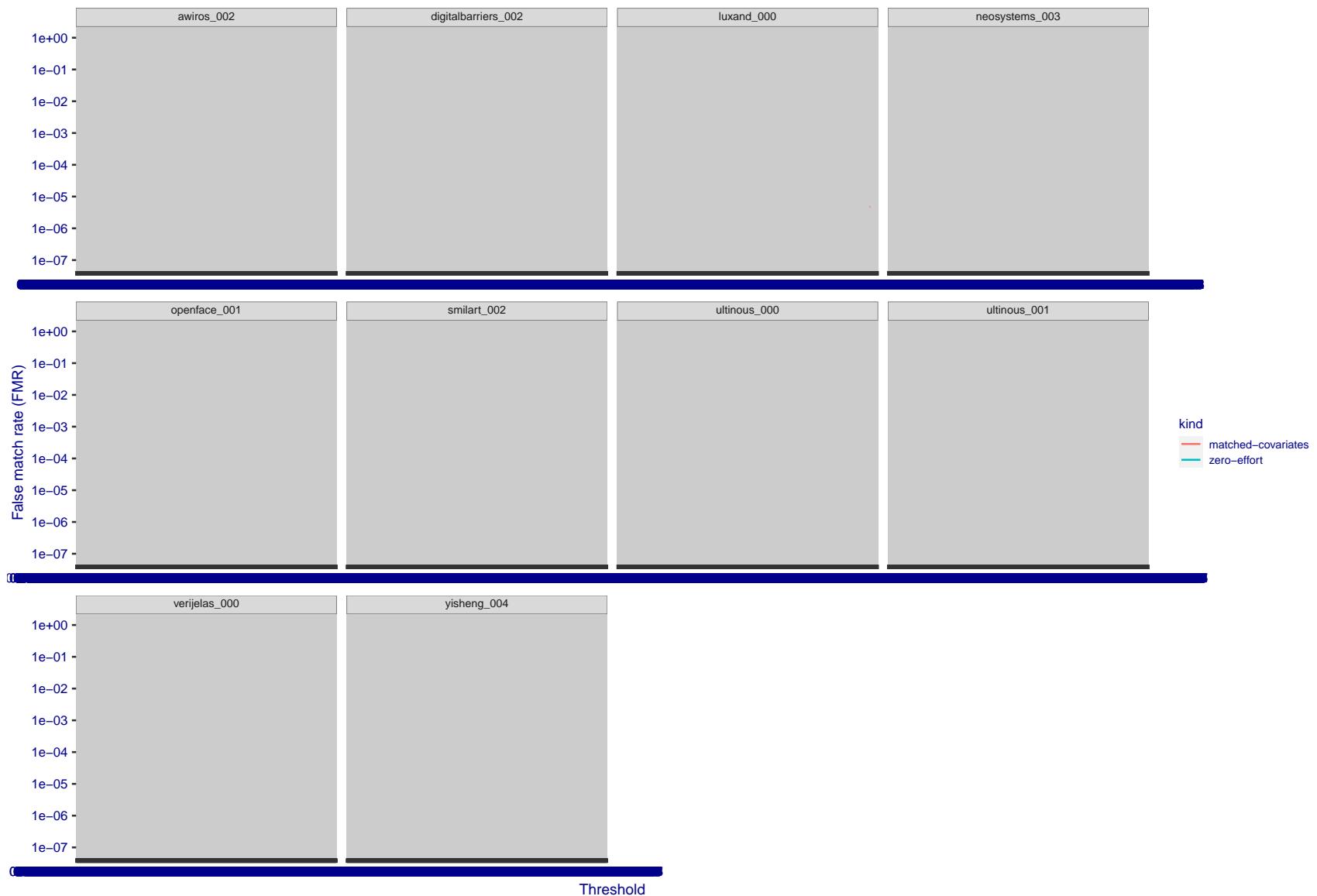


Figure 285: For the visa images, the false match calibration curves show FMR vs. threshold, T . The blue (lower) curves are for zero-effort impostors (i.e. comparing all images against all). The red (upper) curves are for persons of the same-sex, same-age, and same national-origin. This shows that FMR is underestimated (by a factor of 10 or more) by using a zero-effort impostor calculation to calibrate T . As shown later (sec. 3.6), FMR is higher for demographic-matched impostors.

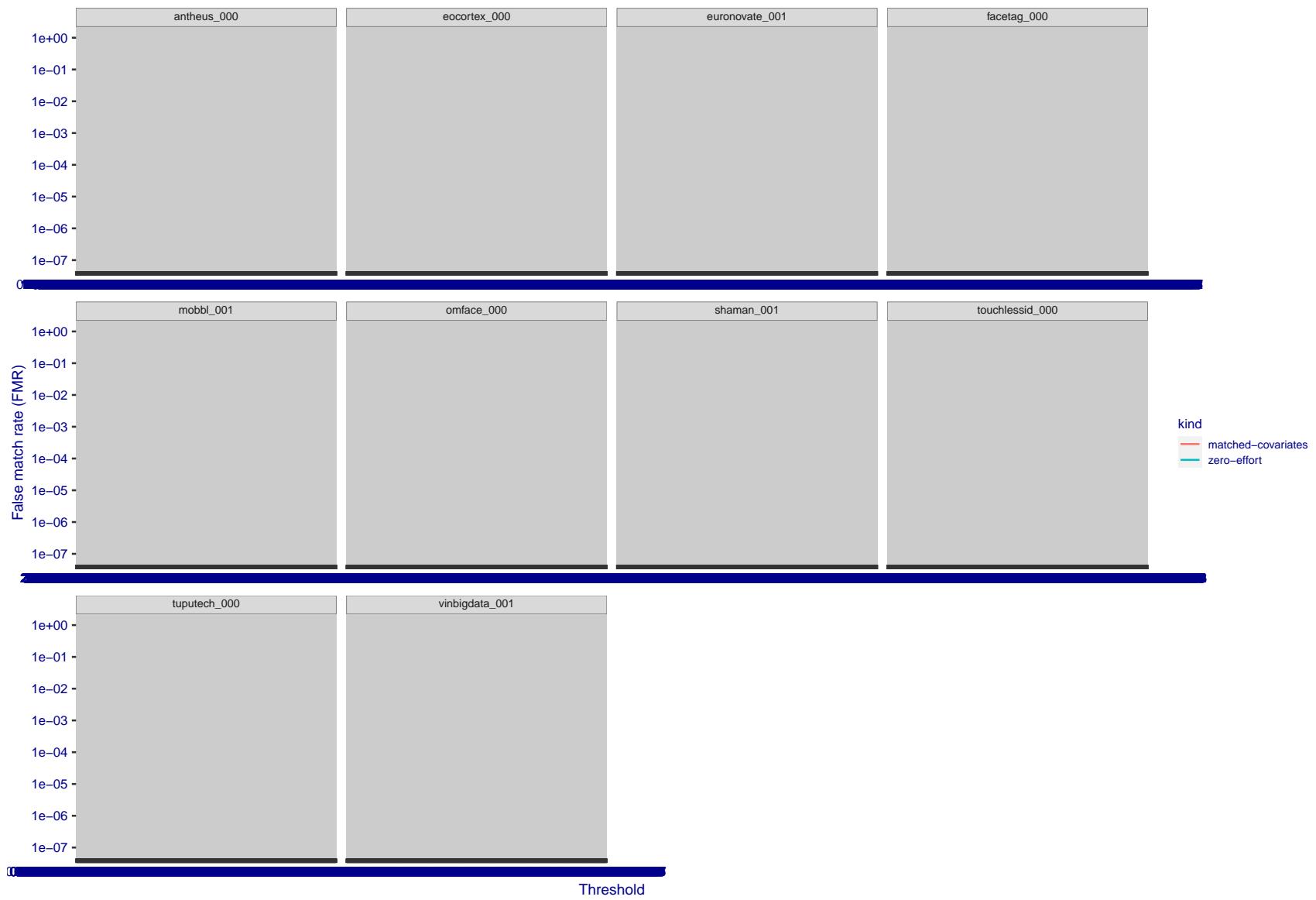


Figure 286: For the visa images, the false match calibration curves show FMR vs. threshold, T . The blue (lower) curves are for zero-effort impostors (i.e. comparing all images against all). The red (upper) curves are for persons of the same-sex, same-age, and same national-origin. This shows that FMR is underestimated (by a factor of 10 or more) by using a zero-effort impostor calculation to calibrate T . As shown later (sec. 3.6), FMR is higher for demographic-matched impostors.

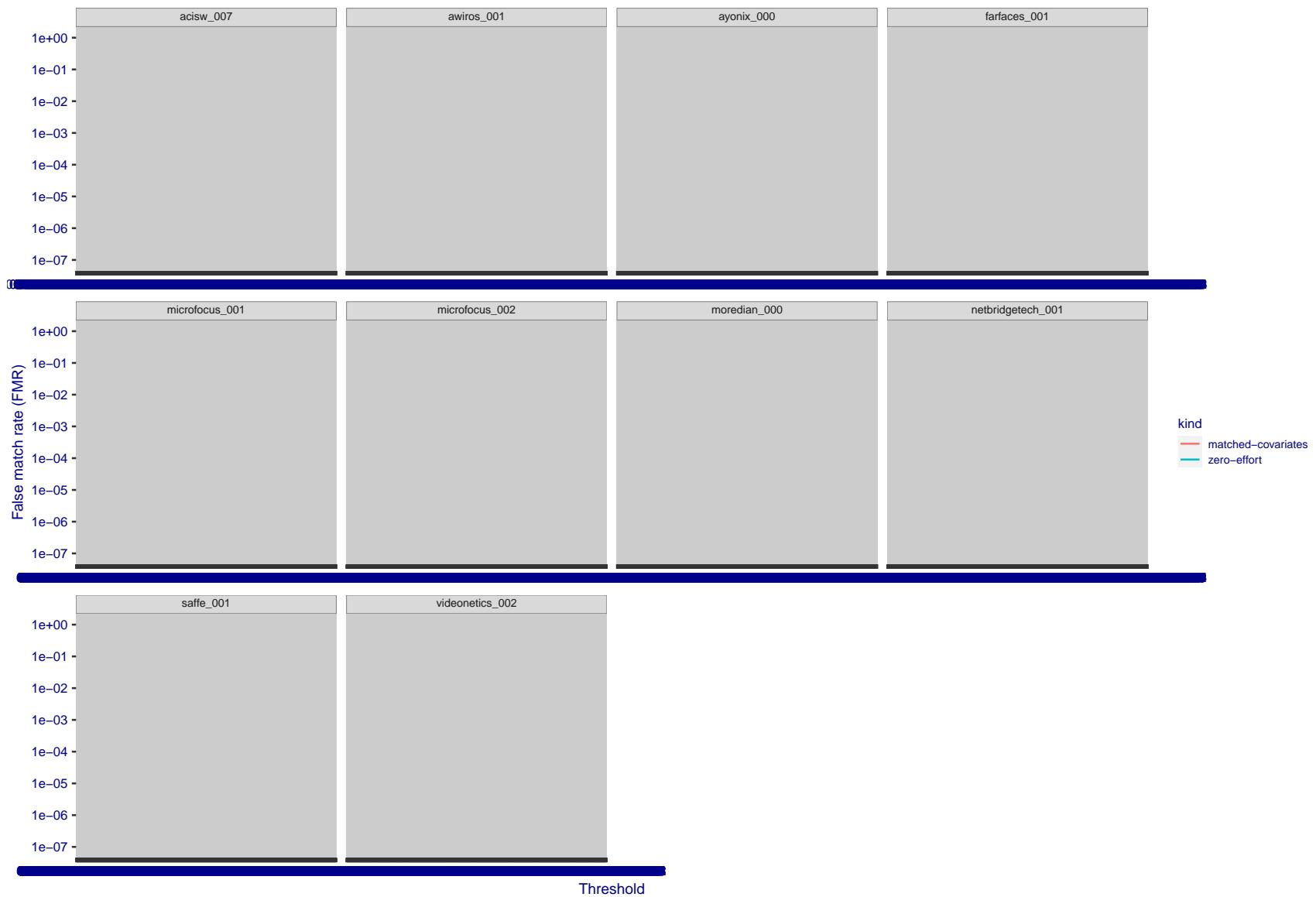


Figure 287: For the visa images, the false match calibration curves show FMR vs. threshold, T . The blue (lower) curves are for zero-effort impostors (i.e. comparing all images against all). The red (upper) curves are for persons of the same-sex, same-age, and same national-origin. This shows that FMR is underestimated (by a factor of 10 or more) by using a zero-effort impostor calculation to calibrate T . As shown later (sec. 3.6), FMR is higher for demographic-matched impostors.

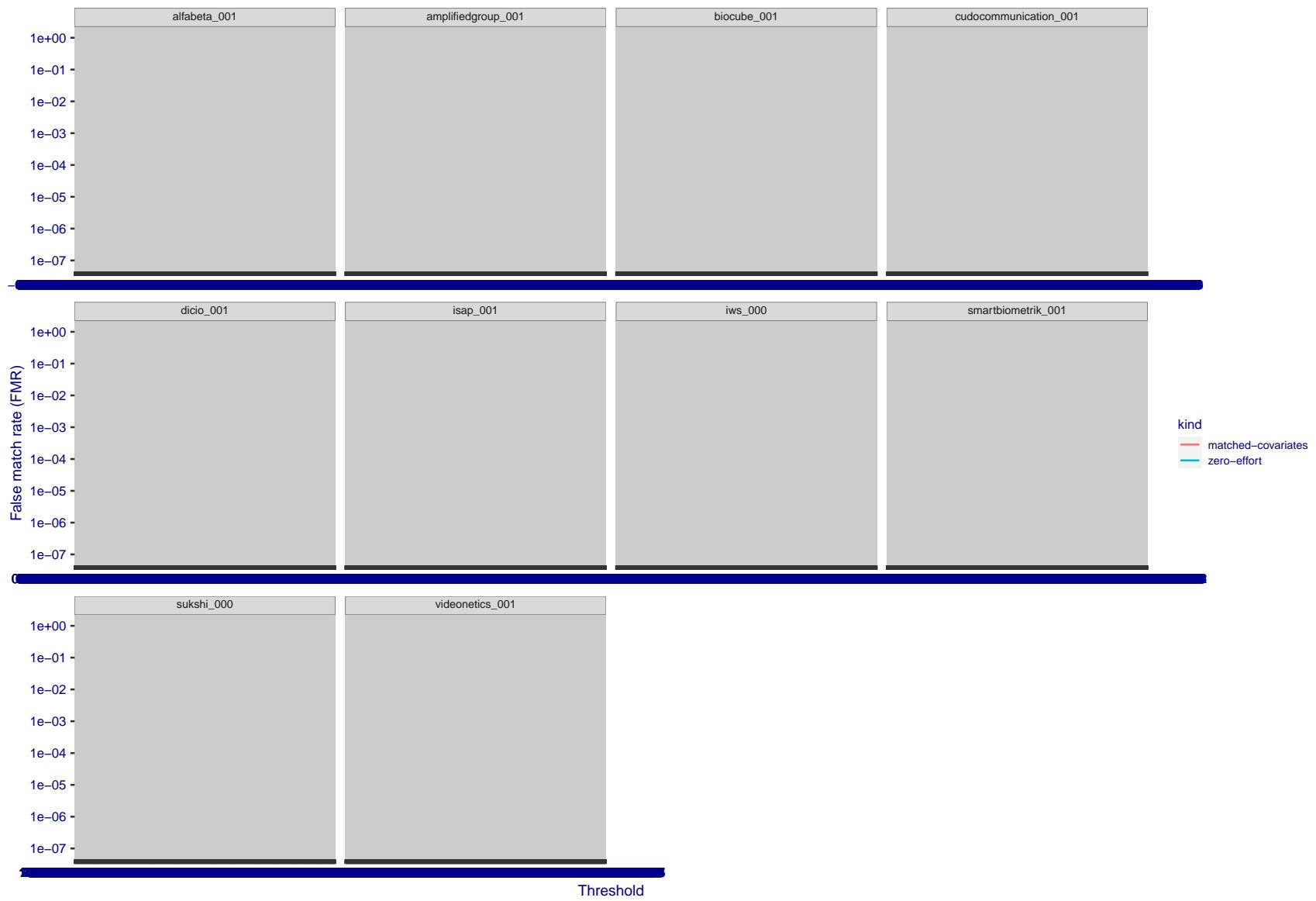


Figure 288: For the visa images, the false match calibration curves show FMR vs. threshold, T . The blue (lower) curves are for zero-effort impostors (i.e. comparing all images against all). The red (upper) curves are for persons of the same-sex, same-age, and same national-origin. This shows that FMR is underestimated (by a factor of 10 or more) by using a zero-effort impostor calculation to calibrate T . As shown later (sec. 3.6), FMR is higher for demographic-matched impostors.

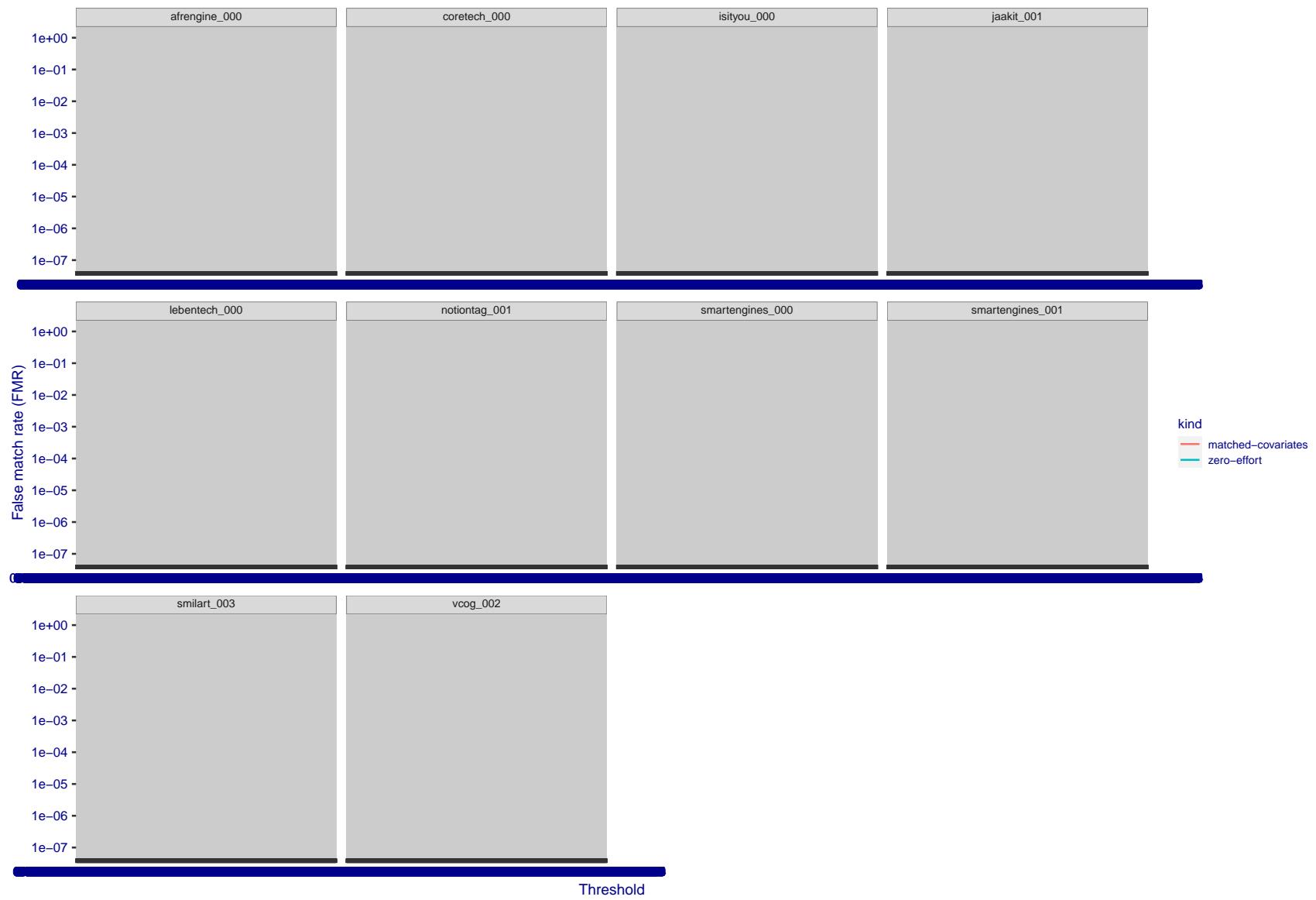


Figure 289: For the visa images, the false match calibration curves show FMR vs. threshold, T . The blue (lower) curves are for zero-effort impostors (i.e. comparing all images against all). The red (upper) curves are for persons of the same-sex, same-age, and same national-origin. This shows that FMR is underestimated (by a factor of 10 or more) by using a zero-effort impostor calculation to calibrate T . As shown later (sec. 3.6), FMR is higher for demographic-matched impostors.

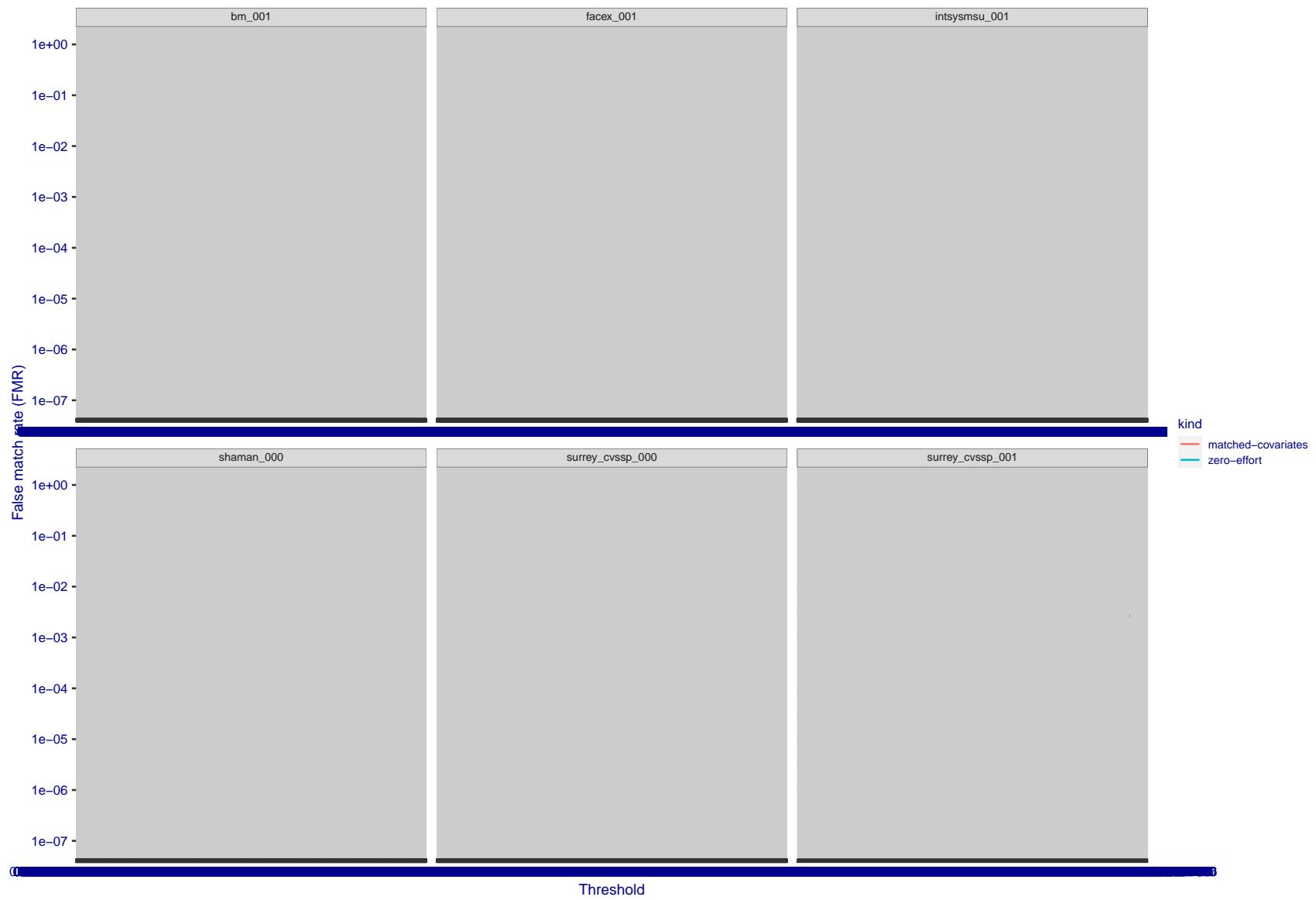


Figure 290: For the visa images, the false match calibration curves show FMR vs. threshold, T . The blue (lower) curves are for zero-effort impostors (i.e. comparing all images against all). The red (upper) curves are for persons of the same-sex, same-age, and same national-origin. This shows that FMR is underestimated (by a factor of 10 or more) by using a zero-effort impostor calculation to calibrate T . As shown later (sec. 3.6), FMR is higher for demographic-matched impostors.

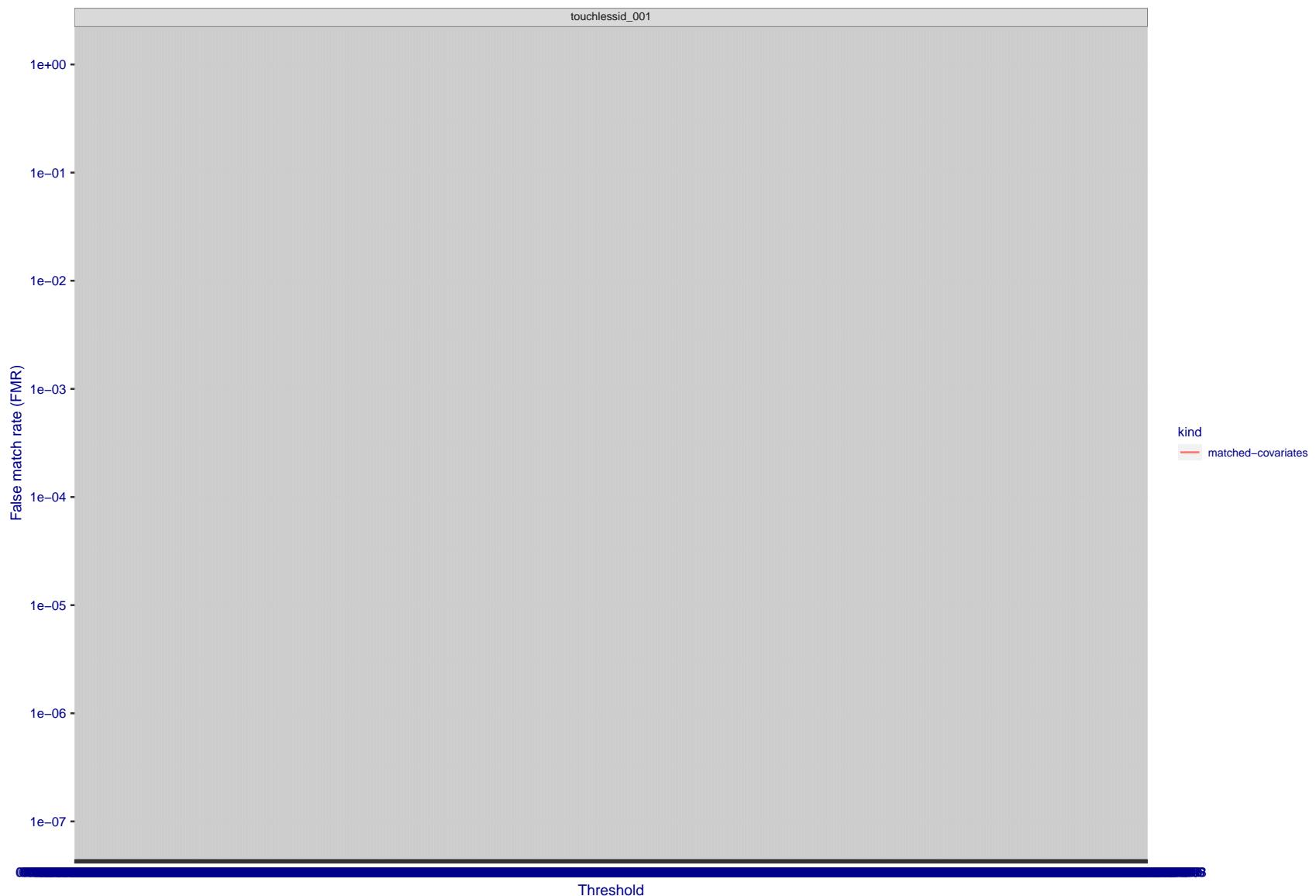


Figure 291: For the visa images, the false match calibration curves show FMR vs. threshold, T . The blue (lower) curves are for zero-effort impostors (i.e. comparing all images against all). The red (upper) curves are for persons of the same-sex, same-age, and same national-origin. This shows that FMR is underestimated (by a factor of 10 or more) by using a zero-effort impostor calculation to calibrate T . As shown later (sec. 3.6), FMR is higher for demographic-matched impostors.

3.5 Genuine distribution stability

3.5.1 Effect of birth place on the genuine distribution

Background: Both skin tone and bone structure vary geographically. Prior studies have reported variations in FNMR and FMR.

Goal: To measure false non-match rate (FNMR) variation with country of birth.

Methods: Thresholds are determined that give $FMR = \{0.001, 0.0001\}$ over the entire impostor set. Then FNMR is measured over 1000 bootstrap replications of the genuine scores. Only those countries with at least 140 individuals are included in the analysis.

Results: Figure 330 shows FNMR by country of birth for the two thresholds.

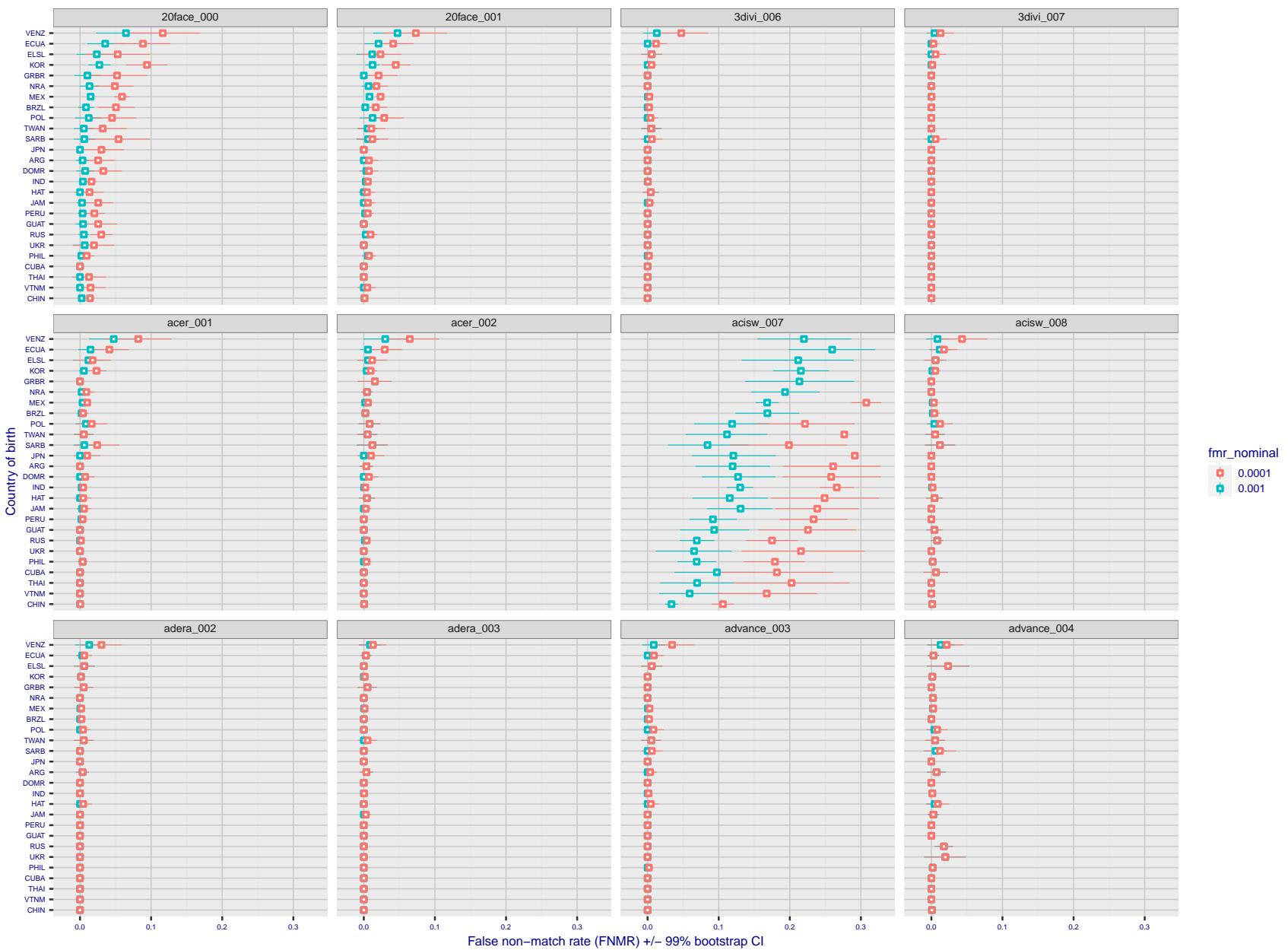


Figure 292: For the visa images, the dots show FNMR by country of birth for two globally set operating thresholds corresponding to $FMR = \{0.001, 0.0001\}$ computed over all on the order of 10^{10} impostor scores. The FMR in each bin will vary also - see subsequent impostor heatmaps in sec. 3.6.1. The figures shows an order of magnitude variation in FNMR across country of birth; these effects are likely due quality variations, then demographics like age and race. The error rates in some cases are zero, and in others the DET is flat so the error rates at the two thresholds are identical. The lines span 1% and 99% of bootstrap replicated FNMR estimates.

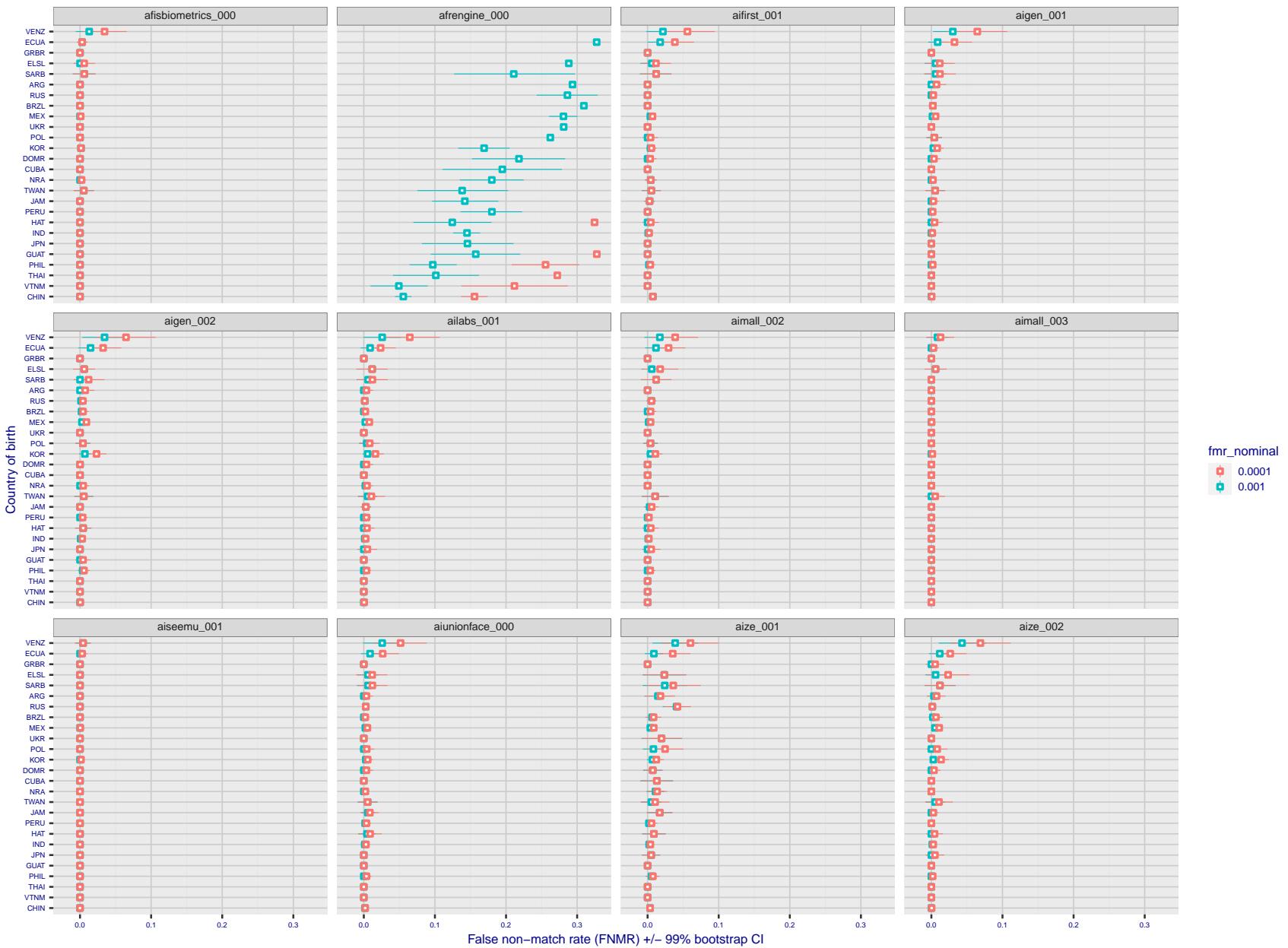


Figure 293: For the visa images, the dots show FNMR by country of birth for two globally set operating thresholds corresponding to $FMR = \{0.001, 0.0001\}$ computed over all on the order of 10^{10} impostor scores. The FMR in each bin will vary also - see subsequent impostor heatmaps in sec. 3.6.1. The figures shows an order of magnitude variation in FNMR across country of birth; these effects are likely due quality variations, then demographics like age and race. The error rates in some cases are zero, and in others the DET is flat so the error rates at the two thresholds are identical. The lines span 1% and 99% of bootstrap replicated FNMR estimates.

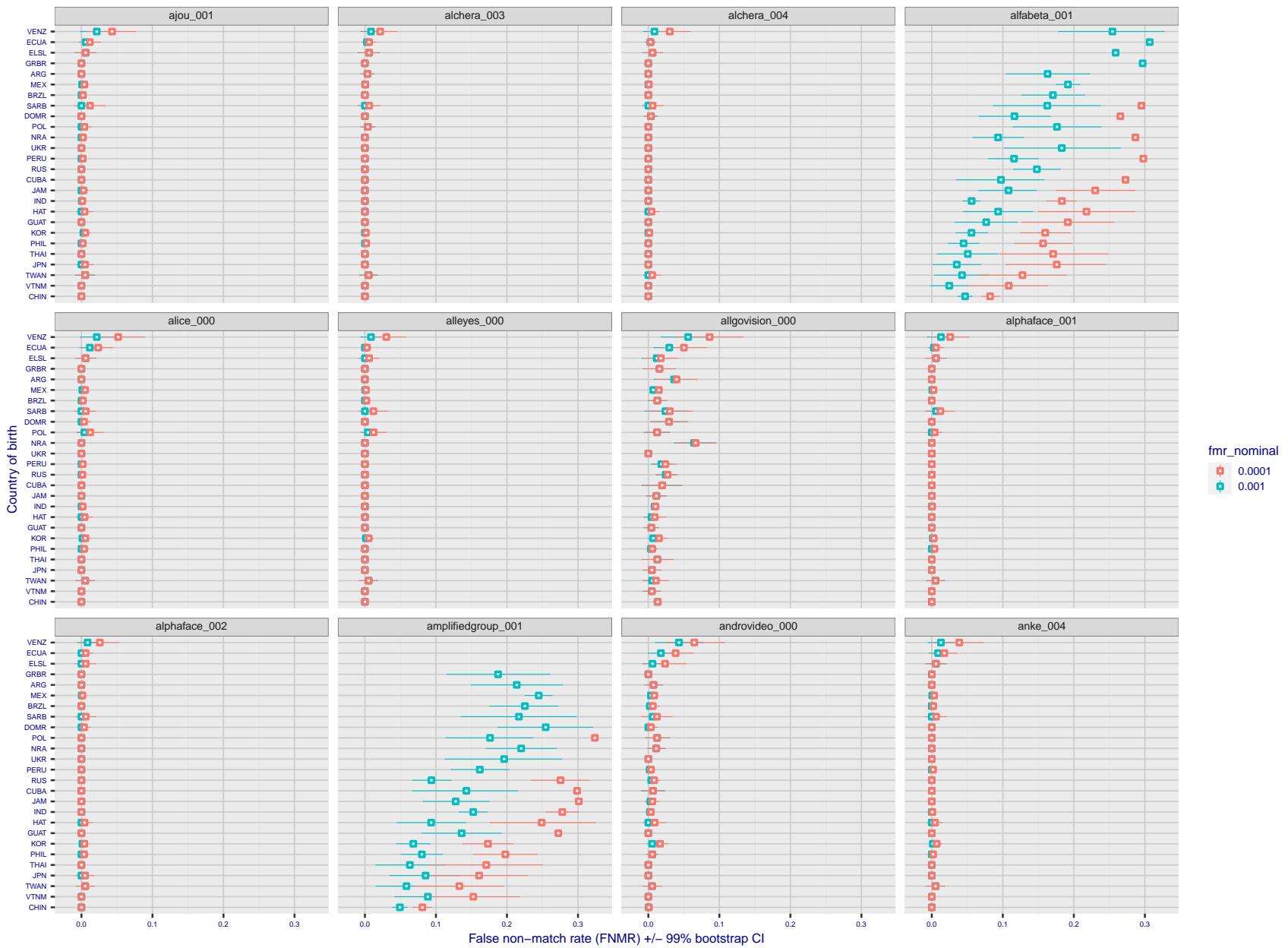


Figure 294: For the visa images, the dots show FNMR by country of birth for two globally set operating thresholds corresponding to $FMR = \{0.001, 0.0001\}$ computed over all on the order of 10^{10} impostor scores. The FMR in each bin will vary also - see subsequent impostor heatmaps in sec. 3.6.1. The figures shows an order of magnitude variation in FNMR across country of birth; these effects are likely due quality variations, then demographics like age and race. The error rates in some cases are zero, and in others the DET is flat so the error rates at the two thresholds are identical. The lines span 1% and 99% of bootstrap replicated FNMR estimates.

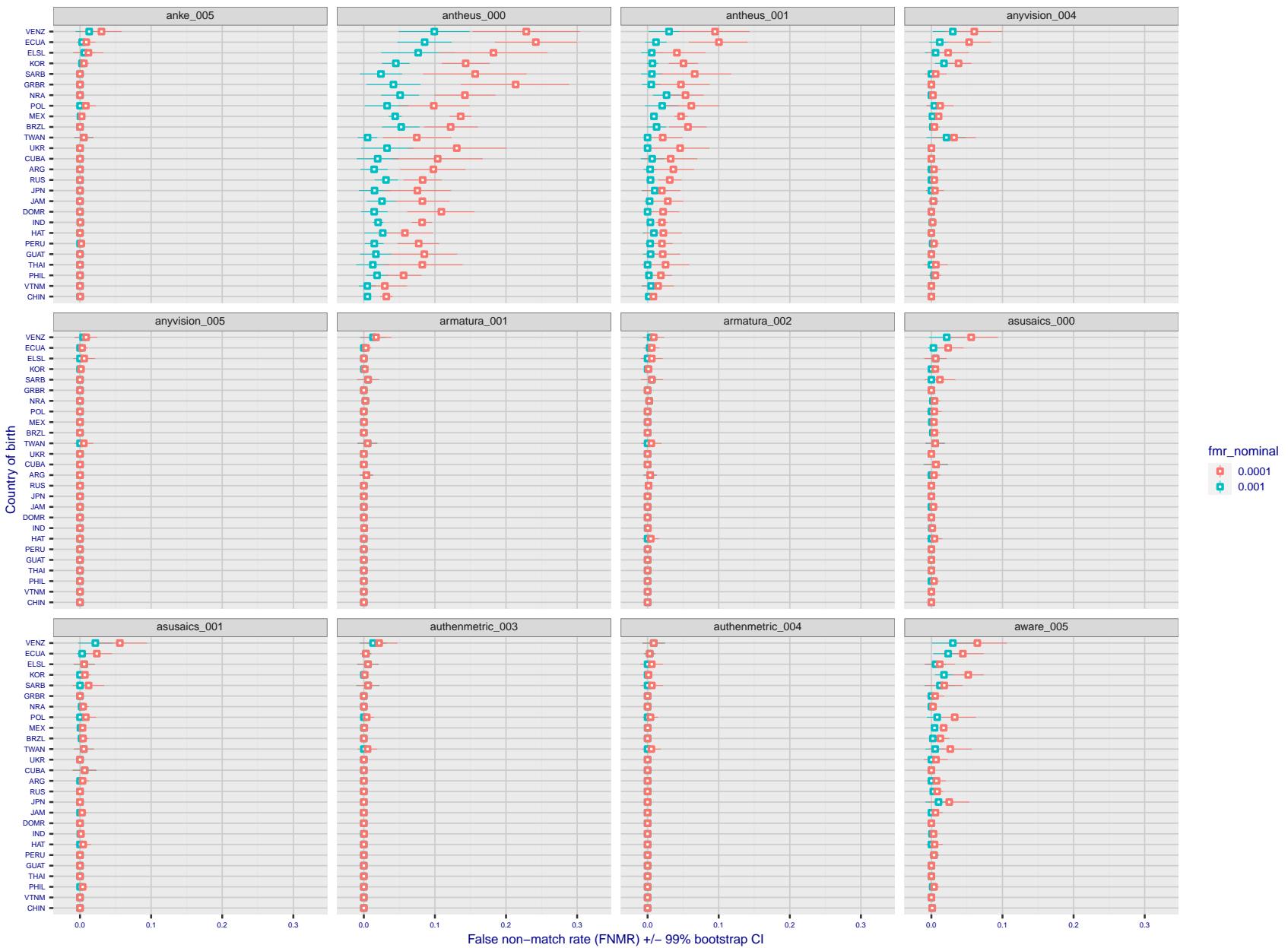


Figure 295: For the visa images, the dots show FNMR by country of birth for two globally set operating thresholds corresponding to $FMR = \{0.001, 0.0001\}$ computed over all on the order of 10^{10} impostor scores. The FMR in each bin will vary also - see subsequent impostor heatmaps in sec. 3.6.1. The figures shows an order of magnitude variation in FNMR across country of birth; these effects are likely due quality variations, then demographics like age and race. The error rates in some cases are zero, and in others the DET is flat so the error rates at the two thresholds are identical. The lines span 1% and 99% of bootstrap replicated FNMR estimates.

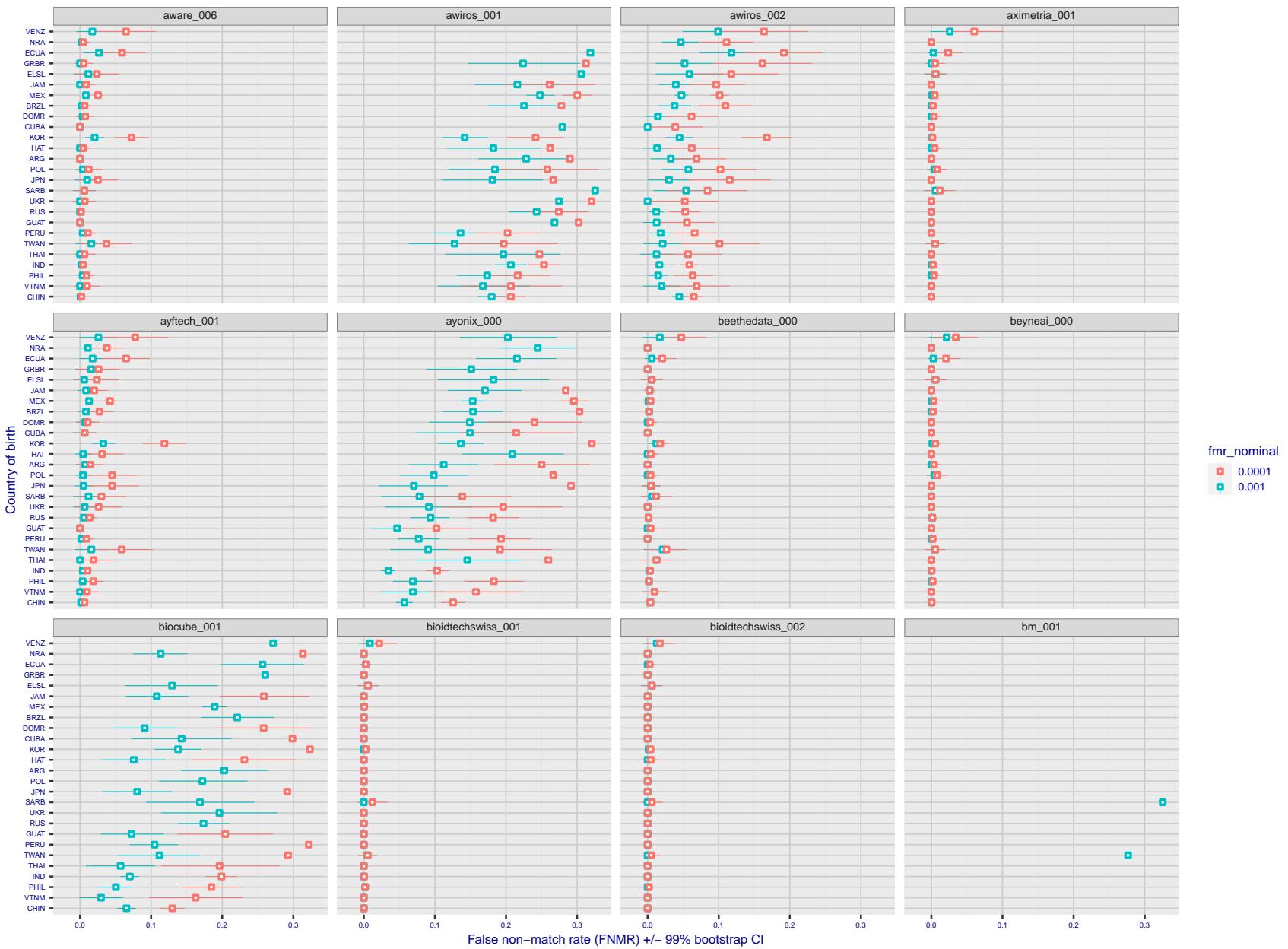


Figure 296: For the visa images, the dots show FNMR by country of birth for two globally set operating thresholds corresponding to $FMR = \{0.001, 0.0001\}$ computed over all on the order of 10^{10} impostor scores. The FMR in each bin will vary also - see subsequent impostor heatmaps in sec. 3.6.1. The figures shows an order of magnitude variation in FNMR across country of birth; these effects are likely due quality variations, then demographics like age and race. The error rates in some cases are zero, and in others the DET is flat so the error rates at the two thresholds are identical. The lines span 1% and 99% of bootstrap replicated FNMR estimates.

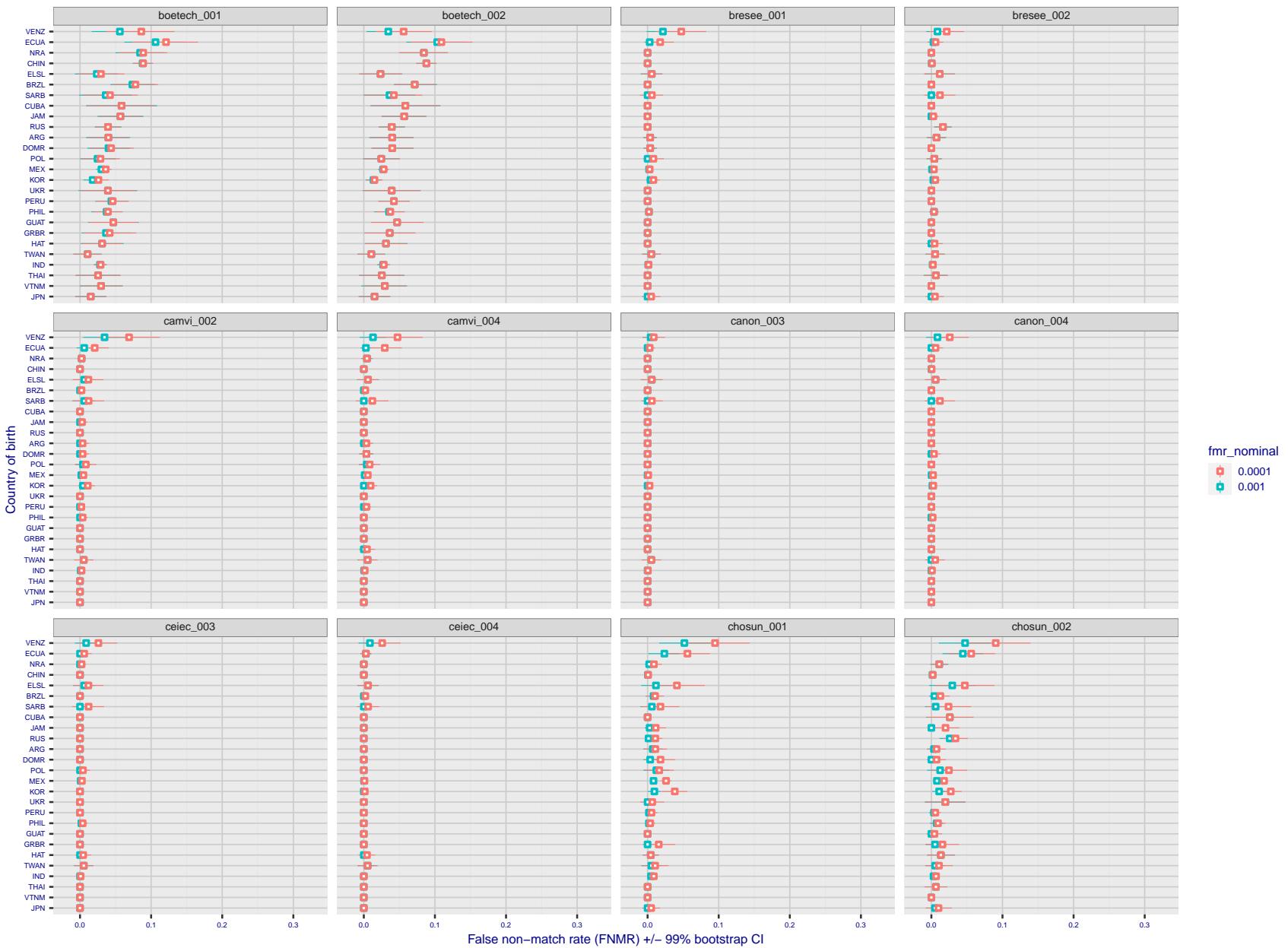


Figure 297: For the visa images, the dots show FNMR by country of birth for two globally set operating thresholds corresponding to $FMR = \{0.001, 0.0001\}$ computed over all on the order of 10^{10} impostor scores. The FMR in each bin will vary also - see subsequent impostor heatmaps in sec. 3.6.1. The figures shows an order of magnitude variation in FNMR across country of birth; these effects are likely due quality variations, then demographics like age and race. The error rates in some cases are zero, and in others the DET is flat so the error rates at the two thresholds are identical. The lines span 1% and 99% of bootstrap replicated FNMR estimates.

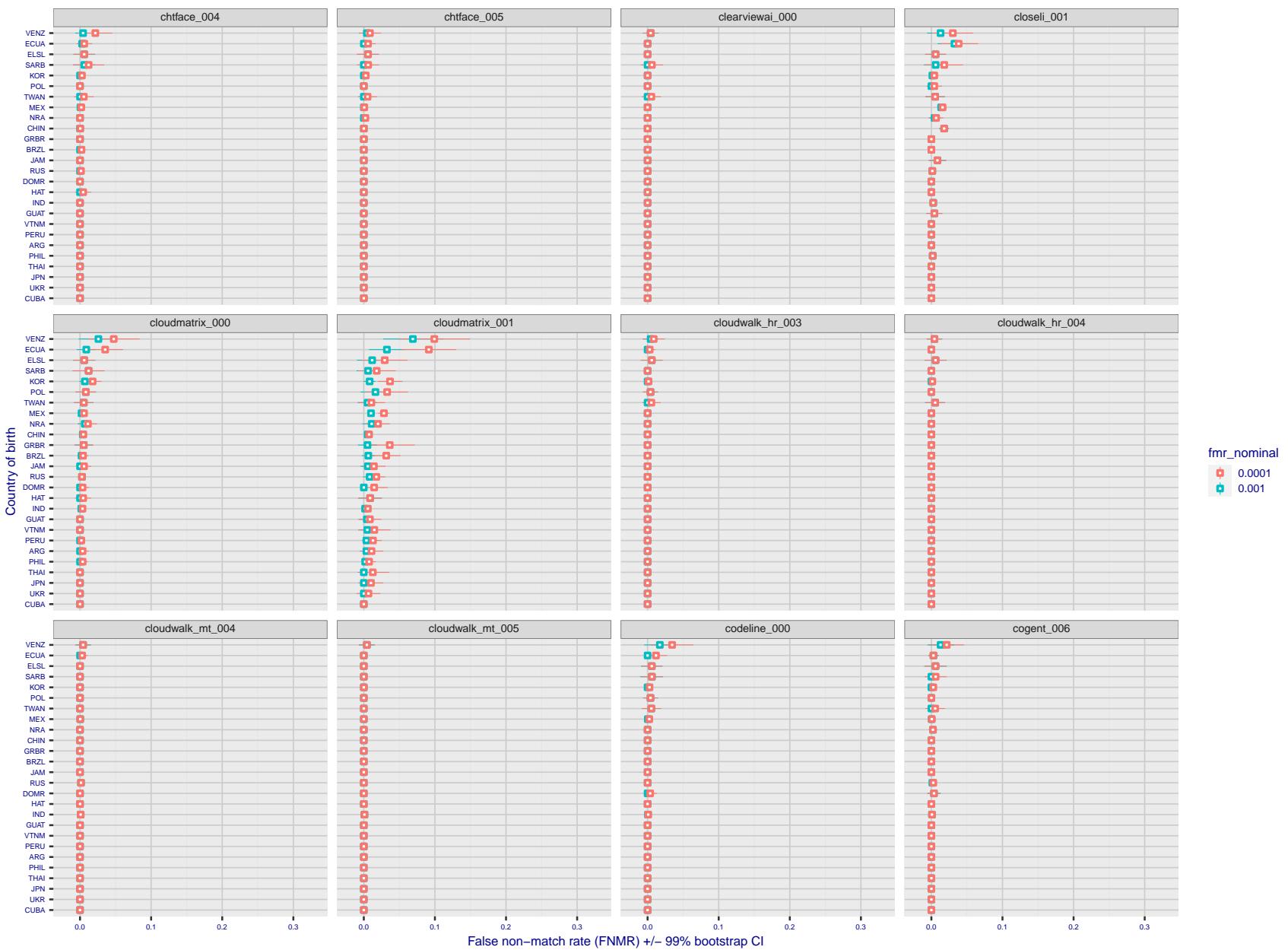


Figure 298: For the visa images, the dots show FNMR by country of birth for two globally set operating thresholds corresponding to $FMR = \{0.001, 0.0001\}$ computed over all on the order of 10^{10} impostor scores. The FMR in each bin will vary also - see subsequent impostor heatmaps in sec. 3.6.1. The figures shows an order of magnitude variation in FNMR across country of birth; these effects are likely due quality variations, then demographics like age and race. The error rates in some cases are zero, and in others the DET is flat so the error rates at the two thresholds are identical. The lines span 1% and 99% of bootstrap replicated FNMR estimates.

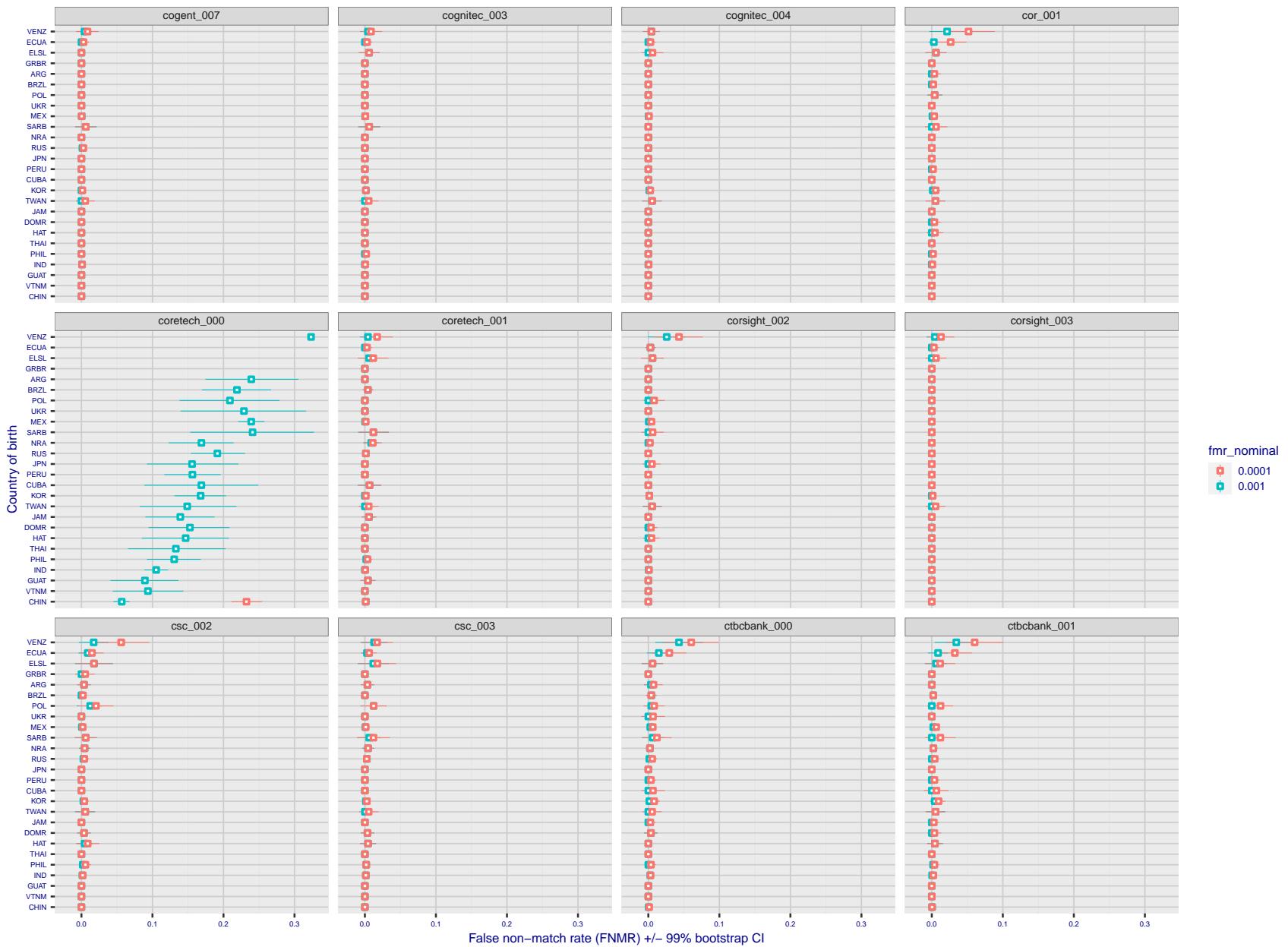


Figure 299: For the visa images, the dots show FNMR by country of birth for two globally set operating thresholds corresponding to $FMR = \{0.001, 0.0001\}$ computed over all on the order of 10^{10} impostor scores. The FMR in each bin will vary also - see subsequent impostor heatmaps in sec. 3.6.1. The figures shows an order of magnitude variation in FNMR across country of birth; these effects are likely due quality variations, then demographics like age and race. The error rates in some cases are zero, and in others the DET is flat so the error rates at the two thresholds are identical. The lines span 1% and 99% of bootstrap replicated FNMR estimates.

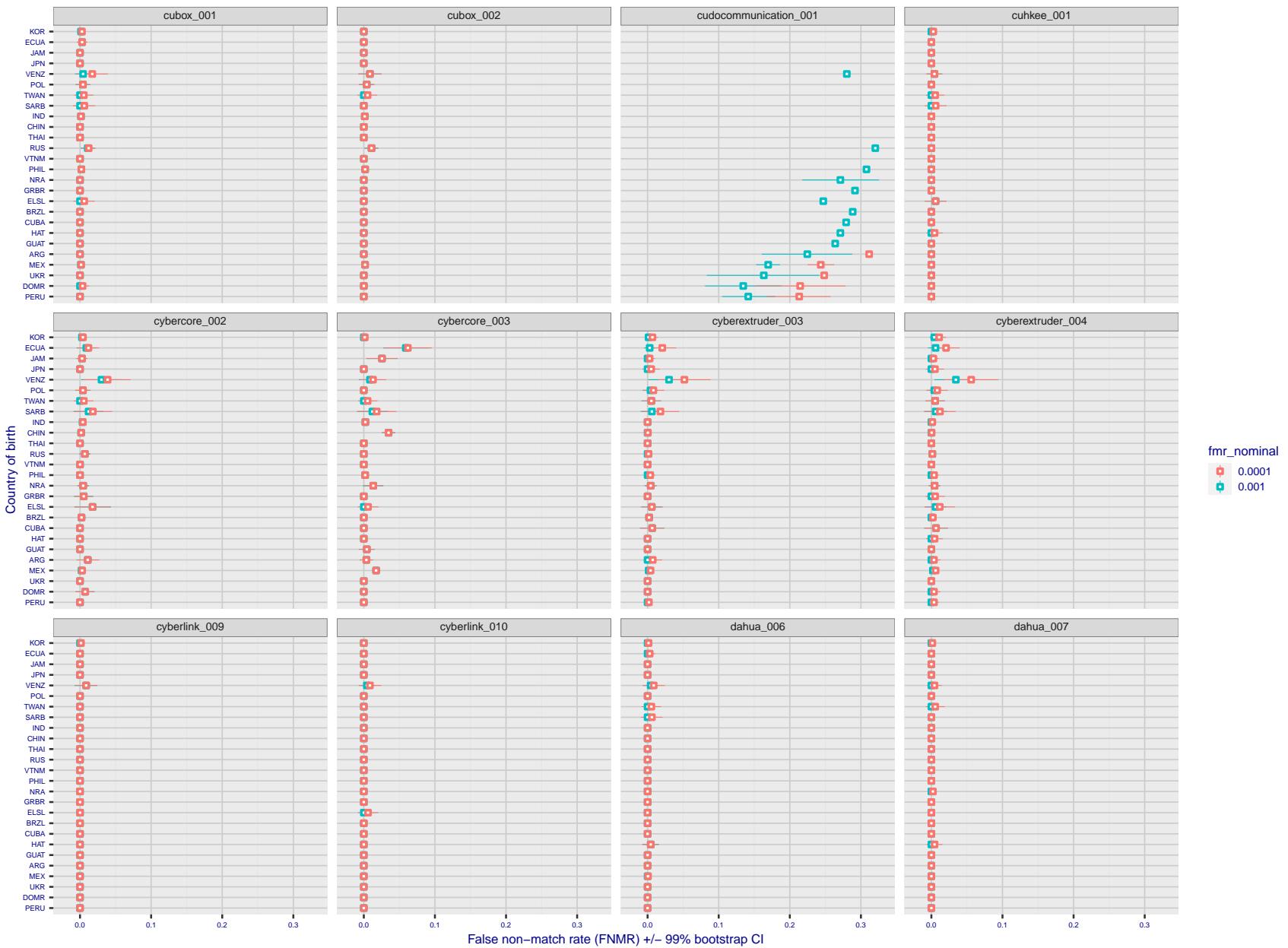


Figure 300: For the visa images, the dots show FNMR by country of birth for two globally set operating thresholds corresponding to $FMR = \{0.001, 0.0001\}$ computed over all on the order of 10^{10} impostor scores. The FMR in each bin will vary also - see subsequent impostor heatmaps in sec. 3.6.1. The figures shows an order of magnitude variation in FNMR across country of birth; these effects are likely due quality variations, then demographics like age and race. The error rates in some cases are zero, and in others the DET is flat so the error rates at the two thresholds are identical. The lines span 1% and 99% of bootstrap replicated FNMR estimates.

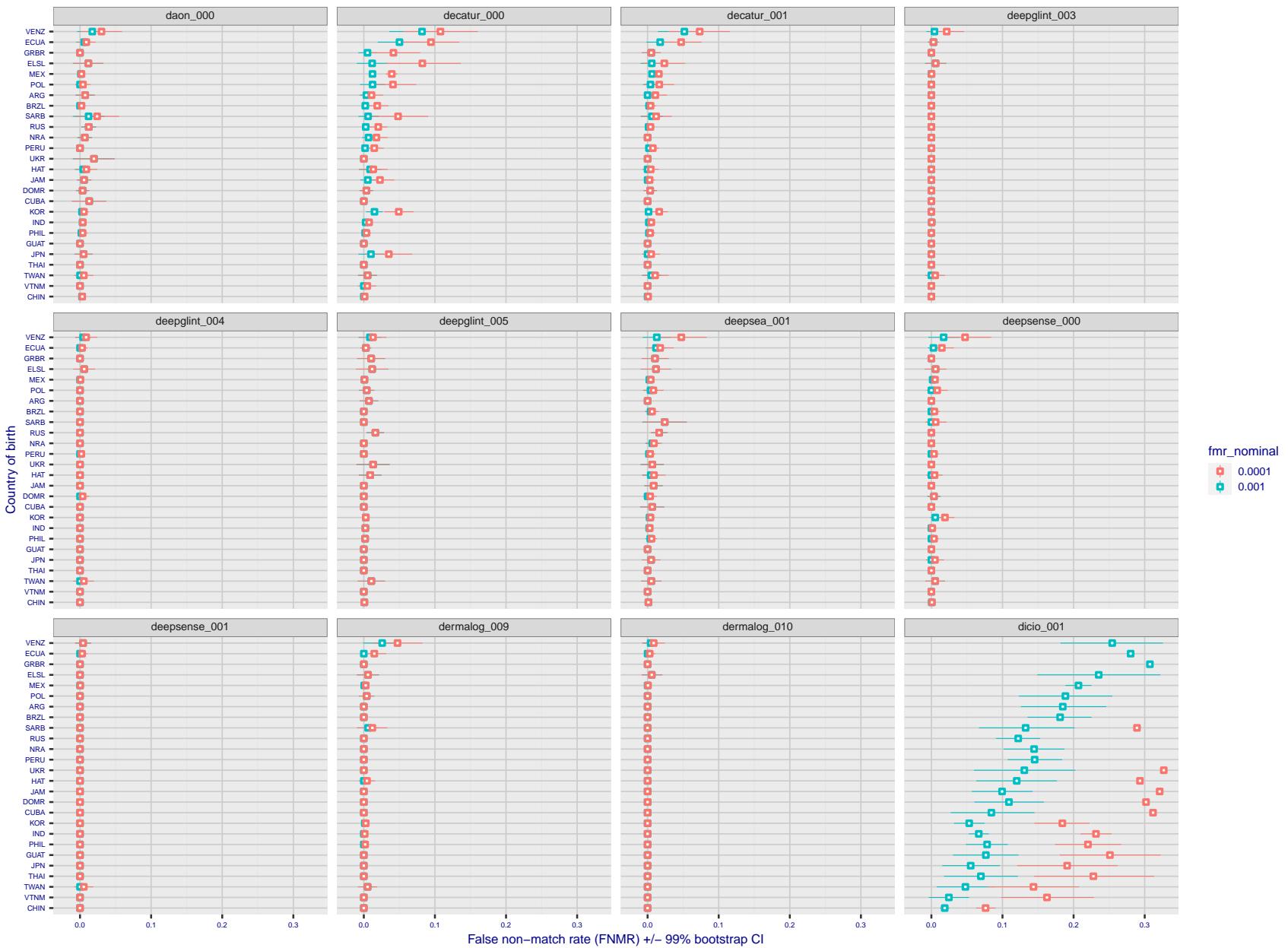


Figure 301: For the visa images, the dots show FNMR by country of birth for two globally set operating thresholds corresponding to $FMR = \{0.001, 0.0001\}$ computed over all on the order of 10^{10} impostor scores. The FMR in each bin will vary also - see subsequent impostor heatmaps in sec. 3.6.1. The figures shows an order of magnitude variation in FNMR across country of birth; these effects are likely due quality variations, then demographics like age and race. The error rates in some cases are zero, and in others the DET is flat so the error rates at the two thresholds are identical. The lines span 1% and 99% of bootstrap replicated FNMR estimates.

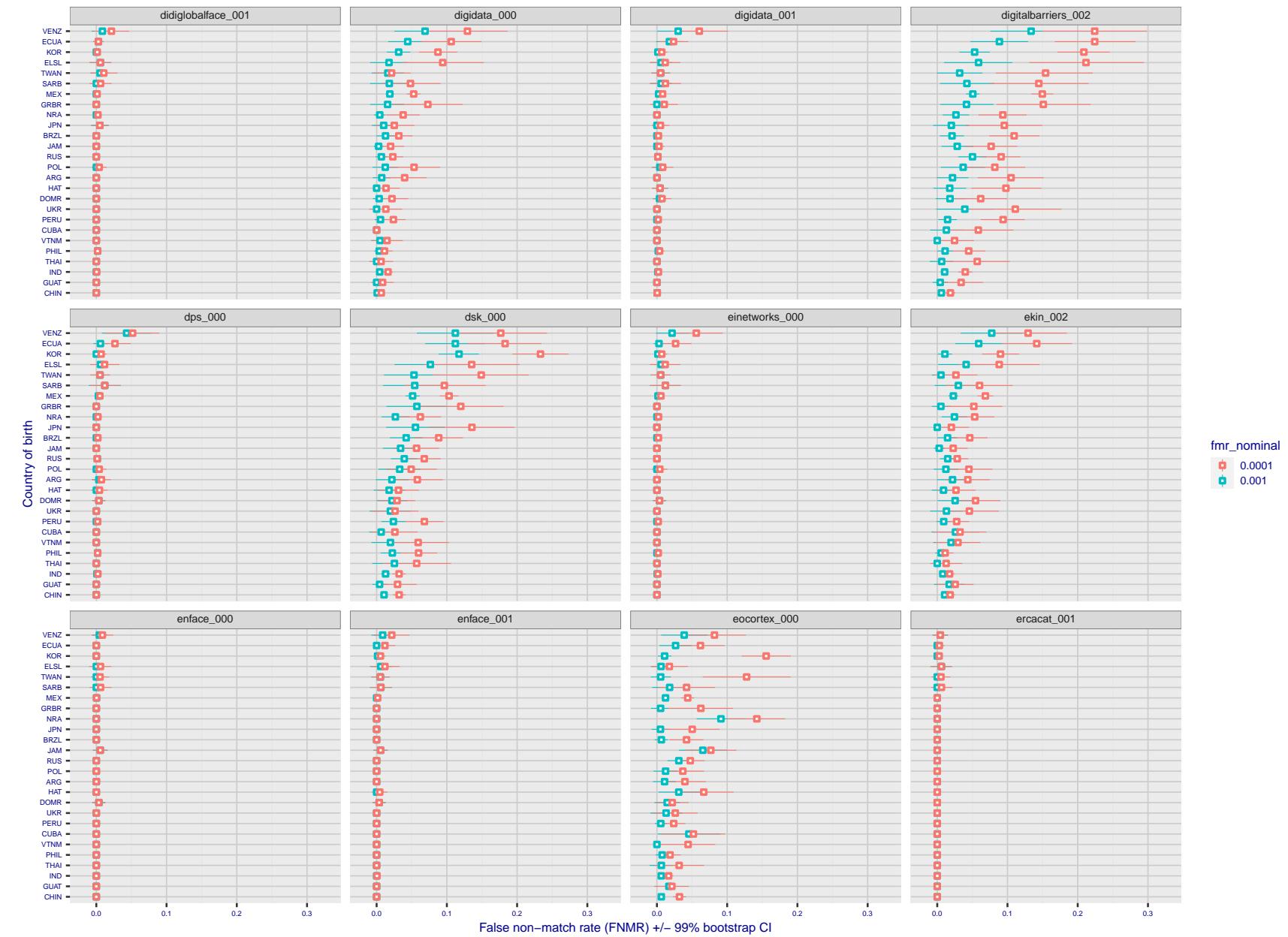


Figure 302: For the visa images, the dots show FNMR by country of birth for two globally set operating thresholds corresponding to $FMR = \{0.001, 0.0001\}$ computed over all on the order of 10^{10} impostor scores. The FMR in each bin will vary also - see subsequent impostor heatmaps in sec. 3.6.1. The figures shows an order of magnitude variation in FNMR across country of birth; these effects are likely due quality variations, then demographics like age and race. The error rates in some cases are zero, and in others the DET is flat so the error rates at the two thresholds are identical. The lines span 1% and 99% of bootstrap replicated FNMR estimates.

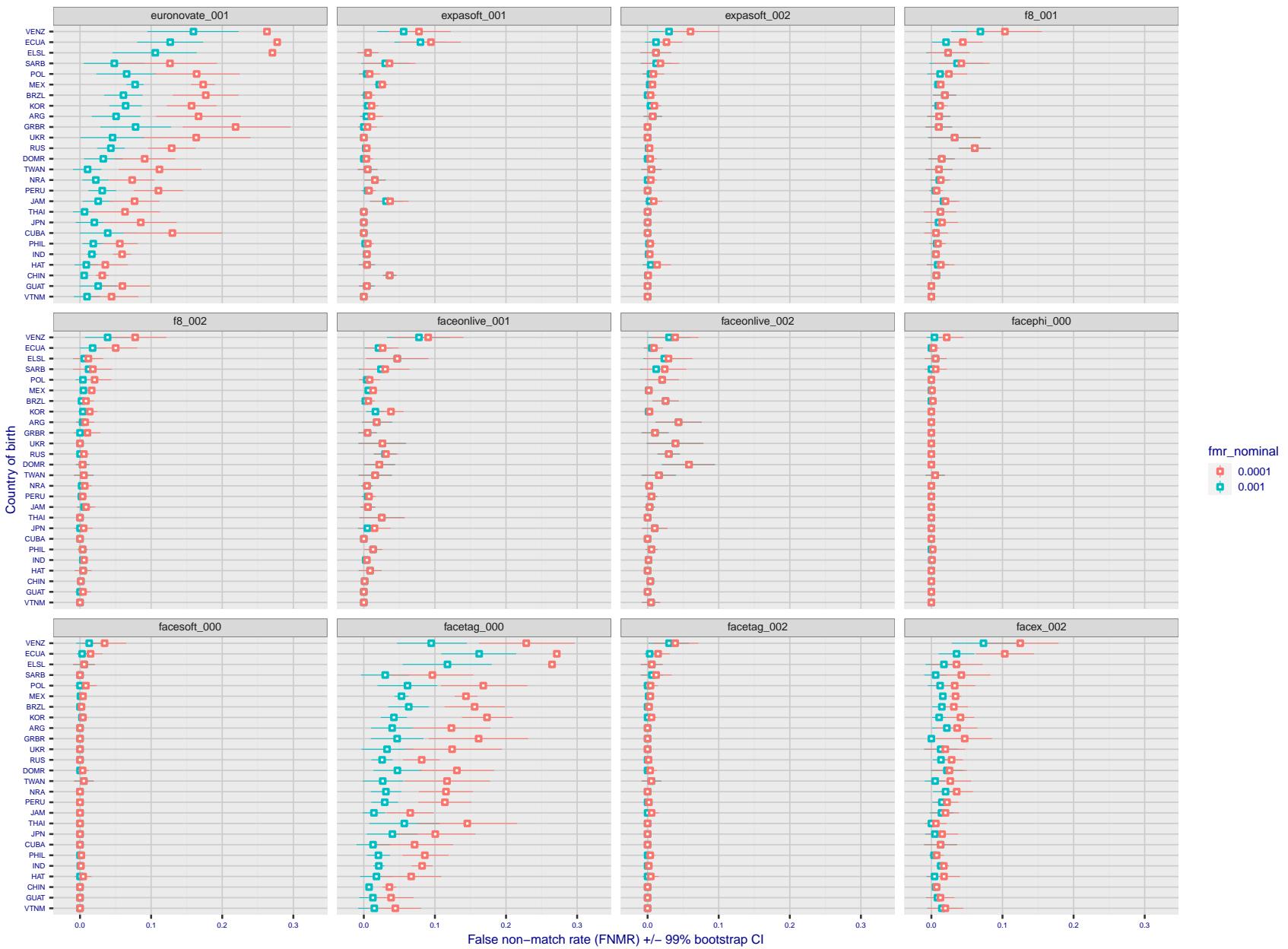


Figure 303: For the visa images, the dots show FNMR by country of birth for two globally set operating thresholds corresponding to $FMR = \{0.001, 0.0001\}$ computed over all on the order of 10^{10} impostor scores. The FMR in each bin will vary also - see subsequent impostor heatmaps in sec. 3.6.1. The figures shows an order of magnitude variation in FNMR across country of birth; these effects are likely due quality variations, then demographics like age and race. The error rates in some cases are zero, and in others the DET is flat so the error rates at the two thresholds are identical. The lines span 1% and 99% of bootstrap replicated FNMR estimates.

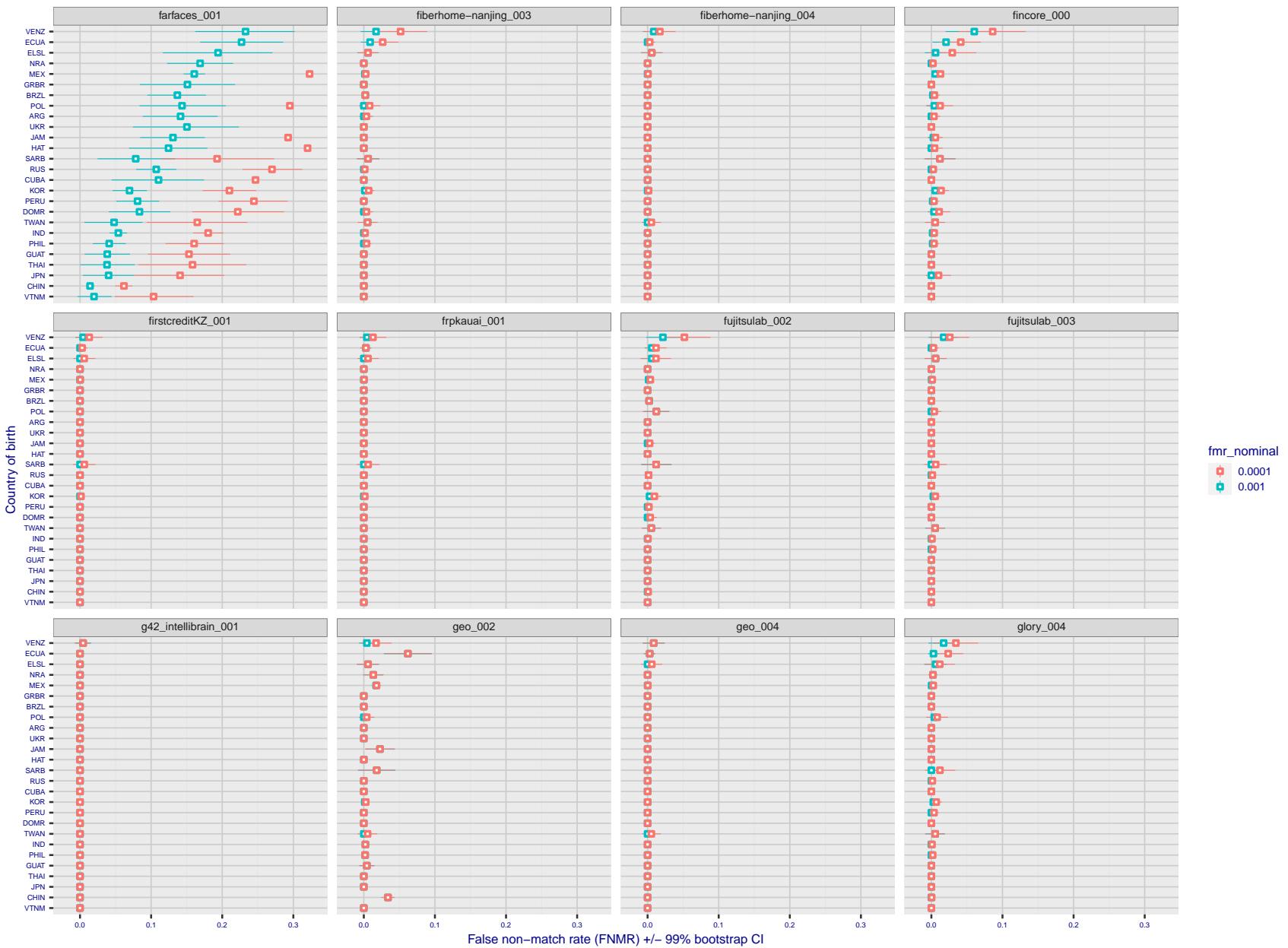


Figure 304: For the visa images, the dots show FNMR by country of birth for two globally set operating thresholds corresponding to $FMR = \{0.001, 0.0001\}$ computed over all on the order of 10^{10} impostor scores. The FMR in each bin will vary also - see subsequent impostor heatmaps in sec. 3.6.1. The figures shows an order of magnitude variation in FNMR across country of birth; these effects are likely due quality variations, then demographics like age and race. The error rates in some cases are zero, and in others the DET is flat so the error rates at the two thresholds are identical. The lines span 1% and 99% of bootstrap replicated FNMR estimates.

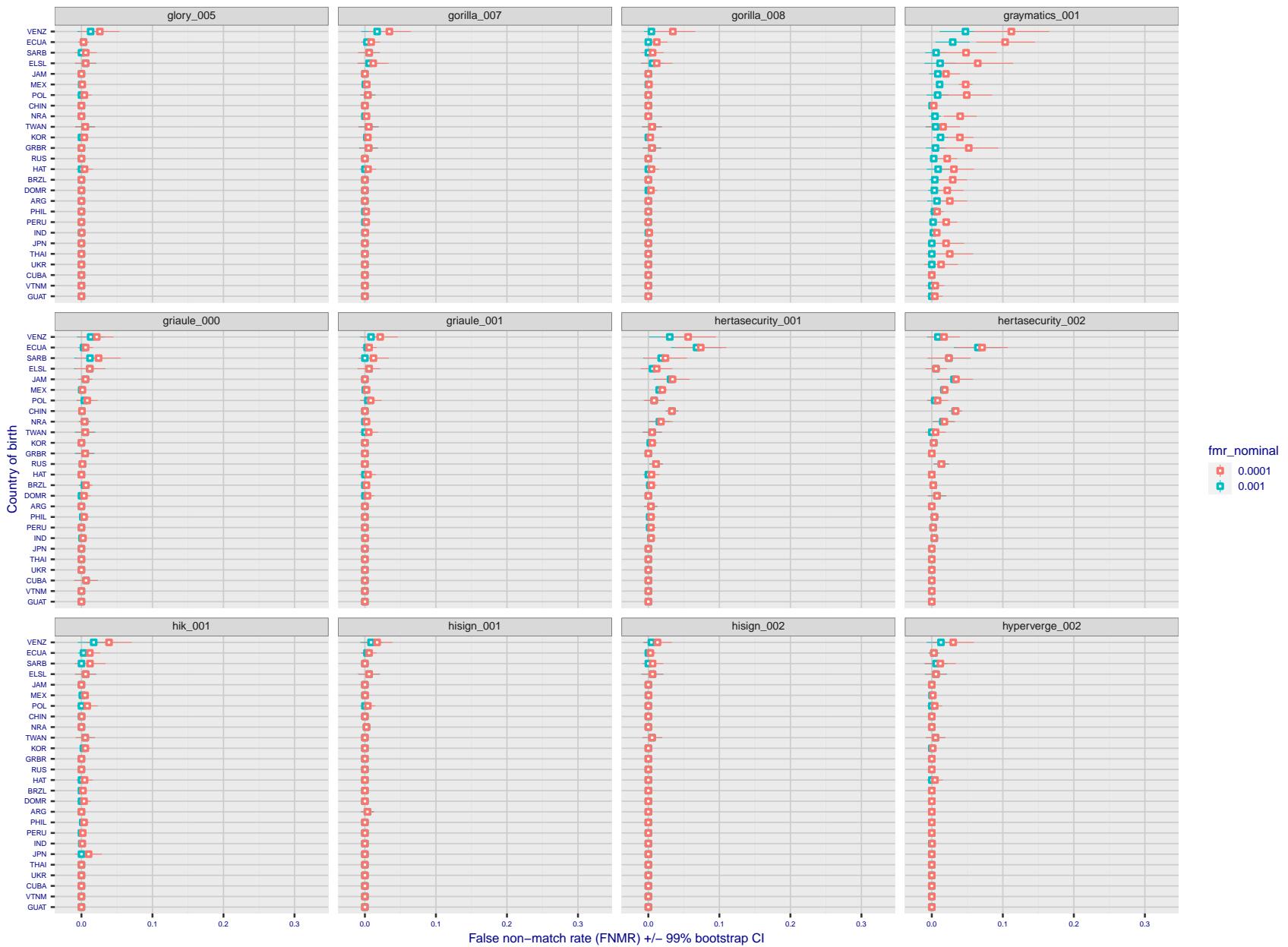


Figure 305: For the visa images, the dots show FNMR by country of birth for two globally set operating thresholds corresponding to $FMR = \{0.001, 0.0001\}$ computed over all on the order of 10^{10} impostor scores. The FMR in each bin will vary also - see subsequent impostor heatmaps in sec. 3.6.1. The figures shows an order of magnitude variation in FNMR across country of birth; these effects are likely due quality variations, then demographics like age and race. The error rates in some cases are zero, and in others the DET is flat so the error rates at the two thresholds are identical. The lines span 1% and 99% of bootstrap replicated FNMR estimates.

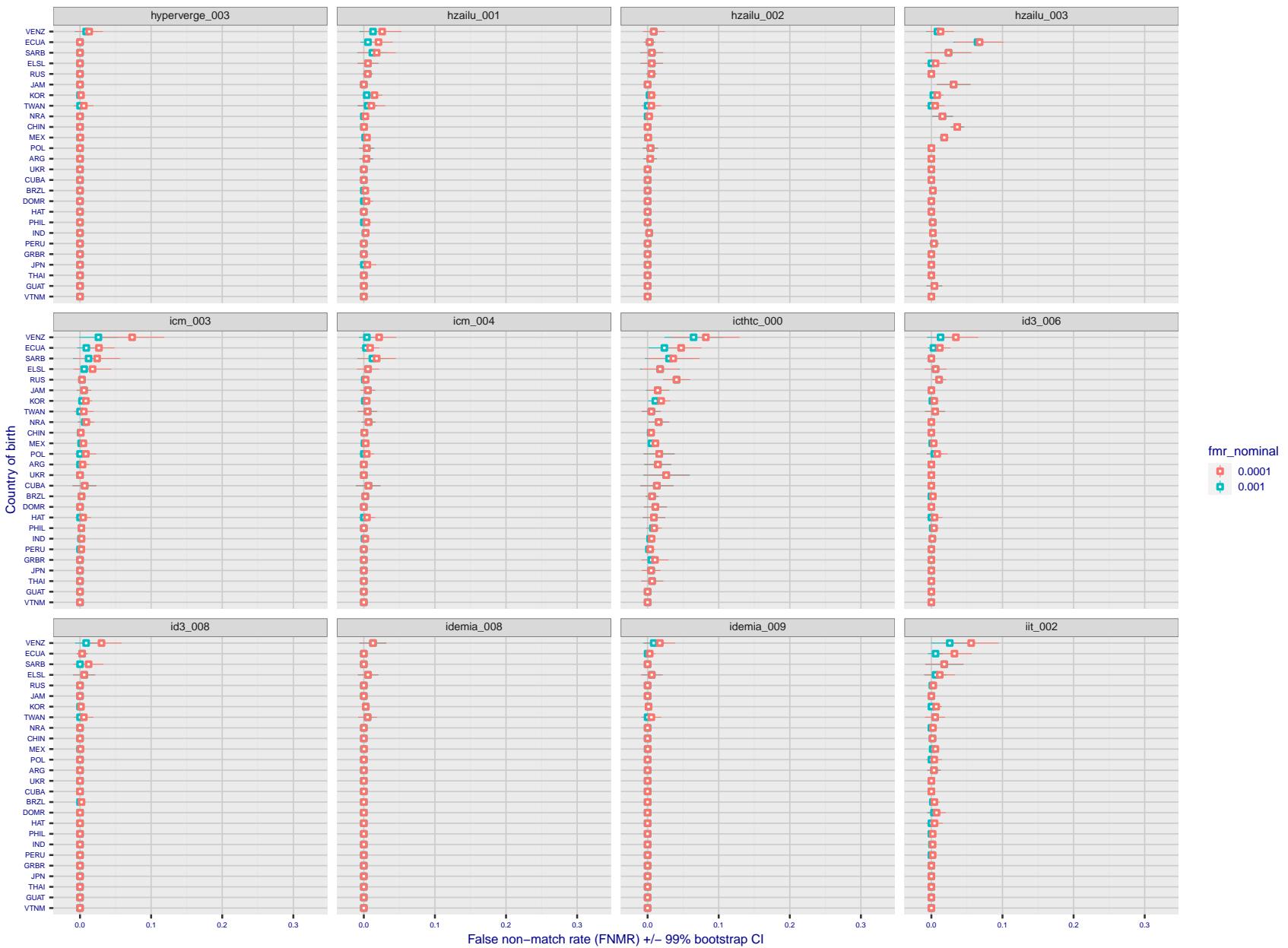


Figure 306: For the visa images, the dots show FNMR by country of birth for two globally set operating thresholds corresponding to $FMR = \{0.001, 0.0001\}$ computed over all on the order of 10^{10} impostor scores. The FMR in each bin will vary also - see subsequent impostor heatmaps in sec. 3.6.1. The figures shows an order of magnitude variation in FNMR across country of birth; these effects are likely due quality variations, then demographics like age and race. The error rates in some cases are zero, and in others the DET is flat so the error rates at the two thresholds are identical. The lines span 1% and 99% of bootstrap replicated FNMR estimates.

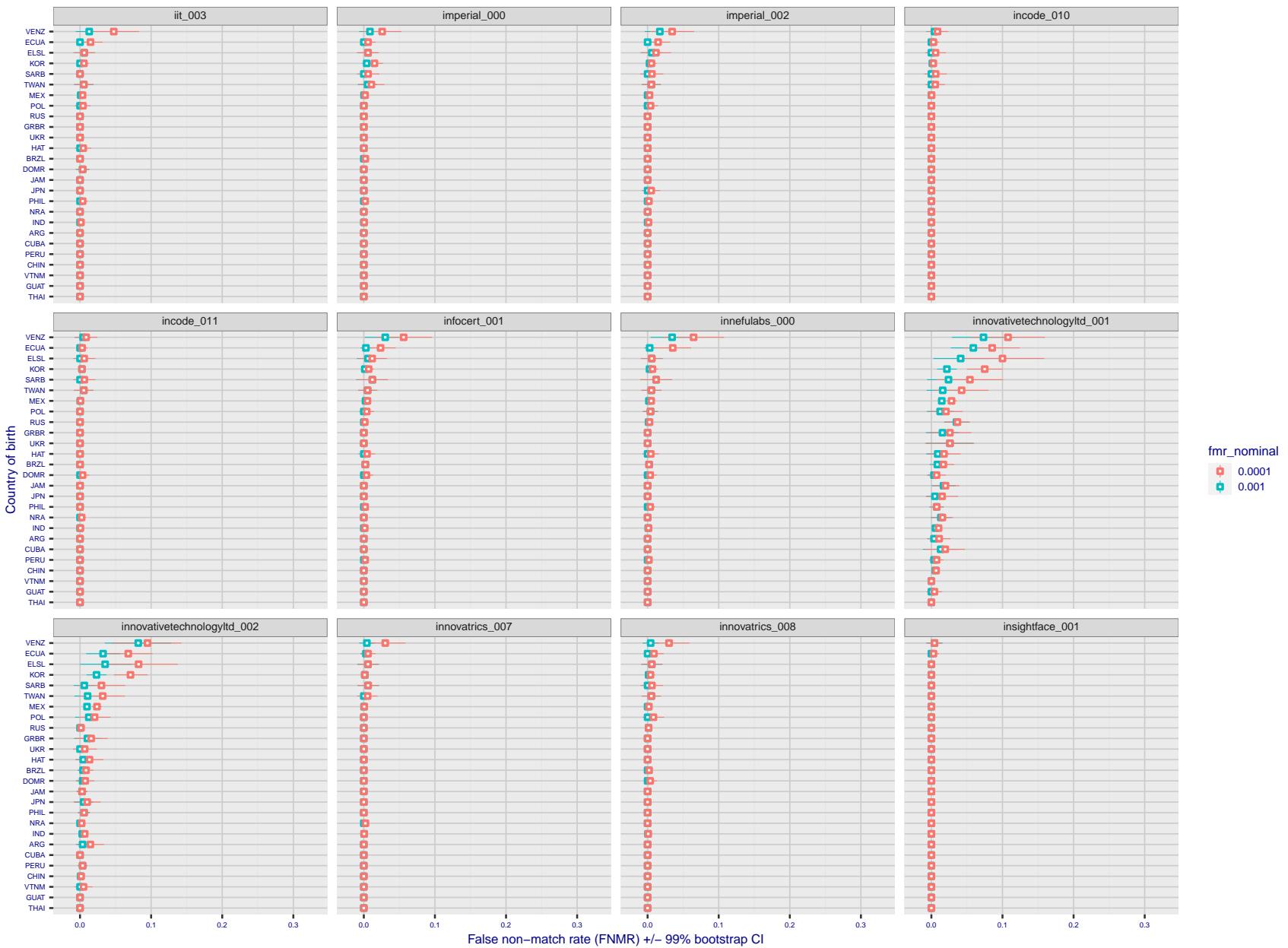


Figure 307: For the visa images, the dots show FNMR by country of birth for two globally set operating thresholds corresponding to $FMR = \{0.001, 0.0001\}$ computed over all on the order of 10^{10} impostor scores. The FMR in each bin will vary also - see subsequent impostor heatmaps in sec. 3.6.1. The figures shows an order of magnitude variation in FNMR across country of birth; these effects are likely due quality variations, then demographics like age and race. The error rates in some cases are zero, and in others the DET is flat so the error rates at the two thresholds are identical. The lines span 1% and 99% of bootstrap replicated FNMR estimates.

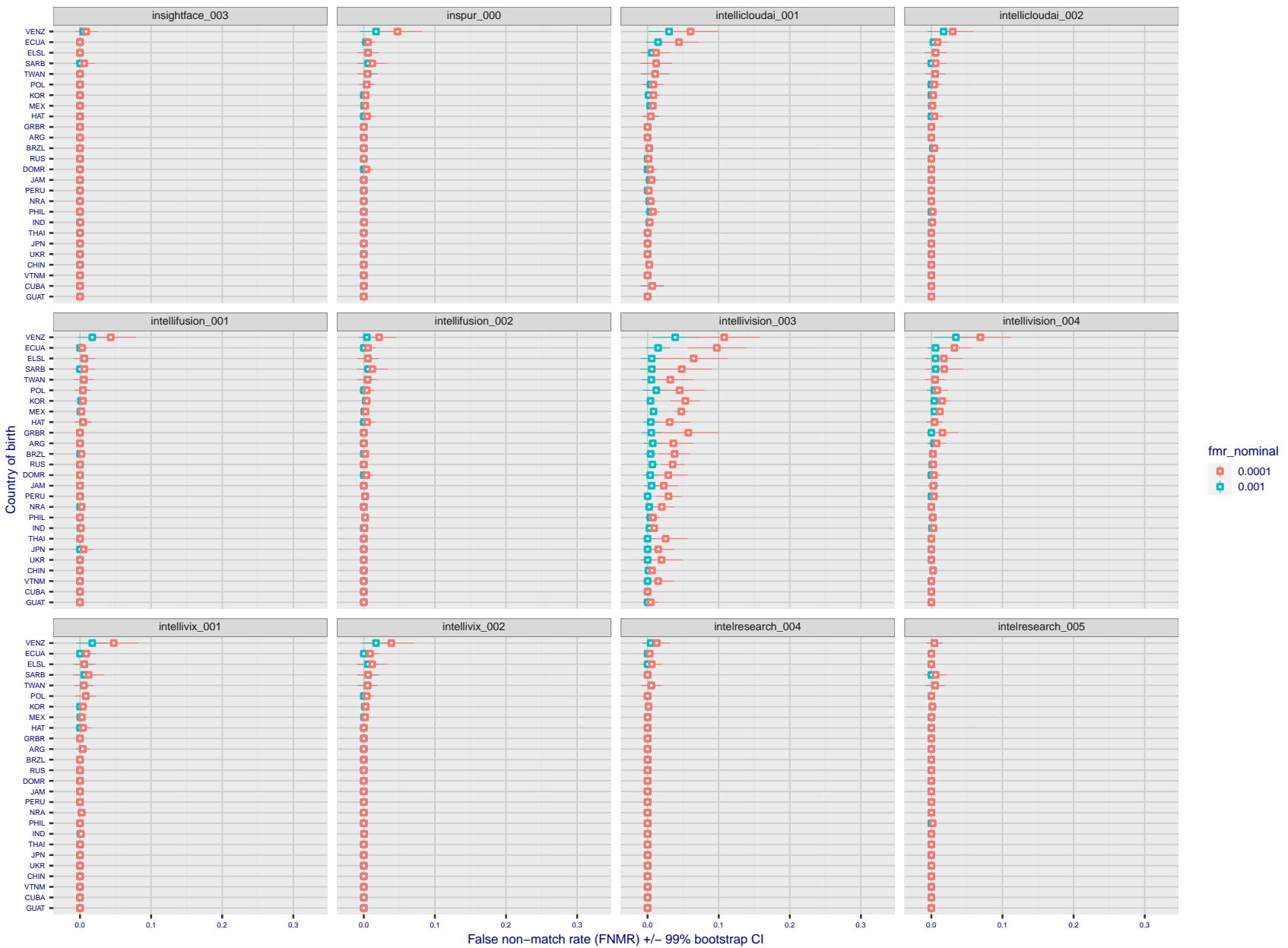


Figure 308: For the visa images, the dots show FNMR by country of birth for two globally set operating thresholds corresponding to $FMR = \{0.001, 0.0001\}$ computed over all on the order of 10^{10} impostor scores. The FMR in each bin will vary also - see subsequent impostor heatmaps in sec. 3.6.1. The figures shows an order of magnitude variation in FNMR across country of birth; these effects are likely due quality variations, then demographics like age and race. The error rates in some cases are zero, and in others the DET is flat so the error rates at the two thresholds are identical. The lines span 1% and 99% of bootstrap replicated FNMR estimates.

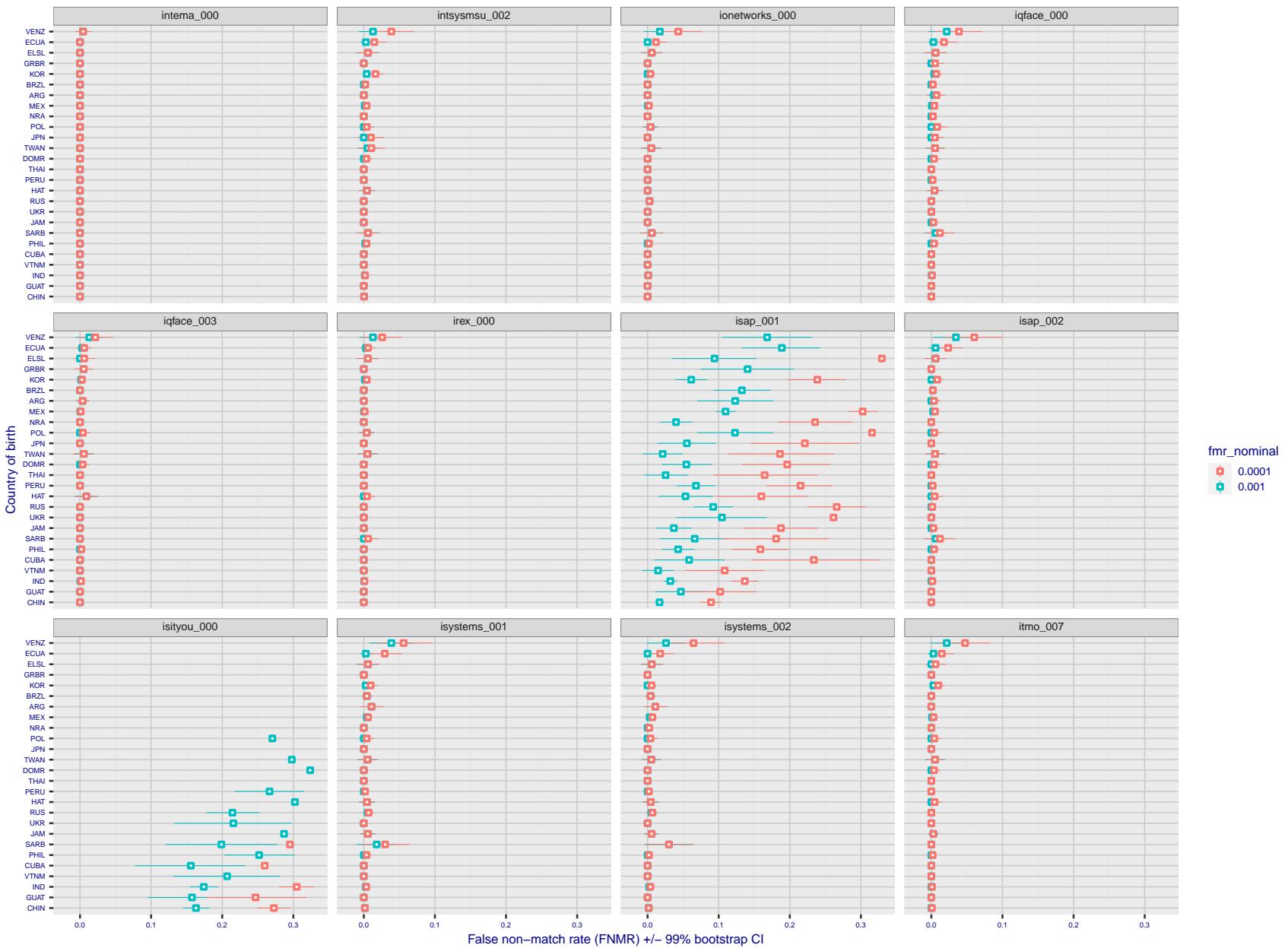


Figure 309: For the visa images, the dots show FNMR by country of birth for two globally set operating thresholds corresponding to $FMR = \{0.001, 0.0001\}$ computed over all on the order of 10^{10} impostor scores. The FMR in each bin will vary also - see subsequent impostor heatmaps in sec. 3.6.1. The figures shows an order of magnitude variation in FNMR across country of birth; these effects are likely due quality variations, then demographics like age and race. The error rates in some cases are zero, and in others the DET is flat so the error rates at the two thresholds are identical. The lines span 1% and 99% of bootstrap replicated FNMR estimates.

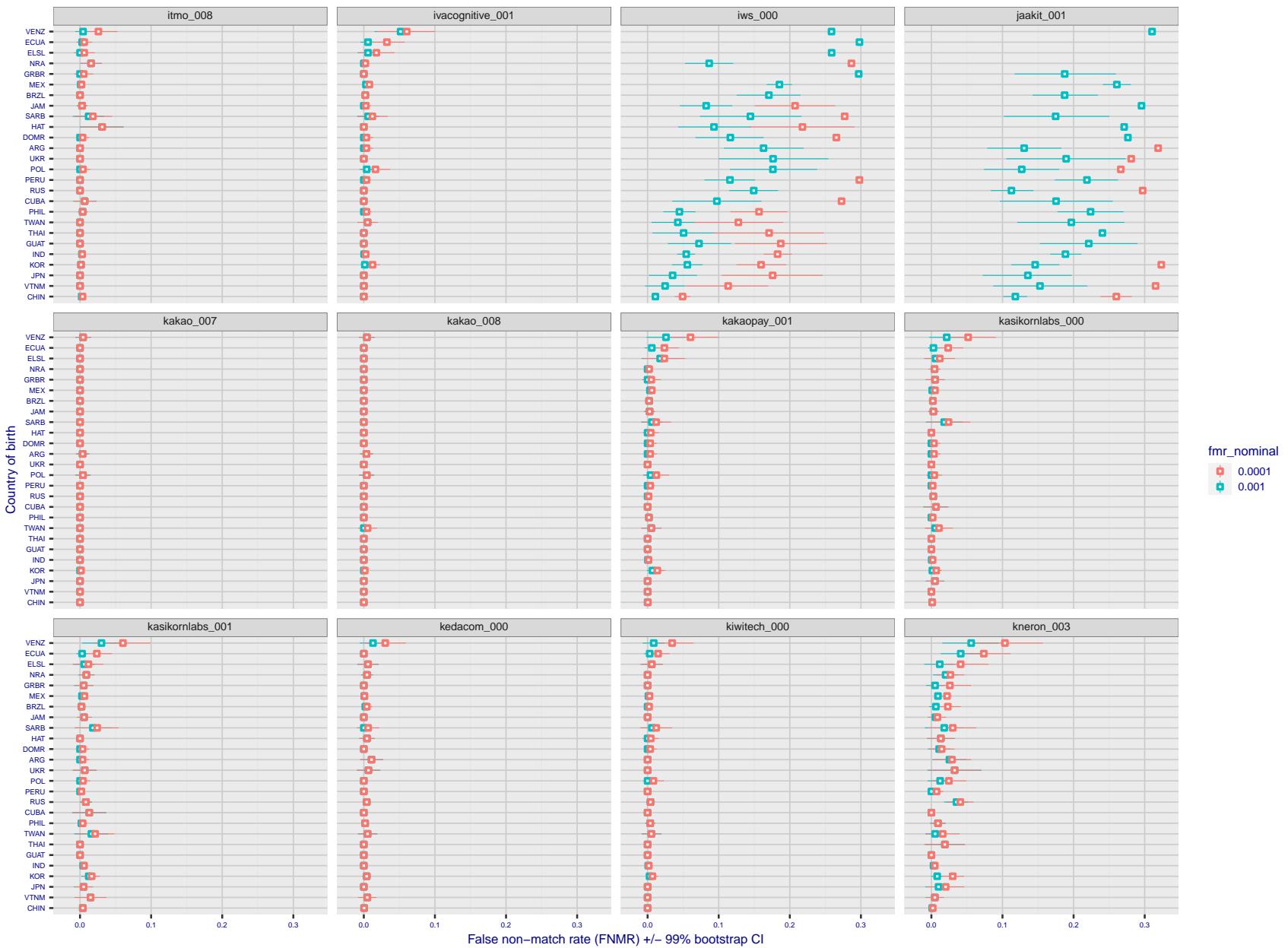


Figure 310: For the visa images, the dots show FNMR by country of birth for two globally set operating thresholds corresponding to $FMR = \{0.001, 0.0001\}$ computed over all on the order of 10^{10} impostor scores. The FMR in each bin will vary also - see subsequent impostor heatmaps in sec. 3.6.1. The figures shows an order of magnitude variation in FNMR across country of birth; these effects are likely due quality variations, then demographics like age and race. The error rates in some cases are zero, and in others the DET is flat so the error rates at the two thresholds are identical. The lines span 1% and 99% of bootstrap replicated FNMR estimates.

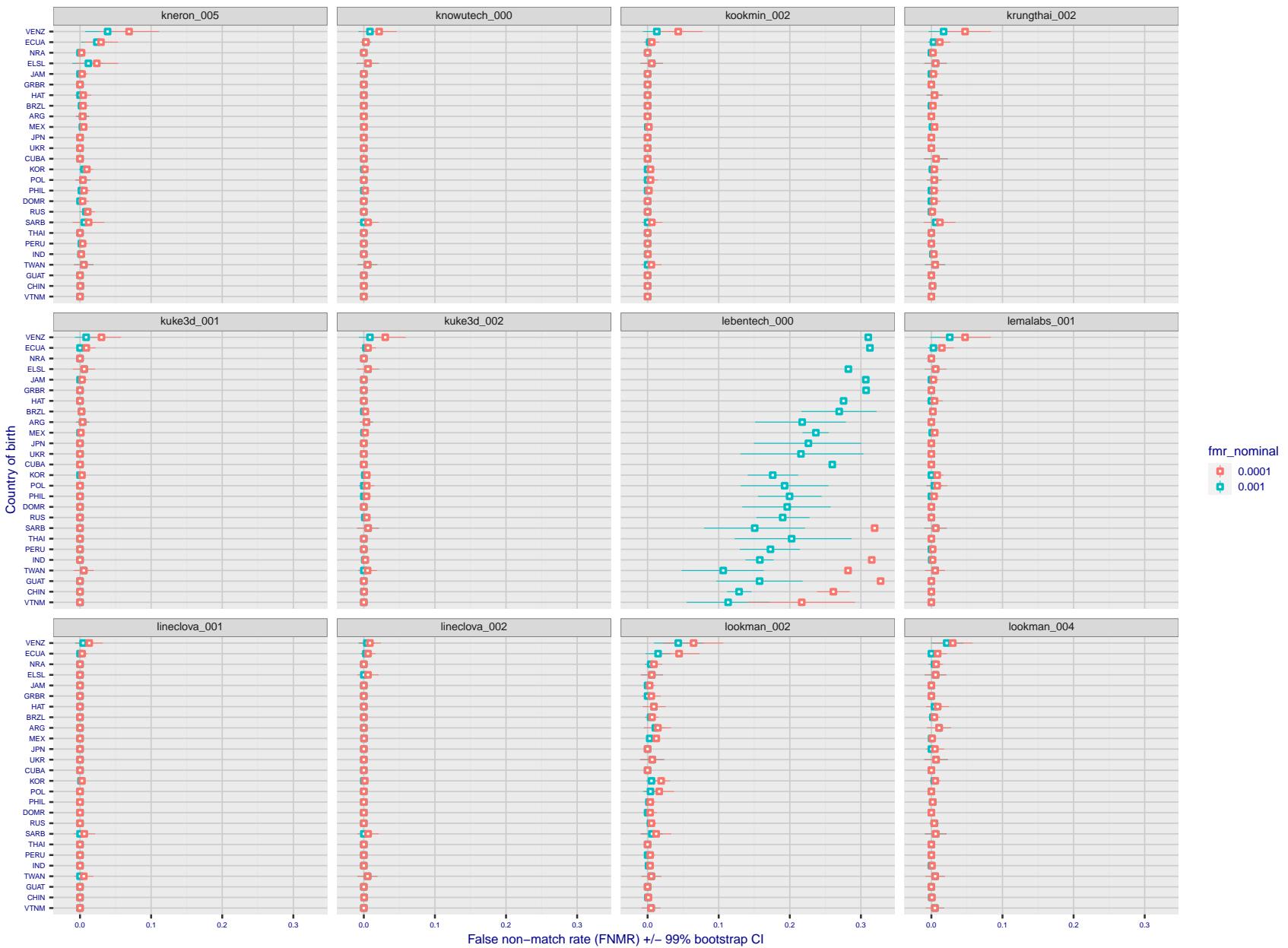


Figure 311: For the visa images, the dots show FNMR by country of birth for two globally set operating thresholds corresponding to $FMR = \{0.001, 0.0001\}$ computed over all on the order of 10^{10} impostor scores. The FMR in each bin will vary also - see subsequent impostor heatmaps in sec. 3.6.1. The figures shows an order of magnitude variation in FNMR across country of birth; these effects are likely due quality variations, then demographics like age and race. The error rates in some cases are zero, and in others the DET is flat so the error rates at the two thresholds are identical. The lines span 1% and 99% of bootstrap replicated FNMR estimates.

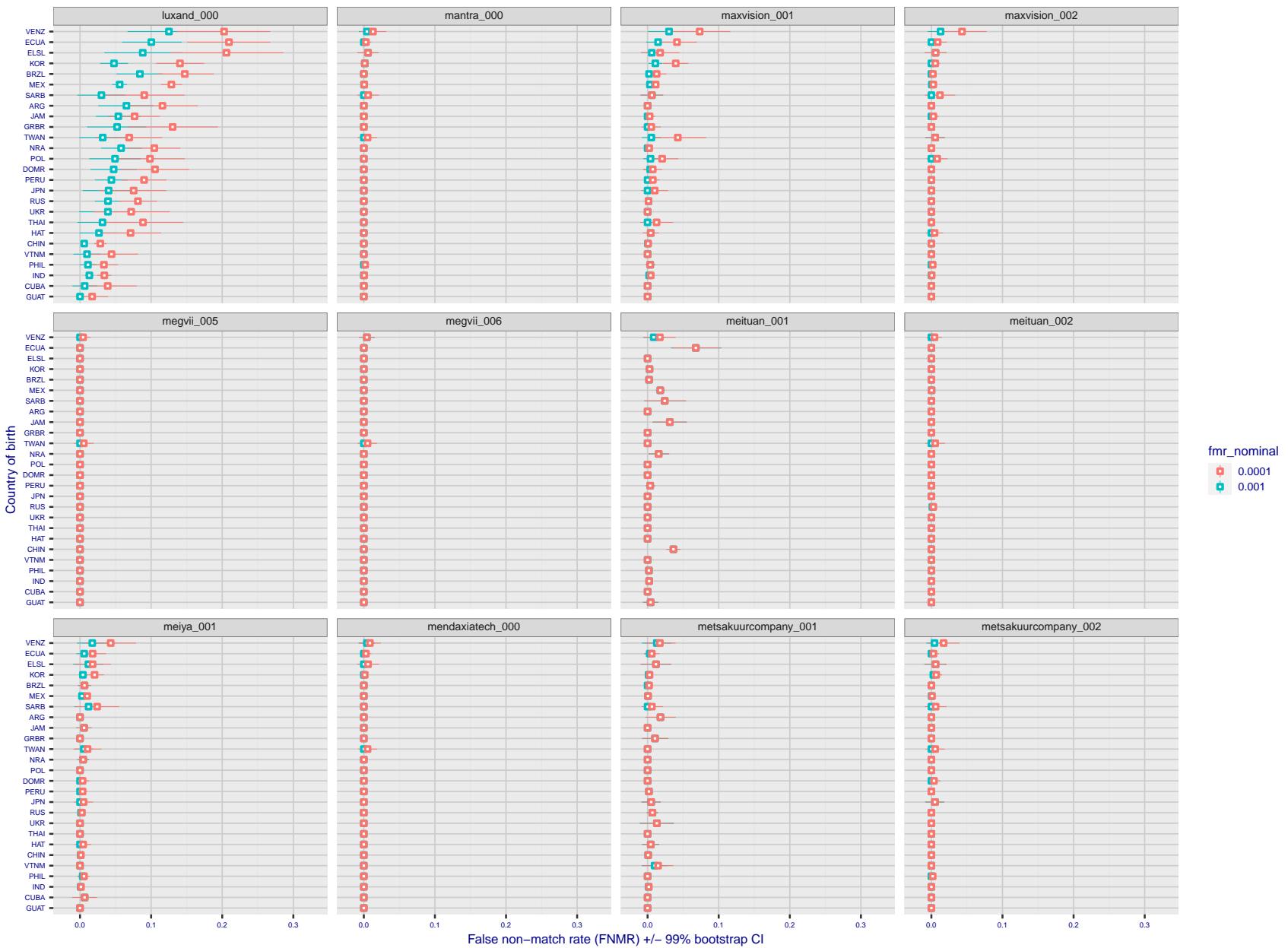


Figure 312: For the visa images, the dots show FNMR by country of birth for two globally set operating thresholds corresponding to $FMR = \{0.001, 0.0001\}$ computed over all on the order of 10^{10} impostor scores. The FMR in each bin will vary also - see subsequent impostor heatmaps in sec. 3.6.1. The figures shows an order of magnitude variation in FNMR across country of birth; these effects are likely due quality variations, then demographics like age and race. The error rates in some cases are zero, and in others the DET is flat so the error rates at the two thresholds are identical. The lines span 1% and 99% of bootstrap replicated FNMR estimates.

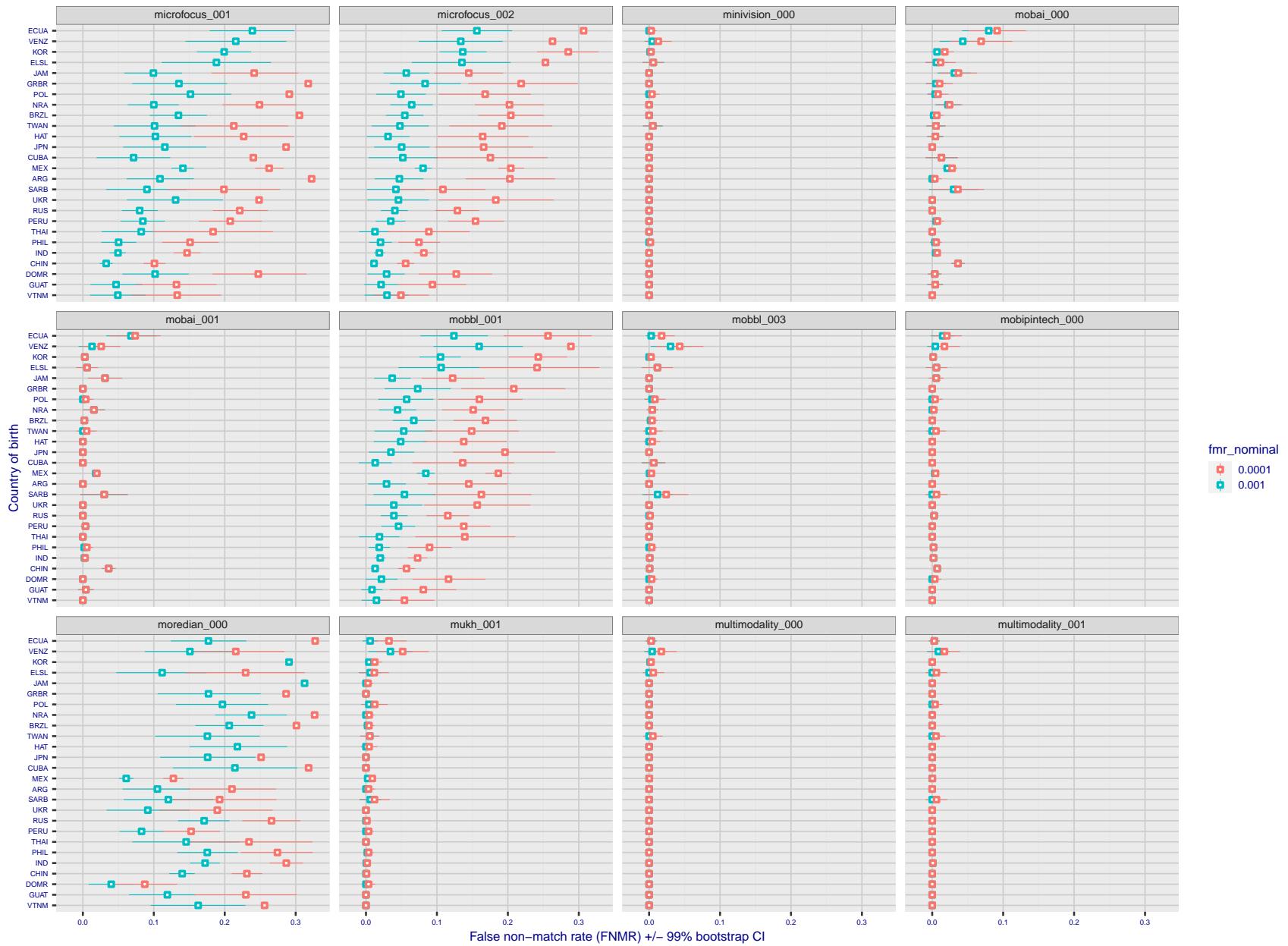


Figure 313: For the visa images, the dots show FNMR by country of birth for two globally set operating thresholds corresponding to $FMR = \{0.001, 0.0001\}$ computed over all on the order of 10^{10} impostor scores. The FMR in each bin will vary also - see subsequent impostor heatmaps in sec. 3.6.1. The figures shows an order of magnitude variation in FNMR across country of birth; these effects are likely due quality variations, then demographics like age and race. The error rates in some cases are zero, and in others the DET is flat so the error rates at the two thresholds are identical. The lines span 1% and 99% of bootstrap replicated FNMR estimates.

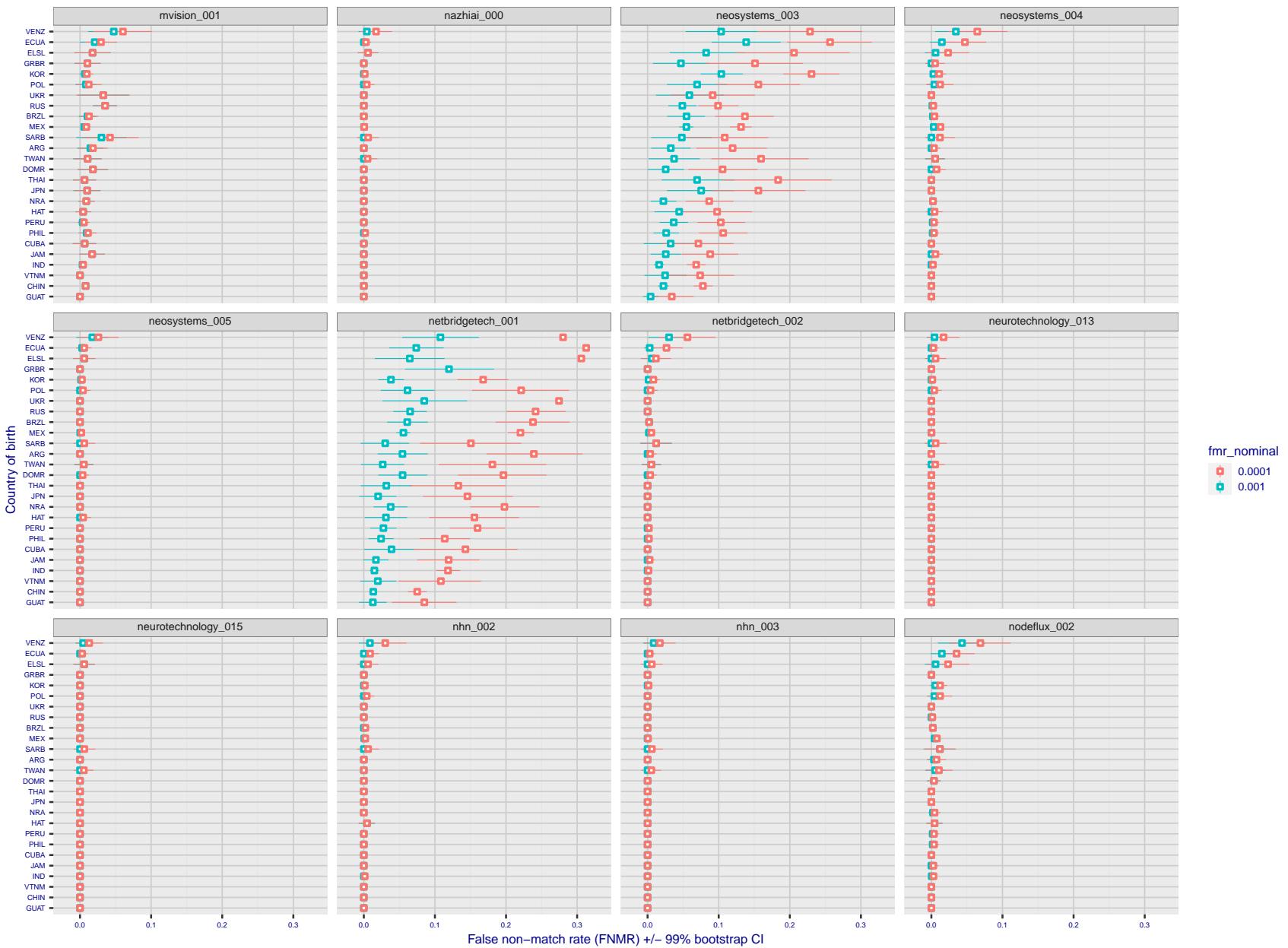


Figure 314: For the visa images, the dots show FNMR by country of birth for two globally set operating thresholds corresponding to $FMR = \{0.001, 0.0001\}$ computed over all on the order of 10^{10} impostor scores. The FMR in each bin will vary also - see subsequent impostor heatmaps in sec. 3.6.1. The figures shows an order of magnitude variation in FNMR across country of birth; these effects are likely due quality variations, then demographics like age and race. The error rates in some cases are zero, and in others the DET is flat so the error rates at the two thresholds are identical. The lines span 1% and 99% of bootstrap replicated FNMR estimates.

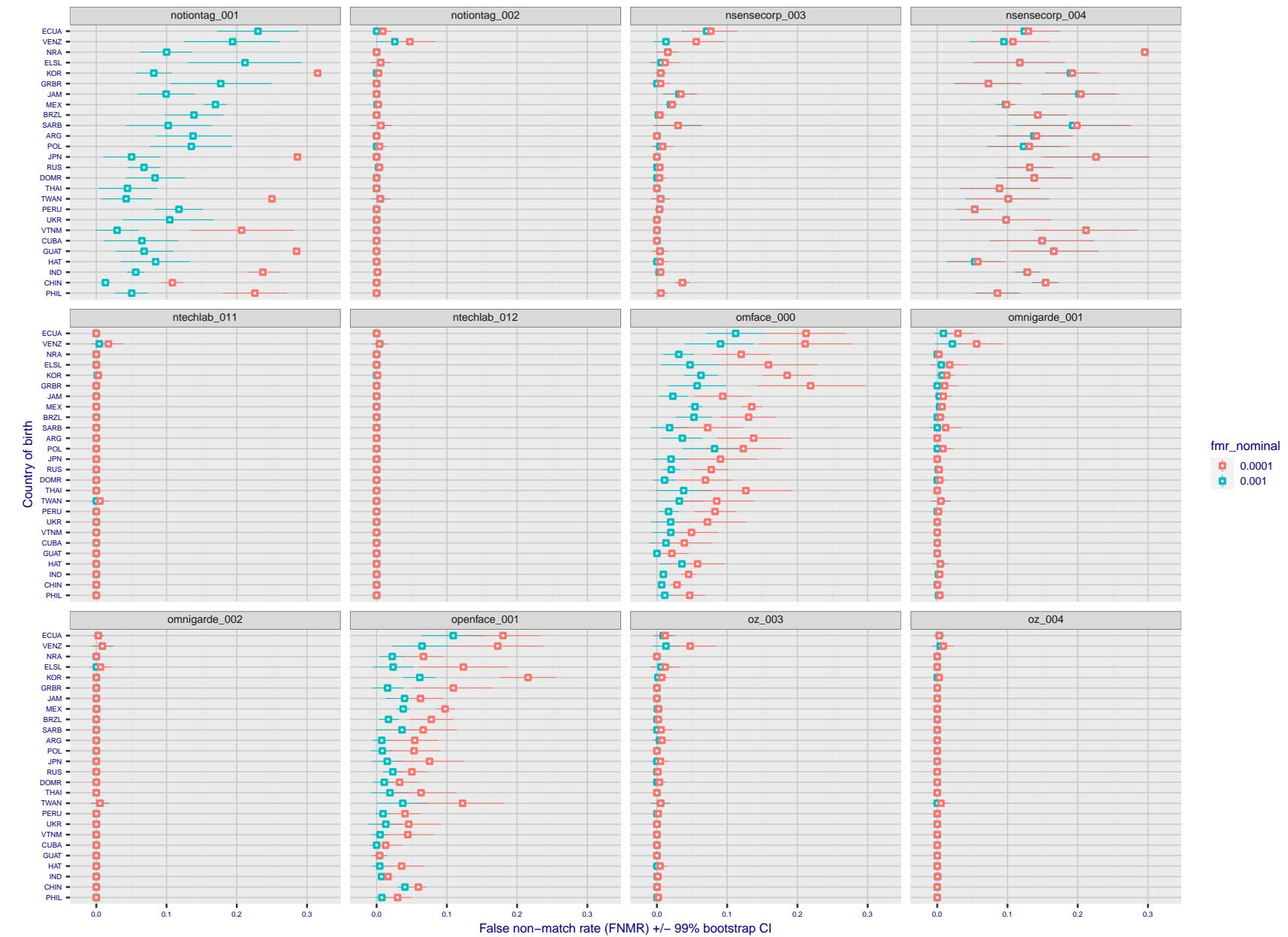


Figure 315: For the visa images, the dots show FNMR by country of birth for two globally set operating thresholds corresponding to $FMR = \{0.001, 0.0001\}$ computed over all on the order of 10^{10} impostor scores. The FMR in each bin will vary also - see subsequent impostor heatmaps in sec. 3.6.1. The figures shows an order of magnitude variation in FNMR across country of birth; these effects are likely due quality variations, then demographics like age and race. The error rates in some cases are zero, and in others the DET is flat so the error rates at the two thresholds are identical. The lines span 1% and 99% of bootstrap replicated FNMR estimates.

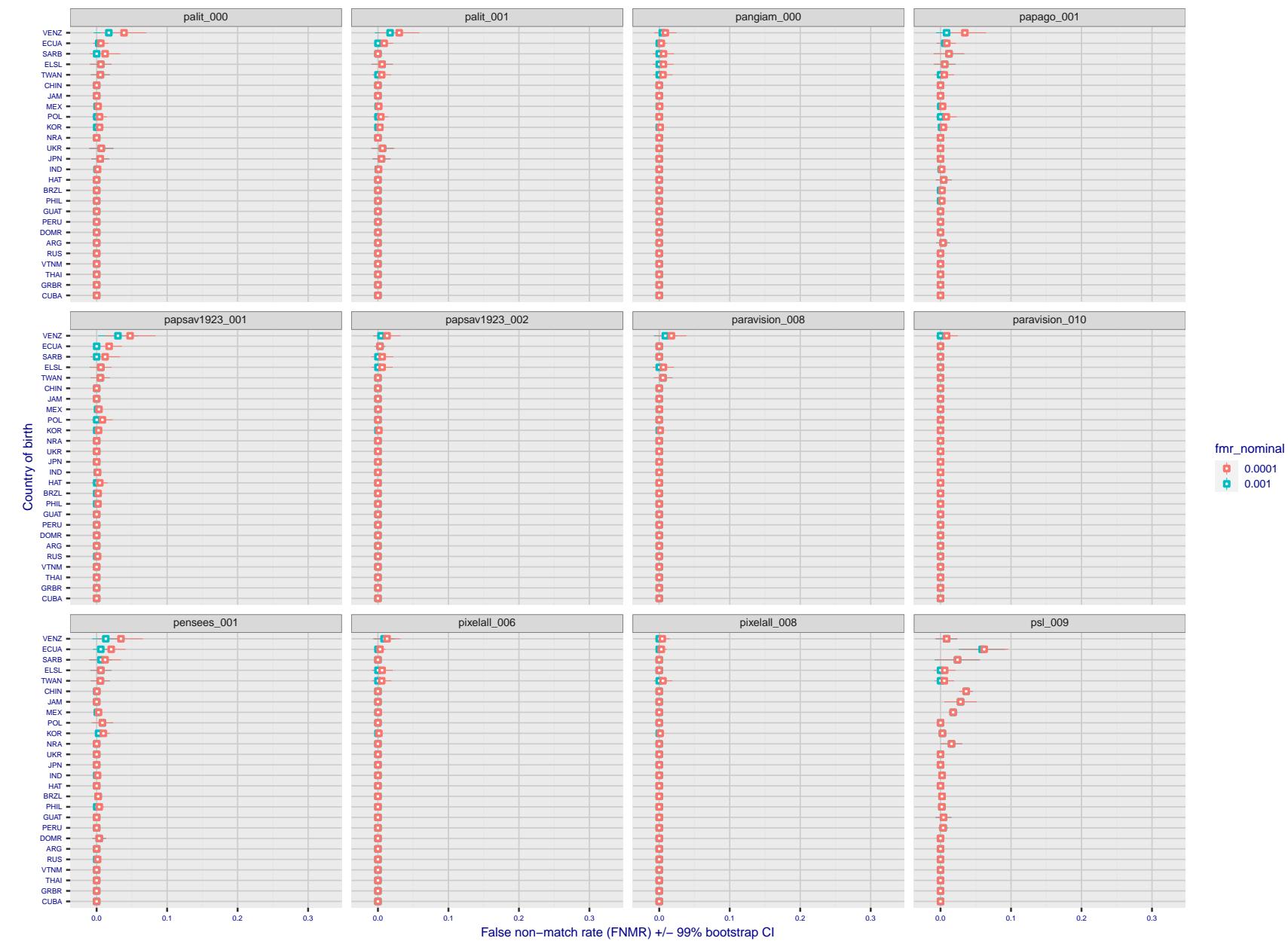


Figure 316: For the visa images, the dots show FNMR by country of birth for two globally set operating thresholds corresponding to $FMR = \{0.001, 0.0001\}$ computed over all on the order of 10^{10} impostor scores. The FMR in each bin will vary also - see subsequent impostor heatmaps in sec. 3.6.1. The figures shows an order of magnitude variation in FNMR across country of birth; these effects are likely due quality variations, then demographics like age and race. The error rates in some cases are zero, and in others the DET is flat so the error rates at the two thresholds are identical. The lines span 1% and 99% of bootstrap replicated FNMR estimates.

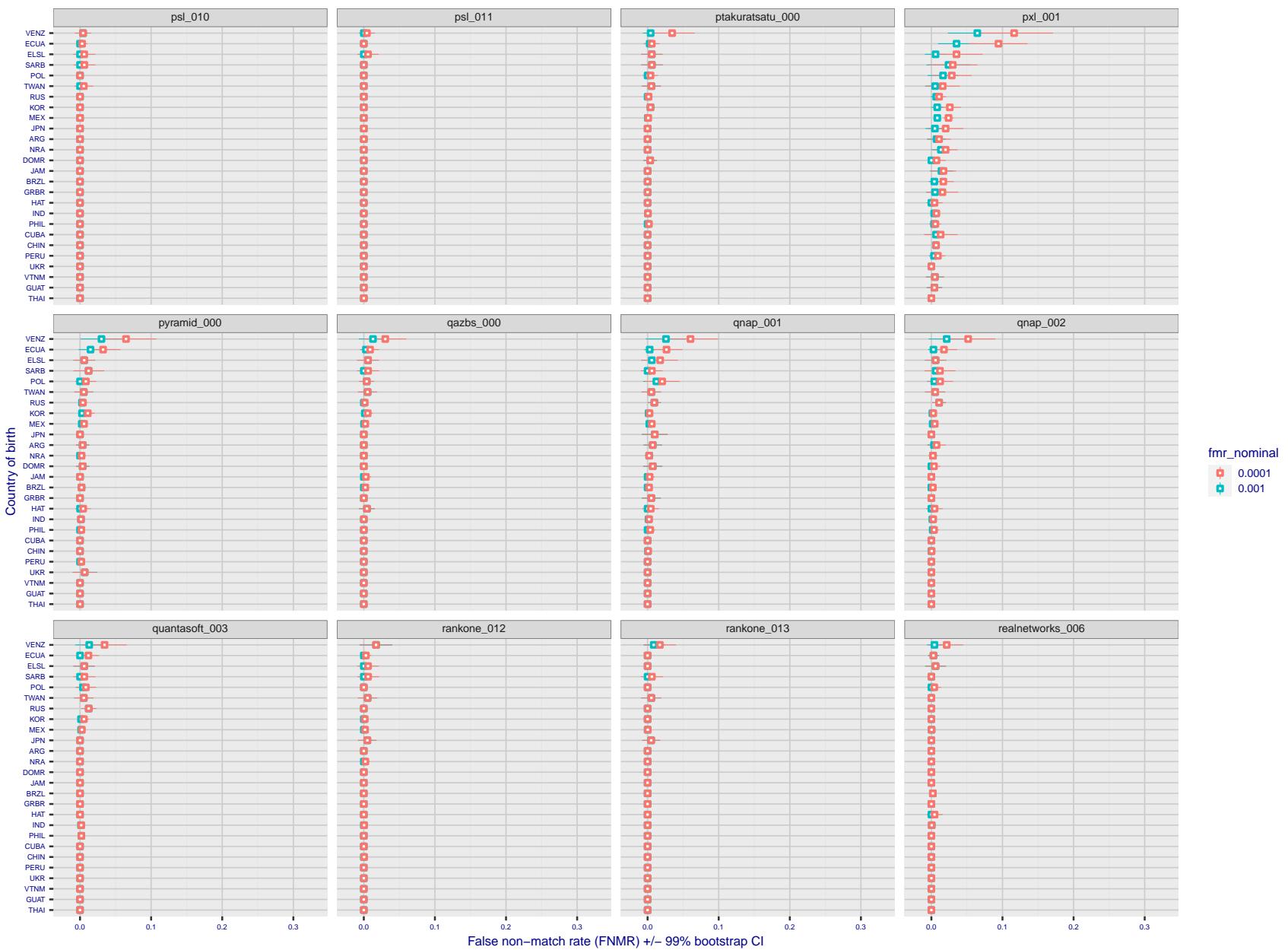


Figure 317: For the visa images, the dots show FNMR by country of birth for two globally set operating thresholds corresponding to $FMR = \{0.001, 0.0001\}$ computed over all on the order of 10^{10} impostor scores. The FMR in each bin will vary also - see subsequent impostor heatmaps in sec. 3.6.1. The figures shows an order of magnitude variation in FNMR across country of birth; these effects are likely due quality variations, then demographics like age and race. The error rates in some cases are zero, and in others the DET is flat so the error rates at the two thresholds are identical. The lines span 1% and 99% of bootstrap replicated FNMR estimates.

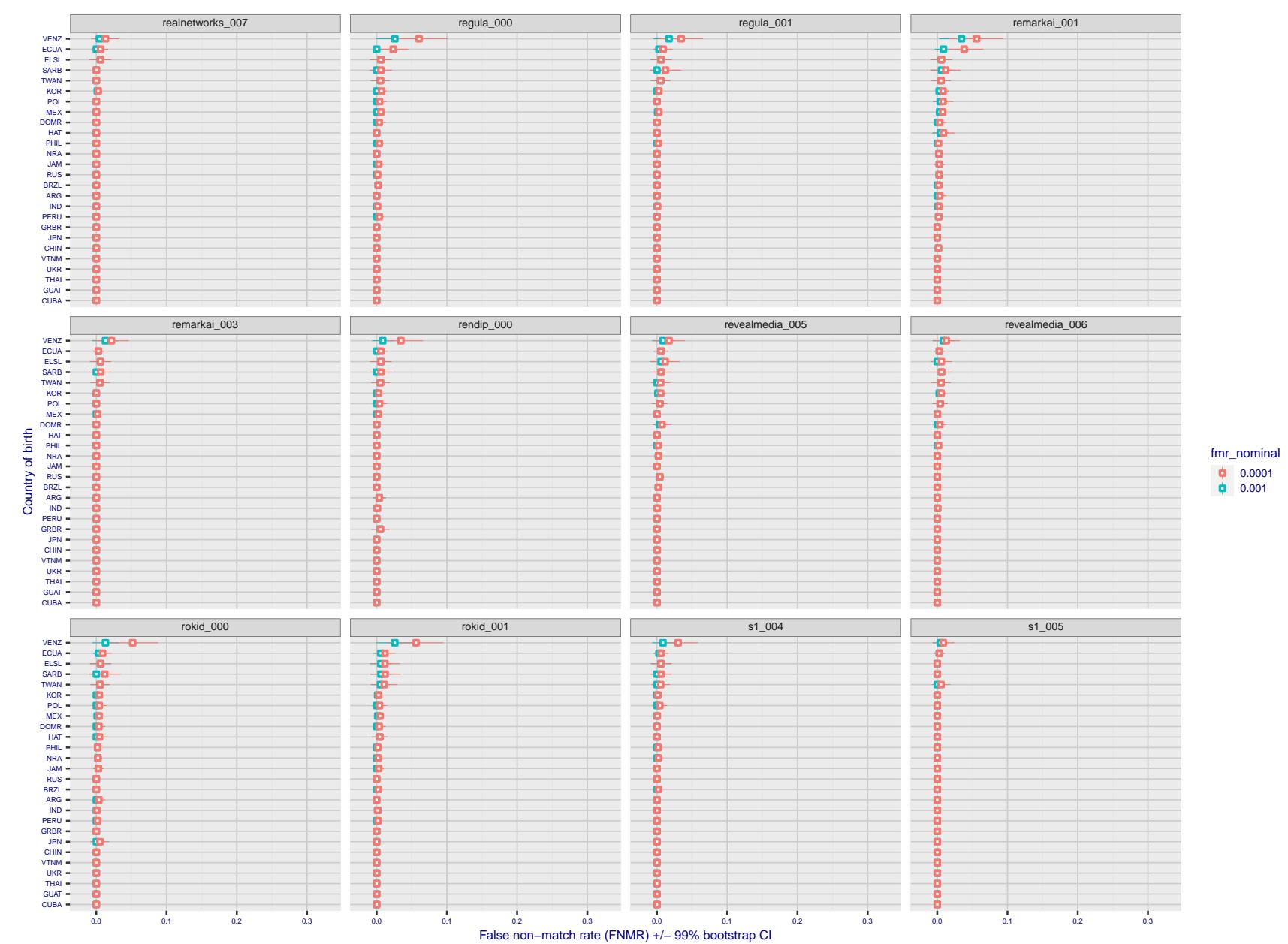


Figure 318: For the visa images, the dots show FNMR by country of birth for two globally set operating thresholds corresponding to $FMR = \{0.001, 0.0001\}$ computed over all on the order of 10^{10} impostor scores. The FMR in each bin will vary also - see subsequent impostor heatmaps in sec. 3.6.1. The figures shows an order of magnitude variation in FNMR across country of birth; these effects are likely due quality variations, then demographics like age and race. The error rates in some cases are zero, and in others the DET is flat so the error rates at the two thresholds are identical. The lines span 1% and 99% of bootstrap replicated FNMR estimates.

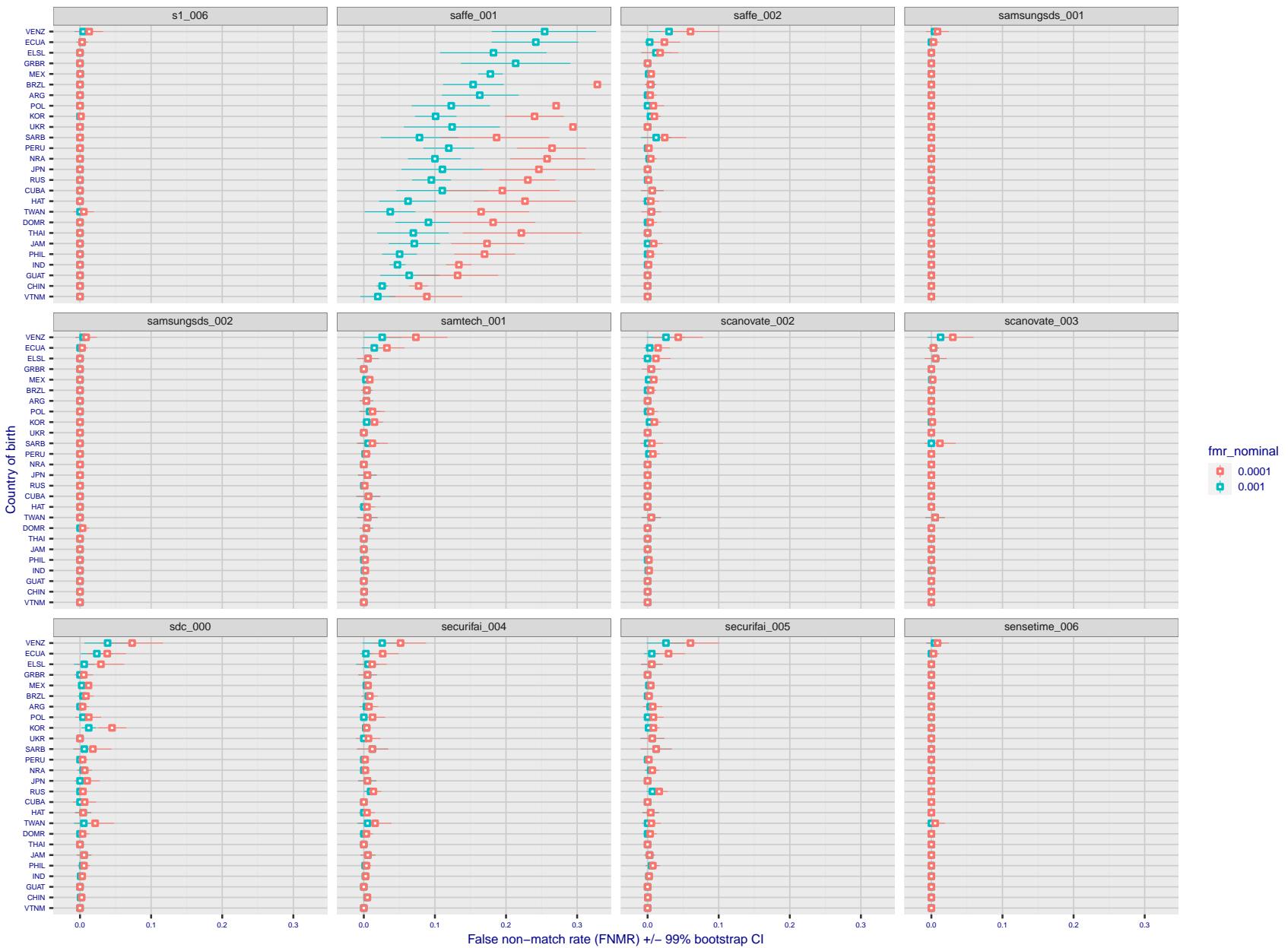


Figure 319: For the visa images, the dots show FNMR by country of birth for two globally set operating thresholds corresponding to $FMR = \{0.001, 0.0001\}$ computed over all on the order of 10^{10} impostor scores. The FMR in each bin will vary also - see subsequent impostor heatmaps in sec. 3.6.1. The figures shows an order of magnitude variation in FNMR across country of birth; these effects are likely due quality variations, then demographics like age and race. The error rates in some cases are zero, and in others the DET is flat so the error rates at the two thresholds are identical. The lines span 1% and 99% of bootstrap replicated FNMR estimates.

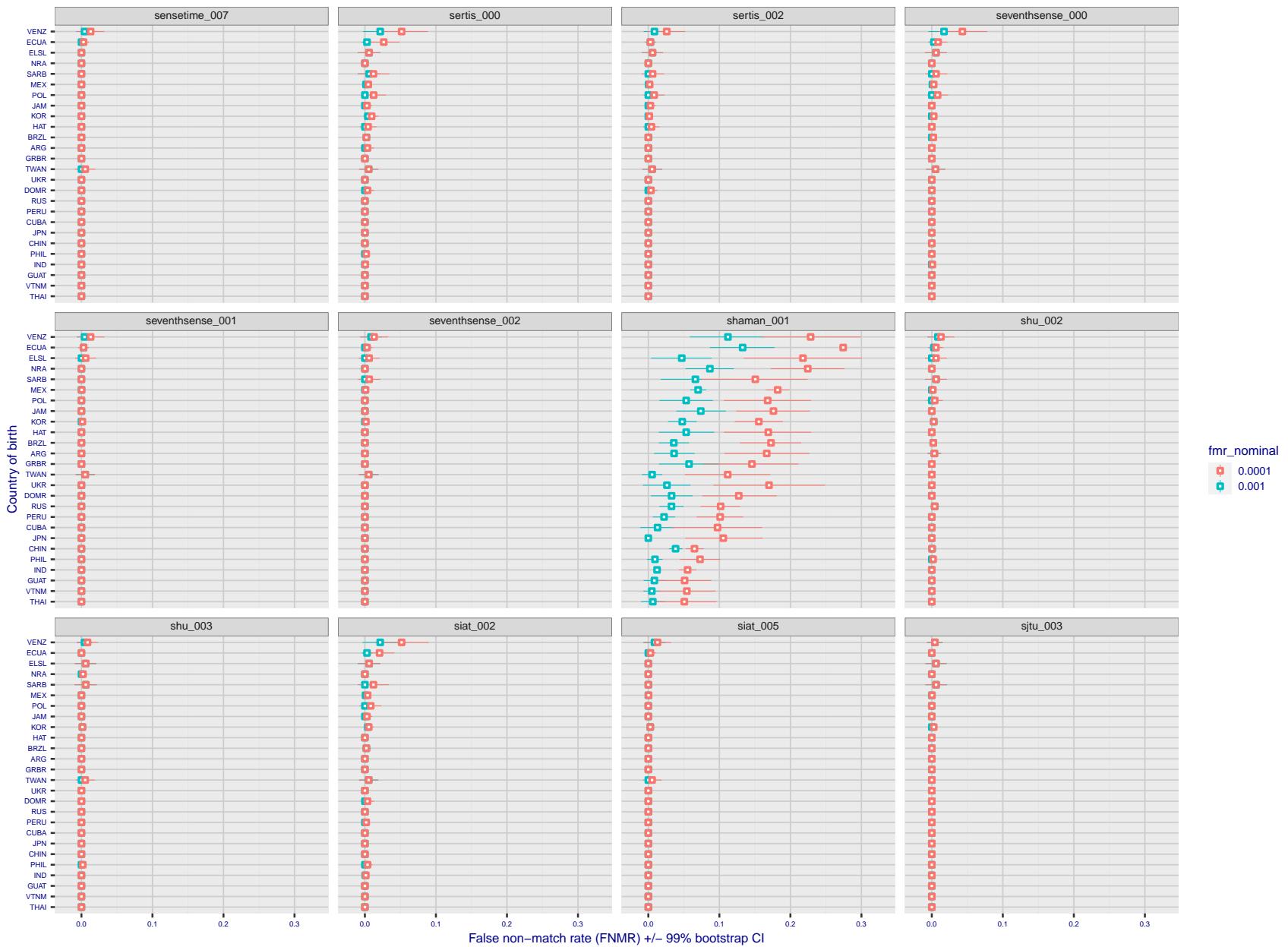


Figure 320: For the visa images, the dots show FNMR by country of birth for two globally set operating thresholds corresponding to $FMR = \{0.001, 0.0001\}$ computed over all on the order of 10^{10} impostor scores. The FMR in each bin will vary also - see subsequent impostor heatmaps in sec. 3.6.1. The figures shows an order of magnitude variation in FNMR across country of birth; these effects are likely due quality variations, then demographics like age and race. The error rates in some cases are zero, and in others the DET is flat so the error rates at the two thresholds are identical. The lines span 1% and 99% of bootstrap replicated FNMR estimates.

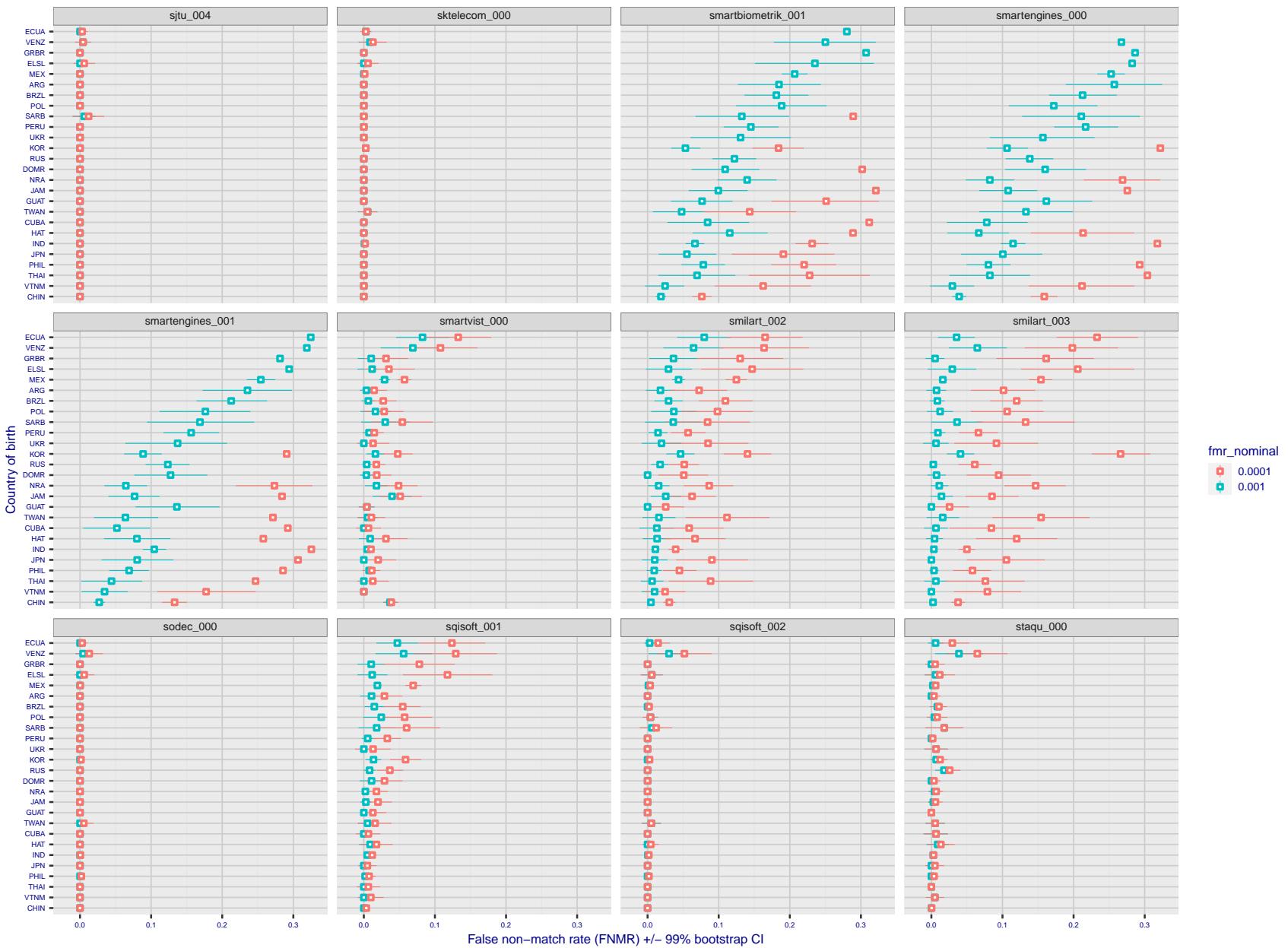


Figure 321: For the visa images, the dots show FNMR by country of birth for two globally set operating thresholds corresponding to $FMR = \{0.001, 0.0001\}$ computed over all on the order of 10^{10} impostor scores. The FMR in each bin will vary also - see subsequent impostor heatmaps in sec. 3.6.1. The figures shows an order of magnitude variation in FNMR across country of birth; these effects are likely due quality variations, then demographics like age and race. The error rates in some cases are zero, and in others the DET is flat so the error rates at the two thresholds are identical. The lines span 1% and 99% of bootstrap replicated FNMR estimates.

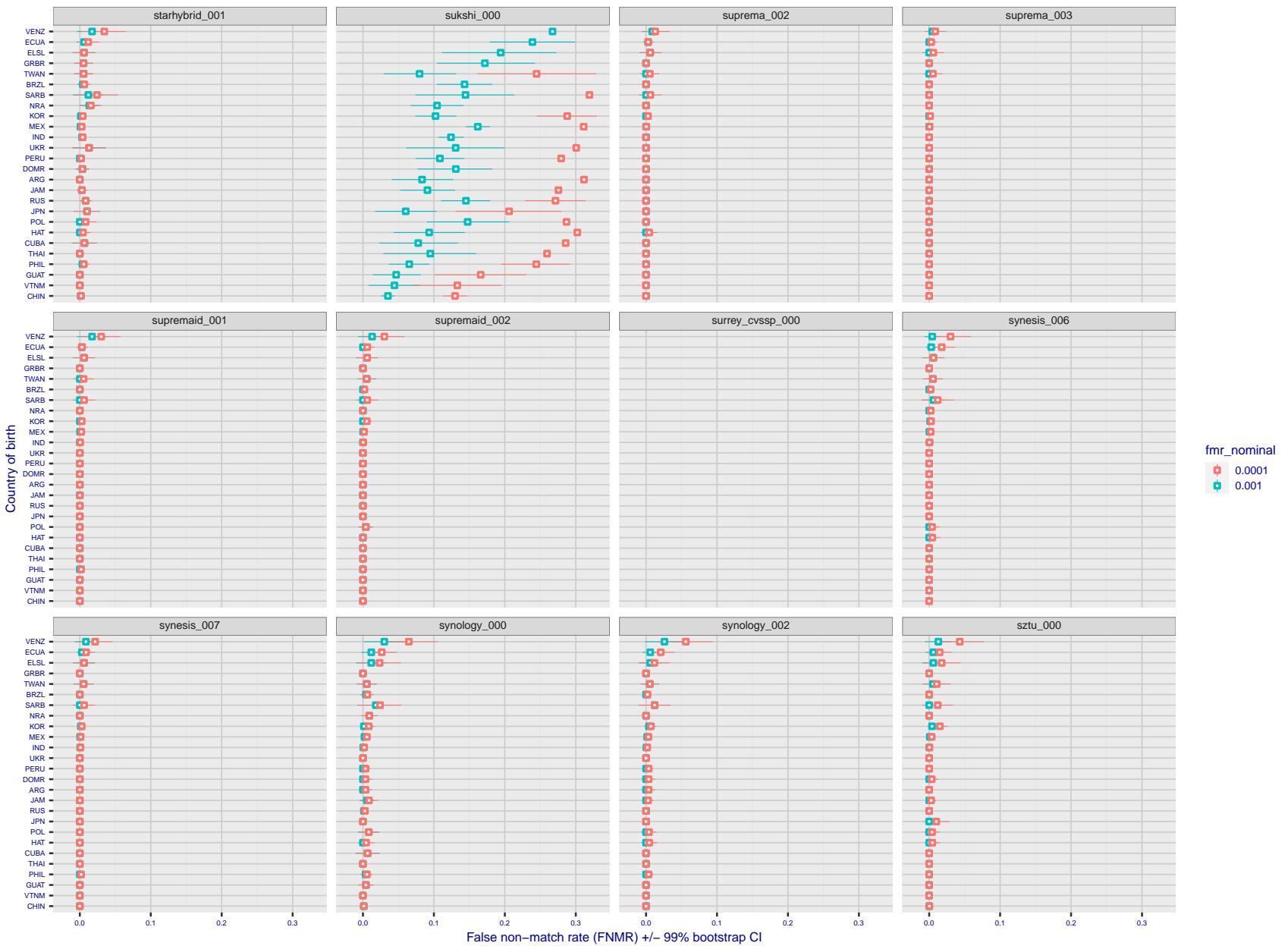


Figure 322: For the visa images, the dots show FNMR by country of birth for two globally set operating thresholds corresponding to $FMR = \{0.001, 0.0001\}$ computed over all on the order of 10^{10} impostor scores. The FMR in each bin will vary also - see subsequent impostor heatmaps in sec. 3.6.1. The figures shows an order of magnitude variation in FNMR across country of birth; these effects are likely due quality variations, then demographics like age and race. The error rates in some cases are zero, and in others the DET is flat so the error rates at the two thresholds are identical. The lines span 1% and 99% of bootstrap replicated FNMR estimates.

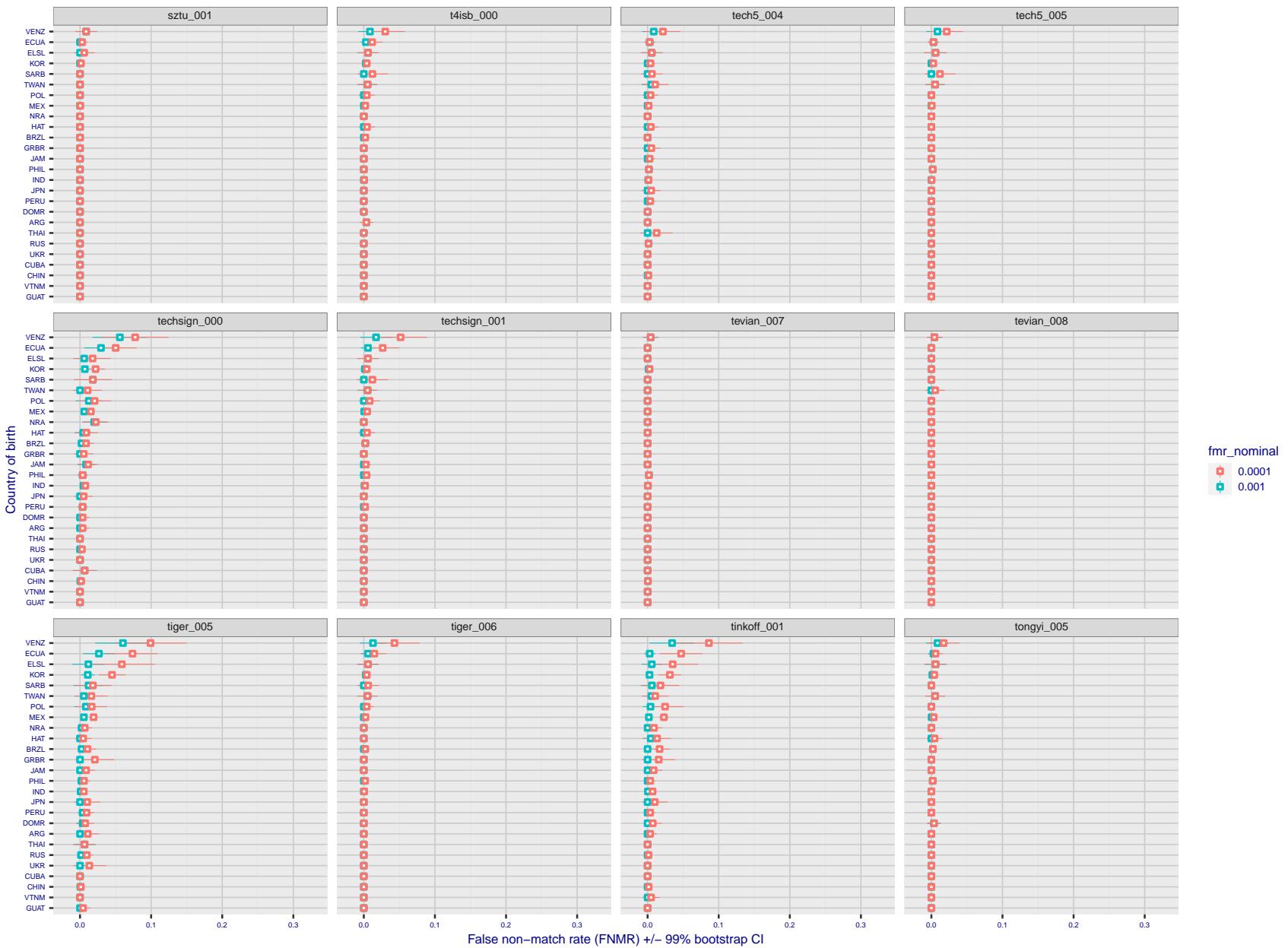


Figure 323: For the visa images, the dots show FNMR by country of birth for two globally set operating thresholds corresponding to $FMR = \{0.001, 0.0001\}$ computed over all on the order of 10^{10} impostor scores. The FMR in each bin will vary also - see subsequent impostor heatmaps in sec. 3.6.1. The figures shows an order of magnitude variation in FNMR across country of birth; these effects are likely due quality variations, then demographics like age and race. The error rates in some cases are zero, and in others the DET is flat so the error rates at the two thresholds are identical. The lines span 1% and 99% of bootstrap replicated FNMR estimates.

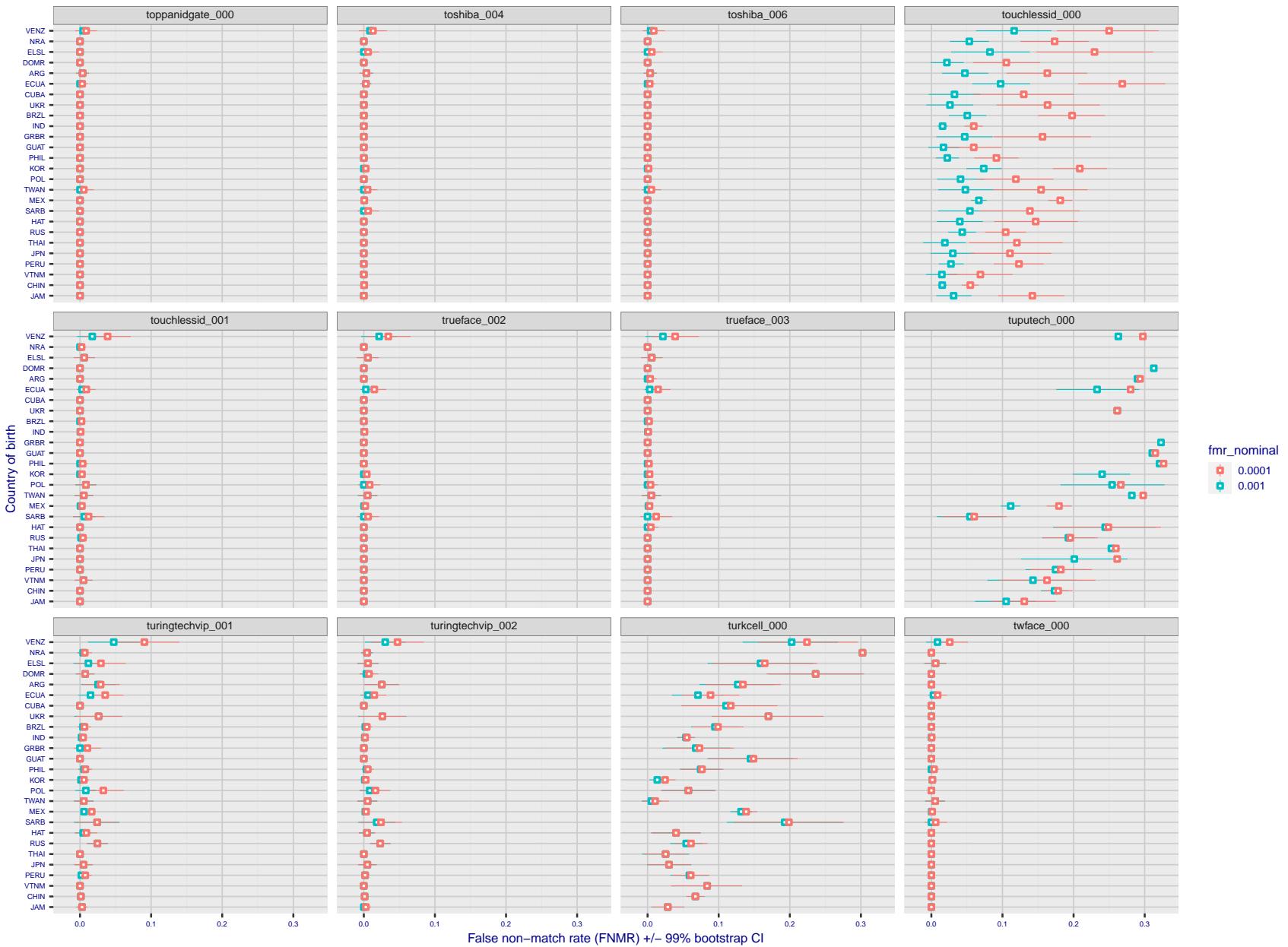


Figure 324: For the visa images, the dots show FNMR by country of birth for two globally set operating thresholds corresponding to $FMR = \{0.001, 0.0001\}$ computed over all on the order of 10^{10} impostor scores. The FMR in each bin will vary also - see subsequent impostor heatmaps in sec. 3.6.1. The figures shows an order of magnitude variation in FNMR across country of birth; these effects are likely due quality variations, then demographics like age and race. The error rates in some cases are zero, and in others the DET is flat so the error rates at the two thresholds are identical. The lines span 1% and 99% of bootstrap replicated FNMR estimates.

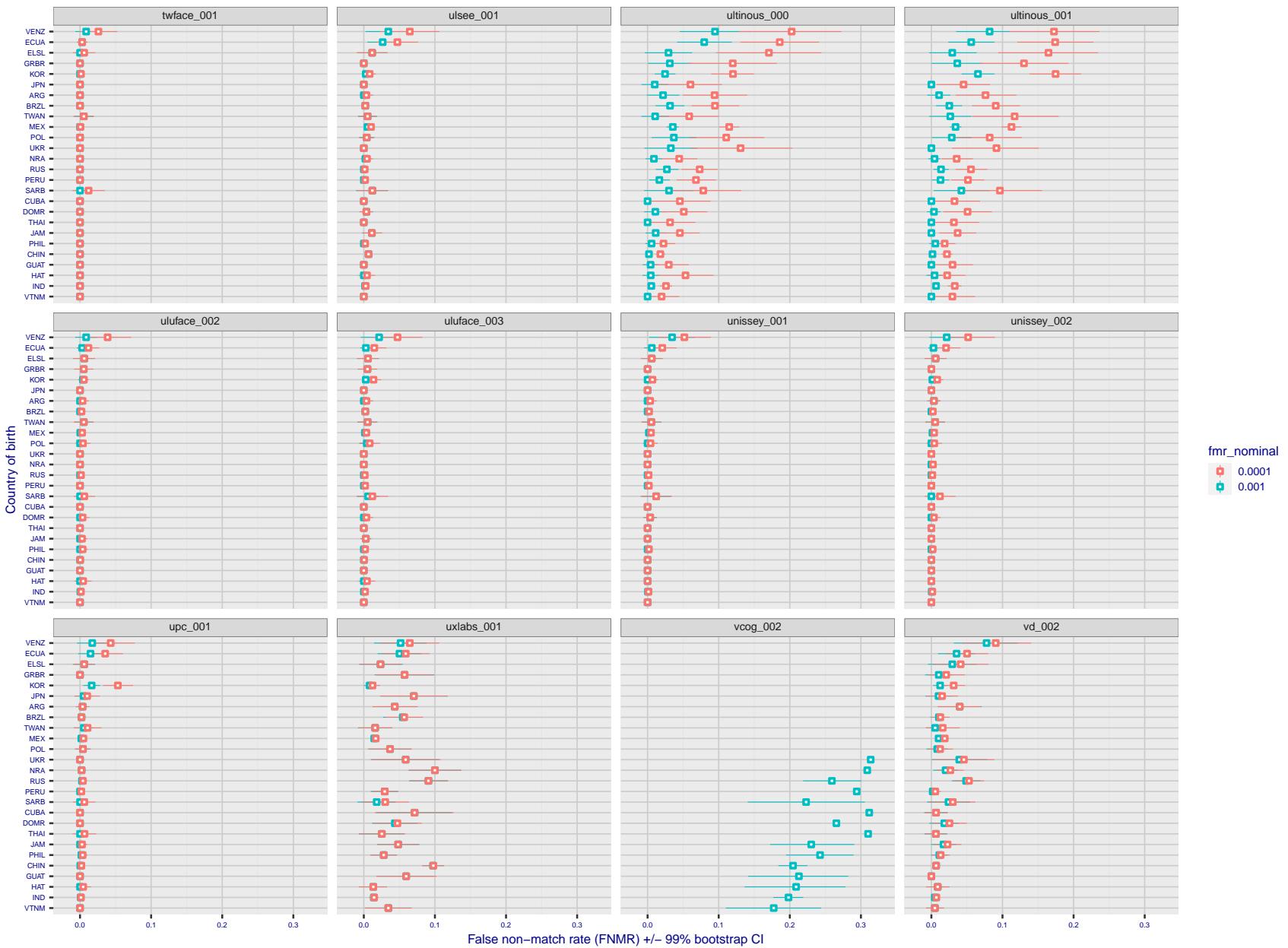


Figure 325: For the visa images, the dots show FNMR by country of birth for two globally set operating thresholds corresponding to $FMR = \{0.001, 0.0001\}$ computed over all on the order of 10^{10} impostor scores. The FMR in each bin will vary also - see subsequent impostor heatmaps in sec. 3.6.1. The figures shows an order of magnitude variation in FNMR across country of birth; these effects are likely due quality variations, then demographics like age and race. The error rates in some cases are zero, and in others the DET is flat so the error rates at the two thresholds are identical. The lines span 1% and 99% of bootstrap replicated FNMR estimates.

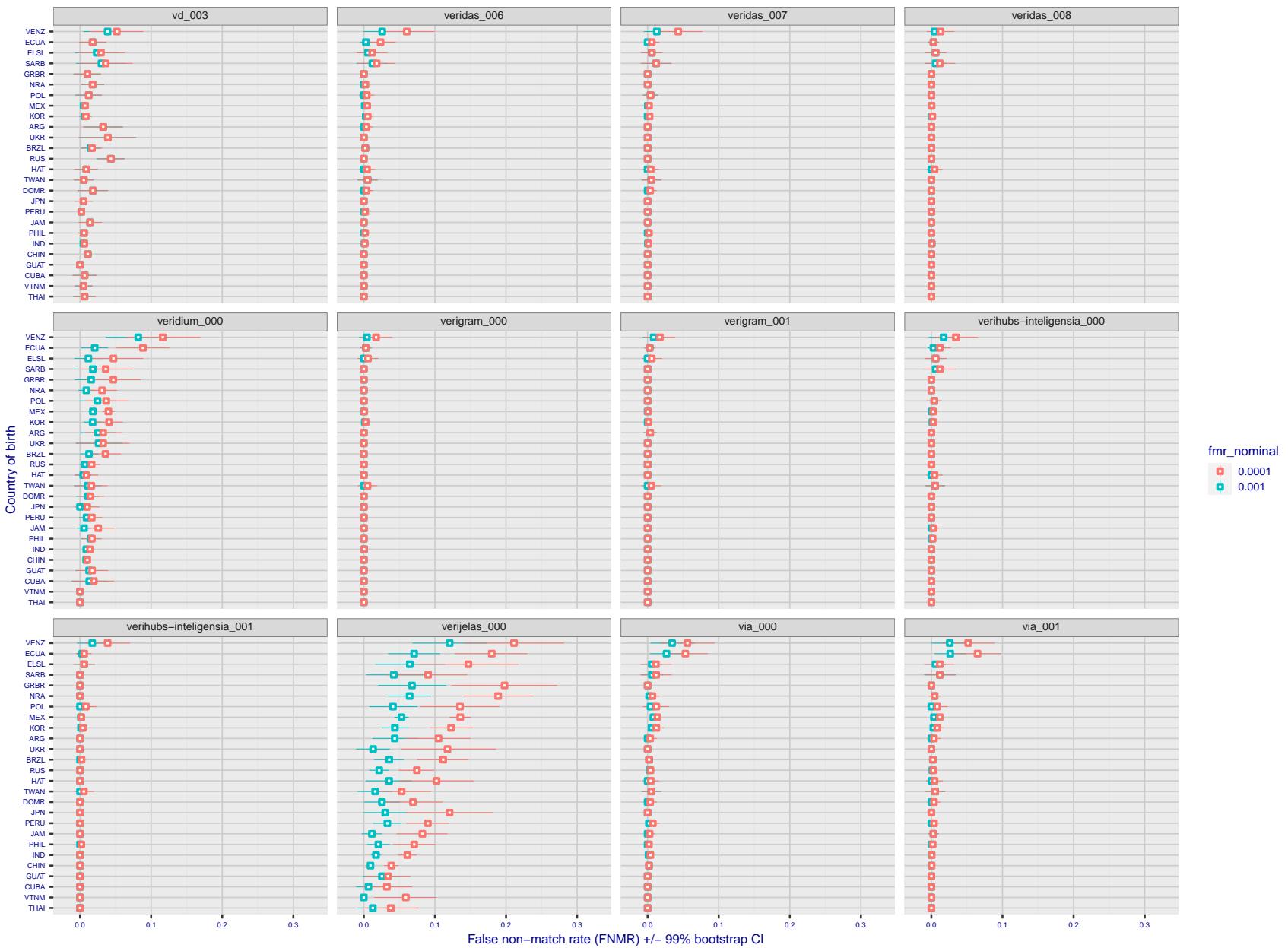


Figure 326: For the visa images, the dots show FNMR by country of birth for two globally set operating thresholds corresponding to $FMR = \{0.001, 0.0001\}$ computed over all on the order of 10^{10} impostor scores. The FMR in each bin will vary also - see subsequent impostor heatmaps in sec. 3.6.1. The figures shows an order of magnitude variation in FNMR across country of birth; these effects are likely due quality variations, then demographics like age and race. The error rates in some cases are zero, and in others the DET is flat so the error rates at the two thresholds are identical. The lines span 1% and 99% of bootstrap replicated FNMR estimates.

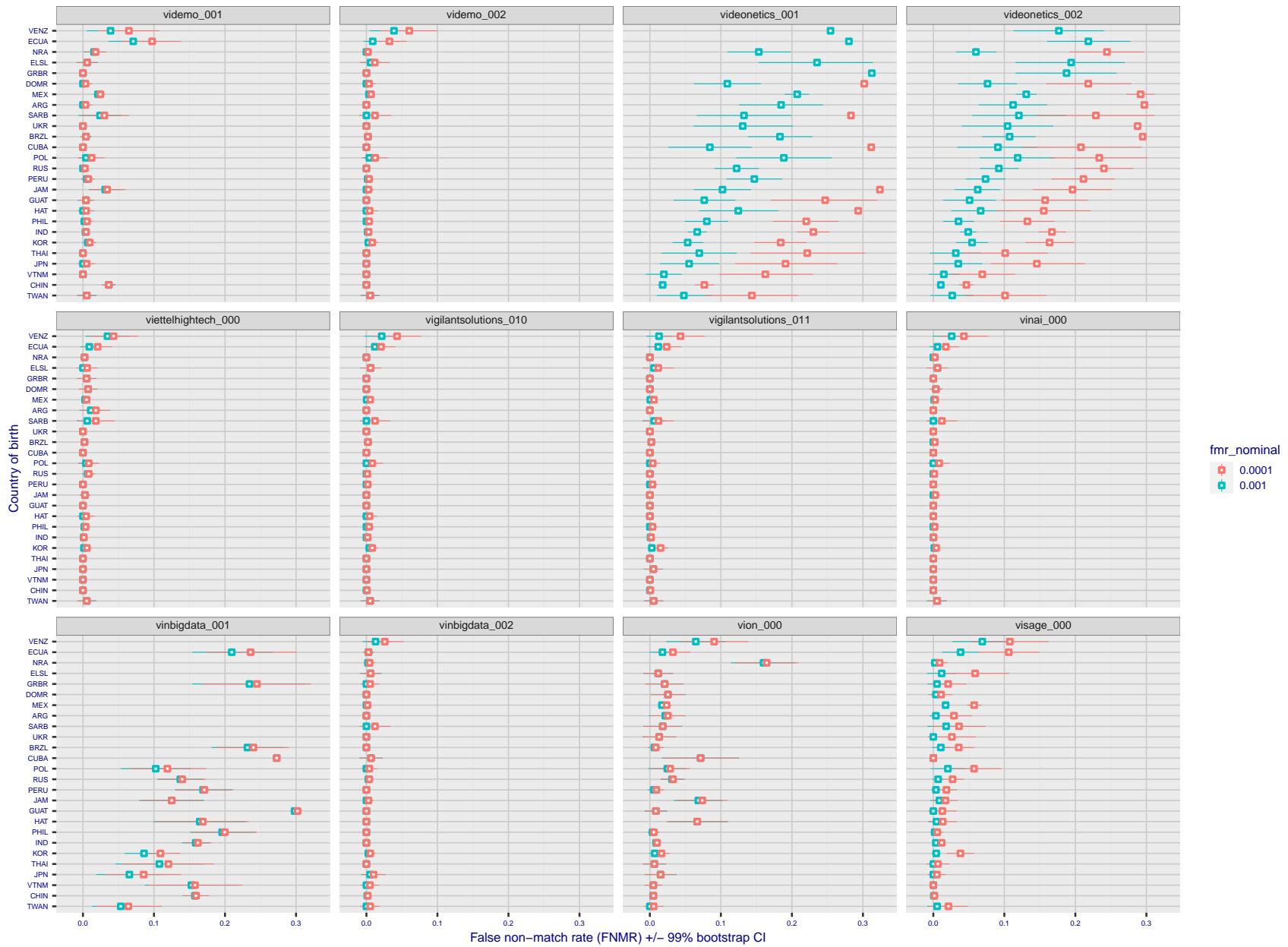


Figure 327: For the visa images, the dots show FNMR by country of birth for two globally set operating thresholds corresponding to $FMR = \{0.001, 0.0001\}$ computed over all on the order of 10^{10} impostor scores. The FMR in each bin will vary also - see subsequent impostor heatmaps in sec. 3.6.1. The figures shows an order of magnitude variation in FNMR across country of birth; these effects are likely due quality variations, then demographics like age and race. The error rates in some cases are zero, and in others the DET is flat so the error rates at the two thresholds are identical. The lines span 1% and 99% of bootstrap replicated FNMR estimates.

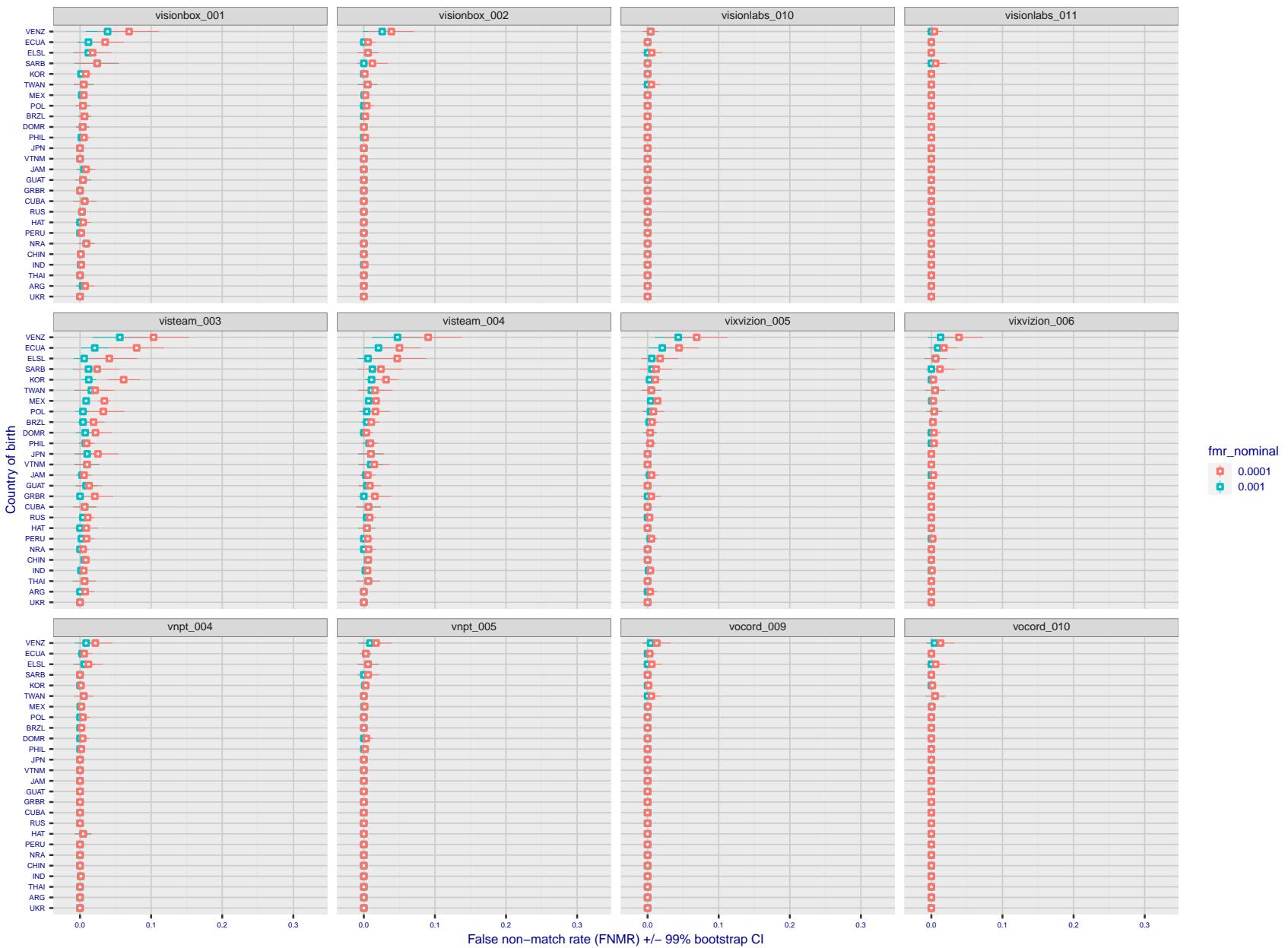


Figure 328: For the visa images, the dots show FNMR by country of birth for two globally set operating thresholds corresponding to $FMR = \{0.001, 0.0001\}$ computed over all on the order of 10^{10} impostor scores. The FMR in each bin will vary also - see subsequent impostor heatmaps in sec. 3.6.1. The figures shows an order of magnitude variation in FNMR across country of birth; these effects are likely due quality variations, then demographics like age and race. The error rates in some cases are zero, and in others the DET is flat so the error rates at the two thresholds are identical. The lines span 1% and 99% of bootstrap replicated FNMR estimates.

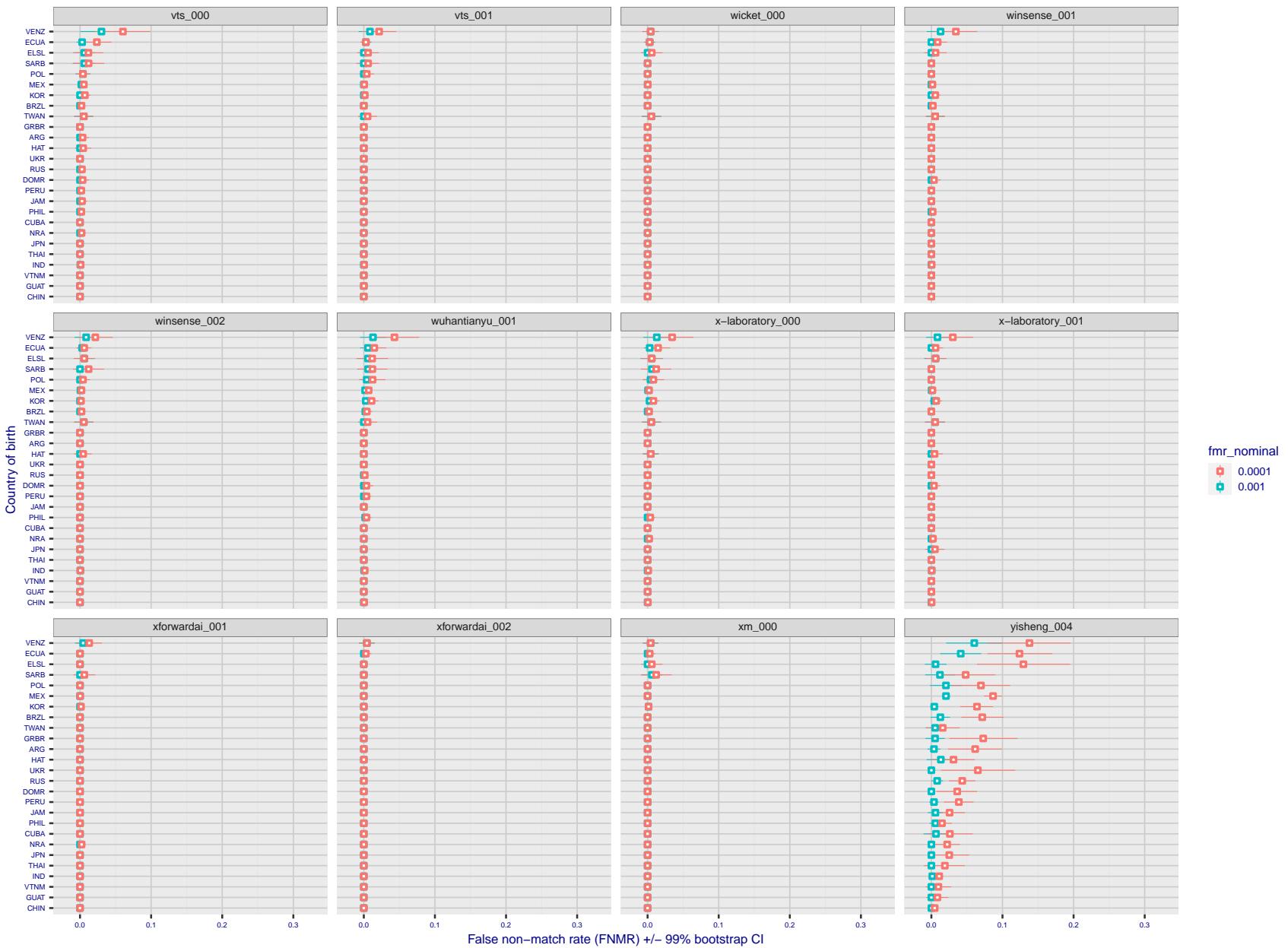


Figure 329: For the visa images, the dots show FNMR by country of birth for two globally set operating thresholds corresponding to $FMR = \{0.001, 0.0001\}$ computed over all on the order of 10^{10} impostor scores. The FMR in each bin will vary also - see subsequent impostor heatmaps in sec. 3.6.1. The figures shows an order of magnitude variation in FNMR across country of birth; these effects are likely due quality variations, then demographics like age and race. The error rates in some cases are zero, and in others the DET is flat so the error rates at the two thresholds are identical. The lines span 1% and 99% of bootstrap replicated FNMR estimates.

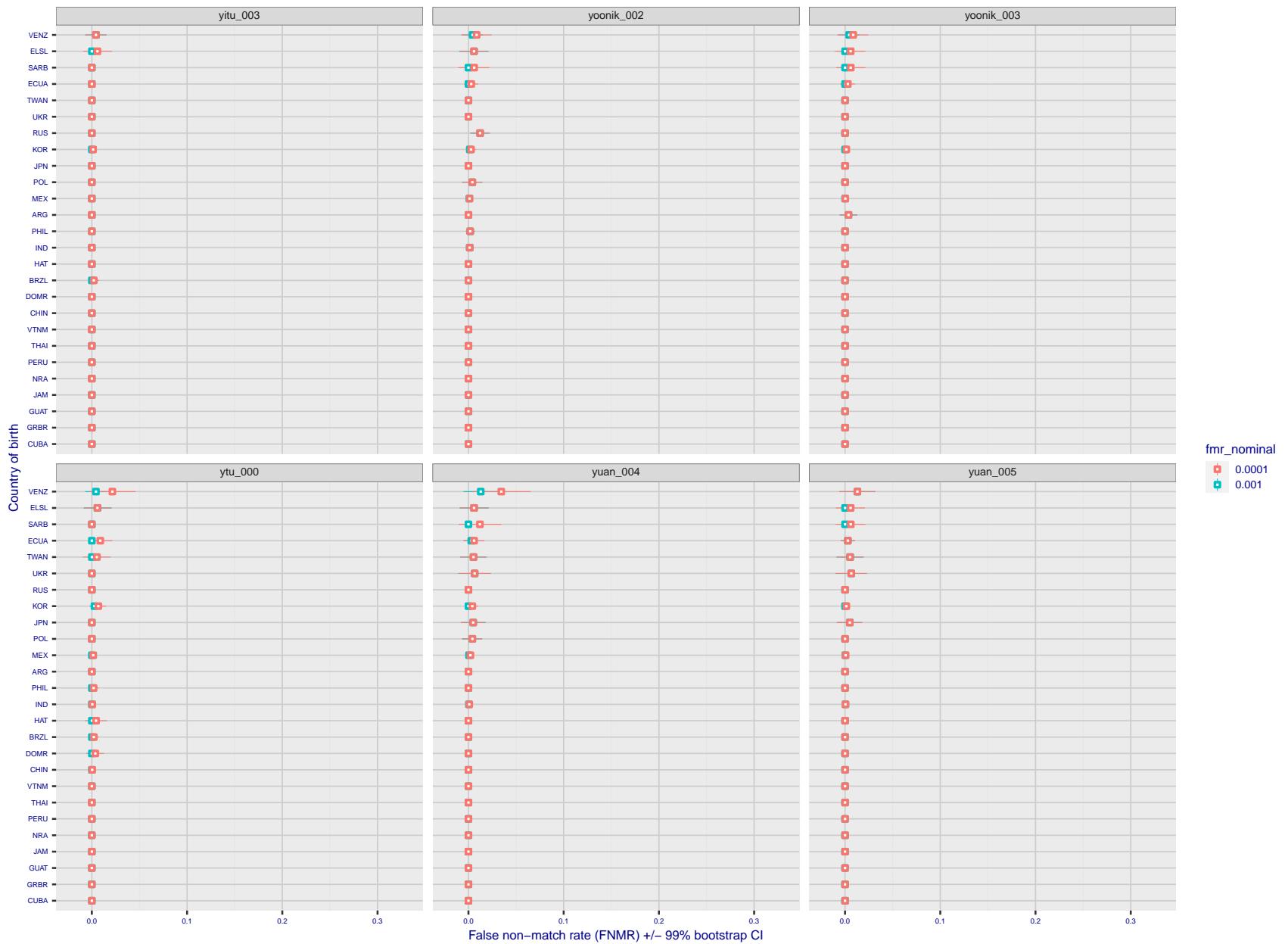


Figure 330: For the visa images, the dots show FNMR by country of birth for two globally set operating thresholds corresponding to $FMR = \{0.001, 0.0001\}$ computed over all on the order of 10^{10} impostor scores. The FMR in each bin will vary also - see subsequent impostor heatmaps in sec. 3.6.1. The figures shows an order of magnitude variation in FNMR across country of birth; these effects are likely due quality variations, then demographics like age and race. The error rates in some cases are zero, and in others the DET is flat so the error rates at the two thresholds are identical. The lines span 1% and 99% of bootstrap replicated FNMR estimates.

Caveats: The results may not relate to subject-specific properties. Instead they could reflect image-specific quality differences, which could occur due to collection protocol or software processing variations.

3.5.2 Effect of ageing

Background: Faces change appearance throughout life. This change gradually reduces similarity of a new image to an earlier image. Face recognition algorithms give reduced similarity scores and more frequent false rejections.

Goal: To quantify false non-match rates (FNMR) as a function of elapsed time in an adult population.

Methods: Using the mugshot images, a threshold is set to give FMR = 0.00001 over the entire impostor set. Then FNMR is measured over 1000 bootstrap replications of the genuine scores.

Results: For the visa images, Figure 359 shows how false non-match rates for genuine users, as a function of age group.

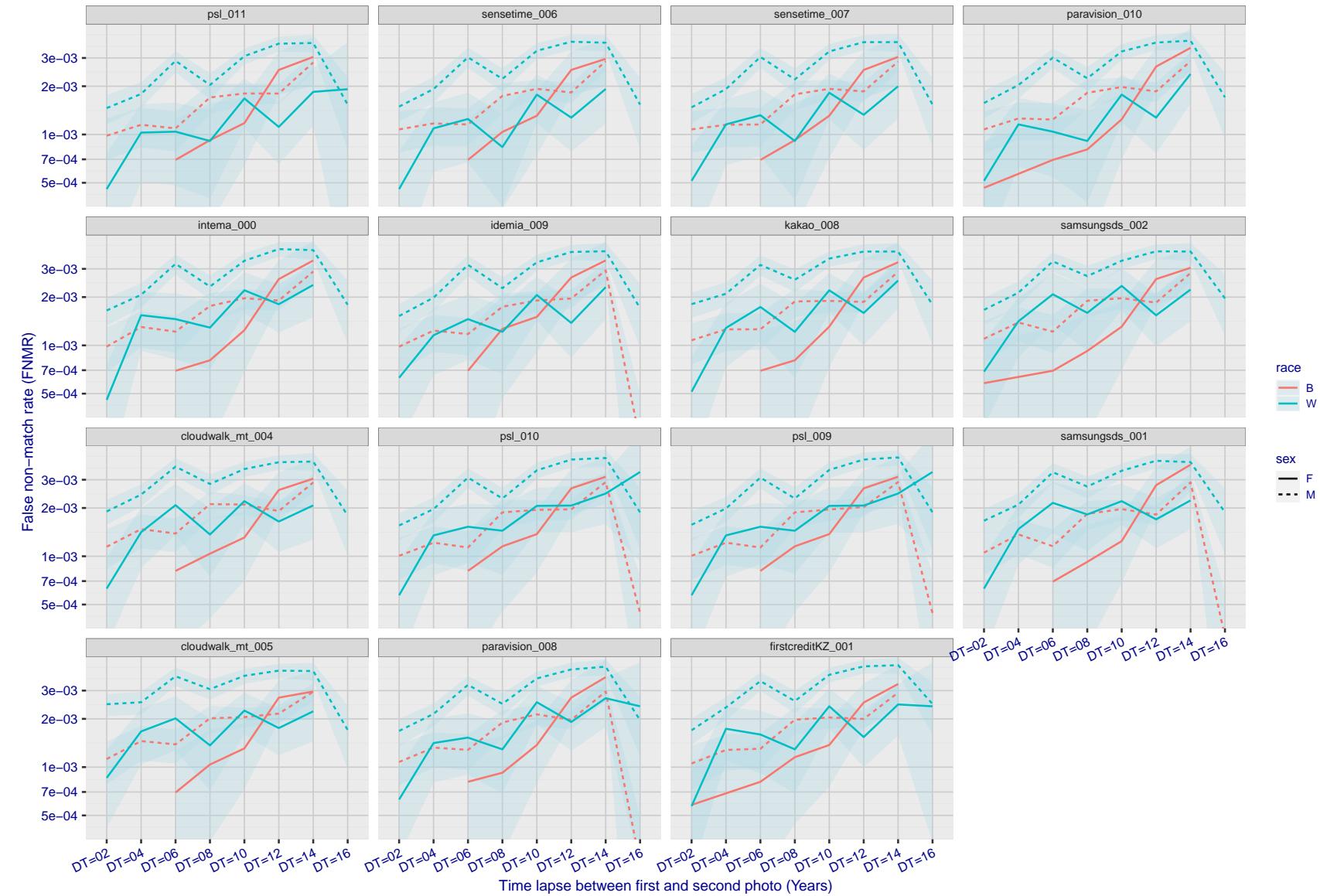


Figure 331: For the mugshot images, FNMR as a function of elapsed time between initial enrollment and second verification images. The panels appear most accurate first, and vertical scale changes on each page. The four traces correspond to images annotated with codes for black female, black male, white female, white male. The threshold is fixed for each algorithm to give $FMR = 0.00001$ over all (10^8) impostor comparisons. For short time-lapses, the most accurate algorithms give very few errors ($FNMR < 0.001$) so that the uncertainty estimates are high.

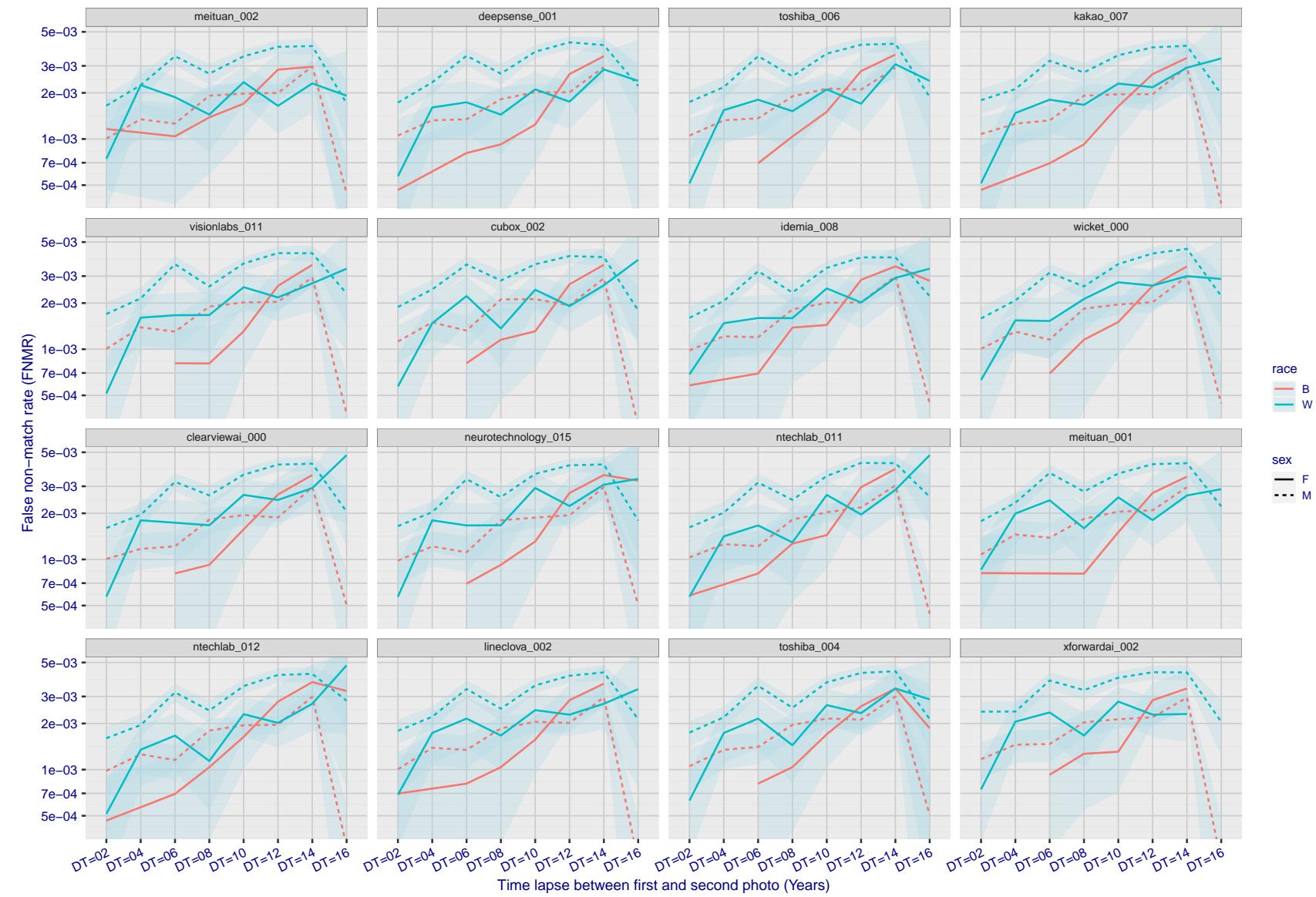


Figure 332: For the mugshot images, FNMR as a function of elapsed time between initial enrollment and second verification images. The panels appear most accurate first, and vertical scale changes on each page. The four traces correspond to images annotated with codes for black female, black male, white female, white male. The threshold is fixed for each algorithm to give FMR = 0.00001 over all (10^8) impostor comparisons. For short time-lapses, the most accurate algorithms give very few errors (FNMR < 0.001) so that the uncertainty estimates are high.

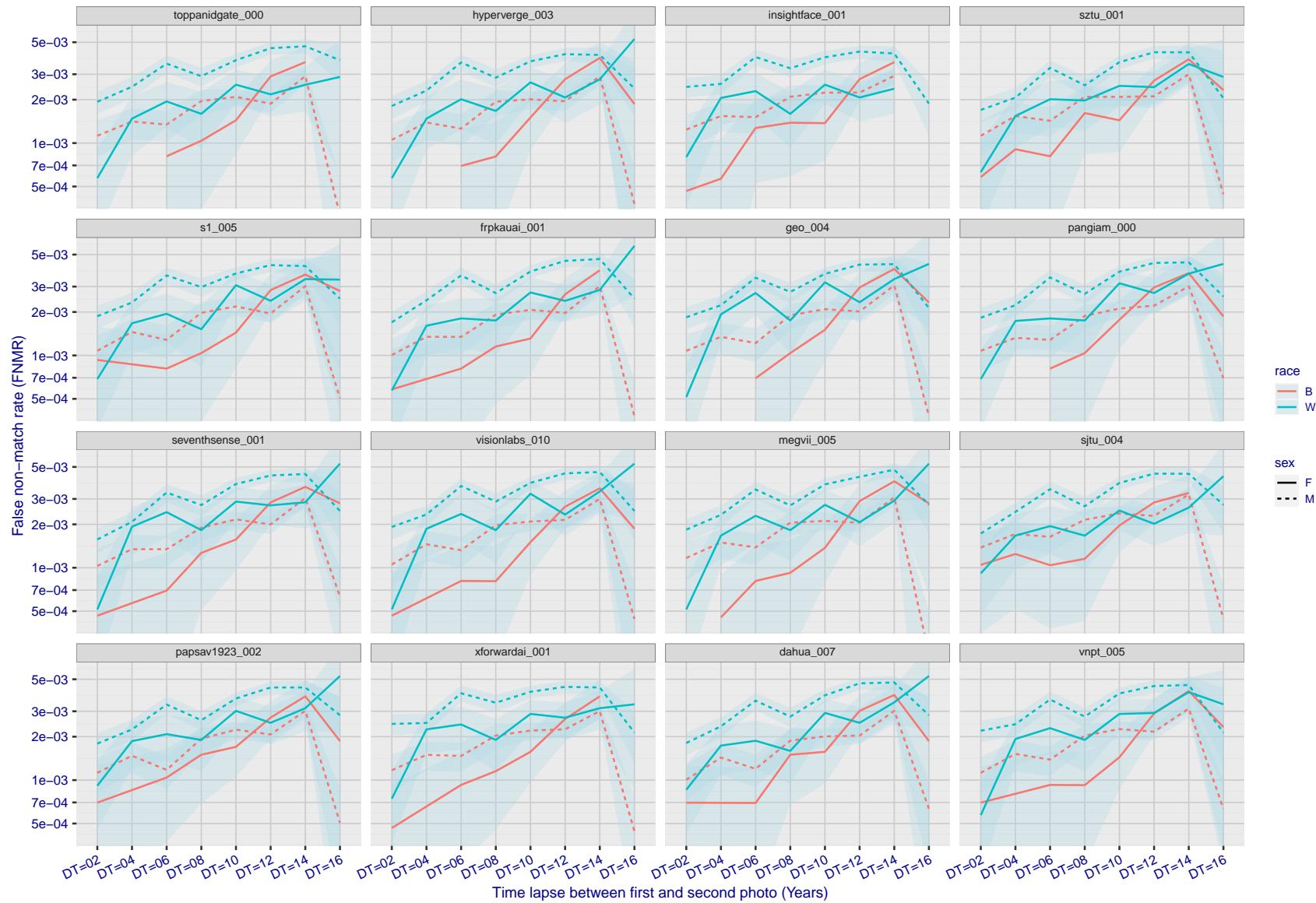


Figure 333: For the mugshot images, FNMR as a function of elapsed time between initial enrollment and second verification images. The panels appear most accurate first, and vertical scale changes on each page. The four traces correspond to images annotated with codes for black female, black male, white female, white male. The threshold is fixed for each algorithm to give $FMR = 0.00001$ over all (10^8) impostor comparisons. For short time-lapses, the most accurate algorithms give very few errors ($FNMR < 0.001$) so that the uncertainty estimates are high.

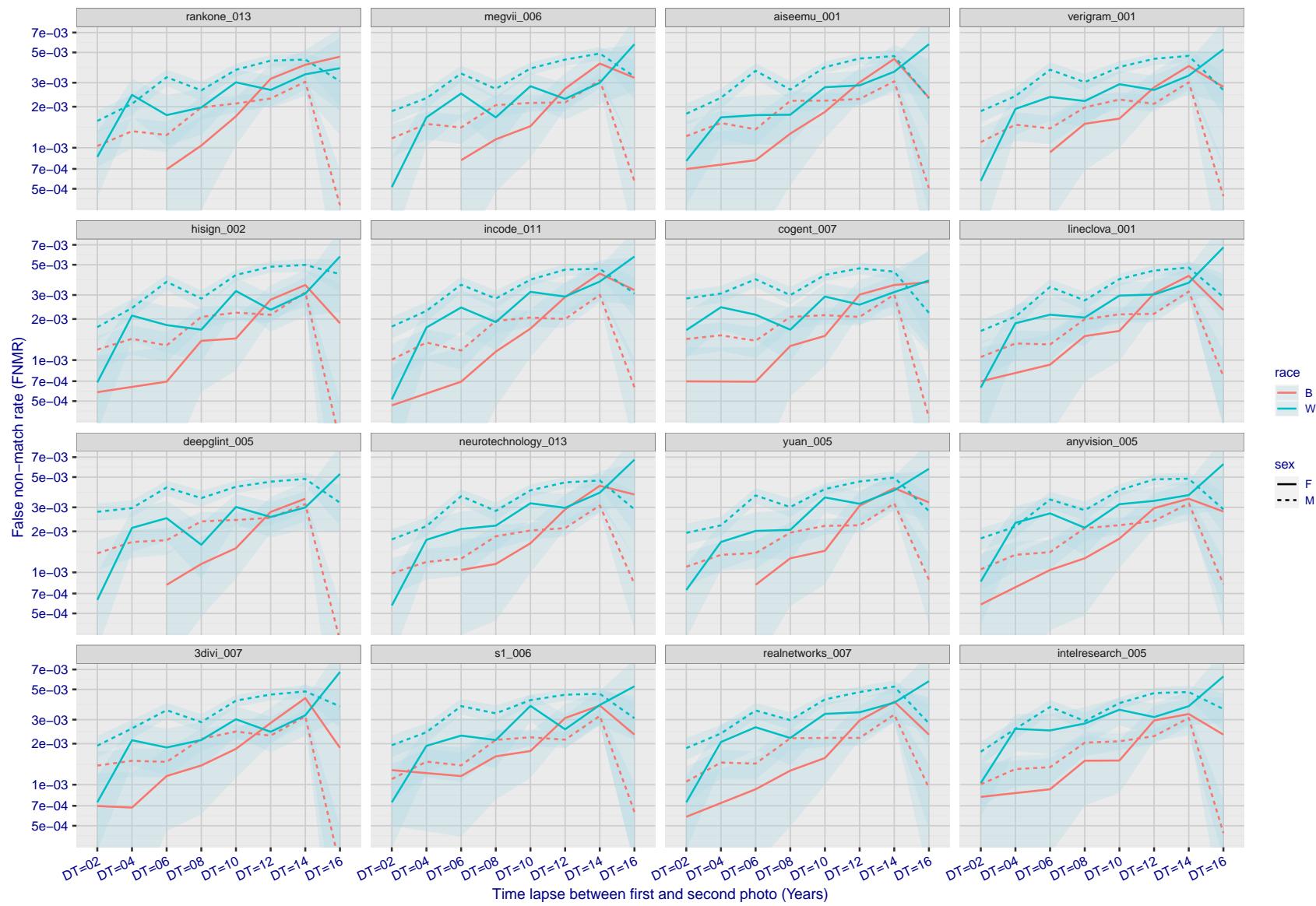


Figure 334: For the mugshot images, FNMR as a function of elapsed time between initial enrollment and second verification images. The panels appear most accurate first, and vertical scale changes on each page. The four traces correspond to images annotated with codes for black female, black male, white female, white male. The threshold is fixed for each algorithm to give FMR = 0.00001 over all (10^8) impostor comparisons. For short time-lapses, the most accurate algorithms give very few errors (FNMR < 0.001) so that the uncertainty estimates are high.

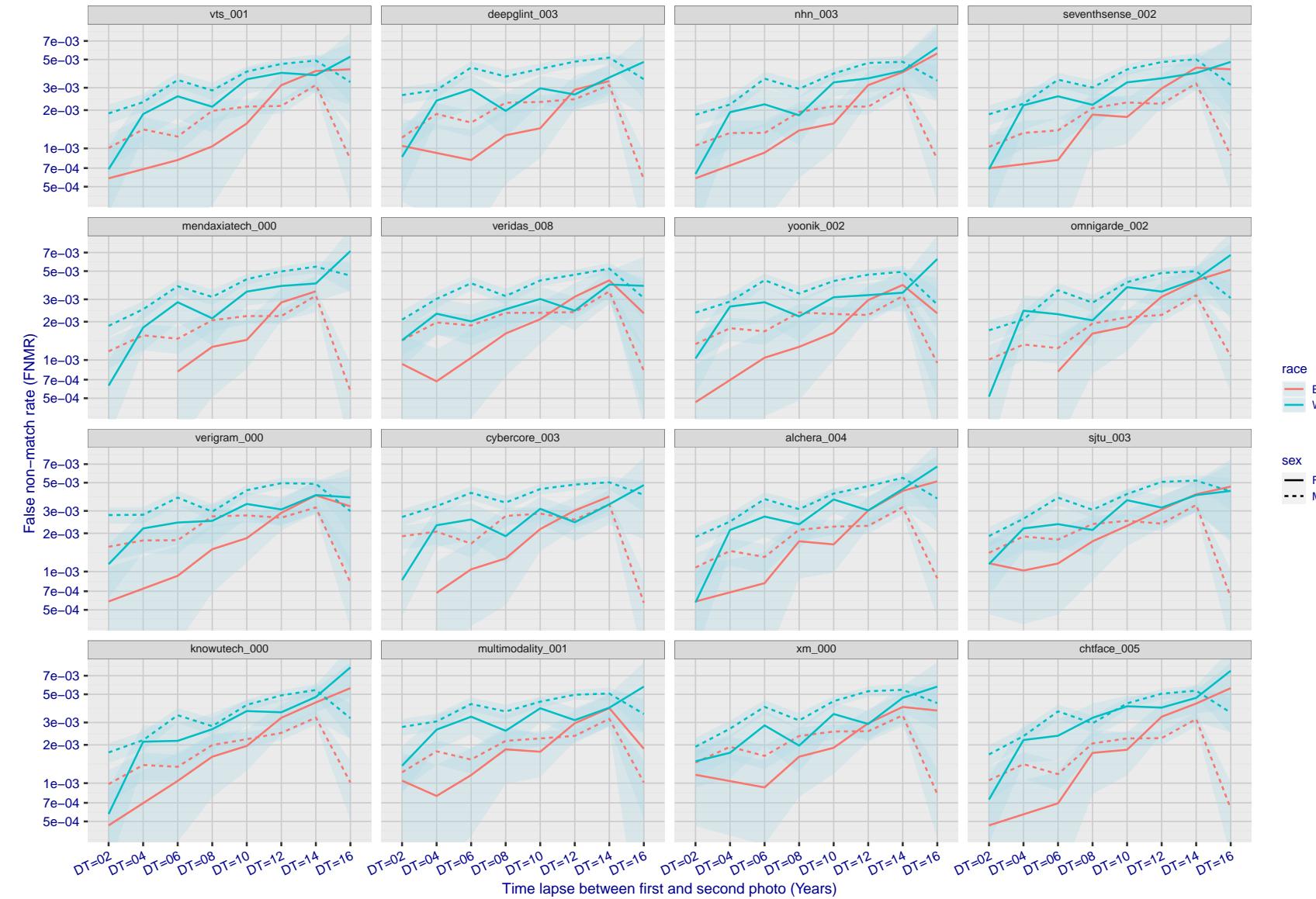


Figure 335: For the mugshot images, FNMR as a function of elapsed time between initial enrollment and second verification images. The panels appear most accurate first, and vertical scale changes on each page. The four traces correspond to images annotated with codes for black female, black male, white female, white male. The threshold is fixed for each algorithm to give $FMR = 0.00001$ over all (10^8) impostor comparisons. For short time-lapses, the most accurate algorithms give very few errors ($FNMR < 0.001$) so that the uncertainty estimates are high.

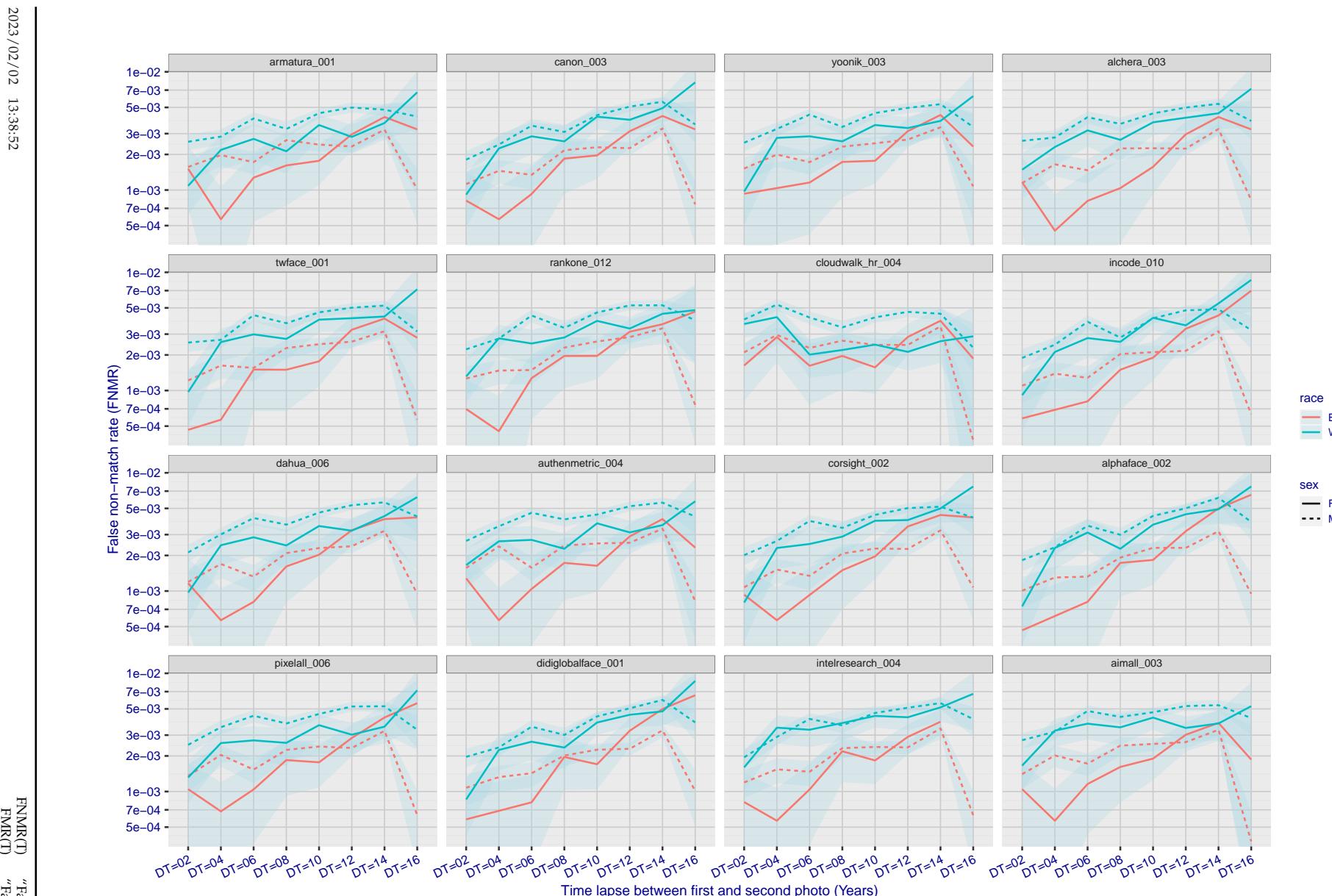


Figure 336: For the mugshot images, FNMR as a function of elapsed time between initial enrollment and second verification images. The panels appear most accurate first, and vertical scale changes on each page. The four traces correspond to images annotated with codes for black female, black male, white female, white male. The threshold is fixed for each algorithm to give $FMR = 0.00001$ over all (10^8) impostor comparisons. For short time-lapses, the most accurate algorithms give very few errors ($FNMR < 0.001$) so that the uncertainty estimates are high.

2023/02/02 13:38:52

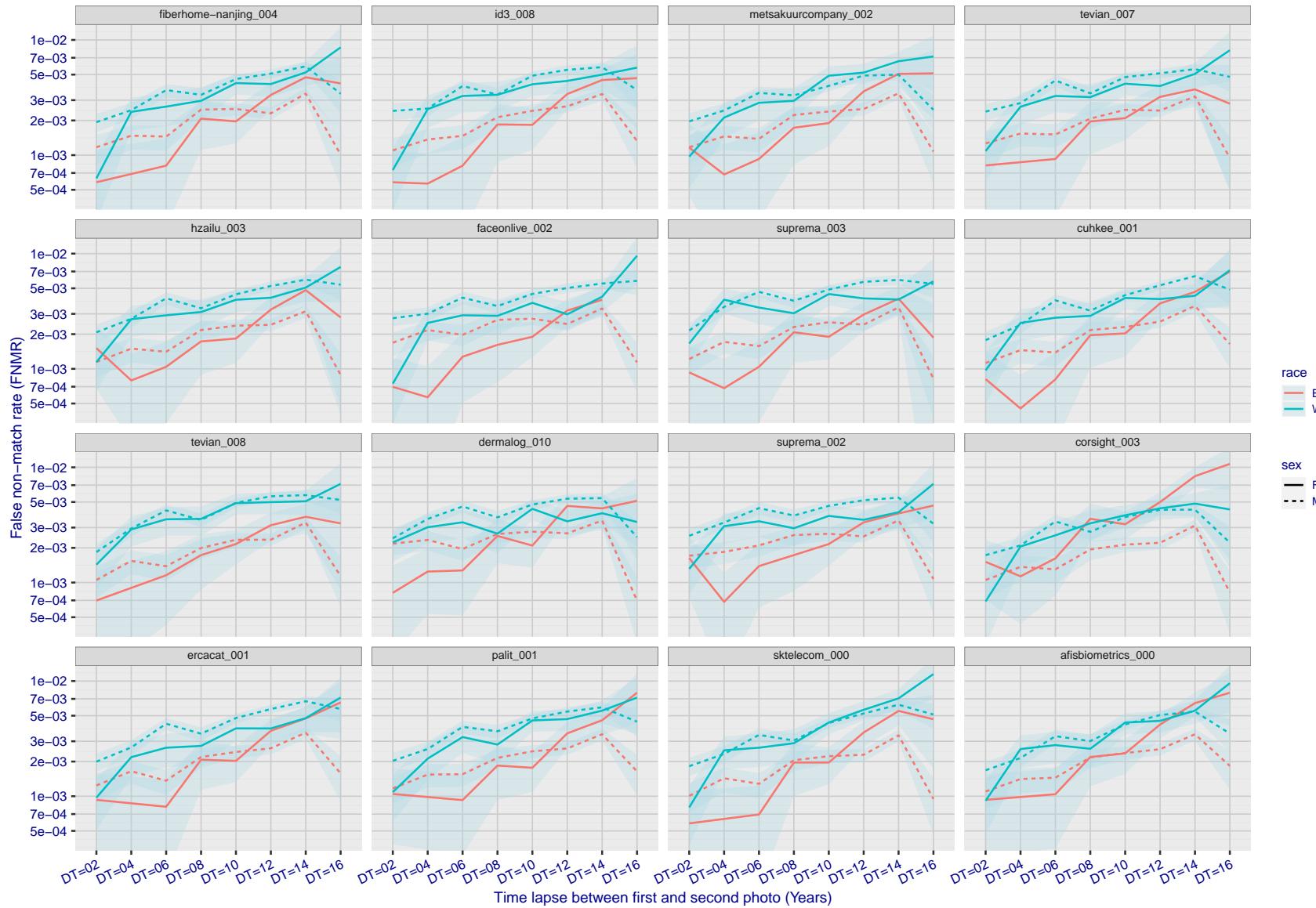
FNMR(T)
FMR(T)
"False non-match rate"
"False match rate"

Figure 337: For the mugshot images, FNMR as a function of elapsed time between initial enrollment and second verification images. The panels appear most accurate first, and vertical scale changes on each page. The four traces correspond to images annotated with codes for black female, black male, white female, white male. The threshold is fixed for each algorithm to give FMR = 0.00001 over all (10^8) impostor comparisons. For short time-lapses, the most accurate algorithms give very few errors (FNMR < 0.001) so that the uncertainty estimates are high.

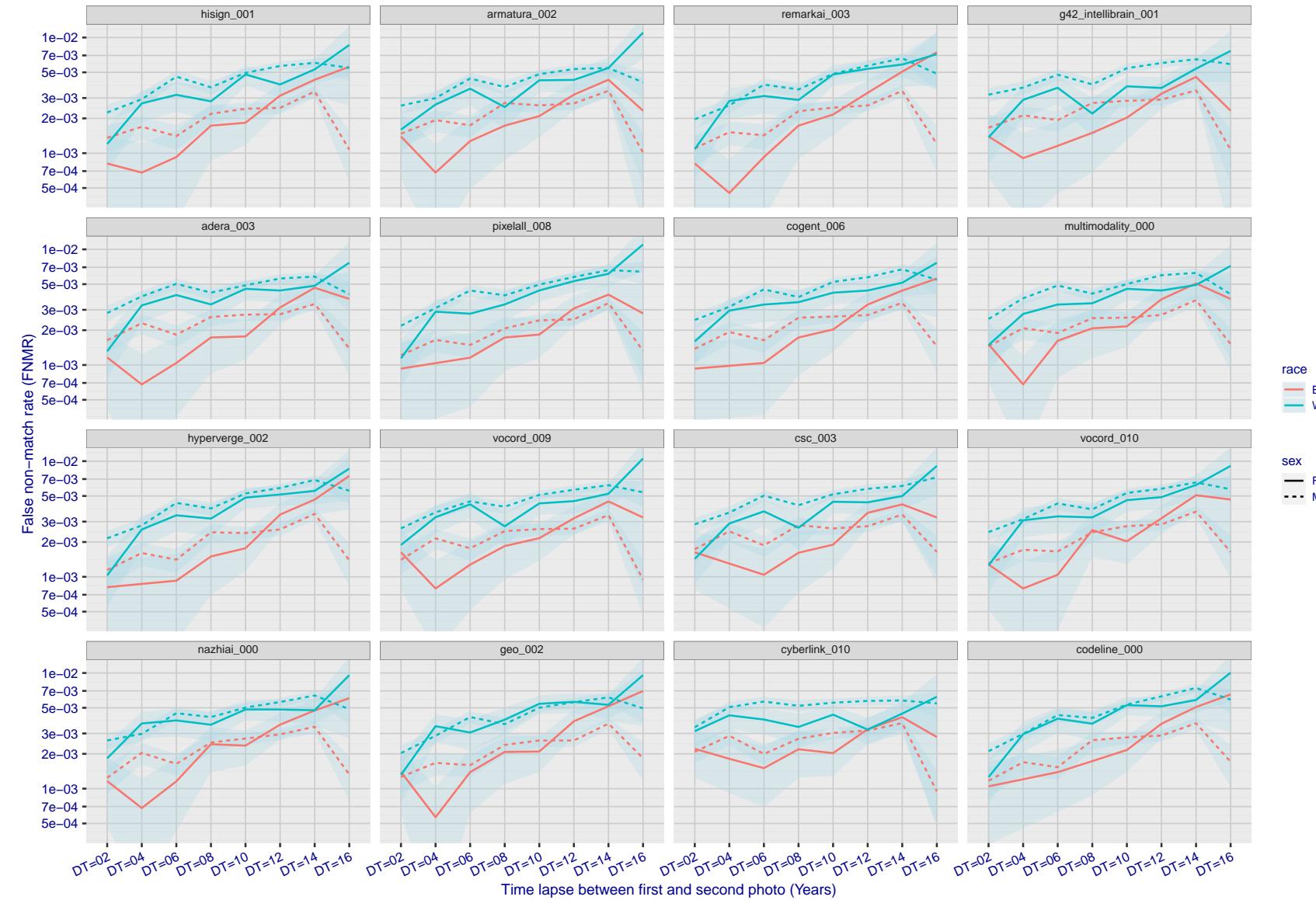


Figure 338: For the mugshot images, FNMR as a function of elapsed time between initial enrollment and second verification images. The panels appear most accurate first, and vertical scale changes on each page. The four traces correspond to images annotated with codes for black female, black male, white female, white male. The threshold is fixed for each algorithm to give FMR = 0.00001 over all (10^8) impostor comparisons. For short time-lapses, the most accurate algorithms give very few errors (FNMR < 0.001) so that the uncertainty estimates are high.

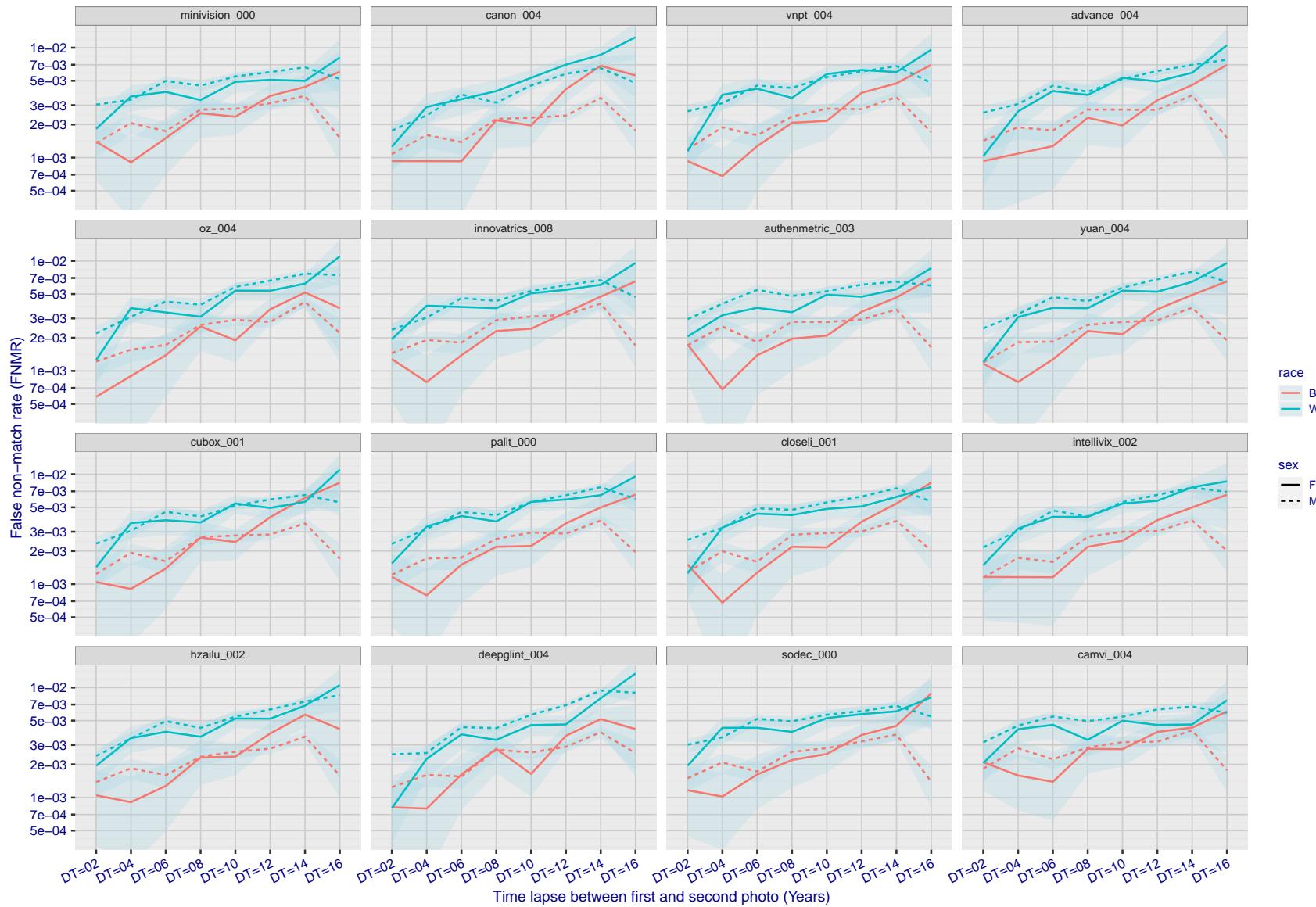


Figure 339: For the mugshot images, FNMR as a function of elapsed time between initial enrollment and second verification images. The panels appear most accurate first, and vertical scale changes on each page. The four traces correspond to images annotated with codes for black female, black male, white female, white male. The threshold is fixed for each algorithm to give $FMR = 0.00001$ over all (10^8) impostor comparisons. For short time-lapses, the most accurate algorithms give very few errors ($FNMR < 0.001$) so that the uncertainty estimates are high.

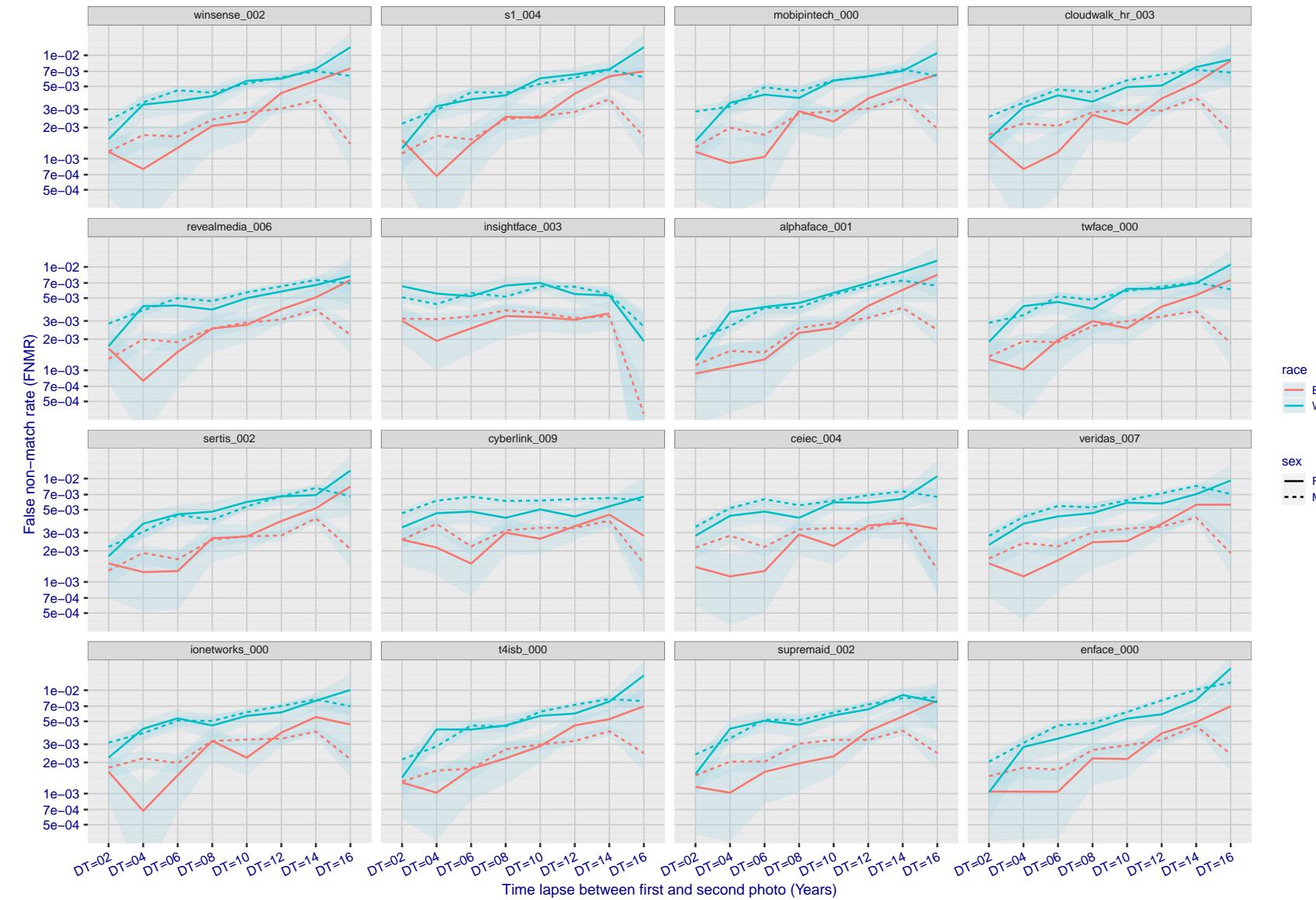


Figure 340: For the mugshot images, FNMR as a function of elapsed time between initial enrollment and second verification images. The panels appear most accurate first, and vertical scale changes on each page. The four traces correspond to images annotated with codes for black female, black male, white female, white male. The threshold is fixed for each algorithm to give $FMR = 0.00001$ over all (10^8) impostor comparisons. For short time-lapses, the most accurate algorithms give very few errors ($FNMR < 0.001$) so that the uncertainty estimates are high.

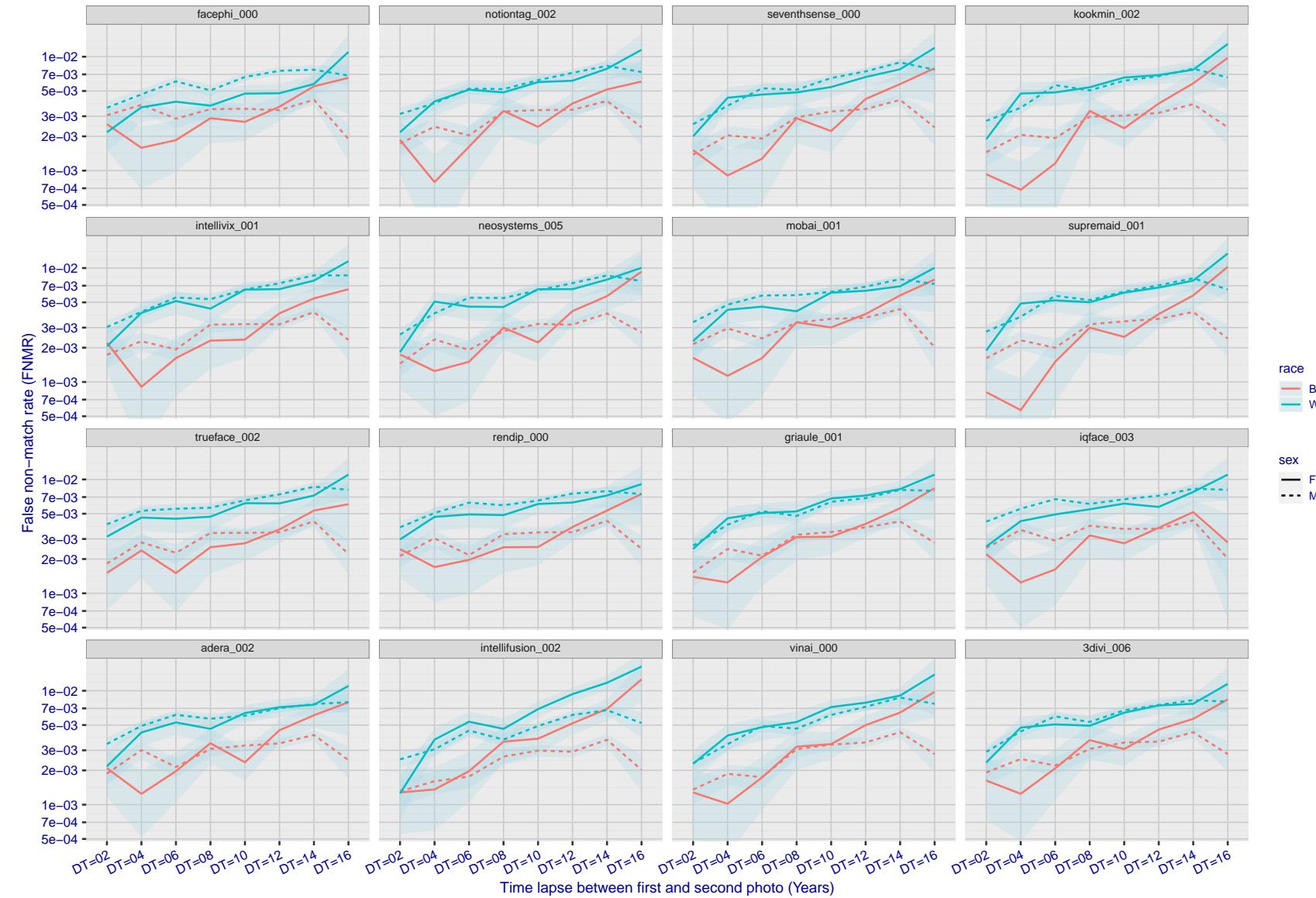


Figure 341: For the mugshot images, FNMR as a function of elapsed time between initial enrollment and second verification images. The panels appear most accurate first, and vertical scale changes on each page. The four traces correspond to images annotated with codes for black female, black male, white female, white male. The threshold is fixed for each algorithm to give $FMR = 0.00001$ over all (10^8) impostor comparisons. For short time-lapses, the most accurate algorithms give very few errors ($FNMR < 0.001$) so that the uncertainty estimates are high.

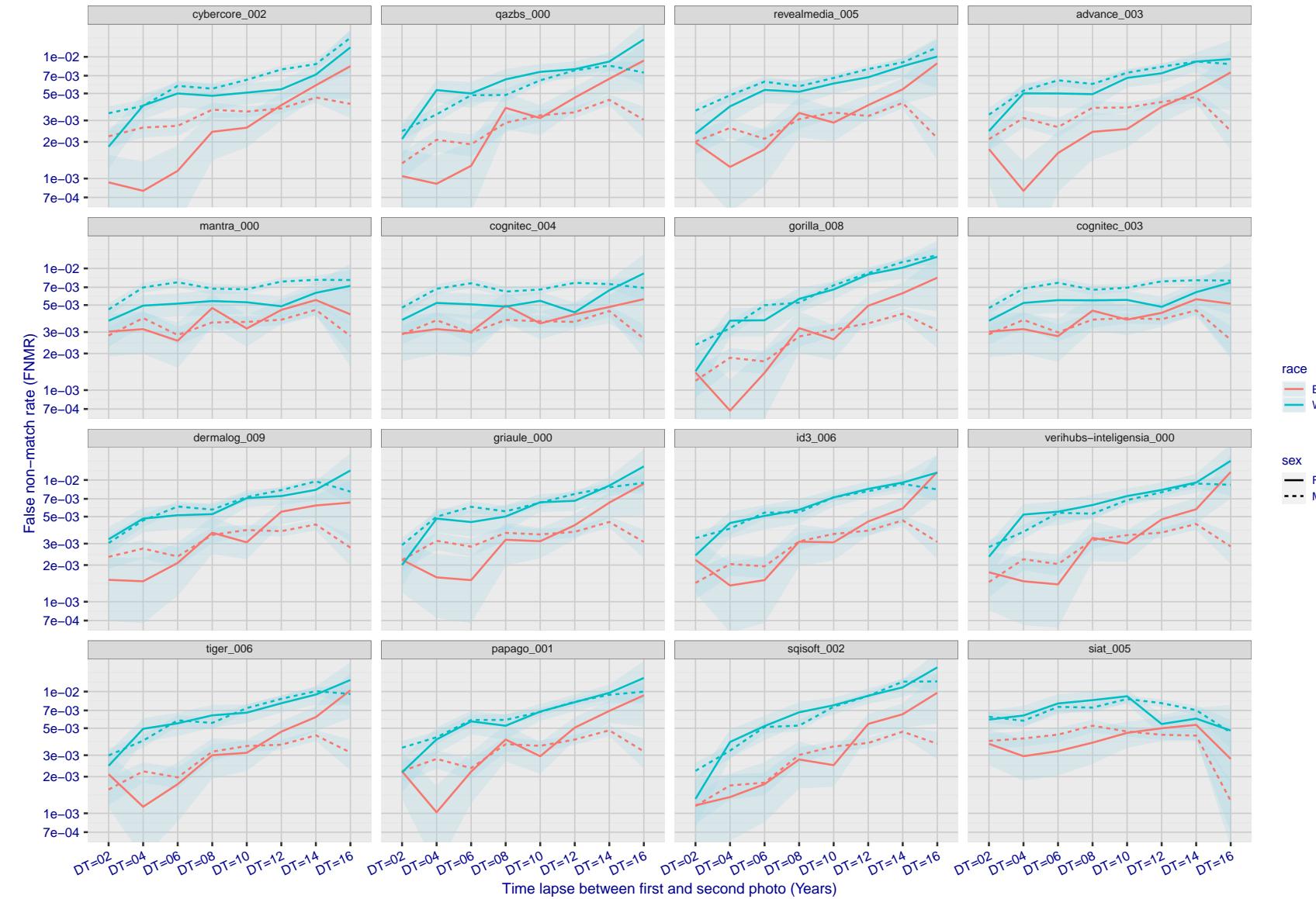


Figure 342: For the mugshot images, FNMR as a function of elapsed time between initial enrollment and second verification images. The panels appear most accurate first, and vertical scale changes on each page. The four traces correspond to images annotated with codes for black female, black male, white female, white male. The threshold is fixed for each algorithm to give $FMR = 0.00001$ over all (10^8) impostor comparisons. For short time-lapses, the most accurate algorithms give very few errors ($FNMR < 0.001$) so that the uncertainty estimates are high.

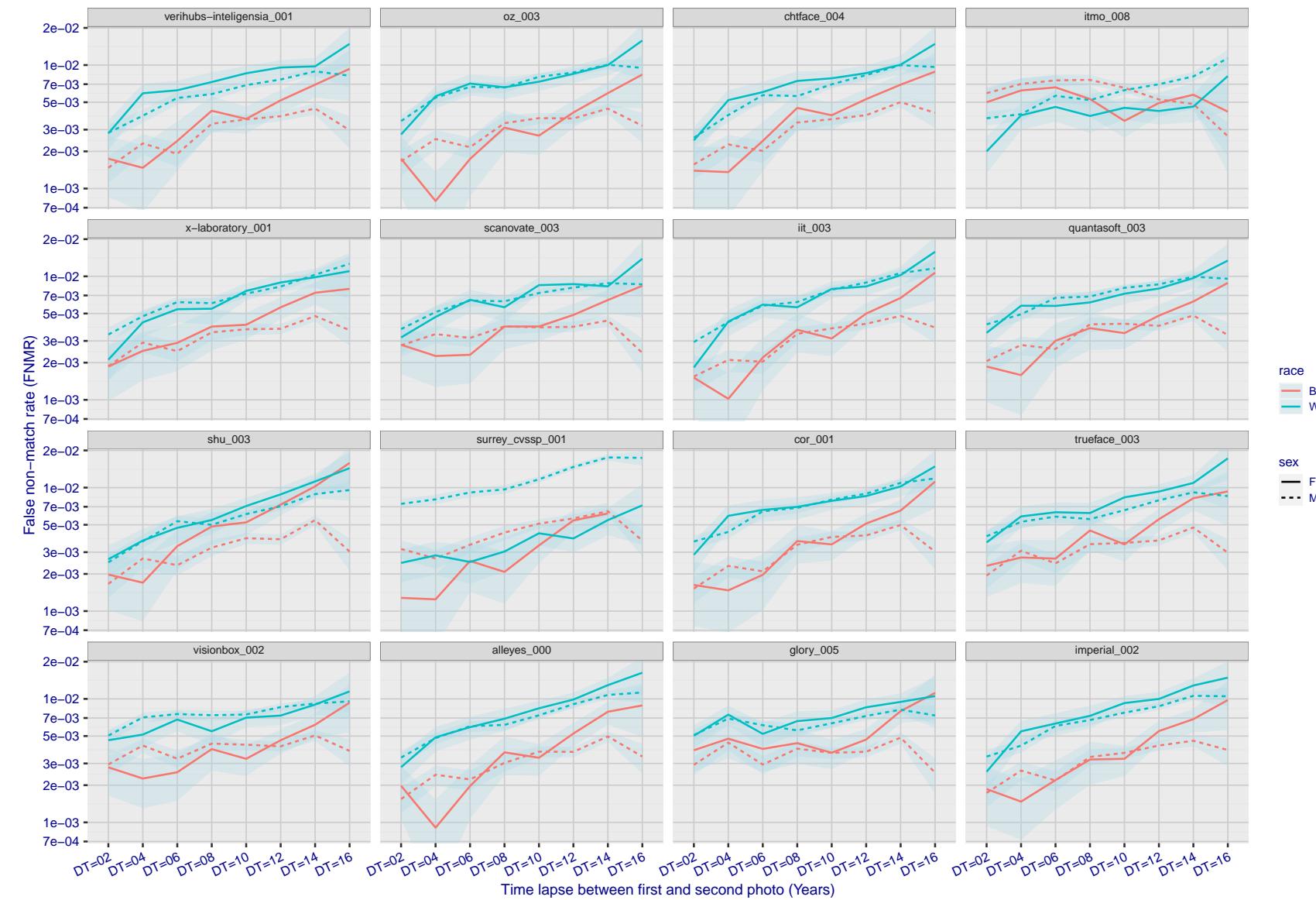


Figure 343: For the mugshot images, FNMR as a function of elapsed time between initial enrollment and second verification images. The panels appear most accurate first, and vertical scale changes on each page. The four traces correspond to images annotated with codes for black female, black male, white female, white male. The threshold is fixed for each algorithm to give $FMR = 0.00001$ over all (10^8) impostor comparisons. For short time-lapses, the most accurate algorithms give very few errors ($FNMR < 0.001$) so that the uncertainty estimates are high.

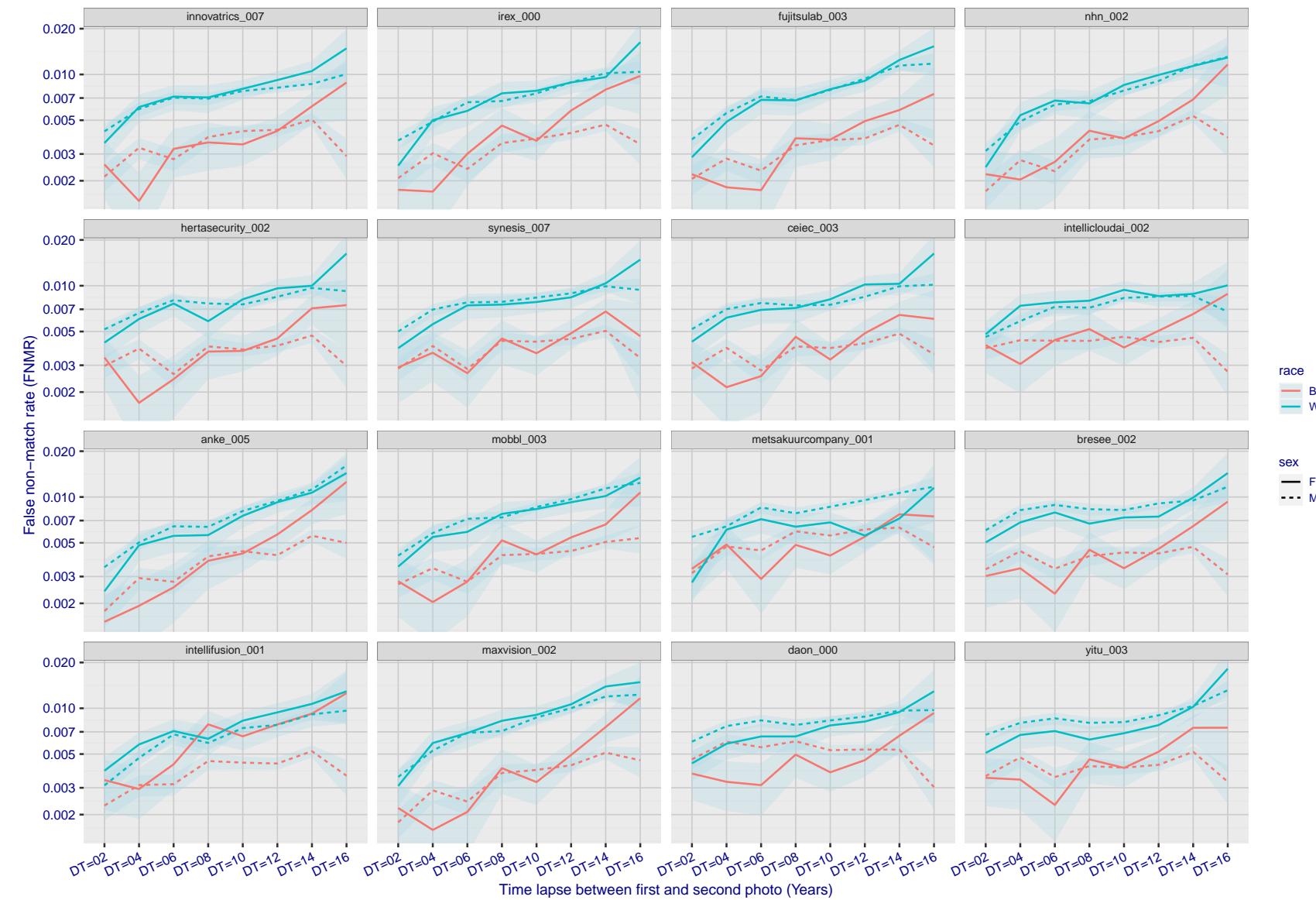


Figure 344: For the mugshot images, FNMR as a function of elapsed time between initial enrollment and second verification images. The panels appear most accurate first, and vertical scale changes on each page. The four traces correspond to images annotated with codes for black female, black male, white female, white male. The threshold is fixed for each algorithm to give FMR = 0.00001 over all (10^8) impostor comparisons. For short time-lapses, the most accurate algorithms give very few errors (FNMR < 0.001) so that the uncertainty estimates are high.

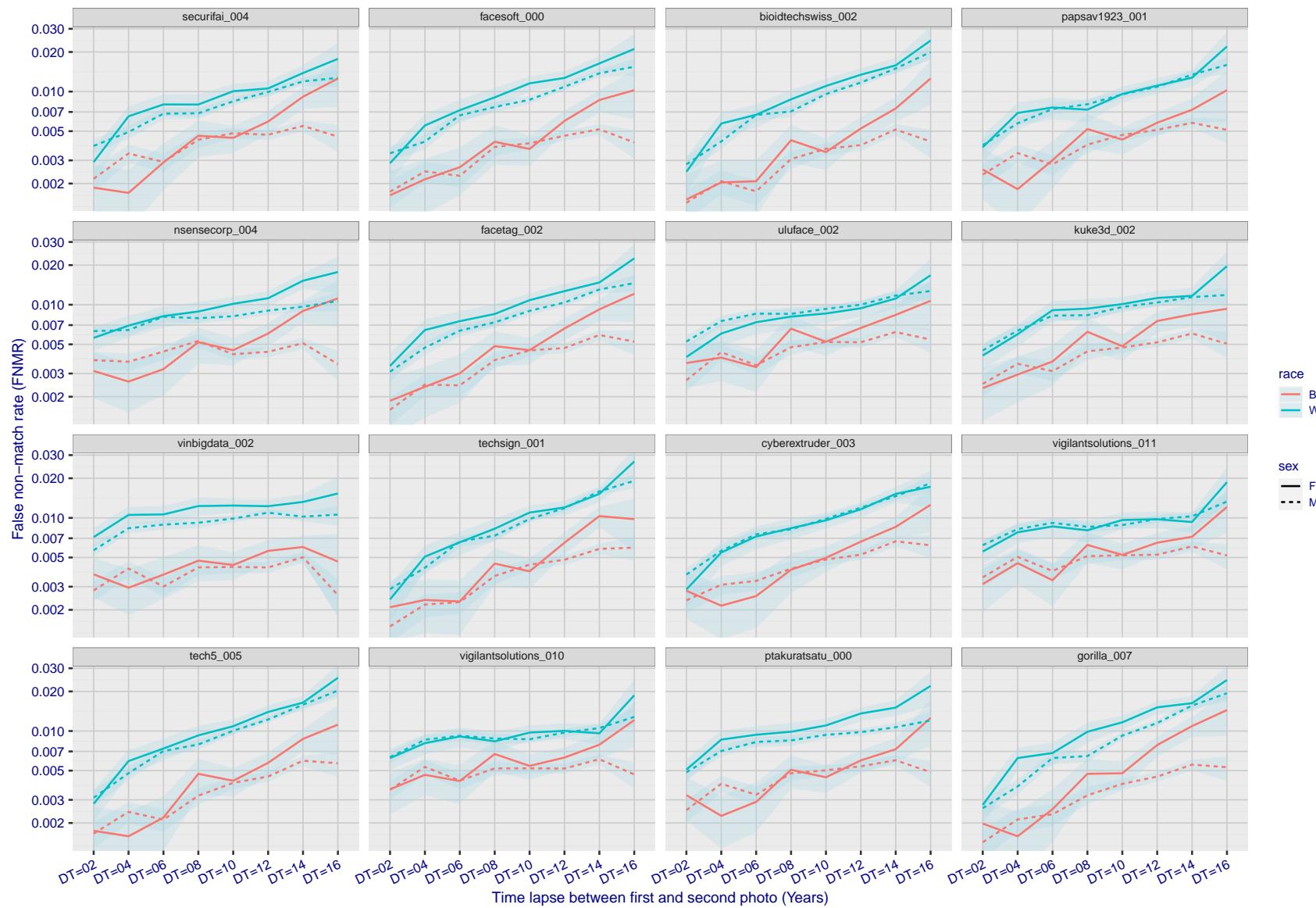


Figure 345: For the mugshot images, FNMR as a function of elapsed time between initial enrollment and second verification images. The panels appear most accurate first, and vertical scale changes on each page. The four traces correspond to images annotated with codes for black female, black male, white female, white male. The threshold is fixed for each algorithm to give $FMR = 0.00001$ over all (10^8) impostor comparisons. For short time-lapses, the most accurate algorithms give very few errors ($FNMR < 0.001$) so that the uncertainty estimates are high.

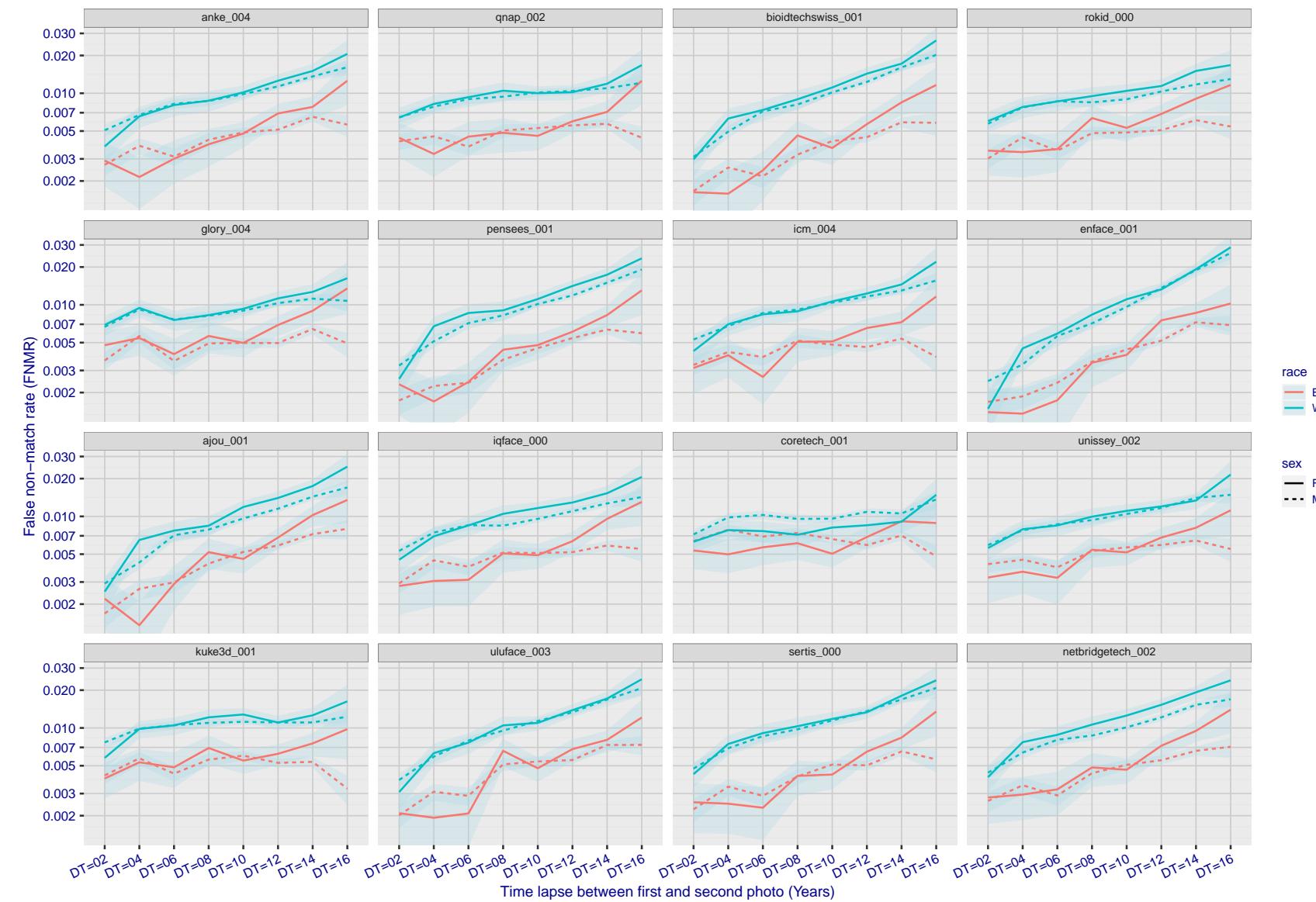


Figure 346: For the mugshot images, FNMR as a function of elapsed time between initial enrollment and second verification images. The panels appear most accurate first, and vertical scale changes on each page. The four traces correspond to images annotated with codes for black female, black male, white female, white male. The threshold is fixed for each algorithm to give FMR = 0.00001 over all (10^8) impostor comparisons. For short time-lapses, the most accurate algorithms give very few errors (FNMR < 0.001) so that the uncertainty estimates are high.

2023/02/02 13:38:52

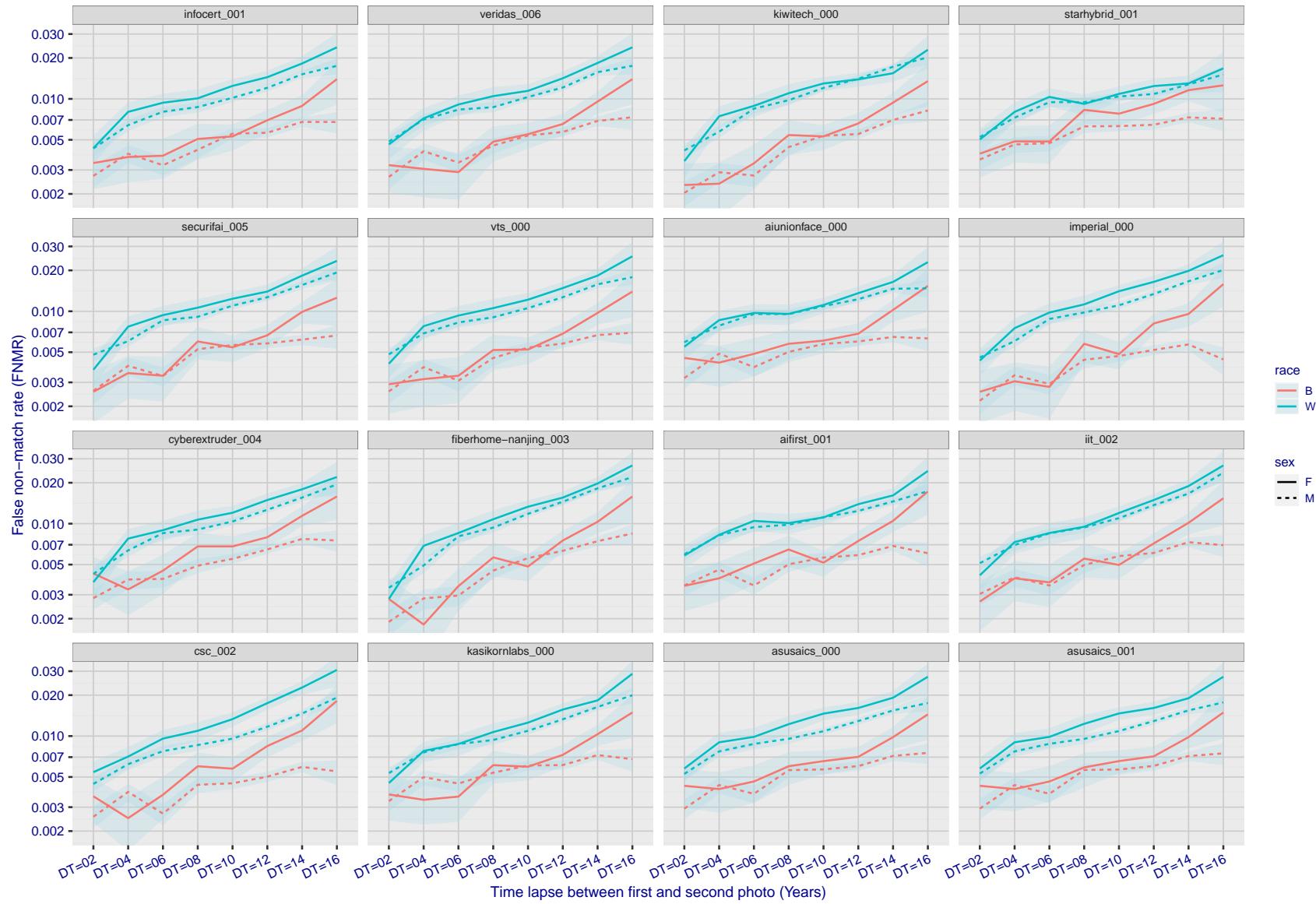


Figure 347: For the mugshot images, FNMR as a function of elapsed time between initial enrollment and second verification images. The panels appear most accurate first, and vertical scale changes on each page. The four traces correspond to images annotated with codes for black female, black male, white female, white male. The threshold is fixed for each algorithm to give FMR = 0.00001 over all (10^8) impostor comparisons. For short time-lapses, the most accurate algorithms give very few errors (FNMR < 0.001) so that the uncertainty estimates are high.

FNMR(T)
FMR(T)
"False match rate"

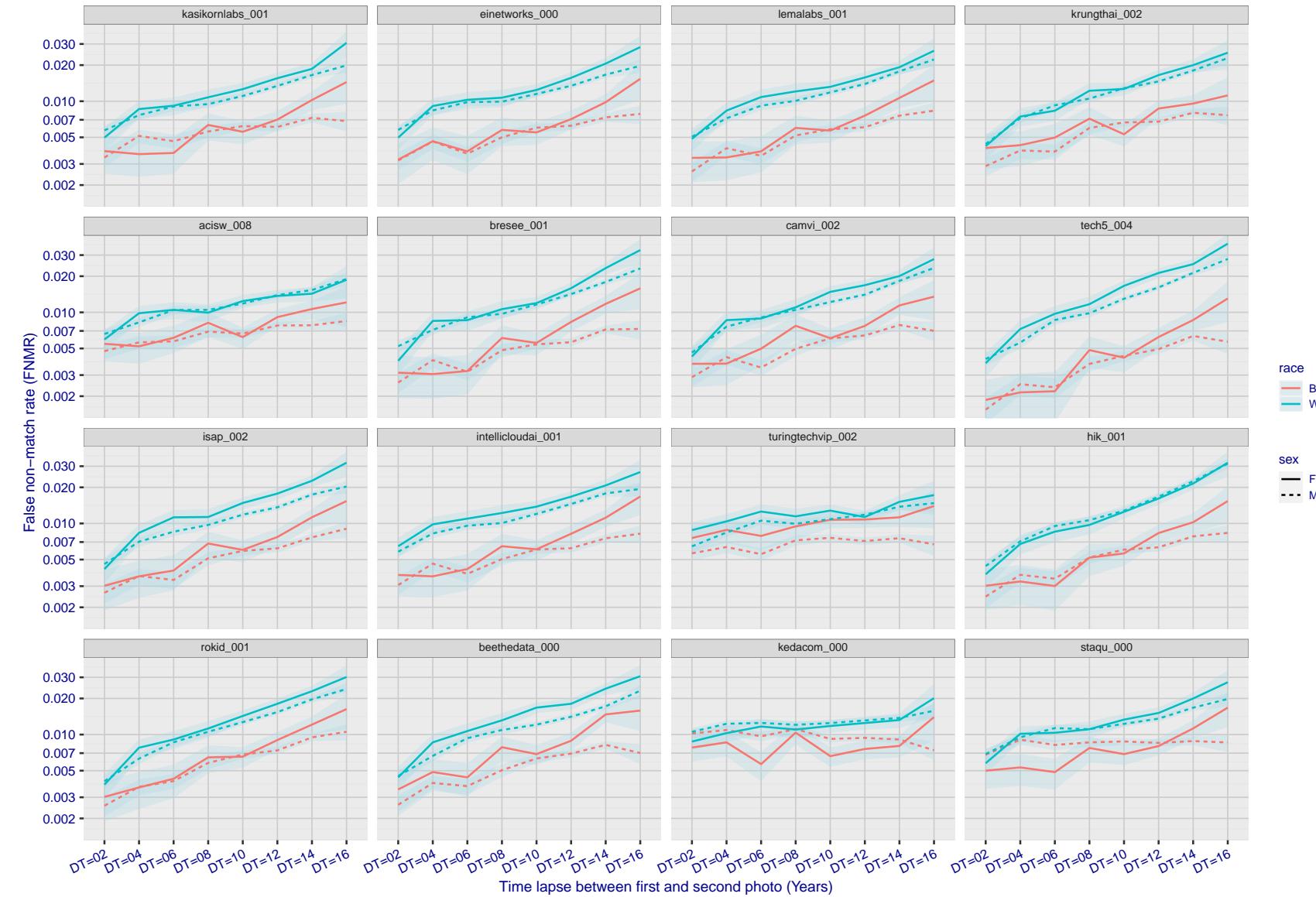


Figure 348: For the mugshot images, FNMR as a function of elapsed time between initial enrollment and second verification images. The panels appear most accurate first, and vertical scale changes on each page. The four traces correspond to images annotated with codes for black female, black male, white female, white male. The threshold is fixed for each algorithm to give $FMR = 0.00001$ over all (10^8) impostor comparisons. For short time-lapses, the most accurate algorithms give very few errors ($FNMR < 0.001$) so that the uncertainty estimates are high.

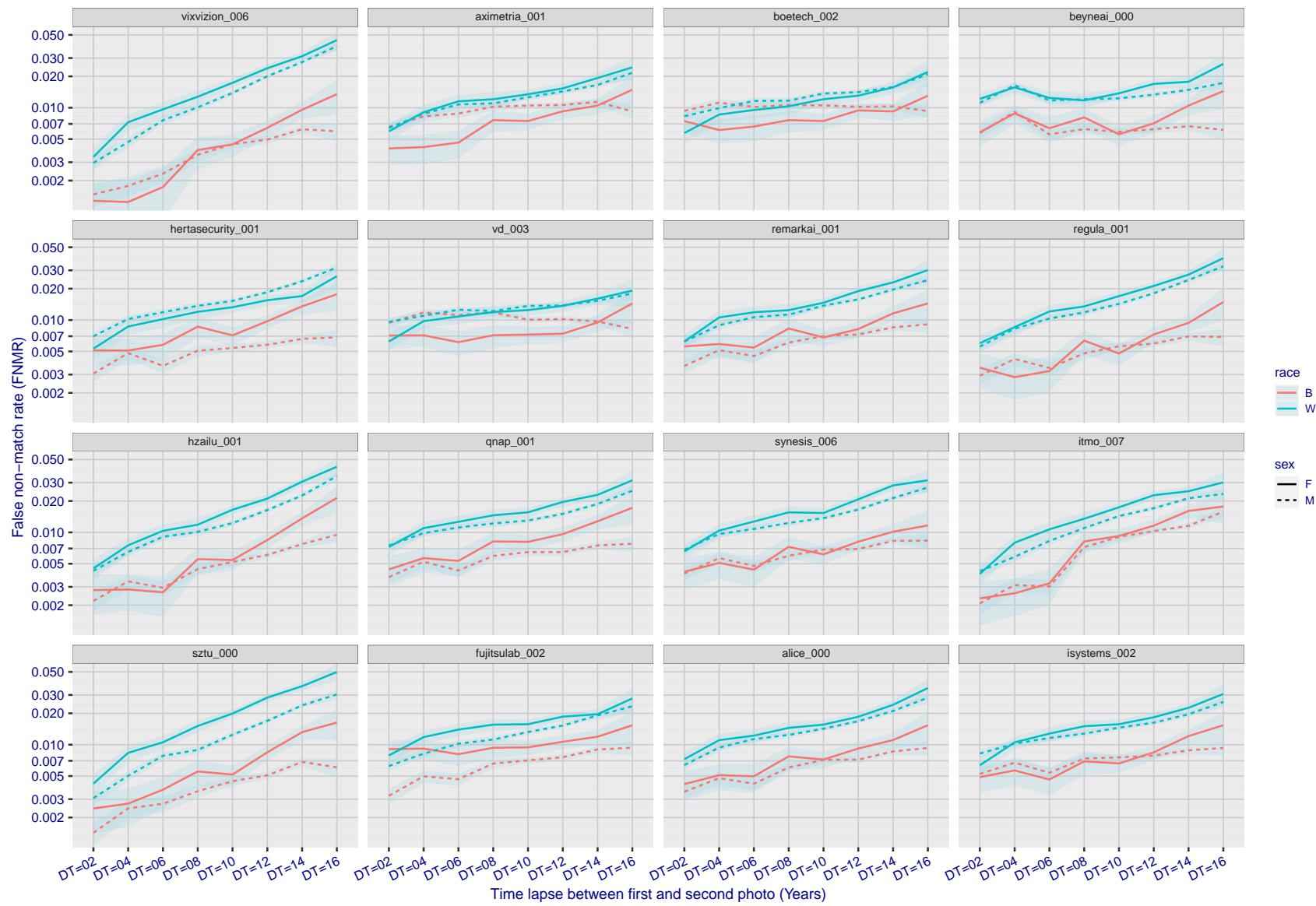


Figure 349: For the mugshot images, FNMR as a function of elapsed time between initial enrollment and second verification images. The panels appear most accurate first, and vertical scale changes on each page. The four traces correspond to images annotated with codes for black female, black male, white female, white male. The threshold is fixed for each algorithm to give FMR = 0.00001 over all (10^8) impostor comparisons. For short time-lapses, the most accurate algorithms give very few errors (FNMR < 0.001) so that the uncertainty estimates are high.

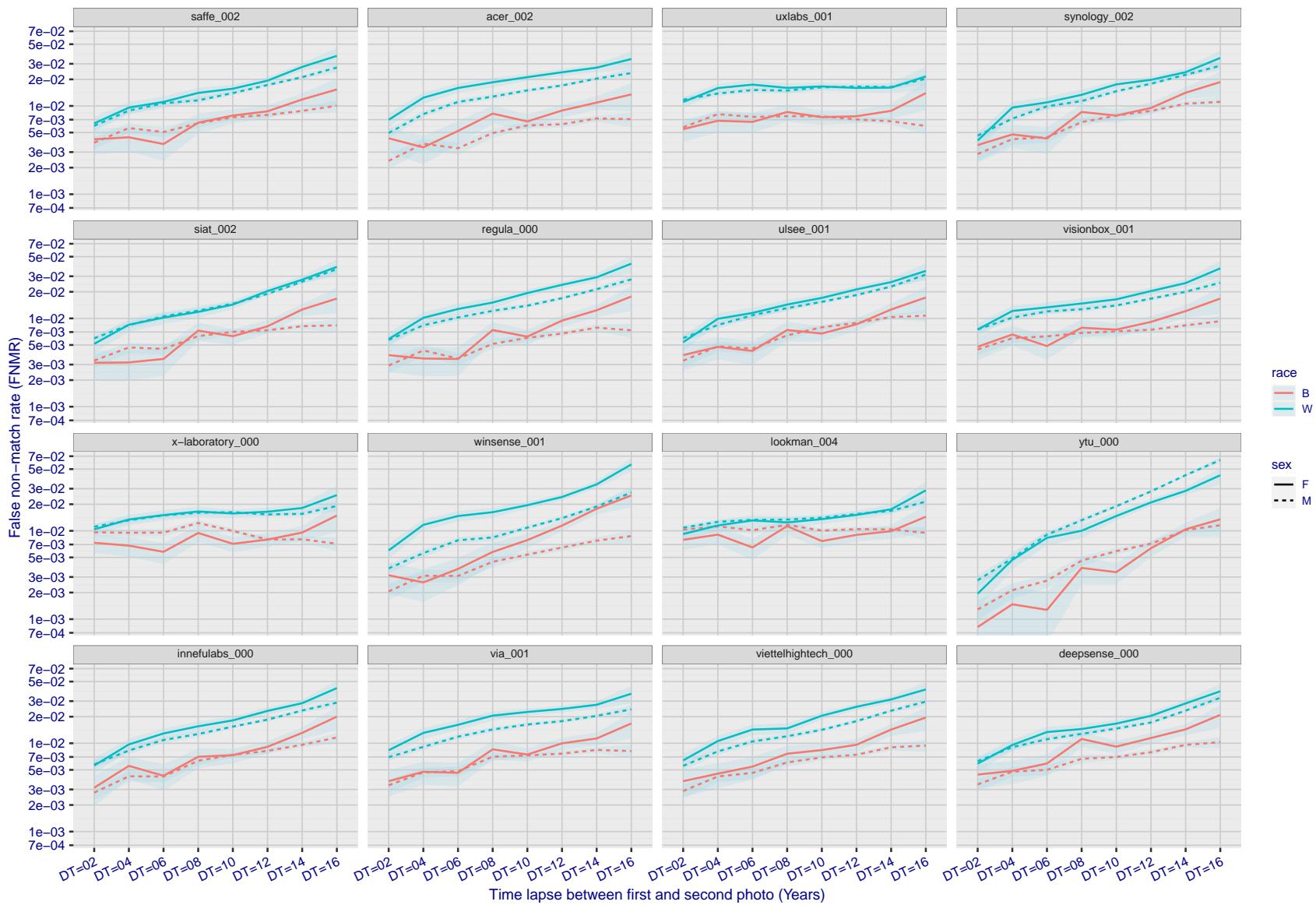


Figure 350: For the mugshot images, FNMR as a function of elapsed time between initial enrollment and second verification images. The panels appear most accurate first, and vertical scale changes on each page. The four traces correspond to images annotated with codes for black female, black male, white female, white male. The threshold is fixed for each algorithm to give $FMR = 0.00001$ over all (10^8) impostor comparisons. For short time-lapses, the most accurate algorithms give very few errors ($FNMR < 0.001$) so that the uncertainty estimates are high.

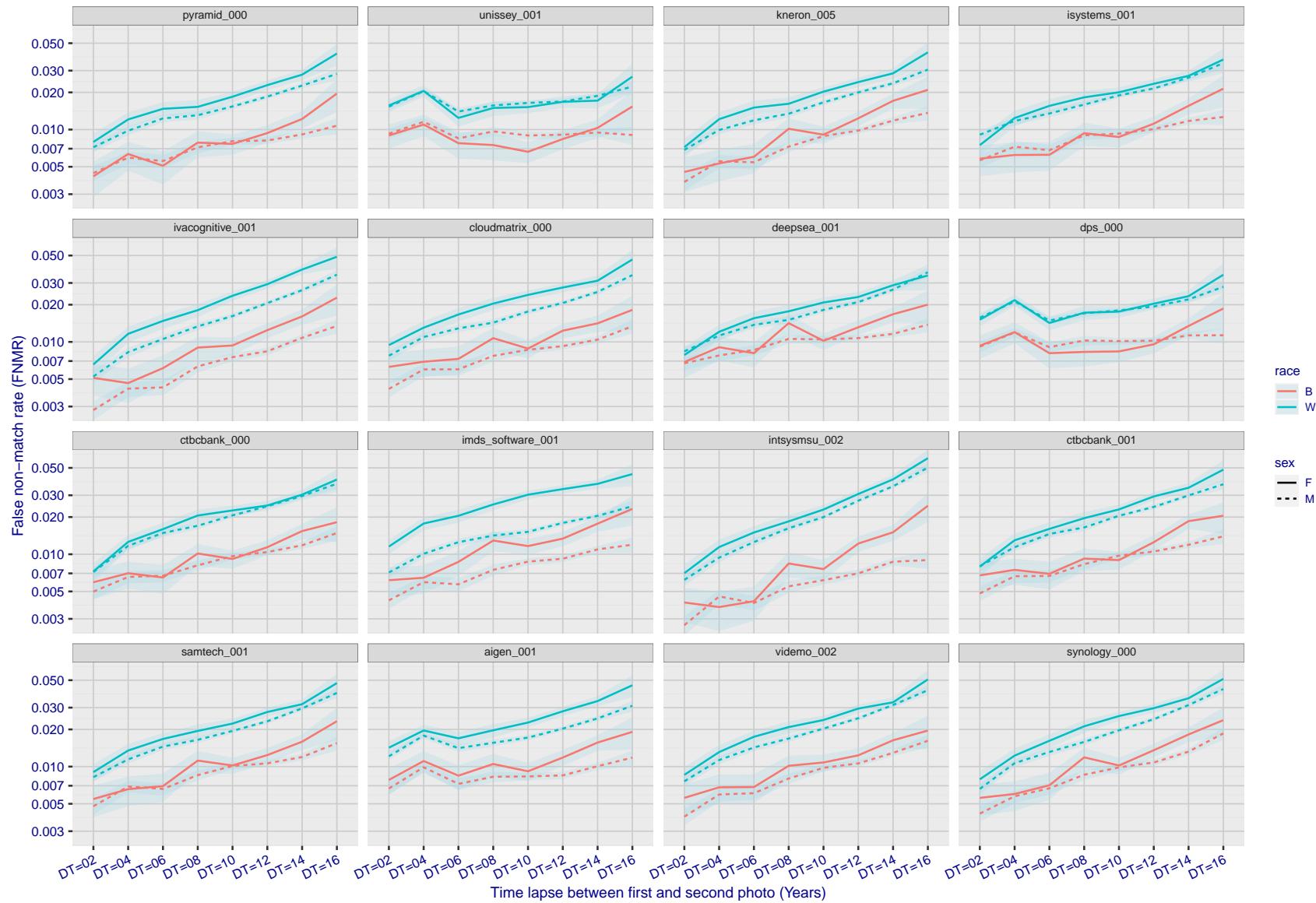


Figure 351: For the mugshot images, FNMR as a function of elapsed time between initial enrollment and second verification images. The panels appear most accurate first, and vertical scale changes on each page. The four traces correspond to images annotated with codes for black female, black male, white female, white male. The threshold is fixed for each algorithm to give FMR = 0.00001 over all (10^8) impostor comparisons. For short time-lapses, the most accurate algorithms give very few errors (FNMR < 0.001) so that the uncertainty estimates are high.

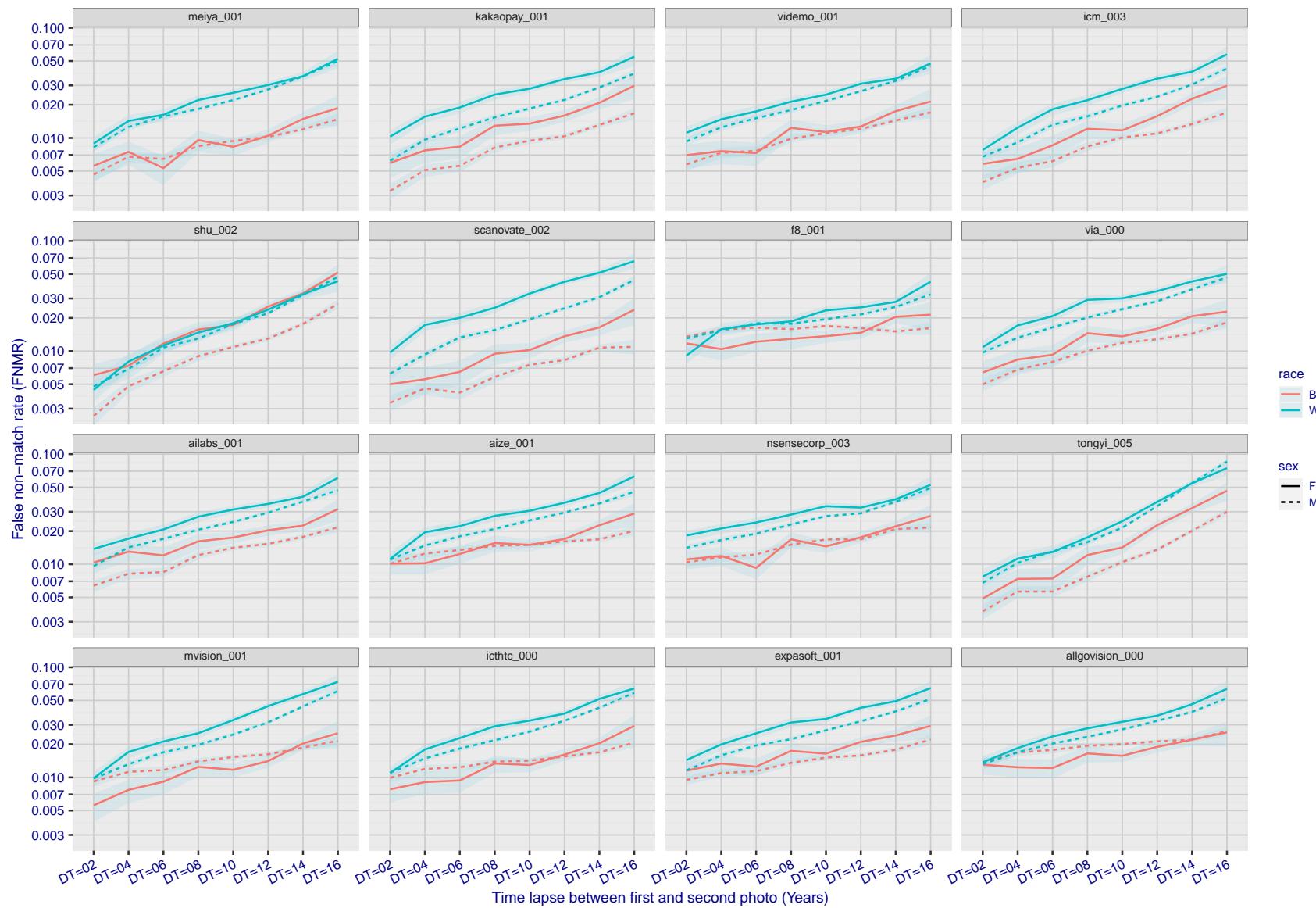


Figure 352: For the mugshot images, FNMR as a function of elapsed time between initial enrollment and second verification images. The panels appear most accurate first, and vertical scale changes on each page. The four traces correspond to images annotated with codes for black female, black male, white female, white male. The threshold is fixed for each algorithm to give FMR = 0.00001 over all (10^8) impostor comparisons. For short time-lapses, the most accurate algorithms give very few errors (FNMR < 0.001) so that the uncertainty estimates are high.

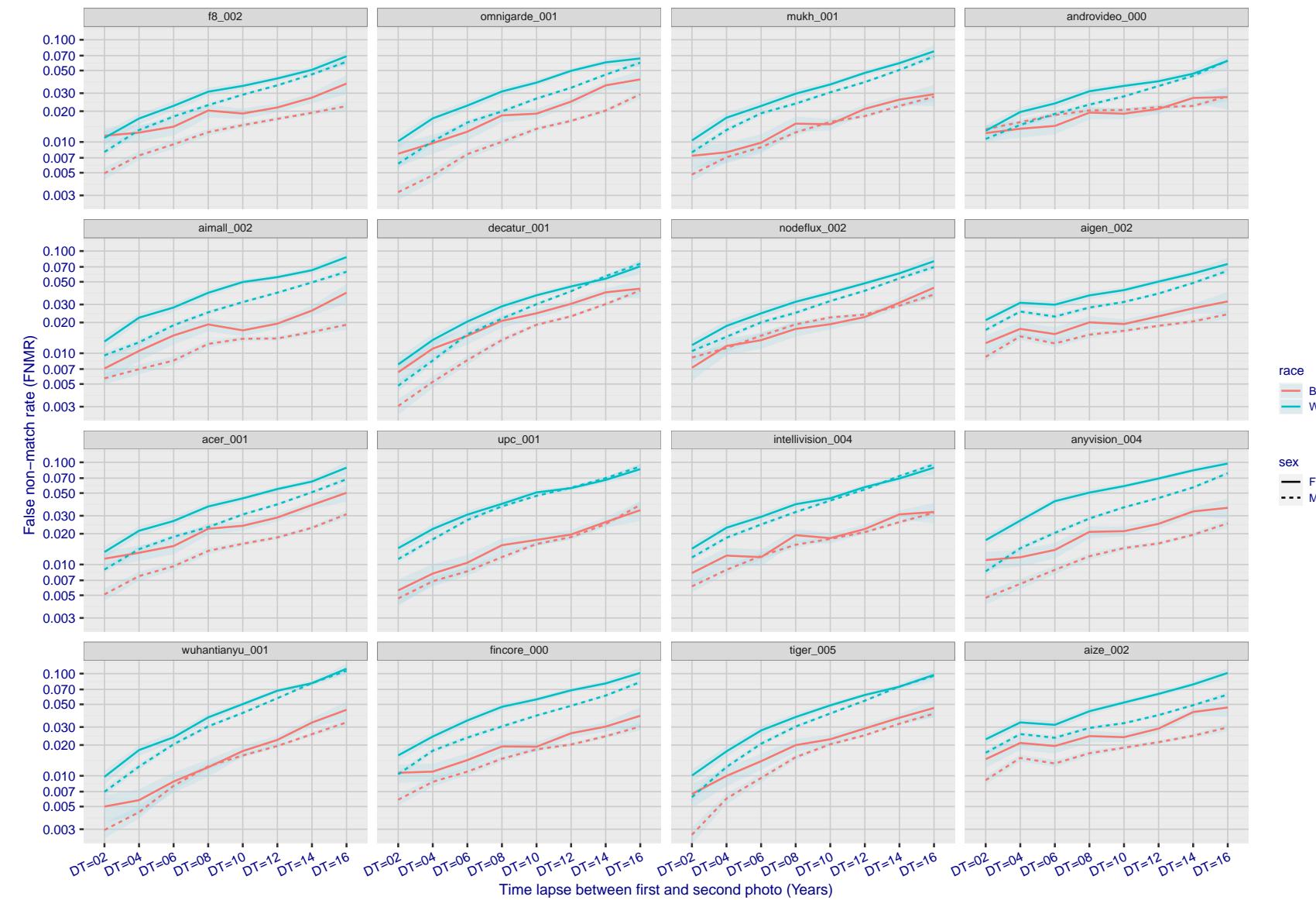


Figure 353: For the mugshot images, FNMR as a function of elapsed time between initial enrollment and second verification images. The panels appear most accurate first, and vertical scale changes on each page. The four traces correspond to images annotated with codes for black female, black male, white female, white male. The threshold is fixed for each algorithm to give FMR = 0.00001 over all (10^8) impostor comparisons. For short time-lapses, the most accurate algorithms give very few errors (FNMR < 0.001) so that the uncertainty estimates are high.

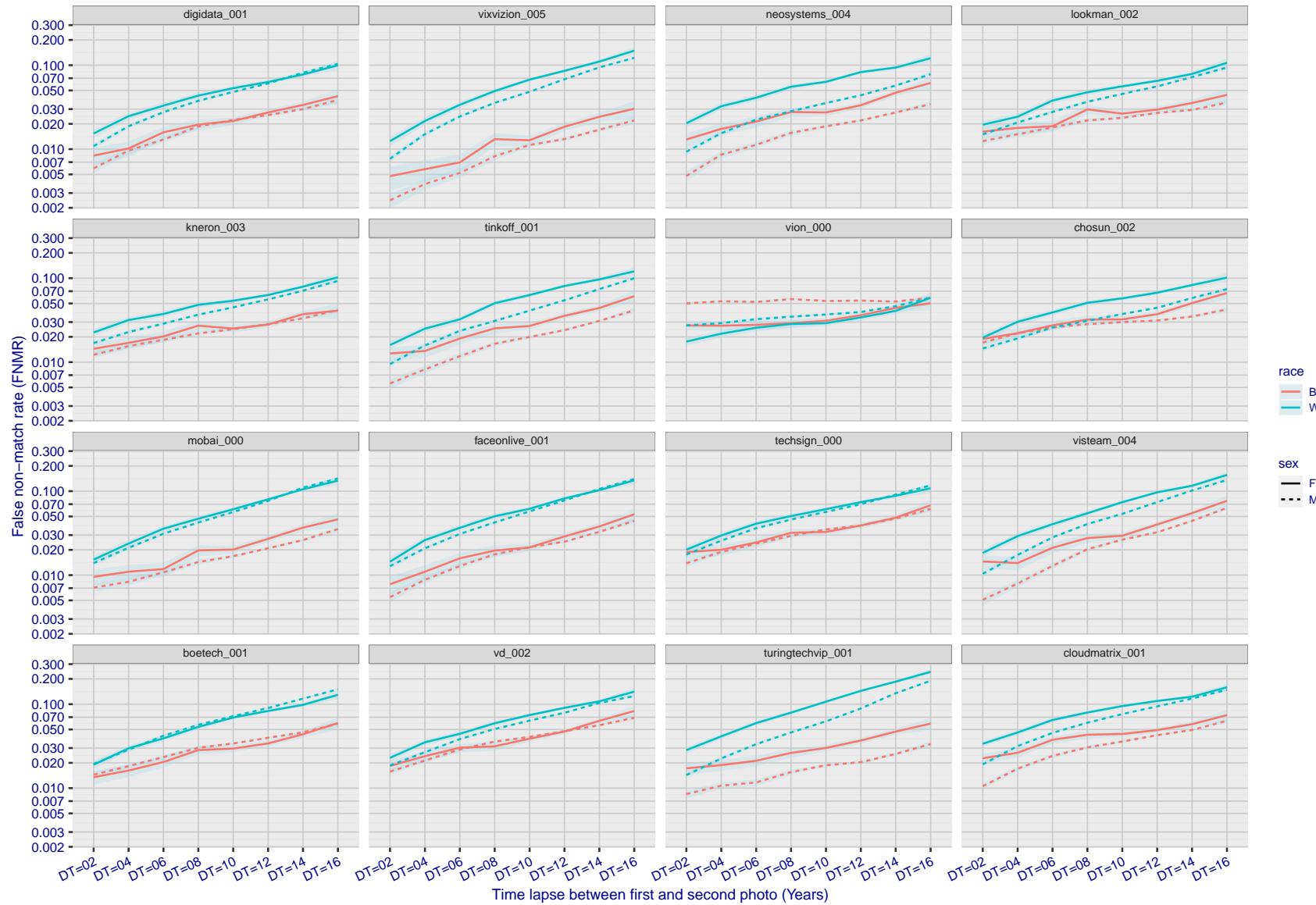


Figure 354: For the mugshot images, FNMR as a function of elapsed time between initial enrollment and second verification images. The panels appear most accurate first, and vertical scale changes on each page. The four traces correspond to images annotated with codes for black female, black male, white female, white male. The threshold is fixed for each algorithm to give FMR = 0.00001 over all (10^8) impostor comparisons. For short time-lapses, the most accurate algorithms give very few errors (FNMR < 0.001) so that the uncertainty estimates are high.

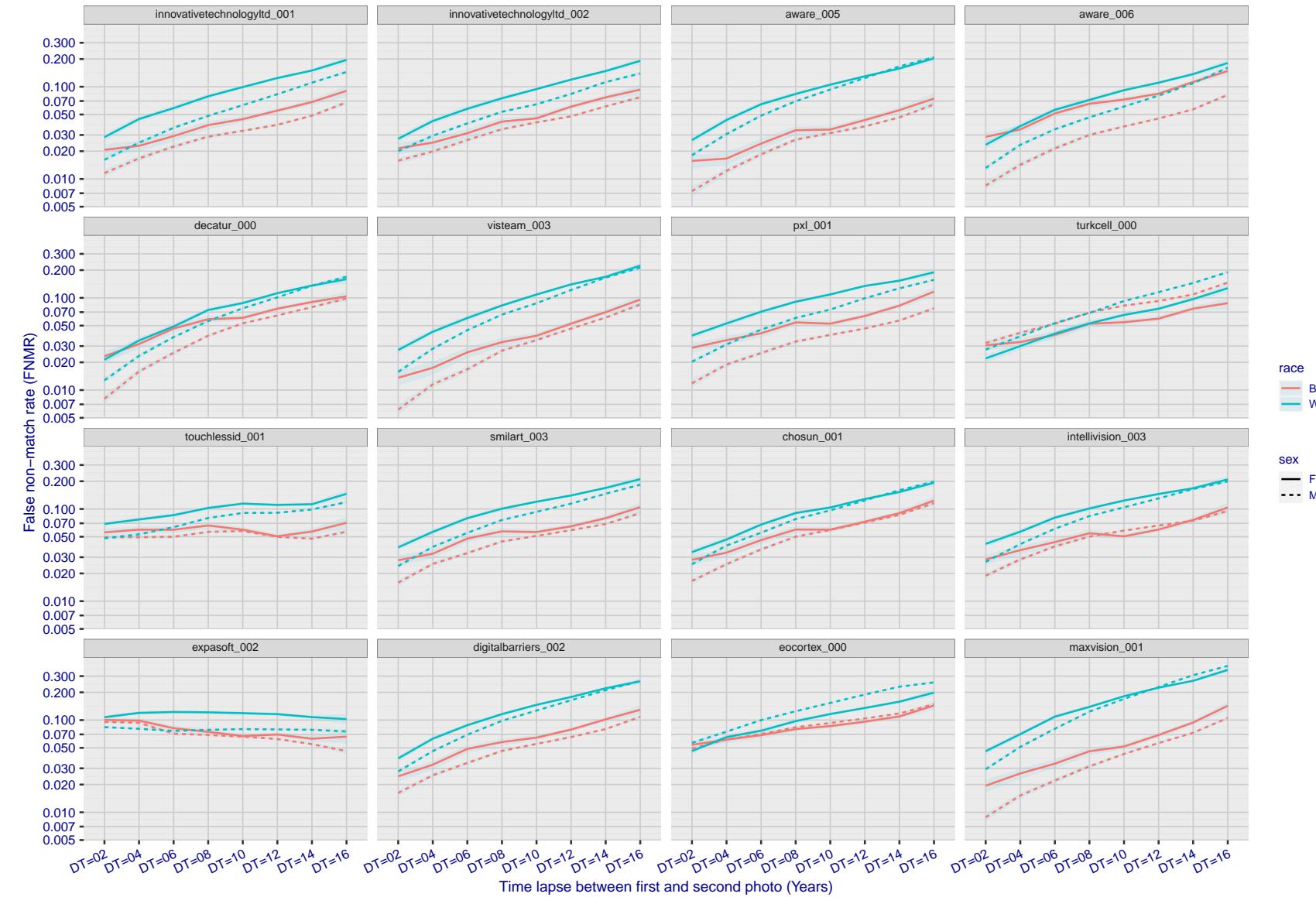


Figure 355: For the mugshot images, FNMR as a function of elapsed time between initial enrollment and second verification images. The panels appear most accurate first, and vertical scale changes on each page. The four traces correspond to images annotated with codes for black female, black male, white female, white male. The threshold is fixed for each algorithm to give FMR = 0.00001 over all (10^8) impostor comparisons. For short time-lapses, the most accurate algorithms give very few errors (FNMR < 0.001) so that the uncertainty estimates are high.

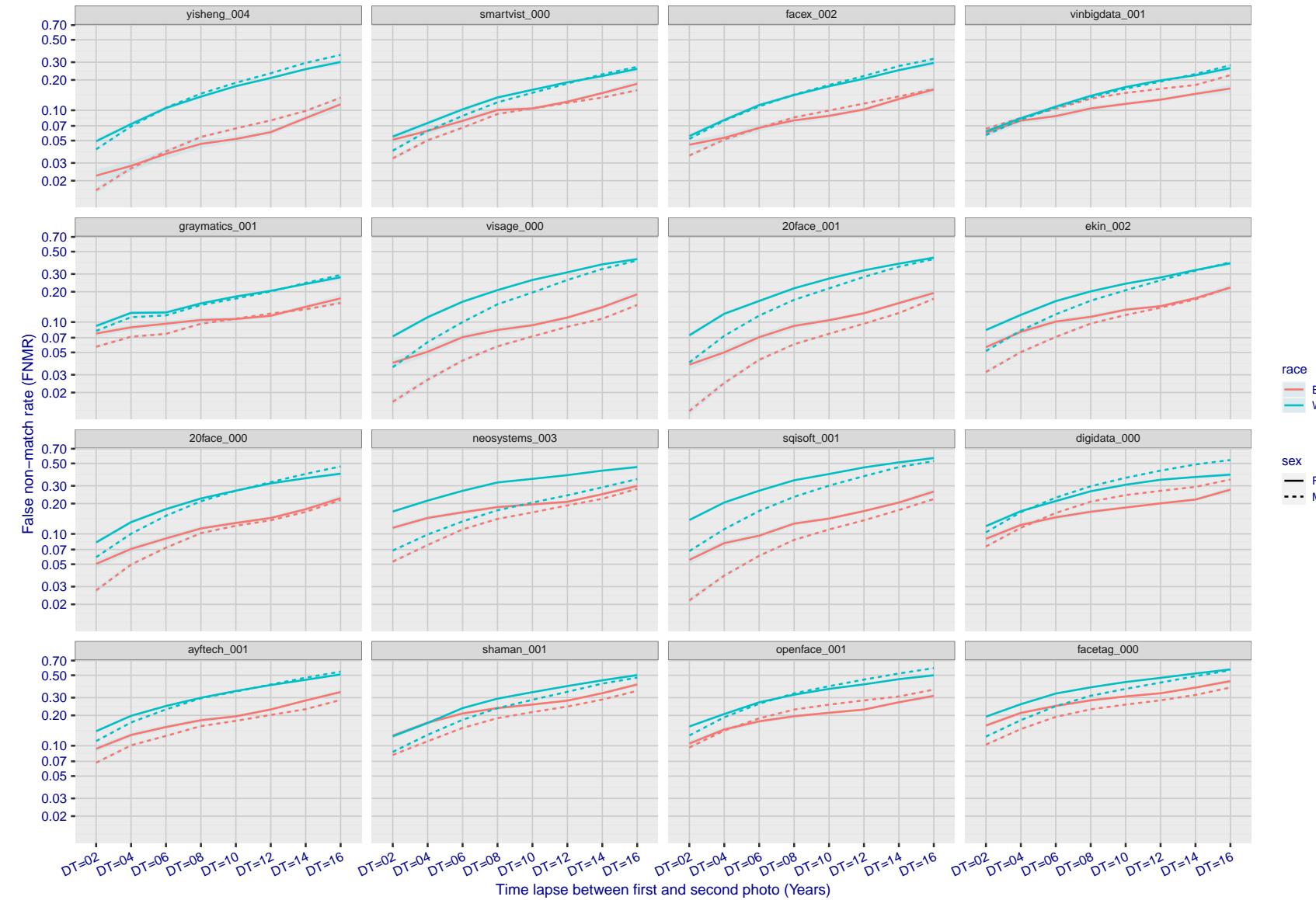


Figure 356: For the mugshot images, FNMR as a function of elapsed time between initial enrollment and second verification images. The panels appear most accurate first, and vertical scale changes on each page. The four traces correspond to images annotated with codes for black female, black male, white female, white male. The threshold is fixed for each algorithm to give FMR = 0.00001 over all (10^8) impostor comparisons. For short time-lapses, the most accurate algorithms give very few errors (FNMR < 0.001) so that the uncertainty estimates are high.

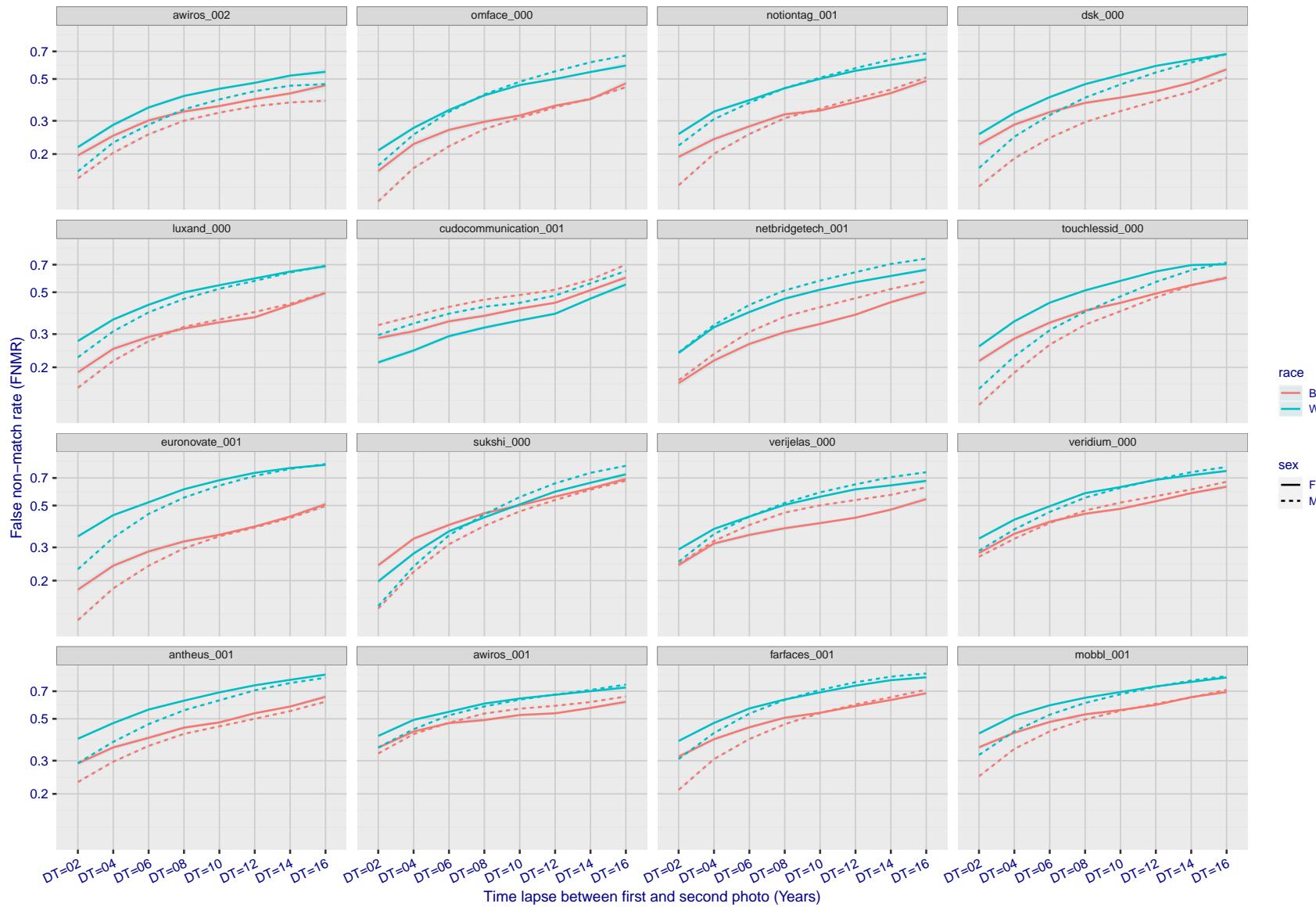


Figure 357: For the mugshot images, FNMR as a function of elapsed time between initial enrollment and second verification images. The panels appear most accurate first, and vertical scale changes on each page. The four traces correspond to images annotated with codes for black female, black male, white female, white male. The threshold is fixed for each algorithm to give FMR = 0.00001 over all (10^8) impostor comparisons. For short time-lapses, the most accurate algorithms give very few errors (FNMR < 0.001) so that the uncertainty estimates are high.

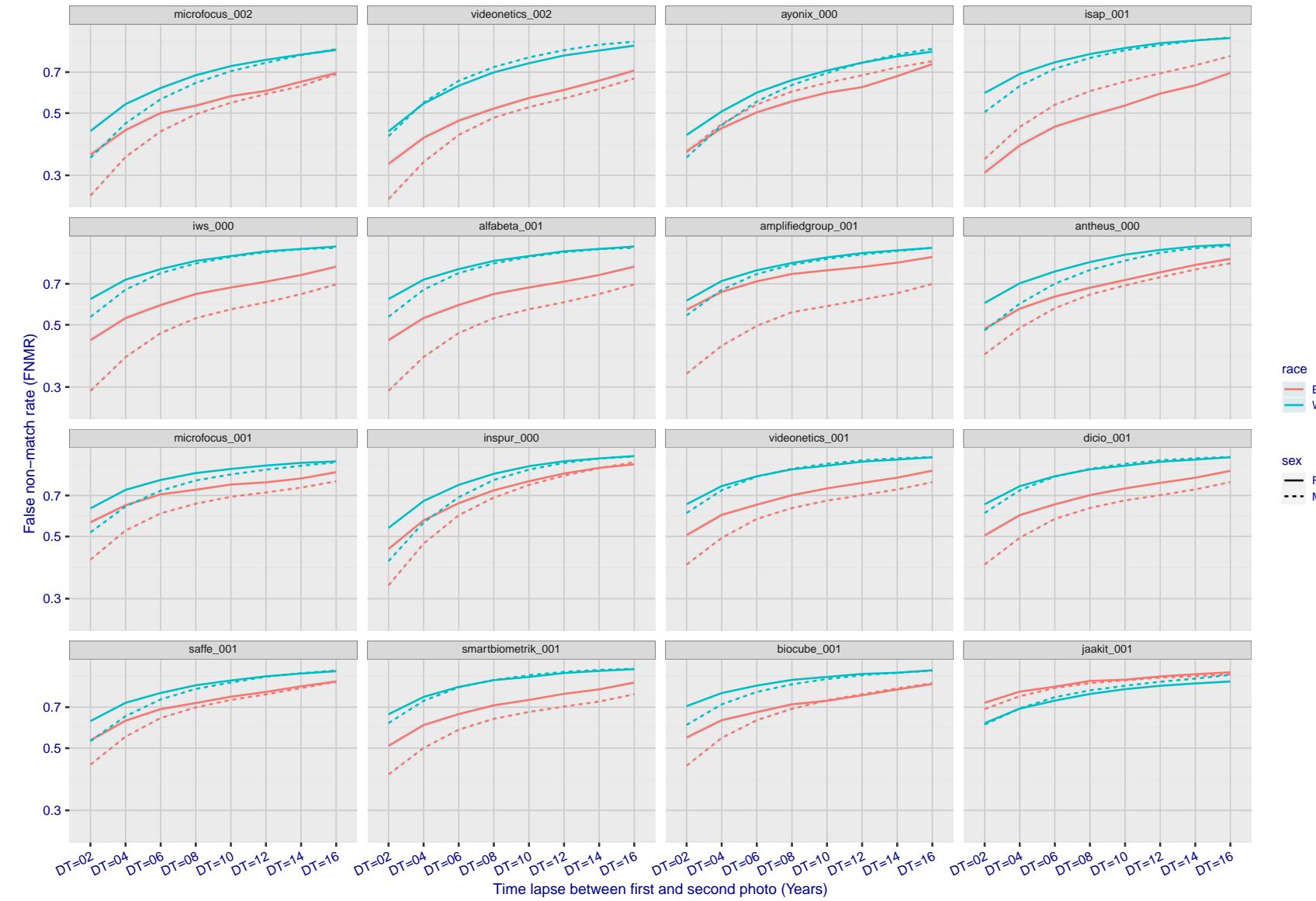


Figure 358: For the mugshot images, FNMR as a function of elapsed time between initial enrollment and second verification images. The panels appear most accurate first, and vertical scale changes on each page. The four traces correspond to images annotated with codes for black female, black male, white female, white male. The threshold is fixed for each algorithm to give $FMR = 0.00001$ over all (10^8) impostor comparisons. For short time-lapses, the most accurate algorithms give very few errors ($FNMR < 0.001$) so that the uncertainty estimates are high.

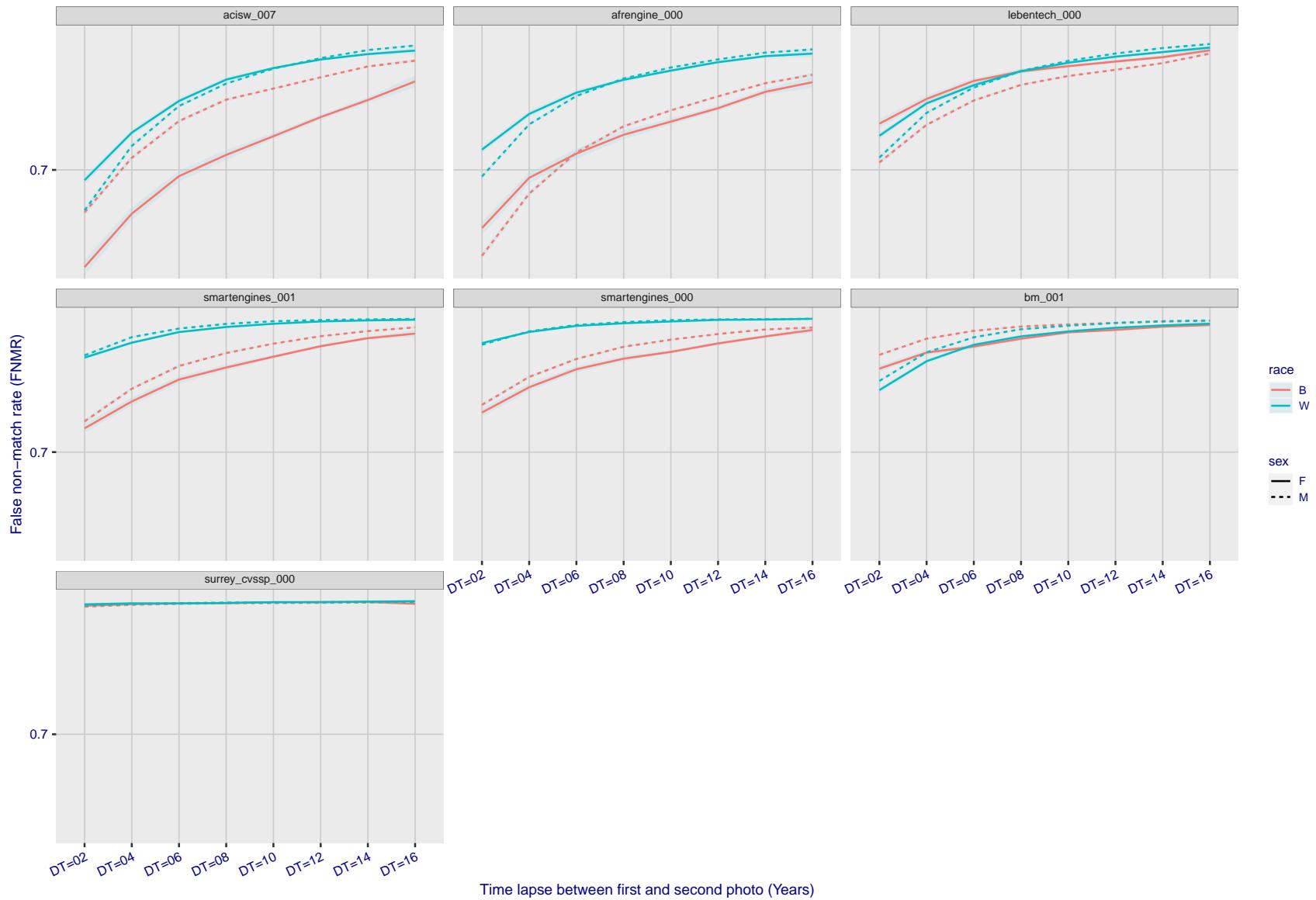


Figure 359: For the mugshot images, FNMR as a function of elapsed time between initial enrollment and second verification images. The panels appear most accurate first, and vertical scale changes on each page. The four traces correspond to images annotated with codes for black female, black male, white female, white male. The threshold is fixed for each algorithm to give FMR = 0.00001 over all (10^8) impostor comparisons. For short time-lapses, the most accurate algorithms give very few errors (FNMR < 0.001) so that the uncertainty estimates are high.

3.5.3 Effect of age on genuine subjects

Background: Faces change appearance throughout life. Face recognition algorithms have previously been reported to give better accuracy on older individuals (See NIST IR 8009).

Goal: To quantify false non-match rates (FNMR) as a function of age, without an ageing component.

Methods: Using the visa images, which span fewer than five years, thresholds are determined that give FMR = 0.001 and 0.0001 over the entire impostor set. Then FNMR is measured over 1000 bootstrap replications of the genuine scores.

Results: For the visa images, Figure 398 shows how false non-match rates for genuine users, as a function of age group.

The notable aspects are:

- ▷ Younger subjects give considerably higher FNMR. This is likely due to rapid growth and change in facial appearance.
- ▷ FNMR trends down throughout life. The last bin, AGE > 72, contains fewer than 140 mated pairs, and may be affected by small sample size.

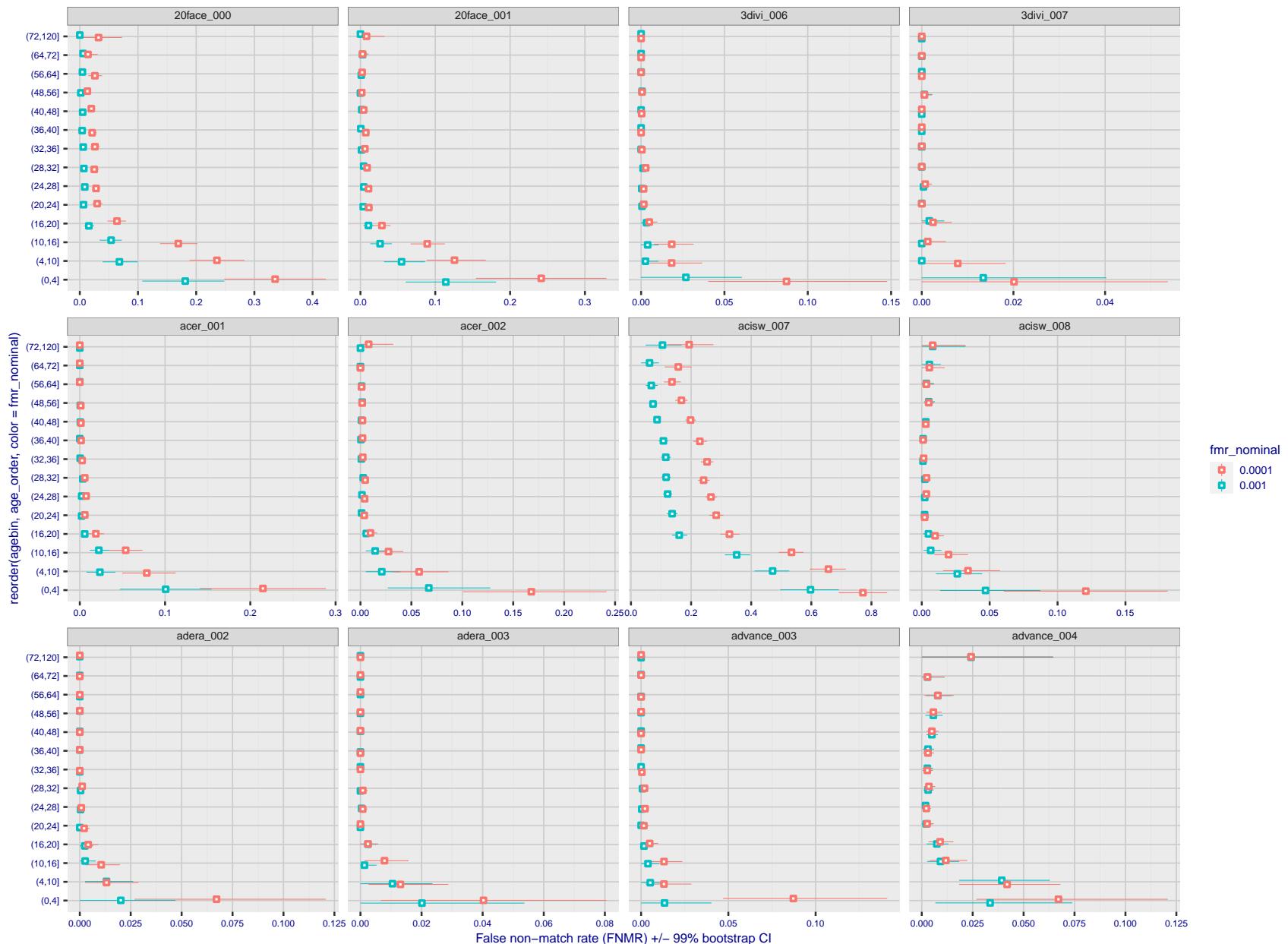


Figure 360: For the visa images, the dots show FNMR by age group for two operating thresholds corresponding to $FMR = \{0.001, 0.0001\}$ computed over all on the order of 10^{10} impostor scores. The FMR in each bin will vary also - see subsequent impostor heatmaps in sec. 3.6.2. Given a pair of face images taken at different times, we assign the comparison to the bin that is the arithmetic average of the subject's ages. This plot shows only the effect of age, not ageing. The number of comparisons in each bin is generally in the thousands, however the first and last bins are computed over 149 and 124 respectively. The error rates in some (adult) cases are zero, and in others the DET is flat so the error rates at the two thresholds are identical. The lines span 1% and 99% of bootstrap replicated FNMR estimates.

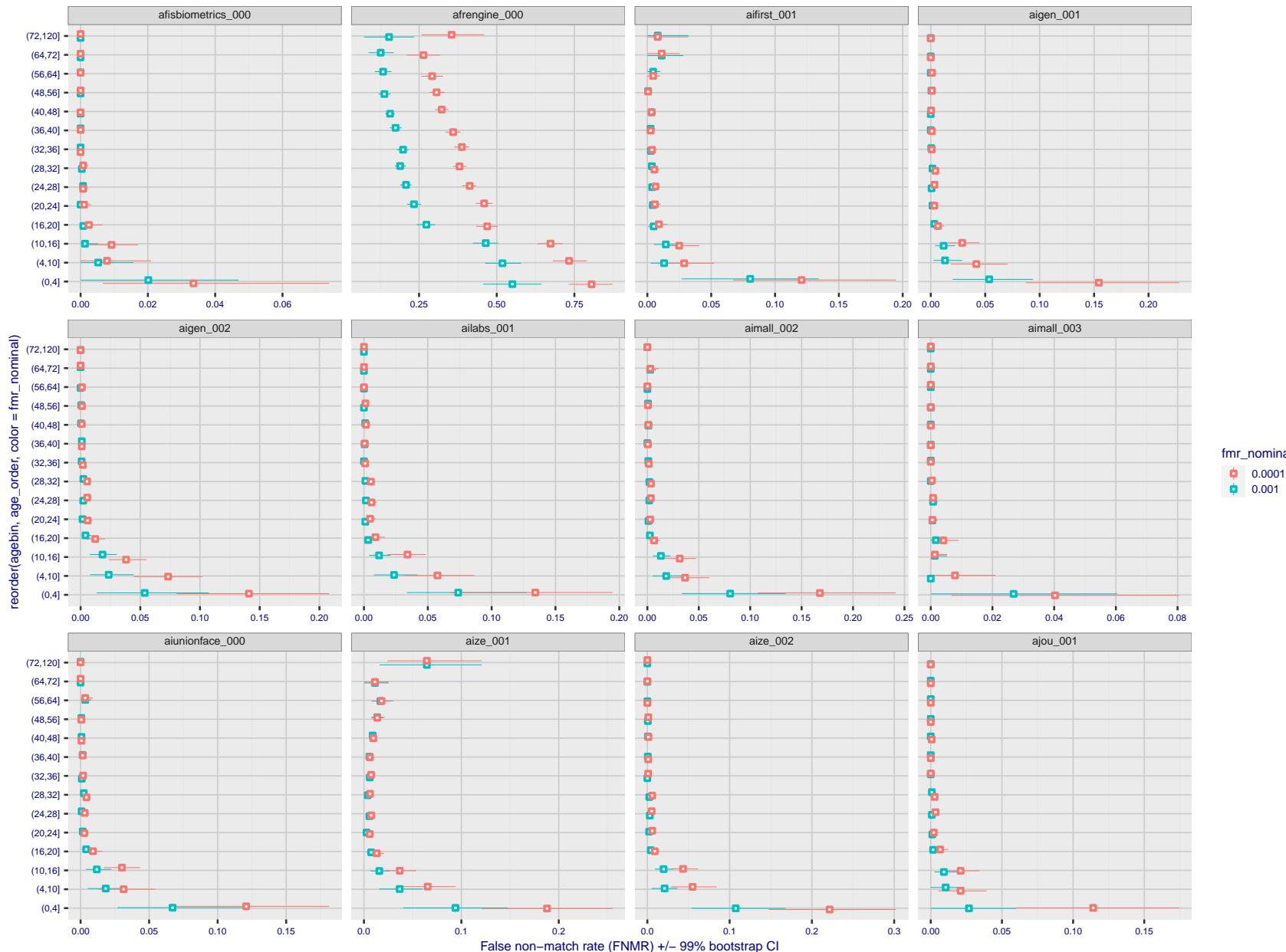


Figure 361: For the visa images, the dots show FNMR by age group for two operating thresholds corresponding to $FMR = \{0.001, 0.0001\}$ computed over all on the order of 10^{10} impostor scores. The FMR in each bin will vary also - see subsequent impostor heatmaps in sec. 3.6.2. Given a pair of face images taken at different times, we assign the comparison to the bin that is the arithmetic average of the subject's ages. This plot shows only the effect of age, not ageing. The number of comparisons in each bin is generally in the thousands, however the first and last bins are computed over 149 and 124 respectively. The error rates in some (adult) cases are zero, and in others the DET is flat so the error rates at the two thresholds are identical. The lines span 1% and 99% of bootstrap replicated FNMR estimates.



Figure 362: For the visa images, the dots show FNMR by age group for two operating thresholds corresponding to $FMR = \{0.001, 0.0001\}$ computed over all on the order of 10^{10} impostor scores. The FMR in each bin will vary also - see subsequent impostor heatmaps in sec. 3.6.2. Given a pair of face images taken at different times, we assign the comparison to the bin that is the arithmetic average of the subject's ages. This plot shows only the effect of age, not ageing. The number of comparisons in each bin is generally in the thousands, however the first and last bins are computed over 149 and 124 respectively. The error rates in some (adult) cases are zero, and in others the DET is flat so the error rates at the two thresholds are identical. The lines span 1% and 99% of bootstrap replicated FNMR estimates.

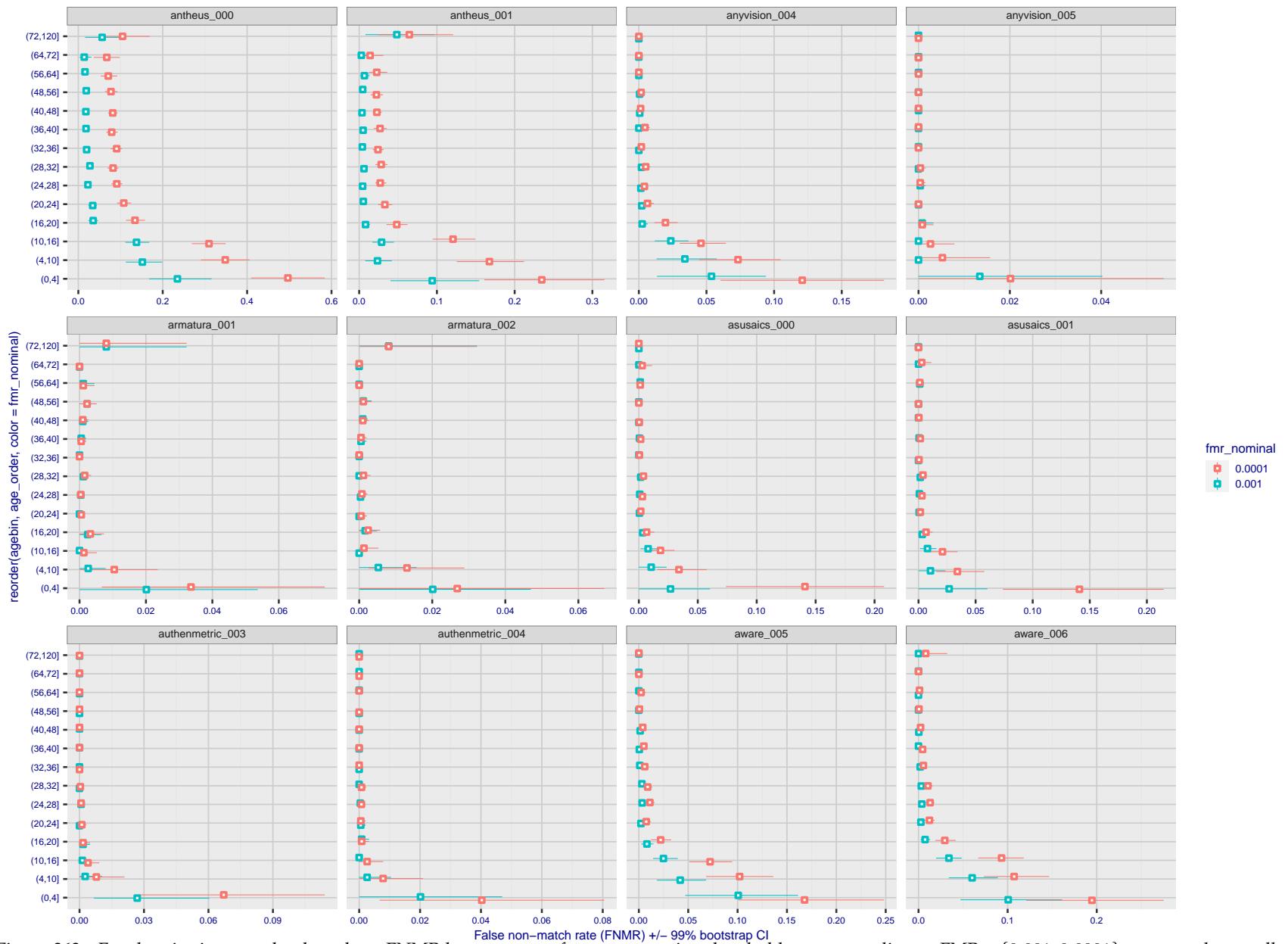


Figure 363: For the visa images, the dots show FNMR by age group for two operating thresholds corresponding to $FMR = \{0.001, 0.0001\}$ computed over all on the order of 10^{10} impostor scores. The FMR in each bin will vary also - see subsequent impostor heatmaps in sec. 3.6.2. Given a pair of face images taken at different times, we assign the comparison to the bin that is the arithmetic average of the subject's ages. This plot shows only the effect of age, not ageing. The number of comparisons in each bin is generally in the thousands, however the first and last bins are computed over 149 and 124 respectively. The error rates in some (adult) cases are zero, and in others the DET is flat so the error rates at the two thresholds are identical. The lines span 1% and 99% of bootstrap replicated FNMR estimates.

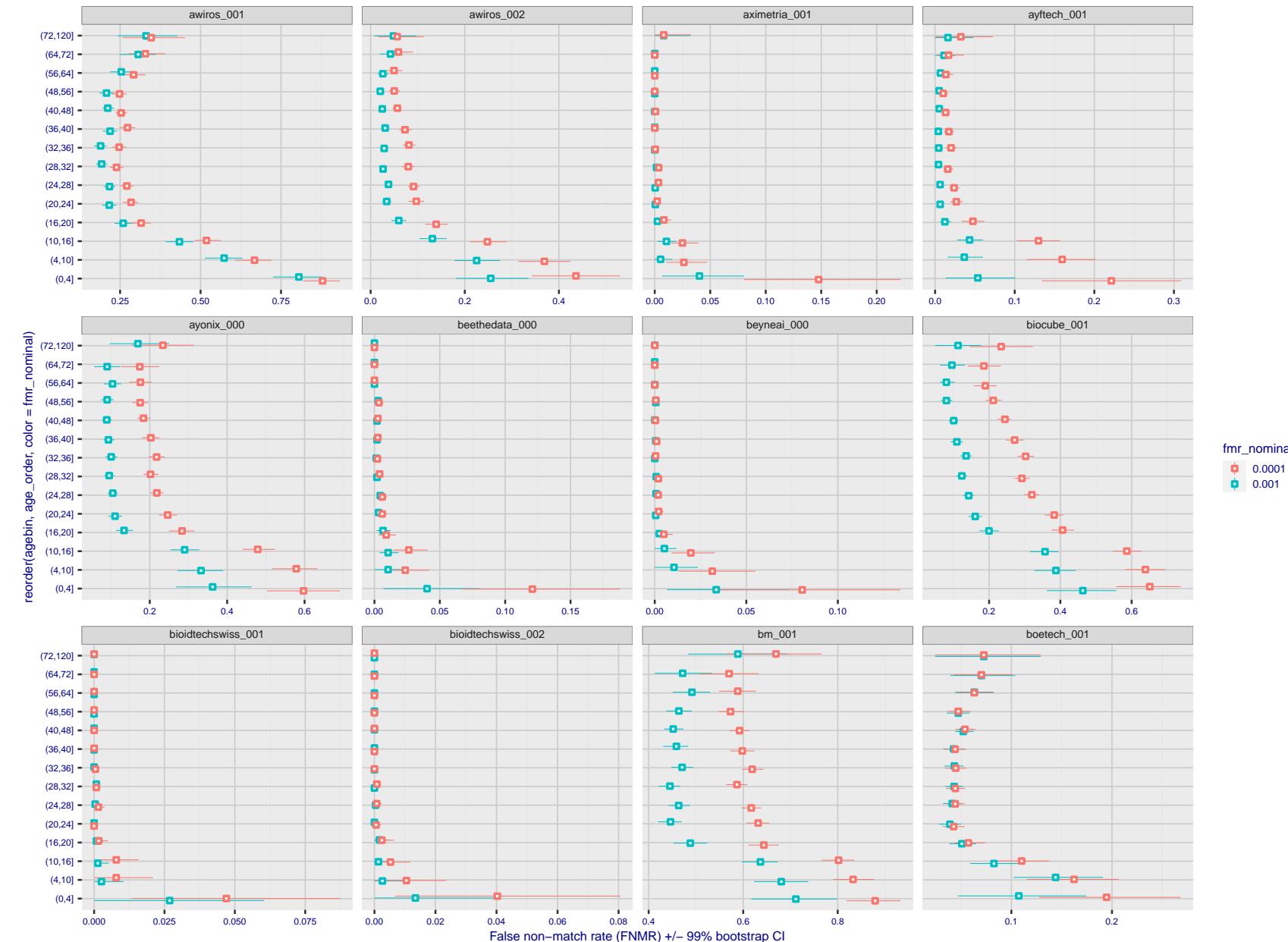


Figure 364: For the visa images, the dots show FNMR by age group for two operating thresholds corresponding to $FMR = \{0.001, 0.0001\}$ computed over all on the order of 10^{10} impostor scores. The FMR in each bin will vary also - see subsequent impostor heatmaps in sec. 3.6.2. Given a pair of face images taken at different times, we assign the comparison to the bin that is the arithmetic average of the subject's ages. This plot shows only the effect of age, not ageing. The number of comparisons in each bin is generally in the thousands, however the first and last bins are computed over 149 and 124 respectively. The error rates in some (adult) cases are zero, and in others the DET is flat so the error rates at the two thresholds are identical. The lines span 1% and 99% of bootstrap replicated FNMR estimates.

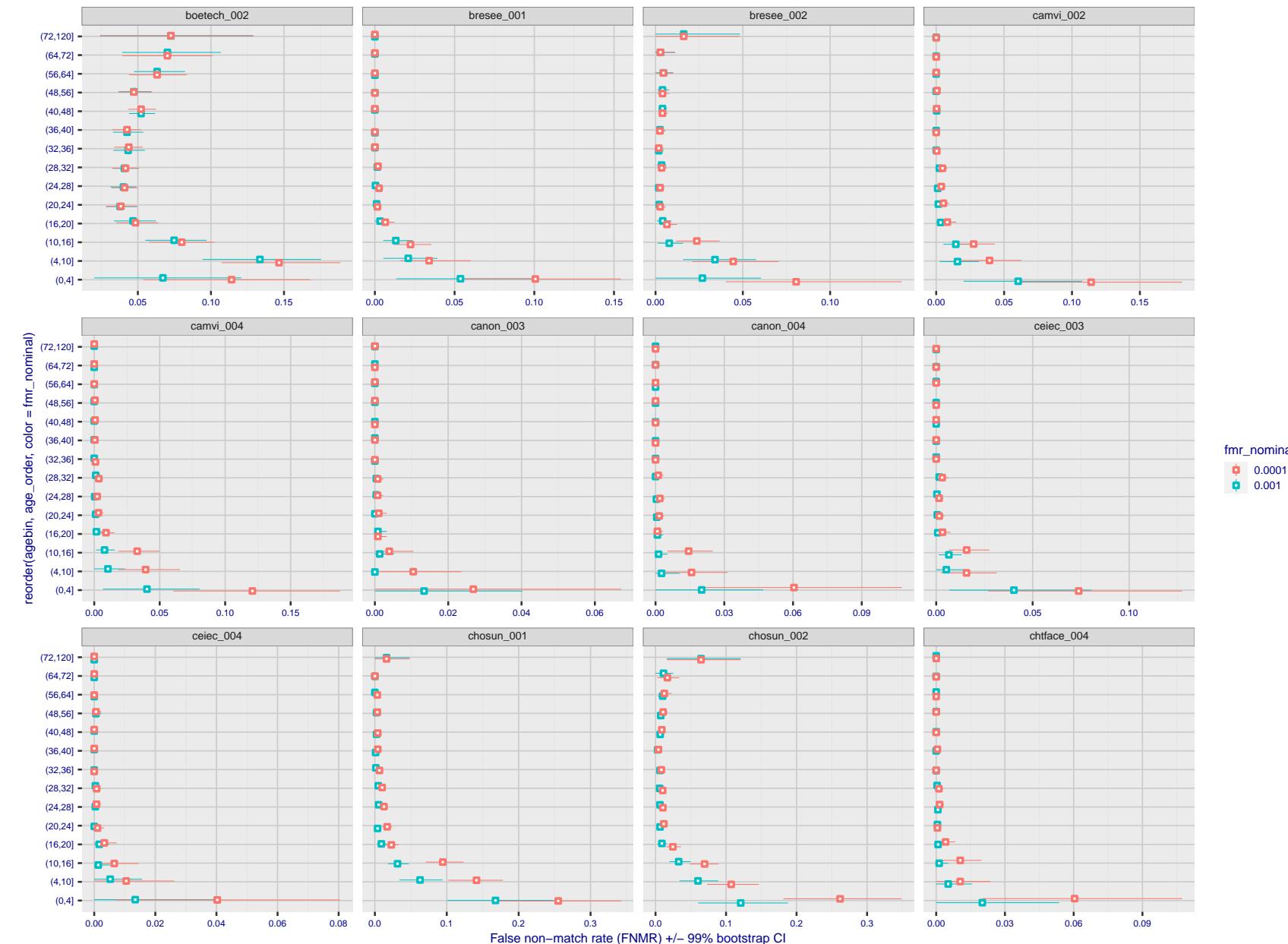


Figure 365: For the visa images, the dots show FNMR by age group for two operating thresholds corresponding to $FMR = \{0.001, 0.0001\}$ computed over all on the order of 10^{10} impostor scores. The FMR in each bin will vary also - see subsequent impostor heatmaps in sec. 3.6.2. Given a pair of face images taken at different times, we assign the comparison to the bin that is the arithmetic average of the subject's ages. This plot shows only the effect of age, not ageing. The number of comparisons in each bin is generally in the thousands, however the first and last bins are computed over 149 and 124 respectively. The error rates in some (adult) cases are zero, and in others the DET is flat so the error rates at the two thresholds are identical. The lines span 1% and 99% of bootstrap replicated FNMR estimates.



Figure 366: For the visa images, the dots show FNMR by age group for two operating thresholds corresponding to $FMR = \{0.001, 0.0001\}$ computed over all on the order of 10^{10} impostor scores. The FMR in each bin will vary also - see subsequent impostor heatmaps in sec. 3.6.2. Given a pair of face images taken at different times, we assign the comparison to the bin that is the arithmetic average of the subject's ages. This plot shows only the effect of age, not ageing. The number of comparisons in each bin is generally in the thousands, however the first and last bins are computed over 149 and 124 respectively. The error rates in some (adult) cases are zero, and in others the DET is flat so the error rates at the two thresholds are identical. The lines span 1% and 99% of bootstrap replicated FNMR estimates.

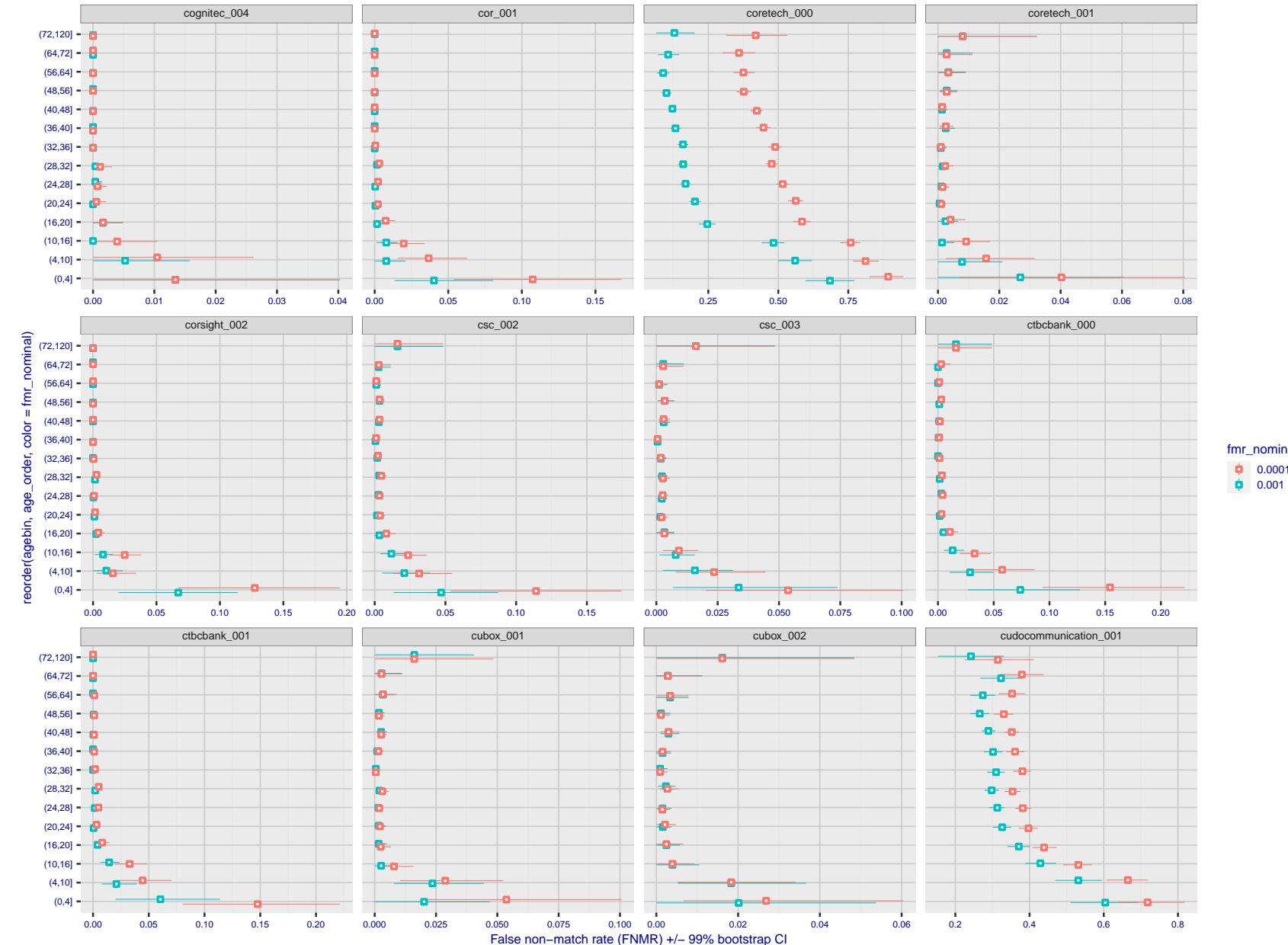


Figure 367: For the visa images, the dots show FNMR by age group for two operating thresholds corresponding to $FMR = \{0.001, 0.0001\}$ computed over all on the order of 10^{10} impostor scores. The FMR in each bin will vary also - see subsequent impostor heatmaps in sec. 3.6.2. Given a pair of face images taken at different times, we assign the comparison to the bin that is the arithmetic average of the subject's ages. This plot shows only the effect of age, not ageing. The number of comparisons in each bin is generally in the thousands, however the first and last bins are computed over 149 and 124 respectively. The error rates in some (adult) cases are zero, and in others the DET is flat so the error rates at the two thresholds are identical. The lines span 1% and 99% of bootstrap replicated FNMR estimates.



Figure 368: For the visa images, the dots show FNMR by age group for two operating thresholds corresponding to $FMR = \{0.001, 0.0001\}$ computed over all on the order of 10^{10} impostor scores. The FMR in each bin will vary also - see subsequent impostor heatmaps in sec. 3.6.2. Given a pair of face images taken at different times, we assign the comparison to the bin that is the arithmetic average of the subject's ages. This plot shows only the effect of age, not ageing. The number of comparisons in each bin is generally in the thousands, however the first and last bins are computed over 149 and 124 respectively. The error rates in some (adult) cases are zero, and in others the DET is flat so the error rates at the two thresholds are identical. The lines span 1% and 99% of bootstrap replicated FNMR estimates.

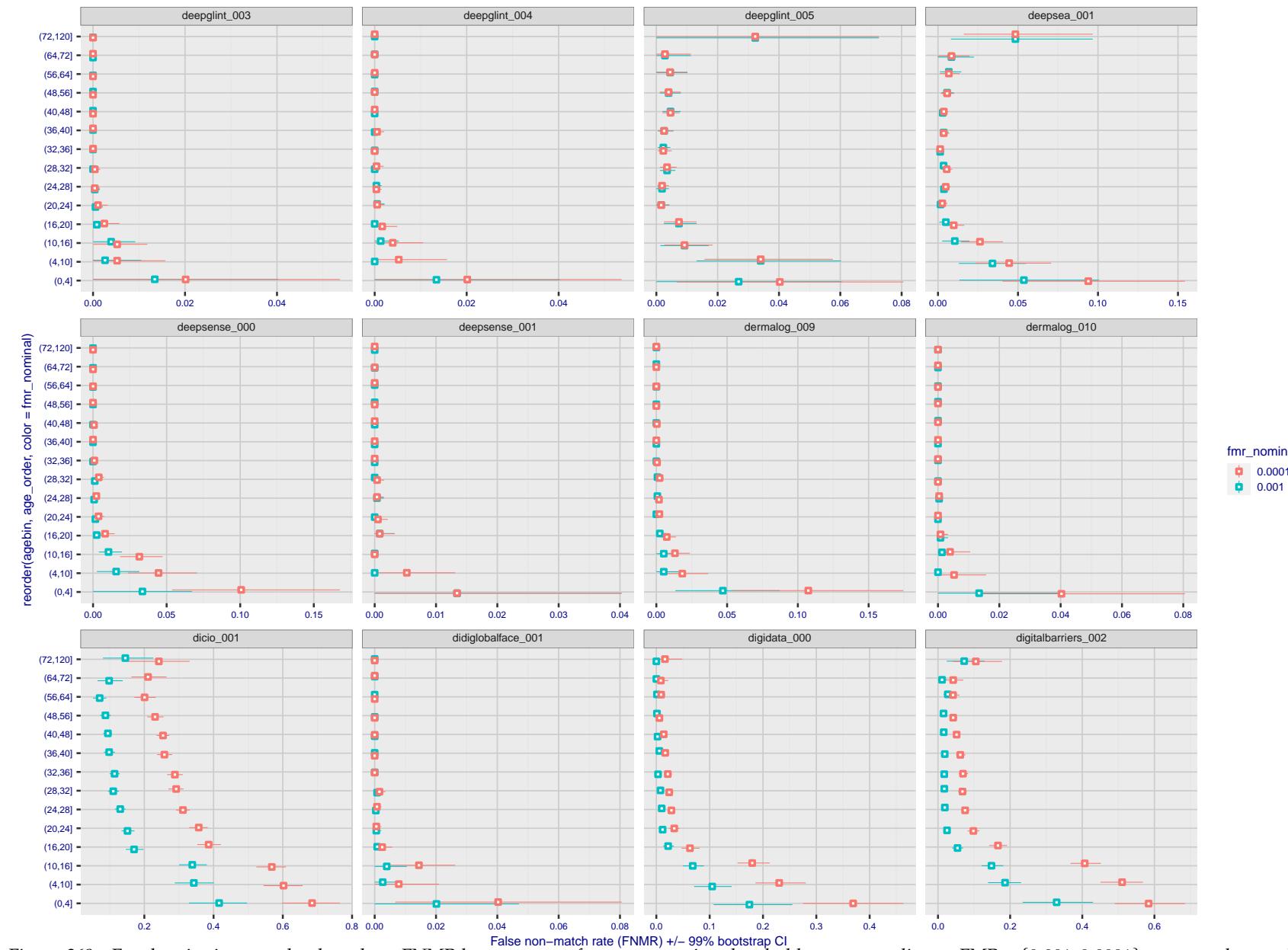


Figure 369: For the visa images, the dots show FNMR by age group for two operating thresholds corresponding to $FMR = \{0.001, 0.0001\}$ computed over all on the order of 10^{10} impostor scores. The FMR in each bin will vary also - see subsequent impostor heatmaps in sec. 3.6.2. Given a pair of face images taken at different times, we assign the comparison to the bin that is the arithmetic average of the subject's ages. This plot shows only the effect of age, not ageing. The number of comparisons in each bin is generally in the thousands, however the first and last bins are computed over 149 and 124 respectively. The error rates in some (adult) cases are zero, and in others the DET is flat so the error rates at the two thresholds are identical. The lines span 1% and 99% of bootstrap replicated FNMR estimates.

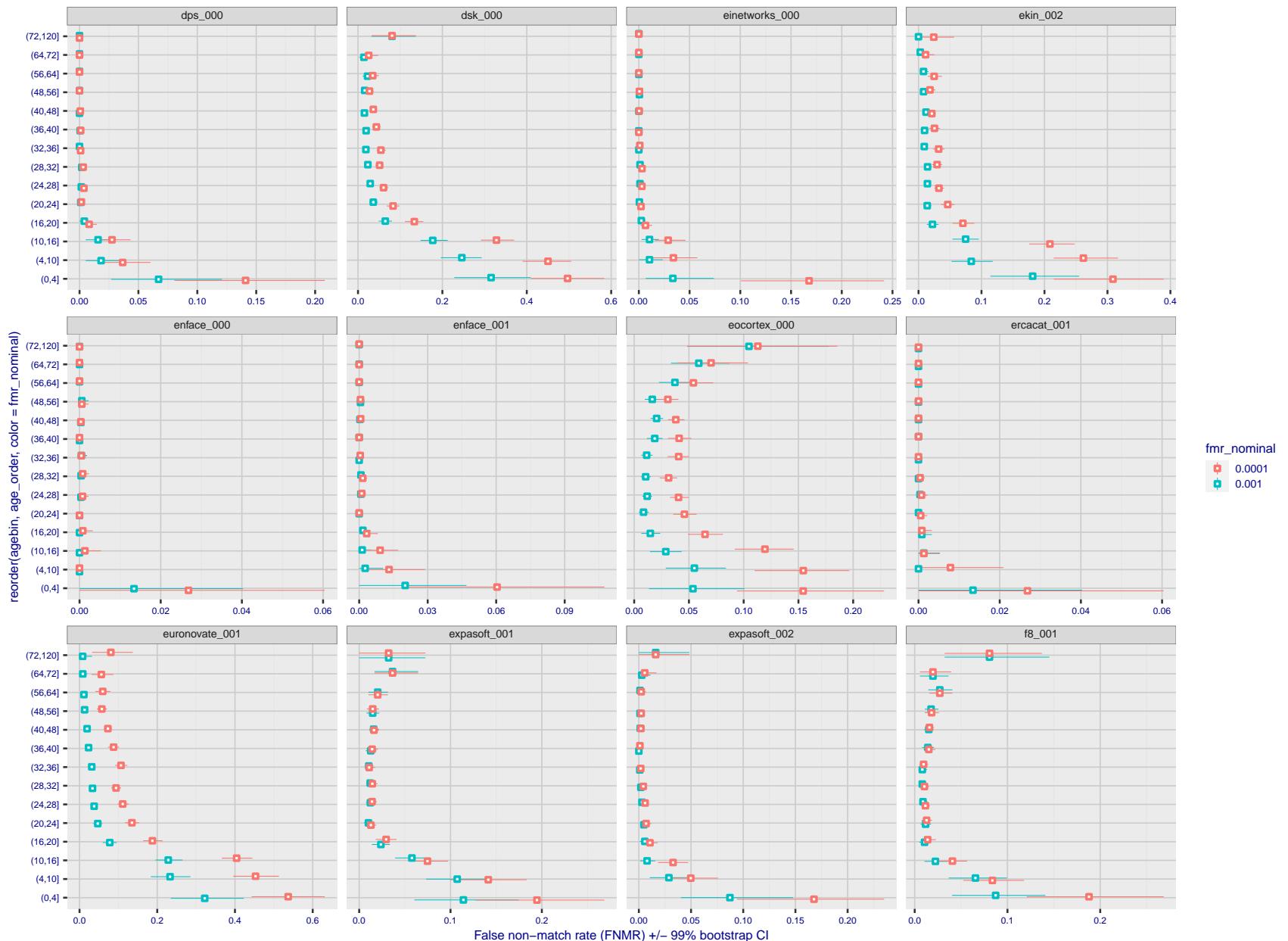


Figure 370: For the visa images, the dots show FNMR by age group for two operating thresholds corresponding to $FMR = \{0.001, 0.0001\}$ computed over all on the order of 10^{10} impostor scores. The FMR in each bin will vary also - see subsequent impostor heatmaps in sec. 3.6.2. Given a pair of face images taken at different times, we assign the comparison to the bin that is the arithmetic average of the subject's ages. This plot shows only the effect of age, not ageing. The number of comparisons in each bin is generally in the thousands, however the first and last bins are computed over 149 and 124 respectively. The error rates in some (adult) cases are zero, and in others the DET is flat so the error rates at the two thresholds are identical. The lines span 1% and 99% of bootstrap replicated FNMR estimates.

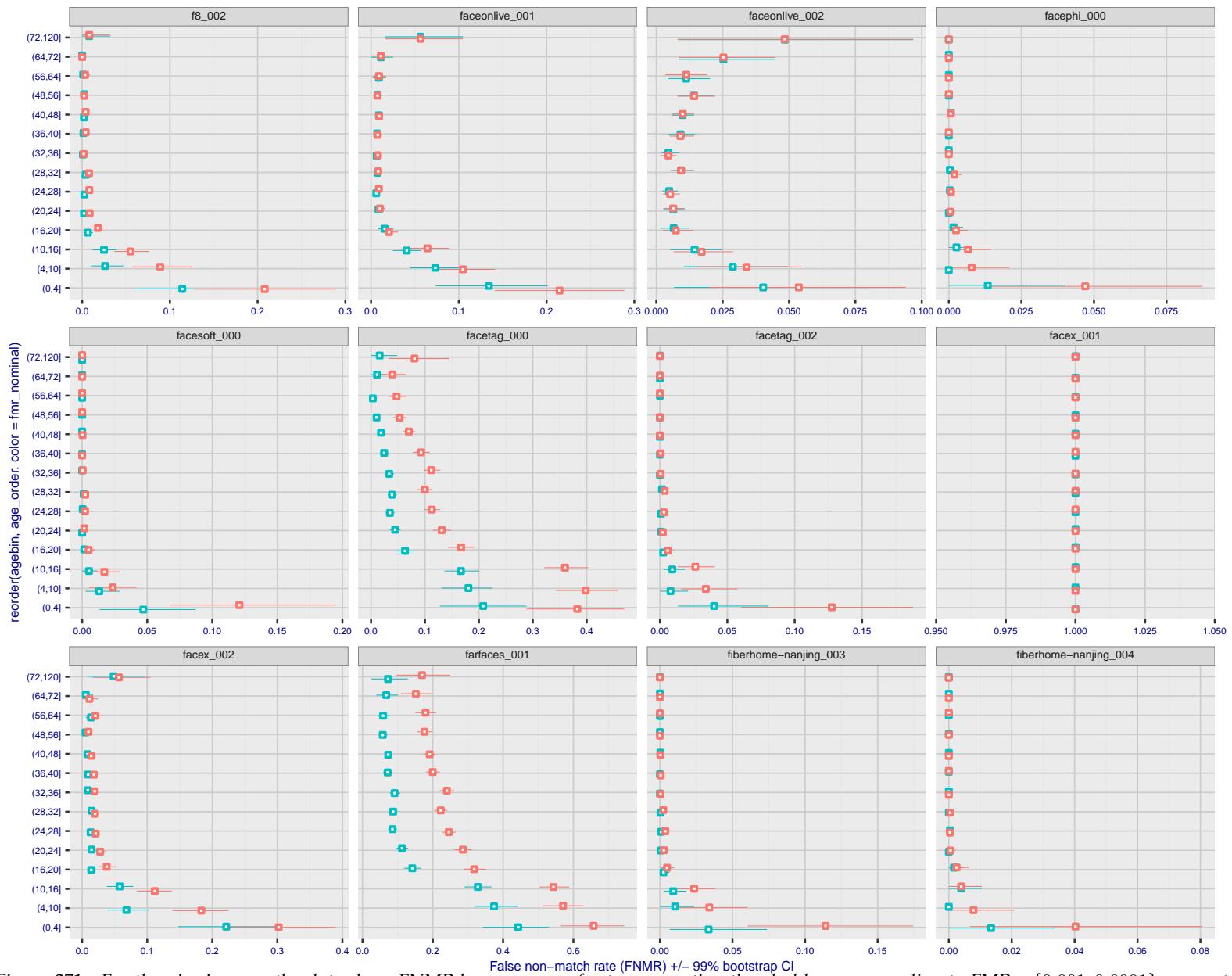


Figure 371: For the visa images, the dots show FNMR by age group for two operating thresholds corresponding to $FMR = \{0.001, 0.0001\}$ computed over all on the order of 10^{10} impostor scores. The FMR in each bin will vary also - see subsequent impostor heatmaps in sec. 3.6.2. Given a pair of face images taken at different times, we assign the comparison to the bin that is the arithmetic average of the subject's ages. This plot shows only the effect of age, not ageing. The number of comparisons in each bin is generally in the thousands, however the first and last bins are computed over 149 and 124 respectively. The error rates in some (adult) cases are zero, and in others the DET is flat so the error rates at the two thresholds are identical. The lines span 1% and 99% of bootstrap replicated FNMR estimates.

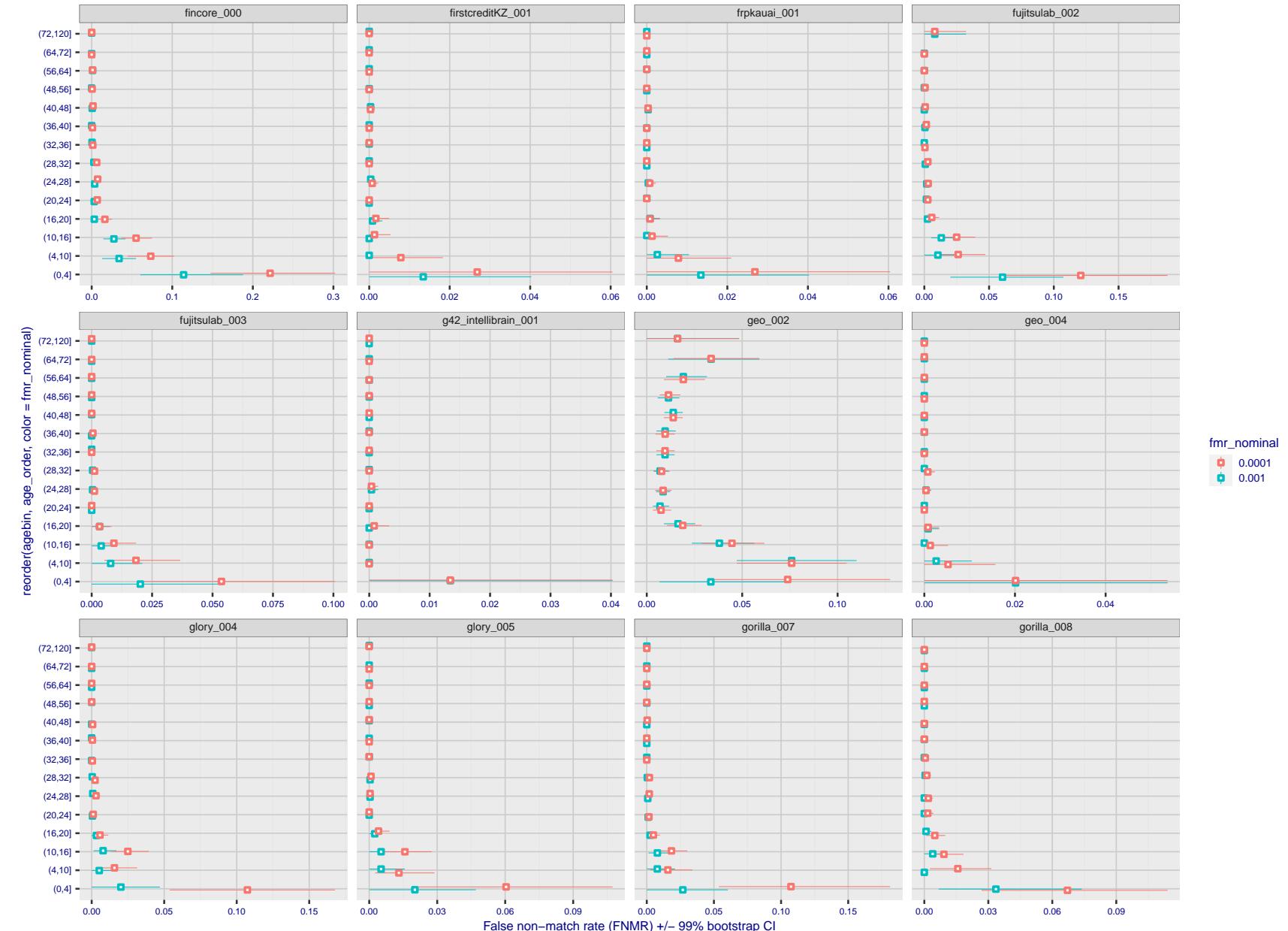


Figure 372: For the visa images, the dots show FNMR by age group for two operating thresholds corresponding to $FMR = \{0.001, 0.0001\}$ computed over all on the order of 10^{10} impostor scores. The FMR in each bin will vary also - see subsequent impostor heatmaps in sec. 3.6.2. Given a pair of face images taken at different times, we assign the comparison to the bin that is the arithmetic average of the subject's ages. This plot shows only the effect of age, not ageing. The number of comparisons in each bin is generally in the thousands, however the first and last bins are computed over 149 and 124 respectively. The error rates in some (adult) cases are zero, and in others the DET is flat so the error rates at the two thresholds are identical. The lines span 1% and 99% of bootstrap replicated FNMR estimates.

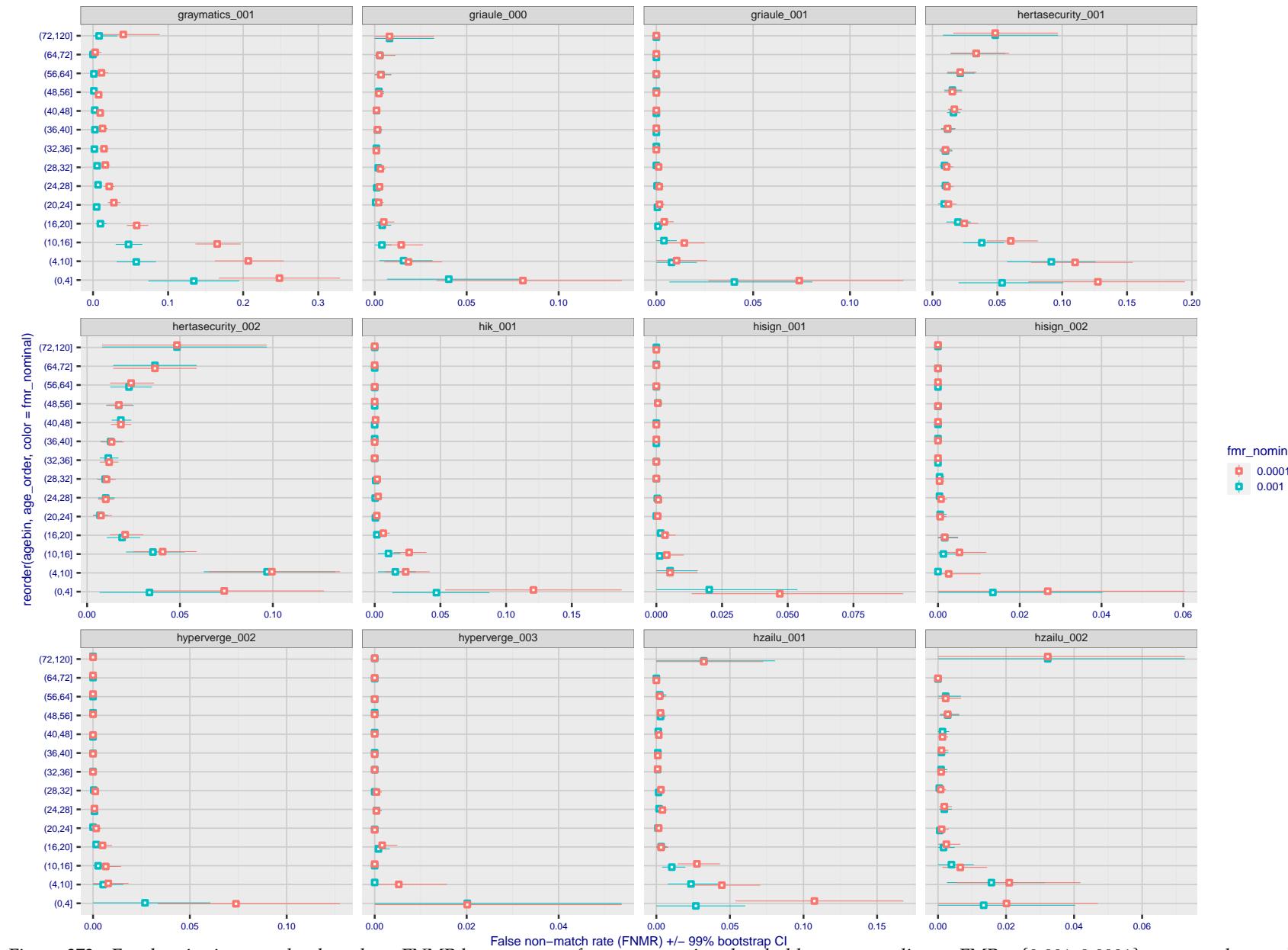


Figure 373: For the visa images, the dots show FNMR by age group for two operating thresholds corresponding to $FMR = \{0.001, 0.0001\}$ computed over all on the order of 10^{10} impostor scores. The FMR in each bin will vary also - see subsequent impostor heatmaps in sec. 3.6.2. Given a pair of face images taken at different times, we assign the comparison to the bin that is the arithmetic average of the subject's ages. This plot shows only the effect of age, not ageing. The number of comparisons in each bin is generally in the thousands, however the first and last bins are computed over 149 and 124 respectively. The error rates in some (adult) cases are zero, and in others the DET is flat so the error rates at the two thresholds are identical. The lines span 1% and 99% of bootstrap replicated FNMR estimates.

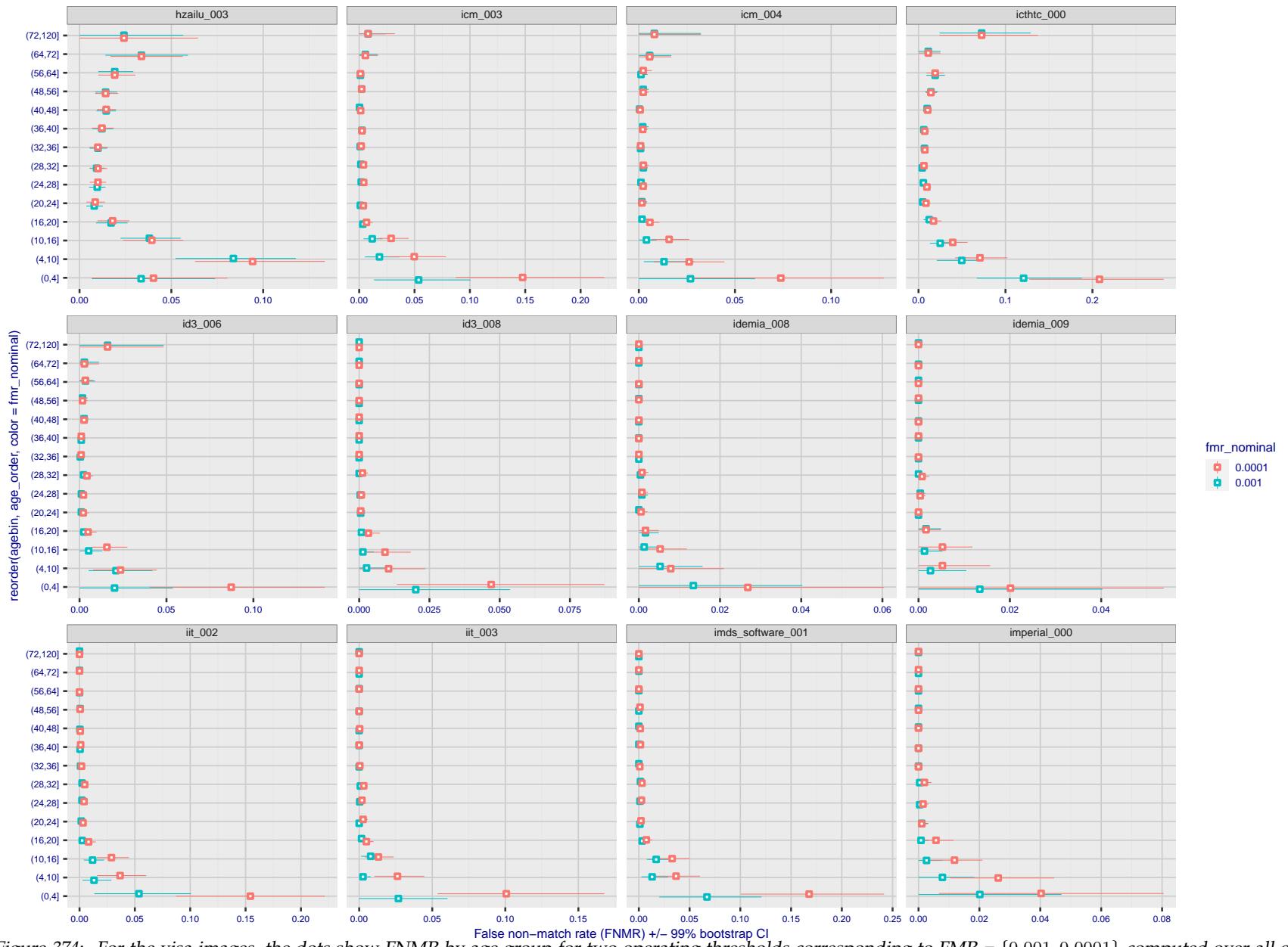


Figure 374: For the visa images, the dots show FNMR by age group for two operating thresholds corresponding to $FMR = \{0.001, 0.0001\}$ computed over all on the order of 10^{10} impostor scores. The FMR in each bin will vary also - see subsequent impostor heatmaps in sec. 3.6.2. Given a pair of face images taken at different times, we assign the comparison to the bin that is the arithmetic average of the subject's ages. This plot shows only the effect of age, not ageing. The number of comparisons in each bin is generally in the thousands, however the first and last bins are computed over 149 and 124 respectively. The error rates in some (adult) cases are zero, and in others the DET is flat so the error rates at the two thresholds are identical. The lines span 1% and 99% of bootstrap replicated FNMR estimates.

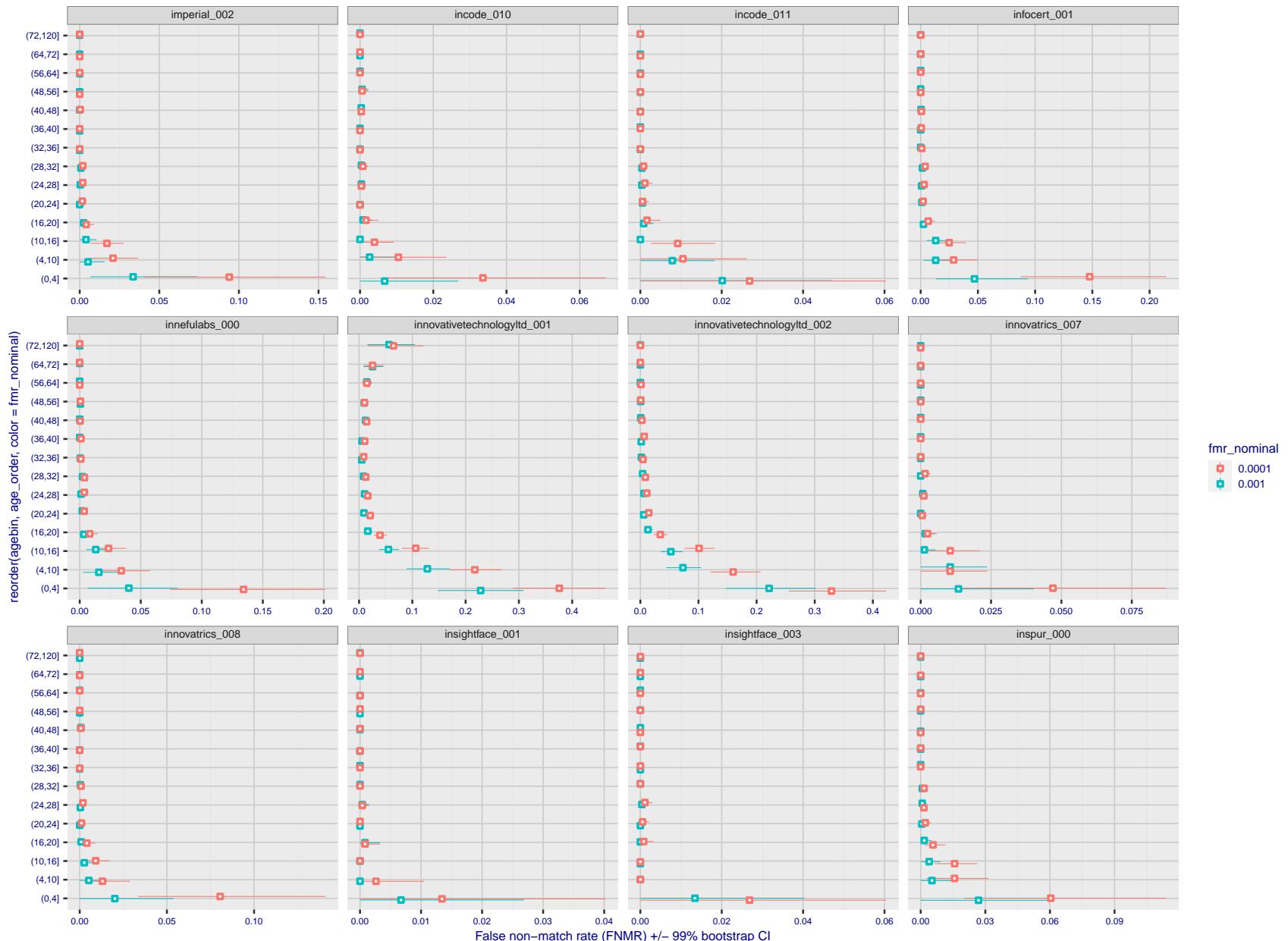


Figure 375: For the visa images, the dots show FNMR by age group for two operating thresholds corresponding to $FMR = \{0.001, 0.0001\}$ computed over all on the order of 10^{10} impostor scores. The FMR in each bin will vary also - see subsequent impostor heatmaps in sec. 3.6.2. Given a pair of face images taken at different times, we assign the comparison to the bin that is the arithmetic average of the subject's ages. This plot shows only the effect of age, not ageing. The number of comparisons in each bin is generally in the thousands, however the first and last bins are computed over 149 and 124 respectively. The error rates in some (adult) cases are zero, and in others the DET is flat so the error rates at the two thresholds are identical. The lines span 1% and 99% of bootstrap replicated FNMR estimates.



Figure 376: For the visa images, the dots show FNMR by age group for two operating thresholds corresponding to $FMR = \{0.001, 0.0001\}$ computed over all on the order of 10^{10} impostor scores. The FMR in each bin will vary also - see subsequent impostor heatmaps in sec. 3.6.2. Given a pair of face images taken at different times, we assign the comparison to the bin that is the arithmetic average of the subject's ages. This plot shows only the effect of age, not ageing. The number of comparisons in each bin is generally in the thousands, however the first and last bins are computed over 149 and 124 respectively. The error rates in some (adult) cases are zero, and in others the DET is flat so the error rates at the two thresholds are identical. The lines span 1% and 99% of bootstrap replicated FNMR estimates.

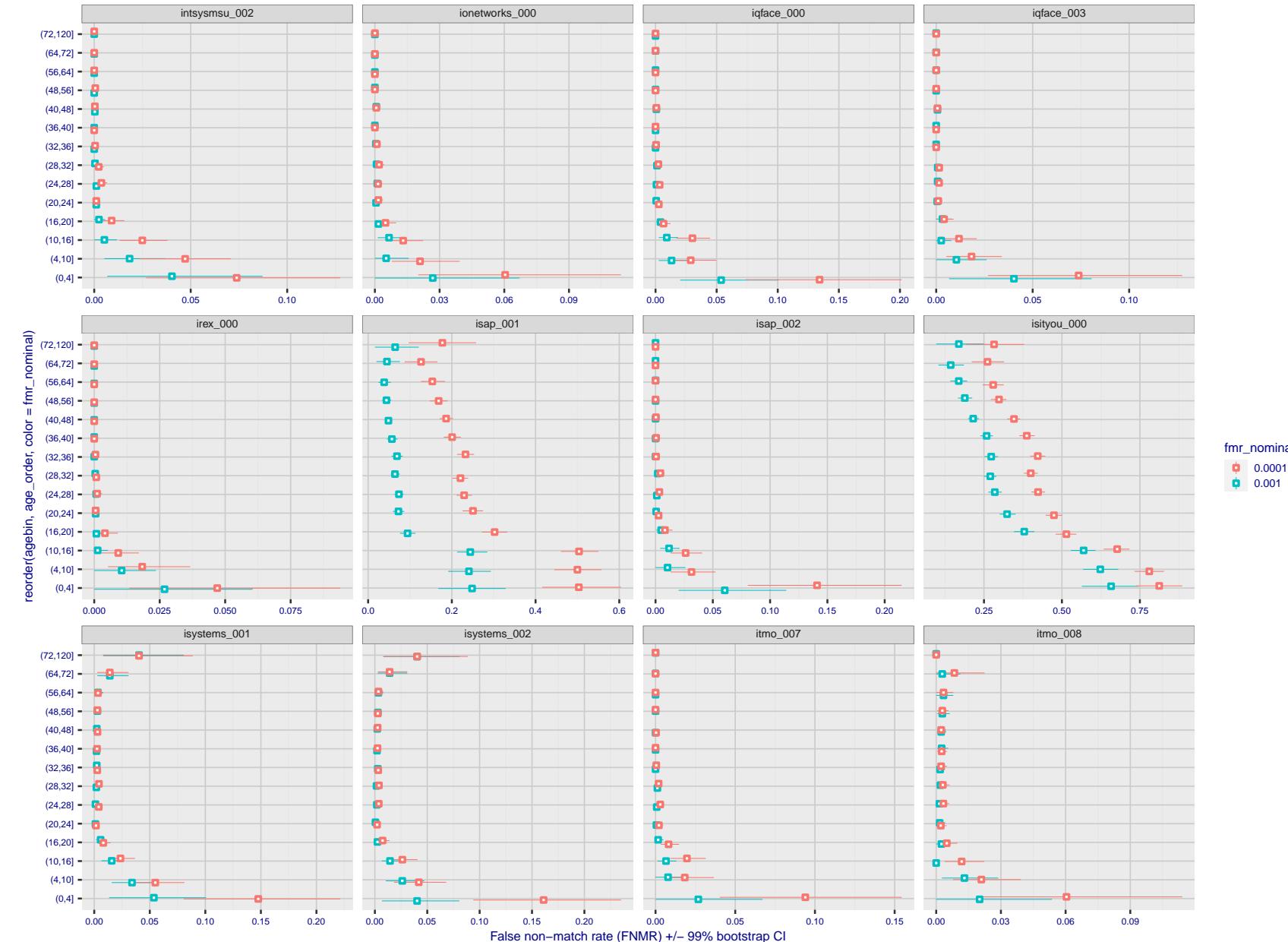


Figure 377: For the visa images, the dots show FNMR by age group for two operating thresholds corresponding to $FMR = \{0.001, 0.0001\}$ computed over all on the order of 10^{10} impostor scores. The FMR in each bin will vary also - see subsequent impostor heatmaps in sec. 3.6.2. Given a pair of face images taken at different times, we assign the comparison to the bin that is the arithmetic average of the subject's ages. This plot shows only the effect of age, not ageing. The number of comparisons in each bin is generally in the thousands, however the first and last bins are computed over 149 and 124 respectively. The error rates in some (adult) cases are zero, and in others the DET is flat so the error rates at the two thresholds are identical. The lines span 1% and 99% of bootstrap replicated FNMR estimates.

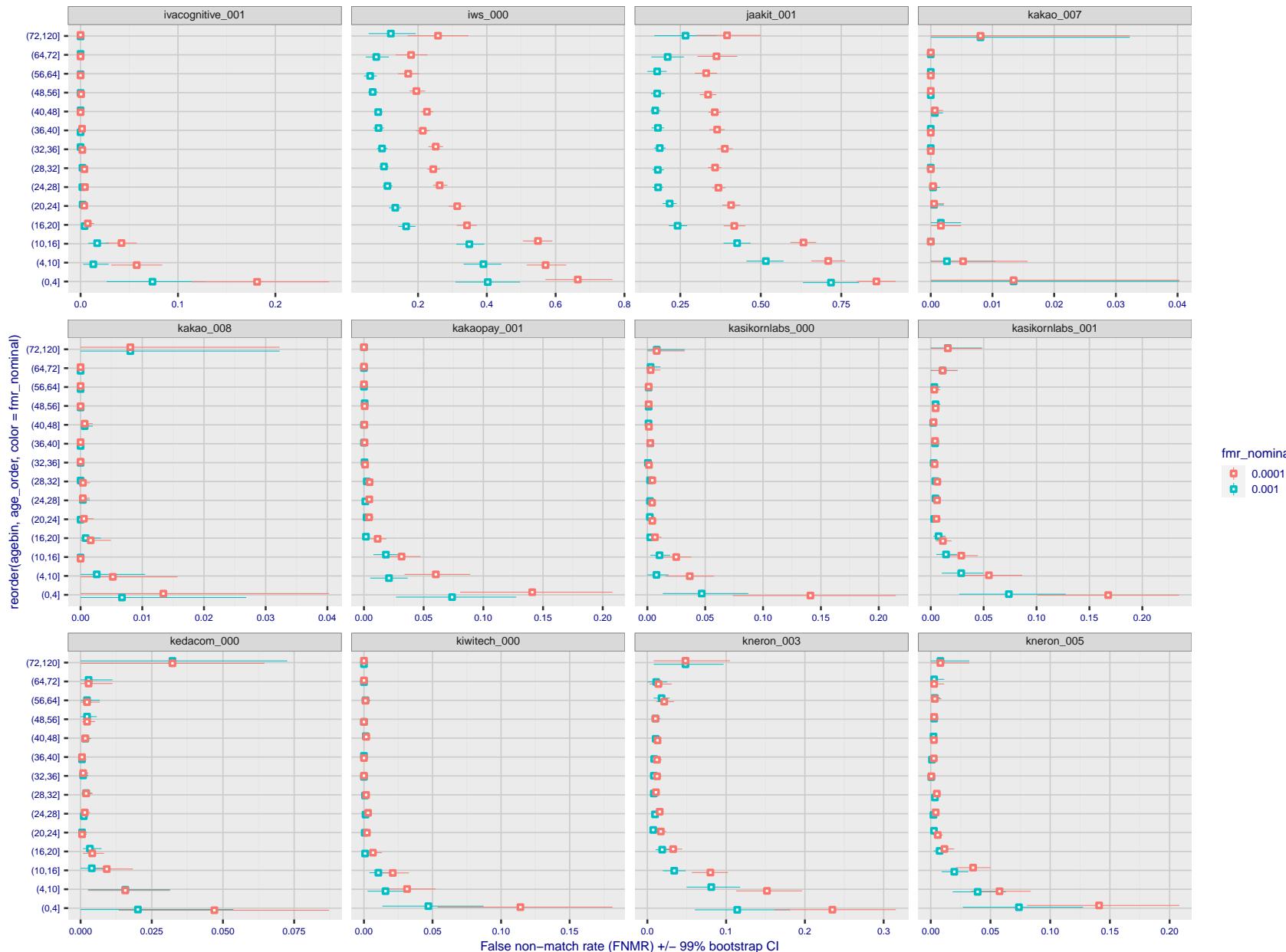


Figure 378: For the visa images, the dots show FNMR by age group for two operating thresholds corresponding to $FMR = \{0.001, 0.0001\}$ computed over all on the order of 10^{10} impostor scores. The FMR in each bin will vary also - see subsequent impostor heatmaps in sec. 3.6.2. Given a pair of face images taken at different times, we assign the comparison to the bin that is the arithmetic average of the subject's ages. This plot shows only the effect of age, not ageing. The number of comparisons in each bin is generally in the thousands, however the first and last bins are computed over 149 and 124 respectively. The error rates in some (adult) cases are zero, and in others the DET is flat so the error rates at the two thresholds are identical. The lines span 1% and 99% of bootstrap replicated FNMR estimates.



Figure 379: For the visa images, the dots show FNMR by age group for two operating thresholds corresponding to $FMR = \{0.001, 0.0001\}$ computed over all on the order of 10^{10} impostor scores. The FMR in each bin will vary also - see subsequent impostor heatmaps in sec. 3.6.2. Given a pair of face images taken at different times, we assign the comparison to the bin that is the arithmetic average of the subject's ages. This plot shows only the effect of age, not ageing. The number of comparisons in each bin is generally in the thousands, however the first and last bins are computed over 149 and 124 respectively. The error rates in some (adult) cases are zero, and in others the DET is flat so the error rates at the two thresholds are identical. The lines span 1% and 99% of bootstrap replicated FNMR estimates.

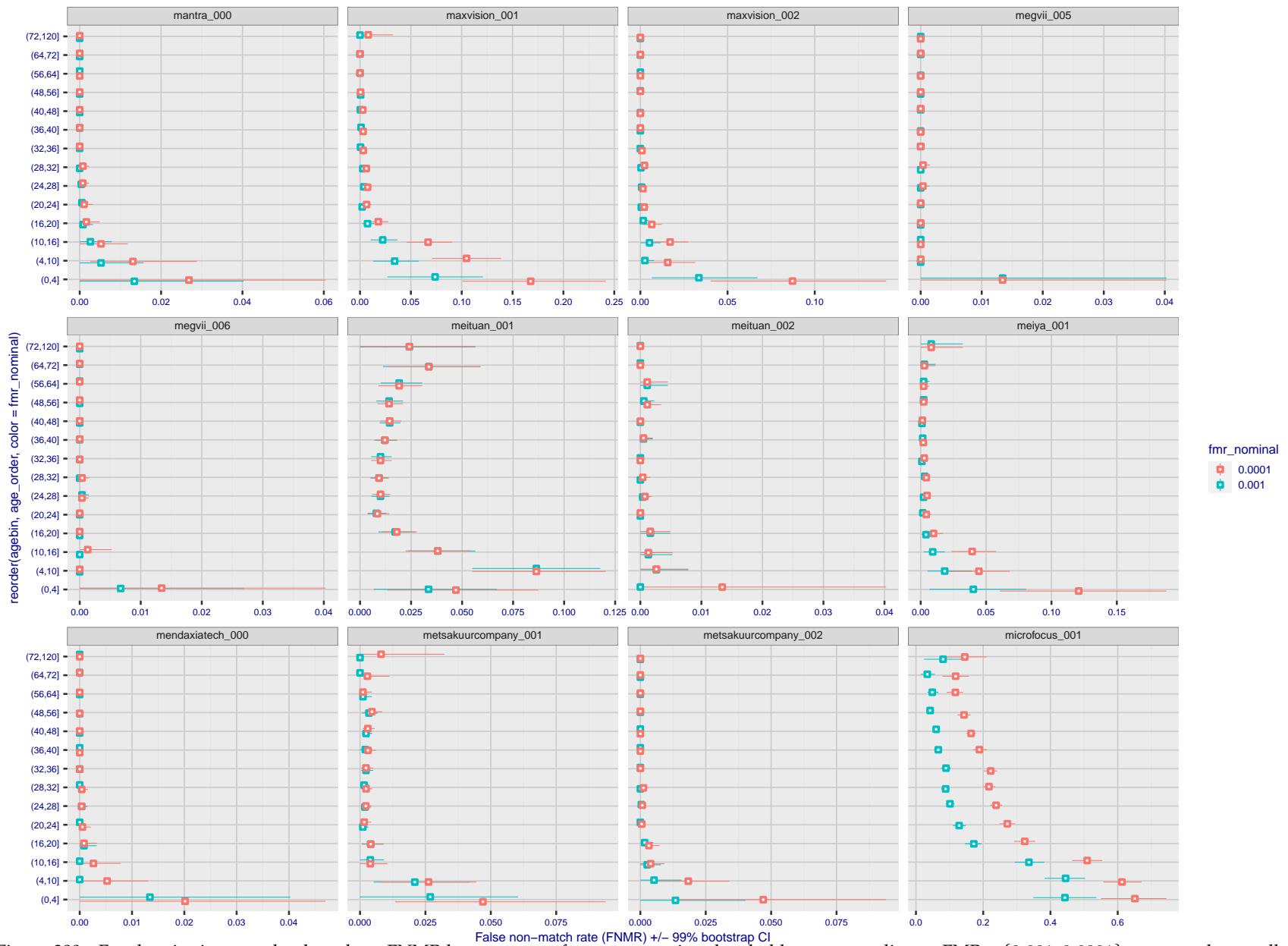


Figure 380: For the visa images, the dots show FNMR by age group for two operating thresholds corresponding to $FMR = \{0.001, 0.0001\}$ computed over all on the order of 10^{10} impostor scores. The FMR in each bin will vary also - see subsequent impostor heatmaps in sec. 3.6.2. Given a pair of face images taken at different times, we assign the comparison to the bin that is the arithmetic average of the subject's ages. This plot shows only the effect of age, not ageing. The number of comparisons in each bin is generally in the thousands, however the first and last bins are computed over 149 and 124 respectively. The error rates in some (adult) cases are zero, and in others the DET is flat so the error rates at the two thresholds are identical. The lines span 1% and 99% of bootstrap replicated FNMR estimates.

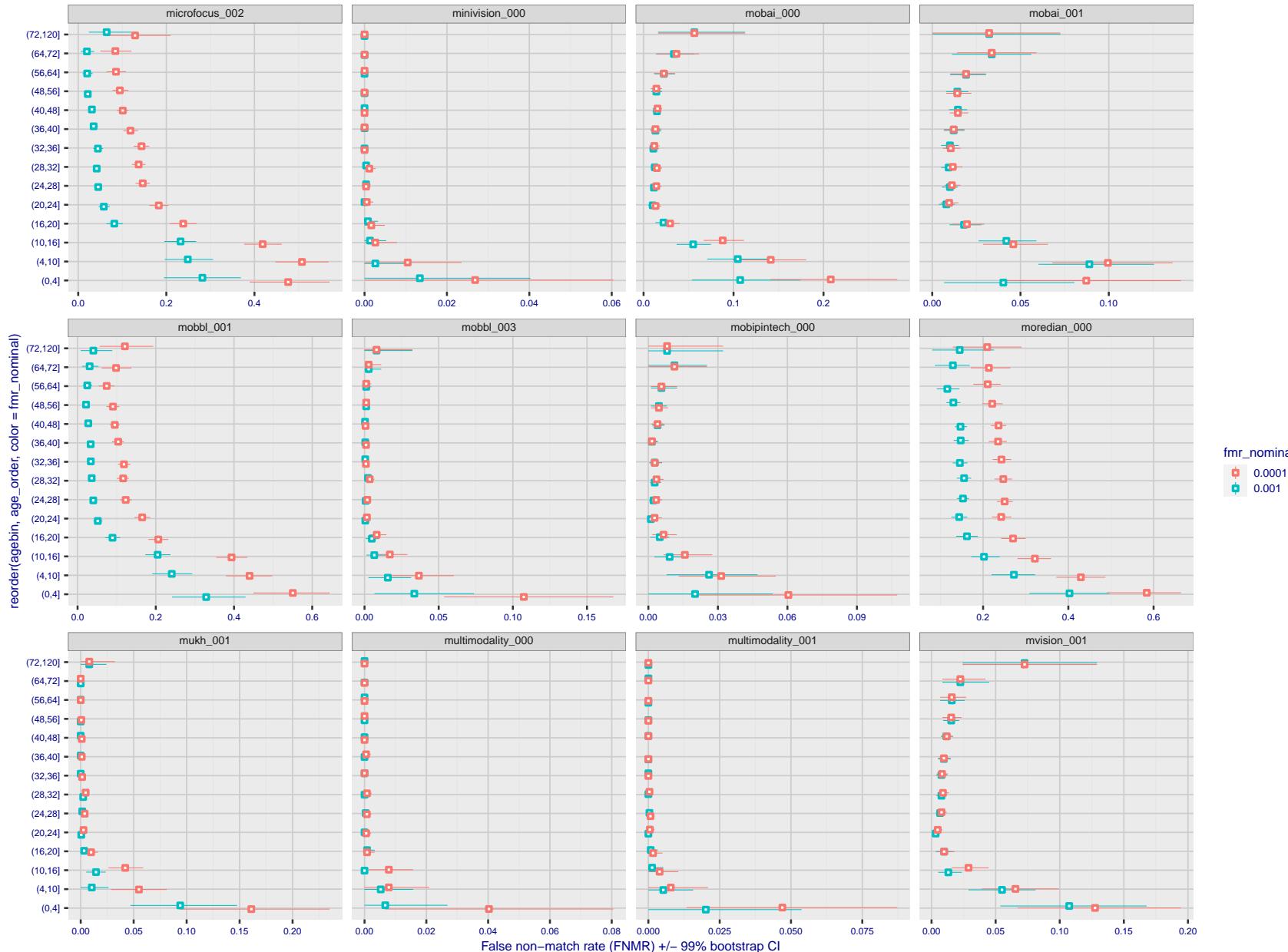


Figure 381: For the visa images, the dots show FNMR by age group for two operating thresholds corresponding to $FMR = \{0.001, 0.0001\}$ computed over all on the order of 10^{10} impostor scores. The FMR in each bin will vary also - see subsequent impostor heatmaps in sec. 3.6.2. Given a pair of face images taken at different times, we assign the comparison to the bin that is the arithmetic average of the subject's ages. This plot shows only the effect of age, not ageing. The number of comparisons in each bin is generally in the thousands, however the first and last bins are computed over 149 and 124 respectively. The error rates in some (adult) cases are zero, and in others the DET is flat so the error rates at the two thresholds are identical. The lines span 1% and 99% of bootstrap replicated FNMR estimates.

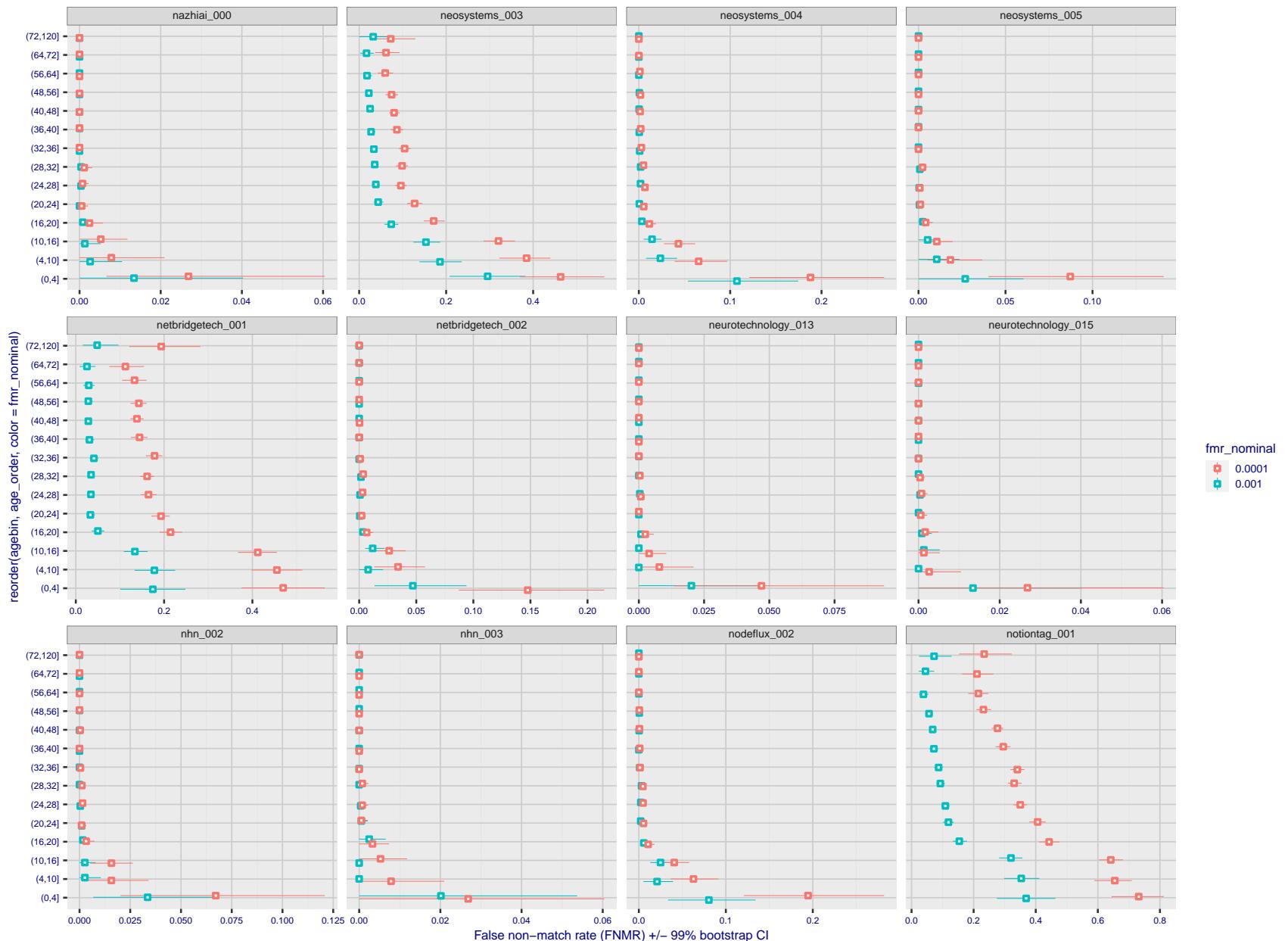


Figure 382: For the visa images, the dots show FNMR by age group for two operating thresholds corresponding to $FMR = \{0.001, 0.0001\}$ computed over all on the order of 10^{10} impostor scores. The FMR in each bin will vary also - see subsequent impostor heatmaps in sec. 3.6.2. Given a pair of face images taken at different times, we assign the comparison to the bin that is the arithmetic average of the subject's ages. This plot shows only the effect of age, not ageing. The number of comparisons in each bin is generally in the thousands, however the first and last bins are computed over 149 and 124 respectively. The error rates in some (adult) cases are zero, and in others the DET is flat so the error rates at the two thresholds are identical. The lines span 1% and 99% of bootstrap replicated FNMR estimates.

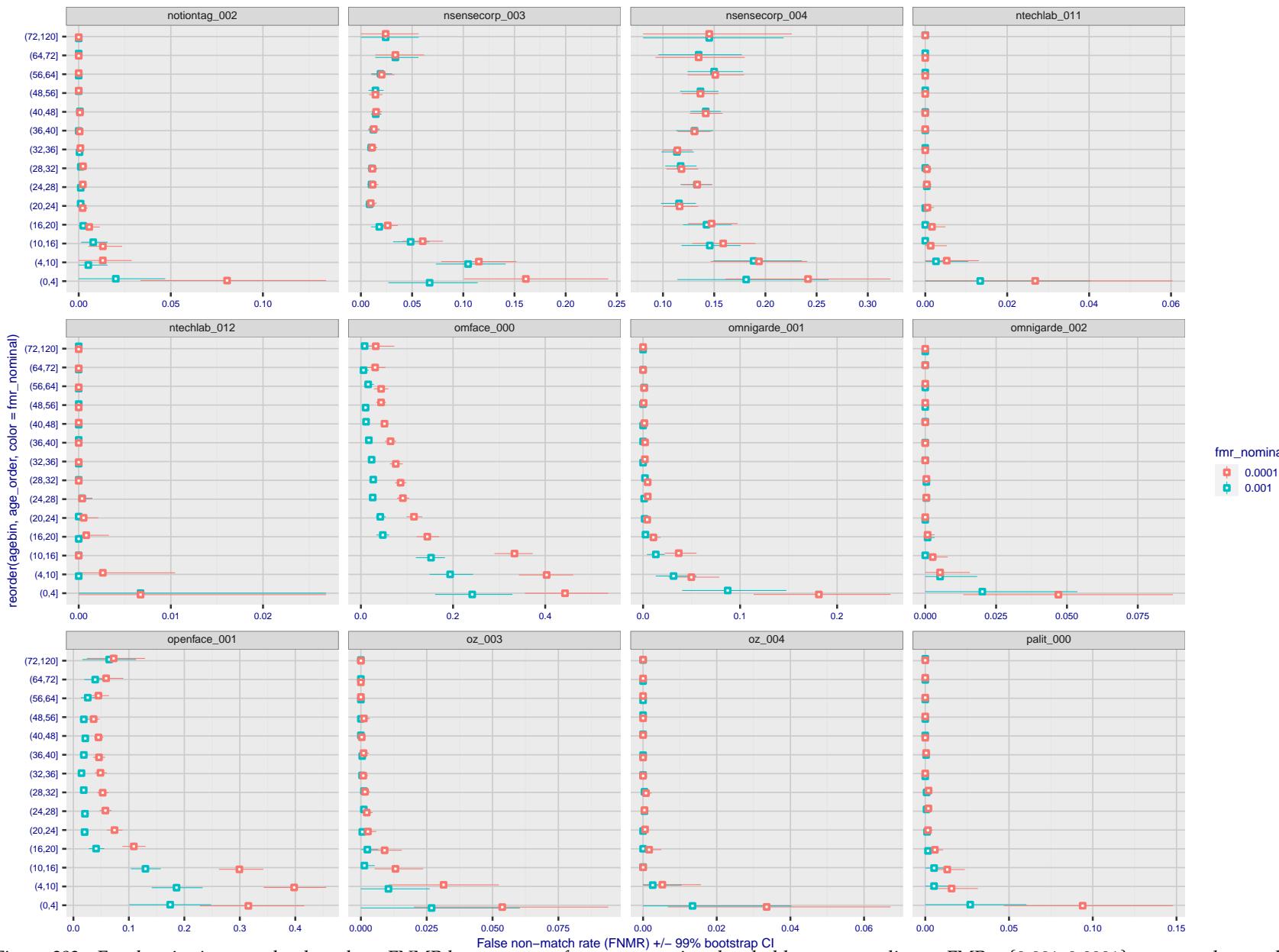


Figure 383: For the visa images, the dots show FNMR by age group for two operating thresholds corresponding to $FMR = \{0.001, 0.0001\}$ computed over all on the order of 10^{10} impostor scores. The FMR in each bin will vary also - see subsequent impostor heatmaps in sec. 3.6.2. Given a pair of face images taken at different times, we assign the comparison to the bin that is the arithmetic average of the subject's ages. This plot shows only the effect of age, not ageing. The number of comparisons in each bin is generally in the thousands, however the first and last bins are computed over 149 and 124 respectively. The error rates in some (adult) cases are zero, and in others the DET is flat so the error rates at the two thresholds are identical. The lines span 1% and 99% of bootstrap replicated FNMR estimates.



Figure 384: For the visa images, the dots show FNMR by age group for two operating thresholds corresponding to $FMR = \{0.001, 0.0001\}$ computed over all on the order of 10^{10} impostor scores. The FMR in each bin will vary also - see subsequent impostor heatmaps in sec. 3.6.2. Given a pair of face images taken at different times, we assign the comparison to the bin that is the arithmetic average of the subject's ages. This plot shows only the effect of age, not ageing. The number of comparisons in each bin is generally in the thousands, however the first and last bins are computed over 149 and 124 respectively. The error rates in some (adult) cases are zero, and in others the DET is flat so the error rates at the two thresholds are identical. The lines span 1% and 99% of bootstrap replicated FNMR estimates.

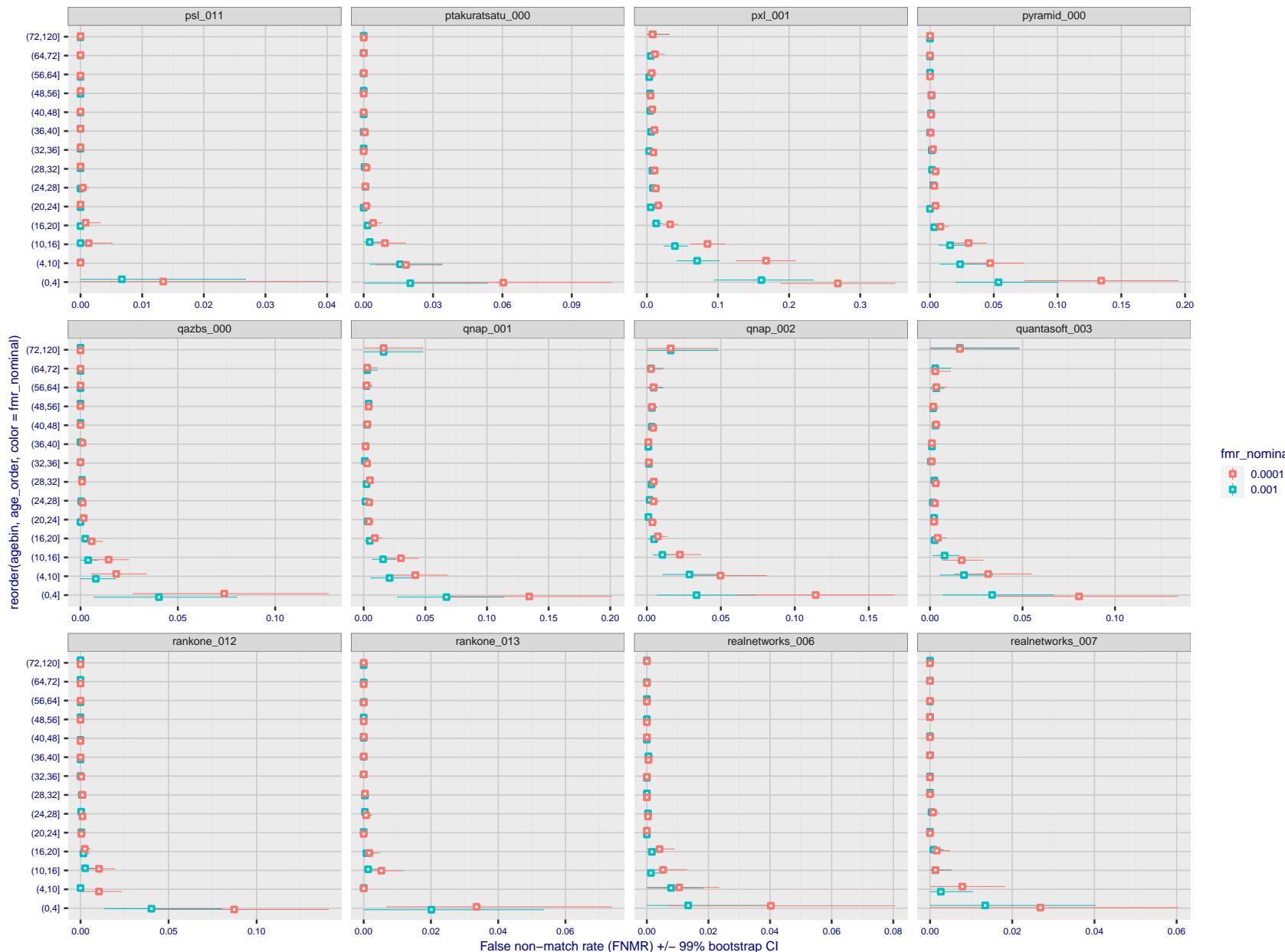


Figure 385: For the visa images, the dots show FNMR by age group for two operating thresholds corresponding to FMR = {0.001, 0.0001} computed over all on the order of 10^{10} impostor scores. The FMR in each bin will vary also - see subsequent impostor heatmaps in sec. 3.6.2. Given a pair of face images taken at different times, we assign the comparison to the bin that is the arithmetic average of the subject's ages. This plot shows only the effect of age, not ageing. The number of comparisons in each bin is generally in the thousands, however the first and last bins are computed over 149 and 124 respectively. The error rates in some (adult) cases are zero, and in others the DET is flat so the error rates at the two thresholds are identical. The lines span 1% and 99% of bootstrap replicated FNMR estimates.

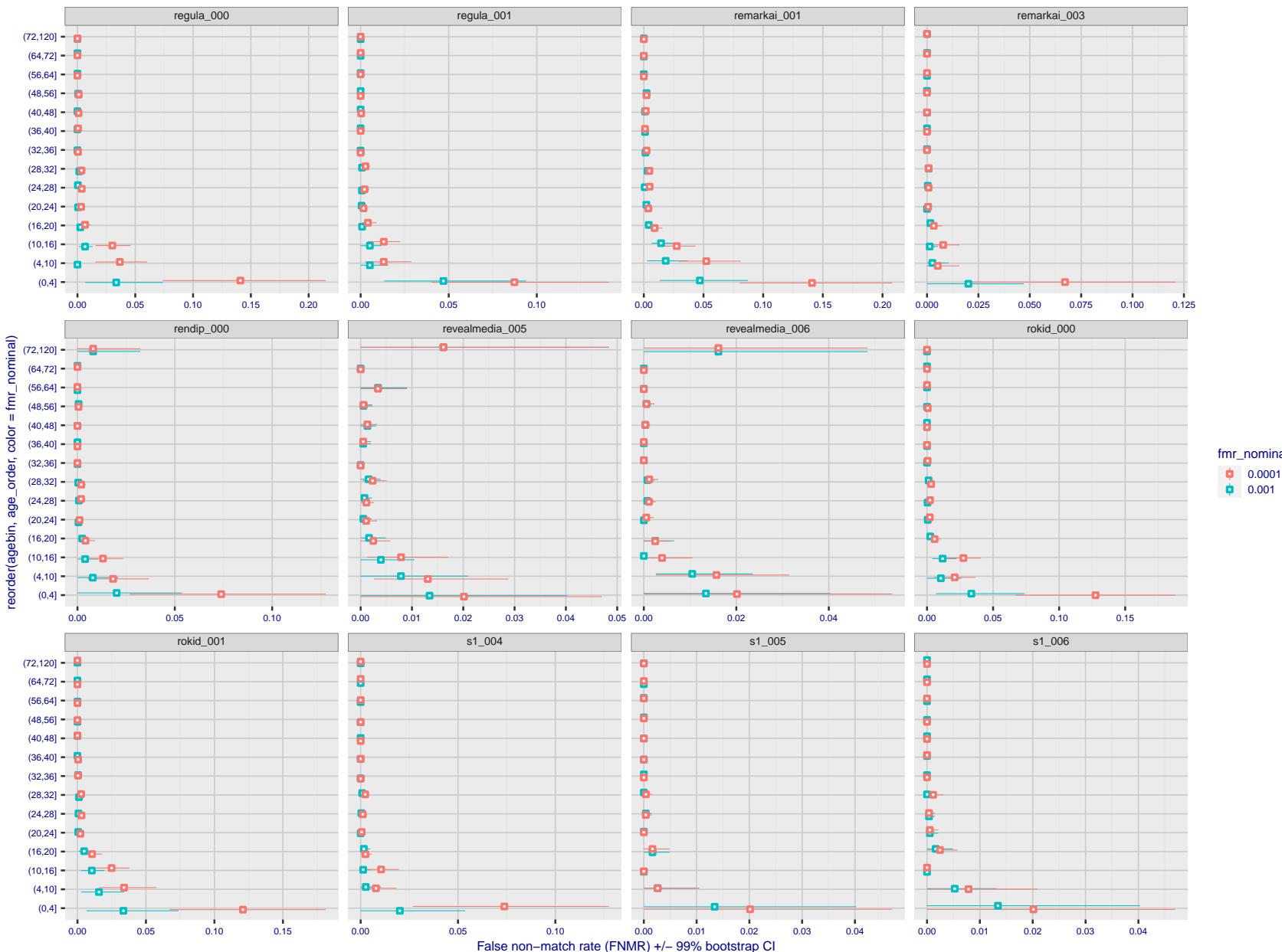


Figure 386: For the visa images, the dots show FNMR by age group for two operating thresholds corresponding to $FMR = \{0.001, 0.0001\}$ computed over all on the order of 10^{10} impostor scores. The FMR in each bin will vary also - see subsequent impostor heatmaps in sec. 3.6.2. Given a pair of face images taken at different times, we assign the comparison to the bin that is the arithmetic average of the subject's ages. This plot shows only the effect of age, not ageing. The number of comparisons in each bin is generally in the thousands, however the first and last bins are computed over 149 and 124 respectively. The error rates in some (adult) cases are zero, and in others the DET is flat so the error rates at the two thresholds are identical. The lines span 1% and 99% of bootstrap replicated FNMR estimates.



Figure 387: For the visa images, the dots show FNMR by age group for two operating thresholds corresponding to $FMR = \{0.001, 0.0001\}$ computed over all on the order of 10^{10} impostor scores. The FMR in each bin will vary also - see subsequent impostor heatmaps in sec. 3.6.2. Given a pair of face images taken at different times, we assign the comparison to the bin that is the arithmetic average of the subject's ages. This plot shows only the effect of age, not ageing. The number of comparisons in each bin is generally in the thousands, however the first and last bins are computed over 149 and 124 respectively. The error rates in some (adult) cases are zero, and in others the DET is flat so the error rates at the two thresholds are identical. The lines span 1% and 99% of bootstrap replicated FNMR estimates.

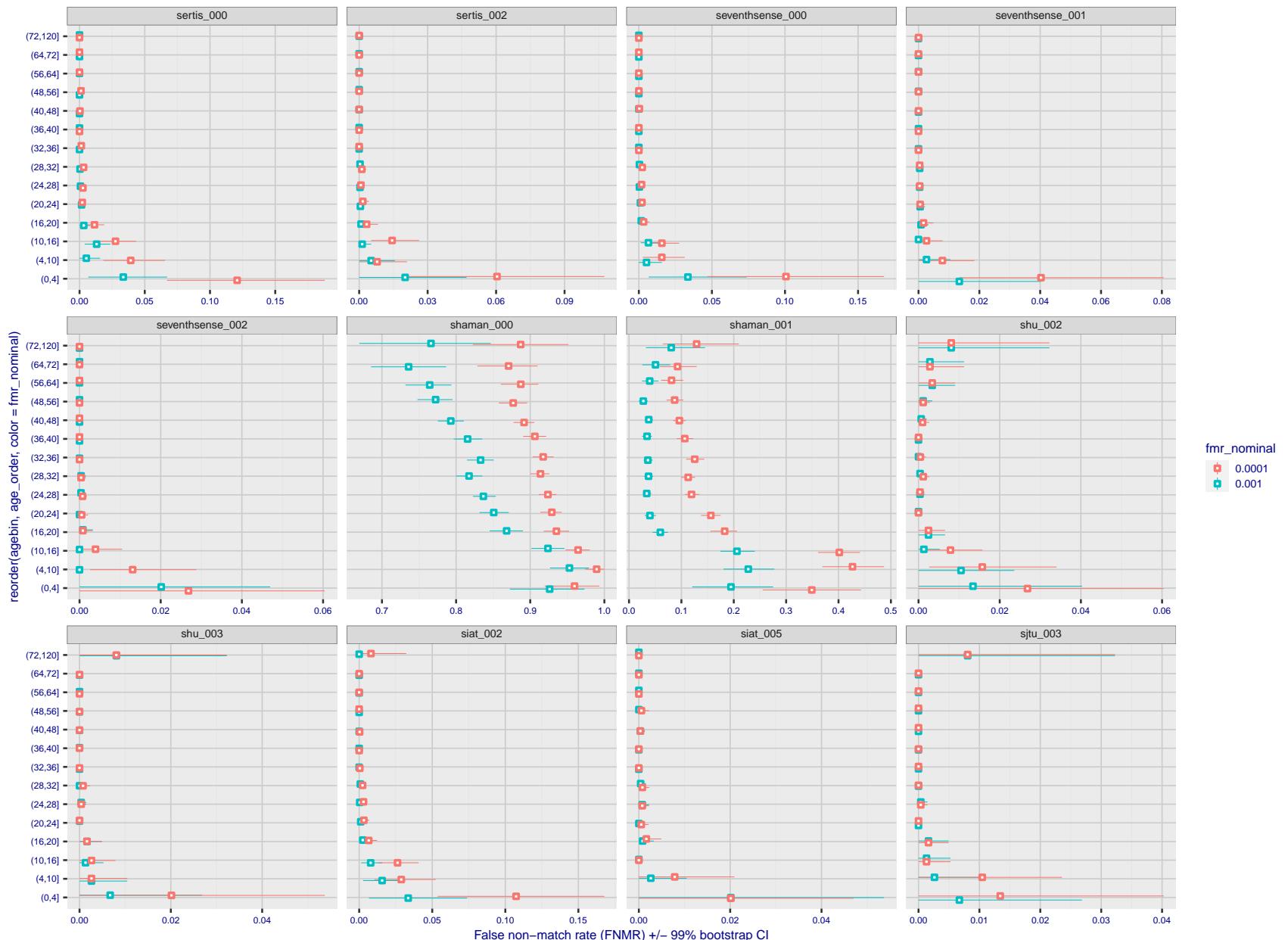


Figure 388: For the visa images, the dots show FNMR by age group for two operating thresholds corresponding to $FMR = \{0.001, 0.0001\}$ computed over all on the order of 10^{10} impostor scores. The FMR in each bin will vary also - see subsequent impostor heatmaps in sec. 3.6.2. Given a pair of face images taken at different times, we assign the comparison to the bin that is the arithmetic average of the subject's ages. This plot shows only the effect of age, not ageing. The number of comparisons in each bin is generally in the thousands, however the first and last bins are computed over 149 and 124 respectively. The error rates in some (adult) cases are zero, and in others the DET is flat so the error rates at the two thresholds are identical. The lines span 1% and 99% of bootstrap replicated FNMR estimates.

2023/02/02 13:38:52

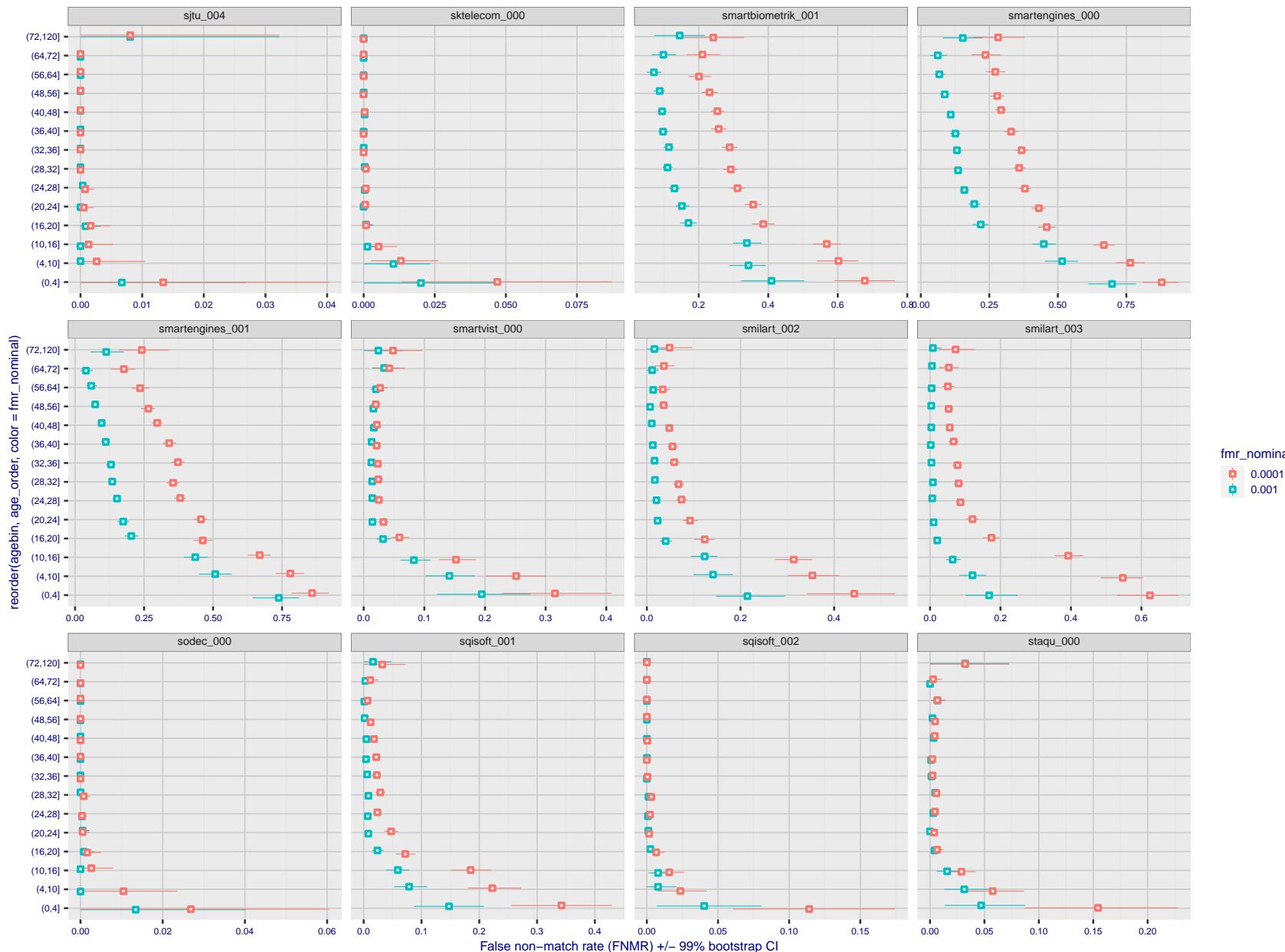


Figure 389: For the visa images, the dots show FNMR by age group for two operating thresholds corresponding to $FMR = \{0.001, 0.0001\}$ computed over all on the order of 10^{10} impostor scores. The FMR in each bin will vary also - see subsequent impostor heatmaps in sec. 3.6.2. Given a pair of face images taken at different times, we assign the comparison to the bin that is the arithmetic average of the subject's ages. This plot shows only the effect of age, not ageing. The number of comparisons in each bin is generally in the thousands, however the first and last bins are computed over 149 and 124 respectively. The error rates in some (adult) cases are zero, and in others the DET is flat so the error rates at the two thresholds are identical. The lines span 1% and 99% of bootstrap replicated FNMR estimates.

FNMR(T)
FMR(T)
"False non-match rate"
"False match rate"

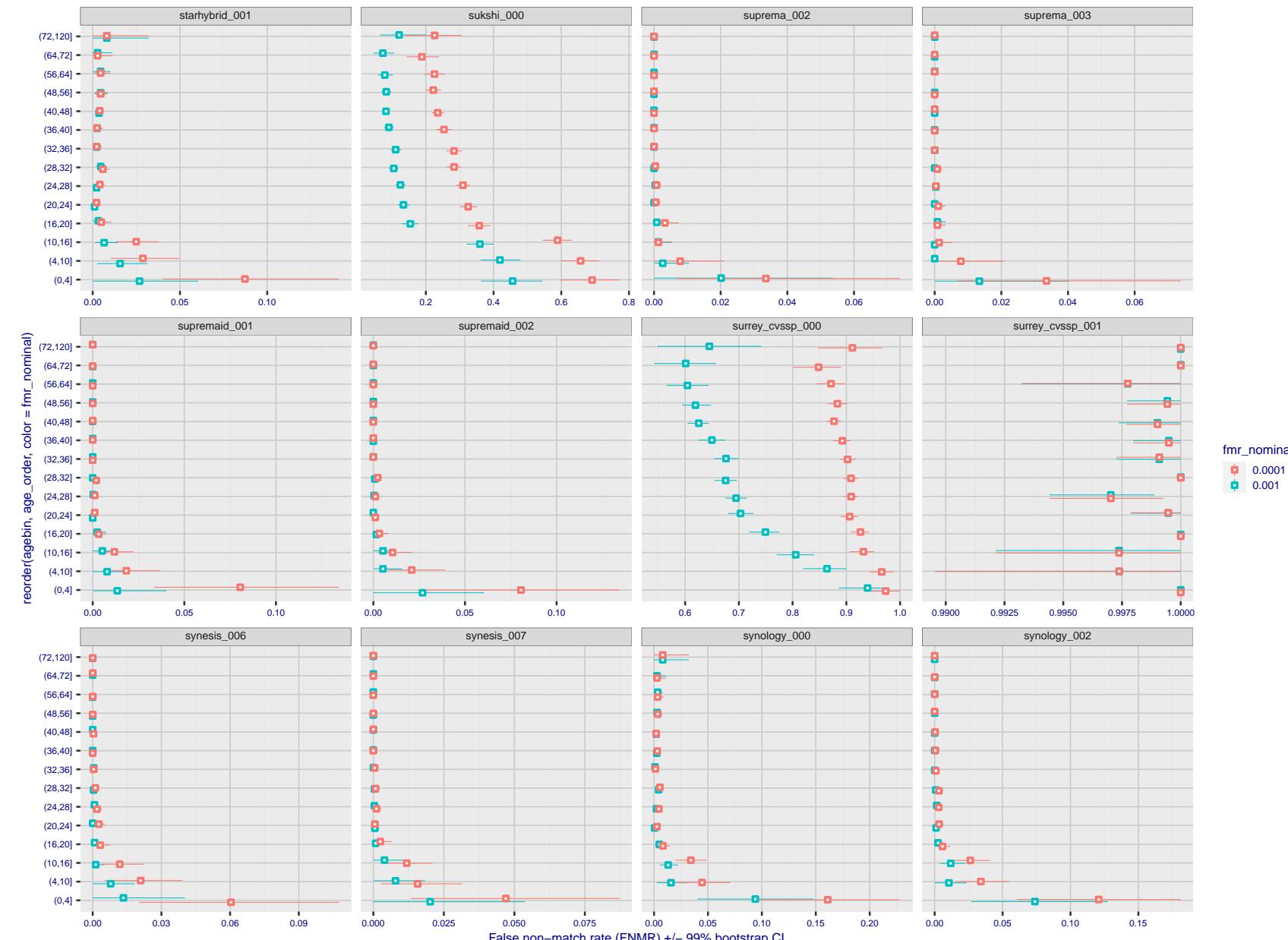


Figure 390: For the visa images, the dots show FNMR by age group for two operating thresholds corresponding to $FMR = \{0.001, 0.0001\}$ computed over all on the order of 10^{10} impostor scores. The FMR in each bin will vary also - see subsequent impostor heatmaps in sec. 3.6.2. Given a pair of face images taken at different times, we assign the comparison to the bin that is the arithmetic average of the subject's ages. This plot shows only the effect of age, not ageing. The number of comparisons in each bin is generally in the thousands, however the first and last bins are computed over 149 and 124 respectively. The error rates in some (adult) cases are zero, and in others the DET is flat so the error rates at the two thresholds are identical. The lines span 1% and 99% of bootstrap replicated FNMR estimates.



Figure 391: For the visa images, the dots show FNMR by age group for two operating thresholds corresponding to $FMR = \{0.001, 0.0001\}$ computed over all on the order of 10^{10} impostor scores. The FMR in each bin will vary also - see subsequent impostor heatmaps in sec. 3.6.2. Given a pair of face images taken at different times, we assign the comparison to the bin that is the arithmetic average of the subject's ages. This plot shows only the effect of age, not ageing. The number of comparisons in each bin is generally in the thousands, however the first and last bins are computed over 149 and 124 respectively. The error rates in some (adult) cases are zero, and in others the DET is flat so the error rates at the two thresholds are identical. The lines span 1% and 99% of bootstrap replicated FNMR estimates.



Figure 392: For the visa images, the dots show FNMR by age group for two operating thresholds corresponding to $FMR = \{0.001, 0.0001\}$ computed over all on the order of 10^{10} impostor scores. The FMR in each bin will vary also - see subsequent impostor heatmaps in sec. 3.6.2. Given a pair of face images taken at different times, we assign the comparison to the bin that is the arithmetic average of the subject's ages. This plot shows only the effect of age, not ageing. The number of comparisons in each bin is generally in the thousands, however the first and last bins are computed over 149 and 124 respectively. The error rates in some (adult) cases are zero, and in others the DET is flat so the error rates at the two thresholds are identical. The lines span 1% and 99% of bootstrap replicated FNMR estimates.

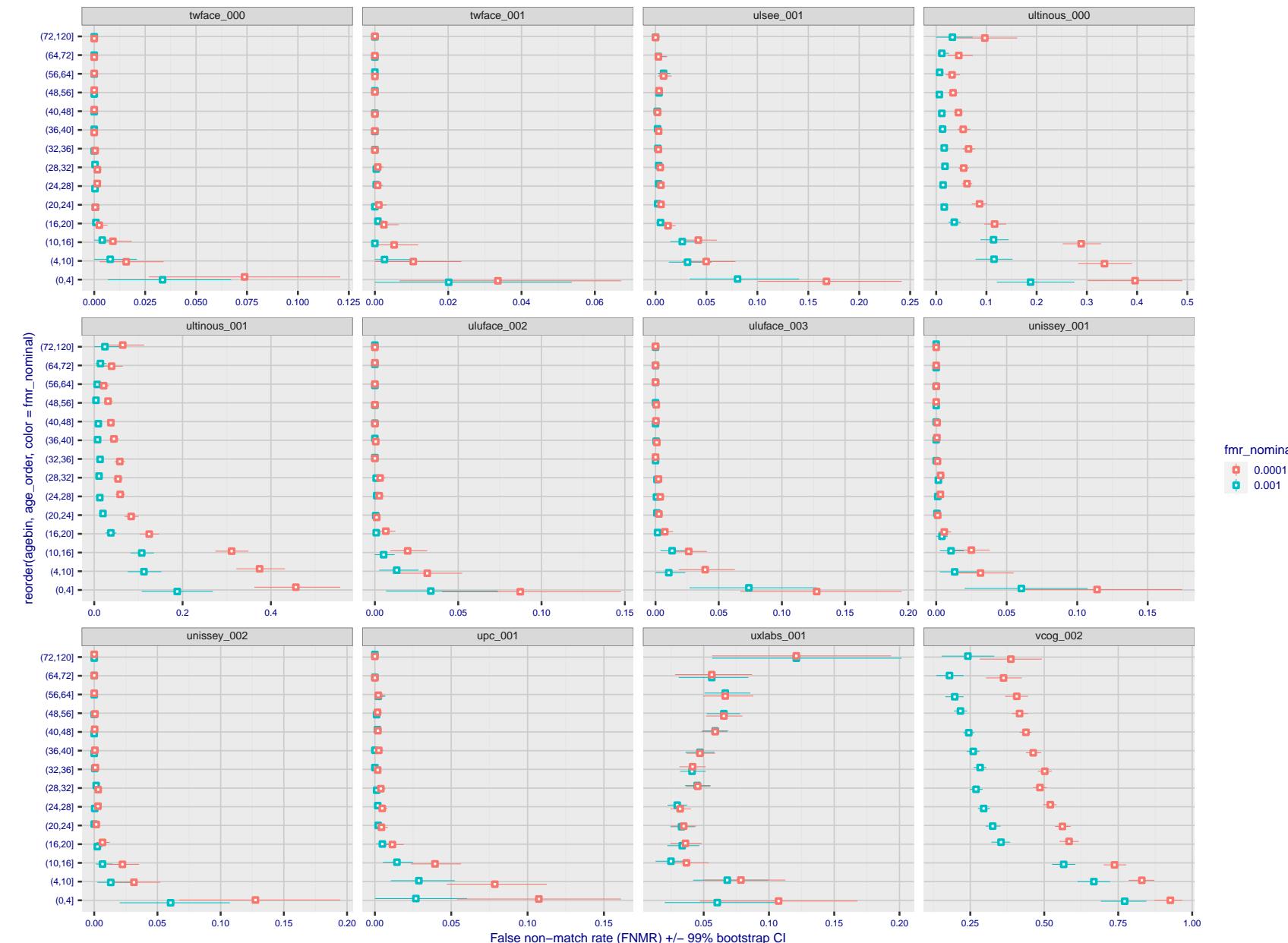


Figure 393: For the visa images, the dots show FNMR by age group for two operating thresholds corresponding to $FMR = \{0.001, 0.0001\}$ computed over all on the order of 10^{10} impostor scores. The FMR in each bin will vary also - see subsequent impostor heatmaps in sec. 3.6.2. Given a pair of face images taken at different times, we assign the comparison to the bin that is the arithmetic average of the subject's ages. This plot shows only the effect of age, not ageing. The number of comparisons in each bin is generally in the thousands, however the first and last bins are computed over 149 and 124 respectively. The error rates in some (adult) cases are zero, and in others the DET is flat so the error rates at the two thresholds are identical. The lines span 1% and 99% of bootstrap replicated FNMR estimates.

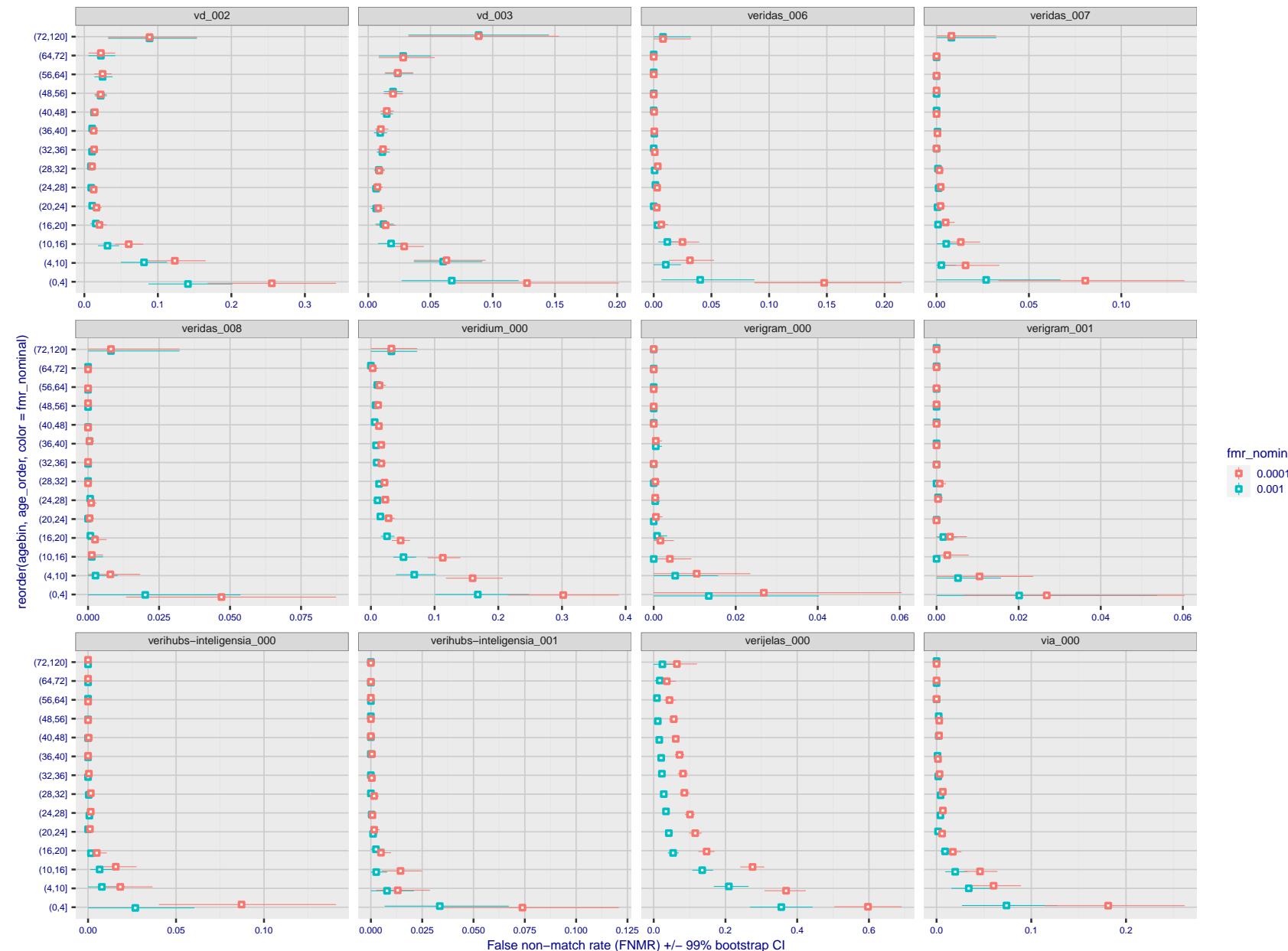


Figure 394: For the visa images, the dots show FNMR by age group for two operating thresholds corresponding to $FMR = \{0.001, 0.0001\}$ computed over all on the order of 10^{10} impostor scores. The FMR in each bin will vary also - see subsequent impostor heatmaps in sec. 3.6.2. Given a pair of face images taken at different times, we assign the comparison to the bin that is the arithmetic average of the subject's ages. This plot shows only the effect of age, not ageing. The number of comparisons in each bin is generally in the thousands, however the first and last bins are computed over 149 and 124 respectively. The error rates in some (adult) cases are zero, and in others the DET is flat so the error rates at the two thresholds are identical. The lines span 1% and 99% of bootstrap replicated FNMR estimates.

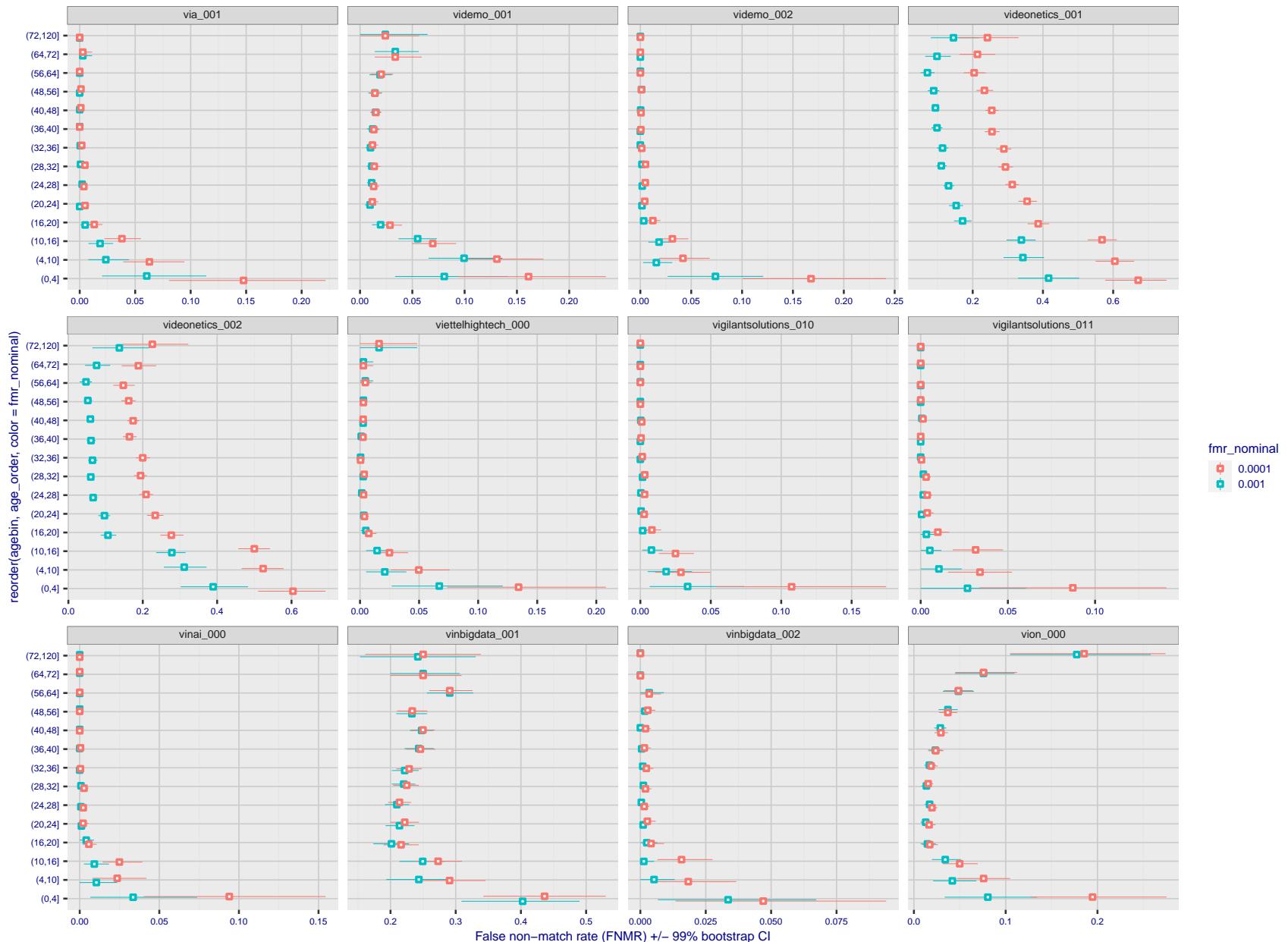


Figure 395: For the visa images, the dots show FNMR by age group for two operating thresholds corresponding to $FMR = \{0.001, 0.0001\}$ computed over all on the order of 10^{10} impostor scores. The FMR in each bin will vary also - see subsequent impostor heatmaps in sec. 3.6.2. Given a pair of face images taken at different times, we assign the comparison to the bin that is the arithmetic average of the subject's ages. This plot shows only the effect of age, not ageing. The number of comparisons in each bin is generally in the thousands, however the first and last bins are computed over 149 and 124 respectively. The error rates in some (adult) cases are zero, and in others the DET is flat so the error rates at the two thresholds are identical. The lines span 1% and 99% of bootstrap replicated FNMR estimates.



Figure 396: For the visa images, the dots show FNMR by age group for two operating thresholds corresponding to $FMR = \{0.001, 0.0001\}$ computed over all on the order of 10^{10} impostor scores. The FMR in each bin will vary also - see subsequent impostor heatmaps in sec. 3.6.2. Given a pair of face images taken at different times, we assign the comparison to the bin that is the arithmetic average of the subject's ages. This plot shows only the effect of age, not ageing. The number of comparisons in each bin is generally in the thousands, however the first and last bins are computed over 149 and 124 respectively. The error rates in some (adult) cases are zero, and in others the DET is flat so the error rates at the two thresholds are identical. The lines span 1% and 99% of bootstrap replicated FNMR estimates.

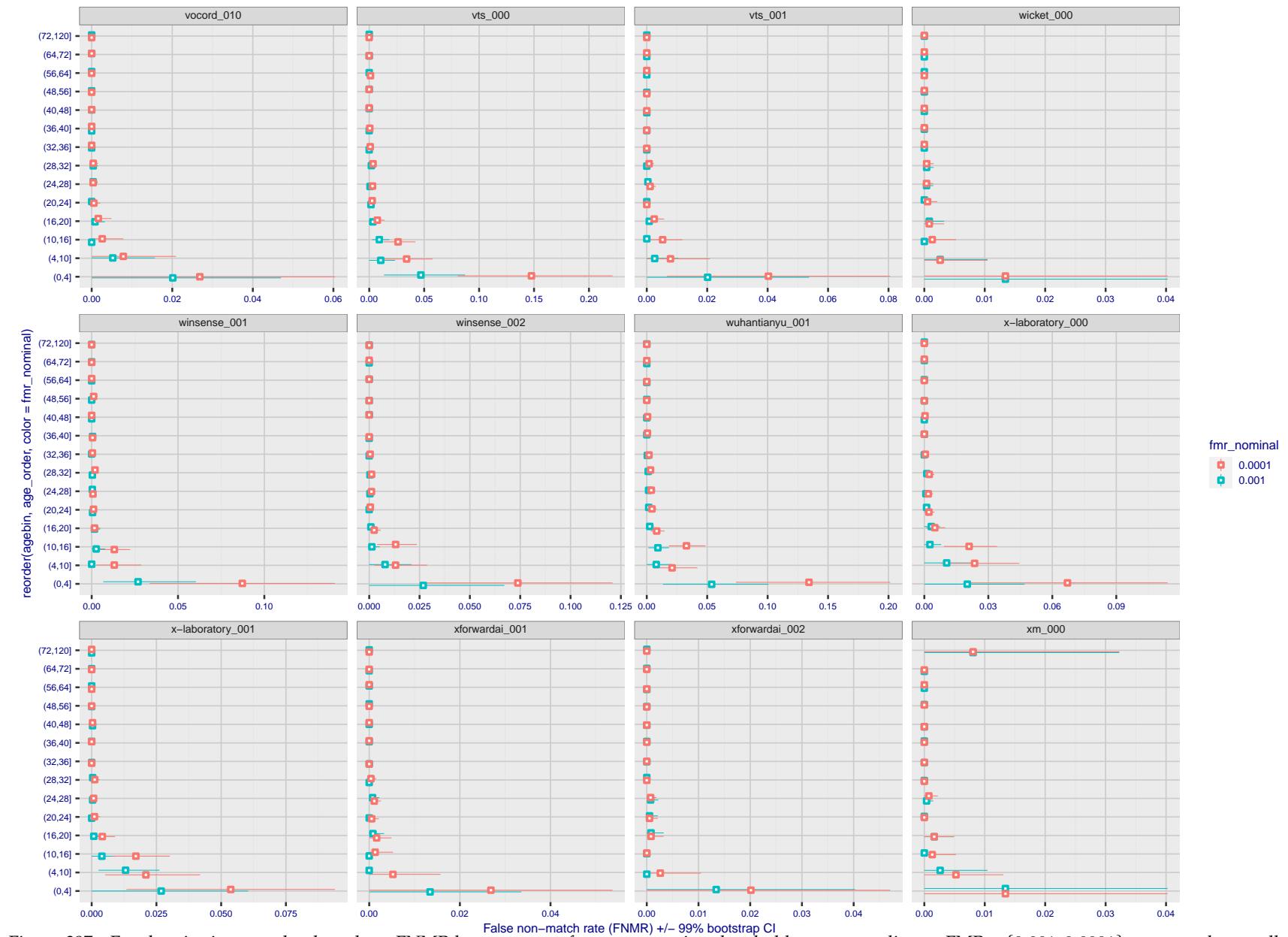


Figure 397: For the visa images, the dots show FNMR by age group for two operating thresholds corresponding to $FMR = \{0.001, 0.0001\}$ computed over all on the order of 10^{10} impostor scores. The FMR in each bin will vary also - see subsequent impostor heatmaps in sec. 3.6.2. Given a pair of face images taken at different times, we assign the comparison to the bin that is the arithmetic average of the subject's ages. This plot shows only the effect of age, not ageing. The number of comparisons in each bin is generally in the thousands, however the first and last bins are computed over 149 and 124 respectively. The error rates in some (adult) cases are zero, and in others the DET is flat so the error rates at the two thresholds are identical. The lines span 1% and 99% of bootstrap replicated FNMR estimates.



Figure 398: For the visa images, the dots show FNMR by age group for two operating thresholds corresponding to $FMR = \{0.001, 0.0001\}$ computed over all on the order of 10^{10} impostor scores. The FMR in each bin will vary also - see subsequent impostor heatmaps in sec. 3.6.2. Given a pair of face images taken at different times, we assign the comparison to the bin that is the arithmetic average of the subject's ages. This plot shows only the effect of age, not ageing. The number of comparisons in each bin is generally in the thousands, however the first and last bins are computed over 149 and 124 respectively. The error rates in some (adult) cases are zero, and in others the DET is flat so the error rates at the two thresholds are identical. The lines span 1% and 99% of bootstrap replicated FNMR estimates.

Caveats: None.

3.6 Impostor distribution stability

3.6.1 Effect of birth place on the impostor distribution

Background: Facial appearance varies geographically, both in terms of skin tone, cranio-facial structure and size. This section addresses whether false match rates vary intra- and inter-regionally.

Goals:

- ▷ To show the effect of birth region of the impostor and enrollee on false match rates.
- ▷ To determine whether some algorithms give better impostor distribution stability.

Methods:

- ▷ For the visa images, NIST defined 10 regions: Sub-Saharan Africa, South Asia, Polynesia, North Africa, Middle East, Europe, East Asia, Central and South America, Central Asia, and the Caribbean.
- ▷ For the visa images, NIST mapped each country of birth to a region. There is some arbitrariness to this. For example, Egypt could reasonably be assigned to the Middle East instead of North Africa. An alternative methodology could, for example, assign the Philippines to *both* Polynesia and East Asia.
- ▷ FMR is computed for cases where all face images of impostors born in region r_2 are compared with enrolled face images of persons born in region r_1 .

$$\text{FMR}(r_1, r_2, T) = \frac{\sum_{i=1}^{N_{r_1, r_2}} H(s_i - T)}{N_{r_1, r_2}} \quad (5)$$

where the same threshold, T , is used in all cells, and H is the unit step function. The threshold is set to give $\text{FMR}(T) = 0.001$ over the entire set of visa image impostor comparisons.

- ▷ This analysis is then repeated by country-pair, but only for those country pairs where both have at least 1000 images available. The countries¹ appear in the axes of graphs that follow.
- ▷ The mean number of impostor scores in any cross-region bin is 33 million. The smallest number of impostor scores in any bin is 135000, for Central Asia - North Africa. While these counts are large enough to support reasonable significance, the number of individual faces is much smaller, on the order of $N^{0.5}$.
- ▷ The numbers of impostor scores in any cross-country bin is shown in Figure 399.

Results: Subsequent figures show heatmaps that use color to represent the base-10 logarithm of the false match rate. Red colors indicate high (bad) false match rates. Dark colors indicate benign false match rates. There are two series of graphs corresponding to aggregated geographical regions, and to countries. The notable observations are:

- ▷ The on-diagonal elements correspond to within-region impostors. FMR is generally above the nominal value of $\text{FMR} = 0.001$. Particularly there is usually higher FMR in, Sub-Saharan Africa, South Asia, and the Caribbean. Europe and Central Asia, on the other hand, usually give FMR closer to the nominal value.
- ▷ The off-diagonal elements correspond to across-region impostors. The highest FMR is produced between the Caribbean and Sub-Saharan Africa.
- ▷ Algorithms vary.

¹These are Argentina, Australia, Brazil, Chile, China, Costa Rica, Cuba, Czech Republic, Dominican Republic, Ecuador, Egypt, El Salvador, Germany, Ghana, Great Britain, Greece, Guatemala, Haiti, Hong Kong, Honduras, Indonesia, India, Israel, Jamaica, Japan, Kenya, Korea, Lebanon, Mexico, Malaysia, Nepal, Nigeria, Peru, Philippines, Pakistan, Poland, Romania, Russia, South Africa, Saudi Arabia, Thailand, Trinidad, Turkey, Taiwan, Ukraine, Venezuela, and Vietnam.

- ▷ We computed the same quantities for a global FMR = 0.0001. The effects are similar.

Caveats:

- ▷ The effects of variable impostor rates on one-to-many identification systems may well differ from what's implied by these one-to-one verification results. Two reasons for this are a) the enrollment galleries are usually imbalanced across countries of birth, age and sex; b) one-to-many identification algorithms often implement techniques aimed at stabilizing the impostor distribution. Further research is necessary.
- ▷ In principle, the effects seen in this subsection could be due to differences in the image capture process. We consider this unlikely since the effects are maintained across geography - e.g. Caribbean vs. Africa, or Japan vs. China.

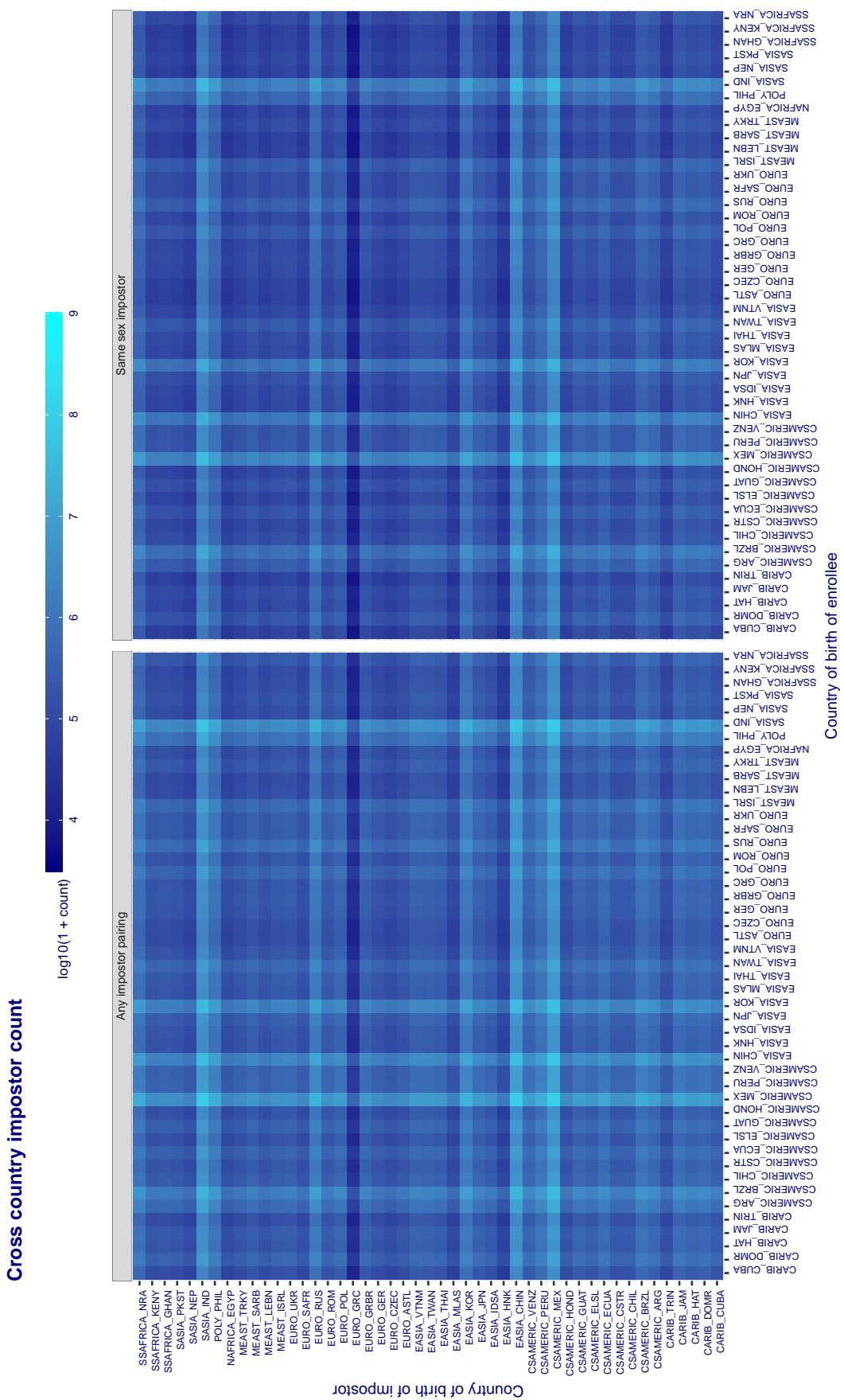


Figure 399: For visa images, the heatmap shows the count of impostor comparisons of faces from different individuals who were born in the given country pair. The FMR heatmaps themselves appear in the 1:1 report cards, for example, [this one](#).

3.6.2 Effect of age on impostors

Background: This section shows the effect of age on the impostor distribution. The ideal behaviour is that the age of the enrollee and the impostor would not affect impostor scores. This would support FMR stability over sub-populations.

Goals:

- ▷ To show the effect of relative ages of the impostor and enrollee on false match rates.
- ▷ To determine whether some algorithms have better impostor distribution stability.

Methods:

- ▷ Define 14 age group bins, spanning 0 to over 100 years old.
- ▷ Compute FMR over all impostor comparisons for which the subjects in the enrollee and impostor images have ages in two bins.
- ▷ Compute FMR over all impostor comparisons for which the subjects are additionally of the same sex, and born in the same geographic region.

Results:

The notable aspects are:

- ▷ Diagonal dominance: Impostors are more likely to be matched against their same age group.
- ▷ Same sex and same region impostors are more successful. On the diagonal, an impostor is more likely to succeed by posing as someone of the same sex. If $\Delta \log_{10} \text{FMR} = 0.2$, then same-sex same-region FMR exceeds the all-pairs FMR by factor of $10^{0.2} = 1.6$.
- ▷ Young children impostors give elevated FMR against young children. Older adult impostor give elevated FMR against older adults. These effects are quite large, for example if $\Delta \log_{10} \text{FMR} = 1.0$ larger than a 32 year old, then these groups have higher FMR by a factor of $10^1 = 10$. This would imply an FMR above 0.01 for a nominal (global) FMR = 0.001.
- ▷ Algorithms vary.
- ▷ We computed the same quantities for a global FMR = 0.0001. The effects are similar.

Note the calculations in this section include impostors paired across all countries of birth.

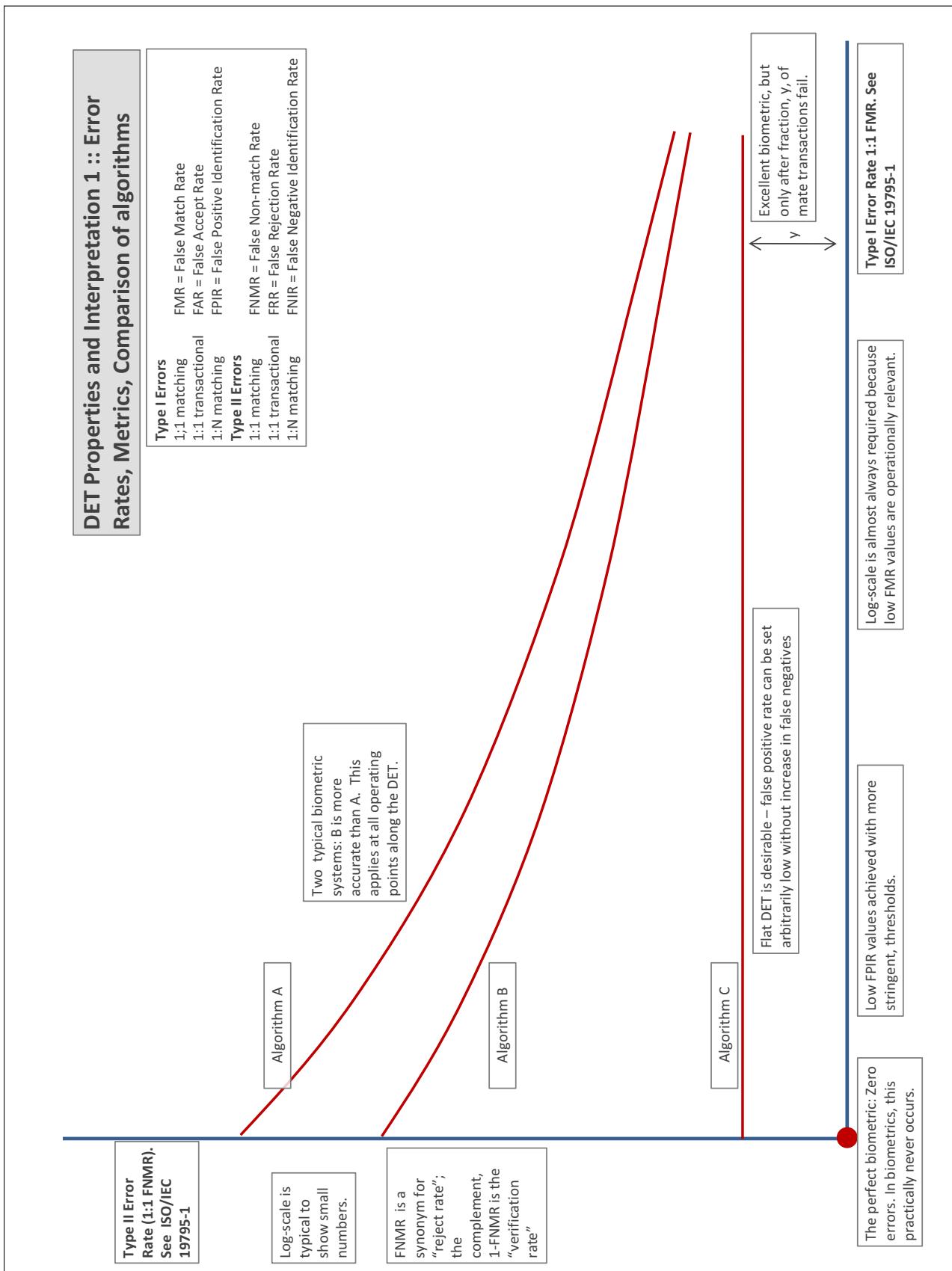
Accuracy Terms + Definitions

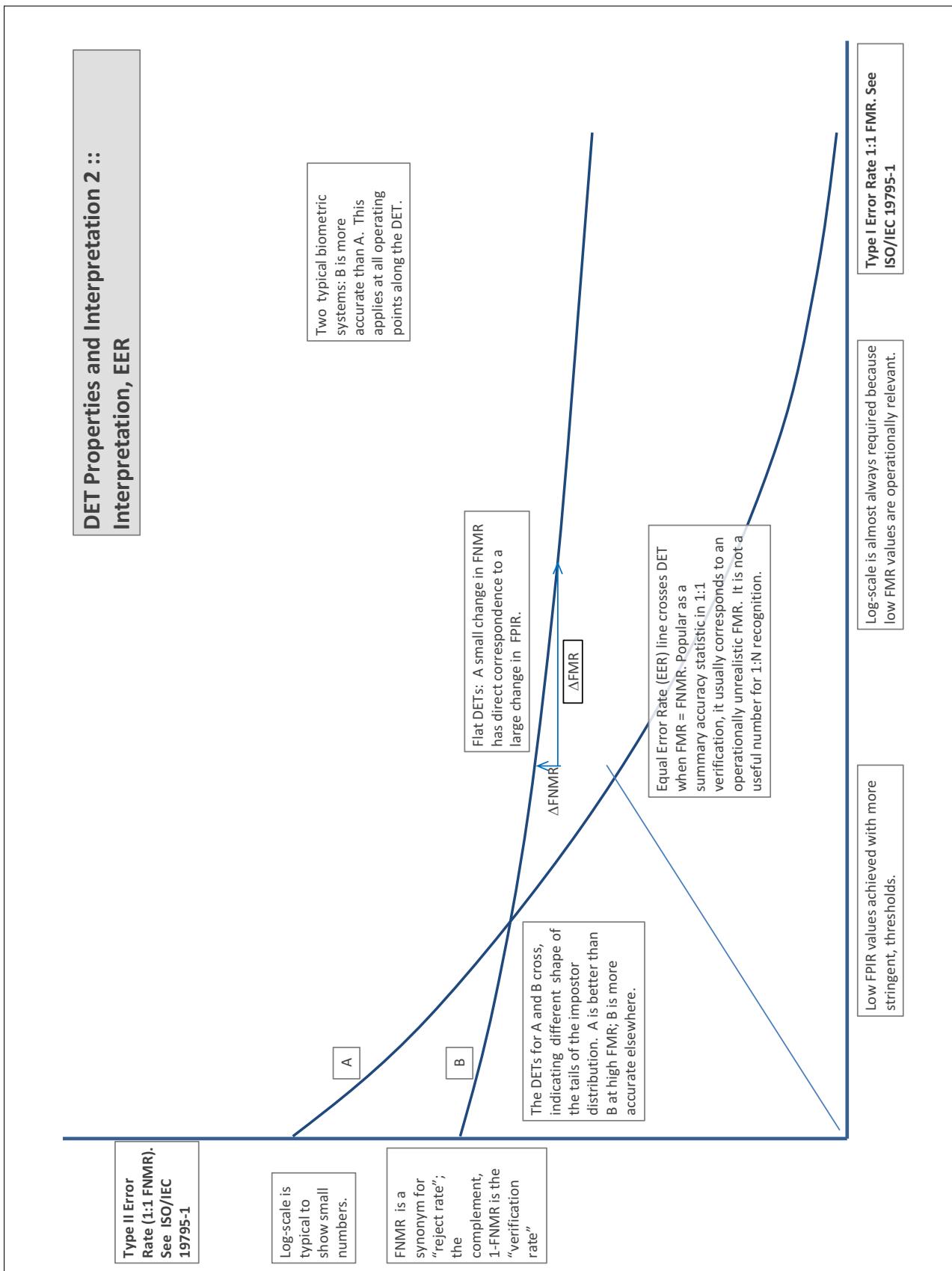
In biometrics, Type II errors occur when two samples of one person do not match – this is called a **false negative**. Correspondingly, Type I errors occur when samples from two persons do match – this is called a **false positive**. Matches are declared by a biometric system when the native comparison score from the recognition algorithm meets some **threshold**. Comparison scores can be either **similarity scores**, in which case higher values indicate that the samples are more likely to come from the same person, or **dissimilarity scores**, in which case higher values indicate different people. Similarity scores are traditionally computed by **fingerprint** and **face** recognition algorithms, while dissimilarities are used in **iris recognition**. In some cases, the dissimilarity score is a distance; this applies only when **metric** properties are obeyed. In any case, scores can be either **mate** scores, coming from a comparison of one person's samples, or **nonmate** scores, coming from comparison of different persons' samples. The words **genuine** or **authentic** are synonyms for mate, and the word **impostor** is used as a synonym for nonmatch. The words mate and nonmatch are traditionally used in identification applications (such as law enforcement search, or background checks) while genuine and impostor are used in verification applications (such as access control).

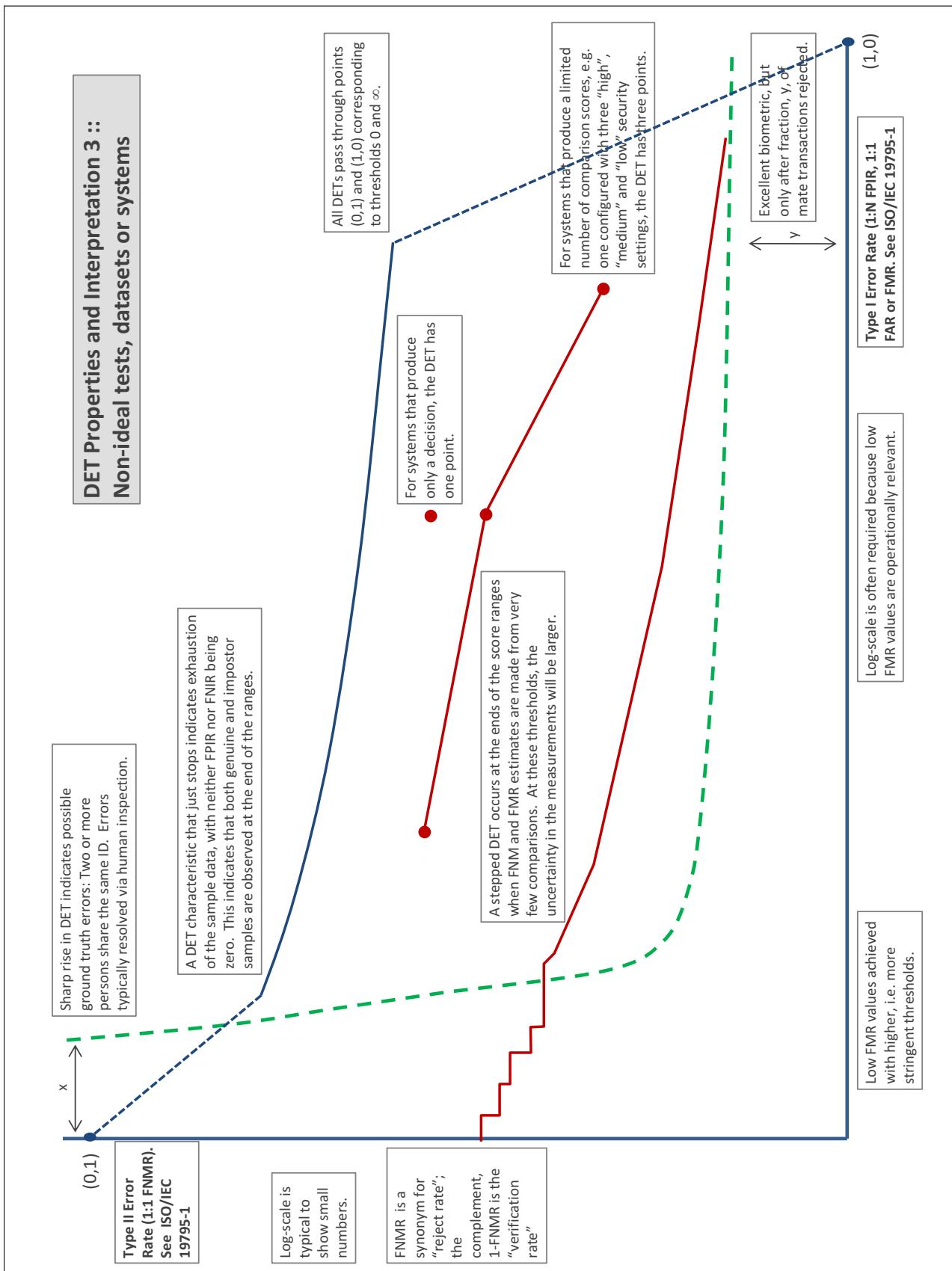
A **error tradeoff** characteristic represents the tradeoff between Type II and Type I classification errors. For verification this plots false non-match rate (FNMR) vs. false match rate (FMR) parametrically with T.

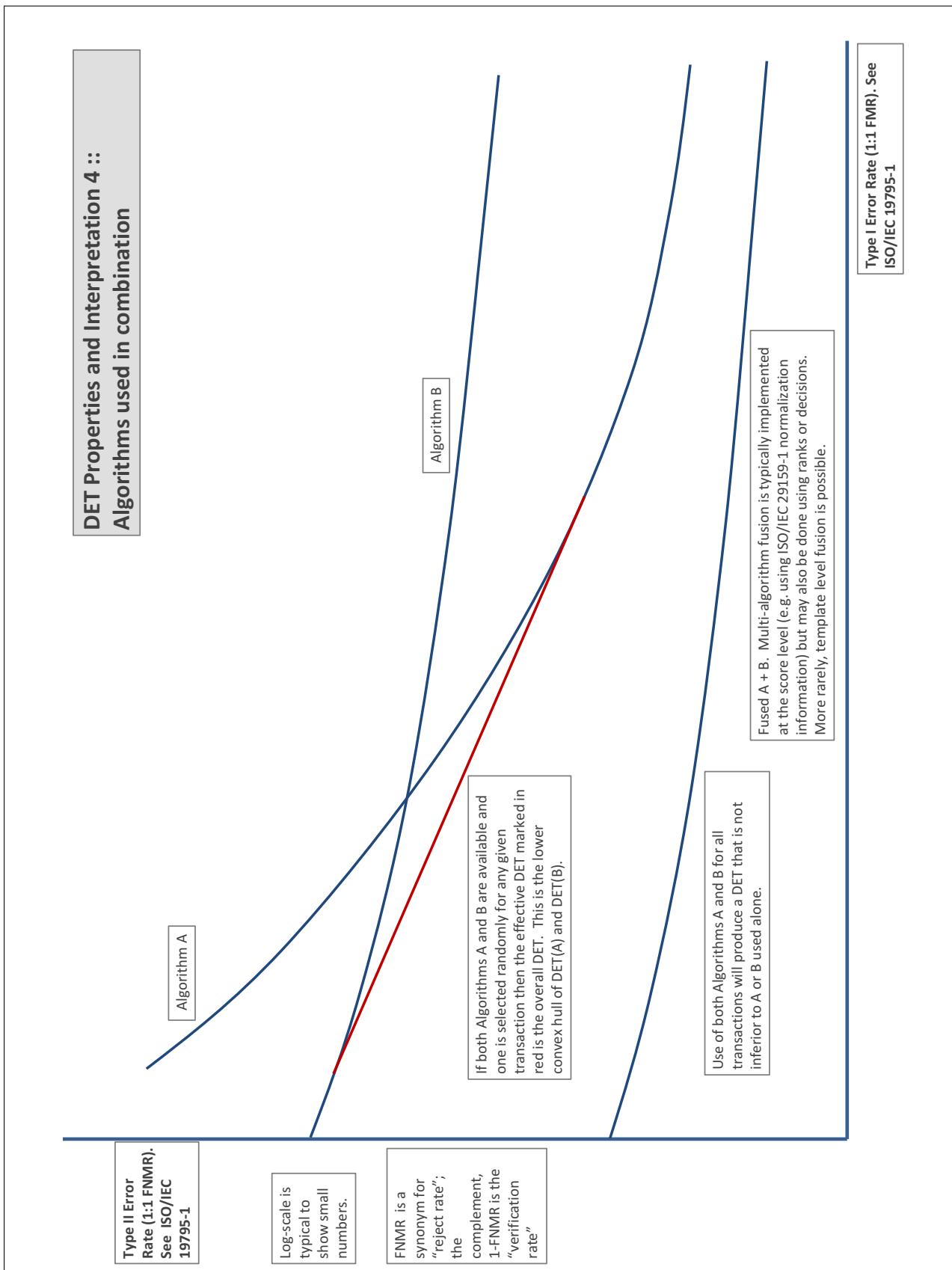
The error tradeoff plots are often called **detection error tradeoff (DET)** characteristics or **receiver operating characteristic (ROC)**. These serve the same function but differ, for example, in plotting the complement of an error rate (e.g., $TMR = 1 - FNMR$) and in transforming the axes most commonly using logarithms, to show multiple decades of FMR. More rarely, the function might be the inverse Gaussian function.

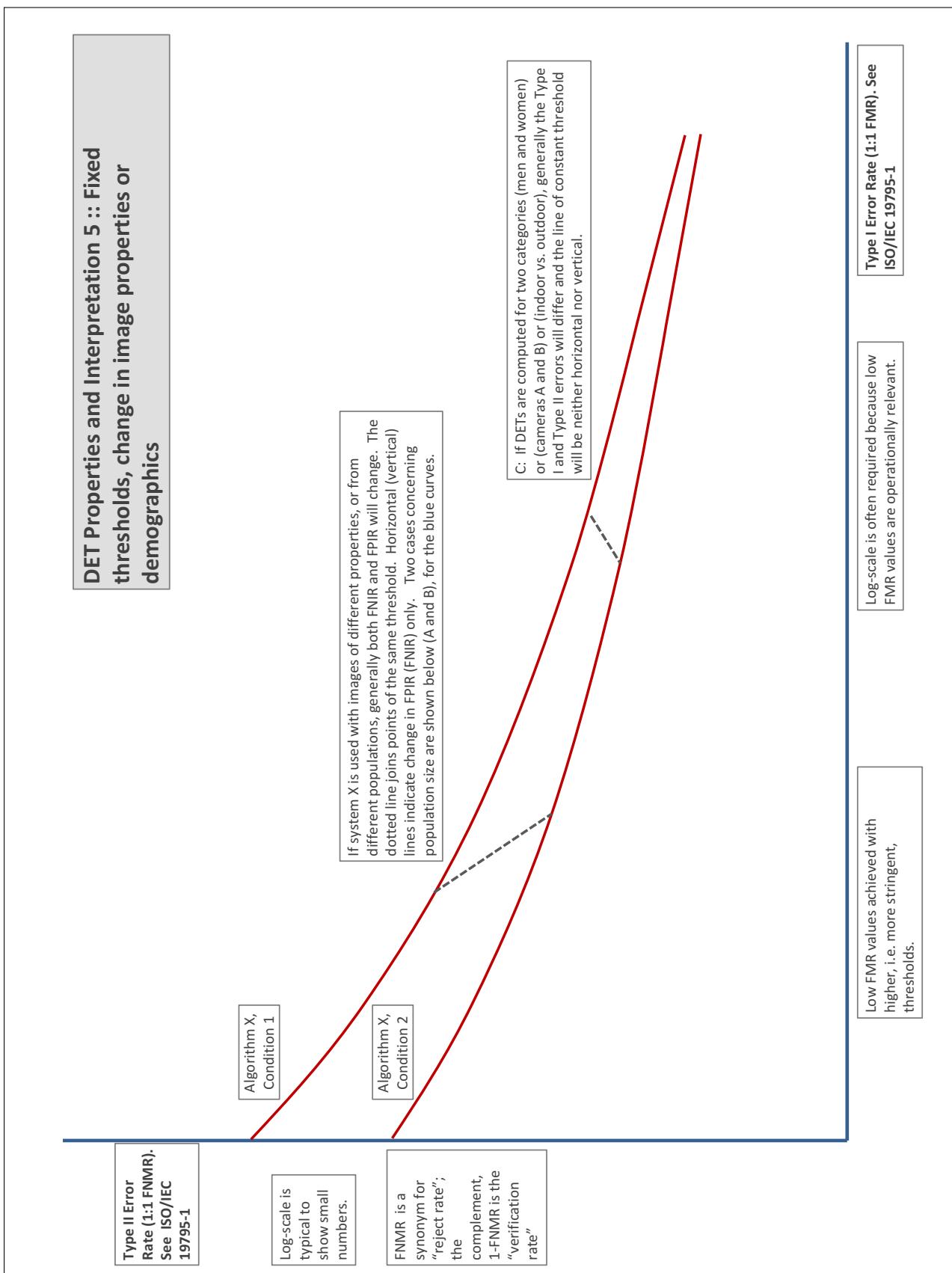
More detail and generality is provided in formal biometrics testing standards, see the various parts of [ISO/IEC 19795 Biometrics Testing and Reporting](#). More terms, including and beyond those to do with accuracy, see [ISO/IEC 2382-37 Information technology -- Vocabulary -- Part 37: Harmonized biometric vocabulary](#)











References

- [1] P. Jonathon Phillips, Amy N. Yates, Ying Hu, Carina A. Hahn, Eilidh Noyes, Kelsey Jackson, Jacqueline G. Cavazos, Géraldine Jeckeln, Rajeev Ranjan, Swami Sankaranarayanan, Jun-Cheng Chen, Carlos D. Castillo, Rama Chellappa, David White, and Alice J. O'Toole. Face recognition accuracy of forensic examiners, superrecognizers, and face recognition algorithms. *Proceedings of the National Academy of Sciences*, 115(24):6171–6176, 2018.